

# Addition and Condensation Polymerization Processes

Publication Date: June 1, 1969 | doi: 10.1021/ba-1969-0091.fw001

In Addition and Condensation Polymerization Processes; Platzer, N.;  
Advances in Chemistry; American Chemical Society: Washington, DC, 1969.





# Addition and Condensation Polymerization Processes

A symposium sponsored by  
the Division of Industrial  
and Engineering Chemistry  
at the 155th Meeting of the  
American Chemical Society,  
San Francisco, Calif.,  
April 1-5, 1968.

**Norbert A. J. Platzer**

*Symposium Chairman*

ADVANCES IN CHEMISTRY SERIES

91

AMERICAN CHEMICAL SOCIETY  
WASHINGTON, D. C. 1969

Coden: ADCSHA

Copyright © 1969

American Chemical Society

All Rights Reserved

Library of Congress Catalog Card 78-102896

PRINTED IN THE UNITED STATES OF AMERICA

# Advances in Chemistry Series

**Robert F. Gould, *Editor***

## *Advisory Board*

Frank G. Ciapetta

William von Fischer

Frederick M. Fowkes

Edwin J. Hart

F. Leo Kauffman

Stanley Kirschner

John L. Lundberg

William E. Parham

Edward E. Smissman



**AMERICAN CHEMICAL SOCIETY PUBLICATIONS**

## FOREWORD

ADVANCES IN CHEMISTRY SERIES was founded in 1949 by the American Chemical Society as an outlet for symposia and collections of data in special areas of topical interest that could not be accommodated in the Society's journals. It provides a medium for symposia that would otherwise be fragmented, their papers distributed among several journals or not published at all. Papers are refereed critically according to ACS editorial standards and receive the careful attention and processing characteristic of ACS publications. Papers published in ADVANCES IN CHEMISTRY SERIES are original contributions not published elsewhere in whole or major part and include reports of research as well as reviews since symposia may embrace both types of presentation.

## PREFACE

Polymer science has advanced to the point where macromolecules can be built at will. They can be designed with flexible or stiff chains, they can be linear or branched, and they can be tailored in length. They can be attached to each other by van der Waals' forces, dipole interaction, hydrogen or ionic bonding, or crosslinking. Amorphous and crystalline polymers may be made from established or new monomers by addition polymerization triggered by free radicals or ions or by condensation, coupling, ring-opening, or ring-closing reactions. The understanding of the relationship between the molecular structure, the kinetics of the process, and the performance characteristics of the product enables us to design better polymers with improved physical properties at reduced cost. Different macromolecules are being designed for different end uses which include fabrics, surface coating or adhesives, structural, automotive, packaging, electrical, glazing, photographic, thermal, medicinal, and other applications.

The first 26 chapters of this volume are devoted to process improvements and the kinetics of addition and condensation polymerization of common monomers. The remaining 22 chapters are concerned with new and better polymers designed for a specific end use or physical property.

### *Process Improvements and Polymerization Kinetics*

**Process Technology.** In commercial addition and condensation polymerization processes reactor design is an important factor for the quality and economics of the polymer. Combining macromolecular kinetics with reactor and process design has led to a new concept called reaction engineering. D. C. Chappellear and R. H. M. Simon review this novel concept in Chapter 1.

**Free-Radical Polymerization in Bulk, Solution, and Suspension.** In free-radical polymerization in bulk, solution, and aqueous suspension the initiator is dissolved in the monomer. Aqueous suspension polymerization is considered as bulk polymerization in droplets. Some polymers, like poly(vinyl chloride) or polyacrylonitrile, are insoluble in the monomers and precipitate during bulk polymerization. The growth of the precipitated chain, which depends on the number of trapped radicals, is

described by O. G. Lewis and R. M. King. Other commercial polymers, like polystyrene or poly(vinyl acetate), remain soluble in their monomers.

Glass-reinforced polyester is manufactured by copolymerizing styrene with unsaturated polyesters between glass fibers. For this copolymerization, enolizable phenylketo compounds may be used as initiator, according to H. Hopff and co-workers. The initiation mechanism is explained by an autoxidation to an active ketohydroperoxide form. The copolymerization proceeds at approximately the same rate as with the usual peroxide initiators, but the reaction is less exothermic, thus preventing crazing, bubble formation, and volume contraction. In the commercial terpolymerization of styrene with 2-ethylhexyl acrylate and glycidyl acrylate high conversion and narrow molecular weight distribution are desirable. The effects of polymerization temperatures and initiation rate on molecular weight, molecular weight distribution, and composition have been studied by A. Ravve and J. T. Khamis.

The kinetics of free-radical polymerization of methyl methacrylate and other monomers with small amounts of  $\text{SO}_2$  and *tert*-butyl hydroperoxide in bulk and solution have been investigated by P. Ghosh and F. W. Billmeyer. The free-radical polymerization of methyl methacrylate, acrylonitrile, and other polymer monomers can be accelerated by adding Lewis acids, like zinc chloride or alkylaluminum chloride. The polar monomer forms a complex with the Lewis acid and becomes more electron accepting. In the presence of a nonpolar olefin or conjugated diene, the complexed polar monomer transfers its charge and copolymerizes readily, as described by N. G. Gaylord and A. Takahashi.

ESR studies of free radical polymerization had been limited to solid state systems. Recently, B. Rånby and K. Takakura were able to explore vinyl polymerization in aqueous solution, using a redox system of  $\text{TiCl}_3$  with  $\text{H}_2\text{O}_2$ .

**Free-Radical Polymerization in Emulsion.** In suspension polymerization, the particle size is fixed by the size of the monomer droplet which contains the initiator. Emulsion polymerization differs from suspension polymerization in that the initiator is dissolved in the aqueous phase and the polymer particle grows during polymerization. Free radicals are generated in the water and diffuse to the monomer-water interface. The length of the polymer chain formed, or equivalently the molecular weight, depends on the rate of free radical arrival and termination. S. Katz, G. M. Saidel, and R. Shinnar present a computation method to calculate the molecular weight distribution for arbitrary rates of free radical arrival and termination.

Vinyl chloride is polymerized in bulk or aqueous suspension to yield a dry-blend resin of porous particle surface. In aqueous emulsion it

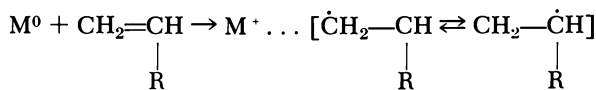
polymerizes into particles of closed surface, used as paste resin. In continuous emulsion polymerization, a broad distribution of particle sizes is obtained, depending on the residence time in the reactor. In the batch emulsion polymerization of styrene, it is possible to obtain a latex of uniform large particle size by seeding the emulsion with particles and controlling the emulsifier concentration. In the batch emulsion polymerization of vinyl chloride this has not been possible. A latex of two particle sizes is obtainable—one about  $1\mu$  which is grown on  $0.4\text{-}\mu$  seeds, and one about  $0.3\mu$  grown as new particle from a micelle. G. Gatta and co-workers discovered that it is possible to produce also a poly(vinyl chloride) of a single large particle size by seeding. This requires not only control of the emulsifier concentration but also a definite ratio of seeded particle surface to the water volume.

Vinyl acetate is polymerized in aqueous emulsion and used widely in surface coating and in adhesives. Copolymerized with vinyl esters of branched carboxylic acids and small quantities of acrylic acid, it gives paint latices of excellent performance characteristics. G. C. Vegter found that a coagulum-free latex of very low residual monomer content can be produced from a mixture of an anionic and a nonionic emulsifier according to a specific operating procedure. The freeze/thaw stability of polymeric latices has been investigated by H. Naidus and R. Hanzes.

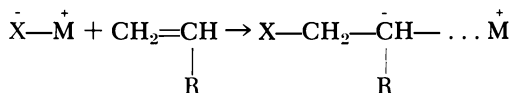
**Radiation-Induced Polymerization.** Polymerization induced by irradiation is initiated by free radicals and by ionic species. On very pure vinyl monomers, D. J. Metz demonstrated that ionic polymerization can become the dominating process. In Chapter 12 he postulates a kinetic scheme starting with the formation of ions, followed by a propagation step *via* carbonium ions and chain transfer to the vinyl monomer. C. Schneider studied the polymerization of styrene and  $\alpha$ -methylstyrene by pulse radiolysis in aqueous medium and found results similar to those obtained in conventional free-radical polymerization. She attributes this to a growing polymeric benzyl type radical which is formed partially through electron capture by the styrene molecule, followed by rapid protonation in the side chain and partially by the addition of H and OH to the double vinyl bond. A. S. Chawla and L. E. St. Pierre report on the solid state polymerization of hexamethylcyclotrisiloxane by high energy radiation of the monomer crystals.

**Anionic Polymerization.** Anionic polymerization is limited to non-polar monomers with carbon-to-carbon double bonds. It takes place in the presence of catalysts capable of generating carbanions—*e.g.*, alkali metals, metal hydrides, metal alkyls, amides, and Grignard reagents. The

initiating step may occur in two principal ways, as follows:



anion radical



anion

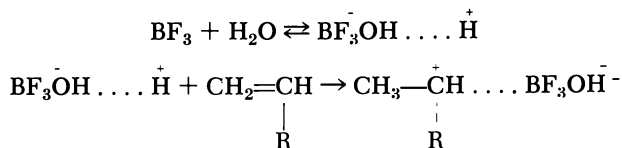
$M^+$  represents the positive counterion, also called “gegenion,” which, in many cases, accompanies the growing chain. Propagation occurs through successive addition of monomer molecules to the charged or “living” ends of the growing chains. Anionic polymerization involves several kinds of anionic species propagating simultaneously. M. Szwarc distinguishes between free ions, contact ion pairs, solvent-separated ion pairs, triple ions, complexed ion pairs, and others. He determined the activation energies of the various types of growth and the heats of the different transformations. If the propagation step is much faster than the initiating step, two or more polymers differing in chain length and stereospecificity are obtained. This was demonstrated in the polymerization of methyl methacrylate with Grignard or organolithium catalyst. V. N. Sokolov and I. Y. Poddubny propose a mechanism for the stereospecific polymerization of dienes. They also assume a dynamic equilibrium during the catalyst complexing and the subsequent polymer chain propagation. In their experiments, butenyllithium- and butenylmagnesium chloride were used as catalysts.

Catalysts of the Ziegler-Natta type are applied widely to the anionic polymerization of olefins and dienes. Polar monomers deactivate the system and cannot be copolymerized with olefins. J. L. Jezl and co-workers discovered that the “living” chains from an anionic polymerization can be converted to free radicals by the reaction with organic peroxides and thus permit the formation of block copolymers with polar vinyl monomers. In this novel technique of combined “anionic-free radical” polymerization, they are able to produce block copolymers of most olefins, such as alkylene, propylene, styrene, or butadiene with polar vinyl monomers, such as acrylonitrile or vinyl pyridine.

**Cationic Polymerization.** Cationic polymerization is initiated by the transfer of a cation from the catalyst to the monomer. It allows a wider choice of monomers with double bonds, including carbonyls, cyclic ethers, and lactones. The ion may be within a carbonium or an oxonium ion. Friedel-Crafts halides, like  $\text{AlCl}_3$  or  $\text{Al}(\text{C}_2\text{H}_5)\text{Cl}_2$ , are strong Lewis acids and initiate the polymerization directly. Weak Lewis acids need a

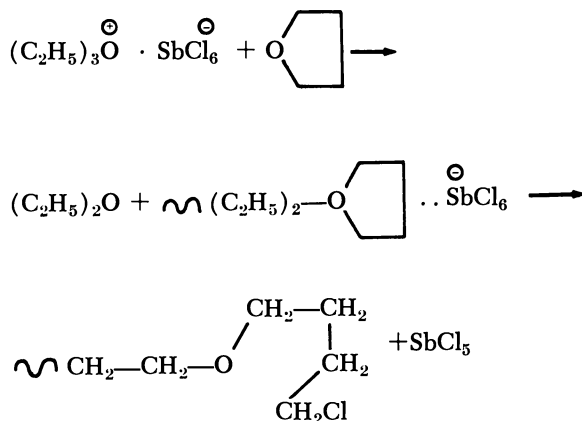


cocatalyst to aid cation transfer. Such cocatalysts may be a small amount of water, HCl, an ether, or another solvent. It is even possible that in the case of a strong Lewis acid a small amount of water or another proton donor acts as a cocatalyst:



$\text{BF}_3\text{OH}^-$  represents the negative counterion, also called gegenion. Propagation proceeds through the insertion of a new monomer molecule on the carbonium ion between the two charges. J. P. Kennedy and G. E. Milliman studied the cationic polymerization with a weak Lewis acid, like trialkylaluminum. They required a Lewis base, like *tert*-butyl chloride, as a cocatalyst. They assume the formation of a complex catalyst in the polymerization of isobutylene and other olefins. V. A. Kormer and co-workers studied the stereospecific polymerization of 1,3-butadiene with bis( $\pi$ -allylnickel halides) and Lewis acids. They found that the strength of the bond between the transition metal and the growing chain influences the structure of the polybutadiene formed.

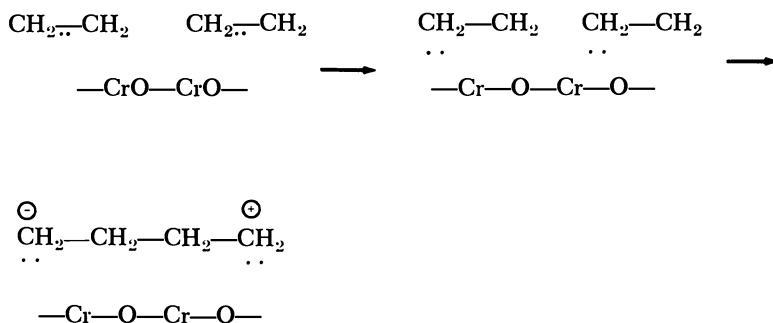
The initiation mechanism for cationic polymerization of cyclic ethers, vinyl amines, and alkoxy styrenes has been investigated by A. Ledwith. He used stable cations, like tropylium or triphenylmethyl cations with stable anions, like  $\text{SbCl}_6^-$ , and distinguished between three initiation reactions: cation additions, hydride abstraction, and electron transfer. One of the typical examples of cationic polymerization, in which the propagating species is the oxonium ion, is the polymerization of tetrahydrofuran. P. and M. P. Dreyfuss studied this polymerization with the triethyloxonium salts of various counterions and established an order of



stability for  $\text{PF}_6^-$ ,  $\text{SbF}_6^-$ ,  $\text{BF}_4^-$ , and  $\text{SbCl}_6^-$  anions. It had been difficult to copolymerize tetrahydrofuran or other oxonium type species with carbonium type species like styrene. Y. Yamashita discovered that certain monomers, like trioxane or 1,3-dioxolane would form carbonium ions with  $(\text{C}_2\text{H}_5)_2\text{OBF}_3$ , but oxonium ions with  $(\text{C}_2\text{H}_5)_3\text{OBF}_4$ , and would copolymerize with either one of the above species.

During the initial polymerization of trioxane with  $(\text{C}_4\text{H}_9)_2\text{OBF}_3$  in melt or solution, no solid polymer is formed, and the reaction medium remains clear. Using a high resolution NMR spectroscope, C. S. H. Chen and A. Di Edwardo observed the appearance of soluble linear polyoxymethylene chains. In the cationic copolymerization of trioxane with 1,3-dioxolane, V. Jaacks found also that a soluble copolymer forms first and turns later into a crystalline copolymer of different composition. Crystallization and polymerization proceed simultaneously in the solid phase.

**Polymerization with Complex Catalysts.** High density polyethylene reached a domestic production of 1.25 billion pounds in 1968. It is made either with a stereospecific Ziegler-Natta catalyst or on a supported chromium oxide catalyst. The latter forms a complex with the silica-alumina and is activated by treatment with air and steam at elevated temperature. The mechanism is such that electrons are donated to the catalyst in order to be returned under polymerizational-promoting conditions, consequently lowering the energy of the system:



It is, however, more complex than this because the silica-alumina support affects also the polymerization. A. Clark describes the correlation between the chromium trioxide and the silica-aluminum support. He also shows the effect of the catalyst activation temperature on the molecular weight of the polyethylene formed.

Cycloolefins can be polymerized by a ring-opening mechanism with complex tungsten-aluminum catalyst, according to K. W. Scott and co-workers. The polymer formed is unsaturated and is either elastomeric or rigid, depending on the monomer and degree of polymerization.

## *Polymers at Will and the Limitations*

A typical example showing that we are able to build macromolecules at will is given by C. P. Pinazzi and co-workers in the first chapter of the second section, Chapter 27. They report how model polyenes can be built and how they react. In Chapter 28 K. F. O'Driscoll illustrates the limitations in polymerization. For every vinyl monomer, a ceiling temperature exists, above which depropagation exceeds polymerization. If two vinyl monomers are copolymerized at a temperature at which one depropagates, the polymer formed will have an unusual composition and sequence distribution.

Occasionally, low molecular weight polymers are required as sealants, adhesives, or in rocket solid propellants. F. P. Baldwin and co-workers report on the manufacture of a low molecular weight carboxy terminated product made by depropagating ozonization of a higher molecular weight polyisobutylene.

**Polymers of High Strength and Toughness.** All polymer chains, regardless of their detailed structure, have about the same strength of *ca.* 2,000,000 p.s.i.g. since they are formed by C—C, C—N, C—O, or C—S covalent bonds. However, the tensile strength of commercial thermoplastics is only 3000–17,000 p.s.i.g. and depends primarily on the interaction between the polymeric chains. Interaction between chains is affected either by secondary forces, such as the van der Waals' forces, dipole-dipole attraction, and hydrogen bonding or by primary forces, such as crosslinking by ionic or covalent bonding. Its effectiveness can be increased by lengthening the chains or by arranging the chains in a crystalline structure. In selecting a polymerization process, it is important to know the phase of the monomer and polymer since the phase affects the configuration and crystallinity of the product. V. A. Kargin shows the importance of the phase in Chapter 30 on the formation of liquid crystals and the analogy of the nucleation of polymers to the nucleation in crystallography.

The possibility of fracture on impact can be reduced by dispersing an elastomeric phase uniformly through the rigid material, as it is done in polyblends or better in grafting vinyl monomer upon rubber. H. Bartl and D. Hardt describe the manufacture of a tough rigid PVC by grafting vinyl chloride upon an elastomeric ethylene–vinyl acetate copolymer.

The internal cross-linking of styrene copolymers is dealt with in the chapter of R. N. Haward, B. M. Parker and E. F. T. White, who prepared a copolymer of styrene and hydroxyethyl methacrylate and crosslinked the copolymer with hexamethylene diisocyanate.

**Light Weight Polymers.** In many instances, lighter weight, thermal insulation, and cushioning effects are considered more important than

strength. During the last 15 years, a number of light weight thermoplastic and thermoset foams with closed and open cellular structure have been developed using volatile foaming or chemical blowing agents. A. R. Ingram reviews various processes for making expandable polystyrene which can be molded or extruded into foam. A new expandable resin is a copolymer of 1-butene with sulfur dioxide where excess  $\text{SO}_2$  acts as a foaming agent. Its manufacture by suspension polymerization is reported by J. Chatelain.

**Non-flammable Plastics.** Non-flammable plastics are required as structural material in commercial buildings and for many automotive, electronic, and electrical applications. From the thermoplastics, only the halogen-containing polymers, polyamides, polycarbonate, poly(phenylene oxide), polysulfone, and polyimides are self-extinguishing. Flammable plastics can be made self-extinguishing by incorporating fire retardants or by adding mineral fillers. A novel version of making ABS (acrylonitrile-butadiene-styrene graft copolymer) non-flammable, without reducing softening temperature, is by incorporating bis(dibromopropyl) fumarate as a fourth monomer. This is described by W. Cummings and R. E. Stark.

**Modified Surfaces.** It is frequently desirable to change the surface of a polymer. Nonpolar surfaces of plastics are characterized by static electricity buildup, non-wetting, poor adhesion, low printability, and poor dyeing. These disadvantages can be overcome by grafting polar vinyl monomers upon the surface by irradiation. A. S. Hoffman describes radiation grafting of polyelectrolytes upon nonpolar surfaces, and A. Chapiro and co-workers discuss radiation grafting of acrylic acid and vinyl pyridene upon Teflon films.

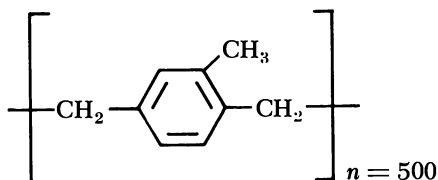
On the other hand, it might be desirable to reduce the hygroscopicity of certain polymers. J. C. Arthur deals with radiation grafting of vinyl monomers upon cotton cellulose.

**Transparent Polymers.** Amorphous thermoplastics, like poly(methyl methacrylate), polystyrene, SAN, PVC, or the cellulose esters are transparent and used for glazing, photographic film, blown bottles, or clear packaging containers. Only a few crystalline thermoplastics, like poly(4-methyl-1-pentane), where the crystalline and the amorphous phases have almost identical refractive indexes, or polycarbonate, which has smaller crystals than the wavelength of light, are also transparent. R. Kosfeld and co-workers analyzed the mobility of methyl groups in polycarbonate, poly(methyl methacrylate) and poly( $\alpha$ -methyl styrene) by NMR spectroscopy.

Generally, to make glass-clear polymers, we must prevent crystallization. This can be accomplished by placing bulky side groups on the main chains. Changing from a crystalline to an amorphous configuration

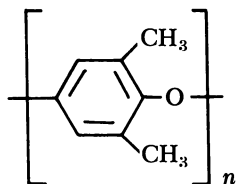
results in less rigidity and lower heat deflection temperature. To maintain high temperature performance, the backbone must be stiffened by placing aromatic rings into the main chains. Two typical examples are a glass clear amorphous aromatic polyamide with three methyl side chains and a phenylated polyphenylene. The polyamide is made by polycondensation of trimethylhexamethylenediamine with terephthalic acid, as described by G. Bier. The phenylated polyphenylene is made by a Diels-Alder reaction of bicyclopentadieneone with diacetylene, as described by J. K. Stille and co-workers.

**Heat-Resistant Polymers.** One of the greatest disadvantages of the commodity plastics in comparison with natural building materials is their low softening temperature. By building an inflexible aromatic or heterocyclic ring into the chain, the softening temperature can be raised significantly. Linear *p*-polyphenylene by itself is a very crystalline, brittle, insoluble, and infusible polymer because its chain is essentially inflexible. Chain flexibility may be introduced by inserting flexible hinges, like alkyl, —O—, —CO—, —NH—, —N<sub>2</sub>—, —S—, or —SO<sub>2</sub>— groups between the rings. Poly-*p*-xylylene



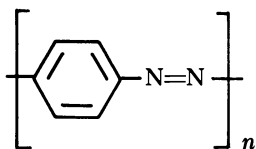
has —CH<sub>2</sub>—CH<sub>2</sub>— as a flexible hinge and a melting point of 400°C. It is made by a novel vapor deposition polymerization process, as described by its inventor, W. F. Gorham.

Poly(phenylene oxide) has —O— as a flexible hinge. It is made by

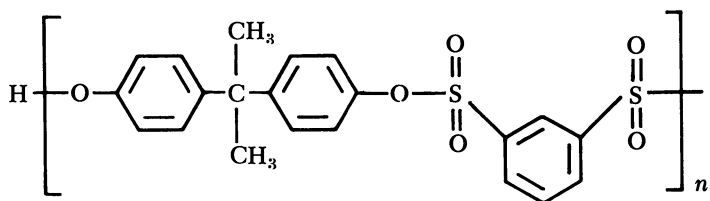
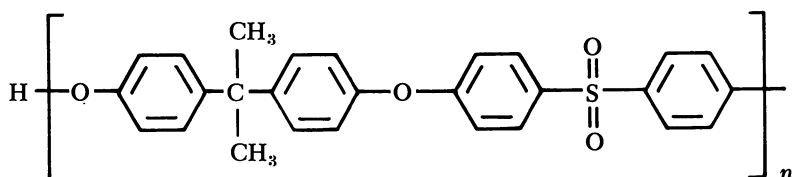


oxidative coupling with cuprous chloride in pyridine. Beginning with a phenol having two methyl side chains, the polymer remains amorphous with a heat deflection temperature of 204°C. (at 66 p.s.i.g.) and can be thermoprocessed. The process and its mechanism are reviewed by G. D. Cooper and A. Katchman.

Oxidative coupling is also to be used to prepare azopolymers from



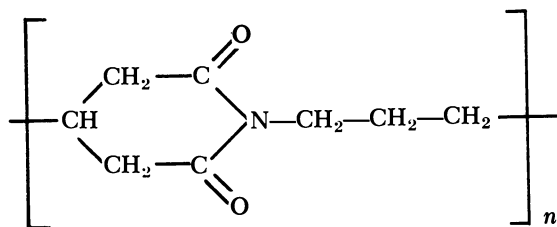
aromatic diamines with cuprous chloride or dimethyl acetamide or its mixture with pyridine, as reported by H. C. Bach and W. B. Black. Bisphenol-A (*p,p*-isopropylidene diphenol), made by the reaction of phenol with acetone, is one of the components in the condensation polymerization of polycarbonate and phenoxy, as well of polysulfones and polysulfonates.



The polysulfones are made by condensation polymerization of the potassium salt of bisphenol-A with dichlorodiphenyl sulfone, as discussed by S. R. Schulze and A. L. Baron. The polysulfonates are made from bisphenol-A and disulfonyl chlorides. They are more brittle than polysulfone and have been suggested by R. J. Schlott and co-workers to be used in copolymers with linear polyesters to improve the hydrolytic stability of the latter.

The polyimides are the best developed class of high temperature polymers with exceptional oxidation resistance. They are generally based on the condensation polymerization of aromatic dianhydrides with diamines forming a soluble polyamic acid, followed by intermolecular cyclodehydration to the insoluble polydiimide. Their maximum use temperature is 358°C. Recently H. Reimschuessel prepared a polyimide

from  $\beta$ -carboxymethylated caprolactam by opening the lactam ring followed by intermolecular cyclodehydration:



Semi-ladder polymers, possessing aromatic and hetero rings, are prepared by condensation polymerization and cyclodehydration from aromatic dicarboxylic or dicarbonyl compounds with aromatic tetraamines of diaminophenols or aminothiophenols. They are used in composites with glass cloth or high strength whiskers, or as adhesive for metal to metal bond. They are characterized by good strength properties from very low temperatures (as  $-260^{\circ}\text{C}.$ ) to very high temperatures ( $320^{\circ}$ – $650^{\circ}\text{C}.$ ). C. Berry and co-workers discuss novel high temperature materials developed for the Air Force: BBB (poly(bisbenzimidazo benzo phenanthroline-dione)) and BBL, both made by condensation polymerization of naphthalenetetracarboxylic acid with either tetraaminobiphenyl or tetraaminobenzene. These polymers are finding increased use in space-craft technology.

### **Conclusion**

The first 26 chapters represent a cross-section of the numerous processes available for the polymerization of common monomers. Through the understanding of process kinetics and through novel technology, we are able to build better polymers from these monomers. The remaining 22 chapters should leave the reader with the impression that we can build new or modified polymers at will and design them for specific end uses.

NORBERT A. J. PLATZER

Springfield, Mass.  
January 1969

# Polymerization Reaction Engineering

DAVID C. CHAPPELEAR<sup>1</sup> and ROBERT H. M. SIMON

Monsanto Co., Process Technology Department, Hydrocarbons and Polymers Division, Springfield, Mass.

*The rational design of a reaction system to produce a desired polymer is more feasible today by virtue of mathematical tools which permit one to predict product distribution as affected by reactor type and conditions. New analytical tools such as gel permeation chromatography are beginning to be used to check technical predictions and to aid in defining molecular parameters as they affect product properties. The vast majority of work concerns bulk or solution polymerization in isothermal batch or continuous stirred tank reactors. There is a clear need to develop techniques to permit fuller application of reaction engineering to realistic nonisothermal systems, emulsion systems, and systems at high conversion found industrially. A mathematical framework is also needed which will start with carefully planned experimental data and efficiently indicate a polymerization mechanism and statistical estimates of kinetic constants rather than vice-versa.*

Owing to a recent increase in theoretical treatments of polymerization kinetics, processes, and reactor design, chemical engineers are becoming increasingly active in a field where physical chemists primarily published. This paper reviews the theoretical tools now available and attempts to identify the work needed to make a fundamental approach more useful in practice. The broader field of chemical reactor engineering is itself relatively new, with the first modern text by Brotz (10) and by Walas (56) appearing in 1958 and 1959, respectively. Of the several thousand pages that have appeared since 1958, however, only a few deal with polymerization reactors, hardly sufficient recognition of their commercial importance. The recent activity seems triggered by the avail-

<sup>1</sup> Also staff member, Department of Chemical Engineering, University of Massachusetts, Amherst, Mass.



ability of a more general reactor theory coupled with advances in mathematical and analytical techniques which permit the much more complex problems of polymerization reactions to be treated quantitatively. One also hopes that there has been a recognition of the already existing commercial need.

Why hasn't this recent polymerization reaction engineering theory been used more? To answer this question, we should first define what we mean by chemical reaction engineering as opposed to reactor design or chemical kinetics. The coupling of the chemical to the physical processes of mixing and transport phenomena on a macro scale distinguishes this field from chemical kinetics. The terms "reaction engineering" and "reactor design" or "reactor engineering" are frequently used interchangeably. By the more general term "reaction engineering," we mean to include the optimal operation of existing reactors to produce better products at lower cost as well as the process design of new reactors.

The role of reaction engineering in a commercial endeavor depends on the approach used for commercialization. Two simplified approaches are shown in Figures 1 and 2. In both cases, we move from a definition of desired product properties to some useful commercial application, with profits to make the endeavor worthwhile. In the polymer field, we sell product properties, not chemical structure. The degree of commercial success depends on: (1) how well we define and meet the properties needed in the market; (2) how quickly we move, and how little we iterate in reaching this objective; (3) how economically we produce our product in the long term.

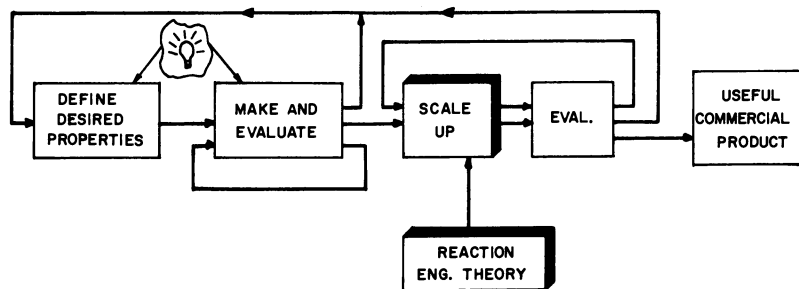


Figure 1. Traditional approach to commercialization of a polymer

The first of these approaches could be called "traditional." New varieties and variations of polymers are made and evaluated in the laboratory against targeted properties or less well defined applications. There is considerable iteration both within the laboratory and with the marketing function. As Zeman (58) pointed out in his somewhat different approaches, the lightbulb of inspiration is necessary to initiate or allow

this approach to succeed. Once a product passes laboratory tests, it is scaled up to a pilot plant and, after iteration, to a new or existing plant. The primary role of reaction engineering shown by the highlighted boxes is to aid this scaleup. Since with polymers, as distinguished from simple chemicals, the process influences the properties obtained, the die is frequently cast on the type of process and even key process conditions before the process engineer can apply his theory. If time is critical, additional iteration for a different process becomes difficult to justify "at this time," even though the process, longer term, may not be the most economical.

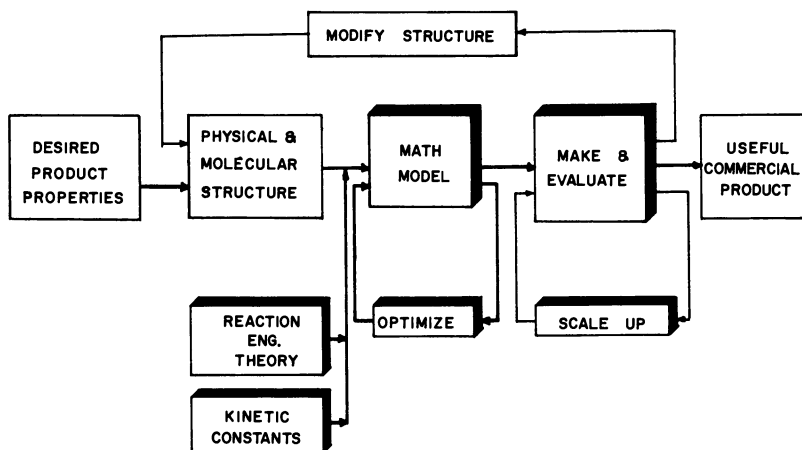


Figure 2. Idealized fundamental approach to commercialization of a polymer

Intuitively, the second or "fundamental" approach shown in Figure 2 is preferred. It has less empiricism, less iteration, and should be more likely to hit the target in big new markets with better optimized products and processes and therefore larger profits. Better theory and measurements have permitted the prediction of properties from structure and, to some extent, the specification of products in terms of molecular structure, morphology, etc. Reaction engineering (the highlighted boxes) is utilized early to guide research toward the optimum combination of product and process. If the kinetic constants and other physical properties are known or can be determined, reaction engineering can be used to define a mathematical model of a process to give the desired molecular structure. Iteration and optimization can then be done quickly on a computer to determine the optimum choice of a reactor type, size, configuration, and operating conditions. The desired polymer can then be made on a bench scale, evaluated, and, with necessary structural modifications, scaled up

to commercial production. If one's confidence in the mathematical model is good, the number of steps in scaleup can be reduced along with the number of experiments at each scale.

We should be realistic in acknowledging the difficulties of this second, idealized approach. There is a real attempt to move in this direction, but what are the factors that stand in its way? Is quantitative reaction engineering theory inapplicable in systems of real commercial interest? Might it apply if it were better known? Even where it applies, are kinetic constants available or readily obtainable? All of these barriers exist to some extent.

This paper attempts to indicate what has been done and what might be needed for broader application. In practice, one is presently forced at best to a compromise between the two approaches with theoretical steps bypassed until they become available.

Polymerization reaction engineering *per se* is a new field. Its beginning is somewhat arbitrary, but we can pick as the pioneering work the 1947 paper by Denbigh (14). He showed not only the great difference in molecular weight distribution obtained from a continuous stirred tank (CSTR) and a batch reactor, but that the CSTR gave a narrower molecular weight distribution (MWD) when termination was important and broader when it wasn't. There is, of course, a significant body of earlier literature on batch polymerization kinetics. Only more recently have more chemical engineers become interested in carving out a section of this field. It is obvious that the field is expanding particularly in the chemical engineering area. It is therefore appropriate to attempt to extrapolate current trends, and, where appropriate, to try to influence some new ones.

Some possible subdivisions of the field are listed in Table I. We can characterize the type of polymerization process—*i.e.*, mass, suspension, emulsion, etc.—and the type of reactor and how it is operated. The chemical classification of the reaction affects the mathematics as well as the product. The last distinction is between the rate of product formation and the distribution of the products obtained.

**Table I. Coordinates or Subdivisions of the Field**

Mass—Suspension—Emulsion  
 Tank—Tubular  
 Batch—Continuous  
 Transient—Steady State  
 Addition—Condensation  
 Theory—Experiment  
 Kinetics—Mixing  
 Analytical—Numerical  
 Rate—Distribution

We have found it useful to consider a technical field analogous to a portion of multidimensional space, where we impose coordinates to define the location of a particular work. The most obvious coordinate is time. The subdivisions mentioned above are other possible coordinates.

To define the character and nature of the field, we must wander among the published literature and define its boundaries with adjacent fields of polymerization kinetics, rheology, transport phenomena, etc. One measure of the extent of a field is the number of times you cross your own tracks in searching references given in new papers. From this, we would guess that the field consists of several hundred references. Most of these are from the overlapping part of polymerization kinetics.

### *Organization of the Review*

In the following section on reactor and process types, the preponderance of work on mass/solution polymerization is pointed out with a brief review of the more limited work on suspension and emulsion polymerization. In another broad view of the field (the next section) the distinction between polymerization rate and product distribution is discussed, particularly the preoccupation with molecular weight distribution.

The second major section of the paper treats the mathematical formulation of reactor design theory, extending the "reactor operator" concept to polymerization reactors to separate the physical processes characterizing the different reactor types from the chemical kinetics which characterize the different types of polymerizations. Thus, all permutations of these need not be treated separately. The solutions of the resulting equations to yield molecular weight distribution are introduced, followed by a review of seven specific mathematical techniques for solving the equations. The applications of these to the solutions for specific kinetic schemes in batch and CST reactors are then reviewed. This is followed by a treatment of the special considerations required for tubular reactors that deviate from the ideal of plug flow behavior. The review is concluded with a section on experimental methods, stressing the problems caused by high conversions in commercially important systems.

**Reactor and Process Types.** It is interesting to subdivide previous work not covered by reactor and process type (Table II). This could be considered a particular two-dimensional projection of the multidimensional space along the coordinates of reactor type and process type. The number of references in each subsection of the field is shown. Obviously, the greatest amount of work has been done in batch, mass/solution polymerization. This is undoubtedly because of the relative simplicity of the mathematical formulation as much as the commercial importance of this case. The same comment applies to the extension of mass/solution

kinetics to CSTR's. Although more difficult to experiment with in a laboratory, steady-state CSTR's are theoretically and mathematically simpler to analyze kinetically, particularly with short-lived chain reactions. The simplest model of a tubular reactor, the plug flow reactor, is mathematically equivalent to a batch reactor, as many authors including Denbigh (14) have noted. With the high viscosities and low diffusivities in polymerization reactors, the assumption of plug flow is usually invalid. More detailed tubular models are relatively complex, with particular interactions between flow and diffusion that will be treated separately in a later section. In addition, operational problems have made this type of reactor less popular commercially.

**Table II. Number of Literature Reference Subdivided by Reactor and Polymerization Process Types**

	<i>Batch</i>	<i>Tubular</i>	<i>CSTR</i>
Mass/soln.	57	7	28
Suspension	5	1	3
Emulsion	12	0	2

The remainder of this review treats the preponderance of work in mass/solution processes. As shown in Table II, relatively little has been done with suspension and emulsion polymerization theory, particularly with continuous reactors. It is worthwhile to highlight some of this work.

Batch suspension reactors are, theoretically, the kinetic equivalent of water-cooled mass reactors. The major new problems are stabilization of the viscous polymer drops, prediction of particle size distribution, etc. Particle size distribution was found to be determined early in the polymerization by Hopff *et al.* (28, 29, 40). Church and Shinnar (12) applied turbulence theory to explain the stabilization of suspension polymers by the combined action of protective colloids and turbulent flow forces. Suspension polymerization in a CSTR without coalescence is a prime example of the segregated CSTR treated by Tadmor and Biesenberger (51) and is discussed below. In a series of papers, Goldsmith and Amundson (23) and Luss and Amundson (39) studied the unique control and stability problems which arise from the existence of the two-phase reaction system.

Although there have been several references on the theory of emulsion polymerization kinetics, it is surprising that its commercial importance and multiphase kinetics have not generated more interest. Smith and Ewart (46) predicted a constant rate of polymerization per particle, based on initiation in the water phase and three ranges of radical concentration per particle. Van der Hoff (55) confirmed this for concentrations

less than  $10^{14}$  particles/ml. but found it to fail at higher particle concentrations.

Stockmeyer (47), O'Toole (41), and Ugelstadt *et al.* (53) have treated the theory where there is more than one radical per particle, leading to higher rates. Katz *et al.* (33) discuss the calculation of MWD in these cases.

**Rate and Distribution.** The distinction between polymerization rate and distribution is particularly important with polymers. Rate considerations answer questions of quantity. What is the conversion per pass? What reactor size is required? Will monomer recovery be needed?

Product distribution concerns yield and selectivity. This is usually more important where more than one product is possible from given reactants. In polymers, where by-products cannot be economically separated, distribution is doubly important because it helps determine product quality. Product distribution and properties are thus a function of the polymerization process.

By far the most widely studied distribution parameter is the molecular weight distribution (MWD), which includes the various average molecular weights. This is because of the considerable effect of molecular weight on physical properties and also because it was the first fundamental polymer parameter to yield to experimental measurement. Although most theoretical work is done with linear polymers, these concepts and methods have been used for grafting and crosslinking. Scanlan (44), for example, was the first to use Z-transforms, in this case for crosslinking and chain scission reactions. In copolymers and terpolymers, parallel questions of composition distribution can be treated, again by extending the above methods. A recent paper (48), for instance, shows the effect of reactor type on composition distribution using a model where elements of the reacting mass are alternately mixed and segregated in various types of reactors.

This review concentrates on MWD in linear polymers. Although it has been approached on a statistical basis in batch reactors, the more usual and general kinetic analysis will also answer all rate questions in the process of defining the MWD.

### **Mathematical Formulation**

**Physical Processes.** The formulation of the reaction engineering problem is best handled by characterizing separately the physical and chemical processes. The physical processes can be symbolized by an operator,  $R(Y)$ , defining the differential accumulation, flow, and diffusion which characterize each type of reactor. These operators are generalizations of those proposed by Hulbert and Kim (32). The chemical processes are

characterized by the production and destruction of each species with the characteristic form for each kinetic mechanism. These independent physical and kinetic expressions can then be combined in all possible configurations to describe the net effect in a specific type of reactor.

Three forms of the reactor operator,  $R(Y)$ , are shown in Figure 3. These are generally differential operators which operate on each monomer and polymer species to describe the effects of accumulation and the physical processes which move material in and out of the reactor or reactor element. The concentration of a specific species is given by the variable  $Y$ . In a simple batch reactor, the reactor operator,  $R_B$ , is merely defined as the rate of accumulation of a certain species with time per unit volume of reactor—*i.e.*, the rate of change of concentration of the species.

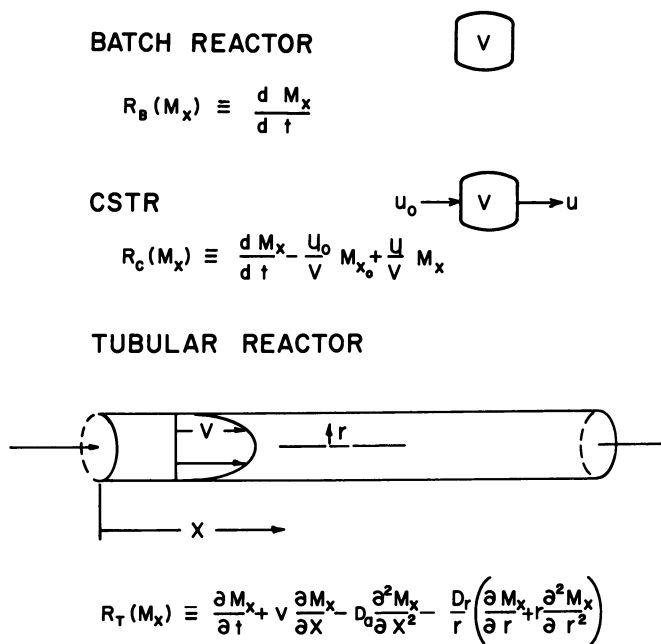


Figure 3. Reactor operators for three reactor types

The CSTR operator,  $R_C$ , has an identical term to describe accumulation under transient operation. The algebraic sum of the two other terms indicates the difference of in-flow and out-flow of that species. This operator also describes semibatch or semicontinuous operation in cases where the volume can be assumed to be essentially constant. In the more general case of variable volume,  $V$  must be included within the differential accumulation term. At steady state, it is a difference equation of the same form as the differential equation for a batch reactor.

Figure 3 also shows the reactor operator for a tubular reactor,  $R_T$ . Again, there is an accumulation term which goes to zero at steady state. The convection term is the product of velocity and concentration gradient, with the last terms indicating effects of radial and axial diffusion. The differential equations are never solved with both diffusion terms. As discussed later, the apparent axial diffusivity differs from the radial diffusivity. If diffusivity varies appreciably with varying temperature or concentration within the reactor, the more general form, including the diffusivities within the differential terms, must be used. In its simplest form—a plug-flow reactor—the concentration is assumed invariant with radial position, and an average velocity is used. The other limiting case occurs when the velocity varies with radius, but there is no mixing or diffusion between the different annuli despite the resulting concentration gradients. This is discussed below. Other reactor types are used but are usually considered as extensions or combinations of the above types.

**Reaction Mechanisms.** Polymerization reactions can be characterized in several ways. For our purposes, they are best characterized by typical mechanisms which determine the kinetic formulations. The formulation is generally that used by Tadmor (50) who also presented a comprehensive review of previous work on MWD.

The mechanisms and resulting kinetic equations are shown in Figure 4. Other mechanisms are possible as well as modifications of these—*e.g.*, disproportion termination of chain reactions, and condensation between unlike monomers. The left sides of the equations represent the reactor operator (note that all resulting differential equations are nonlinear because of the second-order propagation and termination reactions). To this is added the complexity of considering separate equations for the thousands of separate species frequently required to define completely commercially useful polymers. Solution by direct application of classical techniques is impractical or impossible in most cases; even direct numerical solution is often difficult. Simplifying assumptions or special mathematical techniques must be used (described below in the calculations of MWD).

**Molecular Weight Distributions.** The calculation of molecular weight distributions from assumed kinetic mechanisms has its basis in classical polymerization kinetic theory. It is probably the most widely studied aspect of polymerization reaction engineering theory. Separate equations, usually ordinary differential equations, are solved to give the product polymer distribution as a function of chain length and time. The kinetic mechanism and constants are taken as known. These kinetic calculations embrace the calculation of monomer conversion with time and the various average molecular weights, although expressions for these can often be derived directly.



The various mathematical techniques used to obtain MWD with different combinations of mechanisms in different reactor types are surveyed. As Wei and Prater (57) stated for heterogeneous catalysis, and Benson (6) for kinetics in general, the chief difficulties are not the solutions of the kinetic equations once the mechanisms and constants are known. The real problem is the application of solutions to experimental data to determine fundamental mechanisms and constants which may be useful under other conditions. Too few investigators have noted this.

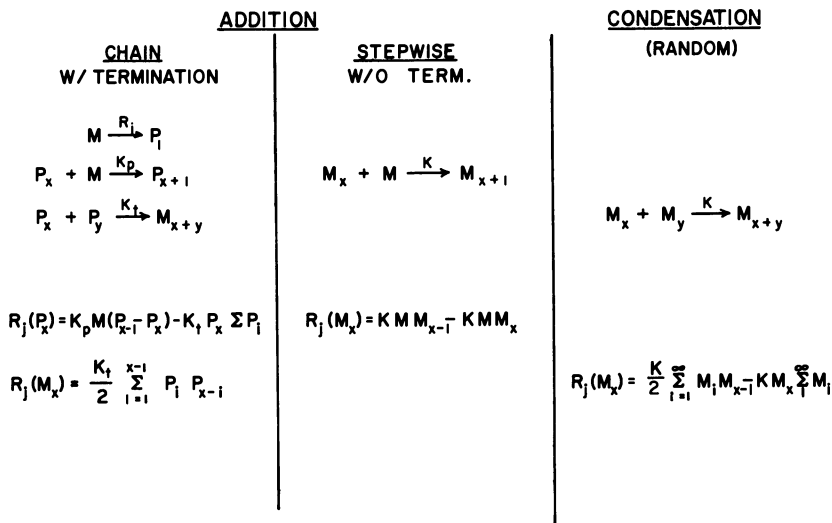


Figure 4. Typical polymerization reaction mechanisms

Another limitation of most work to date is that relatively few cases of theoretically determined MWD's have been checked against experimentally determined values. In many instances, experimentally determined kinetic parameters from the literature have not even been used; parameters were chosen instead for computational convenience and gave misleading results. The works of Hamielec and co-workers represent notable exceptions to the above. Using carefully controlled batch experiments, MWD determination by gel permeation chromatography (GPC), Hamielec *et al.* (25) obtained good agreement with theoretical calculations based on parameters at low viscosities. Duerksen *et al.* (17) did the same for CSTR's.

**Mathematical Techniques.** The polymerization kinetic equations are usually too difficult to solve directly without simplifying assumptions or special mathematical techniques used alone or in combination (*see* Table III, p. 13). Most of these techniques have been reviewed by Zeman (58).

**PSEUDO-STEADY-STATE ASSUMPTION (PSSA).** This assumption, limited to chain reactions with termination, states that the absolute value of the rate of change of free radicals with time is so small relative to the other terms in the differential equations for free radicals, that it can be set equal to zero. Aris (3) refers to this as an

. . . example of a notion of great usefulness which at first sight appears to be hopelessly ill formed. To say that certain intermediates or complexes are present only in small concentrations and that, therefore, their derivatives can be set equal to zero is mathematically nonsensical. It is notorious that a bound on a function imposes no bound on its derivative, however great the simplification of equations that may result from this optimism may be. Yet in many cases, the application of the theory of singular perturbations may show that this is justified . . .

In polymerization kinetics, the PSSA has alternately been justified and used on the one hand, and cautioned against and avoided on the other, usually at a great expense of time on the part of the investigator, computer, and reader. In the latter case, one gets the impression that this is caused more by the unpalatability of its usual formulation, as indicated above by Aris, than to its real failure in cases of interest. Most workers who have considered specific systems feel that it holds for free radical polymerization over all but the shortest transients. A criterion for its permissible use was derived by Bamford *et al.* (4).

**CONTINUOUS VARIABLE APPROACH TO CHAIN LENGTH.** Since only whole numbers of monomer units can add to a chain, the molecular weight distribution is necessarily discrete. This can be approximated by a continuous distribution with some error, particularly at small chain lengths. However, it permits an infinite series of equations for species differing only in chain length to be reduced to a single differential equation with the chain length as a variable. This will be a partial differential equation in chain length and time for batch and other transient reactors and an ordinary differential equation in chain length for steady state CSTR's. Bamford and Tompa (5) show that the equations for a specific species can be approximated by a Taylor series in chain length, truncated after the first derivative term. Zeman and Amundson (60) extend this to the second derivative term. The reduction in the number of equations provides simplification for subsequent solutions by analytical methods, including the use of continuous transforms and numerical techniques. An objection to this technique (35) is that short chains, which lead to the greatest inaccuracies, are the most numerous at all times during a condensation polymerization.

**LAPLACE TRANSFORMS.** If chain length is converted to a continuous variable, and the resulting equations can be linearized, Laplace transforms may be used to transform the chain length variable to solve the equations. In condensation and many realistic free radical polymeriza-

tions, however, the equations cannot be linearized. Exceptions are free radical cases, treated by Bamford and Tompa (5), with combination termination and disproportionation where monomer concentration is held constant, and the PSSA is made.

Another approach is to transform the time variable in the original equations where chain length is discrete (57). Monomer termination permits linearization in this particular case.

**Z-TRANSFORM.** Z- (zeta) transforms, defined as follows, are the most recent and widely used technique for calculating molecular weight distributions.

$$P(Z,t) \equiv \sum_{x=1}^{\infty} Z^{-x} P_x = 0 + P_1 \frac{1}{Z} + P_2 \frac{1}{Z^2} + \dots + P_n \frac{1}{Z^n} + \dots$$

They are discrete transforms and can therefore operate directly on the separate equations for each species, reducing them to one expression. Nonlinear terms arising from condensation polymerization can be handled and, with some difficulty, so can realistic terminations in free radical polymerization. They are a special case of the generating functions and can be used readily to calculate directly the moments of the distribution, and thus, average molecular weights and dispersion index, etc. Abraham (2) provided a short table of Z-transforms and showed their use with stepwise addition.

**EIGENZEIT TRANSFORMATION.** This simple change of variable first proposed by Dostal and Mark (16) linearizes equations when a monomer appears in every term. The quantity  $Mdt$  is defined as a new variable  $dZ$ . It is widely used for stepwise polymerization without termination. It is mentioned to avoid confusion with the Z-transform. In one paper, both transformations were used in the same equation, and both were referred to in connection with the letter Z.

**MOMENTS.** The  $n$ th moment of a molecular weight distribution is defined as follows:

$$Q_n \equiv \sum_{x=1}^{\infty} X^n P_x$$

As mentioned above, the moments of the molecular weight distribution can be determined without solving for the distribution directly. Moments can be calculated from the Z-transforms,

$$\lim_{z \rightarrow 1} (-1)^n \left[ \left( Z \frac{\partial}{\partial Z} \right)^n P(Z,t) \right] = \sum_{x=1}^{\infty} X^n P_x = Q_n$$

They can also be obtained by writing and solving differential equations in terms of moments rather than in terms of specific molecular species as shown by Katz and Siedel (34). Once obtained, the moments can then

be used to determine parameters of interest such as averages and dispersion indices or used to construct an approximation of the distribution *via* Laguerre polynomials as shown by Bamford and Tompa (5).

**NUMERICAL TECHNIQUES.** The digital computer has been an extremely versatile tool for elucidating polymerization kinetics and molecular weight distributions. It has been used directly to solve hundreds of individual differential equations for the individual molecular species, but here even large computers run out of storage space in molecular weight ranges of commercial interest. Numerical techniques have also been used in combination with the above techniques and to evaluate complex analytical solutions. Chen and Spencer (11), for instance, have presented a method of numerical inversion of Z-transforms using the fast Fourier transform.

**Chain Reaction with Termination.** More work has been done on this mechanism, using free radical polymerization as the principle example. As shown in Table IV, batch polymerization has received far more interest within this area than the simpler case of continuous polymerization in a stirred tank, presumably because of commercial laboratory practice. The limited work on tubular reactors is not shown and will be discussed separately later.

**Table III. Key to Mathematical Techniques Used to Calculate Molecular Weight Distributions**

P	=	Pseudo-steady-state assumption
C	=	Continuous variable for chain length
L	=	Laplace transforms
Z	=	Z-transforms
E	=	Eigenzeit transform
M	=	Moments of distribution
N	=	Numerical techniques

**Table IV. Mathematical Techniques Used for MWD in Chain Addition<sup>a</sup>**

	<i>Batch</i>		<i>CSTR</i>	
Gee and Melville (21)	P		Denbigh (14)	
Liu and Amundson (37)		N	Ray (42)	ZMN
Liu and Amundson (38)		Z N	Laurence (36)	ZM
Bamford and Tompa (5)	PCL	N	Zeman and Amundson (59)	C
Zeman and Amundson (59, 60)	CL	EN	Tadmor and Biesenberger (51)	M
Hamielec <i>et al.</i> (31)	P	N	Duerksen and Hamielec (17)	
Hui and Hamielec (30)	P	N	Duerksen and Hamielec (18)	N
Chen and Spencer (11)	P	Z N		

<sup>a</sup> Letters represent first-letter abbreviations from Table III.

**BATCH REACTORS.** One of the classic works in this area is by Gee and Melville (21), based on the PSSA for chain reaction with termination. Realistic mechanisms of termination, disproportionation, and combination, are treated with a variety of initiation kinetics, and analytical solutions are obtained. Liu and Amundson (37) solved the simultaneous differential equations for batch and transient stirred tank reactors by using digital computer without the PSSA. The degree of polymerization was limited to 100; the kinetic constants used were not typical and led to radical lifetimes of hours and to the conclusion that the PSSA is not accurate in the early stages of polymerization. In 1962 Liu and Amundson used the generating function approach and obtained a complex iterated integral which was later termed inconvenient for computation (37). The example treated was monomer termination.

Zeman and Amundson (60) used the continuous variable approach, followed by a numerical integration of the differential equations. One case of combination termination was briefly discussed, although most examples were for monomer termination. The bimodal distribution predicted under certain temperature conditions with monomer termination is made up of a broad peak of inactive polymer with a sharp higher molecular weight peak of active polymer. This effect would not be significant where active polymer concentrations are orders of magnitude less than dead polymer concentrations. Despite the lack of pertinence of many of their examples, the pioneering work of Amundson and co-workers has been important in demonstrating the tractability of polymerization kinetics with today's mathematical techniques and in interesting other chemical engineers in these approaches. Katz and Seidel (34) also used the continuous variable technique but simplified the problem by solving only for the moments of the distribution with termination by combination or disproportionation. Transfer to monomer and solvent and the gel effect were also discussed.

Hamielec, Hodgins, and Tebbins (25) justified and used the PSSA with the solution and bulk polymerization of styrene. They calculated that the steady state was approached in a few thousandths of a second. Their equations for dead polymer were numerically integrated for 5000 species and, as previously mentioned, experimentally confirmed.

**CONTINUOUS STIRRED TANK REACTORS. (CSTR).** The first analysis of continuous reactors for polymerization was by Denbigh (14). He treated the same mechanisms in a CSTR that Gee and Melville (21) had treated in a batch reactor. The problem is simpler in a steady state CSTR since the equation for each dead and live specie is an algebraic rather than a differential equation. These are solved sequentially. The PSSA is not needed. He predicted a narrower molecular weight distribution for a continuous chain polymerization than for the same polymerization carried

out batchwise, based on the fact that the average lifetime of a growing chain is orders of magnitude less than the mean hold time of the CSTR.

Tadmor and Biesenberger (51) extended this work to segregated CSTR's where the individual regions of the reactor are molecularly segregated, although the over-all residence time distribution is the same as an ideal homogeneous CSTR. The effect of segregation in this case is to broaden molecular weight distribution. An example of segregation would be continuous suspension polymerization without coalescence. An intermediate case would be a highly viscous reactor where mixing on a molecular scale is necessarily slow.

Tadmor and Biesenberger (51) used the PSSA and the calculation of moments in the case of a segregated CSTR for chain reaction with termination. Although the effect on conversion with long chains is small, the effect of segregation at significant conversions is to broaden molecular weight distribution from that obtained in a homogeneous CSTR.

With combination termination and no chain transfer, the dispersion indices for all reactor types approach the instantaneous value of  $D_N = 1.5$  as conversion is decreased.  $D_N$  is defined as the ratio of weight to number average molecular weight. The steady state homogeneous CSTR gives  $D_N = 1.5$  at all conversions. In one example,  $D_N$  from a segregated CSTR increased to 3.5 at 80% conversion and to 5 at the limit of 100% conversion. The corresponding values for a batch reactor were 1.8 and 5. With poor mixing, a CSTR may thus give broader MWD as measured by  $D_N$  than a batch reactor. The breadth of the distribution as measured by standard deviations however is roughly comparable for batch reactors and segregated CSTR's at equivalent conversions.

Duerksen, Hamielec, and Hodgins (17) solved for conversions and MWD's in a CSTR by standard methods, using kinetic constants from the literature. They performed experiments on the polymerization of styrene in benzene, measuring MWD by GPC and obtained good agreement at viscosities of less than 10 cp. The propagation rate was corrected for the effect of solvent, using the method of Henrici-Olivé (26). The effect of recycle and split addition of feed with a series of three CSTR's was recently treated by Hui and Hamielec (30). The inclusion of the viscosity effect leads to an increase in conversion and molecular weight with recycle of dead polymer alone.

In a very interesting paper, Ray (42) has applied the methods of optimal design, for instance, minimizing the breadth of the molecular weight distribution within other constraints. He used generating functions to solve for the moments of the distribution and peak-seeking methods for reaching the optimum. One and two CSTR's were considered with combination termination as well as transfer to monomer.

**Stepwise Addition without Termination.** This mechanism has been used to treat so-called stepwise "condensations," such as  $\epsilon$ -caprolactam, as well as other ring-opening polymerizations, such as ethylene oxide (Table V). It may also apply to the "living polymers" treated by Szwarc (49), although these systems are very sensitive to impurities. The distinguishing characteristic relative to chain addition with termination is that the lifetime of the growing molecule is at least as long as the hold time in a batch or continuous reactor. Molecular weight therefore becomes a function of how long the particular molecules have had to react.

**Table V. Mathematical Techniques Used for MWD in Stepwise Addition without Termination**

<i>Batch</i>		<i>CSTR</i>	
Dostal and Mark (16)	E	Denbigh (14)	
Gee and Melville (21)	E	Laurence (36)	ZM
Abraham (2)	Z	Tadmor and Biesenberger (51)	
Kilkson (35)	Z	Kilkson (35)	ZM

$$1 \leq D_N \leq 2$$

**BATCH POLYMERIZATION.** The case of stepwise polymerization without termination was originally treated by Dostal and Mark (16) by using the Eigenzeit transformation to linearize the equations, as discussed earlier. Gee and Melville (21) extended this by the same technique to a case where the propagation rate constant varied with molecular size, contrary to the usual assumption. In the case of stepwise polymerization without termination, batch reactions can give a very narrow (Poisson) distribution. Abraham (2) and Kilkson (35) both showed that the use of the Z-transform simplified the handling of this type of mechanism.

**CONTINUOUS STIRRED TANK REACTORS.** Denbigh (14) also treated stepwise addition without termination as the limiting case where the half-life of the growing chain is relatively long. He predicted that a single CSTR would give a broader distribution than the batch reactor for this mechanism. As before, algebraic equations can be solved for each species sequentially. In this case, the variation in residence time distribution has a preponderant effect on variation in the MWD of the polymer chains since they all continue to grow. This outweighs the effect of constant monomer concentration, which leads to a narrower distribution in chain reactions with termination.

Kilkson (35) also treated stepwise addition in a CSTR, using Z-transforms and calculating the moments of the distribution. The dispersion index was shown to increase from the lower limit of 1 for a batch reactor at high conversions, and to approach 2 in the CSTR at high residence time.

This was the second mechanism for which Tadmor and Biesenberger (51) obtained analytical solutions for segregated as well as homogeneous CSTR's. Calculation of only the moments of the distribution was used in the more complex cases. The results indicate that the distribution in a segregated CSTR is somewhat broader than in a batch reactor but narrower than in a homogeneous CSTR. The dispersion index is a function of average chain length as well as conversion. In the limit of zero conversion, this functionality approaches that of a homogeneous CSTR—*i.e.*, increasing to 2 as chain length increases. In the limit of 100% conversion, this functionality approaches that of a batch reactor—*i.e.*, increasing to a maximum of 1.25 then decreasing to approach 1 with increasing chain length.

In another paper, Biesenberger and Tadmor (9) indicated that a series of CSTR's would exhibit behavior approaching that of a batch or plug-flow reactor, narrowing MWD in the case of stepwise addition without termination and broadening MWD for chain addition with termination. This would be expected from the narrower residence time distribution overriding the effect of greater variability in monomer concentration. Using Z-transforms and the Eigenzeit transform, a program for feed rate of initiator to a semibatch reactor was developed to keep the MWD as narrow as possible. They also developed a temperature program for the same purpose in a batch chain reaction. Hoffman *et al.* (27), Beste and Hall (7), and Vandegaer and Douglas (45) developed similar temperature and feed programs for keeping a narrow MWD in a free radical batch reaction. These authors, however, used the criterion of keeping the average degree of polymerization constant without calculating the actual MWD.

An interesting example of transient CSTR operations is the effect of cycling monomer or initiator feed concentrations, studied by Laurence and Vasudevan (36) using Z-transforms. Both stepwise addition without termination and chain addition with termination were treated. In the former case, using kinetic constants for  $\epsilon$ -caprolactam, slight broadening in MWD relative to steady state under the average conditions was found for both kinds of oscillatory feed. Using the kinetic constants for styrene with the chain mechanism, significant molecular weight broadening was obtained with cyclic operation. Ray (43) presented a related study, including the effects with condensation polymerization.

**Condensation Polymerization.** As shown previously, condensation polymerization is characterized by polymer chains that combine both with each other and with monomer units to give larger chains capable of further reaction (Table VI). Like stepwise addition without termination,



it is characterized by chain lifetimes at least as long as reactor hold times. The fact that any monomer or polymer can react with any other gives rise to the term "random" condensation.

**BATCH POLYMERIZATION.** Batch polymerization with this mechanism was first treated by Flory (19) using a statistical development. The same results were obtained by Biesenberger (8) using a kinetic analysis with an analytical solution. This was also one of the cases treated by Kilksen (35) using Z-transforms. In the simple cases, his result reduces to the Flory, or random, MWD with the dispersion index of 2. In more complex cases, he solves directly for the moments of the distribution. The Z-transform is probably the most powerful tool for solving condensation MWD problems; the convolution theorem allows the nonlinear product terms in the kinetic equation to be handled conveniently.

**Table VI. Mathematical Techniques Used for MWD in Condensations**

<i>Batch</i>		<i>CSTR</i>	
Flory (19)		Biesenberger (8)	(N)
Kilksen (35)	ZM	Kilksen (35)	ZM
		Abraham (1)	Z (N)
		Smith and Sather (45)	(N)

$$2 \leq D_N \leq \infty$$

**CONTINUOUS STIRRED TANK REACTORS.** Biesenberger (8) solved for the MWD with condensation polymerization in a CSTR, analogous to the treatment Denbigh (14) provided for the other two mechanisms. In this case, the variable residence time distribution leads to an extremely broad MWD with even the maximum *weight* fraction at the lowest molecular weight (monomer). The dispersion index approaches infinity as the condensation is driven to completion in a stirred tank reactor. A sequential analytical solution of the algebraic equations was obtained with a numerical evaluation of the consecutive equations.

Kilksen (35) solved this case using Z-transforms and obtained the moments of the distribution for a number of cases, including the use of chain stoppers. Such chain stoppers, monofunctional compounds which prevent further polymerization, limit the molecular weight and the extreme spreading of the MWD that otherwise arises, making it approach the Flory distribution ( $D_N = 2$ ) at high conversions.

Abraham (1) used Z-transforms with numerical evaluation to handle the transient behavior of a CSTR for this mechanism. Smith and Sather (45) had earlier attempted analytical and numerical solution of this transient CSTR. The large number of equations and storage limitations of even large computers limited them to degrees of polymerization of less than 75.

**Tubular Reactors.** The simplest model of a tubular reactor, the plug-flow reactor at steady state is kinetically identical to a batch reactor. The time variable in the batch reactor is transformed into the distance variable by the velocity. An axial temperature gradient can be imposed on the tubular reactor as indicated by Gilles and Schuchmann (22) to obtain the same effects as a temperature program with time in a batch reactor. Even recycle with a plug flow reactor, treated by Kilksen (35) for stepwise addition without termination and condensation, could be duplicated in a batch reactor with holdback between batches.

A more complex model is that of a completely segregated tubular reactor, as discussed by Denbigh (15), where account is taken of differences with radial position of velocity and, therefore, residence time and concentration. Diffusion and mixing between annuli or along an annulus is taken as negligible. Like the plug flow case, the only term in the operator is the convection term, but this now varies with radius. The equations can be solved as an infinite series of batch reactors and an integral average composition calculated at the outlet. Cintron-Cordero, Mostello, and Biesenberger (13) treated this case with a power law fluid and all three of the basic reaction mechanisms. Even at its worst, the broadening of the residence time distribution and the resultant kinetic effects on polymerization are not as severe as in a segregated CSTR. The flattening of the velocity profile caused by a shear thinning fluid minimizes the effect, with plug flow as the limiting case. The effect on MWD is as expected from the above: broadening as compared with MWD from batch or plug-flow reactors for condensation and stepwise additions without termination. In a chain reaction with disproportionation termination, the effects of radial temperature gradients were determined by numerical integration. The admittedly limiting assumption was made that variations in conversion and, therefore, viscosity did not affect the velocity profiles. The system exhibited ignition phenomena, with small changes in parameters causing the axis of the tube to abruptly run out of control, going to completion at very high temperatures with resulting very wide MWD's.

Another limiting case is plug flow with axial diffusion. Although this case is unlikely to be found in practice because of velocity profiles and radial diffusion, it turns out to be a good model when radial diffusion is fast enough to minimize radial concentration gradients despite velocity gradients. In this case the axial diffusion constant,  $D_a$ , is a Taylor diffusion constant which varies inversely with the molecular or eddy diffusion constant. Taylor (52) gives criteria for this limiting case *vs.* that of segregated flow discussed above. Chen and Spencer (11) have calculated an example of this case for stepwise addition without termination. Z-transforms were used with numerical integration of the transformed

equations and numerical inversion. As expected, behavior approaches that of a homogeneous CSTR as axial diffusion becomes infinite. For application, one should determine the validity of this model at high values of axial diffusion.

### *Experimental*

The classical procedures used by the chemist or engineer to obtain polymerization rate data have usually involved dilatometry, sealed ampoules, or samples withdrawn from model reactors—batch, tubular, and CSTR's alone or in various combinations. These rate data, together with data on molecular weight can be used to obtain the chain initiation constant and certain ratios such as  $k_p^2/k_t$  and  $k_{tr}/k_p$ . Some basic relationships are shown in Figure 5. To determine individual rate constants such as  $k_p$  and  $k_t$ , other techniques are needed. For example, by periodic photochemical initiation it is possible to obtain  $k_p/k_t$ . If the ratio  $k_p^2/k_t$  (discussed above) is also known,  $k_p$  and  $k_t$  can each be calculated. Typical techniques are described by Flory (20).

Until comparatively recently most published data, both on over-all rates as well as individual rate constants, have been developed from work with dilute solutions or at low degrees of conversion. There have been very good reasons for this, among which can be cited many experimental difficulties in dealing with high viscosity solutions, the complications brought about by the gel effect (frequently encountered at conversions of 15% or less, depending on the monomer), and further complexities at higher conversions where diffusional and viscous effects become even more pronounced.

In practical reactor design, however, the engineer has been faced with critical problems occurring at conversions and temperatures considerably beyond the range where published data and theory can be directly applied. He has been therefore obliged to rely largely on empirical and semitheoretical methods.

In recent years, considerable work has been devoted to polymerization reactions of vinyl monomers at higher conversions which permit useful quantitative interpretation of the results. A useful review of studies of the gel effect, chain transfer reactions, and new theoretical postulates and studies at elevated conversions has been presented by Gladyshev and Rafikov (24). This accumulated work has demonstrated the effects of conditions at elevated conversions not only on the termination rate constant, but on initiator efficiency, propagation rate constants, and therefore, the concentration of macroradicals. A rigorous quantitative theory, however, has not yet been developed.

CHAIN ADDITION WITH TERMINATIONBATCH - PSSA

$$\lambda \equiv \frac{K_t^{1/2}}{R_i^{1/2} K_p} \quad \alpha \equiv K_t^{1/2} R_i^{1/2} / K_p M_0$$

RATE

$$- \frac{dM}{dt} = \frac{1}{\lambda} M \quad ; \quad M = M_0 e^{-t/\lambda}$$

MWD

$$\frac{dP_x}{dM} = - \left( \frac{x-1}{2} \right) \left( \frac{\alpha}{M/M_0} \right) \left( \frac{M/M_0}{\alpha + M/M_0} \right)$$

$$\bar{X}_w = \frac{3(1+M/M_0)}{2\alpha} + 2$$

$$\alpha/\lambda = \frac{R_i}{M_0} \quad \alpha\lambda = \frac{K_t}{K_p^2 M_0}$$

Figure 5. Interrelations between primary rate constants, polymerization rate, and MWD (long chain approximation)

GPC has become especially useful in polymerization reaction engineering since it permits comparatively rapid and precise determination of MWD. As shown in Figure 5,  $\bar{X}_w$  obtainable from the MWD in a batch reactor can be used to determine the initiation rate constant as well as  $k_p^2/k_t$  assuming the pseudo-steady state, the absence of chain transfer, and termination by combination. Similar relationships with CSTR's are available.

In theory, by feeding the MWD and experimental rate data into a mathematical model containing a variety of polymerization mechanisms, it should be possible to find the mechanism which explains all the experimental phenomena and to evaluate any unknown rate constants. As pointed out by Zeman (58), as long as there are more independent experimental observations than rate parameters, the solution should, in principle, be unique. This approach involves critical problems in choice of experiments and in experimental as well as computational techniques. We are not aware of its having yet been successfully employed. The converse—namely, predicting MWD from different reactor types on the basis of mathematical models and kinetic data—has been successfully demonstrated, however, as discussed above. The recent series of interesting papers by Hamielec *et al.* is a case in point.

Duerksen and Hamielec (18) extended earlier work to a number of steady state CSTR's in series and included the effect of viscosity. Deviations in MWD determined by GPC were used to calculate the changes in initiator efficiency and termination rate constant. Relatively good fits could be obtained at higher viscosities. Hui and Hamielec (30) extended these calculations to a transient CSTR and batch reactor with numerical integration of the ordinary differential equations using a Runge-Kutta technique. Only every 20th radical polymer species was stored for subsequent calculation of every 20th species of dead polymer. By this technique, computer storage was saved, and results could be obtained for degrees of polymerization ranging to several thousand. Relatively good agreement between computed and measured MWD's was again obtained using the viscosity correction.

### **Conclusion**

The rational design of a reaction system to produce a polymer with desired molecular parameters is more feasible today by virtue of mathematical tools which permit prediction of product distribution. New analytical tools such as gel permeation chromatography are being used to check theoretical predictions and to help define molecular parameters as they affect product properties. There is a laudable trend away from arbitrary rate constants, but systems other than styrene need to be treated in depth. A critical review of available rate constants would be useful. Theory might be applied more broadly if it were more generally recognized that molecular weight distributions as well as rates can be calculated from combinations of constants based on the pseudo-steady-state assumption. These are more easily determined than the individual constants in chain reactions.

The mathematical complexity involved with temperature variations has limited most of the studies cited in this paper to the isothermal case. Since few commercial polymerization reactor systems can or should operate isothermally, there is a clear need to develop techniques to permit fuller application of reaction engineering to nonisothermal systems. In polymerizations as in simpler reactions, changes in temperature or temperature profile can have larger effects on rate and distribution than even reactor type.

Greater application of polymerization reaction engineering within the commercial context requires further theoretical development in high conversion systems of interest. A mathematical framework is needed which will start with carefully planned experimental data and efficiently indicate a polymerization mechanism and statistical estimates of kinetic constants, rather than vice-versa. Better cross-communication between

physical chemistry and engineering, and particularly between the industrial and academic investigators, will stimulate the growth of this important field from the viewpoint of utility as well as scientific progress.

### Acknowledgment

The authors thank those who have made manuscripts available prior to publication. They also acknowledge support by the Monsanto Co., which has made this review possible, and the many references and suggestions from their colleagues.

### Literature Cited

- (1) Abraham, W. H., *Chem. Eng. Sci.* **21**, 327-336 (1966).
- (2) Abraham, W. H., *Ind. Eng. Chem.* **2**, 221 (1963).
- (3) Aris, R., *Ind. Eng. Chem.* **58**, 9 (1966).
- (4) Bamford, C. H. *et al.*, "The Kinetics of Vinyl Polymerization," Butterworth, London, 1958.
- (5) Bamford, C. H., Tompa, H., *Trans. Faraday Soc.* **50**, 1097 (1954).
- (6) Benson, S. W., "The Foundations of Chemical Kinetics," McGraw-Hill, New York, 1960.
- (7) Beste, L. F., Hall, H. R., *Makromol. Chem.* **1**, 121 (1966).
- (8) Biesenberger, J. A., *A.I.Ch.E. J.* **11**, 369 (1965).
- (9) Biesenberger, J. A., Tadmor, Z., *Polymer Eng. Sci.* **6**, 299 (1966).
- (10) Brotz, W., "Fundamentals of Chemical Reaction Engineering," Addison-Wesley, Reading, Mass., 1965.
- (11) Chen, P. Y., Spencer, J. L., presented at the 63rd National Meeting, A.I.Ch.E., St. Louis, Mo. (1968).
- (12) Church, J. M., Shinnar, R., *Ind. Eng. Chem.* **53**, 479 (1961).
- (13) Cintron-Cordero, Mostello, R. A., Biesenberger, J. A., personal communication, Stevens Institute of Technology (1968).
- (14) Denbigh, K. G., *Trans. Faraday Soc.* **43**, 643 (1947).
- (15) Denbigh, K. G., *J. Appl. Chem.* **1**, 227 (1951).
- (16) Dostal, H., Mark, H., *Z. Physik. Chem.* **B29**, 299 (1935).
- (17) Duerksen, J. H., Hamielec, A. E., Hodgins, J. W., *A.I.Ch.E. J.* **13**, 1807 (1967).
- (18) Duerksen, J. H., Hamielec, A. E., *J. Polymer Sci. Pt. C* **25**, 155-166 (1968).
- (19) Flory, P. J., *J. Am. Chem. Soc.* **58**, 1877 (1936).
- (20) Flory, P. J., "Principles of Polymer Chemistry," Cornell University Press, Ithaca, N. Y., 1953.
- (21) Gee, G., Melville, H. M., *Trans. Faraday Soc.* **40**, 240 (1944).
- (22) Gilles, E. D., Schuchmann, H., *Chem. Ing. Tech.* **38**, 1278 (1966).
- (23) Goldsmith, R. P., Amundson, N. R., *Chem. Eng. Sci.* **20**, 195, 449, 477, 501 (1965).
- (24) Gladyshev, G. P., Rafikov, S. R., *Russian Chem. Rev.* **35**, 405-415 (1966).
- (25) Hamielec, A. E., Hodgins, J. W., Tebbens, K., *A.I.Ch.E. J.* **13**, 1087 (1967).
- (26) Henrici-Olive, G., Olive, S., *Z. Physik. Chem. (Frankfurt)* **48**, 35 (1966).
- (27) Hoffman, R. F. *et al.*, *Ind. Eng. Chem.* **56**, 51 (1964).
- (28) Hopff, V. H. *et al.*, *Makromol. Chem.* **78**, 24, 34, 274, 282, 286 (1964).
- (29) Hopff, V. H., Löchner, F., *Makromol. Chem.* **84**, 261 (1965).

- (30) Hui, A. W. T., Hamielec, A. E., presented at the 63rd National Meeting A.I.Ch.E., St. Louis, Mo. (1968).
- (31) Hui, A. W. T., Hamielec, A. E., *J. Polymer Sci. Pt. C* **25**, 167-189 (1968).
- (32) Hulbert, H. M., Kim, Y. G., *Ind. Eng. Chem.* **58** (9), 20 (1966).
- (33) Katz, S. *et al.*, *ADVAN. CHEM. SER.* **91**, 145 (1969).
- (34) Katz, S., Seidel, G. M., *A.I.Ch.E. J.* **13**, 319 (1967).
- (35) Kilkson, H., *Ind. Eng. Chem., Fundamentals* **3**, 281 (1964).
- (36) Laurence, R. L., Vasudevan, G., personal communication (1968).
- (37) Liu, S. L., Amundson, H. R., *Rubber Chem. Technol.* **34**, 995 (1961).
- (38) Liu, S. L., Amundson, N. R., *Chem. Eng. Sci.* **17**, 797 (1962).
- (39) Luss, D., Amundson, N. R., *Chem. Eng. Sci.* **22**, 267 (1967).
- (40) Mangaraj, D., Patra, S., Roy, P. C., *Makromol. Chem.* **81**, 175 (1965).
- (41) O'Toole, J. T., *J. Polymer Sci.* **9**, 1291 (1965).
- (42) Ray, W. H., *Can. J. Chem. Eng.* **45**, 356 (1967).
- (43) Ray, W. H., "Abstracts of Papers," 155th Meeting, ACS, March-April 1968, L45.
- (44) Scanlon, J., *Trans. Faraday Soc.* **52**, 1286 (1956).
- (45) Smith, N. H., Sather, G. A., *Chem. Eng. Sci.* **20**, 15 (1965).
- (46) Smith, W. W., Ewart, R. H., *J. Chem. Phys.* **16**, 592 (1948).
- (47) Stockmeyer, W. H., *J. Polymer Sci.* **24**, 314 (1957).
- (48) Szabo, T. T., Nauman, E. B., presented at the 63rd National Meeting, A.I.Ch.E., St. Louis, Mo. (1968).
- (49) Szwarc, M., *Nature* **178**, 1168 (1956).
- (50) Tadmor, Z., Ph.D. Thesis, Stevens Institute of Technology (1966).
- (51) Tadmor, Z., Biesenberger, J. A., *Ind. Eng. Chem., Fundamentals* **5**, 336 (1966).
- (52) Taylor, G. I., *Proc. Roy. Soc. (London)* **A219**, 186 (1953).
- (53) Ugelstadt, J., Mork, P. C., Aasen, J. O., *J. Polymer Sci. A1* **5**, 2281 (1967).
- (54) Vandegaer, J. E., Douglas, D. G., *J. Appl. Polymer Sci.* **11**, 1079 (1967).
- (55) Van der Hoff, M. M. E., *J. Phys. Chem.* **60**, 1250 (1956).
- (56) Walas, S. M., "Reaction Kinetics for Chemical Engineers," McGraw-Hill, New York, 1959.
- (57) Wei, J., Prater, C. D., *Advan. Catalysis* **13**, 203 (1962).
- (58) Zeman, R. J., *Can. Chem. Eng. Conf., 17th, Niagara Falls* (1967).
- (59) Zeman, R. J., Amundson, N. R., *A.I.Ch.E. J.* **9**, 297 (1963).
- (60) Zeman, R. J., Amundson, N. R., *Chem. Eng. Sci.* **20**, 637 (1965).

RECEIVED May 6, 1968.

# Free Radical Polymerization Kinetics of Immobilized Chains

## Bulk Polymerization of Acrylonitrile

O. G. LEWIS and R. M. KING, JR.

Central Research Division, American Cyanamid Co., Stamford, Conn. 06904

*A kinetic study was made of the polymerization at 50°C. of acrylonitrile and acrylonitrile-benzene mixtures catalyzed by azodiisobutyronitrile, using a mercury dilatometer specially designed to maintain isothermal conditions even at high rates of polymerization. A plot of rate vs. catalyst concentration,  $I$ , on logarithmic scales is a curve, the rate varying as  $I^{0.89}$  at  $I = 10^{-4}\text{M}$ —but as  $I^{0.33}$  at  $I = 10^{-2}\text{M}$ . These results were accounted for by generalizing the usual steady-state kinetic scheme for radical chain reactions, taking into account geminate termination and termination by primary radicals. Certain functions of the rate constants for the component reactions were estimated and found to be consistent with published values.*

It is well known that the presence of precipitated polymer can influence the course of polymerization. In bulk acrylonitrile polymerization the effects are most dramatic and have been the subject of many studies. The literature on this subject has been reviewed by Bamford *et al.* (4) by Thomas (29), and by Peebles (23). Under conditions where the system becomes heterogeneous owing to precipitation of small particles of polymer, a protracted acceleration period is observed at the start of polymerization, and the final rate is found to depend on the 0.8 power of the concentration of free radical initiator. Unusual post-polymerization effects are observed in photoinitiated polymerization of acrylonitrile, owing to the presence of trapped radicals which can be detected by electron spin resonance. None of the detailed mechanisms proposed to



account for these observations have found general acceptance, and several different expressions have been derived to account for the kinetic results.

The work described here was undertaken on the premise that measurements of the number of particles, total particle surface, and concentration of trapped radicals are needed in conjunction with rate measurements over a wide range of initiation rate and monomer concentration to understand more thoroughly the important factors in this type of heterogeneous polymerization. However, as will become apparent from the results reported here, variations in particle number and total surface are small and have little effect on the polymerization rate. Under our conditions trapped radicals were present in too low a concentration to be detected and cannot account for the peculiar features of the reaction kinetics.

The mechanism can be best understood within the framework of the conventional theory of radical chain kinetics, provided that certain of the usual simplifying assumptions are omitted. A solution is given to the problem of steady-state polymerization rate as a function of monomer and initiator concentration, taking into account termination reactions of primary radicals and recombination of geminate chains arising from the same initiation event. This model is shown to account for the kinetic data reported herein. With appropriate rate constants it should be generally applicable to radical polymerizations.

### *Microscopic Observations*

The polymer precipitates initially in the form of roughly spherical aggregates of small particles. A typical example is shown in the electron micrograph in Figure 1. The aggregates are fairly uniform in size. The diameters of the aggregates sampled at different degrees of conversion were taken from electron micrographs, and it was found that the calculated number of particles per milliliter of polymerizing solution was constant, indicating that polymerization takes place entirely on or within the existing aggregates, and no new aggregates are formed beyond about 0.4% conversion. A study of the aggregates formed in bulk polymerization at 50°C. revealed that the number increased roughly as the square root of the concentration of azodiisobutyronitrile (AIBN) initiator concentration, from about  $7 \times 10^{10}$  ml.<sup>-1</sup> at  $10^{-4}M$  of AIBN to  $7 \times 10^{11}$  ml.<sup>-1</sup> at  $10^{-2}M$ . The rate of polymerization increased as the initiator concentration to an exponent significantly higher than 0.5, as we shall see later, so that the rate per aggregate must also increase with initiation rate.

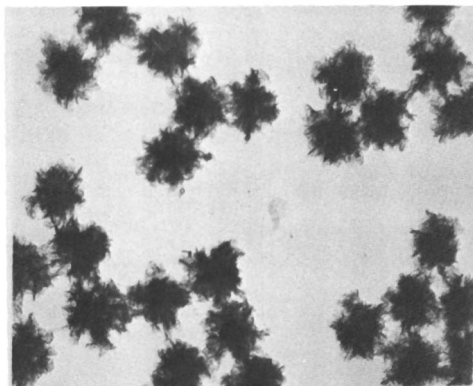


Figure 1. Particles from bulk polymerization of acrylonitrile at 50°C. AIBN concentration,  $3 \times 10^{-3}M$

### Surface Area

The aggregates of precipitated polyacrylonitrile particles are highly porous, as can be seen in the electron micrograph. The total surface is very large and can be measured by the B.E.T. nitrogen adsorption method, after removal of the unreacted monomer. Table I gives the results of a series of bulk polymerizations carried to different conversions at 50°C. The specific surface decreases gradually, presumably because the interstitial volume becomes filled by polymerization within the aggregates. However, the total surface is still an increasing function of time. The suspension becomes very difficult to handle above about 25% conversion, and no results were obtained in this region. It is quite possible that the total surface levels off above 25% conversion, where the polymerization rate becomes constant.

The specific surface was measured over a very wide range of AIBN concentration (Table II). All the measurements were made at 10–15%

Table I. Specific Surface of Particles Formed in Bulk Polymerization of Acrylonitrile at 50°C.

$$[AIBN] = 1.3 \times 10^{-3}M$$

<i>Time, min.</i>	<i>Conversion, %</i>	<i>B.E.T. Area, sq. meters/gram</i>
20	0.79	155
30	2.2	150
45	4.1	134
75	10.0	116
90	10.3	109
180	26.1	84

**Table II. Specific Surface of Particles Formed in Bulk Polymerization of Acrylonitrile at 50°C.**

Conversion = 10-15%

[AIBN], M	$R_p$ , mole/liter/sec.	B.E.T. Area, sq. meters/gram
$7.4 \times 10^{-5}$	$1.2 \times 10^{-5}$	89
$2.0 \times 10^{-4}$	$5.8 \times 10^{-5}$	85
$6.6 \times 10^{-4}$	$2.2 \times 10^{-4}$	121
$7.6 \times 10^{-4}$	$2.9 \times 10^{-4}$	107
$1.3 \times 10^{-3}$	$3.9 \times 10^{-4}$	109
$4.0 \times 10^{-3}$	$9.4 \times 10^{-4}$	123
$1.0 \times 10^{-2}$	$1.8 \times 10^{-3}$	98
$2.0 \times 10^{-2}$	$2.2 \times 10^{-3}$	94

conversion. The range of areas is admittedly rather large, and no explanation for this is offered, but the differences do not seem to be correlated with initiator concentration or rate of polymerization. As a first approximation, it will be assumed that the surface area is independent of the rate of initiation.

#### *Benzene-Acrylonitrile Mixtures*

Polyacrylonitrile is also quite insoluble in benzene, so that dilution of the monomer with benzene does not change the heterogeneous polymerization in any essential way. The effect of dilution on the specific surface is shown in Table III. There is a discernible trend toward lower surface areas at low acrylonitrile concentration. This is also evident in electron micrographs (Figure 2), where the particles from a benzene-acrylonitrile mixture are more compact and dense in appearance than those in Figure 1. Nevertheless, the surface is still extensive, and this has profound effects on the rate of polymerization.

**Table III. Specific Surface of Particles Formed in Polymerization of Acrylonitrile-Benzene Mixtures at 50°C.**

[AIBN] =  $2 \times 10^{-2}M$

Acrylonitrile-Benzene	B.E.T. Area, sq. meters/gram
100/0	117
98/2	94.4
60/40	71.7
40/60	45.7
20/80	25.5
15/85	89.0
10/90	43.7

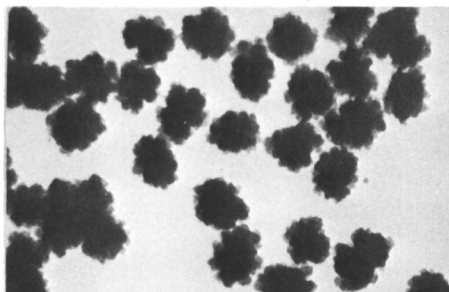


Figure 2. Particles from polymerization of 80/20 benzene acrylonitrile mixture at 50°C. AIBN concentration,  $3 \times 10^{-3}M$

### Kinetic Results

The rate of polymerization was measured dilatometrically, using mercury as the confining liquid. Dilatometers of conventional design and 5–10-ml. capacity were found to give erratic results at high rates of polymerization, owing presumably to inadequate rate of removal of the heat of reaction from the almost solid suspension of particles. Hence, a “J” type dilatometer was built with a flattened reaction cell so that the monomer solution was confined within a uniformly thin space between mercury and a thin glass wall. A schematic is shown in Figure 3. The volume of monomer solution was 1 ml. delivered by micropipet, except at high polymerization rates where it was necessary to reduce the volume to 0.1 ml. No measurements of temperature within the cell were attempted, but the achievement of substantially isothermal conditions could be deduced indirectly from the fact that the measured rate was independent of volume, below a critical volume which decreased as the initiator concentration increased.

Acrylonitrile was washed with phosphoric acid, then with sodium carbonate, then dried over calcium hydride and distilled (b.p., 77.6–77.9°C./760 mm. Hg). AIBN was recrystallized from cold methanol. Solutions were made by volume at 25°C., and the required amount was pipetted into the dilatometer cell. The cell was connected to the capillary by a lightly greased ground glass joint. The cell contents were frozen with liquid nitrogen, then evacuated on a high vacuum line. After several cycles of thawing, freezing, and pumping, the stopcock was closed, and the dilatometer removed from the vacuum line. The mercury in the bulb was first warmed in the 50°C. bath, then poured through the capillary into the cell. The cell was immediately mounted in the bath, and measurements of the column height were taken at intervals with a cathetometer.

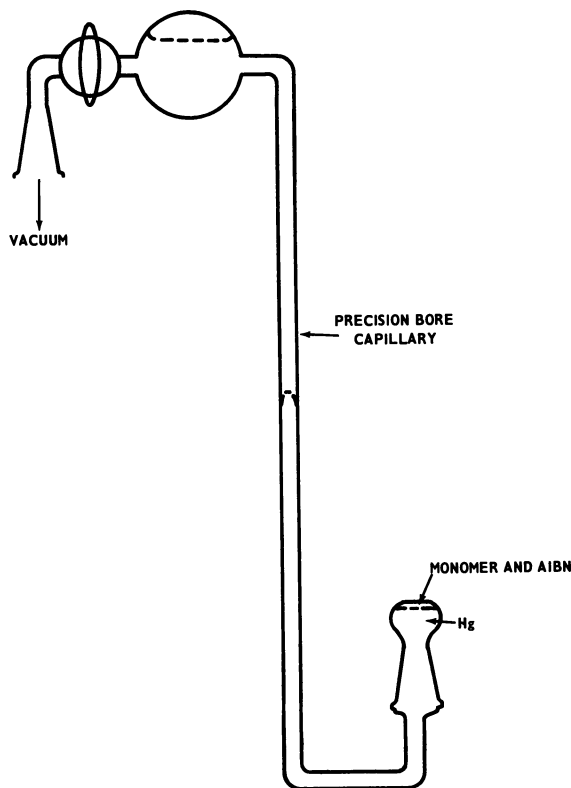


Figure 3. Schematic of dilatometer

A typical rate curve is shown in Figure 4. The measured contraction has been converted to percent conversion by means of a calibration constant derived from a number of direct measurements of polymer formed in the dilatometer cell. The measurements were timed from the instant the dilatometer was placed in the bath. At the highest rates of initiation, the constant rate stage was achieved in less than 10 min., indicating that thermal equilibration of this assembly is rapid compared with whatever process is responsible for the gradual acceleration observed in Figure 4 up to 15% conversion (120 min.). The protracted acceleration period is not caused by the presence of a retarder since it is only observed when polymer precipitates during the reaction (4). Above 15% conversion the rate is constant. At about 45% conversion the agglomerates become too closely packed to contract further, and the rate can no longer be measured by dilatometry.

It should be noted that because of the insolubility of the polymer, there is no change in monomer concentration at the particle interface in

bulk polymerization. Hence, the constant rate is not a fortuitous compensation of increasing radical concentration and decreasing monomer concentration, but indeed represents a steady-state rate.

The effect of using too large a volume of solution in the dilatometer is to extend the acceleration period, resulting in too high a rate. This is symptomatic of nonisothermal conditions.

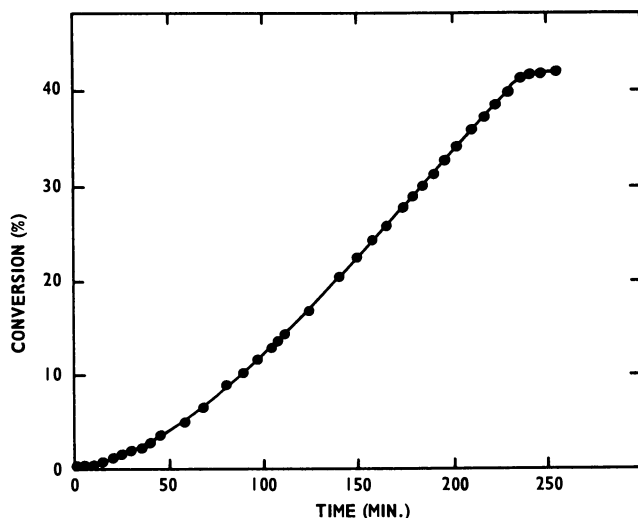


Figure 4. Bulk polymerization of acrylonitrile at 50°C. AIBN concentration,  $2.07 \times 10^{-3}M$

The rate of polymerization in the constant rate period is shown in Figure 5 as a function of AIBN concentration, both on logarithmic scales. At low concentrations of initiator ( $I$ ) the rate varies as  $I^{0.89}$ , but the slope drops as low as 0.33 at high rates of initiation. Similar results have been reported by Chapiro and Sebban-Danon (12) for polymerizations initiated by ionizing radiation at 19°C. Initiator exponents significantly higher than the "normal" value of 0.5 have been reported by many workers (6, 10, 17, 25, 30, 31) for the polymerization of acrylonitrile under heterogeneous conditions.

Polymerization of acrylonitrile-benzene mixtures at 50°C. resulted in a monomer exponent of about 1.7 in the rate expression. This is also in agreement with previous work (17, 20, 28, 31) on heterogeneous polymerization of acrylonitrile but not with homogeneous systems where a monomer exponent of unity is expected (4).

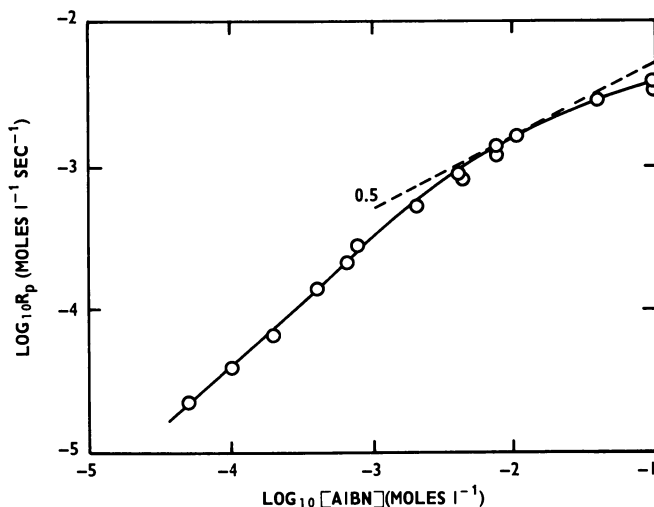


Figure 5. Rate of bulk polymerization of acrylonitrile at 50°C. as a function of AIBN concentration

### Trapped Radicals

Bamford and Jenkins (8) discovered high concentrations of stable free radicals in polyacrylonitrile produced by heterogeneous bulk polymerization. The initial estimate of  $5 \times 10^{16}$  per ml. was derived from measurement of the decoloration of diphenylpicrylhydrazyl. It was postulated that the growing polymer radical can be trapped mechanically in the precipitated polymer and hence shielded from reaction with other radicals. Termination by radical trapping was advanced by Thomas and Pellon (30), and later by Imoto and Takatsugi (17), as an explanation for the high initiator exponent in the rate expression. Radical trapping is a first-order process, and the simultaneous occurrence of first- and second-order termination reactions would give rise to initiator exponents between 0.5 and 1.0. Bamford and Jenkins (7) objected to such mechanistic schemes on the grounds that a very small fraction of the radicals generated actually become trapped, so that the kinetics should be affected to a negligible extent. Measurements of the lifetime of the kinetic chain in heterogeneous acrylonitrile polymerization tend to support this view. Using a thermocouple method for taking non-steady-state measurements under essentially adiabatic conditions, Bengough (10) found that even in the presence of precipitated polymer a steady state is established within minutes of the commencement of irradiation of a photosensitized solution. This means that long lived radicals must contribute little toward the over-all rate of polymerization.

Recently, even higher concentrations of trapped radicals have been observed by electron spin resonance. Bamford *et al.* (5) found up to  $1.3 \times 10^{17}$  radicals per ml., and Ingram *et al.* (18) found  $3.5 \times 10^{17}$  per ml. in the photopolymerization of acrylonitrile at 20°C. At the same time, it was found that the concentration was greatly reduced when polymerization was carried out at higher temperatures, and Bamford *et al.* were unable to detect any radicals at 60°C.

Repeated attempts in this laboratory to demonstrate the presence of unpaired electrons in polyacrylonitrile initiated by AIBN at 50°C., using a Varian spectrometer, have failed to detect any signal at all. Measurements have been made both at room temperature and at -196°C., and we believe that we could have detected concentrations as low as  $10^{14}$  radicals per ml. Hence, it is not possible under the conditions reported here to account for the kinetic results by the mechanism of first-order termination of growing chains by entrapment in precipitated polymer. This is not to say, however, that under other conditions, such as photo-initiated polymerization at low temperature, the trapped radicals are unimportant to the kinetics of polymerization.

### **Mechanism**

Peebles (23) has proposed that three separate loci of polymerization exist during the heterogeneous polymerization of acrylonitrile. These are:

(1) The solution phase. Radicals are generated in the monomer-rich liquid phase, and hence polymer chains must be initiated in this phase.

(2) The surface phase. While this may not be a separate phase in the thermodynamic sense, adsorption of a growing radical on the particle surface would confine the reaction to this locus throughout much of the life of the chain.

(3) The interior phase. Precipitated polymer chains are expected to be tightly coiled. A coiled radical would have reduced reactivity since there is a high probability that the radical end will be occluded within the coil. Trapped radicals are presumed to be deeply buried in the interior phase.

Occlusion of growing radicals within the precipitated polymer has been emphasized by Bamford and co-workers (4) as the paramount factor in the kinetics of heterogeneous polymerization. The following argument endeavors to show that at least under the conditions discussed here the kinetic results can be accounted for by considering surface polymerization only.

It is well known that the acceleration in rate at high conversion (Trommsdorff effect) in the bulk homogeneous polymerization of vinyl monomers is caused by a marked increase in the concentration of growing radicals (21). Despite this, at still higher conversion the reaction virtually



stops, even though unreacted monomer is still present in amounts up to 5% (9, 16, 21). This can only be caused by a reduction in propagation rate constant by many orders of magnitude, caused by vitrification of the system. If the temperature is raised above the glass temperature of the polymer, polymerization resumes and proceeds to completion (21). Polymerization of acrylonitrile in the interior phase of the precipitated particles can therefore make a significant contribution to the over-all rate only if the polymerization temperature is above the glass temperature of the interior phase. The composition and properties of the particles may be inferred from the properties of homogeneous castings of polyacrylonitrile. These can be made by an ingenious technique devised by Shavit, Konigsbuch, and Oplatka (26), in which fresh monomer is continuously supplied to the casting so that the interstices between particles ultimately fill with polymer, resulting in optically clear, consolidated material. Pellon *et al.* (24) found that the monomer content of such castings was about 5%, even after 5 days at 40°C. The monomer content could be reduced to less than 0.3% by heating to 80°C. or above (24). We conclude, therefore, that the precipitated phase contains about 5% monomer, has a glass temperature of about 80°C., and does not polymerize appreciably below 80°C.

The amount of polymer formed in the solution phase must also be greatly restricted. Even assuming that all of the radicals are generated in the solution phase, they become insoluble after adding only perhaps five or 10 monomer units (23). Precipitation should occur rapidly on existing nuclei such as the surface of already precipitated polymer. Hence, the large surface of the particle constitutes an efficient radical trap which maintains the concentration of radicals in the solution phase at a very low level. The situation is comparable with that in emulsion polymerization. An analysis similar to that of Smith (27) for the emulsion polymerization of styrene shows that the average lifetime of a radical in the solution phase is sufficient to add only one to 10 acrylonitrile units before the radical collides with a polymer particle.

The preceding discussion has led us to the conclusion that the surface is the only locus of polymerization which needs to be considered in the heterogeneous polymerization of acrylonitrile. Radicals arrive at the surface at a rate determined by the decomposition of the initiator and efficiency of initiation. Propagation occurs on the surface at a rate determined by the activity of monomer at the surface. By analogy with emulsion polymerization, where monomer diffuses into the particles rapidly enough to maintain near equilibrium activity (14), we assume that the activity of the monomer adsorbed on the particle surface is approximately equal to the mole fraction in solution. The propagation rate constant is presumably influenced somewhat by the presence of the solid surface.

The principal difference from homogeneous polymerization is that the rate constant for bimolecular termination should be greatly reduced since the growing chains are an integral part of a solid particle. Termination of growing chains by initiator radicals can become an important reaction, as has already been proposed (13). It has also been shown that under conditions where chain mobility is very low, there is a high probability of termination between chains arising from the same initiator molecule (1, 3). This arises from the fact that in the early stages of growth the chain lies closer to its "twin," on the average, than to other radicals. The probability of "geminate chain termination," as it has been called (1), increases as the radical concentration decreases or as conditions favor less chain mobility.

The kinetic scheme developed below for these conditions is perfectly general for homogeneous or heterogeneous polymerization. Geminate chain termination and termination by initiator radicals are ordinarily neglected in simple kinetic schemes, but they must be included in any case where the growing chain is immobilized, as by adsorption in a heterogeneous polymerization, or as a result of high viscosity in homogeneous polymerization.

The use of the steady-state approximation is justified on the basis of two separate, independent observations. Firstly, after sufficient polymer has accumulated, the rate remains constant over an extended range of conversion (Figure 4). Secondly, Bengough's measurements (10) of the non-steady-state kinetics of acrylonitrile polymerization show that a steady state is established within minutes, whereas the polymerization continues for hours.

### *Kinetic Scheme*

The subject of the kinetics of vinyl polymerization by radical mechanisms is treated exhaustively in a book by Bamford, *et al.* (4) and more briefly in many textbooks of polymer chemistry. The polymerization of vinyl monomers is a chain reaction in which the primary reactions are:

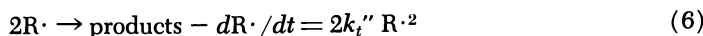
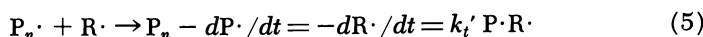
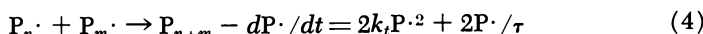
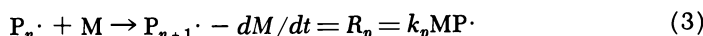
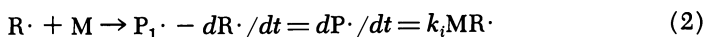
(1) Initiation. The initiator (I) decomposes to form free radicals ( $R\cdot$ ), which initiate the growth of polymer by sequential addition of monomer molecules. The fraction ( $f$ ) which successfully initiate chains is called the efficiency of initiation.

(2) Propagation. Each radical adds monomer to form longer and longer molecules ( $P\cdot$ ), each having one unpaired electron. Except for the initiator radical, all the radicals are assumed to add monomer with equal reactivity and at a rate which is first order in monomer concentration.

(3) Chain transfer. The radical undergoes a displacement reaction to form a new free radical species. Unless the new radical is very inefficient in initiating new chains, there is no effect on the over-all kinetics.

(4) Termination. Two radicals react to form one or two molecules having no unpaired spins. If the radicals are assumed randomly distributed in space, the termination rate is second order in radical concentration. Under conditions where diffusion is restricted, however, the twin chains initiated by radicals from the same initiator molecule may remain close together for a time, so that termination has a higher probability than in the case of random distribution of radicals. This case has been discussed by Allen and Patrick (1, 3). It results in a rate expression formally equivalent to a reaction first order in radical concentration, with half-life  $\tau$ . Termination by initiator radicals is also taken into account here.

The following reactions summarize the scheme:



The concentrations of reactants are represented by  $I$  = initiator,  $R\cdot$  = initiator radicals,  $M$  = monomer,  $P_n\cdot$  = macroradicals of degree of polymerization  $n$ , and  $P_{n+m}$  = polymer formed by combination of radicals of length  $n$  and  $m$ .

Assuming steady-state conditions in all radical species we can write

$$dR\cdot/dt = 0 = 2fk_d I - k_i MR\cdot - k_t' P\cdot R\cdot - 2k_t'' R\cdot^2 \quad (7)$$

and

$$dP\cdot/dt = 0 = k_i R\cdot M - 2k_t P\cdot^2 - 2P\cdot/\tau - k_t' P\cdot R\cdot \quad (8)$$

Hence,

$$P\cdot = \frac{1}{k_t' R\cdot} [2fk_d I - k_i R\cdot M - 2k_t'' R\cdot^2] \quad (9)$$

and

$$R\cdot = \frac{2k_t P\cdot^2 + \frac{2}{\tau} P\cdot}{k_i M - k_t' P\cdot} \quad (10)$$

Using Equation 3 we can combine the above expressions for  $P\cdot$  and  $R\cdot$  to obtain an expression only in  $R_p$  which is, after some rearranging,

$$\begin{aligned} & \left(\frac{k_i \tau}{k_p}\right) \left(1 - 4 \frac{k_t k_t''}{k_t'^2}\right) \frac{R_p^4}{M^3} + \left(1 - 8 \frac{k_t k_t''}{k_t'^2}\right) \frac{R_p^3}{M^2} \\ & - \left[ \left(4 \frac{k_t k_t''}{k_t'^2}\right) \frac{1}{M} \left(\frac{k_p}{k_i \tau}\right) + M \left(\frac{k_i \tau}{k_p}\right) \left(\frac{k_i^2 k_p^2}{k_t'^2}\right) - (f \tau k_p) \frac{k_d I}{M} \right] R_p^2 \\ & - \left[ \left(\frac{k_i^2 k_p^2}{k_t'^2}\right) M^2 + 2 \left(\frac{k_i k_p}{k_t'}\right) (f \tau k_p) M k_d I \right] R_p + \frac{k_i^2 k_p^2}{k_t'^2} (f \tau k_p) M^3 k_d I = 0 \end{aligned} \quad (11)$$

The above can be expressed as a function of four parameters ( $\beta$ 's) as follows:

$$\frac{\beta_4(1-4\beta_3)}{M^3} R_p^4 + \frac{(1-8\beta_3)}{M^2} R_p^3 - \left( \frac{4\beta_3}{M\beta_4} + \frac{M\beta_4}{\beta_1^2} - \frac{k_d I}{M\beta_2} \right) R_p^2 - \left( \frac{M^2}{\beta_1^2} + \frac{2Mk_d I}{\beta_1\beta_2} \right) R_p + \frac{M^3 k_d I}{\beta_1^2 \beta_2} = 0 \quad (12)$$

where

$$\beta_1 = \frac{k_t'}{k_i k_p} \quad (13)$$

$$\beta_2 = \frac{1}{f\tau k_p} \quad (14)$$

$$\beta_3 = \frac{k_i k_t''}{k_i'^2} \quad (15)$$

$$\beta_4 = \frac{kt\tau}{k_p} \quad (16)$$

Thus, the system is basically a four parameter one, and estimation of these  $\beta$ 's will provide all of the information obtainable concerning the seven rate constants.

We used the Gauss procedure to search iteratively for values of the  $\beta$ 's which will make  $\Sigma [\ln (R_p \text{ observed}) - \ln (R_p \text{ calculated})]^2$  a minimum. The reason for taking the logarithm of  $R_p$  was a statistical one stemming from the fact that the errors in  $R_p$  seemed proportional to the value of  $R_p$ . The log transformation makes the error variance approximately constant over the range.

In solving the function for  $R_p$  it was necessary to use a numerical scheme to get roots of the quartic equation and then decide which root was the meaningful one. Since this would have been too time consuming, we decided to use Newton's method, with the observed value of  $R_p$  as a first guess, and tentatively accept the value on which the method converged as the meaningful root. This proved to be a workable approach.

Upon convergence of the iterative procedure and using the least-squares estimates of the parameters herein reported, the other roots of the quartic were investigated at each of these data points. In all cases, there was one other positive root ( $R_p$ ) and either two negative or two complex roots. The second positive root was in all cases further from the observed value of  $R_p$  than the root which was selected by Newton's method. Furthermore, it was found that in all cases for which we had data this second positive root when substituted in the original equations gave a negative value of  $R_p$ . Thus, our numerical procedure led to the proper least squares solution.

The nature of the roots of the quartic, independent of the data and values of the parameters was also investigated. A complete derivation of this is given in the Appendix and is summarized here:

(1) There will always be one and only one positive root ( $R_p$ ) which will satisfy both Equations 9 and 10 and the physical restriction that  $R \cdot$  must be positive.

(2) There may or may not be a second positive root ( $R_p$ ). In any event, it will not satisfy the physical restriction that  $R \cdot$  be positive.

**Table IV. Calculated and Observed Rates of Polymerization of Acrylonitrile at 50°C.**

$I \times 10^5$	$M$	$R_p \times 10^5$		95% Confidence Limits	
		Observed	Predicted	Lower	Upper
4.89	14.79	2.74	2.21	1.92	2.53
10.1		5.14	4.49	3.94	5.12
19.6		5.74	8.49	7.50	9.60
19.8		7.54	8.57	7.57	9.69
39.9		15.8	16.4	14.7	18.3
65.9		23.2	25.6	23.1	28.2
75.8		29.3	28.8	26.2	31.7
130.0		38.7	44.7	41.0	48.8
207.0		58.7	63.5	58.4	69.0
401.0		96.8	99.3	91.2	108
755.0		117	144	132	158
765.0		136	145	133	159
1030.0		180	170	155	186
2000.0		243	231	212	254
3900.0		316	301	277	328
9970.0		418	401	369	437
7.55		5.19	3.38	2.96	3.86
2090.0		224	236	216	258
3080.0		274	276	253	301
4320.0		316	312	287	339
5180.0		372	332	306	360
6230.0		403	352	324	381
7450.0		384	371	342	402
8710.0		451	387	357	421
9250.0		465	393	362	427
10500.0	14.79	383	407	373	443
2000.0	1.51	6.45	5.13	3.99	6.59
2000.0	3.02	13.5	18.5	15.0	22.7
2000.0	6.03	78.9	60.2	53.9	67.3
2000.0	9.05	111	114	106	123
2000.0	15.08	235	238	217	261
2000.0	15.08	237	238	217	261
6090.0	3.017	21.0	22.1	18.9	25.8
6090.0	6.034	56.1	79.0	71.0	87.8
10600.0	3.017	25.0	23.4	18.4	29.7
10590.0	6.034	75.9	86.3	73.9	101

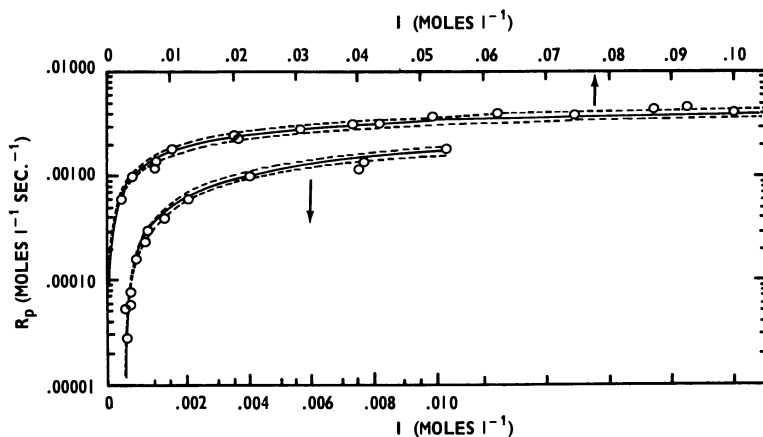


Figure 6. Comparison of predicted rate of bulk polymerization of acrylonitrile at 50°C. with experimental data

— Predicted by Equation 12 with parameters shown in Table V  
 -- 95% confidence limits  
 ○ Observed values

The lower curve which uses the lower scale is an enlargement of the left-hand section of the upper curve

(3) Any other roots ( $R_p$ 's) of the quartic will be either negative or complex, both of which can be ruled out on physical grounds.

While the iterative scheme adopted did not, in this instance, lead to extraneous roots, this possibility can be avoided completely by using the form given in the Appendix (Equation 23) for any future least squares estimation. This form does not possess the unwanted root.

Table IV lists the 36 sets of experimental conditions, the measured  $R_p$ , the calculated  $R_p$ , and the 95% approximate confidence limits for  $R_p$  at these conditions. For all of the data at constant monomer concentration ( $M = 14.79M$ ) a plot of  $R_p$  vs.  $I$  (Figure 6) is provided, showing the observed values in relation to the smooth curve formed by the calculated values.

Once least squares values of the  $\beta$ 's were obtained, it was desirable to extract from them as much information as possible about the original parameters. To do so, we make one further statement concerning the relations between the rate constants for mutual termination of polymeric radicals of different size. It has been shown (2) that termination rates in free radical polymerizations are determined by diffusion rates rather than chemical factors. The relative displacement of two radicals undergoing Brownian motion with diffusion coefficients  $D$  and  $D''$  also follows the laws of Brownian diffusion with diffusivity  $D' = D + D''$  (11). It

follows from this and the definitions of the rate constants, Equations 4, 5, and 6 that

$$k_t' = \frac{k_t + k_t''}{2} \quad (17)$$

Then the following functions of the original parameters which are of interest were expressed in terms of the estimated  $\beta$ 's:

$$f\tau k_p = \frac{1}{\beta_2} \quad (18)$$

$$\frac{k_t}{fk_p^2} = \beta_2\beta_4 \quad (19)$$

$$\frac{k_t'}{fk_p^2} = \left[ \frac{1 + \sqrt{1 - \beta_3}}{\beta_3} \right] [\beta_2\beta_4] \quad (20)$$

$$\frac{k_t''}{fk_p^2} = \left[ \frac{2 + 2\sqrt{1 - \beta_3}}{\beta_3} - 1 \right] [\beta_2\beta_4] \quad (21)$$

$$\frac{k_i}{fk_p} = \left[ \frac{1 + \sqrt{1 - \beta_3}}{\beta_1\beta_3} \right] [\beta_2\beta_4] \quad (22)$$

The estimated values of the  $\beta$ 's and of the original parameters are shown in Table V. Despite the wide range of initiator and monomer concentrations used, it is not possible to obtain precise estimates of this many parameters from the data. In particular,  $\beta_3$  is very poorly defined for this system. Notice that the geometric mean approximation is equivalent to  $\beta_3 = 1$  (see Equation 15). For a diffusion-controlled bimolecular reaction the arithmetic mean is appropriate as shown above, and this is reflected in the fact that  $\beta_3$  is significantly less than 1.

The order of magnitude of the lifetime of a geminate pair,  $\tau$ , can be estimated from the value of  $f\tau k_p$  in Table V and literature values for  $k_p$  in homogeneous polymerization. A recent compilation (23) shows wide discrepancies between reported values of  $k_p$  for acrylonitrile in solution, but it is apparently in the range of  $10^3$  to  $10^4$  at  $50^\circ\text{C}$ . For discussion we take  $f$  to be of order unity, and assume that  $k_p$  is independent of the solvent medium. It then follows that  $\tau = 1.2$  to  $16$  sec., in agreement with direct measurements by Bengough (10) in bulk polymerization at  $25^\circ\text{C}$ . Radical lifetimes of this magnitude are consistent with the assumption of a steady state after a minute or so of reaction time.

Literature values of  $k_t/k_p^2$  for acrylonitrile in homogeneous solution at  $50^\circ\text{C}$ . are 39 mole sec./liter in dimethyl sulfoxide, and 150 mole sec./liter in dimethylformamide (31). Since immobilization of the chains by adsorption should greatly reduce  $k_t$  without drastically affecting  $k_p$ , our value of 0.02–0.7 mole sec./liter (Table V) is reasonable for heterogeneous

conditions. The primary radicals, diffusing freely in solution, undergo termination at a rate comparable with the polymer chains under homogeneous conditions. Hence, the value of  $k_i''/fk_p^2 = 40$  mole sec./liter in Table V is in excellent agreement with that for the polymer in dimethyl sulfoxide.

**Table V. Estimates of Parameters with 95% Approximate Confidence Limits**

$$\beta_1 = (3.3 \pm 2.8) \times 10^4 \text{ mole sec./liter}$$

$$\beta_2 = (7.0 \pm 1.0) \times 10^{-5} \text{ mole/liter}$$

$$\beta_3 = (4 \pm 40) \times 10^{-2}$$

$$\beta_4 = (5 \pm 5) \times 10^3 \text{ sec.}$$

---


$$f\tau k_p = (1.4 \pm 0.2) \times 10^4 \text{ liters/mole}$$

$$\frac{k_i}{fk_p^2} = (3.6 \pm 3.4) \times 10^{-1} \text{ mole sec./liter}$$

$$\frac{k_i'}{fk_p^2} = (2 \pm 20) \times 10 \text{ mole sec./liter}$$

$$\frac{k_i''}{fk_p^2} = (4 \pm 40) \times 10 \text{ mole sec./liter}$$

$$\frac{k_i}{fk_p} = (6 \pm 60) \times 10^{-4}$$

The ratio  $k_i/fk_p$  can be estimated from published data in the following way. The primary radical formed by decomposition of azodiisobutyronitrile is structurally similar to the terminal unit of a polymethacrylonitrile radical, and we can therefore assume that its reactivity towards acrylonitrile is similar. Designating acrylonitrile monomer and radical with the subscript 1 and methacrylonitrile with subscript 2, we can write

$$k_i/k_p = k_{21}/k_{11} = k_{21}k_{22}/k_{22}k_{11}$$

However, the ratio  $k_{22}/k_{21}$  is the reactivity ratio  $r_2$  for copolymerization of acrylonitrile with methacrylonitrile, so that

$$k_i/k_p = k_{22}/r_2k_{11}$$

The literature values, all at 60°C., are  $k_{22} = 184$  liter/mole/sec. (15),  $r_2 = 2.68$  (19), and the two reported values for acrylonitrile  $k_{11} = 1960$  and 11,600 liters/mole/sec. (23). These values give  $k_i/k_p = 5.9 \times 10^{-3}$  or  $3.5 \times 10^{-2}$ . The smaller value agrees with the upper limit given in Table V.



## Appendix

### *The Nature of the Roots*

To determine the nature of the roots of the quartic equation (Equation 12) without regard to the magnitudes of the positive quantities  $M$ ,  $k_d$ ,  $\beta_1$ ,  $\beta_2$ ,  $\beta_3$ , and  $\beta_4$ , it was necessary to return to the two original equations (Equations 9 and 10). After solving Equation 9 for  $R\cdot$  and using Equations 3, 13, 14, 15, and 16, we get:

$$\frac{k_t''R\cdot}{k_t} = \left[ - \left( \frac{M}{4} + \frac{\beta_1 R_p}{4M} \right) \pm \sqrt{\left( \frac{M}{4} + \frac{\beta_1 R_p}{4M} \right)^2 + k_d I \frac{\beta_1^2 \beta_3}{\beta_2 \beta_4}} \right] \quad (9a)$$

and for Equation 10 we get:

$$\frac{k_t''R\cdot}{k_t} = 2\beta_1\beta_3R_p \left[ \begin{array}{c} \frac{R_p}{M} + \frac{1}{\beta_4} \\ \frac{M^2}{\beta_1} - R_p \end{array} \right] \quad (10a)$$

The quartic equation (Equation 12) is then merely the result of equating Equations 9a and 10a and performing the necessary algebra. Geometrically, the roots of the quartic are the intersections of the curves plotted as a function of  $R_p$ . Let us examine the mathematical properties of Equations 9a and 10a so that we can understand the nature of the roots of the quartic. Once we have the mathematics in hand, we can add physical restrictions. For convenience we shall denote the expression for  $k_t''R\cdot/k_t$  in Equation 9a by  $F_1(R_p)$  and that contained in Equation 10a by  $F_2(R_p)$ . There are two branches of  $F_1(R_p)$ : the one using the positive square root remains strictly positive [ $F_1(R_p)^+$ ], while the one using the negative square root remains always negative [ $F_1(R_p)^-$ ]. The derivative of  $F_1(R_p)$  is:

$$F_1'(R_p) = \frac{-\beta_1}{4M} \left[ 1 \mp \frac{\left[ \frac{M}{4} + \frac{\beta_1 R_p}{4M} \right]}{\left[ \left( \frac{M}{4} + \frac{\beta_1 R_p}{4M} \right)^2 + k_d I \frac{\beta_1^2 \beta_3}{\beta_2 \beta_4} \right]^{1/2}} \right]$$

Since the "plus or minus" part of this expression is strictly less than 1,  $F_1'(R_p)$  is strictly negative. We have therefore established:

(1)  $F_1(R_p)^+$  is a non-negative, non-increasing function of  $R_p$ , which can be shown to grow positively without limit as  $R_p$  becomes large negatively and to approach zero as  $R_p$  grows large positively.

(2)  $F_1(R_p)^-$  is a strictly negative, non-increasing function of  $R_p$ , which can be shown to approach zero as  $R_p$  grows large negatively and to grow negatively without limit as  $R_p$  grows large positively.

Several things can be seen readily about the behavior of  $F_2(R_p)$  and are tabulated below ( $\epsilon$  is a small positive quantity).

$R_p$	$F_2(R_p)$
$-\infty$	$\infty$
$-M/\beta_4$	0
0	0
$[M^2/\beta_1] - \epsilon$	large positive
$M^2/\beta_1$	discontinuous
$[M^2/\beta_1] + \epsilon$	large negative
Greater than $M^2/\beta_1$	strictly negative
$\infty$	$-\infty$

It can also be shown that in the interval where  $R_p$  is greater than 0 and less than  $M^2/\beta_1$ ,  $F_2(R_p)$  is a strictly positive non-decreasing function. This is done by showing that the ratio  $F_2(R_p + e)/F_2(R_p)$  for any positive  $e$  less than  $([M^2/\beta_1] - R_p)$  is strictly greater than 1. If we write this ratio:

$$\frac{F_2(R_p + e)}{F_2(R_p)} = \left[ \frac{(R_p + e)}{R_p} \right] \left[ \frac{R_p\beta_4 + M + e\beta_4}{R_p\beta_4 + M} \right] \left[ \frac{M^2 - \beta_1 R_p}{M^2 - \beta_1 R_p - \beta_1 e} \right]$$

the first two brackets are each greater than 1 for any positive value of  $R_p$ . Of the positive values of  $R_p$ , only those less than  $M^2/\beta_1$  will make the third bracket greater than 1.

Therefore, since  $F_1(R_p)^+$  is positive at  $R_p = 0$ , positive at  $R_p = M^2/\beta_1$ , and monotonic decreasing in this interval, and since  $F_2(R_p) = 0$  at  $R_p = 0$  and monotonically grows without bound as  $R_p$  approaches  $M^2/\beta_1$ , there must be one and only one intersection of the two functions in the interval. The region  $R_p < 0$  is physically meaningless, so any roots there will be unacceptable. Similarly, for  $R_p > M^2/\beta_1$ , roots will be unacceptable since  $F_2(R_p)$  is strictly negative in this region, and while  $R_p$  is positive,  $R \cdot$  is implied to be negative.

Therefore, one and only one root of the quartic equation has physical meaning. If it is desired to estimate  $\beta$ 's for other polymerization systems, a better way of writing the function is in its most elementary form. That is, merely equating Equations 9a and 10a [eliminating the negative square root in Equation 9a since it gives negative  $R \cdot$ 's].

$$\begin{aligned} -\left(\frac{M}{4} + \frac{\beta_1 R_p}{4M}\right) + \left[\left(\frac{M}{4} + \frac{\beta_1 R_p}{4M}\right)^2 + k_d I \frac{\beta_1^2 \beta_3}{\beta_2 \beta_4}\right]^{1/2} \\ = 2\beta_1 \beta_3 R_p \left[ \frac{\frac{R_p}{M} + \frac{1}{\beta_4}}{\frac{M^2}{\beta_1} - R_p} \right] \end{aligned} \quad (23)$$

This form will assure that in using Newton's Method to solve for  $R_p$ , the extraneous positive root (giving negative  $R \cdot$ ) will never be found since it does not satisfy the equation in this form.

### Acknowledgments

We are indebted to A. M. Thomas for the electron microscope measurements, R. A. Herrmann and G. F. Yates for the surface area determinations, and W. G. Hodgson for performing the ESR spectroscopy.

### Literature Cited

- (1) Allen, P. E. M., Patrick, C. R., *Nature* **191**, 1194 (1961).
- (2) Allen, P. E. M., Patrick, C. R., *Makromol. Chem.* **47**, 154 (1961).
- (3) Allen, P. E. M., Patrick, C. R., *Trans. Faraday Soc.* **59**, 1819 (1963).
- (4) Bamford, C. H., Barb, W. G., Jenkins, A. D., Onyon, P. F., "The Kinetics of Vinyl Polymerization by Radical Mechanisms," Academic Press, New York, 1958.
- (5) Bamford, C. H., Ingram, D. J. E., Jenkins, A. D., Symons, M. C. R., *Nature* **175**, 894 (1955).
- (6) Bamford, C. H., Jenkins, A. D., *Proc. Roy. Soc. (London)* **A216**, 515 (1953).
- (7) Bamford, C. H., Jenkins, A. D., *J. Polymer Sci.* **14**, 511 (1954).
- (8) *Ibid.*, **20**, 405 (1956).
- (9) Bengough, W. I., Melville, H. W., *Proc. Roy. Soc. (London)* **A230**, 429 (1955).
- (10) Bengough, W. I., *Proc. Roy. Soc. (London)* **A260**, 205 (1961).
- (11) Chandrasekhar, S., *Rev. Mod. Phys.* **15**, 1 (1943).
- (12) Chapiro, A., Sebban-Danon, J., *J. Chim. Phys.* **54**, 776 (1957).
- (13) Durup, J., Magat, M., *J. Polymer Sci.* **18**, 586 (1955).
- (14) Flory, P. J., "Principles of Polymer Chemistry," p. 210, Cornell University Press, Ithaca, N. Y., 1953.
- (15) Grassie, N., Vance, E., *Trans. Faraday Soc.* **52**, 727 (1956).
- (16) Hayden, P., Melville, H. W., *J. Polymer Sci.* **43**, 201 (1960).
- (17) Imoto, M., Takatsugi, H., *Makromol. Chem.* **23**, 119 (1957).
- (18) Ingram, D. J. E., Symons, M. C. R., Townsend, M. G., *Trans. Faraday Soc.* **54**, 409 (1958).
- (19) Mark, H., Immergut, B., Immergut, E. H., Young, L. J., Beynon, K. I., "Copolymerization," G. W. Ham, Ed., Appendix A, Interscience, New York, 1964.
- (20) Nakatsuka, K., *Chem. High Polymers Japan* **15**, 43 (1958).
- (21) Nishimura, N., *J. Macromol. Chem.* **1**, 257 (1966).
- (22) Noyes, R. M., *J. Am. Chem. Soc.* **77**, 2042 (1955).
- (23) Peebles, L. H., Jr., "Copolymerization," Chap. IX, Interscience, New York, 1964.
- (24) Pellon, J. J., Smyth, N. M., Kugel, R. L., Valan, K. J., Thomas, W. M., *J. Appl. Polymer Sci.* **10**, 429 (1966).
- (25) Prevot-Bernas, A., Sebban-Danon, J., *J. Chim. Phys.* **53**, 418 (1956).
- (26) Shavit, N., Konigsbuch, M., Oplatka, A., British Patent **964,533** (1964); French Patent **1,398,711** (1965); German Patent **1,225,390** (1966); Israeli Patent **14410** (1962); Italian Patent **685,058** (1963).

- (27) Smith, W. V., *J. Am. Chem. Soc.* **70**, 3695 (1948).
- (28) Srinivasan, N. T., Santappa, M., *Makromol. Chem.* **26**, 80 (1958).
- (29) Thomas, W. M., *Advan. Polymer Sci.* **2**, 401 (1961).
- (30) Thomas, W. M., Pellon, J. J., *J. Polymer Sci.* **13**, 329 (1954).
- (31) Tokura, N., Matsuda, M., Yazaki, F., *Makromol. Chem.* **42**, 108 (1960).
- (32) White, E. F. T., Zissell, M. J., *J. Polymer Sci. A* **1**, 2189 (1963).

RECEIVED April 1, 1968.

## Keto-Enol Tautomers as Polymerization Initiators

H. HOPFF, E. KLEINER, and S. H. EL-DIN

Swiss Federal Institute of Technology, Department of Industrial and Engineering Chemistry, Zurich 6, Switzerland

*Aryl-substituted enolizable keto compounds initiate the copolymerization of unsaturated polyesters with styrene. Gel times of the same order as those obtained with conventional peroxide initiators can be attained; exotherms, however, are considerably lower, this latter effect being of technological interest—e.g., casting resins. Since a radical mechanism has been proved, it is postulated that radicals result from keto hydroperoxides which have been formed from the aryl-substituted enols via autoxidation. Steric effects and resonance may partly account for differences in the catalytic activity of some and for the inhibiting effect of other ketones and enols. NMR spectroscopy indicates further that cis-trans isomerism may influence the catalytic effectiveness of pure enols.*

The initiating effect of phenylacetaldehyde on the copolymerization of unsaturated polyesters with vinyl monomers has been described (9). The copolymerization proceeds at approximately the same rate as with the usual peroxide catalysts, but the reaction is much less exothermic; hence, the effects of "too rapid" a polymerization such as fissures, bubble formation, and volume contraction do not occur. Investigation of a series of compounds of the benzene family showed that only enolizable phenyl-keto compounds were initiators (7).

Aromatically substituted enols are easily autoxidized to the keto-hydroperoxide form (4, 5, 6, 10, 11, 12, 16), which, we postulate, would then initiate a radical polymerization. A radical mechanism is proved by the inhibiting effect of quinone and  $\alpha,\alpha'$ -diphenylpicrylhydrazyl and by the fact that the polymer yield is directly proportional to the square root of the initiator concentration (7).

Enolization is catalyzed in acidic polyester styrene solutions, and chelated enol tautomers should be more probable than the keto form in styrene, a nonpolar solvent. The tertiary hydroperoxide intermediates that are proposed by this mechanism should, furthermore, be unstable in an acid medium (8, 18).

The purpose of this work was to correlate catalytic activity with chemical structure for various aromatic and heterocyclic carbonyl compounds. Gel time, gel time as a function of initiator concentration, and gel time as a function of temperature were used to measure catalytic activity for the unsaturated polyester styrene systems used throughout this work.

### *Experimental*

All experiments were carried out with 20 grams of Vestopal A, an unsaturated polyester resin from Chemische Werke Hüls, containing approximately 30% styrene as solvent and comonomer. The NMR spectra were taken with a Varian Associates model A-60 spectrograph.

**Initiators.** All keto compounds tested were analytically pure. 1[2-*N*-Methylpyrrolyl]2-propanone, a hitherto unknown compound, was synthesized in 20% yield from *N*-methylpyrrolaldehyde using a Darzens glycidyl ester condensation:

b.p. = 67°–68°C. at 0.35 mm. and 74°–75.5°C. at 0.8 mm.;  $n_D^{20} = 1.5128$ ;  $d^{20} = 1.016$  grams/cc.; the corrected melting point of semicarbazone recrystallized from ethanol and sublimed: 151.2°–151.6°C.;  $C_9H_{14}N_4O$  (MW: 194.243): found, N = 28.85%; calcd., N = 28.85%.

The infrared spectrum shows a characteristic keto band at 1715  $cm^{-1}$ , the  $-CH_2-CO-$  absorption at 1400–1440  $cm^{-1}$ , the  $-CO-CH_3-$  absorption at 1355–1360  $cm^{-1}$ , and an *N*-methyl absorption at 2890  $cm^{-1}$ .

The NMR spectrum taken in carbon tetrachloride gives a singlet (methylene group too far away for interaction) at 2.01 p.p.m. which is attributed to the methyl group, a signal at 3.45 p.p.m. attributed to the *N*-methyl protons, and a signal at 3.52 p.p.m. attributed to the methylene protons. Signals at 5.9 and 6.42 p.p.m. are assigned to pyrrole nucleus protons. Integral ratio indicates the keto form in carbon tetrachloride.

**Arylcarbonyl Compounds as Initiators for Unsaturated Polyester/Styrene Copolymerization Systems.** GEL TIME DETERMINATION and REACTION CURVES. Ten blanks (gel time of 20 grams Vestopal A without initiator) gave a mean deviation from the average of  $\pm 3.3\%$  and a maximum deviation of  $\pm 7.2\%$ . Five measurements with 1-phenyl-2-propanone as initiator gave a mean deviation from the average of  $\pm 3.3\%$  and a maximum deviation of 7.7%. An experimental error of  $\pm 10\%$  was therefore assumed and proved correct by spot checks. The exceptions (not used in the discussions) are most probably caused by the insolubility of the initiators in the reaction medium.

The initiator was weighed into a test tube (radius = 10 mm.), 20 grams of fresh (stored at 0°C.) unsaturated polyester/styrene solution (Vestopal A) were added, the mixture was stirred well with a glass rod,

and a thermometer was introduced. When the arbitrarily chosen starting temperature of 18°C. had been reached, the test tube was placed in an oil bath of the desired temperature (regulated to  $\pm 0.2^\circ\text{C}$ .), and the gel time meter (Mol-Rez gel time meter of the Mol-Rez Division, American Petrochemical Corp.) was started (the starting position of the weight always being the same and a new weight being used for each measurement). The reaction temperature was read every 1–2 minutes.

Table I. Initiators of the Ar—CH—CHO Type at 100°C.

Initiator	Concentration		Gel Time, min.	Temperature Maximum, °C. after (min.)
	Moles/liter polyester	wt. %		
Thiophene- acetaldehyde	0.193	2.08	4.8 $\pm$ 0.5	104.7 (12)
Phenyl- acetaldehyde	0.193	2	6.0 $\pm$ 0.6	110.3 (19)
Hydratropa- aldehyde	0.193	2.2	3.6 $\pm$ 0.3	124 (12)
Benzoyl- peroxide	0.193	4	2.4 $\pm$ 0.2	160 (4)
Azoiso- butyronitrile	0.193	2.7	2.4 $\pm$ 0.2	164 (3, 5)
$\alpha$ -Thienyl- malonic acid diurethane <sup>a</sup>	0.0146	0.36	20 $\pm$ 2	102.8 (30)
$\text{R—CH} \begin{array}{l} \text{NHCOOC}_2\text{H}_5 \\ \text{NHCOOC}_2\text{H}_5 \end{array}$				
$\text{R} = \text{C}_4\text{H}_3\text{S} \text{—CH}_2\text{—}$				
Blank			123.2 $\pm$ 12.3	

<sup>a</sup> A compound which decomposes in acidic polyester resin at high temperature to give  $\alpha$ -thiopheneacetaldehyde.

## Results

Initiators of the Ar—CH—CHO Type. Tables I and II show the

following results:

(a) 1[2-Furyl]2-propanone gives a shorter gel time (approximately 30% shorter) than that obtained with 1-phenyl-2-propanone.

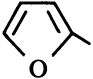
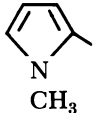
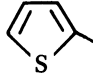
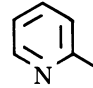
(b) 1[2-Pyridyl]2-propanone inhibits the copolymerization.

(c) The carbonyl initiators give temperature maxima that are considerably lower than those obtained with the conventional peroxide initiators.

The enol rather than the keto tautomer is the intermediate leading to the ketohydroperoxide form (through autoxidation). The catalytic effectiveness of carbonyl compounds would therefore be expected to be directly proportional to their degree of enolization and the reactivity of their enol forms.

For 1[2-pyridyl]2-propanone it is quite possible that the resonance energy of the pyridine nucleus is high enough to stabilize the initiating radical (resulting from the enolic double bond or rather the peroxide or ketohydroperoxide therefrom) to such an extent that it acts as an inhibitor.

Table II. Initiators of the Ar—CH<sub>2</sub>—CO—CH<sub>3</sub> Type<sup>a</sup>

Initiator	Concentration, Wt. %	Gel Time, min.	°C. after (min.) Temperature Maximum
	2.06	4.8 ± 0.5	107.4 (20)
	2.26	6.0 ± 0.6	102.2 (10)
	2.33	6.0 ± 0.6	103.3 (13)
	2.23	8.4 ± 0.8	107.2 (21)
	2.23	>240	— —
Blank		123 ± 12.3	

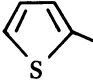
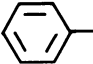
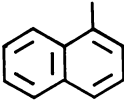
<sup>a</sup> 0.193 Mole/liter polyester at 100°C.

The heat evolved should be the same for copolymerizations initiated by both carbonyl compounds and conventional peroxides. The marked difference in the exotherm can be explained by assuming that there is no



induction period for the keto-enol mechanism, that initiation proceeds smoothly throughout (oxygen inhibits normally), and that the rate of radical generation is much less sensitive to increasing temperature than for benzoyl peroxide. Support for this argument can be found in Table V; a 60°C. rise in temperature reduces the gel time only fourfold, considerably greater changes would be expected for benzoyl peroxide.

**Table III. Initiators of the Ar—CH—CO—COOC<sub>2</sub>H<sub>5</sub> Type<sup>a</sup>**

Initiator	Wt. %	Gel Time, min.	Temperature Maximum °C. after (min.)	Appearance of Copolymer
Ar = 	3.8	>209	—	—
	3.6	4.8 ± 0.5	111 (17)	colorless
	4.4	8.4 ± 0.8	105 (38)	colorless
Blank		123.2 ± 12.3	—	—

<sup>a</sup> 0.193 Mole/liter polyester at 100°C.

**Initiators of the Ar—CH—CO—COOC<sub>2</sub>H<sub>5</sub> Type. Tables III, IV,**



and V show the following results:


(a)  $\alpha$ -Cyanophenyl pyruvic acid ethyl ester is a more active initiator than the corresponding naphthyl compound. The difference in activity using 0.193 mole/liter polyester at 100°C. is approximately 30%. Tables IV and V show that the phenyl ester is more active than its naphthalene counterpart in all concentrations and at every temperature.

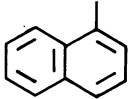
(b)  $\alpha$ -Cyanothiophene pyruvic acid ethyl ester inhibits the copolymerization.

To correlate chemical structure with catalytic activity for these compounds we investigated the keto-enol equilibria with the help of the iron chloride enol test, infrared, and NMR spectra. According to Meyer

Table IV. Initiators of the Ar—CH—CO—COOC<sub>2</sub>H<sub>5</sub> Type<sup>a</sup>

|  
CN

Initiator concentration, × 10 <sup>-4</sup>	5.85	29.3	58.5	293	585
Initiator:					
Ar = 					
wt. %	0.011	0.055	0.11	0.55	1.1
Gel time, min.	19.2 ± 2	10.8 ± 1	8.4 ± 0.8	6.0 ± 0.6	4.8 ± 0.5
Temperature maximum, °C.	103.8	105.5	108	108.9	108
Hardening time, <sup>b</sup> min.	28	30	20	17	20

Initiator:					
Ar = 					
wt. %	0.013	0.065	0.13	0.65	1.3
Gel time, min.	37.2 ± 4	25.2 ± 3	19.2 ± 2	10.8 ± 1	9.6 ± 1
Temperature maximum, °C.	102.5	102.8	103.3	104.5	104
Hardening time, <sup>b</sup> min.	44	32	31	28	24

<sup>a</sup> Gel time = *f*. Initiator concentration in moles/liter polyester at 100°C. All copolymers colorless.

<sup>b</sup> Time to reach maximum temperature.

(14) these compounds, all crystalline at room temperature, should be either 100% enols or 100% ketones. Factors affecting the already one-sided equilibria would therefore be mainly solvent medium and temperature. The enolic form of these compounds is favored *a priori*:

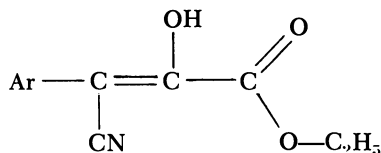

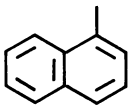


Table V. Initiators of the Ar—CH—COOC<sub>2</sub>H<sub>5</sub> Type<sup>a</sup>

	$\begin{array}{c} \text{Ar—CH—COOC}_2\text{H}_5 \\   \\ \text{CN} \end{array}$				
Temperature, °C.	60	70	80	100	120
Initiator					
Ar =					
	1.1 wt. %				
Gel time, min.	16.8 ± 2	13.2 ± 1	9.6 ± 1	4.8 ± 0.5	3.6 ± 0.4
Temperature maximum, °C.	61.2	71.7	83	108.2	128
Hardening time, min.	34	32	30	20	15
Initiator					
Ar =					
	1.3 wt. %				
Gel time, min.	68.4 ± 7	33.6 ± 3	23.8 ± 2	9.6 ± 1	6.0 ± 0.6
Temperature maximum, °C.	60.2	71.2	81.2	104	127
Hardening time, min.	75	36	36	24	18

<sup>a</sup> Gel time = *f* (temperature). Initiator concentration,  $585 \times 10^{-4}$  mole/liter polyester. All copolymers colorless.

There are three different resonance possibilities for the enolic double bond—*viz.*, with the aromatic nucleus, with the cyano, and with the carbonyl group. Furthermore, the  $\alpha$ -hydrogen of the keto form would be acidic owing to the presence of the cyano group. Accordingly, all three compounds gave positive reactions to the iron chloride enol test. Further proof for the enol form in the crystalline state is given by the infrared spectra taken in Nujol and Fluorolube.

The  $\alpha$ -cyano- $\alpha$ -naphthyl pyruvic acid ethyl ester shows a hydroxyl band at 3190 cm.<sup>-1</sup> which is attributed to chelation (very strong intramolecular hydrogen bonding) (2). At 1717 cm.<sup>-1</sup> it gives the  $\alpha,\beta$ -unsaturated carbonyl band of the enol form (lit. Ref. 2, 1715–1730 cm.<sup>-1</sup>). The phenyl ester shows the same bands at 3190 and 1717.5 cm.<sup>-1</sup>, respectively, whereas the thiophene ester spectrum shows intermolecular hydrogen bonding at 3310 cm.<sup>-1</sup>. Since the  $\alpha$ -keto ester carbonyl band of the keto

form ( $1740\text{--}1755\text{ cm}^{-1}$ ) is missing for all three compounds, the enol form with intra- and intermolecular hydrogen bonding can be assumed. Styrene, a nonpolar solvent, should favor the enol forms, at least for the naphthyl and phenyl esters.

The influence of high temperature on the keto-enol equilibrium was studied using NMR spectra and trifluoroacetic acid (TFE); the modified Shoolery rule (3) was used to identify the methine signal of the keto form which should appear at 5.3 p.p.m. as a singlet. [Trifluoroacetic acid identifies the hydroxyl proton signal. An exchange takes place between the acid proton and the hydroxyl proton resulting in a combined TFE/OH signal which usually appears at lower field than the OH signal.] Three NMR spectra were taken for each ester—in deuteriochloroform at room temperature, in deuteriochloroform at room temperature with TFE, and in deuterobromoform at  $80^\circ$  or  $100^\circ\text{C}$ . According to the spectra all three compounds are enols at room and at higher temperatures.

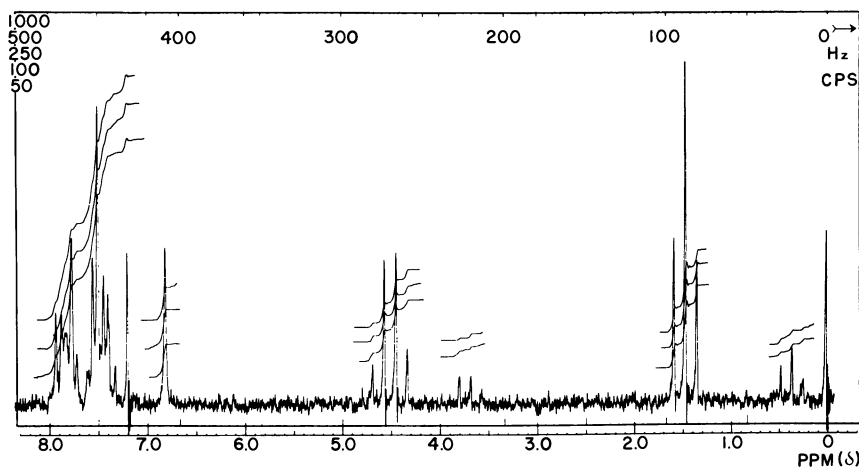


Figure 1. NMR spectrum of  $\alpha$ -cyano- $\alpha$ -naphthyl pyruvic acid ethyl ester in deuteriochloroform at room temperature. The three naphthyl ester spectra are given here. The spectra of the other two esters were interpreted in a similar manner

**NMR SPECTRUM IN DEUTEROCHLOROFORM AT ROOM TEMPERATURE.** The spectrum in Figure 1 shows a methyl triplet at 1.5 p.p.m. and a second methyl triplet at 0.38 p.p.m. which we attribute to the cis-enol form. The shift to higher field is attributed to the shielding effect of the benzene nucleus. The Stuart model shows that the methyl group of the cis-enol form can lie over the middle of one of the benzene nuclei. We assume from the integral ratio of the methyl proton signals that approximately

20% of the enol form is *cis*. There is no methine singlet between 2.5 and 6 p.p.m.; the quadruplet signal at 4.5 p.p.m. corresponds to two protons—*viz.*, the methyl protons of the ester. The signals between 7.3 and 8 p.p.m. are attributed to the naphthalene nucleus; the signals at 7.23 and 6.8 p.p.m. are attributed to chloroform and the hydroxyl proton, respectively.

**NMR SPECTRUM IN DEUTEROCHLOROFORM AT ROOM TEMPERATURE WITH TFE.** As Figure 2 shows, the addition of TFE caused the signal at 6.8 p.p.m. to disappear giving a new TFE/OH signal at 8 p.p.m. We therefore assign the signal at 6.8 p.p.m. to the hydroxyl proton of the enol form.

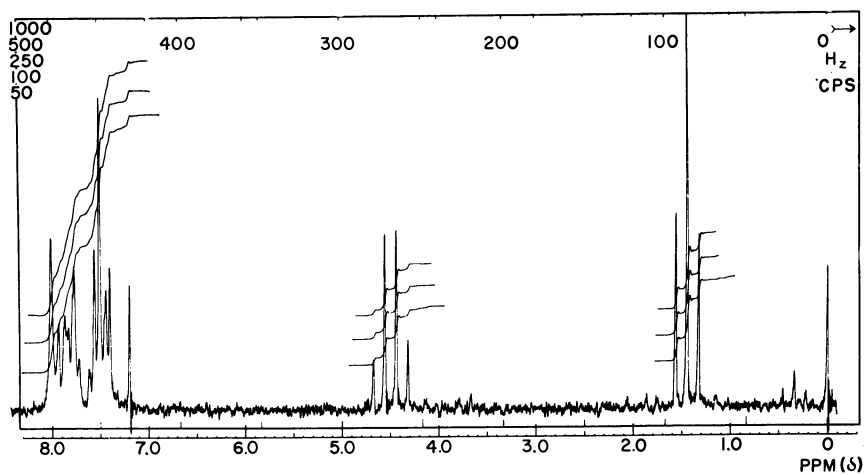


Figure 2. NMR spectrum of  $\alpha$ -cyano- $\alpha$ -naphthyl pyruvic acid ethyl ester in deuteriochloroform with TFE

**NMR SPECTRUM IN DEUTEROBROMOFORM AT 100°C.** The spectrum in Figure 3 is unchanged compared with Figure 1 except that the hydroxyl proton now gives a signal at 6.6 p.p.m. It appears from the methyl integral ratio that the *cis/trans*-enol equilibrium has not shifted.

The greater catalytic activity of the phenyl ester compared with that of the naphthyl ether can be attributed to the fact that there are two isomeric forms of the latter (approximately 20% *cis* and 80% *trans*), the open *trans* form being more susceptible to peroxide formation through autoxidation (equimolar quantities were compared). This is in agreement with results obtained for the benzene series (7).

Stuart models show that nucleus resonance stabilization of the enol double bond is possible only for the thiophene ester. It is possible that resonance stabilization of the radical resulting from the enolic double bond (with the peroxide or ketohydroperoxide forms as intermediates)

is responsible for the inhibiting properties shown by this ester. Since thiophene acetaldehyde and 1-[2-thienyl]-2-propanone are efficient initiators, the inhibiting properties cannot be attributed to the thiophene nucleus.

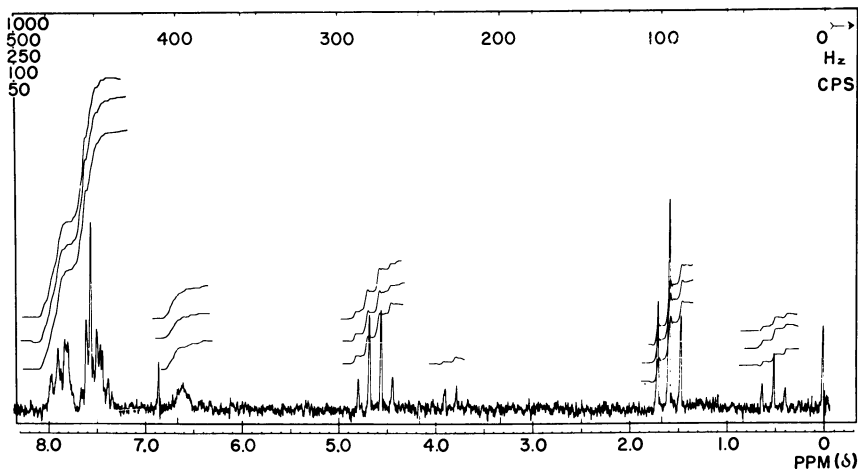
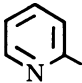



Figure 3. NMR spectrum of  $\alpha$ -cyano- $\alpha$ -naphthyl pyruvic acid ethyl ester in deuterobromoform at 100°C.

Table VI. Initiators of the Ar—CH—CO—Ar Type<sup>a, b</sup>

Initiator	Wt. %	Gel Time, min.	Temperature Maximum, °C. after (min.)	Appearance of Copolymer
Ar = 	3.5	9.6 ± 1	100.5 (16)	red
	3.5	7.2 ± 0.7	103 (8)	colorless

<sup>a</sup> 0.193 Mole/liter polyester at 100°C.

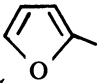
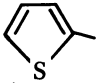

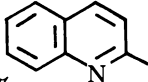
<sup>b</sup> The gel times for  $\alpha$ -furoin and  $\alpha$ -thenoin were not reproducible within the experimental margin of error ( $\pm 10\%$ ) and are hence not included.

<sup>c</sup> Average taken from seven measurements. Mean deviation from the average,  $\pm 8.3\%$ .

Initiators of the Ar—CH—CO—Ar Type. Table VI shows that the

hydroxyketones (0.193 mole/liter polyester at 100°C.) are not particularly efficient initiators. Furthermore the true gel times for  $\alpha$ -furoin and

Table VII. Initiators of the

<i>Initiator Concentration</i> × 10 <sup>-4</sup>	5.85
Initiator	
Ar = 	
wt. %	0.0096
Gel time, min.	57.6 ± 6 <sup>b</sup>
Temperature maximum, °C.	102.5
Hardening time, min.	68
Appearance	colorless
Initiator	
Ar = 	
wt. %	0.011
Gel time, min.	67.2 ± 7
Temperature maximum, °C.	101
Hardening time, min.	73
Appearance	colorless
Initiator	
Ar = 	
wt. %	0.011
Gel time, min.	144 ± 14
Hardening time, min.	—
Appearance	colorless
Initiator	
Ar = 	
wt. %	0.016
Gel time, min.	4.8 ± 0.5
Temperature maximum, °C.	102.5
Hardening time, min.	11
Appearance	brown yellow

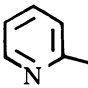
**Ar—CH—CO—Ar Type<sup>a</sup>**

$$\begin{array}{c} | \\ \text{OH} \end{array}$$

29.3	58.5	293	585
0.048	0.096	0.48	0.96
27.6 ± 3	19.2 ± 2	10.8 ± 1	12.0 ± 1.2°
102.9	103	101.8	101.3
36	25	11	14
colorless	colorless	colorless	pale yellow
0.055	0.11	0.55	1.1
22.8 ± 2	14.4 ± 1	9.6 ± 1	15.6 ± 2 <sup>d</sup>
102.5	103.7	102.1	—
31	20	11	—
pale yellow	pale yellow	reddish brown	—
0.055	0.11	0.55	1.1
78 ± 8	38.4 ± 4	15.6 ± 2°	10.8 ± 1
80	48	21	14
colorless	colorless	colorless	colorless
0.080	0.16	0.80	1.6
4.8 ± 0.5	4.8 ± 0.5	4.8 ± 0.5	3.6 ± 0.4
101.1	100.5	100.1	100.1
9	10	14	15
wine red	deep red	black violet	black violet



Table VII.

Initiator Concentration $\times 10^{-4}$	1.11	2.75	5.85
Initiator Ar = 			
mg; wt. %	0.4; 0.002	1; 0.005	2.14; 0.011
Gel time, min.	$26 \pm 3$	$3.6 \pm 0.4$	$3.6 \pm 0.4^f$
Temperature maximum, °C.	—	—	101.4
Hardening time, min.	—	—	16
Appearance	pale yellow	pale yellow	pale yellow

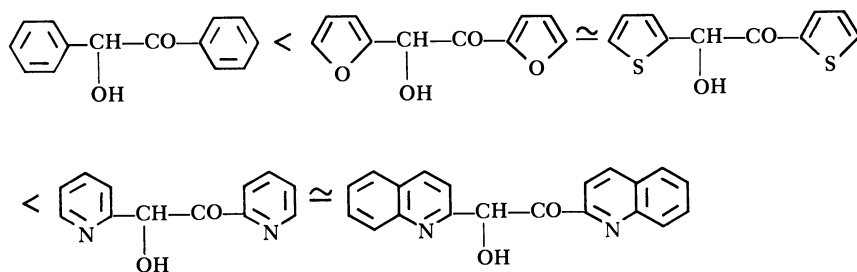
<sup>a</sup> Gel time =  $f$ . Initiator concentration is in moles/liter at 100°C.

<sup>b</sup> Measurement repeated: 62.3 minutes—*i.e.*, inside experimental error margin.

<sup>c</sup> Five measurements gave a mean deviation from the average of 8.7%.

<sup>d</sup> Gel time for this concentration was not reproducible within the error margin of  $\pm 10\%$ . However, since all values obtained were higher than for the next lower con-

$\alpha$ -thenoin could not be measured. Table VII gives a better picture of the catalytic properties of these compounds (gel time =  $f(c)$  at 100°C.). Comparing the gel times for initiator concentrations between  $5.85 \times 10^{-4}$  and  $293 \times 10^{-4}$  moles/liter polyester gives, in the order of catalytic efficiency:



The reaction curves for this group are characterized by extremely low temperature maxima (maximum value at 100°C.; 103°C.). For  $\alpha$ -pyridoin the gel time is not indirectly proportional to the amount of initiator used as would be expected. At first, the gel time is independent of the initiator concentration ( $5.85 \times 10^{-4}$  to  $293 \times 10^{-4}$  mole/liter polyester) and then rises with the next higher concentration to give a 50% higher value, whereby all values obtained were reproducible (*see* Tables VI and VII). The same effect is shown in Table VIII in which gel time is plotted as a

## Continued

29.3	58.5	293	585
11.7; 0.055	21.4; 0.11	117; 0.55	214; 1.1
3.6 ± 0.4 <sup>e</sup>	3.6 ± 0.4 <sup>e</sup>	3.6 ± 0.4 <sup>e</sup>	3.6 ± 0.4 <sup>e</sup>
101	101	101.5	101.8
11	10	12	14
pale yellow	orange yellow	orange	red orange

centration, the real value must also be higher, and we have given the lowest value obtained.

<sup>e</sup> Measurement repeated: 15.6 minutes—*i.e.*, inside experimental error margin.

<sup>f</sup> Measurement repeated seven times: same value.

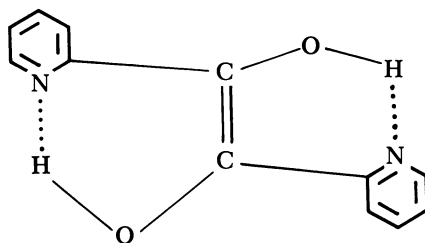
<sup>g</sup> Measurement repeated three times: same value.

function of temperature for two initiator concentrations  $5.85 \times 10^{-4}$  and  $585 \times 10^{-4}$  moles/liter polyester. At 80°, 100°, and 120°C., the gel times were the same for both concentrations; at 60° and 40°C., however, shorter gel times (outside the margin of error) were obtained with the lower concentration of initiator.

Since the gel time increases again when less than a minimum quantity of initiator is used (*see* Table VII), we find a concave parabolic function with plateau-like minimum (or a concave saddle curve) for the gel time =  $f(c)$  function.

It is possible that for  $\alpha$ -pyridoin a minimum quantity is enough to start a copolymerization, a sizable excess causing retardation through recombination with the initiator radical. To determine this minimum quantity of initiator, the concentration was lowered to  $2.75 \times 10^{-4}$  mole/liter polyester (1 mg. per 20 grams polyester-styrene solution = 0.005 wt. %); the same gel time of 3.6 minutes was obtained (Table VII). The gel time rose, however, to 26 minutes when the concentration was lowered to  $1.11 \times 10^{-4}$  mole/liter polyester, 0.4 mg. or 0.002 wt. %. The temperature maxima for all concentrations of this compound at 100°C. did not exceed 102°C.

$\alpha$ -Pyridoin differs from the other hydroxyketones of this type in that in crystalline form in neutral and in weakly acidic solution it is a pure ene-diol, stabilized by intramolecular hydrogen bonding.



N—H chelation is not possible for  $\beta$ - and  $\gamma$ -pyridoin owing to steric hindrance, and hence these compounds have not been isolated (17).

Benzoin,  $\alpha$ -furoin, and most probably  $\alpha$ -thenoin, however, are oxyketones in the solid state and in carbon tetrachloride. This has been

Table VIII.  $\alpha$ -Pyridoin<sup>a</sup>

Temperature, °C.	40	60	80	100	120
$585 \times 10^{-4}$ moles/liter; 214 mg.					
1.1 wt. %					
Gel time, min.	$21.6 \pm 2$	$9.6 \pm 1$	$4.8 \pm 0.5$	$3.6 \pm 0.4$	$2.4 \pm 0.2$
Temperature maximum, °C.	40.8	61.5	82.2	101.8	122
Hardening time, min.	24	12	10	14	20
Appearance	pale yellow	yellow	orange	orange red	red
$5.85 \times 10^{-4}$ moles/liter; 2.14 mg.					
0.011 wt. %					
Gel time, min.	$15.6 \pm 2$	$7.2 \pm 0.7$	$4.8 \pm 0.5$	$3.6 \pm 0.4$	$2.4 \pm 0.2$
Temperature maximum, °C.	41.1	64.6	82.7	101.4	122.5
Hardening time, min.	17	16	9	16	14
Appearance	pale yellow	pale yellow	pale yellow	pale yellow	yellow

<sup>a</sup> Gel time =  $f$  (temperature). Initiator concentrations  $5.85 \times 10^{-4}$  and  $585. \times 10^{-4}$  moles/liter polyester.

proved chemically by Cramer and Krum (1) and physically by Luettker and Marsen (13).

The above shows why  $\alpha$ -pyridoin is more active than benzoin, furoin, and thenoin.  $\alpha$ -Chinaldoin which has the same chelation possibilities as  $\alpha$ -pyridoin and whose infrared spectrum is practically identical gives the same gel times. The second benzene nucleus does not raise the catalytic efficiency.

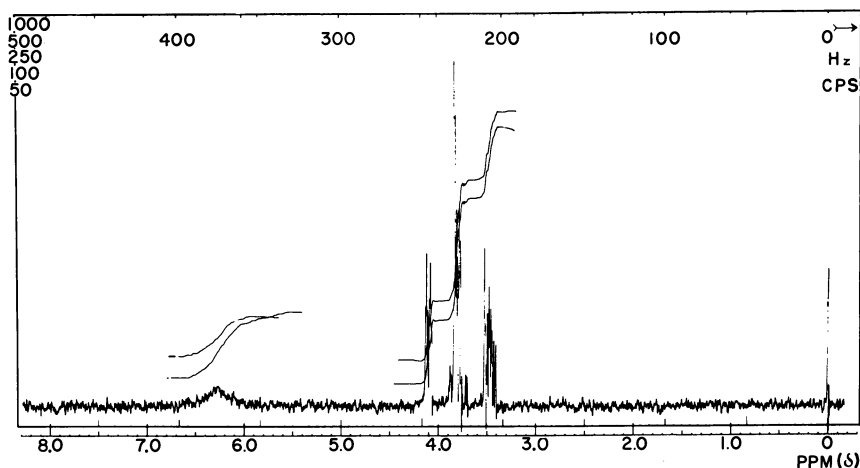


Figure 4. NMR spectrum of  $\alpha$ -pyridoin in deuteriochloroform at room temperature

$\alpha$ -Furoin and  $\alpha$ -thenoin are better initiators than benzoin. A possible explanation is that owing to steric hindrance the enolic double bond of the latter cannot be resonance stabilized by the nucleus (Stuart models).

The  $\alpha$ -pyridoin ene-diol structure cannot be completely planar (13). This indicates that the initiating radical derived from the ene-diol or rather from the ketohydroperoxide form of this compound cannot be so strongly resonance stabilized as to cause inhibition as was postulated for 1[2-pyridyl]2-propanone.

The effect of high temperatures on  $\alpha$ -pyridoin was studied using NMR (Figures 4, 5, and 6). The spectrum in deuteriochloroform at room temperature (Figure 4) shows the ABCD spectrum of an  $\alpha$ -substituted pyridine compound between 6.6 and 8.2 p.p.m. and no methine proton singlet (to be expected at approximately 5.2 p.p.m. according to the modified Shooley rule). A signal for the two chelated hydroxyl protons at 12.6 p.p.m. is shifted to higher field by the addition of TFE (Figure 5) as apparently the N—H chelation signal appears at lower field strength

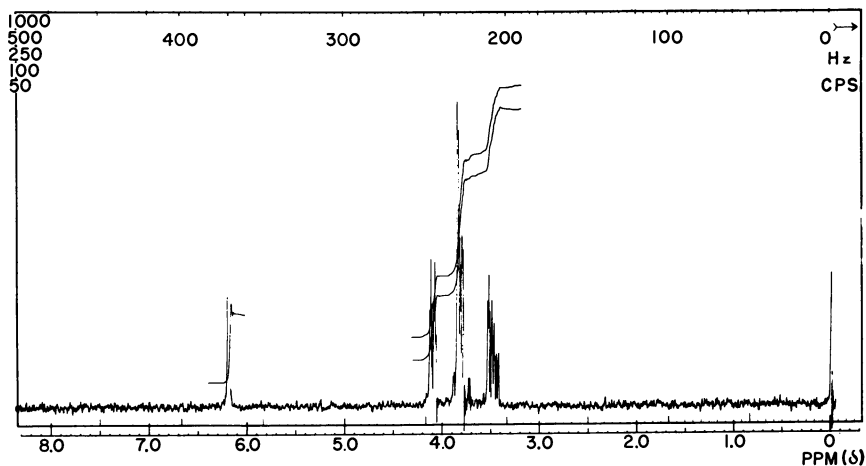


Figure 5. NMR spectrum of  $\alpha$ -pyridoin in deuteriochloroform with TFE

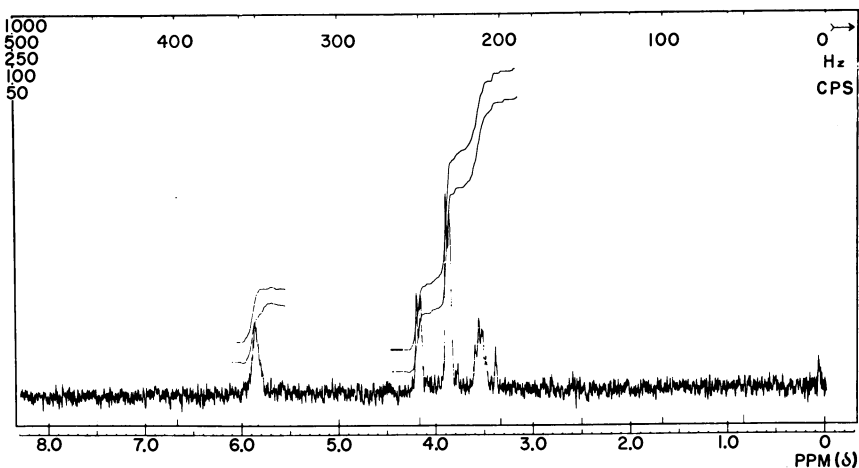


Figure 6. NMR spectrum of  $\alpha$ -pyridoin in deuterobromofrom at 100°C.

than the TFE signal itself. The spectrum in deuterobromofrom at 100°C. (Figure 6) shows an N—H chelation signal shift to higher field, indicating that chelation is somewhat weakened at this high temperature (15); otherwise the spectra taken at room temperature and 100°C. are identical. Therefore,  $\alpha$ -pyridoin remains a pure ene-diol at 100°C. in bromoform, a polar solvent. Owing to chelation the ene-diol form can also be expected at high temperature in styrene, a nonpolar solvent.

**Acknowledgment**

The authors thank C. Bernasconi for his help in interpreting the NMR spectra.

**Literature Cited**

- (1) Cramer, F., Krum, W., *Ber.* **86**, 1586 (1953).
- (2) Cross, A., "Practical Infrared Spectroscopy," pp. 37, 64, Butterworth, London, 1960.
- (3) Dailey, B., Shoolery, J., *J. Am. Chem. Soc.* **77**, 3977 (1955).
- (4) Fuson, R., Jackson, H., *J. Am. Chem. Soc.* **72**, 1637 (1950).
- (5) Fuson, R., Maynert, E., Shenk, W., *J. Am. Chem. Soc.* **67**, 1939 (1945).
- (6) Fuson, R., McKusick, B., Spangler, F., *J. Am. Chem. Soc.* **67**, 597 (1945).
- (7) Hopff, H., Kleiner, E. K., *Chimia* **19**, 99 (1964).
- (8) Houben-Weyl, "Methoden der Organischen Chemie," Band VIII/III p. 66, Verlag Thieme, Stuttgart, 1952.
- (9) Kleiner, E. K., Dissertation ETH, Prom. Nr. 3071, Zürich, 1961.
- (10) Kohler, E., *Am. Chem. J.* **36**, 177, 529 (1906).
- (11) *Ibid.*, **37**, 369 (1907).
- (12) Kohler, E., Thompson, R., *J. Am. Chem. Soc.* **59**, 887 (1937).
- (13) Lüttke, W., Marsen, H., *Z. Elektrochem.* **57**, 680 (1953).
- (14) Meyer, K. H., *Ber.* **45**, 2843 (1912).
- (15) Pimentel, G., McClellan, A., "The Hydrogen Bond," p. 146, Freeman and Co., San Francisco and London, 1960.
- (16) Rigaudy, J., *C. r. Heb. Séances. Acad. Sci.* **226**, 1993 (1948).
- (17) "Ullmanns Encyclopädie der Technischen Chemie," 3. Aufl., p. 475, 1963.
- (18) Walling, C., "Free Radicals in Solution," p. 503, Wiley, London, 1957.

RECEIVED November 18, 1968.

## Terpolymerization Parameters

A. RAVVE and J. T. KHAMIS

Corporate R & D, Continental Can Co., Chicago, Ill.

*In the terpolymerization of styrene, 2-ethylhexyl acrylate, and glycidyl acrylate a continuous-addition type of technique was used, and attempts were made to achieve maximum conversions. Relationships were sought between molecular weights, molecular weight distributions, reaction temperature, initiator concentration, half-life of the initiator, and rate of monomer-initiator addition. The molecular weights of the products depended strongly upon reaction temperature and on the rate of initiator decomposition. Narrower molecular weight distributions resulted from the use of initiators with shorter half-lives.*

The theory of free-radical addition polymerization, described in numerous publications (2, 3, 4, 17, 21), makes it clear that radical chain-growth reactions of polymers are regulated by statistical laws. Because of their statistical character the products from these reactions must be heterodisperse. The ranges extend from a single unit upward, depending upon kinetic details of the reactions.

With changes occurring in concentrations of the reacting species during the reaction, the probability that the radical will propagate also changes progressively. This results in wider average molecular weight distributions than the most probable ones. As a result, molecular weight distributions occurring in vinyl polymers follow complicated patterns and force annoying qualifications upon all attempts at generalizations.

It was shown that in multichain polymers the molecular weight distribution,  $\bar{X}_w/\bar{X}_n$ , is equal to 2 when chain transfer is taking place. When, however, chain transfer is absent,  $\bar{X}_w/\bar{X}_n = 1.5$ . In actual practice, typical  $\bar{X}_w/\bar{X}_n$  values for vinyl polymers prepared to high conversion seldom exceed 5. Special cases like autoacceleration are exceptions where values as high as  $\bar{X}_w/\bar{X}_n = 10$  were reported (5).

The ratio of monomer to catalyst must be maintained constant or as close to constant as possible during the reaction to obtain polymer chains

of uniform length. In practice, the initiator tends to be depleted at a rate different from the monomer. To minimize this phenomenon, multiple charges of initiator and/or monomer are often conducted when polymerizations are carried to high conversions. Hoffman and co-workers (11) demonstrated how polymers may be obtained which have narrower distributions by feeding initiators or monomers to batch polymerizations at rates determined from basic equations. Further (18, 19), monomer and initiator can be added simultaneously at such rates that steady-state conditions might tend to predominate, leading to somewhat narrower distributions.

### ***Scope of This Work***

This is a study of solution polymerization of styrene, 2-ethylhexyl acrylate, and glycidyl acrylate. Such a terpolymer is typical of components in commercial thermosetting systems (20). As such, in commercial batch preparations, high conversions are desirable, and control is needed over molecular weights of the products. In addition, narrow molecular weight distribution often offers many rheological advantages (10). Information was sought, therefore, on the extent of reproducibility and on the degree of variation occurring in both molecular weight and its distribution.

The terpolymerizations described were carried out by a continuous feed method, unless stated otherwise, where both the monomer mixture and the initiator were added together continuously to the reaction kettle (18). The variables studied were (1) effects of initiators with different half-lives, (2) effects of variations in temperature, and (3) effects of variations in concentrations of initiators. Attempts were also made to study the extent of heterogeneity in the products.

Most polymerization reactions were carried out on two commercial mixtures of monomers without any prior purification or removal of inhibitors. The products were compared with polymers from reactions with purified monomers and against other batches of commercial monomers to test reproducibility. Commercial monomers were used to approximate industrial conditions, where economic considerations may often make purification steps undesirable.

### ***Experimental***

The monomers used were (1) styrene, rubber grade, Dow Chemical Co., 99.2% of pure styrene with 12 p.p.m. of *p-tert*-butylcatechol inhibitor; (2) 2-ethylhexyl acrylate (Celanese Corp.) 99.0% purity by weight with 50 p.p.m. of monomethyl ether of hydroquinone; (3) glycidyl acrylate (Dow Chemical Co.) 90% purity with 0.1% monomethyl ether of hydro-



quinone. Most of the impurity in this monomer was epichlorohydrin. Mixture A contained by weight 50% styrene, 35% 2-ethylhexyl acrylate, and 15% glycidyl acrylate with a total of 174 p.p.m. of inhibitors. Mixture B contained by weight 68.5% styrene, 20% 2-ethylhexyl acrylate, and 11.5% glycidyl acrylate, with a total of 133 p.p.m. of inhibitors. Monomers used for kinetic studies were purified by fractional vacuum distillation.

**Polymerization.** All liter-size batches were carried out in three-necked, round-bottomed flasks equipped with mechanical stirrers, reflux condensers, dropping funnels, nitrogen atmosphere, a thermowell for a thermocouple, and a heating mantle connected to an electronic temperature controller (temperatures were controlled within  $\pm 1^\circ\text{C}$ .). A 133-gram portion of the solvent was placed into the flask, the temperature raised to the desired level, and 400 grams of monomer mixture containing the initiator were added dropwise over the desired time.

Larger batches were prepared in an identical manner except that pilot plant stainless steel kettles were utilized, with temperature control of  $\pm 2^\circ\text{C}$ . However, when a 150-gallon kettle was used, control of only  $\pm 4^\circ\text{C}$ . was achieved.

The extent of conversion was obtained by determining the total polymer present and by vapor phase chromatography (VPC) of the solution.

**Molecular Weight Determinations.** The polymers obtained were subjected to gel permeation chromatography (15) using three, 4-foot gelled polystyrene columns (Waters Associates), pore sizes  $10^5$ ,  $10^4$ ,  $10^3$  A., with tetrahydrofuran as the solvent. The weight and number average molecular weights were then calculated with the aid of a General Electric basic language digital computer. The average weight per angstrom of 53.5 was obtained from calculations using molecular models.

Light scattering measurements were carried out on a Brice-Phoenix photometer in three solvents—tetrahydrofuran, toluene, and methyl isobutyl ketone. The values of  $H_c/\tau$  and  $\sin^2 \theta/2 + 10c$  were calculated, where  $c$  is concentration, with the aid of a computer.

Number average molecular weights were determined in toluene using a Mechrolab high speed membrane osmometer with Schleicher and Schuell, type U.O. very dense cellophane membranes. Previous work has established that under these conditions diffusion of this type of polymer through the membrane is not detectable at molecular weights down to about 6000 (18).

Viscosities of the terpolymers were measured in toluene at  $20^\circ\text{C}$ . in an Oswald-Fenske viscometer. Analyses for oxirane oxygen were carried out by titrating with HBr in acetic acid (19).

**Polymer Fractionations.** The first type was conducted by separating a whole polymer into different molecular sizes using gel permeation chromatography (GPC). The effluent was passed into a fraction collector which collected 5-cc. portions.

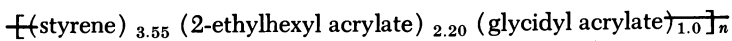
The second fractionation was carried out by selective precipitations. A whole polymer was dissolved in acetone, and methanol was added until a haze developed. The solution was cooled overnight at  $-20^\circ\text{C}$ .

A precipitate separated, yielding Fraction 1. This procedure was repeated several times until a haze would no longer develop from successive alcohol additions. The resulting liquid was evaporated on a rotary evaporator to yield the last fraction (Fraction 4).

### Results and Discussion

Reactivity ratios for the three-component system used in this investigation were reported by Khamis (13): styrene,  $r_{12} = 0.91$ ,  $r_{13} = 0.73$ ; 2-ethylhexyl acrylate,  $r_{21} = 0.29$ ,  $r_{23} = 0.98$ ; glycidyl acrylate,  $r_{31} = 0.25$ ,  $r_{32} = 1.08$ .

From the Alfrey-Goldfinger equation (1), the composition of the product from monomer mixture A should be:



Analysis of the products obtained by continuous feed type polymerization at 138°C. with 3% dicumyl peroxide was:

After 0.5 hours:

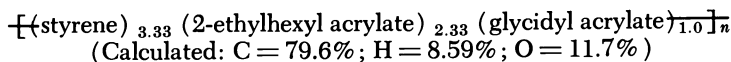


and upon completion of the addition (1.5 hours):



Here styrene entered the chains faster at the outset of the reaction, but as it progressed, chains with amounts of glycidyl acrylate greater than theoretical formed. When monomer-initiator addition was complete and heating and stirring maintained for an additional 1.5 hours (holding period), the polymer composition, found by combustion analysis, was: C = 79.75%; H = 9.1%; O = 11.24%.

This corresponds to a terpolymer composition of:



Upon completion of the addition of the monomers-initiator mixture, at the end of the 90-minute period, some unreacted monomers were still present in the reaction vessel. When heating and stirring were continued for an additional 90 minutes, all the monomer was polymerized. Thus, to achieve maximum conversion, a holding period appears necessary. During such a holding period more chain transferring can be expected, with the result that the products will have broader molecular weight distributions.

Nevertheless, if the greatest conversion can be achieved during the feed period, then final products may not be drastically affected. This appears true at least with the monomers and conditions used in these experiments as shown in Table I.

**Table I. Effect of Holding Time during Terpolymerization<sup>a</sup>**

Time Past Addition, hrs.	Molecular Weight by GPC		
	$\bar{M}_w$	$\bar{M}_n$	$\bar{M}_w/\bar{M}_n$
0	38,200	16,800	2.3
1.0	41,500	16,200	2.6
1.5	40,000	16,400	2.5

<sup>a</sup> At 138°C., 3% dicumyl peroxide, monomer mixture B, and xylene solvent.

Table II shows molecular weight distributions of products from monomer mixtures A and B using 3% dicumyl peroxide as initiator. The molecular weight distributions of the products from the six polymerizations are 3 or less. When, however, the percent of dicumyl peroxide was decreased in the reaction mixture, considerably wider molecular weight distributions resulted (Table III). With less initiator, the chains grow longer and terminate more often by chain transfer.

**Table II. Polymerization with 3% Dicumyl Peroxide Initiator<sup>a</sup>**

Polymer	Batch Size	Monomer Mixture	Molecular Weight by GPC		
			$\bar{M}_w$	$\bar{M}_n$	$\bar{M}_w/\bar{M}_n$
I	1 liter	A	62,700	20,800	3.0
II	10 gal.		60,900	23,100	2.6
III	10 gal.		70,800	29,800	2.4
VII	150 gal.		77,000	30,000	2.6
IV	10 gal.	B	43,100	16,000	2.7
V	10 gal.		39,700	14,800	2.7
VI	10 gal.		40,800	16,600	2.5

<sup>a</sup> At 138°C., addition time, 1.5 hours; hold time, 1.5 hours; conversion, essentially 100%.

Table IV shows the effect of initiator concentration when *tert*-butyl peroxide, an initiator with a longer half-life is used. Increasing the amount of this initiator from 1 to 3% by weight has resulted in a decrease in both the molecular weight and in the molecular weight distribution. However, the molecular weight distributions were still quite wide. Further, when purified monomers were used, the product had a lower molecular weight and a narrower molecular weight distribution. Thus, an appreciable number of initiating radicals appear to be lost to inhibitors in such commercial reaction mixtures.

The amount of thermal initiation which takes place at 138°C. and its effect on molecular weights and their distributions were also studied. Two batches were polymerized thermally using monomer mixture A.

**Table III. Effect of Initiator Concentration Using Dicumyl Peroxide<sup>a</sup>**

Polymer	Initiator, %	Molecular Weight by GPC		
		$\overline{M}_w$	$\overline{M}_n$	$\overline{M}_w/\overline{M}_n$
VIII	1	148,300	33,100	4.5
IX	2	84,200	21,700	3.9
X	3	62,700	20,800	3.0
XI <sup>b</sup>	2	102,400	27,562	4.1
Pure monomers	2	—	23,800	—
			(by osmotic pressure)	

<sup>a</sup> Monomer mixture A, 138°C., 1-liter size; conversion, essentially 100%.

<sup>b</sup> This batch was not prepared by continuous feed method. Instead, a 50% solution of all reactants in xylene was placed into the flask, and the reaction mixture was heated to 138°C. and stirred under N<sub>2</sub> till full conversion was achieved.

**Table IV. Effect of Initiator Concentration Using Di-*tert*-butyl Peroxide<sup>a</sup>**

Polymer	Initiator, %	Molecular Weight by GPC		
		$\overline{M}_w$	$\overline{M}_n$	$\overline{M}_w/\overline{M}_n$
XII	1	568,000	63,900	8.9
Avg. for 4 batches as shown in Table VII	2	228,000	35,600	6.4
XIII	3	124,300	23,900	5.2
Purified monomers	2	144,193	25,000	5.8

<sup>a</sup> At 138°C., addition time, 1.3 hrs.; hold time, 1.5 hrs.; size, 1 liter; conversion, essentially 100%, monomer mixture A.

**Table V. Effect of Temperature on Molecular Weight and on Its Distribution<sup>a</sup>**

Polymer	Reaction Temp., °C.	Molecular Weight by GPC		
		$\overline{M}_w$	$\overline{M}_n$	$\overline{M}_w/\overline{M}_n$
XVI	130	572,500	59,700	9.6
Avg. for 4 batches as shown in Table VII	138	228,000	35,600	6.4
XXVIII <sup>b</sup>	150	73,600	17,700	4.2

<sup>a</sup> 2% Di-*tert*-butyl peroxide, monomer mixture A, batch size, 1 liter; conversion, essentially 100%.

<sup>b</sup>  $\overline{M}_n$  by osmotic pressure = 18,500.

Table VI. Effect of  
*Molecular*

<i>Polymer</i>	<i>Monomer Mixture</i>	<i>Initiator, %</i>	$\bar{M}_w$
X	A	DCP, 3	62,700
XIII	A	DTBP, 3	124,300
XVII	A	BzP, 3	36,800
XVIII	B	BPIC, 3	38,600
XIX <sup>b</sup>	A	AZBN, 2	33,100

<sup>a</sup> Addition time, 1.5 hrs.; hold time, 1.5 hrs.; size of batch, 1 liter.

<sup>c</sup> Legend: DCP, dicumyl peroxide. DTBP, di-*tert*-butyl peroxide. BzP, benzoyl peroxide. BPIC, butyl peroxy isopropyl carbonate. AZBN, azobisisobutyronitrile.

Table VII. Reproducibility of Polymerizations<sup>a</sup>  
*Molecular Weight by GPC*

<i>Polymer</i>	$\bar{M}_w$	$\bar{M}_n$	$\bar{M}_w/\bar{M}_n$
XX	229,200	43,000	5.3
XXI <sup>b</sup>	236,400	30,200	7.8
XXII	226,600	38,500	5.9
XXIII	219,800	31,000	7.1
Average	228,000	35,600	6.4

<sup>a</sup> Monomer mixture A, 2% *tert*-butyl peroxide, 138°C., in xylene. Batch size, 1 liter; conversion, essentially quantitative.

<sup>b</sup>  $\bar{M}_n$  by osmotic pressure = 30,400.

One reaction was not carried out by continuous addition but as a 50% solution in xylene at 138°C. for eight hours.  $\bar{M}_w$  was found by GPC to be 301,000 and  $\bar{M}_n$  to be 113,700 with  $\bar{M}_w/\bar{M}_n = 2.6$ . The second reaction was carried out by continuous addition. Here the conversion was somewhat lower (8–10%). The  $\bar{M}_w$  was found to be 318,600, and  $\bar{M}_n$  was 115,400.  $\bar{M}_w/\bar{M}_n = 2.8$ . Thus, it appears that only small amounts of thermal polymerizations occur at this temperature and that their contributions to the product are relatively small. Table V illustrates the effect of variation in temperature and Table VI the effect of using initiators of different half-lives. The results of these effects are predictable.

The reproducibility of these polymerizations was studied by preparing four batches under identical conditions. The results are presented in Table VII. The average of the molecular weights for these four batches was then used to compare with other batches where effects of variations

**Different Initiators<sup>a</sup>***Weight by GPC*

$\bar{M}_n$	$\bar{M}_w/\bar{M}_n$	Solvent	Reaction Temp., °C.	Half-Life of Init. Reaction Temp., hours
20,800	3.0	Xylene	138	0.7
23,900	5.2	Xylene	138	3.0
16,700	2.2	Toluene	110	0.12
15,400	2.5	Xylene	138	0.1
15,700	2.2	Benzene	80	0.9

<sup>b</sup> After 8 hours the conversion was still only 63%. Reaction was not carried out by the continuous feed method but instead in a 50% benzene solution.

in batch sizes were studied. Results are presented in Table VIII. The high ratios of  $\bar{M}_w/\bar{M}_n$  for the polymers listed are probably caused by autoacceleration.

When both monomer and initiator are added simultaneously, the rate of monomer and initiator addition to the reaction doesn't appear to be very critical. This was shown in a study of homopolymerization of styrene (19) and appears to be true in this terpolymerization (Table IX). Variations in  $\bar{M}_w/\bar{M}_n$  appear small. However, there is a decrease in  $\bar{M}_w$

**Table VIII. Effect of Batch Sizes<sup>a</sup>**

Polymer	Batch Size	Molecular Weight by GPC		
		$\bar{M}_w$	$\bar{M}_n$	$\bar{M}_w/\bar{M}_n$
Avg. for 4 batches shown in Table VII	1 liter	228,000	35,600	6.4
XXV	10 gal.	243,000	38,000	6.4

<sup>a</sup> 2% Di-*tert*-butyl peroxide, monomer mixture A, 138°C., in xylene.

**Table IX. Effects of Monomer-Initiator Addition Rate<sup>a</sup>**

Polymer	Addition Time, hrs.	Molecular Weight by GPC		
		$\bar{M}_w$	$\bar{M}_n$	$\bar{M}_w/\bar{M}_n$
XXII	1½	226,800	38,500	5.9
XXVI <sup>b</sup>	2	187,100	31,400	6.0
XXVII	3	165,900	26,800	6.2

<sup>a</sup> Monomer mixture A, 2% DTBP, 138°C., in xylene; holding time, 1½ hrs.; conversion, essentially 100%.

<sup>b</sup>  $\bar{M}_n$  by osmotic pressure = 27,000.

with an increase in addition time. This may be caused by lower concentration of monomers in the solvent during the early stages of the reactions.

Polymer XVI (Table V) was fractionated into four portions by fractional precipitation. The molecular weights of each fraction were then determined by GPC. The intrinsic viscosity of each fraction was obtained and used to calculate  $K$  and  $a$  values of the Mark-Houwink equation (12, 16) using  $\bar{M}_w$  determined by GPC. This is presented in Table X.

Table X. Fractionation of Polymer XVI<sup>a</sup>

	$[\eta]$	$\bar{M}_w$ by GPC	$\bar{M}_v$
Whole Polymer	—	572,500	—
Fraction 1	1.525	802,300	858,769
Fraction 2	0.3650	161,400	140,700
Fraction 3	0.1315	37,941	38,673
Fraction 4	0.0530	13,746	12,838

<sup>a</sup> From these data,  $K = 3.1097 \times 10^{-5}$ ;  $a = 0.79047$ ;  $[\eta] = 3.1097 \times 10^{-5} \bar{M}_v^{0.79047}$ .

Infrared data on all fractions of Polymer XX (Table X) collected by both methods of fractionation revealed no discernible differences by comparison of any two fractions.

However, to test polymer heterogeneity, which we believe must exist, light scattering data were obtained on this polymer in three different solvents: toluene, tetrahydrofuran, and methyl isobutyl ketone.

Bushuk and Benoit (7) demonstrated that inordinately high molecular weights (apparent) will result from light scattering data for copolymers owing to fluctuations in their chain compositions. Thus, a comparison of  $\bar{M}_w$  obtained with light scattering in solvents of different polarities should be a significant aid in establishing heterogeneity. The weight average molecular weights were found to be: in tetrahydrofuran, 338,000; in toluene, 234,500; and in methyl isobutyl ketone, 345,000. This information coupled with results of chemical analysis indicates that the terpolymer is heterogeneous.

Analysis of data obtained from reactions with mixtures of purified monomers (18) permitted calculations of  $K_p^2/K_t$  and kinetic chain lengths for these terpolymerization reactions using the following two relationships (6, 9):

$$K_p^2/K_t = 2 R_p^2/K_p^2/K_t = 2 R_p^2/[M]^2 [I] f k_d$$

and

$$\nu = K_p [M] / 2 (K_t f k_d [I])^{1/2}$$

where  $R_p$  is the rate of polymerization,  $M$  is the monomer concentration,  $I$  is the initiator concentration,  $f$  is the initiator efficiency, and  $\nu$  is the

kinetic chain length. The information on the kinetic chain length then in turn permitted estimation of  $M_n$  by using an average for the weight of the units in the terpolymer. Thus, the terpolymer formed from monomer mixture A will have an average unit weight of 134. For polymerization at 138°C., using 2% *tert*-butyl peroxide, values were calculated which are shown in Table XI. Initiator efficiency,  $f$ , for diluted systems (9), was assumed to be 0.5.

**Table XI. Calculated Values of  $K_p^2/K_t$ , Kinetic Chain Length, and Molecular Weights**

Time, sec.	$R_p$ , moles/liter $\times 10^{-4}$	$K_p^2/K_t$	$\nu$	$\bar{M}_n^a$
600	3.55	0.2346	182	24,800
1200	7.01	0.2894	232	31,600
1800	8.39	0.3071	230	31,400
3600	8.75	0.3732	205	28,000
5400	7.54	0.4038	184	25,000

<sup>a</sup> Average  $\bar{M}_n$  calculated from the kinetic chain length = 28,200.

The average value of  $\bar{M}_n$  shown above, compared with the measured values (18) of 27,500, suggests that much of the termination is by transfer. The measured  $\bar{M}_n$  values for terpolymers formed under the same conditions but with commercial monomer mixtures averaged  $\bar{M}_n = 37,400$  (Table VIII). Such higher molecular weights are probably results of initiator loss to inhibitors.

The results evolved from the data obtained on polymerizations initiated by 2% dicumyl peroxide are shown in Table XII.

**Table XII. Calculated Values of  $K_p^2/K_t$ , Kinetic Chain Length, and Molecular Weights**

Time, sec.	$K_p^2/K_t$ , moles/liter $\times 10^{-1}$	$\nu$	$\bar{M}_n^a$
600	1.21	95.2	12,700
1200	1.51	126	16,900
1800	1.64	130	17,400
3600	2.08	138	18,500
5400	2.26	118	15,800

<sup>a</sup> Average  $M_n$  calculated from kinetic chain length = 16,300.

The above values are also based on an assumed initiator efficiency of 0.5 owing to the presence of solvent (9). Comparison of the calculated  $\bar{M}_n$  with the measured value (18) ( $\bar{M}_n = 23,830$ ) indicates that a considerable amount of termination occurred by combination.



### Conclusions

The general conclusions which can be drawn from the data presented are:

(1) The molecular weights of the products depend strongly on temperature; hence, good control is essential.

(2) Choice of initiators must include considerations of reaction conditions, initiator efficiency, and rate of initiator decomposition.

(3) Narrower molecular weight distributions resulted from use of initiators with shorter half-lives.

### Literature Cited

- (1) Alfrey, T., Jr., Goldfinger, G., *J. Chem. Phys.* **12**, 322 (1944).
- (2) Bamford, C. H., Barb, W. G., Jenkins, A. D., Onyon, P. F., "The Kinetics of Vinyl Polymerization by Radical Mechanisms," Academic Press, New York, 1958.
- (3) Bevington, J. C., "Radical Polymerization," Academic Press, New York, 1961.
- (4) Billmeyer, Jr., F. W., "Textbook of Polymer Science," Interscience, New York, 1962.
- (5) Billmeyer, Jr., F. W., Stockmayer, W. H., *J. Polymer Sci.* **5**, 121 (1950).
- (6) Burnett, G. M., "Mechanisms of Polymer Reactions," Interscience, New York, 1954.
- (7) Bushuk, W., Benoit, H., *Can. J. Chem.* **36**, 1616 (1958).
- (8) Durbetaki, A. J., *Anal. Chem.* **28**, 2000 (1956).
- (9) Flory, P. J., "Principles of Polymer Chemistry," Cornell University Press, Ithaca, N. Y., 1953.
- (10) Hanle, J. E., Merz, E. H., Mesrobian, R. B., *J. Polymer Sci. C-12*, 185 (1966).
- (11) Hoffman, R. F., Schreiber, S., Rosen, G., *Ind. Eng. Chem.* **56** (5), 51 (1964).
- (12) Houwink, R., *J. Prakt. Chem.* **157**, 15 (1940).
- (13) Huque, M. M., Jaworzyn, J., Goring, D. A. I., *J. Polymer Sci.* **39**, 9 (1959).
- (14) Khamis, J. T., *Polymer* **6**, 98 (1965).
- (15) Maley, L. E., *J. Polymer Sci. C-8*, 253 (1965).
- (16) Mark, H., *Z. Elektrochem.* **40**, 413 (1934).
- (17) Ravve, A., "Organic Chemistry of Macromolecules," M. Dekker, Inc., New York, 1967.
- (18) Ravve, A., Khamis, J. T., Mallavarapu, L. X., *J. Polymer Sci. A-3*, 1775 (1965).
- (19) Ravve, A., Khamis, J. T., *J. Macromol. Sci. A1* (8), 1423 (1967).
- (20) Ravve, A., Khamis, J. T., U. S. Patent **3,306,883** (Feb. 28, 1967); **3,323,946** (June 6, 1967).
- (21) Tanford, C., "Physical Chemistry of Macromolecules," Wiley, New York, 1961.

RECEIVED October 2, 1967.

# Polymerization of Methyl Methacrylate and Other Vinyl Monomers Activated by Low Concentrations of SO<sub>2</sub>

PREMAMOY GHOSH and FRED W. BILLMEYER, JR.

Rensselaer Polytechnic Institute, Troy, N. Y. 12181

*Low concentrations of SO<sub>2</sub> and TBHP were used to initiate the polymerization of MMA and other vinyl monomers. DPPH and hydroquinone do not inhibit this MMA polymerization. End-group analysis indicates the incorporation of sulfonate and hydroxyl end groups in the polymers, and copolymerization results (MMA-isoprene and MMA-acrylic acid) with this SO<sub>2</sub>-TBHP initiator system and AIBN are in good agreement. The over-all polymerization appears to be primarily radical in nature. Inert solvents (benzene, toluene, and xylene) enhance the rate of polymerization of MMA but not of other vinyl monomers (AN, Sty, VA, EMA, MA, etc.). An initiation mechanism involving monomer and solvent appears to be predominant in the case of MMA, while with other monomers an initiation reaction involving only the monomer is predominant.*

**I**t has been observed recently (14, 15) that catalytic concentrations of sulfur dioxide can easily initiate the polymerization of methyl methacrylate, ethyl methacrylate, *n*-butyl methacrylate, and styrene at or near room temperature but fails to initiate polymerization in other monomers such as acrylonitrile, acrylamide, methyl acrylate, ethyl acrylate, vinyl acetate, and vinyl pyridine under similar conditions. However, in the presence of catalytic concentrations of sulfur dioxide and a hydroperoxide, such as *tert*-butyl hydroperoxide, all the above monomers polymerize readily. The results of further investigations on vinyl polymerization in the presence of low concentrations of sulfur dioxide are reported here.

### Experimental

Methyl methacrylate (MMA), ethyl methacrylate (EMA), *n*-butyl methacrylate (*n*-BMA), styrene (Sty), acrylonitrile (AN), vinyl acetate (VA), methyl acrylate (MA), isoprene (IP), and isobutyl vinyl ether (IBVE) were all dried over anhydrous barium oxide and distilled at or below 25°C. (except *n*-BMA, 35°–40°C.) under low nitrogen pressure. Acrylic acid (AA) was dried over anhydrous sodium sulfate and distilled under vacuum before use.

Baker anhydrous sulfur dioxide of 99.98% purity was used without further purification. Sulfur dioxide was passed through the respective monomers, kept at 0–5°C., and the dissolved SO<sub>2</sub> content was determined iodometrically in each case, running a control experiment side by side. *tert*-Butyl hydroperoxide (TBHP), supplied by the Monomer-Polymer Laboratories of the Borden Chemical Co., was used as obtained without further purification.

All solvents used were reagent grade and were distilled once before use in polymerization experiments. The polymerization rate at a specified temperature was followed gravimetrically, using methanol or petroleum ether as the nonsolvent; in some cases (where mentioned) a dilatometric technique was also used. All polymerization experiments were done in clean borosilicate glass tubes, sealed in the usual manner under a vacuum of 10<sup>-2</sup>–10<sup>-3</sup> mm. Hg, following two freezing and thawing cycles.

Intrinsic viscosities were measured in benzene at 30°C. using a Cannon-Ubbelohde viscometer with flow time greater than 200 sec. Results are expressed in deciliters/gram and for poly(methyl methacrylate) (PMMA) were converted to molecular weights by the following equations (4, 12):

$$[\eta] = 7.24 \times 10^{-5} \bar{M}_n^{0.76}$$

$$\text{or } [\eta] = 5.2 \times 10^{-5} \bar{M}_w^{0.76}$$

Gel permeation chromatography (GPC) was carried out with a Waters model 100 gel permeation chromatograph using tetrahydrofuran as the solvent at room temperature. A series of columns of gel porosity 10<sup>6</sup>, 10<sup>5</sup>, 10<sup>4</sup>, and 10<sup>3</sup> Å. (Waters designations) was used, and the system was calibrated with PMMA samples of known molecular weight, each of narrow distribution, following the usual procedures (21). A plot of log (molecular weight) against effluent count for the peak of the curve for each known molecular weight standard was used for calibration. Experimental points for polymers of molecular weight higher than about 6 × 10<sup>5</sup> did not fall on the straight-line calibration curve in the lower molecular weight region. Experimental calibration beyond 9 × 10<sup>5</sup> molecular weight could not be done because of nonavailability of standard polymer fractions. An approximate extrapolated line in the higher molecular weight region was used as the calibration curve for distribution analysis. The column system had a plate count of 1240 plates/ft.

## Results

Preliminary studies (15) of the kinetics of MMA polymerization initiated by TBHP and  $\text{SO}_2$  showed that the rate of polymerization ( $R_p$ ) had a square root dependence on initiator concentration, and the monomer exponent was 1.5 (the monomer variation having been done by adding varying amounts of methanol)—*i.e.*,  $R_p = K [\text{TBHP}]^{0.5} [\text{SO}_2]^{0.5} [\text{M}]^{1.5}$ . On the other hand, if the monomer variation were done by adding benzene, an interesting result occurred: considerably higher rates of polymerization were observed on adding small amounts of benzene, and the rate passed through a maximum with increasing benzene concentration. Similar results were obtained in the presence of toluene, xylene, chlorobenzene, chloroform, tetrahydrofuran, acetone, methyl ethyl ketone, and cyclohexanone. The rate-enhancing effect was more pronounced in the presence of tetrahydrofuran and the ketones.

**Effect of Free Radical Inhibitors.** Polymerization of MMA induced by the TBHP- $\text{SO}_2$  system is not inhibited in the presence of hydroquinone or diphenylpicrylhydrazyl (DPPH). Using 0.0075M TBHP and 0.004M  $\text{SO}_2$ , bulk polymerization of MMA was carried out at 30°C. (a) in the absence and (b) in the presence of 0.0006M DPPH, and the results based on dilatometric studies are given in Figure 1. Polymerization is somewhat retarded in Case b up to about 15 min., and at this point the violet color of the medium is completely destroyed. Polymerization proceeds thereafter at about the same rate as in Case a. The molecular weight of Polymer b is lower than that of Polymer a. On purification by repeated precipitation, Polymer b appears very light brown/yellow in color and exhibits appreciable absorption in the near ultraviolet-visible region (Figure 2) indicating that fragments of DPPH are being incorporated in the polymer during polymerization. The polymerization rate in the presence of hydroquinone is not quite reproducible; no inhibition period is observed, but some retardation is apparent at high hydroquinone concentration. The polymers obtained show absorption in the ultraviolet region (Figure 2), indicating that they are incorporating hydroquinone.

**End Group Analysis.** Using  $^{35}\text{S}$ -labeled sulfur dioxide as the initiator Ghosh and O'Driscoll (15) have shown that under conditions of less than  $2 \times 10^{-2}\text{M}$   $\text{SO}_2$ , little or no sulfur is detected in the PMMA prepared. Quantitative analysis of end groups by dye techniques is rendered uncertain and obscure by the very high molecular weight ( $[\eta] \simeq 5-10$ ) of the  $\text{SO}_2$ -initiated polymers. With the hydroperoxide-sulfur dioxide initiator system, however, the molecular weight of the polymers obtained is fairly low in comparison ( $[\eta] \simeq 0.1-1.5$ ), and the incorporation of sulfonate and hydroxyl end groups in the polymer is possible if the process is of a free radical type (24). By using the dye partition technique to determine

sulfonate (13) and hydroxyl (16) end groups, it is found that PMMA, initiated by the TBHP-SO<sub>2</sub> system (concentration of each initiator component being in the region of 10<sup>-3</sup> to 10<sup>-2</sup>M), has on the average about 1–1.5 end groups (sulfonate and hydroxyl combined) per chain, with the sulfonate end group content varying between 0.5–0.9 per chain. Interestingly, no hydroxyl end group is found in polymers prepared in the presence of DPPH or hydroquinone, and only about 0.8–1.0 sulfonate end group per chain is observed in these cases. Polymers prepared in the presence of high concentrations of SO<sub>2</sub> (>0.8–1M) in the TBHP-SO<sub>2</sub> initiator system give a relatively intense response to the dye test for sulfoxy end groups; the rate of polymerization under this condition is relatively slow, and increased incorporation of sulfur dioxide in the polymer probably takes place by copolymerization of free sulfur dioxide or a sulfur dioxide–monomer complex.

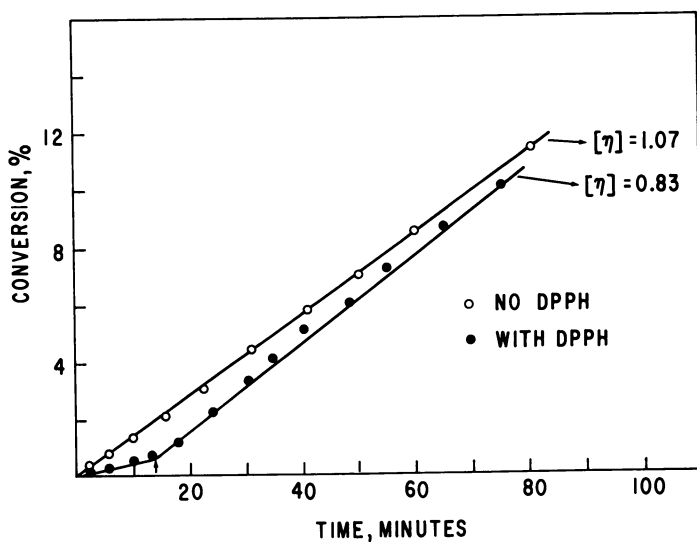


Figure 1. Polymerization of MMA at 30°C. using TBHP-SO<sub>2</sub> initiator system

**Molecular Weight Distribution.** The molecular weight distribution of a few PMMA samples initiated in bulk by SO<sub>2</sub>, TBHP-SO<sub>2</sub>, or TBPH at 30°C. has been examined by GPC. The description of the samples studied is given in Table I. All the polymers were obtained at low conversions (<15%) at 30°C. The molecular weight distribution for each sample was computed, and the distribution ratio  $\overline{M}_w/\overline{M}_n$  for the four samples as obtained from GPC data is shown in Table I. For Sample 3, having intrinsic viscosity 1.07, the GPC weight average molecular weight  $\overline{M}_w$  and number average molecular weight  $\overline{M}_n$  values are in fairly close

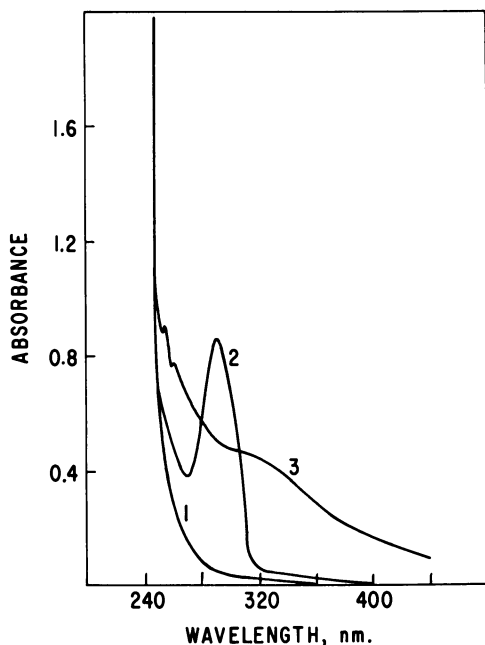


Figure 2. Absorption spectra of PMMA samples prepared with (1) no added reagent, (2) hydroquinone and (3) DPPH. Initiator system: TBHP-SO<sub>2</sub>. (The unit of wavelength is the nanometer, nm., formerly called the millimicron, mμ). Concentration of polymer solution: 2.5% in chloroform

agreement with the respective values calculated from the intrinsic viscosity. For the other three polymers, having very high molecular weights, the GPC molecular weight  $\bar{M}_w$  is much smaller than that calculated from the intrinsic viscosity. This discrepancy with the very high molecular weight polymer suggests that the resolution in the higher molecular weight region is poor, and this is substantiated by the shape of the chromatograms for these samples, showing a sharp rise in the detector response in the higher molecular weight (lower effluent count) region. The uncertainty in calibration in this region (owing to extrapolation) is also a factor to be considered.

**Thermogravimetric Analysis.** PMMA prepared by initiation with low concentrations of sulfur dioxide at or near room temperature has been found to incorporate from negligible amounts to trace quantities of SO<sub>2</sub> at chain ends and/or at any other part of the chain presumably by copolymerization (15). Thermogravimetric analysis of a few PMMA samples prepared in the presence of SO<sub>2</sub> under varied conditions has

Table I. PMMA Samples for GPC Analysis

Sample	Initiator, M	[ $\eta$ ]	$\overline{M}_w$		$\frac{\overline{M}_w}{\overline{M}_n}$
			from GPC	from [ $\eta$ ]	
1	SO <sub>2</sub> (3.75)	6.7	$3.96 \times 10^6$	$5.26 \times 10^6$	1.67
2	SO <sub>2</sub> (0.0037)	7.4	$3.98 \times 10^6$	$6.03 \times 10^6$	1.85
3	TBHP (0.007)	1.07	$5.06 \times 10^5$	$4.73 \times 10^5$	1.75
4	SO <sub>2</sub> (0.004) TBHP (0.03)	5.08	$2.41 \times 10^6$	$3.67 \times 10^6$	1.55

been done to see if the incorporation of SO<sub>2</sub>, in trace quantities, affects the thermal properties of the polymers. Five PMMA samples were studied: (1) du Pont Lucite 140, (2) initiated by SO<sub>2</sub> (4.25M) in bulk at 30°C., (3) initiated by SO<sub>2</sub> (0.0375M) in bulk at 30°C., (4) initiated by 0.05M TBHP at 30°C., (5) initiated by TBHP (0.01M) and SO<sub>2</sub> (0.004M) at 30°C. Polymers 2–5 were isolated by precipitation in petroleum ether (40°–60°C.) and then dried in air and finally in vacuum at 40°C. The numbered curves in Figure 3 represent the thermograms of the respective samples. The thermograms of Samples 2, 3, and 4 appear more or less comparable, showing a very slow decomposition (given by loss in weight) beginning at about 130°–150°C. and a fast decomposition beginning at about 300°C. for Samples 2 and 3 and at about 290°C. for Sample 4. Sample 5 shows much lower thermal stability, decomposing in three stages. It leaves a very fine brown residue beyond about 400°C.,

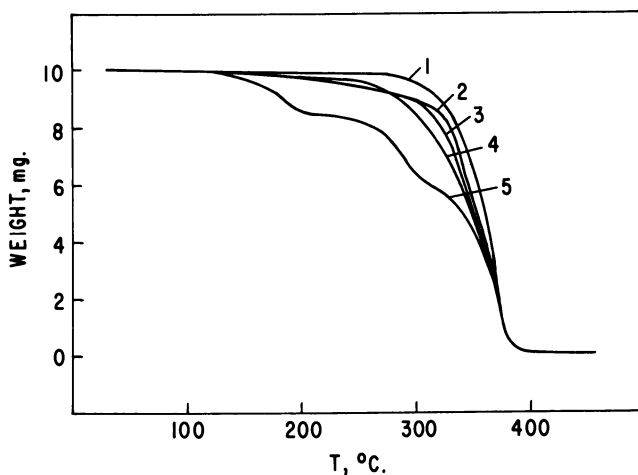


Figure 3. Dynamic thermogravimetric analysis of PMMA samples. Heating rate, 5°C./min., with a steady flow of nitrogen, 80 ml./min.

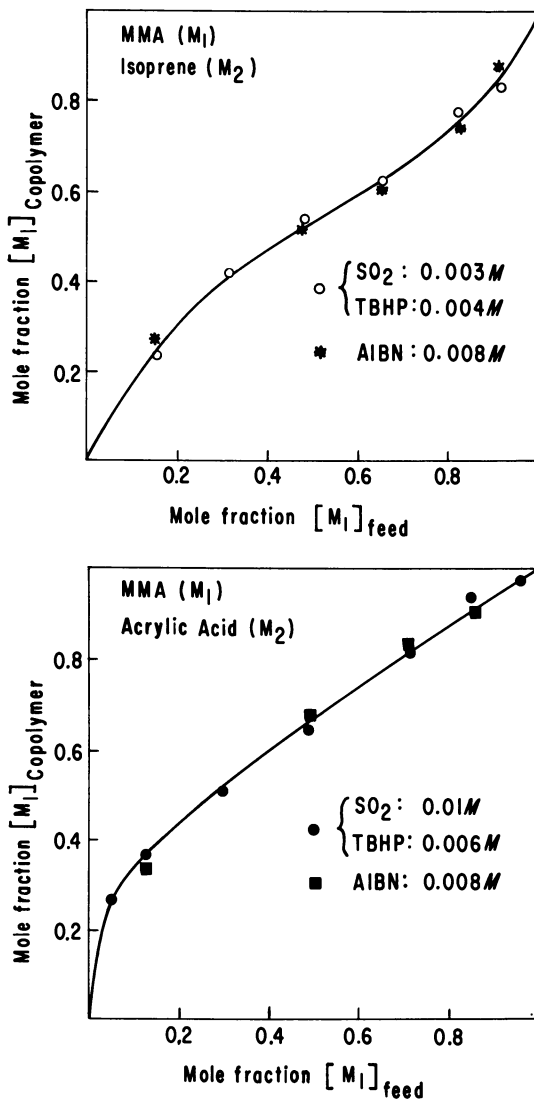


Figure 4. Copolymer composition curves  
 Top: MMA-isoprene. Bottom: MMA-acrylic acid.  
 Temperature: (A) 30°C. for TBHP-SO<sub>2</sub> system and  
 65°C. for AIBN system; (B) 30°C. for both the  
 initiator systems

while the other samples leave no residue. Sample 1 decomposes quickly, beginning at about the same region as Samples 2 and 3.

**Copolymerization.** Copolymerization of MMA ( $M_1$ ) with both isoprene and acrylic acid ( $M_2$ ) was carried out using both the TBHP-SO<sub>2</sub> system and azobisisobutyronitrile (AIBN) as the initiator, and the com-



positions of the respective copolymers obtained at low conversions ( $\sim 5\%$ ) with the two initiator systems have been compared (Figure 4). Isoprene and acrylic acid were chosen as the second monomers because of the wide difference in their physical and chemical properties. The reactivity ratios for these two copolymer systems have not been reported in the literature. In each binary system investigated herein, the results for the two initiator systems agree closely. Compositions of the MMA-isoprene copolymers were determined by estimating unsaturation in the copolymer samples, employing a modified bromination method (17, 18) to determine polyisoprene unsaturation, while those for the MMA-AA copolymers were determined by estimating the carboxylic acid content of the purified copolymers in acetone solution by titration with methanolic sodium hydroxide. The reactivity ratios for the copolymers were derived graphically by the method of intersection. For the MMA-isoprene system,  $r_1 = 0.60$ , and  $r_2 = 0.47$ ; for the MMA-AA system,  $r_1 = 1.59$ , and  $r_2 = 0.21$ . This  $r_1$  value of 1.59 is in good agreement with  $r_1 = 1.28$  for the same system reported by Palit and Ghosh (23) where the carboxyl content in the copolymers, prepared under limiting condition of very low  $M_2/M_1$  ratio in the feed monomer mixture, was determined by a sensitive dye interaction method.

### Discussion

Acrylonitrile, methyl methacrylate, vinyl acetate, and styrene were polymerized at  $30^\circ\text{C}$ . in bulk using the same concentration of  $\text{SO}_2$  and TBHP as the initiator components. The yield curves are given in Figure 5. The initial (steady) rates in moles/liter/sec. are  $6.2 \times 10^{-3}$ ,  $0.83 \times 10^{-3}$ ,  $1.9 \times 10^{-3}$ , and  $0.019 \times 10^{-3}$ , respectively for AN, MMA, VA, and Sty. These rates are thus in the proportion 1 : 0.13 : 0.31 : 0.0031. From values of  $k_p/k_t^{1/2}$  at  $30^\circ\text{C}$ . for radical polymerization, taken from the literature (7) the rates would be expected to be in the proportion 1 : 0.11 : 0.26 : 0.016. Thus, they appear to be in the same order as expected for radical polymerization.

Isobutyl vinyl ether (IBVE) is known to polymerize by cationic mechanisms (5, 27). It has been found, however, that  $\text{SO}_2$ , dissolved in IBVE, turns the system to a brown viscous liquid on standing overnight in air; when the solution is allowed to stand in vacuum, there is little change in 24 hours, but gain in viscosity and gradual darkening of the medium occur in about 3-4 days. The rate of polymerization is enhanced by the presence of TBHP, and using high concentration of TBHP ( $>0.5M$ ), the polymer obtained is found insoluble, presumably owing to crosslinking. In all cases the final yield of polymer is low ( $\sim 2-10\%$

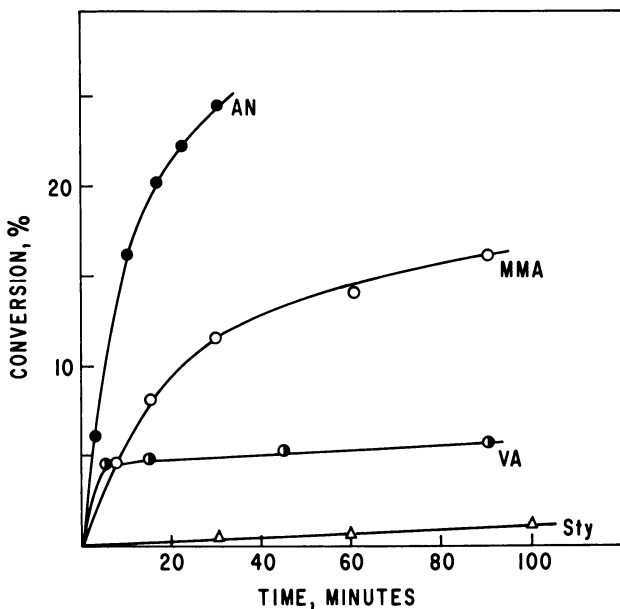


Figure 5. Polymerization of AN, MMA, VA, and Sty at 30°C. using fixed concentrations of  $\text{SO}_2$  and TBHP

in 3–5 days). The intrinsic viscosity of the soluble polymers obtained is in the range of 0.04–0.1 dl./gram, as determined in benzene solution at 30°C.

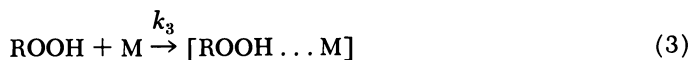
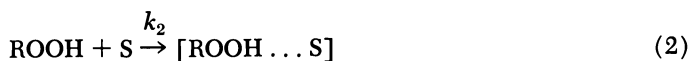
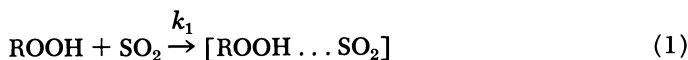
Some interesting solvent effects observed in the TBHP– $\text{SO}_2$ -initiated polymerization of MMA have been mentioned before. It has been further observed that when polymerization of MMA and AN is carried out in the presence of alcohols, the rate of polymerization is in the order: methanol > ethanol > isopropyl alcohol > *tert*-butyl alcohol, cyclohexanol. This suggests that the over-all polymerization mechanism (or the initiation mechanism itself) depends on the polar contribution of the alcohol. A similar observation was made by Imoto *et al.* with a benzoic anhydride–dimethylaniline *N*-oxide system as the initiator (20).

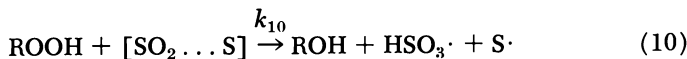
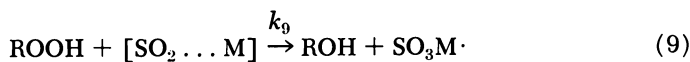
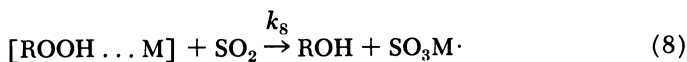
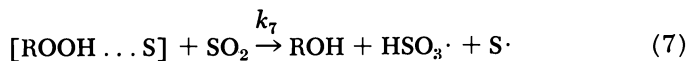
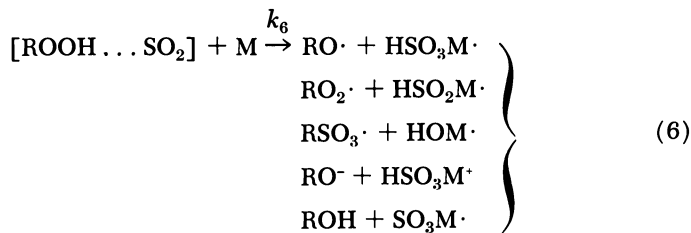
Although the polymerization of AN in bulk and also in the presence of 5–15% alcohol was heterogeneous, that of MMA in the presence of the alcohol remained homogeneous. Radical occlusion undoubtedly took place in the AN polymerizations, but this complication has not been considered in detail.

**Mechanism.** The ability of  $\text{SO}_2$  to participate in complex formation with unsaturated hydrocarbons and a host of other compounds such as amines, ethers, phenols, and aromatic hydrocarbons is known (2, 6, 11, 22).  $\text{SO}_2$  has been found to initiate polymerization of some monomers

such as the methacrylates and styrene at room temperature but not of some other monomers such as AN, acrylamide, the acrylates, and vinyl acetate. This indicates that the  $\text{SO}_2$  complexes formed with the latter monomers are relatively stable compared with those formed with the former monomers. Low concentrations of TBHP easily initiate the polymerization of all the above monomers in the presence of  $\text{SO}_2$  at room temperature. It appears that the stability of the  $\text{SO}_2$  complexes with the latter monomers does not arise from cyclic sulfone formation, and the use of *n*-butyl sulfone with TBHP does not cause these monomers to polymerize at room temperature.

When the hydroperoxide, TBHP, is used, polymerization is much faster than when a peroxide such as *tert*-butyl peroxide or benzoyl peroxide is used along with  $\text{SO}_2$  as the initiator. Thus, it may be assumed that TBHP reacts more rapidly with  $\text{SO}_2$  than do other peroxides to give free radicals or also may form complexes with  $\text{SO}_2$  and probably with the monomers as well (25) to give less stable species, thus bringing down the energy barrier for the initiation reaction.  $\text{SO}_2$  in methanol solution shows a strong absorption at 275 nm. It is greatly and rapidly reduced in the presence of an equivalent amount of TBHP, which does not show any significant absorption at that wavelength. The non-inhibitory effect of DPPH and hydroquinone on polymerization initiated by the TBHP- $\text{SO}_2$  system and the ability to initiate polymerization of isobutyl vinyl ether indicates that the polymerization concerned is not of typical free radical type; on the other hand, copolymerization data and end group studies suggest that the TBHP- $\text{SO}_2$ -initiated polymerization is, by and large, radical in nature. The importance of environment on the TBHP- $\text{SO}_2$ -initiated polymerization was clearly shown when the polymerization was carried out in the presence of different solvents. The following reactions may possibly take place before propagation of the chain reaction sets in:





ROOH stands for TBHP, and the species in the brackets represent respective complexes. In Reactions 7 and 10 abstraction of a hydrogen atom from the solvent molecule, S, is considered. Reactions between two or more complexes are neglected for simplicity; radical generation involving dissociation of the binary complexes as such is considered insignificant and therefore neglected. The rate of initiation,  $R_i$ , can then be expressed as

$$\begin{aligned}
 R_i = &k_1 k_6 [\text{ROOH}] [\text{SO}_2] [\text{M}] + k_2 k_7 [\text{ROOH}] [\text{SO}_2] [\text{S}] + \\
 &k_3 k_8 [\text{ROOH}] [\text{SO}_2] [\text{M}] + k_4 k_9 [\text{ROOH}] [\text{SO}_2] [\text{M}] + \\
 &k_5 k_{10} [\text{ROOH}] [\text{SO}_2] [\text{S}]
 \end{aligned}$$

Thus,  $R_i$  may be simply expressed as:

$$R_i = K_a [\text{ROOH}] [\text{SO}_2] [\text{M}] + K_b [\text{ROOH}] [\text{SO}_2] [\text{S}] \quad (11)$$

If termination of polymerization is bimolecular in nature, then

$$R_i = R_p^2 \cdot \frac{2k_t}{k_p^2} \cdot \frac{1}{[\text{M}]^2}$$

where  $R_p$  = rate of polymerization,  $k_p$  and  $k_t$  are rate constants for propagation and termination, respectively. Hence,

$$\begin{aligned}
 R_p^2 \cdot \frac{2k_t}{k_p^2} \cdot \frac{1}{[\text{M}]^2} &= K_a [\text{ROOH}] [\text{SO}_2] [\text{M}] + K_b [\text{ROOH}] [\text{SO}_2] [\text{S}] \\
 \text{OR, } \frac{R_p^2 \cdot 2k_t}{k_p^2 [\text{ROOH}] [\text{SO}_2] [\text{M}]^3} &= K_a + K_b \frac{[\text{S}]}{[\text{M}]} \quad (12)
 \end{aligned}$$

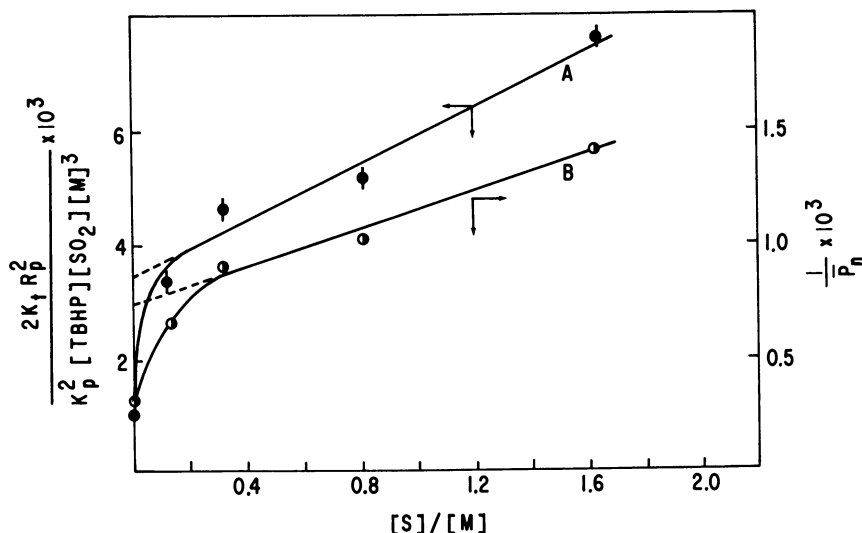


Figure 6. Polymerization of MMA in benzene solution at 30°C.  
 (A), Left-hand expression of Equation 12  
 (B),  $1/P_n$ , plotted against  $[S]/[M]$

Table II. Polymerization of MMA at 30°C. in Benzene Solution<sup>a</sup>

$[S]/[M]$	$[M], M$	$R_p \times 10^4,$ $M/sec.$	$[\eta]$	$2A'' R_p^2$ $C[M]^3$
0	9.36	1.761	0.99	0.00092
0.135	8.44	2.921	0.53	0.00339
0.324	7.49	2.812	0.43	0.00462
0.812	5.62	1.897	0.38	0.00500
1.645	3.98	1.395	0.30	0.00757

<sup>a</sup>  $[TBHP] = 0.0075M$ ;  $[SO_2] = 0.004M$ ;  $C = [TBHP][SO_2] = 3 \times 10^{-5}$ ;  $A'' = k_t/k_p^2 = 3.69 \times 10^2$ .

According to the initiation mechanism given above, a plot of the left hand expression against  $[S]/[M]$  in solution polymerization would give a straight line if termination is bimolecular in nature. Such a plot for the polymerization of MMA in benzene at 30°C. and at constant concentrations of TBHP and  $SO_2$  is given in Figure 6, Curve A, and the results are given in Table II. The values of  $k_p$  and  $k_t$  for free radical polymerization of MMA at 30°C. are taken from the literature (7). A reasonably good linear plot is obtained over a wide range of  $[S]/[M]$ , excepting points at near-bulk or bulk polymerization. In the solution polymerization of MMA at high temperature initiated by cumene hydroperoxide, Tobolsky and Matlak (25) also observed effects of this kind in the presence of solvents such as benzyl alcohol or dimethylaniline, but no solvent effect

was noticed with benzene. Burnett and co-workers (1, 10) also reported an enhanced rate of MMA polymerization in the presence of some halogenated benzenes, but no solvent effect was reported for benzene.

The difference between the intercept obtained by extrapolating the straight line portion of Figure 6, Curve A, to zero  $[S]/[M]$  and the experimental value of the ordinate at zero solvent concentration is significant. A plot of reciprocal degree of polymerization ( $1/P_n$ ) against  $[S]/[M]$  has similar characteristics (Figure 6, Curve B); the molecular weight of the polymer at zero  $[S]/[M]$  is higher than that obtained from the intercept given by extrapolating the straight line at high  $[S]/[M]$  region. The slope of this line is  $0.4 \times 10^{-3}$ , and this is apparently much higher than the expected chain transfer constant for benzene at 30°C. The slope of the straight line portion of Curve A (Figure 6) gives the value  $2.5 \times 10^{-3}$  for  $K_b$  in Reaction 12 for the present system. The value of  $K_a$  as given by the intercept on extrapolating the linear portion of Curve A to zero  $[S]/[M]$  is  $3.4 \times 10^{-3}$ , while the experimental value of the ordinate at zero  $[S]/[M]$  is  $0.93 \times 10^{-3}$ .

Similar observations were made with TBHP-SO<sub>2</sub>-initiated polymerization of MMA at 50°C. using benzene, toluene, and xylene as solvents and at 60°C. using chloroform as the solvent (Figure 7). Among the three aromatic hydrocarbons used, the rate enhancement is of the order: xylene > toluene > benzene.

**Polymerization of Some Other Vinyl Monomers.** The polymerization of acrylonitrile (AN) with TBHP-SO<sub>2</sub> initiator system occurs at a fairly high rate with little inhibition period. A log-log plot of rate of polymerization  $R_p$  in bulk at 30°C. vs. the product of the concentrations of TBHP and SO<sub>2</sub> gives a straight line having a slope of 0.75. The rate varies directly with the 1.8 power of monomer concentration (Figure 8), the monomer variation being done with benzene as the solvent. Polymerization proceeds at an enhanced rate in the presence of low concentrations of tetrahydrofuran, acetone, and cyclohexanone but is appreciably slower in the presence of higher alcohols and dimethyl formamide. Hydroquinone (0.01M) produces a small inhibition period (~2-3 min. using 0.0025M SO<sub>2</sub> and 0.01M TBHP), and the polymerization proceeds at a very retarded rate thereafter. Under the same conditions, 0.0012M DPPH induces an inhibition period of 3 hours, and about 8-10% conversion to polymer takes place in about a week thereafter. The purified polymer is faint yellow and shows significant absorption in the visible/near-ultraviolet region, indicating the incorporation of fragments of DPPH in the polymer. The over-all activation energy of AN polymerization by the TBHP-SO<sub>2</sub> initiator system is 8.74 kcal./mole.

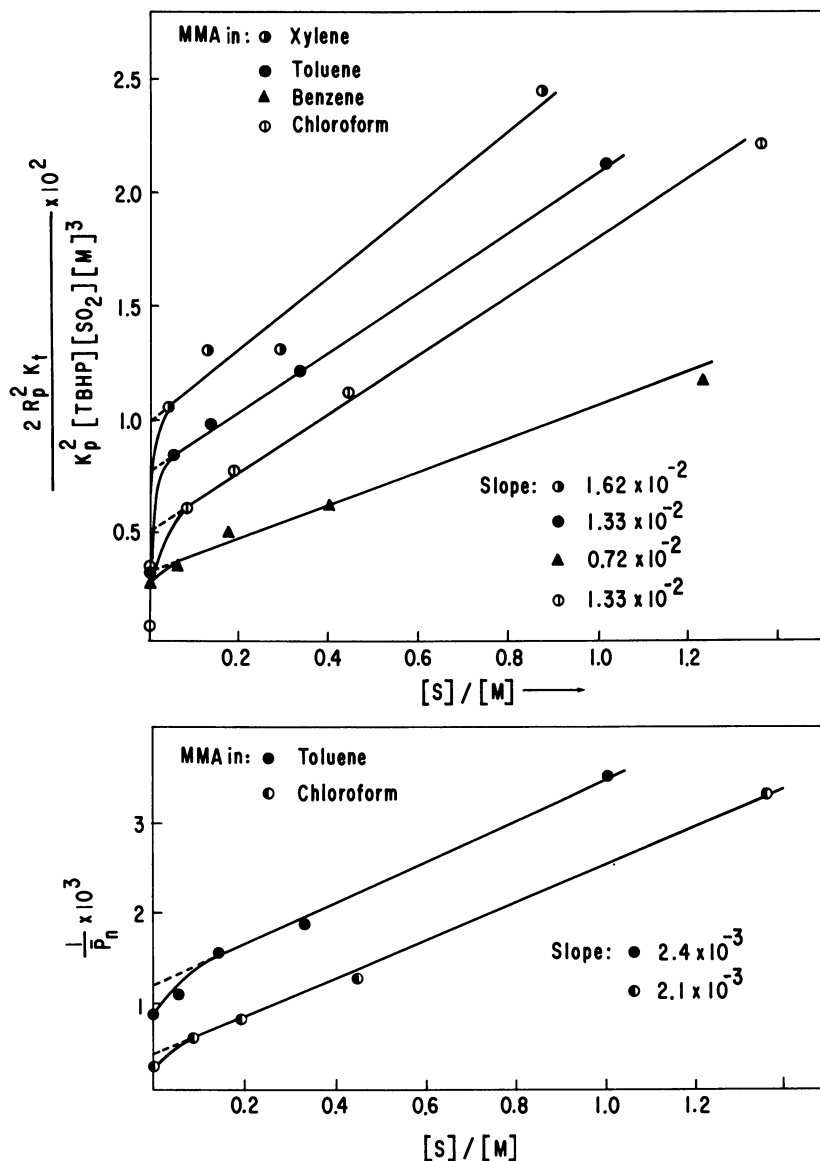


Figure 7. Polymerization of MMA at 50°C. in benzene, toluene, and xylene solution and at 60°C. in chloroform solution  
 Top: left-hand expression of Equation 12 plotted against  $[S]/[M]$   
 Bottom:  $1/P_n$  vs.  $[S]/[M]$  for polymerization in toluene

Polymerization of some other vinyl monomers such as EMA, *n*-BMA, VA, Sty, and MA was studied in the presence of certain solvents using the TBHP-SO<sub>2</sub> initiator system. Tetrahydrofuran, acetone, and cyclo-

hexanone enhanced the rate of polymerization of all these monomers, but benzene, toluene, or xylene did not. The rate dependence on monomer concentration, using benzene as the diluent for the various monomers, is shown in Figure 8. The slopes of the logarithmic straight-line plots of  $R_p$  vs.  $[M]$  for these monomers are between 1.5 and 1.8. Only MMA is different, showing a maximum in the plot.

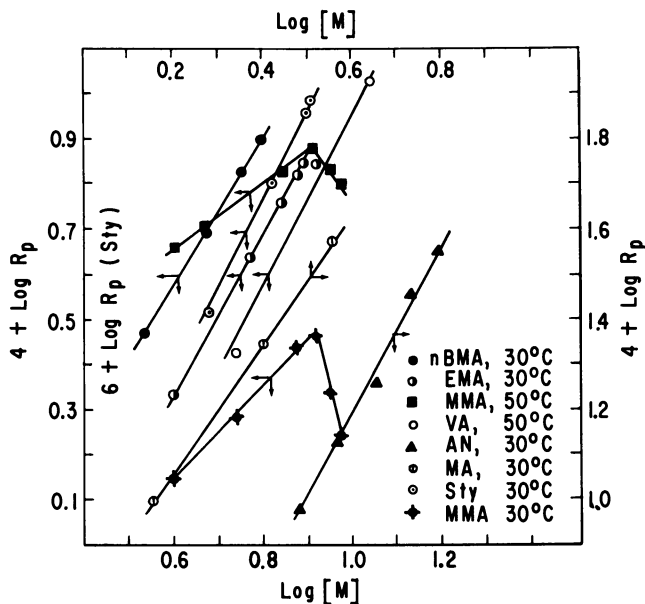


Figure 8.  $\log R_p$  vs.  $\log [M]$  for various monomers  
Initiator, TBHP- $\text{SO}_2$  system. Slope: AN = 1.8, MA = 1.5, VA  
= 1.8, Sty = 1.8, n-BMA = 1.6, EMA = 1.6

The plot of the left-hand expression of Equation 12 against  $[S]/[M]$ , where S stands for benzene, for some of these monomers is shown in Figure 9. For methyl acrylate the rate measurements were done dilatometrically at high  $[S]/[M]$  ratio to avoid difficulties owing to gelation and heat buildup. The slope of the plots in Figure 9 is negative (or negligible compared with the value of the intercept as for MA), indicating that benzene does not participate in the initiation step in the polymerization of these monomers. The monomer exponent of 1.5–1.8 for these monomers (except MMA) indicates that the initiator–monomer initiation reaction is dominant, and the initiator–solvent initiation reaction is negligible. For MMA in benzene solution, in the high solvent concentration region the log-log plot of  $R_p$  vs.  $[M]$  shows an order in  $[M]$  close to the value of 1 (Figure 8) indicating, according to the initiation mechanism detailed above, the predominance of an initiator–solvent initiation reac-



tion (25). Plots of  $(1/P_n)$  vs.  $[S]/[M]$  for some of the monomers polymerized in benzene solution are given in Figure 10; in each case the slope is higher than the expected chain transfer constant for benzene in the respective systems (8).

Thus, in the present system of polymerization initiated by TBHP-SO<sub>2</sub>, MMA behaves quite differently from other monomers such as Sty, EMA, n-BMA, AN, VA, etc. The precise reason for this difference is not under-

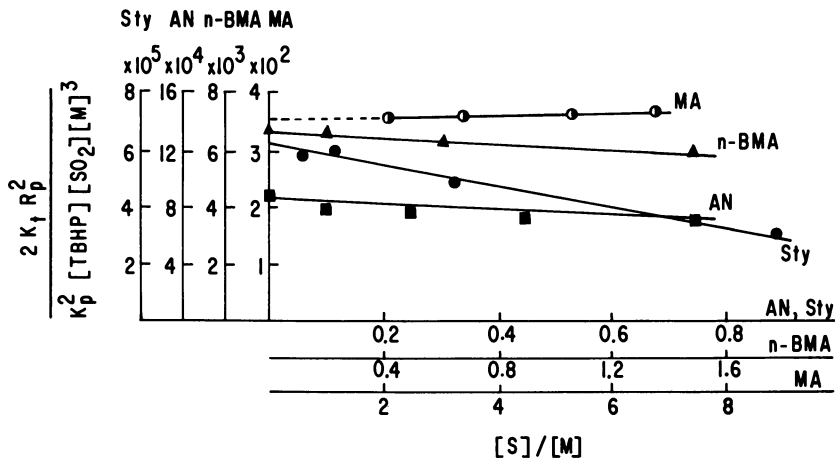


Figure 9. Left-hand expression of Equation 12 vs.  $[S]/[M]$  for the polymerization of MA, n-BMA, AN, and Sty in benzene solution  
Slope: MA =  $0.21 \times 10^{-3}$ , n-BMA =  $0.5 \times 10^{-3}$ , AN =  $-2 \times 10^{-4}$ , and Sty =  $-4 \times 10^{-5}$

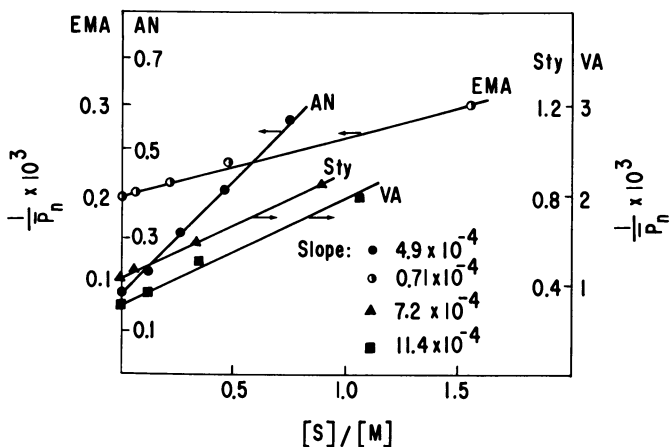


Figure 10.  $1/P_n$  vs.  $[S]/[M]$  for the polymerization of AN, EMA, VA, and Sty at 30°C. in benzene solution initiated by TBHP-SO<sub>2</sub> system

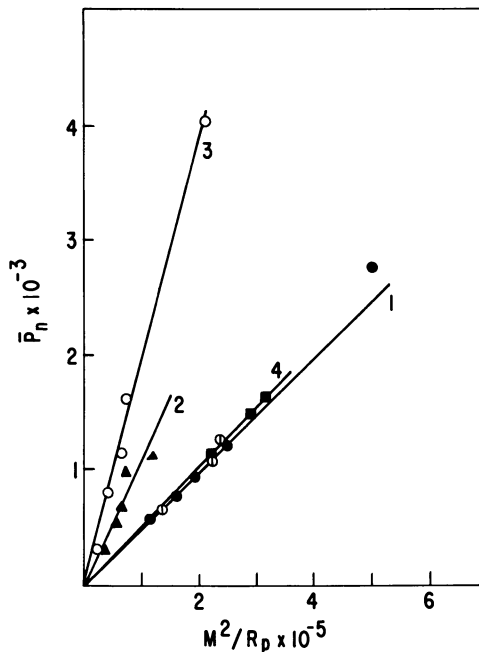


Figure 11.  $P_n$  vs.  $[M]^2/R_p$  for the polymerization of MMA

- (1) In benzene solution at 30°C.
- (2) In toluene solution at 50°C.
- (3) In chloroform solution at 60°C. at varying monomer concentration
- (4) In benzene solution at 30°C. and varying initiator concentration

■,  $[M] = 8.2M$

○,  $[M] = 4.68M$

Initiator system: TBHP-SO<sub>2</sub>

stood from our experiments; the enhanced rate of polymerization in the presence of some ketones and tetrahydrofuran for all the monomers can, on the other hand, be explained in terms of the observation of Uebereiter and Rabel (26)—*i.e.*, it arises from activation of the hydroperoxide by hydrogen bond formation between the peroxy hydrogen of the hydroperoxide and the ketonic or etherial oxygen.

While considering the rate-enhancing effect of bromobenzene in MMA polymerization initiated by AIBN, Henrici-Olivé and Olivé (19) noted that the effect can be explained as the consequence of electron donor-acceptor complex formation between polymer radicals and monomer or solvent molecules. Based on this view, these authors have shown that in polymerization in active solvents (which enhance the rate), the degree of polymerization  $P_n$  appears as a linear function of  $M^2/R_p$  with

zero intercept (19), assuming the absence of any side reactions. For MMA polymerization in benzene, toluene, and chloroform (which show the rate-accelerating effect), using TBHP-SO<sub>2</sub> as the initiator, fairly good linear plots of  $P_n$  vs.  $M^2/R_p$ , passing through the origin, have been obtained (Figure 11). Thus, it appears that our experimental results can also be explained in the light of the hypothesis of Henrici-Olivé and Olivé.

On reviewing and reinvestigating the polymerization of MMA in the presence of halogenated benzenes and other aromatic solvents, Bamford and Brumby (3) have shown that the dependence of the rate of polymerization on the nature of the solvent arises partly from the viscosity dependence of the termination coefficient and partly from the dependence of the propagation rate constant on the nature of the solvent, and that the rate of initiation is not influenced by the nature of the solvent. Their results are compatible with the hypothesis of Henrici-Olivé and Olivé, but they contradict the suggested mechanism of Burnett *et al.* (1, 10) which considers solvent participation in the initiation step.

The above authors (1, 3, 10, 19) did not observe any rate-enhancing effect in MMA polymerization in the presence of benzene. However, using TBHP-SO<sub>2</sub> as the initiator system for the polymerization of MMA, we have observed enhanced rates in the presence of benzene and also in the presence of toluene, xylene, chlorobenzene, chloroform, etc. Kinetic analysis indicates that these solvents take part in the initiation process, and the treatment of data relating the degree of polymerization and rate of polymerization shows that the hypothesis of Henrici-Olivé and Olivé is also compatible with our results.

### Acknowledgment

Financial support of this work by the National Aeronautics and Space Administration under Grant NsG-100 is sincerely acknowledged. The thermogravimetric analyses were obtained through the courtesy of J. Chiu, Plastics Department, E. I. du Pont de Nemours & Co., Experimental Station, Wilmington, Del., and for this we express our sincere thanks. We also appreciate the assistance and cooperation of R. N. Kelley of our laboratories in obtaining the GPC data.

### Literature Cited

- (1) Anderson, D. B., Burnett, G. M., Gowan, A. C., *J. Polymer Sci. A*, **1**, 1465 (1963).
- (2) Andrews, L. J., Keefer, R. M., *J. Am. Chem. Soc.* **73**, 4169 (1951).
- (3) Bamford, C. H., Brumby, S., *Makromol. Chem.* **105**, 122 (1967).
- (4) Baxendale, J. H., Bywater, S., Evans, M. G., *J. Polymer Sci.* **1**, 237 (1940).

- (5) Blanke, G. J., Carbon, A. M., *J. Polymer Sci. A-1* **4**, 1813 (1966).
- (6) Booth, D., Dainton, F. S., Ivin, K. J., *Trans. Faraday Soc.* **55**, 1293 (1959).
- (7) Brandrup, J., Immergut, E. H., Eds., "Polymer Handbook," pp. II-(57-65), Interscience, New York, 1966.
- (8) *Ibid.*, pp. II-(77-133).
- (9) *Ibid.*, pp. IV-(1-45).
- (10) Burnett, G. M., Dailey, W. S., Pearson, J. M., *Trans. Faraday Soc.* **61**, 1216 (1965).
- (11) Dainton, F. S., Ivin, K. J., *Discussions Faraday Soc.* **2**, 376 (1947).
- (12) Fox, T. G., Mason, H. F., Cohn, E. S., unpublished work (cited in Ref. 9).
- (13) Ghosh, P., Chadha, S. C., Mukhrejee, A. R., Palit, S. R., *J. Polymer Sci. A* **2**, 4433 (1964).
- (14) Ghosh, P., O'Driscoll, K. F., *J. Polymer Sci. B*, **4**, 519 (1966).
- (15) Ghosh, P., O'Driscoll, K. F., *J. Macromol. Sci. A*, **1**, 1393 (1967).
- (16) Ghosh, P., Sengupta, P. K., Pramanik, A., *J. Polymer Sci. A*, **3**, 1725 (1965).
- (17) Ghosh, P., Sengupta, P. K., *J. Appl. Polymer Sci.* **11**, 1603 (1967).
- (18) Gowans, W. J., Clark, F. W., *Anal. Chem.* **24**, 529 (1952).
- (19) Henrici-Olivé, G., Olivé, S., *Makromol. Chem.* **96**, 221 (1966).
- (20) Imoto, M., Sato, T., Takemo, K., *Makromol. Chem.* **95**, 117 (1966).
- (21) Johnson, J. F., Porter, R. S., Cantow, M. J. R., *Rev. Macromol. Chem.* **1**, 393 (1966).
- (22) Maine, P. A. D., *J. Chem. Phys.* **26**, 1036, 1042, 1049 (1937).
- (23) Palit, S. R., Ghosh, P., *J. Polymer Sci.* **58**, 1225 (1962).
- (24) Schulz, R. C., Banihaschemi, A., *Makromol. Chem.* **64**, 140 (1963).
- (25) Tobolsky, A. V., Matlak, L. R., *J. Polymer Sci.* **55**, 49 (1961).
- (26) Uebereiter, K., Rabel, W., *Makromol. Chem.* **68**, 12 (1963).
- (27) Yamaka, H., Takakura, K., Hayashi, K., Okamura, S., *J. Polymer Sci. B*, **4**, 509 (1966).

RECEIVED April 1, 1968.

# 6

## Donor–Acceptor Molecular Complexes in Alternating Copolymerization and in the Polymerization of Metal Halide-Complexed Vinyl Monomers

NORMAN G. GAYLORD and AKIO TAKAHASHI

Gaylord Associates Inc., Newark, N. J. 07104

*Polar monomers containing pendant nitrile or carbonyl groups complex with Lewis acids with a resultant increase in their electron-accepting ability relative to that of the uncomplexed monomer. Complexed monomer participates in a one-electron transfer reaction with uncomplexed monomer or another electron donor monomer—e.g., olefin or conjugated diene—to form a charge transfer complex, which is a dipolar, diradical species analogous to the proposed intermediate in certain Diels–Alder reactions. The charge transfer complex may open spontaneously—e.g., olefin–acrylonitrile–alkylaluminum halide, styrene–methyl methacrylate–alkylaluminum halide, isoprene–acrylonitrile–zinc chloride—or under the influence of free radicals—e.g., olefin–or allyl monomer–acrylonitrile–zinc chloride. The process involves spontaneous or radical-initiated homopolymerization of a Lewis acid activated, diradical charge transfer complex.*

The free radical initiated polymerization of polar monomers containing pendant nitrile and carbonyl groups—e.g., acrylonitrile and methyl methacrylate—in the presence of metal halides such as zinc chloride and aluminum chloride, is characterized by increased rates of polymerization (2, 3, 4, 5, 10, 30, 31, 32, 33, 34, 53, 55, 65, 66, 75, 76, 77, 87). Imoto and Otsu (30, 33, 34) have attributed this effect to the formation of a complex between the polar group and the metal halide. The enhanced reactivity of the complexed monomer extends to copolymerization with uncomplexed monomers, such as vinylidene chloride, which are readily responsive to

free radical polymerization, wherein  $Q$  and  $e$  values and the reactivity ratio for the complexed monomer are increased (22, 23, 30, 32). However, monomers such as allylic and olefinic compounds, which are poorly responsive in free radical initiated polymerizations, are more readily copolymerized with the complexed than the uncomplexed polar monomer (35, 72, 73). In this paper, the contribution of donor-acceptor interactions in copolymerization to the reactivity of metal halide-complexed monomers is examined.

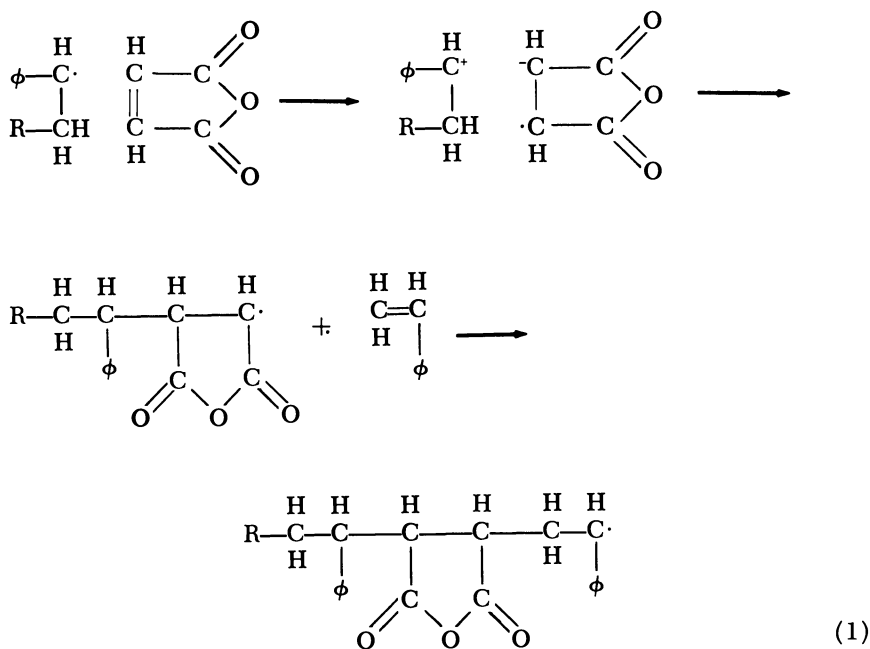
### *Donor-Acceptor Interactions in Polymerization*

The effect of polarity on vinyl monomer copolymerization has long been recognized and is a major factor in the  $Q, e$  scheme and copolymerization theory. Mayo, Lewis, and Walling tabulated a number of vinyl monomers into an "average activity" series and an electron "donor-acceptor series" (62). The activity series showed the effect of substituents on the ease with which an ethylene derivative reacted with an average radical and on stabilizing the radical which was formed thereby. The electron donor-acceptor series indicated the ability of the substituents to serve as donors or acceptors in radical-monomer interactions. It is significant that in both series the dominant factor is the radical-monomer interaction.

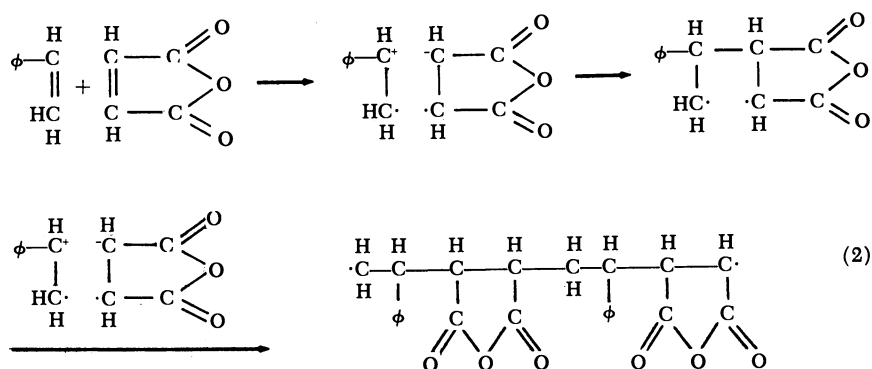
It was further indicated that copolymerization of two monomers which were close together in the donor-acceptor series gave a random copolymer, while monomers which were well separated in the series had a marked tendency to give an alternating copolymer.

In contrast to the radical-monomer interaction in the transition state proposed by Mayo and Walling (62, 63), the formation of a molecular complex between the electron donor monomer and the electron acceptor monomer—*i.e.*, monomer-monomer interaction—has been proposed as the contributing factor in the free radical alternating copolymerization of styrene and maleic anhydride (8) as well as sulfur dioxide and mono- or diolefins (6, 9, 12, 13, 25, 41, 42, 43, 44, 61, 79, 80, 88). Walling and co-workers (83, 84) did note a relationship between the tendency to form molecular complexes and the alternating tendency and considered the possibility that alternation involved the attack of a radical on a molecular complex. However, it was "the presence in the transition state of polar resonance forms resembling those in the colored molecular complexes" which led to alternation in copolymerization (84).

The significant distinction between these proposals lies in the nature of the components participating in the transition state. Thus, the radical-monomer interaction involves a one-electron transfer from the growing radical to the electron acceptor monomer.



In contrast, the donor monomer-acceptor monomer interaction involves a one-electron transfer from the donor monomer to the acceptor monomer to form a charge transfer complex. The latter undergoes homopolymerization through a radical mechanism to give an alternating copolymer.



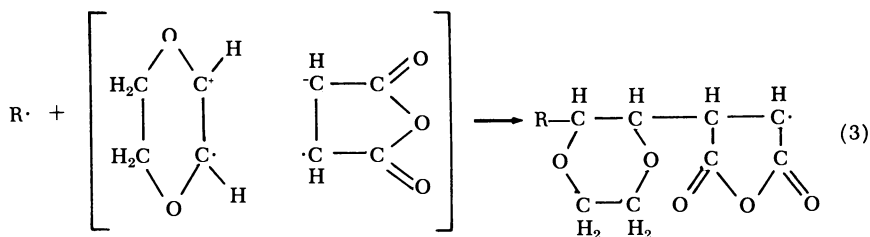
Thus, the radical-monomer interaction involves a monoradical species which successively adds monomer units in an alternating copolymerization, while the monomer-monomer interaction involves the homopolymerization of a charge transfer complex through a diradical coupling

mechanism—*i.e.*, alternating copolymers result from complex homopolymerization and not through copolymerization.

Iwatsuki and Yamashita (46, 48, 50, 52) have provided evidence for the participation of a charge transfer complex in the formation of alternating copolymers from the free radical copolymerization of *p*-dioxene or vinyl ethers with maleic anhydride. Terpolymerization of the monomer pairs which form alternating copolymers with a third monomer which had little interaction with either monomer of the pair, indicated that the polymerization was actually a copolymerization of the third monomer with the complex (45, 47, 51, 52). Similarly, copolymerization kinetics have been found to be applicable to the free radical polymerization of ternary mixtures of sulfur dioxide, an electron donor monomer, and an electron acceptor monomer (25, 44, 61, 88), as well as sulfur dioxide and two electron donor monomers (42, 80).

The diradical nature of the intermediate in the copolymerization of monomers through a charge transfer intermediate has been suggested by Zutty *et al.* (88) as a result of studies on the copolymerization and terpolymerization of monomer systems containing bicycloheptene and sulfur dioxide. The third monomer apparently enters the copolymer chain as a block segment, while the donor-acceptor monomer pair enter the chain in a 1:1 molar ratio, irrespective of the ratio present in the monomer mixture.

Similar results have been noted in terpolymerizations involving the *p*-dioxene-maleic anhydride (49, 51, 52) and vinyl ether-maleic anhydride (45, 49) and vinyl ether-fumaronitrile (49) monomer pairs. Iwatsuki and Yamashita (46) concluded that the molecular complex formed between *p*-dioxene and maleic anhydride is attacked on the *p*-dioxene side by a radical to yield the maleic anhydride radical which is considered to be the main growing radical. Thus, a monoradical propagation step is considered operative.

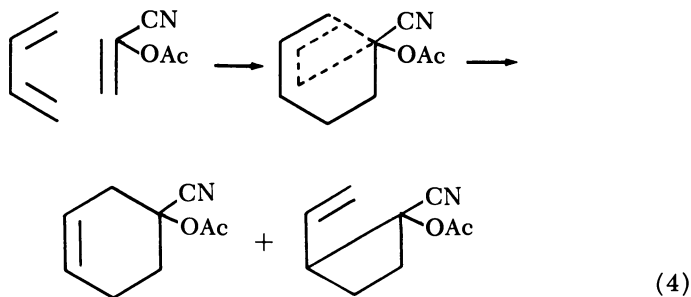


Actually, the diradical and monoradical species in Reactions 2 and 3, respectively, are the same since both involve the participation of the complex as a diradical species. The termination and propagation steps in these reactions are related in that the interaction between two radicals

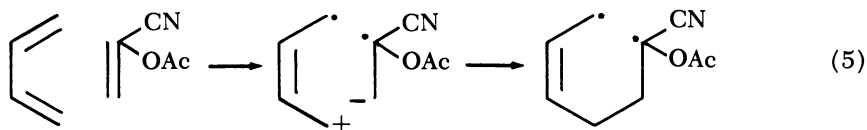


is a propagating step when coupling results and a terminating step when disproportionation occurs. Thus, in contrast to conventional free radical polymerization mechanisms, charge transfer mechanisms involve propagation not only by polymer radical–monomer or polymer radical–complex interactions but also by polymer radical–polymer radical interactions. This leads to the conclusion that while solvents play a role in determining the participation of the third monomer in a ternary polymerization (49), they may be involved to only a limited extent in the termination step. This is confirmed by the absence of chlorine in the terpolymers of *p*-dioxene–maleic anhydride–acrylonitrile prepared in chloroform solution (49) and the ability to prepare methyl vinyl ketone–maleic anhydride copolymers with benzoyl peroxide in nitrobenzene solution (74).

The participation of diradical species in charge transfer reactions has been demonstrated in the most widely recognized example of donor–acceptor interaction—*i.e.*, the Diels-Alder reaction. The two-step nature of this reaction has recently been proposed in the isolation of both four- and six-membered ring products in the thermal and photochemical reaction of butadiene and  $\alpha$ -acetoxyacrylonitrile (14, 56).



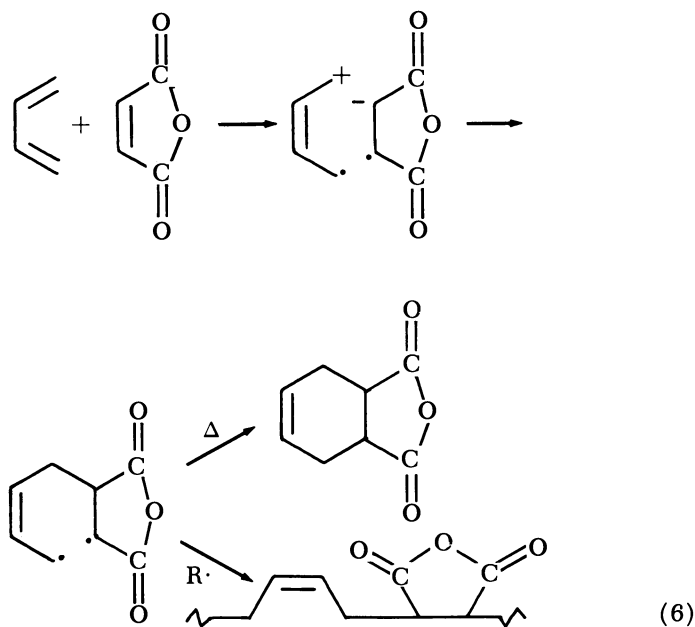
The common intermediate has appreciable diradical structure, and the products result from the alternative modes of its collapse through different transition states.



Although the Diels-Alder reaction of a conjugated diene, such as butadiene or isoprene, with maleic anhydride, has been known to yield tetrahydrophthalic anhydride, it has recently been shown (81, 85) that alternating copolymers are prepared under the influence of ionizing radiation (81) or free radical initiators (81, 85). The participation of the charge transfer complex as a common intermediate in both adduct

and alternating copolymer formation is confirmed by the greater than 74% *cis*-1,4 microstructure of the copolymer, whereas conventional free radical polymerizations (*e.g.*, homopolymerization of butadiene or copolymerizations of butadiene with styrene, acrylonitrile, dimethyl maleate, or fumaronitrile) yield polymer containing less than 25% *cis*-1,4 unsaturation (85).

The proposed reaction mechanism (81) invokes a charge transfer complex which converts to a resonance stabilized diradical. The latter leads to a Diels-Alder adduct as a result of intramolecular coupling. However, when the diradical intermediate is attacked by a free radical, it is opened, and an alternating copolymer results from intermolecular coupling.



The participation of Diels-Alder type intermediates in polymerization was considered by Hill *et al.* (26) in 1939 as a result of the elucidation of the structures of the butadiene homopolymer and the butadiene-methyl methacrylate copolymer resulting from thermal polymerization in emulsion. The considerable amount of alternating 1,4 and 1,2 structures in the homopolymer and the predominantly 1,4 structure of the butadiene in the copolymer which contained more than 50% alternating units of butadiene and methyl methacrylate led to the proposal that the reaction proceeded through a Diels-Alder "dimer complex" or "activated complex." Chain initiation involved a thermal reaction in which the activated com-

plex opened "in an environment which favored chain growth rather than ring closure and chain propagation involved adding on the complex to the growing end of the chain."

Gindin, Abkin, and Medvedev (21) observed several of the characteristics of copolymerizations involving charge transfer intermediates in the benzoyl peroxide-catalyzed copolymerization of butadiene with acrylonitrile and methacrylonitrile. Irrespective of the initial concentrations, polymerization ceased when one of the components was consumed. The butadiene-acrylonitrile copolymer had a 67% alternating structure, while the butadiene-methacrylonitrile copolymer had an 80% alternating structure.

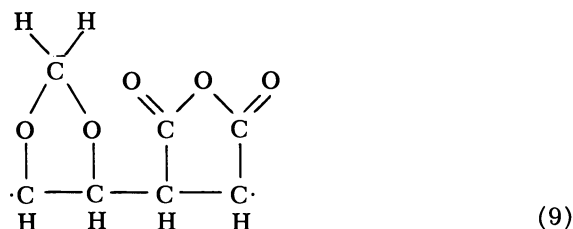
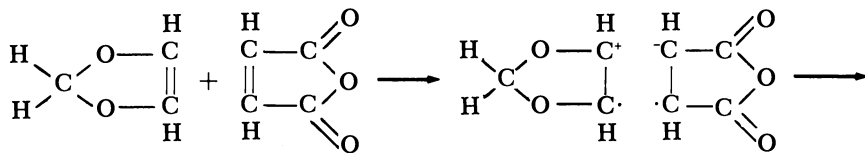
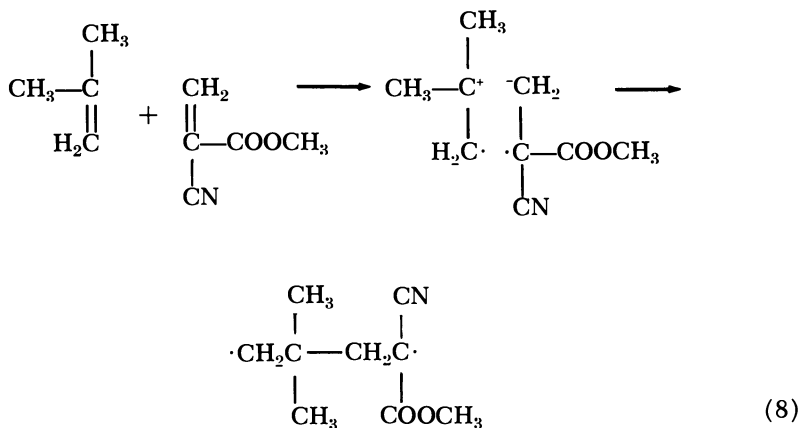
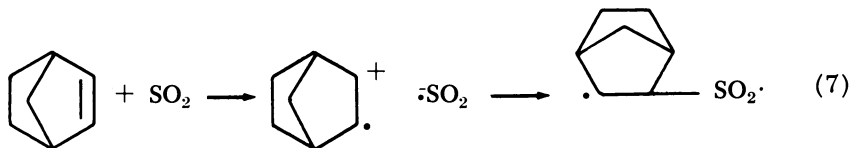
Although donor-acceptor interactions were recognized as playing an important role in copolymerization reactions during the period when the basic principles of copolymerization theory were being formulated, except for isolated instances, monomer-monomer interactions were not considered until recently. The formation of copolymers containing a greater than 1:1 ratio of donor-acceptor components is a function of conversion and the homopolymerizability of the monomers. Thus, 2:1 and 3:1 styrene-maleic anhydride copolymers apparently result from the interaction of a growing polystyrene chain with the 1:1 monomer pair, the coupling of a growing polystyrene chain with a growing alternating copolymer chain, or the addition of styrene monomer to a chain end containing a 1:1 monomer pair. The former are the more probable interactions in view of the failure to obtain copolymers containing excess maleic anhydride and the formation of block copolymers in the ternary compositions containing bicycloheptene-sulfur dioxide or *p*-dioxene-maleic anhydride.

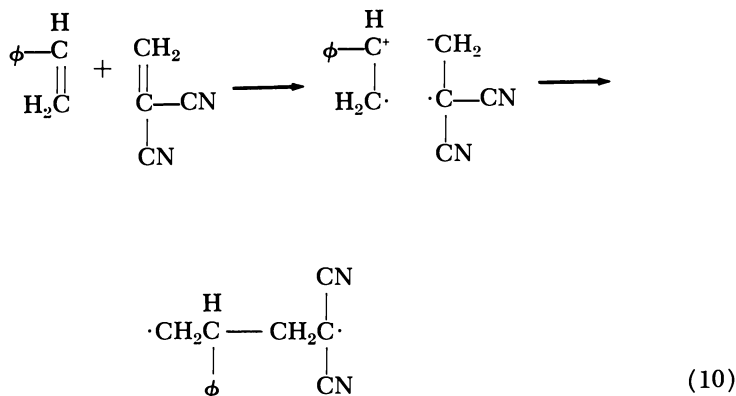
### *Influence of Complex Stability on Copolymerizability*

The charge transfer complex resulting from the one-electron transfer from the electron donor monomer to the electron acceptor monomer has a stability which varies as a function of the internal resonance stabilization. The degree of stabilization apparently determines the ease with which the diradical complex opens, and consequently the stability of the complex determines whether the copolymerization occurs spontaneously or under the influence of heat, light, or free radical attack.

Spontaneous 1:1 copolymerization has been noted when sulfur dioxide was bubbled through bicycloheptene at  $-40^{\circ}\text{C}$ . (88), when isobutylene was bubbled through methyl  $\alpha$ -cyanoacrylate (54), when 1,3-dioxole was mixed with maleic anhydride (17), and when vinylidene cyanide was mixed with styrene (20), the latter reactions at room temperature. None of these monomers undergoes homopolymerization under the same experi-

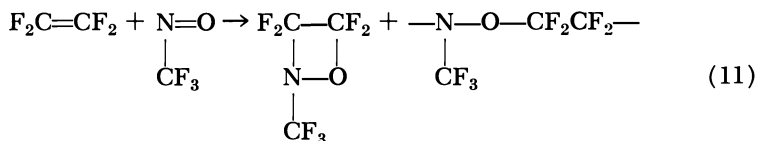
mental conditions. Apparently, the electron-donating characteristics of bicycloheptene, isobutylene, and 1,3-dioxole and the electron-accepting characteristics of sulfur dioxide, methyl  $\alpha$ -cyanoacrylate, and maleic anhydride, respectively, are sufficiently strong that the one-electron transfer reaction occurs readily, and the resultant complex is unstable.



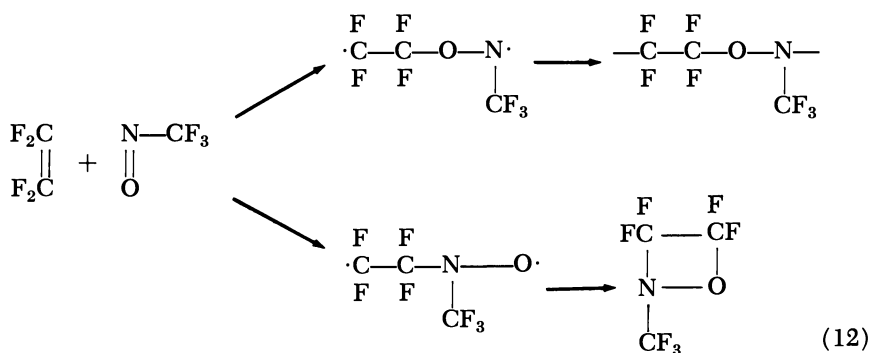


Szwarc (54) has postulated that isobutylene and the  $\alpha$ -cyanoacrylate interact to give a highly polar dimer, and the resultant copolymer should have a head-to-head, tail-to-tail structure. He has further suggested that this would exemplify a case intermediate between polymerization of diradicals and polymerization of zwitterions. As shown in Reaction 8, the electron-donating substituents on the  $\beta$ -carbon of the isobutylene convert the latter to a stronger donor than the  $\alpha$ -carbon. While the electron-withdrawing substituents on the  $\beta$ -carbon of the  $\alpha$ -cyanoacrylate convert it to an acceptor, the electron deficiency is partially compensated by a shift of electrons from the  $\alpha$ -carbon, converting the latter to an electron acceptor. The resulting charge transfer complex leads to the normal head-to-tail, tail-to-head structure. The two-step ion coupling and diradical opening is actually the intermediate case proposed by Szwarc.

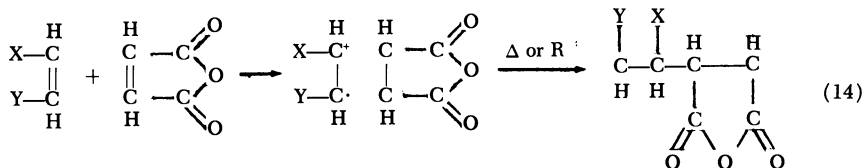
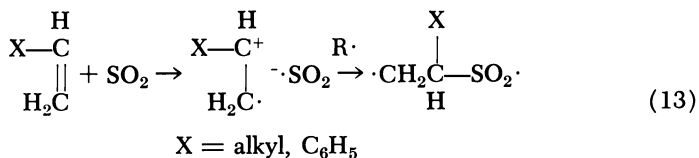
Another case of essentially spontaneous copolymerization is the low temperature reaction of trifluoronitrosomethane with tetrafluoroethylene to give a mixture of cyclic adduct and polymer (7).



Considerable evidence has been presented in support of a diradical mechanism for this reaction (11). An interesting aspect of this reaction is the proposal of two different diradical species, one favoring chain growth and polymer formation and the other favoring intramolecular coupling and adduct formation.

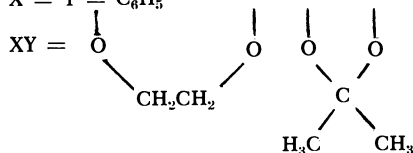


The interactions of  $\alpha$ -olefins or styrene with sulfur dioxide (16) or  $\alpha$ -olefins (24, 58, 78), *trans*-stilbene (64), styrene (1, 63), *p*-dioxene (52), 2,2-dimethyl-1,3-dioxole (17), or alkyl vinyl ethers (1, 63) with maleic anhydride yield charge transfer complexes which are stable and generally readily detectable either visually or by their ultraviolet absorption spectra. However, under the influence of a sufficiently energetic attack in the form of heat or free radicals, the diradical complexes open, and alternating copolymers are formed.

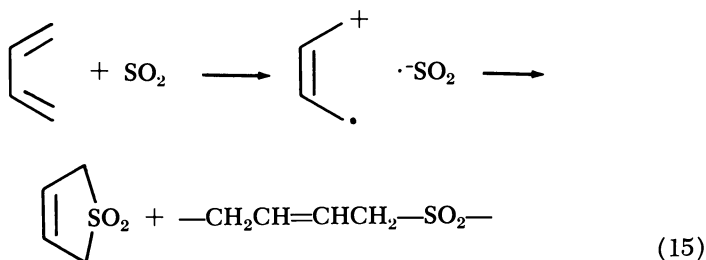


X = alkyl, C<sub>6</sub>H<sub>5</sub>, O-alkyl Y = H

X = Y = C<sub>6</sub>H<sub>5</sub>



The intermediate case where a complex is formed but opening occurs spontaneously to only a limited extent is illustrated by the reaction of butadiene or other conjugated dienes with sulfur dioxide (16). When the two components react, a cyclic adduct and a linear alternating copolymer are produced simultaneously.



Under the influence of heat, free radicals, or radiation the yield of copolymer is increased, and the yield of adduct is decreased (19). This is analogous to the diene-maleic anhydride interaction in the existence of a common intermediate in both adduct and copolymer formation. However, in the Diels-Alder case adduct formation occurs so readily that the copolymer does not normally accompany the adduct. When the intermediate complex is exposed to radiation, both copolymer and adduct are formed (81). The direct analogy of the diene-sulfur dioxide reaction to the diene-maleic anhydride reaction is the greater than 75% cis-1,4 unsaturation of the copolymer in both cases.

When charge transfer intermediates are formed, they are apparently capable of pursuing three different reaction paths: (a) intramolecular diradical coupling yielding a 1:1 adduct, (b) intermolecular diradical coupling yielding an alternating 1:1 copolymer, or (c) no reaction until the input of sufficient energy drives the reaction to follow Paths a or b.

### **Catalysis of Complex Formation**

The interaction of a strong electron donor with a strong electron acceptor results in a spontaneous one-electron transfer and the formation of a charge transfer complex. Once the complex is formed, it may follow one or more of the paths already discussed. However, the one-electron transfer reaction does not readily occur unless the monomers are sufficiently strong in their electron-donating or accepting character. Mayo and Walling (62) have already indicated this in their observation that random copolymers are formed when the two monomers are close together in the donor-acceptor series, while there is a marked tendency for alternation with monomers which are widely separated in the series.

Increasing the electron-accepting character of an electron acceptor monomer would result in a greater separation in the donor-acceptor relationship with a given electron donor monomer. As a result there would be an increased tendency for alternation in the copolymerization.

A further consequence of the ease of complex formation may be a more rapid copolymerization, although the complex may form an adduct or await the input of sufficient energy to open.

In our work on copolymerizations involving charge transfer intermediates, it has been noted that when a mixture of styrene and maleic anhydride is heated to 80°C. in the presence of benzoyl peroxide, an extremely exothermic reaction occurs, and in a sealed system the temperature rises from 80° to 250°C. within three minutes, and the conversion is quantitative.

Similarly, whereas the Diels-Alder reaction is accelerated at elevated temperatures, under polymerization conditions, the reaction of isoprene and maleic anhydride is extremely exothermic, and the relative amounts of adduct and copolymer are temperature dependent. It has been reported (81) that the rate of copolymerization is very fast compared with the rate of homopolymerization of the diene or the dienophile, and the energy of activation is approximately 5 kcal./mole. Although the rate of copolymerization increases at elevated temperatures, the simultaneous adduct formation which also occurs more readily at elevated temperatures limits the maximum rate to lower temperatures.

Catalysis of the diene-dienophile Diels-Alder reaction was not considered feasible until recently. Thus, although those adducts which were difficult to form could be produced at elevated temperatures and after prolonged reaction times, it was not considered possible to catalyze the reaction so that it would proceed under milder conditions.

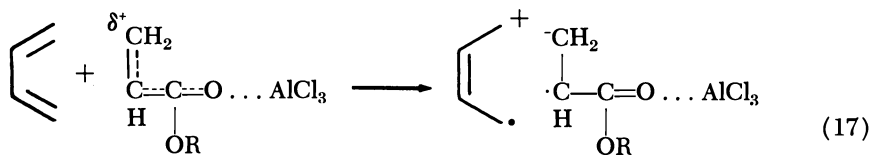
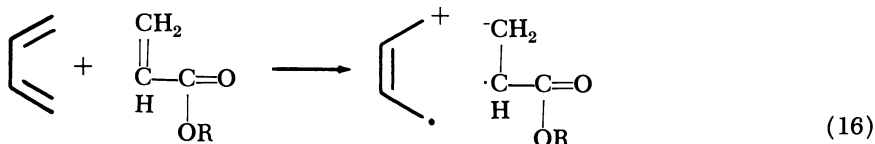
Within the last few years, it has conclusively been demonstrated that the Diels-Alder reaction is susceptible to catalysis with Lewis acids or Friedel-Crafts catalysts such as aluminum chloride (15, 18, 36, 37, 38, 39, 40, 57, 67, 68, 69, 70, 71, 82, 86). As a result of catalysis, it was possible to change the following:

- (1) Time-temperature-yield relationship—*i.e.*, increase the yield of adduct produced at a lower temperature after a shorter reaction time
- (2) Ratio of geometric isomers
- (3) Ratio of exo and endo isomers
- (4) Optical activity of adduct

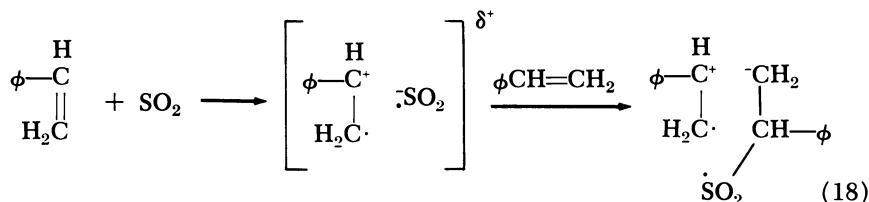
Since the latter effects result from a change in the transition state, it has been proposed that the aluminum chloride complexes with the polar group in the dienophile and influences the structure of the transition state. The catalysis can be considered to involve a greater electron-accepting character of the complexed dienophile compared with the



uncomplexed dienophile. As a consequence, the one-electron transfer from the electron donor diene occurs more readily, increasing the yield of diradical charge transfer complex.



Analogous to the influence of an electron acceptor such as a Lewis acid on the electron accepting character of a polar monomer, a strong electron acceptor is apparently capable of decreasing the electron donating character of an electron donor monomer. As a result, the electron-accepting characteristics of the donor monomer are increased relative to the unmodified monomer. Alternatively, a strong electron acceptor may increase the electron-accepting ability of a donor-acceptor complex, resulting in complexation with an additional molecule of the electron donor monomer. The formation of a copolymer containing two moles of styrene per mole of sulfur dioxide in the presence of an excess of the latter has been attributed (6) to a reaction of styrene with a 1:1 complex of styrene-sulfur dioxide.



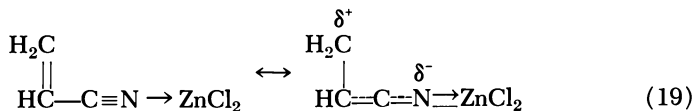
The polysulfones from vinyl chloride and vinyl bromide also contain two moles of vinyl halide per mole of sulfur dioxide (59, 60), apparently as a result of a similar reaction.

### *Homopolymerization of Metal Halide-Complexed Monomers*

The free radical initiated homopolymerization of acrylonitrile and methyl methacrylate in the presence of zinc chloride was characterized by an increase in the reaction rate and the molecular weight with increas-

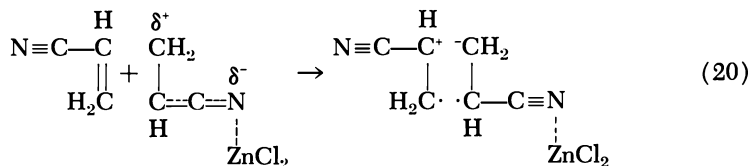
ing zinc chloride content (3, 30, 34). An equimolar complex could be isolated and polymerized much more readily than the uncomplexed monomer, either thermally or under the influence of free radicals or ultraviolet or gamma ray irradiation (33).

The greater reactivity in the presence of equimolar amounts of zinc chloride may result from the delocalization of the electrons in the double bond of the complexed monomer.



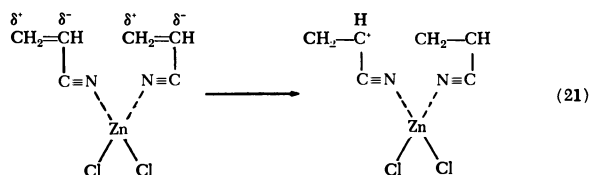
This has been proposed by Imoto and Otsu (33, 34) and confirmed by the molecular orbital calculations of Tazuke *et al.* (76, 77). A similar explanation has been advanced for the increased reactivity of vinylpyridines and vinylimidazoles in the presence of zinc salts (76, 77). Superdelocalizability as a result of conjugation with the metal salt results in spontaneous thermal polymerization.

Increased reactivity in the presence of less than equimolar amounts of zinc salt may result from the greater reactivity of the complexed monomer toward the growing chain end or by the formation of a complex between uncomplexed monomer and complexed monomer.



The increased reactivity of propagating radicals complexed with the metal salt towards uncomplexed monomer has been postulated (87) to account for the increased susceptibility of methyl methacrylate to ultraviolet light or free radicals in the presence of aluminum chloride or aluminum bromide. A similar explanation has been considered to account for the enhanced reactivity in the methyl methacrylate-zinc chloride and acrylonitrile-zinc chloride polymerization systems. However, the complex shown in Reaction 20 must equally be considered.

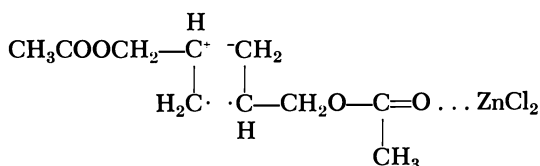
In the case of equimolar or less than equimolar metal salt concentrations, the salt may act as a bifunctional unit.



A similar association phenomena has been proposed (3) in the methyl methacrylate-zinc chloride system. The formation of "organized mobile monomer arrays" has been suggested to account for the accelerated polymerization of methyl methacrylate in the presence of aluminum bromide (87) and allyl alcohol and allyl acetate in the presence of zinc chloride (55, 87).

Russian workers have proposed that the increased activity of allyl acetate and allyl alcohol in free radical or gamma ray initiated polymerization in the presence of zinc chloride may be connected with the decreased degradative chain transfer with complexed monomer or the activation of the stabilized allyl radical in the complexed monomer—*i.e.*, the conversion of degradative chain transfer to effective transfer (55, 87). However, these explanations have been partially rejected as inadequate.

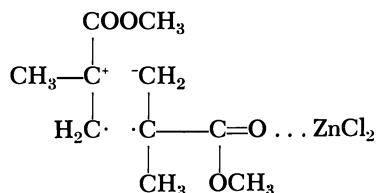
A more probable explanation is the formation of the charge transfer complex between uncomplexed and complexed monomer.



The homopolymerization of the complex would account for the increased reactivity.

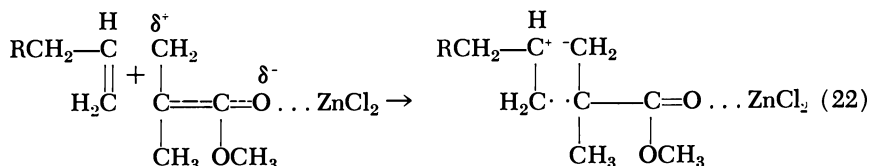
### *Copolymerization of Metal Halide-Complexed Monomers*

The most significant observation in the radical copolymerization of methyl methacrylate with vinylidene chloride in the presence of zinc chloride is the increase in the  $Q$  and  $e$  values of methyl methacrylate, the increase in the  $r_1$  value of methyl methacrylate, and the decrease in the  $r_2$  value of vinylidene chloride (30). Although it has been proposed that these results arise from the increased reactivity of the complexed methyl methacrylate monomer, a more likely explanation is the homopolymerization of a methyl methacrylate-complexed methyl methacrylate complex accompanied by the copolymerization of methyl methacrylate with vinylidene chloride.



An analogous situation would hold in the copolymerization of acrylonitrile with vinylidene chloride in the presence of zinc chloride (32).

The free radical copolymerization of methyl methacrylate or acrylonitrile in the presence of zinc chloride with allylic compounds such as allyl alcohol, allyl acetate, and allyl chloride or butene isomers such as isobutylene, 1-butene, and 2-butene is characterized by the incorporation of greater amounts of comonomer than is noted in the absence of zinc chloride (35). Analogous to the radical homopolymerization of allylic monomers in the presence of zinc chloride, the increase in the electron-accepting capability of the methyl methacrylate or acrylonitrile as a result of complexation results in the formation of a charge transfer complex which undergoes homopolymerization and/or copolymerization with a polar monomer-complexed polar monomer complex.



This explanation is more feasible than one based upon decreased degradative chain transfer with complexed monomer or the conversion of degradative to effective chain transfer in the presence of zinc chloride since it is improbable that the butene isomers would be complexed with zinc chloride.

The scope of this reaction is eloquently given in a patent (72) describing the copolymerization of polar with nonpolar monomers in the presence of a Friedel-Crafts and a free radical initiator. In the process "a polar monomer which contains strongly negative groups and that responds to free radical initiation but not Friedel-Crafts type of polymerization is complexed with a Friedel-Crafts halide, and then the complexed monomer is copolymerized, under anhydrous conditions, in the presence of a free radical initiator with a nonpolar monomer that responds to Friedel-Crafts but not free radical polymerization."

The polar monomers cited include acrylic acid, acrylic esters, methacrylic acid, methacrylic esters, acrylonitrile, methacrylonitrile, acrolein, and vinyl acetate. While this list is reasonable, it also includes vinyl halides and vinylidene halides, although no examples with the latter are given. In view of the fact that the vinyl and vinylidene halides do not form complexes with Friedel-Crafts catalysts, these monomers would not be expected to be operable, as demonstrated by the results of Imoto (30).

The "non-polar olefins or only mildly polar substituted olefins" cited include ethylene, propylene, isobutylene, 1-hexene, 2-methyl-1-pentene,  $\alpha$ -methylstyrene, isopropenyltoluene, and vinyl ethers.

Although the Friedel-Crafts halides which are listed include the typical halides of aluminum, boron, iron, titanium, and zinc, as well as others, all examples except one utilize zinc chloride as the complexing agent.

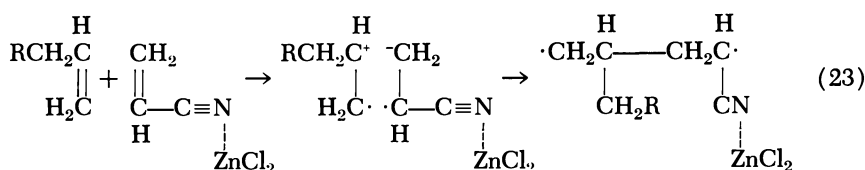
The combined effect of zinc chloride and benzoyl peroxide is clearly shown in the results of the copolymerization of 2-methyl-1-pentene and acrylonitrile at 60°C. (72) (Table I).

**Table I. Copolymerization of 2-Methyl-1-pentene and Acrylonitrile at 60°C.**

Catalysts, moles		Time, hr.	Yield (based on AN), %
$Bz_2O_2$	$ZnCl_2$		
0.0017	0	6.3	0
0	0.2	6.1	8.5
0.0004	0.2	1.1	60

The products in the olefin-polar monomer reactions were shown to be copolymers by elemental analysis and solubility in acetone, a non-solvent for the homopolymers.

Although the structures of these copolymers were not indicated, it is probable that the olefin and polar monomer are alternating units in accordance with the scheme in Reaction 23. It is also probable that the presence of excess polar monomer in the copolymer, as indicated in some examples, results from copolymerization of the polar monomer-complexed polar monomer complex or with the olefin-complexed polar monomer complex or concurrent homopolymerization of the two complexes.

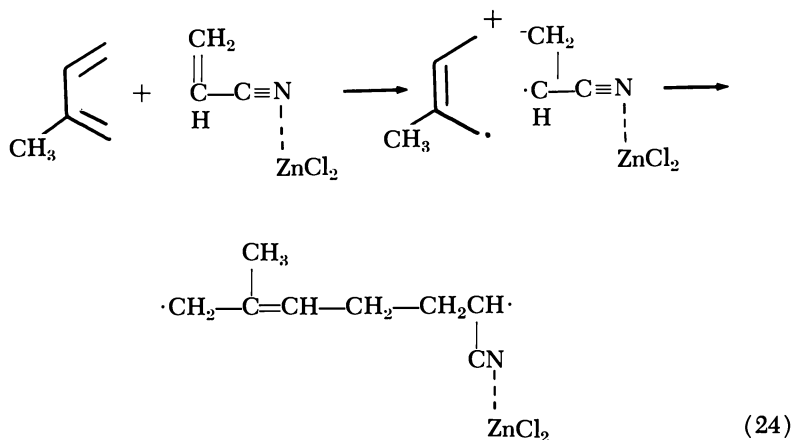


In view of the failure to produce any polymer in the presence of peroxide and the absence of zinc chloride, probably caused by the slow rate of radical formation at 60°C., it is also unlikely that the excess polar monomer enters by the coupling of a growing chain with a radical from the diradical complex. It is significant, however, that a very small concentration of radicals is sufficient to open the complex.

Owing to the insolubility of the polar monomer-zinc chloride complex, handling of the reaction mixture is difficult. However, a second patent (73) describes an improved process wherein the polar monomer is utilized in considerable excess with no effect on the polar monomer content of the resulting copolymer, in contrast to the results from a conventional free radical polymerization. This is consistent with the mechanism shown in Reaction 23 and essentially eliminates the participation of a polar monomer-complexed polar monomer complex.

The process improvement patent (73) also describes the preparation of an acrylonitrile-isoprene copolymer using azobisisobutyronitrile as free radical initiator and zinc chloride as complexing agent. The reaction is carried out using 1-50 moles of acrylonitrile per mole of isoprene and a 10:1 molar ratio of acrylonitrile to zinc chloride. The copolymer, obtained in 16.8% yield (calculated as a 1:1 copolymer), contains 48.2 weight % of acrylonitrile, corresponding to a 1.2:1 acrylonitrile-isoprene molar ratio, and is soluble in acetone and chloroform, in marked contrast to the solubility of the corresponding copolymer prepared with free radical initiators.

This copolymer is apparently an essentially completely alternating copolymer resulting from the greater electron-donating power of the isoprene compared with that of an olefin.



As a result of the enhanced electron-accepting capability of the complexed acrylonitrile, interaction with a strong electron donor such as a conjugated diene should result in the formation of a charge transfer complex capable of undergoing spontaneous opening in the absence of a free radical catalyst.

The probable correctness of this hypothesis was indicated by an earlier qualitative observation, made during an investigation of the cyclo-

polymerization of conjugated dienes with Lewis acid catalysts, that the addition of one drop of isoprene to a mixture of acrylonitrile and ethylaluminum dichloride resulted in an exothermic reaction and the formation of a solid product. However, the nature of this product—*i.e.*, whether it was an isoprene-acrylonitrile copolymer or polyacrylonitrile—was not determined.

Further evidence for the hypothesis was found in the patent describing the isoprene-acrylonitrile-zinc chloride system (23). On adding a four-fold excess of isoprene to an equimolar mixture of acrylonitrile and zinc chloride, in the absence of a free radical catalyst, an exothermic reaction occurs after approximately 30 minutes. The recovered polymer is insoluble in hydrocarbons, chloroform, and acetone. This eliminates polyisoprene and the alternating copolymer. The yield of product is 12%, calculated a polyacrylonitrile, compared with the 16.8% yield of copolymer obtained when excess acrylonitrile and a free radical catalyst are used.

To elucidate the nature of the product and confirm the postulated copolymerization, the reaction of isoprene and butadiene with acrylonitrile in the presence of zinc chloride was investigated. In the absence of solvent or in the presence of a small amount of benzene, the addition of a small amount of isoprene to an equimolar mixture of acrylonitrile and zinc chloride results in spontaneous polymerization, and the solution turns orange.

Table II. Copolymerization of Isoprene (I)

No.	Diene	Solvent, ml.	Catalyst, <sup>b</sup> grams	Temp., °C.
1	I			70-37
2				-78-23
3		Benzene 50	AIBN 0.15	55
4		Benzene 50	TBPP 1.34	60-70
5		Heptane 50	TBPP 1.34	60-70
6		Heptane 50	TBPP 1.34	70
		Dioxane 10		
7	B	Heptane 50	TBPP 1.34	60-70
		Dioxane 10		
8		Heptane 50	TBPP 1.34	60
		Dioxane 10		

<sup>a</sup> AN 10.6 grams (0.2 mole), diene 13.6 grams (0.2 mole), ZnCl<sub>2</sub> 27.3 grams (0.2 mole).

<sup>b</sup> AIBN = azobisisobutyronitrile; TBPP = *tert*-butyl peroxyphthalate.

<sup>c</sup> A = diene added to AN-ZnCl<sub>2</sub> complex; B = diene-AN added to ZnCl<sub>2</sub>; C = diene-AIBN added to AN-ZnCl<sub>2</sub> in solvent; D = diene-AN-TBPP added to ZnCl<sub>2</sub> in solvent; E = diene added to AN-TBPP in solvent, ZnCl<sub>2</sub> absent.

As shown in Table II, in the absence of a free radical catalyst, the reaction of isoprene with acrylonitrile in the presence of zinc chloride results in a less than 10% yield of product containing 66–74 mole % acrylonitrile. In the presence of both free radical catalyst and zinc chloride the yield of product is greatly increased. The product contains more than 85 mole % acrylonitrile when the isoprene and catalyst are added to precomplexed acrylonitrile.

The addition of a mixture of monomers and catalyst to a suspension of zinc chloride in benzene or heptane gives 56 and 77% yield, respectively, of methanol-insoluble product containing *ca.* 57 mole % of acrylonitrile in both cases. Extraction of the product from the reaction carried out in heptane gave 8% of a DMF-soluble fraction which contained 90.9 mole % acrylonitrile and 92% of a DMF-insoluble fraction which contained 52.8% acrylonitrile, close to the theoretical value for an equimolar copolymer. In addition, the reaction mixture gave a 3.9% yield of a methanol-soluble fraction which contained 28.5 mole % acrylonitrile.

In the absence of zinc chloride, the free radical catalyzed polymerization of isoprene and acrylonitrile gave a 19% yield of copolymer containing more than 40% acrylonitrile.

The effects of an equimolar amount of zinc chloride and the presence of a free radical catalyst in the copolymerization of equimolar amounts of acrylonitrile and isoprene at 60°–70°C. are summarized in Table III.

#### or Butadiene (B) with Acrylonitrile (AN)<sup>a</sup>

Time, hr.	Polymer		Procedure <sup>c</sup>
	Yield, %	AN, %	
3	3.3	66.3	A
3	9.7	74.4	B
0.16	30.3	85.6	C
1.5	56.3	57.7	D
1.5	77.3 <sup>d</sup>	56.7	D
1.5	18.7	44.0	E
1.5	84.5	55.7	D
1.5	4.4	54.9	E

<sup>a</sup> 92% DMF-insoluble fraction contains 52.8 mole % AN, 8% DMF-soluble fraction contains 90.9 mole % AN. Reaction mixture also yields 3.9% methanol-soluble fraction which contains 28.5 mole % AN.

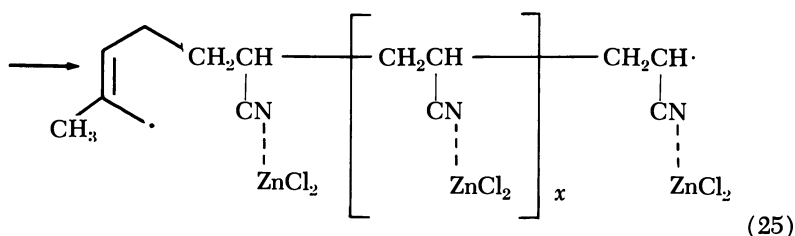
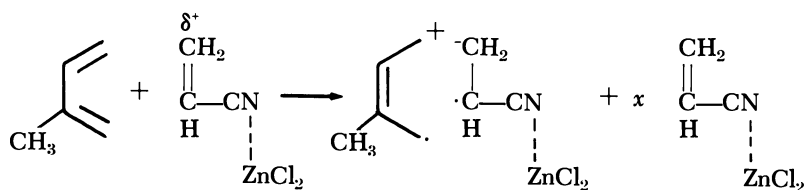


**Table III. Copolymerization of Acrylonitrile and Isoprene at 60–70°C.**

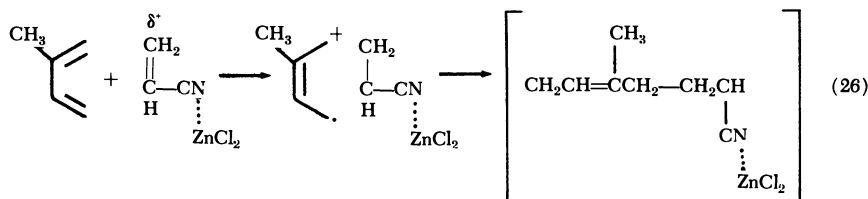
TBPP	ZnCl <sub>2</sub>	Yield (based on AN + I), %	AN in Polymer, mole %
Present	Absent	18.7	44
Absent	Present	3–10	66–74
Present	Present	71	53

Three reactions apparently occur simultaneously—*i.e.*,

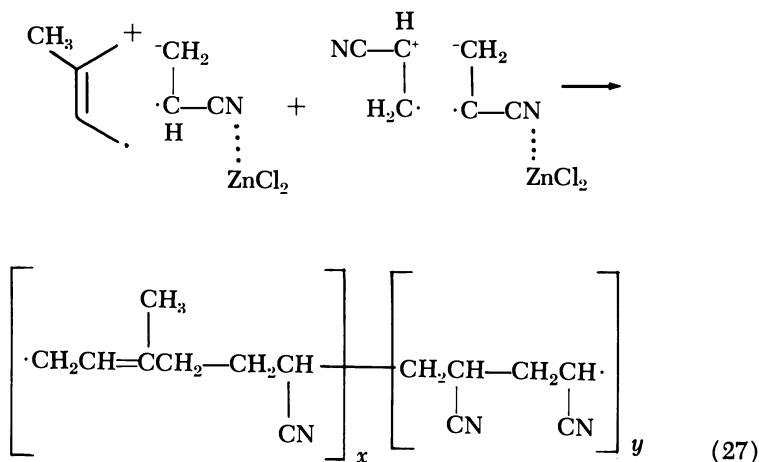
(1) Homopolymerization of complexed acrylonitrile initiated by a one-electron transfer from isoprene monomer:



(2) Spontaneous homopolymerization of the (isoprene-complexed acrylonitrile) complex:



(3) Spontaneous copolymerization of the (isoprene-complexed acrylonitrile) complex with an (acrylonitrile-complexed acrylonitrile) complex:



Reactions 25 and 27 differ in the acrylonitrile content.

In the absence of a free radical catalyst, Reaction 25 is dominant, particularly when precomplexed acrylonitrile is present, accompanied by Reaction 27. In the presence of both a free radical catalyst and zinc chloride, Reactions 25, 26, and 27 occur simultaneously. In addition, Reactions 26 and 27 are initiated by free radicals.

Similar results are obtained in the copolymerization of butadiene and acrylonitrile (Table IV).

**Table IV. Copolymerization of Butadiene with Acrylonitrile**

No.	TBPP	ZnCl <sub>2</sub>	Yield, %	AN, %	Copolymer		
					Microstructure, %		
					<i>trans</i> -1,4	<i>cis</i> -1,4	1,2
1	Present	Absent	4.4	54.9	68.5	17.3	14.1
2	Present	Present	84.5	55.7	86.1	9.7	4.8

The microstructure of the copolymer produced in the absence of zinc chloride is reasonably consistent with the analysis of a commercial free radical 1:1 copolymer—*i.e.*, 20.6% *cis*-1,4 and 73.8% *trans*-1,4 structure. The increased 1,4 content in the polymer produced in the presence of zinc chloride is consistent with the postulated charge transfer complex mechanism.

Hirooka *et al.* (27, 29) recently reported that an equimolar mixture of acrylonitrile and ethylaluminum dichloride form a complex whose infrared spectrum is similar to that of the acrylonitrile-zinc chloride complex of Imoto *et al.* (33). The complex is a liquid above 0°C. and

crystallizes below  $-10^{\circ}\text{C}$ . It is stable and does not undergo homopolymerization under nitrogen.

The addition of propylene to the complex suspended in toluene or the addition of ethylaluminum dichloride to a mixture of propylene and acrylonitrile in the presence or absence of solvent at  $-78^{\circ}\text{C}$ . resulted in a rapid reaction to yield a high molecular weight 1:1 copolymer, irrespective of the initial ratio of monomers. Neither propylene nor acrylonitrile undergo homopolymerization under the same conditions.

The high molecular weight copolymer is soluble in acetonitrile, acetone, and acetic anhydride which are non-solvents for the homopolymers. Similar 1:1 copolymers are produced when ethylene, 1-hexene, 1-octadecene, isobutylene, or styrene is substituted for propylene (29).

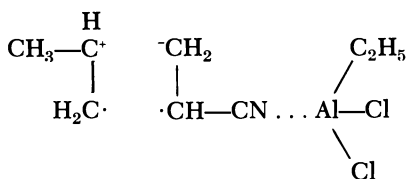
No reaction occurs when triethylaluminum, aluminum chloride, stannic chloride, titanium tetrachloride, diethylzinc or triethylboron are used in lieu of an organoaluminum halide or sesquihalide.

Hirooka has proposed that the products are alternating copolymers produced through "complex copolymerization" and that the latter process differs from that of Imoto and Otsu (30, 33, 34) in which a free radical initiator is necessary for the random copolymerization of olefins with acrylonitrile or methyl methacrylate in the presence of zinc chloride.

As previously discussed, the copolymers produced in the zinc chloride-free radical system are not necessarily random copolymers but are probably the result of the copolymerization of the acrylonitrile-complexed acrylonitrile complex with the olefin-complexed acrylonitrile complex. Further, the olefin-alkylaluminum halide complexed acrylonitrile complex only differs from the olefin-zinc chloride complexed acrylonitrile complex in degree rather than in kind—*i.e.*, the former is an unstable charge transfer complex capable of spontaneous uncoupling of the diradical system followed by intermolecular diradical coupling, while the latter is a stable charge transfer complex requiring radical attack to uncouple the diradical system.

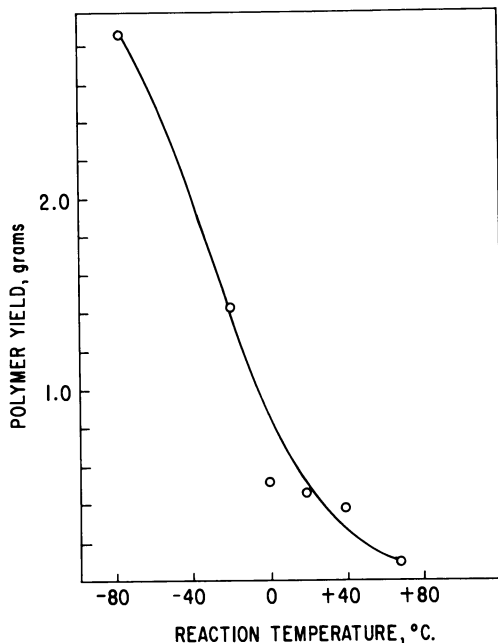
In order to confirm this hypothesis, in the absence of oxygen-free radical catalysts effective at  $-78^{\circ}\text{C}$ ., the temperature dependence of the propylene-acrylonitrile copolymerization in the presence of ethylaluminum dichloride was investigated.

As shown in Figure 1, the yield of copolymer is extremely temperature dependent, indicating that either the acrylonitrile-ethylaluminum dichloride complex is unstable or the propylene-ethylaluminum dichloride complexed acrylonitrile complex is not formed as the temperature is increased.



In later communications (27, 28) Hirooka reported that in addition to acrylonitrile, other conjugated monomers such as methyl acrylate and methyl methacrylate formed active complexes with organoaluminum halides, and the latter yielded high molecular weight 1:1 alternating copolymers with styrene and ethylene. However, an unconjugated monomer such as vinyl acetate failed to copolymerize with olefins by this technique.

Although the infrared spectra of the equimolar styrene-methyl acrylate or methyl methacrylate copolymers prepared in the presence of ethylaluminum sesquichloride and the equimolar copolymers prepared with azobisisobutyronitrile are very similar, the nuclear magnetic resonance spectra of the former are distinctly different from the latter and



*Figure 1. Dependence of complex stability (i.e., polymer yield) on reaction temperature. Propylene, 50 grams; acrylonitrile, 2 grams; ethylaluminum dichloride, 50 mmoles; toluene, 30 ml.; reaction time, 30 min.*

have simpler and well-separated patterns. It is therefore concluded that the copolymers produced by the complexing system are alternating copolymers (28).

Since the styrene-methyl acrylate and styrene-methyl methacrylate copolymers could be prepared in toluene solution at 25°C., it became possible to investigate the influence of free radicals on the ethylaluminum sesquihalide complexed system. 2-Methylpentanoyl peroxide (Lucidol R-226), having a half-life of 10 hours at 27°C. in 0.2M solution in mineral spirits was used as the free radical source at 25°C.

Two styrene-methyl methacrylate ratios were examined: 61.5/38.5 and 20/80 (Table V). Although the results with the two ratios cannot be compared since the reactions were carried out under different conditions, the results with different catalyst systems for the same ratio are comparable (Table VI).

**Table V. Copolymerization of Styrene and Methyl Methacrylate**

<i>Reactants:</i>						
S/MMA mole ratio	_____	61.5/38.5	_____	_____	20/80	_____
Styrene, grams	_____	5.0	_____	_____	3.12	_____
moles	_____	0.048	_____	_____	0.03	_____
Methyl methacrylate, grams	_____	3.0	_____	_____	12.0	_____
moles	_____	0.03	_____	_____	0.12	_____
Toluene, ml.	50	50	50	50	50	50
AlEt <sub>1.5</sub> Cl <sub>1.5</sub> , mmoles	0	30	30	0	30	30
Peroxide, gram	0.69	0	0.69	0.69	0	0.69
mmoles	3	0	3	3	0	3
<i>Conditions:</i>						
Temp., °C.	25	25	25	30	30	30
Time, min.	30	30	30	60	60	60
<i>Polymer:</i>						
Yield, grams	trace	0.19	1.00	0.15	0.75	2.12
% <sup>a</sup>	—	3.1	14.6	—	12.3	34.6
[ $\eta$ ] <sup>b</sup>	—	—	—	0.03	1.14	0.89
Analyses, ° % C	—	75.18	76.11	67.70	74.96	74.78
% H	—	7.97	7.74	7.92	8.03	8.01
Methyl methacrylate, mole %	—	53.7	51.5	77.1	54.2	54.8

<sup>a</sup> Calculated as 1:1 copolymer.

<sup>b</sup> Intrinsic viscosity measured at 25°C. in cyclohexanone.

<sup>c</sup> Calculated analysis for 1:1 copolymer: C, 76.45; H, 7.89.

Although the yield of copolymer is higher when the organoaluminum halide is used as catalyst in lieu of the peroxide, the combination of the two gives a 3-5 times higher yield. However, since the product is essentially the same 1:1 copolymer in either case, as compared with the entirely

Table VI. Copolymerization of Styrene and Methyl Methacrylate

		Initial S/MMA mole ratio			
		61.5/38.5		20/80	
		Copolymer			
Peroxide	$AlEt_{1.5}Cl_{1.5}$	Yield, grams	% MMA	Yield, grams	% MMA
Present	Present	0	—	0.15	77.1
Absent	Absent	0.19	53.7	0.75	54.2
Present	Present	1.00	51.5	2.12	54.8

different composition obtained by using the radical catalyst alone, the higher yield is obviously not an additive effect. The interaction of the Lewis acid and the peroxide resulting in an increased rate of radical generation can also be eliminated since the intrinsic viscosities of the polymers are similar and high compared with the low value obtained with the radical catalyst alone (Table V).

Figure 2 indicates how the results differ from those in a normal radical, anionic, or cationic polymerization. The data confirm the postu-

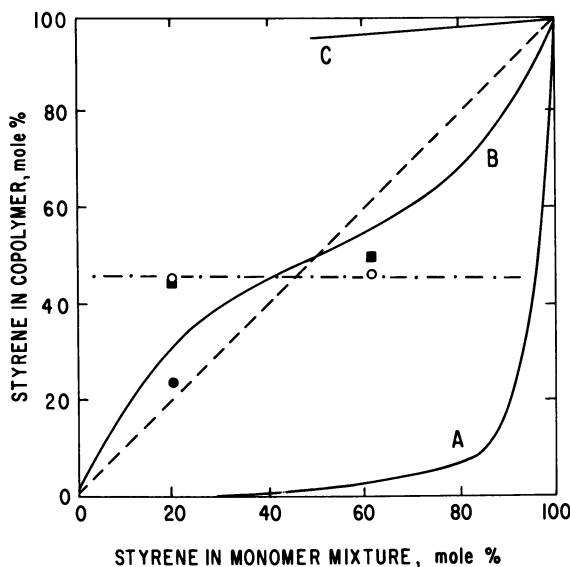


Figure 2. Copolymerization of styrene and methyl methacrylate

- A: Anionic catalysis
- B: Radical catalysis
- C: Cationic catalysis
- : Radical catalyst, this work
- :  $AlEt_{1.5}Cl_{1.5}$ , this work
- : Radical catalyst plus  $AlEt_{1.5}Cl_{1.5}$

late that the ethylaluminum halide-complexed system is of the same type as the zinc chloride-complexed system. They differ only in that the zinc chloride system requires the input of energy, in the present instance in the form of free radicals, to initiate the opening of the charge transfer complex, while the organoaluminum halide system undergoes spontaneous opening to an extent, and additional opening occurs under radical attack.

Hirooka (29) has proposed that copolymerizations of this type be named "complex copolymerization." Russian workers (55) have suggested that polymerizations initiated by radical catalysts in the presence of a complexing agent be called "complex-radical processes." Both polymerizations are more appropriately considered as polymerizations through activated charge transfer complexes, in which the Lewis acid or metal halide catalyzes the formation of the complex, and free radicals may or may not be necessary to initiate the homopolymerization of the complex.

### *Experimental*

**Copolymerization of Isoprene and Acrylonitrile.** Anhydrous zinc chloride (heated at 240°C. for 1 hour *in vacuo*), 27.3 grams (0.2 mole), was weighed into a 300-ml. reaction flask fitted with a thermometer, serum cap, and reflux condenser. Benzene, 50 ml., was added, and the reaction mixture was heated to 70°C. under nitrogen. A mixture of 10.6 grams (0.2 mole) acrylonitrile, 13.6 grams (0.2 mole) isoprene, and 1.34 grams of a 75% solution of *tert*-butyl peroxyvalate in hexane was added slowly. After 2 ml. of monomer mixture were added, the reaction mixture solidified. The mass was broken up with a spatula and the remainder of the monomer mixture was added. The temperature fell and was maintained at 55°C. during the addition. After 15 minutes the temperature was raised to 65°C., and refluxing was continued under nitrogen for 1.5 hours. The reaction mixture was poured into a Waring mixer and agitated with DMF. The resultant slurry was mixed with a large quantity of methanol to give a white precipitate. The latter was stirred with a small quantity of aqueous HCl, filtered, washed with methanol and dried *in vacuo* at 50°C. overnight. The yield of methanol-insoluble product was 13.6 grams (56.3%).

Analysis: found: C, 72.26; H, 7.98; N, 12.96; ash 0.1. Calc. for 1:1 copolymer: 7, 79.30; H, 9.15; N, 11.56.

Evaporation of the filtrate gave 1.39 grams of a hard material which was not identified further.

**Copolymerization of Butadiene and Acrylonitrile.** The same procedure was used except that the zinc chloride was stirred in a mixture of 30 ml. heptane and 15 ml. dioxane. Butadiene, acrylonitrile, and *tert*-butyl peroxyvalate were dissolved in 20 ml. heptane. The yield of polymer was 18.1 grams (84.5%).

Analysis: found: C, 75.33; H, 7.93; N, 14.26. Calc. for 1:1 copolymer: C, 78.46; H, 8.46; N, 13.07.

**Copolymerization of Propylene and Acrylonitrile.** Into a three-necked, round-bottomed flask equipped with a thermometer, Teflon-coated magnetic stirrer bar, reflux condenser, and gas inlet and outlet were added 30 ml. of toluene and 2 grams of distilled acrylonitrile. Nitrogen was bubbled through the solution, and all reactions were carried out under a nitrogen atmosphere.

The solution was cooled to  $-20^{\circ}\text{C}$ ., and 50 mmoles of  $\text{AlEtCl}_2$  were added dropwise to prepare the AN- $\text{AlEtCl}_2$  complex. The solution of complex was warmed to the desired temperature and 50 grams of propylene which had been passed through columns containing KOH pellets and molecular sieves were passed into the reaction mixture in 30 min. The reaction is so rapid that reaction times longer than 5-6 min. make no difference in this polymer yield. The reaction solution was then poured into a large amount of methanol to precipitate the polymer, which was filtered, washed with fresh methanol, and dried to constant weight. If necessary, the polymer was dissolved in acetone and reprecipitated from methanol.

**Copolymerization of Styrene and Methyl Methacrylate.** Using the same apparatus as described above, 40 ml. of toluene and the required amount of methyl methacrylate were mixed, and nitrogen was bubbled through the solution. Ethylaluminum sesquihalide or a 1:1 premixed  $\text{AlEt}_2\text{Cl}-\text{AlEtCl}_2$  mixture was added slowly, keeping the temperature at  $25^{\circ}-30^{\circ}\text{C}$ . under a nitrogen atmosphere. The mixture was stirred for about 5 min., and a solution of 10 ml. toluene, the required amount of styrene, and 0.69 gram of R-226 was added.

After addition of the styrene solution, the reaction mixture temperature was maintained at  $30^{\circ}\text{C}$ . and stirred for 30 or 60 min. The reaction solution was then poured into 1 liter of methanol which contained 0.1 gram of hydroquinone and allowed to settle. After filtration, the precipitate was washed with fresh methanol and dried to constant weight.

Analysis: for 61.5/38.5 S/MMA initial charge: found: C, 76.11; H, 7.74. For 20/80 S/MMA initial charge: found: C, 74.78; H, 8.01. Calc. for 1:1 copolymer: C, 76.45; H, 7.89.

### Literature Cited

- (1) Alfrey, T., Bohrer, J. J., Mark, H., "Copolymerization," Interscience, New York, 1952.
- (2) Arthur, J. C., Jr., Blovin, F. A., *J. Appl. Polymer Sci.* **8**, 2813 (1964).
- (3) Bamford, C. H., Brumby, S., Wayne, R. P., *Nature* **209**, 292 (1966).
- (4) Bamford, C. H., Jenkins, A. D., *J. Polymer Sci.* **29**, 355 (1958).
- (5) Bamford, C. H., Jenkins, A. D., Johnston, R. J., *Proc. Roy. Soc. (London)* **A241**, 364 (1957).
- (6) Barb, W. G., *Proc. Roy. Soc. (London)* **A212**, 66, 177 (1952).
- (7) Barr, D. A., Haszeldine, R. N., *J. Chem. Soc.* **1955**, 1881; **1956**, 3424.
- (8) Bartlett, P. D., Nozaki, K., *J. Am. Chem. Soc.* **68**, 1495 (1946).
- (9) Booth, D., Dainton, F. S., Ivin, K. J., *Trans. Faraday Soc.* **55**, 1293 (1959).
- (10) Bovey, F. A., *J. Polymer Sci.* **47**, 480 (1960).



- (11) Crawford, G. H., Rice, D. E., Landrum, B. F., *J. Polymer Sci.* **A1**, 565 (1963).
- (12) Dainton, F. S., Bristow, G. M., *Proc. Roy. Soc. (London)* **A229**, 509, 525 (1955).
- (13) Dainton, F. S., Ivin, K. J., *Proc. Roy. Soc. (London)* **A212**, 207 (1952).
- (14) Dilling, W. L., Little, J. C., *J. Am. Chem. Soc.* **89**, 2741 (1967).
- (15) Farmer, R. F., Hamer, J., *J. Org. Chem.* **31**, 2418 (1966).
- (16) Fettes, E. M., Davis, F. O., "Polyethers, Part III, Polyalkylene Sulfides and Other Polythioethers," N. C. Gaylord, Ed., Chap. XV, p. 225, Interscience, New York, 1962.
- (17) Field, N. D., *J. Am. Chem. Soc.* **83**, 3504 (1961).
- (18) Fray, G. I., Robinson, R., *J. Am. Chem. Soc.* **83**, 249 (1961).
- (19) Fujioka, S., Shinohara, Y., Hayashi, K., *Kogyo Kagaku Zasshi* **69**, 330 (1966).
- (20) Gilbert, H., Miller, F. F., Averill, S. J., Carlson, E. J., Folt, V. L., Heller, H. J., Stewart, F. J., Schmidt, R. F., Trumbull, H. L., *J. Am. Chem. Soc.* **78**, 1669 (1956).
- (21) Gindin, L., Abkin, A., Medvedev, S., *J. Phys. Chem. (U.S.S.R.)* **21**, 1269 (1947); *Chem. Abstr.* **42**, 5715c (1948).
- (22) Haas, H. C., *Makromol. Chem.* **80**, 232 (1964).
- (23) Haas, H. C., Karlin, E. R., *J. Polymer Sci.* **9**, 588 (1952).
- (24) Hanford, W. E., U. S. Patent **2,396,785** (March 19, 1946); **2,378,629** (June 19, 1945).
- (25) Hayashi, H., Ito, I., Saegusa, T., Furukawa, J., *Kogyo Kagaku Zasshi* **65**, 1634 (1962).
- (26) Hill, R., Lewis, J. R., Simonsen, J. L., *Trans. Faraday Soc.* **35**, 1067, 1073 (1939).
- (27) Hirooka, M., *Kobunshi* **16**, 1172 (1967).
- (28) Hirooka, M., Yabuuchi, H., Iseki, J., Nakai, Y., *J. Polymer Sci., A-1* **6**, 1381 (1968).
- (29) Hirooka, M., Yabuuchi, H., Morita, S., Kawasumi, S., Nakaguchi, K., *J. Polymer Sci.* **B5**, 47 (1967).
- (30) Imoto, M., Otsu, T., Harada, Y., *Makromol. Chem.* **65**, 180 (1963).
- (31) Imoto, M., Otsu, T., Ito, T., *Bull. Chem. Soc. Japan* **36**, 310 (1963).
- (32) Imoto, M., Otsu, T., Murata, K., *Kogyo Kagaku Zasshi* **66**, 1900 (1963).
- (33) Imoto, M., Otsu, T., Nakabayashi, M., *Makromol. Chem.* **65**, 194 (1963).
- (34) Imoto, M., Otsu, T., Shimizu, S., *Makromol. Chem.* **65**, 174 (1963).
- (35) Imoto, M., Otsu, T., Yamada, B., Shimizu, A., *Makromol. Chem.* **82**, 277 (1965).
- (36) Inukai, T., Kasai, M., *J. Org. Chem.* **30**, 3567 (1965).
- (37) Inukai, T., Kojima, T., *J. Org. Chem.* **31**, 1121 (1966).
- (38) *Ibid.*, p. 2032.
- (39) *Ibid.*, **32**, 869 (1967).
- (40) *Ibid.*, p. 872.
- (41) Ito, I., Hayashi, H., Saegusa, T., Furukawa, J., *Kogyo Kagaku Zasshi* **65**, 703, 1634 (1962).
- (42) Ito, I., Hayashi, H., Saegusa, T., Furukawa, J., *Makromol. Chem.* **55**, 15 (1962).
- (43) Ito, I., Saegusa, T., Furukawa, J., *Kogyo Kagaku Zasshi* **65**, 1878 (1962).
- (44) Ito, M., Kuri, Z., *Kogyo Kagaku Zasshi* **70**, 1011 (1967).
- (45) Iwatsuki, S., Murakami, M., Yamashita, Y., *Kogyo Kagaku Zasshi* **68**, 1967 (1965).
- (46) Iwatsuki, S., Nishio, K., Yamashita, Y., *Kogyo Kagaku Zasshi* **70**, 384 (1967).
- (47) Iwatsuki, S., Shin, M., Yamashita, Y., *Makromol. Chem.* **102**, 232 (1967).

- (48) Iwatsuki, S., Tanaka, Y., Yamashita, Y., *Kogyo Kagaku Zasshi* **67**, 1467 (1964).
- (49) Iwatsuki, S., Yamashita, Y., *J. Polymer Sci., A-1* **5**, 1753 (1967).
- (50) Iwatsuki, S., Yamashita, Y., *Kogyo Kagaku Zasshi* **67**, 1470 (1964).
- (51) *Ibid.*, **68**, 1138, 1963 (1965).
- (52) Iwatsuki, S., Yamashita, Y., *Makromol. Chem.* **89**, 205 (1965).
- (53) Kargin, V. A., Kabanov, V. A., Zubov, V. P., *Vysokomolekul. Soedin.* **2**, 765 (1960).
- (54) Kinsinger, J. B., private communication, through M. Szwarc, *Makromol. Chem.* **35**, 132 (1959).
- (55) Kulikova, V. P., Savinova, I. V., Zubov, V. P., Kabanov, V. A., Polak, L. S., Kargin, V. A., *Vysokomolekul. Soedin.* **9**, 299 (1967).
- (56) Little, J. C., *J. Am. Chem. Soc.* **87**, 4020 (1965).
- (57) Lutz, E. F., Bailey, G. H., *J. Am. Chem. Soc.* **86**, 3899 (1964).
- (58) Martin, M. M., Jensen, N. P., *J. Org. Chem.* **27**, 1201 (1962).
- (59) Marvel, C. S., Dunlap, L. H., *J. Am. Chem. Soc.* **61**, 2709 (1939).
- (60) Marvel, C. S., Glavis, F. J., *J. Am. Chem. Soc.* **60**, 2622 (1938).
- (61) Matsuda, M., Iino, M., Tokura, N., *Makromol. Chem.* **52**, 98 (1962).
- (62) Mayo, F. R., Lewis, F. M., Walling, C., *J. Am. Chem. Soc.* **70**, 1529 (1948).
- (63) Mayo, F. R., Walling, C., *Chem. Rev.* **46**, 191 (1950).
- (64) Montgomery, L. K., Schueller, K., Bartlett, P. D., *J. Am. Chem. Soc.* **86**, 622 (1964).
- (65) Otsu, T., Yamada, B., Imoto, M., *J. Macromol. Chem.* **1**, 61 (1966).
- (66) Parrod, J., Monteiro, H., *Compt. rend.* **251**, 2026 (1960).
- (67) Robinson, R., Fray, G. I., British Patent **835,840** (1960).
- (68) Sauer, J., Kredel, J., *Angew. Chem. Intern. Ed.* **4**, 989 (1965).
- (69) Sauer, J., Kredel, J., *Tetrahedron Letters* **1966**, 731.
- (70) *Ibid.*, p. 6359.
- (71) Sauer, J., Lang, D., Wiest, H., *Chem. Ber.* **97**, 3208 (1964).
- (72) Serniuk, G. E., Thomas, R. M., U. S. Patent **3,183,217** (May 11, 1965); British Patent **946,052** (Jan. 8, 1964).
- (73) Serniuk, G. E., Thomas, R. M., U. S. Patent **3,278,503** (Oct. 11, 1966).
- (74) Strzelecki, L., *Bull. Soc. Chim. France* **1967**, 2659.
- (75) Sumitomo, H., Kobayashi, K., Hachihama, Y., *Kogyo Kagaku Zasshi* **67**, 1658 (1964).
- (76) Tazuke, S., Okamura, S., *J. Polymer Sci.* **B5**, 95 (1967).
- (77) Tazuke, S., Tsuji, K., Yonezawa, T., Okamura, S., *J. Phys. Chem.* **71**, 2957 (1967).
- (78) Thomas, R. M., Sparks, W. J., U. S. Patent **2,373,067** (April 3, 1945).
- (79) Tokura, T., Matsuda, M., *Kogyo Kagaku Zasshi* **64**, 501 (1961); **65**, 1095 (1962).
- (80) Tokura, N., Matsuda, M., Anakawa, K., *J. Polymer Sci.* **A2**, 3355 (1964).
- (81) Tsuda, Y., Sakai, T., Shinohara, Y., *I.U.P.A.C. Intern. Symp. Macromol. Chem. Tokyo-Kyoto, Japan* **3**, 44 (1966).
- (82) Walborsky, H. M., Barash, L., Davis, T. C., *Tetrahedron* **19**, 2333 (1963).
- (83) Walling, C., Briggs, E. R., Wolfstirn, K. B., Mayo, F. R., *J. Am. Chem. Soc.* **70**, 1537 (1948).
- (84) Walling, C., Seymour, D., Wolfstirn, K. B., *J. Am. Chem. Soc.* **70**, 1544 (1948).
- (85) Yamashita, Y., Iwatsuki, S., Kokubo, T., *I.U.P.A.C. Intern. Symp. Macromol. Chem. Tokyo-Kyoto, Japan* **1**, 23 (1966).
- (86) Yates, P., Eaton, P., *J. Am. Chem. Soc.* **82**, 4436 (1960).

- (87) Zubov, V. P., Lachinov, M. B., Golubov, V. B., Kulikova, V. P., Kabanov, V. A., Polak, L. S., Kargin, V. A., *I.U.P.A.C. Intern. Symp. Macromol. Chem., Tokyo-Kyoto, Japan* **2**, 56 (1966).
- (88) Zutty, N. L., Wilson, C. W., III, Potter, G. H., Priest, D. C., Whitworth, C. J., *J. Polymer Sci.* **A3**, 2781 (1965).

RECEIVED March 25, 1968.

## ESR Studies of Vinyl Polymerization in Solution

KOICHI TAKAKURA and BENGT RÅNBY

The Royal Institute of Technology, Stockholm, Sweden

*The radical polymerization in aqueous solution of a series of monomers—e.g., vinyl esters, acrylic and methacrylic acids, amides, nitriles, and esters, dicarboxylic acids, and butadiene—have been studied in a flow system using ESR spectrometry. Monomer and polymer radicals have been identified from their ESR spectra.  $\beta$ -Coupling constants of vinyl ester radicals are low (12–13 gauss) and independent of temperature, tentatively indicating that the  $\beta$ -CH<sub>2</sub> group is locked with respect to the  $\alpha$ -carbon group. In copolymerization studies, the low reactivity of vinyl acetate has been confirmed, and increasing reactivity for maleic acid, acrylic acid, acrylonitrile, and fumaric acid in this order has been established by quantitative evaluation of the ESR spectra. This method offers a new approach to studies of free radical polymerization.*

One of the most promising advances in the application of electron spin resonance (ESR) studies to polymer chemistry has been the direct observation of transient free radicals involved in radical polymerization. Until recently, ESR studies of radical polymerization have been limited to solid-state systems or stiff gels in which the free radicals are more or less stabilized or trapped. The very short lifetime and the low concentration of the radicals in liquid systems precluded their analysis in liquids. Recently, however, Dixon and Norman (7, 8, 9) developed a rapid-mixing flow method which made it possible to observe well-resolved ESR spectra of short lived free radicals, using redox reactions for initiation. The redox system they used consists of acidified aqueous solutions of titanous chloride (TiCl<sub>3</sub>) and hydrogen peroxide (H<sub>2</sub>O<sub>2</sub>). On mixing the two reactants, hydroxyl radicals are formed rapidly. If a suitable

substrate is present in the system, the HO radicals react with it to produce the substrate radical which can be observed by ESR. The application of the flow method to investigate radical polymerization was first made by Fischer (11, 12, 13, 14, 15) mainly on acrylic and methacrylic monomers, while vinyl esters and butadiene were studied in this laboratory (33, 36). More recently, Todd *et al.* (6, 21) studied alkenes, vinyl fluoride, and vinyl chloride using the flow method. For all the monomer systems reported so far, ESR spectra attributed to monomer radicals formed by addition of an initiating radical to a monomer molecule, have been recorded. For certain monomers, the ESR spectra caused by growing polymer radicals have been observed, usually at higher monomer concentration.

On the other hand, Livingston and Zeldes (25, 26) have recently developed a flow technique combined with ultraviolet irradiation to study short-lived radicals in solution. They recorded well resolved ESR spectra of radicals obtained from a number of alcohols by hydrogen abstraction using  $H_2O_2$  as photosensitizer. No study, however, on the addition reaction to vinyl compounds has yet been reported.

The ESR method combined with a flow system should be very powerful for studying short lived transient radicals during vinyl polymerization in solutions. As will be made clear later, however, the conditions for the reaction occurring in the flow cell are quite different from the conventional solution polymerization studied during a steady-state process. Nevertheless, the hyperfine structure of the ESR spectra observed by the flow technique, can provide straightforward information on the structure, concentration, reactivity, and even the steric conformation of the transient radicals involved, particularly at the initial stage of the polymerization.

As a new approach, we have made ESR studies of polymerization and copolymerization mainly of vinyl esters using the rapid-mixing flow method. In addition to our work, studies by several workers in the same field are reviewed.

### **Experimental**

An aqueous flow system of the type described by Dixon and Norman (7, 8) was used. Two aqueous solutions acidified with sulfuric acid were used—*i.e.*, one is a  $TiCl_3$  solution and the other a solution of an oxidizing agent (*e.g.*,  $H_2O_2$ , hydroxylamine, or *tert*-butyl hydroperoxide), both solutions containing suitable amounts of monomer. The two solutions were mixed rapidly in the flow system immediately before they entered the flat cell in the ESR cavity (for details, *cf.* Ref. 36).

Unless otherwise stated, the reacting solutions we used were (a) an acidified (0.022M  $H_2SO_4$ ) aqueous  $TiCl_3$  (0.015M) and (b) either an

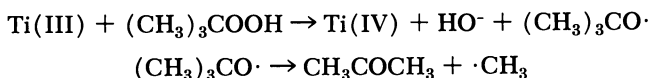
acidified (0.022M H<sub>2</sub>SO<sub>4</sub>) aqueous H<sub>2</sub>O<sub>2</sub> solution (0.2 ~ 0.3M) or an acidified aqueous hydroxylamine hydrochloride (0.5M). The flow rate was about 4 ml./sec. giving a time lag from mixing to entering into the ESR cell of about 0.02 sec. The ESR measurements were carried out using an X-band spectrometer with 100 kc./sec. field modulation (Japan Electron Optics Laboratory Co., Ltd., model JES-3B) at room temperature (22° ± 2°C.). The magnetic field was calibrated with proton magnetic resonance signals. The *g* values were measured with the spectrum of 1,1-diphenyl-2-picrylhydrazyl in methanol solution as a reference standard.

### Results and Discussion

**Initiator Systems.** The initiators used in this investigation are hydroxyl, amino, and methyl radicals, generated from the rapid reactions of Ti(III) with H<sub>2</sub>O<sub>2</sub>, NH<sub>2</sub>OH, and *tert*-butyl hydroperoxide, respectively, all in acidified aqueous solutions. Extensive ESR studies of free radical species from the reaction of Ti(III) with H<sub>2</sub>O<sub>2</sub> have been made by several workers (4, 7, 8, 19, 20, 27, 28, 36). In general, two ESR signals have been reported—*i.e.*, a principal peak at low magnetic field (Peak 1), and a minor peak at high field (Peak 2). However, there is no general agreement on the assignment of these two ESR signals, and conflicting proposals have been presented. We believe that the HO radicals which attack monomer molecules in this system show no ESR signal. The HO radicals are highly reactive and, therefore, are too short-lived to reach a steady-state concentration large enough for observation. According to our recent work (34) Peaks 1 and 2 in this system are unambiguously interpreted as being caused by HO<sub>2</sub>· and HO· radicals, respectively, both coordinated with Ti(IV) ions or a Ti(IV)–H<sub>2</sub>O<sub>2</sub> complex.

Addition reactions of amino radicals, ·NH<sub>2</sub>, to a number of vinyl monomers have been studied by Corvaja *et al.* (5). No ESR spectrum arising from free ·NH<sub>2</sub> radicals, however, has yet been observed, probably because of the high reactivity and low concentration also in this case.

Methyl radicals are also produced with Ti(III) ions in aqueous solution, probably according to the reaction:



The formation of CH<sub>3</sub> radicals is concluded from the observation of a quartet spectrum with separation of about 23 gauss in this system (7, 8).

Recently we found (3) that radical species from reactions in a Fenton's reagent (Fe(II)–EDTA + H<sub>2</sub>O<sub>2</sub>) can be used as initiator in the flow system, especially for vinyl compounds containing carboxylic

groups—*e.g.*, acrylic and maleic acid. Fenton's reagent was first used for ESR studies by Shiga (29). He reported that in the oxidation of alcohols, this reaction system produced free radicals characterized as  $\omega$ -oxidized products in which the furthest position from the alcoholic OH was the main point of attack. However, the exact nature of the reacting species in this redox system has not been revealed as yet.

To obtain monomer and polymer radicals of concentrations large enough for ESR analysis ( $\geq 10^{-6}M$ ) the initiation rate must be much faster than in conventional polymerizations. In the initiating system of  $Ti(III)-H_2O_2$ , the rate of initiation was estimated to be  $\geq 10^{-2}$  mole/liter/sec.

**Acrylic and Methacrylic Monomers.** Fischer *et al.* (5, 11, 12, 13, 14, 15) have studied extensively the transient free radicals formed by addition of  $HO\cdot$ ,  $\cdot NH_2$ ,  $\cdot CH_3$ , and  $\cdot CH_2OH$  radicals to a variety of acrylic and methacrylic monomers. The addition of  $\cdot CH_2OH$  radicals to the monomers could be achieved with a large excess of methanol present in the  $Ti(III)-H_2O_2$  system (5). They have obtained well-resolved spectra assigned to the monomer radicals resulting from the addition of the four initiating radicals mentioned (R) to the monomer molecules. All these radicals have the structure  $R-CH_2-\dot{C}X_1X_2$  and not  $R-CX_1X_2-\dot{C}H_2$ . This result agrees with the general concept that the methylene group of  $CH_2=CX_1X_2$  is normally more reactive toward free radical addition than the substituted carbon atom. For some monomers—*e.g.*, acrylic and methacrylic acid—well-defined ESR spectra attributed to growing polymer radicals were also observed when the monomer concentration was increased. For acrylic acid (AA) the spectrum of monomer radicals was replaced by that of the polymer radicals at a monomer concentration of  $1.5 \times 10^{-1}$  mole/liter (14). The coupling constants for the various radicals obtained in Fischer's work (14, 18) are summarized in Table I.

The variation in the  $\beta$ -coupling constant ( $a_{H\beta}$ ) of  $R-CH_2-\dot{C}X_1X_2$  radicals with different R groups (*cf.*, Table I) has been interpreted satisfactorily as being caused by steric hindrance of the R group attached to the  $\beta$ -carbon atom (15). This is in agreement with the current theory of  $H_\beta$ -coupling related to conformation described by Equation 1 (23).

$$a_{H\beta} = \beta_{H\beta} \cdot \rho_\alpha \cdot \cos^2 \theta \quad (1)$$

where  $\theta$  is the angle between the axis of the  $2p_z$  orbital of the unpaired electron and the direction of the  $C^\beta-H$  bond, projected on a plane perpendicular to the direction of the  $C^\alpha-C^\beta$  bond. If the two  $\beta$ -protons are equivalent, the  $a_{H\beta}$  values can be given by Equation 2 (14).

$$a_{H\beta} = \beta_{H\beta} \cdot \rho_\alpha \cdot 1/4 (3 - 2 \cos^2 \phi) = \beta_{H\beta} \cdot \rho_\alpha \cdot \overline{\cos^2 \theta} \quad (2)$$

Table I. Coupling Constants for Radicals from Acrylic and Methacrylic Acids and Acrylonitrile

Radical	Coupling Constants (gauss)				Ref.
	$a_H^\alpha$	$a_H^\beta$	$a_H^{CH_3}$	$a_N$	
HO—CH <sub>2</sub> — $\dot{C}H$   COOH	20.45	27.58	—	—	14
CH <sub>3</sub> —CH <sub>2</sub> — $\dot{C}H$   COOH	20.17	23.78	—	—	15
NH <sub>2</sub> —CH <sub>2</sub> — $\dot{C}H$   COOH	21.17	25.03	—	3.40	5
HOCH <sub>2</sub> —CH <sub>2</sub> — $\dot{C}H$   COOH	20.23	22.81	—	—	5
HO—CH <sub>2</sub> — $\dot{C}CH_3$   COOH	—	19.98	23.03	—	14
HO—(CH <sub>2</sub> —CH ) <sub>n</sub> —CH <sub>2</sub> — $\dot{C}H$     COOH COOH	22.62 20.67	21.34 22.06	—	—	14
CH <sub>3</sub> —CH <sub>2</sub> — $\dot{C}CH_3$   COOH	—	15.37	21.83	—	15
NH <sub>2</sub> —CH <sub>2</sub> — $\dot{C}CH_3$   COOH	—	16.98	24.19	4.96	5
HO—CH <sub>2</sub> — $\dot{C}CH_3$   COOH	—	14.45	22.27	—	5
HO—(CH <sub>2</sub> —CCH <sub>3</sub> ) <sub>n</sub> —CH <sub>2</sub> — $\dot{C}CH_3$     COOH COOH	—	11.04 13.75	22.45	—	14
HO—CH <sub>2</sub> — $\dot{C}H$   CN	20.10	28.15	—	3.53	14
CH <sub>3</sub> —CH <sub>2</sub> — $\dot{C}H$   CN	20.10	25.19	—	3.53	15
NH <sub>2</sub> —CH <sub>2</sub> — $\dot{C}H$   CN	20.45	23.75	—	3.25	5
HOCH <sub>2</sub> —CH <sub>2</sub> — $\dot{C}H$   CN	20.08	22.89	—	3.44	5



where  $\phi$  is the free rotation angle between the projection of the  $C^\alpha-R$  bond and the axis of the  $2p_z$  orbital representing the average position of the substituent R as illustrated in Figure 1.  $\beta_{HB}$  is 58.6 gauss (10), and  $\cos^2 \theta$  is an average for all angles  $\theta$  attained.

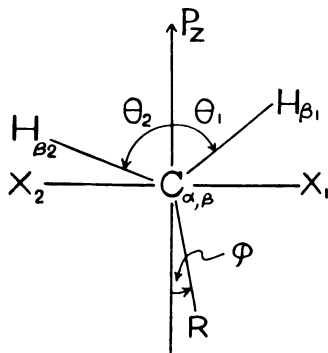
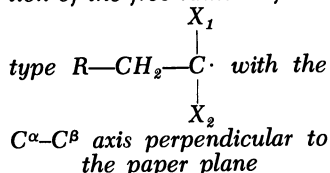
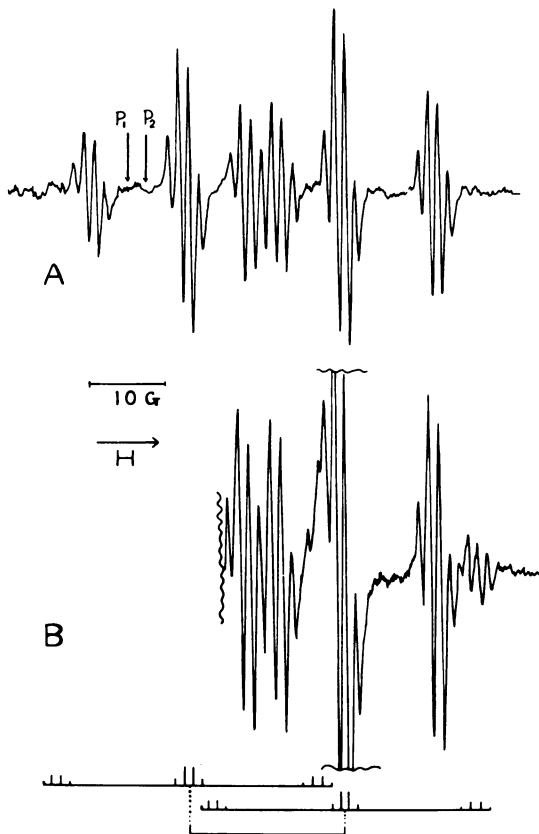


Figure 1. Steric conformation of the free radical of the



With increasing bulkiness of the substituent R, in the order HO,  $CH_3$ ,  $NH_2$ , and  $CH_2OH$ , the  $a_{HB}$  values in most cases tend to decrease. This indicates that the angle of free rotation  $\phi$  decreases. The smaller  $a_{HB}$  value for polymer radicals of AA can be explained in a similar way as being caused by the much higher bulkiness of the group (*i.e.*, the chain) attached to the  $\beta$ -carbon atom. From the observed spectra, however, it is difficult to distinguish between dimer, trimer, and further growing radical because the variation in the  $a_{HB}$  values with the degree of polymerization is not significant.

Methacrylic acid (MAA) showed an ESR spectrum with well resolved hyperfine structure consisting of 16 lines during redox polymerization in a flow system (13, 14). This spectrum was assigned unambiguously to the growing polymer radicals. The two  $\beta$ -protons are apparently not equivalent since they show two different coupling constants (Table I). Describing the conformation, the angles  $\theta_1$  and  $\theta_2$  for  $\beta_1$ - and  $\beta_2$ -protons were  $63.1^\circ$  and  $56.4^\circ$ , respectively, indicating that the R group of long chains in  $R-CH_2-C(CH_3)(COOH)$  is entirely locked in relation to the  $\alpha$ -carbon atom. Moreover, this spectrum leads us to the conclusion that the so-called "5 + 5 line" spectrum which has been reported previously for irradiated methacrylic polymers in the solid state is indeed



**Figure 2.** ESR spectra of vinyl acetate (VAc) radicals initiated with the system  $H_2O_2$ - $TiCl_3$ :  $[H_2O_2] = 1.1 \times 10^{-1}M$ ,  $[TiCl_3] = 7 \times 10^{-3}M$ , and  $[H_2SO_4] = 2.2 \times 10^{-2}M$

**A:** Monomer radical spectrum at  $[VAc] = 5.5 \times 10^{-2}M$ .  $P_1$  and  $P_2$  indicate the position of Peaks 1 and 2, respectively, which appear from the initiator in the absence of monomer

**B:** Monomer radical and polymer radical spectra overlapping at  $[VAc] = 3.2 \times 10^{-1}M$ . The stick spectrum shows the hyperfine lines assigned to the polymer radicals

caused by polymer radicals. On the basis of the steric structure and internal rotation of propagating radicals derived from the ESR spectra, Fischer (17) discussed the relative occurrence of isotactic and syndiotactic units in the polymer. The kinetic study of redox polymerization of AA initiated by  $\cdot CH_3$  radicals in aqueous media in the flow system has been made by Fischer (16). The rate constants obtained under the initiation conditions of  $R_1 = 1.83 \times 10^{-2}$  mole/liter/sec. were  $k_p = 0.64 \times$

$10^5$  liters/mole/sec., and  $k_t = 1.52 \times 10^8$  liters/mole/sec., both of which were about one order of magnitude higher than for usual solution polymerization. This was interpreted as being caused by the much shorter chain length of the propagating radicals.

**Vinyl Esters.** Various vinyl esters have been studied in our laboratory (33, 35, 36). The spectra from vinyl acetate radicals (VAc $\cdot$ ) in the system of  $H_2O_2 + TiCl_3$  are shown in Figure 2. Spectrum A obtained at an ordinary monomer concentration of  $5 \times 10^{-2}$  mole/liter can be described as a doublet of triplets of narrow quartets ( $g = 2.0031$ ). It was assigned to the monomer radical  $HO-CH_2-\dot{C}H(OCOCH_3)$ . Spectrum B in Figure 2 show half of the spectrum obtained at saturated VAc concentration—*i.e.*, about 0.3 mole/liter. Weak signals superimposed on the spectrum of VAc monomer radicals are possibly ascribed to growing polymer radicals. The weak signals  $P_1$  and  $P_2$  in Figure 2A are probably caused by a residue of the initiating system ( $HOO\cdot$  and  $HO\cdot$  in complex form) as described previously (34).

Using  $HO\cdot$  radicals as initiator, ESR spectra for isopropenyl acetate (IPAc), vinyl propionate (VPr), vinyl butyrate (VBu), and vinyl crotonate (VCr) were obtained at monomer concentrations below 0.1 mole/liter. IPAc gave the spectrum of a quartet of triplets. Each line split further into a narrow quartet owing to the expected very weak coupling with the three protons in the acetate group (as shown in Figure 3). VPr and VBu gave almost the same spectra as VAc except for the narrow triplets arising from the two protons next to the carbonyl in the ester group. The spectrum from VCr was rather weak. The splitting arising from the ester protons could not be resolved in this case.

Assignment of the observed spectra to vinyl ester monomer radical is verified by using  $\cdot NH_2$  radicals as initiator. We have observed the spectra from these vinyl esters which showed the expected coupling with the nitrogen atom of the  $NH_2$  group attached to the  $\beta$ -carbon. Coupling with the  $\beta$ -protons was almost the same as that observed for the corresponding HO-adduct radicals. VAc showed an ill-resolved spectrum of low intensity, probably because of the low reactivity of this monomer toward  $\cdot NH_2$  radicals as suggested from its very low  $Q$  value (0.026) in the  $Q, e$  scheme of copolymerization (22) (the  $Q$  values are considered as a measure of mean reactivity of monomer toward free radical addition). IPc and VPr, however, showed well-resolved spectra. The spectrum of VPr is shown in Figure 4 where the triplets with the same intensity of components arising from the nitrogen are clearly observed. The coupling constants obtained for HO- and  $NH_2$ -adduct radicals of various vinyl esters are listed in Table II. For comparison,  $CH_3\dot{C}HOCOCH_3$  radicals obtained by Smith *et al.* (30) from ethyl acetate by hydrogen abstraction in a flow system are listed also. The spin

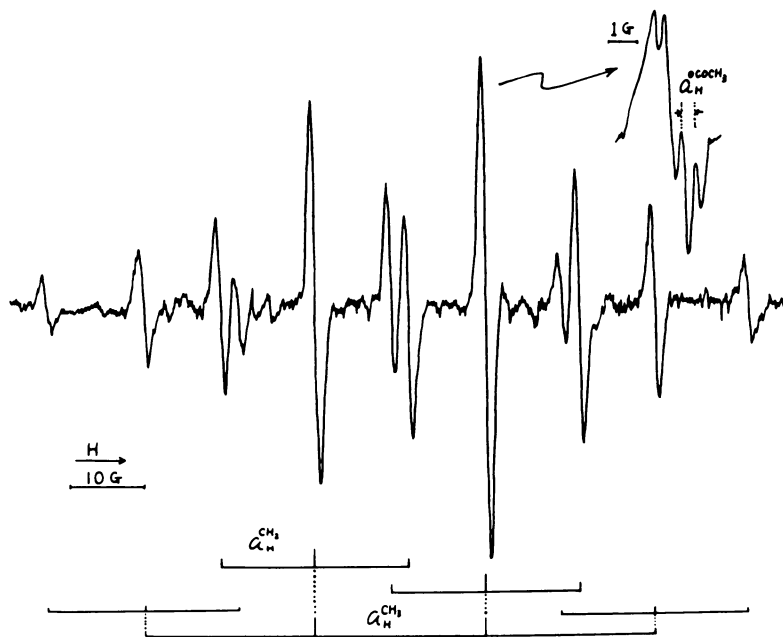


Figure 3. ESR spectrum of isopropenyl acetate (IPAc) radicals initiated with the system  $H_2O_2-TiCl_3$  at  $[IPAc] = 4.6 \times 10^{-2}M$ ,  $[H_2O_2] = 1.5 \times 10^{-2}M$ ,  $[TiCl_3] = 7 \times 10^{-3}M$ , and  $[H_2SO_4] = 2.2 \times 10^{-2}M$

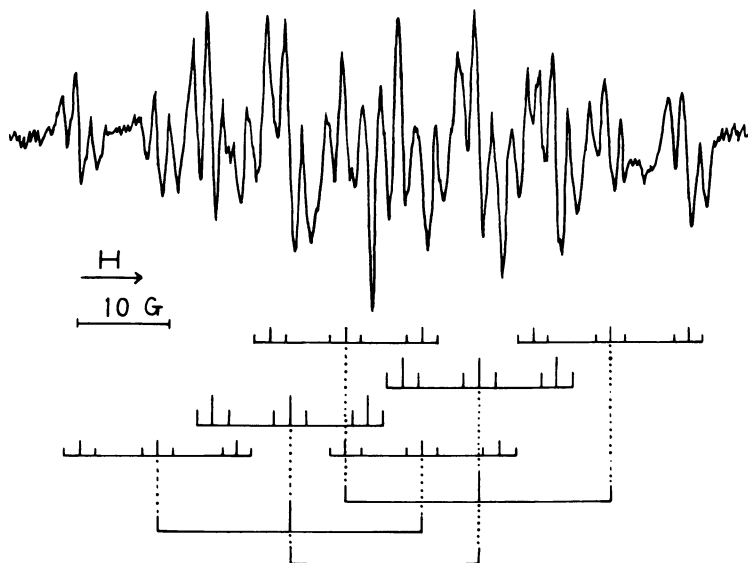


Figure 4. ESR spectrum from vinyl propionate (VPr) radicals initiated with the system  $NH_2OH-TiCl_3$  at  $[VPr] = 5.6 \times 10^{-2}M$ ,  $[NH_2OH] = 2.5 \times 10^{-2}M$ ,  $[TiCl_3] = 7 \times 10^{-3}M$ , and  $[H_2SO_4] = 2.2 \times 10^{-2}M$

Table II. Coupling Constants and Spin Densities

Substrate	Initiator	Radicals	Coupling
			$a_{H^\alpha}$
VAc	HO·	HO—CH <sub>2</sub> — $\dot{C}H$ (OCOCH <sub>3</sub> )	20.3 ± 0.1
IPAc	HO·	HO—CH <sub>2</sub> — $\dot{C}(CH_3)$ (OCOCH <sub>3</sub> )	—
	H <sub>2</sub> N·	H <sub>2</sub> N—CH <sub>2</sub> — $\dot{C}(CH_3)$ (OCOCH <sub>3</sub> ) <sup>b</sup>	—
VPr	HO·	HO—CH <sub>2</sub> — $\dot{C}H$ (OCOCH <sub>2</sub> CH <sub>3</sub> )	20.2 ± 0.1
	H <sub>2</sub> N·	H <sub>2</sub> N—CH <sub>2</sub> — $\dot{C}H$ (OCOCH <sub>2</sub> CH <sub>3</sub> ) <sup>b</sup>	20.5 ± 0.1
VBu	HO·	HO—CH <sub>2</sub> — $\dot{C}H$ (OCOCH <sub>2</sub> C <sub>2</sub> H <sub>5</sub> )	20.1 ± 0.1
VCr	HO·	HO—CH <sub>2</sub> — $\dot{C}H$ (OCOCH=CHCH <sub>3</sub> )	20.4 ± 0.3
EAc <sup>c</sup>	HO·	CH <sub>3</sub> — $\dot{C}H$ (OCOCH <sub>3</sub> )	18.8 ± 0.7

<sup>a</sup> Designations  $\alpha$  and  $\beta$  refer to the position relative to the carbon which bears the unpaired electron.

<sup>b</sup> In acid media they are protonated—*i.e.*, H<sub>3</sub>N<sup>+</sup>—CH<sub>2</sub>— $\dot{C}H$ (OCOR').

<sup>c</sup> Obtained from the  $a_{H^{CH_3}}$  values. The average value of  $\Delta$ (OCOCH<sub>3</sub>) obtained from

densities for these radicals were determined from the  $\alpha$ -CH<sub>3</sub> coupling constants of IPAc monomer radicals using Fischer's data (14, 18).

When methyl radicals were used as initiator, no detectable amount of VAc radicals was obtained under any experimental conditions. The reactivity of VAc is apparently very low compared with the results for acrylic monomers (14). These findings are, however, in agreement with the data from methyl affinity studies by Szwarc (32), who reported the reactivity of VAc monomer towards methyl radicals to be about 1/40th that of acrylonitrile (AN) and methyl methacrylate.

As seen from Table II, all the vinyl ester monomer radicals show almost the same, very small  $\beta$ -coupling constants independent of the ester group. Comparing these values with those for CH<sub>3</sub> $\dot{C}H$ OCOCH<sub>3</sub> radicals, one notices that the  $a_{H\beta}$  value is much less when one of the hydrogens of methyl group attached to the trivalent carbon is replaced with a substituent such as HO or NH<sub>2</sub> group. There is no significant variation in the  $a_{H\beta}$  values for VAc monomer radicals with temperature—*i.e.*, 12.0 gauss (8°C.), 12.2 gauss (20°C.), and 12.8 gauss (~50°C.). These results indicate that the vinyl ester monomer radicals have the  $\beta$ -CH<sub>2</sub> group locked with respect to the  $\alpha$ -carbon group in such a way that the two hydrogens remain equivalent. The free rotation angle  $\phi$  calculated from the  $a_{H\beta}$  values using Equation 2 are as follows: 0° for HO—VAc· radical, 14° for HO—IPAc· radical, 0° and 15° for HO— and NH<sub>2</sub>—VPr· radicals, respectively, and 45° for CH<sub>3</sub> $\dot{C}H$ OCOCH<sub>3</sub>. This means that  $\theta$  is nearly 60° for both methylene hydrogens and that the R group (R = HO or NH<sub>2</sub>) of R—CH<sub>2</sub>— $\dot{C}H$ (OCOCH<sub>3</sub>) is above or below the radical plane. This phenomenon cannot be understood as being caused by enhanced bulkiness of the substituent R, attached to

## for Various Vinyl Ester Monomer Radicals

Constants <sup>a</sup>				Spin Density
$a_H^{CH_3}$	$a_H^\beta$	$a_H^{OCOR'}$	$a_N^{NH_2}$	$\rho_\alpha$
—	12.2 ± 0.1	1.30 ± 0.04	—	0.836
22.5 ± 0.1	12.5 ± 0.1	0.40 ± 0.03	—	0.768 <sup>c</sup>
23.0 ± 0.1	13.1 ± 0.1	unresolved	8.2 ± 0.1	0.785 <sup>c</sup>
—	12.3 ± 0.1	1.61 ± 0.05	—	0.836 <sup>d</sup>
—	14.2 ± 0.1	1.62 ± 0.05	8.3 ± 0.1	0.855 <sup>d</sup>
—	12.1 ± 0.2	1.34 ± 0.04	—	0.836 <sup>d</sup>
—	12.3 ± 0.3	unresolved	—	0.836 <sup>d</sup>
24.0 ± 0.9	—	1.44 ± 0.8	—	0.819

the  $\rho_\alpha$  values was 0.104, which agrees well with the value 0.109 calculated from the data for ethyl acetate.

<sup>d</sup>  $\Delta(OCOR')$  is assumed to be 0.104, irrespective of R group.

<sup>c</sup> Ethyl acetate, from Ref. 30.

the  $\beta$ -carbon. It seems more likely that some type of intramolecular interaction leading to a locked conformation is operative in this case. At the moment two probable explanations are conceivable. The first is a formation of intramolecular hydrogen bond between the hydrogen of the  $\beta$ -hydroxyl group or  $\beta$ -amino group and the carbonyl oxygen of the ester group, giving a seven-membered ring structure. From a molecular model, this conformation seems to be feasible although the whole structure is not planar. The other interpretation is a titanium chelate of two vinyl ester monomer radicals in which titanium ions may be coordinated between the two polar side groups.

The formation of HO adduct radicals of VAc is mainly related to the concentration of initiator, monomer, and sulfuric acid. The intensity of the signal is affected strongly by the  $H_2O_2/TiCl_3$  molar ratio. The maximum intensity was obtained with a ratio close to  $r = 15$ . With decreasing ratio below 10, either by increasing the  $TiCl_3$  concentration or by decreasing the  $H_2O_2$  concentration, the intensity of the ESR signal was decreased considerably. According to simple kinetics, however, the highest intensity is expected at a molar ratio of unity (2). When the  $H_2O_2/TiCl_3$  ratio was kept constant at the optimal value  $r = 16$  with increasing initiator concentration, the intensity at first increased, passed through a maximum, and then decreased. After adding a small amount of ferric chloride, which is known to be a radical scavenger in the reaction system, the signal intensity decreased markedly down to the ESR noise level. These results suggest that species like Ti(IV) ions, derived from the redox reaction, may take part in the termination—*e.g.*, through a process of electron transfer, as previously proposed by Bamford *et al.* (1).

Such scavenging effects of metal halides seem to be enhanced for reactive radicals having negative  $e$  values, such as the VAc radicals.

As seen from Spectrum B in Figure 2 weak signals caused by VAc polymer radicals were observed at saturated monomer concentration. However, no more distinct spectrum than this one has been obtained so

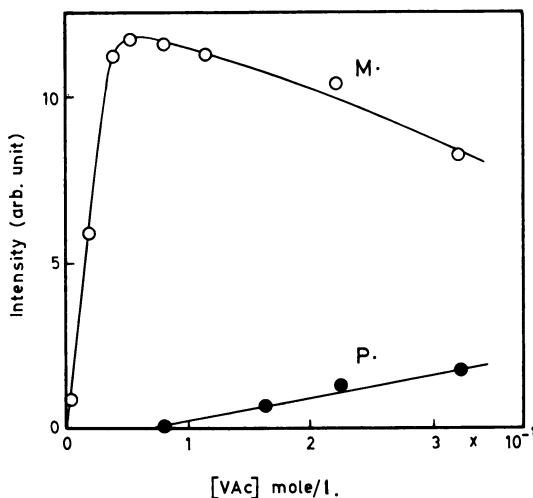


Figure 5. Intensity of monomer ( $M\cdot$ ) and polymer radical ( $P\cdot$ ) spectra at increasing VAc concentration and other conditions as given in Figure 2

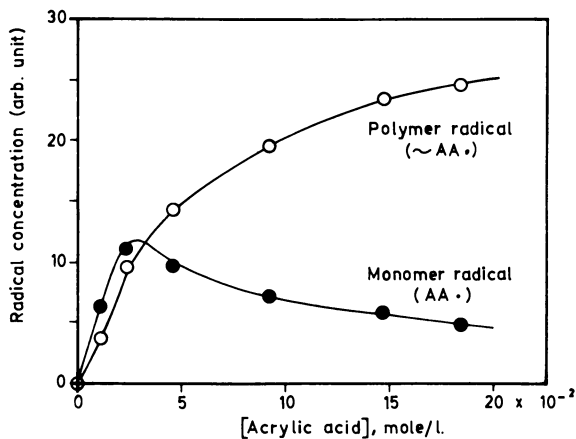


Figure 6. Radical concentrations from ESR signal intensities of monomer and polymer radicals of acrylic acid (AA) at increasing concentrations. Reaction conditions same as in Figure 5

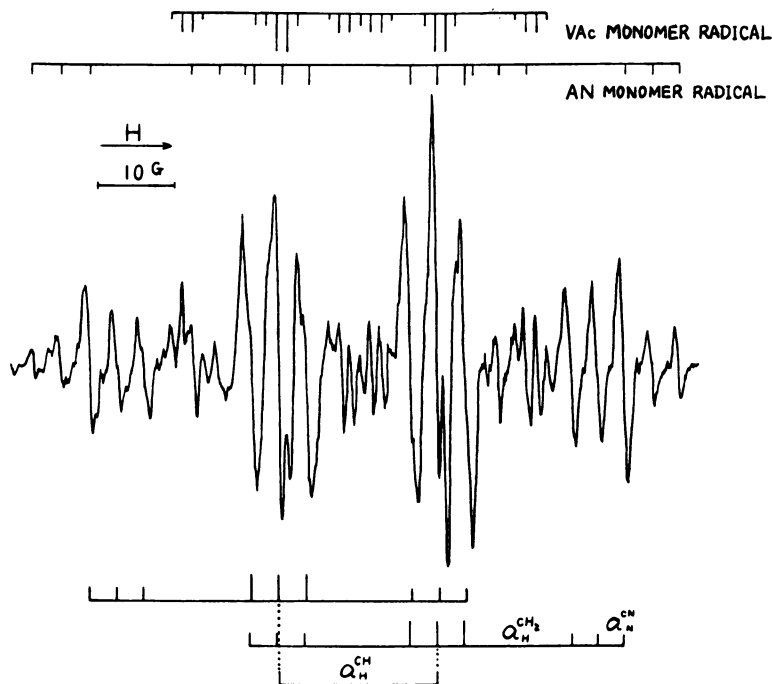


Figure 7. ESR spectrum for a polymerizing system of vinyl acetate (VAc) and acrylonitrile (AN) in aqueous solution. The predominant spectral component is assigned to the radical  $\text{HOCH}_2\text{CH}(\text{OCOCH}_3)\text{-CH}_2\text{CH}(\text{CN})$ . Concentrations are  $5.5 \times 10^{-2}\text{M}$  of VAc and  $1.9 \times 10^{-2}\text{M}$  of AN—i.e., a molar ratio of VAc/AN = 75/25. The stick spectra at the top show the expected relative intensities of the hyperfine lines for VAc and AN monomer radicals

far, owing to the limited solubility of the monomer. The coupling constants obtained from this spectrum are  $a_{\text{H}}^{\alpha} = 20.3$  gauss,  $a_{\text{H}}^{\beta} = 17.5$  gauss, and  $a_{\text{H}}^{\text{OCOCCH}_3} = 1.3$  gauss. The formation of VAc monomer and polymer radicals at increasing monomer concentrations is shown in Figure 5. In most cases, no polymer-like substance could be detected in the reaction streams immediately after mixing the two solutions. The very low concentration of VAc polymer radicals is in marked contrast to the results for acrylic monomers (14) for which intense, well-resolved spectra arising from polymer radicals are easily obtained even at monomer concentrations below  $5 \times 10^{-2}$  mole/liter. For comparison, data obtained for AA under identical conditions in our work are given in Figure 6. These results suggest that the highly reactive VAc radicals could terminate preferentially with species such as  $\text{HO}\cdot$  radicals, VAc monomer radicals, or titanium ions in the flow system rather than undergo propagation. This is probably caused by the low reactivity of VAc as a



monomer. As reported elsewhere (33), however, introduction of small amounts of a more reactive second monomer such as AN into the VAc system has given a well resolved spectrum attributed to the initial copolymer radicals resulting from addition of comonomer to the VAc monomer radicals—*e.g.*, HO—VAc—AN·.

**Copolymerization of VAc with Various Comonomers.** The monomer mixtures used in our experiments were VAc as monomer  $M_1$  and AN, AA, MAA, acrylamide (AAm), maleic acid (MA), and fumaric acid (FA) as monomer  $M_2$  (33). All the ESR spectra obtained from the binary monomer systems containing vinyl ester and small amounts of  $M_2$

Table III. Coupling Constants for Free Radicals

<i>Radical</i>	<i>Monomer Substrate</i>
$\text{HO}\dot{\text{C}}\text{H}_2\text{CH}(\text{CN})$	AN <sup>a</sup>
$\text{HOCH}_2\text{CHCH}_2\dot{\text{C}}\text{H}(\text{CN})$	VAc + AN
$\begin{array}{c}   \\ \text{OCOCH}_3 \\ \text{HOCH}_2\text{CCH}_3\text{CH}_2\dot{\text{C}}\text{H}(\text{CN}) \end{array}$	IPAc + AN
$\begin{array}{c}   \\ \text{OCOCH}_3 \\ \text{HOCH}_2\dot{\text{C}}\text{H}(\text{COOH}) \\ \text{HOCH}_2\text{CHCH}_2\dot{\text{C}}\text{H}(\text{COOH}) \end{array}$	AA <sup>a</sup>
$\begin{array}{c}   \\ \text{COOH} \\ \text{HOCH}_2\text{CHCH}_2\dot{\text{C}}\text{H}(\text{COOH}) \end{array}$	AA <sup>a</sup>
$\begin{array}{c}   \\ \text{COOH} \\ \text{HOCH}_2\text{CHCH}_2\dot{\text{C}}\text{H}(\text{COOH}) \end{array}$	VAc + AA
$\begin{array}{c}   \\ \text{OCOCH}_3 \\ \text{HOCH}(\text{COOH})\dot{\text{C}}\text{H}(\text{COOH}) \\ \text{HOCH}_2\text{CHCH}(\text{COOH})\dot{\text{C}}\text{H} \end{array}$	MA or FA <sup>a</sup>
$\begin{array}{c}   \qquad   \\ \text{OCOCH}_3 \quad \text{COOH} \\ \text{HOCH}_2\dot{\text{C}}\text{CH}_3(\text{COOH}) \\ \text{HOCH}_2\text{CCH}_3\text{CH}_2\dot{\text{C}}\text{CH}_3 \end{array}$	VAc + MA or VAc + FA
$\begin{array}{c}   \qquad   \\ \text{COOH} \quad \text{COOH} \\ \text{HOCH}_2\dot{\text{C}}\text{CH}_3(\text{COOH}) \\ \text{HOCH}_2\text{CCH}_3\text{CH}_2\dot{\text{C}}\text{CH}_3 \end{array}$	MAA <sup>a</sup>
$\begin{array}{c}   \qquad   \\ \text{COOH} \quad \text{COOH} \\ \text{HOCH}_2\text{CCH}_3\text{CH}_2\dot{\text{C}}\text{CH}_3 \end{array}$	MAA <sup>a</sup>
$\begin{array}{c}   \\ \text{COOH} \\ \text{HOCH}_2\text{CHCH}_2\dot{\text{C}}\text{CH}_3(\text{COOH}) \end{array}$	VAc + MAA
$\begin{array}{c}   \\ \text{OCOCH}_3 \\ \text{HOCH}_2\dot{\text{C}}\text{H}(\text{CONH}_2) \end{array}$	AAm
$\begin{array}{c}   \\ \text{OCOCH}_3 \\ \text{HOCH}_2\text{CHCH}_2\text{CH}(\text{CONH}_2) \end{array}$	VAc + AAm

showed predominant, new signals assigned to the radical species HO-(vinyl ester)-M<sub>2</sub>·. These spectra are distinguishable from the corresponding monomer radical spectra of HO-M<sub>2</sub>· by the difference in the  $a_{H\beta}$  values. The initial copolymer radicals are characterized by their low  $a_{H\beta}$  values. No evidence of the reverse type of copolymer radicals—*i.e.*, HO-M<sub>2</sub>-VAc· was observed. A typical spectrum obtained for the system VAc-AN is shown in Figure 7.

The coupling constants for the initial copolymer radicals are given in Table III together with those of the corresponding monomer radicals. The monomer radicals included give coupling constants, which are in

### Obtained from Single and Binary Monomer Systems

#### *Coupling Constants, gauss*

$a_H^\alpha$	$a_H^\beta$	Others
20.1 ± 0.1	28.2 ± 0.1	$a_N^C = 3.45 \pm 0.07$
20.3 ± 0.2	20.6 ± 0.2	$a_N^C = 3.42 \pm 0.07$
20.0 ± 0.2	19.3 ± 0.2	$a_N^{CN} = 3.33 \pm 0.07$
20.6 ± 0.1	27.8 ± 0.2	
21.1 ± 0.2	22.6 ± 0.2	
20.4 ± 0.2	21.2 ± 0.2	
20.80 ± 0.05	12.7 ± 0.1	
20.75 ± 0.05	11.1 ± 0.1	
—	19.9 ± 0.1	$a_H^{CH_3} = 23.0 \pm 0.1$
—	13.8 ± 0.2	$a_H^{CH_3} = 22.4 \pm 0.2$
	11.0 ± 0.2	
—	15.5 ± 0.2	$a_H^{CH_3} = 22.4 \pm 0.2$
	9.5 ± 0.2	$a_H^{CONH_2} = 1.8 \pm 0.3$
20.1 ± 0.3	26.6 ± 0.3	$a_N^{CONH_2} = 2.0 \pm 0.3$
20.0 ± 0.3	21.0 ± 0.3	$a_H^{CONH_2} = 1.8 \pm 0.3$
		$a_N^{CONH_2} = 2.0 \pm 0.3$

\* The results are in agreement with Fischer's data (14).

good agreement with data reported by Fischer (14). The smaller  $a_{\text{HB}}$  values indicate that the rotation of the  $\text{RCH}_2$  group around the  $\text{C}-\text{C}$  bond is restricted to a greater extent in the copolymer radicals than in the corresponding monomer radicals. This is probably caused by steric hindrance of the bulky VAc units R, attached to the  $\beta$ -carbon atom. In comparison, the HO groups on the corresponding monomer radicals are small.

The relative concentrations of the various radical species during copolymerization have been estimated from the intensities of the ESR spectral components. Typical results obtained from the VAc-MA and VAc-FA system are shown in Figure 8, giving the relative radical concentration as a function of comonomer concentration. The addition of small amounts of  $\text{M}_2$  (molar ratio  $\text{M}_2/\text{M}_1 \leq 0.05$ ) in each case caused a sharp decrease in the concentration of VAc monomer radicals, while the

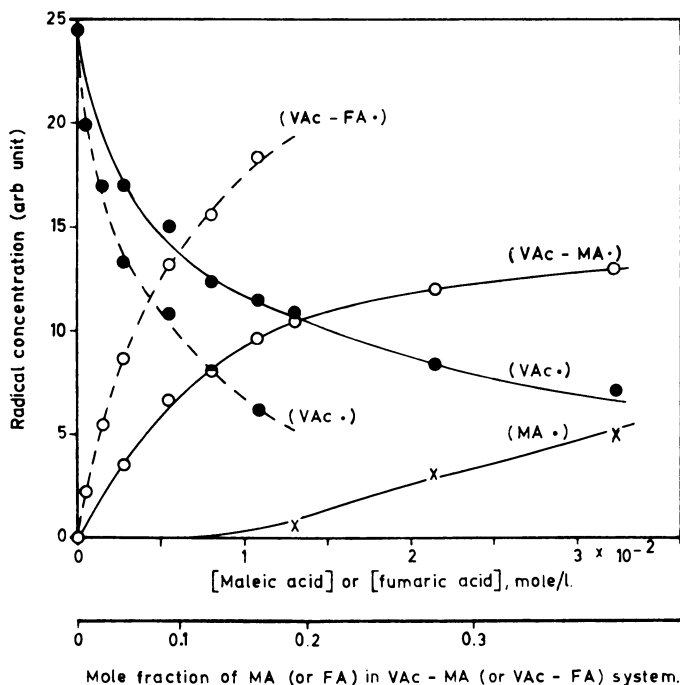


Figure 8. Concentration of different radicals measured from ESR spectra during copolymerization of vinyl acetate (VAc) with maleic acid (MA) and of VAc with fumaric acid (FA) at different molar concentrations of MA in the VAc-MA system and FA in the VAc-FA system, respectively. (VAc·) and (MA·) refer to monomer radicals and (VAc-MA·) and (VAc-MA·) to the copolymer radicals observed.  $[\text{VAc}] = 5.5 \times 10^{-2}\text{M}$ ;  $[\text{MA}]$  or  $[\text{FA}]$ : variable

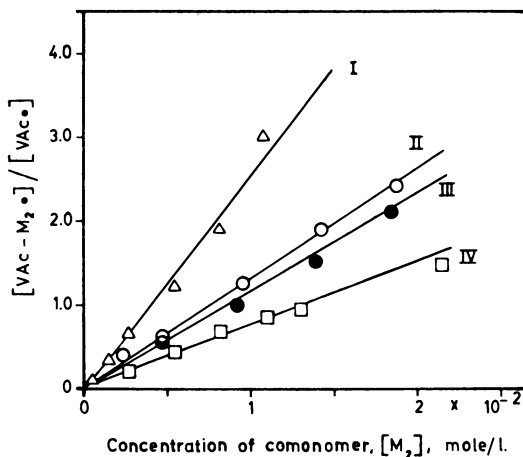


Figure 9. Plots of concentration ratio  $[VAc-M_2\cdot]/[VAc\cdot]$  vs. concentration of comonomer  $M_2$  for the systems (I) VAc-FA, (II) VAc-AN, (III) VAc-AA, and (IV) VAc-MA

FA = fumaric acid

AN = acrylonitrile

AA = acrylic acid

MA = maleic acid

$[VAc] = 5.5 \times 10^{-4}M$  (constant)

concentration of the corresponding copolymer radicals  $VAc-M_2\cdot$  increased. This indicates a rapid reaction of VAc monomer radicals with  $M_2$  resulting in an almost instantaneous transformation to  $VAc-M_2\cdot$  radicals. MA and FA gave the same ESR spectrum as expected. FA (trans isomer) reacted much faster than MA (cis isomer) with VAc monomer radicals.

Plots of the radical concentration ratio  $[VAc-M_2\cdot]/[VAc\cdot]$  vs. concentration of  $M_2$  are shown in Figure 9. The data give straight lines with a characteristic slope, which is a measure of the relative rate of conversion of  $HO-VAc\cdot$  to  $HO-VAc-M_2\cdot$  for the different  $M_2$  comonomers. The results obtained are in good agreement with the reported reactivity ratios (22) for these VAc copolymerization systems as shown in Table IV. The conversion rates (*i.e.*, slope coefficients in Figure 9) can be correlated with the reciprocals of  $r_1$  values on a qualitative basis. The enhanced reactivity of FA compared with AA and AN is described as a higher value of both  $Q$  and  $e$  for FA. The difference in reactivity between FA and MA is most reasonably interpreted in terms of steric effects. It is interesting that the reactivity values for VAc monomer radicals derived from the initial copolymerization reaction step are in harmony with the data for the reported copolymerization kinetics, although the reaction

**Table IV. Conversion Rates of  $M_1\cdot$  to  $M_1-M_2\cdot$  Radicals and  $r_1$  Values from ESR Data**

System		Conversion Rate, liters/mole ( $M_1\cdot + M_2\cdot \rightarrow$ $M_1-M_2\cdot$ )	$r_1$	$1/r_1$	Q, e Values for $M_2$	
$M_1$	$M_2$				Q	e
VAc	Maleic acid	$0.8 \times 10^2$	0.12	8.3	0.09	1.27 (dimethyl maleate)
VAc	Acrylic acid	$1.2 \times 10^2$	0.10	10.0	1.15	0.77
VAc	Acrylonitrile	$1.3 \times 10^2$	0.061	16.4	0.60	1.20
VAc	Fumaric acid	$2.5 \times 10^2$	0.023 <sup>a</sup>	43.5	0.76	1.49 (dimethyl fumarate)
VAc	Methacrylic acid	—	0.01	100.0	2.34	0.65
VAc	Acrylamide	—	0.016 <sup>a</sup>	62.5	1.18	1.30
IPAc	Acrylonitrile	$0.6 \times 10^2$	0.032 <sup>a</sup>	31.2	0.60	1.20
Acrylic acid	Acrylic acid	$0.3 \times 10^2$	—		1.15	0.77

<sup>a</sup> Calculated from Q,e values.

conditions in the flow system are different from the usual polymerization conditions.

**Miscellaneous Monomers.** Butadiene has been studied using HO· radicals as initiator in our laboratory (36). The observed spectrum is probably caused by the radical  $\text{HO}-\text{CH}_2\text{CHCH}=\text{CH}_2 \rightleftharpoons \text{HO}-\text{CH}_2\text{CH}=\text{CH}-\text{CH}_2$ , formed by hydroxyl addition to the monomer. The major product of the reaction of hydroxyl radicals generated from the system of ferrous ions and  $\text{H}_2\text{O}_2$  with butadiene is known to be 1,8-dihydroxy-2,6-octadiene (21). This product would result from the dimerization of  $\text{HOCH}_2-\text{CH}=\text{CH}-\text{CH}_2$ . Griffiths *et al.* (21) have also studied butadiene, and they obtained almost the same spectrum. In addition, they recorded the spectrum obtained by the addition of  $\cdot\text{NH}_2$  to butadiene. The spectrum, however, was highly complex, presumably because isomeric radicals were formed, and an unequivocal assignment was not possible. Griffiths *et al.* also studied ethylene, vinyl chloride, and vinyl fluoride. The spectra obtained were assigned to the monomer radicals formed by hydroxyl radical addition to the terminal methylene group of the monomers. However, no spectrum attributed to propagating radicals has been observed, probably because of the very limited solubility—and resulting low concentration—of these monomers in aqueous media.

In addition to the above-mentioned monomers, various acrylic and methacrylic esters, methacrylonitrile, itaconic acid, crotonic acid, methyl vinyl ketone, allyl alcohol, allyl amine etc., have been studied by Fischer

*et al.* (5, 14). All the monomers show well-resolved spectra arising from monomer radicals. Recently, Smith *et al.* (31) studied allyl alcohol in detail using the Ti(III) + H<sub>2</sub>O<sub>2</sub> system and obtained weak signals arising from a growing polymer radical. The coupling constants for some of the monomer radicals are summarized in Table V. The small  $a_{\text{HB}}$  values recorded for HO-adduct radicals of vinyl fluoride and vinyl chloride may be interpreted as steric effects arising from certain intermolecular interaction in an analogous way as described for the HO adduct radicals of vinyl esters.

**Table V. Coupling Constants for HO-Adduct Radicals of Butadiene, Vinyl Fluoride, and Vinyl Chloride**

Radicals	Coupling Constants, gauss			Ref.
	$a_{\text{H}}^{\alpha}$ (doublet)	$a_{\text{H}}^{\beta}$ (triplet)	$a_{\text{X}}$	
HO—CH <sub>2</sub> — $\dot{\text{C}}\text{H}$ —CH=CH <sub>2</sub>	14.9	13.8, 12.6	—	36
HO—CH <sub>2</sub> — $\dot{\text{C}}\text{H}$ —CH=CH <sub>2</sub>	14.4, 4.0	13.4, 12.4	—	21
HO—CH <sub>2</sub> — $\dot{\text{C}}\text{H}$   F	19.1	11.2	57.6 (X = F)	21
HO—CH <sub>2</sub> — $\dot{\text{C}}\text{H}$   Cl	17.7	14.4	3.0 (X = Cl)	21

### Conclusion

By applying a flow method using rapid redox initiation, ESR studies of vinyl polymerization in solutions have been made. This approach has provided new information on the transient free radicals involved, particularly at the initial stage of polymerization. Although the information obtained is significantly helpful for studying ordinary polymerization, the situation in the flow system is quite different from the normal solution polymerization. In this investigation, considerably high concentration of initiator is required, and turbulent flow on mixing may affect the reaction condition appreciably. As a consequence the effect of diffusion should be taken into account, especially when we determine rate constants and monomer reactivity ratios for the reactions occurring in the flow system.

### Acknowledgment

This research program is supported by MALMFONDEN—Swedish Foundation for Scientific and Industrial Development.

**Literature Cited**

- (1) Bamford, C. H., Jenkins, A. D., Johnston, R., *J. Polymer Sci.* **29**, 355 (1958).
- (2) Baxendale, J. H., Evans, M. G., Park, G. S., *Trans. Faraday Soc.* **42**, 155 (1946).
- (3) Ciubotariu, C., Rånby, B., unpublished data.
- (4) Chiang, Y. S., Craddock, J., Mickewich, D. M., Turkevich, J., *J. Phys. Chem.* **70**, 3509 (1966).
- (5) Corvaja, C., Fischer, H., Giacometti, G., *Z. physik. Chem., N.F.* **45**, 1 (1965).
- (6) Dewing, J., Longster, G. F., Myatt, J., Todd, P. F., *Chem. Commun.* **1965**, 391.
- (7) Dixon, W. T., Norman, R. O. C., *Nature* **196**, 891 (1962).
- (8) Dixon, W. T., Norman, R. O. C., *J. Chem. Soc.* **1963**, 3119.
- (9) Dixon, W. T., Norman, R. O. C., Buley, A. L., *J. Chem. Soc.* **1963**, 3625.
- (10) Fessenden, R. W., Schuler, R. H., *J. Chem. Phys.* **39**, 2147 (1963).
- (11) Fischer, H., *Z. Naturforsch.* **18a**, 1142 (1963).
- (12) *Ibid.*, **19a**, 267 (1964).
- (13) Fischer, H., *J. Polymer Sci.* **B2**, 529 (1964).
- (14) Fischer, H., *Z. Naturforsch.* **19a**, 866 (1964).
- (15) Fischer, H., Giacometti, G., *J. Polymer Sci. Pt. C*, 2763 (1967).
- (16) Fischer, H., *Makromol. Chem.* **98**, 179 (1966).
- (17) Fischer, H., *Kolloid-Z. Z. Polymere* **206**, 131 (1965).
- (18) Fischer, H., *Z. Naturforsch.* **20a**, 428 (1965).
- (19) Fischer, H., private communication.
- (20) Fischer, H., *Ber. Bunsenges. Phys. Chem.* **71**, 685 (1967).
- (21) Griffiths, W. E., Longster, G. F., Myatt, J., Todd, P. F., *J. Chem. Soc. B* **1967**, 530.
- (22) Ham, G. E., Ed., "Copolymerization," Interscience, New York, 1964.
- (23) Heller, C., McConnell, H. M., *J. Chem. Phys.* **32**, 1535 (1960).
- (24) Kharasch, M. S., Arimoto, F. S., Nudenberg, W., *J. Org. Chem.* **16**, 1556 (1951).
- (25) Livingston, R., Zeldes, H., *J. Chem. Phys.* **44**, 1245 (1966).
- (26) Livingston, R., Zeldes, H., *J. Am. Chem. Soc.* **88**, 4333 (1966).
- (27) Piette, L. H., Bulow, G., Loeffler, K., *Am. Chem. Soc., Div. Petrol. Chem. Preprints*, April 1964.
- (28) Sicilio, F., Florin, R. E., Wall, L. A., *J. Phys. Chem.* **70**, 47 (1966).
- (29) Shiga, T., *J. Phys. Chem.* **69**, 3805 (1965).
- (30) Smith, P., Pearson, J. T., Wood, P. B., Smith, T. C., *J. Chem. Phys.* **43**, 1535 (1965).
- (31) Smith, P., Wood, P. B., *Can. J. Chem.* **45**, 649 (1967).
- (32) Szwarc, M., *J. Polymer Sci.* **16**, 367 (1955).
- (33) Takakura, K., Rånby, B., *J. Polymer Sci.* **B5**, 83 (1967); *IUPAC Symp. Macromol. Chem.*, Brussels-Louvain, 1967.
- (34) Takakura, K., Rånby, B., *J. Phys. Chem.* **72**, 164 (1968).
- (35) Takakura, K., Rånby, B., *J. Polymer Sci.*, in press.
- (36) Yoshida, H., Rånby, B., *J. Polymer Sci.* **C16**, 1333 (1967).

RECEIVED March 27, 1968.

# Molecular Weight Distribution for Polymerization in Two-Phase Systems

## The Case of Several Growing Radicals

STANLEY KATZ and REUEL SHINNAR

Department of Chemical Engineering, The City College, C.U.N.Y.,  
New York, N. Y. 10031

GERALD M. SAIDEL

Department of Biomedical Engineering, Case Western Reserve University,  
Cleveland, Ohio 44106

*A method for obtaining the molecular weight distribution in two-phase polymerization systems such as emulsion polymerization is presented. The polymerization process occurring in the dispersed phase is modeled as a Markov process with random arrival and termination of radicals and continuous polymer growth. Earlier studies in which a dispersed-phase particle is assumed to contain (1) zero or one radical or (2) a large number of radicals are encompassed as limiting cases. The most significant variation in the weight-to-number average  $X_w/X_n$  is found to occur when the mean number of radicals  $\langle n \rangle$  lies between 1/2 and 1. For given rates of arrival and growth, distributions with  $\langle n \rangle$  near 1/2 have about the same number average, but they differ markedly in variance.*

**I**n emulsion polymerization and in some suspension polymerizations, free radicals are generated in a continuous phase and diffuse into a dispersed-phase particle or droplet where polymerization takes place (5). The molecular weight distributions or, equivalently, the polymer size distributions of these systems depend on the relative rates of radical arrival and termination. Frequently in emulsion polymerization the radicals are terminated so quickly that each particle in the dispersed phase



contains no more than one radical at any time. The opposite situation occurs in suspension polymerization where the termination rates are so low with respect to the arrival rates that the dispersed phase is considered to contain a virtual continuum of growing radicals. Under each limiting condition a theoretical analysis of the polymer size distribution can be greatly simplified.

Experimental studies show, however, that these limiting approximations must be used with caution. For example, with some emulsion polymerization systems the mean number of radicals per particle may run from one-half to several depending on the size of the particle (1). Assuming that the polymerization process is stationary with known rates of radical arrival and termination, Stockmayer (6) and O'Toole (3) have shown how to calculate not only the mean number of radicals but the entire number distribution as well. Until now, no methods of the same generality seem to exist for calculating the polymer size distribution.

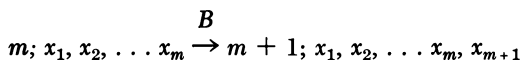
A method is presented here which yields the polymer size distribution for arbitrary rates of radical arrival and termination. Furthermore, from this analysis one can see when each of the limiting cases is applicable. The computations are all carried out under stationary conditions with the rates of radical arrival, propagation, and termination constant. Under transient conditions the computations would be much more difficult. For the limiting cases, however, the moments of the polymer size distributions under transient conditions can be found (4).

Two-phase polymerization is modeled here as a Markov process with random arrival of radicals, continuous polymer (radical) growth, and random termination of radicals by pair-wise combination. The basic equations give the joint probability density of the number and size of the growing polymers in a particle (or droplet). From these equations, suitably averaged, one can obtain the mean polymer size distribution.

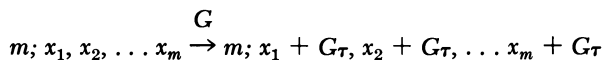
### *Polymerization as a Markov Process*

We can develop a stochastic model for two-phase polymerization by following the changes in the number and size of the growing polymers (or radicals) with time in an arbitrary particle of a system. [For a more general discussion of probability methods in particulate systems see Ref. 7.] Let us say that at some time  $t$  the particle contains  $m$  radicals of sizes  $x_1, x_2, \dots, x_m$  (in order of their appearance) with probability density  $p_m(x_1, x_2, \dots, x_m; t)$ . Since a polymer chain is usually long, we take the chain length or polymer size to be a continuous variable. Now, we assume that in a short time interval  $[t, t + \tau]$  changes in the particle occur by these processes:

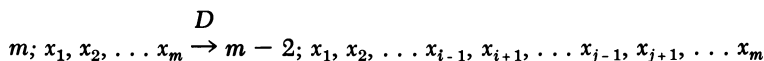
(1) A radical may enter the particle with probability  $B\tau$



(2) Each radical in the particle grows or increases its size, deterministically, by  $G\tau$



(3) Any two radicals—*i.e.*, growing polymers—may terminate by combination with probability  $D\tau$



Macroscopically, we interpret  $B$ ,  $G$ , and  $D$  as the mean rates of radical arrival (birth), propagation (growth), and termination (death) per radical pair; for analytical convenience, we assume that  $B$ ,  $G$ , and  $D$  are constant.

In taking the growth and termination rates  $G$  and  $D$  to have the same values for radicals of all sizes, we are assuming that no radicals are trapped, all being equally accessible both to monomer and to each other. These rates would otherwise depend on the ages and therefore the sizes of the radicals involved. The assumption that all radicals are equally accessible is quite reasonable in suspension polymerization and other two-phase polymerizations in immiscible liquids (*e.g.*, see Ref. 2) but might not always apply to cases in which the dispersed particles grow, such as in precipitation and emulsion polymerization. The size dependence of  $G$  and  $D$  can be incorporated into our stochastic model but only at the expense of very considerable analytical and numerical difficulties. Accordingly, we limit ourselves here to the case of constant parameters generally treated in the literature.

Returning then to the random mechanism sketched above, we find that the (conditional) probability density that the "state" of a particle changes from  $m$  radicals of sizes  $x_1, x_2, \dots, x_m$  to  $n$  radicals of sizes  $y_1, y_2, \dots, y_n$  in short time interval  $[t, t + \tau]$  is given by:

$$\begin{aligned} p_{mn}(x_1, \dots, x_m, y_1, \dots, y_n; \tau) \\ = B\tau \delta_{n,m+1} \delta(y_1 - x_1) \dots \delta(y_m - x_m) \delta(y_{m+1}) \\ + D\tau \delta_{n,m-2} \sum_{i < j} \delta(y_1 - x_1) \dots \delta(y_{i-1} - x_{i-1}) \delta(y_i - x_{i+1}) \\ \dots \delta(y_{j-2} - x_{j-1}) \delta(y_{j-1} - x_{j+1}) \dots \delta(y_{m-2} - x_m) \\ + [1 - B\tau - (m/2) D\tau] \delta_{nm} \delta(y_1 - x_1 - G\tau) \\ \dots \delta(y_m - x_m - G\tau) + o(\tau) \end{aligned} \quad (1)$$

where  $\delta_{ij}$  is the Kronecker delta,  $\delta(x)$  is the delta function, and the symbol  $o(\tau)$  is an order of magnitude smaller than  $\tau$ . The first term of this expression is the probability density that the  $m + 1$  radical, of vanishingly small size, enters the particle and the other  $m$  radicals change negligibly. In the second term, we take into account the probability that any pair of radicals may combine. If neither of the former events occurs, we must consider the continuous growth of radicals as given in the third term.

To find the (absolute) probability that the particle has  $n$  radicals of sizes  $y_1, y_2, \dots, y_n$  at time  $t + \tau$ , we use the following relation based on the Markov property:

$$p_n(y_1, \dots, y_n; t + \tau) = \sum_m \int p_{mn}(x_1, \dots, x_m, y_1, \dots, y_n; \tau) p_m(x_1 \dots x_m; t) dx_1, \dots, dx_m \quad (2)$$

By substituting Equation 1 into Equation 2, we find

$$\begin{aligned} p_n(y_1 \dots y_n; t + \tau) &= B\tau p_{n-1}(y_1, \dots, y_{n-1}; t) \delta(y_n) - G\tau \sum_j \frac{\partial p_n}{\partial y_j}(y_1, \dots, y_n; t) \\ &+ D \sum_{i < j} \int p_{n+2}(y_1, \dots, y_{i-1}, r, \dots, y_{j-2}, s, \dots, y_n; t) dr ds \\ &+ [1 - B\tau - \binom{n}{2} D\tau] p_n(y_1, \dots, y_n; t) + o(\tau) \end{aligned} \quad (3)$$

where the unspecified sums are taken over all positive integers and the integrals over all real values. If we expand the term on the left side of the equation about  $t$ , divide by  $\tau$ , and let  $\tau \downarrow 0$ , then we find

$$\begin{aligned} \frac{\partial p_n(y_1, \dots, y_n)}{\partial t} &= -G \sum_j \frac{\partial p_n(y_1, \dots, y_n)}{\partial y_j} - [B + \binom{n}{2} D] p_n(y_1, \dots, y_n) \\ &+ B p_{n-1}(y_1, \dots, y_{n-1}) \delta(y_n) \\ &+ D \sum_{i < j} \int p_{n+2}(y_1, \dots, y_{i-1}, r, \dots, y_{j-2}, s, \dots, y_n) dr ds \end{aligned} \quad (4)$$

The equation is simpler to work with when the argument of the probability density function is symmetric. To achieve this symmetry, we define a new probability density  $p_n(y_1, y_2, \dots, y_n)$  with random ordering of radicals sizes in the argument:

$$\bar{p}_n(y_1, y_2, \dots, y_n) = \frac{1}{n!} \sum_{\text{all perm.}} p_n(y_1, y_2, \dots, y_n)$$

where we sum over all  $n!$  permutations. Performing this operation on Equation 4, we arrive at

$$\begin{aligned} \frac{\partial \bar{p}_n(y_1, \dots, y_n)}{\partial t} = & -G \sum_j \frac{\partial \rho_n(y_1, \dots, y_n)}{\partial y_j} - [B + \binom{n}{2} D] p_n(y_1, \dots, y_n) \\ & + B/n \sum_j \bar{p}_{n-1}(y_1, \dots, y_{j-1}, y_{j+1}, \dots, y_n) \delta(y_j) \\ & + \binom{n+2}{2} D \int \bar{p}_{n+2}(y_1, \dots, y_n, r, s) dr ds \end{aligned} \quad (5)$$

In this study we consider just the stationary process—*i.e.*, we set the time derivatives equal to zero.

### *Size Distribution of Dead Polymer*

From the pair-wise combinations of growing polymer, we can get the mean size density  $f(z)$  of dead polymers of size  $[z, z + dz]$ :

$$f(z) = \frac{\sum_n \binom{2}{n} \int \bar{p}_n(y_1, \dots, y_n) \delta(y_1 + y_2 - z) dy_1 \dots dy_n}{\sum_u \binom{n}{u} \int \bar{p}_n(y_1, \dots, y_n) dy_1 \dots dy_n} \quad (6)$$

This mean polymer size density is just what would be obtained from the average over all particles in the system. For convenience in computing  $f(z)$  we introduce the following probability functions:

$$\theta_n = \int \bar{p}_n(y_1, \dots, y_n) dy_1 \dots dy_n \quad (7)$$

$$\phi_n(y_1) = \int \bar{p}_n(y_1, \dots, y_n) dy_2 \dots dy_n \quad (8)$$

$$\rho_n(z) = \int \bar{p}_n(y_1, \dots, y_n) \delta(y_1 + y_2 - z) dy_1 \dots dy_n \quad (9)$$

where  $\theta_n$  is the probability that a particle has  $n$  growing polymers, and  $\phi_n(y_1) dy_1$  is the joint probability of choosing a growing polymer of size  $[y_1, y_1 + dy_1]$  in presence of  $n$  of them. In terms of the above functions, the polymer size distribution is

$$f(z) = \frac{\sum_n \binom{n}{2} \rho_n(z)}{\sum_n \binom{n}{2} \theta_n} \quad (10)$$

By appropriate integrations of Equation 5, we obtain under stationary conditions:

$$0 = \theta_{n-1} - \theta_n + (D/B) \left\{ \binom{n+2}{2} \theta_{n+2} - \binom{n}{2} \theta_n \right\} \quad (11)$$

$$\frac{G}{B} \frac{d\phi_n(y_1)}{dy_1} = (1/n) \{ \theta_{n-1} \delta(y_1) - \phi_{n-1} \} + \phi_{n-1} - \phi_n + (D/B) \left\{ \binom{n+2}{2} \phi_{n+2} - \binom{n}{2} \phi_n \right\} \quad (12)$$

$$\frac{2G}{B} \frac{d\rho_n(z)}{dz} = (2/n) \{ \phi_{n-1}(z) - \rho_{n-1} \} + \rho_{n-1} - \rho_n + (D/B) \left\{ \binom{n+2}{2} \rho_{n+2} - \binom{n}{2} \rho_n \right\} \quad (13)$$

Following Stockmayer (6), we get the solution to Equation 11.

$$\theta_n = \frac{1}{\sqrt{2} n!} \left( \frac{2B}{D} \right)^{n/2} \frac{I_{n-1} \left( \sqrt{\frac{8B}{D}} \right)}{I_1 \left( \sqrt{\frac{16B}{D}} \right)} \quad (14)$$

where  $I_m$  represents a modified Bessel function of order  $m$ . From Equation 14 we also get the mean number of growing polymers to be

$$\langle n \rangle = \sum_n n \theta_n = \sqrt{\frac{B}{D}} \frac{I_0 \left( \sqrt{\frac{16B}{D}} \right)}{I_1 \left( \sqrt{\frac{16B}{D}} \right)} \quad (15)$$

and from Equation 11

$$\sum_n \binom{n}{2} \theta_n = B/2D \quad (16)$$

Since the equations for  $\phi_n(y_1)$  and  $\rho_n(z)$  do not readily yield an analytic solution, we obtain a numerical solution. To simplify the numerical computations, we deal with cumulative distributions of the "tails," that is, with the fractions of polymer having molecular weights above specified levels:

$$\Phi_n(y) = \int_y^\infty \phi_n(y_1) dy_1 \quad (17)$$

$$P_n(y) = \int_y^\infty \rho_n(z) dz \quad (18)$$

In terms of these functions, Equations 12 and 13 become

$$\frac{G}{B} \frac{d\phi_n}{dy} = (1 - 1/n) \Phi_{n-1} - \Phi_n + D/B \left[ \binom{n+2}{2} \Phi_{n+2} - \binom{n}{2} \Phi_n \right]; \quad y > 0, n \geq 1 \quad (19)$$

$$\frac{2G}{B} \frac{dP_n}{dy} = (2n) \Phi_{n-1} + (1 - 2/n) P_{n-1} - P_n + D/B \left[ \binom{n+2}{2} P_{n+2} - \binom{n}{2} P_n \right]; \quad y > 0, n \geq 2 \quad (20)$$

with

$$\Phi_n(0) = P_n(0) = \theta_n$$

These systems of equations can be solved by truncating them at a sufficiently large value of  $n$ , say  $N$ , such that  $\Phi_N(y)$  and  $P_N(y)$  contribute negligibly to the size distributions.

The cumulative distribution of the tail of the polymer size is found from Equations 10, 16, and 18 to be

$$F(y) = \int_y^\infty f(z) dz = \frac{2D}{B} \sum_n \binom{n}{2} P_n(y) \quad (21)$$

We can also get the moments of  $f(z)$  which are defined by:

$$\mu_k = \int z^k f(z) dz = k \int z^{k-1} F(z) dz \quad (22)$$

From a combination of Equations 9, 10, and 16, the first moment can be written as:

$$\mu_1 = \frac{2D}{B} \sum_n \binom{n}{2} \int z p_n(y_1, \dots, y_n) \delta(y_1 + y_2 - z) dz$$

Using the symmetry of  $\bar{p}_n(y_1, \dots, y_n)$  and Equations 7 and 17, we get

$$\mu_1 = \frac{4D}{B} \sum_n \binom{n}{2} \int_0^\infty \Phi_n(y) dy \quad (23)$$

But by integration of Equation 19 over  $y > 0$ , we see that

$$-\frac{G}{B} \theta_n = (1 - 1/n) \tilde{\Phi}_{n-1} - \Phi_{n-1} + D/B \left[ \binom{n+2}{2} \tilde{\Phi}_{n+2} - \binom{n}{2} \tilde{\Phi}_n \right], \quad n \geq 1$$

where

$$\tilde{\Phi}_n = \int_0^\infty \Phi_n(y) dy$$

Furthermore, this equation multiplied by  $n$  and summed over all positive values of  $n$  yields

$$\frac{G}{B} \sum_n n \theta_n = \frac{2D}{B} \sum_n \binom{n}{2} \tilde{\Phi}_n \quad (24)$$

If we combine Equations 23 and 24, then

$$\mu_1 = \frac{2G}{B} \sum_n n \theta_n = \frac{2G}{B} \langle n \rangle \quad (25)$$

Hence, the mean polymer size  $\mu_1$  is directly proportional to the mean number of growing polymers  $\langle n \rangle$ .

With respect to the moments of the size distribution, it is common to define the number-average degree of polymerization  $X_n$  and the corresponding weight average  $X_w$ :

$$X_n = \mu_1 \quad X_w = \mu_2 / \mu_1$$

A measure of the spread of the distribution is given by the ratio of weight average to number average, which is related to the variance of the distribution according to:

$$\frac{\text{Var} [X]}{\mu_1^2} = \frac{\mu_2}{\mu_1^2} - 1 = \frac{X_w}{X_n} - 1$$

### Limiting Size Distributions

Although numerical solutions are required when the number of radicals in a particle is arbitrary, we can get analytic solutions for the limiting cases from a previous study by Sidel and Katz (4). The details are worked out in the Appendix. In the limit as  $D/B \uparrow \infty$  (zero or one radical in a particle), the stationary size distribution of dead polymer is

$$f(z) = \frac{B}{G} \cdot \exp \left[ -\frac{B}{G} z \right]$$

for which

$$X_n = G/B \quad X_w/X_n = 2$$

For later comparison we express the cumulative distribution of the tail on a normalized scale:

$$F(t) = \int_{y(t)}^{\infty} f(z) dz = e^{-t}$$

where

$$y(t) = X_n t = \frac{G}{B} t$$

In the other limiting situation  $D/B \downarrow 0$  (a large number of radicals in a particle) the size distribution of dead polymer is given by

$$f(z) = \frac{D}{B} \left( \frac{B}{G} \right)^2 z \cdot \exp \left[ -\left( \frac{D}{B} \right)^{1/2} \left( \frac{B}{G} \right) z \right]$$

for which

$$X_n = \frac{2G}{B} \left( \frac{B}{D} \right)^{1/2} \quad X_w/X_n = 3/2$$

Again we write the cumulative distribution of the tail on a normalized scale as

$$F(t) = \int_{y(t)}^{\infty} f(z) dz = (2t + 1) e^{-2t}$$

where

$$y(t) = X_n t = \frac{2G}{B} \left( \frac{B}{D} \right)^{1/2} t$$

### Discussion of Results

From a numerical solution of Equations 19 and 20 we obtain the polymer size distribution for different values of the ratio  $D/B$  of termination to arrival rates. Figure 1 shows two distributions that essentially encompass the range of variation as plots of the fraction  $F(t)$  of polymer having size greater than  $X_n t$ , where  $X_n$  is the number average. The values of  $D/B$  for which the limiting cases provide suitable approximations can be seen in Figure 2, where the number average is in the form  $(B/2G) X_n = \langle n \rangle$ , the mean number of growing polymers, together with the corresponding weight average  $(B/2G) X_w$  and their ratio  $X_w/X_n$  are plotted

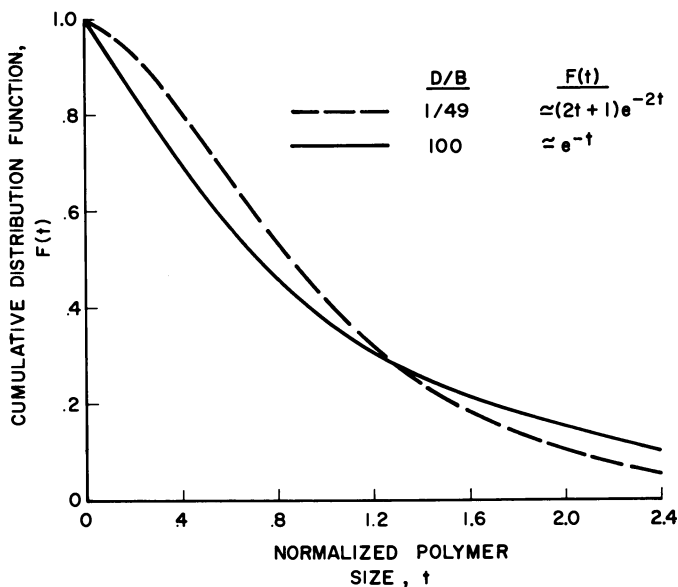


Figure 1. Limiting polymer size distributions

$F(t)$  = Polymer fraction with size greater than  $X_n t$   
 $X_n$  = Number average  
 $B$  = Arrival rate  
 $D$  = Termination rate per radical pair



as functions of  $\sqrt{D/B}$ . We see here that in order to make the leading moments  $X_n$  and  $X_w$  agree well with the limiting case  $D/B \uparrow \infty$ , we must still take  $D/B$  of the order of 100, while to get good agreement in  $X_n$  and  $X_w$  at the other end of the range, we need only go down to  $D/B$  of the order of 0.1.

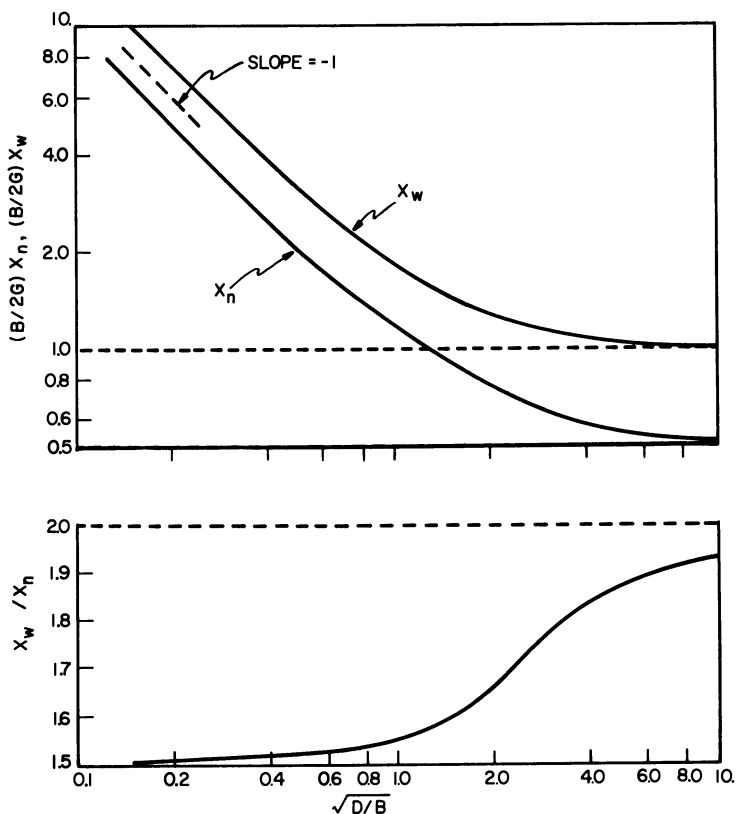


Figure 2. Moments of the size distribution

- $X_n$  = Number average  
 $X_w$  = Weight average  
 $B$  = Arrival rate  
 $G$  = Growth rate  
 $D$  = Termination rate per radical pair  
 $\langle n \rangle = \frac{B}{2G} X_n = \text{Mean number of growing radicals}$

From Figure 2 we may also make an illuminating comparison between the behavior of  $X_w/X_n$  and that of  $\langle n \rangle$ . For values of  $\langle n \rangle$  larger than 5 or so, the value of  $X_w/X_n$  is very close to the limiting value, 1.5, for infinite  $\langle n \rangle$ . Even for  $\langle n \rangle = 2$ , the difference is small. As far as the leading moments go, we may confidently treat by continuum

methods the two-phase heterogeneous polymerizations for which  $\langle n \rangle$  is larger than 2.

The most significant change in  $X_w/X_n$  occurs when  $\langle n \rangle$  lies between 1/2 and 1. As a consequence, relatively small deviations from  $\langle n \rangle = 1/2$  cause the variance of the molecular weight distribution to be substantially different from that of an exponential distribution. According to Gerens (1), emulsion polymerization will often be in this range of  $\langle n \rangle$ , and the results presented here might give one a qualitative insight into the effect of such deviations on the molecular weight distribution. Unfortunately, data on molecular weight distributions or even the moments of the distribution with respect to  $D/B$  do not appear in the literature.

It should, however, be pointed out that in the case of a non-ideal emulsion polymerization,  $D$  and therefore  $\langle n \rangle$  change slowly with time owing to the growth of the particle. Under these conditions our calculations do not give the final molecular weight distribution of the product but only the distribution for the incremental amount of dead polymer formed during a short time interval in which  $D$  can be considered constant. A more complete dynamic analysis of emulsion polymerization is given by Saidel and Katz (4) for the limiting cases.

## Appendix

### *Limiting Polymer Size Distribution*

Following Ref. 4, the polymer size distribution in the Smith-Ewart limit  $D/B \uparrow \infty$  can be developed from the probability equations:

$$\frac{dp_0(t)}{dt} = B \left[ \int p_1(x, t) dx - p_0(t) \right]$$

$$\frac{\partial p_1(x, t)}{\partial t} + G \frac{\partial p_1(x, t)}{\partial x} = B[p_0(t) \delta(x) - p_1(x, t)]$$

where  $p_0(t)$  is the probability that a given particle contains no radical at time  $t$ , and  $p_1(x, t) dx$  is the probability that the particle contains one radical of size  $[x, x + dx]$ . Here again  $B$  and  $G$  are the rates of radical arrival and growth. Under stationary conditions, where the time dependence disappears, we find

$$p_0 = \int p_1(x) dx = \frac{1}{2}$$

and

$$\frac{dp_1(x)}{dx} = \frac{B}{G} \left[ \frac{1}{2} \delta(x) - p_1(x) \right]$$

Since this equation is equivalent to

$$\frac{dp_1(x)}{dx} = -\frac{B}{G} p_1(x) \quad x > 0$$

with

$$p_1|_{x=0} = \frac{B}{2G}$$

we see at once that

$$p_1(x) = \frac{B}{2G} \cdot \exp \left[ -\frac{B}{G} x \right] \quad x > 0$$

Since the situation is stationary, we may simply identify the size distribution of dead polymer with that of growing polymer:

$$f(x) = \frac{p_1(x)}{\int p_1(x) dx} = \frac{B}{G} \cdot \exp \left[ -\frac{B}{G} x \right]$$

To find the polymer size distribution in the opposite limiting case, where  $D/B \downarrow 0$ , we start with phenomenological equation

$$\frac{\partial r(x,t)}{\partial t} + G \frac{\partial r(x,t)}{\partial x} = B \delta(x) - Dr(x,t) \int r(y,t) dy$$

where  $r(x,t) dx$  is not a probability but rather the number of growing radicals of size  $[x, x + dx]$  at time  $t$ . Under stationary conditions, where the time dependence disappears, this becomes an ordinary differential equation in  $r(x)$  which can again readily be solved. Letting

$$n = \int r(y) dy$$

the total number of growing radicals present, we find

$$\frac{dr(x)}{dx} = \frac{B}{G} \delta(x) - \frac{nD}{G} r(x)$$

This has the solution

$$r(x) = \frac{B}{G} \cdot \exp \left[ -\frac{nD}{G} x \right] \quad x > 0$$

from which, by integration

$$n = \left( \frac{B}{D} \right)^{1/2}$$

so that

$$r(x) = \frac{B}{G} \cdot \exp \left[ -\frac{B}{G} \left( \frac{D}{B} \right)^{1/2} x \right]$$

Conditions being stationary, we may calculate the size distribution of dead polymer by catching two growing radicals at the moment they terminate each other and accounting, with suitable weighing, for the sum of their sizes. We find

$$\begin{aligned} f(z) &= \frac{\iint r(x) r(y) \delta(x+y-z) dx dy}{\iint r(x) r(y) dx dy} \\ &= \frac{\int r(x) r(z-x) dx}{\left( \int r(x) dx \right)^2} \\ &= \left( \frac{B}{G} \right)^2 \frac{D}{B} z \cdot \exp \left[ -\frac{B}{G} \left( \frac{D}{B} \right)^{1/2} z \right] \end{aligned}$$

### **Acknowledgment**

The work reported here was supported in part under NSF Grant No. GK-943.

### **Literature Cited**

- (1) Gerens, H., *Z. Electrochem.* **60**, 400 (1956).
- (2) Goldstein, R. P., Amundson, N. R., *Chem. Eng. Sci.* **20**, 195 (1965).
- (3) O'Toole, J. T., *J. Appl. Polymer Sci.* **9**, 129 (1965).
- (4) Sidel, G. M., Katz, S., *J. Polymer Sci.*, in press.
- (5) Schildknecht, C. E., "Polymer Processes," Interscience, New York, 1956.
- (6) Stockmayer, W. H., *J. Polymer Sci.* **24**, 314 (1957).
- (7) Katz, S., Shinnar, R., *Ind. Eng. Chem.*, in press.

RECEIVED April 1, 1968.

## Growth of Polymer Particles in Vinyl Chloride Emulsion Polymerization

G. GATTA, G. BENETTA, G. P. TALAMINI, and G. VIANELLO

Montecatini Edison S.p.A., Research Center of Petrochemical Division,  
Porto Marghera Venezia, Italy

*In the seeded emulsion polymerization of some monomers—e.g., styrene—it is possible to obtain final latexes with uniform, large particles by adjusting, during polymerization, the quantity of added emulsifier; the formation of new particles is prevented by the limited amount of emulsifier. For vinyl chloride, limited emulsifier is not sufficient to prevent the formation of new particles; in fact, to obtain a monodispersed latex, the surface of the particles seeded in a given water volume must be controlled. It is assumed that the growth of new nuclei is related either to the rate of formation of primary useful radicals or to the rate that these are taken by the surface of sized particles.*

For some polymers it has been shown that monodispersed latexes with large particle sizes can be obtained by a seeding technique (10, 11). According to this technique, some particles of a preformed latex are grown by polymerizing monomer on them which is added continually during the process together with emulsifier. To obtain monodispersed final latexes, the addition of the emulsifier must be adjusted accurately (limited emulsifier); in fact, the surface of the seeded particles must never be saturated in order to prevent the formation of new particles.

Few works have appeared on the seeded emulsion polymerization of vinyl chloride (VC). Giskehaug (5) recently used this technique in a kinetic study of the emulsion polymerization of VC, but he has not determined the number and distribution of particles in the final latexes. Kotlyar *et al.* (6) do not give sufficient experimental data for an exhaustive analysis of the results; moreover, most of the growth experiments seem to have been carried out in the presence of free emulsifier. The data reported in some industrial patents (1, 9) point out only the impor-

tance of the way in which emulsifier is added to produce the desired characteristics of the final product. A multiple reseeded technique (7) has been suggested to obtain uniform, large particles, but it is very elaborate and time consuming.

In the present work the conditions used to obtain uniform growth of the seeded particles, in a single step, in the emulsion polymerization of VC, are reported (4), in particular, we show that limited emulsifier is not sufficient to prevent new particle formation. A qualitative interpretation of results is suggested.

### **Experimental**

All polymerizations were carried out at a temperature of 55°C. either in a 50-gallon kettle (Experiments A, B, C) or in a 100-gallon kettle (Experiments D, E); in both cases, reactors were glass lined and fitted with a device for feeding soap solution and VC continuously.

The potassium persulfate-sodium bisulfite redox system was used as the initiator for Experiments A, B, C, D, whereas potassium persulfate only was used in Experiment E. Quantities of initiator were chosen accurately so that the reaction rate was always about the same.

The polymerization procedure was as follows: water and the other additives were introduced, deaeration followed, some of the VC was added, and the reaction was started. The remaining VC and soap solution were introduced continuously, following a procedure that took into account particle total surface, so that at each moment added quantities never reached complete saturation. As soon as the kettle pressure reached 75 p.s.i.g., the reactor was vented, and the following determinations were carried out on the resulting latexes: solids percent, surface tension, particle size, and diameter distribution [measured by electron microscope (Philips model E-M-200 type PW 6000) calibrated with polystyrene latex (Dow):  $\phi = 0.365$  and  $\phi = 0.557 \mu$ ]. Particles were counted, and diameters were measured with a particle size analyzer (Zeiss, model TG-Z3). High purity VC and distilled water were used. Potassium persulfate and sodium bisulfite were C. Erba reagent grade. The soap used was Empicol Ser (a product of Marchon Italiana), as received. The active ingredient is sodium lauryl sulfate = 88%. All the quantities in weight, mentioned in the present work, refer to the product as such.

**Experiment A—Initial Seed Latexes for Growth Experiments.** Four different PVC latexes were prepared for use as seeds in growth experiments according the well-known batch procedure. The properties of these seeds are given in Table I.

**Experiment B—Growing Particle Size of Seed Latex No. 2.** Water (90 kg.), vinyl chloride (13.27 kg.), and seed latex No. 2 (7.85 kg.) (2.73 kg. solids) were placed in the kettle. About one hour after the start of the reaction, 64 kg. of the remaining VC was fed continuously, while simultaneously a solution of 0.336 kg. Empicol Ser in 2.0 kg. water was introduced, continuously, dropwise. Vinyl chloride (64 kg.) and soap (0.336 kg.) were introduced by the following procedure. In the

first hour of reaction 23.5 kg. of VC and 62.5 grams of soap were introduced; during the second hour 23.5 kg. VC and 87.5 grams soap were added; during another hour, 17 kg. VC and 186 grams soap were added. About four and a half hours from the beginning, the reaction was complete. Runs 63 and 67 were carried out according to the described procedure; the conversions were 89.6 and 90.0% respectively, and the latex surface tensions were 66.6 and 66.1 dynes/cm.

Table I. Properties of Seed Latexes

Seed No.	Conversion, %	Solids, %	Particle Diameter, A.	$\sigma$ , A. <sup>a</sup>	$\sigma v$ , % <sup>b</sup>	Surface Tension, dynes/cm.
1	90.6	35.3	4200	120	8.8	—
2	88.6	34.8	4000	115	8.7	62
3	75.0	31.0	3100	66	6.6	—
4	27.3	14.1	2290	100	13.2	66.3

<sup>a</sup> Standard deviation of particle diameter.

<sup>b</sup> Coefficient of volume variation.

**Experiment C—Growing Particle Size of Seed Latex No. 1.** The procedure used for Experiment B was followed, except that 8.95 kg. of seed latex No. 1 (3.16 kg. solids) and 12.84 kg. of VC were initially placed in the kettle. Run 72 was done by this procedure, and a 94.0% conversion resulted; the surface tension of the latex was 65.0 dynes/cm.

**Experiment D—Growing Particle Size of Seed Latex No. 3.** Quantities of H<sub>2</sub>O, VC, and seed (*see* Table I) are given in Table II. A total of 720 grams of soap was introduced dropwise during the reaction. Empicol Ser was dissolved in water. Conversion was about 90% for all runs.

Table II. H<sub>2</sub>O, VC, and Seed Used in Experiment D

Latex Run	H <sub>2</sub> O, kg.		Dry Seed No. 3, kg.	VC Feed, kg.		Reaction Time, hours: min.	Solids in Final Latex, %
	Initial	Final		1st	2nd		
913	222.8	269	2.6	36.0	154	6	39.2
945	223.0	269	2.9	35.7	154	5:30	39.0
951	223.3	269	5.76	32.8	154	5:30	39.4
952	223.0	269	7.2	31.4	154	5:30	39.8
953	223.0	269	8.65	30.0	154	5:15	39.1
954	222.5	269	11.5	27.1	154	5	40.5
962	222.5	269	11.5	27.1	154	5:30	40.2
1277	223.0	269	15.7	22.9	154	4:26	38.8
1278	223.0	269	23.5	15.1	154	4:42	40.2
1279	223.0	269	31.4	161.2 <sup>a</sup>	—	4:20	40.0
941	223.1	269	48.4	144.2 <sup>a</sup>	—	4:45	40.9

<sup>a</sup> All the VC was introduced, continuously, at the beginning of the reaction.

**Experiment E—Growing Particle Size of Seed Latex No. 4.** The quantities of water, VC, seed (Table I) and soap used in these polymerizations are given in Table III. In Runs 935, 1313, and 1314 all the VC was

**Table III. H<sub>2</sub>O, VC, Seed, and Soap Used in Experiment E**

Latex Run	H <sub>2</sub> O, kg.		Dry Seed No. 4, kg.	VC Monomer, kg.	Empicol Ser, kg.	Reaction Time, hours: min.	Solids in Final Latex, %
	Initial	Final					
936	139.6	147	21.2	108.5	0.325	3:55	44.2
937	143.4	147	10.6	60.3	0.162	3:10	30.6
938	144.0	147	8.5	50.6	0.130	2:45	26.7
939	145.0	147	6.35	41.0	0.0975	2:05	22.8
935	147.0	147	4.24	31.5	0	1:30	17.5
940	147.0	147	4.24	70.0	0	3	30.6
1313	147.0	147	2.12	35.0	0	—	—
1314	147.0	147	1.06	17.5	0	—	—

introduced at the beginning of the run; in the other runs, part of the VC was placed initially in the kettle, and the remaining VC was fed during the reaction. In Runs 936, 937, 938, and 939 only the proper soap solution was introduced continuously drop by drop. The amount of Empicol Ser is different in each run, and it was calculated, on the grounds of particle surface increase, that the surface saturation would never be reached. In Runs 935, 940, 1313, and 1314 no soap was added because the low solids percent of final latex assures latex stability. All runs were made at constant reaction rate; since quantities of VC subjected to polymerization are quite different, reaction times are different. Conversions were always about 90%.

### Results

**Seed Latexes.** In preparing the four different PVC latexes to be used as seeds in growth experiments, uniform-sized particles were obtained, as shown in Figure 1. [The main properties of the seed latexes have been given in Table I.] The amount of soap required to coat the particles completely was determined for each latex by the method of surface tension. An example of these determinations is given in Figure 2 for seed latex No. 2, where an aqueous dispersion of the seed latex at 3.55% solids was used. Figure 2 also shows the surface tension variation of aqueous soap solutions. In the absence of particles the surface tension decreases sharply up to a soap concentration of 0.0045%; at higher concentrations, the values are practically constant. In the presence of 3.55% of seed latex No. 2 surface tension becomes practically constant at a much higher soap concentration because the soap molecules are adsorbed on the polymer particles up to complete saturation of their surface.



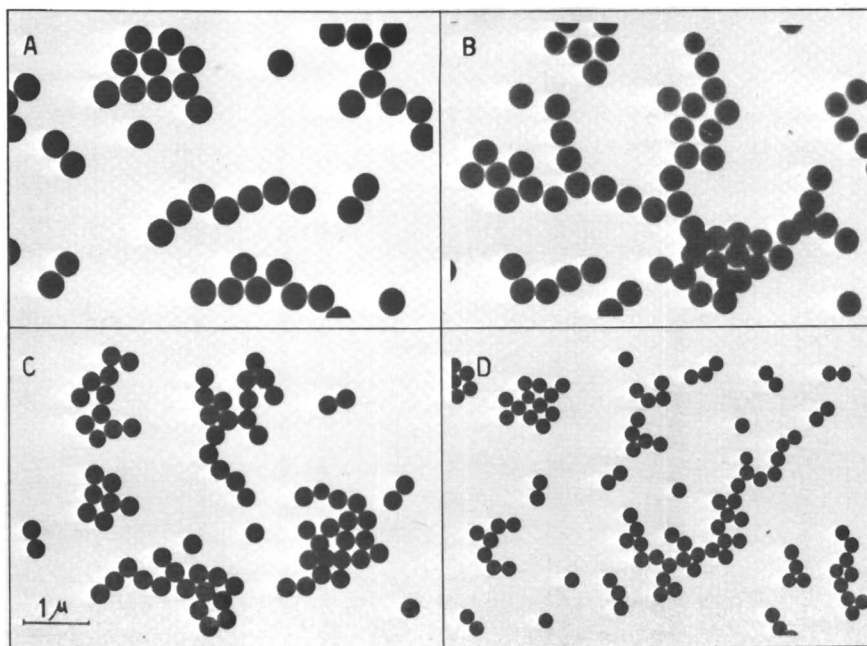


Figure 1. Electron micrographs of seeds used in growth experiments

- (A) Seed No. 1
- (B) Seed No. 2
- (C) Seed No. 3
- (D) Seed No. 4

The amount of soap required for complete coverage of the particle surface lies in the range 1.62–1.94 mg./10<sup>20</sup> sq. A. Taking into account the value of covering power of sodium lauryl sulfate as reported in literature, the value of 1.62 is preferred (2, 3).

**Growing Particle Size.** According to Vandegaer's (10) procedure, the total surface (*TS*) of all the particles during the growth can be calculated, so that the emulsifier addition can be adjusted not to exceed the 100% surface saturation, thus preventing formation of new particles. The following equations were used:

$$\phi = \phi_i [(X + a)/a]^{1/3} \quad (1)$$

$$TS = \frac{6a}{\phi_i \cdot \rho} [(X + a)/a]^{2/3} \quad (2)$$

$\phi$  = diameter of particles in cm., at time *t*

$\phi_i$  = initial diameter of particles

$X$  = grams of VC added at time  $t$

$a$  = grams of seed solids per 100 grams latex

$\rho$  = PVC density = 1.4 grams/ml.

$TS$  = total surface (in square centimeters) of particles in 100 grams of latex.

Two experiments in growing seed No. 2 were carried out—Runs 63 and 67 (Experiment B); 7.85 kg. of seed latex (34.8% solids) were introduced ( $a = 2730$  grams). Calculated values of  $TS$  and of  $\phi$  for different values of  $X$  are reported in Table IV.

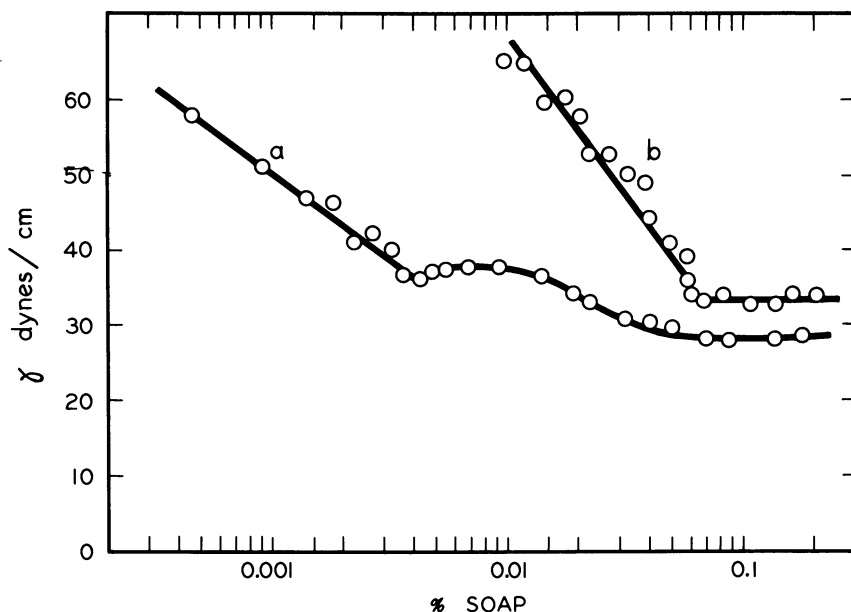


Figure 2. Surface tension vs. soap concentration with (b) and without (a) latex present

During the first stage of growth, no soap was introduced to prevent formation of new particles; only the small amount of soap introduced with the seed is present (this is neglected in the calculations). During this stage, since the solids content is very low, no coagulation is observed. For the same reason, when conversion is high, soap is added in an amount to cause less than 100% saturation. The final latex has a surface tension greater than 60 dynes/cm., which shows how low the concentration of free emulsifier is in water.

During these stages small samples of the latex were taken, with great care to avoid coagulation; the particle sizes were measured by

electron microscopy. Unexpectedly, we observed the formation of new particles, which grow in competition with the seed particles (Table V).

**Table IV. Calculations for Growth Experiment B  
(Runs 63 and 67)**

X, grams	(X + 2730)	(X + 2730) <sup>2/3</sup>	T.S.,	Weight of Empicol		$\phi$ , A.
			sq. A. $\times 10^{-22}$	Required <sup>a</sup>	Used	
0	2730	195.33	292	47	0	4000
7270	10000	464.15	694	112	0	6166
13270	16000	635.01	950	154	0	7211
36770	39500	1214.50	1815	294	62.5	9746
60270	63000	1583.29	2367	384	150.0	10875
77270	80000	1856.59	2772	449	336.0	12332

<sup>a</sup> Amount needed for 100% saturation.

**Table V. Results of Growth Experiment B**

Run	Polymerization Time (from beginning of reaction), min.	Solids, %	Numerical Distribution of Particles in Latex
63	0	—	Monodispersed around 4000 A.
	70	9.30	Two groups around 1300 and 6100 A.
	170	29.75	Three groups around 500, 3200, 9500 A.
	295	40.46	Three groups around 750, 4200, 11500 A.
67	0	—	Monodispersed around 4000 A.
	155	26.0	Two groups around 2500 and 9200 A.
	270	39.0	Three groups around 800, 3800, 11500 A.
	300	40.46	Three groups around 1500, 4200, 12500 A.

The percent numerical distribution of particles, at different polymerization times, is plotted in Figures 3 and 4 and is shown in Figure 5. Each group of particles exhibits a fairly uniform distribution around a main diameter (the one indicated in Table V). Diameter dispersion is wide; for example, we have calculated the  $\sigma$  value for the sample taken at 70 minutes in Run 63 and for the sample taken at 300 minutes in Run 67. They are reported in Table VI. In a few cases, diameter distribution is not strictly gaussian in nature.

By observing diameter distribution in the final latex, one can recognize the following: some large particles, resulting from the growth of the seed; a second group of particles, which clearly results from the growth of particles formed in a nucleation phase at the beginning of polymerization (*see* sample taken at 70 minutes in Run 63 and the one taken at 155 minutes in Run 67); finally a third group with very small diameters whose origin is obscure.

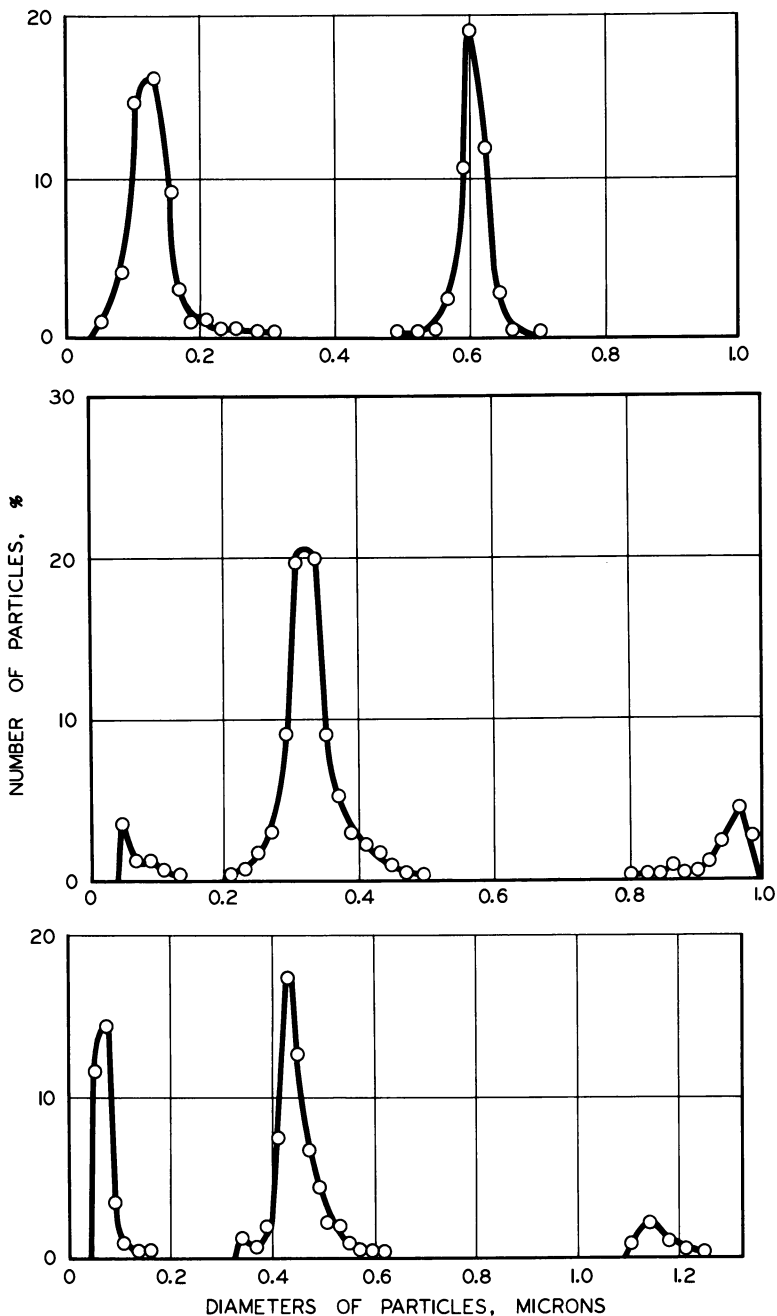
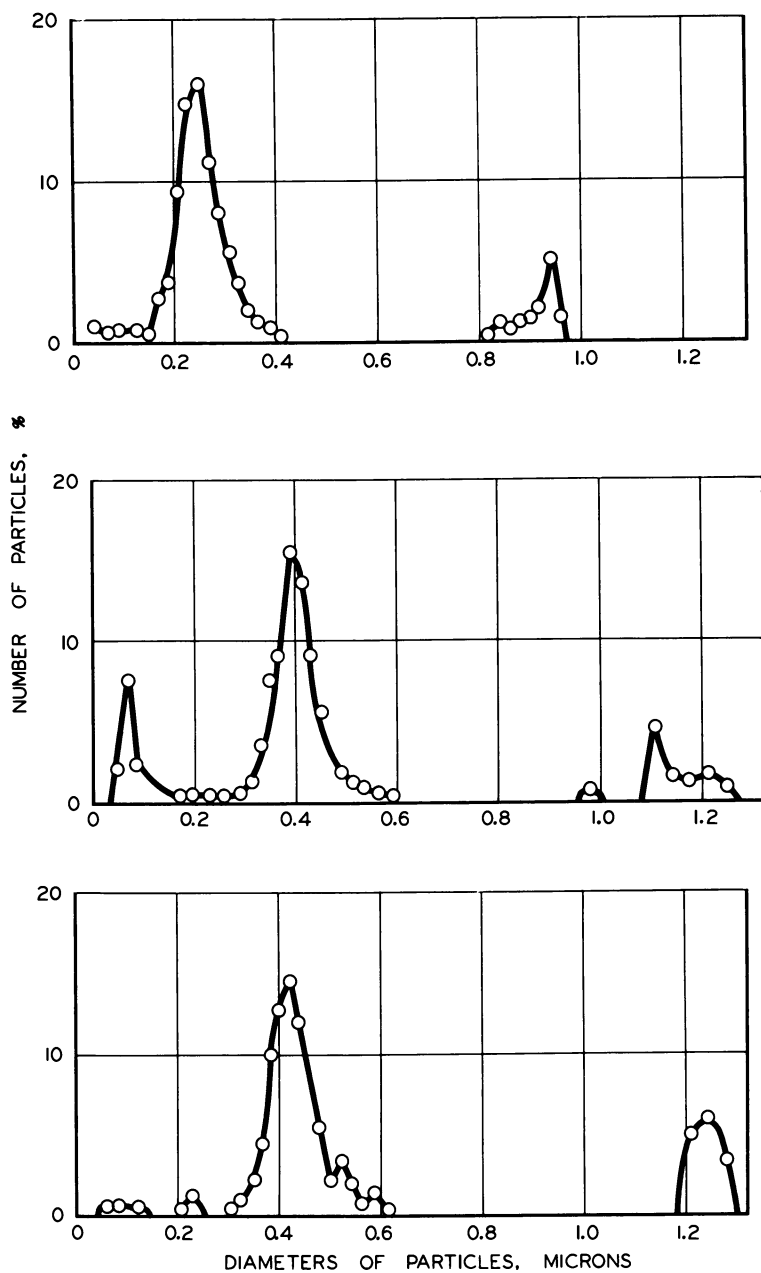


Figure 3. Run 63: numerical distribution of particles at different polymerization times

Top: after 70 min. Middle: after 170 min. Bottom: after 295 min.



**Figure 4.** Run 67: numerical distribution of particles at different polymerization times

Top: after 155 min. Middle: after 270 min. Bottom: after 300 min.

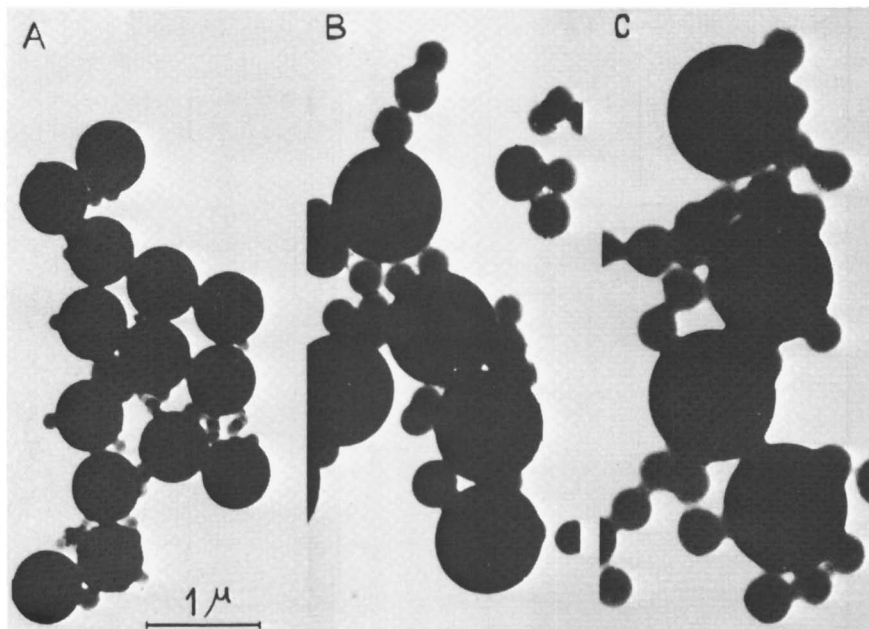


Figure 5. Run 63: electron micrographs of the particles obtained at different polymerization times

(A) after 70 min.

(B) after 170 min.

(C) after 295 min.

Table VI.  $\sigma$ -Values for Experiment B

Run	Sampling Times, min.	Mean Diameter, A.	$\sigma$ , A.
63	70	1300	380
		6100	220
67	300	1500	670
		4200	530
		12500	510

To confirm the results of Runs 63 and 67, another growth experiment (Experiment C, of Run 72) was carried out, using seed latex No. 1. A total of 8.95 kg. of seed latex was used, at 35.3% solids—*i.e.*,  $a = 3160$ . According to Equations 1 and 2, values of  $TS$  and  $\phi$  for different values of  $X$  were obtained and are given in Table VII. As in the previous cases small samples of latexes were taken during polymerization, and the particles were photographed. The results are in Table VIII.

**Table VII. Calculations for Growth Experiment C (Run 72)**

X	X + 3160	(X + 3160) <sup>2/3</sup>	TS, Sq. A. × 10 <sup>-22</sup>	Weight of Empicol Ser, grams		φ, A.
				Required	Used	
0	3160	215.34	322.36	52	0	4200
6840	10000	464.15	694.8	112	0	6176
12840	16000	635.01	950.6	154	0	7212
36340	39500	1214.50	1818.1	294	62.5	9746
59840	63000	1583.29	2370.2	384	150.0	11392
76840	80000	1856.59	2779.3	450	336.0	12332

**Table VIII. Results of Growth Experiment C, Run 72**

Sampling Times (from beginning of reaction), min.	Solids, %	No. of Counted Particles	Numerical Distribution of Particles in Latex
0	—	580	Monodispersed around 4200 A.
45	6.4	372	Two groups around 1100, 6000 A.
137	21.0	442	Three groups around 800, 2300, 8200 A.
273	41.0	538	Three groups around 600, 3700, 11000 A.

Experiment C confirms the previous results. Other growth experiments were carried out with seed latexes No. 3 and 4. In a first series of runs (Experiment D) seed No. 3 ( $\phi = 3100$  A.) was grown by introducing different amounts of seed in each polymerization run, so that the ratio of the total introduced monomer to the weight of seed ( $M/P$ ), ranges from 3 to 73 as a maximum. Polymerizations were carried out, as before, using the redox system potassium persulfate–sodium bisulfite as activator and using an amount of sodium lauryl sulfate always less than the amount required for complete coverage of the particle surface (details are given in the Experimental Section). The results are reported in Table IX and in Figure 6. Runs 954 and 962 are similar and were conducted to test the reproducibility of results.

In another series of runs (Experiment E), various amounts of seed No. 4 were introduced ( $\phi = 2290$  A.). The following modifications were made in the polymerization procedure:

(a) Potassium persulfate alone was used as activator, in such a concentration that the polymerization rate was almost the same as with the redox system.

(b) The  $M/P$  ratio was kept within a narrow range. For the first five runs (see Table X) the  $M/P$  ratio ranges from 5.12 to 7.38. For the other experiments, since the amount of seed was very small (and therefore the amount of VC to be introduced would have been too small), the  $M/P$  ratio had to be increased to 16.51. However, two identical runs

were made, with two different  $M/P$  ratios—*i.e.*, 7.38 (Run 935) and 16.51 (Run 940), and similar results were obtained.

The main results are reported in Table X. In the last two series of experiments, poly- or monodispersed latexes were obtained according to the adopted formulation.

### *Discussion and Conclusions*

In the experiments which were carried out in absence of free soap, new groups of particles arising from new nucleation phases appeared in the final latexes; in other experiments monodispersed final latexes were obtained. If the experimental data are rearranged according to the surface value  $S$  (per ml. of initial water) of seed or according to the number of seeded particles (per ml. of initial water) (Table XI), it is possible to notice that, for the two series of experiments using seeds with  $\phi = 3100$  and 2290 A., uniform growth of seed particles begins only above a certain value of  $S$  or correspondingly of  $N$ .  $S$  and  $N$  are calculated according to the following equations:

$$S = \frac{b \cdot 6}{\phi \cdot \rho} \cdot 10^{24}$$

$$N = \frac{b}{\frac{\pi}{6} \cdot \phi^3 \cdot \rho} \cdot 10^{24}$$

$b$  = grams seed/ml. initial water at 55°C.

$\phi$  = seed diameter, A.

$\rho$  = density of PVC (1.4 grams/ml.)

**Table IX. Results of Growth Experiment D**

Run	$M/P$	No. of Counted Particles	Numerical Distribution of Particles in Final Latex
913	73.0	2338	Three groups around: 1100, 4250, 10000 A. 1100, 4250, 8600 A. 800, 3300, 8100 A. 900, 2900, 7500 A. 900, 2500, 6900 A. 900, 1800, 6600 A. 700, 2000, 6800 A.
945	72.96	355	
951	32.43	229	
952	25.75	426	
953	21.27	362	
954	15.75	637	
962	15.75	233	
1277	11.26	160	
1278	7.19	194	
1279	5.13	184	Monodispersed around: 6360 A. 5900 A. 5200 A. 4300 A.
941	2.98	428	



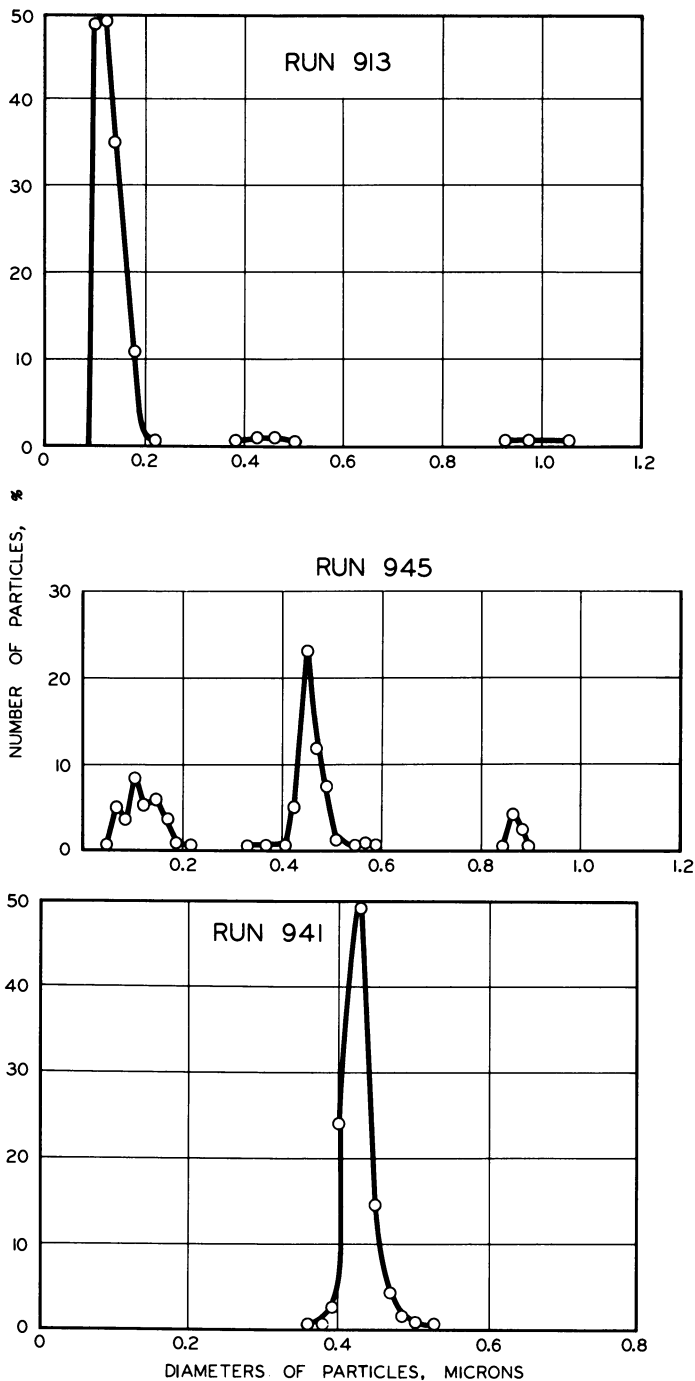
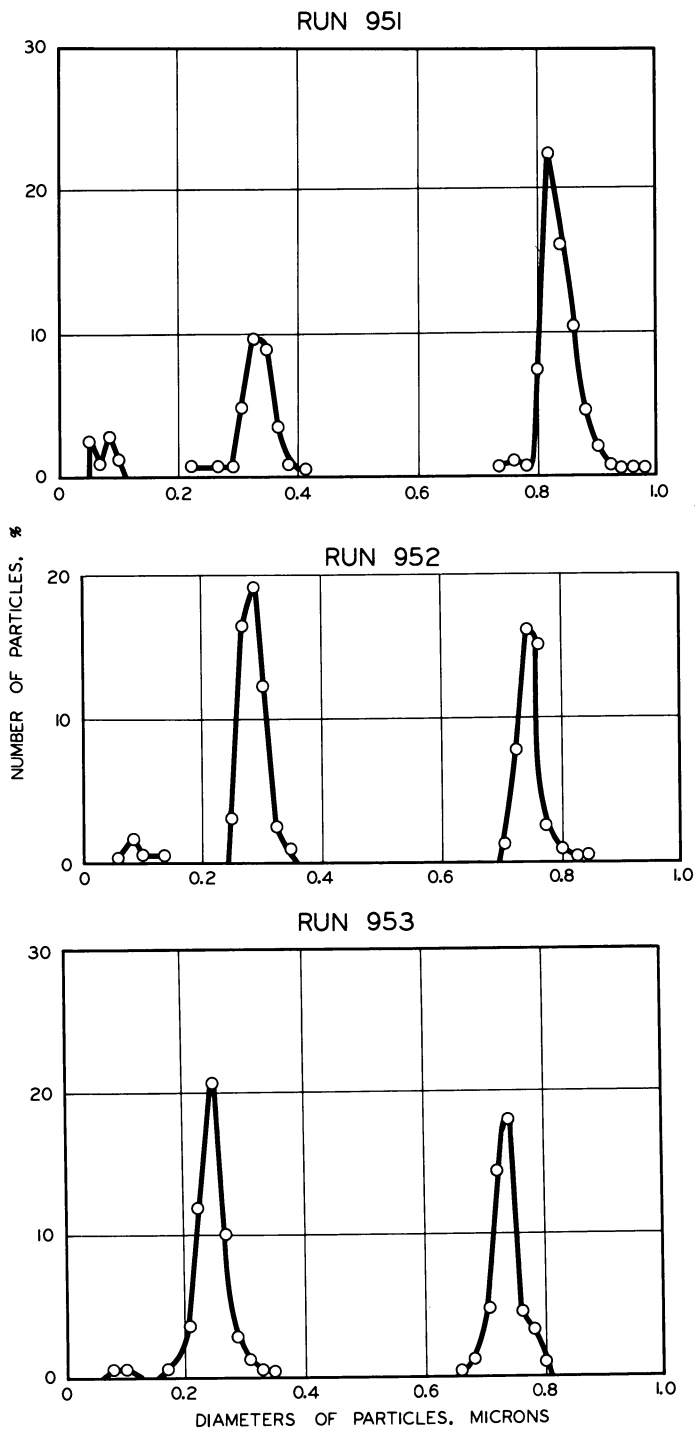
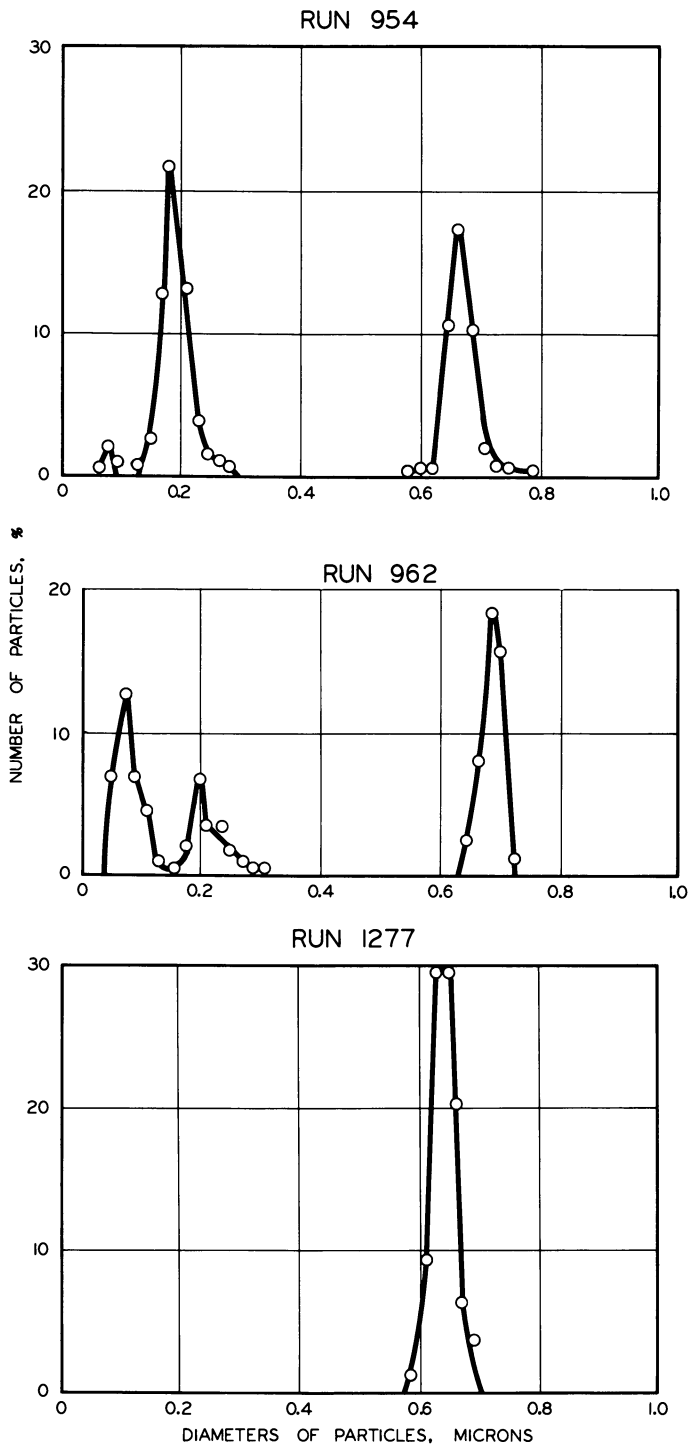
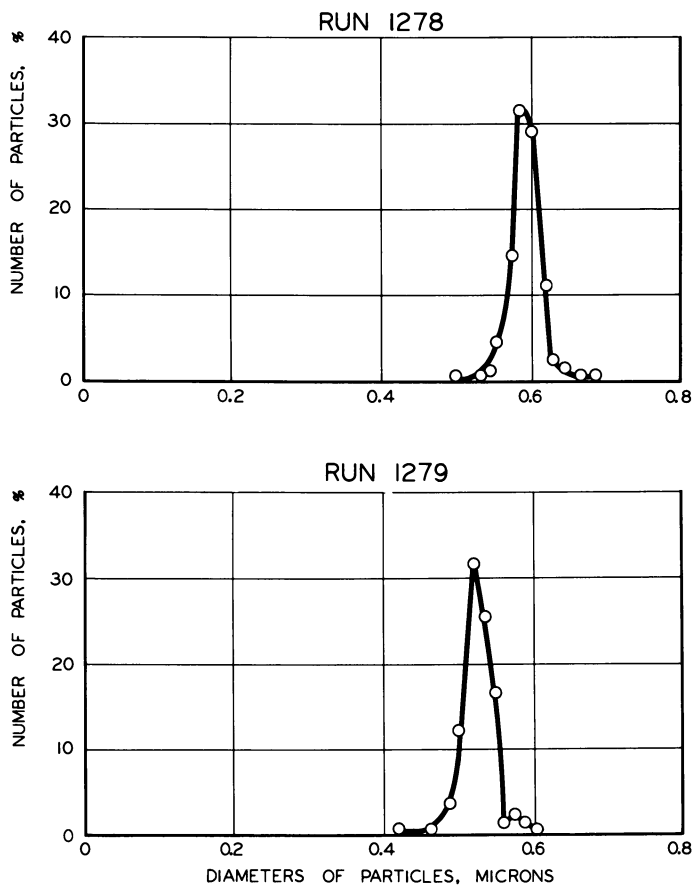


Figure 6. Numerical distribution of particles in final latex of different runs





**Table X. Results of Growth Experiment E**

Run	M/P	No. of Counted Particles	Numerical Distribution of Particles in Final Latex
936	5.12	421	Monodispersed around: 3900 A.
937	5.69	245	3700 A.
938	5.95	325	3900 A.
939	6.45	480	3900 A.
935	7.38	304	3700 A.
940	16.51	301	5400 A.
1314	16.51	305	Two groups around: 2300, 5700 A.
1313	16.51	394	2600, 5500 A.

From the available experimental data, in the experiments with  $\phi = 3100$  A., uniform growth begins in the range of  $S = 0.7 \times 10^{20}$  to  $0.96 \times 10^{20}$  A. and in the range of  $N = 2.34 \times 10^{12}$  to  $3.16 \times 10^{12}$ . Similarly, in

the experiments with seed  $\phi = 2290$  A., uniform growth begins in the range of  $S$  from  $0.26 \times 10^{20}$  to  $0.53 \times 10^{20}$  sq. A. and in the range of  $N$  from  $1.6 \times 10^{12}$  to  $3.24 \times 10^{12}$ . For small seed sizes, such as those used here, the limiting value of  $S$  seems to increase with increasing diameter; the limiting value of  $N$  seems to be more constant. To confirm this behavior, we are carrying out many growth experiments on seeds with diameters in the range 1000–6000 A., using the conditions as in Experiment D—*i.e.*, varying the initial amount of seed so that the number  $N$  of seeded particles per ml. water and the respective surface  $S$  are varied

**Table XI. Results of Growth Experiments**

Run	$S \times 10^{-20}$ , Sq. A. (per ml. $H_2O$ initial)	$N \times 10^{-12}$ (per ml. $H_2O$ initial)	$\phi_i$ , A.	M/P	Distribution of Particles in Final Latex
72	0.312	0.307	4200	24.31	Polydispersed
63	0.285	0.569	4000	28.30	Polydispersed
67	0.285	0.559	4000	28.30	Polydispersed
913	0.155	0.514	3100	73.07	Polydispersed
945	0.177	0.588	3100	72.96	
951	0.352	1.168	3100	32.43	
952	0.440	1.462	3100	25.75	
953	0.529	1.756	3100	21.27	
954	0.705	2.340	3100	15.75	
962	0.705	2.340	3100	15.75	
1277	0.961	3.168	3100	11.26	Monodispersed
1278	1.438	4.771	3100	7.19	
1279	1.922	6.376	3100	5.13	
941	2.960	9.825	3100	2.98	
1313	0.133	0.8105	2290	16.51	Polydispersed
1314	0.266	1.621	2290	16.51	
940	0.533	3.243	2290	16.51	Monodispersed
935	0.533	3.243	2290	7.38	
939	0.809	4.923	2290	6.45	
938	1.091	6.636	2290	5.95	
937	1.366	8.311	2290	5.69	
936	2.885	17.07	2290	5.12	

widely. Thus, for each seed diameter it is possible to determine the range of  $N$  and  $S$  values over which the seed growth behavior is varied. Preliminary results of two sets of experiments with  $\phi = 4570$  and  $5700$  A., respectively, are reported in Table XII, together with previously reported results of experiments with  $\phi = 2290$  and  $3100$  A.

$S$  and  $N$  values cannot be plotted as functions of  $\phi_i$  since sufficient experimental results are not available, although the results adequately describe the phenomenon qualitatively. The smaller the seed particle

size, the higher seems to be the limiting number of particles (per ml. of aqueous phase) to which the system approaches. If the number of seeded particles is less than that limiting value, polymer molecules formed in the aqueous phase give rise to new nuclei, in which polymerization occurs in competition with aqueous-phase polymerization. The limiting value of  $N$  increases, whereas the  $S$  value obviously decreases (Table XII) with decreasing seed diameter.

**Table XII. Range of  $S$  and  $N$  Values of Seed Particles Over Which Growth Behavior Varies (uniform at higher values)**

$\phi_1$ , A.	$S \times 10^{-20}$ , Sq. A.	$N \times 10^{-12}$
2290	0.26-0.53	1.62-3.24
3100	0.70-0.96	2.34-3.16
4570	0.53-1.07	0.94-1.88
5700	0.62-1.29	0.79-1.58

This behavior can be explained as follows. Vinyl chloride is moderately soluble in water (8); thus, the initiator radicals react with VC molecules dissolved in water, and polymerization begins. If there are no polymer particles present, a particle is supposed to be formed for each primary radical. If there are a few particles present, some of the primary or growing radicals may be captured by polymer particles. If the capture rate is equal to that of formation of primary radicals, no new particles form.

The capture rate is proportional to the particle's total surface. The formation rate of new particles is given by Equation 3.

$$\frac{dN}{dt} = R_i - K(TS) \quad (3)$$

$R_i$  is the formation rate of primary useful radicals,  $K$  is the capture rate of particles per unit surface, and  $TS$  is the total surface. In order for no new particles to form ( $dn/dt = 0$ ), it is necessary that:

$$(TS)_1 = \frac{R_i}{K} \quad (4)$$

Therefore, at a constant value of  $R_i$  and  $K$ , there is a surface value above which no new particles form. In growth experiments where the surface was increased gradually, no formation of new particles could be observed above a certain surface value, and latexes appeared monodispersed. For spherical particles, capture rate per unit surface ( $K$ ) is inversely proportional to particle radius; in fact we have:

$$K = \frac{Dc^*}{r} \quad (5)$$

where  $D$  is the diffusion constant,  $c^*$  is the radical stationary concentration in the aqueous phase, and  $r$  is the particle radius. From Equations 4 and 5 it appears that the limiting surface above which no new particles form, increases with increasing particle size. This agrees with our experimental results (*see* Table XII). If  $N$  is the number of particles with radius  $r$ , giving total surface  $TS$ ,

$$TS = 4\pi r^2 N$$

From Equations 4 and 5 we can obtain Equation 6 for the limiting number  $N$ , above which new particles do not form.

$$N_1 = \frac{R_i}{4\pi r D c^*} \quad (6)$$

It follows that the limiting number of particles decreases with increasing dimension of particles, also in agreement with our experimental results.

The growth ratio  $M/P$  of introduced monomer to the initially present seed polymer seems to have no effect. In fact, although most cases of uniform growing have been obtained with small  $M/P$  ratios, some runs carried out with almost equal  $M/P$  ratios (Runs 940 and 962) have given opposite results.

Behavior of VC in emulsion-seeded polymerization is quite different from that of other vinyl monomer such as styrene and vinyl toluene. For instance, in styrene-seeded polymerization, Vanderhoff (11) did not observe any anomalous seed growing. He reports uniform growing for a mixture of two seeds with a  $\phi = 2640$  and 5570 A., respectively, by seeding  $0.193 \times 10^{12}$  particles/ml.  $H_2O$ , whose surface per ml. of water is, according to our calculations, equal to  $0.121 \times 10^{20}$  sq. A.

Therefore, Vanderhoff (11) obtained uniform growing with styrene with values of  $N$  and  $S$  with which VC would have exhibited a new nucleation phase. In the above mentioned work by Vandegaer (10), in his growth Experiments B and D with poly(vinyl toluene) seed (initial diameters 1420 and 1470 A.) he obtained uniform growing. Unfortunately we cannot compare our results because we do not know the  $S$  and  $N$  limiting values for seeds of PVC having such small diameters.

The differences in behavior between VC and styrene would be related to different water solubilities of monomers, as well as to different values of the constant  $D$  of radicals into the polymer particles.

### Acknowledgment

The authors thank F. Gheda, A. Finzi, and G. Valori for their help in the experimental work.

**Literature Cited**

- (1) B. F. Goodrich Co., British Patent **1,036,468** (1966).
- (2) Brodnyan, J. G., Brown, G. L., *J. Colloid Sci.* **15**, 76 (1960).
- (3) Corso, C., Bedeschi, M., *Materie Plastiche* **12**, 1165 (1961).
- (4) Ferri, A., Gatta, G., Benetta, G., Talamini, G. P., Italian Patent **794,693** (1967).
- (5) Giskehaug, K., *Symp. Chem. Polymerization Proc., London, 1965*, preprint.
- (6) Kotlyar, I. B., Mukhina, I. A., Soviet Plastics (March 8, 1966).
- (7) Peggion, E., Testa, F., Gatta, G., *Chim. Ind.* **46**, 9 (1964).
- (8) Peggion, E., Testa, F., Talamini, G. P., *Makromol. Chem.* **71**, 173 (1964).
- (9) U. S. Rubber Co., British Patent **753,832** (1956).
- (10) Vandegaer, J. E., *J. Appl. Polymer Sci.* **9**, 2929 (1965).
- (11) Vanderhoff, J. W., Vitkuske, J. F., Bradford, E. B., Alfrey, T. Jr., *J. Polymer Sci.* **20**, 225 (1956).

RECEIVED March 18, 1968.



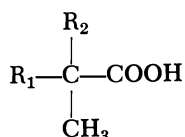
## Emulsion Copolymerization of Vinyl Esters of Branched Carboxylic Acids with Vinyl Acetate

G. C. VEGTER

Koninklijke/Shell-Laboratorium, Amsterdam, The Netherlands

*Vinyl esters of trialkylacetic acids copolymerize randomly with vinyl acetate. Such copolymers show excellent performance in paint latices. A variant of the monomer emulsion addition procedure for preparing latices yielded stable, coagulum-free products with very low residual monomer content. In this technique the initial reactor charge, consisting of part of the water, anionic emulsifier, initiator, and neutralizing agent, is heated to the reaction temperature. A monomer emulsion, containing all the monomers and non-ionic emulsifier as well as the balance of the other ingredients is then added gradually. The reproducibility of the process is, irrespective of the scale of operation, very good when a relatively large proportion of the anionic emulsifier is present in the initial reactor charge.*

The use of Versatic acids as the base material to manufacture alkyd resins was described a few years ago (2, 4, 5, 6, 7, 12, 15, 16, 17). These acids are prepared by the acid-catalyzed reaction between olefins, carbon monoxide, and water. Owing to rearrangements in the intermediate carbonium ion, they are nearly all trialkylacetic acids, of which one alkyl group is invariably methyl.



It appeared that the incorporation of these branched acids into saturated alkyds contributed to the chemical resistance and outdoor durability—especially color and glass retention—of the final stoved films.

More recent investigations revealed that the vinyl esters of these branched acids are excellent base materials for preparing paint latices (3, 8, 9, 10, 11, 13, 14). Their use as comonomer in vinyl acetate copolymer latices imparts improved alkali resistance and weatherability to the paint films.

These investigations were concentrated on the vinyl ester of Versatic 911, the acid derived from C<sub>8</sub>–C<sub>10</sub> olefins. This product will be referred to further as VV 911. The copolymerization of VV 911 with vinyl acetate, especially the emulsion copolymerization, was studied extensively. This paper describes the copolymerization characteristics of VV 911, a process developed for latex manufacture, and the reasons for its excellent reproducibility.

### **Relative Reactivity Ratios**

According to literature data vinyl esters of saturated aliphatic carboxylic acid copolymerize randomly with each other (1), the monomers being incorporated into the copolymer in about the same ratio at which they are present in the monomer mixture. This means that for practical purposes the relative reactivity ratios  $r_1$  and  $r_2$  can be taken to be equal and unity.

To check whether vinyl esters of strongly branched acids behave differently, mixtures of vinyl acetate and VV 911 in molar ratios of 1/3, 1/1, and 3/1 were polymerized in bulk to a conversion of about 10%, using benzoyl peroxide as initiator at 50°C. The reaction mixtures were then diluted with benzene, and the polymers were precipitated with methanol. After five further dissolutions in benzene and precipitation with methanol the polymers were freeze dried from their solutions in benzene and analyzed for carbon content. The results given in Figure 1 show that, at least for practical purposes, the assumption that  $r_1 = r_2 = 1$  is valid, and at any time during the polymerization random copolymers are formed at any vinyl acetate–VV 911 ratio.

### **Emulsion Polymerization Procedure**

Many polymerizations are performed by the emulsion technique to prepare a polymeric substance. The latex obtained is then coagulated, and the polymer is isolated. A paint latex, however, is used as such in the paint formulation, which leads to some special requirements for its stability, such as storage, mechanical, electrolyte, and freeze/thaw stability.

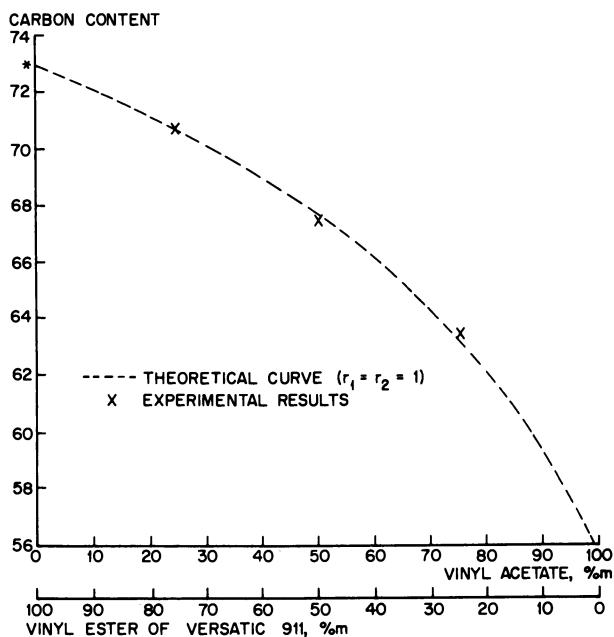


Figure 1. Carbon content (wt. %) as a function of the composition (moles) of vinyl acetate-VV 911 copolymers. Asterisk (\*) denotes 72.88% carbon found for poly(VV 911)

Another important aspect of the entire latex's being applied in the paint is that the ingredients used for latex preparation cannot be removed and will influence the performance of the ultimate paint film. Emulsifiers especially can have an adverse effect in this respect, and it is therefore desirable to use as small an amount as possible to obtain the desired stability.

For vinyl acetate-VV 911 copolymer latexes a suitable recipe was developed and is given in Table I. These latexes have excellent stability and impart superior performance to paints.

The small amount of acrylic acid is required to ensure freeze/thaw stability of the latex at a pH of 7 or higher and contributes to its mechanical stability. The anionic emulsifier (Fenopon SF 78) regulates the particle size and contributes to the stability of the system during latex preparation. The nonionic emulsifier (Tergitol NP 40) is required to obtain sufficient electrolyte stability and contributes to the mechanical and the freeze/thaw stability of the latex. Borax is used as a neutralizing agent.

Of the various methods of latex preparation known and practiced, a variant of the emulsion-addition method was chosen for further investigation because the reaction temperature is easy to control and coagulum

formation is easier to prevent than in the monomer-addition technique. Redox recipes were not considered in connection with the desirability to keep the amount of ingredients as low as possible and because of the observed difficulties to obtain conversions above 99.5%.

**Table I. Ingredients Used in Preparing Vinyl Acetate-VV911 Latexes**

<i>Ingredient</i>	<i>Parts by Weight</i>
Vinyl acetate	52.5
VV 911	46.5
Acrylic acid	1.0
Water (deionized)	85
Fenopon FS 78 (85% active material) <sup>a</sup>	1.0
Tergitol NP 40 <sup>b</sup>	2.5
Potassium persulfate	0.5
Borax	0.5

<sup>a</sup> Sodium alkylbenzene sulfonate from Antara Chemicals.

<sup>b</sup> Nonylphenol condensed with on an average 20 moles of ethylene oxide per mole, from Union Carbide Chemical Co.

An initial reactor charge was prepared by dissolving 0.1 part by weight (pbw) of potassium persulfate, 0.05 pbw of borax, and 0.6 pbw of Fenopon FS 78 in 25 pbw of denioized water. The rest of the ingredients were used as follows for preparing a monomer feed emulsion. In the 60 pbw of water left were dissolved 2.5 pbw of Tergitol NP 40, 0.4 pbw of Fenopon SF 78, 0.4 pbw of potassium persulfate, and 0.45 pbw of borax. To this solution 100 pbw of the monomer mixture were added with stirring. The monomer feed emulsion thus obtained was stable for about one day.

The reactor, a 750-ml. conical glass flask provided with a stainless steel anchor-type stirrer, which contained the initial charge, was then heated to 80°C., and the monomer feed emulsion was added gradually with stirring in about 2½ hours. The temperature was kept at 80°C. After addition of the emulsion, stirring was continued for another 2 hours, the temperature being kept at 80°C. The latex then was cooled with stirring to room temperature. Monomer conversion was 99.8%, the pH 4-4.5.

#### ***Variation in Emulsifier Distribution Ratio between Monomer Feed Emulsion and Initial Reactor Charge***

An important variable for paint latexes is their particle size, which influences properties such as their stability, viscosity, and pigment-binding properties.

Since emulsifiers determine the particle size of the latex, we studied the influence of the distribution ratio of the emulsifiers between monomer feed emulsion and initial reactor charge on the latex properties. We found that small amounts of the nonionic emulsifier in the initial reactor charge caused coagulation during latex preparation. Hence, the total

amount of nonionic emulsifier required had to be added with the monomer feed emulsion. Variation in the amount did not affect the particle size.

The distribution ratio of the anionic emulsifier, however, greatly affected the particle size, as illustrated in Figure 2. It was practically unaffected as long as more than about 15% of the anionic emulsifier was in the initial reactor charge. A further reduction of this amount, however, led to a steep increase in particle size.

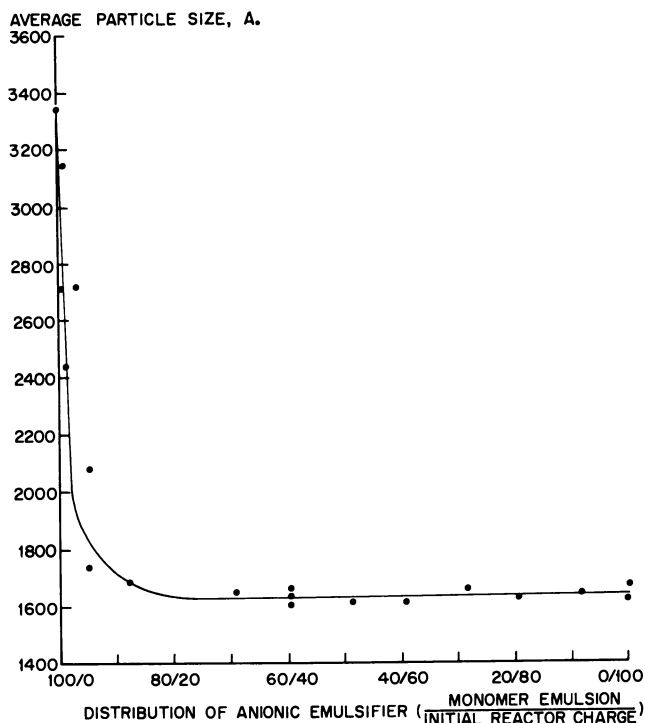


Figure 2. Influence of distribution of anionic emulsifier on average particle size

Since the total recipe is the same for all distribution ratios and the differences are introduced mainly at the beginning of the latex preparation, the initial conditions are very important for particle size.

To gain a better understanding of this phenomenon we followed the number of particles in the reactor with time during the monomer emulsion addition for three different distribution ratios of the anionic emulsifier. The ratios 40/60, 97/3, and 100/0 were chosen because they gave different particle sizes of the ultimate latex: the first on the flat part of the curve in Figure 2, the second just in the bend, and the third on the

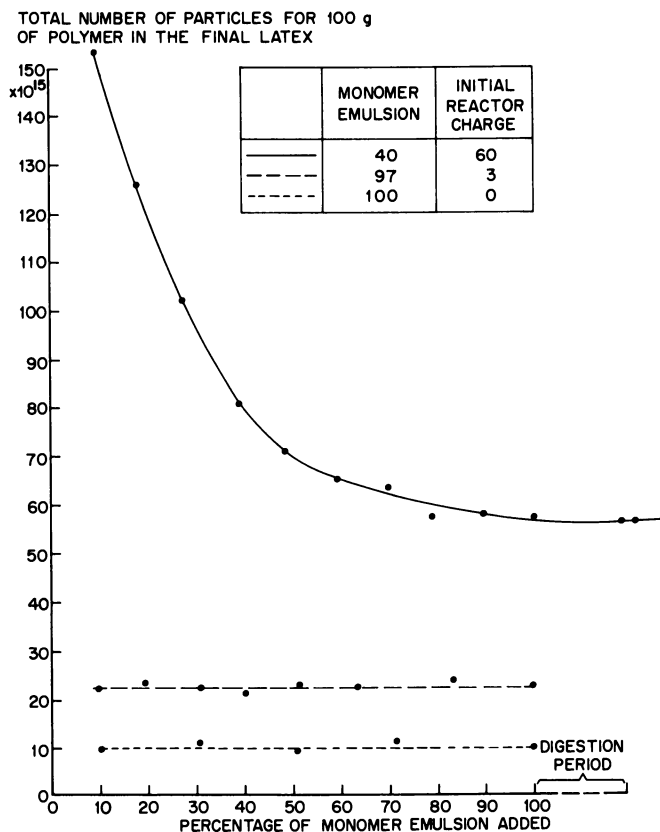


Figure 3. Number of particles during the addition period for different partitions of the anionic emulsifier

extreme left. The number of particles was derived from the known amount of monomer mixture added at any stage, and the average particle size determined *via* turbidity measurements.

The results of these experiments are depicted in Figure 3. They show that the number of particles formed in the initial stages of the latex preparation depends on the amount of anionic emulsifier present. When this amount was small, few particles were formed, and their number remained constant during further latex preparation. Thus, after initial particle formation, only a growth of existing particles took place.

When a large amount of anionic emulsifier was initially present in the reactor, many particles were formed. This number decreased during the latex preparation because not enough emulsifier was added with the monomer feed emulsion to keep the surface of the particles covered. Controlled agglomeration of polymer particles occurred to a stage where

the total surface area of the particles had become so small that the amount of anionic emulsifier present just provided the stability required under the conditions of the experiment. Thus, when more particles are initially formed than can be stabilized by the amount of anionic emulsifier added later, the ultimate average particle size is determined by the total amount of anionic emulsifier used in the latex formulation. When fewer particles are initially formed, the final average particle size is determined by the number of these particles. Figure 2 shows that when, under our conditions, more than about 15% of the anionic emulsifier was present in the initial reactor charge, the average particle size was independent of the distribution ratio, indicating that it was determined only by the total amount of anionic emulsifier present.

In actual fact, under these conditions the average particle size of the latexes was readily reproducible, but poorly so when less than 15% of the anionic emulsifier was present in the initial reactor charge. This can be understood by realizing that the number of particles formed initially cannot be very reproducible. Small variations in the induction period, for instance, will affect this number considerably because anionic emulsifier is added with the monomer feed emulsion.

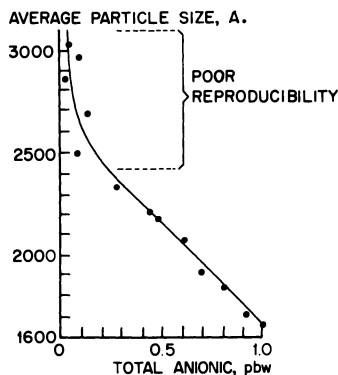


Figure 4. Influence of total amount of anionic emulsifier on average particle size at a constant 40/60 distribution over monomer feed emulsion and initial reactor charge

#### ***Variation in the Amount of Anionic Emulsifier***

The above-mentioned influence of the total amount of anionic emulsifier on the particle size of the latex was checked by varying this total amount, the 40/60 distribution between monomer feed emulsion and initial reactor charge being kept constant. The results of these experi-

ments are given in Figure 4. In Figure 5 they are compared with those obtained by changing the distribution ratio of anionic emulsifier at constant total concentration. The essential difference between the two series of experiments is the amount of anionic emulsifier on the monomer feed emulsion, indicated by the figures near the curve. Points of the two curves on any vertical line drawn through the graph relate to two experiments in which only the amount of anionic emulsifier in the monomer feed emulsion differs. Variation in this amount influences the average particle size considerably, which agrees with our previous statement that in the region of controlled agglomeration the average particle size is governed by the total amount of anionic emulsifier and is thus very reproducible. In fact, identical results were obtained when working on a 750-ml., a 20-liter, or a 250-liter scale.

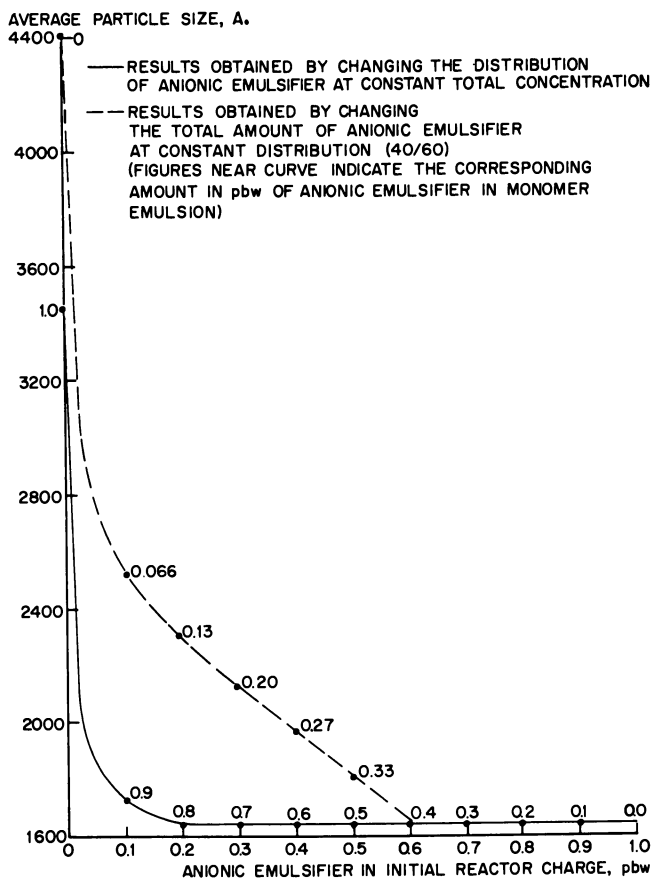


Figure 5. Influence of distribution ratio and total amount of anionic emulsifier on average particle size



### Particle Size Distribution

The particle size distribution of various latices, prepared *via* the above monomer emulsion addition technique, was determined with the aid of an ultracentrifuge. It was found to be invariably of the log-normal type, as shown in Figure 6, independent of the way the particles are formed. This illustrates that the agglomeration of particles during latex preparation, when the initial reactor charge contained more than 15% of the anionic emulsifier, is a random and not a selective process.

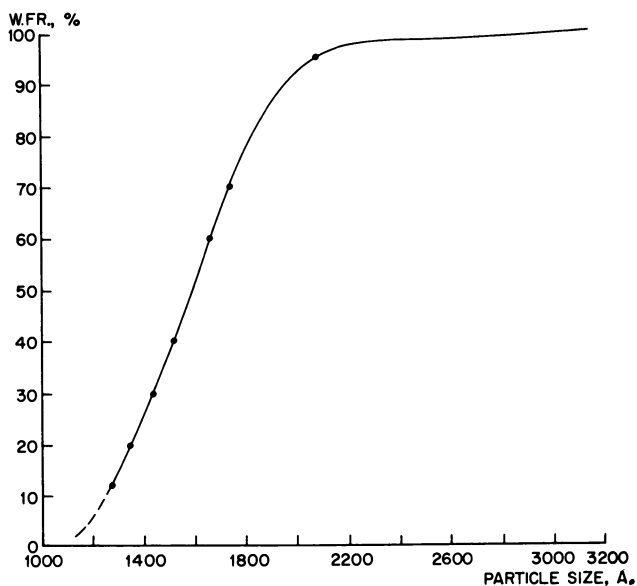


Figure 6. Particle size distribution of a latex

### Conclusions

Vinyl esters of trialkylacetic acid copolymerize randomly with vinyl acetate. Paint latices with a very low residual monomer content, based on vinyl acetate-VV 911 copolymers, can be prepared reproducibly *via* a variant of the monomer emulsion addition technique, when a relatively large part of the anionic emulsifier is present in the initial reactor charge.

### Literature Cited

- (1) Adicoff, A., Buselli, A., *J. Polymer Sci.* **21**, 340 (1956).
- (2) Brockman, A. L. S., Moore, W. V., *Paint Mfg.* **32**, 423 (1962).

- (3) Bruin, P., Oosterhof, H. A., Vegter, G. C., Vogelzang, E. J. W., *F.A.T.I.P.E.C. Congr.*, 7th, 1964, 49.
- (4) Goppel, J. M., Bruin, P., Zonsveld, J. J., *F.A.T.I.P.E.C. Congr.*, 6th, 1962, 31.
- (5) Herzberg, S., *F.A.T.I.P.E.C. Congr.*, 6th, 1962, 319.
- (6) Herzberg, S., *F.A.T.I.P.E.C. Congr.*, 7th, 1964, 387.
- (7) Kreps, R. W. F., *Fette, Seifen, Anstrichmittel* **66**, 1072 (1964).
- (8) Oosterhof, H. A., *J. Oil Color Chemists' Assoc.* **48**, 256 (1965).
- (9) Reader, C. E. L., Oosterhof, H. A., *F.A.T.I.P.E.C. Congr.*, 8th, 1966, 440.
- (10) Reader, C. E. L., Gastineau, G., *Double Liaison* **125**, 642 (1966).
- (11) Tsatsos, W. T., Illman, J. C., Tess, R. W., *Paint Varnish Prod.* **55**, 46 (1965).
- (12) Vegter, G. C., Oosterhof, H. A., *Fette, Seifen, Anstrichmittel* **68**, 283 (1966).
- (13) *Ibid.*, **69**, 79 (1967).
- (14) Vegter, G. C., Grommers, E. P., *J. Oil Color Chemists' Assoc.* **50**, 72 (1967).
- (15) Vogelzang, E. J. W., *J. Oil Color Chemists' Assoc.* **46**, 89 (1963).
- (16) Vogelzang, E. J. W., Oosterhof, H. A., *F.A.T.I.P.E.C. Congr.*, 7th, 1964, 381.
- (17) Vogelzang, E. J. W., *Farbe Lack* **71**, 455 (1965).

RECEIVED April 1, 1968.

## Freeze/Thaw Stability of Polymer Emulsions

HAROLD NAIDUS and ROGER HANZES

Northeastern University, Boston, Mass. 02115

*The freeze/thaw (F/T) stability of a polymer emulsion serves as a macroscopic probe for investigating the properties of the average particle in a polymer emulsion. A review of the factors which contribute to this stability is included. A study of styrene-ethyl acrylate-methacrylic acid polymers shows the existence of a minimum in the plot of minimum weight percent acid required for F/T stability vs. the minimum film formation temperature (MFT) of the polymer. This is considered to be a function of both the amount of associated surfactant and the minimum acid content. Thus, both the type of surfactant and the copolymer ratio—i.e., MFT—play major roles. Chain transfer between radicals and polyether surfactant resulting in covalently bonded surfactant-polymer combinations is important in interpreting the results.*

In the past 20 years a fragmented literature has grown around the phenomena related to freezing and thawing of polymer emulsions. Although much of the patent literature, by far the major source of information, focuses primarily upon specific methods for preparing freeze thaw (F/T) stable polymer emulsions, it has been possible to classify arbitrarily the various methods used. The major factors contributing to the stability of emulsions to freezing and thawing appear to fall into three classes: (a) copolymerization with vinyl carboxylic acids, (b) grafting of monomer to surface-active agents, and (c) postadditions of glycols, salts, surfactants, etc. to the emulsion.

Classes a and b imply the requirement of a covalently bonded, non-diffusible protective layer to achieve F/T stability, whereas Class c involves either a freezing-point lowering (glycols, salts) or additional stabilization (surfactants), presumably in emulsions already moderately stable to freezing and thawing.

These three factors do not appear to be independent of one another—*i.e.*, a polymer emulsion containing insufficient carboxylate ions to be F/T stable may frequently be made stable to the particular set of F/T tests by incorporating one of the addends of Class c.

### **Factors Affecting F/T Stability**

**Copolymerization with Vinyl Carboxylic Acids.** The acids usually suggested for this method include maleic and fumaric acids and their half esters, crotonic, itaconic, methacrylic, and acrylic acid. The latter three appear to be most generally preferred. On occasion, the amides of these acids are suggested for achieving the same end result (24). Suggested specifically for butadiene–styrene latexes are these acids at about 0.05–10 wt. % based on total monomer. The latex should be adjusted to pH 8–11 (28, 29). For copolymerization with vinyl acetate (2) and acrylic monomers (18) identical acid monomers are suggested. Use of such latexes is claimed to give F/T stable emulsion floor polishes (25) and paints (16).

A closely related patent (17) describes a method in which very high concentrations of  $K_2S_2O_8$  are used to initiate styrene–butadiene emulsion polymerizations, and F/T stability is claimed. In view of the well-known sulfate end group formation resulting from the use of persulfates, it would appear plausible that such end groups have been linked to the unsaturated polymer by radical transfer as well as by normal initiation and termination and thus function as non-diffusible anions to protect the particles during freezing and thawing.

**Grafting of Monomer to Surface-Active Agents.** A recent patent claims the preparation of a F/T stable poly(vinylacetate–vinylbenzoate) copolymer emulsion in the presence of a graft polymer of vinylacetate on a polyalkylene glycol (21).

A publication of the Celanese Chemical Co. (18) describes the preparation of a highly crosslinked vinyl acetate homopolymer prepared with poly(vinyl alcohol) stabilizer in which the poly(vinyl alcohol) contains about 12% residual acetyl groups, and a very reactive redox–initiator system is used:  $H_2O_2$  and zinc formaldehyde sulfoxylate. It has been shown (21) that this emulsion exhibits improved F/T stability compared with similar emulsions made with other colloids and less reactive initiating systems. In view of the work of Wheeler (31, 32), in which he points out the relative ease with which the hydrogens of the acetyl group undergo chain transfer, one may visualize the partially acetylated poly(vinyl alcohol) as a multifunctional chain transfer agent participating in the polymerization reaction so as to create a highly branched or cross-linked polymer (Figure 1). The product therefore would contain dis-

persed particles of poly(vinyl acetate) of higher glass temperature ( $T_g$ ) than linear poly(vinyl acetate) and would have associated with it a closely adhering layer of covalently bonded, non-diffusible colloid. Both are likely to contribute to improved F/T stability. Experimentally, this polymer is not 100% soluble. There are several patents on F/T stable poly(vinyl acetate) polymer emulsions which may be interpreted in a similar light (6, 11). For example, in Ref. 6 the following statement appears:

These advantages (wet rub and gloss) may be attributed to the fact that during the polymerization process, there are formed grafted copolymers of vinyl acetate and the water soluble colloids present in the polymerizing medium. These graft copolymers possess marked surface activity and contribute to the stabilization of the emulsion in which they are formed. . . .

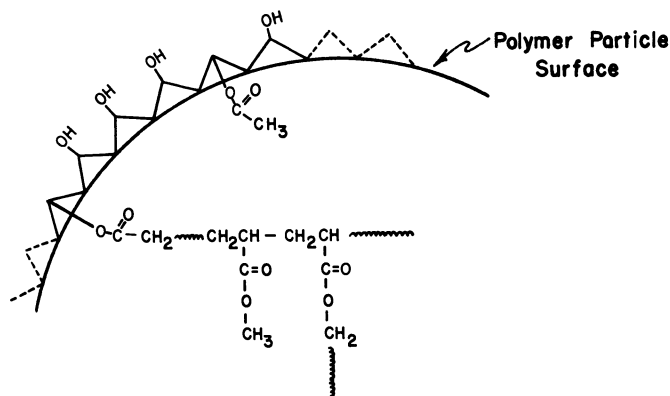


Figure 1. Postulated participation of poly(vinyl alcohol) in emulsion polymerization (schematic)

The emulsion polymerization of styrene with shellac salt stabilizer yields a highly crosslinked, F/T stable emulsion from which it is not possible to extract all the shellac by conventional means (21). This may be interpreted in a similar manner although it has not, as yet, been possible to determine the sites on the shellac which undergo chain transfer.

Both the poly(vinyl acetate)–poly(vinyl alcohol) and styrene–shellac examples of colloid participation in the polymerization require much investigation especially with respect to whether grafting to the colloid occurs in aqueous solutions or at the particle surface. The former would appear more likely for the relatively water soluble vinyl acetate monomer, while the latter should be favored for the less soluble styrene. In any case, both would result in identical particle stabilization.

**Postadditions.** Although definitive experiments have yet to be carried out, present information leads us to assume that emulsion polymers that

are particularly unstable to freezing and thawing cannot be made stable by postadditions in a F/T test which requires that the emulsion be frozen solid. That is, the suggested addition of glycols and the other freezing-point depressants often enhances F/T stability simply by preventing complete freezing under the test conditions. On the other hand, it is equally reasonable to assume that polymer emulsions that are borderline with respect to F/T stability may be nudged over the border by adding compounds which either modify the crystal form of the continuous phase, prevent complete freezing at the test temperatures, or furnish additional stabilization by adsorption on the polymer particles.

It has been suggested, for example, that the addition of ethylene glycol and polyethylene glycols enhances the F/T stability of polymer emulsions (2). Further, the addition of electrolytes has been proposed to achieve the same goal (5). All are freezing-point depressants and may influence the other factors as well.

The addition to poly(vinyl acetate) emulsions of poly(oxyethylene) poly(oxypropylene) glycols is claimed to improve F/T stability (10) as are nitrogen-containing polyalkylene glycols (13). A general treatment of the improvement in F/T stability by adding surfactants is given by Digioia and Nelson (4) and Leonard (14). Both papers indicate that improvement in F/T stability is obtained by adding surfactants.

### ***F/T Stability and Mechanical Stability***

When polymer emulsions are subjected to freezing and thawing or to mechanical shear, the stabilizing layer of each particle (whether ionic or nonionic) is subjected to deformation which permits easier particle-to-particle approach (8, 15, 19, 26, 27) and frequently results in coagulation. Since F/T and mechanical stability appear to be mechanistically related, several authors have undertaken work to elucidate at least one of the stability relationships (8, 15, 19, 26). The first paper measures mechanical stability by subjecting the emulsion to shear at 1100–1400 r.p.m. in a Couette viscometer and records the time required for the onset of coagulation. The author evaluates acrylic copolymers containing methacrylic acid and demonstrates that mechanical stability improves with increasing emulsion particle charge (Figure 2). This is completely consistent with F/T results on similar emulsions (22).

The author notes that his results are consistent with those of Stamberger (27) who worked with a styrene–ethyl hexyl acrylate–acrylic acid emulsion terpolymer. At pH 8, the emulsion was stable to liquid shear, whereas at pH 3, it was unstable. There was little difference in zeta potential of the latex at the two pH values.

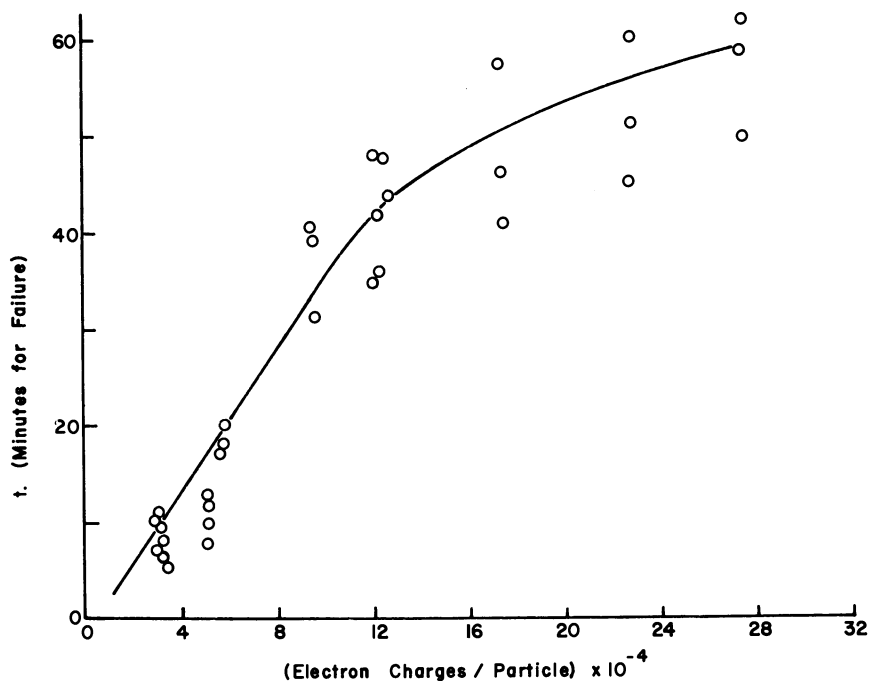


Figure 2. Effect of particle charge on mechanical stability (MAA terpolymer) (after Ref. 8)

### Coagulation by Freezing and Thawing

The freezing and thawing of polymer emulsions has been a well-known method for latex coagulation for many years. In 1959, Barb and Mikucki (1) investigated the particle size of the coagulate. The systems chosen were polystyrene copolymer emulsions stabilized with cationic surfactants. By evaluating the coagulate through a three-sieve system having spacings of approximately 178, 104, and 66 $\mu$ , it was possible to correlate the distribution of coagulate particle sizes with the rate of freezing, the rate of thawing, the time interval between freezing and thawing, the concentration of the emulsion, the emulsifier concentration and type, latex particle diameter, and polymer type.

Of all these variables, only the freezing rate, the emulsion concentration, and the polymer type appeared to have a significant effect upon the appearance and particle size distribution of the polymer coagulate. In a styrene-acrylonitrile (S-AN) copolymer series, those of higher softening point give finer, less agglomerated coagulate (see Table I).

**Table I. Coagulate Particle Size and Polymer Softening Point (1)**

<i>Polymer</i>	<i>Softening Point</i>	<i>Coagulate Retained by 178<math>\mu</math> Sieve (wt. %)</i>
Styrene (S)	102	56
75/25 S-AN	110	33
10/90 S-AN	200	negligible

Our results differ significantly from these observations. Emulsifier and monomer types appear to play a much more complex role than implied above.

### *Experimental*

**Minimum Film Formation Temperature (MFT).** Equipment described by Protzman and Brown (24) was built, calibrated, and used for all measurements. A series of 25% emulsions, adjusted to pH 9.5 with  $\text{NH}_3$ , was used throughout unless otherwise indicated.

**Polymerization.** The procedure described in Ref. 22 was followed, except that the redox-initiated system involving styrene required a 100% increase in redox initiators and a 50% increase in Triton X-405. The polymerization formula used in all the styrene systems was:

	<i>Weight, grams</i>
Monomers	288.9
Triton X-405	39.6
$\text{H}_2\text{O}$ (distilled)	368.0
Glacial acetic acid	(to pH 2.5)
$(\text{NH}_4)_2\text{S}_2\text{O}_8$ (4% aq.)	60.4
$\text{Na}_2\text{S}_2\text{O}_5$ (10% aq.)	26.0

[In those experiments with sodium lauryl sulfate (SLS), the same dry weight as for Triton X-405 was used for emulsion stability. The appropriate adjustment in  $\text{H}_2\text{O}$  was made as well. Triton X-405 is a poly(ethoxylated) octyl phenol containing about 40 moles ethylene oxide per mole and used as supplied by Rohm & Haas Co. at 70% solids.]

All the emulsions appeared to have similar particle sizes, estimated to be in the range of 0.1–0.5 $\mu$ . The monomers were all polymerization grade and polymerized without purification since no significant difference in induction period or rate was observed with distilled monomer.

**Methacrylic Acid Content in Polymer.** One gram of methanol-precipitated, water-washed, dried polymer was dissolved in 100 ml. tetrahydrofuran (THF) and titrated to a faint pink phenolphthalein end point with 0.055 *n*-benzyltrimethylammonium hydroxide in THF. The base was standardized by potentiometric titration against 0.01N acetic acid in methanol. The value for a non-acid containing polymer of the same series was used as a blank. All analyses were within 5% of the theoretical value.

**Other Procedures.** Residual monomer content, solids content, viscosities, F/T stability, and surface tension were determined as described



in Ref. 22. All infrared data were obtained with a Beckman IR 5A infrared spectrophotometer.

### Results and Discussion

**Methyl Methacrylate–Ethyl Acrylate–Methacrylic Acid (MMA–EA–MAA) Terpolymers.** In an earlier paper (22, 23) values for the MFT of each of a series of acrylic copolymer emulsions were obtained by calculating  $T_g$  values using the equation of Wood (34), ignoring the presence of methacrylic acid. These were then converted to MFT values using available literature data (20, 24) and by extrapolating and interpolating the straight line obtained. The MFT values for these identical emulsions at pH 9.5 have now been determined experimentally, and these data are compared in Table II. Values for MFT's below 0°C. could not be obtained experimentally.

Table II. MFT Values for MMA/EA/MAA Emulsion Polymers

MMA–EA	MAA, wt. %	MFT, °C.	
		(calc.)	(exp.)
100/0	0.4	109	108.1
80/20	0.86	78	78.6
50/50	1.13	32	30.0

It appears that use of the Wood formula for calculating  $T_g$  values combined with the use of literature data relating MFT and  $T_g$  was reliable for obtaining previously unknown MFT values despite the presence of small amounts of acid in the polymer and a likely difference in polymerization method.

**Styrene–Ethyl Acrylate (S–EA) Copolymers.** At the inception of the research on F/T stability, it was evident that more than one polymer system would require investigation before adequate conclusions could be drawn regarding the various pertinent parameters. These include, in addition to the previous considerations, surfactant type and amount as a function of polymer type.

To this end, work has been initiated on a series of somewhat less polar styrene–ethyl acrylate–methacrylic acid emulsion polymers. The first major difference encountered in changing from the MMA–EA–MAA to the S–EA–MAA polymers was the need for at least a 50% increase in surfactant to obtain a coagulate-free emulsion for the 100% styrene *vs.* 100% methyl methacrylate. The determination of the minimum weight percent of MAA required to yield a F/T stable emulsion for various copolymers gave the results listed in Table III.

**Table III. F/T and MFT Data for S/EA/MAA Copolymers Stabilized with Triton X-405**

S-EA Ratio	MAA, wt. %	F/T Stable	MFT, °C.		
			pH Unadjusted <sup>a</sup>	pH 9.5 with NH <sub>3</sub>	pH 9.5 with NaOH
100/0	0	no	101.4	—	—
100/0	0.834 <sup>b</sup>	yes	—	102.2	—
75/25	0	no	77.1	76.4	—
75/25	0.34 <sup>b</sup>	yes	74.6	74.5	74.3
50/50	0	no	—	—	—
50/50	0.82 <sup>b</sup>	yes	—	35.5	—

<sup>a</sup> The pH of unadjusted emulsions ranged from 2 to 2.5.

<sup>b</sup> These values for wt. % MAA are the minimum required for F/T stability using NH<sub>3</sub> to pH 9.5.

These data show that for the low levels of acid in the pH range considered, MFT values are relatively insensitive to methacrylic acid content. On the other hand, in the SLS system, the 100% S polymer requires 4.4% MAA for F/T stability, and the MFT becomes 113°C.

To see more clearly the marked differences in MFT relationships between these polymers and the MMA-EA-MAA polymers (22), Figure 3 has been constructed to compare the data of the two series.

Among the questions which become apparent from Figure 3 and which require explanation are:

(a) Since the MFT's of 100% MMA and 100% S emulsions are not too different (382° and 375°K.), why does the latter require appreciably more MAA to achieve F/T stability?

In emulsion systems, an equilibrium between surfactant associated with the particles and free surfactant is considered to exist—*i.e.*,



where S(assoc.) may include both adsorbed and chemically combined surfactant.

If one makes the reasonable assumption, consistent with colloid stability theory, that F/T stability is a direct function of the total thickness of the minimum hydration layer required for F/T stability,  $(H)_m$ , which is in turn a function of both the minimum carboxylate ion content,  $w_m$ , and the associated surfactant, then

$$\text{F/T stability} \cong (H)_m = aw_m + b S(\text{assoc.}) \quad (2)$$

Since it was observed that a 50% increase in surfactant was required to prepare a coagulate-free polystyrene emulsion compared with poly-(methyl methacrylate) emulsion, it appears clear that for poly-S emulsion Equation 1 is shifted to the right compared with poly-MMA emulsion.

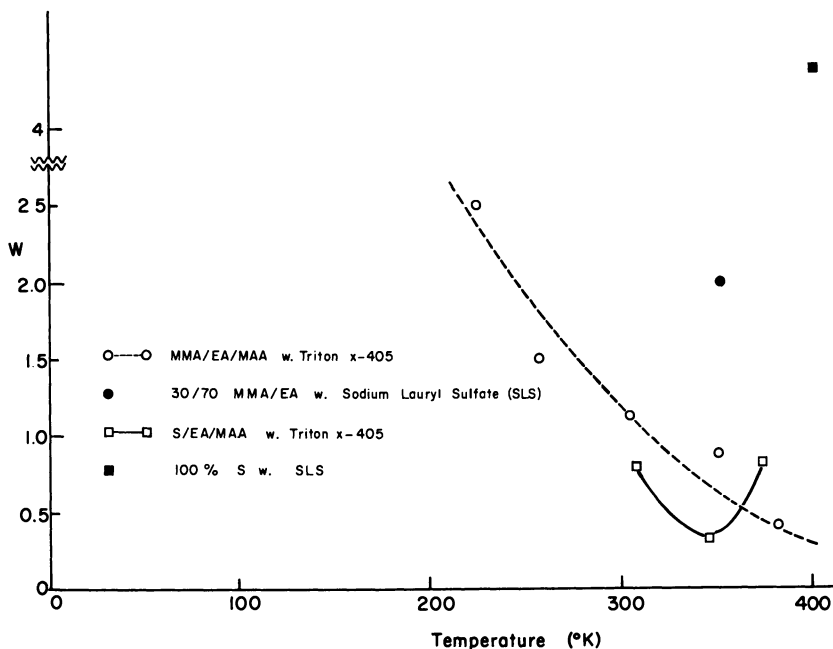


Figure 3. Minimum weight percent acid required for F/T stability vs. MFT ( $^{\circ}\text{K}$ .)

Under F/T conditions, desorption of surfactant presumably occurs more readily with the poly-S emulsion as a new equilibrium is established (a slight surface-tension lowering was observed after each F/T cycle throughout the series.) This conclusion is further substantiated by the exceptional increase in minimum weight percent acid required for poly-S in SLS (black square) compared with the 80/20 MMA-*EA* in SLS (black dot) despite the fact that less than one-half as much SLS was used in the latter case. Thus, it appears that poly-S is a less favorable surface for surfactant adsorption and as predicted by Equation 2 more carboxylate ions are required to obtain F/T stability.

(b) Why does the 75/25 S-*EA* polymer require even less acid than 100% poly-MMA which has a higher MFT ( $347.5^{\circ}$  vs.  $382^{\circ}\text{K}$ .)?

Since the styrene series contains more surfactant than the methyl methacrylate series and since the ethyl acrylate has afforded increased surfactant adsorptivity to the styrene by a mechanism to be proposed under Question d, the equilibrium suggested by Equation 1 is shifted markedly to the left, resulting in lower requirements for carboxylate ions to achieve F/T stability.

(c) When replacing Triton X-405 by SLS weight for weight, why is the minimum weight percent acid necessary for F/T stability increased

so markedly despite the fact that the Triton X-405 represents many fewer moles?

By virtue of the chemical structure of the two surfactants, it would appear reasonable that many more moles of water per mole surfactant would be associated with the Triton X-405 than the SLS and thus effectively increase the hydration layer thickness. On the other hand, this would not necessarily maintain the equilibrium represented by Equation 1 shifted sufficiently far to the left following multiple F/T cycles. Maintenance of an equilibrium shifted to the left can only be assured if the surfactant is covalently bonded to the polymer particle by some means. By invoking certain well-known chemical phenomena and by analogy with the poly(vinyl alcohol)-poly(vinyl acetate) system (Figure 1), it becomes possible to recognize that a polyether, like Triton X-405, would tend to undergo chain transfer during an emulsion polymerization reaction, whereas it is much less likely with SLS. It has been shown (31) that the chain transfer constants of alcohols at the —OH group is low, about equal to that of aliphatic hydrocarbons, in agreement with the high dissociation energies of the bonds involved. When transfer does take place, it occurs at the  $\alpha$ -hydrogen. With ethers, both the autoxidation to form hydroperoxides (9, 29) and transfer with radicals (3) occur at the  $\alpha$ -hydrogen.

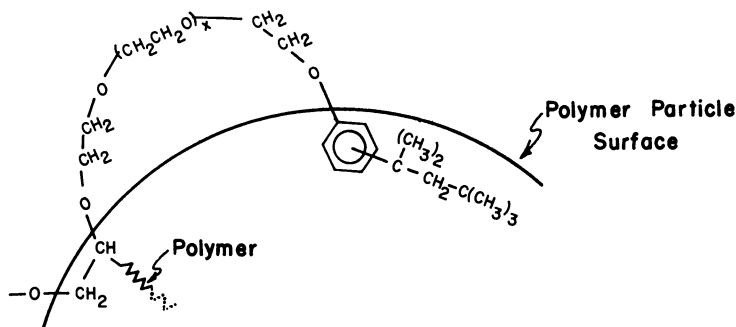
Radical transfer reactions involving polyethers of the poly(ethylene oxide) type are well known (7). Heating polyethylene glycols of various molecular weights at 140°C. with dicumyl peroxide for 2.5 hours has resulted in a gel fraction explained by transfer at the  $\alpha$ -carbon followed by combination of the polymer radicals. Further, poly(ethylene oxide) dissolved in MMA and heated in the presence of benzoyl peroxide results in grafted copolymer.

In a highly favorable medium, containing a reactive redox-initiating pair, transfer is likely to occur either in the aqueous phase or at the particle surface. In either case, the surfactant will reside at a particle surface bound to the polymer by one or more covalent bonds (*see* Figure 4).

To follow up this reasoning, we subjected reprecipitated polystyrene to spectrographic analysis. Emulsion polymer at its unadjusted pH was precipitated in 10-fold excess of methanol (a solvent for Triton X-405), dried, dissolved in toluene (a nonsolvent for the Triton), filtered, and the toluene solution was added to a 10-fold excess of methanol. About 1.5% of the polymer remained as a fine dispersion which could not be precipitated or separated by the addition of water or by centrifugation, thus exhibiting characteristics to be expected of a polystyrene graft to Triton X-405. [The value of 1.5% is completely consistent with the calculated value of about 18% by weight of Triton X-405 which could be associated

with a polystyrene particle of  $0.1\mu$  diameter assuming complete surface coverage by the Triton X-405. From the Rohm and Haas literature, Triton X-405 has an area per molecule of 88 sq. A. and a molecular weight of about 1900 grams per mole.]

The infrared spectrum of the precipitated polystyrene at this stage exhibited no absorption using thermally polymerized polystyrene in the reference beam. A 3.5% solution of dried Triton X-405 in chloroform showed intense adsorption at about  $1100\text{ cm.}^{-1}$ , characteristic of the ether linkage.



Reviews in Macromolecular Chemistry

Figure 4. Chain transfer with polyethoxylated octylphenol (schematic) (7)

The dispersed polymer was evaporated to dryness to yield a low softening point residue exhibiting complete solubility in  $\text{CCl}_4$  and no water solubility. The spectrum of this material (3% in  $\text{CCl}_4$ ) was taken using a solution of the precipitated polymer of the same sample in the reference beam. Strong absorption was observed at about  $1110\text{ cm.}^{-1}$ , and the rest of the spectrum was essentially identical to that of Triton X-405.

It has also been observed consistently that frozen and thawed samples of non-F/T stable emulsions prepared with Triton X-405 and SLS exhibit significantly different characteristics. In the frozen and thawed samples of SLS-stabilized emulsions, the pseudo-crystalline coagulate separates cleanly leaving a relatively clear supernatant liquid. In the Triton X-405 samples, a white, swollen amorphous coagulate is obtained with an opaque supernatant liquid. These combined observations lend credence to the conclusion that Triton X-405 molecules are bound chemically to the polymer particles.

(d) Why does the styrene series exhibit a marked minimum?

There appear to be several factors playing simultaneous roles in the S-EA polymer series. An increase in minimum weight percent acid

required for F/T stability would be predicted for increased EA content on purely MFT considerations by analogy with the MMA-EA series (22). On the other hand, acrylate radicals have a transfer constant for toluene about 310 times that of styrene (30) which, by analogy, would increase its capability of transfer with the polyether, Triton X-405. Moreover, the greater solubility of EA in water compared with S would increase the probability of transfer in the favorable aqueous environment. Both these influences would increase the quantity of surfactant associated with the polymer particle.

Thus, at relatively low EA contents, it appears that the increase in hydration layer thickness associated with the increase in bonded surfactant far outweighs the influence of the decrease in MFT. At higher EA levels, it appears that the relative influence of the two factors is reversed.

(e) Are the data of Figure 3 and Table III valid for alkalies other than  $\text{NH}_3$  or at different surfactant levels?

In an earlier paper (22) studies on a commercial latex as a model system indicated clearly no difference in F/T results when  $\text{NH}_3$  or NaOH was used to adjust pH. It is now observed that at the minimum acid levels, the quantity of alkali and not pH is the controlling factor. Thus, Table IV shows that less NaOH than  $\text{NH}_3$  is required to obtain pH 9.5, but an equal number of equivalents is necessary to achieve F/T stability. Moreover, as might have been expected, if more than the minimum acid content is present, F/T stability can be obtained at a lower pH so long as an equivalent amount of alkali is added—*i.e.*, as long as the same concentration of carboxylic acids are converted to carboxylate ions.

**Table IV. Alkali and pH Requirements for F/T Stability in Triton X-405 Stabilized Styrene Copolymer Emulsions**

<i>Polymer</i>	<i>Acid, %</i>	<i>Base, meq.</i>	<i>pH</i>	<i>F/T Stability</i>
100% S	0.834 <sup>a</sup>	0.158 ( $\text{NH}_3$ )	9.5	stable
	1.2	0.158 ( $\text{NH}_3$ )	9.15	stable
	0.834 <sup>a</sup>	-----( $\text{NH}_3$ )	9.15	unstable
75/25 S-EA	0.34 <sup>a</sup>	0.158 ( $\text{NH}_3$ )	9.5	stable
		0.048 (NaOH)	9.5	unstable
		0.158 (NaOH)	11.8	stable

<sup>a</sup> Minimum wt. % acid for F/T stability.

In the 100% S emulsion stabilized by SLS, a sample containing 3% MMA was not F/T stable but became stable following addition of an amount of Triton X-405 equal to the SLS originally used. This was expected on the basis of the previous arguments and is consistent with the

literature which recommends postaddition of surfactants to improve F/T stability.

### Conclusions

(1) The Wood equation (33) is suitable for calculating  $T_g$  values for emulsion copolymers.

(2) At low MAA levels ( $< 1\%$ ) neither the acid content, the pH, nor the type of alkali affect the measured value of the MFT.

(3) Nonionic polyethoxylated surfactants exemplified by Triton X-405, tend to chain transfer in redox-initiated emulsion polymerizations and become chemically bound to the polymer.

(4) SLS tends to be less associated with emulsion polymer particles than does a polyethoxylated octylphenol.

(5) Polystyrene has a lower affinity for surfactant than acrylic polymer.

(6) The results confirm that transfer agents (in this case Triton X-405) have higher transfer constants with acrylate radicals than with styrene radicals.

(7) It is possible to convert a carboxyl-containing emulsion polymer which is not F/T stable to one which is stable by the addition of surfactant.

(8) It is the absolute amount of alkali used in neutralization which controls F/T stability and not the pH.

(9) F/T stability is controlled by the carboxylate ion content and not the carboxylic acid content, although with sufficient alkali these are probably synonymous.

### Literature Cited

- (1) Barb, W. G., Mikucki, W., *J. Polymer Sci.* **37**, 499 (1959).
- (2) Belgian Patent **644,919** (1964).
- (3) Cass, W. E., *J. Am. Chem. Soc.* **69**, 500 (1947).
- (4) Digioia, F. A., Nelson, R. A., *Ind. Eng. Chem.* **45**, 745 (1953).
- (5) Fikentscher, H., Berkert, H., Newfeld, E., Plötz, German Patent **1,055,239** (1959).
- (6) Guest, D. V., Lord, F. W., Peace, W., British Patent **854,346** (1960).
- (7) Gurgiolo, A. E., *Rev. Macromol. Chem.* **1**(1), 136, 160 (1966).
- (8) Hatala, R. J., *Am. Chem. Soc., Div. Org. Coatings Plastics Chem., Preprints* **24**(1), 257 (1964).
- (9) Hawkins, E. G. E., "Organic Peroxides," van Nostrand, Princeton, N. J., 1961.
- (10) Holdsworth, R. S., German Patent **1,093,558** (1960).
- (11) Kahrs, K. H., Koch, G., Jeckel, P., Bork, S., German Patent **1,071,954** (1959).
- (12) Kahrs, K. H., Staller, A., Wolfgang, J., U. S. Patent **3,301,805** (1967).
- (13) Kahrs, K. H., Starck, W., German Patent **1,123,470** (1962).
- (14) Leonard, F. J., *Offic. Dig. Federation Paint Varnish Prod. Clubs* **28**, 441 (1956).

- (15) Mast, W. E., Fisher, C. H., *Ind. Eng. Chem.* **41**, 790 (1949).
- (16) McDowell, M. J., Hill, T. B., U. S. Patent **3,309,331** (1967).
- (17) Miller, V. A., Bebb, R. L., Masch, J. H., U. S. Patent **2,822,341** (1958).
- (18) "Monomer References," Celanese Chemical Co., pp. 102, 652A.
- (19) Muroi, S., Nomura, J., *Kogyo Kagaku Zasshi* **68**, 1800 (1965).
- (20) Myers, R., Schulz, R., *J. Appl. Polymer Sci.* **4**, 81 (1960).
- (21) Naidus, H., unpublished work.
- (22) Naidus, H., King, A. P., *Am. Chem. Soc., Div. Polymer Chem., Preprints* **7(2)**, 860 (1966); *J. Polymer Sci.*, in press.
- (23) Okamura, S., Motoyama, T., *Bull. Chem. Soc. Japan* **28**, 61 (1955).
- (24) Protzman, T. F., Brown, G. L., *J. Appl. Polymer Sci.* **4**, 81 (1960).
- (25) Smith, T. V., Vetren, R. E., U. S. Patent **2,233,224** (1956).
- (26) Stamberger, P., *J. Phys. Chem.* **61**, 127 (1957).
- (27) Stamberger, P., *J. Colloid Sci.* **10**, 194 (1955).
- (28) Tess, R. W., VanEss, P. R., U. S. Patent **3,202,625** (1965).
- (29) VanEss, P. R., Tess, R. W., U. S. Patent **3,202,627** (1965).
- (30) Walling, Cheves, "Free Radicals in Solution," Wiley, New York, 1957.
- (31) Wheeler, O. L., Ernst, S. L., Crozier, R. N., *J. Polymer Sci.* **8**, 409 (1952).
- (32) Wheeler, O. L., Lavin, E., Crozier, R. N., *J. Polymer Sci.* **9**, 157 (1952).
- (33) Wood, L., *J. Polymer Sci.* **28**, 319 (1950).
- (34) Zobrin, Yu. I., Russian Patent **115,676** (1958); **166,141** (1964).

RECEIVED March 14, 1968.



## Radiation-Induced Ionic Polymerization

D. J. METZ

Brookhaven National Laboratory, Upton, N. Y. 11973

*Sufficient experimental data from several laboratories now exist to describe the conditions under which the radiation-induced ionic propagation of many pure liquid vinyl monomers can be observed. The kinetic data and electrical conductivity measurements establish the ionic nature of the reaction; scavenger studies appear to establish the preponderant role played by the carbonium ion in propagating the polymerization. On the basis of a single propagating species, it is possible to write a simple mechanism to describe the process. Limiting values of several of the kinetic rate constants can be estimated, notably the rate constant for reaction between a bare carbonium ion and a vinyl double bond. These rate constants are compared with similar constants arrived at in chemically initiated free radical, carbonium ion and carbanion polymerization. Several shortcomings of the present scheme are discussed.*

Although most of the original studies of radiation-initiated liquid-phase vinyl polymerizations pointed unequivocally to initiation and propagation by free radicals, sufficient evidence is now available to establish that under proper conditions ionic species may also be formed which are capable of not only contributing to but almost entirely dominating the over-all process. The proper conditions under which this can be established are simply purity and dryness (another form of purity), but the degree of purity which must be achieved partially explains why the free radical behavior, and not the ionic process, was the first to be observed. The following discussion outlines briefly the technique of preparing samples, the kinetic evidence on which propagating ions are postulated, some of the evidence for the nature of the propagating ions, and one suggested mechanism for the radiation-induced ionic polymerization which has limited usefulness.

During this paper, many questions will be raised for which only partial answers can be given. In an emerging field such as this, that is to be expected. In this way we hope to arrive at a fairly complete understanding of not only radiation-induced polymerization but the broader field of liquid-phase organic radiation chemistry.

### **Sample Preparation**

As we shall see below, the levels of impurity, including the ubiquitous impurity—water, that can successfully destroy the desired ionic contribution to the polymerization process may be as low as  $10^{-7}M$ . Therefore, vigorous purification methods for monomer, glassware, and any additives must be used. The particular method of sample preparation which we have used in our laboratory is outlined below and described in detail elsewhere (29, 30). Most other workers in this field use methods comparable in principle but differing in details. The several steps involved are as follows:

- (a) Monomer purification. Fractionation in 6-foot packed column under a reduced pressure of dry helium.
- (b) Bake-out. All glassware and drying agent (silica gel) are baked at  $500^{\circ}C$ . for 36 hours at  $10^{-7}$  torr.
- (c) Monomer degassing. Freeze-thaw cycling; final sealing at  $<10^{-6}$  torr.
- (d) Drying of monomer. Equilibration over previously dried silica gel.
- (e) Isolation. Distillation into reaction vessel.

All of these operations are accomplished in such a way that monomer never passes through any stopcocks, thereby avoiding contamination by grease. These operations require the use of glass breakseals and several parallel sub-manifolds on the high vacuum line. We are still unhappy about the amount of contamination that must be introduced by the flame-sealing of the final reaction vessel, but it appears to be a source of contamination with which we must live.

The cleansing action of the high temperature, low pressure treatment of the glassware appears to be a very important step in the over-all preparation of the sample. Without it, even rigorously dried monomer may not exhibit the intended ionic polymerization (29, 34).

### **Evidence for Ionic Nature**

Several kinetic criteria can be employed to elucidate the nature of the propagating species in vinyl polymerizations. The results of the application of these criteria, as exemplified by styrene, are shown in Table I. This monomer has been chosen in this discussion mainly because

it polymerizes under radiation, by both free radical and ionic mechanisms, at measurable rates and with relatively high molecular and kinetic chain lengths, and reasonably good sets of experimental data are available.

Since the dose rate exponent of both the rate of polymerization and the average molecular chain length, as well as the over-all temperature coefficient, vary so markedly between the dry and the wet conditions, and the latter are accepted as being indicative of a free radical process, it becomes tempting to describe the dry process as being non-radical, and, by logical exclusion, ionic. Both the extreme sensitivity to water, ammonia, and amines and the data from the copolymerization with  $\alpha$ -methylstyrene further support this thesis.

**Table I. Kinetic Behavior of Styrene Polymerization Initiated by Radiation Under Wet (Radical) and Dry (Ionic) Conditions**

Kinetic Parameter	Wet (radical)	Dry (ionic)
$R_p \propto I^\beta$	$\beta = 0.50$ (9)	$0.62 \leq \beta \leq 1$ (29, 30, 34, 35)
$\overline{DP} \propto I^\gamma$	$\gamma = -0.50$ (9)	$\gamma \approx 0$ (18, 33)
$E_a$ (rate)	$E_a \approx 7$ kcal. (9)	$-6 < E_a < +2$ kcal. (25)
$E_a'$ ( $\overline{DP}$ )	$E_a' \approx 5$ kcal. (1)	$E_a' \approx 0$ (25)
Copolymerization	$r_1 = 2.2 \pm 0.2$ (34)	$r_1 = 0.25 \pm 0.25$ (34)
with $\alpha$ -methylstyrene ( $M_2$ )	$r_2 = 0.6 \pm 0.2$ (34)	$r_2 = 8.5 \pm 4.0$ (34)
Sensitivity to impurities:		
H <sub>2</sub> O	None	very high (18, 29, 30, 33, 34, 35)
O <sub>2</sub>	High	high (25, 33)
DPPH	High	high (33)
N <sub>2</sub> O		slight (35)
CO <sub>2</sub>		slight (7)
NH <sub>3</sub> , amines		very high (35)

There is further evidence that the two processes differ at a given dose rate and temperature by the relative values of the absolute rates of polymerization for wet and dry monomer. These can differ by as much as four orders of magnitude, the dry sample being the more rapid. That the removal of water and impurities does not merely enhance the rate of formation of initiating free radicals was demonstrated by Potter *et al.* (29) by showing that in a given sample the rate of thermal polymerization at 40°C. of the dry monomer was unaffected, the intensity dependence of the ultraviolet-initiated rate of polymerization being 0.5, whereas the dose rate dependence of the  $\gamma$ -ray-initiated polymerization was 1.0.

In addition to the data on the dose rate dependence of the rate of polymerization, it has been observed that the average degree of polym-

erization of styrene under dry conditions is essentially independent of both the dose rate and the temperature. (Although some small dependencies on these two parameters have been observed (25), they are very small, and do not begin to approach the analogous dependencies in the wet-radical system.) These observations, together with the actual values of polymerization rates and molecular weight, lead to the conclusion that molecular chains are terminated by a rapid and essentially temperature-independent chain transfer mechanism.

As an example, for styrene at 0°C. the following data are typical (30): rate of polymerization = 14.5%/hour, dose rate =  $2.2 \times 10^3$  rads/hour, average DP  $\approx 10^3$ . Since 1 rad corresponds to the absorption of 100 ergs/gram of material, it can be demonstrated, on the basis of the above values, that approximately  $6 \times 10^5$  monomer units are incorporated into polymer for each 100 e.v. of energy absorbed. In conventional radiation chemistry terminology this would be expressed as  $G_{(-\text{monomer})} \approx 6 \times 10^5$ . If no chain transfer occurred, it would then follow that

$$G_{(\text{Initiation})} = \frac{G_{(-\text{monomer})}}{\text{DP}} \approx 6 \times 10^2 \quad (1)$$

This would imply that approximately six initiating centers were formed per electron volt of energy absorbed. Such a value cannot be reconciled with any known ion yields in either the gaseous or condensed phases, requiring that the origin of most molecular chains is regenerative chain transfer rather than direct radiation-induced initiation. This type of behavior—termination by chain transfer—is not indicated by the data on wet styrene, where typical values are  $G_{(-\text{monomer})} \approx 300$  (9) and  $G_{(\text{Initiation})} \approx 0.6$  (9).

The evidence in the case of styrene, where both modes of radiation-induced polymerization can be conveniently studied, is quite convincing that reduction of the concentration of water changes the predominating mode of propagation from purely free radical to essentially ionic. Evidence for an ionic propagation initiated by radiation has also been obtained in pure  $\alpha$ -methylstyrene (3, 24), isobutylene (12, 32), cyclopentadiene (5),  $\beta$ -pinene (2), 1,2-cyclohexene oxide (11), isobutyl vinyl ether (6), and nitroethylene (38), although the radical process in these monomers is extremely difficult, if not impossible, to study.

### *Nature of the Propagating Species*

Rather than approach the answer to this question by reviewing the possible intermediates formed either directly or indirectly by the absorption of high energy radiation in an organic liquid, let us look at some of the experimental data obtained by different techniques in various mono-

mers. These data come essentially from three sources: (1) scavenger studies, (2) electrical conductance, and (3) pulse radiolysis. Supporting evidence also comes from studies of monomers dispersed in frozen glassy hydrocarbon solvents, based on optical (13) and electron spin resonance (37) spectroscopy.

**Scavenger Studies.** Of all the scavengers that are effective in quenching the radiation-induced ionic polymerization, water is perhaps the most pernicious and elusive, even if it may not be the most effective or diagnostic additive. The limit of detectability of water lies somewhere around 5 p.p.m. or approximately  $10^{-4}M$ . Attempts in our laboratory to correlate the rate of polymerization of  $\alpha$ -methylstyrene with residual water concentration have indicated that differences in the polymerization rate of one to two orders of magnitude are observed in samples all of which show a water concentration less than 5 p.p.m. (26). Also, in view of the exhaustive drying and baking which must be followed generally to obtain reproducible data in "pure" systems, addition of traces of water to dry monomers appears doomed to failure in any quantitative sense because there is really no way of knowing how much water has been adsorbed onto the previously dried glassware between the water reservoir and the monomer sample.

In addition to these difficulties, water is not the best diagnostic additive since it can terminate both carbonium ion and carbanion propagations effectively, although apparently it is specific for ionic as opposed to free radical chain reactions.

On the other hand, several "known" free radical scavengers, such as oxygen, DPPH, and benzoquinone, have been reported to interfere seriously with the radiation-induced ionic polymerization of isobutylene (10) and styrene (25, 34). Apparently these free radical scavengers are also capable of reacting with the radiation-generated ionic propagation species and must no longer be considered as discriminating scavengers for free radicals.

Perhaps the best qualitative and quantitative scavenger studies in these ionic polymerizations have been made with ammonia and several amines. Busler, Martin, and Williams (8) have shown that, at  $-78^{\circ}C$ . the initial polymer yield from irradiated cyclopentadiene increases linearly with the ratio of  $[C_5H_6]/[NH_3]$  over the range 1–10. This would be consistent with a mechanism in which all growing chains are terminated by reaction with ammonia, according to:

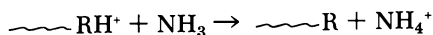
$$G_{(-C_5H_6)} = G_{(initiation)} \frac{k_p [C_5H_6]}{k_r [NH_3]} \quad (2)$$

where  $k_p$  and  $k_r$  are the propagation and retardation (with ammonia) rate constants, respectively.

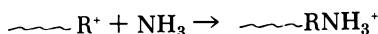
The same authors observed (8) that at equal mole fractions, ammonia, ethyl-, diethyl-, and triethylamine were approximately equivalent in their efficiency in inhibiting the polymerization of cyclopentadiene.

Ueno *et al.* (35) have reported similar behavior for styrene. In their work, at 30°C. and a dose rate of  $2.42 \times 10^{14}$  e.v. cc.<sup>-1</sup> sec.<sup>-1</sup>, there was an approximate inverse linear relationship between the rate of polymerization of styrene and the concentration of triethylamine, between  $10^{-6}$  and  $10^{-4}M$  amine. Ammonia and amines have also been observed to inhibit the polymerization of isobutyl vinyl ether (6) and  $\alpha$ -methylstyrene (17).

Liquid ammonia can be used as a solvent in the anionic polymerization of styrene initiated chemically (15). Moreover, the basic nature of ammonia and amines needs no further justification. These data appear to lead to the tentative conclusion that the growing species in these systems is the positively charged carbonium ion, which may terminate with ammonia (and amines) either by a proton transfer mechanism or an addition reaction to form a nonpolymerizing ammonium ion (8)—*viz.*,



or



A recent study of the radiation-induced polymerization of nitroethylene (38) indicates that the predominant propagating species in this monomer is an anion. This is based on scavenger studies utilizing HBr, substantiated by a study of the electron-trapping capabilities of this monomer in irradiated 2-methyltetrahydrofuran glass (38).

**Electrical Conductivity.** Hayashi *et al.* (14) have made electrical conductivity measurements in irradiated styrene,  $\alpha$ -methylstyrene, and isobutyl vinyl ether. The observed specific conductivities in these monomers were of the same order of magnitude, at a given dose rate, as that measured in cyclohexane. Since the *G* values for ion production in most hydrocarbon liquids are approximately the same, they concluded that the conducting species in the monomer systems must have had approximately the same molecular size as cyclohexane. Also, since the observed specific conductances of the three monomers and that of cyclohexane showed a square-root dependence on the dose rate, they concluded that the behavior of kinetically independent oppositely charged carriers was being observed, with very little effect of the applied field on the recombination process.

Making several plausible assumptions (14), an average mobility of a growing polystyrene ion (final DP = 500) was calculated to be  $4 \times 10^{-5}$  sq. cm. volt<sup>-1</sup> sec.<sup>-1</sup>. The mobility of a positive or negative cyclohexane

ion can be calculated from the Nernst-Einstein equation, by assuming that the diffusion coefficient of the ion is the same as the self-diffusion coefficient of the solvent. This results in a value of  $\mu_+ = \mu_- = 4 \times 10^{-4}$  sq. cm. volt<sup>-1</sup> sec.<sup>-1</sup>. Based on these calculations, Hayashi *et al.* (14) concluded that the conductivity of the polymerizing ion is much too low to account for the conductivity data, and an oppositely charged small ion of greater mobility must be the major contributor to the observed conductance. These workers identified the polymeric ion as the carbonium ion of styrene, and the small, mobile negative ion as probably either the monomeric styrene anion radical or a low molecular weight propagating anion (14).

**Pulse Radiolysis.** Several investigations of styrene (32) and  $\alpha$ -methylstyrene (20, 24) under rigorous drying conditions, have been published. Other data (31) on less rigorously dried systems have also been reported, but because of the uncertainties of the effects of impurities, it is difficult to compare the latter with the former. This part of the discussion will be confined to the very pure systems.

Both Katayama (20) and Metz (24) have reported the observation of a radical anion of extremely short half-life in pulsed, dry  $\alpha$ -methylstyrene. This species is extremely sensitive to water and oxygen.

In a slightly more detailed study of dry styrene, Metz *et al.* (23) have reported similar observations. They tentatively identified a species with broad absorption maximum at 370 m $\mu$ , decaying with a first-order half-life of approximately 4  $\mu$ sec., extremely sensitive to water, sensitive to oxygen, insensitive to N<sub>2</sub>O, and formed with an apparent radiolytic yield (measured immediately after a 0.2- $\mu$ sec. pulse) of  $G \approx 0.15$ , as the styryl radical anion.

This species, superimposed on several longer-lived species is shown in Figure 1 as the sharp spike at the beginning of the decay curve. When this species is observed in a pulse, the corresponding kinetics shown by the sample conform to the maximum rates reported by both Potter *et al.* (30) and Ueno *et al.* (35). On the other hand, for samples in which this species is not observed (because of improper sample preparation) the observed rate of polymerization is approximately one-half or one-third less (depending on dose rate) than the maximum rates, but still 10<sup>3</sup> times higher than the free radical rates.

These observations would tend to confirm the contention that the major contribution to the ionic polymerization is probably the carbonium ion (as not yet observed in pulse radiolysis), with a smaller but significant contribution from the propagating anion (24).

At this point, then, the data appear to indicate that in most of the monomers which have been studied so far—cyclopentadiene,  $\beta$ -pinene, styrene,  $\alpha$ -methylstyrene, isobutylene, and isobutyl vinyl ether—the pre-

dominating propagating species is a carbonium ion of some sort. In one case—nitroethylene—the propagating species is probably an anion. In all cases, however, the role of the oppositely charged ion is not entirely accounted for, and, as we shall see below, generally is neglected for the sake of simplicity.

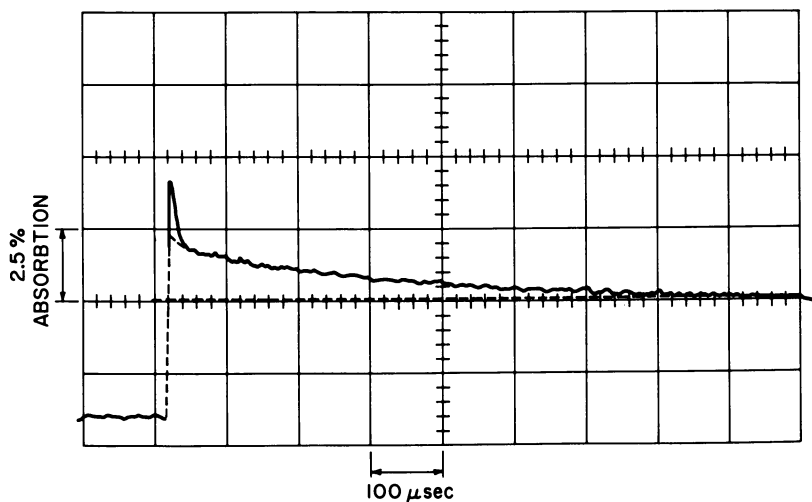


Figure 1. Absorption at 370  $m\mu$  vs. time after pulse for very dry styrene

### **Suggested Kinetic Scheme**

Any postulated kinetic scheme must incorporate several important empirical observations, as follows:

- (1) Formation of ions.
- (2) Propagation by ionic species.
- (3) Chain transfer to monomer.
- (4) Chain termination by impurity (first-order in propagating species).
- (5) Chain termination by charge recombination (second-order in species formed by initiation step).
- (6) Steady-state assumption.

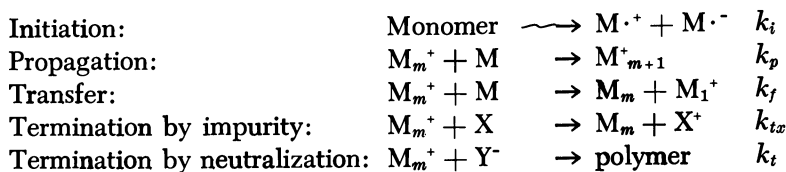
In addition to fulfilling these requirements, a full treatment of the kinetics would also allow for regeneration of impurity and radiolytic formation of inhibitor.

Regeneration of impurity is dictated by the failure to observe any acceleration in the rate of polymerization with conversion, of most monomers studied, because of consumption of inhibitor. Radiolytic formation of inhibitor is suggested by the fact that in most monomers studied,



despite rigorous drying and purification, the square-root dependence of rate on intensity, which must be approached at zero impurity level, has not been achieved.

The following reactions have been offered as a modified description of the radiation-induced polymerization of several vinyl monomers. The symbolism and nomenclature is that used by Williams *et al.* (36), wherein, after eliminating the contribution of anionic initiation and/or propagation, the principal propagating species is considered to be a carbonium ion. Thus,



where  $[Y^-]$  would represent the total negative ion concentration.

Application of the steady-state assumption and the restriction of over-all electrical neutrality lead to the expression:

$$R_p = \frac{R_i k_p [M]}{(k_t R_i)^{1/2} + k_{tx} [x]} = R_i k_p [M] \tau' \quad (3)$$

and  $1/\tau' = (1/\tau) + (1/\tau_s)$ , where  $\tau'$  is the mean lifetime of the propagating species, related to the average lifetimes of two parallel processes—termination by impurity ( $\tau_s$ ) and termination by neutralization ( $\tau$ ).

Under such conditions that  $k_{tx} [x] \gg (k_t R_i)^{1/2}$ , where termination of molecular chains is governed by reaction with impurity, it can be shown (22, 27) that

$$\frac{1}{\overline{DP}} = \frac{1}{\overline{DP}_0} + \frac{k_{tx} [x]}{k_p [M]} \quad (4)$$

where  $\overline{DP}_0$  is the average degree of polymerization in the absence of impurity. A plot of  $1/\overline{DP}$  vs.  $[x]/[M]$  should allow an evaluation of  $k_{tx}/k_p$ , and evaluation of the latter as a diffusion-controlled rate constant in an ion-dipole interaction on the basis of the Smoluchowski-Debye theory would allow an estimate of  $k_{tx}$  to be made. This has been done for cyclopentadiene (5) and leads to the value of  $k_{tx} \approx 10^{10} M^{-1} \text{ sec}^{-1}$  and corresponding orders of  $k_p \approx 10^8 \text{ }^{\pm 1} M^{-1} \text{ sec}^{-1}$ .

On the basis of electrical conductivity, it can be shown (14) that

$$\frac{1}{\tau} = 3.6 \times 10^{12} \frac{\pi \sigma}{\epsilon} \quad (5)$$

where  $\sigma$  is the specific conductance,  $3.6 \times 10^{12}$  represents a conversion factor, and  $\epsilon$  is the bulk dielectric constant of the medium. This equation

is based on the assumption that termination of kinetic chains is by charge neutralization. Thus, measurement of specific conductance allows a calculation of  $\tau$ —the average lifetime for recombining ions—and, from Equation 6

$$k_p = \frac{R_p}{[M]\tau R_i} \quad (6)$$

which assumes that  $\tau \gg \tau'$ . This condition should be approached in all cases at high enough dose rates and is characterized by the empirical observation that

$$R_p \propto I^{0.50}$$

Thus,  $k_p$  can be approximated independently by electrical conductance measurements in conjunction with kinetic measurements.

Combining these two types of experiments—scavenger studies and electrical conductance measurements—it is possible to arrive at limits on the value of  $k_p$  for any monomer undergoing this process. Williams *et al.* (36) have done this for several monomers, and the results are shown in Table II along with other data. The values of the propagation rate constants for styryl carbonium (free) ion, carbanion (free), carbanion (associated with  $\text{Na}^+$ ), free radical, and carbonium ion (associated with gegenions) are shown. The range of values is from  $4 \times 10^{-3}$  to  $3.5 \times 10^6 M^{-1} \text{ sec}^{-1}$ . Based on available data, it is apparent that the free styryl carbonium ion is much more reactive than any of the other styryl species.

Also shown in Table II are the propagation rate constants for several other free carbonium ions and one free carbanion.

**Table II. Selected Propagation Rate Constants in Addition Polymerization**

Monomer	Propagation Species	$k_p$ , $M^{-1} \text{ sec}^{-1}$	T, °C.	Initiator	Solvent	Ref.
Styrene	carbonium ion	$3.5 \times 10^6$	15	radiation	bulk	36
	carbanion	$6.5 \times 10^4$	25	styryl anion	THF	4
		$1.3 \times 10^5$	25	styryl anion	THF	16
	ion pair	80	25	styryl anion	THF	4
	free radical	35	20	— $\text{Na}^+$		
	ion pair	17	25		bulk	21
				$\text{HClO}_4$	$\text{C}_2\text{H}_4\text{Cl}_2$	28
	ion pair	$4 \times 10^{-3}$	30	$\text{I}_2$	$\text{C}_2\text{H}_4\text{Cl}_2$	19
$\alpha$ -Methylstyrene	carbonium ion	$3 \times 10^6$	30	radiation	bulk	17
Isobutyl vinyl ether	carbonium ion	$3 \times 10^5$	$\approx 30$	radiation	bulk	36
Cyclopentadiene	carbonium ion	$6 \times 10^8$	-78	radiation	bulk	5
Nitroethylene	carbanion	$6 \times 10^7$	10	radiation	bulk	38

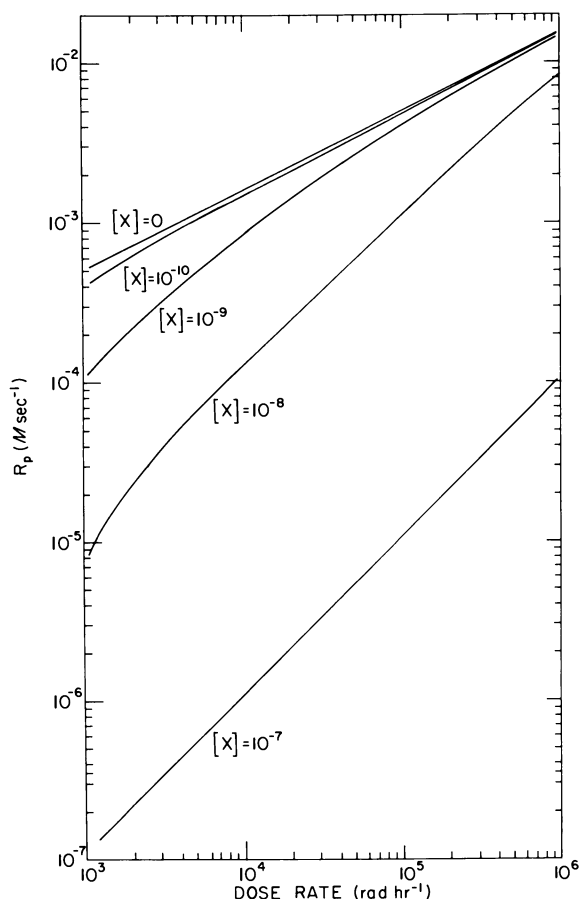


Figure 2. Theoretical plots of Equation 3 for various values of impurity concentration, assuming:

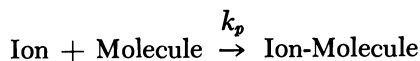
$$G_{(ions)} = 0.1$$

$$k_t = 2 \times 10^{11} \text{ M}^{-1} \text{ sec}^{-1}$$

$$k_{tx} = 1 \times 10^{10} \text{ M}^{-1} \text{ sec}^{-1}$$

$$k_p = 5 \times 10^6 \text{ M}^{-1} \text{ sec}^{-1}$$

A singular contribution that a detailed study of radiation-induced ionic polymerization can make to fundamental processes, then, is that the rate constants for the family of reactions typified by



may be estimated without the complicating effects of the ever-present regenerations of chemically formed organic ions.

Williams *et al.* (36) have pursued the predictions of Equation 3 further by assuming reasonable values for the rate constants involved and have shown that the observed change of dose rate dependence with increasing dryness (and hence absolute value of the rate of polymerization) for both styrene (30, 35) and  $\alpha$ -methylstyrene (24) can be predicted semiquantitatively. For styrene they assumed the following values (36):

$$G_{(\text{ions})} = 0.1 \text{ (based on most published determinations)}$$

$$k_t = 2 \times 10^{11} M^{-1} \text{ sec.}^{-1} \text{ (based on ion lifetimes measured by conductivity)}$$

$$k_{tx} = 1 \times 10^{10} M^{-1} \text{ sec.}^{-1} \text{ (diffusion-controlled value)}$$

$$k_p = 5 \times 10^6 M^{-1} \text{ sec.}^{-1} \text{ [see Equation 6]}$$

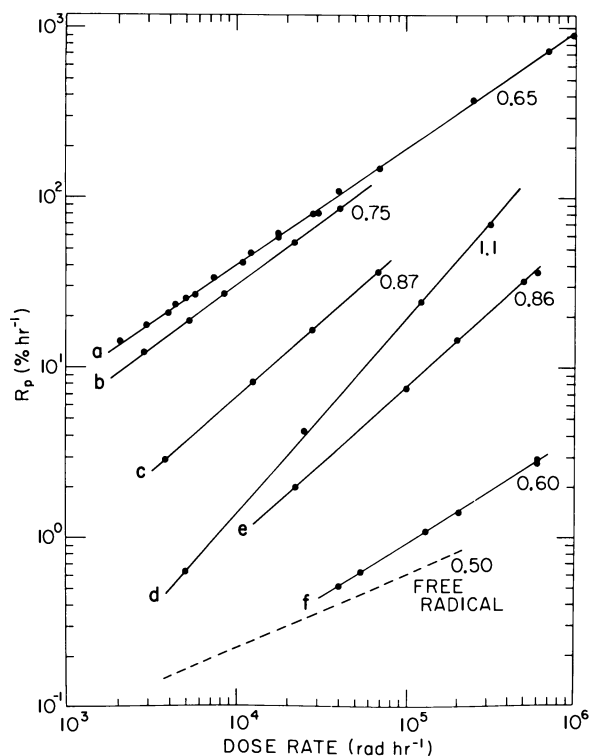


Figure 3. Empirical data for styrene polymerization showing variation of  $R_p$  vs. dose rate and the dose rate dependence of  $R_p$  as impurity level decreases (data taken at  $0^\circ\text{C}$ .)

Figure 2 shows a plot of Equation 3, using the above assumed values, with the concentration of impurity,  $[x]$ , as the adjustable parameter. It is readily seen that at  $[x] \approx 10^{-7} M$ , the polymerization rate may be several orders of magnitude below the maximum (impurity free) rate,

and the observed dependence of the rate on the dose rate should be almost unity.

Figures 3 and 4 show empirical data, of the above form, for styrene (30) and  $\alpha$ -methylstyrene (24), respectively. Only in the latter case is the predicted square-root behavior observed, but the general predictions of Equation 3 are followed by both monomers.

It is interesting to calculate the approximate impurity levels of the samples for which the kinetic data are presented in Figures 3 and 4. Table III summarizes these approximations, based on Equation 3 and the rate constants given in Reference 36 for the two monomers in question. The comparison has been made on the basis of the slopes of the experimental curves between  $10^4$  and  $10^5$  rads/hour and the corresponding values of the calculated curves in the same interval. For both monomers, the values of impurity concentrations over which dramatic changes in rate constants given in Ref. 36 for the two monomers in question. ample explanation of the failure of all early studies, especially for styrene, to uncover any mechanism other than the free radical kinetics.

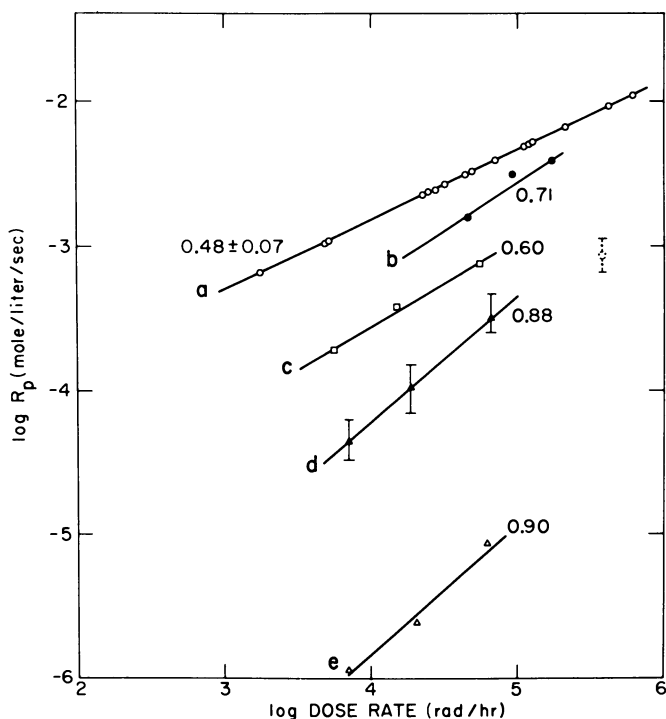


Figure 4. Empirical data for  $\alpha$ -methylstyrene showing variation of  $R_p$  vs. dose rate and dose rate dependence of  $R_p$  as impurity level decreases (data taken at  $0^\circ\text{C}.$ )

**Table III. Estimated<sup>a</sup> Impurity Concentrations**

Curve <sup>b</sup>	Styrene, M	$\alpha$ -Methylstyrene, M
a	$>10^{-10}$	$\sim 0$
b	$\sim 10^{-10}$	$>10^{-9}$
c	$\sim 10^{-8}$	$<10^{-8}$
d	$>10^{-8}$	$>10^{-8}$
e	$>10^{-8}$	$\sim 10^{-7}$
f	$<10^{-7}$	—

<sup>a</sup> Utilizing Equation 3.<sup>b</sup> Refers to curves in Figures 3 and 4.

It is also of some interest to look at the values of other kinetic parameters that can be calculated for styrene using Equations 3 and 6. These are shown in Table IV. Thus, although the average lifetime of the ions and their steady-state concentrations are quite low compared with radicals, this is overcompensated by the much higher intrinsic reactivity toward propagation. Thus, the ionic propagation, in the absence of terminating impurities, clearly can be several orders of magnitude higher than the radical process. However, exceedingly small concentrations of inhibitors are sufficient to mask completely these ionic effects.

**Table IV. Some Kinetic Parameters for Styrene**

Dose Rate		Lifetimes of Charge Carriers, msec. <sup>a</sup>	Steady-State Concentration of Ions, <sup>b</sup> M	Rate of Polymer- ization, <sup>b</sup> M sec. <sup>-1</sup>
e.v. cc. <sup>-1</sup> sec. <sup>-1</sup>	rads/hour			
$1 \times 10^{13}$	$6 \times 10^2$	710	$1 \times 10^{-11}$	$4 \times 10^{-4}$
$1 \times 10^{14}$	$6 \times 10^3$	180	$3 \times 10^{-10}$	$1 \times 10^{-3}$
$1 \times 10^{15}$	$6 \times 10^4$	47	$1 \times 10^{-10}$	$4 \times 10^{-3}$

<sup>a</sup> Ref. 14.<sup>b</sup> Calculated using Equation 3 and assuming  $[x] = 0$ .**Shortcomings of Proposed Kinetic Scheme**

According to the proposed mechanism (36):

$$R_p = \frac{R_i k_p [M]}{(k_t R_i)^{1/2} + k_{tx} [x]} \quad (3)$$

which may be subjected to analysis.

In the first place, if Equation 3 depicts the behavior of the system correctly, two observations must follow. The temperature behavior of  $R_p$  predicted by Equation 3 should be of the form

$$R_p(T) = \frac{R_i [M] A_p e^{-E_p/RT}}{R_i^{1/2} A_t^{1/2} e^{-E_t/2RT} + A_{tx} e^{-E_{tx}/RT} [x]} \quad (7)$$

in which  $R_t$  is assumed to be temperature independent. Although this equation would predict a changing "apparent" temperature coefficient for the rate of polymerization, it would *not* predict a change from negative to positive values with increasing temperature. This type of behavior has been observed and reported for styrene by both Ueno *et al.* (35) and Potter *et al.* (30), with the observed maximum rate of polymerization occurring at slightly different values of temperature and dose rate.

Secondly, Equation 3 predicts that

$$R_p \rightarrow I^{0.5}$$

at high enough dose rates. The data which are available on styrene cover three orders of magnitude of dose rate—from  $10^3$  to  $10^6$  rads/hour—and, to the best approximation, the dose rate exponent is 0.62 (30, 34). One determination of  $R_p$  at extremely high dose rates ( $\approx 10^{12}$  rads/hour) indicates that this order of dependence extends to even this high dose rate (24).

In general, in only one system studied so far, the  $\alpha$ -methylstyrene system, has a 0.5 order dependence on dose rate been observed in the  $10^3$  to  $10^6$  rads/hour range (24). This failure of other systems to approach the predicted square-root behavior might be ascribed to a radio-lytically formed inhibitor—a unimolecular terminating agent. This eventuality is not incorporated into the scheme now under discussion.

On the basis of the proposed kinetic scheme, it would be predicted that the number average degree of polymerization would be given by

$$\overline{DP}_n = \frac{k_p[M]}{k_t[M^+] + k_f[M] + k_{tx}[x]} \quad (8)$$

Inserting the assumed values (36) of  $k_p$ ,  $k_t$ , and  $k_{tx}$  and letting  $[x] = 3 \times 10^{-10}M$ , corresponding to  $R_p \propto I^{0.60}$ ,

$$\overline{DP}_n \approx \frac{5 \times 10^6}{(2.3 + k_f)} \quad (\text{at } 1 \times 10^{15} \text{ e.v. cc.}^{-1} \text{ sec.}^{-1}) \quad (9)$$

Pepper (7) has shown that for a  $\overline{DP}$  calculated on the basis of intrinsic viscosity and yielding a  $\overline{DP}_{vis} \approx 5 \times 10^2$ ,  $\overline{DP}_n \approx 1 \times 10^2$ . Taking this latter value and using Equation 9

$$k_f \approx 10^4$$

Johnson and Metz (18) and Metz *et al.* (25) have consistently reported  $\overline{DP}$ 's, based on intrinsic viscosities, of the order of  $7 \times 10^2$  to  $8 \times 10^2$ , whereas Pepper (7) and Ueno (34) have consistently reported values of  $5 \times 10^2$ . Metz's (18) early data were obtained at impurity levels much greater than  $[x] = 3 \times 10^{-10}M$ , and, based on rates of polymerization, Metz's (25, 30) and Ueno's (34) data essentially refer to the same low level of  $[x] \approx 10^{-10}M$ . To rationalize the almost two-fold discrepancy

in average molecular weights on the basis of an impurity reaction is unreasonable in view of the mechanism and rate constant values assumed.

Furthermore, since most molecular chains must be terminated by regenerative chain transfer, and hence the molecular weight is governed by the competition between propagation and transfer, by the assumed mechanism, no dependence of  $\overline{DP}$  on dose rate would be expected. Metz *et al.* (25) have reported preliminary data which would question this.

### Conclusion

The development of the study of radiation-induced ionic polymerization of liquid vinyl monomers has been a story of the struggle against adventitious impurities. The contribution of several workers has led to the establishment of preparative techniques which yield reproducible data.

In many cases studied, the predominant contribution to the propagation process is apparently made by a carbonium ion. The details of the formation of a normal carbonium ion from the originally formed carbonium ion radical is not yet clear. The fate of the ejected electron is likewise unclear.

Assuming a single-ion (carbonium ion) propagation step and based on scavenger studies with ammonia and amines and on electrical conductance measurements, rate constants for the propagation reaction (ion-molecule reaction) can be estimated. These estimates are free of the correction that one has to apply (or ignore) for chemically generated ion pair ionic polymerization, but are subject to other limitations imposed by different assumptions in the treatment of the data.

Undoubtedly, the order-of-magnitude estimates of the rate constants derived from these studies are reasonably valid. Continued work should provide an even clearer picture of the many details of the process which, to this point, have been either neglected or minimized.

### Literature Cited

- (1) Ballantine, D. S., Colombo, P., Glines, A., Manowitz, B., *Brookhaven Natl. Lab. Rept.* **229** (1953).
- (2) Bates, T. H., Best, J. V. F., Williams, F., *J. Chem. Soc.* **1962**, 1531.
- (3) Best, J. V. F., Bates, T. H., Williams, F., *Trans. Faraday Soc.* **58**, 192 (1962).
- (4) Bhattacharya, D. N., Lee, C. L., Smid, J., Szwarc, M., *J. Phys. Chem.* **69**, 612 (1963).
- (5) Bonin, M. A., Busler, W. R., Williams, F., *J. Am. Chem. Soc.* **87**, 199 (1965).
- (6) Bonin, M. A., Calvert, M. L., Miller, W. L., Williams, F., *Polymer Letters* **2**, 143 (1964).



- (7) Burns, F. W., O'Connor, R. M., Pepper, D. C., *Polymer Letters* **B5**, 1059 (1967).
- (8) Busler, W. R., Martin, D. H., Williams, F., *Discussions Faraday Soc.* **36**, 102 (1963).
- (9) Chapiro, A., "Radiation Chemistry of Polymeric Systems," Chap. 5, Interscience, New York, 1962.
- (10) Collinson, E., Dainton, F. S., Gillis, H. A., *J. Phys. Chem.* **63**, 909 (1959).
- (11) Cordischi, D., Lenzi, M., Mele, A., *J. Polymer Sci., Pt. A-1* **3**, 3421 (1965).
- (12) Davison, W. H. T., Pinner, S. H., Worrall, R., *Proc. Roy. Soc. (London)* **A252**, 187 (1959).
- (13) Hamill, W. H., Guarino, J. P., Roynane, M. R., Ward, J. A., *Discussions Faraday Soc.* **36**, 169 (1964).
- (14) Hayashi, K., Yamazawa, Y., Takagaki, T., Williams, F., Hayashi, K., Okamura, S., *Trans. Faraday Soc.* **63**, 1489 (1967).
- (15) Higginson, W. E. C., Wooding, N. S., *J. Chem. Soc.* **1952**, 760.
- (16) Hostalka, H., Schulz, G. V., *Polymer Letters* **3**, 1043 (1965).
- (17) Hubman, E., Taylor, R. B., Williams, F., *Trans. Faraday Soc.* **62**, 88 (1966).
- (18) Johnson, C. L., Metz, D. J., *Am. Chem. Soc., Div. Polymer Chem., Preprints* **4**, 440 (1963).
- (19) Kanoh, N., Higashimura, T., Okamura, S., *Makromol. Chem.* **56**, 65 (1962).
- (20) Katayama, M., Hatada, M., Hirota, K., Yamazaki, H., Ozawa, Y., *Bull. Chem. Soc. (Japan)* **38**, 851 (1965).
- (21) Matheson, M. S., Auer, E. E., Beuilacqua, E. B., Hart, E. J., *J. Am. Chem. Soc.* **73**, 1700 (1951).
- (22) Mayo, F. R., *J. Am. Chem. Soc.* **65**, 2324 (1943).
- (23) Metz, D. J., Potter, R. C., Thomas, J. K., *J. Polymer Sci., Pt. A-1* **5**, 877 (1967).
- (24) Metz, D. J., *ADVAN. CHEM. SER.* **66**, 170 (1967).
- (25) Metz, D. J., Potter, R. C., Bretton, R. H., *J. Polymer Sci.*, in press.
- (26) Metz, D. J., unpublished work.
- (27) Overberger, C. G., Endres, G. F., Monaci, A., *J. Am. Chem. Soc.* **78**, 1969 (1956).
- (28) Pepper, D. C., Reilly, P. J., *J. Polymer Sci.* **58**, 639 (1962).
- (29) Potter, R. C., Johnson, C. L., Metz, D. J., Bretton, R. H., *J. Polymer Sci., Pt. A-1* **4**, 419 (1966).
- (30) Potter, R. C., Bretton, R. H., Metz, D. J., *J. Polymer Sci., Pt. A-1* **4**, 2295 (1966).
- (31) Schneider, C., Swallow, A. J., *J. Polymer Sci.* **B4**, 277 (1966).
- (32) Taylor, R. B., Williams, F., *J. Am. Chem. Soc.* **89**, 6359 (1967).
- (33) Ueno, K., Hayashi, K., Okamura, S., *J. Polymer Sci.* **B3**, 363 (1965).
- (34) Ueno, K., Hayashi, K., Okamura, S., *Polymer* **7**, 431 (1966).
- (35) Ueno, K., Williams, F., Hayashi, K., Okamura, S., *Trans. Faraday Soc.* **63**, 1478 (1967).
- (36) Williams, F., Hayashi, K., Ueno, K., Hayashi, K., Okamura, S., *Trans. Faraday Soc.* **63**, 1501 (1967).
- (37) Williams, F., private communication.
- (38) Yamaoka, H., Williams, F., Hayashi, K., *Trans. Faraday Soc.* **63**, 376 (1967).

RECEIVED April 1, 1968. Work performed under the auspices of the U. S. Atomic Energy Commission.

# Pulse Radiolysis of Styrene and $\alpha$ -Methylstyrene

CHRISTEL SCHNEIDER

Institute for Physical Chemistry, University of Cologne,  
5 Cologne, West Germany

*Information can be obtained by pulse radiolysis studies on the nature and reactions of transient species formed in styrene and  $\alpha$ -methylstyrene. A very short-lived species showing an absorption in the range 350–400  $m\mu$  has been identified as the monomer anion radical formed through electron capture by a monomer molecule. Besides the anion, a second longer-lived species with an absorption maximum at about 320  $m\mu$  appeared which was identified as the polymerizing styrene radical  $\sim\text{CH}_2\text{CHC}_6\text{H}_5$ . Pulsing of an aqueous solution of styrene showed an additional absorption at 345  $m\mu$  owing to a hydroxy cyclohexadienyl radical formed by addition of OH to the benzene ring of the styrene molecule.*

**D**uring the past few years pulse radiolysis has yielded valuable information about excited molecules, ionic species, and free radicals produced in irradiated systems (3, 4). However, it has been applied mainly to aqueous systems where results of great general interest have been obtained—*e.g.*, the detection of the solvated electron (6, 13). Only since about 1965 has this technique been applied to polymerizing systems where, although much is known about the reaction kinetics, there is still little direct information on the nature of the initiating species and on the growing radicals. Up to now, styrene and  $\alpha$ -methylstyrene are the monomers which have been studied under pulsed irradiation. These monomers are well suited to such studies because of the profound knowledge of their polymerization kinetics which exists and because they can be polymerized by anions or cations as well as by free radicals; this has been proved by using various conventional catalysts and by initiating polymerization through ionizing radiation under extreme conditions.

Pulse radiolysis studies on styrene and  $\alpha$ -methylstyrene have been carried out independently by three research groups using comparable facilities and optical detection methods. There is good agreement among the authors' results with regard to the general pattern on the nature and even on the possible mechanism of formation of the transient species while such agreement is often lacking in the kinetic data obtained or in the effects produced by adding other reactants. This paper summarizes information obtained by pulse radiolysis on the nature and reactions of transient species formed in styrene and  $\alpha$ -methylstyrene.

### *Anions*

The formation of the styrene and  $\alpha$ -methylstyrene anion under pulsed irradiation of monomers in the pure state and in dilute solutions has been clearly indicated from the absorption spectra obtained.

Katayama *et al.* (10, 11, 12) reported on the appearance of absorption maxima at about 350 and 546  $m\mu$  with a shoulder at about 420  $m\mu$  in the pulsing of extremely dry  $\alpha$ -methylstyrene sealed in a quartz cell. The absorptions have been shown to be sensitive to traces of water, and the kinetics of the absorption at 3663 Å. showed two kinds of intermediates, one of which ( $A_{1/2} \sim 25 \mu\text{sec.}$ ) was regarded as the radical anion. Metz and co-workers (16), using ultrapure styrene observed a very short-lived transient absorbing at 370  $m\mu$ . The sensitivity of this species to water indicated strongly that it was an ion, which the authors think is partially responsible for the kinetics of polymerization observed under extremely dry conditions (19, 20). Oxygen decreased the initial height of the absorption and slowed the decay rate of this species, while addition of  $N_2O$  showed no effect at all. Both authors tentatively identified the species observed as the styrene anion radical formed through electron capture by a styrene molecule. The species decayed according to first-order kinetics with a half-life of about 4  $\mu\text{sec.}$  obtained at 370  $m\mu$  by Metz compared with 25  $\mu\text{sec.}$  reported by Katayama for all three absorption maxima.

The formation of a styrene and  $\alpha$ -methylstyrene anion, absorbing at about 390  $m\mu$ , was shown by Schneider and Swallow (23, 24, 25), even for conventionally purified monomers which had not been treated to remove traces of water. The nature and reactions of this transient were studied in more detail in dilute solutions of styrene in different solvents. A solution ( $10^{-3}M$ ) of styrene in cyclohexane showed, immediately after the pulse, a spectrum with a distinct absorption band at 390  $m\mu$  (Figure 1), similar to that observed by Keene *et al.* (14). However, the intensity of the absorption was irreproducible during a series of experiments, probably because of the varying moisture content of the air and of the

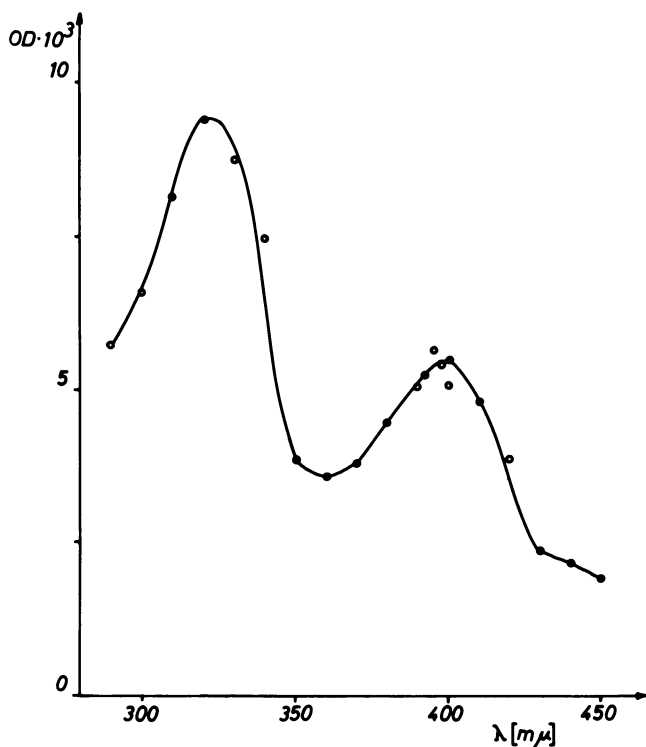


Figure 1. Absorption spectrum of a deaerated  $10^{-3}M$  solution of styrene in cyclohexane, taken immediately after a  $2\text{-}\mu\text{sec.}$  pulse of  $\sim 5000$  rads

glassware used. The influence of impurities on the  $390\text{ m}\mu$  absorption was checked by adding small amounts of water, methanol, chloroform, carbon tetrachloride or *n*-butylamine or by saturating the solution with  $N_2O$ . All additives considerably reduced or even removed the  $390\text{-m}\mu$  absorption, the strongest effects being exerted by the halogenated compounds and  $N_2O$ , both of which act as electron scavengers (Figure 2). Pulsing of dilute solutions of styrene in hexane showed similar results. Schneider and Swallow concluded that the species absorbing at  $390\text{ m}\mu$  was the styrene anion. This finding was supported by the fact that pulsed dilute solutions of styrene ( $5 \times 10^{-4}$  to  $5 \times 10^{-3}M$ ) in aliphatic alcohols and water no longer show the broad absorption band of the solvated electron observed for the irradiated pure solvents in the visible region of the spectrum (1, 22). However, no absorption at about  $390\text{ m}\mu$ , as would be expected for the anion formed through capture of the solvated electron by the styrene could be observed. This is explained by rapid protonation of the anion in solvents like water or aliphatic alcohols.

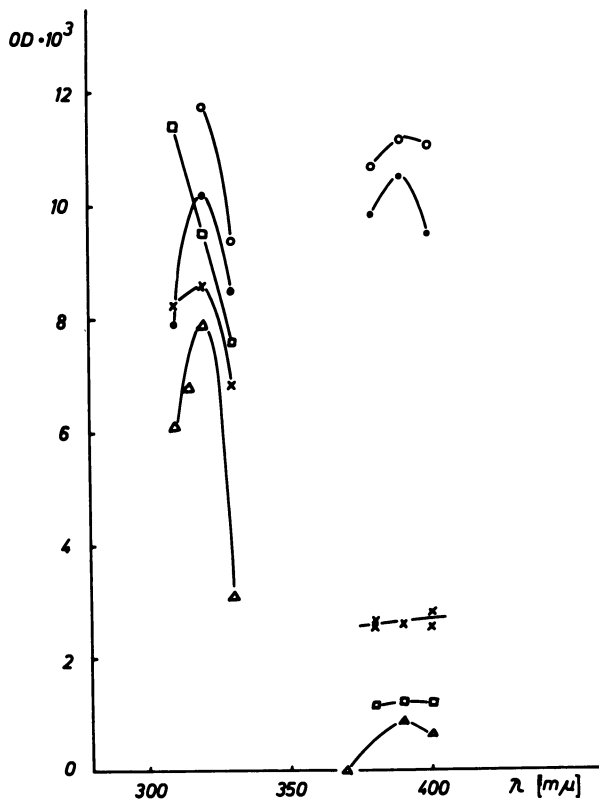


Figure 2. Influence of small amounts ( $10^{-3}M$ ) of additives on the absorption spectrum of a  $10^{-3}M$  solution of styrene in cyclohexane; dose rate:  $\sim 5000$  rads/pulse

- Cyclohexane (aerated)
- Cyclohexane (dried)
- × Water added
- △ Methanol added
- $CCl_4$  added

The styrene anion was extremely short lived when cyclohexane and hexane were used as solvents, but contrary to the findings of Katayama *et al.* and of Metz *et al.*, Schneider and Swallow stated that the decay of the anion followed second-order kinetics with a first half-life of about  $3-4 \mu\text{sec.}$  for styrene ( $10^{-3}M$ ) in cyclohexane and hexane. Evaluation of the decay curves at  $390 m\mu$  led to values for  $k/\epsilon \approx 7 \times 10^6 \text{ cm. sec.}^{-1}$  for styrene in the pure state and  $k/\epsilon = 3.8 \pm 0.6 \times 10^7 \text{ cm. sec.}^{-1}$  for a  $10^{-3}M$  solution of styrene in cyclohexane. The decay kinetics were not influenced by varying the dose rate of the pulse by a factor of about 6, thus confirming that the decay is second order. If a  $G$  value of 0.2 is assumed for the formation of free ions in hydrocarbons, an extinction coefficient

of about  $6 \times 10^3 M^{-1} \text{ cm.}^{-1}$  for pure styrene and  $8 \pm 3 \times 10^3 M^{-1} \text{ cm.}^{-1}$  for the cyclohexane solution was calculated from the dose rate (5000 rads/pulse) and the optical density obtained immediately at the end of a pulse. Thus, decay constants of  $k = 6 \times 10^{10} M^{-1} \text{ sec.}^{-1}$  for styrene in the pure state and  $k = 3 \times 10^{11} M^{-1} \text{ sec.}^{-1}$  for styrene in cyclohexane were obtained, which are not inconsistent with a diffusion-controlled ion-ion recombination reaction (5, 9).

$\alpha$ -Methylstyrene behaved like styrene with respect to the absorption spectra and the decay kinetics. From the findings of the different authors obtained under different conditions one must conclude that ions are always produced in a substantial number, regardless of the purity of the monomers, but the successful propagation of these ions requires extreme purity.

### Cations

The role of cations in the pulse radiolysis of styrene and  $\alpha$ -methylstyrene is not yet clear. Using frozen glasses, Shida and Hamill (26) and Williams (27) have seen absorptions with peaks at 350 and 650  $m\mu$  for styrene and  $\alpha$ -methylstyrene. Bands have also been seen previously (24) at 460 or 475  $m\mu$ . Perhaps the species responsible for the shoulders seen by Schneider and Swallow between 340 and 370  $m\mu$  is a cation, whose absorption overlaps that of the anion radical. This could explain the diminution of the absorption intensity round 390  $m\mu$  when *n*-butylamine was added. However, there was no evidence for an absorption band at longer wavelengths.

### Radicals

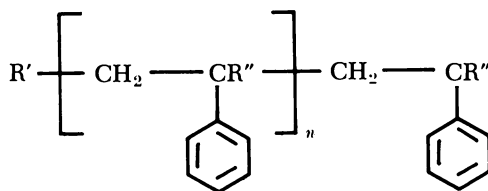
Katayama *et al.* have reported that the species absorbing at 350, 420, and 546  $m\mu$  in  $\alpha$ -methylstyrene in the pure state is sensitive to both water and DPPH, both of which were also found to suppress the polymerization reaction. They suggest, therefore, that it is the anion radical which is responsible for the polymerization of  $\alpha$ -methylstyrene. In addition, they observed a transient which decayed very slowly ( $t_{1/2} \sim 5 \text{ msec.}$ ) and which was regarded to be probably the free radical.

In addition to the anion, Metz and co-workers, when pulsing ultra-pure styrene, observed a second, longer-lived species with an absorption maximum at 320–330  $m\mu$ . It was unaffected by addition of water or oxygen and decayed according to first-order kinetics with a half-life of

about 220  $\mu\text{sec}$ . By comparison with work done on the  $\gamma$ -irradiation of bromoethylbenzene by Hamill *et al.* (8) and on the flash photolysis of ethylbenzene and benzyl compounds by Porter and co-workers (17, 18), the American authors tentatively identify this species as the styrene radical  $\text{C}_6\text{H}_6\dot{\text{C}}\text{HCH}_3$ . Based on their dosimetry value and the initial optical density obtained and taking a  $G$  value for radical formation in styrene of 0.35 (2), they calculate an extinction coefficient at 320  $m\mu$  for this species of  $\epsilon = 7 \times 10^3 M^{-1} \text{cm}^{-1}$ . Metz *et al.*, however, note that two of the results are difficult to understand if the species is indeed a radical—*i.e.*, the first-order decay and the apparent insensitivity of the species to oxygen.

Schneider and Swallow showed that repetitive pulsing of styrene in the pure state and in different solvents using  $10^4$  pulses (2  $\mu\text{sec.}/\text{pulse}$ ,  $\approx 3 \times 10^{17}$  e.v./gram pulse) at a frequency of 50 pulses/sec. yielded polystyrene in each case. The amount of polymer formed and its molecular weight were determined. The effect of dose rate variation on the amount and molecular weight as well as addition of radical scavengers and studies on copolymer formation showed results similar to those found in the conventional free radical polymerization of styrene. From the degree of polymerization and the rate of polymer formation a rate constant for mutual chain termination of  $k_t = 1.1 \times 10^6 M^{-1} \text{sec}^{-1}$  was calculated. Correspondingly, the polymerizing radical showed a mean lifetime  $\tau$  of about 0.5 sec.

Besides the absorption of the anion at about 390  $m\mu$ , the absorption spectra of pulsed styrene and  $\alpha$ -methylstyrene, taken by Schneider and Swallow show broad and rather intense absorptions round 320  $m\mu$ . These absorptions are influenced only slightly by water but are eliminated in the presence of iodine. Oxygen decreases the initial height of the absorption and also causes an apparent change in the decay kinetics (Figure 3). The decay in the deaerated solution did not fit first- or second-order kinetics, but if the decay after about 0.5 msec. is regarded as second order, a value of  $k/\epsilon < 1.3 \times 10^3 \text{cm. sec}^{-1}$  is obtained for styrene. Combination with a molar extinction coefficient  $\epsilon = 1.2 \times 10^4 M^{-1} \text{cm}^{-1}$  (7) led to a decay rate constant  $k \leq 1.6 \times 10^7 M^{-1} \text{sec}^{-1}$ , which is in reasonable agreement with values given in the literature for the termination rate constant  $k_t$  of styrene polymerization and the value of  $1.1 \times 10^6 M^{-1} \text{sec}^{-1}$  derived from the polymerization experiments under pulsed conditions. From the effect of additives on the 320- $m\mu$  absorption, the kinetic data obtained and considerations already mentioned in connection with Metz's work the authors attribute the absorption in large part to a resonance-stabilized growing polymer radical of the benzyl type: where  $R'$  is the initiating group and  $R''$  is H for styrene and  $\text{CH}_3$  for  $\alpha$ -methylstyrene.



Both groups—Metz, Potter, and Thomas and Schneider and Swallow—observed an additional very long-lived absorption at 310 to 320  $m\mu$  which may be caused by more than one species. The absorption decays, in the dark, over many hours while it is photolyzed by light in seconds or minutes, and its nature is not yet clear.

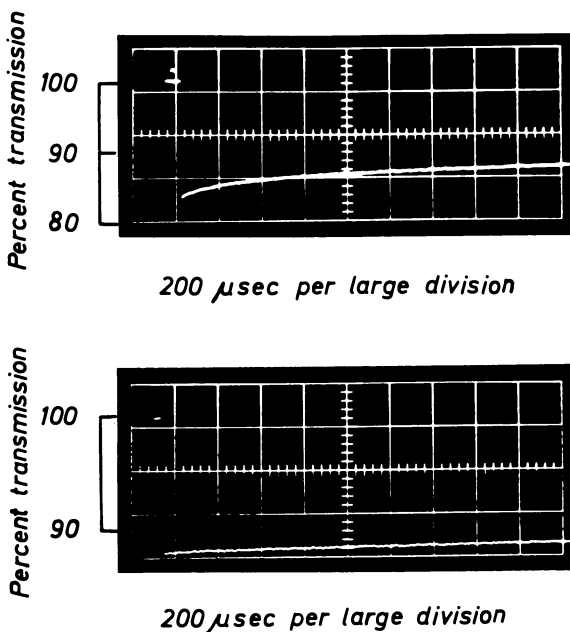


Figure 3. Oscilloscope traces of pulsed deaerated styrene at 315  $m\mu$  after a 2- $\mu$ sec. pulse of  $\sim 2000$  rads (top) and  $\sim 5000$  rads (bottom) in the presence of oxygen

When an aqueous solution of styrene or  $\alpha$ -methylstyrene ( $5 \times 10^{-4}$  to  $5 \times 10^{-3}M$ ) was pulsed, Schneider and Swallow observed a group of intense and distinct absorption bands obviously caused by different radical species, while the absorption of the hydrated electron could no longer be observed (Figure 4). The absorption obtained at 345  $m\mu$  for styrene and 350  $m\mu$  for  $\alpha$ -methylstyrene is caused mainly by a hydroxy-cyclohexa-



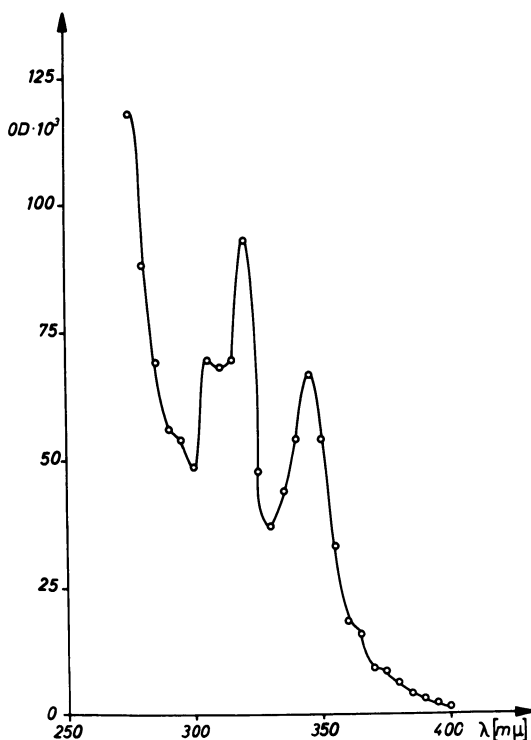


Figure 4. Absorption spectrum of an acidified aqueous solution of styrene ( $5 \times 10^{-4}$ M, pH = 1.26), taken immediately after a 2- $\mu$ sec. pulse of  $\sim 5000$  rads

Table I. Pulse Radiolysis Results

Short Lived Species	$\lambda_{max}$ [m $\mu$ ]	Sensitive to			
		H <sub>2</sub> O	O <sub>2</sub>	DPPH	N <sub>2</sub> O
Katayama <i>et al.</i>	$\sim 350$				
	$\sim 420$	yes		yes	
	546				
Metz <i>et al.</i>	370	yes	yes		no
Schneider and Swallow	$\sim 390$	yes			yes
	[390]	[yes]	little		[yes]
<b>Long Lived Species</b>					
Metz <i>et al.</i>	320	no		no	no
Schneider and Swallow	$\sim 320$	no	yes	yes	no
	[320]	[no]	[yes]		

\* Values in brackets refer to dilute solutions of styrene in cyclohexane.

dienyl radical formed by addition of OH to the benzene ring of the styrene molecule. This was shown by saturating the solution with  $N_2O$  ( $10^{-4}M$ ) which converts all hydrated electrons to OH, thus doubling the intensity of the absorption. On the other hand, adding formate or aliphatic alcohols almost eliminated the 345-m $\mu$  absorption completely by capturing the OH radicals. Pulsing of acidified aqueous styrene solutions (pH = 2.76 and pH = 1.26) gave absorption spectra which did not differ significantly from that in neutral solution, either with respect to the wavelengths of the absorptions or to the intensities. The species observed is rather short lived and decays according to a second-order reaction with a rate constant in the range  $7.4 \times 10^8$  to  $2.9 \times 10^9 M^{-1} sec^{-1}$ ; the exact value, however, depends on the acidity of the solution.

In the ultraviolet region, two absorption maxima, one at 320 m $\mu$  and a weaker one at 305 m $\mu$  were observed; their intensities were increased slightly by  $N_2O$  and were decreased by about half when formate or alcohols were added. The absorption, which is rather long lived, is again attributed to the growing substituted benzyl radical. The splitting of the absorption, which could not be detected in the organic monomer solutions, is suggested by the authors to support this assignment because the benzyl radical itself is known to have absorptions at 306 and 317 m $\mu$  (15). It is assumed that the benzyl type radical is formed partly through electron capture by the styrene molecule followed by rapid protonation in the side chain and partly by addition of H and OH to the double vinyl bond.

Table I summarizes some of the results on the pulse radiolysis of styrene and  $\alpha$ -methylstyrene obtained by the different authors. Although

#### Obtained on Styrene and $\alpha$ -Methylstyrene<sup>a</sup>

Kinetics of Decay, Order	Half-Life, [ $\mu sec.$ ]	$\epsilon_{\lambda_{max}}$	Decay Constant, k	Assignment
first	$\sim 25$		$\sim 4.0 \times 10^4$	(styrene) <sup>-</sup>
first	$\sim 4$	$1 \times 10^4$ (G $\sim 0,15$ )	$\sim 2.5 \times 10^5$	(styrene) <sup>-</sup>
second		$\sim 6 \times 10^3$	$\sim 6 \times 10^{10}$	(styrene) <sup>-</sup>
second		[ $\sim 8 \times 10^3$ ]	[ $3 \times 10^{11}$ ]	
first	220	$7 \times 10^3$	$4.5 \times 10^3$	$C_6H_5\cdot CHCH_3$
second		$\sim 1.2 \times 10^4$	$1.6 \times 10^7$	$C_6H_5\cdot CHCH_3$
second				

there is already a great deal of information on the nature and reactions of the transient species, there are still many questions which need to be clarified.

### Acknowledgments

The author thanks his colleagues, especially A. J. Swallow, for helpful discussions.

### Literature Cited

- (1) Adams, G. E., Baxendale, J. H., Boag, J. W., *Proc. Roy. Soc. (London)* **A277**, 549 (1964).
- (2) Chapiro, A., "Radiation Chemistry of Polymeric Systems," Interscience, New York, 1962.
- (3) Dorfman, L. M., Matheson, M. S., *Progr. Reaction Kinetics* **3** (1965).
- (4) Ebert, M., Keene, J. P., Swallow, A. J., Baxendale, J. H., Eds., "Pulse Radiolysis," Academic Press, New York, 1965.
- (5) Freeman, G. R., *J. Chem. Phys.* **46**, 2822 (1967).
- (6) Hart, E. J., Boag, J. W., *J. Am. Chem. Soc.* **84**, 4090 (1962).
- (7) Hagemann, R. J., Schwarz, H. A., *J. Phys. Chem.* **71**, 2694 (1967).
- (8) Hamill, W. H., Guarino, J. P., Ronayne, M. R., Ward, J. A., *Discussions Faraday Soc.* **36**, 169 (1964).
- (9) Hummel, A., Allen, A. O., *J. Chem. Phys.* **44**, 3426, 3431 (1966).
- (10) Katayama, M., Hatada, M., Hirota, K., Yamazaki, H., Ozawa, Y., *Bull. Chem. Soc. (Japan)* **38**, 851 (1965).
- (11) Katayama, M., *Bull. Chem. Soc. (Japan)* **38**, 2208 (1965).
- (12) Katayama, M., Yamazaki, H., Ozawa, Y., Hatada, M., Hirota, K., *Nippon Kagaku Zasshi* **87**, 37 (1966).
- (13) Keene, J. P., *Nature* **197**, 47 (1963).
- (14) Keene, J. P., Land, E. J., Swallow, A. J., *J. Am. Chem. Soc.* **87**, 5284 (1965).
- (15) McCarthy, R. L., MacLachlan, A., *Trans. Faraday Soc.* **56** (1960).
- (16) Metz, D. J., Potter, R. C., Thomas, J. K., *J. Polymer Sci., Pt. A-1* **5**, 877 (1967).
- (17) Porter, G., Strachan, E., *Trans. Faraday Soc.* **54**, 1595 (1958).
- (18) Porter, G., Windsor, M. W., *Nature* **180**, 187 (1957).
- (19) Potter, R. C., Johnson, C. L., Metz, D. J., Bretton, R. H., *J. Polymer Sci., Pt. A-1* **4**, 419 (1966).
- (20) Potter, R. C., Bretton, R. H., Metz, D. J., *J. Polymer Sci., Pt. A-1* **4**, 2295 (1966).
- (21) Ronayne, M. R., Guarino, J. P., Hamill, W. H., *J. Am. Chem. Soc.*, **84**, 4230 (1962).
- (22) Sauer, M. C., Arai, S., Dorfman, L. H., *J. Chem. Phys.* **42**, 708 (1965).
- (23) Schneider, C., Swallow, A. J., *Proc. Tihany Symp. Radiation Chem., 2nd, Akademiai Kiado, Budapest*, 1967.
- (24) Schneider, C., Swallow, A. J., *J. Polymer Sci., Pt. B* **4** (1966).
- (25) Schneider, C., Swallow, A. J., *Makromol. Chem.* **114**, 155, 172 (1968).
- (26) Shida, T., Hamill, W. H., *J. Chem. Phys.* **44**, 4372 (1966).
- (27) Williams, F., private communication.

RECEIVED March 25, 1968.

# The Solid State Polymerization of Hexamethylcyclotrisiloxane

A. S. CHAWLA and L. E. ST. PIERRE

McGill University, Montreal, Quebec, Canada

*The solid state polymerization of hexamethylcyclotrisiloxane has been investigated over the temperature range  $-196^{\circ}$  to  $60^{\circ}\text{C}$ . The rates of polymerization have been related to the presence of ion scavengers,  $\text{H}_2\text{O}$ ,  $\text{NH}_3$ , in the monomer and to the size of the crystals. Using large crystals dried over sodium, G values of polymerization of  $11 \times 10^3$  were obtained at  $50^{\circ}\text{C}$ . This is five times larger than previously reported values. The reaction is concluded to be surface initiated and to be terminated at a crystal face or at a defect.*

The ability of high energy radiation to initiate polymerization of monomers in the crystalline state was first reported more than a decade ago (14) and has been an active area of investigation for both radiation and polymer researchers. The field has seen outstanding progress during this period (2, 3, 7, 13) but despite these advances, many important questions still remain only partially answered. Few, if any, systems have been investigated in sufficient detail to yield adequate answers to questions concerning the nature and the site of initiation, the nature of the propagating species, the effect of impurities, and the roles of crystal structure and size (8, 9). Because of this lack of understanding, reproducibility continues to be a major problem for investigators in the field and, indeed, it is not difficult to discover in the literature direct contradictions in results reported from two different laboratories.

In this chapter we report some results from an intensive investigation of the radiation-induced polymerization of a single monomer—hexamethylcyclotrisiloxane—which by virtue of its ease of polymerization and very high solid state vapor pressure affords an opportunity for comment on two of the points mentioned above.

The first reported solid-state polymerization of this monomer was that of Lawton, Grubb, and Balwit (6) in 1956. Subsequent studies involving irradiation initiation have been reported by Burlant and Taylor (1), and Trofimova *et al.* (15); recently Prut *et al.* (12) reported the results of a study of the solid polymerization in which they used  $\text{SnCl}_4$  as the initiator.

This chapter deals mainly with two aspects of solid state polymerization—the effect of impurities and the effect of crystal size on the rates of polymerization. From the conclusions drawn, a reaction mechanism is proposed.

### **Experimental**

Detailed experimental procedures are reported elsewhere (4). However, brief descriptions of these techniques follow.

**Monomer Preparation.** The hexamethylcyclotrisiloxane used in these experiments was supplied through the courtesy of W. L. Robb of the Silicone Products Department, General Electric Co. It was purified through repeated sublimation and recrystallization and exhibited, by VPC analysis, an impurity level of less than 1 part in 1000. (m.p.,  $64.5^\circ\text{C}.$ )

**Polymerization Technique.** Owing to the difficulty in obtaining reproducible results, comparisons were made only between samples of the same "batch." A batch was prepared by having the monomer in each of 10 or 12 tubes all derived from the same master sample and all equilibrated with the same vapor before sealing off.

The customary procedure used in sample preparation was as follows: a tube containing  $\sim 50$  grams of prepurified and silica dried monomer was connected to a vacuum line and degassed through repeated meltings. Monomer was then distilled simultaneously to each of the many tubes connected to a manifold. When approximately 2 grams were in each tube, the tubes were sealed under vacuum. Small crystals were then formed in the tubes by melting the monomer and quick quenching it in liquid nitrogen.

**Drying of Monomer.** The monomer was dried by contacting it with finely dispersed sodium. The sodium was melted and degassed by holding it under a vacuum ( $10^{-5}$  mm. Hg) for 3 hours at  $400^\circ\text{C}.$  The tube containing the sodium was then closed off, and monomer was distilled into it from a previously attached sidearm, separated by a breakoff. The tube was then heated and shaken to disperse the sodium. After 4 hours contact at  $70^\circ\text{C}.$  between the monomer and the sodium, the system was reconnected to the vacuum line, degassed, and the dried monomer was distilled into the reaction tubes as previously described.

**Addition of Impurities to Monomer.** Minute amounts of  $\text{H}_2\text{O}$  and  $\text{NH}_3$  were, in some cases, added to the monomer under controlled conditions. This was done by connecting 0.5-cc. thin walled ampoules to the vacuum line and equilibrating them with known vapor pressures of impurities. The ampoules were sealed off and placed in a reaction tube. At any time desired, the contaminant was mixed with the reactant by simply shaking the reaction tube, thus causing the ampoule to break.

**Growth of Large Crystals.** Large crystals were grown in the reaction tubes by cooling the empty end of a tube containing very small crystals. Mass transfer was effected through sublimation. The temperature of crystal growth was 25°C. with a temperature gradient of 2.5°C. being maintained between the ends of the tube.

**Irradiation.** The irradiation source was a cobalt-60 Gammacell 220 (Canadian Atomic Energy Limited) operating at a dose rate of  $3.7 \times 10^4$  rads/hr.

Temperature control during irradiation was effected by placing the tubes in holes in a thermostatted aluminum block.

**Isolation of Products.** Following irradiation, the reaction tubes were weighed and opened. Unreacted monomer was then pumped off, and the tube was re-weighed. Polymer yields were calculated from the weight differences.

### Results and Discussion

**Effect of Impurities.** The initial polymerizations were done using monomer which had been dried and vacuum transferred. The drying, however, did not involve the sodium treatment. Such polymerizations yielded results of a highly irreproducible nature (Figure 1) and caused us to commence the drying procedures discussed above. Using monomer which had been dried rigorously, we were able to increase yields and to accomplish reproducibility, as is shown by the solid line in Figure 1. The yields, using the dried monomer, were considerably higher than those reported by previous workers in the field, and it was assumed that the differences were caused by higher levels of impurities in their monomers. Lawton, Grubb, and Balwit (6) had irradiated their samples in open dishes and thus undoubtedly had appreciable quantities of water present, and while Burland and Taylor (1) did their work in vacuum, no special drying procedures were reported.

Before expanding on the role of impurities in defining polymerization rates and yields, it must be acknowledged that there is a dose-rate effect which may be a contributing factor to the discrepancies mentioned. Reports of such an effect have been made, but they are at variance as to the nature of the change in kinetics associated with changes in dose rates (1, 6, 15). In the current work the dose rates have been kept constant.

To test the effect of impurity levels, very small quantities of  $\text{NH}_3$  and  $\text{H}_2\text{O}$  were added to monomer which had been dried vigorously. The results (Figure 2) show a marked effect down to exceedingly low concentrations, and both  $\text{H}_2\text{O}$  and  $\text{NH}_3$  are observed to be strong inhibitors. That such strong inhibition should occur with these agents suggests the mechanism to be ionic and evokes comparison with the results of Williams and Okamura (16). Those investigators observed similar rate effects in  $\text{H}_2\text{O}$ -contaminated styrene during radiation polymerization. They pro-

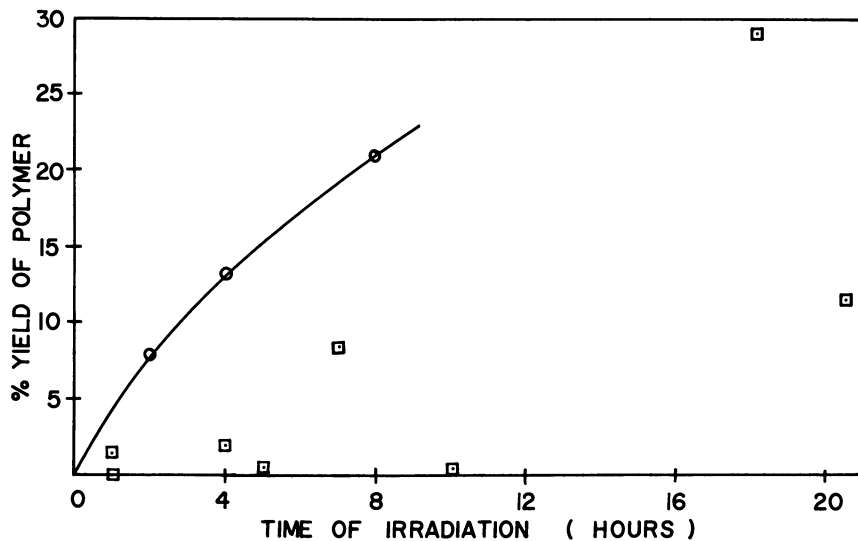


Figure 1. Polymer yield vs. irradiation time

○ Sodium dried monomer  
 □ Silica dried monomer

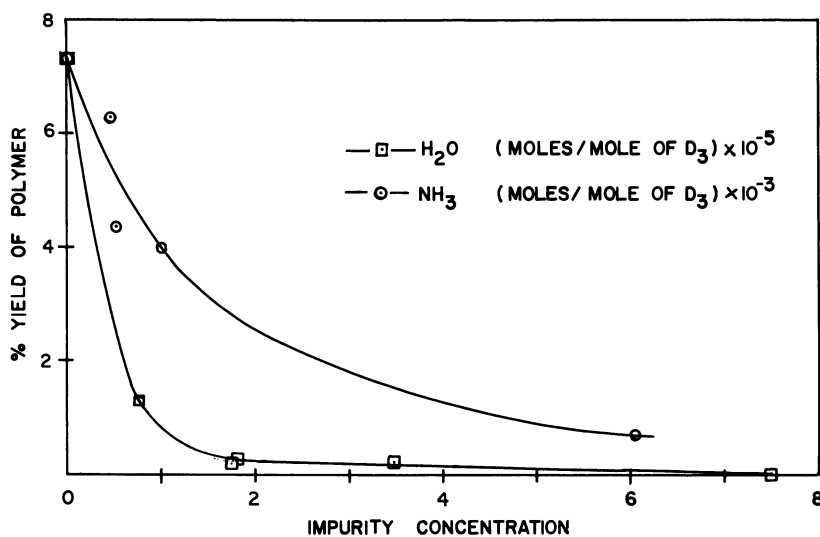


Figure 2. Effect of impurities on polymer yields in hexamethylcyclotri-siloxane

□ H<sub>2</sub>O  
 ○ NH<sub>3</sub>

pose an ionic polymerization with the cations playing a predominant role. Quenching with water is proposed to take place *via* hydrogen transfer, neutralizing the propagating species.

The present observations could well be explained on the same basis since hexamethylcyclotrisiloxane polymerizes *via* both anionic and cationic mechanisms (5). (No evidence exists to date for free radical polymerizations.) The greater activity of H<sub>2</sub>O as an inhibitor, as compared with NH<sub>3</sub>, is explained on the basis of a more rapid ion transfer. Since this would be a hydrogen ion rather than a hydride ion, it further suggests an anion as the primary polymerization species in the present polymerization. The authors feel, however, that further work is required before definite conclusions can be drawn regarding the polymerization mechanism or mechanisms.

**Effect of Crystal Size.** The effect of crystal size on the polymerization rate in radiation-induced polymerizations has been the subject of much discussion (8, 9). However, since small levels of impurities have been demonstrated to have such profound effects, it has been difficult to compare meaningful rate data obtained on large crystals in one reaction vessel with those for small crystals in another. Hexamethylcyclotetrasiloxane allows a unique opportunity for experimentation into this size effect since, owing to the high vapor pressure of the solid (10), it is possible to grow large crystals from small crystals in the same tube, after purification is complete. Thus, crystals of both sizes exist in exactly the same environment.

Large crystals were grown, in the manner described previously, in the empty ends of tubes containing small crystals. The total samples were then irradiated, and the yields from each end of the reaction tube were determined. Figure 3 shows the increase in rate with crystal size. It demonstrates a marked improvement in rate and is explicable in any one of three ways. First, should the termination occur at a surface, the larger crystals would allow a longer chain propagation. Secondly, the large crystals could, by virtue of an extra sublimation, be purer and therefore less susceptible to impurity inhibition. Thirdly, the large crystals may contain fewer defects. Since termination can be expected to occur at defects as well as at crystal faces, a diminution in such sites would enhance the kinetic chain length. The x-ray data of Peyronel (11) have been interpreted to show a diminished defect concentration in the large crystals. The analysis is, however, not quantitative in terms of numbers of defects but only points to fewer in the large crystals. Selection between Factors 1 and 3 is thus not possible at this time. Notwithstanding, the work of Peyronel shows that Factors 1 and 3 are both associated with crystal size.



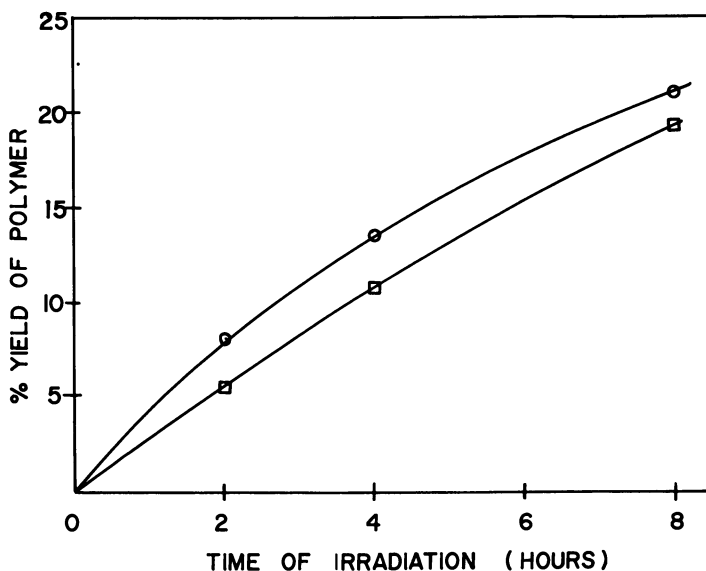


Figure 3. Effect of crystal size on polymerization yields

○ Large crystals  
 □ Small crystals

The importance of Factor 2, the extra sublimation of the large crystals, was quickly discounted by a simple experiment. Large and small crystals were prepared in the same tube in the usual manner by growing the large crystals in the empty end of a tube containing small crystals. The tube was then sealed off at the center, and the large crystals were melted quickly and quenched to yield small crystals. These had now been subjected to one more sublimation than those in the opposite end of the tube. Irradiation was then performed as before, and the respective yields were determined. The monomers in both ends gave the same yields. The enhancement observed in Figure 1 is thus a crystal size effect and is not caused by different impurity levels.

Table I.  $G_{(\text{Monomer})}$

Temperature, °C.	L-G-B (4)	B-T (5)	T-B-K (6)	Present Work
30	30	800	750	5,050
50	80	2200	1680	11,510

The combination of careful purification and the use of large crystals results in rates of polymerization and polymer yields far in excess of those otherwise obtainable (Table I).

**Literature Cited**

- (1) Burlant, W., Taylor, C., *J. Polymer Sci.* **42**, 547 (1959).
- (2) Chapiro, A., "High Polymers," Vol. 15, pp. 236-246, Interscience, London, 1962.
- (3) Charlesby, A., *Rept. Progr. Phys.* **28**, 463 (1965).
- (4) Chawla, A. S., St. Pierre, L. E., *J. Polymer Sci.*, in press.
- (5) Kantor, S. W., Grubb, W. T., Osthoff, R. C., *J. Am. Chem. Soc.* **76**, 5190 (1954).
- (6) Lawton, E. J., Grubb, W. T., Balwit, J. S., *J. Polymer Sci.* **19**, 455 (1956).
- (7) Morawetz, H., "Physics and Chemistry of the Organic Solid State," Vol. 1, Chap. 4, Interscience, New York, 1963.
- (8) Okamura, S., Hayashi, K., Kitanishi, Y., *J. Polymer Sci.* **58**, 925 (1962).
- (9) Okamura, S., Obayashi, E. K., Takeda, M., Tomikawa, K., Higashimura, T., *J. Polymer Sci. C4*, 827 (1964).
- (10) Osthoff, R. C., Grubb, W. T., Burkhard, C. A., *J. Am. Chem. Soc.* **75**, 2227 (1953).
- (11) Peyronel, G., *Accad. Lincei* **15**, 402 (1953).
- (12) Prut, E. V., Trofimova, G. M., Yenikolopyan, N. S., *Vysokomolekul. Soedin* **6**, 2103 (1964).
- (13) Restaino, A. J., Mesrobian, R. B., Morawetz, H., Ballantine, D. S., Dienes, G. J., Metz, D. J., *J. Am. Chem. Soc.* **78**, 2939 (1956).
- (14) Schmitz, J. V., Lawton, F. J., *Science* **113**, 718 (1951).
- (15) Trofimova, G. M., Barkalov, I. M., Kuz'mina, S. S., Gol'danskii, V. I., Yenikolopyan, N. S., *Dokl. Akad. Nauk, SSSR*, **161**, 882 (1965).

RECEIVED April 1, 1968.

## Mechanisms of Propagation of Ionic Polymerizations

M. SZWARC

State University College of Forestry at Syracuse University,  
Syracuse, N. Y. 13210

*Ionic polymerization is propagated by various species (free ions, ion pairs, triple ions, etc.). Solvents, counterions, solvating agents, etc. affect in different ways the reactivities of free ions and of ion pairs. The existence of different types of ion pairs is revealed by ESR spectroscopy. The application of ESR for such studies is reviewed, and the potentialities of the method illustrated by suitable examples. The role of water in cationic polymerization is discussed. Water can act as a terminating agent of cationic polymerization either as single  $H_2O$  molecules or as agglomerates such as  $(H_2O)_2$ . It is suggested that a single  $H_2O$  molecule acts as a Brønsted base, while  $(H_2O)_2$ , or higher agglomerates act as Lewis bases. This changes the kinetics of termination and affects profoundly the behavior of the system.*

While radical homopolymerization involves one species only—viz., a growing free radical—several distinct entities may contribute to ionic propagation. In a classic ionic polymerization the growing polymers are endowed with electrically charged active ends, the charge being negative in anionic systems and positive in cationic processes. However, because the reacting solution must be electrically neutral, an equal number of oppositely charged ions, referred to as counterions, must be present in the system. In solvents of high dielectric constant and strong solvating power the ions may remain free, especially in dilute solutions, and the polymerization is performed then by free ions—e.g., by carbanions or carbonium ions. In less powerfully solvating media of relatively low dielectric constant the oppositely charged ions combine into ion pairs and these could be the carriers of the reaction. In a general case both free ions and ion pairs may contribute to the propagation,

and if  $k_f$  denotes the rate constant of the free ion and  $k_{\pm}$  that of ion pairs, the *observed* propagation constant  $k_p$  is given by

$$k_p = \gamma k_f + (1 - \gamma) k_{\pm}$$

where  $\gamma$  denotes the fraction of growing ends present as free ions.

Ions and ion pairs remain usually in equilibrium with each other—*e.g.*,



and then  $\gamma^2 C / (1 - \gamma) = K_{\text{diss}}$ ,  $C$  denoting the concentration of all the growing species. For  $\gamma \ll 1$ , a case often encountered in practice, the approximation

$$\gamma = K_{\text{diss}}^{1/2} / C^{1/2}$$

is valid. One finds then that the observed propagation constant  $k_p$  is given by

$$k_p = k_{\pm} + (k_f - k_{\pm}) K_{\text{diss}}^{1/2} / C^{1/2},$$

which was verified for many anionic polymerizations. Its reliability is illustrated in Figure 1 (6). Other examples are discussed in recent monograph by the writer (31).

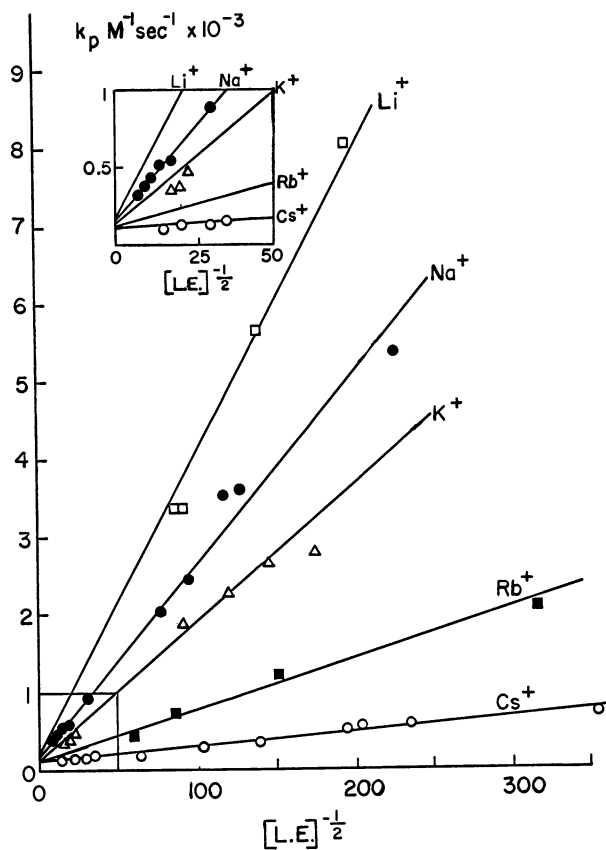
In the presence of another electrolyte, sharing a common counterion with the growing polymer, the above relation must be modified (26). For example, the addition of  $\text{Na}^+, \text{BPh}_4^-$  to living sodium polystyrene,  $\sim\text{S}^-, \text{Na}^+$ , retards its polymerization, and the propagation constant is then independent of the concentration of living polymers—*viz.*,

$$k_p = k_{\pm} + (k_f - k_{\pm}) K_{\text{diss}} / [\text{Na}^+]$$

This result is caused by the fact that most of the sodium ions are formed through the dissociation of the salt, and thus,  $\gamma / (1 - \gamma) = K_{\text{diss}} / [\text{Na}^+]$ .

It follows that the kinetic results permit us to find  $k_f$  and  $K_{\text{diss}}$  because in the absence of the boride the slope of the line  $k_p$  vs.  $1/C^{1/2}$  gives  $(k_f - k_{\pm}) K_{\text{diss}}^{1/2}$ , whereas the slope of the line  $k_p$  vs.  $1/[\text{counterion}]$ , obtained in the presence of the salt gives  $(k_f - k_{\pm}) K_{\text{diss}}$ . The propagation constant  $k_{\pm}$  may be found from either plot; it is given by the intercept of the respective lines.

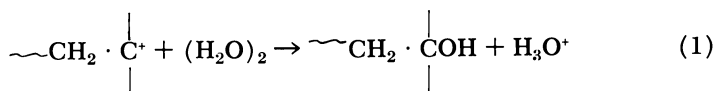
The equilibrium between ions and ion pairs is not maintained in all polymerizing systems. For example, the cationic polymerization induced by ionizing radiation produces the positive and negative ions, the latter initiating a free carbonium ion propagation which is terminated by their collision with negative ions. Such a collision destroys the free ions, and hence their stationary, but not the equilibrium, concentration is determined by their rate of formation and destruction.



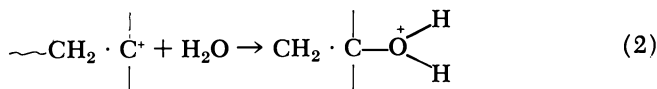
Journal of Physical Chemistry

Figure 1. Linear dependence of the observed propagation constant,  $k_p$ , of living polystyrene polymerization on  $[\text{living polymers}]^{-1/2}$  for  $\text{Li}^+$ ,  $\text{Na}^+$ ,  $\text{K}^+$ ,  $\text{Rb}^+$ , and  $\text{Cs}^+$  salts in THF at  $25^\circ\text{C}$ .

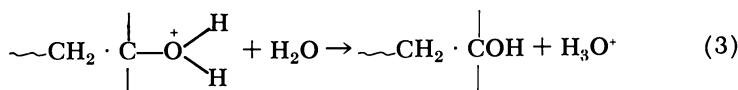
The cation-anion annihilation provides the main mode for termination in extraordinarily dry systems. Traces of water terminate propagation in a most efficient way, and then the termination is first order with respect to the growing polymers. It is interesting to digress here and discuss this writer's ideas about the role of water in such processes. Under normally achieved states of "dryness" the concentration of water in a hydrocarbon monomer is probably sufficiently high to maintain the dissolved water in its dimeric form,  $(\text{H}_2\text{O})_2$  or, at least, to allow a second molecule of water to collide with carbonium ion associated with one  $\text{H}_2\text{O}$  prior to the decomposition of such an associate. Thus, the termination involves processes such as



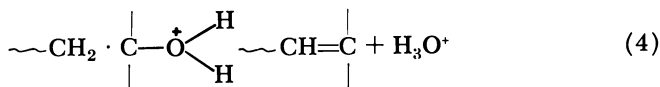
or



followed by the reaction



When the concentration of water is exceedingly low, Reaction 2 is not followed by 3, but the associate decomposes—*i.e.*,



The eventual collision between  $\text{H}_3\text{O}^+$  and a negative center regenerates then the water molecule and destroys the negative ion. Hence,  $(\text{H}_2\text{O})_2$  or higher agglomerates react with carbonium ions as Lewis bases, alcohol is formed, and one water molecule is destroyed. Therefore, the termination of polymerization proceeds simultaneously with the destruction of the terminator. However, at very low water concentration, the single  $\text{H}_2\text{O}$  molecule eventually reacts as a Brönsted base—*i.e.*, as a proton acceptor (Reaction 4). In this process the polymerization is terminated, but the terminator is not destroyed. This accounts for the experimental results—*viz.*, the last trace of moisture cannot be removed from the monomer by prolonged irradiation (24, 37).

To what extent are the reactivities of free ions influenced by the nature of solvent? The required information is available at present for anionic systems only although it is hoped that some data pertaining to cationic polymerization will be available soon. Extensive studies of polymerization of living polystyrene showed that  $k_t$  is affected only slightly by the solvent; the relevant values are listed in Table I. Similar observations were reported for living poly- $\alpha$ -methylstyrene (11). In fact, even the activation energies of propagation are virtually unaffected by the change of solvent—*e.g.*, for the  $\sim\text{S}^-$  growth the activation energies appear to be in the range 5–6 kcal./mole in many different solvents (31).

In this respect the behavior of ion pairs dramatically contrasts with that of free ions. Table II provides some data for various salts of  $\sim\text{S}^-$ . Its inspection shows that  $k_{\pm}$  may vary by a factor as large as 1000 ( $k_{\pm}$  for the propagation of  $\sim\text{S}^-\text{Na}^+$  at 25°C. is about  $4M^{-1} \text{sec.}^{-1}$  in dioxane but about  $3600M^{-1} \text{sec.}^{-1}$  in dimethoxyethane). Moreover, the

pattern of reactivities for a series of alkali salts may depend on the solvent—e.g.,  $\sim\text{S}^-\text{Li}^+$  salt is the least reactive, and the  $\sim\text{S}^-\text{Cs}^+$  salt is the most reactive when the polymerization takes place in dioxane. The order of reactivities is reversed in tetrahydrofuran.

This observation, as well as other facts, led to the conclusion that ion pairs may exist in various forms which could differ greatly in their reactivities. The nature of ion pairs is revealed by various studies (34), and the ESR technique applied to paramagnetic ion pairs provides probably the most penetrating and powerful tool for such investigations. Indeed, the very first direct evidence for the existence of ion pairs as independent molecular species was furnished by Weissman's ESR studies of sodium naphthalenide (1, 2). In the following years the ESR method revealed many interesting phenomena which acquaint us with the thermo-

**Table I. Absolute Rate Constants of Propagation by Free Polystyryl Anions in Different Solvents at 25°C.**

<i>Solvent</i>	$k_p$ , liter mole <sup>-1</sup> sec. <sup>-1</sup>	<i>Ref.</i>
Tetrahydrofuran	63,000–65,000	26
Dimethoxyethane	~40,000	27
2-Methyltetrahydrofuran	27,000–30,000 (?)	15
Tetrahydropyrene	59,000–72,000	14
Tetrahydrofuran–dioxane mixtures	~60,000	36
Tetrahydrofuran–benzene mixtures	40,000–70,000	39

**Table II. Propagation by Living Polystyrene Salts in Various Solvents at 25°C.**

<i>Solvent</i>	$k_{\pm}$ , liter mole <sup>-1</sup> sec. <sup>-1</sup>					<i>Ref.</i>
	<i>Li</i> <sup>+</sup>	<i>Na</i> <sup>+</sup>	<i>K</i> <sup>+</sup>	<i>Rb</i> <sup>+</sup>	<i>Cs</i> <sup>+</sup>	
Living Polystyrene Salts						
Dioxane	0.9	3.4 6.5	20 28	21.5 34	24.6 15	7 12 9, 12, 22
Benzene (non-associated)			47	24	18	
Tetrahydropyrene	<10 <sup>a</sup>	14, 12 <sup>a</sup> 10	73	83	53	25 3, 4
2-Methyltetrahydrofuran	57	11	7.5		22	15
Tetrahydrofuran	~160	80	~100(?)	~50	25	5, 6
Dimethoxyethane		3600			~150	27
Living Poly- $\alpha$ -methylstyrene Salts						
Dioxane		0.02	0.1	0.06		12
Tetrahydropyrene	2.6	0.047	0.25	0.35	0.26	13
Tetrahydrofuran		0.04				40

<sup>a</sup> Aging the solution inhibits the reaction making  $k_{\pm}$  smaller.

dynamics and kinetics of various processes leading from one type of ion pair to another.

ESR spectroscopy is useful in studies of ion pairs if one of the ions is paramagnetic and the other contains an atom whose nucleus has spin different from 0. These conditions do not confer on the ion pairs any special properties; in principle, they behave like any other ion pairs. However, they are necessary to make the ESR investigations feasible. For example, sodium naphthalenide possesses one odd electron moving within the framework of naphthalene moiety. Therefore, this species responds in ESR spectrometer, and the resulting ESR spectrum shows 25 hyperfine lines arising from the interaction of the odd electron with the four  $\alpha$ -type and four  $\beta$ -type protons present in each naphthalene molecule. The association of the naphthalenide ion with a sodium cation changes the observed spectrum—*viz.*, each of the 25 lines shows further splitting into four (1, 2) because the odd electron may now interact with Na nucleus which has spin 3/2. The magnitude of the resulting splitting constant  $a_{\text{Na}}$  measures the probability of finding the odd electron on the Na nucleus, and hence, its value changes as the position of  $\text{Na}^+$  in respect to naphthalenide<sup>-</sup> is altered.

The existence of two different types of ion pairs is revealed in the ESR spectrum by the difference in  $a_{\text{Na}}$ . An example is provided by recent studies of sodium naphthalenide in tetrahydropyran in the presence and absence of tetraglyme (20). The relevant spectra are shown in Figure 2. The large splitting constant,  $a_{\text{Na}} = 1.2$  gauss, seen in the spectrum observed in the absence of tetraglyme (Figure 2a) is replaced by the small splitting constant,  $a_{\text{Na}} = 0.4$  gauss (Figure 2b), when tetraglyme was added to the investigated solution.

The above change of spectrum was noted when the concentration of tetraglyme was about 0.2M. Under these conditions *all* the “ordinary” sodium naphthalenide pairs,  $\text{Na}^+\text{N}\cdot^-$ , were converted into “glymated” pairs,  $\text{Na}^+\text{G}\cdot\text{N}\cdot^-$ . When the concentration of tetraglyme is sufficiently low—*e.g.*, 0.006M, only a fraction of the “ordinary” pairs become solvated by glyme, and then both sets of hyperfine lines appear in the spectrum. This is seen in Figure 3.

Spectra shown in Figure 3 may be obtained at various glyme concentrations. Their examination permits us to determine the stoichiometry and the equilibrium constant of the reaction: “ordinary”  $\text{Na}^+\text{N}\cdot^-$  (*i.e.*, surrounded by THP molecules) + glyme  $\overset{k_1}{\rightleftharpoons} \overset{k_{-1}}{\text{“glymated”}} \text{Na}^+\text{N}\cdot^-$ . Thus, it was found (20) that only one molecule of glyme participates in the solvation, and the equilibrium constant of the solvation was determined to be about  $200M^{-1}$  at 25°C. The broadening of the lines observed in



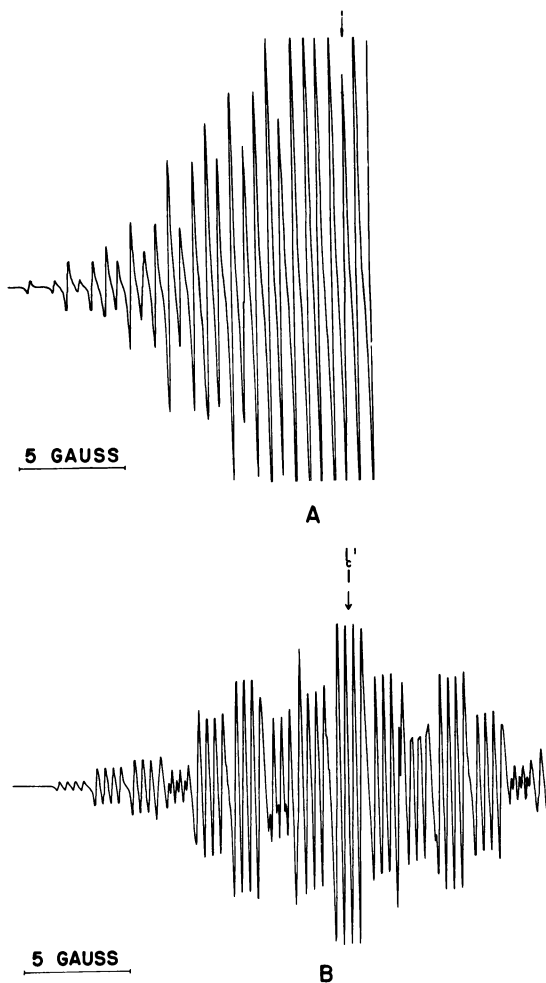


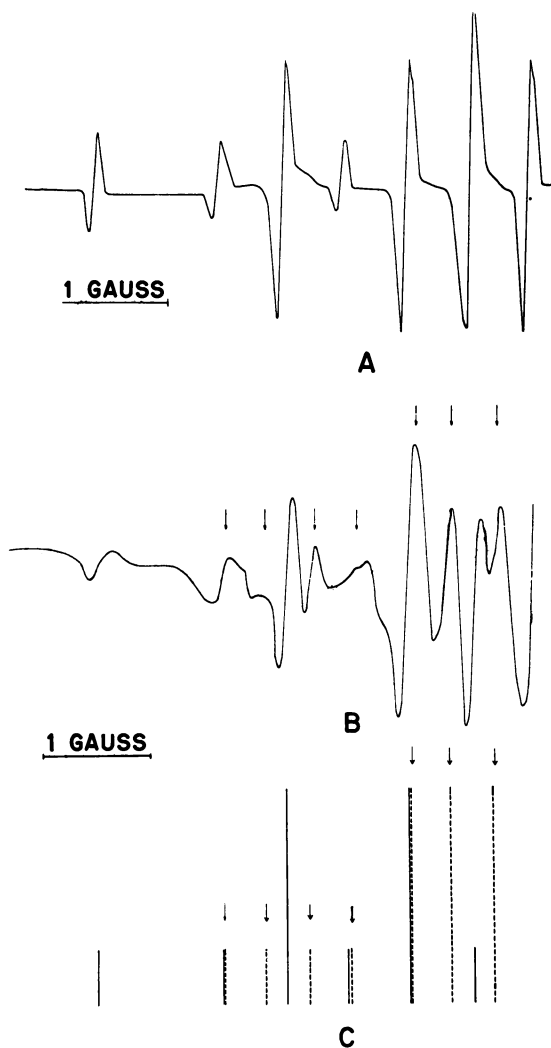
Figure 2. ESR spectra of sodium naphthalenide

A: In tetrahydropyran—tight pair,  $a_{Na} = 1.2$  gauss

B: On addition of 0.2M tetraglyme—loose pair  
 $a_{Na} = 0.4$  gauss

the spectrum allows us to calculate the rate constants of “glymation” ( $k_1$ ) and of the collapse of a “glymated” pair into an “ordinary”  $Na^+, N^-$  ( $k_{-1}$ ). The former was found to be about  $10^7 M^{-1} \text{ sec}^{-1}$  and the latter about  $10^5 \text{ sec}^{-1}$ .

The simultaneous presence of two types of ion pairs was revealed in the above discussed investigation by the two sets of hyperfine lines appearing in the ESR spectrum. This was possible because interconversion



*Figure 3. Low field wing of ESR spectrum of  $\text{Na}^+\text{N}^{\cdot-}$  in THP at 27°C.*

*a: In the absence of glyme*

*b: In the presence of 0.006M tetraglyme*

*c: Stick model showing both types of ion pairs.*

*Tight pairs, full lines; loose pairs, dotted lines*

is relatively slow in this system. However, when interconversion of the different types of ion pairs is fast, only one set of lines is seen in the investigated spectrum, its relevant  $a_{\text{Na}}$  being the average of  $a_{\text{Na}}$ 's of the two interconverting pairs. For example, in a relatively good solvent an equi-

librium may be established between pairs in which the ions are in close contact and therefore interact only weakly with the surrounding solvent (owing to the weak  $A^+B^-$  dipole moment) and those separated by solvent and strongly interacting with its molecules (17, 38) (the  $A^+B^-$  dipole moment is then large). We refer to the first type of ion pairs as the tight ones and to the other as the loose ones. The two types are in equilibrium, and if  $(1 - f)$  and  $f$ , respectively, denote the fractions present in each form, the equilibrium constant  $K_{\text{sep}}$ , is given by the ratio  $f/(1 - f)$ . The latter increases at lower temperatures because the process of ion separation is exothermic (21, 34). Thus, if  $a_1$  and  $a_2$  are the respective counterion splitting constants of such pairs the observed splitting constant,  $a_{\text{obs}}$ , should be

$$a_{\text{obs}} = (1 - f)a_1 + fa_2$$

whenever the interconversion is fast. It is plausible that  $a_1 \gg a_2$  and, therefore,  $a_{\text{obs}}$  is expected to decrease with decreasing temperature. The equilibrium constant,  $K_{\text{sep}}$ , could be determined at each temperature if  $a_1$  and  $a_2$  are known and are temperature independent. It is possible that the last condition is valid, at least approximately, in some systems although in principle the individual  $a$ 's are temperature dependent.

The above treatment was applied successfully by Hirota and his students (18, 19) in their studies of ion pairs in several solvents. Thus, they determined the equilibrium constants and heats of conversion of ion pairs involving various alkali metals and also investigated the kinetics of their inter-conversions.

Although the ESR studies of ion pairs give the most detailed information about such systems and provide valuable data about the thermodynamics, as well as about kinetics of the interconversion, other methods of investigations are also important. An interesting spectrophotometric technique was developed in our laboratory by Smid and Hogen-Esch (21). Their work led to the understanding of various factors which affect the ability of ethereal solvents to interact with alkali ions of fluorenyl salts.

The review presented above compels us to accept the idea of various types of ion pairs which may contribute to reactivity. For example, the propagation of  $\sim S^-, Na^+$  in tetrahydrofuran seems to involve the loose  $\sim S^-, (THF)_n, Na^+$  ion pairs which, probably, are many times more reactive than the "ordinary" tight ion pairs. Because the proportion of the former increases at lower temperatures, the rate of propagation could be enhanced by cooling the polymerizing solution. This is indeed the case (26), and the relevant Arrhenius plot of  $\log k_{\pm}$  vs.  $1/T$  is shown in Figure 4. The negative "activation energy" implies that the heat of conversion of the unreactive tight ion pairs into the reactive loose ones is

greater than the genuine activation energy of propagation of the loose  $\sim S^-(THF)_nNa^+$  pairs.

Lowering the temperature increases the fraction of the more reactive pairs, and this may more than balance the retarding effect of activation energy and lead to the apparent "negative" activation energy. The gain is voided, however, when the conversion of contact pairs into solvent-separated pairs is high, and then  $E_{\pm}$  becomes positive although  $-\Delta H_s$  is still greater than  $E_s$ . This behavior is observed in the polymerization of  $\sim S^-, Na^+$  performed in dimethoxyethane (27). Owing to the bidentate nature of this solvent, the fraction of loose, solvent-separated pairs present in this system is much larger than in tetrahydrofuran. Consequently, the observed  $k_{\pm}$  is substantially higher—e.g.,  $3600M^{-1} \text{ sec}^{-1}$  at  $25^{\circ}\text{C}$ . compared with  $80M^{-1} \text{ sec}^{-1}$  found in tetrahydrofuran. Therefore, the relevant Arrhenius line passes through a maximum (see Figure 4) at an accessible temperature (actually at  $0^{\circ}\text{C}$ .).

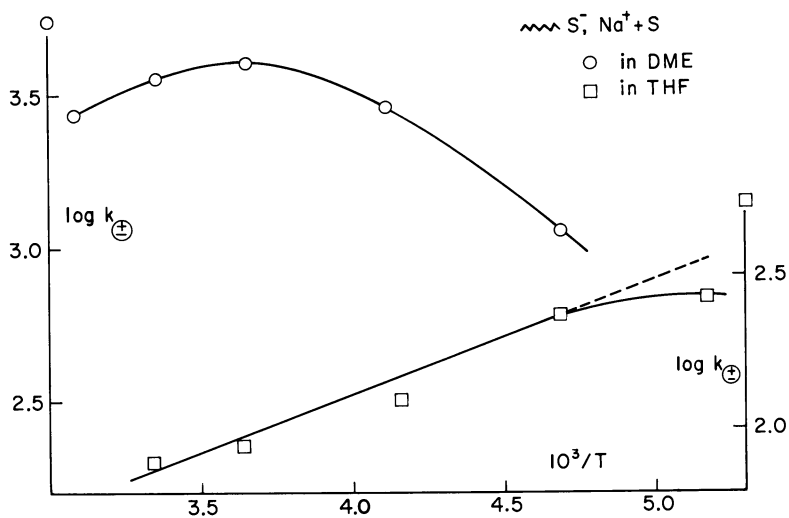
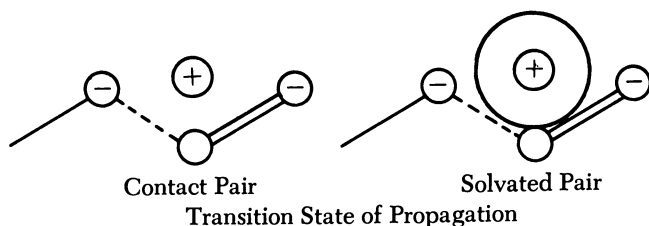


Figure 4. Arrhenius plot of the propagation constant,  $k_{\pm}$ , of sodium polystyryl polymerization in THF (lower curve) and in dimethoxyethane (upper curve). Note the negative "activation energy" (the lower curve) and the maximum in the upper curve

Why is a loose, solvent-separated pair more reactive than a tight contact pair? A contact pair involves a small, bare cation which becomes partially dissociated in the transition state as shown in the following diagram. This hinders the propagation. The partial dissociation may be unnecessary for the separated pair because the cation is large (owing to its solvation).



Furthermore, the latter reaction may involve a "push-pull" mechanism which could make the separated ion pair more reactive even than the free ion. It seems, indeed, that  $E_s < E_.$ , but the entropy of activation is more negative for the separated ion pair than for the free  $\sim S^-$  ion.

Change in the structure of ion pair may have an enormous effect upon its reactivity. The  $\sim S^-, Na^+$  tight ion pairs propagate with a rate constant which is not greater than  $15M^{-1} \text{ sec.}^{-1}$  at  $25^\circ\text{C}$ . Thus, the  $k_{\pm}$  of the tight pairs was found to be  $3-6M^{-1} \text{ sec.}^{-1}$  in dioxane, about 10-12 in tetrahydropyran, and its value is probably similar in tetrahydrofuran. At the same temperature the very loose pairs formed in tetrahydrofuran or dimethoxyethane (often referred to as solvent-separated pairs) propagate with rate constant  $20,000-30,000M^{-1} \text{ sec.}^{-1}$ —i.e., they are only slightly less active than the free  $\sim S^-$  ions (26, 27). Recent studies (28) of  $\sim S^-, Na^+$  polymerization in tetrahydropyran in the presence of tetraglyme showed that the  $\sim S^-, \text{glyme}, Na^+$  pairs propagate with rate constant of about  $4000M^{-1} \text{ sec.}^{-1}$  (at  $25^\circ\text{C}$ .). In fact, the addition of tetraglyme has a dramatic effect on the rate of polymerization (29) as shown in Figure 5. The 100-fold increase in the rate of propagation arising from the addition of only  $3.10^{-3}M$  tetraglyme is caused by two factors: (1) the conversion of the ordinary tight  $\sim S^-, Na^+$  into the reactive "glymated" pair, and (2) the increase in the fraction of free  $\sim S^-$  ions arising from the conversion of the free  $Na^+$  ions surrounded by THP into "glymated"  $Na^+$  ions. The mathematical treatment of this problem and its experimental verification is outlined in Ref. 29.

The solvation of ion pairs may also arise from intramolecular interaction. For example, the high reactivity of living poly(2-vinylpyridine) is probably caused by the intramolecular solvation of the  $Na^+$  ion by the adjacent pyridine rings (16, 23, 32). Interesting example of such a solvation has been discovered by Smets and van Beylen (30), who studied anionic polymerization of *p*- and *o*-methoxystyrene. The ion pair of the latter living polymer, but not of the former, showed exceptional reactivity, and the model reveals that only the *o*-methoxy group can participate in the intramolecular solvation.

Solvation also has an important effect upon the stereochemistry of the propagation. Extensive studies of this subject by Fox, Glusker, and

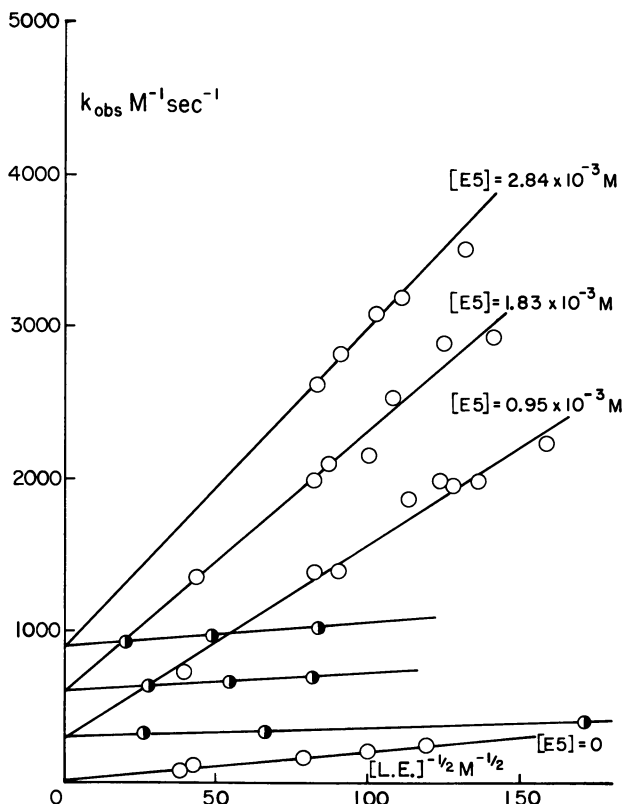


Figure 5. Propagation constant  $k_{obs}$  of sodium polystyryl propagation in tetrahydrofuran in the presence of various amounts of tetraglyme. Half-shaded points, in the presence of  $\text{Na}^+, \text{BPh}_4^-$

their co-workers, as well as the recent studies by Schuerch, Bovey, and their associates have been reviewed by this writer (33).

Finally, one should realize that higher agglomerates than ion pairs may exist in the polymerizing systems. These species are particularly abundant in systems involving  $\text{Li}^+$  counterions. A comprehensive and authoritative review of this subject was presented by Bywater (10), and some additional material was reviewed by this writer (29). Polymers possessing two growing ends may form intramolecular triple ions (8, 35). This phenomenon leads to the dependence of the reactivity of living polymers on their degree of polymerization.

The existence of different types of growing ends makes the ionic polymerization more complex than the radical polymerization. Studies of these systems are therefore fascinating, and the results are valuable

because they shed much light upon the mechanisms of other ionic reactions observed in organic chemistry.

### *Acknowledgment*

The support of this work by the National Science Foundation is gratefully acknowledged.

### *Literature Cited*

- (1) Adam, F. C., Weissman, S. I., *J. Am. Chem. Soc.* **80**, 1518 (1958).
- (2) Atherton, N. M., Weissman, S. I., *J. Am. Chem. Soc.* **83**, 1330 (1961).
- (3) Barnikol, W. K. R., Schulz, G. V., *Makromol. Chem.* **68**, 211 (1963).
- (4) *Ibid.*, **86**, 298 (1965).
- (5) Bhattacharyya, D. N., Lee, C. L., Smid, J., Szwarc, M., *Polymer* **5**, 54 (1964).
- (6) Bhattacharyya, D. N., Lee, C. L., Smid, J., Szwarc, M., *J. Phys. Chem.* **69**, 612 (1965).
- (7) Bhattacharyya, D. N., Smid, J., Szwarc, M., *J. Phys. Chem.* **69**, 624 (1965).
- (8) Bhattacharyya, D. N., Smid, J., Szwarc, M., *J. Am. Chem. Soc.* **86**, 5024 (1964).
- (9) Böhm, L., Barnikol, W. K. R., Schulz, G. V., *Makromol. Chem.* **110**, 222 (1967).
- (10) Bywater, S., *Advan. Polymer Sci.* **4**, 66 (1965).
- (11) Comyn, J., Dainton, F. S., Harpell, G. A., Hui, K. M., Ivin, K. J., *J. Polymer Sci. Pt. B* **5**, 965 (1967).
- (12) Dainton, F. S., East, G. C., Harpell, G. A., Hurworth, N. R., Ivin, K. J., LaFlair, R. T., Pallen, R. H., Hui, K. M., *Makromol. Chem.* **89**, 257 (1965).
- (13) Dainton, F. S., Hui, K. H., Ivin, K. J., private communication.
- (14) Fisher, M., Smid, J., Szwarc, M., to be published.
- (15) Fisher, M., van Beylen, M., Smid, J., Szwarc, M., to be published.
- (16) Fisher, M., Szwarc, M., to be published.
- (17) Grunwald, E., *Anal. Chem.* **26**, 1696 (1954).
- (18) Hirota, N., *J. Am. Chem. Soc.* **90**, 3603 (1968).
- (19) Hirota, N., Carraway, R., Schook, W., *J. Am. Chem. Soc.* **90**, 3611 (1968).
- (20) Höfelmann, K., Jaguar-Grodzinski, J., Szwarc, M., *J. Am. Chem. Soc.* **91**, 4645 (1969).
- (21) Hogen-Esch, T. E., Smid, J., *J. Am. Chem. Soc.* **88**, 307 (1966).
- (22) Ivin, K. J., unpublished data.
- (23) Lee, C. L., Smid, J., Szwarc, M., *Trans. Faraday Soc.* **59**, 1192 (1963).
- (24) Potter, R. C., Bretton, R. H., Metz, D. J., Johnson, C. L., *J. Polymer Sci. Pt. A-1* **4**, 419 (1966).
- (25) Roovers, J. E. L., Bywater, S., *Trans. Faraday Soc.* **62**, 701 (1966).
- (26) Shimomura, T., Tölle, K. J., Smid, J., Szwarc, M., *J. Am. Chem. Soc.* **89**, 796 (1967).
- (27) Shimomura, T., Smid, J., Szwarc, M., *J. Am. Chem. Soc.* **89**, 5743 (1967).
- (28) Shinohara, M., Smid, J., Szwarc, M., *Chem. Commun.* in press.
- (29) Shinohara, M., Smid, J., Szwarc, M., *J. Am. Chem. Soc.* **90**, 2175 (1968).
- (30) Smets, G., van Beylen, M., private communication.

- (31) Szwarc, M., "Carbanions, Living Polymers and Electron Transfer Processes," Chap. VII, Interscience, 1968.
- (32) *Ibid.*, pp. 455-456, 544-546.
- (33) *Ibid.*, pp. 426-472.
- (34) Szwarc, M., *Accounts Chem. Res.* **2**, 87 (1969).
- (35) Tardi, M., Rouge, D., Sigwalt, P., *European Polymer J.* **3**, 85 (1967).
- (36) van Beylen, M., Bhattacharyya, D. N., Smid, J., Szwarc, M., *J. Phys. Chem.* **70**, 157 (1966).
- (37) Williams, F., Okamura, S. *et al.*, *Trans. Faraday Soc.* **63**, 1478, 1501 (1967).
- (38) Winstein, S., Clippinger, E., Fainberg, A. H., Robinson, G. C., *J. Am. Chem. Soc.* **76**, 2597 (1954).
- (39) Worsfold, D. J., Bywater, S., *J. Phys. Chem.* **70**, 162 (1966).
- (40) Worsfold, D. J., Bywater, S., *Can. J. Chem.* **36**, 1141 (1958).

RECEIVED March 12, 1968.



# Multistate Stereospecific Polymerization Mechanism

## Structure of Metallyls and Their Activity in Diene Polymerization

V. N. SOKOLOV and I. Y. PODDUBNY

S. V. Lebedev Synthetic Rubber Research Institute, Leningrad, USSR

*The structure and chemical properties of metal-allyl compounds ( $\pi$ -allylic, "dynamic" and  $\sigma$ -allylic) which can be considered as models of a living polymer chain in butadiene polymerization have been studied. The polymerization of dienes proceeds only in "dynamic" allylic systems through the metal-ligand  $\pi$ -bond in  $\pi$ -,  $\sigma$ -isomers.*

Since the discovery of Ziegler-Natta catalysts, the efforts of many scientists have been directed toward elucidating the mechanism of stereospecific polymerization. As a result of extensive investigations during the last decade a theory of stereospecific polymerization has been proposed. Some authors (2, 11, 16) suggest that  $\pi$ -complexes participate in polymerization. However, since not all results can be explained using the proposed hypotheses, further investigations seem worthwhile.

It is generally accepted that the most valuable information on polymerization mechanism can be obtained by studying the polymer chain unit adjacent to a catalyst active site since the latter determines the structure of polymer chain formed.

For diene hydrocarbons such a unit is represented by:



Since spectroscopic investigations of such a structure in real polymer chains present difficulties owing to the low concentration of the unit in the polymer (even for low molecular weight polymers), model compounds have been used widely in polymerization studies.

In our studies an attempt was made to obtain detailed information on the mechanism of stereospecific diene polymerization initiated by several catalyst systems. To this end the structure and some chemical reactions of compounds used as models of the system "catalyst-growing polymer chain" were studied in detail.

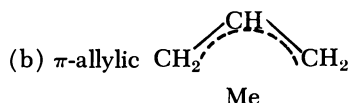
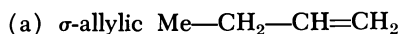
### *Structure and Reactions of Model Catalyst Systems*

For organometallic compounds the catalyst-growing polymer chain system can be represented as



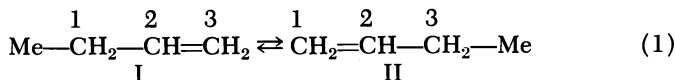
Various possible configurations of such a system may be represented by corresponding model metal allylic compounds.

According to data reported in the literature at least three types of metal allylic compounds are usually distinguished:



in which the electron density is distributed uniformly among three carbon atoms, and:

(c) "dynamic" allylic



in which the protons of all methylene groups become capable of free rotation about the metal-carbon bond as a result of rapid exchange between I and II.

It seemed reasonable to investigate some physical and chemical properties as well as the catalytic activity of all types of metal allylic compounds, and hence we chose compounds for our investigations.

Butenyllithium and butenylmagnesium chloride were used as "dynamic" allylic compounds. The former was selected because of the ability of lithium catalysts to provide high rates of diene polymerization and to give stereoregular polymers; the latter was selected for its availability and simplicity of synthesis.

**Experimental.** Butenylmagnesium chloride was prepared from crotyl chloride and magnesium chips in ether. Decomposition reactions of butenylmagnesium chloride were carried out at room temperature using  $H_2O$  and  $D_2O$ . Butenes were condensed at  $-20^\circ C$ . and analyzed on a FB-4 Shandon ionization chromatograph.

The NMR spectra were measured with JEOL spectrometer JNM-3H-60. Low temperatures were obtained with the variable Dewar inserts. Tetramethylsilane (TMS) was used as an internal standard. The solutions were degassed before use, and tubes were sealed under argon.

Crotyllithium was synthesized from tetracrotyltin and butyllithium in pentane and purified by reprecipitation from dimethyl ether with the help of pentane (17).

Bis( $\pi$ -crotylpalladium chloride) was prepared by the reaction of palladium chloride solution in 50% acetic acid with crotyl chloride at  $+30^\circ\text{C}$ . (19).

The specific electrical conductivity of the solutions was measured in a cell with plane-parallel electrodes, the cell constant being  $6.5 \times 10^{-2} \text{ cm}^{-1}$ . In all cases the specific electrical conductivity was low ( $1 \times 10^{-9} \text{ ohm}^{-1} \text{ cm}^{-1}$ ); hence, it was possible to neglect polarization on electrodes and to use direct current.

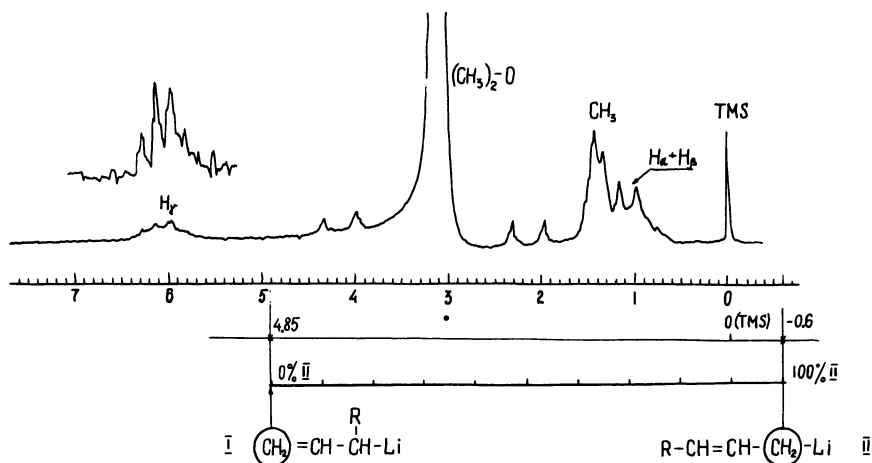
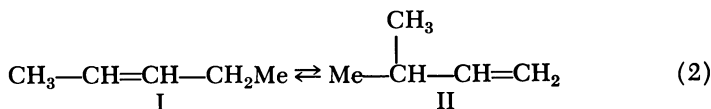


Figure 1. NMR spectrum of  $\text{C}_4\text{H}_7\text{Li}$  in dimethyl ether at  $20^\circ\text{C}$ . and scale for estimating the tautomer ratio by  $\text{CH}_2$  group chemical shift

**Results.** As the data in the literature show, the NMR spectrum of allyl magnesium bromide in ether solution (15) can be interpreted most easily by assuming that a rapid exchange of two isomeric forms occurs. The rate of this exchange is very high, and at  $-80^\circ\text{C}$ . it is more than 1000 times per second.

Similar to allylmagnesium bromide the NMR spectrum of butenylmagnesium bromide can be interpreted on the basis of rapid exchange between two isomers (14, 21)



Our NMR spectrum of butenyllithium in dimethyl ether (Figure 1) is similar to the spectrum given in Ref. 7; this spectrum and the spectrum of butenylmagnesium chloride are considered typical for such compounds.

The position of the methylene group in both spectra is significantly different from that in the spectra of the corresponding metal alkyl compounds and could be considered generally as a measure of the isomer ratio. For rapid exchange between two tautomeric forms, whose spectra are known, the ratio of the tautomeric forms could be calculated by using the additivity of CH<sub>2</sub> group chemical shift.

$$\tau_{\text{CH}_2} = \tau_{\text{I}}P_{\text{I}} + \tau_{\text{II}}P_{\text{II}} \quad (3)$$

where P<sub>I</sub> and P<sub>II</sub> are the portion of I and II isomers,  $\tau_{\text{I}}$  and  $\tau_{\text{II}}$  are the chemical shifts of CH<sub>2</sub> group in I and II isomers.

With butenylmagnesium chloride and butenyllithium attempts to obtain spectra of each isomer failed. Hence, an approximate method was

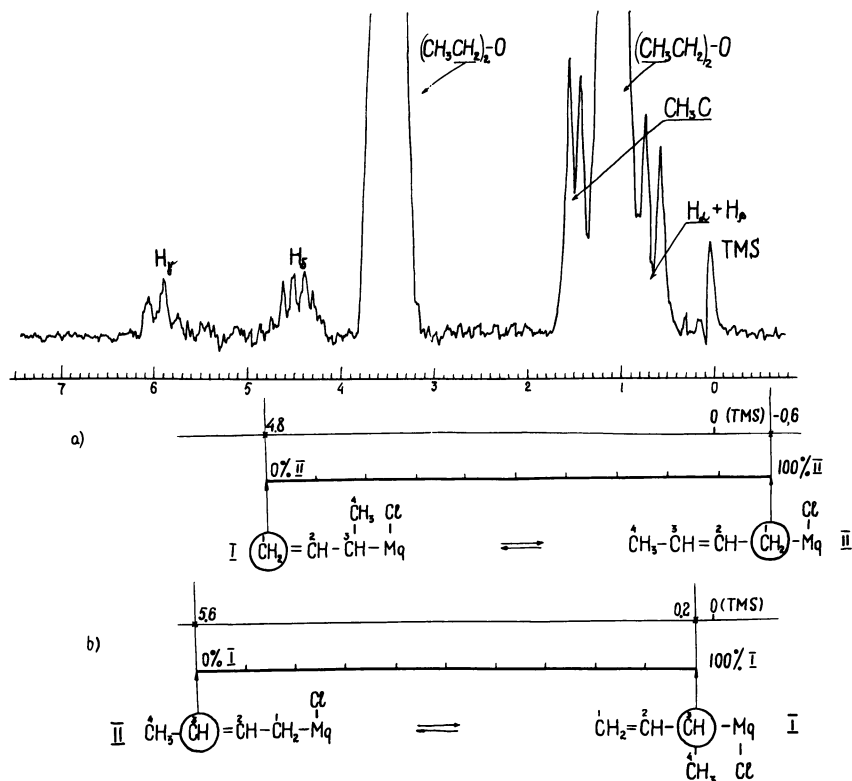


Figure 2. NMR spectrum of  $\text{C}_4\text{H}_7\text{MgCl}$  in diethyl ether at  $20^\circ\text{C}$ . and scale for estimating the tautomer ratio by  $\text{CH}_2$  and  $\text{CH}$  group chemical shift

used to estimate the ratio of the two dynamic isomers. This method uses known chemical shifts of CH<sub>2</sub> group as extreme points, and the isomer ratio is estimated by the CH<sub>2</sub> group position on the scale (Figure 2).

It is obvious that the protons of methylene group occupy two positions—one accounting for the metal, the other being the vinyl methylene group (Isomer II).

As a model compound for Isomer II the CH<sub>2</sub> group of stable (undergoing no exchange) Me-allylic compounds (such as Sn(C<sub>3</sub>H<sub>5</sub>)<sub>4</sub>,  $\tau_{\text{CH}_2} = 4.85$ ) can be used, corresponding Me-alkyl compounds (such as butylmagnesium halide,  $\tau_{\text{CH}_2} = -0.6$ ) as model compounds for Isomer I.

Certainly, CH<sub>2</sub> group chemical shift values of model compounds cannot correspond exactly to those of allylic compounds, and there will be some error in the estimated ratios.

A similar scale can be designed for the  $\tau_{\text{CH}}$  group. The tautomeric ratio scale for lithium designed this way is represented in Figure 1.

It follows from Figure 1 that  $K_e = 65/35$  for butenyllithium in dimethyl ether. From Figure 2 it is seen that for C<sub>4</sub>H<sub>7</sub>MgCl in ether a I:II ratio = 3:1. From the temperature dependence of the NMR spectrum of C<sub>4</sub>H<sub>7</sub>MgCl in solution it has been found that the position of CH<sub>2</sub> and CH groups changes slightly but regularly with temperature. Corresponding  $K_e$  values obtained at various temperatures are given in Figure 3; for the two isomers  $\Delta E = 660$  cal./mole.

Hydrolysis products studied by NMR spectroscopy and gas chromatography (Table I) showed 1-butene to be the main decomposition

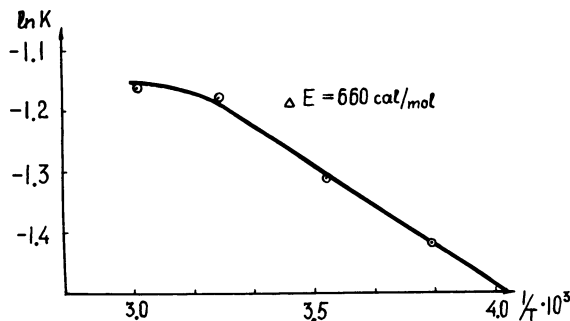


Figure 3. Temperature dependence of equilibrium constants of two C<sub>4</sub>H<sub>7</sub>MgCl forms in diethyl ether

product. The  $\alpha$ - to  $\beta$ -butene ratio was determined from NMR spectrum as the ratio of intensities of the A to B regions (Figure 4A)

$$\frac{\alpha\text{-butenes}}{\beta\text{-butenes}} = \frac{B/2}{A/6} \quad (4)$$

**Table I. Structure of Metal-Crotyl Complexes and Composition of Their Hydrolysis Products<sup>a</sup>**

Complex	Solvent	Composition of Hydrolysis Products				
		I : II Isomer Ratio		NMR		
		I	II	1-Butene	2 Butene	
				cis, %	trans, %	
C <sub>4</sub> H <sub>7</sub> MgCl	Et <sub>2</sub> O	75	25	72	16	12
C <sub>4</sub> H <sub>7</sub> Li	C <sub>6</sub> H <sub>6</sub> + (CH <sub>3</sub> ) <sub>2</sub> O	65	35	60	18	22
C <sub>4</sub> H <sub>7</sub> PdCl	DMSO	34	66	40	45	15

<sup>a</sup> Hydrolysis temperatures: 20°C. for C<sub>4</sub>H<sub>7</sub>MgCl and C<sub>4</sub>H<sub>7</sub>Li; 100°C. for C<sub>4</sub>H<sub>7</sub>PdCl.

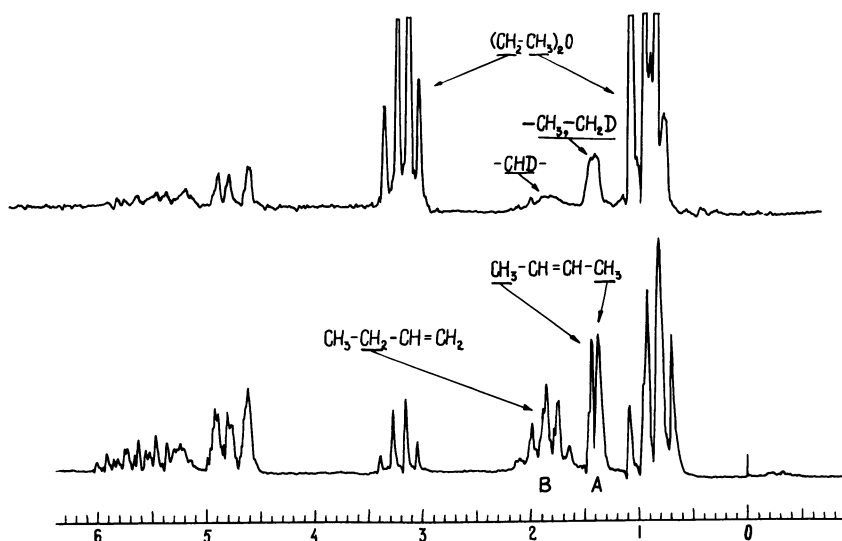


Figure 4. NMR spectrum of hydrolysis (A) and deuterolysis (B) products of C<sub>4</sub>H<sub>7</sub>MgCl in diethyl ether at 20°C.

Deuterolysis results in the same ratio. Simple calculation (from Spectrum 4B) shows that deuterium addition occurs in the  $\gamma$ -position of the metal atom.

The electrical conductivity of C<sub>4</sub>H<sub>7</sub>Li · (CH<sub>3</sub>)<sub>2</sub>O in toluene increased with temperature (Figure 5) up to 100°–110°C. and then decreased. The increase in electrical conductivity is higher than could be expected from a change in ion mobility owing to a temperature increase. Hence, the phenomena should be attributed to some other process (discussed below).

Electrical conductivity increased sharply on adding butadiene (Figure 10) and then decreased to its original level; further addition of butadiene resulted in the same effect.

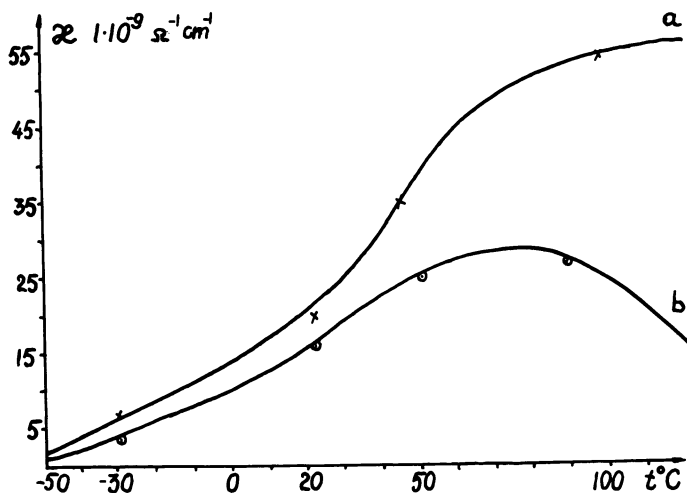


Figure 5. Temperature dependence of electrical conductivity of  $C_4H_7Li \cdot (CH_3)_2O$  in toluene

- (a) 0.25 mole/liter  
(b) 0.1 mole/liter

Some typical  $\pi$ -allylic compounds— $\pi$ -allyl- and  $\pi$ -crotylpalladium halides—have been investigated. In nonpolar and slightly polar solvents at room temperature their electron density is uniformly (or nearly uniformly) distributed among three carbon atoms. According to x-ray spectroscopy data the same structure is observed in the crystalline state (22).

The NMR spectra (Figure 6) of these compounds under normal conditions are also characteristic of compounds of this group.

The solutions are nonconducting, and the compounds display no tendency to undergo chemical reactions (hydrolysis, polymerization, etc.). However, as shown later, heating these compounds in the presence of donor reagents causes significant changes in most of their properties (NMR spectra, chemical activity, electrical conductivity, etc.), thus making them similar in properties to the typical "dynamic" allylic compounds.

The spectrum of crotylpalladium chloride in  $CDCl_3$  solution containing dimethyl sulfoxide (Figure 6) displays a transition to the dynamic structure at room temperature; this transition appears to be completed at  $110^\circ C$ .

The equilibrium constant ( $K_e$ ) at elevated temperature can be estimated using NMR spectrum. However, the scale to estimate  $K_e$  cannot be designed in the way previously mentioned since the spectrum of alkyl palladium is unavailable.

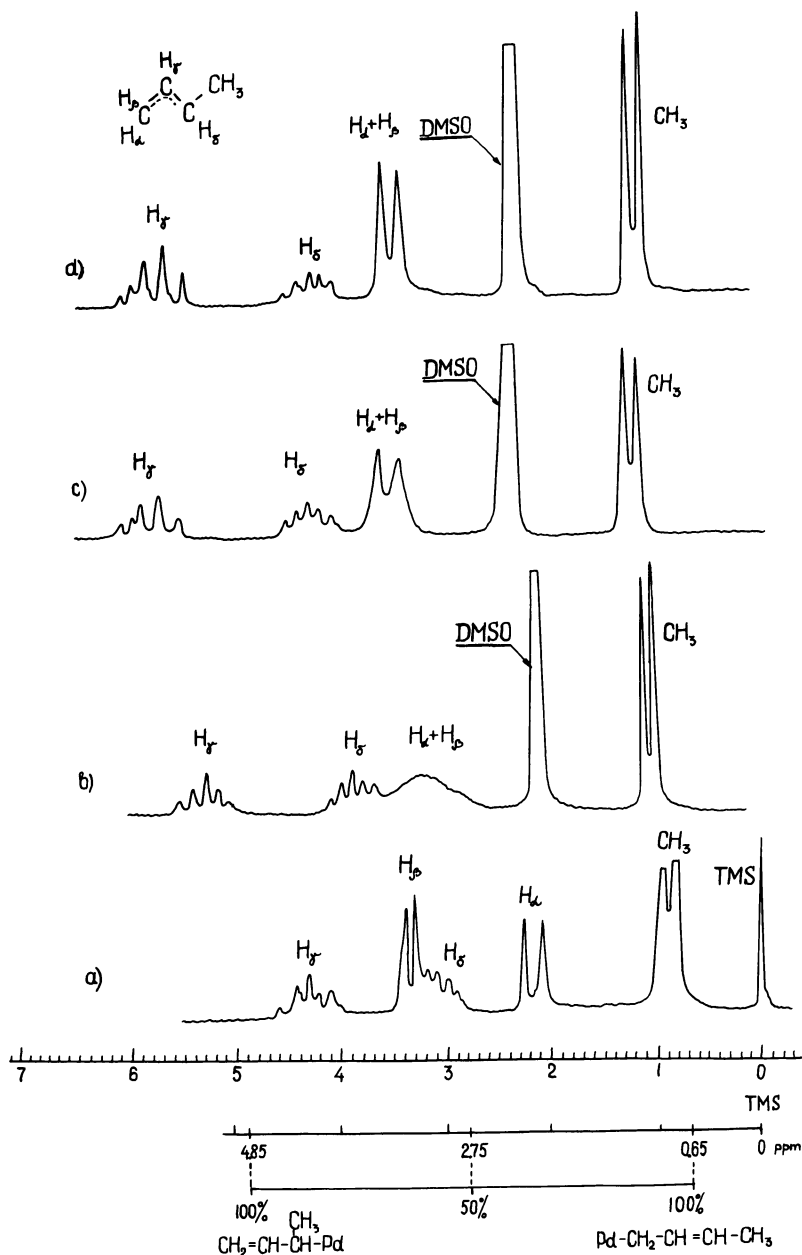


Figure 6. NMR spectra of:

(a)  $(C_4H_7PdCl)_2$  in benzene at 20°C.

(b)  $C_4H_7PdCl \cdot DMSO$  in  $CDCl_3$ , 20°C.

(c) Same at 80°C.

(d) Same at 110°C.

$[C_4H_7PdCl_2] = 0.1 \text{ mole/liter}$



In this case  $\tau = 4.85$  corresponds to 100% (II);  $\tau = 2.75$  (half the distance between two doublets of  $\pi$ -allylic groups in nonpolar solvents) corresponds to I:II = 50:50.

The electrical conductivity of butenylpalladium chloride solutions, which is low at low temperatures even in the presence of donor reagents, increases as the transition of the NMR spectrum of the  $\pi$ -allylic type occurs to the "dynamic" type (Figure 7).

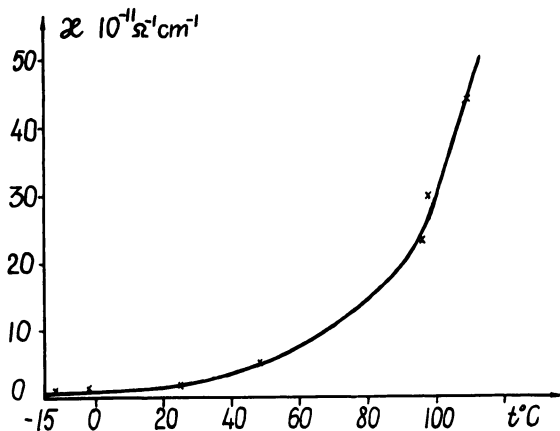


Figure 7. Temperature dependence of electrical conductivity of  $C_4H_7PdCl \cdot DMSO$  in toluene

Addition of butadiene to  $\pi$ -allylic type structure solutions does not change the electrical conductivity whereas with "dynamic" type structure solution a stepwise change takes place.

Similarly,  $\pi$ -allylic structure solutions show no tendency toward hydrolysis unlike dynamic structures which hydrolyze readily.

For  $C_4H_7PdCl \cdot DMSO$  the main product of hydrolysis at 100°C. proved to be 2-butene (Table I).

Typical  $\sigma$ -allylic compounds are tetraallyl- and tetrabutenyln. Their chemical properties differ strongly from the analogous properties of "dynamic" allylic compounds.  $R_4Sn$  possesses low electric conductivity, does not hydrolyze (even at elevated temperatures), and has no catalytic activity towards dienes. The addition of butadiene also does not cause any change in electric conductivity. The NMR spectra of these compounds which differ from the spectra of  $\pi$ -allylic and "dynamic" compounds remain unchanged over the range  $-90^\circ$  to  $180^\circ C$ . (Figure 8).

**Discussion.** It follows from the traditional representation of a dynamic allylic system that the exchange occurs between two  $\sigma$ -allylic isomers, the transformation of one isomer into the other is instantaneous,

the first isomer is necessarily transformed into the second one, and vice-versa. Also, high electric conductivity of the "dynamic" systems is not accounted for at all.

The fact that the transition of the spectrum from a  $\pi$ -allylic to a "dynamic" one is accompanied by a change in the properties of these compounds show that "dynamic" allylic compounds of Li, Mg, and Pd have the same nature.

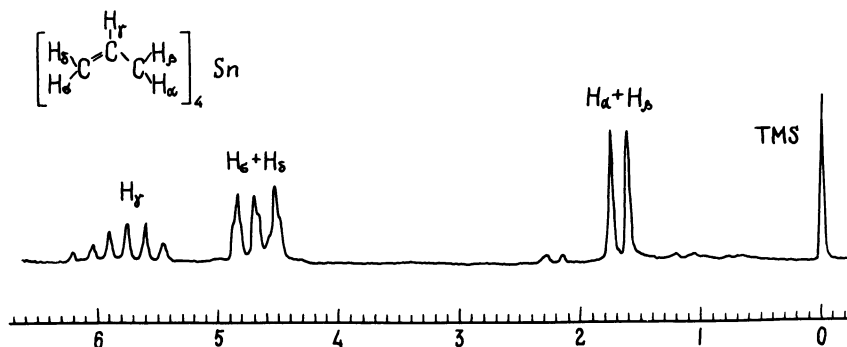
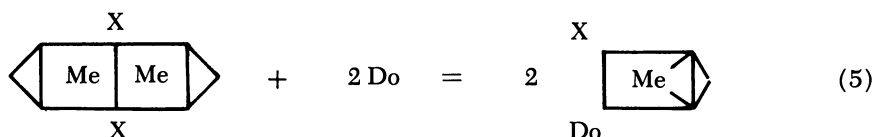


Figure 8. NMR spectrum of  $(\delta\text{-C}_3\text{H}_5)_4\text{Sn}$  in pyridine at  $20^\circ\text{C}$ .

Bis( $\pi$ -allylpalladium chloride) (in which the  $\pi$ -allyl group occupies two coordination sites) reacts with donor reagents:



giving  $\pi$ ,  $\sigma$ -compounds (12).

At elevated temperatures and in the presence of stronger donor reagents the transition of the  $\pi$ -allylic group into a "dynamic" one occurs.

According to Refs. 18, 19, and 20 this involves insertion of one more donor molecule into the coordination sphere of a metal, giving a short lived  $\sigma$ -allylic compound.

Our data show that the changes in the spectrum are accompanied by a change in the number of ions in the system, and hence ionic forms are involved also in the exchange.



If the exchange does not occur (as in the case of static  $\sigma$ -allylic compounds), the electrical conductivity is hardly observed.

If only the excited form participates in the exchange, the only possible mechanism will be an intramolecular one. This contrasts with the experimentally established fact that in organometallic compounds a rapid intermolecular exchange occurs (4, 8, 18).

Being in ionic form the organic anion and metal atom become kinetically independent, resulting in recombination by an intramolecular and intermolecular mechanism (this can easily explain the ligand exchange in organometallic compounds).

Taking into account the above assumptions the energy diagram of the complexes investigated was designed (Figure 9).

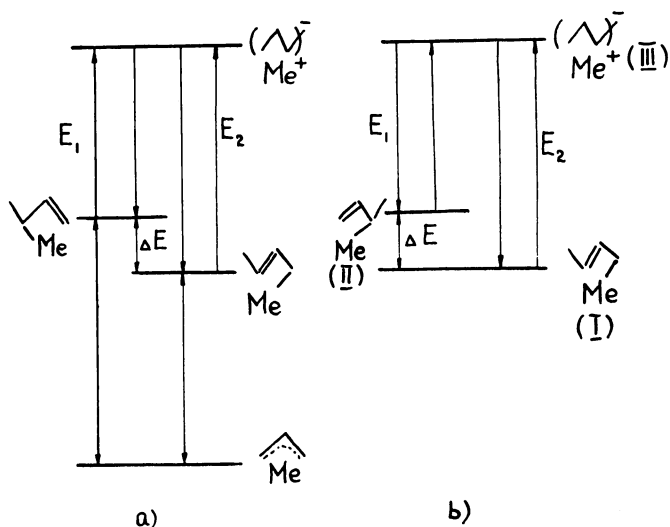
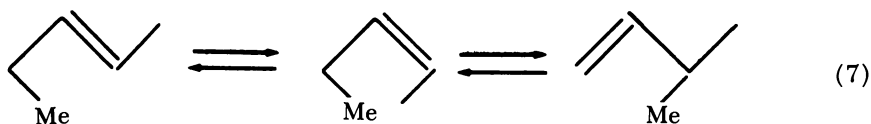


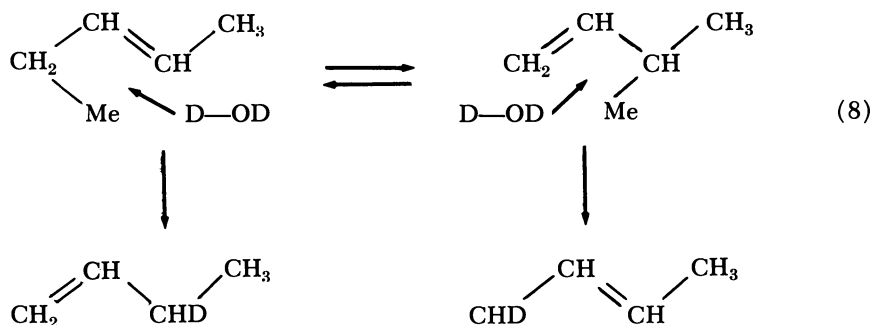
Figure 9. Energy diagram of "dynamic" allylic (b) and  $\pi$ -allylic systems (a)

The "dynamic" allylic system may be represented as resulting from the exchange of  $\pi$ -,  $\sigma$ -isomers (through excited or ionic forms):



With this representation two reaction routes are possible: one through the metal-carbon  $\sigma$ -bond and the other through the  $\pi$ -bond.

The data in Table I can be interpreted unambiguously—*i.e.*, hydrolysis occurs through the metal-ligand  $\pi$ -bond.



Data on the deuterolysis of butenylmagnesium chloride allow us to draw the same conclusions—*i.e.*, the CHD/CH<sub>2</sub>D ratio, determined from the NMR spectra of deuterated butenes, supports the assumption of addition through the  $\pi$ -bond.

**Conclusions.** The following conclusions can be drawn:

(1) Various types of metal allylic compounds differ significantly in their physical and chemical properties. “Dynamic” allylic compounds exhibit the highest chemical activity.

(2)  $\pi$ -Allylic compounds may undergo transition to a “dynamic” form under the influence of certain factors (*e.g.*, donor reagents and temperature), and the chemical properties are changed accordingly.

(3) “Dynamic” allylic compounds are formed as a result of rapid exchange (intra- and intermolecular) between tautomeric  $\pi$ -,  $\sigma$ -forms and an intermediate (ionic) form.

(4) Hydrolysis of “dynamic” allylic compounds proceeds through  $\pi$ -bond with  $\pi$ ,  $\sigma$ -tautomers.

#### *Butadiene Polymerization Initiated by Model Metal-Allylic Compounds*

Metal allylic compounds, whose structure and reactions have been described in the preceding section, were used as catalysts for diene polymerization.

Tetraallyl- and tetrabutenyln (  $\sigma$ -allylic compounds) do not act as initiators of butadiene polymerization even under most favorable conditions (presence of donor additives, elevated temperature). In contrast, butenyllithium, which is considered to be a typical compound of dynamic structure, does initiate polymerization even at temperatures below zero.

$\pi$ -Allyl- and  $\pi$ -crotylpalladium chloride do not react with butadiene under normal conditions. However, as the structure of the compounds undergoes transition to a dynamic one under the influence of donor reagents and increasing temperature, some evidence of a polymerization

reaction is obtained; if the reaction is carried out in the presence of  $C_4H_7PdCl \cdot DMSO$  in benzene at  $70^\circ C.$ , butadiene oligomers are formed slowly.

Polymerization carried out in a cell for electrical conductivity measurement (Figures 9, 10, and 11) showed that addition of monomers to solutions of catalytically active compounds causes a stepwise change in electrical conductivity (20). Since such a change is not observed with inactive forms and compounds ( $\pi$ -allylic and  $\sigma$ -allylic), this effect can be considered indicative of catalytic activity.

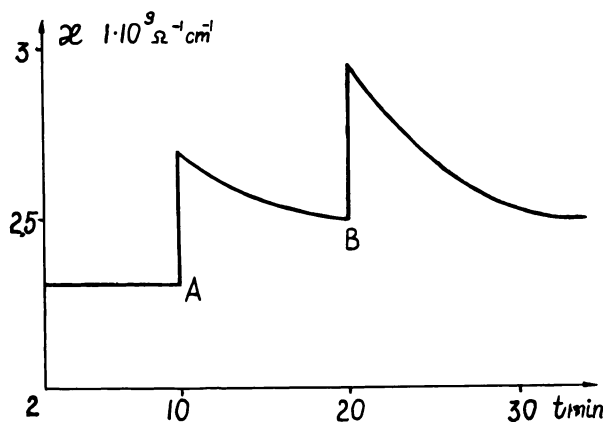
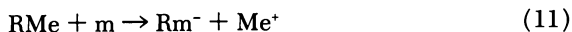


Figure 10. Change in electrical conductivity of  $C_4H_7Li \cdot Met_2O$  toluene solution on butadiene addition at points A and B

Investigation of the effect shows that if initiation and propagation reactions (which in our case coincide) took place in ionic forms, the total amount of ions in solution would remain constant.



For such a mechanism the electrical conductivity should not increase on adding monomer to a catalyst system. An increase can occur if monomer reacts with covalent organometallic forms in such a way that a transition to ionic forms takes place.



The fact that a stepwise change is followed by decrease in electrical conductivity up to its original value (Figures 9 and 10) can be explained

by a recombination of newly formed ions and by a change in their mobility with increasing chain length.



Thus, the ions are not responsible for reactions since they themselves are formed as a result of reactions (including polymerization).

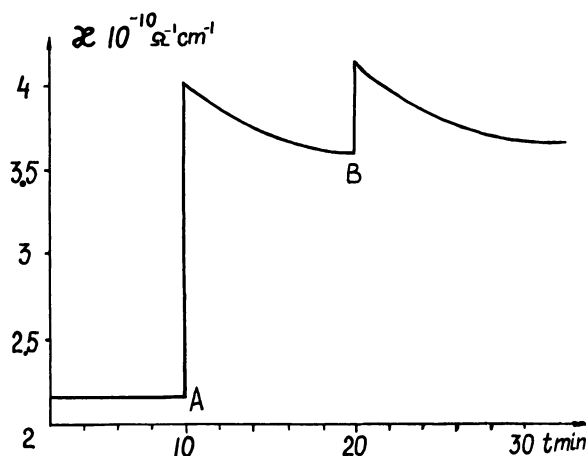
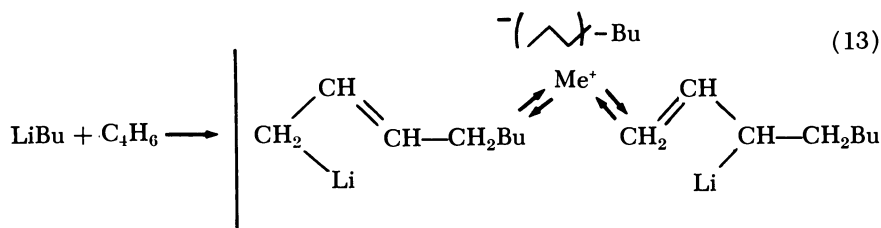


Figure 11. Change in electrical conductivity of  $\text{C}_4\text{H}_7\text{PdCl} \cdot \text{DMSO}$  on butadiene addition (points A and B)

The high rate of diene polymerization initiated by lithium compounds and the availability of much data reported in the literature prompted us to undertake a more detailed investigation. Polymerization was carried out in dimethyl ether in the presence of butyllithium and butenyllithium, with polymerization conditions similar to those used in the investigations of the NMR spectra of butenyllithium.

NMR spectra measurements during butadiene polymerization with BuLi showed that the  $\text{CH}_2$  group line ( $\tau_{\text{CH}_2} = -1.0$ ) disappears at the beginning of reaction, and a new line ( $\tau_{\text{CH}_2} = 1.1$ ) characteristic of the  $\text{CH}_2$  group in  $\text{LiC}_4\text{H}_7$  appears. Chemical shift of this line makes it possible to determine the tautomeric form ratio in a growing polymer chain. The ratio was proved to be I:II = 65:35. Thus, adding the first molecule of monomer to BuLi produces a structure similar to that of the model butenyllithium (the mechanism of the process is not discussed, but it can be treated in the same way as the reaction of chain propagation).



This indicates that the model compound was chosen properly.

As could be expected, the polymer structures obtained with butyllithium and butenyllithium proved to be similar (Table II).

**Table II. Polymerization Results Obtained in the Presence of Butyllithium and Butenyllithium**

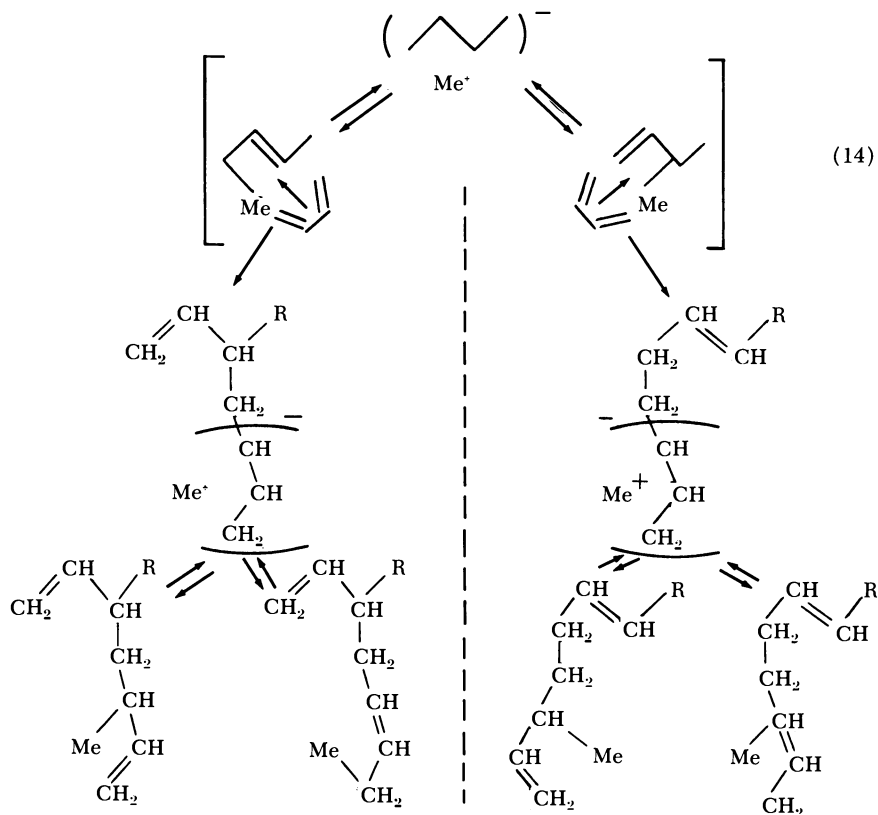
Catalyst	Solvent	Ratio of Tautomers	Polymer
		in the Catalyst, $n_1/n_2$	Structure, 1,2/1,4
LiC <sub>4</sub> H <sub>7</sub>	Met <sub>2</sub> O + C <sub>6</sub> H <sub>6</sub>	65 : 35	70 : 30
		70 : 30	70 : 30
LiBu	Met <sub>2</sub> O + C <sub>6</sub> H <sub>6</sub>	—	70 : 30
		—	70 : 30
C <sub>4</sub> H <sub>7</sub> PdCl	DMSO	34 : 66	35 : 65

The important conclusion from Table II is that the polymer structure—namely, the 1,2- to 1,4- unit ratio is in accordance with the ratio of tautomers in model butenyllithium and C<sub>4</sub>H<sub>7</sub>PdCl. Such a ratio indicates that attack by the monomer as well as hydrolysis (*see* the preceding section) occurs on the metal-carbon  $\pi$ -bond in  $\pi$ ,  $\sigma$ -isomers. In this case the addition of butadiene to the crotyl isomer results in 1,2-units, and its addition to the 2-methyl allylic isomer gives rise to 1,4-units.

The correlation between the data on the electric conductivity of the system in the presence of monomer and those on the relationship between the structures of the catalytic complex and the polymer makes it possible to represent the general polymerization scheme (Reaction 14). In so doing, *cis-trans* isomerism of the polymer chain structure is not dealt with, although the same approach can be applied to this phenomenon as well.

As the scheme shows (Reaction 14), monomer insertion consists of three stages:

(1) Attack by the monomer on the  $\pi$ -bond of the metal-carbon in one of  $\pi$ -,  $\sigma$ -isomers.



(2) Formation of the intermediate complex on a higher energy level at the expense of the monomer energy. The structure of this complex is analogous to its structure in the dynamic system in the absence of the monomer.

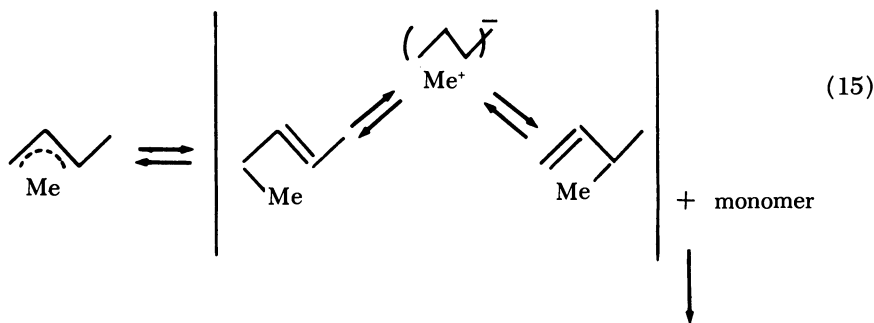
(3) Recombination (intra- or intermolecular) into one of  $\pi$ -,  $\sigma$ -forms in accordance with the probabilities of their existence  $P_1$  and  $P_2$ . In this case the polymer chain length is increased by one unit, and the system returns to its original dynamic state.

Hence, the catalytic complex is not static. In the absence of monomer in the system there exists a process which leads to polymerization on adding the monomer.

As stated above, for compounds having a  $\pi$ -allylic structure, reactions (including polymerization) occur after the compounds are transformed into the dynamic form. Polymerization in the presence of such compounds can be represented by Reaction 15.

It follows from the reversibility of the transition in Reaction 15 (allylic structure to dynamic), which naturally exists during polymeriza-





Polymerization according to Reaction 14

tion, that in this case the kinetic chain termination may proceed by the transition of the catalytic center into the unreactive  $\pi$ -allylic form, in addition to other known ways.

Some years ago Fox and Coleman (5) analyzed a system of two catalytic centers in equilibrium. The polymerization mechanism of such a system existing in several states was referred as a "multistate" one.

It is easy to see that in our case the system exists in several discrete states of one catalytic center, and their ratio affects the polymer chain structure and the polymerization rate.

The mathematical approach followed by the above authors may be applied to our system as well by making due allowance. Therefore, we also use the term "multistate" for the mechanism involved.

### Acknowledgments

This work was done in collaboration with G. M. Khvostik, I. U. Tseretely, E. R. Dolynskaja, G. P. Kondratenko, and N. B. Zaitzev.

### Literature Cited

- (1) Ashby, E. C., Smith, M. B., *J. Am. Chem. Soc.* **86**, 4364 (1964).
- (2) Bagdasarian, A. H., Frolov, V. M., Dolgoplosk, B. A., *Dokl. Akad. Nauk SSSR* **174**, 587 (1967).
- (3) Brown, T. L., Gerteis, B. L., Bafus, D. A., Ladd, S. A., *J. Am. Chem. Soc.* **86**, 2134 (1964).
- (4) Brown, T. L., Ladd, J. A., *J. Organometal. Chem.* **2**, 373 (1964).
- (5) Coleman, B. D., Fox, T. G., *J. Chem. Phys.* **38**, 1065 (1963).
- (6) Cotton, F. A., Faller, J. W., Musco, A., *Inorg. Chem.* **6**, 618 (1966).
- (7) Dolgoplosk, B. A., Vinogradov, P. A., *et al.*, *J. Polymer Sci., Pt. C* **2625** (1967).
- (8) Fraenkel, C., Adams, D., Williams, J., *Tetrahedron Letters* **1963**, 767.
- (9) Hayes, G., *Bull. Soc. Chim. France* **1963**, 1404.
- (10) Huttel, R., Kratzer, I., *Angew. Chem.* **71**, 456 (1959).

- (11) Kormer, V. A., Babickii, B. D., *et al.*, *Intern. Symp. Macromol. Chem., Prague, 1965, Preprint*, p. 413.
- (12) Mason, R., Russel, D., *Chem. Commun.* **1**, 26 (1966).
- (13) Mojseev, I. I., Fedorovskaja, E. A., Syrkin, Ya. I., *Zh. Neorgan. Chim.* **4**, 2641 (1959).
- (14) Nordlander, J. E., Joung, W. G., Roberts, J. D., *J. Am. Chem. Soc.* **83**, 494 (1961).
- (15) Nordlander, J. E., Roberts, J. D., *J. Am. Chem. Soc.* **81**, 1769 (1959).
- (16) Porri, L., Natta, G., Gallazzi, M. C., *J. Polymer Sci., Pt. C* **2526** (1967).
- (17) Seyferth, D., Gordon, M. E., Damrauer, R., *J. Org. Chem.* **32**, 469 (1967).
- (18) Sinotova, E. I., Vobezkii, M. F., *et al.*, *Radiochim.* **1**, 280 (1960).
- (19) Statton, G. L., Ramey, K. C., *J. Am. Chem. Soc.* **88**, 1327 (1966).
- (20) Vrieze, K., Cossee, P., Maclean, C., Hilbers, C. W., *J. Organometal. Chem.* **6**, 672 (1966).
- (21) Whitesides, G. M., Nordlander, J. E., Roberts, J. D., *J. Am. Chem. Soc.* **84**, 2010 (1962).
- (22) Wilke, G., Bogdanovich, B., Hardt, P., *Angew. Chem.* **5**, 151 (1966).

RECEIVED March 18, 1968.

## Anionic Free Radical Polymers of $\alpha$ -Olefins

JAMES L. JEZL, N. S. CHU,<sup>1</sup> and H. M. KHELGHATIAN

Research and Engineering Department, Avisun Corp., Marcus Hook, Pa.

*Catalysts of the Ziegler type have been used widely in the anionic polymerization of 1-olefins, diolefins, and a few polar monomers which can proceed by an anionic mechanism. Polar monomers normally deactivate the system and cannot be copolymerized with olefins. However, it has been found that the "living" chains from an anionic polymerization can be converted to free radicals in the presence of peroxides to form block polymers with vinyl and acrylic monomers. Vinylpyridines, acrylic esters, acrylonitrile, and styrene are converted to block polymers in good yield. Binary and ternary mixtures of 4-vinylpyridine, acrylonitrile, and styrene, are particularly effective. Peroxides are effective at temperatures well below those normally required for free radical polymerizations. A tentative mechanism for the reaction is given.*

This paper presents a polymerization reaction, as yet unreported in the literature, wherein block polymerization of a free radical type can be caused to take place onto an actively growing chain which had proceeded by an anionic mechanism. Specifically, a Ziegler type of polymerization, such as that of propylene or ethylene, can be interrupted by adding vinylic monomers and an organic peroxide, and a vinyl polymer grown on the end of the polyolefin. For simplicity we will refer to these types as anionic free radical (AFR) polymerizations.

Some reactions between organometallic compounds and peroxides have been reported. Razuvaev and co-workers (5) observed an exothermic reaction between triethylaluminum and benzoyl peroxide in benzene. At a reaction temperature of 25°–30°C. the reaction gave diethylaluminum benzoate and ethyl benzoate. At higher temperature

<sup>1</sup> Present address: Union Carbide Corp., Tarrytown, N. Y.

no definite compounds could be isolated from the complex product. Vyazankin (9) reported a reaction between benzoyl peroxide and diethyltin ethylate, which led to the formation of ethoxydiethyltin benzoate and ethyl benzoate. Reaction between aluminum isopropoxide and benzoyl peroxide has been found to form acetone, 2-propanol, isopropyl benzoate, and benzoic acid (6). From patent literature we learn that organometallic aluminum compounds polymerize vinyl acetate at low temperatures in the presence of a peroxide (3). An Italian patent (8) specifies the use of trialkylboron with benzoyl peroxide, lauroyl peroxide, and azobisisobutyronitrile for the polymerization of ethylene, propylene, styrene, and other vinyl monomers. Recently, E. B. Milovskaya and her co-workers (4) reported the polymerization of acrylonitrile and vinyl acetate in the presence of trialkylaluminum and a peroxide. These monomers were polymerized at a temperature well below that of the simple decomposition of the peroxide used, although the polymerization was believed to be a radical-initiated process. From these it can be concluded that organometallic compounds can react with peroxides and that such mixtures do promote polymerization of suitable vinyl compounds. However, we find no references to mixed polymerizations of the type under discussion. Some of the practical implications of these polymers are given in the patent literature (1).

A major objective of our research has been to introduce polar groups into polyolefin molecules. With the anionic type of catalysts, copolymerization is very difficult because most nonhydrocarbon vinylic monomers deactivate the catalyst system and stop olefinic polymerization. However, by the AFR route, the desired olefin is completely polymerized before polar monomers are introduced so that high yields of product are possible.

In the present paper we pay special attention to block polymers with polypropylene and polyethylene as the initial anionic block. However, both crystalline and amorphous block polymers of ethylene and propylene, butadiene, and several other olefins and dienes have been made by the AFR technique. The second or free radical block has been made from 4-vinylpyridine, 2-methyl-5-vinylpyridine, and mixtures with other monomers, as well as a number of acrylic monomers. Vinyl chloride, vinylidene chloride, vinyl acetate, and several related monomers have not been successfully copolymerized.

### **Experimental**

**Materials.** Polymerization grades of propylene and ethylene, obtained from Sun Oil Co., were used without further purification. Vinylpyridines were obtained from Borden Chemical Co. Before use, the monomers were purified by vacuum distillation to remove inhibitors. Acrylonitrile, from Distillation Products Industries, was purified by distil-

lation. All acrylates were obtained from Rohm and Haas Co. and were vacuum distilled before use. Commercial peroxides were used without purification. A polymerization grade hexane was used as solvent medium. It contained about 15% isohexanes and 85% *n*-hexane. Before use it was dried over molecular sieves and purged of O<sub>2</sub> with dry high purity nitrogen.

**Polymerization.** Propylene was polymerized in 250-ml. pressure bottles. Into an oxygen-free, dried bottle were added 100 ml. of dry hexane and 1 mmole each of AA·TiCl<sub>3</sub> (Stauffer) and diethylaluminum chloride (Texas Alkyl) under the air-free, water-free conditions required for anionic types of polymerizations. The bottle was equipped with a Teflon-lined bar stirrer, was capped with a perforated metal cap equipped with neoprene disc, and was placed into a 70°C.-thermostatted bath. Propylene was introduced to a pressure of 40 p.s.i.g. by a syringe needle which had been inserted into the bottle through the neoprene disc. For 3 hours of polymerization the contents of the bottle were agitated constantly with a magnetic stirrer. Excess pressure was then released, and the bottle was cooled to room temperature. The desired amounts of polar monomers and peroxide were added in a prescribed sequence, and the bottle was returned to the thermostatted bath at the desired temperature and stirred for a specified length of time, usually overnight. The anionic catalyst was deactivated with 10 ml. methanol, and solid polymer was filtered away from suspending solvent. The solid polymer was washed with hexane, methanol, dilute HCl in methanol, dilute NaOH in methanol, 1:1 methanol-water mixture, and lastly methanol, at each step subjecting the mixture to intimate mixing in a Waring Blendor. After being dried overnight under reduced pressure, the polymer was weighed. Infrared spectroscopy was used wherever possible to assess polymer composition.

### *Results and Discussion*

**Vinylpyridines.** Vinylpyridines form block polymers readily by the AFR route with polypropylene as the substrate. Block formation is increased by the presence of acrylonitrile and/or styrene as comonomer. Each of these will form block polymers with polypropylene under certain conditions.

Of the three most common vinylpyridines, 4-vinylpyridine and 2-methyl-5-vinylpyridine are approximately equivalent in terms of the amount incorporated into block polymers, while 2-vinylpyridine is about one-fourth as reactive.

**PEROXIDES.** The need for a peroxide to bring about the desired reaction is demonstrated in Table I for mixtures of 2-methyl-5-vinylpyridine and acrylonitrile. Without benzoyl peroxide, little or no incorporation of monomers into insoluble polymer takes place. At 70°C. a higher level of peroxide is needed for maximum conversion of both monomers to block polymers than at lower temperatures. Plateaus or maxima are attained at 0.10, 0.15, and 0.25 gram of benzoyl peroxide at 30°, 50°, and

**Table I. Effect of Peroxide Concentration and Temperature on Block Formation**2-Methyl-5-vinylpyridine and Acrylonitrile on Polypropylene<sup>a</sup>

Temperature, °C.	Peroxide, Benzoyl gram	Conversion, %	
		2-Methyl-5-vinylpyridine	Acrylonitrile
30	0.00	nil	nil
	0.05	5	4
	0.10	26	23
	0.15	26	21
	0.20	28	27
	0.25	29	22
50	0.00	nil	nil
	0.05	5	3
	0.10	20	23
	0.15	29	39
	0.20	23	31
70	0.00	nil	nil
	0.10	8	7
	0.15	9	10
	0.20	14	15
	0.25	21	31
	0.30	18	28

<sup>a</sup> 100 ml. hexane, ca. 20 grams active polypropylene powder, 2 grams of 2-methyl-5-vinylpyridine, 2.4 grams acrylonitrile; sequence of addition: MVP, ACN, Bz<sub>2</sub>O<sub>2</sub>; time of free radical polymerization, 16 hours.

70°C., respectively. Maximum conversions of both acrylonitrile and 2-methyl-5-vinylpyridine are obtained at about 50°C. It is interesting that the free-radical reaction takes place at 30°C., particularly since the peroxide used (benzoyl peroxide) normally is not effective at temperatures below 70°C. This suggests that the anionic catalyst components take part in the free radical reaction. This appears to be the exclusive reaction at the lower temperatures. At higher temperatures homogeneous polymerization of monomers and possibly a random grafting reaction also occur to a significant extent. However, inactive polypropylene powder does not undergo low temperature block or graft formation with the comonomers used. The active ends with catalyst moieties attached thereto appear necessary for the reaction.

Other peroxides—2,6-dichlorobenzoyl peroxide; lauroyl peroxide, *tert*-butyl hydroperoxide, and methyl ethyl ketone peroxide—are also highly effective for the free radical reaction at low temperatures. On the other hand, azobisisobutyronitrile (AIBN) is ineffective. Hence, the mechanism cannot be simple, free radical formation which then initiates polymerization.

**MONOMER CONCENTRATION.** When 2-methyl-5-vinylpyridine is used alone, the incorporation or conversion of the monomer to block polymer is low, of the order of 10% of monomer used. However, conversion of vinylpyridine is increased greatly by the presence of acrylonitrile (Table II). Table II also shows that a lower temperature favors conversion, with 50°C. being optimum. Conversion at 70°C. is lower than at 30°C., even when twice the peroxide is used.

**Table II. Effect of Comonomer Composition on Conversion to Block Polymers**

2-Methyl-5-vinylpyridine and Acrylonitrile on Polypropylene*				
Temperature, °C.	Acrylonitrile, grams	Benzoyl Peroxide, gram	Conversion, %	
			2-Methyl-5-vinylpyridine	Acrylonitrile
2-Methyl-5-vinylpyridine at 2.0 grams				
30	0.0	0.20	9	—
	0.8		12	6
	1.6		18	20
	2.4		29	25
	3.2		36	36
50	0.0	0.20	11	—
	0.8		14	16
	1.6		20	43
	2.4		32	48
	3.2		35	51
70	0.0	0.40	10	—
	0.8		13	21
	1.6		15	23
	2.4		21	26
	3.2		27	35
2-Methyl-5-vinylpyridine at 1.0 gram				
	0.8		19	—
	1.6		24	25
	2.4		35	35
	3.2		37	38

\* 100 ml. hexane, approx. 20 grams active polypropylene; sequence of addition: MVP, ACN, Bz<sub>2</sub>O<sub>2</sub>; time of free radical polymerization, 16 hours.

The amount of vinyl pyridine used has some effect on incorporation of acrylonitrile. At half the level of 2-methyl-5-vinylpyridine (1.0 gram) a smaller conversion of acrylonitrile is noted. However, conversion of 2-methyl-5-vinylpyridine is increased somewhat at the lower level.

ORDER OF ADDITION OF BENZOYL PEROXIDE. Block polymerization proceeds best when polar monomers are added before the peroxide. When benzoyl peroxide is added before the monomers, monomer conversion is reduced drastically. The longer the time lapse between addition of peroxide and addition of monomers, the more dramatic is the effect (Table III). When monomers are added first, the time lapse before addition of peroxide is not critical.

**Table III. Effect of Order of Addition on Conversion to Block Polymers**

2-Methyl-5-vinylpyridine and Acrylonitrile on Polypropylene<sup>a</sup>

<i>Order of Addition</i>	<i>Conversion, %</i>	
	<i>MVP</i>	<i>ACN</i>
Bz <sub>2</sub> O <sub>2</sub> , MVP, ACN (almost simultaneously)	27	28
Bz <sub>2</sub> O <sub>2</sub> , 10 min., MVP, ACN	8	5
Bz <sub>2</sub> O <sub>2</sub> , 60 min., MVP, ACN	5	Trace
MVP, ACN, Bz <sub>2</sub> O <sub>2</sub> (almost simultaneously)	40	49
MVP, 10 min.; ACN, Bz <sub>2</sub> O <sub>2</sub>	38	50
MVP, 10 min.; ACN, 10 min.; Bz <sub>2</sub> O <sub>2</sub>	41	58

<sup>a</sup> 100 ml. hexane, *ca.* 20 grams active polypropylene powder, 2.0 grams 2-methyl-5-vinylpyridine, 2.4 grams acrylonitrile, 0.15 gram benzoyl peroxide. Monomers and peroxide added at 0–5°C.; free radical polymerization at 30°C. for 16 hours.

Although the reaction between the peroxide and the growing end of the anionic polymer chain is very rapid, the subsequent free radical polymerization reaction is relatively slow. Data in Table IV show that the conversions of methylvinylpyridine and acrylonitrile increase with increasing polymerization time. More than 4 hours are required for maximum reaction.

**Table IV. Effect of Duration of Free Radical Polymerization on Monomer Conversion to Block Polymers**

2-Methyl-5-vinylpyridine-Acrylonitrile System<sup>a</sup>

<i>Time of Free Radical Polymerization, hours</i>	<i>Monomer Conversion, %</i>	
	<i>MVP</i>	<i>ACN</i>
1	14	14
2	20	21
3	21	21
4	28	26
16	32	44

<sup>a</sup> 100 ml. hexane, *ca.* 15 grams active polypropylene powder, 2.0 grams 2-methyl-5-vinylpyridine and 2.4 grams acrylonitrile added 10 minutes apart, 0.2 gram benzoyl peroxide; free radical polymerization made at 30°C.



A study of the disappearance of benzoyl peroxide as a function of time at 30°C. shows immediate decomposition of one-fourth to one-half of the peroxide. After about 5 minutes the rate of decomposition becomes slow, and some peroxide persists after 20 hours.

**ORDER OF ADDITION OF POLAR MONOMERS.** The order of addition of methylvinylpyridine and acrylonitrile also plays an important part in the incorporation of the monomers. Conversions to block polymers are higher when methylvinylpyridine is added first (Table V). When methylvinylpyridine is added first, the mixture retains the usual purple color of  $TiCl_3$ , and the color does not change upon addition of acrylonitrile. However, when acrylonitrile is added first, the color changes rapidly to brown, which then persists.

**Table V. Effect of Order of Addition of Comonomers on Conversion to Block Polymers**

2-Methyl-5-vinylpyridine and Acrylonitrile on Polypropylene<sup>a</sup>

Order of Addition	Minutes between Addition	Monomer Conversion, %	
		MVP	ACN
MVP, ACN	5	17	19
	10	16	15
	15	6	30
ACN, MVP	5	8	40
	10	4	nil
	15	nil	nil

<sup>a</sup> 100 ml. hexane, *ca.* 20 grams active polypropylene powder, 2.0 grams 2-methyl-5-vinylpyridine, 2.4 grams acrylonitrile, 0.2 gram benzoyl peroxide; free radical polymerization at 70°C. for 16 hours.

The color change and the sensitivity of conversion to order of addition of monomers and peroxide indicate that in order to obtain an AFR polymer the polar monomers must first be complexed or allowed to react with the active or "living" end of the anionic polymer chain, or otherwise "solvate" it before the polymer chain is attacked by the peroxide. Success or failure of the subsequent free radical block polymerization depends on the nature of the complex or reaction product formed. The resultant species are no longer active for propylene polymerization. The necessity of complex formation has also been observed by Milovskaya and co-workers (4). They have shown that vinyl chloride, a weak complexing agent, can be polymerized effectively with triethylaluminum peroxide only when it is present with a more active complexing compound such as an ester or an ether.

**STYRENE AS COMONOMER.** At room temperature styrene and acrylonitrile are incorporated into block polymers to a limited extent when used as single monomers. If the free radical polymerization temperature is decreased to 0°C., the conversion of acrylonitrile increases, but little effect is noted on styrene. Styrene, on the other hand, can be incorporated at elevated temperatures.

The effect of styrene on conversion of 2-methyl-5-vinylpyridine and acrylonitrile is quite dramatic, as shown in Table VI. Surprisingly, the incorporation of both methylvinylpyridine and acrylonitrile increases with the addition of styrene, but styrene itself is not incorporated to any appreciable extent. The low temperature of block polymerization (30°C.) may have been responsible for this selectivity. In subsequent work to be reported on at a later date, it was observed that styrene itself can be introduced as a block during the anionic portion of the polymerization, and that this anion was particularly attractive as an anchor for free radical block formation. From this it may be concluded that styrene serves mainly in the anionic rather than the free radical phase of the block polymerization.

**Table VI. Effect of Styrene on Block Formation**  
2-Methyl-5-vinylpyridine and Acrylonitrile on Polypropylene<sup>a</sup>

	Conversion, %		
	MVP	ACN	Styrene
MVP-Styrene	19	—	trace
MVP-ACN (2.4 grams)	52	57	—
MVP-ACN (2.4 grams)-St	84	84	trace
St-ACN	—	<5	trace
ACN (1.6 grams)-St	—	14	trace
Styrene	—	—	trace
ACN	—	0-5	—
MVP	6	—	—

<sup>a</sup> 100 ml. hexane, *ca.* 20 grams active polypropylene powder, 1.0 gram 2-methyl-5-vinylpyridine, 1.6-2.4 grams acrylonitrile, 1.8 grams styrene, 0.2 gram benzoyl peroxide; free radical polymerization at 30°C. for 16 hours.

**EFFECT OF SUBSTRATE.** Several comparisons were made to establish the effect of substrate on conversion of methylvinylpyridine and acrylonitrile. Relative effectiveness in the ethylene-propylene series were: ethylene-propylene copolymer > polyethylene > polypropylene on a relativity scale of 4:3:2. The fact that chains terminated with polyethylene blocks are better substrates than polypropylene blocks suggests that random grafting on the backbone is not a major part of the reaction at low polymerization temperatures. The higher conversion on polyethylene

blocks is also consistent with the observation that a greater number of active catalyst sites are generated when ethylene is polymerized than when propylene is polymerized.

**ACTIVE AND INERT SUBSTRATES.** Since acrylonitrile, methylvinylpyridine, and mixtures of the two compounds all can be polymerized by  $(C_2H_5)_2AlCl-TiCl_3$  and benzoyl peroxide, it is desirable to study the free radical reaction in the presence of inert polypropylene powder and to compare its final product with the AFR polymerization under otherwise similar conditions. Deactivated, dry polypropylene powder in hexane suspension was treated with  $(C_2H_5)_2AlCl-TiCl_3$ , methylvinylpyridine, acrylonitrile, and benzoyl peroxide in a prescribed manner. The results are summarized in Table VII. When deactivated dry polypropylene powder was treated with monomers and peroxide, the amount of insoluble polar copolymer decreased as free radical temperature decreased, while for AFR polymer (active polypropylene) this amount of insoluble polar copolymer increased as temperature decreased. The polymerized comonomers in the active polymer were much less extractable than in the inert powder.

In addition to the AFR block polymer, there is also some copolymer of methylvinylpyridine and acrylonitrile. The amount of this copolymer varies with both the free radical temperature and the amount of benzoyl peroxide used. At room temperature, the AFR polymerization appears to be the main reaction. Both comonomers in the polymer made with inert polypropylene powder at room temperature are found at much lower levels than in the AFR polymer. Furthermore, the polar polymer made with active polypropylene at room temperature is essentially non-extractable. At 50°C. under the condition used the product isolated seemed to be a 50–50% mixture of block polymer and free copolymer.

**Table VII. Comparison of Block Formation with Active and Inert Substrates**

2-Methyl-5-vinylpyridine and Acrylonitrile on Polypropylene<sup>a</sup>

Substrate	Free Radical Temp., °C.	Benzoyl Peroxide, gram	Conversion, %			
			Unextracted		Extracted	
			MVP	ACN	MVP	ACN
Active	30	0.1	34	39	31	44
Inactive	30	0.1	6	trace	trace	trace
Active	50	0.2	24	37	14	19
Inactive	50	0.2	32	45	8	8

<sup>a</sup> Two grams 2-methyl-5-vinylpyridine, 3.2 grams acrylonitrile, 0.1–0.2 gram benzoyl peroxide.

Scans by differential thermal analysis show a broadening of the polypropylene melting peak for the AFR polymer as the temperature of free radical polymerization decreases. Samples from inert polypropylene powder do not exhibit this same phenomenon. This suggests that for the AFR polymerization, more methylvinylpyridine and acrylonitrile are incorporated on the polypropylene chain as the free radical polymerization temperature is decreased. The AFR polymerization is favored by low temperatures.

In summary, the data obtained from the comparative studies of the AFR polymer with active and inert polypropylene powder further support our view that an active polypropylene chain is necessary and that the copolymer block in AFR polymerization does not exist as a mixture with polypropylene but is tied to the polypropylene. The studies also rule out the possibility of a graft polymerization for which active polymer would not be necessary.

**Acrylic Esters.** Acrylic esters are also polymerizable by the AFR technique. Response to conditions is somewhat different from vinylpyridine.

Acrylates which have been tried successfully are methyl methacrylate (MMA), ethyl acrylate (EA), methyl acrylate (MA), *N,N*-dimethylaminoethyl methacrylate (DMAEMA), *N,N*-diethylaminoethyl acrylate (DMAEA), *tert*-butylaminoethyl methacrylate (BAEMA), and a 30% aqueous solution of hydroxyethyl methacrylate (HEMA). Most studies were made with *N,N*-dimethylaminoethyl methacrylate since its basic group would render the polymer dyeable with acid dyes.

In the absence of benzoyl peroxide, no discernible conversion of acrylic esters has been observed under the conditions used for AFR polymerization. At levels of 0.1–0.3 gram of peroxide and 0.5–5.0 ml. of dimethylaminoethyl methacrylate, conversion to graft polymers was observed at 70°C. for 16 hours with an active polypropylene slurry, as shown in Table VIII.

Incorporation of acrylates into polypropylene can be increased by increasing the amount of acrylate or by increasing the amount of peroxide at a given acrylate level. Although the amount of acrylate found in the insoluble AFR polymer increased as the amount of acrylate present increased, the relative efficiency of conversion decreased as the amount used increased. The acrylate content was determined from the —COOR absorbance per mil of the AFR polymer. When peroxide was added before the polar monomer, poor incorporation of the monomer resulted.

**EFFECT OF WATER.** It was observed quite by accident that addition of a small amount of water increased the conversion of *N,N*-dimethylaminoethyl methacrylate or the corresponding acrylate into block polymers (Table IX). On the other hand, acrylates such as methyl meth-

acrylate and ethyl acrylate showed a decrease in monomer incorporation by the addition of water. *tert*-Butylaminoethyl methacrylate was unaffected by addition of water. When *N,N*-dimethylaminoethyl methacrylate was copolymerized with other acrylates such as methyl methacrylate or ethyl acrylate, addition of water enhanced the incorporation of *N,N*-dimethylaminoethyl methacrylate, while the incorporation of methyl methacrylate was suppressed. As a matter of fact, no disappearance of monomeric methyl methacrylate was seen by gas chromatography when water was used. Despite this, methyl methacrylate and other acrylates increased the incorporation of *N,N*-dimethylaminoethyl methacrylate in AFR polymers.

**Table VIII. Effect of Change of Concentration of Acrylate or Peroxide on Block Formation**

Dimethylaminoethyl Methacrylate on Polypropylene<sup>a</sup>

DMAEMA Used, cc.	$Bz_2O_2$ Used, gram	DMAEMA Incorporation, %	
		in Polymer	Conversion
0.5	0.1	trace	trace
1.0	0.1	0.3	5
2.0	0.1	0.4	4
3.0	0.1	0.4	2
5.0	0.1	0.7	2
3.0	0.0	0.0	0
3.0	0.1	0.4	2
3.0	0.2	0.6	4
3.0	0.3	0.7	4

<sup>a</sup> 100 ml. hexane, ca. 20 grams active polypropylene powder, dimethylaminoethyl methacrylate, benzoyl peroxide; free radical polymerization, 16 hours at 70°C.

Addition of water has been found to be the best way to improve the effective use of *N,N*-dimethylaminoethyl methacrylate. Adding 0.4 ml. of water to the mixture before adding *N,N*-dimethylaminoethyl methacrylate and benzoyl peroxide increased incorporation of *N,N*-dimethylaminoethyl methacrylate tenfold. Water was not beneficial for polymerizations with vinylpyridine.

At present, the role of water in this type AFR polymerization is unclear. It seems likely that water changes the nature of the complex or solvating nature of the active ends of the anionic chain. Because of the hydrophobic aliphatic polymer chain, a polar compound such as water probably can approach the catalyst site to solvate or complex the environment of the active center without destroying the C—metal bond. This water barrier may prevent water-insoluble monomer from penetrating the reaction site, while with a water-soluble acrylate, the presence of the

water might assist in interaction with the active site. The fact that water addition can destroy excess alkylaluminum may also contribute to increasing the incorporation of the *N,N*-dimethylaminoethyl methacrylate, although it cannot explain the different effects of water on *N,N*-dimethylaminoethyl methacrylate and methyl methacrylate.

**Table IX. Effect of Water on Conversion of Acrylate Esters to Block Polymers<sup>a</sup>**

<i>Monomer</i>		$H_2O$ , <i>ml.</i>	$Bz_2O_2$ , <i>gram</i>	$-COOR$ , <i>abs./mil.</i>
Methyl acrylate (MA)	2.0	—	0.10	0.008
	2.0	0.40	0.10	trace
Methyl methacrylate (MMA)	2.0	—	0.10	0.023
	2.0	0.40	0.10	trace
Ethyl acrylate (EA)	2.0	—	0.10	0.013
	2.0	0.40	0.10	trace
<i>tert</i> -Butylaminoethyl methacrylate	2.0	—	0.10	0.025
	2.0	0.40	0.10	0.032
Dimethylaminoethyl acrylate (DMAEA)	1.0	—	0.10	0.015
	1.0	0.40	0.10	0.027
DMAEA + EA	1.0, 1.0	—	0.10	0.026
	1.0, 1.0	0.40	0.10	0.073
Dimethylaminoethyl methacrylate (DMAEMA)	2.0	—	0.10	0.015
	2.0	0.15	0.10	0.037
	2.0	0.40	0.10	0.107
	2.0	5.0	0.10	0.110
	1.0	0.40	0.15	0.108
DMAEMA + MMA	1.0, 1.0	—	0.20	0.063
	1.0, 1.0	0.40	0.20	0.161
	1.0, 1.0	0.40	0.15	0.122
DMAEMA + HEMA	1.0, 0.3	0.70	0.10	0.188
	1.0, 0.6	1.40	0.10	0.310

<sup>a</sup> 100 ml. hexane, *ca.* 25 grams active polypropylene powder; order of addition:  $H_2O$ , acrylate, peroxide; free radical polymerization, 70°C. for 16 hours.

Comparison of conversion of *N,N*-dimethylaminoethyl methacrylate and *N,N*-dimethylaminoethyl acrylate shows that the former is more effective than the latter for AFR polymer preparation under comparable conditions. Among the three amine-containing acrylates, *tert*-butylaminoethyl methacrylate is the least effective compound for AFR polymeriza-

tion. Its low effectiveness may be caused by the bulkiness of the *tert*-butyl group, and/or the presence of hydrogen on the amino group.

**EFFECT OF PEROXIDES.** In addition to benzoyl peroxide, lauryl-, acetyl-, 2,4-dichlorobenzoyl-, and methyl ethyl peroxide, and *tert*-butyl hydroperoxide were studied and gave satisfactory results. The effectiveness of the peroxide is relatively independent of the half-life of the peroxide (Table X). By contrast, the catalyst AIBN is much less satisfactory, as found for methylvinylpyridine and acrylonitrile. The difference between these peroxides and AIBN suggests that the AFR polymer is not formed by a simple uncatalyzed free radical system which would give a graft polymer or a simple mixture of polypropylene and polyacrylate. It is well known that for the polymerization of acrylates AIBN is at least as good if not better than peroxide in initiating the free radical reaction (2).

**Table X. Effect of Different Peroxides on Block Formation with Dimethylaminoethyl Methacrylate<sup>a</sup>**

Peroxide Used, 0.4 mmole	Hexane Insol., grams	DMAEMA Incorporated, %		Half-Life at 70°C. in C <sub>6</sub> H <sub>6</sub> , hours <sup>b</sup>
		in Polymer	Conversion	
Benzoyl	14.5	3.1	24	13
Lauroyl	15.4	0.8	6	3.5
Acetyl	14.5	0.7	5	8.1
<i>tert</i> -Butyl hydro	12.7	1.2	8	>10,000
2,4-Dichlorobenzoyl	13.0	2.6	18	1.3
Methyl ethyl ketone	15.1	0.9	8	280±

<sup>a</sup> DMAEMA 2.0 ml., H<sub>2</sub>O 0.4 ml.; order of addition: H<sub>2</sub>O, DMAEMA, peroxide; free radical polymerization, 16 hours at 70°C.

<sup>b</sup> Most of these data supplied by Wallace and Tierman, Inc., Lucidol Division.

As in previous work, all these studies were carried out in a hexane fraction containing 15–20% of mixed isohexane. The successful results obtained rule out the possibility of grafting for it is well known that the efficiency of grafting decreases considerably in the presence of a low molecular weight, chain-transfer agent such as isohexane.

**EFFECT OF SUBSTRATE.** Again, polyethylene and ethylene-propylene copolymers are better substrates for block formation than polypropylene (Table XI). Polyethylene is better than polypropylene, and a polyethylene-polypropylene-polyethylene type of block polymer is better than polyethylene. This agrees with what has been found for AFR polymers containing methylvinylpyridine and acrylonitrile. It also supports our belief that AFR polymers are formed by the growing of a free radical polymer onto active ends of anionic polymer chains. If it were a random grafting reaction, it would be hard to explain why a propylene polymer with a more vulnerable tertiary hydrogen should give a lower

incorporation of polar monomer than a polymer containing ethylene. It is interesting that a polymer containing initial and terminal blocks of polyethylene gives better acrylate incorporation than one with only a terminal polyethylene. This is difficult to explain on the basis of a random grafting reaction but supports our view that a "living" anionic chain is necessary for an AFR polymerization. Ethylene initiates more anionic polymer chains than does propylene, and thus there are more chains to which the subsequent free radical polymer can attach itself.

**Table XI. Effect of Substrate on Conversion of Acrylate Esters to Block Polymers<sup>a</sup>**

Monomer	ml.	Anionic Polymer	H <sub>2</sub> O	-COOR abs./mil
DMAEMA	2.0	Polypropylene (PP)	0.40	0.107
	2.0	Polyethylene (PE)	0.40	0.148
DMAEMA	2.0	PP	—	0.027
	2.0	PP-PE	—	0.060
	2.0	PE-PP-PE	—	0.080
DMAEMA	1.0	PP	—	0.022
	1.0	PP-PE	—	0.027
	1.0	PE-PP-PE	—	0.065
DMAEMA + MMA	1.0 + 1.0	PP	—	0.023
	1.0 + 1.0	PE	—	0.108
DMAEMA + EA	1.0 + 1.0	PP	—	0.024
	1.0 + 1.0	PE	—	0.078
	1.0 + 1.0	PP	0.40	0.120
DMAEMA + MMA	1.0 + 1.0	PP	—	0.085
	1.0 + 1.0	PE-PP-PE	—	0.120
DMAEA + EA	1.0 + 1.0	PP	—	0.047
	1.0 + 1.0	PE-PP-PE	—	0.076

<sup>a</sup> 100 ml. hexane, *ca.* 20 grams active polymer, 0.10 gram benzoyl peroxide; free radical temperature, 70°C. for 16 hours.

**EFFECT OF CATALYST CONCENTRATION.** Since the effectiveness of AFR polymerization should depend on the number of active ends of the anionic polymer chain, it is of interest to study the effect of the change of anionic catalyst concentration on AFR polymer formation. At high catalyst levels the effect of catalyst concentration is difficult to demonstrate, but at low catalyst levels monomer conversion is directly related to the amount of TiCl<sub>3</sub> used (Table XII).



**Table XII. Effect of Catalyst Concentrations on Conversion of Acrylates to Block Polymers<sup>a</sup>**

$TiCl_3$ , mmoles	$Al/Ti$ , molar	$Ti/Bz_2O_2$ , molar	Milliliters			—COOR abs./mil	Conver- sion, %
			DMAEMA	EA	$H_2O$		
0.17	1.35/1	1/2.7	1.2	1.2	0.12	0.030	
0.34	1.35/1	1/1.3	1.2	1.2	0.12	0.064	
0.50	1.2/1	1/0.8	1.0	1.0	0.40	0.109	
1.00	1/1	1/0.4	1.0	1.0	0.40	0.120	
1.00	1/1	1/0.2	1.0	—	0.40	0.042	24
1.00	1/1	1/0.4	1.0	—	0.40	0.062	40
100	1/1	1/0.6	1.0	—	0.40	0.108	68
1.00	1/1	1/0.8	1.0	—	0.40	0.114	65

<sup>a</sup> 100 ml. hexane, ca. 20 grams active powder; free radical polymerization, 70°C. at 16 hours.

The existence of a relationship between anionic catalyst concentration and incorporation of the acrylate again rules out the possibility of a grafting mechanism, but it is consistent with an active chain mechanism. If acrylate entered the polypropylene molecule at random along the backbone of the molecule, which would result in a grafting process, the level of anionic catalyst would be immaterial as long as the total weight of the polypropylene were kept constant.

At high concentrations of  $TiCl_3$  there was a deficiency of peroxide, while at lower concentrations the peroxide was in excess. In the first case, there were sufficient  $RCH_2$ —metal bonds to react with the limited amount of peroxide used, and changes in anionic catalyst concentration probably did not affect the actual number of active C—metal bonds which could react with peroxide. Moreover, in the reaction mixture, other C—metal bonds such as those present on free  $(C_2H_5)_2AlCl$  may compete with the  $RCH_2$ —metal for the peroxide. In fact, it is reasonable to assume that the  $RCH_2$ —metal bond with a bulky polymer chain attached on it should have greater steric hindrance and a smaller reactivity toward the peroxide than the  $C_2H_5$ —Al bond from free alkyl. By decreasing the anionic catalyst concentration without decreasing the amount of the peroxide, we reach a point where there is more than enough peroxide to react with all the  $RCH_2$ —metal bonds which lead to AFR polymers, and further addition of peroxide is of little help. However, we can increase the incorporation of acrylate by keeping the  $(C_2H_5)_2AlCl$  and  $TiCl_3$  concentration high while increasing the concentration of the peroxide.

The effect of the anionic catalyst concentration on the formation of AFR polymers also rules out the possibility of a simple initiation of acrylate polymerization by benzoyl peroxide. If the latter is the case, the yield of the polyacrylate would depend only on the concentration of the peroxide and not on the concentration of the anionic catalyst.

EFFECT OF ADDED TRIETHYLALUMINUM. Excess alkylaluminum should have a suppressive effect on block formation because it should provide a competitive side reaction. To show this, different amounts of alkyl were added to the polypropylene mixture before addition of *N,N*-dimethylaminoethyl methacrylate and peroxide. Data in Table XIII show that the presence of triethylaluminum drastically decreases the incorporation of *N,N*-dimethylaminoethyl methacrylate. Conversion decreases with increasing amounts of triethylaluminum. At the same level of alkyl concentration, an increase in the amount of benzoyl peroxide increases conversion of monomer. These results demonstrate clearly that a portion of benzoyl peroxide is wasted by reaction with the alkyl. Although the radical  $\text{CH}_3\text{CH}_2\cdot$  produced may also initiate the polymerization of the acrylate, the polymer formed is not tied to polypropylene and, therefore, is removed during the solvent-washing step. Since the ratio of *N,N*-dimethylaminoethyl methacrylate to initiator is very low, the molecular weight of the poly(*N,N*-dimethylaminoethyl methacrylate) should be rather low. Only when the poly(*N,N*-dimethylaminoethyl methacrylate) is tied to the polypropylene chain can it withstand the solvent-finishing process without being removed.

BLOCK POLYMER MADE WITH "ACTIVE" AND "INACTIVE" POLYPROPYLENE. Inactive polypropylene powder in hexane suspension was treated with  $(\text{CH}_3\text{CH}_2)_2\text{AlCl}$ ,  $\text{TiCl}_3$ , water, *N,N*-dimethylaminoethyl methacrylate, and benzoyl peroxide under the same conditions used to prepare AFR polymer. Just as for the polypropylene-methylvinylpyridine-acrylonitrile system, the inactive polypropylene did not show evidence of incorporation of the free radical polymer (Table XIV). When inactive polypropylene was used, the  $-\text{COOR}$  absorbance of the polymer was only about 10–30% as great as the  $-\text{COOR}$  absorbance with active polypropylene. With active polymer conversion to block formation increased as the

**Table XIII. Effect of Triethylaluminum on Block Polymerization with Diethylaminoethyl Methacrylate<sup>a</sup>**

DMAEMA, ml.	Mmoles		$-\text{COOR}$ abs./mil
	$\text{Et}_3\text{Al}$	$\text{Bz}_2\text{O}_2$	
2.0	—	0.8	0.056
2.0	1.0	0.8	0.042
2.0	2.0	0.8	0.024
2.0	—	0.4	0.065
2.0	0.5	0.4	0.047
2.0	1.0	0.4	0.038
2.0	2.0	0.4	nil

<sup>a</sup> 100 ml. hexane, ca. 20 grams active polypropylene powder; free radical polymerization at room temperature, 16 hours.

temperature of the free radical polymerization was decreased from 70° to 50°C. This observation is contradictory to data for benzoyl peroxide-initiated acrylate polymerization. The half-life of benzoyl peroxide at 50°C. is about 190 hours, and this peroxide would not be expected to be active at room temperature (7).

**Table XIV. Comparison of Block Formation with Active and Inactive Polypropylene**

Dimethylaminoethyl Methacrylate on Polypropylene<sup>a</sup>

Polypropylene Used	Anionic Catalyst Added	DMAEMA	H <sub>2</sub> O	Bz <sub>2</sub> O <sub>2</sub>	Temp., °C.	—COOR abs./mil
Active	—	1.0	0.4	0.4	70	0.101
Inactive	yes	1.0	0.4	0.4	70	0.040
Active	—	2.0	0.4	0.4	50	0.142
Inactive	yes	2.0	0.4	0.4	50	0.032
Active	—	1.0	0.4	0.4	30	0.094
Inactive	yes	1.0	0.4	0.4	30	0.016
Active	—	1.0	0.4	0.6	30	0.120
Inactive	yes	1.0	0.4	0.6	30	0.015
Inactive	—	2.0	0.4	0.4	30	nil

<sup>a</sup> Active polymer: made *in situ* and not deactivated; inactive polymer: deactivated, washed, and dried under nitrogen. Free radical polymerization order of addition: water, DMAEMA, benzoyl-peroxide; polymerization, 16 hours. Anionic catalyst: 1 mmole AlEt<sub>2</sub>Cl and 1 mmole TiCl<sub>3</sub> (AA).

The poly(*N,N*-dimethylaminoethyl methacrylate) present in the AFR polymer was found to be nonextractable with methyl ethyl ketone, in which the free radical homopolymer is soluble.

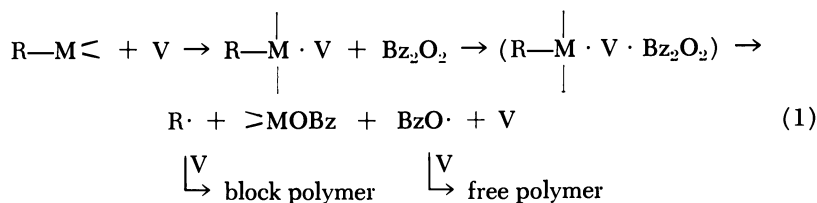
Inactive polypropylene powder, when treated with *N,N*-dimethylaminoethyl methacrylate and benzoyl peroxide in hexane at 30°C. did not possess detectable amounts of —COOR absorbance. The absence of —COOR absorbance in the resultant polymer gives further evidence that *N,N*-dimethylaminoethyl methacrylate either did not polymerize under the conditions used or formed only a very low molecular weight polymer which was washed out by the finishing procedure used. It also established that an active polymer chain is necessary and that poly(*N,N*-dimethylaminoethyl methacrylate) does not exist as a mixture with polypropylene but is tied into the polypropylene chain.

**MECHANISM.** There is ample evidence that the reaction we are dealing with is a block polymerization in which the first block is formed by an anionic mechanism and the second block is formed by a free-radical

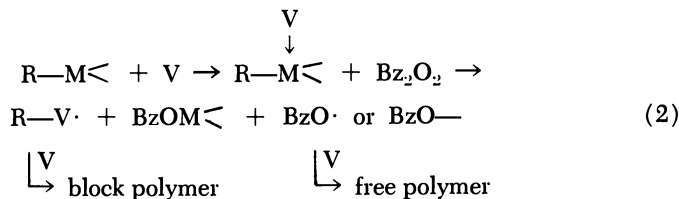
mechanism. At present we can only speculate as to the means whereby the reaction is switched from one mechanism to the other.

The free radical polymerization is probably initiated by the reaction of the peroxide with a metal—carbon bond which has been modified through complexation, solvation, or even chemical interaction with a proper monomer. This "site" is interacted with the peroxide molecule, which is then decomposed in a metal-catalyzed manner to form a free radical terminus on the polymer chain along with an inert metal—peroxide interaction product. Whether the metal in question is aluminum, titanium, or a complex of the two is uncertain since the mechanism of Ziegler type reactions is still uncertain and since all three have been found in separate studies to promote the polymerization of methyl methacrylate in the presence of peroxides. However, the complex between  $\text{AlEt}_2\text{Cl}$  and  $\text{TiCl}_3$  has been observed to have a much greater effect in accelerating the polymerization of methyl methacrylate than either component by itself; hence, the complex appears to be the most likely species.

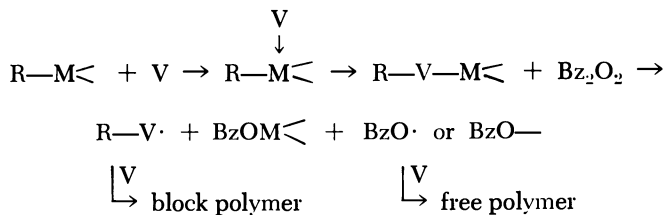
For simplicity we designate the metallic moiety as  $-\text{M}<$ , polymer chain as  $\text{R}\cdot$ , and monomer as  $\text{V}$ . By analogy with the mechanism proposed by Molovskaya *et al.*, we might view the reaction as follows:



If titanium is involved, it seems more probable that the following series of steps occurs:



or in the case of anionic polymerization of the monomer (V):



If the metal is oxidized, as is likely with  $TiCl_3$ , OBz becomes an inactive anion, and this reaction gives rise primarily to block polymers.

Excess alkylaluminum would tend to promote the competitive reaction observed by Milovskaya *et al.*, and, in part, a free polymer would be formed. The fact that alkylaluminum suppresses formation of block polymers tends to support this concept and further suggests that the reaction to form AFR polymer does not reside solely with the aluminum compounds present. In fact, the titanium must be involved to a significant extent.

### Literature Cited

- (1) Avisun Corp., Belgian Patent 694,455 (Aug. 22, 1967).
- (2) Flory, P. J., "Principles of Polymer Chemistry," Chap. IV, Cornell University Press, Ithaca, N. Y., 1953.
- (3) Milovskaya, E. B., Dolgopolskaya, P. I., *Vysokomolekul. Soedin.* **5**, 151 (1963); *Chem. Abstr.* **59**, 764e (1963).
- (4) Milovskaya, E. B., Zhuravleva, T. G., Zamoyskaya, L. V., *J. Polymer Sci. Pt. C* **16**, 899-910 (1967).
- (5) Razuvaev, G. A., Mitrofanova, E. V., Petukhov, G. G., *Zh. Obshch. Khim.* **31**, 2340-2343 (1961); *Chem. Abstr.* **57**, 3464i (1962).
- (6) Razuvaev, G. A., Stepovik, L. P., Mitrofanova, E. V., *Izv. Akad. Nauk SSSR, Ser. Khim.* **1964** (1) 162-164; *Chem. Abstr.* **60**, 9183h (1964).
- (7) Rohm and Haas Co., *Rept. SP-159* (1959).
- (8) Solvic-Industria delle Materie Plastiche S.p.A., Italian Patent 613,707 (appl. July 25, 1959).
- (9) Vyazankin, N. S., Razuvaev, G. A., D'yachkovskaya, O. S., Shchepetkova, O. A., *Dokl. Akad. Nauk SSSR* **143**, 1348-1350 (1962); *Chem. Abstr.* **57**, 8599c (1962).

RECEIVED March 14, 1968.

# Olefin Polymerizations and Copolymerizations with Alkylaluminum-Cocatalyst Systems

## III. Carbonium Ion Polymerizations with Trialkylaluminums and the Characterization of $AlR_3$ -Lewis Base Systems by NMR Spectroscopy

JOSEPH P. KENNEDY and GEORGE E. MILLIMAN

Corporate Research Laboratory, Esso Research and Engineering Co., Linden, N. J.

*Trialkylaluminums are efficient catalysts for isobutylene polymerization in the presence of a suitable cocatalyst—e.g., tert-butyl chloride, in methyl chloride solvent at low temperatures. In the  $AlMe_3$ -MeCl system, investigated by NMR spectroscopy, methyl exchange is very rapid in the  $AlMe_3$  dimer even at low temperatures in the presence of methyl chloride. Methyl chloride enhances the rate of methyl scrambling. In addition to methyl chloride, a variety of other Lewis bases apparently also effect the exchange of methyl groups in  $Al_2Me_6$ . The significance of these findings for the theory of polymerization initiation with trialkylaluminums is discussed.*

Recently we have described (2, 3, 4, 5, 6) and discussed from the theoretical point of view the polymerization and copolymerization of olefins, isoolefins, and aromatic hydrocarbons and dienes using trialkylaluminum and related catalyst systems. Trialkylaluminums—e.g., trimethylaluminum ( $AlMe_3$ ), triethylaluminum ( $AlEt_3$ ), and triisobutylaluminum ( $Al(iBu)_3$ ) or dialkylaluminum halides—e.g., diethylaluminum chloride ( $AlEt_2Cl$ ) are weak Lewis acids and do not initiate the polymerization of cationically polymerizable hydrocarbon monomers in the absence of suitable cocatalysts. For example, isobutylene, an extremely

reactive olefin, can be stirred at reflux or at low temperatures in methyl chloride (MeCl) diluent in the presence of any of these trialkylaluminums, and no polymerization will occur. However, instantaneous and vigorous polymerization occurs immediately after a small amount of a suitable cocatalyst—*e.g.*, *tert*-butyl chloride—is introduced to the quiescent system.

In contrast to these alkylaluminum catalyst systems, the well-known Friedel-Crafts halides—*e.g.*, AlCl<sub>3</sub>, AlEtCl<sub>2</sub>, etc.—rapidly polymerize isobutylene to high molecular weight products in the absence of added cocatalyst. It is usually presumed, but remains to be proved, that traces of moisture or HCl provide the necessary cocatalyst with the latter agents.

During our fundamental studies on the mechanism of carbonium ion polymerizations we became interested in the problem of cocatalysis in trialkylaluminum-initiated polymerizations and decided to elucidate some of the characteristic features of these systems by nuclear magnetic resonance (NMR) spectroscopy. This paper presents some of the intriguing phenomena we encountered with the AlMe<sub>3</sub> and Al<sub>i</sub>Bu<sub>3</sub> in methyl chloride and other solvent systems, in particular an extremely rapid methyl group exchange in the AlMe<sub>3</sub> dimer at very low temperatures and a very weak and a somewhat stronger complexation between Al<sub>2</sub>Me<sub>6</sub> and methyl chloride, and Al<sub>i</sub>Bu<sub>3</sub> and methyl chloride, respectively.

### Experimental

All polymerizations were carried out in a stainless steel enclosure (8). The purity and analysis of isobutylene, methyl chloride, and aluminum chloride have been described (9). The trialkylaluminums (Texas Alkyls, Inc.) were purified by distillation before use; AlEt<sub>2</sub>Cl was treated with NaCl at 80°C. for 2 hours to remove traces of AlEtCl<sub>2</sub>.

**AlMe<sub>3</sub>-*tert*-BuCl in MeCl.** To 15 ml. isobutylene in 60 ml. methyl chloride stirred at -35°C.,  $8.3 \times 10^{-5}$  mole AlMe<sub>3</sub> (0.2 ml. of 4 vol. % AlMe<sub>3</sub> in MeCl solution) was added; no reaction occurred. Subsequently, a total of  $\sim 5.5 \times 10^{-6}$  mole of *tert*-butyl chloride was added dropwise (a 1% *tert*-butyl chloride solution was used); immediate polymerization occurred; the yield was 1.469 grams or 14%; the viscosity average molecular weight was 240,300.

A series of experiments was carried out with this system at -35°, -55°, -78°, and -100°C. The general appearances of the reactions were essentially identical.

**AlMe<sub>3</sub>-*tert*-BuCl in *n*-Pentane.** To a charge of 15 ml. isobutylene in 60 ml. *n*-pentane stirred at -35°C.,  $1.05 \times 10^{-3}$  mole of an AlMe<sub>3</sub> (2 ml. of 8 vol. % AlMe<sub>3</sub>) was added in *n*-pentane solution; no reaction occurred. Subsequently, a *tert*-butyl chloride in *n*-pentane solution was added dropwise until a total of  $1.66 \times 10^{-4}$  mole of *tert*-butyl chloride was introduced (0.9 ml. of a 2% *tert*-butyl chloride in *n*-pentane solution); however, no polymerization occurred, and no methanol-insoluble polymer was formed.

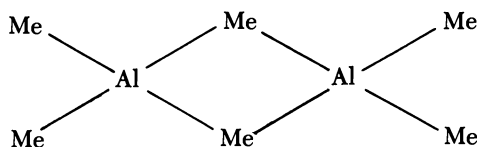
In a similar experiment AlMe<sub>3</sub> and *tert*-butyl chloride were added intermittently over 187 minutes to the above charge until a total of 6.65

$\times 10^{-3}$  mole of  $\text{AlMe}_3$  and  $7.0 \times 10^{-3}$  mole of *tert*-butyl chloride—*i.e.*, approximately equimolar amounts—were added, but no reaction was noticeable, and no methanol-insoluble polymer was formed.

**NMR Spectroscopy.** All samples were sealed under nitrogen. Line width measurements were made on spectra obtained at 100-Hz sweep widths from a Varian A60 NMR spectrometer. The solvent signal was used as a reference for the adjustment of the *y*-axis and curvature controls so that the maximum possible field homogeneity was obtained before the line whose width was to be measured was recorded. Line widths are uncorrected for inhomogeneity or uncertainty broadening. Uncertainty broadening is not expected to contribute significantly to the observed line width. Inhomogeneity broadening is estimated at 0.2–0.3 Hz and therefore should not contribute significantly to any of the observed line widths in Table I except those obtained from the solutions having the two highest methyl chloride concentrations. Sample temperatures were measured by inserting a sample of methanol into the probe and then calculating the temperature using the known temperature dependence of the hydroxyl signal. Chemical shifts were obtained from spectra obtained in a Varian HA 100 NMR spectrometer operating in the HA frequency sweep mode. The signal whose chemical shift was to be measured was recorded at a 50-Hz. sweep width, and the chemical shift was determined by reading the difference in frequency between this signal and the lock (solvent) signal from an electronic counter. The measured chemical shifts are believed to be accurate to  $\pm 0.1$  Hz. Concentrations of the sample components were calculated from the electronic integrals of the components and the molar volumes of the components, assuming ideal solutions.

### Results and Discussion

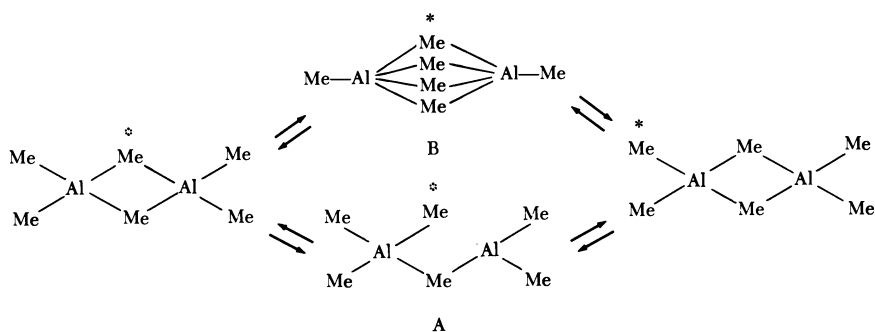
**Characterization of the  $\text{AlMe}_3$ -MeCl System by NMR.** It appears that the  $\text{AlMe}_3$  in methyl chloride system has not been investigated previously by NMR spectroscopy. In related research by other workers, freezing point depression measurements of  $\text{AlMe}_3$  in benzene solution indicated the predominant presence of dimers—*i.e.* (13):



The NMR spectrum of this dimer would be expected to exhibit two signals, in the ratio of 1:2, corresponding to the two magnetically inequivalent methyl groups—*viz.*, bridging and terminal. Indeed, whereas at room temperature the NMR spectra of  $\text{AlMe}_3$  solutions show only one signal for the methyls (7, 8), upon cooling these solutions to  $-30^\circ\text{C}$ . the signal broadens and is very distorted, and at  $-40^\circ\text{C}$ . two slightly broad-



ened signals are observed, one for each of the two types of methyls (Figure 1). [Note added in proof: J. R. McDivitt has recently observed that the 60-MHz. NMR spectrum of  $\text{Al}_2\text{Me}_6$  dissolved in  $\text{MeCl}$  exhibits two signals at  $-85^\circ\text{C}$ . for the methyls attached to aluminum at  $\tau 9.44$  and  $\tau 10.64$  in the ratio 1:2. This observation indicates that bridge-terminal methyl exchange of the trimethylaluminum dimer is slow in methyl chloride at this temperature.] This behavior is typical of exchange and indicates that the bridge and terminal methyl groups equilibrate rapidly at room temperature and that this exchange is retarded significantly at low temperatures. Noting that the activation energy for the exchange is 6–14 kcal./mole and the heat of dissociation of the dimer in the gas phase is 20.2 kcal./mole, Muller and Pritchard (12) postulated that the exchange process was intramolecular, involving either the breaking of one bridge (A) or a deformation of the molecule (B) as shown below.



Ramey *et al.* (14) reproduced these experiments and determined the activation parameters for the exchange as  $\Delta G^\ddagger = 11.0$  kcal./mole,  $\Delta H^\ddagger = 15.6$  kcal./mole and  $\Delta S^\ddagger = 20$  e.u. They stated that on the basis of these data one could not differentiate between the two exchange mechanisms suggested by Muller and Pritchard (12). Ramey *et al.* therefore investigated the mixed alkylaluminum system of  $\text{Al}(\text{Bu})_3$  and  $\text{AlMe}_3$ . Triisobutylaluminum is monomeric in solution (1). Above  $-40^\circ\text{C}$ . they found that the alkyl groups of these aluminum compounds exchange and concluded that the most likely mechanism for the exchange of methyl groups of trimethylaluminum dimer involves the breaking of one of the methyl bridges of the dimer (A).

Williams and Brown (15) also investigated the association and exchange of alkylaluminums. They studied the exchange of methyls between trimethylaluminum and trimethylgallium. In contrast to the earlier workers Williams and Brown concluded that the exchange of methyls of  $\text{Al}_2\text{Me}_6$  involves the dissociation of the dimer into monomers.

McCoy and Allred (10) found intermolecular exchange between the methyls of dimethylcadmium and trimethylaluminum.

Mole (11) found that the reaction of  $\text{AlEt}_3$  with  $\text{AlMe}_3$  to form mixed alkylaluminums was slower in the coordinating solvent pyridine than in benzene. He hypothesized that at least one of the two aluminums participating in the exchange must be pentacoordinated in the transition state. He stated that in the absence of a coordinating solvent the inter-

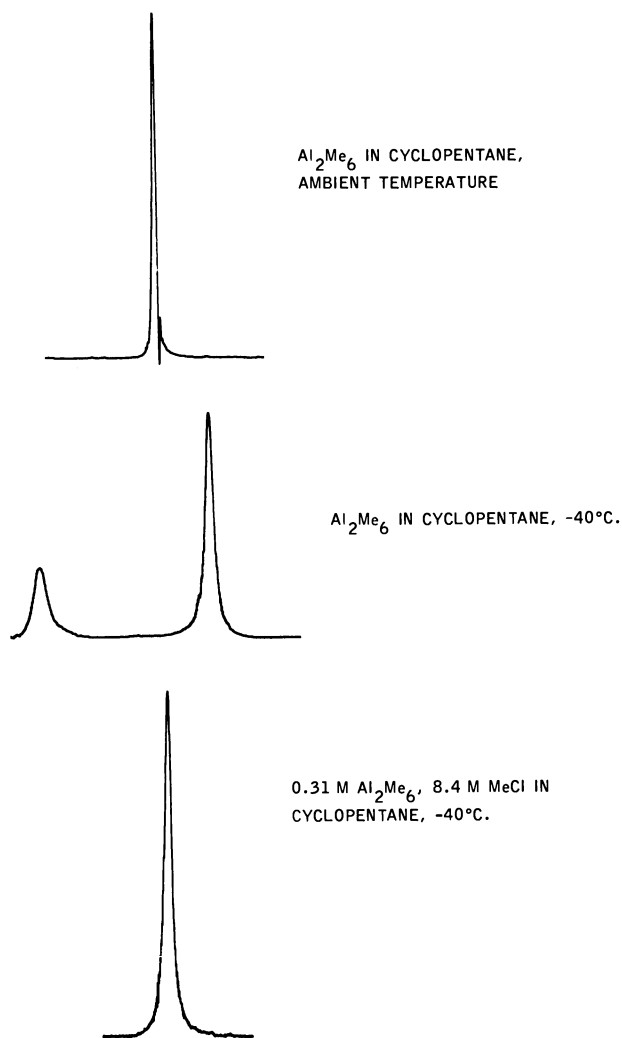
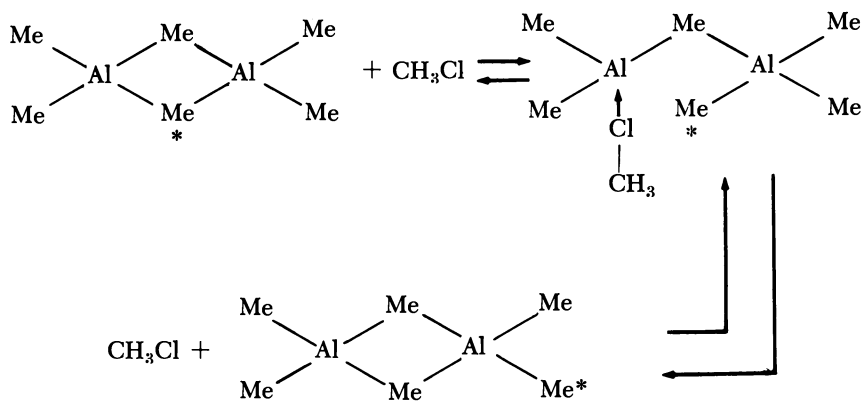


Figure 1. Trimethylaluminum spectra obtained on a Jeolco C60-H NMR spectrometer

molecular exchange of alkyl groups attached to aluminum may involve the collision of a monomer with a dimer or of two dimers.

In our investigation of the NMR spectra of  $\text{AlMe}_3$  and  $\text{Al}i\text{Bu}_3$  in methyl chloride solution at various temperatures, the line width of the methyl signals of  $\text{AlMe}_3$  in solutions of cyclopentane containing various amounts of added methyl chloride were measured, and we obtained values for the chemical shifts of methyl chloride and  $\text{Al}i\text{Bu}_3$  in solutions of these compounds in cyclopentane. In addition we measured the line width of  $\text{AlMe}_3$  in solutions of various Lewis bases.

In preliminary experiments we noted that  $\text{Al}_2\text{Me}_6$  dissolved in  $\text{MeCl}$  exhibits only one reasonably sharp signal in the NMR spectrum at  $-40^\circ\text{C}$ . In contrast, two signals are observed for the methyls attached to aluminum in solutions of  $\text{Al}_2\text{Me}_6$  in cyclopentane at this temperature. The position of the aluminum-methyl signal in  $\text{MeCl}$  solution at  $-40^\circ\text{C}$ . is the same as that in cyclopentane solution of  $\text{Al}_2\text{Me}_6$  at room temperature (Figure 1). Subsequently, we found that at  $-25^\circ\text{C}$ . (a temperature where the rate of methyl exchange in the  $\text{AlMe}_3$  dimer in cyclopentane is less rapid than at room temperature—*i.e.*, where the methyl signal is somewhat broadened but still a single line) the reciprocal of the line width of the methyl signal of  $\text{Al}_2\text{Me}_6$  in cyclopentane solutions depends linearly on the molar concentration of added methyl chloride (Figure 2). In other words, the more methyl chloride that is present, the narrower the single  $\text{Al-CH}_3$  peak at  $\tau = 10.30$  in the NMR spectrum. These observations indicate that methyl group exchange of  $\text{Al}_2\text{Me}_6$  occurs rapidly even at low temperatures in the presence of methyl chloride and that methyl chloride is important in promoting the interconversion of the two types of methyl groups. The following mechanism is proposed to explain the effect of methyl chloride in promoting methyl group exchange in  $\text{Al}_2\text{Me}_6$ :



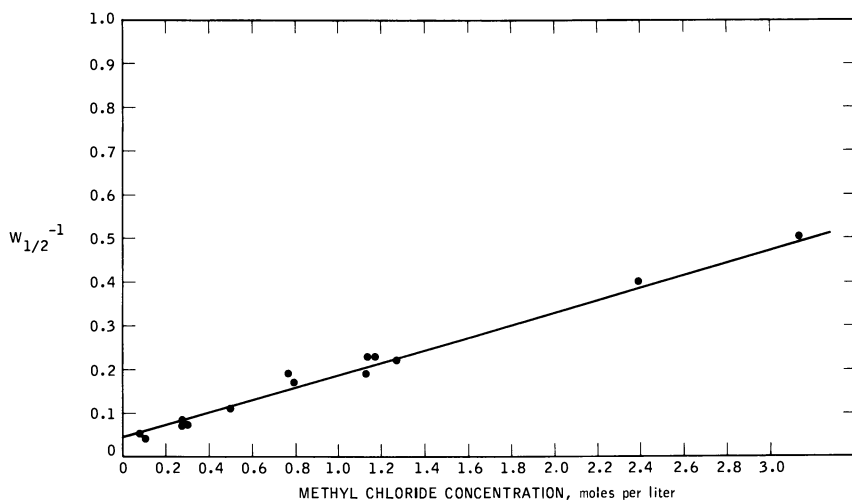


Figure 2. Reciprocal of the line width of trimethylaluminum as a function of methyl chloride concentration at 60 MHz at  $-25^{\circ}\text{C}$ . in cyclopentane solutions

Thus, the  $\text{Al}_2\text{Me}_6$  held together by electron-deficient methyl bridges is opened partially by methyl chloride, and an intermediary single-bridged hypothetical complex,  $\text{Al}_2\text{Me}_6 \cdot \text{MeCl}$  is formed. This complex rearranges readily, resulting in rapid methyl group scrambling. Direct evidence for the interaction between  $\text{Al}_2\text{Me}_6$  and  $\text{MeCl}$  has been obtained and is presented now.

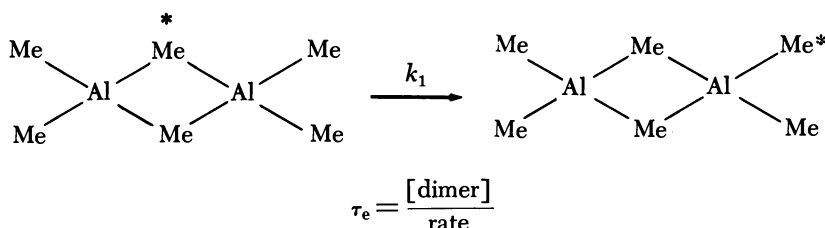
**Interaction between  $\text{Al}_2\text{Me}_6$  and  $\text{MeCl}$  and Evidence for an  $\text{Al}_2\text{Me}_6 \cdot \text{MeCl}$  Complex.** Complex formation between molecules can be detected by accurate chemical shift measurements of protons near the complexing sites. The interaction of a Lewis base such as methyl chloride with an alkylaluminum dimer might also be detected by its effect upon the line-width of the alkyl group even if the amount of complex is very small. For slow exchange of methyl groups between the bridging and terminal positions (two observable signals) of trimethylaluminum dimer solutions in hydrocarbon solvents it has been shown (14) that the  $W_{1/2}$  (the full width at one-half peak height) is related to the average time a methyl spends in one of the two positions ( $\tau_{eA}$ ). This relationship is  $\tau_{eA} = W_{1/2}$  (corr.), where  $W_{1/2}$  (corr.) is the line width ( $W_{1/2}$ ) minus uncertainty and inhomogeneity broadening. For fast methyl exchange (one observable signal) the quantity  $\tau_e$  is defined as

$$\tau_e = \frac{\tau_{eA}\tau_{eB}}{\tau_{eA} + \tau_{eB}}$$

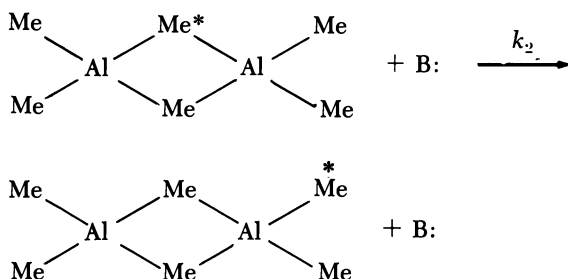
where  $\tau_{eA}$  and  $\tau_{eB}$  are the average times a methyl group spends in a bridging and terminal position, respectively. Furthermore,  $\tau_{eA} = \frac{1}{2}\tau_{eB}$  since there are twice as many terminal as bridging positions. For fast exchange  $\tau_e$  is given by

$$\frac{1}{\tau_e} = \frac{\pi(\Delta\nu)^2}{2W_{1/2}(\text{corr.})}$$

where  $\Delta\nu$  is the difference in chemical shifts of the bridge and terminal methyls in the absence of exchange (14). For an intramolecular exchange process such as shown below,  $\tau_e$  is given by



and therefore  $W_{1/2}$  is independent of [dimer]. In the presence of an added Lewis base [B:] which competes with the above spontaneous process in effecting methyl exchange—*viz.*



$$\tau_e = \frac{[\text{Dimer}]}{k_1[\text{Dimer}] + k_2[\text{Dimer}][\text{B:}]}$$

and therefore

$$k_1 + k_2[\text{B:}] = \frac{\pi(\Delta\nu)^2}{2W_{1/2}(\text{corr.})}$$

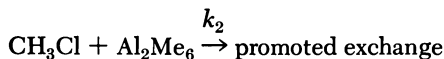
*i.e.*, the reciprocal of the line width would be proportional to the concentration of the Lewis base.

According to our data shown in Table I and Figure 2 the reciprocal of the line width of the exchanging methyl groups of the  $\text{AlMe}_3$  dimer in cyclopentane solvent at  $-25^\circ\text{C}$ . depends linearly on the concentration

**Table I.** NMR Data Obtained from Solutions of Trimethylaluminum and Methyl Chloride in Cyclopentane

[CH <sub>3</sub> Cl]	[Al <sub>2</sub> Me <sub>6</sub> ]	Chemical Shifts of CH <sub>3</sub> Cl, CH <sub>3</sub> Cl-Cyclopentane, Hz. at 100 MHz., Ambient Temp.		
		W <sub>1/2</sub> Al <sub>2</sub> Me <sub>6</sub> , Hz, -25°C.	W <sub>1/2</sub> <sup>-1</sup> , Al <sub>2</sub> Me <sub>6</sub> , Hz <sup>-1</sup> , -25°C.	
0.09	1.65	20.4	0.05	134.7
0.10	0.82	27.6	0.04	134.2
0.28	1.40	14.6	0.07	134.8
0.28	1.50	12.0	0.08	134.9
0.30	0.75	14.1	0.07	134.4
0.50	0.83	9.1	0.11	134.6
0.77	1.50	5.4	0.19	135.4
0.80	1.09	5.9	0.17	135.3
1.13	0.82	5.2	0.19	135.1
1.17	1.40	4.4	0.23	135.9
1.27	0.51	4.5	0.22	135.5
1.37	0.81	4.3	0.23	135.7
2.39	0.84	2.5	0.40	137.0
3.13	1.14	2.0	0.50	137.5
4.23	0.88	1.8	0.56	138.4

of added methyl chloride. This indicates interaction between Al<sub>2</sub>Me<sub>6</sub> and MeCl and the presence of two exchange mechanisms:



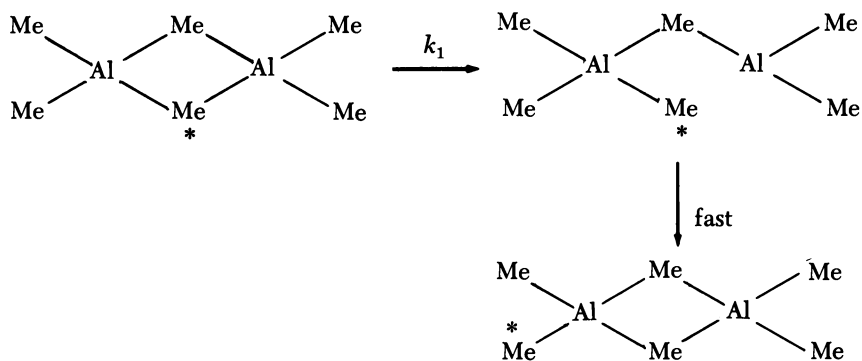
From arguments presented above this scheme requires that

$$k_1 + k_2[\text{CH}_3\text{Cl}] = \frac{\pi(\Delta\nu)^2}{2W_{1/2}}$$

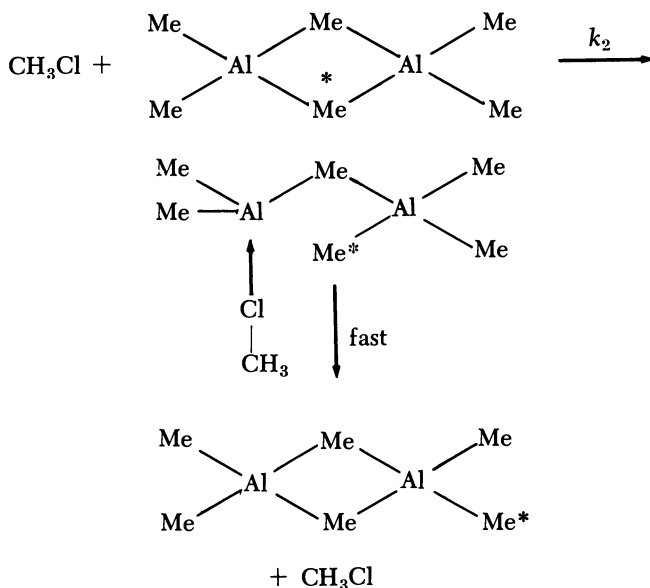
The rate constants,  $k_1$  and  $k_2$ , are calculated from this equation and the line in Figure 2 using the intercept and slope obtained from a least-squares fit for a straight line;

$$k_1 = 366 \text{ sec.}^{-1}, \text{ and } k_2 = 9.9 \times 10^2 \text{ liter/mole/sec.}$$

The value we obtained for  $k_1$  at -25°C. agrees well with that obtained by Ramey *et al.* (14) of 316 sec.<sup>-1</sup> using solutions of trimethylaluminum in cyclopentane. Our scheme therefore is consistent with the experimental data we obtained and with the data which Ramey obtained. We concur with Ramey that the mechanism for the exchange of methyls most likely involves the breaking of one bridge bond:



and suggest furthermore that the methyl chloride interacts with the trimethylaluminum to effect methyl exchange as follows:



The observation that the chemical shift of added methyl chloride in  $\text{Al}_2\text{Me}_6$ -cyclopentane solutions is very close to the chemical shift of the same concentration of methyl chloride in cyclopentane solutions (Figure 3, Tables I and II) indicates that there is little if any  $\text{Al}_2\text{Me}_6 \cdot \text{MeCl}$  complex formed in solutions in cyclopentane. Therefore, the chemical shift of  $\text{MeCl}$  in  $\text{Al}_2\text{Me}_6$ -cyclopentane solutions is a convenient measure of  $\text{MeCl}$  concentration, and the plot of the  $W^{-1/2}$  of  $\text{AlMe}_3$  vs. the chemical shift of  $\text{MeCl}$  in cyclopentane solutions should be linear. This is observed and is illustrated in Figure 4.

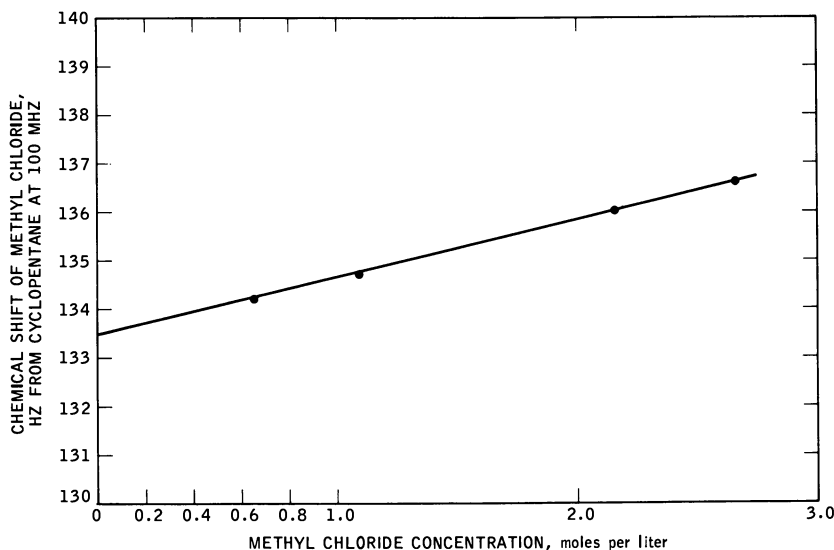


Figure 3. Concentration dependence of the chemical shift of methyl chloride in cyclopentane solutions

Table II. Chemical Shifts of Cyclopentane Solutions of Methyl Chloride

$[CH_3Cl]$	Chemical Shift of $CH_3Cl$ , $CH_3Cl$ -Cyclopentane, Hz. at 100 MHz.
0.65	134.2
1.09	134.7
2.16	136.0
2.66	136.6

While our results indicate clearly an interaction between  $Al_2Me_6$  and methyl chloride, we do not have direct evidence for complex formation. Evidently if a complex such as  $Al_2Me_6 \cdot MeCl$  exists at all, its concentration must be very low. It was theorized that chances to find evidence for the existence of a complex between a trialkylaluminum and methyl chloride would be more successful by using a monomeric trialkylaluminum, such as  $Al-i-Bu_3$ . Experiments with the  $Al-i-Bu_3$ - $MeCl$  system are discussed below.

**Characterization of the  $Al-i-Bu_3$ - $MeCl$  System by NMR.**  $Al-i-Bu_3$  is monomeric in hydrocarbon solutions (1). Evidently the bulky isobutyl groups attached to the aluminum prevent dimerization. Since the size of the chlorine in methyl chloride is certainly much smaller than that of an isobutyl group, we expected complex formation between  $Al-i-Bu_3$  and methyl chloride to occur. To investigate this possibility we prepared



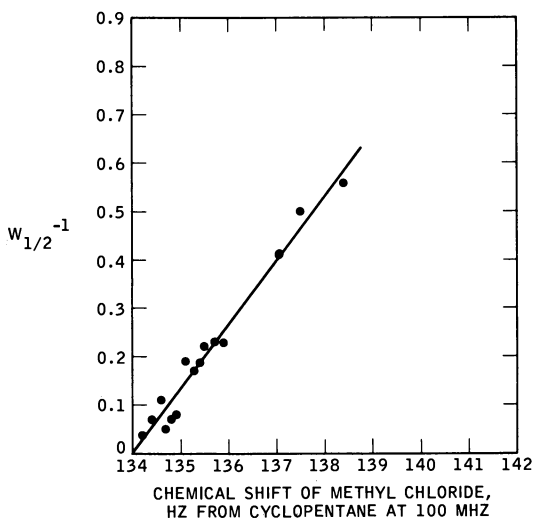


Figure 4. Reciprocal of the line width of trimethylaluminum as a function of the chemical shift of methyl chloride. Measured at  $-25^{\circ}\text{C}$ .; chemical shifts measured at room temperature

Table III. Chemical Shifts of Cyclopentane Solutions of Methyl Chloride and Triisobutylaluminum

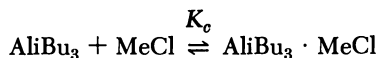
$[\text{CH}_3\text{Cl}]$	$[\text{Al-i-Bu}_3]$	Shift <sup>a</sup> of the Methylene Group of Al-i-Bu <sub>3</sub> , in Cyclopentane, Hz. at 100 MHz.	Shift <sup>a</sup> of Methyl Chloride, in Cyclopentane, Hz. at 100 MHz.
0.10	0.67	-114.7	143.2
0.30	0.66	-115.8	143.2
0.88	0.78	-119.9	142.3
1.10	0.70	-122.0	141.9

<sup>a</sup> Measured from cyclopentane.

solutions of Al-i-Bu<sub>3</sub> in cyclopentane and added various amounts of methyl chloride. Table III and Figures 5 and 6 show our data.

Figure 5 shows the chemical shift of the methylene protons of Al-i-Bu<sub>3</sub> as a function of the ratios of concentrations of  $[\text{Al-i-Bu}_3]/[\text{MeCl}]$  in cyclopentane solution at ambient temperature. The sharp break in the plot at  $\sim 1.7$   $[\text{Al-i-Bu}_3]/[\text{MeCl}]$  suggests complex formation between these compounds. Similarly, the plot of the "corrected" chemical shift of methyl chloride—i.e., the chemical shift of MeCl in Al-i-Bu<sub>3</sub>-cyclopentane solutions minus the chemical shift of MeCl in the same concentration in cyclopentane solutions vs.  $[\text{Al-i-Bu}_3]/[\text{MeCl}]$  (Figure 6), indicate complex formation. Obtaining more chemical shift measurements on

solutions of  $\text{Al}(\text{iBu})_3\text{-MeCl}$  in cyclopentane will lead to the determination of the equilibrium constant  $K_c$  for complex formation.



These results are considered to be strong evidence for complex formation between  $\text{Al}(\text{iBu})_3$  and  $\text{MeCl}$ .

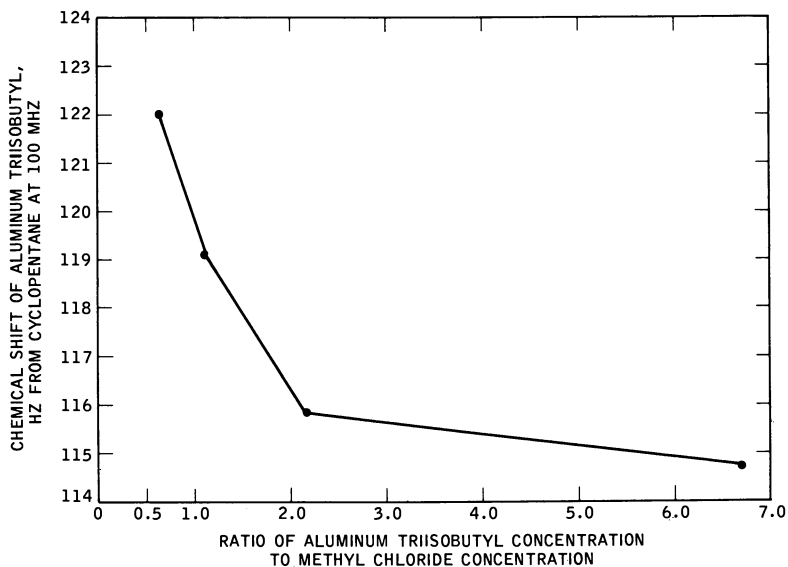


Figure 5. Chemical shift of the methylene protons of triisobutylaluminum as a function of the ratios of concentrations of  $\text{Al}(\text{iBu})_3$  and  $\text{MeCl}$ -cyclopentane solutions

#### Characterizations of Other $\text{Al}_2\text{Me}_6$ -Lewis Base Systems by NMR.

Concurrently with our work with methyl chloride we also investigated a variety of compounds which could be regarded as Lewis bases *vis-a-vis*  $\text{AlMe}_3$ —*e.g.*, ethyl chloride, methylene chloride, isobutylene, styrene, toluene, and butadiene. All these compounds are electron rich because of the presence of chlorine atoms, olefinic unsaturation, or aromatic  $\pi$ -electron systems. It was theorized that, similarly to methyl chloride, these compounds might also enhance the rate of methyl group scrambling in  $\text{Al}_2\text{Me}_6$ . NMR spectra of solutions of  $\text{Al}_2\text{Me}_6$  in these compounds have been obtained at low temperatures, and we have noted that the  $W_{1/2}$  values for the aluminum-methyl signals in these materials are significantly less than that of  $\text{Al}_2\text{Me}_6$  in cyclopentane. Values obtained for  $k_2$  (*see* second reaction scheme on p. 294) using solutions containing these

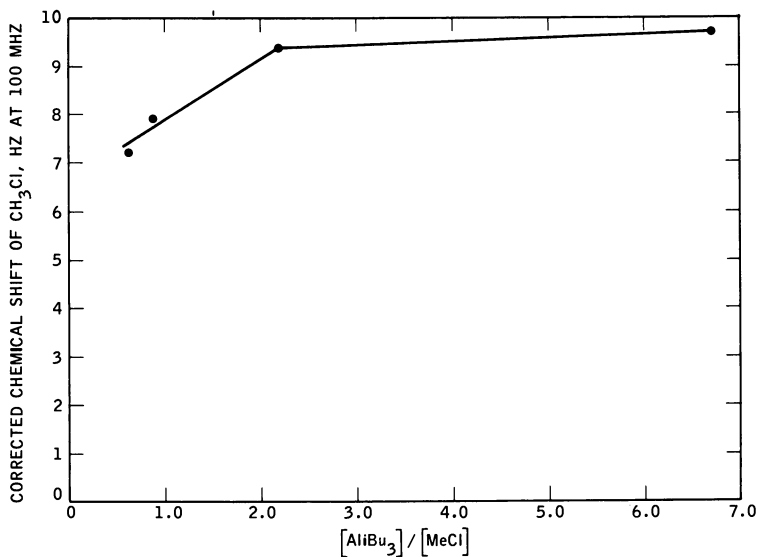


Figure 6. Dependence of the chemical shift of MeCl on AliBu<sub>3</sub>/MeCl ratio

and other Lewis bases may lead to the establishment of a new "basicity" scale for Lewis bases. Such a "basicity" scale would be sensitive not only to electronic effects but also to steric and other factors.

### Conclusion

**A Theory of Initiation and Propagation of Carbonium Ion Polymerizations with Trialkylaluminum Catalysts.** Trialkylaluminums or dialkylaluminum halides in conjunction with suitable cocatalysts in polar solvent are active polymerization catalysts. For example, when cocatalytic amounts of *tert*-butyl chloride are added to a quiescent mixture of trialkylaluminums or dialkylaluminum halides in methyl chloride solvent in the temperature range  $-30^{\circ}$  to  $-100^{\circ}\text{C}$ ., immediate polymerization commences (2, 3, 4, 5, 6).

From this and earlier published results it could be theorized that polymerization initiation involves the "*in situ*" formation of AlCl<sub>3</sub> and/or AlEtCl<sub>2</sub> catalysts from AlR<sub>3</sub> and *tert*-butyl chloride or AlEt<sub>2</sub>Cl and HCl or *tert*-butyl chloride and that one of the former conventional aluminum-containing Friedel-Crafts halides, rather than the AlMe<sub>3</sub>-*tert*-BuCl or AlEt<sub>2</sub>Cl-HCl system, is the active catalytic species. However, several experimental facts speak against this possibility. First, the slopes of the

plots of the log molecular weight ( $MW$ ) of polyisobutylene *vs.*  $1/T$  lines obtained for  $AlCl_3$  and  $AlEt_2Cl$  catalysts on the one hand and  $AlMe_3$  and other trialkyl aluminums (or dialkylaluminum halides) on the other hand are quite different (Figure 7, Refs. 2 and 5). The  $E_{DP}$  (over-all activation energy calculated from the slope of the log  $MW$  *vs.*  $1/T$  plot) is 6.6 kcal./mole for the  $AlCl_3$  and  $AlEt_2Cl$  systems whereas that for the trialkylaluminums and diethylaluminum chloride is 1.7 kcal./mole under essentially identical conditions. If  $AlCl_3$  or  $AlEt_2Cl$  were formed from the latter systems, all the slopes of these lines would be the same—*i.e.*, the effect of temperature on the molecular weights would be the same for all these catalyst systems. Obviously, this is not so, which indicates that the characteristics of these catalysts are in fact dissimilar. The polymerization details (rates, molecular weights, etc.) which are different for the  $AlEt_2Cl/HCl$  system and the conventional  $AlCl_3$  or  $AlEt_2Cl$  systems have been discussed previously (3).

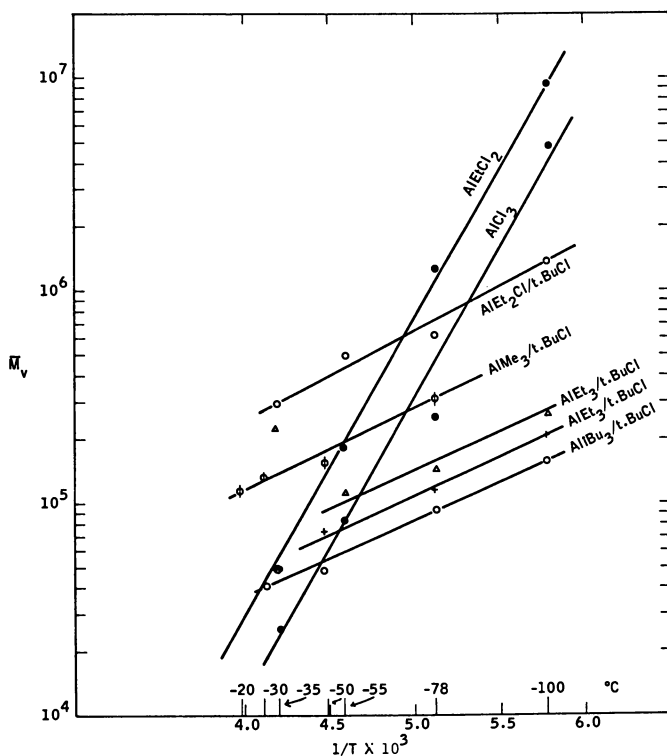
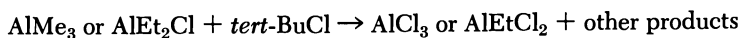


Figure 7. Effect of temperature on the viscosity average molecular weight of polyisobutylene obtained with various aluminum-containing catalyst systems in methyl chloride diluent

Secondly, the  $\text{AlMe}_3$ -*tert*-BuCl catalyst system does not initiate the polymerization of isobutylene in *n*-pentane solvent, whereas  $\text{AlEtCl}_2$  is an efficient catalyst in this solvent.

Thirdly, the cocatalytic amounts of *tert*-butyl chloride required in conjunction with  $\text{AlMe}_3$  or  $\text{AlEt}_2\text{Cl}$  are very small ( $\text{AlMe}_3$  or  $\text{AlEt}_2\text{Cl}$ -*tert*-BuCl  $\leq 10$ ) so that the  $\text{AlCl}_3$  or  $\text{AlEtCl}_2$  which could be formed in the following reaction:



would certainly be insufficient to give the high conversions obtained experimentally.

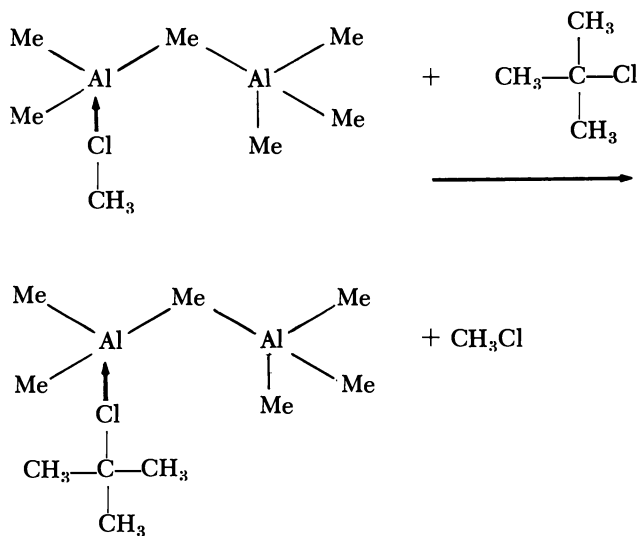
Fourthly, if, as it is usually assumed,  $\text{AlCl}_3$  or  $\text{AlEtCl}_2$  required the presence of cocatalysts presumably in the form of active impurities (*e.g.*,  $\text{H}_2\text{O}$  or  $\text{HCl}$ ) for initiation, it is hard to explain where this cocatalytic impurity would come from since the  $\text{AlR}_3$  or  $\text{AlEt}_2\text{Cl}$  added to the charge would have consumed these active substances before  $\text{AlCl}_3$  or  $\text{AlEtCl}_2$  could have formed.

The different polymerization results obtained with different catalysts in methyl chloride also suggest that the polymerization of isobutylene most likely does not proceed by free ion propagation alone. If free ions were involved in propagation exclusively and the growing species were kinetically independent from the gegenion, products with identical molecular weights would be expected with all these catalysts. Again, this is not observed, which indicates that the gegenion influences the mechanism. Consequently, the concept of associated ion pairs as propagating species must be invoked. Nothing can be said about the nature of this association beyond postulating that the propagating carbonium ions are not entirely free and somehow are influenced by the corresponding gegenions. It is conceivable that associated and free ions coexist and/or are in equilibrium with each other and that this equilibrium is affected by the nature of the solvent, temperature, concentrations, etc.

It is important to emphasize that the  $\text{AlMe}_3$ -*tert*-BuCl system is inactive in *n*-pentane but is very active in methyl chloride solvent as a polymerization catalyst for isobutylene (2). Thus, methyl chloride profoundly affects the active catalytic species in this system. Although the  $\text{AlMe}_3$ -MeCl system is catalytically completely inactive and the addition of *tert*-butyl chloride is necessary to initiate the polymerization of isobutylene, our NMR studies indicate considerable interaction between  $\text{AlMe}_3$  and MeCl.

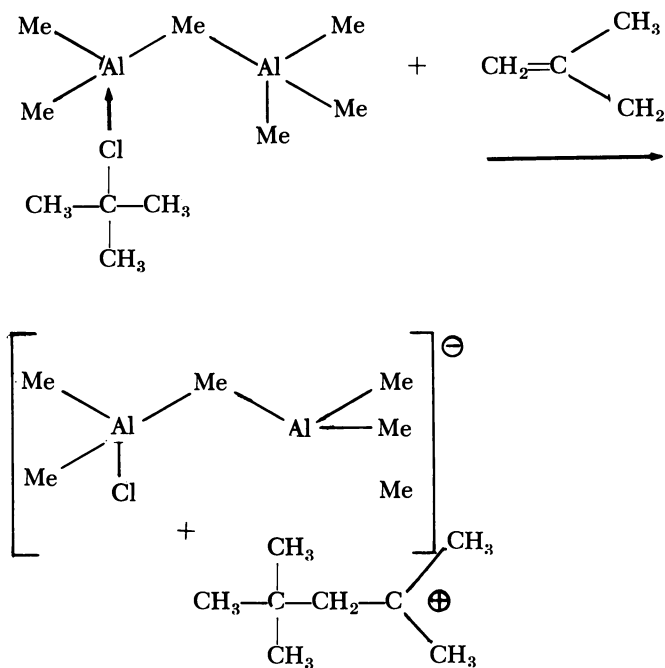
On the basis of these facts the following theory for the initiation of isobutylene polymerization with trialkylaluminums is proposed. At temperatures lower than  $\sim -35^\circ\text{C}$ ., *tert*-butyl chloride does not interact

with  $\text{AlMe}_3$  to the extent that methyl chloride does (7). Conceivably, the *tert*-butyl chloride is able to replace the less basic methyl chloride to form a new complex:



The  $(\text{CH}_3)_3\text{CCl}-\text{Al}_2\text{Me}_6$  bond (complex) should be stronger (more stable) than the  $\text{CH}_3\text{Cl}-\text{Al}_2\text{Me}_6$  bond (complex) because the *tert*-butyl group is a much better electron donor than the methyl group. Conceivably, as the  $(\text{CH}_3)_3\text{CCl}-\text{Al}_2\text{Me}_6$  bond is forming, the  $(\text{CH}_3)_3\text{C}-\text{ClAl}_2\text{Me}_6$  bond is breaking, *i.e.*, an incipient carbonium ion,  $(\text{CH}_3)_3\text{C}^{\oplus}-\text{ClAl}_2\text{Me}_6^{\ominus}$  begins to form. In the presence of a cationically polymerizable olefin this carbonium ion (strong Lewis acid) attacks the monomer (weak Lewis base), and initiation occurs (*see* reaction scheme at top of p. 304). This reaction might be concerted; at the same rate the  $(\text{CH}_3)_3\text{C}^{\oplus}-\text{Cl}^{\ominus}\text{Al}_2\text{Me}_6$  bond is loosened, the  $(\text{CH}_3)_3\text{C}^{\oplus}-\text{C}_4\text{H}_8$  bond is formed; the driving force of the initiation reaction would be the formation of a new C—C bond and a solvated stable ion pair from an unsolvated  $(\text{CH}_3)_3\text{C}-\text{Cl}$  bond and one-half of a double bond. The methyl chloride solvent would help to open the trialkylaluminum dimer and because of its polarity (d.c.  $\sim 15$ ), would solvate and thus stabilize the forming ions. Strong indirect evidence in support of this mechanism is the fact that in the absence of isobutylene, *tert*-butyl chloride yields neopentane (7).

It is of interest to examine the reason for the absence of polymerization in the isobutylene- $\text{Al}_2\text{Me}_6$ -*n*-pentane system. According to our NMR results, methyl group exchange is decidedly faster in the presence of isobutylene than in pure cyclopentane, and consequently if the isobutylene monomer itself is able to interact with  $\text{Al}_2\text{Me}_6$ , by analogy with



methyl chloride, it opens the methyl bridge of  $\text{Al}_2\text{Me}_6$ . Evidently the *tert*-butyl chloride does not displace the isobutylene in the  $\text{C}_4\text{H}_8\text{-Al}_2\text{Me}_6$  complex and initiate the polymerization along the lines proposed above. The reason for this is far from obvious. It could be that the mechanism of methyl group exchange in the  $\text{Al}_2\text{Me}_6\text{-MeCl}$  system is entirely different from that occurring in the  $\text{Al}_2\text{Me}_6\text{-iC}_4\text{H}_8$  system, or that the polar  $\text{MeCl}$  solvent is necessary to solvate the incipient ions because unsolvated species cannot initiate. Further experiments must be performed to answer this question.

### Acknowledgments

We are pleased to acknowledge the help and advice of M. T. Melchior in interpreting NMR spectra.

### Literature Cited

- (1) Hoffman, E. G., *Trans. Faraday Soc.* **58**, 642 (1962).
- (2) Kennedy, J. P., U. S. Patent **3,349,065** (1967).
- (3) Kennedy, J. P., *ACS, Div. Polymer Chem., Polymer Preprints* **7**, 485 (1966).
- (4) Kennedy, J. P., *Intern. Symp. Macromol. Chem., Tokyo, Kyoto, 1966, Abstract* **2.104**.

- (5) Kennedy, J. P., "Polymer Chemistry of Synthetic Elastomers," J. P. Kennedy, E. G. Tornqvist, Eds., Vol. I, Chap. 5A, Wiley, New York, 1968.
- (6) Kennedy, J. P., British Patent **1,094,728** (1967).
- (7) Kennedy, J. P., Melchior, M. T., Milliman, G. E., unpublished results.
- (8) Kennedy, J. P., Thomas, R. M., *ADVAN. CHEM. SER.* **34**, 111 (1962).
- (9) Kennedy, J. P., Thomas, R. M., *J. Polymer Sci.* **45**, 481 (1960).
- (10) McCoy, G. R., Allred, A. L., *J. Am. Chem. Soc.* **84**, 912 (1962).
- (11) Mole, T., *Australian J. Chem.* **18**, 1183 (1965).
- (12) Muller, N., Pritchard, D. E., *J. Am. Chem. Soc.* **82**, 248 (1960).
- (13) Pitzer, K. S., Gutowsky, H. S., *J. Am. Chem. Soc.* **68**, 2204 (1946).
- (14) Ramey, K. C., O'Brien, J. F., Hasegawa, I., Borchert, A. E., *J. Phys. Chem.* **69**, 3418 (1965).
- (15) Williams, K. C., Brown, T. L., *J. Am. Chem. Soc.* **88**, 5460 (1966).

RECEIVED March 11, 1968.



## Stereospecific Polymerization of 1,3-Butadiene Initiated by the Transition Metal $\pi$ -Complexes

V. A. KORMER, B. D. BABITSKIY, and M. I. LOBACH

All-Union Scientific Synthetic Rubber Institute, Leningrad, U.S.S.R.

*The stereospecificity of butadiene polymerization initiated by dimeric  $\pi$ -allylnickel halides depends on the nature of the anion bridges. The formation of cis-1,4 units is favored by chloride complexes; that of trans-1,4 units is favored by iodide complexes. In aqueous medium  $(C_4H_7NiI)_2$  catalyzes butadiene polymerization to the trans-1,4-polymer. Cis-1,4-polybutadiene is produced in presence of the reaction products of  $\pi$ -allylnickel halides and Lewis acids. The stereospecificity of the catalyst is not affected by the nature of the metal atom in the Lewis acid. The mechanism of butadiene polymerization initiated by  $\pi$ -allylnickel halides is discussed. The reactive intermediate in the polymerization catalyzed by  $(C_4H_7NiCl)_2$  or by the reaction products of  $(C_4H_7NiX)_2$  with Lewis acids is presumed to consist of a complex with coordination number 4 containing no halide ligand. The polymerization initiated by  $(C_4H_7NiI)_2$  is presumed to proceed via active complex with the coordination number 5. The reactivity of  $(C_4H_7NiI)_2$  in aqueous medium and the effect of Lewis bases on polymerization process can be interpreted using this assumption. The data reported demonstrate that the polymer microstructure arises from the nature of metal—carbon bonds formed by the transition metal and the growing polymer end.*

**A**lthough the discovery of stereospecific catalysts for olefin polymerization more than a decade ago has led to the development of numerous catalytic systems to produce polymers of different microstructure, the mechanism of catalytic action still remains obscure. The different schemes

proposed to account for controlled propagation are not universally useful since they describe only certain details of the process. The amount of experimental data, sometimes contradictory, indicates that the mechanism of the stereospecific synthesis of polymers is very complex.

The different behavior of the catalysts apparently arises from the nature of the transition metal of the catalyst. It seems reasonable to treat the mechanism of stereospecific olefin polymerization in terms of coordination ionic catalysts, regarding the valence state, coordination number, and nature of ligands of the transition metal as a matter of primary importance. In such an approach the polymerization mechanism is based on the character of metal-carbon bond by which a growing polymer chain is linked to the transition metal.

During olefin polymerization initiated by organometallic complexes the propagating chain is  $\sigma$ -bonded to the transition metal atom. However, for dienes certain conditions might exist (nature of the transition metal, number and nature of ligands, and temperature) where addition of monomer to the polymer chain occurs in a complex with a transition metal in a position allylic to a double bond. Such complexes might rearrange to more stable thermodynamically  $\pi$ -allylic complexes, where all three carbon atoms of the allyl group contribute to the bond with the transition metal atom.

The polymerization of dienes with  $\pi$ -allylic complexes is of great interest since the complexes may be considered as model compounds for a propagating polymer chain.

### *1,3-Butadiene Polymerization Initiated by Bis( $\pi$ -allylnickel Halides)*

Polymerization was carried out in benzene in the presence of bis( $\pi$ -allylnickel halides). The latter were prepared from nickel carbonyl and allyl halide (allyl bromide, crotyl chloride, bromide, or iodide etc.). The results of the polymerization runs are reported in Table I. The data indicate that all of the bis( $\pi$ -allylnickel halides) initiate by themselves the stereospecific butadiene polymerization yielding a polymer with 97–98% 1,4-units. The *cis*-1,4/*trans*-1,4 ratio depends on the halide in the dimeric  $\pi$ -allylnickel halide but not on the nature of allylic ligand. The case of bis( $\pi$ -crotylnickel halides) shows the effect of halide on microstructure, for whereas  $(C_4H_7NiCl)_2$  initiates *cis*-1,4-polybutadiene formation, *trans*-1,4 polymers are produced by  $(C_4H_7NiI)_2$ . The reactivity increase in the series:  $Cl < Br < I$ .

The study also attempted to elucidate the effect of other anions, X, in  $(C_4H_7NiX)_2$  on polymer microstructure. However, none of the complexes with  $X = SCN^-$ ,  $CH_3COO^-$ ,  $CF_3COO^-$ , and  $C_{17}H_{33}COO^-$  initiate

the polymerization alone. [The preparation of these complexes has been reported (19)].

The  $\pi$ -allylic bond is stable against hydrolysis in absence of oxygen (3), and thus the butadiene polymerization initiated by the catalysts mentioned above can be carried out in water. The nature of the halide in bis( $\pi$ -crotylnickel halide) affects the stereospecificity and reactivity of the complex in emulsion polymerization in the same way as in hydrocarbon media (*cf.*, Table II).

**Table I. 1,3-Butadiene Polymerization Initiated by Bis( $\pi$ -allylnickel Halides)<sup>a</sup>**

Catalyst <sup>d</sup>	Catalyst, mmoles	Polymerization Time, hours	Polymer Yield, %	Unit Content, %			$[\eta]$
				1,2	<i>trans</i> -1,4	<i>cis</i> -1,4	
(C <sub>4</sub> H <sub>7</sub> NiCl) <sub>2</sub>	0.3	18	14	2	8	90	0.87 <sup>b</sup>
(C <sub>4</sub> H <sub>7</sub> NiCl) <sub>2</sub>	0.6	12	17	2	10	88	0.46 <sup>b</sup>
[(2-MA)NiCl] <sub>2</sub>	0.62	17	43	2	9	89	
[(1,1-DMA)NiCl] <sub>2</sub>	0.62	17	50	2	9	89	
[(1,3-DMA)NiCl] <sub>2</sub>	0.62	17	22	2	7	91	
[(1-HA)NiCl] <sub>2</sub>	0.62	40	36	2	16	82	
(C <sub>3</sub> H <sub>5</sub> NiBr) <sub>2</sub>	0.26	15	20	3	53	44	
(C <sub>4</sub> H <sub>7</sub> NiBr) <sub>2</sub>	0.37	40	40	2	53	45	
(C <sub>4</sub> H <sub>7</sub> NiI) <sub>2</sub>	0.07	17	58	—	100	—	0.36 <sup>c</sup>
(C <sub>4</sub> H <sub>7</sub> NiI) <sub>2</sub>	1.0	15	100	—	96	4	0.22 <sup>c</sup>

<sup>a</sup> Solvent, benzene; butadiene, 0.2 mole; butadiene concentration, 2.5M; polymerization temperature, 50°C.

<sup>b</sup> In benzene at 20°C.

<sup>c</sup> In cyclohexane at 20°C.

<sup>d</sup> 2-MA = 2-methylallyl, 1,1-DMA = 1,1-dimethylallyl, 1,3-DMA = 1,3-dimethylallyl, 1-HA = 1-isohexenylallyl.

Bis( $\pi$ -crotylnickel chloride) is inactive in water medium; with bromide a low yield of polymer with 50–60% *trans*, 40–50% *cis*-1,4, and 2–3% 1,2-units was obtained. (C<sub>4</sub>H<sub>7</sub>NiI)<sub>2</sub> produces *trans*-1,4-polybutadiene with 14–20% conversion.

The low activity of bromide and inactivity of chloride do not arise from their decomposition since the introduction of the iodide anion into the reaction medium activates the system and transforms its stereospecificity with regard to polymerization in hydrocarbon. Iodide anion addition activates ( $\pi$ -C<sub>4</sub>H<sub>7</sub>NiI)<sub>2</sub> also (Table II).

The emulsifier is not required specifically to obtain polybutadiene in water medium, but the reactivity of the system is affected by the nature of the emulsifier, the nonionic-type reagents producing best results.

**Table II. Emulsion Polymerization of 1,3-Butadiene<sup>a</sup>**

Catalytic System	$(C_4H_7NiX)_2/KI$ , mole ratio	Polymer Yield, %	Unit Content, %		
			1,2	trans 1,4	cis- 1,4
$(C_4H_7NiCl)_2$	—	—	—	—	—
$(C_4H_7NiCl)_2 + KI$	1:6	67	4	82	14
	1:30	85	3	87	10
$(C_4H_7NiBr)_2$	—	6	2	56	42
$(C_4H_7NiBr)_2 + KI$	1:3	28	3	87	10
	1:6	60	3	95	2
	1:30	96	3	86	11
$(C_4H_7NiI)_2$	—	14	2	94	4
$(C_4H_7NiI)_2 + KI$	1:3	26	2	94	4
	1:6	56	2	94	4
	1:30	87	3	89	8

<sup>a</sup> Butadiene, 0.13 mole;  $(C_4H_7NiX)_2$ , 0.35 mmole;  $C_4H_6/H_2O = 1:2$  (wt.); Emulsifier (Tween 80), 5% wt. to monomer. Polymerization temperature, 50°C.; Polymerization time, 17 hours.

### ***1,3-Butadiene Polymerization Initiated by the Catalysts Prepared from Bis( $\pi$ -crotylnickel Halides) and Lewis Acids***

The interaction of bis( $\pi$ -crotylnickel halides) and Lewis acids (B, Al, Ti, V, Mo, W halides, etc.) results in formation of products which are insoluble in hydrocarbons. The compounds initiate stereospecific butadiene polymerization to polymers whose structure is unaffected by the nature of the halide in the initial complex or by the nature of metal in the Lewis acids. The reactivity of the catalysts is higher than that of corresponding bis( $\pi$ -crotylnickel halides) (*cf.*, Table III).

The cis content of polymer obtained with catalysts based on bis( $\pi$ -crotylnickel chloride) and Lewis acids amounts to the same value as for bis( $\pi$ -crotylnickel chloride) only. The stereospecificity of bis( $\pi$ -crotylnickel bromide) and iodide is changed by introducing Lewis acids, and polymers of high cis content are obtained with these catalysts. All Lewis acids favor cis-1,4 polymer formation although the nature of halide affects the phenomenon slightly. Iodine-containing catalysts generally provide polymers with lower cis content than polymers obtained with chloride complexes. The stereospecificity is unaffected by the nature of acidoligand as was demonstrated by polymerization on catalytic system  $(C_4H_7NiX)_2 + TiCl_4$  ( $X = SCN^-$ ,  $CH_3COO^-$ ,  $CF_3COO^-$ ,  $C_{17}H_{33}COO^-$ ) (*cf.*, Table IV).

**Mechanism of Butadiene Polymerization Initiated by  $\pi$ -allylic Complexes**

The "non-classic" structure of  $\pi$ -allylic complexes means that a substituted  $\pi$ -allylic group could exist in two isomer forms (syn and anti). The formation of definite structure depends on the nature of ligands in the inner coordination sphere of the central atom.

**Table III. 1,3-Butadiene Polymerization Initiated by Catalytic Systems of Bis( $\pi$ -crotylnickel Halide) + Lewis Acid<sup>a</sup>**

Catalytic System	T, °C.	Time, hours	Polymer Yield, %	Unit Content, %			
				1,2	trans-1,4	cis-1,4	
$(C_4H_7NiCl)_2 + TiCl_4$	20	1	81	3	5	92	
	+ $VCl_4$	20	0.5	32	2	7	91
	+ $AlCl_3$	30	0.5	70	2	8	90
	+ $MoCl_5$	50	17	82	4	6	90
	+ $WCl_6$	50	15	75	3	7	90
	+ $BCl_3$	30	17	38	2	10	88
	+ $TiBr_4$	20	2	52	3	8	89
	+ $TiI_4$	50	17	60	3	22	75
$(C_4H_7NiBr)_2 + TiCl_4$	20	0.25	51	3	8	89	
	+ $TiBr_4$	30	17	70	3	10	87
	+ $TiI_4$	50	11	70	3	23	74
	+ $AlBr_3$	20	0.5	71	3	13	84
	+ $VCl_4$	30	17	53	4	7	89
	+ $MoCl_5$	30	17	66	2	3	95
	+ $WCl_6$	50	17	90	4	8	88
	$(C_4H_7NiI)_2 + TiCl_4$	20	0.5	86	3	6	91
+ $TiBr_4$		50	25	16	3	20	77
+ $TiI_4$		50	40	11	3	22	75
+ $AlBr_3$		20	6	50	4	22	74
+ $VCl_4$		50	40	56	3	10	87
+ $SnCl_4$		50	37	15	3	6	91
+ $MoCl_5$		50	17	70	6	7	87
$(C_4H_7NiCl)_2 + TiCl_4$		50	18	3 <sup>b</sup>	2	7	91
$(C_4H_7NiI)_2 + TiCl_4$	50	5	13 <sup>b</sup>	3	6	91	

<sup>a</sup> Solvent, benzene;  $(C_4H_7NiX)_2$ , 2.5 mmoles/liter; butadiene, 2.5M;  $(C_4H_7NiX)_2$ /Lewis acid = 1:2 (moles).

<sup>b</sup> Solvent, mesitylene.

In previous publications (7, 14, 17) it was presumed that the microstructure of the ultimate unit of the polybutadiene chain arose from the mode of its attachment to the central atom in the  $\pi$ -allylic complex, so that the syn (or anti) isomer yielded *trans*- (or *cis*)-1,4-enchainment.

**Table IV. 1,3-Butadiene Polymerization Initiated by Catalytic Systems of  $(C_4H_7NiX)_2 + TiCl_4$** 

$\pi$ -Allylic Complex	T, °C.	Time, hours <sup>a</sup>	Polymer Yield, %	Unit Content, %		
				1,2	trans-1,4	cis-1,4
$(C_4H_7NiSCN)_2$	30	2.5	20	2	19	79
	50	17	93	2	27	71
$(C_4H_7NiOOCF_3)_2$	50	18	18	4	9	87
$(C_4H_7NiOOCCH_3)_2$	50	18	90	3	6	91
$(C_4H_7NiOOC_{17}H_{33})_2$	50	18	75	3	6	91

<sup>a</sup> For other polymerization conditions see Table III.

It was demonstrated recently by NMR spectra and by hydrogenation of bis( $\pi$ -crotylnickel halides) that whatever the halogen might be, the  $\pi$ -crotyl group takes the syn configuration (10, 15).

The authors suggested that the structure of bis(syn- $\pi$ -crotylnickel chloride) is inconsistent with the assumed mechanism of cis unit formation. From our point of view the apparent contradiction does not prove anything since in the reactive intermediate the nickel atom might not be linked with halide ligands. Different stereospecificity and reactivity of  $(C_4H_7NiCl)_2$  and  $(C_4H_7NiI)_2$  in hydrocarbon and water media indicate that the nature of active sites is not the same in both cases.

However, the structural identity of polybutadienes prepared with bis( $\pi$ -crotylnickel chloride) and with  $(C_4H_7NiX)_2^+$  Lewis acids system suggests that the nature of the active sites is similar for these catalysts.

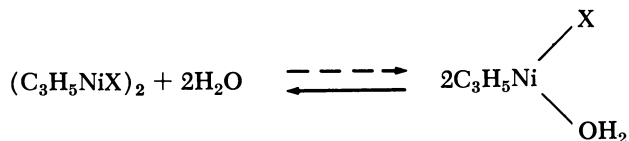
According to several workers (8, 9, 18) the interaction of Lewis acids and crotylnickel halides involves transfer of a halide from the  $\pi$ -allylic complex to metal halide



where X = halide (or another univalent anion); L = monomer or solvent molecule.

The scheme is supported by experimental evidence since the nature of halide or Lewis acid does not contribute to the stereospecificity of catalyst. The retardation of polymerization by this catalyst in the presence of a donor stronger than benzene (mesitylene) also is consistent with this view.

The stability of halide bridges in dimeric  $\pi$ -allylic complexes against the action of bases depends on the nature of the halogen; the chloride complexes are the least stable. According to Burger (3) the dimers of bis( $\pi$ -allylnickel halides) are hydrolyzed with destruction of bridges and monohydrate formation.

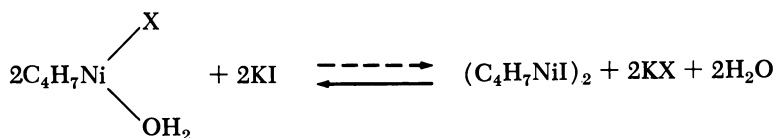


Our results indicate that the transition of bis( $\pi$ -crotylnickel halides) from the hydrocarbon layer into water decreases in the order:



Water phase of the same volume extracts at 20°C. from benzene solution 35% of  $(\text{C}_4\text{H}_7\text{NiCl})_2$ , 26.5%  $(\text{C}_4\text{H}_7\text{NiBr})_2$  and 8.7%  $(\text{C}_4\text{H}_7\text{NiI})_2$  when the initial concentration in benzene is 0.083M and 50%, 39.3% and 17% at an initial concentration of 0.033M.

The nickel content in water decreases strongly on adding potassium, sodium, or lithium iodides. At KI and  $(\text{C}_4\text{H}_7\text{NiCl})_2$  and  $(\text{C}_4\text{H}_7\text{NiBr})_2$  concentrations of 0.033M the nickel content in hydrocarbon phase amounts to 90–95% whereas KCl addition decreases the nickel concentration in water by only 5–10%. The results demonstrate the exchange according to the following reaction.



Thus, the butadiene polymerization in water medium initiated by the catalytic system KI +  $(\text{C}_4\text{H}_7\text{NiX})_2$  (X = Cl, Br) is apparently effected by bis( $\pi$ -crotylnickel iodide). The reactivity and stereospecificity of the latter arise evidently from the stability of iodide bridges to hydrolysis.

Taking into account the lability of the dimer with chloride bridges we suggest that butadiene attacks the bis( $\pi$ -crotylnickel chloride) with destruction of the halide bridges and formation of complexes like those formed by the interaction of crotylnickel halide with Lewis bases:



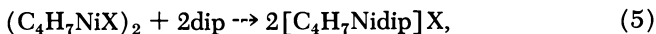
or



The reaction of bis( $\pi$ -crotylnickel halides) with  $\alpha, \alpha'$ -dipyridyl, *o*-phenanthroline, and ethylenediamine provides evidence for this assumption. The type of the complex formed depends on the components ratio —*e.g.*,



and



where X = Cl, Br, J.

Orgel, Chatt *et al.* (4, 5, 6, 16) assumed that the activation energy of transition complex formation is lowered by the strong trans effect of ligands in initial square-planar complex. The transition state is regarded as a five-coordinate complex produced by the bimolecular reaction of the initial complex with a reactant. The trans effect is known to decrease in the order: I > Br > Cl (12). The high catalytic activity of the  $(C_4H_7NiI)_2$  in aqueous medium is caused presumably by the formation of a transition complex with coordination number 5 arising from the catalyst-monomer interaction.

Since the electron density of nickel in bis( $\pi$ -crotylnickel iodide) is high, the formation of five-coordinate complexes is favored for compounds with vacant orbitals readily attached by dative bonds (11). The bases might be classed into two types by this characteristic:

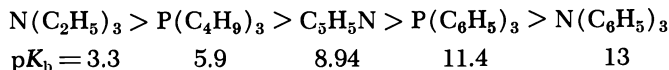
(1) Bases without  $\pi$ - or  $d$ -orbitals which cannot form dative bonds—*e.g.*,  $H_2O$ ,  $Et_2O$ ,  $R_3N$  etc.

(2) Ligands with  $\pi$ - or  $d$ -orbitals—*e.g.*, pyridine, phosphines, etc.

The first class does not affect the polymerization process initiated by  $(C_4H_7NiI)_2$  as demonstrated by polymerization in the presence of  $NR_3$  (with R =  $C_2H_5^-$  or  $C_6H_5^-$ ) in the range of ratios  $(C_4H_7NiI)_2 : NR_3$  from 1:1 to 1:6 (Figure 1).

Bases of the second class decrease the catalyst activity. The polymer yield obtained with bis( $\pi$ -crotylnickel iodide) is significantly higher than that produced by catalysts  $(C_4H_7NiI)_2 + 2B$  [B = pyridine,  $P(C_6H_5)_3$  and  $P(C_4H_9)_3$ ].

The sequence of basicity of the reagents we studied is as follows (1, 13):



The series does not correspond to an inhibiting effect (Figure 1); thus, retardation arises from the donor-acceptor properties of the ligands and not their basicity.

The probability of monomer coordination in the 5th position and the catalytic activity of  $(C_4H_7NiI)_2$  strongly decreases in the presence of electron acceptors—*e.g.*,  $PCl_3$ , *p*-chloroanisole, *p*-iodoanisole etc.

The high catalytic activity of  $[C_4H_7NiD]$   $[C_4H_7NiI_2]$  complexes obtained by the reaction of equimolar quantities of  $(C_4H_7NiI)_2$  and diamines (D =  $\alpha, \alpha'$ -dipyridyl, *o*-phenanthroline, ethylenediamine) demonstrates that the butadiene polymerization may occur at a nickel atom substituted by two iodines.



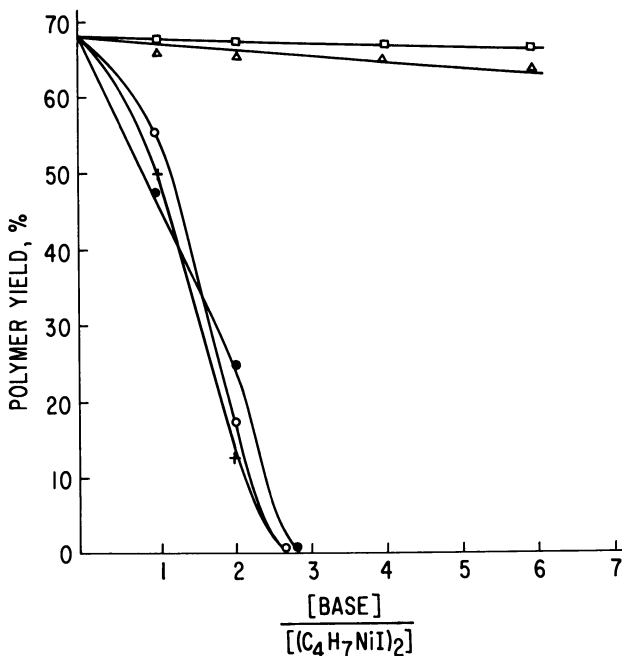


Figure 1. The influence of bases on 1,3-butadiene polymerization initiated by  $(C_4H_7NiI)_2$  in benzene solution. Catalyst concentration, 3 mmoles/liter; polymerization temperature, 50°C.; polymerization time, 15 hours

- $N(C_2H_5)_3$
- △  $N(C_6H_5)_3$
- $C_5H_5N$
- +  $P(C_4H_9)_3$
- $P(C_6H_5)_3$

Our experimental finding supports the view that the active site of butadiene polymerization in the presence of bis( $\pi$ -crotylnickel iodide) is the complex with nickel bound to iodide. Thus, the butadiene addition across syn- $\pi$ -allylic bond produces *trans*-1,4-polybutadiene.

The active center formed by the interaction of butadiene with bis( $\pi$ -crotylnickel chloride) or the products of the reaction of  $(C_4H_7NiX)_2 +$  Lewis acids does not contain halides, and there is no steric hindrance for syn complex to be isomerized into an anti complex, which is more stable thermodynamically according to Bank (2).

The microstructure of polybutadienes prepared with  $\pi$ -allylnickel complexes does not depend on the details of monomer coordination if one of the double bonds is involved (1,2- or *trans*-1,4-structures) or both (*cis*-1,4 structure). This fact is confirmed by results obtained with homogeneous catalytic systems based on  $(C_4H_7NiCl)_2$  and  $GaCl_3$  in

chlorobenzene giving *cis*-1,4-polybutadiene. The reaction of bis( $\pi$ -crotyl-nickel chloride) with  $\text{GaCl}_3$  proceeds according to Reaction 1 and results in the formation of a four-coordinate square-planar complex; two coordinates of the metal atom are occupied by  $\pi$ -allylic ligands, and the other two are free. Introduction of one phosphine or phosphite molecule into the inner coordination sphere does not change the stereospecificity of the catalyst (Table V), although the number of vacant coordinates is reduced to one.

**Table V. 1,3-Butadiene Polymerization Initiated by Catalytic System of  $(\text{C}_4\text{H}_7\text{NiCl})_2 + \text{GaCl}_3^a$**

Catalytic System	Compo- nents, mole ratio	T, °C.	Time, hours	Polymer Yield, %	Unit Content, %		
					1,2	<i>trans</i> - 1,4	<i>cis</i> - 1,4
$(\text{C}_4\text{H}_7\text{NiCl})_2 + \text{GaCl}_3$	1:2	2	1	73	—	22	78
$(\text{C}_4\text{H}_7\text{NiCl})_2 + \text{GaCl}_3 + \text{P}(\text{C}_6\text{H}_5)_3$	1:2:2	5	18	70	6	30	64
$(\text{C}_4\text{H}_7\text{NiCl})_2 + \text{GaCl}_3 + \text{P}(\text{OC}_6\text{H}_5)_3$	1:2:2	2	1,5	76	2	19	79
$(\text{C}_4\text{H}_7\text{NiCl})_2 + \text{GaCl}_3 + \text{P}(\text{C}_4\text{H}_9)_3$	1:2:2	5	18	54	6	24	70
$(\text{C}_4\text{H}_7\text{NiCl})_2 + \text{GaCl}_3 + \text{P}(\text{C}_4\text{H}_9)_3$	1:2:4	50	48	—	—	—	—

<sup>a</sup> Solvent, chlorobenzene;  $(\text{C}_4\text{H}_7\text{NiCl})_2$ , 3 mmoles/liter; butadiene, 2.5M.

In this case it is possible for butadiene to coordinate to nickel by one double bond; it is improbable that a weak base like butadiene would be able to convert a  $\pi$ -allyl group into a  $\sigma$ -group. The 5th coordinate is not realized in this case; no catalytic activity is observed if two phosphine molecules are bonded to the nickel. Our results are confirmed by Wilke's *et al.* work (20, 21) on butadiene polymerization in the presence of  $[\text{C}_3\text{H}_5\text{NiP}(\text{C}_6\text{H}_{11})_3] [\text{AlCl}_4]$  in chlorobenzene.

Our experimental data enable us to state that the microstructure of diene polymers obtained with  $\pi$ -allylic systems depends on the character of metal-carbon bonds between the transition metal and the growing chain end.

**Literature Cited**

- (1) Albert, A., Sergent, E., "Ionization Constants of Acids and Bases," *Chimiya*, Moscow, 1964.
- (2) Bank, S., Schriesheim, A., Rowe, C. A., *J. Am. Chem. Soc.* **87**, 3244 (1965).
- (3) Bürger, G., Ph.D. Thesis, Universität, München, 1962.
- (4) Cardwell, H., *Chem. Ind. (London)* **1955**, 422.
- (5) Chatt, J., Duncanson, L. A., Venanzi, L. M., *Chem. Ind. (London)* **1955**, 749.
- (6) Chatt, J., Duncanson, L. A., Venanzi, L. M., *J. Chem. Soc.* **1955**, 4456.
- (7) Dolgoplosk, B. A., Babitsky, B. D., Kormer, V. A., Lobach, M. I., Tinyakova, E. I., *Dokl. Akad. Nauk SSSR* **164**, 1300 (1965).
- (8) Fischer, E. O., Fichtel, K., *Chem. Ber.* **94**, 1200 (1961).
- (9) *Ibid.*, **95**, 2063 (1962).
- (10) Frolov, V. M., Volkov, A. V., Parenago, O. P., Dolgoplosk, B. A., *Dokl. Akad. Nauk SSSR* **177**, 1359 (1967).
- (11) Gray, H. B., *J. Am. Chem. Soc.* **84**, 1550 (1962).
- (12) Grinberg, A. A., "Introduction to the Chemistry of Coordination Compounds," *Chimiya*, Moscow, 1966.
- (13) Hudson, R. F., "Structure and Mechanism in Organo-Phosphorus Chemistry," *Mir*, Moscow, 1967.
- (14) Kormer, V. A., Babitsky, B. D., Lobach, M. I., Chesnokova, N. N., *Proc. Intern. Symp. Macromol. Chem., Prague, 1965, Preprint* 413.
- (15) Matsumoto, T., Furukawa, Y., *J. Polymer Sci.* **5B**, 935 (1967).
- (16) Orgel, L. E., *J. Inorg. Nucl. Chem.* **2**, 137 (1956).
- (17) Otsuka, S., Kawakami, M., *Koguo Kagaku Zasshi* **68**, 874 (1965).
- (18) Porri, L., Natta, G., Galazzi, M. C., *Proc. Intern. Symp. Macromol. Chem., Prague, 1965, Preprint* 494.
- (19) Simanova, N. P., Lobach, M. I., Babitsky, B. D., Kormer, V. A., *Vysokomol. Soed.* **10B**, 588 (1968).
- (20) Wilke, G., *Proc. Robert A. Welch Foundation Conf. Chem. Res., 9th, Organometal. Compounds, Houston, 1965*, p. 165.
- (21) Wilke, G., Bogdanovic, B., Hardt, P., Heimbach, P., Keim, W., Kröner, M., Oberkirch, W., Tanaka, K., Steinrücke, E., Walter, D., Zimmermann, H., *Angew. Chem.* **78**, 157 (1966).

RECEIVED March 18, 1968.

# Mechanisms for Initiating Polymerization by Stable Organic Cations

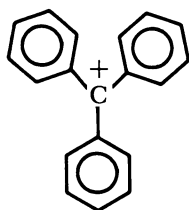
A. LEDWITH

Donnan Laboratories, University of Liverpool, Liverpool 7, England

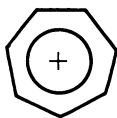
*Use of triphenylmethyl and cycloheptatrienyl cations as initiators for cationic polymerization provides a convenient method for estimating the absolute reactivity of free ions and ion pairs as propagating intermediates. Mechanisms for the polymerization of vinyl alkyl ethers, N-vinylcarbazole, and tetrahydrofuran, initiated by these reagents, are discussed in detail. Free ions are shown to be much more reactive than ion pairs in most cases, but for hydride abstraction from THF, triphenylmethyl cation is less reactive than its ion pair with hexachlorantimonate ion. Propagation rate coefficients ( $k_p$ ) for free ion polymerization of isobutyl vinyl ether and N-vinylcarbazole have been determined in  $\text{CH}_2\text{Cl}_2$ , and for the latter monomer the value of  $k_p$  is  $10^5$  times greater than that for the corresponding free radical polymerization.*

During the past five years we have shown that many stable organic cations are useful initiators for polymerizing reactive olefins and cyclic ethers (1, 2, 3, 4, 5, 27). Compared with more common initiators for cationic polymerization (31), the stable salts allow for complete characterization of the catalyst system and give rapid, highly reproducible polymerizations. In addition many of the salts used are stable indefinitely in the crystalline state, which makes the experimental techniques easy and convenient.

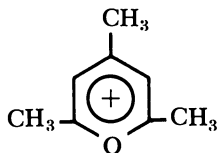
Stabilization of an organic cation occurs whenever the electron-deficient carbon atom is conjugated with aryl groups or with atoms containing unshared pairs of electrons such as oxygen, nitrogen, or sulfur (7). Examples of cations which are useful in polymerization include triphenylmethyl (I), cycloheptatrienyl (tropylium) (II), and various alkyl (III), aryl (IV), and benzopyrylium (V, VI) derivatives.



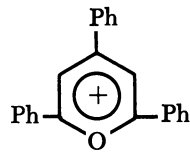
I



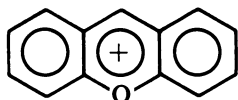
II



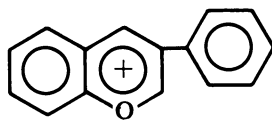
III



IV

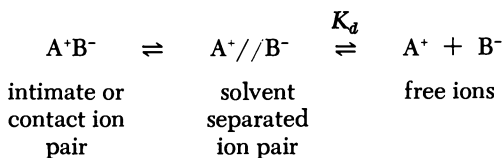


V



VI

Ionic materials ( $A^+B^-$ ) display ion pair dissociation equilibria, and the value of the dissociation constant ( $K_d$ ) varies according to the nature of  $A^+$ ,  $B^-$ , and the dissociating ability of solvents used—*e.g.*,



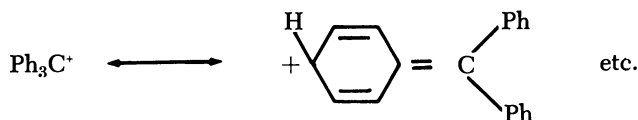
In some cases it is possible to estimate the fraction of solvent-separated ion pairs in equilibrium with contact ion pairs and free ions (37, 43), but conductance measurements yield values for  $K_d$  only. For most cationic (32) and anionic (37) polymerizations it is now clear that the reactivity of free ions is several orders of magnitude greater than that of corresponding ion pairs. Consequently, it is necessary to know  $K_d$  to be able to interpret correctly the reactivity in any ionic polymerization. Table I shows values of  $K_d$  for typical stable organic cations.

This article reviews the experimental evidence, accumulated in our laboratory, relating to different mechanisms involved in reactions of trityl and tropylium ions with reactive olefins and cyclic ethers and outlines the probable effect of ion pair equilibria on these reactions.

### *Polymerization of Alkyl Vinyl Ethers*

**Initiation with Triphenylmethyl Cation.** Triphenylmethyl (trityl) cation derives its stability (7, 30) from resonance between the electro-

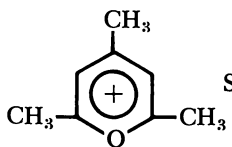
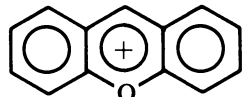
philic carbon atom and the aryl substituents:



This cation can be derived from many different precursors, and we have found the hexachloroantimonate ( $\text{SbCl}_6^-$ ) to be the most stable of the crystalline salts toward hydrolysis and thermal decomposition. Consequently  $\text{Ph}_3\text{C}^+\text{SbCl}_6^-$  has been used throughout this work.

Trityl ion effectively initiates polymerization of olefins having strongly electron-releasing substituents, especially vinyl alkyl ethers (2, 16),

**Table I. Ion-Pair Dissociation Constants ( $K_d$ )<sup>b</sup> for Hexachloroantimonate Salts of Stable Organic Cations in  $\text{CH}_2\text{Cl}_2$  (34)**

Salt	Temp., °C.	$10^4 K_d$ , M
$\text{Ph}_3\text{C}^+\text{SbCl}_6^-$	25	1.9
	0	3.1
	-45	5.3
$\text{Ph}_3\text{C}^+\text{SbCl}_6^-$	25	1.4 <sup>a</sup>
	-45	2.9 <sup>a</sup>
$\text{C}_7\text{H}_7^+\text{SbCl}_6^-$	0	0.3
	-45	0.7
$\left[ \begin{array}{c} \text{CH}_3 \\   \\ \text{Ph}-\text{N}-\text{CH}_2\text{Ph} \\   \\ \text{CH}_3 \end{array} \right]^+\text{SbCl}_6^-$	0	0.6
	-45	1.3
$(\text{C}_2\text{H}_5)_4\text{N}^+\text{SbCl}_6^-$	0	0.7
	-45	1.2
 $\text{SbCl}_6^-$	0	0.6
	-45	0.9
 $\text{SbCl}_6^-$	25	0.1
	0	0.2

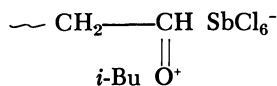
<sup>a</sup> Ref. 22.

<sup>b</sup>  $K_d$  was evaluated according to the procedure described by Szwarc (37). Conductance was measured under high vacuum with computerized evaluation of the data.

*N*-vinylcarbazole, and styrenes (9, 19). Tritylhexachloroantimonate ( $\text{Ph}_3\text{C}^+\text{SbCl}_6^-$ ) dissolves readily in  $\text{CH}_2\text{Cl}_2$ , and in this solvent it is a very effective initiator for polymerizing isobutyl vinyl ether. The polymerizations are completely homogeneous, and reaction rates have been measured by an adiabatic calorimetric technique (8). Initiation is rapid and essentially complete before significant conversion occurs. Termination appears not to be a complicating factor at low temperatures, and hence the rate measurements give an estimate of the propagation rate coefficient,  $k_p$ , from the rate expression:

$$\frac{-d(\text{monomer})}{dt} = k_p[\text{monomer}][\text{Ph}_3\text{C}^+\text{SbCl}_6^-]$$

where  $k_p = 1.5 \times 10^3 M^{-1} \text{ sec}^{-1}$  at  $-25^\circ\text{C}$ . and  $E_a = 6 \text{ kcal./mole}$ . These kinetic measurements were made with isobutyl vinyl ether in the concentration range  $10^{-1}$  to  $10^{-2} M$  and with the concentration of catalyst,  $\text{Ph}_3\text{C}^+\text{SbCl}_6^-$ , in the range  $10^{-4}$  to  $10^{-6} M$ . The ion pair dissociation constant ( $K_d$ ) for  $\text{Ph}_3\text{C}^+\text{SbCl}_6^-$  in  $\text{CH}_2\text{Cl}_2$  at  $-25^\circ\text{C}$ . was measured (Table I) and found to be  $\sim 4 \times 10^{-4} M$ . It follows, therefore, that for the concentrations of salt used as initiator, dissociation into free ions will occur to at least 90% of the amount of salt added. Ion pair dissociation constants for the propagating species:

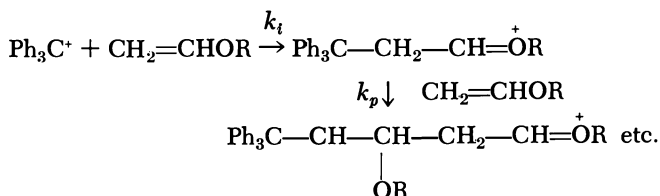


would not be expected to differ by more than one order of magnitude from the values reported in Table I for triphenylmethyl and carbononium salts, and therefore, polymerization of isobutyl vinyl ether initiated in this manner yields propagating species which are largely free cations. The value of  $k_p$ , therefore, relates to the reaction of free cation with monomer. [The experimental data reported here were obtained in a high vacuum apparatus free from greased stopcocks. The solvent  $\text{CH}_2\text{Cl}_2$  was used within 12 hours of final purification (under vacuum) because of deterioration caused by the glass surface.]

Radiation-induced polymerization of isobutyl vinyl ether in bulk leads to an estimate (42) for  $k_p$  of  $10^5 M^{-1} \text{ sec}^{-1}$  at  $30^\circ\text{C}$ . with  $E_a = 6 \text{ kcal./mole}$ . This value, extrapolated to the temperatures used in the present work, yields an estimate of  $k_p$  within one order of magnitude of that now reported. Considering the experimental problems in these vastly different techniques, and the fact that different solvents are involved, such agreement is remarkable and provides support for the assumptions made to evaluate  $k_p$ .

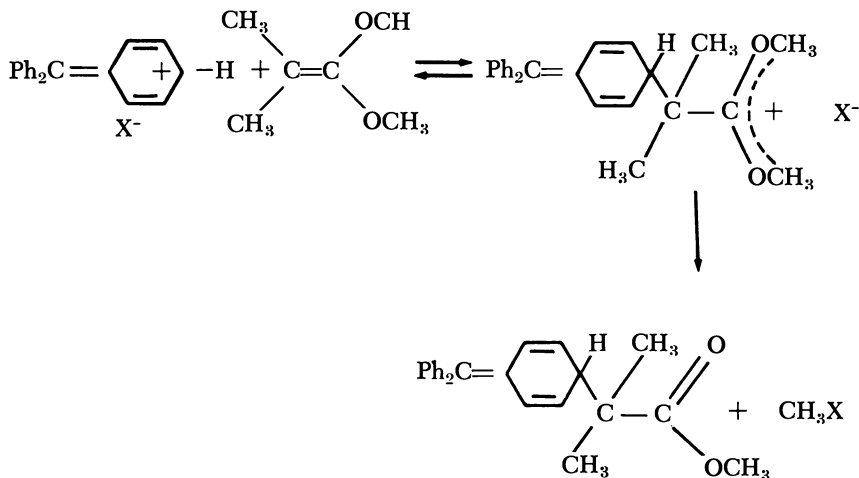
Poly(vinyl isobutyl ether) obtained this way is the typical, low molecular weight, ( $MW = 2000\text{--}8000$ ) amorphous material normally

obtained by homogeneous polymerization. Extensive monomer transfer accounts for the low molecular weights and may be confirmed readily by crude column chromatographic fractionations of polymers prepared with high catalyst concentrations. Aryl end groups are readily detected (by infrared analysis) in some of the fractions but not in others. Significantly, triphenylmethane can not be detected even by GLC analysis, and hence it must be concluded that initiation involves *addition* of trityl cation to the reactive olefin:



It is apparent from the kinetic measurements that  $k_i$  is not significantly less than  $k_p$  for vinyl isobutyl ether, as expected (12) from the greater thermodynamic stability of, for example,  $\text{CH}_3\text{CH}^+\text{OCH}_2\text{CH}_3$  over  $\text{Ph}_3\text{C}^+$ .

As represented above the initiation of vinyl ether polymerization by trityl salts involves reaction of the olefin with the aliphatic carbon atom. It is worth noting, however, that Magee, Winstein, and Heck (18) have shown previously that trityl cation reacts with the related olefin  $(\text{CH}_3)_2\text{C}=\text{C}(\text{OCH}_3)_2$  exclusively in the 4-position of one of the aromatic rings:

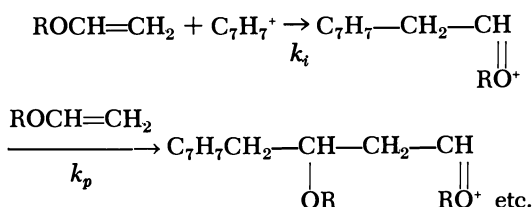


Undoubtedly the latter reaction is one in which steric factors dominate, although the extent to which ion pairing is a contributing cause has not

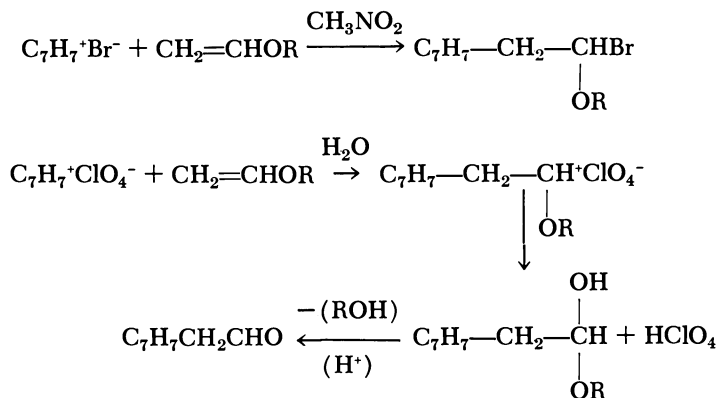


been characterized. Reactivity of trityl cation in the 4-position has also been reported by Kampmeier and his collaborators (23).

**Initiation with Tropylium Ion.** Tropylium hexachlorantimonate reacts with vinyl alkyl ethers in a manner very similar to the reactions of triphenylmethyl salts. Again, rapid initiation is followed by propagation without apparent termination. Termination can be demonstrated to be absent from experiments in which fresh samples of monomer are added to completed polymerizations, whereupon the measured reaction rates parallel those previously recorded (Table II). Molecular weights of the polymers from isobutyl vinyl ether are very similar to those obtained with triphenylmethyl salts as initiators and again give clear evidence for excessive monomer transfer. Gas chromatographic analysis of the reaction mixtures showed that cycloheptatriene (product of hydride abstraction) was not present which indicates clearly that initiation must arise *via* addition of the tropylium ion to the vinyl ether—*i.e.*,



Russian workers (26) have demonstrated that tropylium ion will add to vinyl ethers as indicated below, providing support for the proposed initiation reaction.



As with triphenylmethyl salts, the hexachlorantimonate derivative of tropylium ion is by far the most convenient to handle and to use as a catalyst. In this case, thermal decomposition or hydrolysis of the tropylium salt is almost nonexistent under ordinary conditions, and the catalyst can be prepared conveniently, purified, and stored over long

**Table II. Polymerization of Isobutyl Vinyl Ether with  $C_7H_7^+SbCl_6^-$  in  $CH_2Cl_2$  at  $-25^\circ C$ .**

$[C_7H_7^+SbCl_6^-], M$	$[i-BuOCH=CH_2], 10^2 M$	$10^2 R_p, M \text{ sec.}^{-1}$	MW
7.57	5.52	0.62	3200 <sup>b</sup>
		0.66 <sup>a</sup>	3160 <sup>c</sup>
8.58	5.52	0.75	3100 <sup>b</sup>
		0.74 <sup>a</sup>	3300 <sup>c</sup>

<sup>a</sup> Measured rate of polymerization on adding a second sample of monomer so that  $[i-BuOCH=CH_2]$  was the same as in the initial run.

<sup>b</sup> Molecular weight of a sample prepared independently under identical conditions.

<sup>c</sup> Molecular weight of total polymer yield from successive polymerizations.

periods without change. Detailed kinetic studies on the polymerization of isobutyl vinyl ether (17) demonstrated that the reaction followed the pattern displayed by triphenylmethyl salt initiation and yielded a value for the propagation rate coefficient  $k_p = 2.0 \times 10^3 M^{-1} \text{ sec.}^{-1}$  at  $-25^\circ C$ . This value agrees closely with that obtained from polymerizations initiated by trityl hexachlorantimonate. From the value of the ion pair dissociation constant for  $C_7H_7^+SbCl_6^-$  (Table I) it can be concluded that the initiator is dissociated largely into free ions at the catalyst concentrations employed ( $10^{-4}$  to  $10^{-6} M$ ). The observed close correspondence between values of  $k_p$  obtained for polymerizations initiated by trityl and tropylium ions confirms the conclusions regarding free ion as the propagating species.

### *Polymerization of Tetrahydrofuran*

**Initiation with Triphenylmethyl Cation.** When tetrahydrofuran (THF) is used to dissolve triphenylmethyl hexachlorantimonate at room temperature, there is almost immediate decomposition of the triphenylmethyl cation (6). On the other hand, solutions of the trityl salt in THF can be prepared and stored as deep yellow solutions if maintained at temperatures around  $-80^\circ C$ . At room temperature the initial decoloration of the catalyst is followed rapidly by polymerization of the monomer to poly(tetramethylene oxide), and the actual percentage conversion depends markedly on the temperature. This behavior is typical of systems exhibiting monomer-polymer equilibria (28), and Table III shows values for the equilibrium conversion of monomeric THF to polymeric THF obtained with a variety of catalysts. As for vinyl ether polymerization, it is most convenient to use the trityl hexachlorantimonate salt; however, recourse to Table III shows clearly that above room temperature this anion yields less than the expected equilibrium conversion monomer

to polymer. The true equilibrium conversions for THF polymerization were first demonstrated by Dreyfuss and Dreyfuss (13, 14) using *p*-chlorophenyl diazonium cation as initiator with hexafluorophosphate anion. In later studies (5) we showed that triphenylmethyl hexafluorophosphate similarly yielded the expected equilibrium conversion of monomeric THF, and apparently there is little termination in these systems. Reasons for the lower equilibrium conversion of monomer to polymer when hexachlorantimonate is the gegenion remain to be decided. However, it is clear that it is the anion which contributes to the decay in active centers and to the transfer which occurs because initiation with triphenylmethyl hexachlorantimonate in the presence of inert tetraalkylammonium hexafluorophosphate gives increased conversion and increased molecular weight (5).

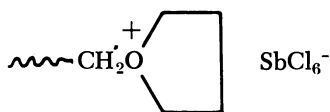
**Table III. Equilibrium Conversion of Monomeric THF to Polymer (Bulk Polymerization)**

<i>Catalyst</i>	<i>Temp., °C.</i>	<i>Polymer at Equilibrium, %</i>
Ph <sub>3</sub> C <sup>+</sup> SbCl <sub>6</sub> <sup>-</sup>	50	43
Ph <sub>3</sub> C <sup>+</sup> PF <sub>6</sub> <sup>-</sup>	50	56
Ph <sub>3</sub> C <sup>+</sup> AsF <sub>6</sub> <sup>-</sup>	50	57
Ph <sub>3</sub> C <sup>+</sup> SbCl <sub>6</sub> <sup>-</sup>	25	73
Ph <sub>3</sub> C <sup>+</sup> PF <sub>6</sub> <sup>-</sup>	25	77
C <sub>7</sub> H <sub>7</sub> <sup>+</sup> SbCl <sub>6</sub> <sup>-</sup>	50	55
PhCO <sup>+</sup> SbCl <sub>6</sub> <sup>-</sup>	50	54
Xanthylum <sup>+</sup> SbCl <sub>6</sub> <sup>-</sup>	50	55
Xanthylum <sup>+</sup> ClO <sub>4</sub> <sup>-</sup>	50	55
Xanthylum <sup>+</sup> FeCl <sub>4</sub> <sup>-</sup>	50	32
( <i>p</i> )ClC <sub>6</sub> H <sub>4</sub> N <sub>2</sub> <sup>+</sup> PF <sub>6</sub> <sup>-</sup>	50	56 <sup>21</sup>
PF <sub>5</sub>	50	56 <sup>22</sup>

Kinetic studies (6) of the polymerization of bulk THF with trityl hexachlorantimonate have established the rate expression:

$$\frac{-d(\text{THF})}{dt} = k_p [\text{THF}] [\text{Ph}_3\text{C}^+\text{SbCl}_6^-]$$

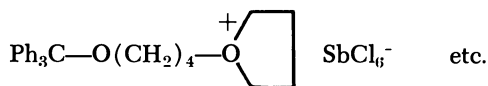
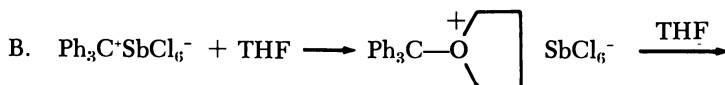
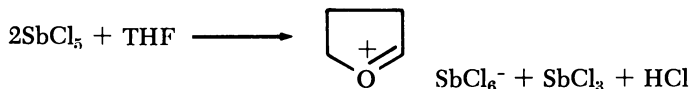
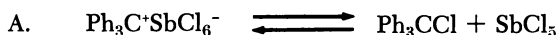
where  $k_p = 1.4 \times 10^{-2} M^{-1} \text{sec}^{-1}$  at 50°C., and  $E_a = 12 \text{ kcal./mole}$ . This value for  $k_p$  compares favorably with corresponding values reported by Vofsi and Tobolsky (40) and Rozenberg *et al.* (33) using BF<sub>4</sub><sup>-</sup> as counterion. From the treatment of Denison and Ramsey (11) and the value of  $K_d$  (Table I) in CH<sub>2</sub>Cl<sub>2</sub> it can be estimated that at the catalyst concentrations employed ( $\sim 10^{-3} M$ ), trityl hexachlorantimonate exists largely as ion pairs in pure THF. The value of  $k_p$  reported above might relate, therefore, to reactions of oxonium ion pairs:



and contrasts sharply with that for free ion propagation in the not unrelated vinyl ether systems—*e.g.*,  $\sim\text{CH}_2-\text{CH}$ .



There are three possible primary reactions leading to initiation of polymerization:

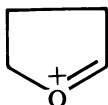


Reaction A was discounted because of the observed kinetic rate expression (6),

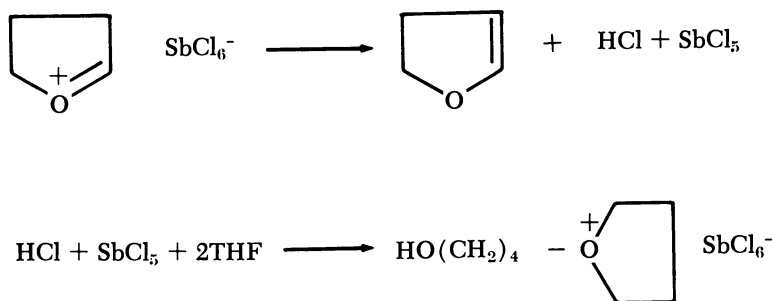
$$\frac{d(\text{Polymer})}{dt} = k_p [\text{THF}] [\text{Ph}_3\text{C}^+\text{SbCl}_6^-]$$

Kuntz (24) demonstrated by NMR techniques that hydride ion transfer (Reaction C) was occurring during polymerization of THF with triphenylmethyl hexachlorantimonate. In more recent work (17), we have shown that the product triphenylmethane can be detected readily by GLC from reaction mixtures allowed to reach equilibration at high temperatures and may be isolated in > 80% yield by chromatography

on neutral alumina. These observations clearly demonstrate that hydride ion transfer (Reaction C) is the predominant reaction when triphenylmethyl salts interact with THF. The fate of the cyclic carboxonium ion:



is less easy to define. One possibility is instant elimination to a dihydrofuran producing HCl and  $\text{SbCl}_5$  which could then function as initiating molecules:



This idea was first suggested by Dreyfuss *et al.* (15) but still requires confirmation for typical polymerization conditions. In recent months, we have studied in detail (41) the kinetics of the reaction between the colored triphenylmethyl salt and THF at temperatures which are much too low for significant polymerization. Reactions were followed spectrophotometrically and demonstrate clearly that in bulk THF solvent the reaction between triphenylmethyl cation and monomeric THF is rapid even as low as  $-40^\circ\text{C}$ . A clean first-order kinetic decay of  $[\text{Ph}_3\text{C}^+\text{SbCl}_6^-]$  was observed, and evaluated rate coefficients are shown in Table IV. The enthalpy of activation for the process was 10 kcal./mole, and GLC analysis of the mixtures even at the lowest temperatures shows clearly that triphenylmethane is formed directly in the decoloration step. Specifically, the reaction between triphenylmethyl hexachlorantimonate and THF in pure THF yields triphenylmethane directly even at temperatures as low as  $-40^\circ\text{C}$ ., at which point there is little or no polymerization. Although formation of triphenylmethane is rapid at low temperatures, initiation of polymerization is somewhat slower, as indicated by the slight initial curvature of typical kinetic curves at temperatures above ambient, and more dramatically by Kuntz and Melchior (25), who demonstrated significant cocatalysis by small amounts of epoxides. Cocatalysis of the polymerization of THF using trityl hexachloroantimonate was effected

conveniently by using propylene oxide, and the cocatalytic effect decreases rapidly with increasing temperature. Additionally, cocatalysis by propylene oxide eliminates the dark colors which are normally observed

**Table IV. Reaction of  $\text{Ph}_3\text{C}^+\text{SbCl}_6^-$  with Pure THF<sup>b</sup>**

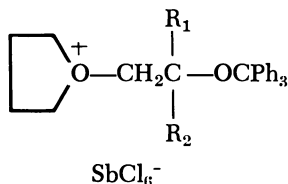
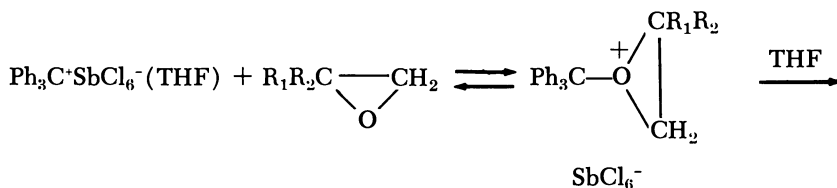
Temp., °C.	$10^3 k$ (observed) <sup>a, c</sup> sec. <sup>-1</sup>
-50	0.79 ± 0.08
-40	2.0 ± 0.2
-33	4.17 ± 0.08
-25	7.8 ± 1.0

<sup>a</sup> Apparent first-order rate coefficients averaged over many kinetic runs in which  $[\text{Ph}_3\text{C}^+\text{SbCl}_6^-]$  varied between  $10^{-4}$  and  $10^{-3}M$ .

<sup>b</sup> Bulk THF  $\equiv 12.3M$  at 25°C.

<sup>c</sup> Reaction rates were followed spectrophotometrically by observing the disappearance of absorption caused by  $\text{Ph}_3\text{C}^+$  at 412 nm.

during the early stages of trityl initiated polymerizations. Kuntz and Melchior (25) suggest, therefore, that propylene oxide functions by reacting directly with trityl ion to give a reactive cyclic oxonium ion in a manner similar to that suggested as initiation reaction B.



Evidence for this suggestion was obtained by NMR spectroscopy of reacting mixtures which showed that triphenylmethane formation was almost eliminated and a trityl ether unit formed when the reaction systems contained propylene oxide. While this interpretation is consistent with most of the experimental work published, Kuntz and Melchior (25) also report that cocatalysis by propylene oxide can be observed when the latter is added several hours after the start of polymeriza-

tion. Consequently, it is likely that the true "dormant" species in these polymerizations has not yet been characterized.

Dynamic equilibrium between trityl cation and THF (Reaction B) could not be demonstrated in pure THF as solvent (41) but has been characterized successfully (10) in methylene chloride solutions (Table V), for THF, tetrahydropyran, and 1,4-dioxane.

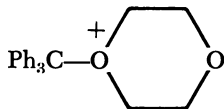
**Table V. Association Constants ( $K_e$ ) for Oxonium Ion Equilibria of  $\text{Ph}_3\text{C}^+\text{SbCl}_6^-$  in  $\text{CH}_2\text{Cl}_2$  at 25.0°C.**

<i>Ether</i> <sup>b</sup>	$K_e$ , <sup>a</sup> $M^{-1}$
Tetrahydrofuran	3.7
Tetrahydrofuran	2.0
1,4-Dioxane	0.5

<sup>a</sup>  $K_e = [\text{Oxonium ion}]_e / [\text{Ph}_3\text{C}^+]_e [\text{Ether}]_e$ , where  $[\text{Ph}_3\text{C}^+]_e$  represents the corrected value for free ion obtained using  $K_d$  from Table I. (Initially  $[\text{Ph}_3\text{C}^+\text{SbCl}_6^-] \approx 2.5 \times 10^{-4} M$ ).

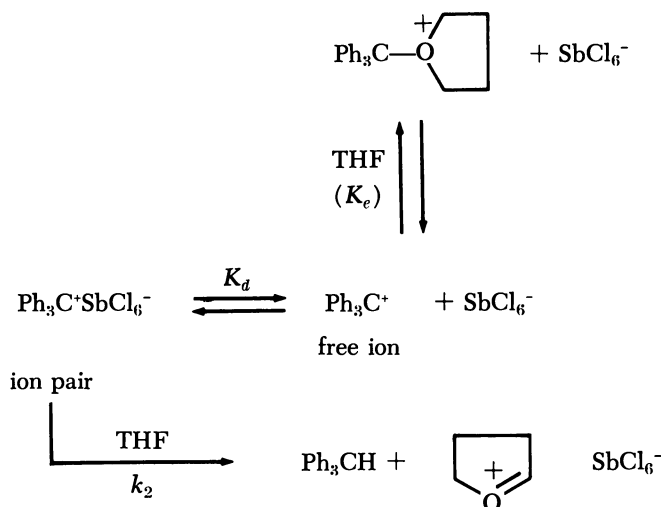
<sup>b</sup>  $[\text{Ether}]$  varied in the range 0.3 to 1.0M.

Dioxane gave the most stable system, and with this ether it was possible to demonstrate dynamic equilibrium by raising and lowering the temperature (Table VI). In addition low temperature quenching ( $\text{H}_2\text{O}$ ) of a  $\text{Ph}_3\text{C}^+\text{SbCl}_6^-$ -dioxane system in  $\text{CH}_2\text{Cl}_2$ , such that > 90% of the trityl content was in the form of colorless oxonium ion:



gave a quantitative recovery of all the trityl content as triphenylcarbinol. This result shows that hydride ion transfer (forming  $\text{Ph}_3\text{CH}$ ) was not significant under the reaction conditions and confirms the proposed oxonium ion equilibrium.

For all three cyclic ethers there was a concurrent slow decay of the equilibrium trityl ion concentration leading to formation of triphenylmethane (Reaction C). Thus, in  $\text{CH}_2\text{Cl}_2$ , Reactions B and C occur simultaneously whereas only C is significant in pure THF. Since for  $10^{-4} M$  solution of  $\text{Ph}_3\text{C}^+\text{SbCl}_6^-$ , the salt is > 80% dissociated into free ions in  $\text{CH}_2\text{Cl}_2$  and almost completely associated as ion pairs in pure THF, oxonium ion equilibria involving trityl cation are important only for the free ion. The ion pair reacts preferentially as a hydride abstracting reagent—*i.e.*,



Decay of  $\text{Ph}_3\text{C}^+$  (*i.e.*, formation of  $\text{Ph}_3\text{CH}$ ) follows the rate expression

$$-\frac{d[\text{Ph}_3\text{C}^+]}{dt} = k_2[\text{Ph}_3\text{C}^+\text{SbCl}_6^-][\text{THF}]$$

for both  $\text{CH}_2\text{Cl}_2$  and THF solvents. Extrapolated values of  $k_2$  at  $25^\circ\text{C}$ . are  $21 \times 10^{-3} \text{M}^{-1} \text{sec}^{-1}$  in pure THF and  $6 \pm 3 \times 10^{-3} \text{M}^{-1} \text{sec}^{-1}$  in  $\text{CH}_2\text{Cl}_2$  with  $[\text{THF}] = 0.4 \text{M}$ . Allowing for the probable errors involved in the extrapolation and the fact that two different solvents are involved, it must be concluded that free trityl ion is much less reactive than its ion pair in hydride abstraction from THF. Clearly, this has important

**Table VI. Variation in Absorbance with Temperature for the Equilibrium between  $\text{Ph}_3\text{C}^+\text{SbCl}_6^-$  and 1,4-Dioxane (0.31M) in  $\text{CH}_2\text{Cl}_2$**

Temp., $^\circ\text{C}$ .	Optical Density (OD) <sub>e</sub>	$10^4$ [Total trityl ion] <sub>e</sub> M <sup>a</sup>
25	2.040 <sup>b</sup>	2.55 <sup>b</sup>
25	1.890	2.36
0	1.660	2.16
25	1.895	2.37
-35	1.195	1.38
25	1.780	2.22

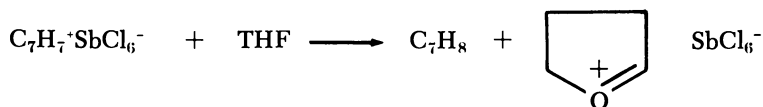
<sup>a</sup> [Total trityl ion]<sub>e</sub> =  $[\text{Ph}_3\text{C}^+]_e + [\text{Ph}_3\text{C}^+\text{SbCl}_6^-]_e$ , values are corrected for density change and quoted as at  $25^\circ\text{C}$ . The sealed system was cooled and reheated in the sequence shown descending the first column.

<sup>b</sup> Before adding dioxane.



consequences for considerations of initiator efficiency and cocatalysis in polymerization of cyclic ethers.

**Initiation with Tropylium Ion.** When cycloheptatrienyl hexachlorantimonate is used as initiator for tetrahydrofuran polymerization, the reactions are somewhat cleaner, and strong colors do not develop as readily as when the corresponding trityl salts are used (17). Rates of initiation are much lower, and the reaction is hardly noticeable at room temperature. However, at 50°C. and above initiation is significant, and the polymerizations proceed almost to the expected theoretical conversion of monomer to polymer even when hexachlorantimonate is the anion (Table III). Therefore, the apparent low equilibrium conversion obtained with the rapidly initiating trityl salts is minimized in this case by the comparatively low rate of consumption of initiator. Once again GLC demonstrates clearly that the initiation reaction involves primarily hydride abstraction from the ether.



Cycloheptatriene ( $\text{C}_7\text{H}_8$ ) is detected readily by GLC, but as before the fate of the cyclic carboxonium ion remains enigmatic. Nevertheless, polymerization of THF proceeds smoothly and reproducibly especially at temperatures above 50°C. Other workers (36) have used triphenylmethyl salts to polymerize trioxane, and the general conclusion remains that hydride abstraction is a primary initiation process, although in all cases there is no clear evidence for the fate of carboxonium ion formed.

### *Polymerization of N-Vinylcarbazole*

Carbazole, like most aromatic amines, oxidizes readily *via* electron transfer. We recognized early that electron transfer may be an important initiation process for polymerizing the *N*-vinyl derivative. Some years ago we showed (29) that cycloheptatrienyl cation could act as an efficient one-electron transfer reagent, producing the appropriate cation radicals from reactive amines such as phenothiazine and tetramethyl-*p*-phenylenediamine. It was also suggested that the product of the reaction between cycloheptatrienyl cation and carbazole itself was the carbazole cation radical. However, our recent work (21) has demonstrated that one-electron oxidation of carbazole leads directly to the 3,3-dicarbazoyle cation radical (VII).

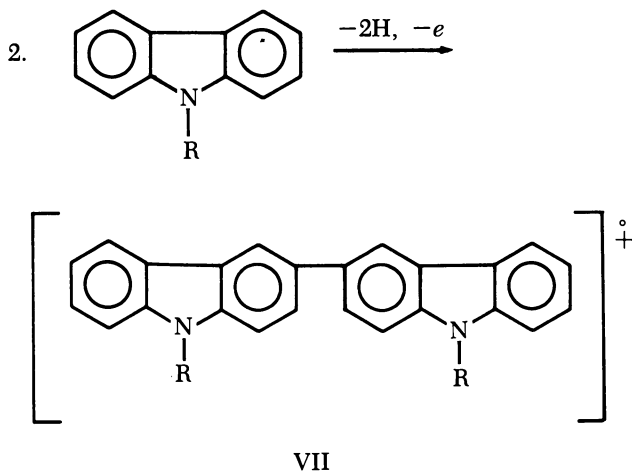


Table VII. Polymerization of *N*-Vinylcarbazole by  $C_7H_7^+SbCl_6^-$  in  $CH_2Cl_2$

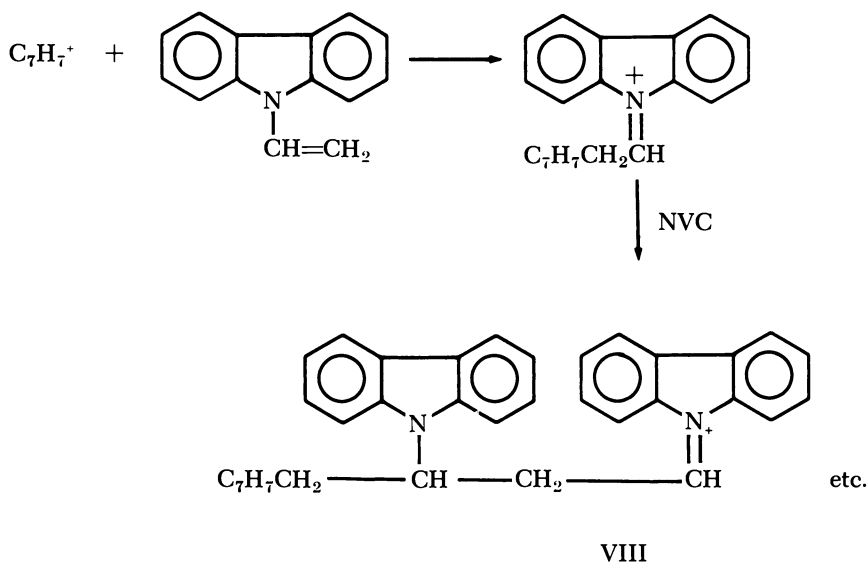
Temp., °C.	[Cat.] $10^6M$	[NVC], $10^2M$	Rate ( $R_p$ ), $M \text{ sec.}^{-1}$	$10^{-5} k_p^a$ $M^{-1} \text{ sec.}^{-1}$	Viscosity Av. Mol. Wt. <sup>b</sup> ( $\times 10^{-5}$ )
0	0.987	5.39	2.60	4.88	2.59
	0.987	5.40	2.42	4.53	1.68
	0.750	5.40	1.97	4.87	1.92
	1.00	2.70	1.15	4.27	1.38
	1.00	4.04	1.87	4.63	1.85
-25	2.00	5.40	1.42	1.31	10.2
	1.75	5.39	1.90	2.01	9.00
	1.50	5.40	1.09	1.35	8.83
	1.00	5.39	0.703	1.30	8.57

<sup>a</sup> Calculated from the rate expression  $R_p = k_p[NVC][C_7H_7^+SbCl_6^-]$ .

<sup>b</sup> Estimated from measurements of intrinsic viscosity in benzene at 25°C. (38).

This in no way detracts from the proved ability of the cycloheptatrienyl cation to oxidize reactive amines, and consequently there is always doubt as to the true nature of the reaction mechanism when tropylium ion initiates polymerization of *N*-vinylcarbazole. We have made a detailed kinetic study of this polymerization (34), using an adiabatic calorimetric technique. Some typical data are shown in Table VII. Initiation is instantaneous and complete, there is no termination, and  $k_p$  is evaluated readily as  $4.6 \times 10^5 M^{-1} \text{ sec.}^{-1}$  at 0°C. with  $E_a = 6 \text{ kcal./mole}$ . By comparing data for the ion pair dissociation constant of  $C_7H_7^+SbCl_6^-$  (Table I) with the catalyst concentrations employed (Table VII) it is apparent that free tropylium ions are the dominant initiating species. It

is also probable that free immonium ions (VIII) are the propagating entities—*i.e.*,



Initiation is represented as simple addition of trolylium ion to the monomer double bond by analogy with reactions of alkyl vinyl ethers.

The value of  $k_p$  now reported for propagation by free cation is approximately five orders of magnitude greater than that for the corresponding free radical reaction in THF (20). Similar differences have already been noted for free cation (42) and free anion (37) propagation of styrene.

Use of stable organic cations to initiate cationic polymerization allows characterization of free ions and ion pairs as intermediates and in some cases facilitates measurement of their respective absolute reactivities. Further work is in progress to extend the range of catalysts and monomers which may react in this way and therefore to extend our knowledge of the absolute reactivity in cationic polymerization.

### Acknowledgment

The studies described here were carried out in the Donnan Laboratories, University of Liverpool with joint supervision by C. E. H. Bawn, C. B. E., F. R. S. Contributions by R. M. Bell, C. Fitzsimmonds, J. Weightman, G. Cowell, D. Sherrington, J. Penfold, P. Bowyer, D. H. Iles, and P. Beresford are gratefully acknowledged. The author also thanks I. Kuntz for an advance copy of his manuscript (25).

**Literature Cited**

- (1) Bawn, C. E. H., *Pure Appl. Chem.* **16**, 285 (1968).
- (2) Bawn, C. E. H., Fitzsimmons, C., Ledwith, A., *Proc. Chem. Soc.* **1964**, 391.
- (3) Bawn, C. E. H., Bell, R. M., Ledwith, A., *Polymer* **6**, 95 (1965).
- (4) Bawn, C. E. H., Carruthers, R. A., Ledwith, A., *Chem. Commun.* **1965**, 522.
- (5) Bawn, C. E. H., Bell, R. M., Fitzsimmons, C., Ledwith, A., *Polymer* **6**, 661 (1965).
- (6) Bell, R. M., Ph.D. Thesis, University of Liverpool, 1963.
- (7) Bethell, D., Gold, V., "Carbonium Ions," Academic Press, London, 1967.
- (8) Biddulph, R., Plesch, P. H., *Chem. Ind.* **1959**, 1482.
- (9) Bonner, T. G., Clayton, J. M., Williams, G., *J. Chem. Soc.* **1958**, 1705.
- (10) Cowell, G. W., Ph.D. Thesis, University of Liverpool, 1966.
- (11) Denison, J. T., Ramsey, J. B., *J. Am. Chem. Soc.* **77**, 2615 (1955).
- (12) Deno, N., Saines, G., Spangler, M., *J. Am. Chem. Soc.* **84**, 3295 (1962).
- (13) Dreyfuss, M. P., Dreyfuss, P., *J. Polymer Sci.* **A4**, 2179 (1966).
- (14) Dreyfuss, M. P., Dreyfuss, P., *Advan. Polymer Sci.* **4**, 528 (1967).
- (15) Dreyfuss, M. P., Westfahl, J. C., Dreyfuss, P., *Macromolecules* **1**, 437, 1968.
- (16) Eley, D. D., Richards, A. W., *Trans. Faraday Soc.* **45**, 436 (1949).
- (17) Fitzsimmons, C., Ph.D. Thesis, University of Liverpool, 1966.
- (18) Heck, R., Magee, P. S., Winstein, S., *Tetrahedron Letters* **1964**, 2033.
- (19) Higashimura, T., Fukushima, T., Okamura, S., *J. Makromol. Sci. (Chem.)* **A1**, 683 (1967).
- (20) Hughes, J., North, A. M., *Trans. Faraday Soc.* **62**, 1866 (1966).
- (21) Iles, D. H., Ledwith, A., *Chem. Commun.* **1968**, 498.
- (22) Kalfoglu, N., Szwarc, M., *J. Phys. Chem.* **72**, 2233 (1968).
- (23) Kampmeier, J. A., Greer, R. P., Meskin, A. J., D'silva, R. M., *J. Am. Chem. Soc.* **88**, 1257 (1966).
- (24) Kuntz, I., *J. Polymer Sci.* **A5**, 193 (1967).
- (25) Kuntz, I., Melchior, M. T., *J. Polymer Sci.*, in press.
- (26) Kursanov, D. N., Vol'pin, M. E., Akhrem, I. S., *Dokl. Akad. Nauk., SSSR* **120**, 531 (1958).
- (27) Ledwith, A., *J. Appl. Chem.* **17**, 344 (1967).
- (28) Ledwith, A., Fitzsimmons, C., "Polymer Chemistry of Synthetic Elastomers," p. 377, J. P. Kennedy, E. G. M. Tornqvist, Eds., Interscience, New York, 1968.
- (29) Ledwith, A., Sambhi, M., *Chem. Commun.* **1965**, 64.
- (30) Olah, G., Schleyer, von R. P., Eds., "Carbonium Ions," Vol. 1, Interscience, London, 1968.
- (31) Plesch, P. H., Ed., "The Chemistry of Cationic Polymerization," Pergamon, Oxford, 1963.
- (32) Plesch, P. H., "Progress in High Polymers," J. C. Robb, F. W. Peaker, Eds., Vol. II, p. 137, Iliffe, London, 1968.
- (33) Rozenberg, B. A., Chekhuta, O. M., Lyudvig, E. B., Cantmakher, A. R., Medvedev, S. S., *Vysokomolekul. Soedin.* **6** (11), 2030 (1964).
- (34) Sherrington, D., Ph.D. Thesis, University of Liverpool, 1969.
- (35) Sims, D., *J. Chem. Soc.* **1964**, 864.
- (36) Smith, B. J. K., Dodd, J. A., Instone, A. T., Partridge, D. B., *J. Polymer Sci.* **B5**, 625 (1967).
- (37) Szwarc, M., "Carbanions, Living Polymers, and Electron-transfer Processes," Interscience, New York, 1968.
- (38) Ubbereiter, K., Springer, J., *Z. Phys. Chem.* **36**, 299 (1963).
- (39) Vol'pin, M. E., Aphrem, I. S., Kursanov, D. N., *Z. Obshch. Khim.* **30**, 159 (1960).

- (40) Vofsi, D., Tobolsky, A. V., *J. Polymer Sci.* **A3**, 3261 (1965).
- (41) Weightman, J. A., Ph.D. Thesis, University of Liverpool, 1968.
- (42) Williams, F., Hayashi, K., Ueno, K., Hayashi, K., Okamura, S., *Trans. Faraday Soc.* **63**, 1501 (1967).
- (43) Winstein, S., Robinson, G. C., *J. Am. Chem. Soc.* **80**, 169 (1958).
- (44) Winstein, S., Appel, B., Baker, R., Diaz, A., *Chem. Soc. (London), Spec. Publ.* **19**, 109 (1965).

RECEIVED April 14, 1969.

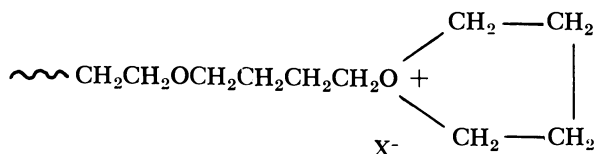
## The Nature and Influence of Gegenions in Tetrahydrofuran Polymerization

PATRICIA DREYFUSS and M. PETER DREYFUSS

B. F. Goodrich Co., Research Center, Brecksville, Ohio 44141

*The effects of gegenion on the polymerization of tetrahydrofuran (THF) indicated that the order of stability was  $PF_6^- \simeq SbF_6^- > BF_4^- \geq SbCl_6^-$ . With all gegenions gel permeation chromatography indicated a rapid broadening of the molecular weight distribution before equilibrium conversion was reached. A narrowing of the distribution occurred after equilibrium conversion. These results suggested that reaction with polymer oxygen is very important in THF polymerizations. Low conversions with  $BF_4^-$  suggested termination. Decreased molecular weights with  $SbCl_6^-$  without a corresponding decrease in percent conversion suggested transfer. The conclusions are based on changes with time of conversion, intrinsic viscosity, and molecular weight distributions. Equivalent concentrations of each gegenion were introduced in the form of triethyloxonium salts. Polymerizations were run in methylene chloride at 30°C.*

**T**etrahydrofuran (THF) polymerizes by ring-opening polycondensation to give a linear polymer usually called polytetrahydrofuran (PTHF) but frequently called poly(tetramethylene oxide). All its known polymerizations occur by a cationic mechanism. The generally accepted growing species is a tertiary oxonium ion,  $R_3O^+X^-$ , of the form:



As in all ionic polymerizations, the oxonium ion is associated with a gegenion or counterion,  $X^-$ . The gegenion  $X^-$  exerts a large influence on the course of the polymerization and affects the properties of the polymer that is formed.

Meerwein and co-workers (16) reported long ago that simple anions such as  $Cl^-$  lead to unstable complexes that decompose to give the ether and the alkyl halide (Reaction 1)



They reported the first stable oxonium ion salts in 1937. These salts all contained complex gegenions such as  $BF_4^-$ ,  $SbCl_6^-$ ,  $AlCl_4^-$ , or  $FeCl_4^-$ . They found (15) that stable oxonium ions, such as triethyloxonium tetrafluoroborate, could initiate the polymerization of THF. Meerwein also recognized that the polymerization of THF is reversible and goes to an equilibrium between monomer and polymer. It is now well established (10) that with suitable choice of gegenion the conversion depends only on temperature and monomer concentration. Meerwein did not study systematically the effect of changing the gegenion.

In 1965 Bawn and co-workers (2) reported a comparison of the effects of changing the gegenion from  $SbCl_6^-$  to  $PF_6^-$  using trityl and tropylium salts as initiators. These workers made their study in bulk polymerizations at 25° and 50°C. Some of their results at 50°C. on the effect of gegenion on conversion and rate are shown in Table I. Using

**Table I. Effect of Gegenion on Conversion and Rate at 50°C. (2)**

<i>Catalyst</i>	<i>Eq. Conv., %</i>	$R_p(PF_6^-)/R_p(SbCl_6^-)$
$\phi_3C^+PF_6^-$	56	—
$\phi_3C^+SbCl_6^-$	43	1.5
$C_7H_7^+SbCl_6^-$	54.5	—

the  $PF_6^-$  gegenion they obtained the 56% equilibrium conversion to polymer previously observed by Sims (21) and Dreyfuss and Dreyfuss (7). However, with  $SbCl_6^-$  gegenion, their percent conversion was lower—namely, 43% with the triphenylmethyl cation and 54.5% with tropylium cation. Bawn and co-workers attributed this difference to termination in the case of the  $SbCl_6^-$  gegenion. The rate of polymerization with the  $PF_6^-$  gegenion was 1.5 times greater than with the  $SbCl_6^-$  gegenion at equal catalyst concentrations. They concluded that this was not a significant difference.

Under the right conditions (10) termination and transfer reactions are unimportant in THF polymerization. By analogy to anionic systems (23), one would expect that the degree of polymerization could be calculated from the relation shown in Equation 2

$$DP = M_0 - M_t / C_0 \quad (2)$$

where  $M_0$  is the initial monomer concentration,  $M_t$  is the monomer concentration at time  $t$ , and  $C_0$  is the initial catalyst concentration. The effects on the degree of polymerization that Bawn and co-workers obtained are shown in Table II.

**Table II. Effect of Gegenion on the Degree of Polymerization (2)**

Catalyst	[Catalyst], $M \times 10^3$	Temp., °C.	Meas. DP/Calcd. DP
$\phi_3C^+PF_6^-$	3.9	50	2.6
$\phi_3C^+SbCl_6^-$	4.0	50	0.47
$\phi_3C^+PF_6^-$	5.4	25	2.6
$\phi_3C^+SbCl_6^-$	4.9	25	0.45

At both 25° and 50°C. the catalysts with the  $PF_6^-$  gegenion gave 2.5 times the calculated DP, and the catalyst with the  $SbCl_6^-$  gegenion gave only one-half the expected DP. Thus, there is considerable doubt about the number of active sites present in polymerizations initiated with these salts.

Kuntz (13) and Dreyfuss *et al.* (8, 9) have used NMR spectroscopy to study the THF polymerizations initiated by trityl salts. The results seem to indicate that the initial reaction that occurs between THF and the carbonium ion or diazonium ion salts is analogous to the one shown in Reaction 3.



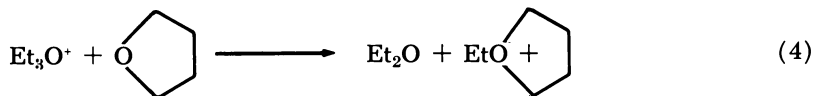
The triphenylmethyl cation reacts with the THF to form triphenylmethane and a protonic acid. We believe that this acid is the true initiator and that its reaction with THF may be slow. This can account in part for the deviations in DP. As Bawn and co-workers pointed out, in the case of the  $SbCl_6^-$  gegenion transfer reactions are probably also important and result in low DP's.

In addition, by-products of the initiation process may consume some of the protonic acid. The most probable by-products are furans, which could interact with the strong acid to form dark-colored resins. Polymerizations initiated with trityl or diazonium salts develop very dark colors which are not characteristic of the growing THF ion.

We have chosen to use preformed triethyloxonium salts as initiators. Polymerizations initiated with these salts remain nearly colorless. The



evidence is good that initiation is the straightforward alkyl exchange reaction shown in Reaction 4.



The most convincing evidence is Vofsi and Tobolsky's (24) work with  $^{14}\text{C}$ -labelled triethyloxonium tetrafluoroborate at  $0^\circ\text{C}$ . They found good agreement among the molecular weights calculated from the amounts of catalyst charged, determined by  $^{14}\text{C}$  end-group analysis and determined by vapor pressure osmometry. Dreyfuss *et al.* have also obtained NMR data on this initiation reaction (9). The spectra are entirely consistent with Reaction 4. No side reactions are indicated.

Initiation appears to be reasonably fast and complete. Both Rozenberg (20) and Ofstead (18) have reported the preparation of polymers with a narrow molecular weight distribution using oxonium ion initiators. The oxonium ion can be formed *in situ*, but Rozenberg (20) has shown that if the catalyst is formed *in situ* the DP will be five to 10 times the value calculated from Equation 2.

The salts used as initiators are all triethyloxonium salts of the formula  $(\text{C}_2\text{H}_5)_3\text{O}^+\text{X}^-$ . The gegenions ( $\text{X}^-$ ) examined are  $\text{BF}_4^-$ ,  $\text{PF}_6^-$ ,  $\text{SbF}_6^-$ , and  $\text{SbCl}_6^-$ . The first and last are well-known compounds and have been used frequently. The other two have been mentioned only in the patent literature (5, 6). These four gegenions probably include all the most common ones used in THF polymerizations except the ones resulting from triethylaluminum-water systems (11). In this case the structure of the gegenion is probably complex and has not yet been established.

### Experimental

**Materials.** TETRAHYDROFURAN. The monomer was refluxed over potassium until a small amount of distillate easily developed the green sodium naphthalene complex. It was then distilled from potassium under nitrogen, and a center cut was stored *in vacuo* in the presence of a sodium naphthalene complex. When needed, the monomer was distilled under high vacuum from the storage vessel into breakseals and weighed.

METHYLENE CHLORIDE. The solvent was refluxed over calcium hydride for at least 12 hours before distillation from calcium hydride under nitrogen.

CATALYSTS. The triethyloxonium salts were all prepared by reaction of epichlorohydrin with the Lewis acid corresponding to the desired gegenion in ether. The method of Meerwein *et al.* (14) was used. They were stored under high vacuum until needed.

$\text{Et}_3\text{O}^+\text{BF}_4^-$  was prepared under dry nitrogen with purified and anhydrous reagents and isolated as described by Meerwein. It was not purified further; m.p.  $94\text{--}95^\circ\text{C}$ .; reported (14),  $92^\circ\text{C}$ . Thereafter, this salt was handled only in a dry box.

$\text{Et}_3\text{O}^+\text{PF}_6^-$  was purified by repeatedly dissolving in methylene chloride and precipitating in ether until the melting point was not raised further. It did not seem to be very hygroscopic and was stable to short exposure to air. The last traces of ether were difficult to remove even under high vacuum; m.p.,  $142\text{--}143^\circ\text{C}$ . reported (6),  $137\text{--}137.5^\circ\text{C}$ . Calcd. for  $\text{C}_6\text{H}_{15}\text{OPF}_6$ : P, 12.48. Found: P, 12.6, 12.6.

$\text{Et}_3\text{O}^+\text{SbF}_6^-$  was oily as first isolated. The crystalline material was obtained by pressing on a clay plate. The salt was purified in the same way as the  $\text{PF}_6^-$  salt; m.p.,  $121\text{--}122^\circ\text{C}$ . Calcd. for  $\text{C}_6\text{H}_{15}\text{OSbF}_6$ : Sb, 35.92. Found: Sb, 36.40, 36.59.

$\text{Et}_3\text{O}^+\text{SbCl}_6^-$  was also purified in the same way as the latter two, but the melting point would not go above  $128\text{--}130^\circ\text{C}$ . (decompn.); reported (14),  $135\text{--}137^\circ\text{C}$ . (decompn.). However, the NMR spectrum did not indicate the presence of any impurities.

**Polymerization Procedure.** The polymerization apparatus consisted of a simple tube with two constrictions. The THF breakseal was attached between the two constrictions. The catalyst solution was prepared in a serum capped nitrogen purged bottle from weighed amounts of oxonium salt and methylene chloride. This solution was made up so that the final catalyst concentration was  $3.25 \times 10^{-3}\text{M}$ , and the THF concentration was  $7.6\text{M}$  (62.5% *v/v* THF). This insured a fluid mixture throughout the polymerization. Under these conditions the equilibrium conversion to polymer was 27.5%—*i.e.*, the equilibrium monomer concentration of THF was  $5.6\text{M}$ .

The required amount of catalyst solution was then transferred by a hypodermic syringe into the nitrogen-purged polymerization apparatus. The catalyst solution was degassed and finally sealed off under high vacuum at the top constriction. THF was added to the catalyst solution at  $-78^\circ\text{C}$ ., and the breakseal was removed by sealing off at the lower constriction. The ampoule was removed from the dry ice, placed in a  $30^\circ\text{C}$ . bath, and shaken. Approximately 2 minutes were required for the reaction mixture to warm to  $30^\circ\text{C}$ . Polymerization was continued at  $30^\circ\text{C}$ . without shaking. We chose  $30^\circ\text{C}$ . because we felt any side reactions would be fast enough to be observed. The initiation reaction should be even more rapid than Vofsi and Tobolsky (24) measured at  $0^\circ\text{C}$ .

The ampoules were removed from the bath at the desired time and opened. The polymerizations were shortstopped by quickly pouring the polymer cement into 30% of its volume of a  $0.15\text{M}$  solution of ammonia gas in THF. This cement was then evaporated in air and finally dried in a vacuum oven to constant weight.

**Intrinsic Viscosity.** Intrinsic viscosities were determined in ethyl acetate at  $30^\circ\text{C}$ . using a Ubbelohde dilution viscometer.

**Molecular Weight Distributions.** Molecular weight distributions were determined with a Waters Associates Model 100 modified to the equivalent of a model 200 gel permeation chromatograph using a five-column series in the  $10^6$ ,  $10^4$ , and  $10^2$  Å. range. The columns used in this

study are described in Table III. The samples were run in THF at 40°C. using a charge of 4.4 mg. of polymer in a 0.25% solution. The flow rate

**Table III. Description of Column Series**

Porosity, A.	Plate Count (plates/ft.)	Pressure, p.s.i.g.
10 <sup>6</sup>	829	29
10 <sup>5</sup>	856	20
10 <sup>4</sup>	1057	20
800	1310	24
100	1263	40

was regulated at 1 cc. per minute. The columns were calibrated using narrow distribution polystyrenes.  $\bar{M}_w$ ,  $\bar{M}_n$ , and  $\bar{M}_w/\bar{M}_n$  ratios were calculated by standard methods for each polymer using an IBM 1130 computer program that gives  $\bar{M}_n$ ,  $\bar{M}_w$ ,  $\bar{M}_w/\bar{M}_n$ , and log intervals. No corrections were made for base line spread owing to diffusion. The degree of polymer swell was assumed to be approximately the same as for polystyrene.

### Results

**NMR Spectra of the Oxonium Salts.** The chemical shifts of the triethyloxonium salts are given in Table IV. The chemical shifts of diethyl ether are included for comparison.

**Table IV. Chemical Shifts**

X <sup>-</sup>	$\delta$ , —CH <sub>2</sub> O—	$\delta$ , —CH <sub>3</sub>
BF <sub>4</sub> <sup>-</sup>	4.79	1.60
PF <sub>6</sub> <sup>-</sup>	4.74	1.60
SbF <sub>6</sub> <sup>-</sup>	4.74	1.62
SbCl <sub>6</sub> <sup>-</sup>	4.88	1.75
C <sub>2</sub> H <sub>5</sub> OC <sub>2</sub> H <sub>5</sub>	3.44	1.15

A typical example of the NMR spectra from which we derived the chemical shifts is given in Figure 1. The familiar spectrum of an ethyl group is apparent. The large peak is the solvent, methylene chloride. The triplet at a  $\delta$  of 1.60 p.p.m. relative to tetramethylsilane is the methyl group and the quartet at a  $\delta$  of 4.79 p.p.m. is the —CH<sub>2</sub>— next to the positive oxygen. The areas are in the expected ratio of 3:2. The chemical shift is downfield from that usually observed for an ethyl group on oxygen. This is the expected result of the polar environment in which these three equivalent ethyl groups exist.

Note that the chemical shifts are very similar for all of these salts, in agreement with their all being triethyloxonium salts supposed. The

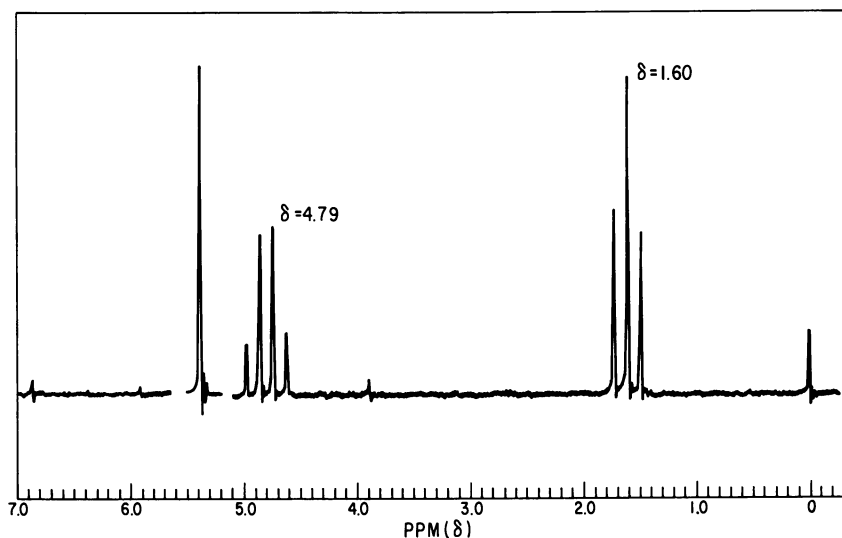


Figure 1. NMR spectrum of triethyloxonium tetrafluoroborate

chemical shifts for the hexachloroantimony salt are even further downfield as a result of the greater deshielding effect of the  $\text{SbCl}_6^-$  ion. All these spectra indicated that the salts were better than 99% pure.

**Time Effect of Gegenion on Percent Conversion and Intrinsic Viscosity.** The effect of gegenion on percent conversion to polymer and on intrinsic viscosity of the polymers is shown in Table V. Duplicates and runs with fresh catalyst solution all followed the same pattern. In the experiment using the  $\text{BF}_4^-$  gegenion at 10 times the usual concentration, the final conversion is increased considerably, although it still falls 2% below the equilibrium conversion.

Table V. Time Effect of Gegenion on Percent Conversion and Intrinsic Viscosity of PTHF

Polymerization, hrs.	Conversion, %				Intrinsic Viscosity, dl./gram			
	$\text{BF}_4^-$	$\text{PF}_6^-$	$\text{SbF}_6^-$	$\text{SbCl}_6^-$	$\text{BF}_4^-$	$\text{PF}_6^-$	$\text{SbF}_6^-$	$\text{SbCl}_6^-$
0.5	6.6	8.6	8.8	9.1	0.38	0.38	0.41	0.41
1.5	12.3, 13.2 <sup>a</sup>	18.4 <sup>a</sup>	19.9	17.5	0.64, 0.58 <sup>a</sup>	0.83 <sup>a</sup>	0.84	0.70
2.5	15.5 <sup>a</sup>	23.8	20.6 <sup>a</sup>	19.0 <sup>a</sup>	0.75 <sup>a</sup>	1.03	0.93 <sup>a</sup>	0.71 <sup>a</sup>
8	20.3	27.5	27.2	25.7	0.91	1.15	1.07	0.70
19	21.6	27.0	27.5	26.7	0.93	1.07	1.12	0.76
68	22.4 <sup>a</sup> , 25.5 <sup>b</sup>	27.3	27.0	27.3 <sup>a</sup>	0.89, 0.2 <sup>b</sup>	1.02	0.99	0.65 <sup>a</sup>

<sup>a</sup> Duplicate or later runs made with fresh catalyst solution.

<sup>b</sup> Run with ten times the catalyst concentration used in all other cases.

**Time Effect of Gegension on Molecular Weight Distribution.** The time effect of gegension on the molecular weights and molecular weight distributions obtained by GPC are shown in Table VI. The molecular weight calculated from the weight of polymer isolated, and the amount of catalyst charged is also shown for comparison.

The data for the narrow distribution polystyrene C-105 are given to provide a standard of comparison for the numbers reported for the experimental polymers. The GPC results indicate a broader distribution than that obtained by sedimentation velocity analysis. Such differences between GPC results and the more traditional measurements have been reported previously (1).

**Table VI. Time Effect of Gegension on GPC Results**

Gegension	Time	$\bar{M}_w/\bar{M}_n$	$\bar{M}_n \times 10^{-4}$	$\bar{M}_w \times 10^{-4}$	$\bar{M}_n \times 10^{-4}$ (Calcd.) <sup>a</sup>
BF <sub>4</sub> <sup>-</sup>	0.5	1.44	0.87	1.25	1.11
	1.5	1.59	1.73	2.76	2.08
	8	1.91	2.56	4.90	3.43
	19	1.98	2.64	5.25	3.65
PF <sub>6</sub> <sup>-</sup>	0.5	1.37	1.04	1.43	1.45
	1.5	1.74	2.64	4.62	3.11
	2.5	1.89	2.77	5.25	4.02
	8	1.96	3.89	7.66	4.65
	19	1.78	3.72	6.64	4.57
	68	1.84	3.45	6.37	4.61
SbCl <sub>6</sub> <sup>-</sup>	0.5	1.29	1.13	1.46	1.54
	1.5	1.68	2.14	3.61	2.95
	8	1.76	1.90	3.36	4.34
	19	1.78	2.20	3.93	4.53
PS-S105 <sup>b</sup>	GPC <sup>c</sup>	1.22	12.30	15.10	—
	SVA <sup>d</sup>	1.04	14.70	15.30	—

<sup>a</sup> Calculated by dividing the weight of polymer isolated by the moles of catalyst charged.

<sup>b</sup> A narrow distribution polystyrene provided by H. W. McCormick (Dow Chemical Co.).

<sup>c</sup> GPC results under our conditions.

<sup>d</sup> Sedimentation velocity analysis results supplied by H. W. McCormick (Dow Chemical Co.).

## Discussion

**Time Effect of Gegension on Percent Conversion.** A comparison of the effect of gegension on the percent conversion is shown in Figure 2. The lower conversion obtained with the BF<sub>4</sub><sup>-</sup> gegension is already obvious at 0.5 hour. By 1.5 hours the conversion is only 70% of that observed with the other gegensions. The effect becomes more noticeable as time con-

tinues. A conversion of about 20% was reached after 8 hours and did not change much thereafter. Equilibrium conversion was not reached even after 68 hours. In the polymerization with this catalyst using 10 times the concentration used in the other experiments, a 25.5% conversion to polymer was obtained. This is only 2% instead of 5% below equilibrium conversion. These results suggest clearly the loss of active centers owing to termination.

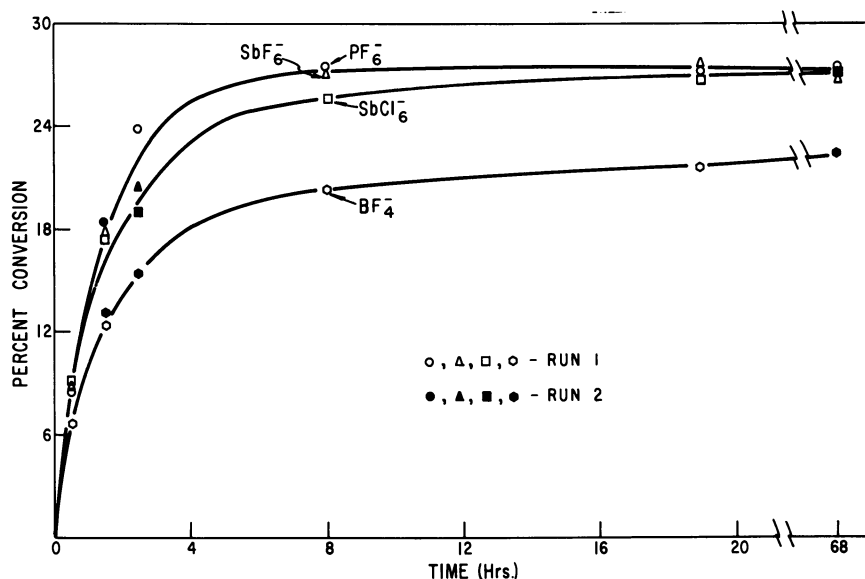


Figure 2. Comparison of time effect of gegenion on percent conversion

In their study at  $0^\circ\text{C}$ . Vofsi and Tobolsky (24) obtained good kinetic results over a limited range of catalyst and monomer concentration without considering a termination term. The catalyst and monomer concentrations in this work fall within this limited range. Obviously, at  $30^\circ\text{C}$ . termination can no longer be ignored.

The rate in the presence of the  $\text{SbCl}_6^-$  gegenion is noticeably slower after 2.5 hours. More than 19 hours were required to reach equilibrium conversion. Clearly the polymerization is slowing down. This could be caused by a loss of active centers through termination or transfer (*see* below).

The  $\text{PF}_6^-$  and  $\text{SbF}_6^-$  gegenions are discussed together because the percent conversion for the  $\text{SbF}_6^-$  and the  $\text{PF}_6^-$  followed approximately the same course. Equilibrium was reached after about 8 hours. It has been shown that there is very little termination (10) with the  $\text{PF}_6^-$

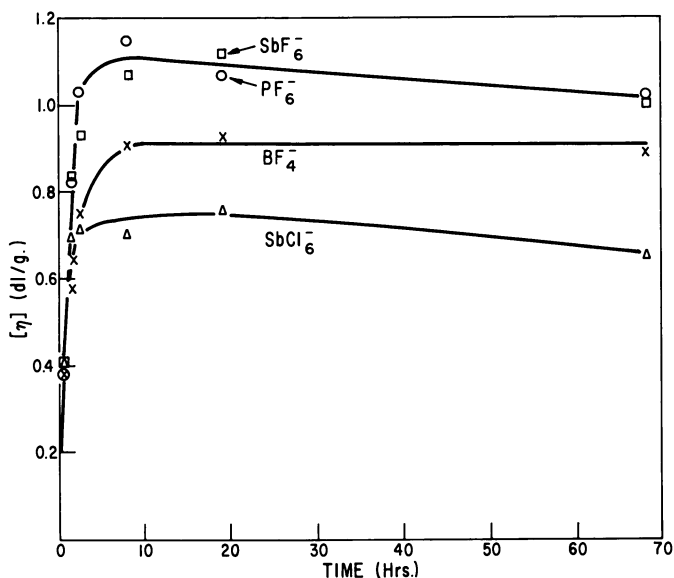
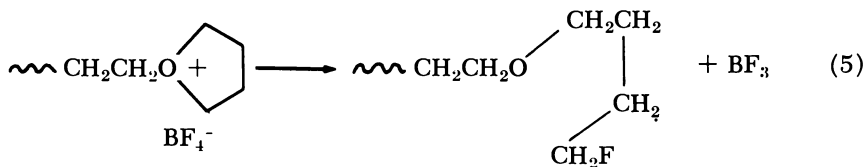


Figure 3. Time effect of gegenion on intrinsic viscosity

gegenion, and these results are consistent with the earlier data. Apparently there is not much termination with the  $\text{SbF}_6^-$  gegenion either.

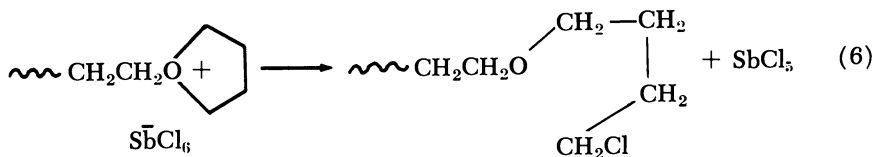
**Time Effect of Gegenion on Intrinsic Viscosity.** Figure 3 shows a comparison of the effects of gegenion on viscosity. For the  $\text{BF}_4^-$  gegenion the intrinsic viscosity reached a value of about 0.9 after 8 hours and like the conversion did not change much with time. Again this suggests termination. The type of termination reaction that has been suggested (15) is shown in Reaction 5.



It is a termination reaction because  $\text{BF}_3$  alone does not initiate polymerization (6) unless a large excess is used.

In the case of the  $\text{SbCl}_6^-$  gegenion a lower maximum intrinsic viscosity (about 0.75) was obtained. The viscosity declined with time. Since the conversion was still increasing during this period, transfer reactions must be very important with the  $\text{SbCl}_6^-$  gegenion. If the reaction analogous to that shown with the  $\text{BF}_4^-$  gegenion occurs (Reaction 6), we

now have a transfer reaction. It is well known (20, 22) that  $\text{SbCl}_5$  alone can initiate polymerization. However, since two molecules of  $\text{SbCl}_5$  are probably required to initiate



one new chain, half an active center is lost by each reaction with  $\text{SbCl}_6^-$ . Hence, in this case there is a combination transfer-termination reaction.

There is little difference between the effects of the  $\text{PF}_6^-$  and  $\text{SbF}_6^-$  gegenions. The viscosity continued to increase up to the equilibrium conversion at 8 hours. After equilibrium conversion, the intrinsic viscosity slowly but steadily decreased with time. It seems that some transfer occurs even with these two gegenions. Alternatively, the effect of transfer to the small amount of ether present may be appearing. An amount of ether equivalent to the catalyst concentration is formed in the initiation step (see Reaction 4).

**Time Effect of Gegenion on GPC Results.** Figure 4 shows some typical normalized gel permeation chromatography results for the  $\text{PF}_6^-$  polymers before equilibrium conversion is reached. The curves shown are for  $\text{PF}_6^-$  polymers after 0.5, 1.5, and 8 hours of polymerization. In agreement with the viscosity results the increase of molecular weight with time is evident. As expected, the distribution starts off quite narrowly. Then it quickly becomes broader.

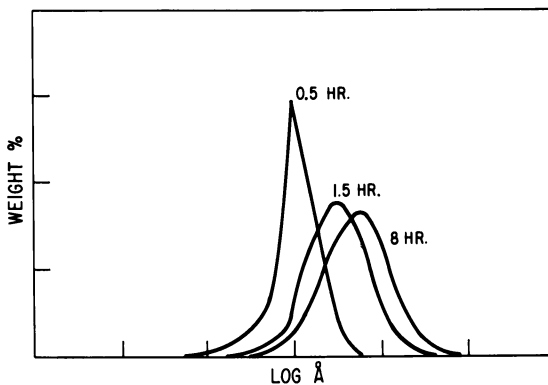
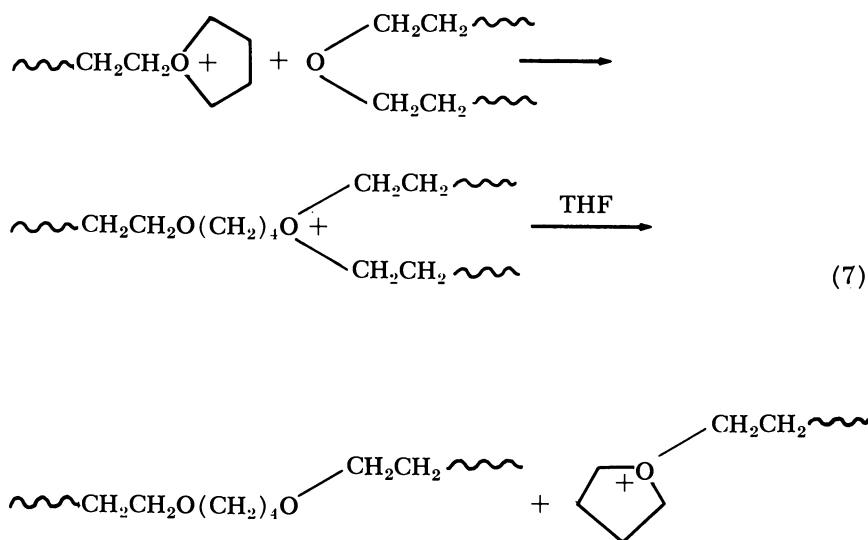


Figure 4. GPC molecular weight distribution curves for  $\text{PF}_6^-$  polymers before equilibrium conversion



This is quite different from what is observed with anionic polystyrene, where the distribution is narrow even at equilibrium conversion. Both systems contain "living" polymers. It has been shown mathematically (4, 17) that eventually the molecular weight distribution of living polymers will become normal—*i.e.*,  $\bar{M}_w/\bar{M}_n$  approaches 2. Miyake and Stockmayer (17) have considered the rate at which this equilibrium distribution is approached. For styrene they concluded that about 80 years would be required for the necessary broadening to occur. Using their equations and the value reported by Rosenberg (20) for the rate of depropagation in THF polymerizations we calculate that under the conditions in these experiments the attainment of a normal molecular weight distribution as a result of the propagation–depropagation process alone would require approximately 20 days. This is so much larger than the time observed in these experiments (1.5 hours) that we feel propagation–depropagation reactions cannot account for the rate of broadening.

It seems more likely that the rapid broadening comes largely from reactions with polymer oxygen as illustrated in Reaction 7.

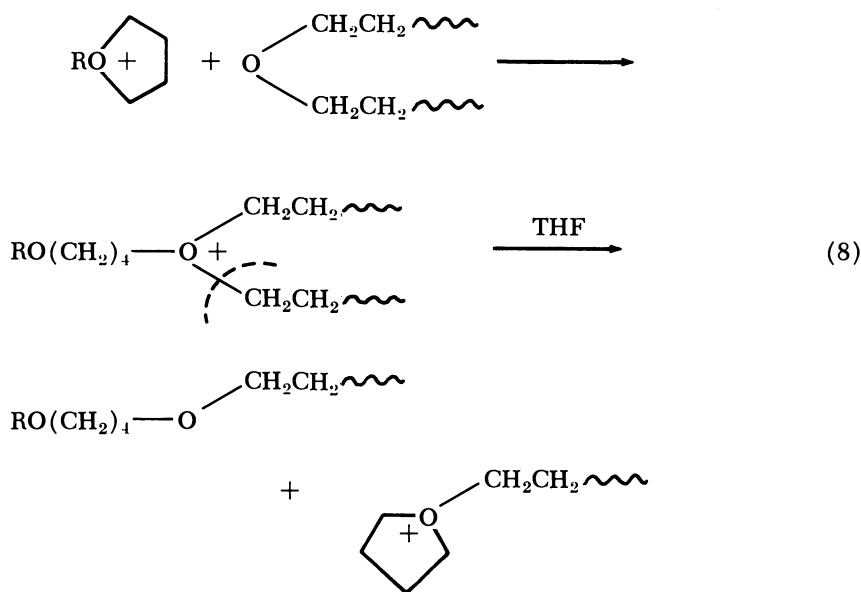


Dreyfuss *et al.* have shown previously that alkyl ethers are reactive in THF polymerizations, and the oxygens of the polymer chain *are* alkyl ether oxygens. The only outcome of this reaction is a randomization of the molecular weight distribution. The number of polymer molecules is not changed, and the number of active sites stays the same.

After equilibrium conversion is reached, a rather surprising decrease in the molecular weight distribution occurred (*see* Table VI). Although

the differences appear small, they are outside the normal experimental error for a series of polymers run at one time. Note that after equilibrium there is a 13% drop in  $\bar{M}_w$  and only a 5% drop in  $\bar{M}_n$  and that the trend in both  $\bar{M}_w$  and  $\bar{M}_n$  is down.

We said earlier that the decrease in viscosity was caused by transfer. This transfer reaction will result in the formation of new polymer chains. If the relatively small chains now react with polymer oxygen as previously shown, something more than just redistribution occurs. Reaction 8 shows that since R is small, an effective chain cleavage is possible. This should result in a more rapid breakdown of the larger molecules because the greater number of oxygens in the longer chains would increase the probability of their reacting. Hence,  $\bar{M}_w$  would decrease more rapidly than  $\bar{M}_n$ , and  $\bar{M}_w/\bar{M}_n$  would tend to decrease.



Gel permeation chromatograms were not obtained on the  $\text{SbF}_6^-$  polymers. However, there is no reason to suspect that these results would differ substantially from the  $\text{PF}_6^-$  results.

For the  $\text{BF}_4^-$  gegenion the initial narrow distribution formed was again followed by a rapid broadening. The viscosity and conversion data suggested that nothing much was happening after 8 hours, and the polymerization died. The GPC data also reflects this.

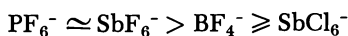
GPC data from the study with the  $\text{SbCl}_6^-$  gegenion are interesting. Here the effects of reaction with polymer oxygen in the presence of a relatively large concentration of new chains are visible. As one would

expect from the viscosity data, both  $\bar{M}_n$  and  $\bar{M}_w$  are substantially lower than in previous cases. This occurred despite the fact that each experiment initially contained the same number of growing centers. Again a rapid broadening of the initial narrow molecular weight distribution occurs, but in this case, the  $\bar{M}_w/\bar{M}_n$  ratio never seems to reach that of a normal distribution. Again this can be explained by the more probable chain cleavage of the longer polymer molecules by the products of the transfer reaction.

Reaction with polymer oxygen seems to occur readily in THF polymerizations. This reaction makes it difficult to prepare narrow distribution polytetrahydrofuran at significant conversions. The calculations of Hermans (12) and Rozenberg *et al.* (19) show that this kind of reaction should lead to the formation of polymer with a random distribution. When the additional complication of transfer reactions leading to new short chains is introduced, reaction with polymer oxygen tends to give a molecular weight distribution somewhat narrower than the normal. This reaction also seems to speed up the effect of transfer reactions, especially those occurring after equilibrium is achieved.

### Conclusions

The order of stability of the gegenions we have studied in THF polymerizations at 30°C. is:



From a chemical standpoint there is little evidence at present to prefer  $\text{PF}_6^-$  over  $\text{SbF}_6^-$  or vice-versa. Both gegenions seem considerably more stable than  $\text{BF}_4^-$  or  $\text{SbCl}_6^-$ . The  $\text{BF}_4^-$  polymerization contains considerable termination, and the  $\text{SbCl}_6^-$  polymerization contains considerable transfer and some termination. It is interesting to note that both results can be explained in terms of a similar reaction with gegenion.

All our studies were made at 30°C. Data in the literature suggest that as the temperature is lowered, these differences will become less because reaction with gegenion becomes much slower. On the other hand the differences will become even more pronounced as the temperature is raised above 30°C. Thus, for high temperature studies the use of  $\text{PF}_6^-$  or  $\text{SbF}_6^-$  is clearly indicated.

### Acknowledgment

We thank J. C. Westfahl for making the NMR measurements and D. Harmon for carrying out the GPC measurements and calculations.

**Literature Cited**

- (1) Alliet, D. F., *Proc. Intern. Symp. Polymer Characterization, Battelle Mem. Inst., Columbus, Ohio, IV-1* (1967).
- (2) Bawn, C. E. H., Bell, R. M., Fitzsimmons, C., Ledwith, A., *Polymer* **6**, 661 (1965).
- (3) British Industrial Plastics Ltd., Netherland Patent Application **6,509,888** (1966).
- (4) Brown, W. B., Szwarc, M., *Trans. Faraday Soc.* **54**, 416 (1958).
- (5) Burrows, R. C., Crowe, B. F., *J. Appl. Polymer Sci.* **6**, 465 (1962).
- (6) Distillers Co., Ltd., Netherland Patent Application **6,612,244** (1967).
- (7) Dreyfuss, M. P., Dreyfuss, P., *J. Polymer Sci., Pt. A-1* **4**, 2179 (1966).
- (8) Dreyfuss, M. P., Westfahl, J. C., Dreyfuss, P., *ACS, Div. Polymer Chem., Polymer Preprints* **7** (2), 413 (1966).
- (9) Dreyfuss, M. P., Westfahl, J. C., Dreyfuss, P., *Macromolecules* **1**, 437 (1968).
- (10) Dreyfuss, P., Dreyfuss, M. P., *Advan. Polymer Sci.* **4**, 528 (1967).
- (11) Furukawa, J., Saegusa, T., "Polymerization of Aldehydes and Oxides," Interscience, New York, 1963.
- (12) Hermans, J. J., *J. Polymer Sci. C* (12), 345 (1966).
- (13) Kuntz, I., *J. Polymer Sci.* **B4**, 427 (1966).
- (14) Meerwein, H., Battenberg, E., Gold, H., Pfeil, E., Willfang, G., *J. Prakt. Chem.* **154**, 83 (1939).
- (15) Meerwein, H., Delfs, D., Morshel, H., *Angew. Chem.* **72**, 927 (1960).
- (16) Meerwein, H., Hinz, G., Hofmann, P., Kroning, E., Pfeil, E., *J. Prakt. Chem.* **147**, 257 (1937).
- (17) Miyake, A., Stockmayer, W. H., *Makromol. Chem.* **88**, 90 (1965).
- (18) Ofstead, E. A., *ACS, Div. Polymer Chem., Polymer Preprints* **6** (2), 674 (1965).
- (19) Rosenberg, B. A., Irzhak, V. I., Enikolopyan, N. S., *Proc. Acad. Sci. USSR* **170**, 888 (1966).
- (20) Rosenberg, B. A., Ludvig, E. B., Gantmakher, A. R., Medvedev, S. S., *J. Polymer Sci. C* (16), 1917 (1967).
- (21) Sims, D., *J. Chem. Soc.* **1964**, 864.
- (22) Sorenson, W. R., Campbell, T. W., "Preparative Methods of Polymer Chemistry," p. 255, Interscience, New York, 1961.
- (23) Szwarc, M., *Advan. Polymer Sci.* **2**, 275 (1960).
- (24) Vofsi, D., Tobolsky, A. V., *J. Polymer Sci.* **A3**, 3261 (1965).

RECEIVED March 25, 1968.

## Block and Random Copolymers by Cationic Copolymerization

YUYA YAMASHITA

Department of Synthetic Chemistry, Faculty of Engineering,  
Nagoya University, Nagoya, Japan

*Although 3,3-bis(chloromethyl)oxetane (BCMO) does not copolymerize with styrene (St), random copolymers are obtained between 1,3-dioxolane (DOL) with St or BCMO by cationic catalyst. The propagating species of cationic polymerization of cyclic formals such as DOL are cations in between a carbonium ion like St and an oxonium ion like BCMO. The living nature of the cationic polymerization of DOL in  $C_2H_4Cl_2$  with  $Et_3OBF_4$  was established, and DOL polymer of molecular weight 160,000 was obtained. Copolymerization of DOL–St attained a molecular weight of 300,000. By adding BCMO to the DOL–St living polymer, block copolymers of DOL–St and DOL–BCMO were obtained.*

In copolymerization by a radical mechanism, random copolymers are obtained in almost every case, but true copolymers are not obtained in copolymerization by a cationic mechanism. Usually copolymers with considerable block character are obtained, or some homopolymer is formed together with the copolymer.

It is generally recognized that copolymerization between monomers with different polarities leads to copolymers with marked block character. In an extreme case the copolymerization product practically consists of a homopolymer mixture. O'Driscoll (7) derived a copolymerization equation showing that monomer consumption is determined by the ratio of the active sites formed at the initiation reaction if cross propagation is negligible. We propose that the difficulty of cross propagation between monomers with different polarities might arise from the different nature of the propagating species.

The predominant propagating species in the cationic polymerization of vinyl monomers is a carbonium ion, but the living end of cyclic ether polymerization is an oxonium ion, and the nucleophilic attack of the ether oxygen of the monomer to the  $\alpha$ -carbon atom of the oxonium ion should be the rate-determining step of the propagation reaction. However, bond breaking between the  $\alpha$ -carbon atom and the oxygen atom of the oxonium ion might proceed in some cases to give more electron-deficient carbon atom in the transition state.

The propagating species in the cationic polymerization can be examined from the copolymerization behavior (21). Cyclic ethers such as tetrahydrofuran (THF) or 3,3-bischloromethyloxetane (BCMO), and cyclic esters such as  $\beta$ -propiolactone ( $\beta$ -PL) or  $\epsilon$ -caprolactone ( $\epsilon$ -CL) are classified as oxonium ion type monomers. Copolymerizations between these monomers are observed easily as in the case of BCMO-THF (12, 13), BCMO- $\beta$ -PL (14, 15), BCMO- $\epsilon$ -CL (16), and THF- $\epsilon$ -CL (21).

Copolymerization between an oxonium ion type monomer and a carbonium ion type monomer has never been carried out successfully. Styrene (St) does not form a copolymer with THF (1), BCMO (1), or  $\beta$ -PL (2, 16). The formation of a homopolymer mixture was confirmed for the St- $\beta$ -PL system (18, 19, 26). The reason for the absence of cross propagation was discussed elsewhere (6), but the reaction of the trityl cation with  $\beta$ -PL and the reaction of the triethyloxonium ion with 1,1-diphenylethylene did show the absence of the bonding reaction (6).

On the other hand, some intermediate monomers can be copolymerized either with St or with THF as in the case of cyclic formals. Cyclic formals such as 1,3-dioxolane (10) (DOL), 1,3-dioxepane (11), and trioxane (3, 4) can be copolymerized randomly with styrene, and the cross sequence can be measured with NMR (10). This suggests that formals and styrene have a similar propagating species. The oxonium ion from formals is apt to react like a carbonium ion because of the resonance stabilization of the derived carbonium ion. It is difficult to consider the propagating species as a true carbonium ion because the carbon atom in the presence of neighboring oxygen atom might not be able to have more than fractional positive charge. The formation of random copolymer between formals and oxonium ion type monomers, on the other hand, suggests that the oxonium ion type monomer and formals have a similar propagating species. DOL can copolymerize with THF, BCMO, and  $\beta$ -PL (8). Thus, we concluded that the propagating species of cationic polymerization of cyclic formals is something in between the carbonium ion and the oxonium ion (24, 25). Hence, it should be possible to copolymerize an oxonium ion type monomer with a carbonium ion type monomer by introducing an intermediate monomer with it. This idea was verified by obtaining random copolymer of  $\beta$ -PL-St-

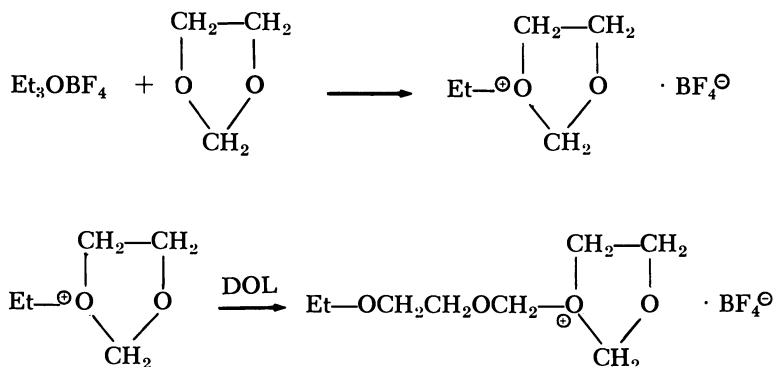
DOL (6), although we could obtain only a homopolymer mixture in the copolymerization of  $\beta$ -PL and St. We intend to obtain a high molecular weight polymer with such a random sequence of cyclic ether and vinyl monomer by using cyclic formals as intermediates.

To obtain a high molecular weight block or random copolymer of the oxonium ion type monomer and carbonium ion type monomer, experimental conditions must be such that termination or transfer reactions are minimized. The living nature of the cationic polymerization of THF (7) is well established, but it has been difficult to obtain a high polymer of styrene or DOL by cationic mechanism. In this paper we demonstrate the living nature of the polymerization of DOL and the high polymer of St-DOL copolymer. Using this technique, we were able to obtain a block copolymer of vinyl monomer and cyclic monomer.

### *Living Polymer of 1,3-Dioxolane*

Polymerization of DOL with cationic catalysts such as  $\text{BF}_3 \cdot \text{Et}_2\text{O}$ ,  $\text{Ac}_2\text{O}-\text{HClO}_4$ , or  $\text{AlEt}_2\text{Cl}-\text{H}_2\text{O}$  in a sealed ampoule under nitrogen yields polymers with molecular weight of less than several thousands (9). To clarify the reason for the low molecular weight, we examined the mechanism of the polymerization of DOL with  $\text{BF}_3 \cdot \text{Et}_2\text{O}$  (22). The polymerization proceeds with complex kinetics, and a complex initiation reaction arises from  $\text{BF}_3 \cdot \text{DOL}$ . In addition, there is evidence for considerable termination and transfer.

On the other hand, the polymerization with  $\text{Et}_3\text{OBF}_4$  proceeds with very simple kinetics, and the following scheme was deduced from the structure of the initiation product and the molecular weight of the polymer (20).



The rate of polymerization follows the standard equation obtained for an equilibrium polymerization without termination and with rapid initiation (20):

$$-\frac{d[M]}{dt} = k_p [C]_o \{ [M] - [M]_e \}$$

where  $[C]_o$  is the initial catalyst concentration, and  $[M]_e$  is the equilibrium monomer concentration.

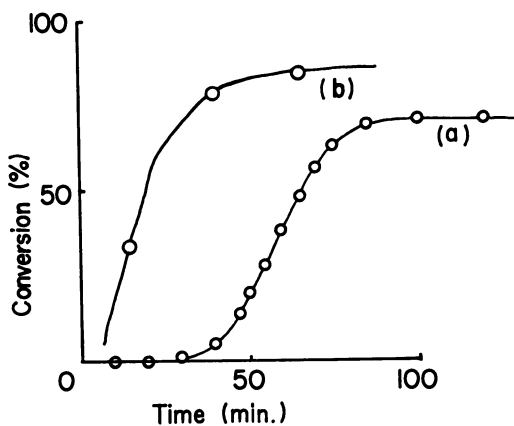


Figure 1. Time-conversion curve for DOL polymerization with  $\text{Et}_3\text{OBF}_4$  at  $30^\circ\text{C}$ .

- (a)  $[M]_o = 4.95$  moles/liter,  $[C]_o = 1.78 \times 10^{-2}$  mole/liter in  $\text{C}_6\text{H}_6\text{Cl}_2$  under  $\text{N}_2$   
 (b)  $[M]_o = 8.65$  moles/liter,  $[C]_o = 1.56 \times 10^{-2}$  mole/liter in  $\text{C}_6\text{H}_6\text{Cl}_2$  under high vacuum

The time-conversion curve (Curve a) shown in Figure 1 was obtained by an experiment in an open system from residual monomer concentration measured by gas chromatography. The thermodynamic data for the equilibrium polymerization were obtained as  $\Delta H_p = -3.6$  kcal./mole and  $\Delta S_p = -14$  cal./mole-degree for the benzene solution (23). The induction period depends upon the reaction between the catalyst and the added water. The degree of polymerization determined by vapor pressure osmometer increases linearly as shown in Figure 2 if the added water is kept low. The absolute rate constant for the propagation was estimated as  $4.3 \times 10^{-2}$  liter/mole-sec. at  $30^\circ\text{C}$ . with an activation energy of 11.7 kcal./mole with  $\text{Et}_3\text{OBF}_4$  in methylene chloride—a value comparable with that of THF. The living nature of DOL is suggested by Figure 2, and the observed degree of polymerization reaches 90% of the



calculated value  $\bar{P} = \frac{[M]_0 - [M]}{[C]_0}$  even in this rough open system if the initial catalyst concentration is sufficiently high to yield polymer molecular weight below 10,000.

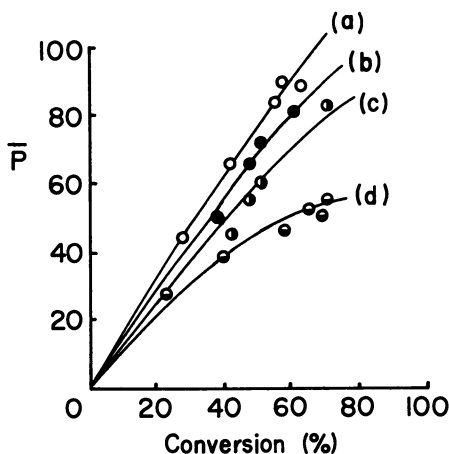


Figure 2. Degree of polymerization vs. conversion of DOL with  $\text{Et}_3\text{OBF}_4$  in  $\text{CH}_2\text{Cl}_2$  at  $30^\circ\text{C}$ .

$[M]_0 = 4.95$  moles/liter,  $[C]_0 = 2.93 \times 10^{-3}$  mole/liter

Added water: (a) none, (b)  $7.2 \times 10^{-3}$  mole/liter, (c)  $14.4 \times 10^{-3}$  mole/liter, (d)  $25.5 \times 10^{-3}$  mole/liter

Because the adventitious water reacts with catalyst to decrease the degree of polymerization by transfer or termination, experiments in high vacuum system are necessary. The following experiment was carried out in a vacuum system kept at  $10^{-6}$  mm. Hg, and DOL was distilled from the stock solution colored with anthracene sodium. The solvent, ethylene dichloride, was dried over calcium hydride and then over barium oxide. The catalyst,  $\text{Et}_3\text{OBF}_4$ , was also prepared in vacuum from the ether solution of epichlorohydrin and  $\text{BF}_3 \cdot \text{Et}_2\text{O}$ , filtered and dissolved in ethylene dichloride, and the necessary amount was charged into the polymerizing system. After polymerization for the desired time at room temperature, the polymer solution was poured into methanol. The molecular weight was determined by membrane osmometer.

Table I shows some experimental results. The induction period decreases to several minutes as shown by Curve b in Figure 1, but it was not possible to eliminate it. The molecular weight reached a value as high as 160,000, still a little lower than the calculated value. Thus, some

termination or transfer reaction might be unavoidable in this system if the polymerization were carried out for a longer time with lower catalyst concentration, and a true living polymer was hardly visualized in this cationic system.

The melting point of high molecular weight crystalline polymer of DOL reached 66.0°C. compared with 55°C. of low molecular weight polymer (9), and since the solubility in benzene decreased, the viscosity measurement was carried out in dimethylformamide.

**Table I. Polymerization of DOL in  $C_2H_4Cl_2$  at 30°C. with  $Et_3OBF_4$**

$[M]_0 = 10.3$  moles/liter,  $[C]_0 = 2.47 \times 10^{-3}$  mole/liter

No.	min. Time,	Conversion, %	Reduced Viscosity <sup>a</sup>	$\bar{M}_n$
1	95	47.5	1.22	—
2	135	76.2	2.45	161,000 <sup>c</sup>
3	240	85.5 <sup>b</sup>	2.63	165,000 <sup>c</sup>

<sup>a</sup>  $\eta_{sp}/C$  in DMF at 30°C.,  $C = 0.3$  gram/100 ml.

<sup>b</sup> Equilibrium conversion calculated from  $[M]_e = 1.5$  moles/liter 85.5%.

<sup>c</sup> Calculated value from  $\bar{M}_n = \frac{[M] - [M]_e}{[C]_0} = 230,000$  and 261,000, respectively.

### ***Block and Random Copolymer of 1,3-Dioxolane, Styrene, and 3,3-Bischloromethyloxetane***

In a previous paper (10), we reported random copolymer of DOL-St using  $BF_3 \cdot Et_2O$  at 0°C. The monomer reactivity ratios were determined as  $r_1$  (DOL) =  $6.5 \pm 0.85$ ,  $r_2$  (St) =  $0.65 \pm 0.07$  at 0°C. in toluene (11), and  $r_1 = 1.9 \pm 0.2$ ,  $r_2 = 0.35 \pm 0.05$  at 25°C. in toluene (10), and  $r_1 = 3.8 \pm 0.5$ ,  $r_2 = 1.4 \pm 0.3$  at 0°C. in nitrobenzene (11). Experiments in a vacuum system were carried out using rigorously dried DOL, St, and ethylene dichloride with  $Et_3OBF_4$ . Although pure St dried over barium oxide showed little tendency to polymerize by this catalyst system, copolymerization of DOL-St occurred and gave a fairly high molecular weight copolymer if the St feed were kept low.

Table II shows some experimental results. In some cases, where a fairly large amount of St monomer was added in the initial feed, the molecular weight of the copolymer is considerably lower than the calculated value, indicating considerable chain breaking reactions during polymerization. However, from initially low St feed, the molecular weight of the copolymer becomes comparable with the calculated value. Presumably, this is caused by solvation of the growing St end by DOL

to prevent chain scission by proton transfer. Thus, we can show the living nature of DOL–St copolymer system.

Table III shows the increase of molecular weight of BCMO polymerization with conversion, although the polymer tends to precipitate. The monomer reactivity ratios of DOL–BCMO copolymerization were previously determined as  $r_1$  (DOL) =  $0.65 \pm 0.05$ ,  $r_2$  (BCMO) =  $1.5 \pm 0.1$  at 0°C. by  $\text{BF}_3 \cdot \text{Et}_2\text{O}$  (8). Table IV shows a preparation of block copolymer of DOL, St, and BCMO. In the first step we polymerized DOL and St; in the second step we added BCMO to this living system. The copolymer obtained showed an increase of molecular weight, and considerable BCMO was incorporated in the copolymer still remaining soluble in ethylene dichloride. The solubility behavior together with the increase of molecular weight with addition of BCMO shows that this polymer consists of block sequences of DOL–St and (St)–DOL–BCMO. This we call block and random copolymer of DOL–St–BCMO. We can deny the presence of BCMO, St, or DOL homopolymers in this system, but some chain-breaking reactions are unavoidable, leading to copolymer mixtures. Thus, the principle of formation of block copolymers by cationic system is partly substantiated.

**Table II. Copolymerization of DOL and St in  $\text{C}_2\text{H}_4\text{Cl}_2$  at 20°C. with  $\text{Et}_3\text{OBF}_4$**

No.	Concentration, moles/liter			Time, hrs.	Yield, %	$\bar{M}_n$	St Content, mole %
	DOL	St	I				
4	4.30	4.28	$3.35 \times 10^{-3}$	5	26.3	$4.19 \times 10^3$	—
5	10.3	1.48	$3.03 \times 10^{-3}$	4	55.9	$2.11 \times 10^5$	6.1
6	5.64	0.565	$6.50 \times 10^{-4}$	91	39.4	$3.06 \times 10^5$	—
7	12.1	1.48	$3.28 \times 10^{-2}$	1	85.5	$1.1 \times 10^4$	8.9

### Experimental

**Materials.** Rectified DOL was dried over calcium hydride and distilled from a stock solution of colored sodium anthracene in a vacuum system. BCMO, St, and ethylene dichloride were purified by the usual procedure and dried with calcium hydride and barium oxide.  $\text{Et}_3\text{OBF}_4$  was prepared in a high vacuum system ( $10^{-6}$  mm. Hg).

**Polymerization.** All experiments were run under a high vacuum system. Monomer was added from a breakseal to the catalyst solution. The polymerization was stopped by pouring the reaction mixture into excess methanol containing phenyl  $\beta$ -naphthylamine, and precipitated polymer was vacuum dried under room temperature.

**Characterization of the Copolymer.** The copolymer composition was analyzed by elementary analysis and NMR. NMR spectra were run at 70°C. on a JNM-C-60 high resolution spectrometer at 60 Mc. in  $\text{CCl}_4$ .

**Table III. Polymerization of BCMO in C<sub>2</sub>H<sub>4</sub>Cl<sub>2</sub> at 0°C<sub>4</sub> with Et<sub>3</sub>OBF<sub>4</sub>**

No.	Concentration, moles/liter		Time, min.	Yield, %	$\eta_{sp}/C^a$
	BCMO	I			
8-1	2.21	$4.42 \times 10^{-3}$	25	15.7	0.385
8-2	2.21	$4.42 \times 10^{-3}$	30	17.4	0.405
8-3	2.21	$4.42 \times 10^{-3}$	40	23.4	0.449
8-4	2.21	$4.42 \times 10^{-3}$	250	36.1	0.475

<sup>a</sup> Measured in cyclohexanone at 60°C. (C = 2 grams/liter).

**Table IV. Block Copolymerization of DOL, St, and BCMO in C<sub>2</sub>H<sub>4</sub>Cl<sub>2</sub> at 30°C. with Et<sub>3</sub>OBF<sub>4</sub>**

First Step: Copolymerization of DOL and St

No.	Concentration, moles/liter			Time, hrs.	Yield, %	M <sub>n</sub>	St Content, %
	DOL	St	I				
9-1	9.82	1.96	$1.05 \times 10^{-2}$	2	24	$4.35 \times 10^3$	4.0

Second Step: Addition of BCMO

No.	BCMO, moles/liter	Time, hrs.	Yield, %	M <sub>n</sub>	Composition, mole %		
					DOL	St	BCMO
9-2	1.91	72	35.8	$5.8 \times 10^3$	85.7	2.6	11.7

As previously described (9), the St content is measured from the peak of the phenyl proton at 2.7–3.1  $\tau$ , the DOL content from the corrected peak area at 5.3  $\tau$  and 6.4  $\tau$ , and the BCMO content from the peak area of 6.5  $\tau$ .

The number average molecular weight was measured in benzene solution by Mechrolab membrane osmometer 502 and also by Hitachi vapor pressure osmometer 115.

### Literature Cited

- (1) Aoki, S., Harita, Y., Otsu, T., Imoto, M., *Bull. Chem. Soc. Japan* **38**, 1922 (1965).
- (2) *Ibid.*, p. 1928.
- (3) Higashimura, T., Tanaka, A., Miki, T., Okamura, S., *J. Polymer Sci., A-1*, **5**, 1927 (1967).
- (4) Höhr, L., Cherdron, H., Kern, W., *Makromol. Chem.* **52**, 59 (1962).
- (5) Dreyfuss, P., Dreyfuss, M. P., *J. Polymer Sci., A-1*, **4**, 2179 (1966).
- (6) Ito, K., Umehara, K., Yamashita, Y., *Kogyo Kagaku Zasshi* **70**, 2040 (1967).
- (7) O'Driscoll, K. F., *J. Polymer Sci.* **57**, 721 (1962).
- (8) Okada, M., Takigawa, N., Iwatsuki, S., Yamashita, Y., Ishii, Y., *Makromol. Chem.* **82**, 16 (1965).

- (9) Okada, M., Yamashita, Y., Ishii, Y., *Makromol. Chem.* **80**, 196 (1964).
- (10) *Ibid.*, **94**, 181 (1966).
- (11) Okada, M., Yamashita, Y., *Kogyo Kagaku Zasshi* **69**, 506 (1966).
- (12) Saegusa, T., Imai, H., Furukawa, J., *Makromol. Chem.* **56**, 55 (1962).
- (13) Saegusa, T., Ueshima, T., Imai, H., Furukawa, J., *Makromol. Chem.* **79**, 22 (1964).
- (14) Tada, K., Saegusa, T., Furukawa, J., *Makromol. Chem.* **71**, 71 (1964).
- (15) Tsuda, T., Shimizu, T., Yamashita, Y., *Kogyo Kagaku Zasshi* **67**, 1661 (1964).
- (16) *Ibid.*, p. 2145.
- (17) *Ibid.*, p. 2150.
- (18) Tsuda, T., Yamashita, Y., *Makromol. Chem.* **86**, 304 (1965).
- (19) Tsuda, T., Yamashita, Y., *Kogyo Kagaku Zasshi* **70**, 553 (1967).
- (20) Yamashita, Y., Okada, M., Kasahara, H., *Makromol. Chem.* **117**, 256 (1968).
- (21) Yamashita, Y., Okada, M., Kozawa, S., unpublished work.
- (22) Yamashita, Y., Okada, M., Suyama, K., *Makromol. Chem.* **111**, 277 (1968).
- (23) Yamashita, Y., Okada, M., Suyama, K., Kasahara, H., *Makromol. Chem.* **114**, 146 (1968).
- (24) Yamashita, Y., Tsuda, T., Okada, M., Iwatsuki, S., *J. Polymer Sci. A-1*, **4**, 2121 (1966).
- (25) Yamashita, Y., Uchikawa, A., *Kogyo Kagaku Zasshi* **71**, 758 (1968).
- (26) Yamashita, Y., Umehara, K., Ito, K., Tsuda, T., *Polymer Letters* **4**, 241 (1966).

RECEIVED March 7, 1968.

# Cationic Polymerization and Copolymerization of Trioxane

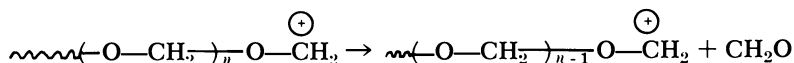
## High Resolution NMR Investigation of Polymerization Mechanism

CATHERINE S. HSIA CHEN and A. DI EDUARDO

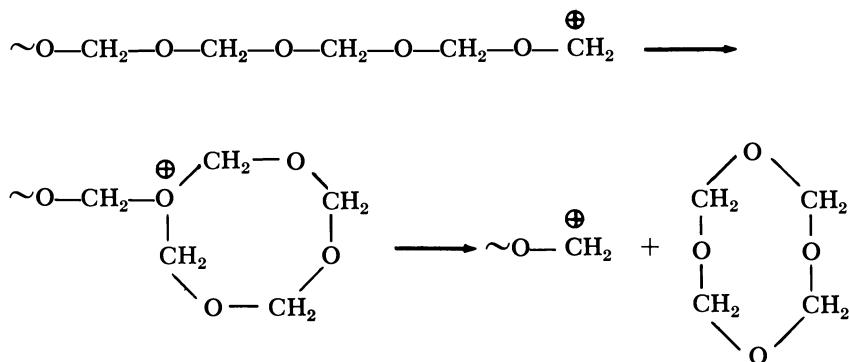
Celanese Research Co., Box 1000, Summit, N. J.

*The polymerization of trioxane has been studied by high resolution nuclear magnetic resonance. In homopolymerization the concentration of open-chain polymers reaches a steady state, independent of catalyst ( $\text{BF}_3 \cdot \text{Bu}_2\text{O}$ ) concentration. In copolymerization with ethylene oxide, ring opening of the ethylene oxide occurs immediately on adding catalyst and is copolymerized completely while the bulk of trioxane still remains. A surprisingly high concentration of formaldehyde builds up during copolymerization, reaching a maximum immediately before formation of solid polymer. Although the maximum formaldehyde concentration varies with ethylene oxide and/or catalyst concentration, the concentration of open-chain polymer remains relatively constant regardless of monomer and/or catalyst concentration.*

In the cationic polymerization and copolymerization of trioxane in the melt or in solution, an "induction period" usually exists, during which no solid polymer is formed and the reaction medium remains clear. Nevertheless, reactions are known to occur during this period. By using  $\text{BF}_3$  or an etherate as catalyst, in homopolymerization, Kern and Jaacks (1) reported the formation of formaldehyde *via* depolymerization of polyoxymethylene cations.



Miki, Higashimura, and Okamura (2) reported the formation of tetraoxane from polyoxymethylene cations by a "back-biting" mechanism:



In the copolymerization with ethylene oxide, Price and McAndrew (3) reported the formation of 1,3-dioxolane, presumably also by a back-biting mechanism. Chromatography has been the most commonly used analytical tool for following these reactions. It appeared that high resolution nuclear magnetic resonance (NMR) spectroscopy should be a good analytical method for monitoring the dynamic polymerization during the clear period before solidification. This paper describes the results of *in-situ* NMR investigations of homopolymerization of trioxane and its copolymerization with ethylene oxide in the melt at 65°C., the polymerization mechanisms based on these results, and the limitation of NMR as an analytical method for trioxane polymerization.

### Experimental

**Materials.** Trioxane (Celanese) was purified by refluxing over metallic sodium followed by distillation (b.p., 114.3°C.). Ampoules of ethylene oxide (Eastman white label) were opened immediately before use. The purity was established by mass spectrometry. Boron trifluoride dibutyl etherate (Eastman white label) was used without further purification.

**NMR Specifications and Calibrations.** The NMR spectra were obtained on a Varian high resolution NMR spectrometer, model A-60-A. The temperature was controlled with a Varian V-6040 variable heater unit. The instrument was tuned to a maximum resolution (0.3 c.p.s.) under reaction conditions (using the monomers) with no catalyst present. All spectra were recorded at 65°C. ( $\pm 1^\circ\text{C}$ ). An accurate chemical shift for the trioxane proton resonance (*vs.* TMS) was obtained by recording a spectrum at low gain. During the actual homo- and copolymerizations, high spectrum amplitudes were used so that new proton in-growth signals could be observed easily. The chemical shifts of these new proton signals

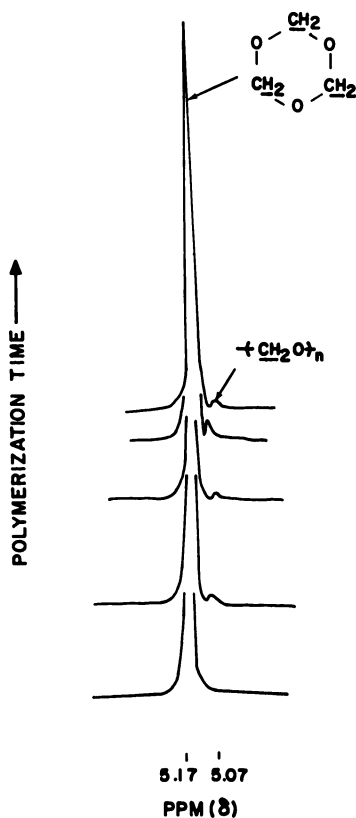


Figure 1. Homopolymerization of trioxane in bulk at 65°C.

were determined using the weak  $^{13}\text{C}$ H resonance peak of trioxane ( $J = 186$  c.p.s.) since in most cases the trioxane proton resonance was appreciably off scale. Intermittently, the spectra were integrated to determine the concentration of different species in the dynamic system. The following model compounds were used to help interpret the new proton signals appearing during the polymerizations: diethylene glycol dimethyl ether, tetraethylene glycol dimethyl ether, and Carbowax 400. Saturated solutions of gaseous formaldehyde in trioxane and trioxane-ethylene oxide mixtures were also recorded to determine the chemical shift of formaldehyde monomer in these matrices.

**Polymerizations.** Polymerizations were carried out in the spectrophotometer, and spectra were recorded at appropriate intervals until solidification took place. Under nitrogen atmosphere and at 65°C., polymerization mixtures were prepared in separate larger glass vessels. After mixing thoroughly, they were transferred to NMR tubes, flushed with nitrogen, and capped immediately. Before adding catalyst to the larger vessel, a sample was withdrawn and placed in the spectrometer for the



dual purpose of optimizing the resolution of the instrument and determining the ethylene oxide content. All glassware, including the NMR tubes, were base treated in an alcoholic KOH bath before final cleaning and drying to eliminate inadvertent polymer formation catalyzed by untreated glass surface.

### Results and Discussion

**Homopolymerization.** Figure 1 shows the spectra of the homopolymerization of trioxane with various concentrations of  $\text{BF}_3 \cdot \text{Bu}_2\text{O}$  catalyst.

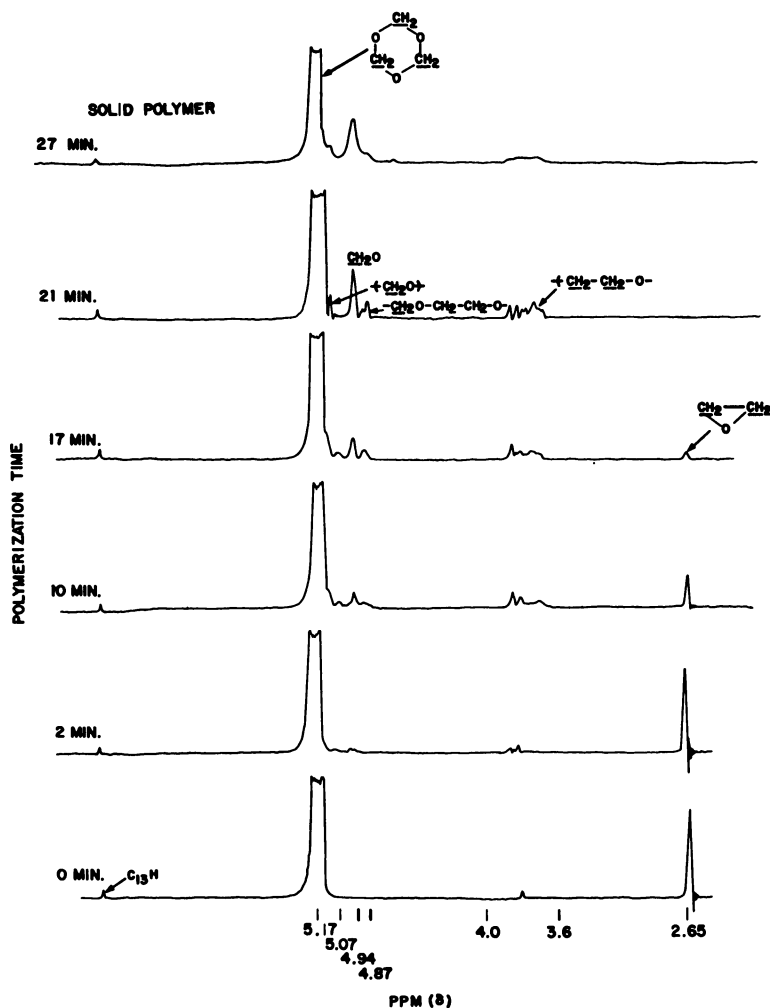


Figure 2. Copolymerization of trioxane with 1.5 mole % ethylene oxide in bulk at 65°C.  $\text{BF}_3 \cdot \text{Bu}_2\text{O}$ :  $1.0 \times 10^{-3}$  mole %

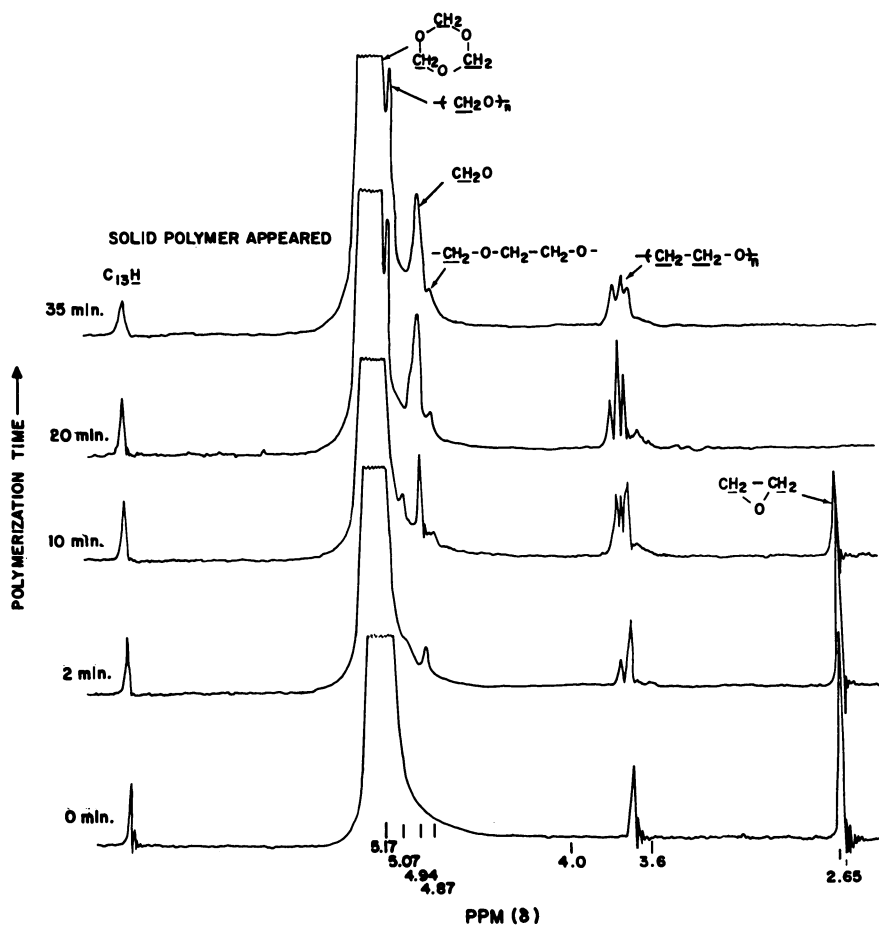


Figure 3. Copolymerization of trioxane with 3.3 mole % ethylene oxide in bulk at 65°C.  $\text{BF}_3 \cdot \text{Bu}_2\text{O}$ :  $1.0 \times 10^{-3}$  mole %

The trioxane proton signal appears at 5.17 p.p.m. (*vs.* TMS). Since the trioxane protons are magnetically equivalent, they appear as a sharp single peak. As the polymerization proceeds, the appearance of a new proton signal occurs at 5.07 p.p.m. This signal appeared and remained relatively constant during the clear period of the polymerization regardless of catalyst concentration. No change in the spectra occurred until the polymer precipitated from solution, when broadening and, consequently, loss of resolution occurred; hence, meaningful spectra could not be obtained. Assignment of this new peak was attributed to the low molecular weight-soluble open-chain polymer—*viz.*,  $(\text{CH}_2\text{—O})_n$ . As would be expected, an increase in catalyst concentration increased the

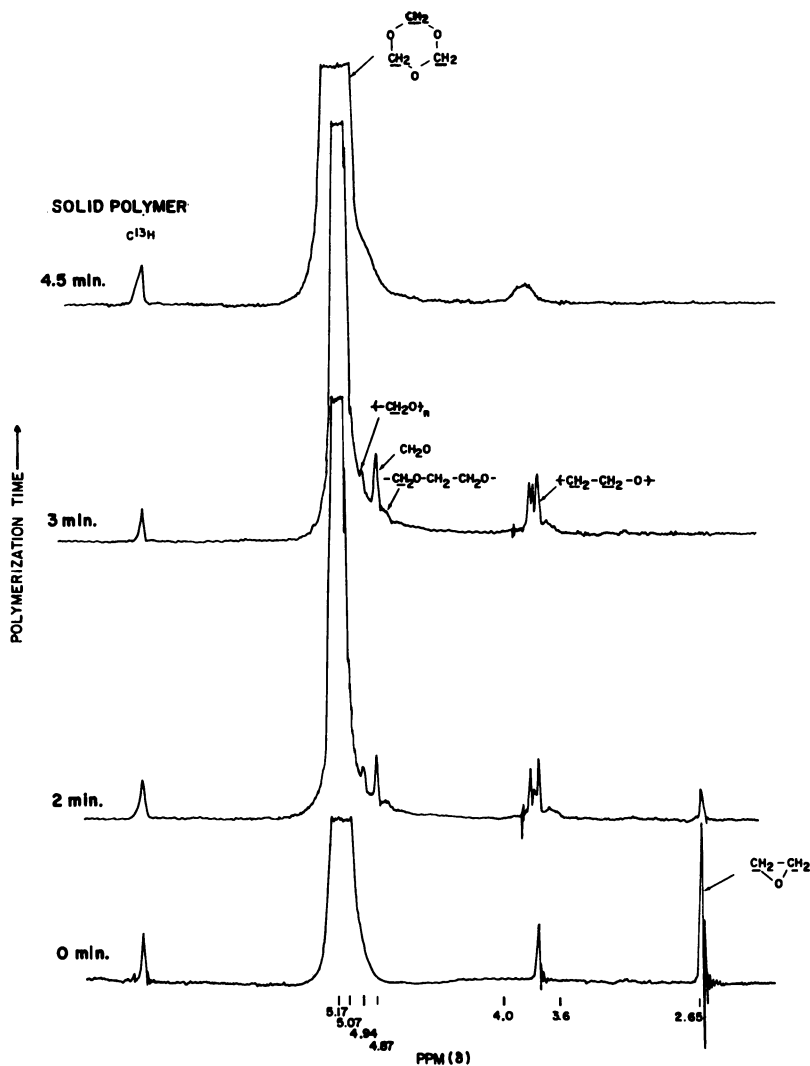


Figure 4. Copolymerization of trioxane with 3.3 mole % ethylene oxide in bulk at  $65^\circ\text{C}$ .  $\text{BF}_3 \cdot \text{Bu}_2\text{O}$ :  $2.2 \times 10^{-3}$  mole %

rate in attaining the steady-state concentration and decreased the clear period of polymerization. No formaldehyde was detectable even with high spectrum amplitude. Kerr and Jaacks (1) reported an equilibrium concentration of 60 mmoles/liter for the homopolymerization of trioxane in methylene chloride at  $30^\circ\text{C}$ . In our systems, the concentration of formaldehyde, if formed, is probably low and therefore will not be de-

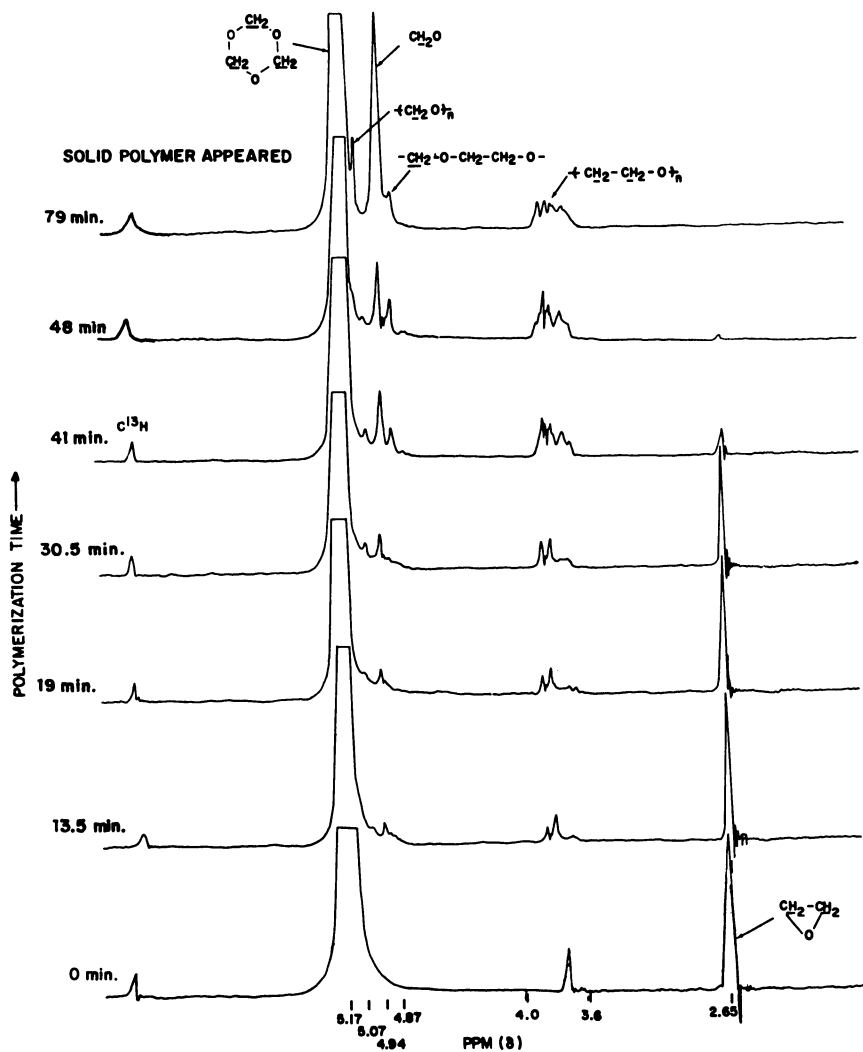


Figure 5. Copolymerization of trioxane with 7.2 mole % ethylene oxide in bulk at 65°C.  $BF_3 \cdot Bu_2O$ :  $2.2 \times 10^{-3}$  mole %

ected by this NMR method. Tetraoxane was not detected in our NMR study for the following reasons: (1) low concentrations, and (2) the chemical shift difference in proton resonance from that of trioxane would probably be negligible.

**Copolymerization with Ethylene Oxide.** Figures 2–6 show the NMR spectra of copolymerization of trioxane and ethylene oxide where the

effects of catalyst concentration and of ethylene oxide concentration can be observed. Features common to all copolymerization investigations are:

(1) Opening of the ethylene oxide ring occurred immediately upon adding catalyst.

(2) The polymerization remained in "clear stage" for some time even after ethylene oxide was no longer detectable.

(3) In-growth of new proton signals appeared. The new proton signals and their assignments are summarized in Table I.

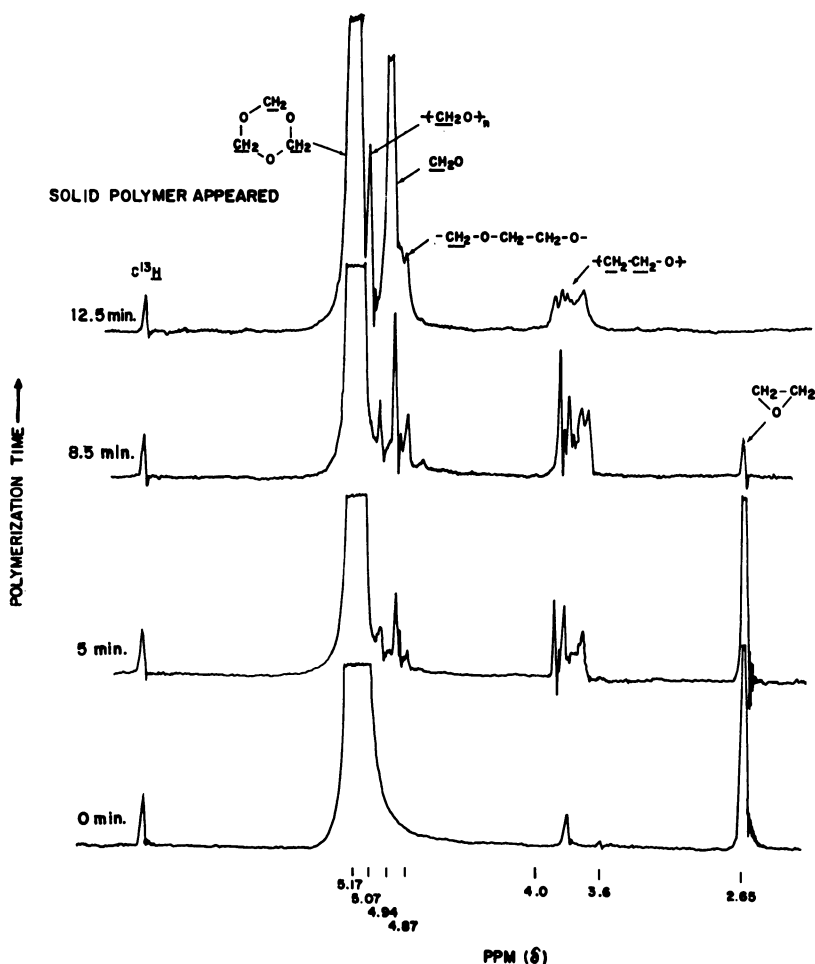
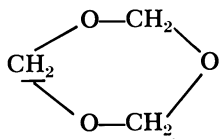
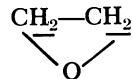


Figure 6. Copolymerization of trioxane with 10 mole % ethylene oxide in bulk at 65°C.  $BF_3 \cdot Bu_2O$ :  $6.0 \times 10^{-3}$  mole %

Although no appreciable difference in the in-growth of new proton signals was observed as the catalyst concentration or the ethylene oxide concentration was varied, differences were observed in the relative intensities of the proton signals—*viz.*, the CH<sub>2</sub>O resonance at 4.94 p.p.m.

**Table I. Assignment of New Proton Signals During the Copolymerization of Trioxane and Ethylene Oxide**

<i>P.p.m. (vs. TMS)</i>	<i>Assignment</i>
5.17	
5.07	$-(\text{CH}_2-\text{O})_n-$
4.94	<u>CH<sub>2</sub>O</u>
4.87	$-\text{CH}_2-\text{O}-\text{CH}_2-\text{CH}_2-\text{O}-$
3.60-4.0 <sup>a</sup>	$-(\text{CH}_2-\text{CH}_2-\text{O})_{1 \geq n \leq 3}-$
2.65	

<sup>a</sup> A <sup>13</sup>CH peak symmetric to the one on the left of the trioxane peak also appears in this chemical shift range.

The concentration of open-chain polymers, similar to what was observed in the homopolymerization, reached a steady state and could be ascertained easily. However, the concentration of CH<sub>2</sub>O increased rapidly as the polymerization progressed, reaching a maximum immediately before precipitation of the polymers. An attempt to measure the maximum formaldehyde concentration was made by integrating the spectra immediately before solidification. This was somewhat difficult since the polymer precipitates from solution rapidly. Therefore, quantitative estimates may not represent the maximum concentrations of CH<sub>2</sub>O but are a close approximation.

The steady-state concentration of open-chain polymers and maximum concentration buildup of CH<sub>2</sub>O under various catalyst and ethylene oxide concentrations are summarized in Table II.

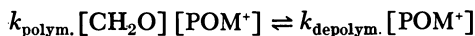
In the present investigation the reactivity and distribution of ethylene oxide observed agreed with previous results (3) using chemical analysis and chromatography. A significant finding was the buildup of surprisingly high CH<sub>2</sub>O concentration during copolymerization in contrast to homo-

polymerization. In separate experiments, it was ascertained that when gaseous  $\text{CH}_2\text{O}$  was bubbled into molten trioxane at  $65^\circ\text{C}$ ., the maximum solubility of  $\text{CH}_2\text{O}$ , before formation of solid polyformaldehyde, was 2–3 mole %; however, when ethylene oxide was present in trioxane, the solubility of  $\text{CH}_2\text{O}$  increased sharply (*see* Figure 7). The formaldehyde

**Table II. Effect of Catalyst and Ethylene Oxide Concentrations on Concentrations of Open-Chain Polymers and Formaldehyde**

<i>Mole %</i>			
<i>Ethylene Oxide</i>	<i>Catalyst</i> ( $\times 10^{-3}$ )	<i>Open-Chain Polymer</i> ( <i>Steady-State</i> )	$\text{CH}_2\text{O}$ ( <i>Max. Measured</i> )
1.5	1.0	3.7	9.0
3.3	1.0	3.5	29
3.3	2.2	3.2	12
7.2	2.2	3.4	28
10	6.0	3.0	28

concentrations were determined by NMR, and the lower-limit detection was 1 mole %. The increased solubility of  $\text{CH}_2\text{O}$  in the copolymerization systems elucidate, at least partially, the lower rates of polymerization and lower molecular weights of polymers invariably obtained in copolymerization compared with homopolymerization. Since  $\text{CH}_2\text{O}$  is formed from the depolymerization of the propagation chains, and at equilibrium,



Therefore, if  $\text{CH}_2\text{O}$  were soluble in the reaction medium, it would be deactivated, and the equilibrium consequently displaced to the left. As a result, depolymerization is favored. Table II shows that an increase in ethylene oxide concentration (*cf.*, Rows 1 with 2 and 3 with 4) increased the maximum buildup of  $\text{CH}_2\text{O}$  concentration. An increase in catalyst concentration (*cf.*, Row 2 with 3) decreased the maximum buildup of  $\text{CH}_2\text{O}$  concentration. The steady-state concentration of open-chain polymers nevertheless was insensitive to both ethylene oxide and catalyst concentrations.

Based on the spectra obtained from copolymerizations (Figures 2–6), the presence of 1,3-dioxolane could not be ascertained. This again might be attributed to low concentrations which could not be detected by NMR. Parallel copolymerization experiments were carried out, vapor-phase aliquots were analyzed during the polymerization by mass spectrometry, and the formation of 1,3-dioxolane was detected.

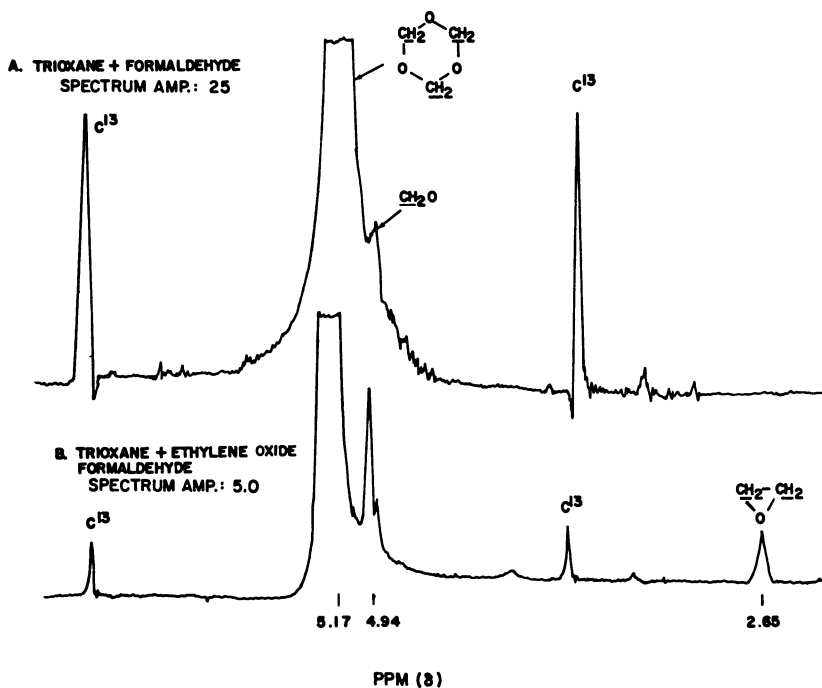


Figure 7. Solubility of  $\text{CH}_2\text{O}$  in trioxane and trioxane-ethylene oxide mixture

### Conclusion

High resolution NMR spectroscopy is advantageous and unique for studying the homo- and copolymerizations of trioxane. Reactions involving changes in proton magnetic resonance which are not ascertained conveniently by other analytical means have been revealed during the "clear period" of polymerization usually regarded as the induction period. The appearance (and equilibrium concentration) of soluble linear polyoxymethylene chains has been determined for the homo- and copolymerizations. The extremely high buildup of formaldehyde concentration during copolymerization has been revealed, and more insight into the polymerization mechanisms has been gained.

NMR, like other instrumental techniques, has limiting factors which preclude complete insight into changes occurring during a chemical reaction. One of the major disadvantages is its limiting sensitivity which precludes detection of chemical moieties at low concentrations. The formation of formaldehyde and/or tetraoxane reported for the homo-polymerizations (1, 2), and 1,3-dioxolane for the copolymerization could not be verified.



The combined techniques of NMR, gas chromatography, and mass spectrometry, together with polymerization kinetics, should be sufficient to understand the complicated mechanism of trioxane polymerization.

***Literature Cited***

- (1) Kern, W., Jaacks, J., *J. Polymer Sci.* **48**, 399 (1960).
- (2) Miki, T., Higashimura, T., Okamura, S., *J. Polymer Sci. Pt. A-1*, **5**, 95 (1967).
- (3) Price, M. B., McAndrew, F. B., *J. Makromol. Sci. Pt. A-1*, **2**, 231 (1967).

RECEIVED March 18, 1968.

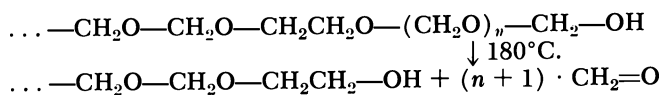
# Cationic Copolymerization of Trioxane and 1,3-Dioxolane

VOLKER JAACKS

Institute of Organic Chemistry, Mainz University, Germany

*In the copolymerization of trioxane with dioxolane, reactivity ratios of dissolved copolymer cations are quite different from those of active centers in the crystalline phase. The former strongly prefer addition of dioxolane. The difference in reactivity ratios between dissolved and precipitated active centers is attributed to the fact that in the solid phase, polymerization and crystallization of the copolymer are simultaneous. The cationic chain ends are assumed to be directly on the crystal surface. Determination of the equilibrium concentrations of formaldehyde confirms this conclusion; dissolved copolymer has a higher tendency to cleave formaldehyde than crystalline polyoxymethylene. In the latter stages of copolymerization the soluble copolymer is degraded gradually to the dioxolane monomer which is incorporated into the crystalline copolymer in an almost random distribution.*

Cationic copolymerization of trioxane with 1,3-dioxolane or other cyclic formals is of particular interest in producing thermally stable polyoxymethylene copolymers (1, 6, 14, 18). Thermal depolymerization starts at the hemiacetalic chain ends but can proceed only up to the nearest dioxolane unit:



After cleavage of  $n + 1$  formaldehyde units, a stable alcoholic end group ( $\dots -\text{CH}_2-\text{CH}_2-\text{OH}$ ) is obtained. A few percent of dioxolane units is sufficient to render the bulk of the copolymer thermally stable.

Unfortunately, neither reactivity ratios are known in copolymerizations of trioxane with cyclic formals, nor has a proper method of determining sequence lengths been developed to date. The weight of the thermally unstable fraction (terminal polyoxymethylene segments) may give some indication as to the distribution of the stabilizing dioxolane units (8). The nearer to random the distribution of the stabilizing comonomer units (and the higher the molecular weight of the copolymer), the smaller is the weight of the unstable fraction. Recently, however, a hydride transfer reaction was discovered which yields methoxy and formate or orthoformate end groups (11). These stable end groups and the formation of some stable macrocyclic polymer (10) impart an additional stabilizing effect. Thus, any conclusion from the thermal stability of a copolymer on the distribution of the stabilizing comonomer units is uncertain. Nevertheless, it is generally assumed that the few comonomer units in commercial polyoxymethylene copolymers are almost randomly distributed, so that blocks of several coherent dioxolane units are virtually absent.

It seems most important, therefore, to know one reactivity ratio— $r_1$  for copolymer cations with terminal trioxane ( $M_1$ ) unit. The second reactivity ratio,  $r_2$ , may be expected to have little significance on the polymerization and on the composition of the copolymer.

### *Elementary Reactions and Kinetics*

For the following reasons Mayo's conventional method for determining reactivity ratios (15) fails in copolymerizations of trioxane (9), and if the reactivity ratios were known, the same reasons would prevent calculation of copolymer compositions:

- (1) Cleavage of formaldehyde from the active centers and polymerization of formaldehyde at the same cationic chain ends (polymerization-depolymerization equilibrium of formaldehyde) (9).
- (2) Cleavage of oxacyclic compounds (cyclic formals) from the cationic chain ends (9, 18).
- (3) Chain transfer by polymer (transacetalization) (9, 18).

Formaldehyde is cleaved from the cationic chain ends much faster than chains propagate by addition of trioxane (13). At the end of the induction period formaldehyde reaches its equilibrium concentration, and from then on the rate of formaldehyde addition at the active chain ends equals the rate of formaldehyde production.

In the copolymerization of trioxane with dioxolane, formaldehyde may also add to copolymer cations with terminal dioxolane unit ( $P_2^+$ ).





copolymerizations with excess trioxane. Each reactivity ratio (*e.g.*,  $r_1$ ) is obtained individually from one experiment or from a series of similar experiments. Copolymerizations are run with a large enough excess of one monomer ( $M_1$ ) so that almost pure poly( $M_1$ ) is obtained containing only very few and single  $M_2$  units. Then  $P_1^+$  comprises a large majority of active centers, and as a first approximation we can neglect monomer consumption arising from reactions of  $P_2^+$ ; a correction for this neglect may be applied if necessary (7). Under these conditions, over-all monomer consumptions are given approximately by the rates of propagation of  $P_1^+$ :

$$\frac{-d[M_1]}{dt} = k_{11}[M_1][P_1^+] \quad (5a)$$

$$\frac{-d[M_2]}{dt} = k_{12}[M_2][P_1^+] \quad (5b)$$

Dividing 5a by 5b yields:

$$\frac{d[M_1]}{d[M_2]} = \frac{k_{11}[M_1]}{k_{12}[M_2]} = r_1 \frac{[M_1]}{[M_2]} \quad (6)$$

Integrating Equation 6 yields Equation 7, which is valid up to unlimited conversions as long as the excess of  $M_1$  over  $M_2$  remains large enough to produce almost pure poly( $M_1$ ):

$$\log \frac{[M_1]_t}{[M_1]_o} = r_1 \log \frac{[M_2]_t}{[M_2]_o} \quad (7)$$

$[M_1]_o$ ;  $[M_2]_o$  = initial concentration of monomers

$[M_1]_t$ ;  $[M_2]_t$  = concentrations of unreacted monomers, after termination of copolymerization

The advantage of this method is that high conversions can be determined conveniently and accurately by gas chromatography of unreacted monomers, without isolating and analyzing the copolymer. In principle, one suitable copolymerization run yields  $r_1$  with the aid of Equation 7. A series of experiments may be carried out—*e.g.*, to various different conversions or starting with different ratios of  $[M_1]/[M_2]$ ;  $\log [M_2]_t/[M_2]_o$  is plotted against  $\log [M_1]_t/[M_1]_o$ . A straight line through zero should be obtained, whose slope equals  $r_1$ .

This method is not affected by the side reactions described above. Elimination and addition of formaldehyde as well as cleavage of oxacyclic compounds and chain transfer by polymer regenerate predominantly  $P_1^+$ , the desired active center. As noted above,  $r_1$  is the more important reactivity ratio in copolymerizations of dioxolane with a large excess of trioxane. The value of  $r_1$  can be determined conveniently by the de-

scribed excess method. By analogy,  $r_2$  should be determined by copolymerization with a large enough excess of dioxolane. Polydioxolane, however, is quite soluble in organic solvents. Therefore, copolymerizations with excess dioxolane are homogeneous. In contrast, the usual copolymerizations with excess trioxane are heterogeneous, owing to the insolubility and crystallinity of the propagating polymer. Since the physical state is expected to influence the reactivities of the active centers, the second reactivity ratio ( $r_2$ ) for polymerization in the crystalline phase cannot be determined by the excess method. No possibility is seen at present to determine  $r_2$ .

### *Rates of Monomer Conversion*

To investigate the copolymerization of trioxane with dioxolane and to determine  $r_1$  by the excess method, a molar ratio of trioxane to dioxolane of 100:1.8 was used. All polymerizations were run in methylene dichloride at 30°C. with  $\text{SnCl}_4$  as initiator. To reduce the influence of formaldehyde production at the beginning of copolymerization, dioxolane was added to the solution of trioxane and initiator only at the end of the induction period—*i.e.*, at the appearance of the first insoluble polyoxymethylene. After various reaction times polymerizations were terminated by adding tributylamine. Monomer conversions were determined by gas chromatography, the liquid phase being injected directly. When conversions were small, isolation and analysis of the copolymer yielded more accurate results.

The concentrations of unreacted monomers were plotted on a logarithmic scale (Figure 1). According to Equation 7 a straight line had been expected with a slope equal to  $r_1$ . However, the curves were quite peculiar. At first dioxolane was consumed much faster than trioxane. Then, after about 50% conversion, the dioxolane concentration remained nearly constant, and predominant consumption of trioxane began. The same shape of conversion curves as in Figure 1 was obtained in copolymerizations with smaller and larger dioxolane concentrations (between 0.01 and 0.1M). In all cases a sharp break occurred after conversion of roughly half the dioxolane. The reason for this phenomenon cannot be that dioxolane simply reached its equilibrium concentration since the break occurred at quite different absolute concentrations of dioxolane, all of which were far below the equilibrium concentration. In the homopolymerization of dioxolane at 30°C. the equilibrium concentration is at  $\sim 2M$  (16).

The fast initial conversion of dioxolane yielded copolymers which are soluble in the reaction medium owing to their high dioxolane content of over 50 mole %. The increase of this soluble copolymer ceased at

about the same time that the break in the conversion curve occurred. At this point a second type of copolymer began to form; it contained so much trioxane (98 mole %) that it was insoluble in the reaction medium and crystallized immediately. For a short time both types of copolymers—soluble and crystalline—propagated simultaneously in the same copolymerization run. In the later stages of copolymerization formation of the crystalline copolymer with high trioxane content was the only monomer-consuming reaction.

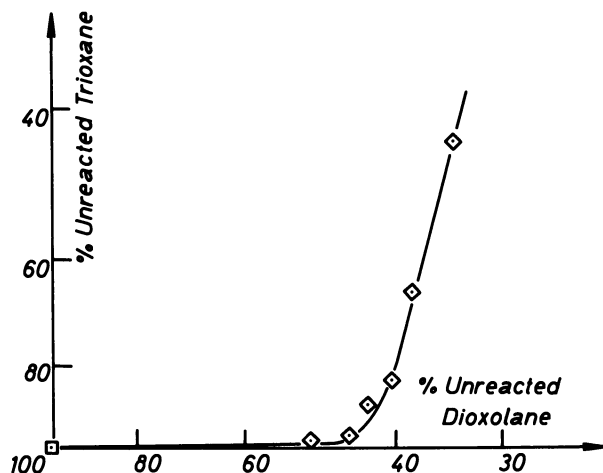


Figure 1. Copolymerization of trioxane (2.5M) with 1.8 mole % of dioxolane at 30°C. in  $\text{CH}_2\text{Cl}_2$ . Concentration of  $\text{SnCl}_4 = 0.017M$

Up to now we have not found reaction conditions permitting exclusive production of insoluble copolymer, which is the desired product in commercial copolymerization of trioxane. Conversion of a large portion of the dioxolane into soluble copolymer could not even be avoided by slow and gradual addition of the comonomer to a homopolymerization run of trioxane in methylene dichloride (9). The same result was obtained in solution copolymerization of trioxane with 8 mole % of 1,3-dioxacycloheptane (dioxepane), and even 1,3-dioxane—which is not homopolymerizable and is a very sluggish comonomer—formed a soluble copolymer in the initial phase of copolymerization (trioxane: 2.5M; 1,3-dioxane: 0.31M;  $\text{SnCl}_4$ : 0.025M in methylene dichloride at 30°C.).

### Estimating Reactivity Ratios

With almost identical monomer concentrations two copolymers of completely different composition were formed—one in solution, the



other in the crystalline phase. In Figure 1 the soluble copolymer containing 70% dioxolane units is formed at [trioxane]/[dioxolane] ratios between 55 and 110. After the break in the conversion curve, crystalline copolymer containing only 2.2 mole % of dioxolane units is formed at monomer concentration ratios between 120 and 70 (owing to the faster consumption of trioxane, the molar ratio decreases again). Soluble copolymer of over 50% dioxolane content was even obtained at initial ratios of monomer concentrations as high as 200.

One possible explanation of the differences in composition could be diffusion control in the crystalline phase. This may have a certain limited importance, but diffusion does not seem to be the main factor governing monomer consumption in the crystalline phase. Otherwise, the ease of diffusion of monomers to the active centers and not chemical reactivity should determine the composition of copolymers. Monomers of similar molecular size and shape show large differences, however, in their rates of copolymerization with trioxane—*e.g.*, a strong decrease in reactivities was observed in the comonomer series 1,3-dioxolane > 1,3-dioxepane > 1,3-dioxane. Furthermore, activation energies in the solution polymerization of trioxane seem too high to be compatible with a diffusion-controlled process (initiation is relatively fast (2, 5) and therefore does not contribute substantially to the over-all activation energy). A second possibility of explaining at least in part the low oxymethylene content of the soluble copolymer could be the fact that formaldehyde is cleaved from dissolved propagating chains with terminal trioxymethylene unit (9). In the initial phase of copolymerization the equilibrium concentration of 0.1 mole CH<sub>2</sub>O/liter is set up by depolymerization of soluble copolymer. However, the addition of formaldehyde to the monomer solution before initiation did not reduce substantially the amount of the dioxolane content of the soluble copolymer (9).

It seems, therefore, that the main reason for the different composition of dissolved and crystalline copolymer is a genuine difference in reactivity ratios in the two phases. Generally speaking, dissolved copolymer cations have a very high affinity for dioxolane monomer, while chains propagating in the crystalline phase prefer addition of trioxane. For a full description and characterization of the system, four reactivity ratios should be known: two for chains propagation in solution ( $r_{1\text{ sol}}$  and  $r_{2\text{ sol}}$ ) and two for propagation in the crystalline phase ( $r_{1\text{ cryst}}$  and  $r_{2\text{ cryst}}$ ). Furthermore, the over-all consumption of each monomer should depend strongly on the ratio of the numbers of active centers in the dissolved and in the crystalline phase. This makes the kinetics of such copolymerizations quite complicated and may cause peculiar effects such as the break in the conversion curve in Figure 1.

Despite these complications, an attempt is made to estimate at least some of these reactivity ratios;  $r_{1\text{crist}}$ —the most important reactivity ratio in the system—can be determined by the excess method described above. The dioxolane content of the crystalline copolymer is small enough to satisfy the conditions for using the method. For reasons which will become apparent later (depolymerization of soluble copolymer) copolymer analysis had to be used rather than direct determination of unreacted monomers by gas chromatography. For analysis, the crystalline copolymers were isolated and hydrolyzed in 0.1*N* aqueous HCl at 95°C. (19). Dioxolane units in the copolymer yielded ethylene glycol and dioxolane, both of which were determined by gas chromatography of the neutralized aqueous solution. The insoluble copolymer isolated after 35% trioxane conversion in the experiment in Figure 1 contained 2.2 mole % of dioxolane units (*i.e.*, 2.2 dioxolane units per 100 trioxymethylene units). Owing to the unusual shape of the conversion curve in Figure 1 an almost constant ratio of monomer concentrations ( $[\text{trioxane}]/[\text{dioxolane}] \sim 100$ ) had been maintained throughout the formation of this crystalline copolymer. Therefore, the differential equation (Equation 6) may be used in this case. We obtain the following approximate value for the reactivity ratio of crystalline copolymer cations with terminal trioxane ( $M_1$ ) unit:

$$r_{1\text{crist}} = \frac{d[M_1]}{d[M_2]} \cdot \frac{[M_2]}{[M_1]} = 45/100 \sim \frac{1}{2}$$

$$\frac{d[M_1]}{d[M_2]} = \frac{100}{2.2} = 45 \text{ is the composition of the copolymer}$$

Hence, dioxolane is slightly more reactive than trioxane toward crystalline polymer cations with terminal trioxane unit. The same result was obtained from similar copolymerization runs.

The soluble copolymer contains too much dioxolane (> 50 mole %) to use the excess method. Even from a monomer mixture of  $[\text{trioxane}]/[\text{dioxolane}] = 200$  a soluble copolymer of *ca.* 50 mole % dioxolane content is formed. There may be two reasons for the high dioxolane content: a very low value of  $r_{1\text{sol}}$  or a very high value of  $r_{2\text{sol}}$ . In the latter case long blocks of coherent dioxolane units should be formed. Formation of blocks of more than 1 or 2 dioxolane units is improbable, however, since dioxolane is present in less than 1/100 of its equilibrium concentration. If two successive dioxolane units have accumulated at the cationic chain end, depropagation to dioxolane monomer is over 100 times faster than addition of another dioxolane unit. We are dealing with a copolymerization with one strongly reversible propagation step. No matter what the actual value of the reactivity ratio  $r_{2\text{sol}}$  is, the effect of the fast depropagation is the same as if  $r_{2\text{sol}}$  were very small. Therefore, the high dioxolane content

of the soluble copolymer must be attributed to a small value of  $r_{1 \text{ sol}}$ . Considering the large excess of trioxane in the monomer mixture and the high dioxolane content of the soluble copolymer it is obvious that dioxolane must have a much higher reactivity than trioxane toward dissolved copolymer cations with terminal trioxane unit:

$$r_{1 \text{ sol}} \ll 0.1$$

This value is at least one order of magnitude smaller than  $r_{1 \text{ cryst}}$ .

The same reason (depropagation of dioxolane-dioxolane blocks) which prevents formation of long dioxolane sequences in solution also applies to polymerization in the crystalline phase. This supports the assumption that most of the dioxolane incorporated into the crystalline copolymer is present as single units and not as longer blocks.

***Reasons for the Differences in Reactivity Ratios Between the Dissolved and Crystalline Phase (Topochemistry of Chain Propagation)***

The chemical structures of propagating chain ends in the dissolved and in the crystalline copolymer are identical. Therefore, differences in the reactivity ratios must be attributed to physical differences in the environment of the copolymer cations.

Such differences in reactivities would be plausible if during chain growth in the solid phase, polymerization and crystallization were simultaneous. This means that a newly added monomer unit is incorporated into the crystal lattice at the same time that it is attached chemically to the polymer chain. This would imply that the cationic chain ends are directly on the crystal surface (simultaneous polymerization and crystallization as symbolized by Model A in Figure 2).

Other possibilities of chain growth are indicated in Figure 2, as proposed by Wunderlich in a general review on crystallization during polymerization (20, 21). In Model B, crystallization of chain segments takes place at some distance from the propagating chain end (successive polymerization and crystallization); the active centers actually remain in the dissolved state. Model C represents the formation of a complete macromolecule in solution; afterward the terminated chain may crystallize. This model is improbable in trioxane polymerization because high molecular weight polyoxymethylene (and copolymers containing predominantly oxymethylene units) is virtually insoluble in the reaction medium and chain propagation is slow enough to give the growing chains time to crystallize. Recently, Model C was ruled out experimentally by Csürös (3). He found that the propagating active centers are predominantly in the crystalline phase.

It is an interesting fundamental question as to which of the remaining models, A and B, is true. To explain our copolymerization results, we

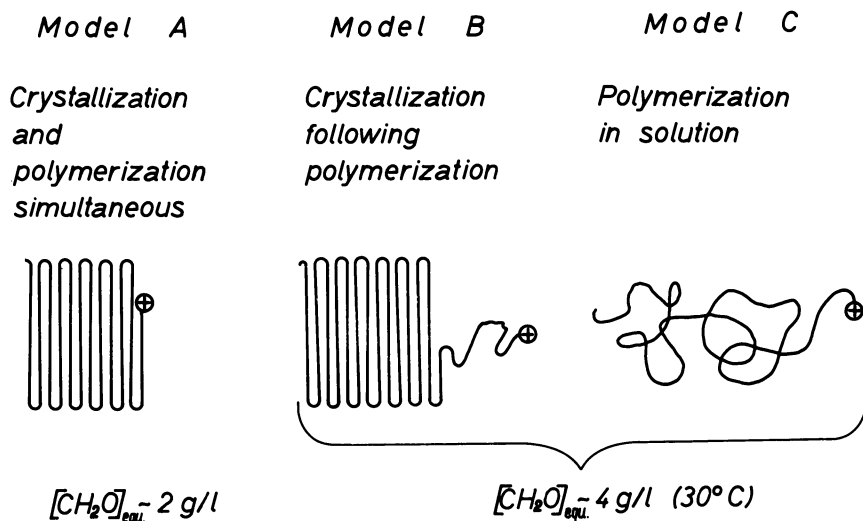


Figure 2. Possible mechanisms of chain propagation in heterogeneous polymerizations

tend to assume the former—simultaneous polymerization and crystallization. This assumption was confirmed by measuring formaldehyde concentrations during the polymerization of trioxane. As noted earlier, monomeric formaldehyde is present in its equilibrium concentration during the homopolymerization of trioxane as well as during copolymerization. Cationic chain ends quickly cleave off formaldehyde and (after the induction period) also add formaldehyde with an equally high velocity. If the cationic chain ends are actually in the crystal lattice (as in Model A), the equilibrium concentration of formaldehyde should be lower than in the case of dissolved cations (Model C). This is because in Model A the entropy and the heat of crystallization ( $\Delta H_{\text{cryst}} \sim -2$  kcal./base mole) come in addition to the entropy and heat of polymerization of formaldehyde ( $\Delta H_{\text{pol}} \sim -6$  kcal./mole).

On the other hand, no difference in equilibrium concentration is expected between Models C and B. In the latter only the “dead” chain segments are crystallized while the cationic active centers, at which depolymerization and polymerization of formaldehyde takes place, are in solution.

In the experimental investigations the soluble copolymer from trioxane and 25 mole % of dioxolane was used as Model C. This is permissible because dioxolane does not cleave off formaldehyde during polymerization. The experimental determination of equilibrium concentrations of formaldehyde during trioxane polymerization is somewhat problematic. Up to now the only available method is extraction of

formaldehyde monomer from the polymerization medium by an aqueous phase. Once dissolved in water, the formaldehyde may be titrated easily by the iodometric or by the sulfite method (17). The disadvantage of this method is that during extraction with water some unstable chain ends may depolymerize to formaldehyde, thus exhibiting a false high formaldehyde concentration. Dissolved oligomeric or copolymer chains especially are susceptible to depolymerization. A more reliable spectroscopic method of determining formaldehyde monomer in the polymerization medium is being developed (4). At present, however, only results of the extraction—titration method are available.

In the homopolymerization of trioxane at 30°C. in methylene dichloride an equilibrium concentration of 2.0 grams  $\text{CH}_2\text{O}$ /liter was found (13). Here chain growth takes place predominantly in the solid phase. In contrast, copolymerization of trioxane (2.8 moles/liter) with dioxolane (0.78 mole/liter) is homogeneous up to a conversion of more than half the dioxolane. In this system higher formaldehyde concentrations were titrated—the highest, 4.2 grams  $\text{CH}_2\text{O}$ /liter, shortly after precipitation of the first insoluble copolymer. Later in the copolymerization the equilibrium concentration decreases again and falls below 3 grams/liter.

The difference in formaldehyde equilibrium concentration between homogeneous and heterogeneous polymerization is large enough to indicate a difference in the physical state of cationic chain ends in the dissolved and in the crystalline polymer. Thus, Model B is ruled out. In the homopolymerization of trioxane and in the heterogeneous copolymerization with small amounts of dioxolane the active centers of chains which have precipitated from the solution predominantly are directly on the crystal surface (Model A). According to Wunderlich (20, 21), this is the first case in addition polymerization where Model A—simultaneous polymerization and crystallization—has been proved experimentally.

The topochemical differences in the physical environment of dissolved and crystallized active centers explain easily the difference in reactivity ratios between the two phases. The gain in free energy arising from immediate crystallization of growing chain ends enhances the incorporation of trioxane into the crystalline copolymer. Simultaneous crystallization is considered an important driving force in copolymerization as well as in the homopolymerization of trioxane. On the other hand, dioxolane units do not fit the crystal lattice of polyoxymethylene and reduce the crystallinity of the polymer. This impedes the incorporation of dioxolane units into the crystalline copolymer.

The observed difference in formaldehyde equilibrium concentration between dissolved and crystalline copolymer chains may affect the copolymer composition in still another manner: part of the formaldehyde,

which is quickly cleaved off from dissolved copolymer cations, will add to active centers in the crystalline phase. Owing to the smaller formaldehyde equilibrium concentration of crystalline copolymer, formaldehyde is withdrawn constantly from the dissolved chains and is absorbed by the crystalline phase. This may be an additional reason for the large difference in composition between dissolved and crystalline copolymer.

### *Further Reactions of the Soluble Copolymer*

There is a further complication in the copolymerization of trioxane with dioxolane. The initially formed soluble copolymer gradually vanishes later in the polymerization (see Figure 3). To discover the reaction mechanism by which the soluble copolymer disappears, the following experiments were made:

(1) The soluble copolymer was isolated, dried, and added to a homopolymerization run of trioxane in methylene dichloride. After a few minutes at 30°C. appreciable amounts of monomeric dioxolane were identified by gas chromatography.

(2) Dioxolane was also formed in the absence of trioxane when the soluble copolymer was simply dissolved in a 0.03M solution of  $\text{SnCl}_4$  in methylene dichloride at 30°C. (conditions similar to those of the copolymerization in Figure 3). Within one hour half of the soluble copolymer was depolymerized under formation of dioxolane monomer and formaldehyde.

These experiments indicate that the disappearance of the soluble copolymer in Figure 3 is caused mainly by depolymerization to dioxolane

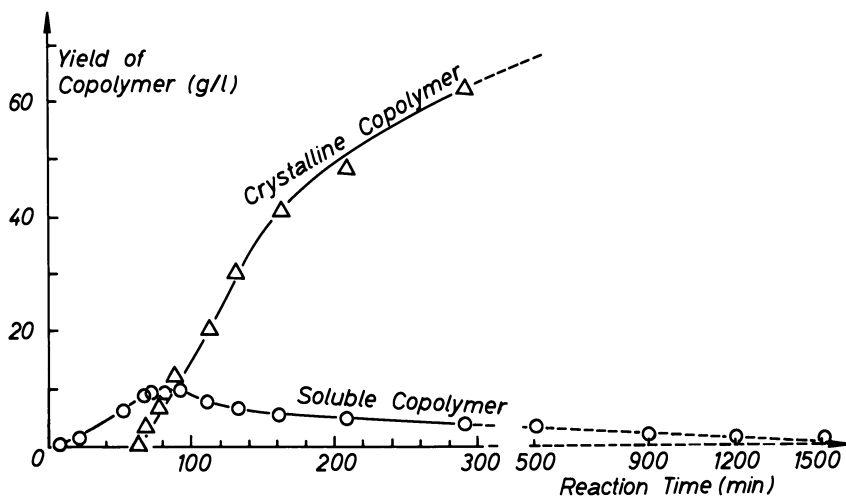


Figure 3. Copolymerization of trioxane with 10 mole % dioxolane in  $\text{CH}_2\text{Cl}_2$  at 30°C. Concentration of trioxane, 2.8M; concentration of  $\text{SnCl}_4$ , 0.025M

and formaldehyde or trioxane. Then the dioxolane monomer is incorporated gradually into the crystalline copolymer. This also explains why in the second stage of copolymerization—after the break of the curve (Figure 1)—the dioxolane concentration remains almost constant and in some cases even increases slightly during further polymerization. The soluble copolymer serves as a kind of reservoir from which the dioxolane monomer is replenished continuously as it is consumed by incorporation into the crystalline copolymer.

It remains to be explained why the soluble copolymer is at first formed and then depolymerized again, although the reaction conditions and monomer concentrations do not change substantially. The answer to this question also lies in the difference in formaldehyde equilibrium concentration between dissolved and crystalline copolymer. As mentioned above, crystalline copolymer cations absorb formaldehyde which has been split off from the dissolved chains. As the number of crystalline active centers increases during copolymerization, the dissolved chains lose formaldehyde at an increasing rate. Eventually, the loss of formaldehyde becomes faster than chain growth of the dissolved copolymer by addition of new trioxane. The dissolved copolymer becomes thermodynamically unstable as the formaldehyde concentration falls below 4 grams/liter. Further, the dioxolane monomer is far below its equilibrium concentration which amounts to 2 moles/liter at 30°C. (16). Therefore, dioxolane units or dioxolane blocks at the cationic chain ends of dissolved copolymer cannot survive either. They eliminate dioxolane by a cationic backbiting mechanism. Thus, the dissolved copolymer vanished gradually.

### Conclusions

One of the most prominent features in the heterogeneous copolymerization of trioxane is the occurrence of two different kinds of active centers—dissolved and crystalline copolymer cations. They have different copolymer reactivity ratios and different tendencies to depolymerize, *i.e.*, different formaldehyde equilibrium concentrations. At first the formation of soluble copolymer with high dioxolane content did not raise much hope for obtaining a crystalline copolymer of good thermal stability from trioxane and dioxolane; but the gradual depolymerization of the soluble copolymer proved to be a useful side reaction which greatly improved the situation. Eventually, the entire complicated process turned out to be quite favorable for the formation of a stable crystalline copolymer with the desired random distribution.

Previously, the best explanation of the almost random distribution of such copolymers had been given by Weissermel, Fischer, Gutweiler, and Hermann (18). They proposed that an extensive transacetalization takes

place during copolymerization. This is a transfer reaction by copolymer; a propagating polymer cation cleaves another macromolecule which may be a soluble copolymer chain (*see* Figure 4). By one such transfer step a long block of soluble copolymer is attached to a chain growing in the crystalline phase. This block must be cleaved repeatedly before a random distribution can result. Furthermore, the fragments would have to be mobile enough to be linked together in a different way. In view of the high crystallinity of the solid copolymer this does not seem probable at moderate temperatures. Even the first transacetalization step (between soluble and crystalline copolymer as in Figure 4) may not be very fast owing to difficulty of diffusion. Thus, the soluble copolymer from trioxane and styrene, which does not depolymerize easily, remained unchanged during further polymerization and was not incorporated into the crystalline phase (9).

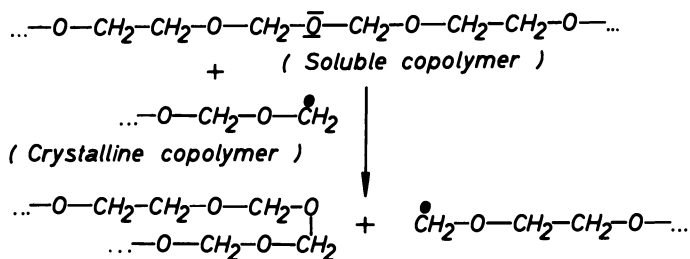


Figure 4. Transfer by polymer in copolymerization of trioxane (transacetalization)

The occurrence and a limited importance of chain transfer by transacetalization cannot be doubted. We proposed this type of reaction for trioxane polymerization as early as 1959 (6) and assumed that intramolecular transacetalization produces some thermally stable macrocyclic polyoxymethylene (10). We have utilized bimolecular chain transfer by polymers to produce thermally stable block copolymers at temperatures over 100°C. [—*e.g.*, with polyesters, polypropylene oxide, or with poly(vinyl butyral)] (12).

In the copolymerization of trioxane with dioxolane, however, depolymerization and regeneration of dioxolane monomer is a faster and more effective way of converting soluble into crystalline copolymer with random distribution. A similar mechanism may hold true for trioxane polymerization with similar comonomers such as 1,3-dioxane, 1,3-dioxacycloheptane and in part even for copolymerization of trioxane with ethylene oxide which also involves formation of some dioxolane and soluble copolymer.



### Acknowledgments

I am indebted to W. Kern for promoting this work and to I. Lehmann for carrying out the experiments. I thank Degussa, Frankfurt/Main for subsidizing our work.

### Literature Cited

- (1) Berardinelli, F. M., Dolce, T. J., Walling, C., *J. Appl. Polymer Sci.* **9**, 1419 (1965).
- (2) Boehlke, K., Ph.D. Dissertation, Mainz, 1969.
- (3) Csürös, Z., unpublished data.
- (4) Hölle, J., unpublished data.
- (5) Jaacks, V., Boehlke, T. K., Eberius, E., *Makromol. Chem.* **118**, 354 (1968).
- (6) Jaacks, V., Ph.D. Dissertation, Mainz, 1959.
- (7) Jaacks, V., *Makromol. Chem.* **105**, 289 (1967).
- (8) *Ibid.*, **84**, 250 (1965).
- (9) *Ibid.*, **101**, 33 (1967).
- (10) *Ibid.*, **99**, 300 (1966).
- (11) Jaacks, V., Frank, H., Grünberger, E., Kern, W., *Makromol. Chem.* **115**, 290 (1968).
- (12) Jaacks, V., Kern, W., *Makromol. Chem.* **83**, 71 (1965).
- (13) Kern, W., Jaacks, V., *J. Polymer Sci.* **48**, 399 (1960).
- (14) Kern, W., Cherdon, H., Jaacks, V., *Angew. Chem.* **73**, 177 (1961).
- (15) Mayo, F. R., Lewis, F. M., *J. Am. Chem. Soc.* **66**, 1594 (1944).
- (16) Plesch, P. H., Westermann, P. H., *J. Polymer Sci. Pt. C*, **16**, 3837 (1968). 1964.
- (17) Walker, J. F., "Formaldehyde," Reinhold Publishing Corp., New York, 1953.
- (18) Weissermel, K., Fischer, E., Gutweiler, K., Hermann, H. D., *Kunststoffe* **54**, 410 (1964).
- (19) Weyland, P., unpublished data.
- (20) Wunderlich, B., *Fortschr. Hochpolymerenforsch.* **5**, 568 (1968).
- (21) Wunderlich, B., *Angew. Chem.* **80**, 1009 (1968).

RECEIVED May 8, 1968.

# Polymerization and Copolymerization of Olefins on Chromium Oxide Catalysts

ALFRED CLARK

Phillips Petroleum Co., Bartlesville, Okla. 74003

*Fundamental aspects of polymerization and copolymerization of olefins on supported chromium oxide catalysts are discussed. Evidence is presented showing that hexavalent chromium is stabilized by the support. The reaction is believed to proceed through a Langmuir-Hinshelwood mechanism on tetrahedral chromium sites. Chain termination occurs predominantly by transfer with monomer. The active site may be formed by interaction of ethylene or other agents such as CO with the tetrahedral chromium site. As chromium content is increased, the efficiency of reaction per chromium atom decreases. The rate-temperature curve for polymerization of ethylene goes through a maximum. Homopolymerization of 1-butene proceeds at one-tenth the rate of its copolymerization with ethylene. The broad distribution of molecular weights obtained is attributed to the broad distribution of adsorption site energies.*

Since the discovery (6) of supported chromium oxide catalysts for polymerization and copolymerization of olefins, many fundamental studies of these systems have been reported. Early studies by Topchiev *et al.* (18) deal with the effects of catalyst and reaction variables on the over-all kinetics. More recent studies stress the nature of the catalytically active species (1, 2, 9, 13, 14, 16, 19). Using ESR techniques, evidence is developed which indicates that the active species are Cr ions in tetrahedral environment. Other recent work presents a more detailed look at the reaction kinetics. For example, Yermakov and co-workers (12) provide evidence which suggests that chain termination in the polymerization of ethylene on the catalyst surface takes place predominantly by transfer with monomer, and Clark and Bailey (3, 4) give evidence that chain growth occurs through a Langmuir-Hinshelwood mechanism.

This chapter reviews and extends some of the fundamental aspects concerned with the nature of the catalyst, the reaction, and the product.

### *The Process*

There are at least two ways of carrying out the process: the solution process and the slurry process.

In the solution process, the reaction is carried out in the presence of an inert hydrocarbon which dissolves the polymer as it is formed. The solvent may contain a portion of cycloparaffin. Both monomer and polymer remain in solution during the reaction while the catalyst is maintained in suspension by agitation. Reaction temperatures range from about 125°–175°C. and reaction pressures from 20–30 atm. The reactor product is withdrawn, and monomer is flashed off and recycled. Suspended catalyst is then removed by filtration, and solvent is flashed from the filtrate with steam.

In the slurry process, the reaction is carried out in a liquid dispersant (paraffinic in nature), in which catalyst and polymer remain in suspension. Reaction temperature is held below 110°C. to prevent dissolution of the polymer. Catalyst does not necessarily remain in the middle of a polymer particle but spalls and is scattered throughout the polymer. The slurry of polymer and hydrocarbon is withdrawn from the reactor and flashed to remove diluent and unreacted olefin for recycle. Because of the high productivities obtained in this process, it is unnecessary to remove catalyst for many polymer applications.

### *The Catalyst*

The catalyst may be prepared by impregnating a silica–aluminum support with an aqueous solution of chromium trioxide. After drying, the catalyst is usually activated in a stream of dry air at temperatures ranging from *ca.* 400°–800°C. Under these conditions catalysts can be prepared with a major percentage of chromium in the form of chromium trioxide. Evidently, the support is not just an inert diluent for chromium oxide by itself is stable only as Cr<sub>2</sub>O<sub>3</sub> at these temperatures. There must be interaction between chromium trioxide and the support which stabilizes the former.

Other evidence of stabilization exists. For example, if a catalyst is prepared by activating the support alone and mixing it with dried, powdered chromium trioxide, no polymerization activity is developed until after the catalyst has been heated to approximately the melting point of chromium trioxide (~197°C.). A slow increase in the polymerization rate occurs as the mixture is heated at temperatures up to

400°C.; at higher temperatures, the increase in polymerization rate is more rapid. These results indicate that high temperature activation is important not only for removing water from the support but also for inducing the stabilizing interaction between the support and chromium trioxide.

Further evidence for stabilization is obtained from reduction profiles of catalysts (11). These profiles were determined from changes in the reduction rate as the temperature of a test sample in contact with hydrogen was increased at a steady rate from 145°–550°C. Hydrogen was circulated continuously over the catalyst, passing through a drying agent on each cycle. Reduction rates,  $\Delta P/\Delta t$ , were determined by measuring pressure drops in small time intervals, and they were plotted against temperature. The heating rate selected was 1.5°C./min. When samples are the same size and similar heating schedules are used, the areas under the curves measure the total amount of reduction.

In Figure 1, the profiles represent the rates of reduction of samples containing different amounts of total chromium from 0.25% to 3.19%. It is evident that reduction starts at a lower temperature the higher the chromium content. The results clearly show that the lower the chromium content, the more resistant the chromium is to reduction.

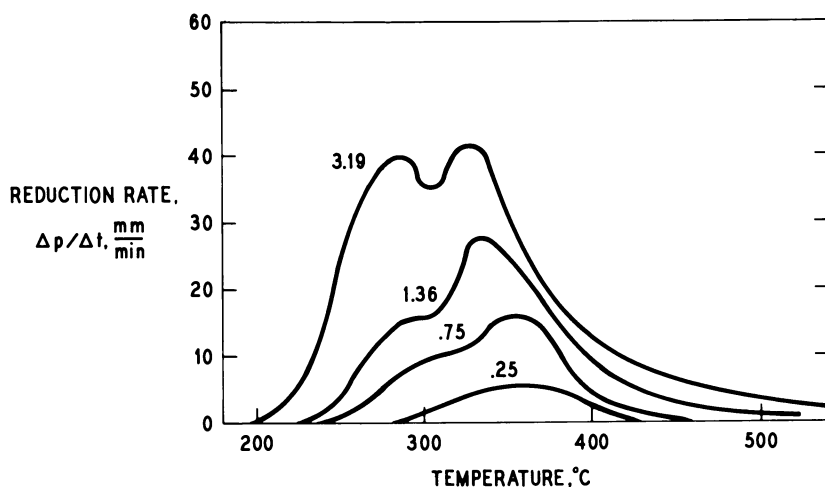


Figure 1. Reduction profiles for air-activated catalysts with varying chromium content

It is interesting to speculate how the support stabilizes the chromium ion against reduction. A reasonable explanation may be based on the views of van Reijen and Cossee (17), who speculate that  $\text{CrO}_4$

tetrahedra are linked to the silica network by sharing corners or edges with  $\text{SiO}_4$  tetrahedra. The amount of chromium so stabilized will be limited, and, as found experimentally, the stability of the high oxidation states of chromium decreases with increasing concentration of chromium on the support not only under reducing conditions but also under oxidizing conditions as in catalyst activation.

### *The Reaction*

Many of the kinetic studies have been done at low pressures and temperatures because accurate kinetic measurements are more difficult to make at high pressures. Those measurements that have been made at high pressures ( $\sim 500$  p.s.i.g.) confirm the approximate first-order relationships obtained at atmospheric pressure and below. Therefore, we believe that the kinetic information obtained at low pressures has general significance. In spite of the indicated first-order behavior, the reaction is undoubtedly complex, and the relative rates of the individual steps may change drastically with pressure. Yet there is no reason to believe that totally different mechanisms operate in the various pressure ranges. Reaction rates at atmospheric pressure and below have been determined by three different techniques:

- (1) Quartz vacuum microbalance, in which the rate of reaction is determined by weighing the polymer produced as a function of time.
- (2) Static system, in which rate of reaction is determined by pressure drop of monomer as a function of time.
- (3) In a flow system using helium diluent.

All three methods gave consistent results. Figure 2 gives a typical low pressure first-order plot.

In a previous publication (4) it was shown that at pressures above 500 p.s.i.g., the rate of reaction ultimately levels out, approaching zero order. This behavior offers evidence that polymerization occurs by reaction of an adsorbed monomer molecule with an adjacently adsorbed monomer molecule or growing polymer chain (Langmuir-Hinshelwood mechanism). If polymerization occurred by reaction of monomer in the gas phase with adsorbed monomer or adsorbed growing polymer chains (Rideal mechanism), the reaction rate should increase without limit as pressure is increased.

The details of the mechanism are not well understood yet. Reasonable speculations based on evidence from ESR measurements have been published by van Reijen and Cossee (17) and by Pecherskaya and Kazanskii (15). Van Reijen and Cossee speculate that the active site in a chromium oxide-silica catalyst is a tetrahedrally coordinated chromium ion. They picture the  $\text{CrO}_4$  tetrahedron linked to the  $\text{SiO}_2$  network by

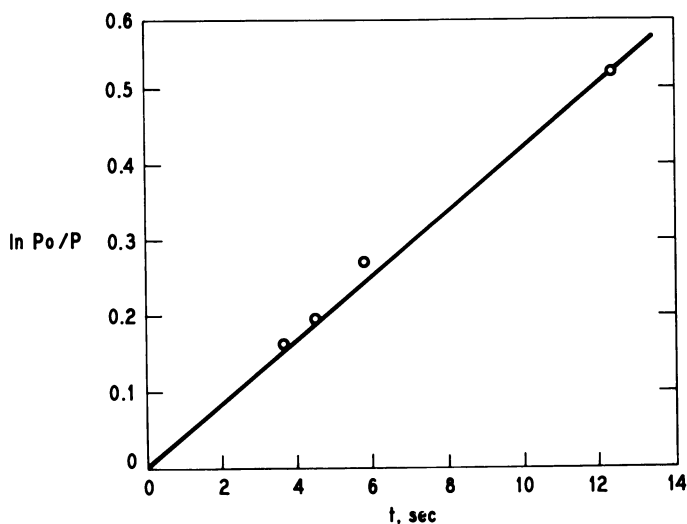


Figure 2. Typical first-order plot polymerization of ethylene over Cr-Si-Al catalyst (low temperature and pressure)

sharing corners or edges with  $\text{SiO}_4$  tetrahedra. Four different ligands of the Cr ion may be distinguished as follows: (1)  $\text{O}^{2-}$  ions shared by a Cr and a Si ion, (2)  $\text{O}^{2-}$  ions pointing outward, (3)  $\text{OH}^-$  ions pointing outward, and (4)  $\text{H}_2\text{O}$  molecules pointing outward. The detailed symmetry of the ligand field will be determined chiefly by the polarization of the oxygen bonds. The  $\text{O}^{2-}$  ion pointing outward will form the most polarized bond; the  $\text{H}_2\text{O}$  molecule pointing outward will form the least polarized bond, and the other two types of bonds will represent intermediate degrees of polarization. It is possible to form (1) a tetrahedron with a predominantly trigonal symmetry formed from one strongly and three intermediately polarized ligands, (2) a tetrahedron with predominantly a mirror symmetry formed by three differently polarized ligands. Pecherskaya and Kazanskii (15) describe the initiation of a polymeric chain reaction as occurring by interaction between the center and a molecule of ethylene, leading to alkylation of the center, and changing from tetrahedral to square pyramidal coordination. The square pyramidal configuration is considered to possess a free ligand which, if filled, produces an octahedral configuration. The free ligand of the square pyramidal structure may adsorb a second ethylene molecule (15) which then inserts itself into the Cr-C bond of the first adsorbed ethylene in a manner similar to that proposed by Cossee (17) in chain propagation for complex Ziegler-Natta catalysts. The work of Yermakov and co-workers (12) presents strong evidence showing that chain termination occurs chiefly by transfer with monomer.

The behavior of the reaction rate as a function of temperature dispels any notion that the reaction is simple. Figure 3 shows that there is a maximum in the first-order rate constant-temperature curve at approximately 80°C. At such a low temperature, the rate-temperature maximum cannot be explained by depolymerization, nor can it be explained by deactivation of the catalyst as a result of more rapid polymer accumulation on the catalyst at higher temperatures since the maximum is obtained for *initial* rates measured as a function of temperature. Theoretical considerations predict that a maximum in the rate-temperature curve may be expected from the Langmuir-Hinshelwood model for polymerization on solid surfaces but not from the Rideal model (5). The rate of reaction for the Langmuir-Hinshelwood model is given by:

$$R = N_o^2 k_r \theta_1^2 (N_o k_r \theta_1 + 2k_d) / k_d \quad (1)$$

where  $N_o$  is the number of polymerization sites per unit catalyst surface;  $\theta_1$ , the fraction of sites covered with monomer;  $k_r = A_r e^{-Q/RT}$ , the reaction velocity constant;  $k_d = A_d e^{-Q/RT}$ , the desorption velocity constant. The activation energy in  $k_r$  for the surface reaction is assumed to be the energy required to remove an adsorbed monomer molecule laterally from its position and is taken equal to the heat of adsorption  $Q$  (4).

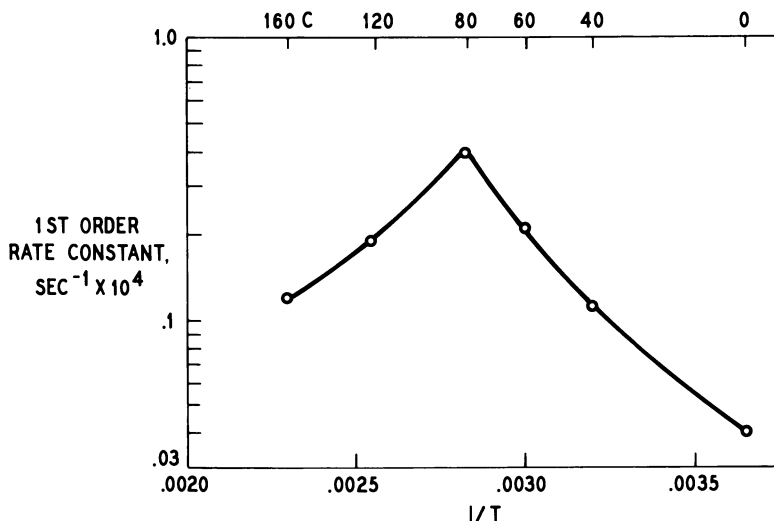


Figure 3. Effect of temperature on polymerization activity

The monomer material balance on the surface at steady state is:

$$b^2\theta_1^3 + cb\theta_1^2 - 2b\theta_1^2 + c\theta_1 + \theta_1 - c = 0, \quad (2)$$

where  $b = k_r N_o / k_a$ ,  $c = k_a P / k_a$ , and  $k_a$  is the velocity constant of adsorption in which the activation energy is assumed to be zero.

Using the Arrhenius form of  $k_r$  and  $k_a$  in Equation 2, we solve for  $e^{Q/RT}$ :

$$e^{Q/RT} = A_d \left( \frac{\theta_1^3}{K^2} + \frac{2}{K} \theta_1^2 + \theta_1 \right) / k_a P \left( 1 - \theta_1 - \frac{\theta_1^2}{K} \right), \quad (3)$$

where  $K = A_d / A_r N_o$ .

Substituting Equation 3 into Equation 1, the result is:

$$R = [k_a P A_r N_o^2 / A_d] [\theta_1 (\theta_1 + 2K) (K - K\theta_1 - \theta_1^2) / (\theta_1 + K)^2]. \quad (4)$$

Taking the derivative with respect to temperature and setting it equal to zero gives:

$$\theta_{1m}^4 + \frac{7}{2} K \theta_{1m}^3 + \frac{9}{2} K^2 \theta_{1m} - K^3 = 0, \quad (5)$$

where  $\theta_{1m}$  is the value of  $\theta_1$  at the rate maximum for given  $K$ . It is interesting to note that  $\theta_{1m}$  is independent of  $T_{\max}$ , the temperature at which a rate maximum is observed.  $T_{\max}$  is a function of pressure. In Equation 5, when  $\theta_{1m}$  is zero,  $K$  is zero;  $\theta_{1m}$  approaches the value  $1/2$  asymptotically as  $K$  increases. This means that for this model rate maxima are not possible when the surface is more than one-half covered with monomer.

If values of  $\theta_{1m}$  and  $K$  from Equation 5 are substituted into the monomer balance Equation 2, the values of  $T_{\max}$  as a function of pressure are obtained. Since  $e^{Q/RT} \geq 1$  ( $T$  and  $Q$  always positive), it is possible to calculate, for each pair of values of  $\theta_{1m}$  and  $K$ , the minimum value of  $A_d / k_a P$  below which a rate maximum is not possible. It may be seen from Table I that after passing through a maximum,  $(A_d / k_a P)_{\min}$  approaches unity asymptotically with increasing  $K$ .

Apparent activation energies have been measured for various chromium contents and supports at low pressures and temperatures far below the rate-temperature maximum. In the temperature range  $-40^\circ$ – $0^\circ\text{C}$ .

**Table I. Criteria for Existence of a Rate Maximum**

K	$\theta_{1m}$	$(A_d / k_a P)_{\min}$
1000	0.5	1.00
100	0.5	1.00
50	0.49	1.01
10	0.43	1.18
1	0.28	1.40
0.1	0.14	1.24
0.01	0.045	0.55
0.001	0.015	0.19
0.0001	0.0045	0.087



on catalysts containing from 0.5 to 2.5% chromium on silica-alumina (85-15), alumina, and silica, activation energies calculated from first-order rate constants remained practically constant at 7-8 kcal. There is danger in trying to interpret activation energies of complex reactions. Possibly the activation energy is associated with the energy of mobility required to move monomer adsorbed on the support to the chromium atom polymerization site. Such energies should correspond roughly with the average energies of adsorption of ethylene on the supports.

It is interesting to note the effect of chromium content on reaction rate at high pressures ( $\sim 500$  p.s.i.g.). Experiments (5) were carried out with normal air-activated catalysts (Figure 4). Catalysts were used with chromium contents ranging from 0.7 to 0.0005 wt. % of the total catalyst. Results of one-hour ethylene polymerization tests at 132°C. and 450 p.s.i.g. with these catalysts, activated at 500°C., are given. As the concentration of chromium was decreased, catalyst charge was increased to compensate for poisoning of catalyst sites by trace impurities and to keep total rate of production about constant.

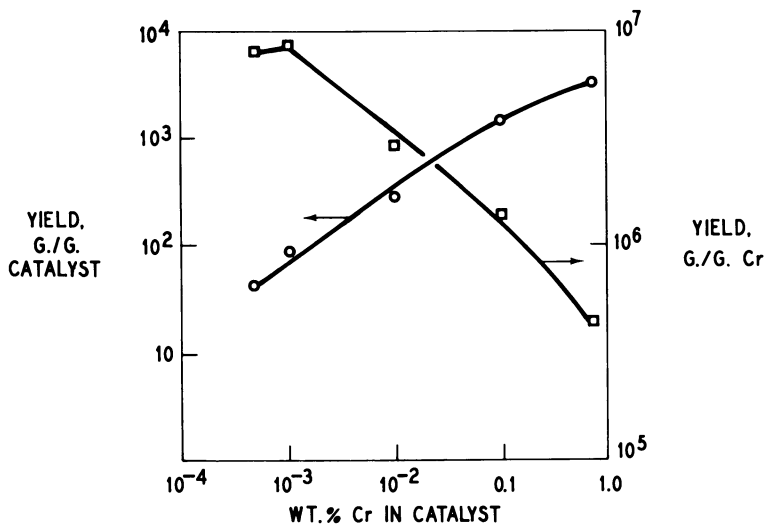


Figure 4. Effect of Cr concentration on catalyst activity

Although polymer yield based on total catalyst decreased sharply, yield based on chromium increased sharply as the chromium content was decreased to 0.001% of the catalyst, and then it leveled out.

In view of the extreme dilution of chromium atoms in the surface, a mechanism involving polymer growth on a single site is indicated strongly. Special locations on the catalyst surface limited in number are

indicated as the best environment for maximum polymerization rate. Efficiency decreases as chromium content increases, but over-all rate is increased, which indicates that other sites provide activity, though at lower rates.

The increase in activity per atom of chromium as chromium content is decreased may be explained by the supposition that ethylene concentration around the catalyst site increases as chromium concentration decreases at a given ethylene pressure. A certain amount of ethylene may be adsorbed on support sites. As chromium is added to the support, some of these sites are covered with chromium, producing new sites, some of which will be occupied by growing polymer chains. Thus, the adsorbed monomer concentration is reduced. It may be reduced further by reaction of adsorbed monomer molecules with growing polymer chains since if this reaction is appreciably faster than the rate of monomer adsorption, then the surface will tend to become denuded of monomer. The assumption that monomer on sites of the support feed into growing chains on chromium sites requires a more complex Langmuir-Hinshelwood mechanism than that described above but no change in general principles. The question arises whether it is possible to explain increased activity per chromium atom with decreasing chromium content by invoking an increasing proportion of active sites with decreasing chromium content. Although this explanation might be true at the higher concentrations of chromium, it would not be expected to hold at very low concentrations where activity per chromium atom is still increasing.

Catalysts which have been heated for one hour at 250°C. with carbon monoxide at 100 mm., cooled to 35°C., and pumped to remove physically adsorbed gas have far greater activities than untreated catalysts at all chromium concentrations (7). At low pressures, CO treatment increases the activity by at least an order of magnitude. As described in a previous publication, on the basis of infrared evidence, it is believed that the CO-treated catalyst is characterized by the presence of a carbon monoxide-chromium complex.

The idea that complex formation may be important in the catalytic process can be carried further. It has been found, for example, that bis-arene chromium complexes supported on silica-alumina are active for ethylene polymerization. These catalysts are prepared by activating the support alone in the usual manner and then impregnating with a hydrocarbon solution of the bis-arene compound at room temperature in the absence of air or other oxidizing agent.

There is a marked difference between the rate of polymerization of ethylene and the higher olefins as shown in Table II (10).

**Table II. Polymerization Rates of Various Monomers**

<i>Monomer</i>	<i>Rate of Polymerization, grams polymer/grams catalyst/hr.</i>
$C_2H_4$	1000
$C_3H_6$	10
$1-C_6H_{12}$	8

However, in the copolymerization of various 1-olefins with ethylene, the rate of copolymerization of the 1-olefin is increased greatly over its rate in homopolymerization. Table III (10) gives the weight ratio of ethylene to comonomer in the feed compared with the ratio in the

**Table III. Copolymerization of Ethylene and 1-Olefins (10)**

<i>Weight Ratio <math>C_2H_4</math> to Comonomer in Feed</i>	<i>Weight Ratio <math>C_2H_4</math> to Comonomer in Polymer</i>	
	<i><math>C_2H_4-C_3H_6</math> Feed</i>	<i><math>C_2H_4-1-C_4H_8</math> Feed</i>
5	12	9
10	19	15
15	25	21
20	32	26
30	44	39

product. With a weight ratio of  $C_2H_4$  to  $1-C_4H_8$  in the feed of 10, the ratio in the polymer is 15. Under these conditions, the over-all polymerization rate is 2000 grams polymer/grams catalyst/hr. The rate of polymerization of 1-butene is calculated to be  $1/16 \times 2000 = 125$  grams/gram-hr., which is more than 10 times the homopolymerization rate.

Copolymers may also be produced with a catalyst containing both chromium oxide and nickel oxide supported on silica-alumina. It is well-known that nickel oxide-silica-alumina by itself makes predominantly butenes from ethylene. In the mixed catalyst, butenes that are formed on nickel oxide copolymerize with ethylene on the chromium oxide to form ethylene-butene copolymers. The fact that infrared shows only ethyl branching in the polymer indicates that the initial product

**Table IV. Polymerization over Nickel Oxide-Chromium Oxide on Silica-Alumina**

<i>Atom Ratio Ni/Cr</i>	<i>Preparation</i>	<i>Density</i>
0	Impregnated	0.959
0.24	Physical mixture	0.941
0.89	Physical mixture	0.939
6.45	Coimpregnated	0.938

from methylene over the nickel oxide sites is 1-butene. This is another example to add to the growing list of dual-function catalysts. The nickel behaves more efficiently in physical mixtures of nickel oxide-silica alumina and chromium oxide-silica alumina than it does in coimpregnated catalysts. Evidently too close proximity of the nickel to chromium deactivates the nickel. This is illustrated in Table IV with data from Hogan (10). The density decreases with increasing 1-butene content of the copolymer.

### *The Product*

In a previous paper (3) it was shown that number average and weight average molecular weights approach a limiting value asymptotically as pressure is increased. Such behavior is in agreement with a Langmuir-Hinshelwood mechanism and in disagreement with a Rideal mechanism provided the terminating step (desorption) is assumed to be spontaneous. If the terminating step is assumed to involve reaction with monomer, the two mechanisms are indistinguishable on the basis of molecular weight-pressure relationships.

Weight average-number average molecular weight ratios, which give a measure of the breadth of molecular weight distribution, are unusually high compared with those obtained in homogeneous systems. In the supported chromium oxide system, ratios of 13 to 15 are common, and values as high as 30 have been observed; in homogeneous systems, values outside the range of 1 to 2 are seldom observed. A logical cause for such broad distribution of molecular weights is the broad distribution of adsorption site energies present on supported chromium oxide catalysts.

Molecular weights of ethylene polymers vary not only with temperature and pressure, they are also functions of activation temperature. Molecular weight decreases as catalyst activation temperature is increased over the range of about 400°-850°C.

Table V gives pertinent experiments for a chromium oxide-silica catalyst.

First, the polymer molecular weight can be increased by decreasing the activation temperature from 850° to 500°C. If the silica is first treated at 850°C. in air, then impregnated with CrO<sub>3</sub> in the absence of moisture, the molecular weight corresponds to the 850°C. treatment rather than the 500°C. treatment. If the silica is wetted after 850°C. treatment, the molecular weight is closer to the 500°C. treatment. It would appear that change of the hydroxyl content of the surface, which is the major effect of the temperature change, is one of the factors that causes changes in molecular weight. It is not known whether this is the result of a change in the rate of propagation, rate of termination, or both. The presence of —OH groups near the chromium atom would be ex-

**Table V. Effect of Activation Temperature on Molecular Weight of Ethylene Polymer**

<i>Catalyst Preparation</i>	<i>Relative MW</i>
(1) CrO <sub>3</sub> -Silica, 850°C. activation	1
(2) CrO <sub>3</sub> -Silica, 500°C. activation	3.5
(3) Silica calcined at 850°C., dry-promoted with CrO <sub>3</sub> , 500°C. activation	1.2
(4) Silica calcined at 850°C., wet-promoted with CrO <sub>3</sub> , 500°C. activation	2.5

pected to control either the rate of propagation, the rate of termination, or both.

Molecular weight also changes with the concentration of chromium on the support (5). For example, the number average molecular weight increases about 40% as chromium concentration decreases from 0.75 to 0.001%. This increase is in line with the supposition put forth above in connection with increasing activity per atom of chromium with decreasing chromium content.

#### *Literature Cited*

- (1) Antuf'ev, V. V., Botinov, M. P., Savin, A. G., Sazhin, B. I., Semenova, A. S., Leitmor, M. I., *Kinetika i Kataliz* **3**, 353 (1962).
- (2) Bukhanaeva, F. M., Pecherskaya, Yu. I., Kazanskii, V. B., Dzis'ko, V. A., *Kinetika i Kataliz* **3**, 358 (1962).
- (3) Clark, A., Bailey, G. C., *J. Catalysis* **2**, 230 (1963).
- (4) *Ibid.*, p. 241.
- (5) Clark, Alfred, *Ind. Eng. Chem.* **59**, 29 (1967).
- (6) Clark, A., Hogan, J. P., Banks, R. L., Lanning, W. C., *Ind. Eng. Chem.* **48**, 1152 (1956).
- (7) Clark, A., Finch, J. N., Ashe, B. H., *Proc. Intern. Congr. Catalysis, 3rd, Amsterdam, 1964*.
- (8) Cossee, P., *J. Catalysis* **3**, 80 (1964).
- (9) Cossee, P., van Reijen, L. L., *Actes Congr. Catalyse, Beuxieme, Paris 2* (1960).
- (10) Hogan, J. P., "High Polymers," G. E. Ham, Ed., Vol. XVIII, Chap. III, Interscience, 1964.
- (11) Holm, V. C. F., Clark, A., *J. Catalysis* **11**, 305 (1968).
- (12) Ivonov, L. P., Yermakov, Yu. I., Gel'bshtein, A. J., *Vysokomol o Soedin.* **9**, 2422 (1967).
- (13) Kazanskii, V. B., Pecherskaya, Yu. I., *Kinetika i Kataliz* **2**, 454 (1961).
- (14) *Ibid.*, **4**, 244 (1963).
- (15) Pecherskaya, Yu. I., Kazanskii, V. B., *Kinetika i Kataliz* **8**, 401 (1967).
- (16) Van Reijen, L. L., Ph.D. Thesis, Technische Hogeschool, Eindhoven (1964).
- (17) Van Reijen, L. L., Cossee, P., *Discussions Faraday Soc.* **41**, 277 (1966).
- (18) Topchiev, A. V., Krentsel, B. A., Perel'man, A. I., Rode, T. V., *Izv. Akad. Nauk SSSR, Otd. Khim. Nauk* **6**, 1079 (1959).
- (19) Voevodskii, V. V., *Proc. Intern. Congr. Catalysis, 3rd, Amsterdam, 1964*.

RECEIVED November 27, 1967.

# Ring-Opening Polymerization of Cycloolefins

## Some Mechanistic Aspects

KENNETH W. SCOTT, NISSIM CALDERON, E. A. OFSTEAD,  
W. A. JUDY, and J. P. WARD

The Goodyear Tire & Rubber Co., Research Division, Akron, Ohio 44316

*The ring-opening polymerization of cycloolefins by  $WCl_6/ROH/AlCl_3$  catalysts is a special case of olefin metathesis, a new reaction operating via a transalkylideneation mechanism. Hence, the ring-opening polymerization site involves the double bond itself rather than a single bond adjacent to the double bond. Ring-opening via a transalkylideneation reaction produces macrocyclics. All observable polymeric species up to the undecamer are monocyclic compounds whose structures depend on the number of carbons per double bond in the monomer. The same macrocyclic species are obtained from either polymerization of monomer or depolymerization of high polymer. This ring-opening polymerization is an equilibrium reaction, and it is predicted that ring-chain equilibrium may be attained if acyclic olefins are available to form chain ends.*

The ring-opening polymerization of unsubstituted cyclo-monoolefins leading to polymers with unsaturated polymeric repeat units having the general formula  $[-(CH_2)_n-CH=CH-]$ , has been reported recently (4, 7, 9, 10). Natta *et al.* (9) demonstrated that the monomers cyclopentene, cycloheptene, cyclooctene, and cyclododecene, when exposed to catalyst combinations derived from  $WCl_6$  and either  $(C_2H_5)_3Al$  or  $(C_2H_5)_2AlCl$ , will undergo ring-opening polymerization leading to their respective polyalkenamers. In addition, unsaturated alicyclic monomers possessing more than one double bond in the ring—namely 1,5-cyclooctadiene and 1,5,9-cyclododecatriene—and the substituted, un-

saturated alicyclic monomers—3-methylcyclooctene and 3-phenylcyclooctene—have been shown to undergo ring-opening polymerization in the presence of  $WCl_6$  and  $C_2H_5AlCl_2$  (4). The latter work demonstrated two basic features of the ring-opening polymerization of cycloolefins by tungsten-based catalysts. First, there is no double bond migration by rearrangement during polymerization, thus maintaining a regular spacing between double bonds in the polymer chain. Secondly, the polymerizability of substituted cycloolefins provides a convenient route to several perfectly alternating interpolymers.

Natta *et al.*, while discussing the thermodynamic factors which influence the polymerizability of cycloolefins, suggested that the ring-opening proceeds by cleavage of carbon-to-carbon single bonds which are  $\alpha$  to the double bond (10) and that the main energy contribution to the driving force of the reaction is ring strain energy (9). In view of our recent results in connection with the recently discovered olefin metathesis reaction (1, 2, 5, 6), Natta's suggestions require drastic revision.

### Experimental

**Materials.** Ethylaluminum dichloride, Texas Alkyls Inc., obtained as a 25% solution in hexane, was diluted with the appropriate amount of benzene (dried over silica gel) to form a 0.2M solution.

Tungsten hexachloride, Climax Molybdenum Co., was purified prior to use by sublimation of the volatile impurities (mostly  $WOCl_4$ ) at  $200^\circ C$ . under a nitrogen atmosphere (G.E. Lamp Grade).

Cyclooctene (CO), 1,5-cyclooctadiene (COD), and 1,5,9-cyclododecatriene (CDT), Columbian Carbon Co., were purified prior to use by distillation from molten sodium under a nitrogen atmosphere.

**Catalyst Preparation.** COMPONENT A. A weighed amount of purified  $WCl_6$  was dissolved in dried benzene, under a nitrogen atmosphere, to form a 0.05M solution. An appropriate amount of ethanol was added to the solution, maintaining a  $WCl_6/C_2H_5OH$  molar ratio of 1.00, and the mixture was allowed to react at room temperature for about 30 minutes. A color change from dark purple to deep red was noticed.

COMPONENT B.  $C_2H_5AlCl_2$  was used as the 0.2M solution in the mixed hexane/benzene solvent (*see above*).

**CO and COD Polymerizations: Effect of Monomer Concentration on Low Molecular Weight Macrocyclics.** The polymerizations were carried out in narrow-mouthed bottles equipped with screw caps which were fitted with self-sealing gaskets and Teflon liners. Each reaction bottle was filled with 100 ml. of the appropriate monomer/benzene solution which had been pretreated by passing through a silica gel column. All operations were conducted under a nitrogen atmosphere. All bottles were injected with 1.0 ml. of Component A followed by 1.0 ml. of Component B, thus obtaining a molar ratio of Al/W/O of 4/1/1. The polymerizations were carried out at room temperature, *ca.*  $25^\circ C$ ., for 30 minutes, then terminated by injecting 4.0 ml. of a terminating solution

prepared by dissolving 6.0 grams 2,6-di-*tert*-butyl-*p*-cresol in 100 ml. of an 80/20 benzene/methanol mixture.

The terminated solutions were transferred quantitatively into pre-weighed receivers where all volatile solvents and residual monomer were removed by evaporation under reduced pressure for 48 hours at 50°C.

The dried products were analyzed for the low molecular weight extractable macrocyclic fraction (described under Analyses).

**CO Polymerization: Effect of Conversion on Low Molecular Weight Macrocyclics.** A series of polymerizations of cyclooctene was carried out in a manner similar to that described above, using a constant monomer concentration of 1.57M. The polymerizations were terminated at various reaction times, thus obtaining different conversions. The products were isolated, processed, and analyzed for percent extractable macrocyclics as described previously.

**CDT Polymerization.** Following the general polymerization procedure described above, 1,5,9-cyclododecatriene was polymerized using 100 ml. of 1.57M solution of monomer in benzene and initiated by 2.0 ml. each of the catalyst Components A and B. The reaction was terminated after 30 minutes, and the product was isolated, processed, and analyzed for the low molecular weight extractable macrocyclic fraction as before.

**Macrocyclics from CO and COD Polymers.** High molecular weight polymer samples, prepared in the CO and COD polymerizations and extracted to remove their respective low molecular weight macrocyclic fractions were dissolved in dried benzene forming a 4% solution of poly-octenamer and also one of poly-1,5-octadienamer.

Into 50 ml. of each of these solutions we added 2.0 ml. of catalyst Component A, followed by 2.0 ml. of Component B. After 30 minutes at room temperature, the reactions were terminated, and the products were isolated as described.

The material was analyzed for newly formed low molecular weight extractable macrocyclics (*see* Analyses).

**Polymers from CO and COD Macrocyclics.** Low molecular weight extractable macrocyclic fractions, obtained from the polyoctenamers and poly-1,5-octadienamers prepared in CO and COD polymerizations by the extraction procedure described in Analyses, were dissolved in benzene, forming 20% solutions. Each 10 ml. solution was treated with 2.0 ml. of catalyst Component A, followed by 2.0 ml. of Component B. The mixtures turned highly viscous within a few minutes, indicating the formation of a high molecular weight material. After 30 minutes, the polymerizations were terminated, and the solid high molecular weight polymers were isolated as described.

## *Analyses*

**Determination of Low Molecular Weight Extractable Macrocyclics.** A weighed sample of dried polymer (about 10 grams) was extracted at room temperature for 72 hours with 100 ml. of a 50/50 hexane/2-propanol extracting mixture, changing the extracting mixture every 24 hours. After drying the extracted polymer in vacuum for 48 hours at 50°C., it was



reweighed, and the weight fraction of extracted material was thus determined.

The extracting liquor containing the oily low molecular weight extractable fraction and some antioxidant (2,6-di-*tert*-butyl-*p*-cresol) was concentrated by evaporation of the volatile solvents and dried in vacuum at 50°C. for further analysis by GLC, NMR, and low voltage mass spectrometry, or used in other experiments as previously described.

**NMR Spectrometry.** The NMR analyses of the high molecular weight extracted polymers and their respective low molecular weight extracted fractions, obtained in the various polymerization reactions of cyclooctene and 1,5-cyclooctadiene, were carried out in 4–6% CCl<sub>4</sub> solutions using the Varian A60 spectrometer at room temperature as previously described (4).

**Gas Chromatography of Macrocyclic Extractables.** Analyses of the various macrocyclic extractable fractions by GLC were performed using an F & M Model 810 Research Chromatograph, equipped with a flame ionization detector, a 20-ft. silicone Hi-Pak column and using helium gas as carrier. The analyses were conducted at a carrier gas rate of 50 cc./min., injection port temperature of 280°C., and programmed at 20°C./min. in the 60–300°C. range and holding isothermally at 300°C. for an additional 8 minutes.

**Low Voltage Mass Spectrometry of Macrocyclic Extractables.** Nominal parent mass analyses of the macrocyclic extractables, obtained from typical polymerization products of cyclooctene and 1,5-cyclooctadiene, were performed on a Model MS-9 double focusing mass spectrometer (Associated Electrical Industries, England) at a resolution of 1/1000 and an emission of 7.0 e.v. Samples were introduced directly into the source chamber by the direct-probe technique. The temperature range during the experiment was 125°–200°C., and the source pressure was maintained in the 0.1–3 × 10<sup>-6</sup> torr range. In addition, a high resolution measurement was carried out on the mass number 220 to identify the two components present at that mass number.

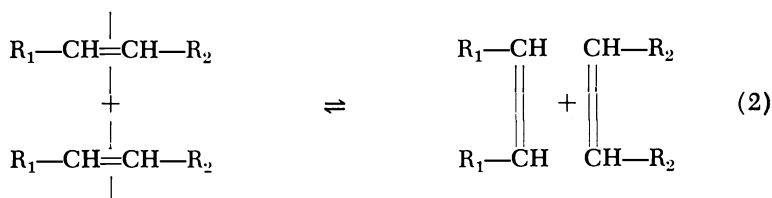
### Results and Discussion

**Metathesis of Cycloolefins.** The same general catalysts which promote the ring-opening polymerization of cycloolefins are also effective in the olefin metathesis reaction in which acyclic internal olefins undergo a unique redistribution process (1, 2, 5, 6).



Analyses of the products obtained from the metathesis of 2-butene and 2-butene-*d*<sub>8</sub> (2, 5) and also from the metathesis of 3-hexene and 2-butene-*d*<sub>8</sub> (5), proved that the interchange process in Reaction 1 definitely does not proceed *via* a simple transalkylation process—*i.e.*, a cleavage and reformation of the carbon-to-carbon single bond situated α to the double bond. The data are, however, consistent with a transalkyldienation process—*i.e.*, a scheme which contemplates an interchange

via cleavage and reformation of the carbon-to-carbon double bond as represented in Reaction 2.



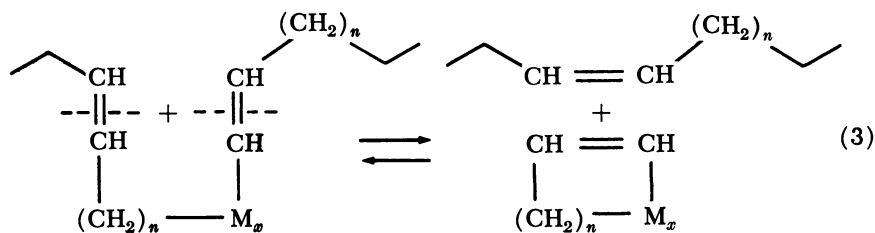
This model compound work provides the basis for our contention that the ring-opening polymerization of cycloolefins, promoted by tungsten-based catalysts is, in fact, a special case of the more general reaction of olefin metathesis. Information obtained from studies of the olefin metathesis reaction on acyclic vinylenic hydrocarbons indicates that the site of cleavage in the polymerization of cycloolefins to form polyalkenamers is not a carbon-to-carbon single bond but the double bond itself and that ring strain energy is not an essential source for the driving force of the polymerization since one is able to conduct the basic reaction on presumably strain-free macrocyclics and even on open chain olefins which, of course, do not possess any ring strain.

The following important implications, which bear directly on the nature of the cycloolefin polymerization, have precipitated out of our understanding of the basic properties of the olefin metathesis reaction.

(a) A given alkylidene portion of a double bond of a cycloolefin monomer, which has undergone metathesis and has thus become an integral part of a higher molecular weight species, remains eligible for further reaction and may participate in additional metathesis steps with other double bonds, which may be constituents of another cycloolefin monomer unit, another macromolecule, or the same macromolecule.

(b) The polymerization possesses the basic features of equilibrium polymerization.

(c) Macrocyclic species, resulting from intermolecular ring enlargement of two smaller rings or from the intramolecular metathesis of two double bonds on the same macromolecule according to Reaction 3 are present in the polymerization mixture at equilibrium.

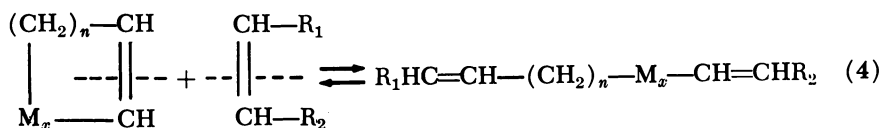


$\text{M}_x$  represents  $x$  polymeric repeat units

(d) The composition of macrocyclic species depends on the spacing between double bonds in the macromolecule (number of methylene groups between neighboring double bonds).

(e) In the absence of all side reactions the application of the olefin metathesis reaction to cycloolefins yields only macrocyclic species.

(f) An olefin metathesis reaction between a macrocyclic species and an acyclic vinylenic compounds leads to scission of the macrocyclic resulting in an open chain polymer whose end groups are the alkylidene moieties of the acyclic vinylenic compound.



Acyclic vinylenic compounds, on reaction in this system, end up only as chain ends of open chain species.

(g) Ring-chain equilibrium occurs when Factors b, c, and f are operative.

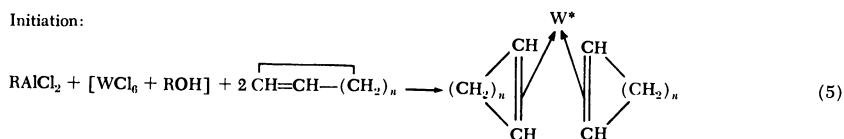
(h) Some control on the configuration of the polymeric double bonds is possible (3).

It has been speculated (5) that the olefin metathesis reaction mechanism involves a four-centered "quasi-cyclobutane" transition state. The three basic steps postulated for the reaction, namely, formation of a bis-olefin-tungsten complex, transalkylidation and olefin exchange, may account, in general, for the initiation and propagation steps in the ring-opening polymerization of cycloolefins. Several modes of termination have been considered, but suitable data to test these are not yet available.

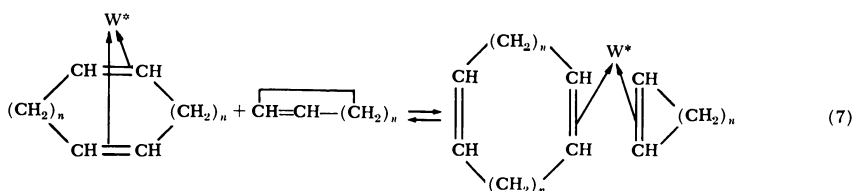
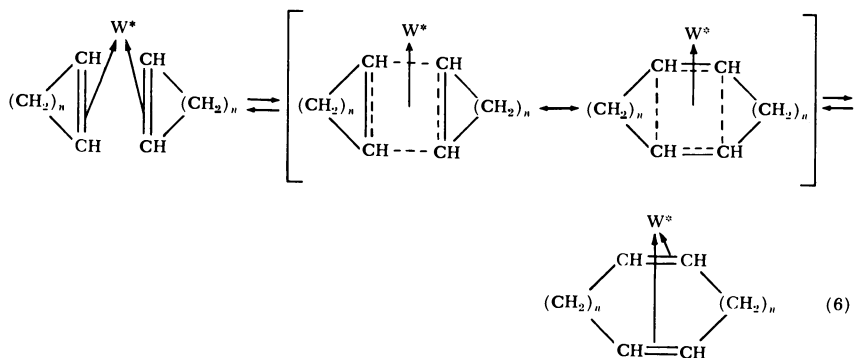
It is possible to suggest a polymerization scheme which is compatible with the mechanism suggested for the olefin metathesis reaction. For conciseness the polymerization scheme shown at the top of the next page assumes the strict absence of any acyclic olefins which might participate in the process.

Reaction 5 (the initiation step) suggests the eventual formation of a complex of two cycloolefin molecules coordinated to tungsten. Reaction 6 indicates that the transalkylidation step results in a macrocyclization of two monomeric rings into a cyclic dimer. This is followed by the olefin exchange step (Reaction 7) whereby a monomer replaces one of the double bonds coordinated to the transition metal. Repetition of Reactions 6 and 7 constitutes the propagation step.  $W^*$  is used in Reactions 5-7 because the exact composition of the remaining ligands about the coordination sphere is not known. For example, the ultimate fate of the ethanol is uncertain. In addition, the participation of Al in the complex

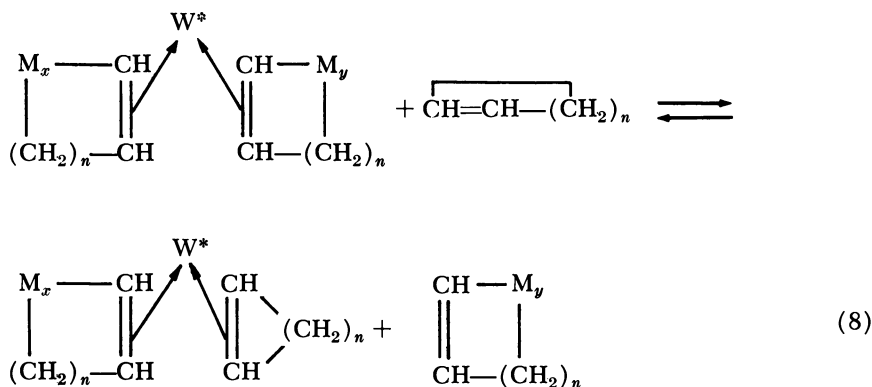
Initiation:



Propagation:

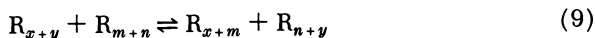


is strongly suspected, and this could occur through a  $\mu$ -chloride bridge to the tungsten. One of the possible termination steps considered involves a version of the olefin exchange step—Reaction 7—as

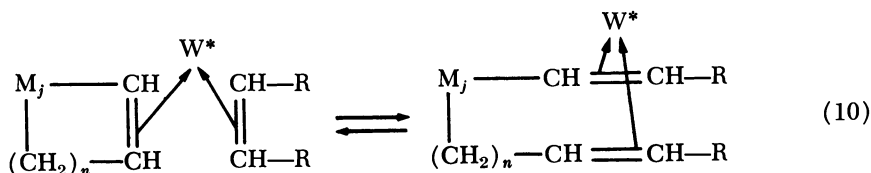


Termination in this polymerization is not completely final since the  $\text{M}_{y+1}$  species formed in Reaction 8 may participate again *via* Reaction 7; hence, Reaction 8 represents a type of chain transfer mode of termination.

In the complete absence of acyclic olefins in the system, this polymerization scheme predicts a macrocyclization mode of propagation, whereby the resulting polymer is a mixture of cyclic macromolecules. A general equilibrium for this process can be represented by Reaction 9:



where  $R_i$  represents a ring of  $i$  polymeric repeat units. However, if minute amounts of acyclic olefins are present to participate in the process (they might originate as products of reaction of the tungsten and aluminum catalyst components, be present as an impurity, or added intentionally) a mixture of rings and open chains will result from the process depicted in Reaction 10.



Under such conditions it is possible to obtain an equilibrium ring-chain system as described by Reaction 11.



where  $C_m$  is a chain of  $m$  polymeric repeat units and  $R_n$  is a ring of  $n$  polymeric repeat units.

Presently available information is insufficient to permit deciding whether the high molecular weight polymers obtained in ordinary polymerizations of cycloolefins consist of macrocyclics alone or mixtures of rings and chains. Nevertheless, the intentional introduction of known amounts of chain ends *via* addition of vinylenic olefins should result in ring-chain equilibrium of the type presented in Reaction 11. For this type of equilibrium, the weight fractions and size distributions of rings and chains present in the system may be compared with the Jacobson and Stockmayer theory (8). Experiments to test theory in this area are currently underway.

### Formation of Macrocyclics

#### Concentration and Conversion Effects on Macrocyclics Formation.

The dependence of the extractable fraction on initial monomer concentration has been determined for cyclooctene and 1,5-cyclooctadiene polymerizations and are plotted in Figure 1. In this set of experiments all polymerizations were carried out to high conversions (88% or higher). The catalyst concentration was maintained constant throughout at an

Al/W/O ratio of 4/1/1. The monomer/catalyst ratio necessarily increased with initial monomer concentration. Figure 1 indicates that large amounts of the extractable fraction are formed in polymerizations carried out in dilute systems.

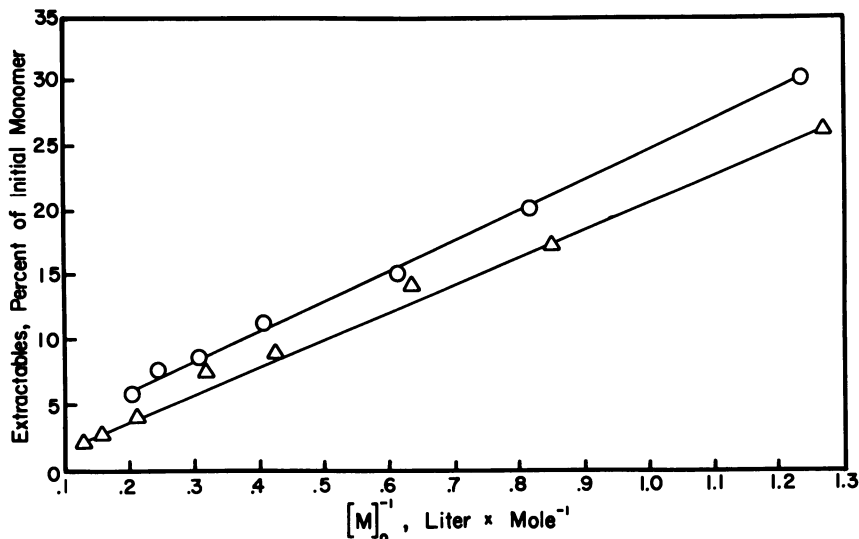


Figure 1. Dependence of extractable macrocyclics on reciprocal of initial monomer concentration,  $[M]_0$ . Polymerizations conducted at  $[W] = 5 \times 10^{-4}$  and  $[Al] = 2 \times 10^{-3}$  for 30 minutes at room temperature. Conversion:  $>88\%$

○: 1,5-Cyclooctadiene  
 △: Cyclooctene

The effect of conversion on extractable fraction formation is presented in Figure 2 for cyclooctene polymerization. All variables were held constant except polymerization time. The results are plotted in two forms. The left plot illustrates the extractable fraction as a percentage of the converted monomer. Note that at low conversions the percent of low molecular weight extractable material on the basis of the reacted monomer is much higher than the final cumulative level attained at the end of the polymerization where conversions reach 90% or higher. The cumulative percentage of the extractables formed on the basis of the initial amount of monomer is plotted on the right side of Figure 2 and increases monotonically to reach a value of 12–13% at high conversions which is typical of a cyclooctene polymerization at  $[M]_0 = 1.57$ .

**Composition of Macrocyclic Extractables.** The quantitative procedure used in this work to separate and determine the level of the low molecular weight oily fraction is based on using a solvent mixture (hex-

ane and 2-propanol) which is capable of dissolving the low molecular weight material which accompanies the very high molecular weight polymer. The present technique commonly isolates fractions having a number-average molecular weight in the 400–500 range. The selection of this specific solvent pair is arbitrary, and other extracting solvent combinations would lead to somewhat different results. Nevertheless, on a comparative basis, the results are valuable for demonstrating basic trends of the ring-opening polymerization of cycloolefins in forming low molecular weight material. Various techniques were used to establish the macrocyclic character of the low molecular weight extractable fraction.

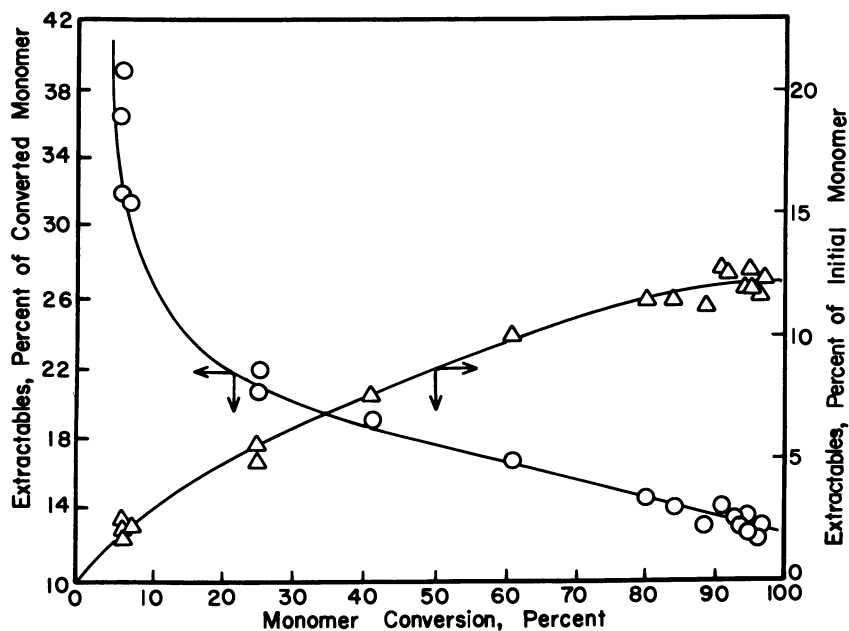


Figure 2. Dependence of extractable macrocyclics on conversion in cyclooctene polymerization.  $[M]_0 = 1.57$ ;  $[W] = 5 \times 10^{-4}$ ;  $[Al] = 2 \times 10^{-3}$ . Room temperature. Polymerization time varied

**Low Voltage Mass Spectrometry.** The nominal parent mass numbers of the various components in the low molecular weight extractable fractions obtained from polyoctenamer and poly-1,5-octadienamer are listed in Table I. Quantitative estimation of the relative amounts of individual components were not carried out owing to experimental difficulties. The large variation in the volatilities of the various oligomers limits this procedure to the determination of molecular weights of the oligomers.

The basic difference between the homologous series of the polymers of CO and COD is that mass numbers found in the CO low molecular

weight extractable fraction consist of "whole" multiples of the monomer, cyclooctene,  $(C_8H_{14})_n = 110n$ , while the COD fraction consists of two series, one of which contains "whole" multiples of the monomer, 1,5-cyclooctadiene,  $(C_8H_{12})_n = 108n$ , and a second series consisting of the "sesqui-" oligomers,  $(C_8H_{12})_n - C_4H_6 = 108n - 54$ .

Alternatively, the COD series can be described as a single series consisting of multiples of half a monomer unit,  $(C_4H_6)_m = 54m$  for  $m \geq 3$ . This indicates that the significant polymeric repeat unit contains only one double bond and is not necessarily an original monomer unit.

In addition to the mass numbers reported in Table I, a peak at 188, corresponding to phenylcyclooctane, and a peak at 186, corresponding to

**Table I. Parent Masses ( $m/e$ ) of Low Molecular Weight Extractable Fractions Obtained from the Polymerization Products of Cyclooctene and 1,5-Cyclooctadiene**

	CO	COD	
	(Oligomers)	(Oligomers)	(Sesquioligomers)
	220 <sup>a</sup>	216	162
	330	324	270
	440	432	378
	550	540	486
	660	648	594
	770	756	702
	880	864	810
	990	972	918
	1100	1080	1026
	1210	—	220 <sup>b</sup>
Homologous Series:	$(C_8H_{14})_n$	$(C_8H_{12})_n$	$(C_8H_{12})_n - C_4H_6$
	$(n \geq 2)$		

<sup>a</sup> A high resolution mass analysis of the 220 peak reveals the presence of two compounds (220.1824 and 220.2190). The 220.1824 corresponds to the antioxidant, di-*tert*-butyl-*p*-cresol, which has a theoretical mass number of 220.1827. The 220.2190 peak corresponds to  $C_{16}H_{28}$  which has a theoretical mass number of 220.2191.

<sup>b</sup> Corresponds to 220.1824 and is thus attributed to antioxidant.

phenylcyclooctene, were observed in the CO and COD series, respectively. These apparently are products of the cationic alkylation of the benzene solvent by the monomers. Mass numbers which could account for the presence of open chain oligomers plus two hydrogens were not detected within the examined region.

**Gas Chromatography Data.** Under the testing conditions used in the GLC analyses it is apparent that the resolution decreases with an increase in temperature. Thus, in Figures 3–7 a tendency of peak broadening is noticed for the higher molecular weight components. Nevertheless, the data are adequate to support an important feature of this work—namely, that this cycloolefin polymerization is reversible.



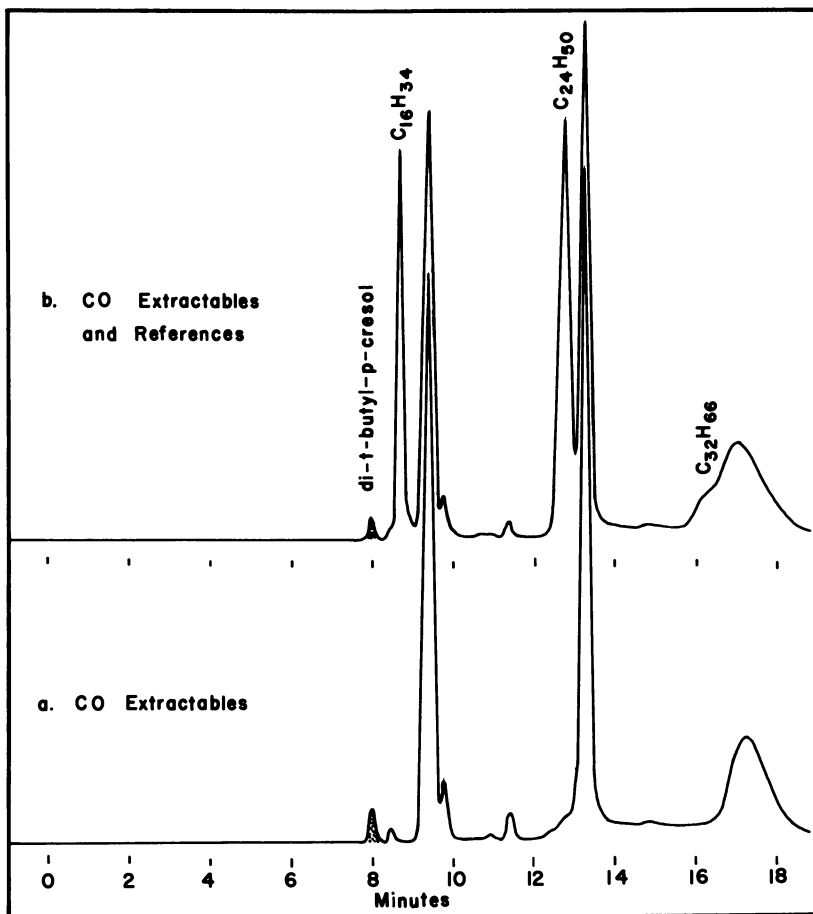


Figure 3. Comparison of chromatograms of cyclooctene extractable macrocyclics with standard reference materials

Figures 3a and 4a show the GLC charts obtained from the CO and COD low molecular weight extractable fractions, respectively. Figures 3b and 4b are chromatograms of the same tested samples with added known standard materials which were all normal paraffins except for 1,5,9-cyclododecatriene (40/60 c,t,t/t,t,t) which was used as a reference material in the COD analysis of Figure 4b. The main peaks in the CO series differ by eight carbons while in the COD series the peaks are spaced at every four carbons.

In comparing the first doublet peak in Figure 4a at an elution time of 6–7 minutes with its counterpart in Figure 4b, to which 1,5,9-cyclododecatriene was added to a reference materials, one finds a perfect overlap

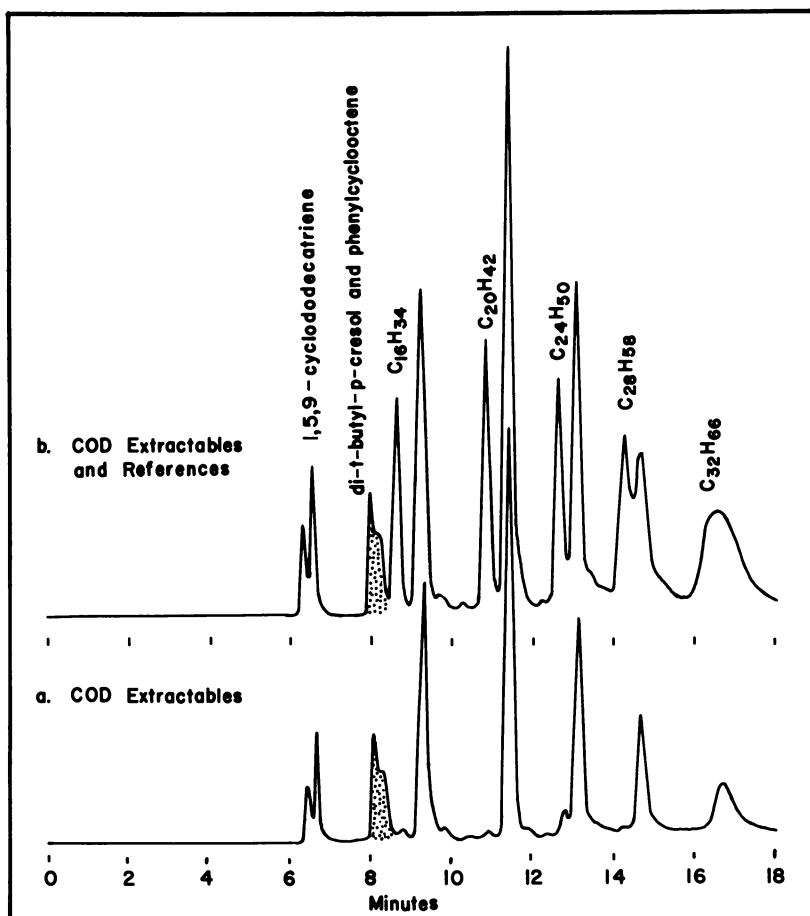


Figure 4. Comparison of chromatograms of 1,5-cyclooctadiene extractable macrocyclics with standard reference materials

of the two peaks. Combined with the data from the low voltage mass spectrometer, where a peak corresponding to a mass of 162 was observed, it is evident that the lowest member of the COD extractable fraction is 1,5,9-cyclododecatriene.

The shaded peaks in the various chromatograms presented in Figures 3–7 are caused by antioxidant and alkylated benzenes whose presence had been confirmed by mass spectrometry.

Figure 5 compares the GLC charts of the low molecular weight extractable fractions obtained from COD and CDT polymerization products. Both samples exhibit the same major peaks up through the component possessing 32 carbons, which is the highest resolvable com-

ponent under the conditions used. All the major components consist of multiples of four carbons. It is also observed, on a semiquantitative basis, that the ratios of peak heights for the  $C_{20}$ ,  $C_{24}$ ,  $C_{28}$ , and  $C_{32}$  components are of the same order of magnitude. This leads to the reasonable conclusion that the spectrum of components in a given sample of an extractable fraction depends primarily on the structure of the polymeric repeat unit. COD and CDT have the same repeat unit,  $-(CH_2)_2-CH=CH-$  and thus will yield similar mixtures of macrocyclic extractable fractions. Similarly, 1,4-polybutadiene, with the same polymeric repeat units as the COD and CDT polymers, gives the same spectrum of macrocyclic species when exposed to these catalysts.

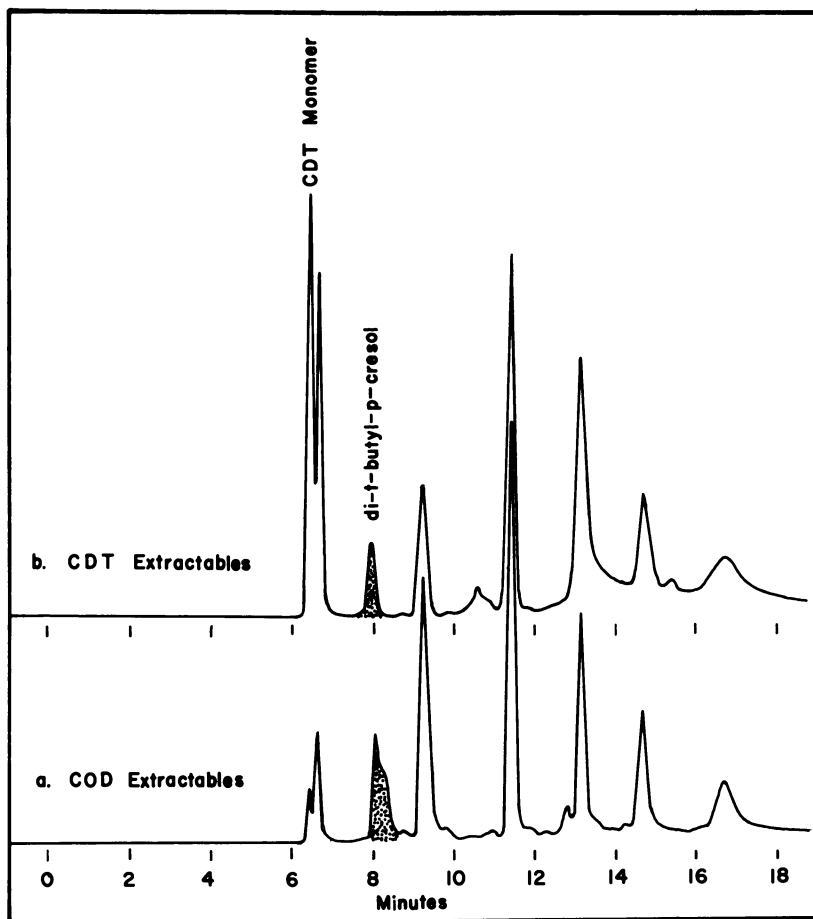
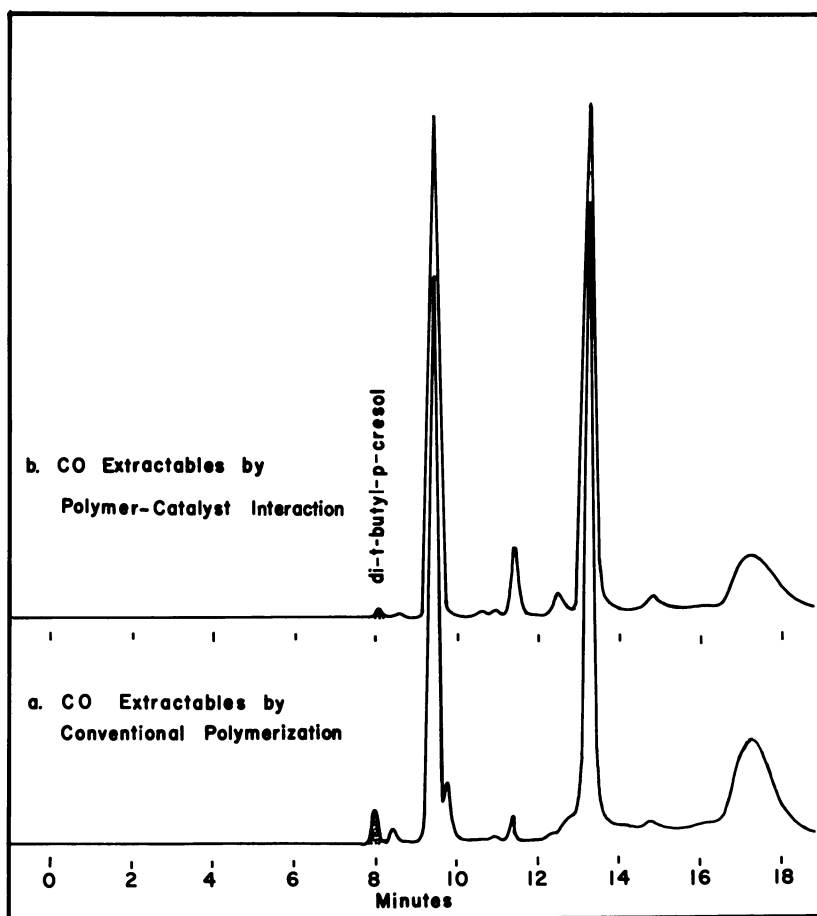


Figure 5. Comparison of chromatograms of 1,5-cyclooctadiene and 1,5-cyclododecatriene extractable macrocyclics

Low molecular weight extractable fractions produced by adding catalyst to dilute solutions of previously extracted high molecular weight CO and COD polymers (Figures 6b and 7b) are compared with "conventional" extractable fractions (Figures 6a and 7a). Obviously, these low molecular weight extractable fractions can be prepared from the polymers in the absence of any monomer, and they bear a marked resemblance to the extractable fractions prepared during polymerization.

**NMR Spectrometry.** Figures 8 and 9 reproduce the NMR spectra of (a) the high molecular weight polymer fraction, (b) the low molecular weight extractable fraction, and (c) the high molecular weight polymer obtained by polymerization of the low molecular weight extractable frac-



*Figure 6. Comparison of cyclooctene extractable macrocyclics obtained by catalyst treatment of high molecular weight polyoctenamer with extractable macrocyclics obtained during cyclooctene polymerization*

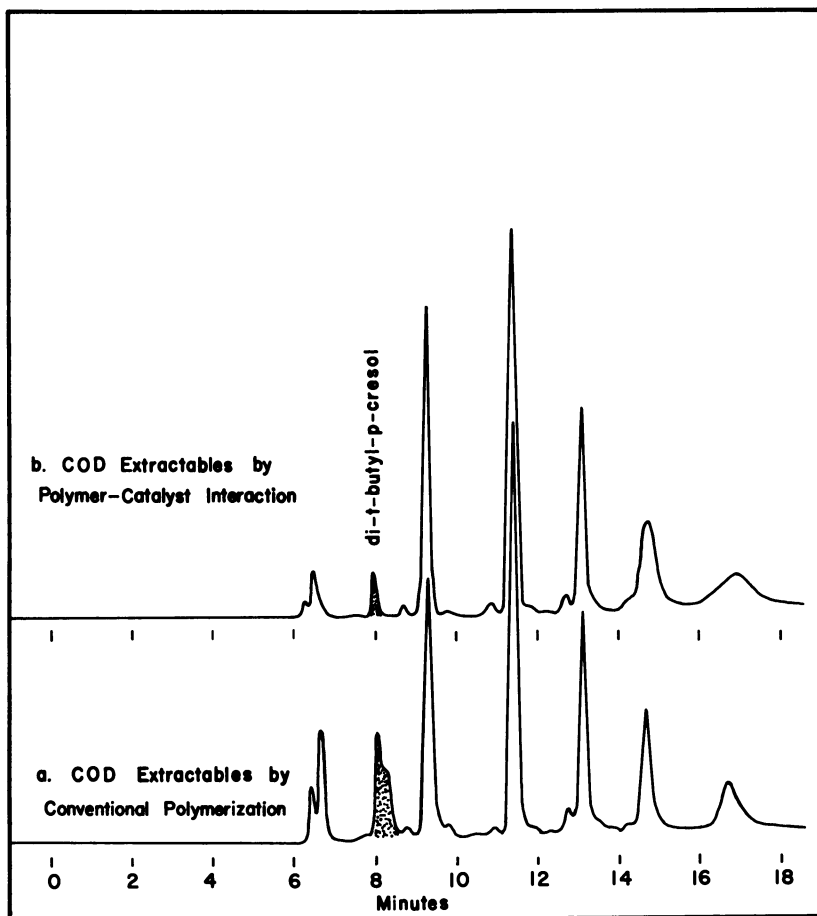
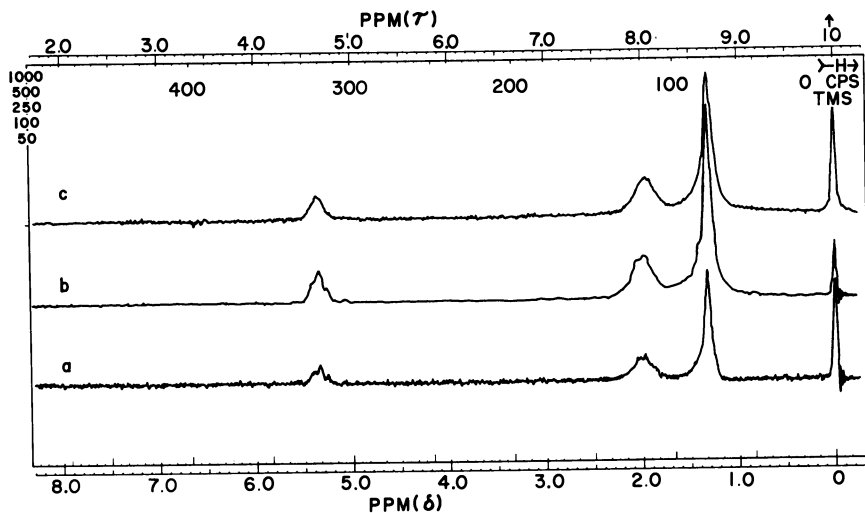


Figure 7. Comparison of 1,5-cyclooctadiene extractable macrocyclics obtained by catalyst treatment of high molecular weight poly-1,5-octadienamer with extractable macrocyclics obtained during 1,5-cyclooctadiene polymerization

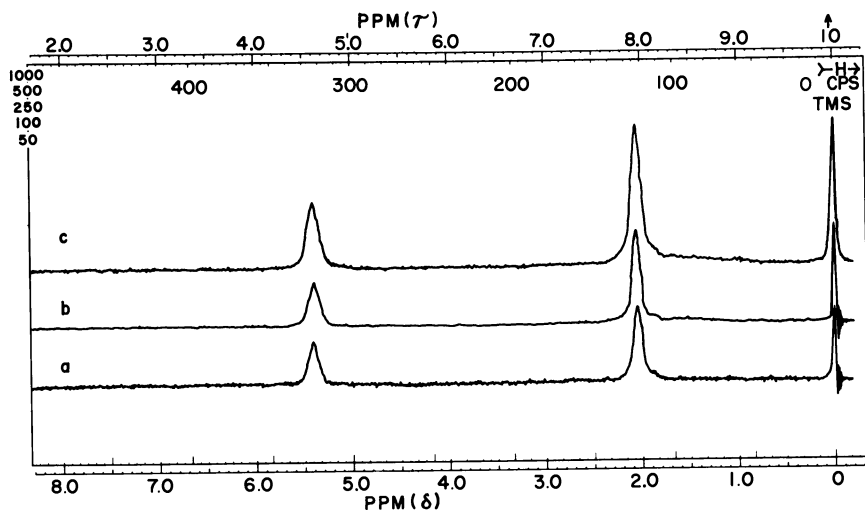
tion, for both the cyclooctene and the 1,5-cyclooctadiene cases. The data clearly demonstrate that for a given monomer these are structurally indistinguishable. Within the limits of NMR resolution, there is no evidence for the presence of any methyl or vinyl group protons in the low molecular weight extractable fractions, and thus open chain species, which might be expected to possess such protons, are not present in significant amounts in the extractable fraction.

Combining the results of NMR, low voltage mass spectrometry, (Table I), and gas chromatography (Figures 3-7) with the undisputed fact that the low molecular weight extractable fractions can be polymer-



**Figure 8.** NMR spectra of polyoctenamer, extractable macrocyclic fraction from polyoctenamer and polyoctenamer obtained by polymerization of the extractable macrocyclic fraction

- (a): Polyoctenamer  
 (b): Extractables from polyoctenamer  
 (c): Polymerized extractables from polyoctenamer



**Figure 9.** NMR spectra of poly-1,5-octadienamer, extractable macrocyclic fraction from poly-1,5-octadienamer, and poly-1,5-octadienamer obtained by polymerization of the extractable macrocyclic fraction

- (a): Poly-1,5-octadienamer  
 (b): Extractables from poly-1,5-octadienamer  
 (c): Polymerized extractables from poly-1,5-octadienamer

ized to high molecular weight polymers leads to the conclusion that the low molecular weight fractions are mixtures of macrocyclic species and essentially free of open chain compounds. As described earlier, open-chain olefins in this system are a source of chain ends, and if any appreciable amount of the low molecular weight fraction consisted of open-chain olefins, one would not be able to polymerize these to a solid, high molecular weight polymer. Since the polymer prepared by polymerizing the extractable macrocyclic fraction is gel-free the macrocyclic fraction must be essentially all monocyclic species because polycyclic species would serve as crosslinkers and could lead to gel formation.

The results above support four basic features, characteristic of cycloolefin polymerization:

(1) The macrocyclic nature of the low molecular weight extractable fraction.

(2) The composition of a given macrocyclic mixture is controlled primarily by its polymeric repeat unit.

(3) Macrocyclics can be prepared, in the absence of monomer, starting from the high molecular weight polymer.

(4) The low molecular weight extracted macrocyclics can be converted to high molecular weight polymer, whose structure is indistinguishable from polymer prepared by the normal polymerization of the respective cycloolefin monomer.

These features are all well understood when it is realized that the above reactions of monomer and polymers are simply examples of the general olefin metathesis reaction which operates *via* a random interchange of alkylidene groups as described in our previous work (1, 2, 5, 6).

### *Additional Mechanistic Aspects*

**Selective Formation of Macrocyclics.** The scheme suggested and supported by the experimental results provides, at least theoretically, a route for attaining equilibrated mixtures of macrocyclic rings of selected sizes, the smallest being one polymeric repeat unit (cyclobutene for poly-1,5-octadienamer and cyclooctene for polyoctenamer) and the largest being a huge macrocyclic with essentially an infinite number of polymeric repeat units. In practice we have not been able to detect any cyclobutene formation in polymerizations involving the  $-(CH_2)_2-CH=CH-$  repeat unit. Even for the eight membered repeat unit  $-(CH_2)_6-CH=CH-$ , the equilibrium concentration of cyclooctene monomer is lower than  $2 \times 10^{-3}M$ . Evidently, in the formation of small- and medium-sized rings from higher molecular weight polyalkenamers configurational

and conformational factors play an important role. All rings permitted by the repeat unit structure and having at least 12 carbons have been detected up to molecular weights of 1000 and higher (Table I).

**Every Double Bond Eligible for Reaction.** In this polymerization system, the double bonds in a given macromolecule may participate in either intermolecular or intramolecular transalkylidenation. The intermolecular process cannot lead to a lowering of the number average molecular weight. This is true regardless of the ring or chain content of the high molecular weight polymer. The intramolecular process, which "pinches off" a macrocyclic ring from a species of higher molecular weight (Reaction 3), does lead to a net lowering of the molecular weight. The ratio between intra- and intermolecular processes, which affects the fraction of macrocyclics formed in the system, will depend inversely on concentration. Figure 1 clearly confirms this expectation. Actually, by exposing a dilute (4%) solution of high molecular weight polymer to the catalyst (*see* Experimental discussion on macrocyclics from CO and COD polymers), where enhancement of the intramolecular transalkylidenation process relative to the intermolecular one takes place, large amounts of extractable macrocyclics are obtained. The reverse is also true since exposing a concentrated (20%) solution of the low molecular weight macrocyclics to the catalyst (*see* Experimental discussion on polymers from CO and COD macrocyclics) yields a high molecular weight polymer. Since these experiments clearly indicate that macrocyclic formation is a reversible, concentration-dependent process, one is led to the conclusion that ring-opening polymerization of cycloolefins by the olefin metathesis reaction is an equilibrium polymerization.

**Equilibrium Polymerization.** The transalkylidenation mechanism provides a convenient reaction path to ring-chain equilibrium for this polymer system. The final, necessary and sufficient condition for ring-chain equilibrium is the presence of chain end groups. This requirement is not too difficult to fulfill since theory (8) suggests that less than 0.1 mole % of acyclic olefin out of the total olefin content will yield ring-chain equilibrium approximating some of our qualitative observations. On this basis, an ultrapure polymerization system will be required to produce very high molecular weight macrocyclic species. The distribution of ring sizes in an equilibrated system will be treated in a future publication.

### ***Acknowledgment***

The authors acknowledge the assistance of J. K. Phillips for the low voltage mass spectra analyses.



*Literature Cited*

- (1) Calderon, N., Chen, H. Y., Scott, K. W., *Tetrahedron Letters* **1967**, 3327.
- (2) Calderon, N., Chen, H. Y., Scott, K. W., "Abstracts of Papers," 154th Meeting, ACS, Sept. 1967, S172.
- (3) Calderon, N., Morris, M. C., *J. Polymer Sci. Pt. A-2*, **5**, 1283 (1967).
- (4) Calderon, N., Ofstead, E. A., Judy, W. A., *J. Polymer Sci. Pt. A-1*, **5**, 2209 (1967).
- (5) Calderon, N., Ofstead, E. A., Ward, J. P., Judy, W. A., Scott, K. W., *J. Am. Chem. Soc.* **90**, 4132 (1968).
- (6) *Chem. Eng. News* **45** (41), 51 (1967).
- (7) Eleuterio, H. C., U. S. Patent **3,074,918** (1963).
- (8) Jacobson, H., Stockmayer, W. H., *J. Chem. Phys.* **18**, 1600 (1950).
- (9) Natta, G., Dall'Asta, G., Bassi, I. W., Carella, G., *Makromol. Chem.* **91**, 87 (1966).
- (10) Natta, G., Dall'Asta, G., Mazzanti, G., *Angew. Chem.* **76**, 765 (1964); see also *Makromol. Chem.* **56**, 224 (1962).

RECEIVED March 22, 1968.

## Chemical Reactions of Model Polyenes and Macromolecular Polyenes

CHRISTIAN P. PINAZZI, GUY LEVESQUE, DANIELE REYX,  
JEAN-CLAUDE BROSSE, and ALAIN PLEURDEAU

Laboratoire de Chimie Organique Macromoléculaire, Collège Scientifique  
Universitaire, Route de Laval, 72-Le Mans, France

*The chemical properties of 1,4-polybutadienes and 1,4-polyisoprenes have been studied on the model substances 4-octene, 4,8-dodecadiene, 4,8,12-hexadecatriene, and their methyl derivatives. Macromolecular models of cyclopropane were synthesized by adding dihalocarbenes, followed by reduction. The macromolecules derived from the polyenes by replacing the double bonds with non-substituted cyclopropanes were prepared under similar conditions. These macromolecules are theoretically strongly analogous to the corresponding polyenes. Starting with the same olefinic models, polyethyleneimine derivatives were prepared by adding carbethoxy nitrene. We tried to synthesize these cyclopropane structures directly, and the ability of dihalocyclopropane and bicyclane (norcarane types) monomers to polymerize were studied. In this connection, spiro-pentane was polymerized; its reaction mechanism is complex, and we have made comparisons with simpler cyclopropanes and bicyclo[n.1.0]alkanes.*

In general, polymers obtained by polymerizing conjugated dienes possess one double bond per structural unit; a study has been undertaken of chemical reactions which can be carried out on these polymers. In previous publications the halogenation of polyenes was continued and extended by using specific brominating and chlorinating agents (15); the dehydrohalogenation reactions which may occur either during substitution reactions or on the addition products have also been demonstrated (16). Considerable differences appeared during the standard reactions depend-

ing on whether they were carried out on 1,4-polyisoprenes, 1,4-polybutadienes, or 1,4-polychloroprene.

It was possible to bring this work to a satisfactory conclusion only by the continued use of "models" of the macromolecules studied. These models consist of ethylenic compounds comprising one or more structural units identical to the structural unit of the polymer. The units are interconnected in a manner identical to that encountered in a regular polymer, and the ends of the chains, which are determined by the method of model synthesis, are most frequently in the form of alkyl groups sufficiently long not to cause marked disturbances in the end groups. This led to the development of a simple method for synthesizing model polyisoprenes consisting of up to four monomer units; an equivalent method of synthesis is being developed for model polybutadienes.

It has been shown that dihalocarbenes react with macromolecular polyenes (17, 18) to yield polycyclopropane type products. This chapter describes the results obtained during characterization of these structures as the result of using models and particularly the preparation of cyclopropane type hydrocarbon macromolecules. Next, the reactions between carbethoxynitrene and polyisoprene type structures are discussed. This work was carried out first and brought to light a previously unknown reaction of this reagent. Finally, several examples are given of cyclopropane polymerization. The structures of all the polymers obtained have not yet been established with certainty and probably will be established only by synthesizing models and comparing the polymers with such models.

### *Experimental Procedure*

The infrared spectra were obtained with a Perkin Elmer 237 spectrophotometer and the NMR spectra with a Varian A 60 A.

**Chemical Modification.** Reactions on the macromolecular polyenes were carried out by procedures described previously (3, 4).  $\text{PhHgCBr}_3$  is obtained by a modification of Seyferth's method (21) from  $\text{PhHgBr}$  and  $\text{HCBr}_3$  in presence of a base. Yields similar to those reported in the literature are obtained more easily by replacing the complex (*tert*-BuOK-*tert*-BuOH) with a solution of sodium *tert*-amylate in benzene as prepared by Conia (24). This reagent was, in fact, used systematically in place of potassium *tert*-butylate; it is easier to use and can be prepared completely free of alcohol.

The dihalocyclopropanes were prepared either by reaction of  $\text{PhHgCBr}_3$  with the ethylenic compound by Seyferth's method or by the reaction of sodium *tert*-amylate with  $\text{CHCl}_3$  or  $\text{CHBr}_3$ . Using an excess of the reagent (2-8 times the stoichiometric amount) the total reaction products are obtained on both models and polyenes with almost quantitative yields.

Tri-*n*-butyltin hydride is obtained by reaction of  $\text{Bu}_3\text{SnCl}$  with excess LAH in ether (4).

The cyclopropanes are prepared either by reduction of the gem-dibrominated derivatives with  $\text{Bu}_3\text{SnH}$  by either the method of Seyferth (24) or by the Simmons-Smith reaction.

*p*-Nitrobenzenesulfonyloxy urethane is prepared by the method of Lwowski (13). Reactions with carbethoxynitrene are carried out at 20°C. in methylene chloride, and the polyisoprene reacts in a mixture of  $\text{CCl}_4$  and  $\text{CH}_2\text{Cl}_2$ .

Physical data on the compounds not already described are collected in Table VI.

**Polymerization. MONOMERS.** The cyclopropane type monomers are prepared either by addition of the dichlorocarbene or by the Simmons-Smith reaction on the corresponding olefins. Most of these compounds have been described. Spiropentane is prepared by the Applequist method (1, 2), by the reaction of zinc with  $\text{C}(\text{CH}_2\text{Br})_4$  in alcohol in the presence of ethylenediaminetetraacetic acid (EDTA). This hydrocarbon is purified until a single NMR signal is obtained at  $\tau = 9.28$ .

**POLYMERIZATION.** Into the tube to be sealed the solvent is introduced; trialkylaluminum is added with a hypodermic syringe, then the metal halide, and finally the monomer. These operations are carried out in an inert atmosphere. The tube and its contents are then immersed in liquid nitrogen, and sealing is effected at a residual pressure of the order of 1 mm. Polymerization is carried out at the temperatures indicated in the text. The tube is opened after cooling, and polymerization is arrested by adding methanol. The reaction mixture is precipitated in 500 ml. of  $\text{CH}_3\text{OH}$  containing 50 ml. 0.1N HCl and is allowed to stand for 24 hours. The polymer is then filtered on a glass filter, redissolved in benzene or THF, and reprecipitated with methanol. The polymer is dried to constant weight under vacuum.

### *Chemical Modifications on Introducing Cyclopropane Systems*

It has been shown that the dihalocarbenes ( $\text{CX}_2$ ) react with macromolecular polyenes to give polydihalocyclopropane type products (17, 18). The transformations effected may be either partial or total on polyisoprenes and polybutadienes. The reactivity of the polychloroprenes is slighter, and they undergo marked conversion only when they react with  $\text{CCl}_2$ . A study was made of the structures obtained and in particular their reduction to polycyclopropane hydrocarbons.

The dihalocyclopropanes are obtained by reaction of ethylenic compounds with carbenes obtained by thermolysis of  $\text{Ph-Hg-CX}_2\text{Br}$  (22) at 80°C. When carried out on polyenes of type A, this reaction can, under certain conditions (17) give rise to completely converted products of type B (Figure 1).

There is little information in the literature permitting the characterization of B; furthermore, the products are only slightly soluble and cannot be studied by NMR. Compounds as similar as possible to B were

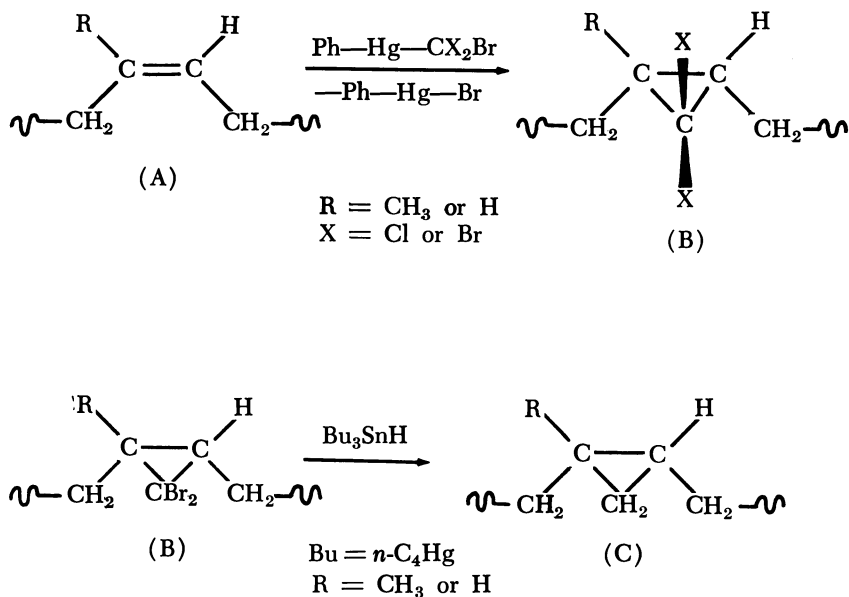


Figure 1. Preparation of dihalocyclopropanes (reduction by tin hydrides)

synthesized and compared with the macromolecular compounds in question. For this purpose, models of Structure A were used, and these reacted with dihalocarbenes. Models of type A are shown in Figure 2. Reasons for choosing these compounds were indicated when their synthesis was described (18).

Models Ia–Va reacted with dihalocarbenes prepared either by  $\alpha$ -elimination (11) or by thermolysis of Ph-Hg-CX<sub>2</sub>Br (22), giving rise to the corresponding dihalocyclopropane derivatives Ib–Vb (Figure 3). It was possible with these derivatives to characterize B, to study the reduction of B (X = Br) to C, and to characterize C.

**Characterization of B.** This study was carried out on (macromolecular and model) products in which all the double bonds were converted to 1,1-dihalocyclopropanes. Products obtained by adding CCl<sub>2</sub> and CBr<sub>2</sub> to each of the model compounds were characterized by conventional methods. Their infrared spectra were examined and compared with those of the corresponding macromolecular compounds. None were found to absorb in the 3000–3100 cm.<sup>-1</sup> region [cyclopropane–CH<sub>2</sub>– (25)], but all gave an intense absorption band in the C–halogen bond region (Table I): 790–850 cm.<sup>-1</sup> for chlorinated products and 700–770 cm.<sup>-1</sup> for brominated products, this band having been reported for B (17, 18). This band, therefore, seems to be characteristic of the dihalo-1,1-cyclo-

propane structure; it disappears when the structure is modified, either by hydrogenation (*see below*) or by conversion to cumulenes (17).

**Preparation of Cyclopropane Hydrocarbon Macromolecules.** The preparation of cyclopropane type macromolecules C was contemplated with interest since this structure actually possesses similarities to those of polyenes A in the matter of local rigidity of the chains either with respect to the cyclopropane or to the double bond. Furthermore, several

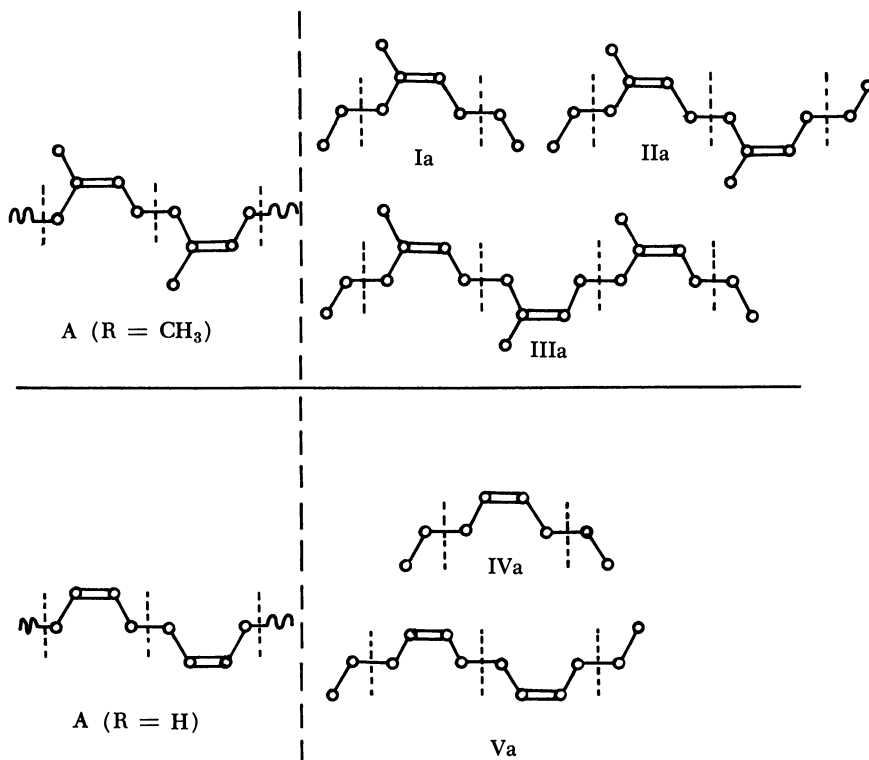


Figure 2. *cis-1,4-Polyisoprene and polybutadiene models*

methods are known by which it is possible theoretically to go from A to C by transfer of the methylene group (11), in particular the Simmons-Smith reaction (26) using  $\text{CH}_2\text{I}_2 + \text{Zn/Cu}$ . When this reaction was carried out with polyenes, polymer crosslinking occurs at the very start of the reaction. Variations of the reaction were also tried and the results are shown in Table II. Note that the Simmons methylene transfer reactions often result in crosslinking. The Seyferth reaction (23) does lead to Structure C but necessitates prolonged heating which degrades the macromolecular chain. On the other hand, by means of the Simmons

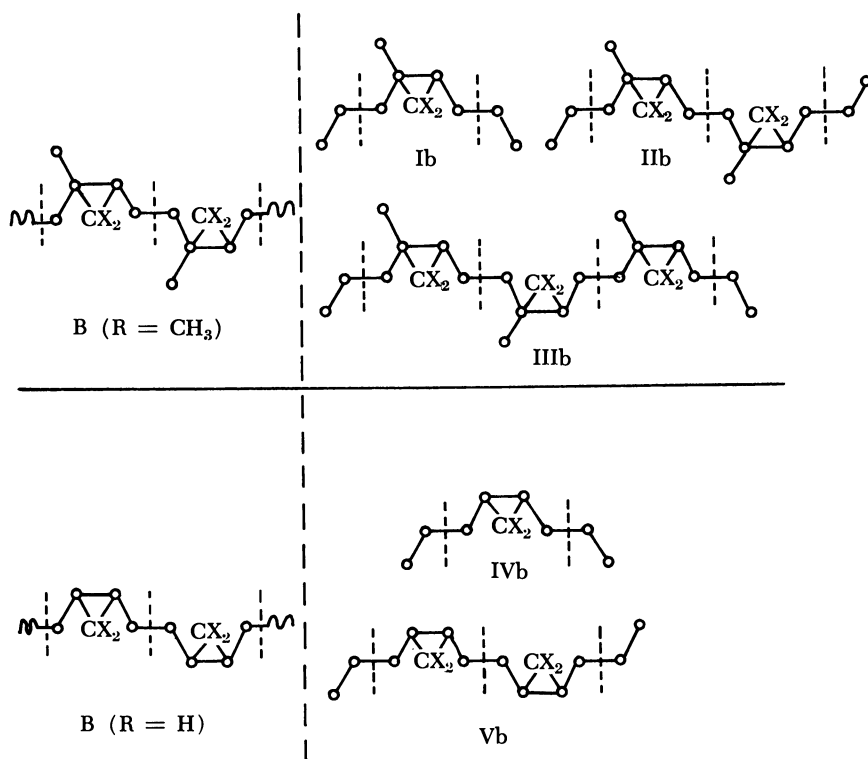


Figure 3. Dihalocyclopropane models

reaction with models Ia–Va, it was found possible to prepare and characterize models Ic–Vc of polycyclopropanes C. Most of these compounds were also prepared by reduction of the dibrominated derivatives.

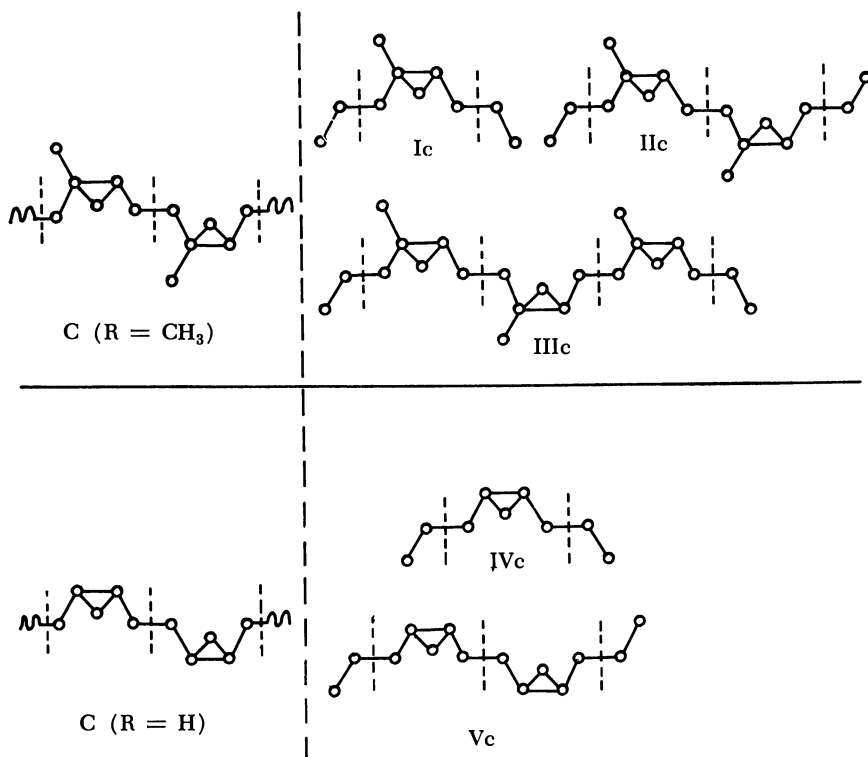
The products C are obtained by reduction of products B ( $X = \text{Br}$ ) by Seyferth's method using  $\text{Bu}_3\text{SnH}$  at  $80^\circ\text{C}$ . (24). This conversion gives yields of more than 95% in the presence of an excess of hydride. The same reaction with B ( $X = \text{Cl}$ ) at  $140^\circ\text{C}$ . only results in the reduction of one halogen; by using other reagents such as  $\text{Ph}_3\text{SnH}$  the same result is obtained, but lower temperatures are possible (*i.e.*, about  $100^\circ\text{C}$ .).

Table I. Infrared Absorption of Structure B in the  $850\text{--}700\text{ cm}^{-1}$  Region

	Ib	IIb	IIIb	$B(R = \text{CH}_3)$	IVb	Vb	$B(R = \text{H})$
X = Cl	825	835	830	835	795	805	810
X = Br	750	740	740	740	725	720	715

**Table II. Methylene Transfer to Macromolecular Polyenes**

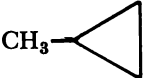
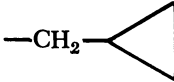
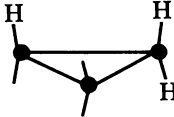
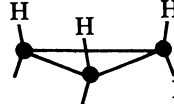
Reagent <sup>a</sup>	Ref.	Solvent (temp.)	Reaction Yield	Crosslinking
CH <sub>2</sub> I <sub>2</sub> + Zn/Cu	26	THF <sup>b</sup> (Reflux)	0	Crosslinking as the reaction starts
PhCO <sub>2</sub> CH <sub>2</sub> ZnI	29	Benzene (20°C.)	High <sup>d</sup>	Insoluble, but good-swelling polymer
CH <sub>2</sub> I <sub>2</sub> + ZnEt <sub>2</sub>	8	THF (Reflux)	Poor	
Ph <sub>2</sub> Hg + ICH <sub>2</sub> HgI	23	Benzene (Reflux, 4 days)	40% <sup>c</sup>	Altered polymer
(BrCH <sub>2</sub> ) <sub>2</sub> Hg	23	Benzene (Reflux, 4 days)	Poor	Altered polymer

<sup>a</sup> Three moles per monomer unit.<sup>b</sup> THF = tetrahydrofuran.<sup>c</sup> Calculated from NMR spectrum.<sup>d</sup> Infrared spectra nearly identical to that of C obtained by reduction of B (X = Br).**Figure 4. Cyclopropane models**



All the compounds shown in Figure 4 give infrared absorption bands at 3050 and 1020  $\text{cm}^{-1}$ , characteristic of  $\text{C}-\text{C}$  (25). The characterization of cyclopropane structures is confirmed by the NMR data given in Table III.

Table III. NMR Spectra of Cyclopropanes<sup>a</sup>

	Ic	IIc	IIIc	C(R = CH <sub>3</sub> )	IVc	Vc	C(R = H)
	9.00 s <sup>b</sup>	9.02 s	9.01 s	9.02 s			
	8.75 b	8.68 b	8.65 b	8.70 b	8.70 b	8.65 b	8.70 b
	9.65- 10.20 m	9.60- 10.20 m	9.60- 10.20 m	9.60- 10.20 m			
					9.50- 10.30 m	9.50- 10.30 m	9.50- 10.30 m

<sup>a</sup> TMS.  $\tau = 10$ .  $\text{CCl}_4$  solution, benzene as internal reference.

<sup>b</sup> Legend: s = sharp peak; b = broad peak; m = multiplet.

The cyclopropane type macromolecules C possess a structure similar to the polyenes A from which they are derived—*i.e.* (as the result of the *cis* addition of the carbenes to the olefins) the *cis* configuration of the original double bond reappears in the ring which is formed; the valence angles are modified only slightly in C compared with those in A; the rigidity of the chain with respect to the double bond is maintained by introducing the ring, whereas the sensitivity to oxidizing agents disappears. These products are similar in physical appearance to the elastomers from which they were prepared; a physicochemical study will reveal if they do, in fact, exhibit the properties of the elastomers.

**Behavior of Carboethoxynitrene toward Polyisoprene Structures.** After studying the reaction of a number of divalent carbon derivatives with polyenes (17, 18), attention was directed to monovalent nitrogen derivatives. Of these, carboethoxynitrene,  $\text{N}-\text{CO}_2\text{Et}$ , gives addition reactions with olefins (12, 13). It can be produced either by photolysis of ethyl azidoformate (12), or by  $\alpha$ -elimination (13) (Figure 5).

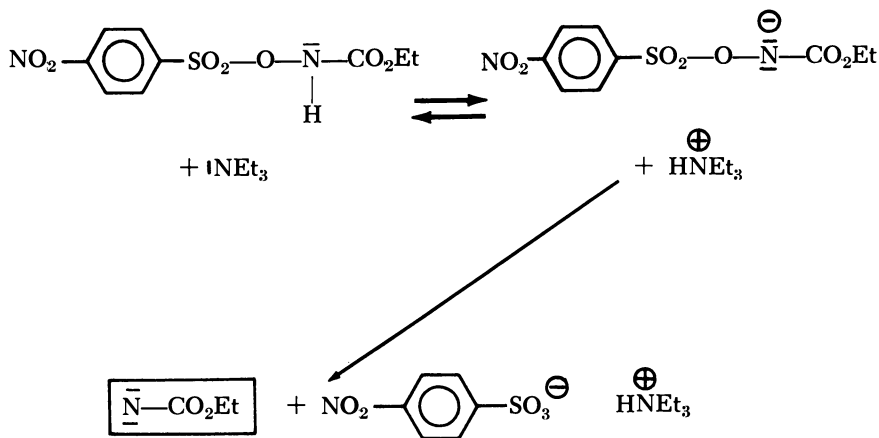


Figure 5. Carbethoxynitrene by  $\alpha$ -elimination (13)

The nitrene obtained by photolysis may under certain conditions be highly radicalar, and this method of preparation, likely to cause cross-linking, was avoided. When prepared by  $\alpha$ -elimination, carbethoxynitrene reacts with cyclohexene to give a mixture consisting of 85% addition product and 15% various substitution products (13). This reaction was used in attempts to prepare macromolecules with a polyethyleneimine structure. A preliminary investigation showed that the polyisoprenes react to a greater extent than the polybutadienes, and the reaction was first studied on model polyisoprenes.

Under Lwowsky's conditions (13), simple models of the 1,4-polyisoprenes (4-methyl-3-heptene, 4-methyl-4-octene, 1-methylcyclohexene, etc.) react with carbethoxynitrene to give mainly substitution products (85%) together with only a small amount (about 15%) of addition product. The latter compound is separable from the other by distillation and is characterized easily by the absence of infrared N—H bands and NMR vinylic protons. The mixed substitution products possess an unexpected special feature—*i.e.*, alongside the triplet arising from the vinylic proton at  $\tau = 4.7$ , there is a doublet at  $\tau = 5.2$  which can be attributed to  $\text{CH}_2=\text{C}<$ . The absorption bands in the infrared spectrum are actually of low intensity but are characteristic at 3080 and 900  $\text{cm}^{-1}$  (the C=C bands at *ca.* 1650  $\text{cm}^{-1}$  overlap with the very intense C=O band at 1700  $\text{cm}^{-1}$ ). Attempts were made to convert the urethane functional group into a less polar functional group to facilitate separation of the various products. A suitable method appears to consist of reducing N-CO<sub>2</sub>Et to N-CH<sub>3</sub> in the presence of lithium aluminum hydride (LAH); this reaction is virtually quantitative (9) and allowed us to obtain the methylamines corresponding to the urethanes.

The above data are also found for the amines obtained by reduction since the double bonds remain untouched by the operating conditions adopted. It is therefore possible to show (the C=O band having disappeared) the presence of two C=C bands at 1660 and 1640  $\text{cm}^{-1}$  and  $\text{>C=CH}_2$  at about 3080 and 900  $\text{cm}^{-1}$ . With NMR, a peak is found at  $\tau = 5.2$  corresponding to  $\text{>C=CH}_2$  (the  $\text{>C=CH}_2$  gives a singlet or a doublet depending on the respective environments of the two protons. This explains the observed change).

The presence of the methyl group at a double bond therefore involves two new effects in the reaction with carbethoxynitrene—namely the predominance of substitution reactions over addition reactions and the formation of a product in which the double bond is displaced (about 20% of the total mixture). In addition to the products of Structures D, E<sub>1</sub>, E<sub>2</sub>, and E<sub>3</sub> expected as the result of Lwowski's work, another product, probably of Structure E<sub>4</sub>, is formed (Figure 6). This is now being checked and necessitates the separation of the products either at the urethane stage or more effectively at the amine stage. Once the structure of this product is established definitely, the conditions affecting its formation remain to be studied, and this may yield an explanation of the reaction mechanism involved.

While awaiting the results of these experiments, the reaction between carbethoxynitrene and the cis-1,4-polyisoprenes was investigated. Using three moles of the reactant per isoprene unit, products were obtained whose analysis indicates a degree of reaction around 100%. These materials are highly viscous and adhere strongly to glass; they are very soluble in methylene chloride, carbon tetrachloride, and THF but are only slightly soluble in benzene. They can be precipitated from solution only by adding aliphatic hydrocarbons since they dissolve fairly well in acetone and methanol, confirming the highly polar nature of the structural units D and E.

Characterization of the structures of these products is facilitated by the study carried out on the model compounds. In the infrared spectra, characteristic N—H absorptions are found at 3320  $\text{cm}^{-1}$  and of C=O at 1705  $\text{cm}^{-1}$ , with a shoulder at 1650  $\text{cm}^{-1}$  (C=C). The NMR spectrum in  $\text{CCl}_4$  confirms the unsaturated nature of the products through the existence of a mass of peaks at  $\tau = 5.0$  probably caused by the superposition of Structures E. The presence of the structural units E<sub>4</sub> cannot be confirmed with certainty because of the unsatisfactory quality of the NMR spectrum. However, the infrared spectrum of the product reduced with LAH shows the presence of  $\text{C=CH}_2$ . This reduced product is slightly soluble in aqueous acids from which it precipitates on adding ammonia; its solubility in organic solvents is very much less than that of the previous product, and it was not possible to study it by NMR.

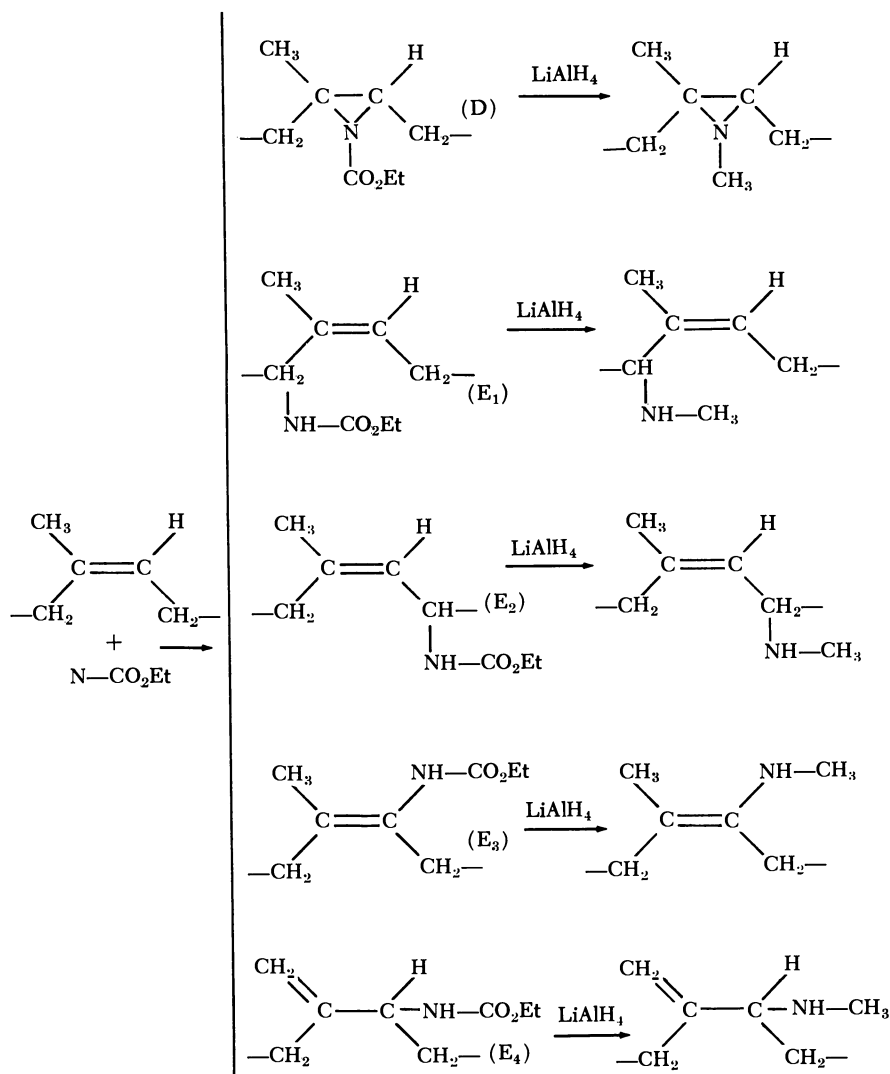


Figure 6. Reaction of carbethoxynitrene with polyisoprenes

It appears, therefore, that the reaction of carbethoxynitrene with the polyenes opens the way to two new kinds of unsaturated macromolecules, one comprising the urethane groups which are the source of hydrogen bonds between the chains, the other free amine functional groups, capable of reacting like weak bases. An important aspect of these reactions lies in the degree of modification which is determined by the amount of reagent used and may therefore vary within considerable proportions.

### Polymerization of Tricentric Systems

Prior knowledge has shown the value of introducing cyclopropane systems into macromolecules. A number of isolated studies have been carried out on the polymerization of such structures (10, 14, 28), principally on cyclopropane (28) and isopropylcyclopropane. Attention was directed toward three types of structures—*i.e.*, the 1,1-dichlorocyclopropanes, the bicyclo[*n*.1.0]alkanes, and the spiro[2.*n*]alkanes. In each case, the effects involved appeared highly complex; the polymers formed have not yet all been characterized, and it is thought that a comparison with the model structures expected from rupture of one or the other of the cyclopropane bonds may be of value.

**Polymerization of 1,1-Dichlorocyclopropanes.** Experiments were first carried out on vinyl dichlorocyclopropanes derived from isoprene and butadiene. The polymers obtained were very different from the cyclopropane macromolecular products already described (17), and it was found that cyclopropane participates in polymerization reactions. The study was therefore repeated in the simplest case—*i.e.*, that of saturated cyclopropane monomers.

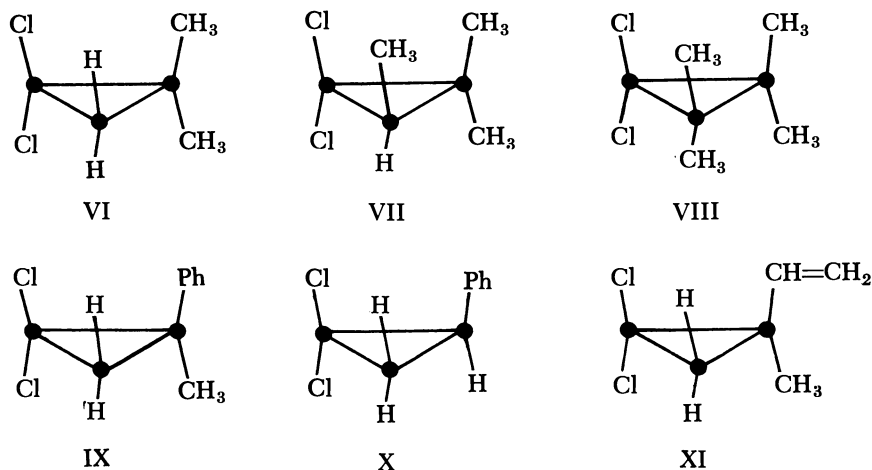


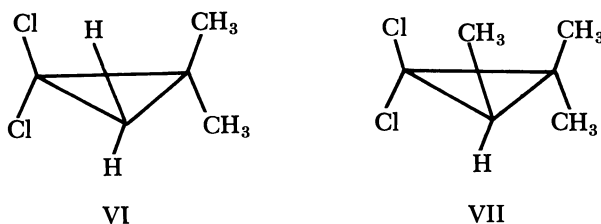
Figure 7. Dichlorocyclopropane monomers

The remarkable stability of the 1,1-dichlorocyclopropane system has been recognized ever since the discovery of the carbenes has enabled them to be prepared easily (6). The structure is, however, destroyed by Lewis acids (27). Therefore, polymerizations were first carried out using cationic catalysts and then Ziegler-Natta catalysts which give better results. A first group of monomers consists of 2,2-dimethyl-, 2,2,3-tri-

methyl-, and tetramethyl-1,1-dichlorocyclopropane (VI, VII, VIII) (Figure 7).

In the presence of catalysts  $\text{Et}_3\text{Al}/\text{TiCl}_4$ ,  $\text{Et}_2\text{AlCl}/\text{TiCl}_4$ , etc. in *n*-hexane at between  $50^\circ$  and  $80^\circ\text{C}$ . in a sealed tube, Monomers VI and VII give varying yields of polymers of average molecular weights ( $M_n$ ; vapor pressure method) of less than 10,000. Some typical examples of polymerization are collected in Table IV.

**Table IV. Polymerization of Dichlorocyclopanes<sup>a</sup>**



Monomer	$\text{Et}_3\text{Al}$ , mmoles	$\text{TiCl}_4$ , mmoles	$\text{Et}_3\text{Al}/$ $\text{TiCl}_4$	$T$ , $^\circ\text{C}$ .	Time, hours	Yield, %	$M_n$
VI (16 mmoles)	4.2	5.4	0.8	80	24	31	900
	2.1	2.7	0.8		24	16	1050
	1.4	1.8	0.8		18	9.5	2250
	1.4	1.8	0.8		50	14	8
VII (14 mmoles)	2.1	2.7	0.8	80	24	9	650
	1.4	1.8	0.8		24	5	800
	0.7	0.9	0.8		31	3.5	1230

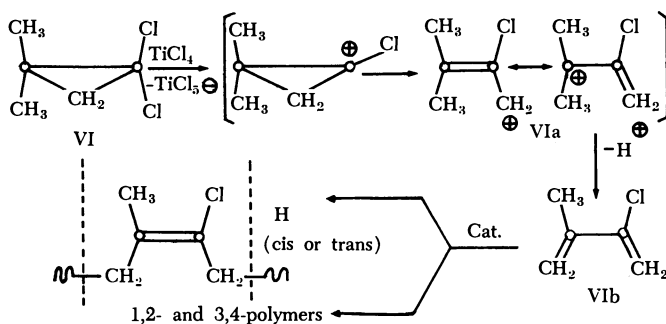
<sup>a</sup> Solvent, hexane (20 ml.).

It should be noted that VIII gives neither polymer nor oligomer under the conditions described, and the yield is smaller with VII than with VI. Moreover, the percentage composition of the polymers does not correspond to that of the monomers; about one atom of chlorine per molecule of monomer is lost when polymerization occurs. The polymer does not possess the characteristics of the cyclopanes. It therefore appears that opening of the cyclopropane ring, dehydrochlorination, and polymerization occur simultaneously.

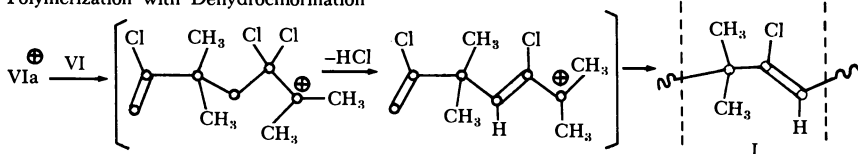
Several modes of reaction are possible, and these are collected in Figure 8. The first assumes that dehydrochlorination occurs first because of the presence of the acid catalyst (the formation of the mesomeric ion VIa being suggested by the work of Skattebol (27)). This intermediate structure may lose a proton, thus giving the conjugated diene VIb which is the product obtained by thermolysis of VI at  $500^\circ\text{C}$ . (7). VIb may then

polymerize to -1,4 (H), -1,2; -3,4 etc. The second possibility would be attack of the monomer by ion VIa, with evolution of HCl during the propagation reaction. This mechanism could give rise to I. Finally, polymerization of VI by the catalyst could lead to the production of unstable gem-dichloro derivatives capable of easy dehydrochlorination (Structure I). The two last modes of polymerization may be accompanied by a rearrangement (Structure J); they also suppose the existence of some unsaturation of the cyclopropane.

#### Dehydrochlorination before Polymerization



#### Polymerization with Dehydrochlorination



#### Polymerization followed by Dehydrochlorination

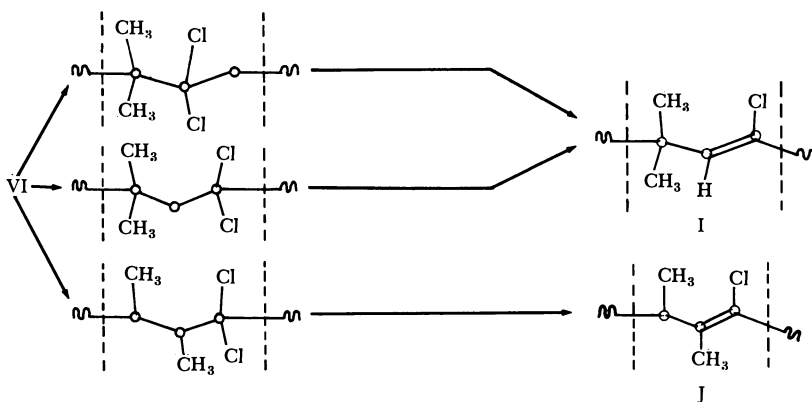


Figure 8. Polymerization of 1,1-dichloro-2,2-dimethylcyclopropane

Data obtained so far on the polymers of VI make it clear that there is a loss of HCl, double bonds are present (infrared evidence and the addition of Br<sub>2</sub>), and there are very few vinylic protons (by NMR). These data are likely to be completed in the near future, but are insufficient to indicate which of the possible structures is correct. However, the most probable ones appear to be H, I, and J which are all compatible with the experimental results.

The absence of polymerization found with VIII may be explained either by the formation of a trimethylchlorobutadiene too hindered to polymerize, or by the absence of protons in the ring which might be necessary for the second mechanism, or even perhaps by the hindrance of the molecule being unsuitable for reaction by the third mechanism. Studies presently in progress are concerned with possible reactions between the complex Ziegler catalyst and the hydrochloric acid liberated. In addition, work is envisaged on this type of polymerization in the presence of a reagent capable of combining with the proton acid formed.

Of the cyclopropane systems containing unsaturated groups, it is 2-methyl-2-phenyl-1,1-dichlorocyclopropane IX which gives results identical to those described in Table V; the same reactions can be described for IX as for VI. 2-Phenyl-1,1-dichlorocyclopropane X also gives polymers, but of much lower solubility than those from IX, it being noted

**Table V. Polymerization of 2-Phenyl-1,1-dichlorocyclopropane at 80°C.**

<i>Monomer,</i> <i>mmoles</i>	<i>Et<sub>3</sub>Al,</i> <i>mmoles</i>	<i>Et<sub>2</sub>AlCl,</i> <i>mmoles</i>	<i>TiCl<sub>4</sub>,</i> <i>mmoles</i>	<i>R<sub>3</sub>Al/</i> <i>TiCl<sub>4</sub></i>	<i>Time,</i> <i>hours</i>	<i>Yield,</i> <i>%</i>
13	2.2		2.7	0.8	24	31
13	1.05		1.35		24	18
13	0.7		0.9		24	14
13	0.35		0.45		24	0.4
13		2.4	2.7	0.9	26	38.4
13		1.2	1.35		23	18.9
13		0.8	0.9		26	14.1
13		0.4	0.45		41	3.9

that X cannot give a conjugated diene of type VIb. However, the ring is capable of reacting with carbocations, and on this assumption, the structural units of the polymer would be fairly rigid, which explains the low solubility of the product. Furthermore, grafting can occur during polymerization. Monomer XI represents the most complex case since, in addition to the possibilities mentioned here, it can give rise to vinyl polymerization which may or may not be associated with opening of the cyclopropane ring.



The results obtained have revealed the complexity of the effects involved during the polymerization of the 1,1-dichlorocyclopropanes. Experiments now in progress will undoubtedly indicate the nature of the structures formed. It will then be possible to study in detail the reactions between these monomers and the Ziegler-Natta catalysts.

**Polymerization of the Bicyclo[*n*.1.0]alkanes.** Some cyclopropane type hydrocarbons have already been polymerized—*i.e.*, cyclopropane (28), 1,1-dimethyl- (10) and isopropylcyclopropane (14), particularly in presence of cationic catalysts. This work has established that a  $\pi$  complex is formed between the active site in the chain and a new molecule of monomer; the complex then develops *via* opening of the cyclopropane ring; in certain cases this opening is accompanied by transfer of a hydride ion (10).

Bicyclo[5.1.0]octane, [6.1.0]nonane and [10.1.0]tridecane XII, obtained from the corresponding cyclenes by the Simmons-Smith method (26), were polymerized in solution in methylene chloride in presence of  $\text{BF}_3\text{-Et}_2\text{O}$ ,  $\text{TiCl}_4$ , or  $\text{SnCl}_4$ . The mixture was placed in a sealed tube and maintained at temperatures between 20° and 80°C. for 60 to 200 hours. The numerous experiments carried out always gave oligomers of a low degree of polymerization—*i.e.*, 2 to 4—but the degrees of conversion were nonetheless relatively high (up to 60%).

Infra spectra of the oligomers obtained show characteristic  $\text{—CH}_2\text{—}$  and  $\text{—CH—}$  bands at 2950, 2920, and 1450  $\text{cm}^{-1}$ . In addition, they all show an absorption of 1375  $\text{cm}^{-1}$  caused by  $\text{CH}_3\text{—}$  groups. This fact is confirmed by NMR spectra having peaks at  $\tau = 8.60$  ( $\text{—CH}_2\text{—}$ ) and  $\tau = 9.18$  ( $\text{CH}_3\text{—}$ ). In addition, characteristic signals are found for vinylic protons ( $\tau = 4.8$ ) and for methyl groups at a double bond ( $\tau = 8.2$ ). The latter are of increasing intensity as the degree of polymerization drops, probably owing to one end of the ethylenic chain.

Polymerization of the bicyclo[*n*.1.0]alkanes studied therefore occurs by opening of the cyclopropane ring and results in the appearance of one methyl group per structural unit.

Cationic polymerization of XII may therefore be visualized in terms of Figure 9 according to which the  $\pi$  complex initially formed between the active site and the monomer is converted into a carbocation with rupture of a C—C bond in the cyclopropane. This cation may be XIIa, b, or c, but only the latter can give rise to Structure M, alone compatible with the experimental data. This change necessitates the transfer of a hydride ion to transform the primary cation XIIc into the more stable tertiary cation XIIId. On this assumption, the termination reaction probably occurs as the result of the displacement of a proton in the alpha position with respect to the  $\text{C}^+$ , which is relatively easy, whereas the steric hindrance around the active site does not favor continued poly-

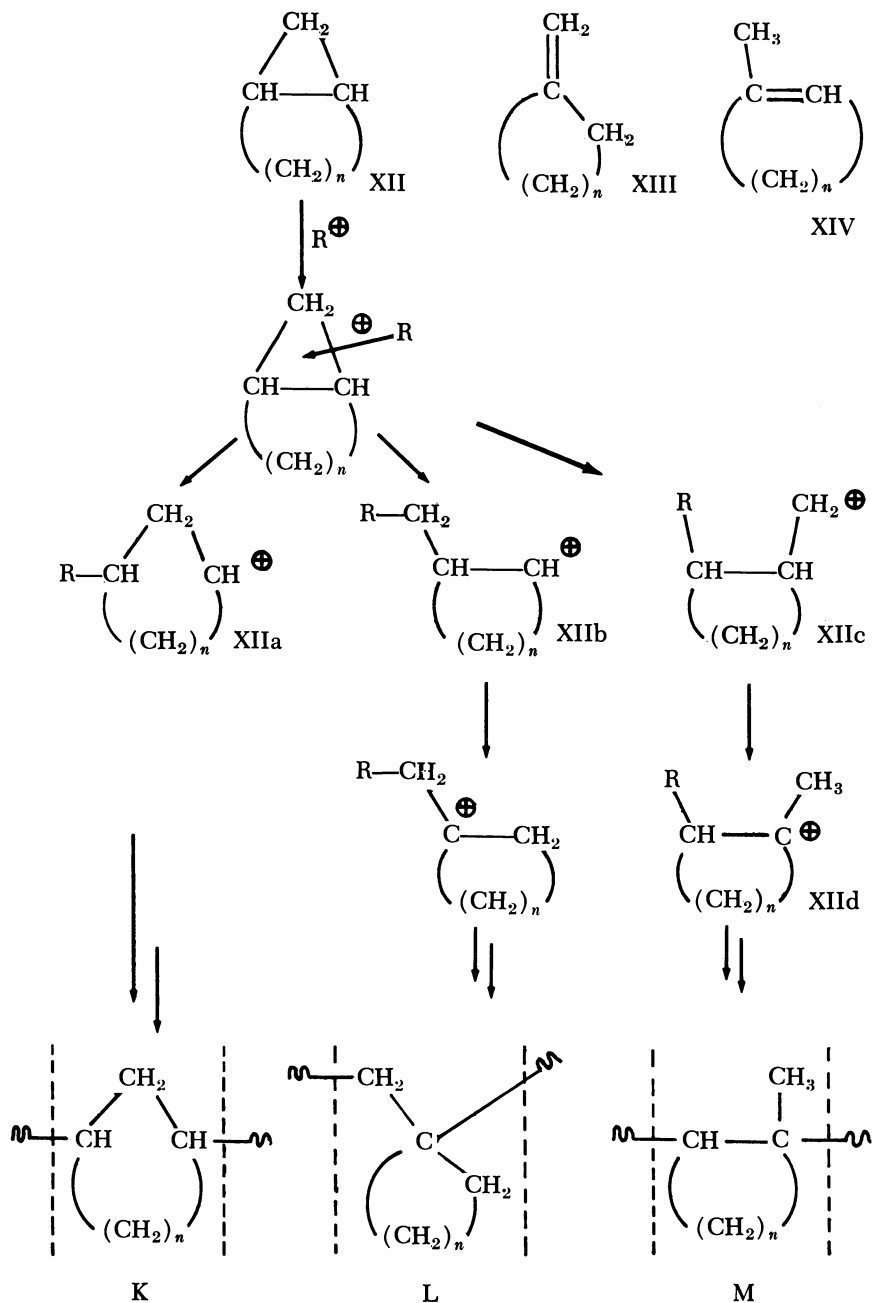
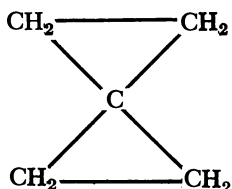


Figure 9. Polymerization of bicyclo[n.1.0]alkanes ( $n = 5, 6, \text{ or } 10$ )

merization. The facts just enumerated confirm these speculations—namely that the degree of polymerization remains very low and there is some unsaturation as a chain end effect.

Polymerization of the methylenecyclanes XIII and methylcyclohexanes XIV, the isomers of XII, was studied independently (19). The oligomers obtained from XIII or XIV have the same structure M as those described in this paper. These results therefore confirm the hypotheses advanced for XII—*i.e.*, opening of the cyclopropane ring and transfer of hydride ion with formation of XIId, the hindered intermediate which polymerizes poorly and undergoes deprotonation easily, which interrupts the polymerization process.

**Polymerization of Spiropentane.** The study of polymerization by opening of the three carbon ring has given a picture of the reactivity of spiro-pentane with respect to various catalysts.



The difficulty in obtaining this monomer in the pure state arises from the fact that the known methods of preparation involve the simultaneous formation of considerable amounts of the isomers of spiro-pentane which are difficult to remove. The method adopted as giving the most satisfactory yields is that of Applequist, Fanta, and Henrickson (1, 2). The spiro-pentane is prepared by reaction of zinc dust with pentaerythrityl tetrabromide in alcohol in presence of the sodium salt of ethylenediamine-tetraacetic acid as complexing agent. The yield of hydrocarbon (spiro-pentane plus various ethylenic compounds) is of the order of 84%. The spiro-pentane is obtained in the pure state by treating the mixture with bromine in dibromomethane. The yield of pure spiro-pentane was found to be 62%.

Radical polymerization experiments, especially with azobisisobutyronitrile, were negative. However, cationic polymerization gave positive results. The Lewis acid type catalysts used appear to possess varying reactivities. In particular, by using  $\text{BF}_3$  and  $\text{BF}_3\text{-Et}_2\text{O}$  it is possible to obtain low molecular weight oils but occasionally at relatively high degrees of conversion. On the other hand, experiments carried out so far with  $\text{TiCl}_4$  and  $\text{SnCl}_4$  give only traces of oligomers. The best results

**Table VI. Physical Data for Cyclopropane Models**

	B.P., °C. (mm. Hg)	$n_D^{20}$
Ic	152 (760)	1.4220
IIc	107-9 (5)	1.4489
IIIc	125 (.2)	1.4608
IVc	140-2 (760)	1.4186
Vc	90 (6)	

have been obtained with Ziegler-Natta type catalysts. Various combinations have been employed—*i.e.*,



Polymerizations carried out in hexane in a sealed tube have elucidated the importance of a number of parameters: yields increase as a function of temperature, with no polymerization at below 20°C., optimum yields correspond to a well-defined amount of catalyst, and concentrations of monomer and catalysts give higher yields at the highest dilutions.

The polymers are obtained in the form of powders which are generally colorless and soluble in benzene, tetrahydrofuran, carbon tetrachloride, etc.

Structural studies are now under way. Infrared spectroscopy and NMR of the polymers obtained exclude the existence of cyclopropane groups, which suggests a polymerization mechanism involving the two spiro-pentane rings, perhaps simultaneously. On the other hand, structures similar to those of cyclized polyisoprene are highly probable. Comparisons of the similarity of structure of polyspiropentane and cyclized isoprene models are now in progress (20). Further, this hypothesis appears to be in agreement with the work of Dall'asta and Manetti (5), who have demonstrated such structures by polymerization of an isomer of spiro-pentane, 1-methylcyclobutene.

### Literature Cited

- (1) Applequist, D. E., Fanta, G. F., Henrickson, B. W., *J. Am. Chem. Soc.* **82**, 2368 (1960).
- (2) Applequist, D. E., Fanta, G. F., Henrickson, B. W., *J. Org. Chem.* **23**, 1715 (1958).
- (3) Conia, J. M., *Bull. Soc. Chim. France* **1950**, 537.
- (4) Considine, W. J., Ventura, J. J., *Chem. Ind. (London)* **1962**, 1683.
- (5) Dall'asta, G., Manetti, R., *Atti. Accad. Nazl. Lincei, Rend., Classe Sci. Fis., Mat. Nat.* **41**, 351 (1966).
- (6) Doering, W. Von E., Hoffmann, A. K., *J. Am. Chem. Soc.* **76**, 6167 (1954).
- (7) Engelsma, J. W., *Rec. Trav. Chim.* **84**, 187 (1965).

- (8) Furukawa, J., Kawabata, N., Nishimura, J., *Tetrahedron* **24**, 53 (1968).
- (9) Gaylord, N. G., "Reduction with Complex Metal Hydrides," p. 636, Interscience, New York, 1956.
- (10) Ketley, A. D., *J. Polymer Sci. Pt. B1*, **2**, 313 (1963).
- (11) Kirmse, W., "Carbene Chemistry," Academic Press, New York, 1964.
- (12) Lwowski, W., Mattingly, T. W., Jr., *J. Am. Chem. Soc.* **87**, 1947 (1965).
- (13) Lwowski, W., Maricich, T. J., *J. Am. Chem. Soc.* **87**, 3630 (1965).
- (14) Naegele, W., Haubenstock, H., *Tetrahedron Letters* **1965**, 4283.
- (15) Pinazzi, C., Gueniffey, H., *Compt. Rend.* **263C**, 915 (1966).
- (16) Pinazzi, C., Gueniffey, H., *Makromol. Chem.* **93**, 109 (1966).
- (17) Pinazzi, C., Levesque, G., *J. Polymer Sci. Pt. C*, **16**, 4695 (1969).
- (18) Pinazzi, C., Gueniffey, H., Levesque, G., Reyx, D., Pleurdeau, A., *Symp. Macromol. Chem., Brussels, 1967*, Preprint 2/83.
- (19) Pinazzi, C., Brosse, J. C., *Compt. Rend.* **266C**, 1136 (1968).
- (20) Pinazzi, C., Reyx, D., unpublished work.
- (21) Seyferth, D., Burlitch, J. M., *J. Organometal. Chem.* **4**, 127 (1965).
- (22) Seyferth, D., Burlitch, J. M., Minasz, R. J., Yick-Pui Mui, J., Simmons, Jr., H. D., Treiber, A. J. H., Dowd, S. R., *J. Am. Chem. Soc.* **87**, 4259 (1965).
- (23) Seyferth, D., Eisert, M. A., Todd, L. J., *J. Am. Chem. Soc.* **86**, 121 (1964).
- (24) Seyferth, D., Yamazaki, H., Allester, D. L., *J. Org. Chem.* **28**, 703 (1963).
- (25) Simmons, H. E., Blanchard, E. P., Hartzler, H. D., *J. Org. Chem.* **31**, 295 (1966).
- (26) Simmons, H. E., Smith, R. D., *J. Am. Chem. Soc.* **80**, 5323 (1958).
- (27) Skattebol, L., Boulette, B., *J. Org. Chem.* **31**, 81 (1966).
- (28) Tipper, C. F. H., Walker, D. A., *J. Chem. Soc.* **1959**, 1352.
- (29) Wittig, G., Jautelat, M. H., *Ann.* **702**, 24 (1967).

RECEIVED April 1, 1968.

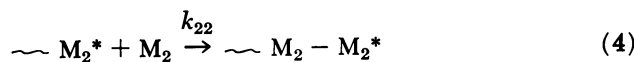
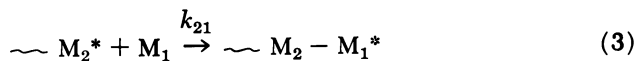
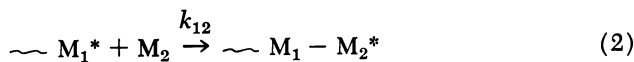
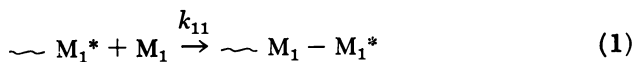
# Copolymerization with Depropagation

KENNETH F. O'DRISCOLL

Department of Chemical Engineering, State University of New York  
at Buffalo, Buffalo, N. Y. 14214

*For every vinyl monomer there exists a ceiling temperature above which it is thermodynamically impossible to convert monomer into high polymer because of the depropagation reaction. If two vinyl monomers are copolymerized under conditions such that one or both may depropagate, the resultant polymer will have an unusual composition and sequence distribution. Existing theoretical and experimental works are reviewed which treat of copolymer composition, rate of copolymerization, and degree of copolymerization.*

The theory and experimental practice of addition copolymerization have been well understood for many years (1). In the simplest form, one considers that four, and only four, propagation reactions are necessary to describe copolymer composition:



Various theoretical approaches all lead to the well known composition equation:

$$\frac{m_1}{m_2} = \frac{[M_1]}{[M_2]} \frac{r_1 \frac{[M_1]}{[M_2]} + 1}{r_2 + \frac{[M_1]}{[M_2]}} \quad (5)$$

where the reactivity ratios are defined as

$$r_1 = k_{11}/k_{12}; \quad r_2 = k_{22}/k_{21} \quad (6)$$

and  $[M_1]$  and  $[M_2]$  are the monomer feed concentrations which produce an instantaneous copolymer containing mole fractions  $m_1$  and  $m_2$  of the two monomers.

Variants of the above have been used to explain unusual data where it was suspected that monomer units penultimate to the chain end (or even further back) were affecting the reaction rate constants (6). Such treatments suffer from a degree of arbitrariness in that the experimental data may not provide an adequate test of the kinetic model (3). In some cases, penultimate unit effect models have been used to interpret unusual data where one might expect depropagation to be important.

Although it has long been recognized (4) that homopolymerization chain reactions can and do depropagate under reaction conditions of practical importance, it was not until recently that the problem of copolymerization with depropagation was attacked. The successful experimental and theoretical treatment of depropagation in anionic homopolymerization (the so-called "living polymers") provided both the incentive to begin the problem of copolymerization with depropagation and a large amount of the necessary thermodynamic data. Since the details of equilibrium homopolymerization have been reviewed elsewhere (4, 9), it will suffice to present the following, oversimplified, thermodynamic considerations.

### *Reversibility of Homopolymerization*

The general reaction to be considered is that of a monomer unit in some particular state  $s$  (where  $s$  is either bulk monomer, solution in a particular solvent, or gas phase) being incorporated in a polymer of chain length  $n$  where the polymer chain is in some particular state  $s'$  (where  $s'$  represents amorphous or crystalline polymer, or polymer in solution). For theoretical purposes,  $s'$  might represent the gaseous state. If such a reaction has achieved equilibrium (Equation 7), the free-energy change for the polymerization  $\Delta G_p$  will be zero (Equation 8).

$$nM(s) \rightleftharpoons \frac{1}{n} (M)_n(s') \quad (7)$$

$$\Delta G_p = \Delta H_p - T\Delta S_p \quad (8)$$

Consequently,

$$T_c = \Delta H_p / \Delta S_p = \Delta H_p / (\Delta S_p^\circ + R \ln a_M) \quad (9)$$

where  $\Delta S_p^\circ$  is the standard entropy change accompanying polymerization when the monomer activity,  $a_M$ , is unity.  $T_c$  is a critical temperature for polymerization: if both  $\Delta S_p$  and  $\Delta H_p$  are negative,  $T_c$  is a "ceiling" temperature above which it is thermodynamically impossible to convert monomer into polymer of chain length  $n$ ; if both are positive, it is a "floor" temperature below which it is thermodynamically impossible to convert monomer into polymer of chain length  $n$ .

Equation 9 suggests several points about  $T_c$ . Obviously, it will be affected by conditions which affect the monomer activity or the heat of polymerization. Since these terms will be affected by the reaction medium, the critical temperature obviously depends on that. It is also important to stress that for every monomer concentration (or activity) there is a corresponding critical temperature; this can be restated by noting that for every temperature there will be a corresponding equilibrium monomer concentration. In fact, the equilibrium monomer concentrations of most polymerizations are so low ( $10^{-3}$  to  $10^{-9}M$ ) that they defy precise measurement. Nevertheless, in particular cases they may be sufficiently high to cause concern over potential effects on the physical or physiological properties of the polymer. Most vinyl polymerizations exhibit ceiling temperatures of  $100^\circ$ – $300^\circ C$ . since the heats of polymerization are on the order of  $-20$  kcal./mole and the entropies of polymerization are approximately  $-30$  cal./degree/mole. Polymerizations of ring compounds to linear polymers may show ceiling temperatures as in the case of tetrahydrofuran ( $60^\circ$ – $70^\circ C$ .) or floor temperatures as in the case of sulfur ( $160^\circ C$ .) and selenium ( $80^\circ C$ .).

### ***Reversibility of Copolymerization***

If one applies these considerations on homopolymerization to copolymerization, it is easy to appreciate that any or all of Reactions 1 through 4 may, in a particular copolymerization, be of such a reversible character that depropagation must be considered. Lowry was the first to construct a successful theory concerning this (11). He postulated several cases, the simplest of which considered only Reaction 4 to be reversible.



In his kinetic analysis of the copolymer composition that would be formed, the usual steady-state assumptions were made. Lowry also made the important deduction that the rate at which Monomer 2 disappeared from the reaction (and was incorporated into the polymer) depended not simply upon the relative rates of the forward and reverse reaction (4a)



but rather upon the rate of Reaction 3, wherein a run of  $M_2$  units was "capped" by an  $M_1$ , thus preventing depolymerization of that run.

$$-\frac{d[M_2]}{dt} = \sum_{n=1}^{\infty} n k_{21} [(m_2)_n^* [M_1]] \quad (10)$$

where  $[(m_2)_n^*]$  is the concentration of active chains ending in a run of  $n$  consecutive  $M_2$  units.

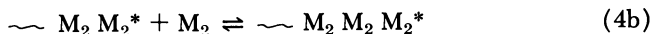
The composition equation for this model was given as (11):

$$\frac{m_2}{m_1} = [M_2](1/(1-\alpha))/(r_1[M_1] + [M_2]) \quad (11)$$

$$\alpha \equiv [(m_2)_{n+1}^*]/[(m_2)_n^*] \text{ for } 0 < n < \infty$$

where  $\alpha$  is a function of the equilibrium constant for Reaction 4a,  $r_2$ , and the monomer concentrations. Note that copolymer composition is a function of the absolute monomer concentrations when depropagation occurs but only of the ratio of monomer concentration when Equation 5 applies.

The second, and more physically realistic, case which Lowry considered, postulated that only Reaction 4b was reversible:



*i.e.*, depropagation occurred whenever three or more  $M_2$  units were at the end of an active chain.

Again using steady-state assumptions and Equation 10, the copolymer composition is given by (11):

$$\frac{m_2}{m_1} = \frac{\beta\gamma - 1 + (1/1 - \beta)^2}{[(r_1 [M_1]/[M_2]) + 1][\beta\gamma + (\beta/1 - \beta)]} \quad (12)$$

where  $\beta$  is defined as  $\alpha$  above except that  $1 < n < \infty$  and

$$\gamma \equiv [(m_2)_1^*]/[(m_2)_2^*]$$

Using  $K$  for the equilibrium constant of Reaction 4b

$$\beta = \frac{1}{2} \left\{ \left( 1 + K [M_2] + \frac{K}{r_2} [M_1] \right) - \left[ \left( 1 + K [M_2] + \frac{K}{r_2} [M_1] \right)^2 - 4 K [M_2] \right]^{1/2} \right\} \quad (13)$$

$$\gamma = 1 - \frac{[M_1]}{r_2 [M_2]} - \frac{\beta}{K [M_2]} \quad (14)$$

$K$  is a thermodynamic constant and is independent of mechanism, while reactivity ratios are kinetic constants and depend on mechanism.

Lowry also considered a third case in which the sequence  $-M_2M_2M_2^*$  could depropagate whether the terminal unit was an  $M_1$

or an  $M_2$ . The resulting equations were too cumbersome for use since they involved series which are slow to converge.

Ivin and Hazell (7) extended Lowry's treatment to include a fourth case where any propagating chain ending in  $M_2$  could depropagate. Such a mechanism has been shown to apply in olefin-sulfur dioxide copolymerizations.

More recently Durgaryan derived (5) a copolymer composition equation assuming reversibility of all propagation reactions, Equations 1-4. He expressed his solution as a pair of simultaneous equations in which the two unknowns (besides kinetic parameters and monomer feed) were copolymer composition and the ratio  $[(m_1)_2^*]/[(m_1)_1^*]$ . At this writing no experimental tests of Durgaryan's equations have appeared.

### *Applications of Lowry Case II*

Ivin and Spensley (10) tested the Lowry Case II model and equations for the anionic copolymerization of vinyl mesitylene ( $M_1$ ) with  $\alpha$ -methylstyrene at 0°C. by varying the total concentration of the two monomers while keeping their mole ratio constant. As pointed out above, theory predicts a dependence on absolute monomer concentration when depropagation occurs. Table I summarizes some of Ivin and Spensley's data.

They also tested (10) Case II for the free radical polymerization of styrene ( $M_1$ ) and methyl methacrylate at 132°C. by the dilution technique. These data are also shown in Table I, where the good agreement between theory and experiment is apparent. The applicability of the theory to different mechanisms of polymerization is a nice verification of the statement that the composition is governed by end-state thermodynamics rather than by mechanism.

**Table I. Comparisons of Copolymer Compositions (9)**

$[M_2], M$	<i>Vinylmesitylene-<math>\alpha</math>-Methylstyrene</i>		<i>Styrene-Methyl Methacrylate</i>		
	$m_2$ (Mole Fraction)		$[M_2], M$	$m_2$ (Mole Fraction)	
	<i>Calcd.</i>	<i>Obsd. (<math>\pm .01</math>)</i>		<i>Calcd.</i>	<i>Obsd. (<math>\pm .01</math>)</i>
3.90	.840	.841	1.376	.856	.860
.575	.750	.790	1.380	.857	.856
.250	.696	.730	0.166	.706	.760
.240	.693	.723	0.165	.707	.740
.054	.659	.660	0.125	.688	.704

Coincidental with Ivin and Spensley, O'Driscoll and Gasparro (12) studied the free radical copolymerization of styrene-methyl methacrylate but at 250°C. The latter workers varied monomer feed ratio over a wide

range at constant total concentration and found the unusual copolymer composition curve shown in Figure 1. Again the Lowry Case II gave excellent fit to the experimental data.

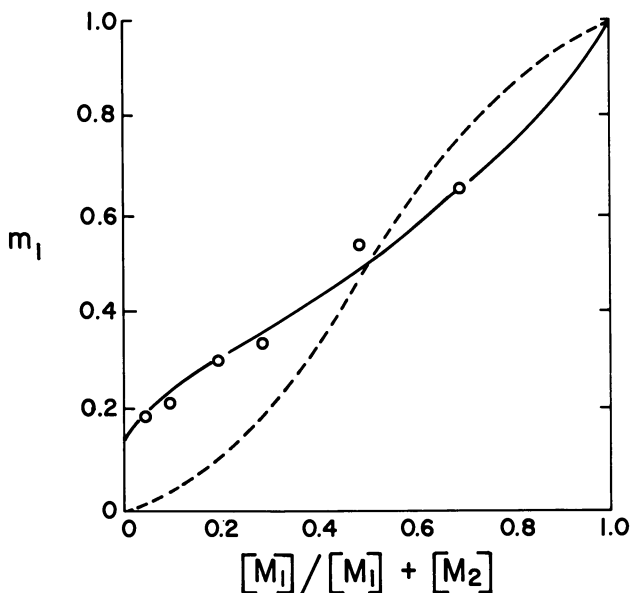


Figure 1. Free radical bulk copolymerization of styrene ( $M_1$ ) with methyl methacrylate ( $M_2$ ) (11). Open circles represent experimental data at 250°C.

— Calculated from Equation 12 ( $r_1 = 0.8$ ,  $r_2 = 0.8$ ,  $K = 0.105$ )

--- Calculated from Equation 5 ( $r_1 = 0.5$ ,  $r_2 = 0.5$ )

O'Driscoll and Gasparro also studied the copolymerization by free radicals of  $\alpha$ -methylstyrene ( $M_2$ ) with either styrene or acrylonitrile as  $M_1$  and found excellent agreement with Case II. They also showed that the limiting composition to be expected as the mole fraction of  $M_1$  in the feed approached zero was accurately given by (12):

$$m_2 = (2 - K [M_2]) / (3 - 2K [M_2]) \quad (15)$$

This equation permits the calculation of equilibrium constants for polymerization-depolymerization from copolymer composition data extrapolated to zero  $M_1$  feed. The agreement between equilibrium constants calculated in this manner from free radical copolymerizations and those obtained from anionic homopolymerizations is shown in Table II, and again emphasizes the thermodynamic character of this work.

**Table II. Comparison of Equilibrium Constants (11)**

$M_1$	$M_2$	$T, ^\circ\text{C.}$	K	
			Ref. 16	from homopolym.
Styrene	$\alpha$ -Methylstyrene	60	.097	.110
		100	.021	.015
Acrylonitrile	$\alpha$ -Methylstyrene	75	.074	.061
Styrene	Methyl methacrylate	250	.102	.079

O'Driscoll and Dickson (13) have extended the Lowry Case II to cover the rate of copolymerization as well as composition. They attribute the apparent increase in termination rate as the depropagating monomer is added to the feed to the predominance of small radicals of the type:  $\text{R}-(\text{M}_2)_n^*$ , where R is an initiator fragment and  $n$  is a very small whole number—1, 2, or 3. Such small radicals, they postulate, would have diffusivities 1000 times greater than polymeric free radicals, and hence the diffusion-controlled, bimolecular termination rate constant would be greatly increased. Using a model for the rate of termination which involves termination reactions between two small radicals, two large radicals, and a small radical with a large radical, it has been shown that the experimentally observed rate of copolymerization can be interpreted precisely. Figure 2 shows a plot for the system styrene- $\alpha$ -methylstyrene at 60°C. The solid line in Figure 2 is calculated according to the equation

$$\frac{R_p}{R_{p,0}} = \left\{ k_{21} [\text{M}_1] \left( r_1 \frac{[\text{M}_1]}{[\text{M}_2]} \left( \gamma + \frac{1}{1-\beta} \right) + 2\gamma + \frac{3-2\beta}{(1-\beta)^2} \right) / \right. \\ \left. \left\{ k_{11} [\text{M}_1]_{\text{bulk}} \left[ \left( \frac{k_{21} [\text{M}_1]}{k_{12} [\text{M}_2]} \left( \gamma + \frac{1}{1-\beta} \right) + \frac{\beta^2}{1-\beta} \right)^2 + \frac{k_{t22}}{k_{t11}} (\gamma + 1 + \beta)^2 \right. \right. \right. \\ \left. \left. \left. + \frac{k_{t12}}{k_{t11}} \left( \frac{k_{21} [\text{M}_1]}{k_{12} [\text{M}_2]} \left( \gamma + \frac{1}{1-\beta} \right) + \frac{\beta^2}{1-\beta} \right) (\gamma + 1 + \beta) \right]^{1/2} \right\} \right\} \quad (16)$$

$k_{t11}$  is the homopolymerization termination rate constant for styrene, and  $k_{t22}$  is determined by extrapolation to pure  $\alpha$ -methylstyrene feed while  $k_{t12}$  is given by the general geometric mean

$$k_{t12} = k_{t11}^{(1-x)} k_{t22}^x \quad (17)$$

where  $x$  is the mole fraction of active chain ends which are small. Experimentally, it was found by extrapolation that  $k_{t22}$  was about  $10^{10}$  which is what one expects for diffusion-controlled bimolecular rate constants for the reaction of small molecules.

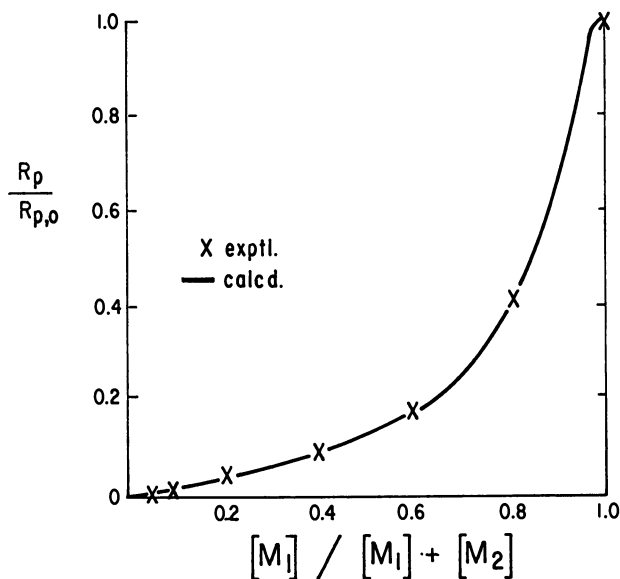


Figure 2. Relative rate of copolymerization of styrene ( $M_1$ ) and  $\alpha$ -methylstyrene ( $M_2$ ) at 60°C. as a function of monomer composition (12)

### Ring Opening Copolymerizations

Tobolsky and Owen (15) extended the Tobolsky-Eisenberg (16) general treatment of homopolymerization equilibria to copolymerization and applied their equations to the copolymerization data of Schenk (14) on selenium and sulfur. In this work the equilibrium degree of polymerization is measured as a function of temperature for total conversion of monomer to polymer. Equilibrium constants for initiation and propagation are derived from homopolymerization experiments.

Recently, Yamashita and co-workers (17) extended Lowry's treatment for use on the cationic copolymerization of 3,3-bis(chloromethyl)-oxacyclobutane (BCMO,  $M_1$ ) with tetrahydrofuran (THF,  $M_2$ ). They find that their data can be interpreted successfully by a model which considers a chain ending in  $M_2$  to add either  $M_1$  or  $M_2$  reversibly, but chains ending in  $M_1$  add both monomers irreversibly. Their equation takes the simple form

$$\frac{m_1}{m_2} = (1 - \alpha) \left( 1 + r_1 \frac{[M_1]}{[M_2]} \right) \quad (16)$$

where  $\alpha$ , as before, is the ratio  $[(m_2^*)_{n+1}]/[(m_2)_n^*]$  and is given by a function of equilibrium constants and  $r_2$  and monomer feed concentrations.

### Summary

The work to date has largely verified the approach of Lowry and extended his models in particular systems. In several cases, the satisfying result appears that one is dealing with thermodynamic control of composition since quantitative data appear to be independent of mechanism. Still to be found is whether the distribution of monomer units in the chain conforms to kinetic or thermodynamic control. Alfrey and Tobolsky (2) have presented a statistical thermodynamic treatment of equilibrium distribution which has not been tested experimentally. A calculation of sequence distribution using still another extension of Lowry's model is presently underway in this laboratory (8).

### Acknowledgments

Support of the author's work mentioned in this review by an unrestricted grant from the Chevron Research Corp. and by the National Science Foundation is greatly appreciated.

### Literature Cited

- (1) Alfrey, T., Bohrer, J., Mark, H., "Copolymerization," Vol. VIII of "High Polymers," Interscience, New York, 1952; updated as Vol. XVIII, G. E. Ham, Ed., 1964.
- (2) Alfrey, T., Tobolsky, A. V., *J. Polymer Sci.* **38**, 269 (1959).
- (3) Berger, M., Kuntz, I., *J. Polymer Sci.* **A2**, 1687 (1964).
- (4) Dainton, F. S., Ivin, K. J., *Quart. Rev.* **12**, 61 (1958).
- (5) Durgaryan, A. A., *Vysokomol. Soyed.* **8**, 780 (1966).
- (6) Ham, G. E., *J. Polymer Sci.* **45**, 169, 177, 183 (1960).
- (7) Hazell, J. E., Ivin, K. J., *Trans. Faraday Soc.* **58**, 176 (1961); **61**, 2330 (1965).
- (8) Howell, J. A., Izv, M., O'Driscoll, K. F., *J. Polymer Sci.*, in press.
- (9) Ivin, K. J., *Pure Appl. Chem.* **4**, 271 (1962).
- (10) Ivin, K. J., Spensley, R. H., *J. Macromol. Sci. (Chem.)* **A1**, 653 (1967).
- (11) Lowry, G., *J. Polymer Sci.* **42**, 463 (1960).
- (12) O'Driscoll, K. F., Gasparro, F. P., *J. Macromol. Sci. (Chem.)* **A1**, 643 (1967).
- (13) O'Driscoll, K. F., Dickson, J. R., *J. Macromol. Sci. (Chem.)* **A2**, 449 (1968).
- (14) Schenk, J., *Physica* **23**, 325 (1957).
- (15) Tobolsky, A. V., Owen, G. D. T., *J. Polymer Sci.* **59**, 329 (1962).
- (16) Tobolsky, A. V., Eisenberg, A., *J. Am. Chem. Soc.* **82**, 289 (1960).
- (17) Yamashita, Y., Kasahara, H., Suyama, K., Okada, M., *Makromol. Chem.* **117**, 242 (1968).

RECEIVED March 18, 1968.

## Preparation of Carboxy-Terminated Polyisobutylene

FRANCIS P. BALDWIN, GILBERT W. BURTON, KARL GRIESBAUM,  
and GEORGE HANINGTON

Enjay Polymer Laboratories, Linden, N. J. 07036

*Carboxy-terminated polyisobutylene (CTPIB) is a low molecular weight, terminally bifunctional liquid rubber. Products of interest have molecular weights of 1800–4000 and functionalities of  $\sim 1.8$  carboxyl groups/molecule. CTPIB is prepared by degradative ozonization in the presence of pyridine of high molecular weight copolymers of isobutylene and 2–4% piperylene. Pyridine-modified ozonization leads to direct formation of acid, peracid, and aldehyde functionality. Ozone and oxygen are the only externally supplied oxidizing agents. The process consists of (a) double bond cleavage with the formation of aldehyde and acid groups, (b) oxidation of aldehyde to acid and peracid, and (c) reduction of peracid to acid. The chemistry of the process is discussed in detail.*

Liquid rubbers are polymeric products used primarily as adhesives, sealants, castable rubbers, and rocket propellant binders. The name liquid rubber comes from the properties of flowing at room temperature and curing to rubbery networks. These materials offer advantages over conventional elastomers in their ease of handling and processing as they can be readily pumped and mixed in low power (relative to normal rubber) equipment with resultant savings.

A liquid rubber must be more than just a low molecular weight counterpart of a conventional elastomer. Because of molecular weight, functionality, and network-formation requirements, a liquid rubber needs to be considered as a polymeric entity of its own. This point has been shown by an analysis of the network formed upon vulcanization of a liquid rubber (3). This analysis compares and contrasts two classes of liquid rubbers: terminally functional and randomly functional prepoly-

mers. The authors show that a terminally bifunctional prepolymer is inherently more desirable than a randomly functional polymer because terminally bifunctional prepolymers meet more easily two important criteria of liquid rubbers—*i.e.*, that they be liquid and cure to a rubbery network. To form vulcanizate networks of comparable strength and elongation, the randomly functional prepolymer as compared with the terminally bifunctional polymer must have higher molecular weight. Thus, the terminally bifunctional material will be inherently more fluid.

To form a good rubbery network upon crosslinking, we wish to minimize the number of chain ends present since they do not help support stress. This is again inherently easier with a terminally bifunctional material since in the ideal case of perfect coupling there would be no chain ends upon crosslinking.

An analysis of network formation shows that terminal bifunctionality must be very close to the ideal of two functional groups per molecule to produce a high quality vulcanizate. The quality of a vulcanizate can be related to the required number average molecular weight,  $M_R$ , of a polymer in an equivalent random network (6).  $M_R$  values can be determined for an idealized network formed by coupling bi- or monofunctional prepolymers—*i.e.*, no nonfunctional molecules—using the expression:

$$M_R = M_N \left( \frac{2\bar{f} - 2}{2 - \bar{f}} \right) + 2M_N$$

where  $M_N$  is the molecular weight of the prepolymers, and  $\bar{f}$  is the average functionality (*see* Appendix for the derivation of this equation and a description of the process involved). Table I shows the results of the calculation using an  $M_N$  of 2000.

**Table I. Correlation of Network Quality with Prepolymer Functionality**

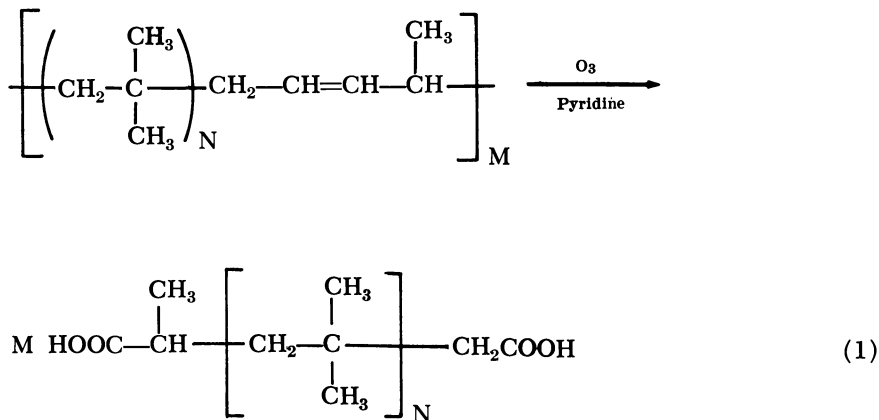
Average Functionality/Molecule	Network Quality, $M_R$
2.00	$\infty$
1.98	200,000
1.95	80,000
1.90	40,000
1.80	20,000
1.50	8,000

It is apparent that small changes in functionality levels close to the ideal of 2.00 can lead to large changes in network perfection. As an example, a small increase from 1.95 to 1.98 functional groups results in a large (over 100%) increase in  $M_R$  and hence a large decrease in chain end dilution. Although this correlation is not numerically exact for real



systems, it does illustrate that nearly perfect terminal bifunctionality is necessary for forming high quality vulcanizates.

Our goal in this work has been the development of a terminally bifunctional liquid rubber. Carboxy-terminated polyisobutylene (CTPIB) approaches a terminally bifunctional polymer. It is made by the ozonization in the presence of pyridine of a high molecular weight, low unsaturation piperylene-isobutylene copolymer as shown in Reaction 1.



The polymer has a polyisobutylene backbone which, because of lack of unsaturation, is resistant to ozone, heat aging, and chemical attack. Carboxyl groups terminate the ends of the chain so that chain extension and crosslinking can be accomplished with a variety of agents.

A typical product has the following characteristics: number average molecular weight,  $\sim 1800$ ; carboxyl assay,  $\sim 1.1$  meq./gram; color, amber; bulk viscosity (Brookfield synchroelectric viscometer):  $70^\circ\text{F}$ ., 8000 poises,  $100^\circ\text{F}$ ., 2000 poises,  $150^\circ\text{F}$ ., 250 poises, and  $250^\circ\text{F}$ ., 15 poises. The product can be cured with polyfunctional epoxides, aziridines, and isocyanates for applications such as thermoset and pressure sensitive adhesives, electronic component encapsulation, rocket propellant binders, epoxy flexibilizers, etc. Detailed vulcanization data can be obtained for the 1800 molecular weight material, EMD-590, from the Enjay Chemical Co., Cranford, N. J.

### *Formation of Carboxy-Terminated Polyisobutylene*

The terminally bifunctional prepolymer, carboxy-terminated polyisobutylene, is prepared by the pyridine-modified ozonization of a copolymer of piperylene (2–4%) and isobutylene. Figure 1 shows a block diagram of the process. The high molecular weight elastomer can be prepared by the conventional techniques of isobutylene–diene copoly-

merization. The polymer is dissolved in an aliphatic hydrocarbon, pentane in the laboratory and hexane in the pilot plant; pyridine is added, and ozonization is begun. Pyridine in the pilot plant has generally been used at a weight that is 20–40% of the polymer weight to produce polymer with  $\sim 1.8$  carboxyl groups/molecule. The temperature should be kept below  $50^\circ\text{C}$ . to avoid ozonolytic degradation of the polyisobutylene portion of the polymers. Pilot plant experiments have been carried out routinely at ambient temperatures. Ozonizations are carried out for sufficient times to cleave all the double bonds and to oxidize subsequently the aldehyde groups formed during ozonization. (The time should be determined for each set of conditions since it depends upon ozone and oxygen rate, etc.) Heating after ozonization is necessary for the decomposition of peracids. Heating is done in the pilot plant by refluxing the hexane cement. Water washing after heating removes pyridine sludge and other oxidation products.

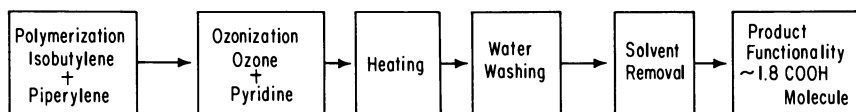


Figure 1. Preparation of CTPIB

Solvent removal after washing leads to a product with functionality of  $\sim 1.8$  carboxyl groups/molecule. Heating time can be reduced and combined with solvent removal, if desired, by vacuum stripping; a vacuum oven is used in the laboratory and a thin-film evaporator in the pilot plant. The product is dark brown and on acidic water washing before solvent removal, becomes pale yellow.

The safety aspects of ozonization—*i.e.*, ozone, pyridine, and solvent toxicity, explosive nature of oxygen–hydrocarbon mixtures, etc., need to be considered in the design and running of any ozonization process, especially large scale operations. However, with the proper design and operating conditions the problems involved are surmountable.

There are many advantages in the formation of a liquid rubber by the pyridine-modified ozonization process. Carboxylic acid prepolymers with terminal functionality are formed directly in a homogeneous hydrocarbon solution. Gaseous reagents—ozone and oxygen—are the only externally supplied oxidizing agents. There are no serious corrosion problems. The operations, including product workup, are quite simple with no stringent restrictions or reaction conditions. Ozonization is quantitative and fast; ozone–oxygen feed rate is the limiting factor on the speed of oxidation.

### Chemistry of the CTPIB Process

The chemistry of the ozonization of olefins has been reviewed (1, 2, 5). Although the exact details of the mechanism(s) have not been elucidated, the Criegee zwitterion mechanism plays an important role in olefin ozonization. According to this mechanism, ozonization occurs in the manner shown in Figure 2.

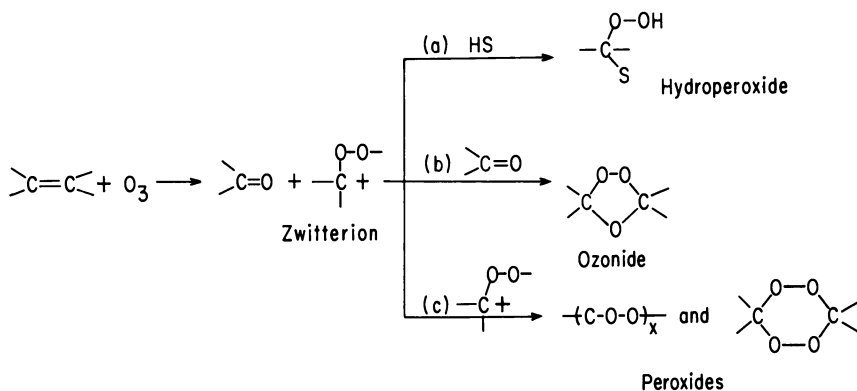


Figure 2. Zwitterion mechanism of ozonization

The products depend on the reaction conditions. In the presence of reactive solvent, such as methanol, Path a dominates. Ozonization in an inert medium leads to ozonide (Path b) and peroxide formation (Path c); the relative yield of ozonide and peroxide depends upon the olefin, solvent, and other reaction conditions.

If terminally bifunctional prepolymers are to be formed by ozonolytic degradation, several restrictions are immediately apparent. Ozonization is best carried out in aliphatic hydrocarbons because they are inert to ozone, they dissolve the original elastomer easily, and they are inexpensive. Formation of ozonides and peroxides should be prevented because they are difficult to convert to useful terminal functionality. The best way to prevent their formation is the reaction of the zwitterion with a nucleophile as in Path a of Figure 2.

Pyridine could function as a nucleophile in ozonization. It is soluble in hydrocarbons and is rather stable towards ozone (8, 11). Pyridine does have a dramatic effect on the course of ozonization. Slomp and Johnson (13) in their work on the ozonolysis of 4,22-stigmastadien-3-one propose that two moles of aldehyde are formed for each mole of double bond oxidized and that pyridine is oxidized to pyridine oxide. They also propose that pyridine oxide oxidizes aldehyde to acid with regeneration of pyridine.

Work on the pyridine-modified ozonization of tetramethylethylene showed that pyridine oxide is not a product of ozonization (8). Most of the pyridine ( $\sim 90\%$ ) remains unchanged during double bond cleavage. Only one mole of acetone, rather than two, is formed for each mole of olefin oxidized. Other work with a disubstituted olefin, *trans*-4-octene, showed that ozonides are formed in the reaction so that the reaction of pyridine with ozonide to form acid and aldehyde cannot occur (9). An NMR study of *trans*-4-octene ozonolysis in the presence of pyridine using 1,2-dichloroethane as the solvent shows that aldehyde and hydroxyl-containing material (carboxylic acid, peracid, and other OH species) are formed directly during double bond cleavage.

**Experimental.** **LABORATORY OZONE GENERATION.** Ozone was generated in a Welsbach model 816 ozone generator. Gas flow rates were determined with the instrument flow meters and are uncorrected. Unless mentioned otherwise the ozone-oxygen stream was taken from the ozone source, and the sample source was not used. Oxygen was used directly from the cylinder (Linde oxygen, U.S.P.) without further purification. Oxygen was delivered to the ozonator from the cylinder at pressures of 10–14 p.s.i.g. The pressure as indicated by the ozonator gage was 6 p.s.i.g. A voltage setting of 85 volts and an oxygen flow 1.5 SLPM were used to get an ozone rate of  $\sim 3.0$  meq./min.

**OZONE PRODUCTION RATE.** The ozone rate was determined by passing the gas stream from the ozone generator into an aqueous 10% potassium iodide solution and titrating the iodine that was liberated with standard sodium thiosulfate solution.

**POLYMER.** The polymer used in laboratory ozonation studies was from a masterbatch of a copolymer of small amounts (2–4%) of piperylene and isobutylene. The polymer was dissolved in hexane, shaken with silica gel to remove any impurities, and precipitated with acetone. The precipitated polymer was washed several times with methanol and then dried in a vacuum oven at 50°C./ $\sim 10$  mm. Hg for 2 days. The resulting material was colorless and had an iodine number of 20.7.

**PYRIDINE.** Fisher Scientific Co. reagent grade pyridine was used without further purification for laboratory operations.

**ACID-WASHED PENTANE.** About 1500 ml. of Phillips *n*-pentane (99 mole % pure) were placed in a 2-liter separatory funnel. The pentane was then shaken thoroughly with the following material in this order: (1) three 100-ml. portions of 20% oleum, (2) two 100-ml. portions of concentrated sulfuric acid, (3) 100 ml. of 50% sulfuric acid-water, (4) 250 ml. of water, (5) two 100-ml. portions of 5% potassium permanganate (to remove any sulfur dioxide), (6) two 100-ml. portions of 10% sodium bisulfite (to remove manganese dioxide), and (7) three 250-ml. portions of water. The pentane was dried partially by standing over Drierite. Final drying was done by refluxing and distilling from phosphorus pentoxide.

**TOTAL ACID TITRATIONS.** A sample (*ca.* 2.5 grams) was removed from the solution, weighed to an accuracy of 0.05 gram, and diluted with 100 ml. of tetrahydrofuran. Triethylamine (2 ml.) was added, and the solution was stirred for 1 minute. A few drops of phenolphthalein indi-

cator (0.75% in methanol) were added, and the solution was titrated with standard methanolic potassium hydroxide (*ca.* 0.01*N*) until a slight pinkish color was noted in the solution. Potentiometric titration is advisable for heavily colored solutions. (For best results the base should be standardized with the indicator).

When ozonizations were run at temperatures below 0°C., the analytical procedure was changed so that after the sample had been withdrawn it was added immediately to the triethylamine before weighing. In this way the cold cement was added to the triethylamine as quickly as possible after it was removed from the ozonization reaction.

**ACTIVE OXYGEN DETERMINATIONS.** A sample (*ca.* 2.5 grams) was removed from the solution, weighed to 0.05 gram, and diluted with about 20 ml. of pentane. Nitrogen was blown over the solution for about 1 minute. The solution was diluted with 100 ml. of isopropyl alcohol; 2 ml. of glacial acetic acid and 1 ml. of saturated potassium iodide solution were then added in that order. Enough water (5–10 ml.) was added to dissolve the potassium iodide precipitate. This mixture was titrated with standard sodium thiosulfate (0.01*N*) to a colorless endpoint. If the mixture were not titrated immediately, a piece of dry ice was added, and the solution was stored in the dark.

**TOTAL ACID OR ACTIVE OXYGEN IN OZONOLYSIS SOLUTIONS.** The results from total acid titrations described previously are meq. of total acid per gram of solution at the particular time when the sample was taken. Similarly the results from active oxygen determinations are meq. of active oxygen per gram of solution. To obtain the total acid or total active oxygen, one must know the total amount of solution. The complicating factor is loss of solvent by oxygen sweeping through the system as the reaction proceeds. Solvent loss can be measured since the initial weight, the final weight, and the amount of samples removed are known over the ozonolysis. Thus, a rate of solvent loss per unit time is known. In actual determinations solvent loss is between 0.2 and 0.3 gram/minute. These rates were used to correct the total amount of solution at any time, ignoring the samples removed. For example, if the solvent loss were 0.2 gram/minute, the initial solutions was 300 grams, and the acid plus peracid titration gave a value of 0.208 meq./gram of solution after 60 minutes, then the total amount of acid in the solution would be [300 minus (0.2) (60)] [0.208] meq. or 60 meq. of total acid in solution. This would also be equivalent to 60 mmoles of total acid in solution. A similar calculation was made in active oxygen determinations to obtain total meq. of active oxygen in solution.

**TYPICAL LABORATORY OZONOLYSIS.** Ozonization cement was prepared by dissolving 50 grams polymer in 300 grams of acid-washed pentane and 15–20 grams of pyridine. This solution, in a 1-liter four-necked round-bottomed flask equipped with a low temperature thermometer, a gas inlet tube, a dry ice-cooled Dewar condenser, and a sampling device, was cooled to ~0°C. in an ice-salt bath or dry ice-isopropyl alcohol bath. The temperature was kept around 0°C. during ozonolysis. The sampling device was a Teflon thermometer adapter which had a gas chromatography silicone rubber injection septum in the top. A stainless steel hypodermic needle was pushed through the septum so that it would reach the solution. A syringe stopcock was placed on the needle

so that a closed system could be maintained. The reflux condenser was attached to a 10% potassium iodide trap.

Ozone was passed into the cooled solution at a rate of *ca.* 3.0 meq./minute. The gas flow rate was 1.5 SLPM. Samples were taken by placing a syringe on the syringe stopcock, opening the syringe stopcock, and withdrawing the sample. When ozonolysis was over, nitrogen was passed into the solution for 5 minutes. Work up was then done in any desired manner—*i.e.*, treatment with triethylamine, acid washing, or simply heating on a steam bath to remove solvent and then heating in a vacuum oven for the desired length of time.

**POLYMER NEUTRALIZATION NUMBER.** A sample of polymer was weighed to the nearest 0.1 mg. (sample sizes of 0.5–1.0 gram). The polymer was dissolved in tetrahydrofuran and if necessary warmed on a steam bath. The solution was titrated with standard potassium hydroxide in methanol using phenolphthalein as indicator. Calculation:

$$\text{KOH Number} = \frac{(\text{ml. of KOH}) (\text{N of KOH}) (56.1)}{\text{grams of sample taken}}$$

**MOLECULAR WEIGHT DETERMINATION.** Molecular weight determinations were made with a Mechrolab vapor pressure osmometer, model 302, in dichlorobenzene solutions at 130°C. The molecular weight of a typical CTPIB prepared in the pilot plant (neutralization no. 62.5 mg. KOH/gram) was determined at various concentrations of dichlorobenzene. The results with concentration in parentheses were: 1782 (7.893 grams/kg.), 1748 (13.743 grams/kg.), and 1835 (22.790 grams/kg.). In this study the average value was 1788 with an average deviation of 1.7%. This error is in the range expected for this method. These results indicate that molecular weight determinations in the concentration range shown need not be corrected for concentration effects. In the work reported here, no corrections have been made.

**POLYMER STRUCTURE.** Unpublished work by Bearden *et al.* (4) shows that there is predominantly trans-1,4 addition of piperylene in the cationic copolymerization of piperylene and isobutylene. Infrared spectroscopic examination shows only an intense 970  $\text{cm}^{-1}$  band and no band at 910  $\text{cm}^{-1}$ . This indicates only 1,2- or 1,4-addition of piperylene with little or no 3,4-addition. An examination by NMR with a time-averaging computer also confirms that there is essentially no 3,4-addition and that 1,2-addition is about 10% of 1,4-addition.

**POLYMER UNSATURATION ANALYSIS.** Unsaturation is determined routinely by an iodine-mercuric acetate procedure (5). The result of this procedure, iodine number (cgrams of iodine/grams of polymer), was correlated to actual unsaturation by an infrared and an NMR study (4). The infrared study showed that the factor of 0.184 is needed to convert iodine number to % unsaturation. The NMR study showed that a factor of 0.196 is needed to convert iodine number to % unsaturation. [As an example, a piperylene-isobutylene copolymer with an iodine number of 20.7 would have unsaturation values of (20.7) (0.196) = 4.05 mole % (NMR) and (20.7) (0.184) = 3.82 mole % (infrared).]

**Results.** The chemistry of the ozonization of a piperylene-isobutylene copolymer was investigated by measuring the amounts of acid and

active oxygen species formed during ozonization of a polymer containing a known amount of unsaturation. In each of the experiments 50 grams of polymer (34–36 mmoles of unsaturation) were ozonized, using pentane, hexane, or heptane as solvent. Pentane was chosen as the primary solvent because of its high volatility, with subsequent ease of removal from the cement after ozonization. Since Phillips *n*-pentane (99 mole %) takes up ozone, it is necessary to acid-wash it to remove impurities. (The term acid-washed pentane means pentane treated as described in the experimental section.)

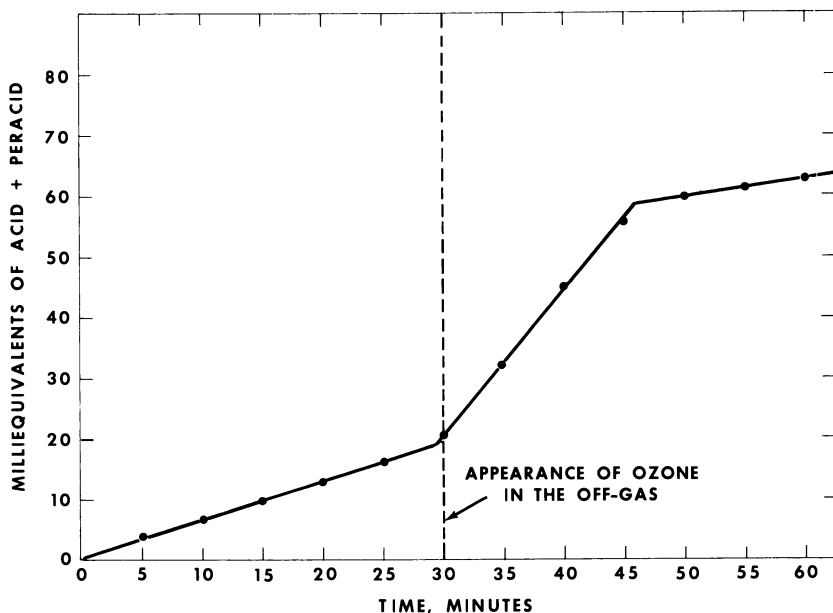


Figure 3. Acid and peracid formation in ozonolyses at 0°C. Average composite of two runs

Polymer, 50 grams (iodine No. 20.7)  
 Pyridine, 15 grams  
 Ozone rate, 3.0 meq./min.  
 Solvent, acid-washed pentane

Both carboxylic acid and peracid are formed during ozonolysis of disubstituted double bonds. The analytical procedure for acid analysis measures the total carboxylic acid and peracid after reduction of peracid to acid with triethylamine, followed by titration with standard base. Results for polymer ozonizations measuring total acid formed as a function of time at 0°C. are shown in Figures 3 and 4, respectively. These show that total acid formation is divided into two stages, which can be separated experimentally by the breakthrough of ozone into the potassium

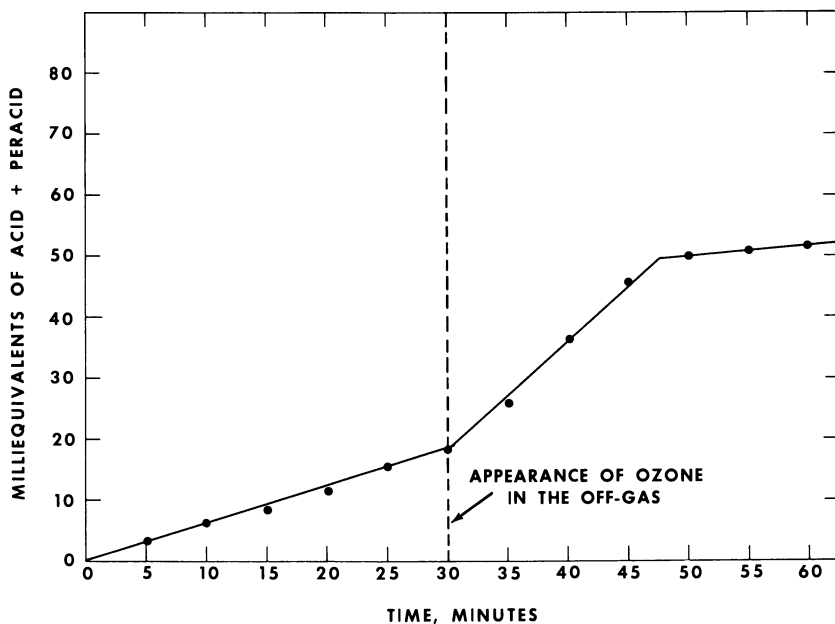


Figure 4. Acid and peracid formation in ozonolyses at  $-25^{\circ}$  to  $-30^{\circ}\text{C}$ . Average composite of two runs. Conditions are same as in Figure 3

iodide trap. At this point, iodine forms in the trap indicating ozone is present in the off-gas. Thus, up to this point all the ozone has reacted with the polymer solution. Acid formation until breakthrough—the first stage—is regarded as coming only from double bond cleavage, while acid formation after breakthrough—the second stage—is considered to arise solely from aldehyde oxidation since a study with model compounds showed that aldehyde was oxidized only after all the double bonds had been cleaved (9). Care must be taken when using ozone breakthrough as a criterion of double bond cleavage. The titration data demonstrate that it could be used as a criterion in this work since ozonization was done under controlled conditions using carefully purified solvent. With other solvents and conditions, breakthrough may be delayed by ozonization of solvent so that it comes closer to the end of oxidation. This has been found to be true under pilot-plant ozonization conditions.

Second stage (aldehyde) oxidation under the conditions of ozone and oxygen rates used is considered to require only about one-half of the time required for double bond cleavage. Thus, polymer oxidation is considered complete in about 45 minutes in the experiments plotted in Figures 3 and 4. Total acid formation after  $\sim 45$  minutes—*i.e.*, the part with the flattest slope—is thought to arise from ozonization of pyridine or solvent and will be considered as such in further discussions.



Figures 3 and 4 illustrate that there is a temperature dependence in acid formation under our experimental conditions because Figure 3 shows  $\sim 59$  mmoles of acid at the end of aldehyde oxidation whereas Figure 4 shows only 50 mmoles of acid. However, temperature dependence occurs only in the aldehyde-oxidation phase since the two plots for acid formation before ozone breakthrough are essentially identical. Furthermore, the temperature of ozonization does not affect final acid formation if the solutions are allowed to warm up with no immediate triethylamine treatment. Thus, upon warming to room temperature the final acid values for  $0^\circ$  and  $\sim -25^\circ\text{C}$ . titration experiments are in the range 65–70 mmoles total acid. (In the  $-25^\circ\text{C}$ . titration experiments care was taken to treat the cold ozonized cement with triethylamine as soon as the cement was removed from the reactor. The cement was not allowed to warm up before triethylamine treatment. As discussed later, triethylamine reduces a species which is capable of forming acid.)

Figure 3 shows that  $\sim 20$  mmoles of total acid have been formed at breakthrough. At the end of aldehyde oxidation  $\sim 59$  mmoles of total acid have been formed. At  $0^\circ\text{C}$ . the second stage of reaction is temperature dependent; the composite value indicates that there is an increase of 6 mmoles of total acid upon standing. No adjustment for temperature dependence is made in the data shown in Figure 3 since the samples were put in a beaker at room temperature and weighed before trimethylamine (at room temperature) was added. At the most any numerical conclusions from the data would be increased by 6 mmoles. This value of 59 mmoles includes acid formation from pyridine or solvent during the aldehyde oxidation stage. If the pyridine oxidation line is extrapolated to breakthrough, acid formation from pyridine or solvent oxidation could amount at the most to 6 mmoles of acid (59 mmoles minus 53 mmoles). Thus, at the end of polymer oxidation 53–59 mmoles of total acid are formed. This means that 33–39 [(53–59) minus (20)] mmoles of acid have been formed in the aldehyde oxidation stage of polymer ozonization.

If we assume as a model that cleavage of one mole of double bond leads to one mole of acid and one mole of aldehyde, we would expect to find  $\sim 35$  mmoles of acid in the first stage and 70 mmoles of acid at the end of aldehyde oxidation. The difference between total acid formation in the first and second stages of reaction should reflect the amount of aldehyde oxidized. The analysis of the total acid titration data indicates that only 57% ( $20/35 \times 100\%$ ) of the expected amount of acid is formed in the first stage. Between 33–39 mmoles of acid are formed in the second stage, which is in the range expected from oxidation of  $\sim 35$  mmoles of aldehyde.

This analysis implies that acid functionality is lost or fails to be formed in the first stage, and not in the second since as only one-half to two-thirds of the expected amount of acid is found after the first stage while the expected amount is found after the second stage. Furthermore, we have probably formed the correct amount of aldehyde in the first stage and oxidized it completely to acid in the second stage.

Active oxygen species—*i.e.* peracids, peroxides, hydroperoxides, etc.—can be determined quantitatively by iodometric titration; however, there is a rate difference in reaction, with peracids reacting instantaneously and peroxides much more slowly. Since peracids are formed in the ozonization of olefins by an ozone-catalyzed oxidation of aldehyde (15), an iodometric titration of the reaction mixture should be a measure of peracid formation. An averaged composite of four active oxygen determinations as a function of time is shown in Figure 5. (The results have been reported in units of meq./2. Most active oxygen analyses involve a two-electron change; as a result, meq./2 represents mmoles of active oxygen and can be used directly in stoichiometric comparisons). Active oxygen determinations were made within 3–4 minutes after removal of the sample.

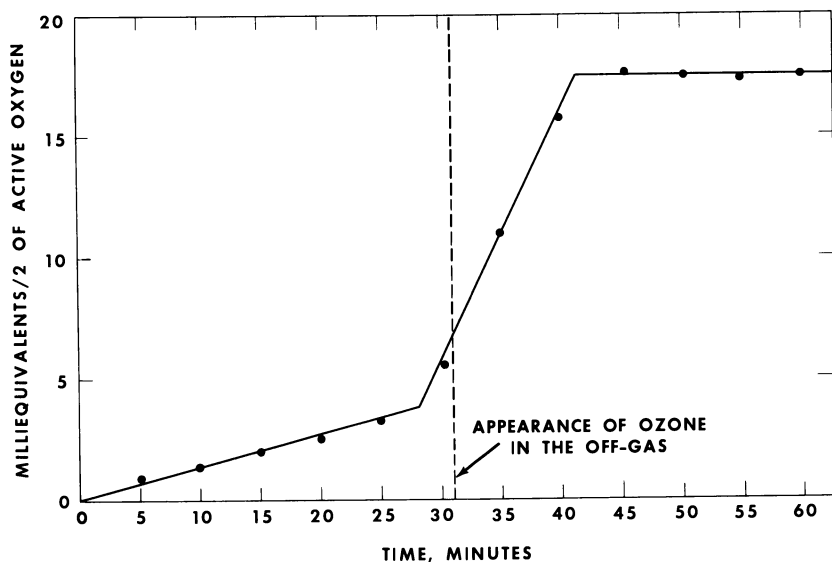


Figure 5. Active oxygen formation in ozonolyses at 0°C. Average composite of four runs. Conditions are same as in Figure 3

After titration of these samples, a piece of dry ice was put in each to give a carbon dioxide blanket; they were stoppered and kept overnight in the dark. The next morning they were titrated further to a

colorless endpoint with sodium thiosulfate. (In all cases blanks were titrated, and suitable corrections were applied.)

The maximum amount of additional iodine that formed upon standing was  $\sim 3$  meq./2. All the additional active oxygen found in these titrations had been formed in the first stage of ozonization—*i.e.*, before ozone breakthrough. There are at least two kinds of active oxygen produced in the reaction. One kind is reduced rapidly, forming iodine while the other reacts more slowly. This has been shown in the active oxygen titrations since iodine is formed in the solutions upon standing. The second kind of active oxygen is probably a peroxide or hydroperoxide and amounts to at least 3 meq./2 in a 50-gram polymer ozonization. This in no way sets a limit on the amount of the second kind of active oxygen since no effort was made to maximize iodine formation.

Figure 5 is a plot of the averaged composite data, and it represents instantaneously titrable active oxygen. As in total acid determinations, active oxygen formation can be divided into two stages which can be differentiated by ozone breakthrough. (Figure 5 illustrates the point about using breakthrough as a criterion of double bond cleavage. In these experiments double bond cleavage has preceded breakthrough by several minutes. This does not affect seriously any conclusions which will be made.) Active oxygen production seems to stop at 40–45 minutes, and this plot also indicates that polymer oxidation is complete at this point. The total of active oxygen formation during double bond cleavage is  $\sim 4$  meq./2 and during aldehyde oxidation is  $\sim 13$  meq./2 (17 minus 4 meq./2). The nature of the active oxygen species formed during double bond cleavage is unknown. This may be peracid from some aldehyde oxidation, or it may represent some type of zwitterion, activated peroxide, etc., formed during double bond cleavage. However, this instantaneously titrable active oxygen represents the maximum amount of peracid that could have been formed.

Analysis of the total acid titration data indicates that 33–39 mmoles of acid and peracid have been formed from aldehyde oxidation. Furthermore, 34–36 mmoles of aldehyde should have been formed in the first stage and oxidized in the second stage. If aldehyde had been oxidized solely to peracid, the active oxygen determination should have showed 34–36 mmoles of peracid instead of at the most 13 mmoles (meq./2). Enough acid but not enough peracid has been formed. This means that there are at least two paths by which aldehyde can be oxidized to acid, one of which involves peracid formation.

The results from total acid and active oxygen determinations impose the following conditions upon any mechanism for polymer oxidation:

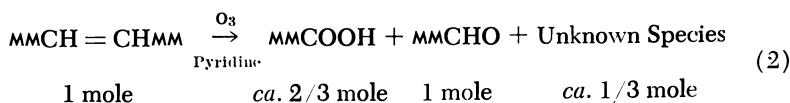
(1) Acid functionality is lost or fails to be formed during double bond cleavage.

(2) The proper amount of aldehyde is formed during double bond cleavage and is oxidized subsequently in the second stage.

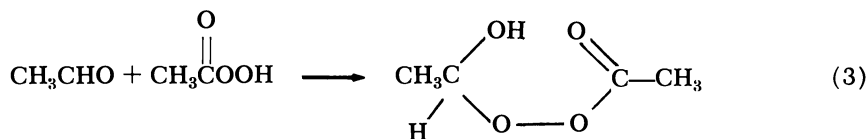
(3) There are at least two paths for aldehyde oxidation.

(4) Aldehyde oxidation must show a temperature dependence.

**Conclusions.** DOUBLE BOND CLEAVAGE IN PYRIDINE-MODIFIED OZONIZATION. Results from total acid titration data indicate that functionality is lost during double bond cleavage. Double bond cleavage can then be represented as shown in Reaction 2.



**MECHANISMS OF ALDEHYDE OXIDATION.** There must be at least two paths for oxidation of aldehyde to acid, and at least one of these must be temperature dependent. One pathway is the ozone-oxygen oxidation of aldehydes to peracids (14). However, peracid can also serve as an oxidizing agent for aldehyde. In the oxidation of acetaldehyde, Reaction 3 is thought to occur (14).



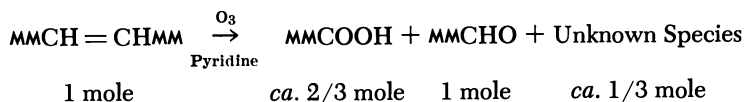
This hemiacetal type of peroxide has been isolated; in fact, a commercial synthesis of peracetic acid is based upon formation of this material (11). These authors state that this peroxide decomposes spontaneously to two molecules of acetic acid and that the decomposition is slow at 0°C. but the rate increases rapidly as the temperature increases. Analogously in polymer oxidation aldehyde could be oxidized by peracid to the hemiperacetal intermediate which then breaks down to form two acid groups.

The temperature dependence of acid formation can be explained by formation of this peroxide with its subsequent decomposition to two molecules of acid. Since the end of the reaction seems to be temperature independent (as measured by the change in slope), aldehyde oxidation stops at the same time in both cases; low temperature favors the preservation of the hemiacetal type of peroxide, and thus less acid formation is seen. Treatment of the cold cement with triethylamine prevents formation of acid on warming by reducing peroxidic material (either peracid or hemiperacetal) to acid and aldehyde, and as a result less acid is titrated. However, when the solution is warmed with no reducing agent

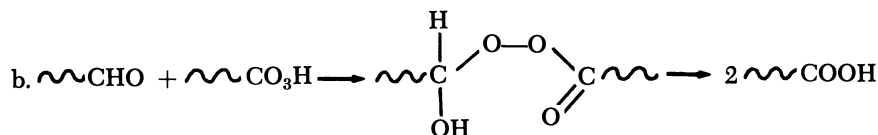
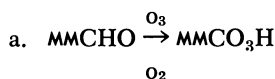
present, the proper amount of acid forms. Temperature dependence could also be accounted for by reduction of other types of peroxides by triethylamine. Further experimental work is needed to determine the nature of the intermediates involved.

**CHEMISTRY OF POLYMER OXIDATION.** The conclusions drawn from the total acid and active oxygen titration data and the results from re-ozonization can be used to form an over-all picture of polymer oxidation. The chemistry of polymer oxidation can be represented as shown below.

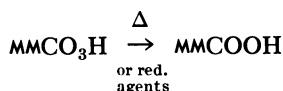
I. Pyridine-Modified Cleavage of the Double Bond:



II. Two Paths of Aldehyde Oxidation:



III. Reduction of Peracid:



## Appendix

### *Derivation of the $M_R$ -Average Functionality Relationship*

Process: Directly couple prepolymers  $\text{AMMA}$  and  $\text{MAA}$  of equal molecular weight. Only perfect and complete coupling of two A units is allowed. At the end of the process, the total number of polymer molecules present must equal one-half the number of monofunctional prepolymers.

Let:  $N_A$  = number of difunctional groups  
 $N_A'$  = number of monofunctional groups  
 $N_T$  = total number of prepolymers  
 $M_T$  = total number of polymer molecules at end of reaction

- $M_N$  = number average molecular weight of prepolymers  
 $\bar{X}_N = N_T/M_T$  = number average degree of polymerization  
 $M_R = (\bar{X}_N)(M_N)$  = number average molecular weight of polymer  
in an equivalent random network  
 $A$  = mole fraction of difunctional prepolymer  
 $1 - A$  = mole fraction of monofunctional prepolymer  
 $\bar{f}$  = average functionality

From the definitions and basic conditions,

$$N_T = N_A/2 + N_{A'} = (N_A + 2N_{A'})/2 \quad (1)$$

$$M_T = N_{A'}/2 \quad (2)$$

$$\begin{aligned} \bar{X}_N &= (N_A + 2N_{A'})/N_{A'} \\ &= N_A/N_{A'} + 2 \end{aligned} \quad (3)$$

By definition:

$$\begin{aligned} N_A/N_{A'} &= \frac{(2) \text{ (mole fraction of difunctional units)}}{(1) \text{ (mole fraction of monofunctional units)}} \\ &= \frac{(2) \text{ (moles of difunctional units)}}{(1) \text{ (moles of monofunctional units)}} \\ &= \frac{2A}{1 - A} \end{aligned} \quad (4)$$

$$\begin{aligned} \bar{f} &= 2(A) + (1)(1 - A) \\ &= A + 1 \end{aligned} \quad (5)$$

By manipulating Equations 3, 4, and 5 and the basic definition of  $M_R$ , one obtains Equation 6 which relates  $M_R$ ,  $M_N$ , and average functionality.

$$M_R = M_N \left( \frac{2\bar{f} - 2}{2 - \bar{f}} \right) + 2M_N \quad (6)$$

### Acknowledgments

We thank L. E. Gastwirt, L. S. Minckler, and R. Slysh for their many helpful discussions and J. I. Adams, E. H. Brozyna, J. K. Creel, N. C. Dispenziere, and D. J. Saliski for their excellent technical assistance.

### Literature Cited

- (1) ADVAN. CHEM. SER. 21 (1959).
- (2) Bailey, P. S., *Chem. Rev.* 58, 925 (1958).
- (3) Baldwin, F. P., Fusco, J. V., Gastwirt, L. E., *Adhesives Age* 22 (Feb. 1967).
- (4) Bearden, R., Taylor, H. H., Drushel, H. V., Hodgeson, J. A., Esso Research Laboratories, Baton Rouge, La., unpublished data.
- (5) Criegee, R., *Rec. Chem. Progr.* 18, 111 (1957).

- (6) Flory, P. J., "Principles of Polymer Chemistry," Chap. XI, Cornell University Press, Ithaca, 1953.
- (7) Gallo, S. G., Wiese, H. K., Nelson, J. F., *Ind. Eng. Chem.* **40**, 1277 (1948).
- (8) Griesbaum, K., *Chem. Commun.* **1966**, 920.
- (9) Griesbaum, K., Burton, G. W., "Abstracts of Papers," 155th Meeting, ACS, April 1965, R 066.
- (10) Kooyman, E. C., Wibaut, J. P., *Rec. Trav. Chem. Pays-Bas* **66**, 705 (1947).
- (11) Phillips, B., Frostick, Jr., F., Starcher, P., *J. Am. Chem. Soc.* **79**, 5982 (1957).
- (12) Sixma, F. L. J., *Rec. Trav. Chem. Pays-Bas* **71**, 1124 (1952).
- (13) Slomp, Jr., G., Johnson, J. L., *J. Am. Chem. Soc.* **80**, 915 (1958).
- (14) Walling, C., "Free Radicals in Solution," p. 411, Wiley, New York, 1957.
- (15) White, H. M., Bailey, P. S., *J. Org. Chem.* **30**, 3037 (1965).

RECEIVED April 1, 1968.

# The Role of Structural Phenomena in Polymerization

V. A. KARGIN

Scientific Committee on High Molecular Compounds, Vavilova St. 32,  
Moscow B-312, U.S.S.R.

*Polymerization is influenced by the physical structure and phase of the monomer and polymer. It proceeds in the monomer, and the chemical configuration of the macromolecules formed depends on whether the monomer is a liquid, vapor, or solid at the moment of polymerization. The influence of structural phenomena is evident in the polymerization of acrylic monomer either as liquids or liquid crystals. Supermolecular structures are formed in solid- and liquid-state reactions during and simultaneously with polymerization. Structural effects can be studied by investigating the nucleation effect of the solid phase of the newly formed polymer as a nucleation reaction by itself and as nuclei for a specific supermolecular structure of a polymer. Structural effects are demonstrated also using macromolecular initiators which influence the polymerization kinetics and mechanism.*

**W**e are accustomed to the notion that during polymerization of monomer molecules are combined into separate macromolecules and that this approximation is almost always sufficient. Actually it is sufficient in most cases in dilute solutions, but if polymerization is accompanied by any phase or structural transitions, including the formation of the polymer as a new phase, one must consider the possibility of structural phenomena affecting the polymerization.

The first, and perhaps most vivid, example is the effect of the structure of a monomer crystal on polymerization in the solid state. The fact that the configuration of the emerging polymer depends directly on the structure of the solid monomer is no longer doubted, having been proved for many cases. Thus, depending on its phase, acetaldehyde polymerizes



to poly(vinyl alcohol) or polyacetal (18); diketene polymerizes to a polyester or a polydiketone (22). A number of cases are known where the crystalline or ordered state of the monomer results in the formation of polymers of regular structure. Long ago it was discovered that the explosive polymerization of solid monomers proceeds often at phase transition points (9, 10, 16). These results have been described (11).

The fact that the structure of a solid monomer influences its polymerization substantially now seems obvious. It is not as clear whether structural phenomena can effect polymerization if the monomer is a liquid. It has long been known that ordered regions or "clusters" exist in liquids, and several years ago it was assumed that in some cases these regions in liquid monomers can influence the polymerization. One of the most vivid examples—namely, polymerization in the liquid-crystalline state—was accomplished by Krentzel and co-workers (1, 2, 3). The object of their study was *p*-methacrylylhydroxybenzoic acid, which forms conventional crystals in the pure state and does not polymerize in the solid state. However, when mixed with alkoxybenzoic acid, it forms liquid crystals of both smectic and nematic forms. Polymerization of *p*-methacrylylhydroxybenzoic acid in various forms of liquid crystals was compared with polymerization of the same substance dissolved in dioxane and dimethylformamide (DMF).

The rate of polymerization is nearly the same in both solvents and is proportional to the monomer concentration and to the square root of initiator concentration.

The molecular weight of the resulting polymer is comparatively small (of the order of dozens of thousands), and at temperatures above 100°C. the monomer does not polymerize completely owing to the establishment of polymerization–depolymerization equilibrium. These features are typical of the radical polymerization of methacrylates.

If *p*-methacrylylhydroxybenzoic acid is mixed with *p*-cetylhydroxybenzoic acid, a smectic form of liquid crystals results, but if it is mixed with *p*-nonylhydroxybenzoic acid, the resulting form is nematic above 104°C. and is smectic below this. This makes it possible to compare the polymerization behavior of the same monomer in solution, where the mutual ordering of its molecules is minimal, in a liquid crystal state with only orientation order (nematic form), and in the liquid-crystal state involving both orientation and coordination order (smectic form).

Polymerization in the liquid crystal state involves a major increase in the molecular weight of the polymer, reaching the hundreds of thousands. The thermodynamic equilibrium between the monomer in smectic liquid crystals and the polymer is shifted completely toward formation of the polymer up to the melting point of the crystal (138°C.). The polymerization rate does not change with the degree of conversion

up to 70–75% conversion and accordingly depends little on the initial monomer concentration. This supports the assumption that polymerization proceeds in ordered regions whose lifetime is sufficiently long compared with the time of chain propagation. When the temperature exceeds the melting point of the liquid crystals (138°C. for the smectic form), the molecular weight drops to 10,000 or 12,000 and the equilibrium monomer concentration increases up to 25%. Thus, a temperature change of a few degrees exerts a considerable effect if it is accompanied by a liquid crystal–liquid phase transformation.

The polymerization rate also increases as the monomer molecules in the liquid become more ordered. Figure 1 shows the kinetic curves of polymerization in solution and in liquid crystals under comparable conditions.

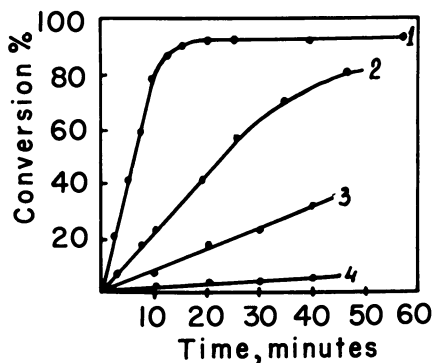


Figure 1. Kinetic polymerization curves of n-MAOBA in DMF solution and in liquid crystals.  $T = 110^{\circ}\text{C}$ .  $[M] = 1.25\text{M}$

- (1) Initiated polymerization in liquid crystal;  $[I_0] = 0.05\text{M}$
- (2) Initiated polymerization in DMF solution.  $[I_0] = 0.05\text{M}$
- (3) Thermal polymerization in liquid crystal
- (4) Thermal polymerization in DMF solution

The ordering may also occur in liquid states especially in those which are able to form liquid crystals. The lower the heat of the phase transition, the higher will be the probability of appearance of heterophasal fluctuations, whose existence has been proved directly for the acids studied (23).

The intermediate region between the liquid and the liquid crystals can be by-passed in ways other than changing the temperature. If an inert solvent is added to the system, the entire interval from a simple

liquid to a liquid crystal can be covered at a constant temperature. Figures 2 and 3 give the dependence of the polymerization rate and intrinsic viscosity of an emerging polymer on the monomer content in a binary solvent [DMF and *p*-nonylhydroxybenzoic acid (*p*-NHBA)] at 90°C. The transition from the liquid to the liquid-crystalline state occurs at a monomer content of 2.3M, but the changes in rate and molecular weight begin long before the phase transition point. Heterophasal fluctuations in the liquid may affect the polymerization quite tangibly.

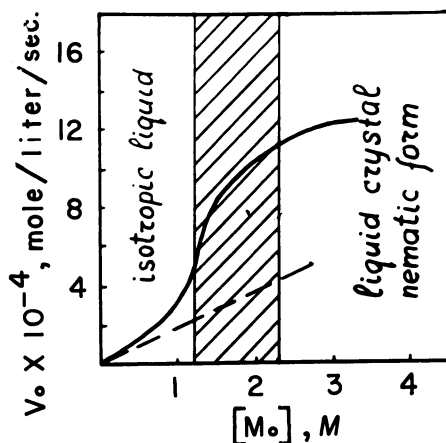


Figure 2. Dependence of n-MAOBA polymerization rate in binary solvent (DMF + *p*-NHBA) on initial monomer concentration.  $T = 90^{\circ}\text{C}$ .  $[I_0] = 0.0025\text{M}$

In other words, if any structural formations appear in the liquid, they may become a new reaction medium in which the polymerization may change substantially. The part of such a medium may be played, as we have seen, by fluctuational formations of monomer molecules; but there is another possibility. The polymer molecules formed during polymerization are often more unevenly distributed in the monomer than in the solvent. They are much more likely to form structures than monomeric substances. The extreme case is the formation of a polymer which is insoluble in the monomer or in the solvent used for polymerization. In this case the polymer formed is evolved as a new phase, and if polymerization occurs inside or on the surface of the particles of this new phase, structural phenomena will naturally begin to play a major part. Perhaps the most vivid example of such a phenomenon is the bulk polymerization of vinyl chloride, whose structural features were studied recently (6, 7). The peculiarities of this process arise from the fact that

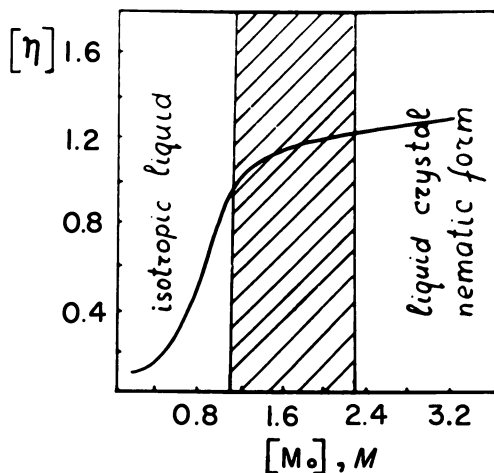


Figure 3. Dependence of  $[\eta]$  of poly(*n*-MAOBA) on initial monomer concentration.  $T = 90^\circ\text{C}$ .  $[I_0] = 0.0025\text{M}$

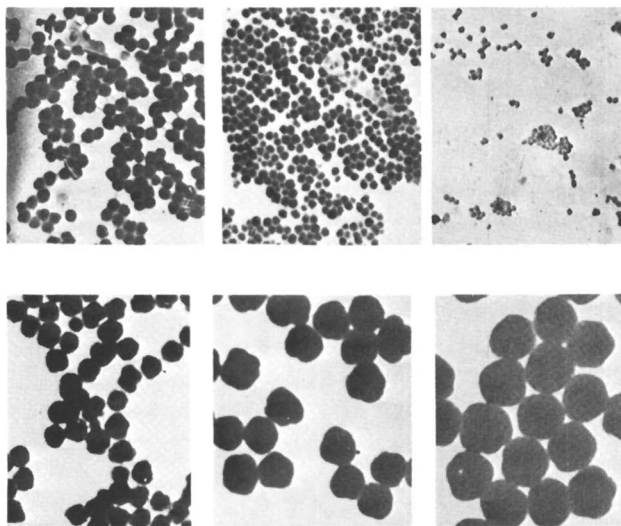


Figure 4. Electron microscope photographs of PVC particles at various stages of conversion. Each photograph is  $1.25\mu$  wide

the polymer is almost insoluble in the monomer, and the monomer dissolves in the polymer to an extent of 10–15%. During radical polymerization the polymer appears as globular formations 600–800 Å in size. The globular structure of the emerging poly(vinyl chloride) (PVC) is retained throughout the polymerization until the solid block is formed.

The number of globules does not change during this process, although each globule enlarges as polymerization proceeds. Figure 4 shows electron microscope photographs of PVC particles at various degree of conversion—*i. e.*, less than 1% to several score percent of conversion. Neither new small globules nor very large ones appear during the polymerization. The size distribution curves of the emerging globules, shown in Figure 5 for various stages of conversion, remain unchanged during polymerization, shifting only along the ordinate axis. Figure 6 shows the relationship between the amount of polymer formed and the cube of its average particle diameter. The linear nature of this dependence indicates that the increase in the amount of polymer is not related to any change in the number of particles but only to an increase in their size. In other words, polymerization occurs practically entirely in the particles already formed. The entire picture comes close to that of emulsion polymerization except that the nuclei of the new phase of the emerging polymer are the medium in which polymerization proceeds.

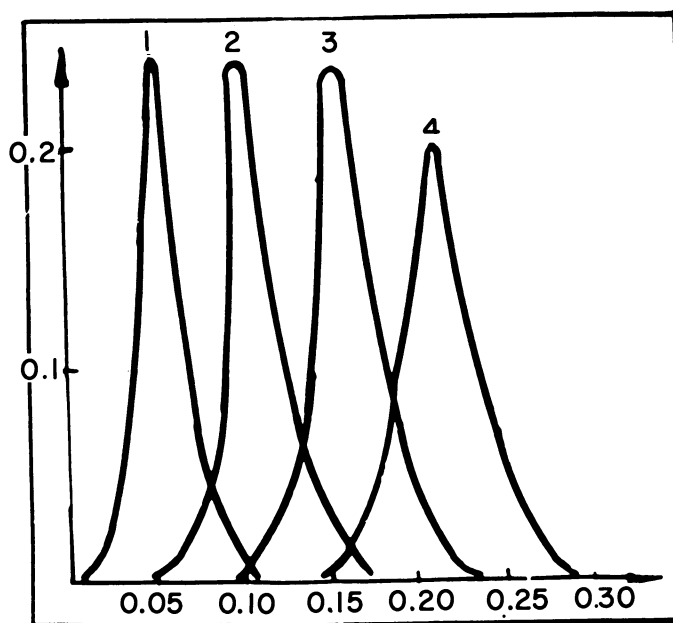


Figure 5. Size distribution curves of emerging globules at various stages of conversion during polymerization

The picture described is the simplest one and is observed only at high rates when PVC globules cannot aggregate. However, if the rate of temperature lowering or the initiator content are decreased, secondary processes occur, caused by aggregation of the PVC globule. On combin-

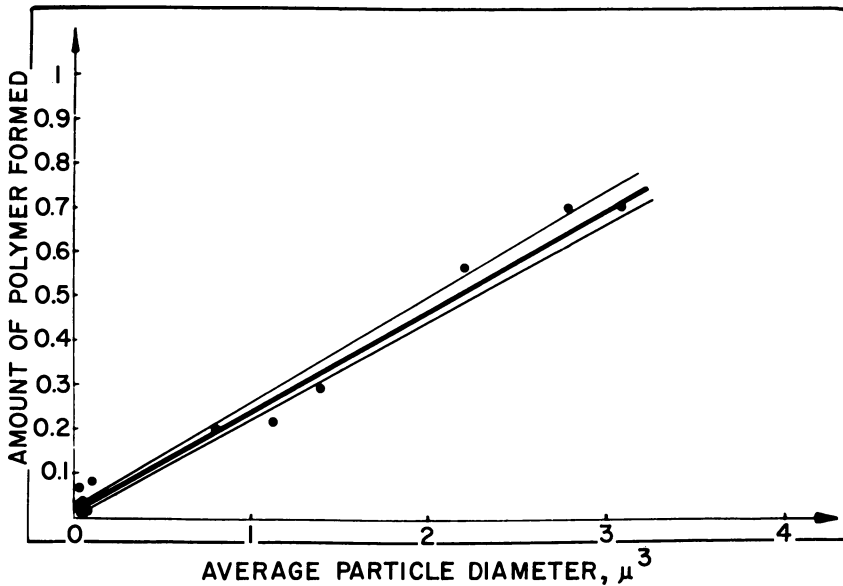


Figure 6. Relationship between the amount of polymer formed and the cube of its average particle diameter

ing into an aggregate, individual particles do not merge like the drops of a liquid but remain separated with interfaces between them. Figure 7 shows electron microscopic photographs of such aggregates (direct image and replica of a fracture). However, this aggregation does not alter the polymerization picture described above. With an increasing degree of conversion, the size of the primary particles (and simultaneously the size of the aggregates) increases. However, their number does not change. Again polymerization proceeds inside the globular structures of PVC.

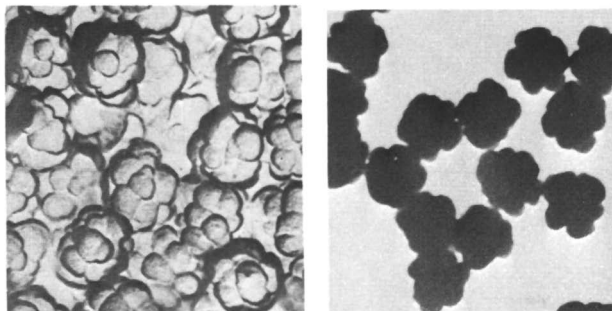


Figure 7. Electron microscope photographs of PVC globular aggregates. Each photograph is  $1.25\mu$  wide

Polymerization in an emerging polymer may also occur when the polymer is soluble in the reaction medium and does not evolve as a separate phase. Sufficiently large structures may arise in solutions for polymerization processes to proceed within them—*e.g.*, polymerization on polymeric initiators. Anionic processes of this type were studied in detail by Platé (15, 20). The initiator used was polystyrene containing lithium, with a molecular weight of 4000–6000; lithium was introduced by its reaction with a complex of butyllithium–tetramethyldiamine. The polymerization rate of styrene in Decalin was studied for such a polymeric catalyst and compared with the polymerization rate in the presence of an equivalent amount of pure butyllithium. In the presence of the polymeric initiator the rate in polar medium was higher (Figure 8), the activation energy decreased slightly (from 8.6 to 6.8 cal./mole), and the

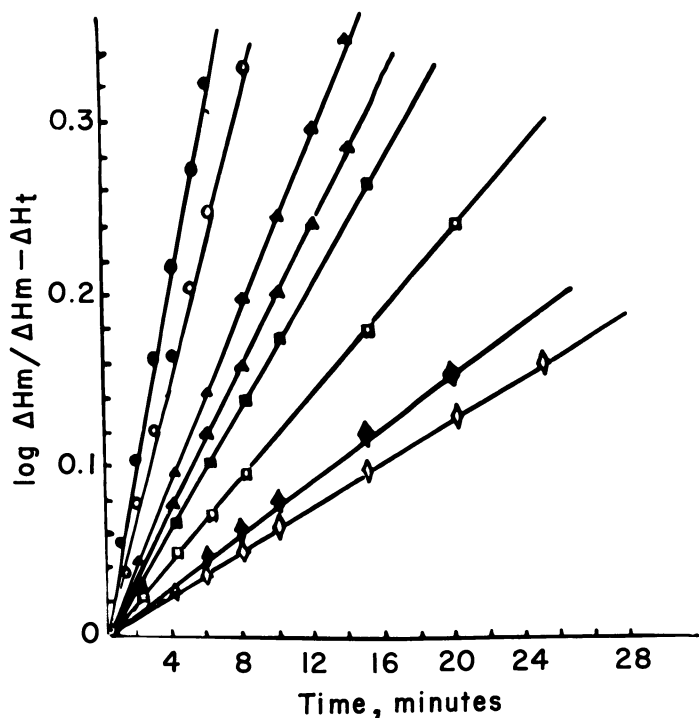


Figure 8. Polymerization of styrene onto PLPS + BuLi mixture and onto pure BuLi at 25°C. in Decalin with tetramethyldiamine.  $[M] = 0.9M$ ;  $[\text{polystyrene}] = 3.9\%$  of monomer. Catalyst concentration, corresponding to each pair of curves from left to right:

- (1)  $1.4 \times 10^{-2}M$
- (2)  $6.5 \times 10^{-3}M$
- (3)  $4.8 \times 10^{-3}M$
- (4)  $2.1 \times 10^{-3}M$

steric factor changed considerably (from  $2 \times 10^5$  to  $3 \times 10^4$ ). Evidently the polymeric chains growing on a polymeric catalyst form comparatively large coils in which further polymerization develops. Inside these coils the monomer concentration is higher than the average concentration in volume. By varying the solvent and polymeric catalyst the rate of polymerization can be either increased or decreased (as in the case of nonpolar medium), owing to the different distribution of the monomer between the solvent and the polymer coil.

In all cases cited, the formation of structures during polymerization resulted in the polymerization reaction's proceeding subsequently within these newly appearing structural formations. The influence of the structural processes was reduced to the appearance of a new polymerization medium, but the formation of polymeric structures during polymerization may result in other effects; the most essential is a change in the thermodynamic conditions of polymerization.

The change in free energy is taken into account during the conversion of monomer molecules into separate macromolecules. However, if polymerization results directly in polymeric structures rather than separate molecules, the total free energy change includes the change in free energy from structural formation as well. This value may be of essential importance, primarily during the formation of polymers with conjugated double bonds and in ring-opening polymerization as well as in the formation of crystalline polymers.

We know of several cases involving the formation of large crystalline structures during polymerization. One example is the growth of crystalline nascent polyethylene on an aluminum wire with a slightly chlorinated surface during the polymerization of ethylene from a benzene solution in the presence of titanium trichloride (5). Figure 9 is a general view of the emerging polyethylene and electron microscope photographs of its individual fibrils. No matter how effective such photographs might be, unfortunately they cannot supply the answer to the question of whether these structures form during the polymerization process itself or are a result of the regrouping of individual chains formed during polymerization. Meanwhile the answer to this question is decisive if we are interested in the influence of structure formation on polymerization. To be certain that no secondary regrouping of finished macromolecules occurs, the entire polymerization test must be carried out at temperatures below the glass transition temperature of the forming polymer—*i.e.*, under conditions where the polymeric molecules are immobile. So far only one set of data exists, obtained at the Moscow University, by polymerizing solid monomers directly in the electron microscope, where polymerization was initiated by the electron beam itself (4, 8, 19). Under these conditions it could be shown for a number of substituted methacrylates and for



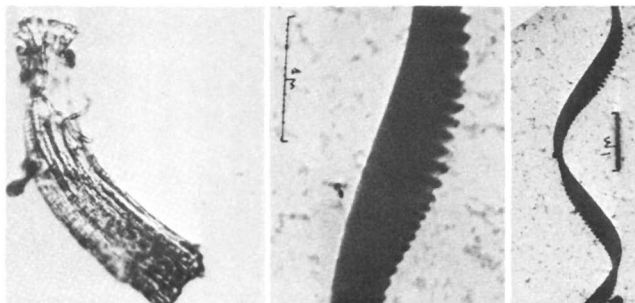


Figure 9. Emerging polyethylene and its individual fibrils

sodium acrylate that at temperatures below the melting point of the monomers and below the softening point of the forming polymers, ordered supermolecular polymeric strictures form directly during polymerization. It is curious that conditions favoring polymerization also result in the formation of more perfect structures. Thus, for phenylmethacrylamide, polymerization with perceptible yields of the polymer, occurs at temperatures  $5^{\circ}$ – $10^{\circ}$  below the melting point of the monomer crystals. Under the same conditions more perfect structures appear. A comparison of the formation of structures from solution (where the conditions would seem to be the most favorable) and during polymerization revealed that the most ordered structures appear during the chemical reactions of formation of the polymeric molecules themselves. All the data suggest that simultaneous growth of clusters of chains is preferable to growth of isolated chains. If these assumptions are true, polymerization in all such cases must be connected closely with evolution of the polymer as a new phase. Hence, the effect of nucleus action should also be observed. This suggests the possibility of existence of polymerization nuclei, similar to the nuclei of crystallization. Such effects were first demonstrated a few years ago in pyridine polymerization.

The last example of structural influence on polymerization is the action of already formed polymeric chains on the formation of new polymeric molecules. During recent years we have been investigating the matrix (templet) polymerization of 4-vinylpyridine on polymeric acids (12, 13, 14). Recently we discovered another peculiar case where the preformed polymer and growing chains participate in the formation of the polymeric substance (17).

Ryan and Fleischer, Jr. (21) found that if isotactic and syndiotactic poly(methyl methacrylate) (PMMA) are mixed, they form a stereo-complex. It might have been supposed that the course of polymerization of methyl methacrylate in the presence of preformed stereoisomers of

PMMA added previously would depend on their structure. Indeed, when polymerization was carried out in the presence of isotactic PMMA, it influenced the formation of new macromolecules, affecting the rate of polymerization, the molecular weights of the polymer formed, and the structure of its molecules. It is natural to assume that these effects are caused by the appearance of a stereocomplex during polymerization between the polymer added beforehand and the growing macroradical. It is also characteristic that the ratio of polymerization rates in the presence and in the absence of the polymer is independent of the concentrations of monomer and polymer added, depending only on their ratio. Viscosity investigations revealed that these solutions are highly crosslinked.

All these tests were run in DMF as solvent. In such a system the templet polymerization cannot be pictured as alignment of the monomer molecules to the polymer molecule serving as the matrix. The interaction between them is comparatively weak, and DMF is a better solvent with respect to monomer than dead polymer. Evidently, comparatively large growing radicals, enriched in the configuration which favors the formation of the stereocomplex, attach themselves to the matrix molecules. Further growth is caused by the matrix molecules. Here we are dealing with a new peculiar type of matrix process. Perhaps it will also furnish new possibilities for stereoregulation in radical polymerization.

These examples of the phenomena which influence structural factors of the polymerization process should always be taken into account. Eventually, they may reveal new possibilities in polymerization phenomena.

### **Literature Cited**

- (1) Amerik, U. B., Krentsel, V. A., *J. Polymer Sci., Pt. C*, **16**, 1383 (1967).
- (2) Amerik, U. B., Konstantinov, N. I., Krentsel, B. A., *Vysokomol. Soyed.* **A9**, 2236 (1967).
- (3) Amerik, U. B., Konstantinov, I. I., Krentsel, B. A., *J. Polymer Sci., Pt. C*, **23**, 231 (1968).
- (4) Azori, M., Plate, N. A., Kargin, V. A., *Proc. Symp. Radiation Chem., 2nd Tihany, Budapest*, 547 (1967).
- (5) Bort, D. N., Minsker, K. S., Okladnov, N. A., Starkman, B. P., Kargin, V. A., *Dokl. Akad. Nauk SSSR* **145**, 787 (1962).
- (6) Bort, D. N., Rylov, E. E., Okladnov, N. A., Starkman, E. P., Kargin, V. A., *Vysokomol. Soyed.* **7**, 50 (1965).
- (7) Bort, D. N., Rylov, E. E., Kargin, V. A., *Vysokomol. Soyed.* **A9**, 303 (1967).
- (8) Kargin, V. A., Azori, M., Platé, N. A., Bandurian, S., *Dokl. Akad. Nauk SSSR* **154**, 1157 (1964).
- (9) Kargin, V. A., Kabanov, V. A., Zubov, V. P., *Vysokomol. Soyed.* **1**, 265 (1959).
- (10) Kargin, V. A., Kabanov, V. A., Papisov, I. M., *J. Polymer Sci., Pt. C*, **4**, 767 (1964).

- (11) Kargin, V. A., Kabanov, V. A., *Zh. Vsesoyuzn. Khim. Obshch. Mendel'eyeva* **9** (6), 602 (1964).
- (12) Kargin, V. A., Kabanov, V. A., Kargina, O. V., *Dokl. Akad. Nauk. SSSR* **161**, 1131 (1965).
- (13) Kargina, O. V., Ulyanova, V. A., Kabanov, V. A., Patrikeyeva, T., Kargin, V. A., *Vysokomol. Soyed.* **A9** (1967).
- (14) Kargina, O. V., Kabanov, V. A., Kargin, V. A., *Symp. Macromol. Chem. Brussels, 1967, Preprint* **1-119**.
- (15) Jampolskaya, M., Platé, N. A., Kargin, V. A., *Vysokomolek. Soyed.* **102**, 152 (1968).
- (16) Miyama, H., Kamashi, M., *J. Polymer Sci., Pt. B*, **9**, 4651 (1963).
- (17) Orlova, O. V., Kargin, V. A., Krentsel, B. A., Amerik, U. B., *Dokl. Akad. Nauk. SSSR*.
- (18) Paussov, I. M., Pisarenko, T. A., Panasenko, A. A., Kabanov, V. A., Kargin, V. A., *Dokl. Akad. Nauk. SSSR* **156**, 669 (1964).
- (19) Plate, N. A., Azori, M., Kargin, V. A., *Vysokomolek. Soyed.* **8**, 764, 1562, 1966.
- (20) Plate, N. A., Jampolskaya, M. A., Davydova, S. L., Kargin, V. A., *Symp. Macromol. Chem., Brussels, 1967, Preprint*.
- (21) Ryan, C. F., Fleischer, P. C., Jr., *J. Phys. Chem.* **69**, 3384 (1965).
- (22) Shreiner, E. S., Zubov, V. P., Kabanov, V. A., Kargin, V. A., *Dokl. Akad. Nauk. SSSR* **156**, 396 (1964).
- (23) Tsvetkov, V. N., Ryumtsev, E. M., *Dokl. Akad. Nauk. SSSR* **176**, 382 (1967).

RECEIVED April 1, 1968.

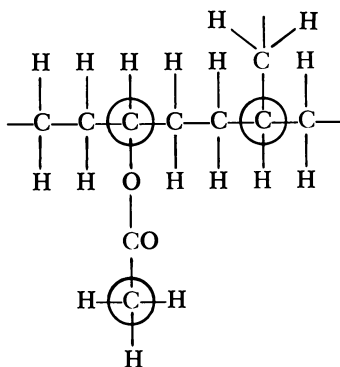
# Graft Polymerization of Vinyl Compounds on Ethylene-Vinyl Acetate Copolymers

HERBERT BARTL and DIETRICH HARDT

Polymerization Department, Central Research Laboratory, Farbenfabriken Bayer AG, 5090 Leverkusen, West Germany

*Ethylene-vinyl acetate copolymers represent a good backbone for the radical graft polymerization of vinyl compounds. The grafting tendency of the vinyl compounds used is proportional to the activity of the monomer radicals, according to Mayo and Walling, in the following order: vinyl chloride, vinyl acetate, ethyl acrylate, methyl methacrylate, and styrene. The dependence of the degree of grafting on monomer type suggests that under the conditions of suspension polymerization, grafting points in the backbone are formed predominantly by transfer reactions of monomeric or primary radicals. In solution polymerization in tert-butyl alcohol, acrylonitrile shows a greater tendency to graft than vinyl chloride or vinyl acetate. This behavior does not follow the activity series of the monomer radical.*

Ethylene and vinyl acetate can be copolymerized in any desired proportion. Depending on their vinyl acetate content, the copolymers, hereafter called EVA copolymers, exhibit very different properties. With a low vinyl acetate content, they are similar to high pressure polyethylene but possess an improved transparency and elasticity. With about 40–50% vinyl acetate, the copolymers show pronounced elastomer properties. With higher contents of vinyl acetate, the copolymers represent soft compounds, and finally, with a very high content of vinyl acetate, their properties approach those of poly(vinyl acetate). Since EVA copolymers, owing to their saturated character, possess excellent resistance to weathering, it seemed interesting to try to combine the elastomer type with approximately 45% vinyl acetate by graft polymerization with monomers forming plastics, such as vinyl chloride or styrene-acrylonitrile to impart to the plastics improved impact resistance.



### Preferred Branching Points of an EVA Copolymer

Because of their content of hydrogen atoms, which can be separated by a radical reaction, ethylene-vinyl acetate copolymers have a good basis for grafting. In earlier papers on the radical crosslinking of EVA copolymers with peroxides, we showed that polyunsaturated compounds, such as triallyl cyanurate, can be incorporated completely in the copolymers by graft reactions (2).

To survey as completely as possible the grafting behavior of EVA copolymers toward various vinyl compounds, our investigations covered the grafting of vinyl acetate, vinylidene chloride, and acrylic and methacrylic esters. As polymerization processes, at first we preferred suspension polymerization to exclude the influence of solvents by terminating or transfer reactions during polymerization. Grafting by emulsion polymerization, in which the EVA copolymer was dissolved in the monomer before polymerization, was difficult because coagulate was formed as polymerization proceeded.

The various monomers were compared as to the degree of grafting and the reaction of the backbone under identical reaction conditions—*i.e.*, only Porofor N (AZBN =  $\alpha, \alpha'$ -azodiisobutyronitrile) was used as the initiator in the same concentration, and the polymerization took place at 60°C. at about equal monomer conversion rate. The backbone used was Levapren 450, an ethylene-vinyl acetate copolymer with a vinyl acetate content of 45% and an average molecular weight of about 100,000. When the starting ratio was two parts of backbone to three parts of monomer and when the conversion was about 75% complete, the resulting polymers contained about 45% of the original backbone and 55% of the polymerized monomers. The degree of grafting was determined by fractionation or extraction, on the basis of the different solution behavior of the EVA copolymers and the grafted products or pure polymers,

respectively. [In determining the degree of grafting by extraction, relatively broad scattering may occur owing to too low solubility differences.]

**Table I. Grafting of Various Monomers on Levapren 450<sup>a</sup>**

<i>Product</i>	<i>Monomer</i>	<i>Grafting of the Monomer, %</i>	<i>Grafting of the Backbone, %</i>	<i>Instructions Processing</i>
1	Styrene	5	8	A
2	Methyl methacrylate	28	29	A
4	Ethyl acrylate	88	38	A
6	Vinylidene chloride	—	67	B
3	Vinyl acetate	95	45	A
5	Vinyl chloride	~100	82	B

<sup>a</sup> Farbenfabriken Bayer AG.

Table I gives the composition of the grafting products investigated. The monomers are listed in the order of their increasing tendency to graft—*i.e.*, in the order of an increase in the degree of grafting of the monomer and of the grafted backbone portion. A similar sequence was determined by Hayes for the grafting of vinyl chloride, vinyl acetate, and styrene by emulsion polymerization on poly(vinyl chloride), polyacrylonitrile, or poly(vinyl acetate) (7). Obviously, the sequence in Table I corresponds to the order of the relative activities of the monomer radicals according to Mayo and Walling.

The dependence of the degree of grafting on monomer type leads to the conclusion that under the polymerization conditions used here the grafting points in the backbone are formed predominantly by transfer reactions of monomer radicals or primary radicals, respectively, obtained by a reaction of initiator and monomer and not by the radicals of the initiator  $\alpha, \alpha'$ -azodiisobutyronitrile. The reaction of the polymer radicals with a hydrogen atom of the backbone, which leads to a homopolymer by chain termination, can also be of minor importance only because in the case of vinyl chloride, for example, when larger proportions of the EVA copolymer are used, no homo-PVC is obtained during grafting (*see* Tables I and II). Thus, it is the highly active vinyl chloride radical that is responsible for the extensive grafting of vinyl chloride, while the inert resonance-stabilized styrene radical imparts only slight grafting.

After investigating the grafting behavior of styrene on polyethylene, Czvikovsky and Dobo emphasized the importance of certain primary radicals for the formation of grafting points (4). The effectiveness of AZBN in forming grafting points has already been shown (1, 3, 8, 9). An argument in support of this is that it is impossible by the action of

AZBN, in contrast to various peroxides, to crosslink EVA copolymers radically, which means that the formation of radicals at the macromolecules does not take place to a sufficient extent.

For vinyl acetate there seems to be a contradiction regarding the extent of grafting of the backbone because it is essentially lower than for vinyl chloride, although the vinyl acetate radical (according to Mayo and Walling) is approximately as active as the vinyl chloride radical. This observation might be accounted for by the poly(vinyl acetate) chains which, during polymerization have been formed and grafted, and compete as a new graftable backbone with the EVA copolymer, in which, according to a well-known reaction, poly(vinyl acetate) branchings are formed. Consequently, a lower proportion of EVA copolymer is grafted than expected.

On the basis of a series of experiments with vinyl chloride, which, owing to its high tendency to graft with the backbone, offers favorable conditions for investigation, let us now consider some influences on the grafting reaction such as proportion, composition, and differences in the molecular weight of the backbone. Table II shows the dependence of

**Table II. Grafting of Vinyl Chloride on Levapren 450 with Increasing Quantities of Levapren**

<i>Product</i>	<i>Content of Backbone, %</i>	<i>Grafting of Vinyl Chloride, %</i>	<i>Grafting of the Backbone, %</i>	<i>Production Instructions</i>
9	6	10-15	90	B
10	24	65-70	81-85	B
11	42	~100	80	B
12	63	~100	60	B

the extent of grafting on the proportion of backbone. The extent of vinyl chloride grafting rises with an increasing quantity of backbone, so that from about 40% backbone content homo-PVC is no longer detectable in the products by fractionation from tetrahydrofuran solution with petroleum ether. For instance, a graft copolymer containing about 50% EVA and 50% PVC has the values of fractional precipitation shown in Table III.

Such graft polymers, which virtually contain all the poly(vinyl chloride) in a grafted condition, can be crosslinked easily with peroxides *via* the EVA copolymer chains. This corresponds to an indirect statement on the degree of grafting of the products.

The degree of reaction of the backbone occurs in the reverse direction: when the quantities are lower than 10%, the backbone is grafted largely down to small low molecular weight proportions extractable from

**Table III. Fractional Precipitation of Graft Copolymer of 50% EVA (45% VAc) and 50% PVC<sup>a</sup>**

Fraction	Amount Precipitated	( $\eta$ )	Chlorine Content
1	37.6	1.85	35.5
2	17.6	1.68	34.2
3	11.5	1.65	33.5
4	12.5	1.54	31.1
5	4.6	1.38	26.2
6	3.3	1.00	5.3
7	2.2	0.72	0.8
R	8.4	0.46	0.2
Loss	2.3	—	—

<sup>a</sup> Solvent, tetrahydrofuran; precipitating agent, petroleum ether.

**Table IV. Grafting of Vinyl Chloride on Ethylene-Vinyl Acetate and Poly(vinyl acetate)**

Product	Proportion of Backbone, %	Vinyl Acetate in the Backbone, %	Degree of Grafting of the Backbone, %	Production Instructions
14	40	17	30	C
7	42	30	50	B
5	41	45	81	B
8	46	66	82	B
15	45	100	~20	D

the product. The dependence of the degree of grafting of the backbone upon the content of vinyl acetate is shown in Table IV. The tendency to graft rises with increasing content of vinyl acetate and reaches its maximum at 45–70% vinyl acetate. As expected, the degree of reaction of the backbone is greater the higher the concentration of the activator. More interesting is the observation that the grafted quantity of backbone depends on the molecular weight (Table V).

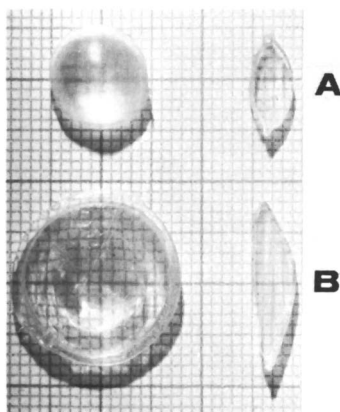
**Table V. Grafting of Vinyl Chloride on Ethylene-Vinyl Acetate Copolymers with Non-uniform Molecular Weight (50% VAC in the Backbone)**

Product	Content of Backbone in the Polymer, %	Molecular Weight	Degree of Grafting of the Backbone, %	Production Instructions
16	26	$\sim 3 \times 10^4$	~20	E
17	27	$3 \times 10^5$	73	E



Two graft polymers of the same composition, which have been prepared under identical conditions and differ only in the molecular weight of the backbone, are compared in Table V. The data show that the high-molecular weight EVA is subject to grafting, as far as quantities are concerned, to a much higher degree than the low molecular weight product.

If one intends to graft on very little monomer, the EVA polymer granules may be swelled slightly with the monomers containing the initiator, dispersed in water, and polymerized (Figure 1). The upper part of Figure 1 shows the EVA copolymer used as a starting product (A) (vinyl acetate content = 45%). The granulated particles have a diameter of about 1 cm. Swelling with vinyl acetate and subsequent polymerization lead to the homogeneous and transparent graft product (B), the particle shape being maintained.



*Figure 1. Grafting of a small amount of monomer onto an EVA polymer*

*A: EVA starting product  
B: Swollen and polymerized*

Polymerization thus takes place at a high backbone concentration so that the backbone becomes much more effective owing to its transfer and terminating reaction. Consequently, with different monomers not only high degrees of grafting are achieved but the grafting reactions can proceed so far that with low quantities of some monomers, partly cross-linked products are obtained (Table VI). This method is also suitable for grafting monomers which are not able to dissolve the EVA copolymer but only swell it more or less. One of these monomers is acrylonitrile, which we could not graft by the method of suspension polymerization because of its poor solvent properties.

**Table VI. Grafting in a Swollen Condition (Instruction F)**

	<i>Polymerized Monomers in the Polymer, %</i>	<i>Solubility<sup>a</sup></i>
Vinyl acetate	5	+
	12	±
	30	±
Vinyl chloride	3	+
	6.5	+
	15	+
Acrylonitrile	12	±
	20	±
	25	-
Styrene	8	+
	20	+
	41	+

<sup>a</sup> + = soluble, ± = partly soluble, - = insoluble.

When grafting acrylonitrile in a swollen condition of the EVA copolymer, only partly soluble or insoluble products are obtained (Table VI). Therefore, we investigated the graft polymerization of acrylonitrile in solution and compared its grafting behavior with that of vinyl chloride and vinyl acetate. The solvent was *tert*-butyl alcohol, which is known to show a very low transfer tendency (Table VII).

**Table VII. Graft Polymerization in Solution (Instruction G)**

	<i>Acrylonitrile</i>	<i>Vinyl Chloride</i>	<i>Vinyl Acetate</i>
Yield, parts by weight	190	110	174
Content of the polymerized monomer in the total polymer, %	47	9	43
Homopolymer in the total polymer, %	0	0	33

When the polymers were analyzed for their content of homopolymer, it was found that the acrylonitrile polymer is soluble in chlorobenzene and the vinyl chloride polymer in toluene. Since chlorobenzene is unable to dissolve polyacrylonitrile and toluene cannot dissolve poly(vinyl chloride), it must be assumed that no homopolymer has been formed. This has been verified by fractionations. It is possible to extract with methanol from the vinyl acetate polymer 33% of a substantially pure polyvinyl acetate with a vinyl acetate content of 95%. Hence, acrylo-

nitrile grafts better in *tert*-butyl alcohol than vinyl acetate, although in the activity series of the monomer radicals it falls after vinyl acetate.

It is also remarkable that vinyl chloride, under the same reaction conditions, polymerizes only slightly. If higher conversion rates of vinyl chloride are desired, it is necessary to use a considerable excess of vinyl chloride over the EVA copolymer or to reduce the quantity of *tert*-butyl alcohol. It seems that during the polymerization in the presence of *tert*-butyl alcohol the solvent inhibits the polymerization of the vinyl chloride. This means that by using a further component—*i.e.*, a solvent—the polymerization conditions in graft polymerization are changed to such an extent that the grafting behavior of the various monomers is completely different.

The physical properties of the graft polymers depend largely on whether the end products—namely the graft polymer, the backbone, and

**Table VIII. Graft Copolymer Containing 8% Ethylene-Vinyl Acetate Copolymer (45% VAc) and 92% PVC<sup>a</sup>**

Physical Properties of the Raw Material			
Property	Test Method	Unit	Value
EVAc content	—	%	ca. 8
Chlorine content	DIN 53.474	%	ca. 52.5
K value (according to Fikentscher)	DIN 53.726	—	ca. 68
Density	DIN 53.479	grams/ml.	ca. 1.35
Bulk density	DIN 53.468	grams/ml.	ca. 0.5
Ash content	—	%	<0.1
Water content	K. Fischer	%	<0.1
Average grain size	—	—	0.1–0.2 mm.
Mechanical Values of Pressed Sheets <sup>b</sup>			
Hardness, kg./cm. <sup>2</sup>	DIN 53.456	10 sec.	900–930
		60 sec.	860–880
Impact strength, cm. kg./cm. <sup>2</sup>	DIN 53.453	20°C.	not broken
		–20°C.	not broken
Impact strength, (notched) cm. kg./cm. <sup>2</sup>	DIN 53.453	20°C.	45–50
		0°C.	8
		–20°C.	5–6
Tensile strength, kg./cm. <sup>2</sup>	DIN 53.504		440
Elongation at break, %	DIN 53.504		50–60
Modulus of elasticity, kg./cm. <sup>2</sup>	DIN 53.457		24000
Vicat, °C.	DIN 53.460		81

<sup>a</sup> The product is a shock-resistant PVC, which may be processed immediately.

<sup>b</sup> Processing temperature, 170°C. Stabilization: 1% Advastab 17M.

perhaps the homopolymers of the monomers used—constitute a polymer mixture compatible in itself. This is largely the case for vinyl chloride graft polymers: when their proportion of vinyl chloride is high, the properties are those of an impact-resistant poly(vinyl chloride); when the proportion of ethylene–vinyl acetate is high, the properties closely resemble a plasticized PVC (5, 6). Graft polymerization of styrene or acrylonitrile, however, leads to predominantly incompatible polymer mixtures. If, however, vinyl chloride is grafted on an EVA copolymer, this is compatible if the content of vinyl chloride is about 50%, with styrene–acrylonitrile copolymers to such an extent that polymer mixtures can be produced which have properties similar to those of ABS-copolymers (10).

Tables VIII and IX show the essential data of the most important graft copolymers regarding application.

**Table IX. Graft Copolymer Containing 50% by Weight of Grafted PVC and 50% by Weight of EVAc Copolymer (45% VAc)<sup>a</sup>**

Raw Material Properties			
<i>Property</i>	<i>Test Method</i>	<i>Unit</i>	<i>Value</i>
EVAc content		%	ca. 50
Chlorine content	DIN 53.474	%	ca. 28
K value (according to Fikentscher)	DIN 53.726	—	ca. 78
Density	DIN 53.479	grams/ml.	ca. 1.16
Bulk density	DIN 53.468	grams/ml.	ca. 0.55
Ash content		%	<0.1
Water content	K. Fischer	%	<0.1
Mechanical Properties			
Shore hardness A/D	DIN 53.505	—	ca. 85/35
Tensile strength	DIN 53.504	kg./cm. <sup>2</sup>	160–190
Elongation at break	Standard Specimen I	%	240–270
Modulus at 100% elongation		kg./cm. <sup>2</sup>	100–120
Tear resistance	DIN 53.515	kg./cm. <sup>2</sup>	35–45
Low temperature flexibility	Schulz-Mehnert	°C.	ca. –50
Low temperature impact resistance	DIN 53.372	°C.	ca. –55

<sup>a</sup> This material may be processed itself as a flexible PVC, the plasticizer being connected to the resin or in mixtures with normal PVC powder with an effective EVA content of about 8–10% as a high impact modified rigid PVC.

### Experimental

**Instruction A.** In a vessel equipped with a high speed stirrer, at *ca.* 20° to 30°C. are placed a solution of 200 grams of Levapren 450 [ethylene-vinyl acetate copolymer with 45% vinyl acetate (commercial product of Farbenfabriken Bayer AG)] and 300 grams of the monomer to be grafted. 0.5 gram of azodiisobutyronitrile is added with stirring, 1000 grams of 0.5% aqueous methyl cellulose solution are introduced, and vigorous stirring is continued until the viscous solution of the aqueous phase is finely dispersed. Polymerization is effected by increasing the temperature while stirring is continued. After the polymerization is complete, the beads formed are isolated, washed with water, and dried *in vacuo* at 40° to 50°C.

Product	Monomer	Polymerization		Content of Levapren 450, %
		15 hrs. at:	+ 10 hrs. at:	
1	Styrene	60°C.	80°C.	43.5
2	Methyl methacrylate	60°C.	70°C.	47
3	Vinyl acetate	55°C.	70°C.	43.5
4	Ethyl acrylate	55°C.	70°C.	46
				crosslinked

**Instruction B.** A solution of an ethylene-vinyl acetate copolymer is prepared in a stirrer autoclave in vinyl chloride (vinylidene chloride) while adding azodiisobutyronitrile; dissolution takes place at 25° to 30°C. for four hours. A 1% methyl cellulose solution is introduced into the autoclave under pressure, the content is stirred vigorously (400 r.p.m.) at 25°C. for two hours, and polymerization is effected by temperature increase at the same speed of agitation. After the polymerization is complete, the bead polymer is isolated, washed with large amounts of water, and dried *in vacuo* at 50°C.

Product	Leva-pren, grams	VAc in Leva-pren, %	Catalyst, grams	Vinyl Chloride, grams	Vinyl- idene Chloride, grams	Methyl Cellulose Solution, grams	T, °C.	Time, hours	Leva-pren in the Polymer, %
5	800	45	2	1200	1200	3000	60	15	44
6	800	45	2			2000	60	15	41
7	800	30	2	1200		2000	62	15	42
8	800	66	2	1200		2000	62	15	46
9	75	45	3	1425		3000	60	15	6
10	300	45	3	1200		3000	60	15	24
11	550	45	3	750		3300	60	15	41
12	750	45	1	750		4000	60	15	63

**Instruction C.** PRODUCT 14. In a stirrer autoclave, 1300 grams of vinyl chloride and 700 grams of an ethylene-vinyl acetate copolymer with 17% vinyl acetate are stirred at 75°C. and then cooled to 40°C. Two grams of azodiisobutyronitrile dissolved in 30-40 ml. of vinyl chloride are introduced under pressure, the solution is stirred at 40°C. for one

hour, and a solution of 20 grams of methyl cellulose in 2000 grams of water is added under pressure. After vigorous agitation at 40°C. for one hour, polymerization is effected at 60°–62°C. for 15 hours with further stirring. The bead polymer obtained has a PVC content of 60% by weight.

**Instruction D. PRODUCT 15.** In a stirrer autoclave, 1200 grams of vinyl chloride, 800 grams of poly(vinyl acetate) (Movilith 30), and 2 grams of azodiisobutyronitrile are stirred at 30°C. for three hours. After adding a solution of 40 grams of methyl cellulose in 4000 grams of water, vigorous stirring is continued at 30°C. for two hours, and polymerization is effected by increasing the temperature to 60°–62°C. for 15 hours. The resulting finely dispersed bead polymer has a PVC content of 55%.

**Instruction E. PRODUCT 17.** The following substances are used in the process of Instruction B: 35 kg. Levapren 450; 115 kg. vinyl chloride; 150 kg. water plus 1.5 kg. methyl cellulose; 50 grams azodiisobutyronitrile. Polymerization is carried out for 13 hours at 61°C. The bead polymer obtained has a PVC content of 73%. Product 16 was made according to Instruction E, using a low molecular weight type of Levapren (molecular weight *ca.*  $3 \times 10^4$ , 43.5% vinyl acetate). The bead polymer obtained has a PVC content of 75%.

**Instruction F. GRAFTING IN SWOLLEN CONDITION.** A total of 300 grams of Levapren 450 are swelled slightly in a solution of 12 grams of methyl cellulose in 1200 ml. water for 24 hours with the monomer at room temperature. Porofor N (0.1%) was previously dissolved in the monomer (referred to the initial quantity of monomer). After swelling, polymerization is effected at 70°C. for 20 hours.

After polymerization, the beads are separated from the aqueous phase by a fine mesh size sieve, washed, and dried *in vacuo* at 50°–60°C. When using vinyl acetate and acrylonitrile as monomers, a slight loss of the swollen monomer owing to diffusion out of the beads must be taken into consideration because of the solubility in water.

**Instruction G. GRAFT POLYMERIZATION IN SOLUTION.** A total of 100 grams of Levapren 450 are dissolved in 300 grams of *tert*-butyl alcohol at 20°C. for five hours; 0.1% of Porofor N (referred to the initial quantity of Levapren) is added, and the mixture is stirred at 70°C. for one hour. Then the monomer is added, and polymerization is effected at 70°C. for 20 hours. The solution is precipitated with water, and the polymer is dried *in vacuo* at 50°–60°C.

### Conclusions

The physical properties of the graft polymers depend largely on whether the end products—namely the graft polymer, the backbone, and perhaps the homopolymers of the monomers used—constitute a polymer mixture compatible in itself. This is largely the case with vinyl chloride graft polymers which, when they contain a high proportion of vinyl chloride, have the properties of an impact-resistant poly(vinyl chloride); when they contain a high proportion of ethylene–vinyl acetate, they are very similar to a plasticized PVC. In the graft polymerization of styrene

or acrylonitrile, however, the polymer mixtures obtained are predominantly incompatible.

### *Acknowledgment*

The authors are grateful to M. Hoffmann for investigations on the structure of graft polymers and interesting discussions on structural problems.

This paper is dedicated to E. Huseman on the occasion of her 60th birthday.

### *Literature Cited*

- (1) Allen, P. W., Ayrey, G., Moore, C. G., *J. Polymer Sci.* **36**, 55 (1959).
- (2) Bartl, H., Peter, J., German patent 1,669,126 (June 3, 1958); *Kautschuk Gummi* **14**, WT23 (1967).
- (3) Bewington, J. C., *J. Chem. Soc.* **1954**, 3707.
- (4) Dobo, J., Czikovsky, T., *J. Polymer Sci. Pt. C.* **16**, 2973 (1967).
- (5) Göbel, W., Bartl, H., Hardt, D., Reischl, A., *Kunststoffe* **5**, 4 (1965).
- (6) Hardt, D., Bartl, H., U. S. Patent 3,358,054 (April 9, 1962).
- (7) Hayes, R. A., *J. Polymer Sci.* **11**, 531 (1953).
- (8) Lazar, M., Rado, R., Pavlinec, J., *J. Polymer Sci.* **53**, 163 (1961).
- (9) Severini, F., Pegoraro, M., Tavazzani, C., Aurello, G., *J. Polymer Sci. Pt. C.* **16**, 2805 (1967).
- (10) Weitzel, H., Göbel, W., Hardt, D., Dinges, K., German patent 1,499,139 (April 21, 1965).

RECEIVED March 19, 1968.

# The Internal Crosslinking of Styrene Copolymers

R. N. HAWARD, B. M. PARKER,<sup>1</sup> and E. F. T. WHITE

Department of Polymer and Fiber Science, The University of Manchester,  
Institute of Science and Technology, Sackville St.,  
Manchester M60 IQD, England

*The crosslinking of styrene-hydroxyethyl methacrylate copolymers by hexamethylene diisocyanate has been studied in toluene solution at 80°C. At high copolymer concentrations the specific viscosity of the solutions increased during reaction owing to the coupling of polymer chains. However, below a certain concentration, which depends on the copolymer composition, the viscosity fell as the reaction proceeded. At very low concentrations, the change in viscosity became independent of concentration. As the intrinsic viscosity decreased, the Huggins constant increased rapidly and the radius of gyration decreased, indicating a marked change in the polymer-solvent interaction. These results are explained on the basis of internal cyclization of the polymer molecule during the crosslinking reaction. Toluene solutions of  $\alpha,\omega$ -dihydroxy polystyrene on reaction with hexamethylene diisocyanate showed similar behavior.*

Any molecule which contains two groups which are able to combine can react either with itself (cyclization) or with another molecule (polymerization). In the general case these reactions can compete, and their relative proportions depend sharply on the concentration of the reactant. This principle was studied some time ago for small molecules by Salomon (26, 27) and Ziegler (38). Obviously, similar possibilities arise for polymers, but so far this subject has not been investigated systematically, although certain special areas have now been studied.

<sup>1</sup> Present address: Materials Department, Royal Aircraft Establishment, Farnborough, Hants, England.



One such area concerns the internal crosslinking which occurs during the preparation of certain thermosetting resins by free radical polymerization. Here the work of Stockmayer (34) and Simpson and co-workers (31, 32) has laid the foundation for subsequent developments. Simpson showed that appreciable internal cyclization takes place during the polymerization of diallyl esters. Where the most favored 5- and 6-membered rings can be formed, Butler has demonstrated that the cyclization reaction can be dominant (7, 8). This field has been reviewed recently by Gibbs and Barton (12). On the other hand, there have been a few direct studies of the internal cyclization of a polymer with the formation of very large rings although Haward and Simpson (15) did provide some evidence for the occurrence of such a process in the copolymerization of styrene and divinylbenzene.

However, up to the present, the knowledge we do have of internal crosslinking in polymers is largely due to the work of Kuhn, who originally calculated the probability of a cyclic configuration in a Gaussian chain (21). Similarly, Kuhn and Majer (23) calculated the expected change in intrinsic viscosity arising from intramolecular ring formation in a polymer, and Kuhn and Balmer (22) went on to study the acetal formation reaction of polyvinyl alcohol by terephthaldehyde ( $\text{OCH} \cdot \text{C}_6\text{H}_4 \cdot \text{CHO}$ ). In their experiments naturally there was a high probability of reaction between neighboring parts of the polymer chain, a situation which was taken into account in the calculation of Kuhn and Majer, but small changes in intrinsic viscosity were nevertheless observed when one molecule of aldehyde reacted with one polymer molecule. Kuhn and Balmer also showed that the observed reduction in intrinsic viscosity became constant at high dilutions. However, in view of the very limited range of these experiments, we felt there was need for further study of the intramolecular crosslinking reactions using polymers which had been prepared especially to contain a controlled number of reactive groups. For this purpose, some copolymers of styrene and hydroxyethyl methacrylate (HEMA) were prepared and characterized (*see* Appendix). These provide starting polymers with a range of hydroxyl content capable of reacting with bifunctional isocyanate to give internally crosslinked molecules. This paper describes the results of a study of these reactions.

### **Experimental**

**Materials.** Styrene-hydroxyethyl methacrylate copolymers were prepared and characterized as described in the Appendix. The copolymers used in this work contained 0.7, 2.2, 3.8, and 9.5 mole % HEMA.

$\alpha,\omega$ -Dihydroxy polystyrene, of molecular weight  $1.2 \times 10^5$ , was prepared by terminating with ethylene oxide the polymer obtained by anionic

polymerization of styrene and was kindly supplied by K. Riches (Shell Chemical Co., Ltd., Carrington).

Hexamethylene diisocyanate was supplied as pure by W. Hopkins of this department (71), having a density of 1.045, and an average equivalent weight of  $83.7 \pm 0.5$  (theoretical equivalent 84.09). The weights of isocyanate used were calculated on the analysis of the particular sample.

*n*-Butyl isocyanate (Aldrich Chemical Co.) ( $n_D^{20} = 1.0461$ ) was used as supplied without further purification.

Toluene (reagent grade) was fractionated, and the middle fraction was stored over sodium wire. This dried toluene was degassed under high vacuum and distilled onto a sodium mirror at room temperature.

All reagents were stored and handled only under anhydrous conditions in a dry box. Glassware was dried at 175°C. and cooled in the dry box. Standard solutions were prepared by weight, and all solvent and solutions were filtered before use.

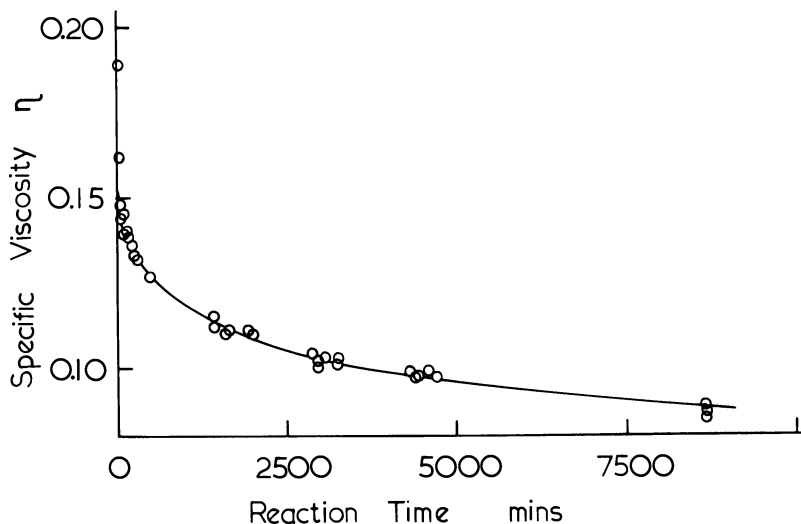


Figure 1. Variation in specific viscosity of a toluene solution of a styrene-hydroxyethyl methacrylate copolymer (2.2 mole % HEMA) on reaction with hexamethylene diisocyanate at 80°C. Polymer concentration 0.047%, (gram/dl.)  $[NCO]_0 : [OH]_0 = 9.5$

**Methods.** VISCOSITY MEASUREMENTS. Crosslinking reactions and reactions with butyl isocyanate were carried out in an Ubbelohde suspended-level viscometer modified to enable reactions to be carried out in an enclosed atmosphere. Viscometers were immersed in an oil bath at 80°C., and flow times were measured over periods of up to 10 days. Specific viscosities,  $\eta$ , were then calculated. In general, runs were followed until the change in viscosity with time had become very small. Flow times were measured frequently enough to allow a smooth curve to be drawn when  $\eta$  was plotted against reaction time; a typical curve is

given in Figure 1. Values of  $\eta$  at particular times were interpolated from such curves. The initial viscosity,  $\eta_0$ , could not be measured directly owing to the finite time taken for the viscometer and solution to reach the reaction temperature, and it was therefore determined by extrapolating the specific viscosity–time curve to zero time. Since  $\eta_0$  is a function of polymer concentration, runs of different concentrations were compared through the function  $\frac{\eta_0 - \eta}{\eta_0}$  which to a first approximation may be considered independent of concentration. The reproducibility of the viscosity change is illustrated in Figure 2.

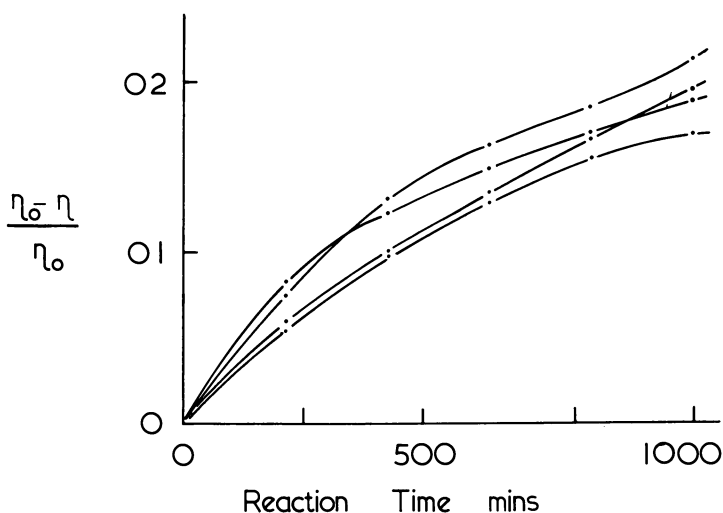


Figure 2. Reproducibility of the viscosity change for replicate crosslinking runs. Styrene–hydroxyethyl methacrylate copolymer (2.2 mole % HEMA) concentration in toluene 0.09% (gram/dl.)  $[NCO]_0 : [OH]_0 = 1$

In many ways it would have been desirable to have obtained a continuous record during the reaction of the intrinsic viscosity,  $[\eta]$ , which can be found by extrapolating to zero concentration of the function  $\eta/c$ . However, no convenient experimental procedure was devised for doing this, and no extrapolation formula could be used since the Huggins constant for the polymer changed during the reaction.

With the styrene–hydroxyethyl methacrylate copolymers some deposition of polymer on the walls of the reaction vessel was generally observed after 7–8 days of reaction. It was difficult to estimate the amount of gel, but in no case was the amount found as much as 4% of the total polymer. Thus, the effect of polymer loss on intrinsic viscosity was small.

**RATE OF REACTION OF THE COPOLYMERS WITH ISOCYANATES.** The reactions were carried out in a three-necked flask open to the atmosphere through a drying tube. Samples were removed at intervals. The isocyanate concentrations were determined using variable space cells in an Infracord 137 spectrophotometer by measuring the intensity of the band at  $4.4 \mu$ . The extinction coefficients were determined using samples of known concentration. Light scattering measurements were made on polymer solutions in toluene at  $25^\circ\text{C}$ . using a Sofica-gonio-diffusiometer.

### Results and Discussion

**Reactions of Styrene Hydroxyethyl Methacrylate Polymers.** The effect of reaction with hexamethylene diisocyanate on the specific viscosities of toluene solutions of the copolymers was studied over a wide range of isocyanate and polymer concentrations. The first feature noted was that the sign of the viscosity change depended on the polymer concentration (Figure 3). Although at high concentrations the viscosity increased, at low concentrations it decreased. Increased viscosity was undoubtedly caused by an increase in molecular weight, but we cannot, at this stage, be certain that the decrease was caused by intramolecular crosslinking.

It has been shown that an increase in the polarity of the polymer molecule owing to an increase in the number of hydroxyl groups caused

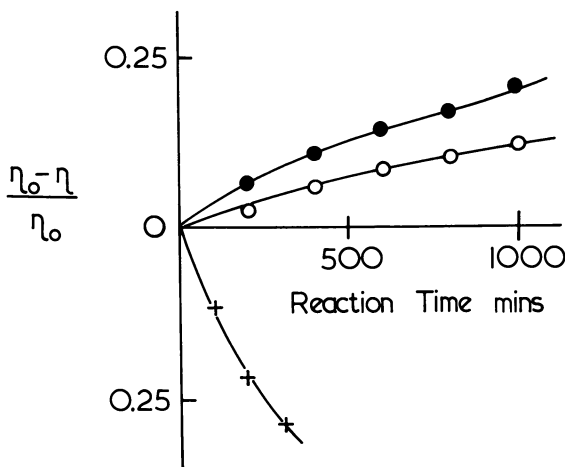


Figure 3. Effect of polymer concentration on the viscosity changes on reaction between styrene-hydroxyethyl methacrylate copolymer (2.2 mole % HEMA) and hexamethylene diisocyanate in toluene at  $80^\circ\text{C}$ .  $[\text{NCO}]_0 : [\text{OH}]_0 = 1$ . Polymer concentrations 0.047% (gram/dl.) (●), 0.134% (gram/dl.) (○), 0.85% (gram/dl.) (+)

a decrease in viscosity (14). It is possible that a similar effect might be the cause of the viscosity decreases observed. Reaction of the polymer molecule with hexamethylene diisocyanate attaches a free polar isocyanate group to the chain and creates a urethane grouping  $\text{—N—C—}$  which

$$\begin{array}{c} \text{H} \quad \text{O} \\ | \quad || \\ \text{—N—C—} \end{array}$$

might be expected to be more polar than the hydroxyl groups owing to the resonance



which would increase electron density on the carbonyl carbon. This could cause a contraction of the molecule owing to increased attraction between polar groups. Therefore, we studied the reaction of the polymer with a monoisocyanate, butyl isocyanate, and showed that although this did cause a decrease in viscosity, it was very small compared with that produced by the diisocyanate under the same conditions (Figure 4). With butyl isocyanate, of course, no crosslinking could occur. The reactions of the polymer with isocyanates (Figure 5) show that the two reactions do indeed take place at approximately the same rate.

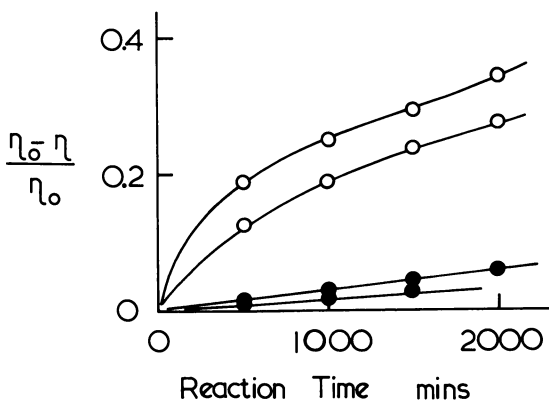


Figure 4. Comparison of viscosity changes on reaction between styrene-hydroxyethyl methacrylate copolymer (2.2 mole % HEMA) and butyl isocyanate ( $\bullet$ ) and hexamethylene diisocyanate ( $\circ$ ) in toluene at  $80^\circ\text{C}$ .

Although reaction with monoisocyanate cannot reproduce the viscosity change caused by the attachment of an unreacted isocyanate to the polymer chain, in view of the small change caused by the formation of urethane, it is unlikely that this could cause an extra decrease in

viscosity large enough to equal that found for reaction with diisocyanate. It is therefore unlikely that viscosity decreases arose simply from changes in the polarity of the polymer molecule.

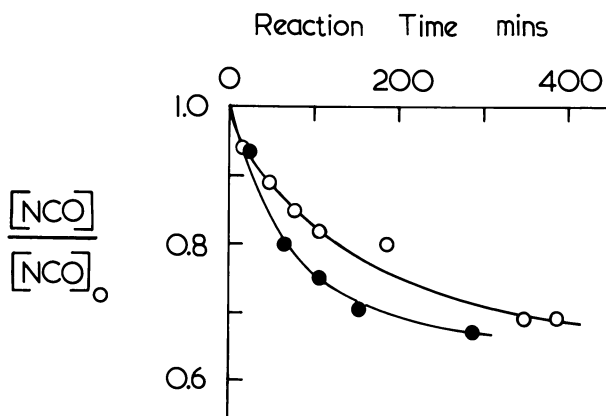


Figure 5. A comparison of decreases in isocyanate concentration during reaction between styrene-hydroxyethyl methacrylate copolymer (2.2 mole % HEMA) in toluene at 80°C. and butyl isocyanate (●) and hexamethylene diisocyanate (○). Polymer concentration 1.87% (grams/dl.)  $[NCO]_0 : [OH]_0 = 1$

The simplest case of a polymer molecule which can undergo either cyclization or chain extension is that in which the groups are situated at each end of the polymer chain (which can react together). An example of this type of polymer is  $\alpha, \omega$ -hydroxy-terminated polystyrene which reacts with a difunctional isocyanate, and our first studies were carried out with this reaction system. Obviously, the chain extension reaction leads to an increased specific viscosity, and cyclization leads to the reverse.

Since it was not possible to obtain a suitable dihydroxypolystyrene of high molecular weight, we were compelled to work with solutions of low specific viscosity. The observed changes in  $\eta$  on reaction with isocyanate were therefore also small. Our measurements were limited to demonstrating the effect of dilution on this system. The rate of change of viscosity,  $-\frac{1}{\eta_0} \frac{d\eta}{dt}$ , derived from the approximate viscosity-linear time curve, was measured during the initial part of the reaction using a 1:1 ratio of isocyanate to hydroxyl. The results given in Figure 6 showed that the expected decrease in  $\eta$  could be observed at the lowest concentrations.

For the styrene-hydroxyethyl methacrylate copolymers, the situation is more complex. To try to determine the nature of the reaction with

hexamethylene diisocyanate, we studied the effect of the copolymer composition and concentration in solution and of the initial ratio of isocyanate to hydroxyl  $[\text{NCO}]_0 : [\text{OH}]_0$ , on the viscosity changes with time.

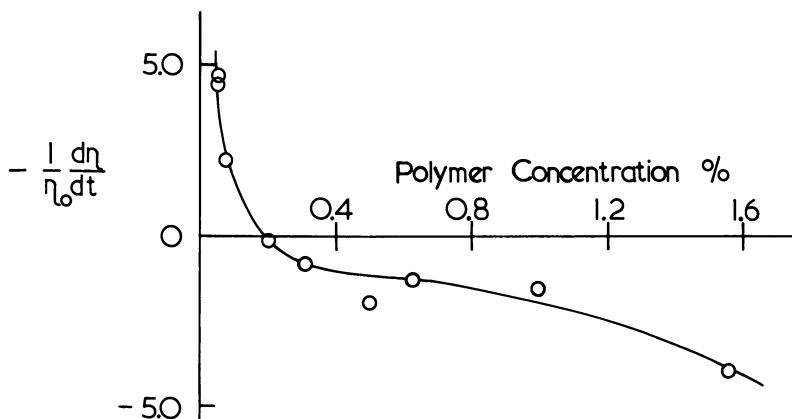


Figure 6. Rate of change of specific viscosity as a function of polymer concentration for the reaction between hexamethylene diisocyanate and  $\alpha, \omega$ -dihydroxy polystyrene in toluene at  $80^\circ\text{C}$ .  $[\text{NCO}]_0 : [\text{OH}]_0 = 1$

Figure 7 illustrates the effect of copolymer composition and of concentration, the curves obtained being at constant reaction time for runs of the same initial reactant ratio. Although different curves refer to different times and ratios, it is clear that increasing HEMA content of the polymer gave a larger viscosity change at both high and low polymer concentrations. Increasing the HEMA content also raised the polymer concentration at which the viscosity change becomes negative. At this point, the viscosity increase arising from the intermolecular reaction balanced the decrease caused by the intramolecular crosslinking and the increase in polarity of the polymer molecule.

Kuhn and Balmer (22) have shown that, as the polymer concentration is decreased, the change in viscosity becomes constant. At these concentrations it was assumed that no intermolecular reaction was taking place. A similar effect is demonstrated for the present system in Figures 7 and 8: for a given initial ratio of isocyanate to hydroxyl and a given reaction time, the polymer concentration had no effect on the viscosity change below a certain point.

The effects of reaction time and initial ratio of reactant concentrations are illustrated in Figures 9–11. In all cases increasing the isocyanate concentration over a wide range increased the change in viscosity. Comparison of Curve 5 (copolymer 2.2 moles % HEMA) in Figure 10 with

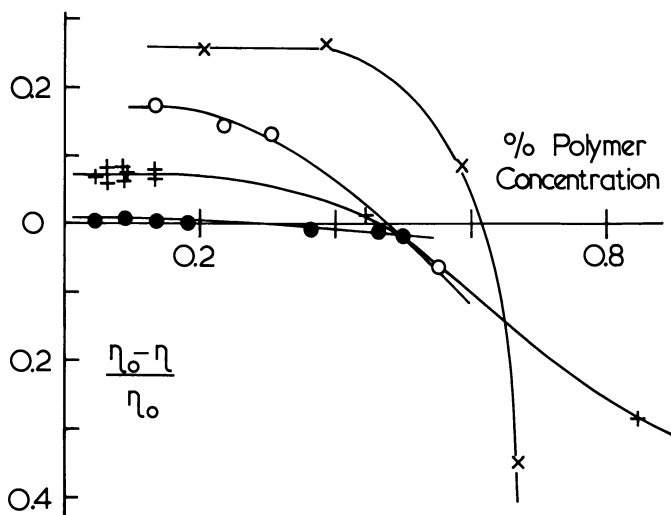


Figure 7. Viscosity changes and polymer concentration for the reaction between hexamethylene diisocyanate and styrene-hydroxyethyl methacrylate copolymers in toluene at 80°C.

	Copolymer, mole % HEMA	$[\text{NCO}]_0 : [\text{OH}]_0$	Reaction Time, min.
●	0.7	50	200
+	2.2	1	200
○	3.8	10	100
×	9.5	10	100

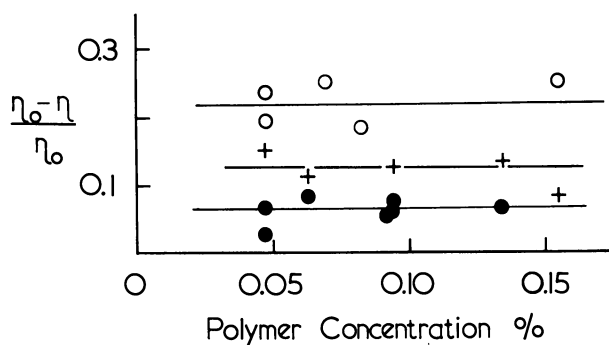


Figure 8. Viscosity changes on reaction between styrene-hydroxyethyl methacrylate copolymer (2.2 mole % HEMA) and hexamethylene diisocyanate in toluene at 80°C. At the ratios  $[\text{NCO}]_0 : [\text{OH}]_0$  of 1 (●), 3 (+) and 10 (○), the reaction times were 200, 400, and 1000 minutes, respectively



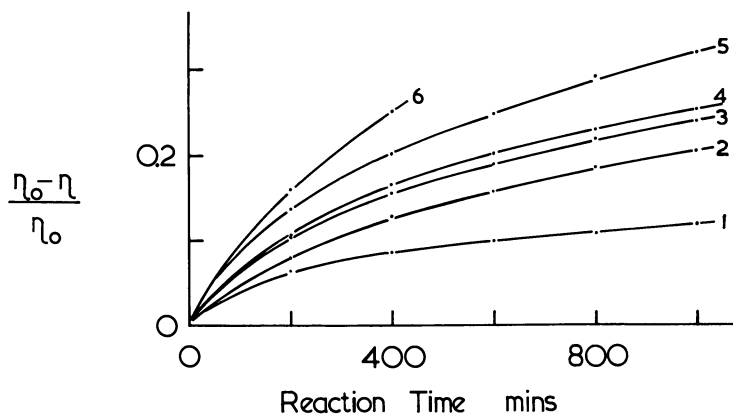


Figure 9. Effect of the initial reactant ratio on the viscosity change during reaction between styrene-hydroxyethyl methacrylate copolymer (2.2 mole % HEMA) and hexamethylene diisocyanate in toluene at 80°C. Polymer concentration 0.134% (gram/dl.)  $[\text{NCO}]_0 : [\text{OH}]_0 = 0.5, 1.1, 4.0, 18.4, 115, \text{ and } 4000$  for Curves 1-6, respectively

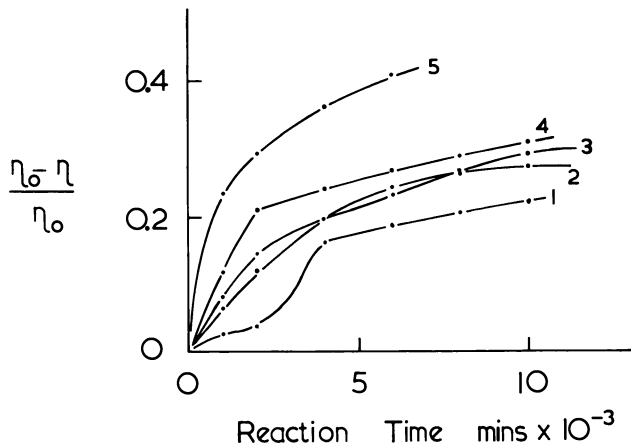


Figure 10. Change in viscosity over long times during reaction between styrene-hydroxyethyl methacrylate copolymer and hexamethylene diisocyanate in toluene at 80°C. Curves 1-4 (copolymer 0.7 mole % HEMA, 0.134% (gram/dl.) solution) had  $[\text{NCO}]_0 : [\text{OH}]_0 = 10^2, 1.5 \times 10^2, 10^3, \text{ and } 10^4$ , respectively. Curve 5 (copolymer 2.2 mole % HEMA, 0.047% (gram/dl.) solution) had  $[\text{NCO}]_0 : [\text{OH}]_0 = 10$ . All solutions have approximately the same  $[\text{OH}]_0$ .

Curves 1–4 (copolymer 0.7 mole % HEMA) shows clearly the difference in the viscosity changes between copolymers. For all curves  $[\text{OH}]_0$  was approximately the same; for Curves 1–4 increasing  $[\text{NCO}]_0$  gave an increased viscosity change, but the change for Curve 5 was even greater than that for Curve 4 despite  $[\text{NCO}]_0$  being 1/1000th as great.

At short reaction times ( $< 1000$  min.) the viscosity decreased smoothly with time, and an increase in the initial isocyanate concentration gave a faster change in viscosity (Figure 9). However, the effect of increasing the isocyanate concentration was small at concentrations greater than  $2 \times 10^{-3}M$  (Figure 11).

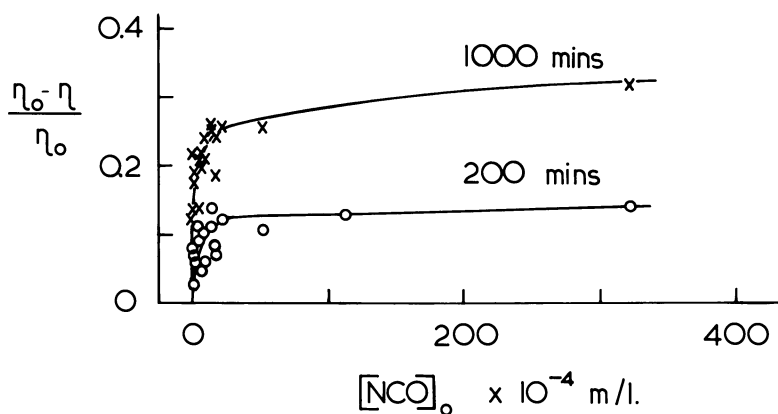
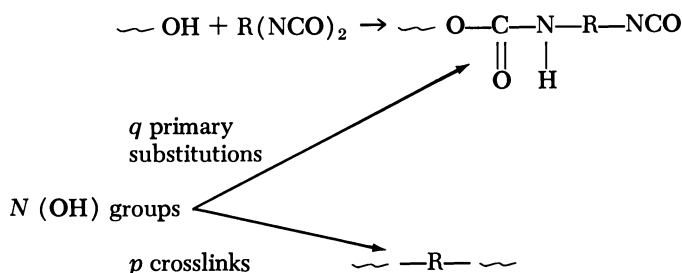


Figure 11. Effect of initial isocyanate concentration on the viscosity changes after 200 minutes (O) and 1000 minutes (X) during reaction between styrene-hydroxyethyl methacrylate copolymer (2.2 mole % HEMA) and hexamethylene diisocyanate in toluene at 80°C. Polymer concentration  $< 0.2\%$  (gram/dl.)

When the reaction time exceeded 1000 minutes, the viscosity continued to fall, but the viscosity–time curve was in some cases no longer smooth (Figure 10). Although this effect was found in a number of runs, its occurrence showed no dependence on any of the reaction variables except time, occurring most frequently between 2000 and 3000 minutes after the start of the reaction. Some of these changes may have been caused by the deposition of small particles of gel on the viscometer.

**Theoretical Effect of Isocyanate Concentration.** If very high isocyanate concentrations were used, we would expect that most of the hydroxyl groups could have reacted before internal crosslinking took place. This argument can be illustrated as follows.

Consider a polymer as providing  $N$  reactive groups within a certain volume of solution. We can then consider the rates of reaction which occur to form  $q$  primary substitutions and  $p$  crosslinks—*i.e.*,



Assuming a first-order reaction for isocyanate and hydroxyl we can then write

$$dp/dt = K_1(q - p)(N - q - p)$$

$$dq/dt = K_2(N - q - p)C$$

where  $C$  is the concentration of isocyanate in the solvent. This equation leads to

$$p = q - \frac{K_2C}{K_1} \left( 1 - \exp \frac{-qK_1}{K_2C} \right)$$

Now we observe that  $K_2C$  can be increased almost without limit whereas  $q$  can never exceed the limited number of reactive groups present in the molecule. Therefore, the situation  $qK_1 \ll K_2C$  will hold at the beginning of the reaction and when  $C$  is very large. Under these conditions it can be shown by expanding the experimental terms as far as the second power of  $\frac{qK_1}{K_2C}$  that:

$$p \approx \frac{q^2K_1}{K_2C}$$

and since  $q$  can never exceed  $q_{(\text{max})}$ , a situation could arise where the amount of crosslinking is reduced as  $C$  increases. Since this has not been observed, perhaps the necessary conditions are difficult to realize because high degrees of reaction of the hydroxyl groups are not obtained. Obviously, the isocyanate-hydroxyl reaction is slow under the experimental conditions shown in Figure 5. Nevertheless, at the highest isocyanate concentrations used some reduction of the amount of internal crosslinking might have been expected. Any possible explanation of these observations is inevitably speculative—*e.g.*, catalysis of the second isocyanate reaction by the attached urethane group might lead to the second reaction following quickly after the first. However, any properly based explanation of these times must depend on better understanding of the apparently complicated processes involved when hexamethylene diisocyanate reacts with alcohols (2, 3, 4, 13, 28).

Other considerations relate to the probable form of the polymer molecule. As the crosslinking proceeds, the volume of the coil will decline so that the internal crosslinking might be expected to accelerate. On the other hand, the occurrence of a cage-like structure might well constrain the molecular motion and slow down the later stages of the reaction substantially.

**Intrinsic Viscosity.** The intrinsic viscosities,  $[\eta]$ , of some of the crosslinked polymers (copolymer 2.2 mole % HEMA) were measured by successive dilution on the reacted solutions. Figure 12 shows that the change in  $[\eta]$  at 25°C. was, within the experimental error, related directly to the change in specific viscosity at 80°C. As Figure 13 shows, crosslinking reduced the intrinsic viscosity of the polymer solution and also altered the slopes of the lines for both  $\eta/c$  and  $\log(1 + \eta)/c$  against  $c$ .

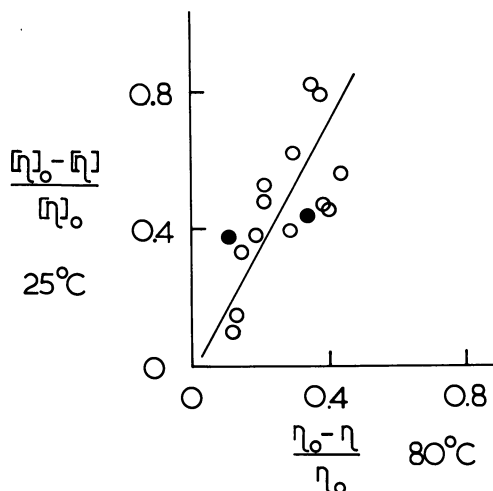


Figure 12. Intrinsic viscosity change at 25°C. and specific viscosity change at 80°C. for styrene-hydroxyethyl methacrylate copolymers, 0.7 mole % HEMA (●) and 2.2 mole % HEMA (○)

The intrinsic viscosity can be related to the specific viscosity by the equation (18):

$$\eta/c = [\eta] + k_1[\eta]^2c$$

A plot of  $k_1$  as a function of  $[\eta]$  is given in Figure 14. As  $[\eta]$  was reduced,  $k_1$  increased rapidly.

This result provides further evidence for an internal crosslinking reaction since intercrosslinking of two polymer molecules and grafting to polymer chains generally increase intrinsic viscosity.

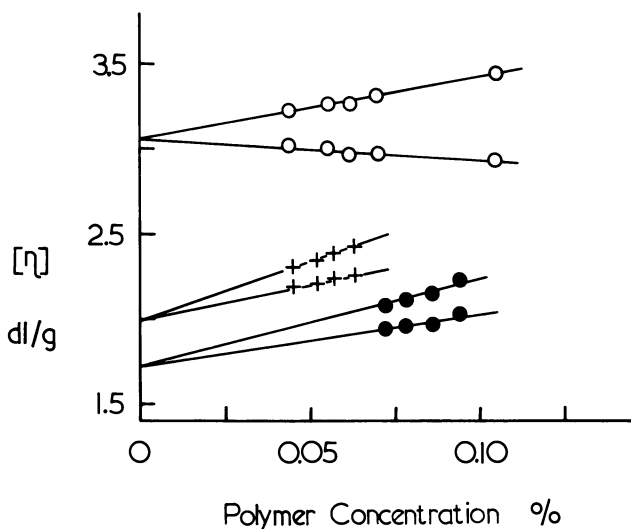


Figure 13. Viscosity functions for styrene-hydroxyethyl methacrylate copolymer (2.2 mole % HEMA) before (○) and after (●+) two typical reactions with hexamethylene diisocyanate in toluene at 80°C.

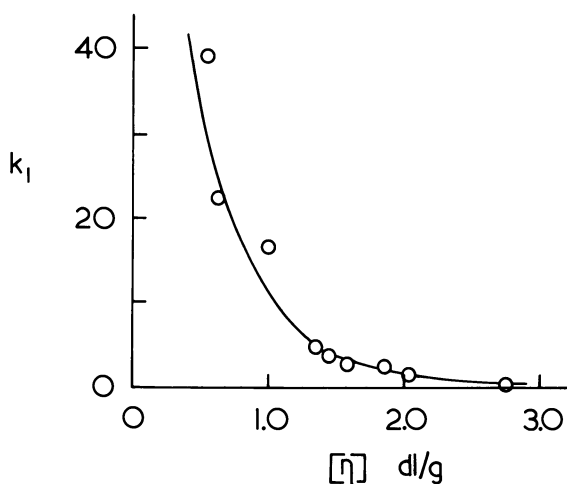


Figure 14. Huggins constant,  $k_1$ , and intrinsic viscosity in toluene at 25°C. for styrene-hydroxyethyl methacrylate copolymer (2.2 mole % HEMA) after crosslinking with hexamethylene diisocyanate in toluene at 80°C.

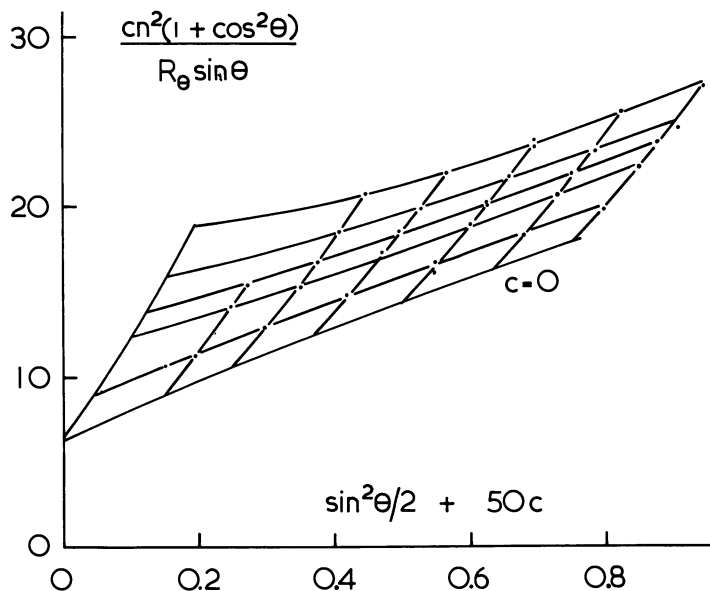
When the intrinsic viscosity of a polymer solution is reduced by changing the solvent or by introducing crosslinks during polymerization,

$k_1$  increases. Alfrey and co-workers (1) measured the intrinsic viscosity of a poly(methyl methacrylate) in solvents of varying solvent power and found that  $k_1$  increased hyperbolically with decreasing  $[\eta]$ . Similarly, for soluble polystyrene crosslinked with divinylbenzene, the higher the divinylbenzene content, the lower the intrinsic viscosity and the higher  $k_1$  (9).

**Table I. Light Scattering for Styrene-Hydroxyethyl Methacrylate Copolymer (3.8 mole % HEMA) before and after Crosslinking with Hexamethylene Diisocyanate**

$$(\eta_o - \eta)/\eta_o = 0.140$$

	<i>Untreated</i>	<i>Crosslinked</i>
$dn/dc$ ml./gram	-0.099	-0.045
$M_w \times 10^{-6}$	1.7, 1.9	1.8
$\langle R_g^2 \rangle_z M_w A.^2$	0.21, 0.26	0.02
$\langle R_g^2 \rangle^{1/2} A.$	600, 700	200
$B \times 10^4$ ml./gram	1.2, 1.7	0.97



**Figure 15. Zimm plot for a styrene-hydroxyethyl methacrylate copolymer (3.8 mole % HEMA) in toluene at 25°C. (8)**

The positive slope of the plot of  $\log(1 + \eta)/c$  against  $c$  in Figure 13 is also evidence for a large change in the polymer-solvent interaction. A similar effect has been observed for polyisobutylene by Baker *et al.* (5).

At 25°C. cyclohexane was a poor solvent for the polymer, and a plot of  $\log(1 + \eta)/c$  showed a positive slope; on raising the temperature, cyclohexane became a better solvent, and the slope decreased, becoming negative at about 45°C.

The values of  $k_1$  reported here are much higher than any found previously. Perhaps this is a result of the deposition of polymer, leading to the use of incorrect values of  $c$  in calculating  $[\eta]$  and  $k_1$ . However, even a loss of polymer of 10%—much higher than anything measured—would cause a 10% increase in  $[\eta]$  but a decrease of only 4% in  $k_1$ .

**Light Scattering.** Light scattering is often used to follow changes in the size of polymer molecules. However, the results were not accurate enough (14) to give a quantitative estimate of the change in the radius of gyration of polymer molecules having different degrees of crosslinking. However, when comparing an internally crosslinked polymer with the original material, the differences proved large enough to be measurable. (The results in Table I and Figures 15 and 16 are an illustration of what could be obtained.) The decrease in the second virial coefficient,  $B$ , was of the order that might be expected, but the change in the radius of

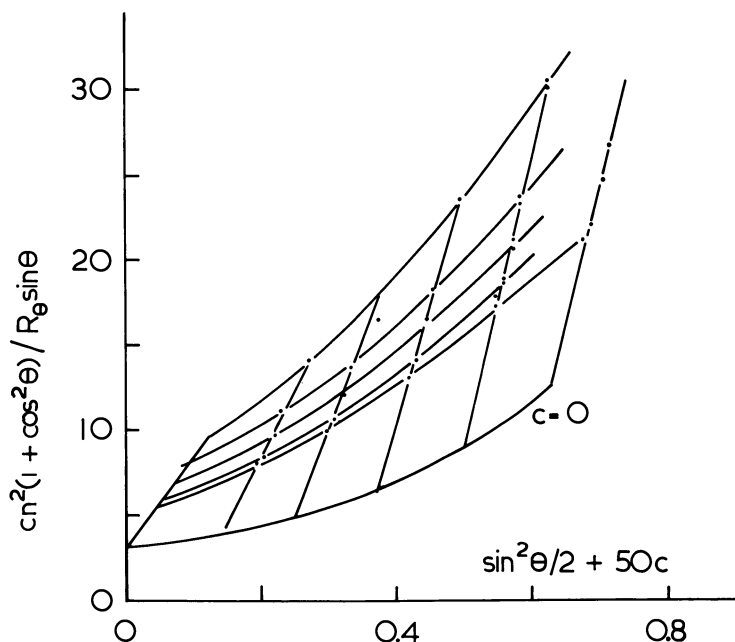


Figure 16. Zimm plot for a styrene-hydroxyethyl methacrylate copolymer (3.8 mole % HEMA) after reaction with hexamethylene diisocyanate,  $\eta_0 - \eta/\eta_0 = 0.14$ . Measurements in toluene at 25°C.

gyration was large. This may have been caused by experimental error in measuring the initial gradient of the curved zero-concentration line. Nevertheless, these results confirm that a reduction in the size of the polymer molecule and in the polymer-solvent interaction had occurred, thus confirming the findings from viscosity.

### *Acknowledgment*

The authors thank the Science Research Council for a special research assistantship for B. M. P.

## Appendix

### *Preparation and Characterization of Styrene-Hydroxyethyl Methacrylate Copolymers*

To study the internal crosslinking of styrene-hydroxyethyl methacrylate copolymers, it was necessary to prepare a range of well characterized materials containing only low concentrations of hydroxyethyl methacrylate. To ensure that the copolymers were of uniform composition, only low monomer conversions were used so that the composition of the monomer mixtures did not change appreciably during the reaction. Low polymerization temperatures were used to obtain high molecular weight copolymers.

### *Preparation of Copolymers*

**Styrene.** Styrene (Shell Chemical Co.) was purified by fractionation under reduced pressure, and the middle fraction, boiling at 30°C. at 10 mm. Hg, was retained.

**Hydroxyethyl Methacrylate (HEMA).** This compound (Rohm and Haas Co.) was supplied as a 30% solution in xylene inhibited with methyl ether hydroquinone and containing methacrylic acid and ethylene dimethacrylate (25). Xylene was removed at 10 mm. Hg, and the residue was fractionated under high vacuum. A fraction boiling at 51°-53°C. at 10<sup>-3</sup> mm. Hg was retained, having  $n_D^{22} = 1.452$ . For 96% HEMA,  $n_D^{25} = 1.451$  (25)  $n_D^{20} = 1.4520$  (30).

The purity of the monomer fraction was checked by gas-liquid chromatography. It was essential to ensure that ethylene dimethacrylate was not present in the monomer since it could cause crosslinking or branching during polymerization and hence affect the macromolecule configuration. For comparison, ethylene dimethacrylate was synthesized by a method based on that of Sigwalt (30). The chromatographic peak of the synthesized ethylene dimethacrylate did not occur in the chro-



matogram of the HEMA fraction, and the hydroxyethyl methacrylate used in the copolymerization was, therefore, assumed to be free from ethylene dimethacrylate.

Styrene copolymers were prepared with a range of monomer feed compositions from 0 to 6 mole % HEMA. The monomers were weighed into flasks, and dissolved gases were removed by repeated freezing with methanol–solid  $\text{CO}_2$  and thawing under high vacuum. The flasks were sealed and heated at  $40 \pm 1^\circ\text{C}$ . for up to 14 days. By this time about 7% conversion had taken place, and the viscosity of the mixture had increased noticeably. The polymer solutions were diluted with methylene chloride, and the polymers were precipitated by the addition of methanol. After washing thoroughly with methanol, the polymer was dried to constant weight at  $40^\circ\text{C}$ . and  $10^{-3}$  mm. Samples were stored in closed jars in a dry atmosphere and were redried occasionally.

The average rate of polymerization was  $2.4 \times 10^{-2}\%$   $\text{hr}^{-1}$  and did not differ significantly over the range of feed compositions.

### Characterization of Copolymers

**Chemical Analysis.** The copolymers were acetylated by refluxing with acetic anhydride in pyridine, and the hydroxyl content was estimated by titration with alkali of the acetic acid produced during acetylation and by hydrolysis of excess anhydride. The procedure adopted was based on that described by Sorensen and Campbell (33). The results of the analyses are given in Table A. At the three lower concentrations of hydroxyl groups all results were averaged from five or more measurements.

**Infrared Analysis.** Polymer solutions of about 1% concentration were prepared in spectroscopic grade chloroform. The absorbance of the band at  $5.8\mu$  ( $\text{C}=\text{O}$  stretching vibration) was measured on an Infracord 137 as a function of polymer concentration and of cell path length. This gave an apparent extinction coefficient for each polymer. From the results of the chemical analyses, the following equation was obtained, which relates the apparent extinction coefficient to the copolymer composition:

$$\epsilon_{\text{app}} = 0.0069 + 0.0370 c'$$

where  $c'$  is the concentration in mole % of HEMA in the copolymer.

**Table A. Composition of Styrene–Hydroxyethyl Methacrylate Copolymers Determined by Chemical Analysis**

Monomer Feed, mole % HEMA	Copolymer Composition mole % HEMA
0.51	$0.68 \pm 0.1$
1.12	$2.2 \pm 0.2$
2.78	$4.1 \pm 0.5$
6.0	9.5

The monomer reactivity ratios could be calculated from Table A and other values by the method of Fineman and Ross (10), but owing to the narrow range of compositions studied only the value of  $r_2$  (referring to the styrene radical) was significant. A value of 0.7 was obtained which may be compared with 0.52 for styrene–methyl methacrylate, and a value of 0.41 calculated from the  $Q - e$  values for hydroxyethyl methacrylate supplied by Rohm and Haas (25).

### *Solution Properties of Copolymers*

**Solution Viscosity.** The intrinsic viscosities  $[\eta]$  of the copolymers were measured for solutions in dry toluene at 25°C. by dilution in an Ubbelohde suspended-level viscometer. Conventional plots of  $\eta/c$  (18) and  $\log(1 + \eta)/c$  (29) were found to be nonlinear for all copolymers where  $\eta$  is the specific viscosity. To get accurate values of the intrinsic viscosities and of the Huggins constants  $k_1$  and  $k_2$ , triple plots were drawn as recommended by Heller (16). These gave the intercept  $1/[\eta]$ , and  $k_1$  and  $k_2$  were determined directly from the initial slopes of the plots

$$c/\eta = 1/[\eta] - k_1c$$
$$c/\log(1 + \eta) = 1/[\eta] + k_2c$$

Values of  $[\eta]$  are given in Table C. The slope constants  $k_1$  and  $k_2$  had values of  $0.32 \pm 0.03$  and  $0.15 \pm 0.03$ , respectively, for all the copolymers studied.

Provided that similar viscosity–molecular weight relationships hold for copolymers of different composition, the variation in viscosity might be caused by a variation in the molecular weight of the polymers. However, the hydroxyethyl methacrylate molecule contains both hydroxyl and carbonyl groups between which interaction such as hydrogen bonding might occur. In a nonpolar solvent—*e.g.*, toluene, the existence of an interaction of this type might be expected to lead to a more tightly coiled molecule than for polystyrene. For copolymers of the same molecular weight, the higher the HEMA content, the lower would be the viscosity. The molecular weights of the copolymers as determined by light scattering are discussed later.

However, to illustrate the effect of solvent on viscosity, we measured the intrinsic viscosities of three copolymers in a polar solvent—benzyl alcohol at 80°C. The two solvents are compared in Table B. Although the intrinsic viscosities of the hydroxyl-containing copolymers are similar in the two solvents, the value for pure polystyrene is much reduced in the polar solvent. This provides indirect evidence for the existence of a smaller coil volume for the copolymer molecules in the nonpolar solvent.

**Table B. Intrinsic Viscosities of Styrene-Hydroxyethyl Methacrylate Copolymers in Polar and Nonpolar Solvents**

Copolymer Composition, mole % HEMA	$[\eta]$ in Toluene, 25°C., dl./gram	$[\eta]$ in Benzyl Alcohol, 80°C., dl./gram
0	5.19	2.27
3.8	2.12	2.07
9.5	1.42	1.51

**Light Scattering.** Light scattering measurements were made on toluene solutions of the copolymers at 4358 Å. and 25°C. using a Sofica photogonio-diffusiometer. Solute refractive indices as a function of polymer concentration were measured in a differential refractometer (Polymer Consultants, Ltd.).

Table C gives the results of several series of measurements. The absolute value of  $dn/dc$  decreases with increasing HEMA content of the polymer. However, it was difficult to obtain reproducible results owing to the absorption of water vapor from the air. Where the angle and concentration lines of Zimm plots are nonlinear, there can be considerable error in determining the common zero intercept: for polystyrene, where this is the case, the error in the intercept gave a variation of  $\pm 30\%$  in the molecular weight. However, for the copolymers the variation was of the order of  $\pm 10\%$ . The error in determining the radius of gyration and

**Table C. Analysis of Toluene Solutions of**

HEMA, mole %	$[\eta]$ dl./gram 25°C.	$M_n \times 10^{-6}$ (osmotic pressure)	$-dn/dc$ , cc./gram
0 <sup>a</sup>	5.19		0.117
0.7	4.16	1.2 <sup>b</sup>	0.113
1.3	4.71		0.108
2.2	3.05		0.106 <sup>c</sup>
3.8	2.12	0.65 0.59 <sup>b</sup>	0.099
9.5	1.42		0.086

<sup>a</sup> Values for polystyrene from the literature for comparison; refractive index increment  $dn/dc = 0.112-0.114$  [Polymer Handbook (Interscience)]. Second virial coefficient  $B = 3.2 \times 10^{-4}$  for  $M_w = 2.5 \times 10^6$  (6).

of  $B$  varied between  $\pm 100\%$  and  $\pm 30\%$ . Table C gives the average values of molecular weight,  $\langle R_g^2 \rangle_z / M_w$  and the second virial coefficient  $B$ .

Although the intrinsic viscosities of the toluene solutions apparently decrease with increasing hydroxyl content of the copolymers, no molecular weight estimates can be made from them since the viscosity-molecular weight relationships are not known for the copolymers. However, for polystyrene the equation  $[\eta]_v = 1.44 \times 10^{-4} M_v^{0.704}$  (37), leads to a viscosity average molecular weight of  $3.0 \times 10^6$  which is in reasonable agreement with the weight average as determined by light scattering.

Both  $\langle R_g^2 \rangle_z / M_w$  and  $B$  show the same trend with increasing hydroxyl content of the copolymer, falling rapidly in the range 0–4 mole % HEMA but showing only a small decrease for the addition of a further 5 mole % HEMA. For a flexible polymer, it has been calculated (35) that  $B$  should decrease from  $5 \times 10^{-4}$  in a good solvent to zero in a poor solvent at the  $\theta$  temperature. There is ample experimental evidence to confirm this for a single polymer in a series of solvents (19). Here we appear to have produced the same effect by varying the composition of the polymer rather than of the solvent.

The value of the radius of gyration for polystyrene derived from these measurements is, at 1385 Å., somewhat higher than previously reported; for example, for a polystyrene of molecular weight  $4 \times 10^6$ , Nottley and Debye (24) obtained a radius of 840 Å.

### Styrene-Hydroxyethyl Methacrylate Copolymers

*Light Scattering at 25°C.*

$M_w \times 10^{-6}$	$B, \text{cc./gram} \times 10^4$	$\langle R_g^2 \rangle_z / M_w, \text{Å.}^2$	$\langle R_g^2 \rangle^{1/2}, \text{Å.}$	$R_g, \text{Å. from viscosity}$
4.3	3.1	0.45	1385	910
3.3	3.4	0.40	1130	780
5.8	3.7	0.49	1680	950
6.3	2.8	0.30	1380	1000
8	2.7	0.22	1310	950
1.7	1.2	0.21	600	510
1.9	1.7	0.26	700	500
7.2	0.7	0.22	1240	660
5.3	0.8	0.30	1280	620

<sup>b</sup> Values determined by K. Riches (Shell Research, Woodstock) using a Mecrolab membrane osmometer.

<sup>c</sup> Interpolated.

For comparison, the radius of gyration can also be calculated from the viscosity and the molecular weight of the polymer by use of the Flory-Fox equation (11):

$$[\eta] = \Phi (6R_g)^2/M$$

where  $\Phi$  is Flory's universal constant. This depends on the interaction between solvent and polymer and has been related to the second virial coefficient,  $B$ , by Krigbaum and Carpenter (20). Appropriate values of  $\Phi$  are, for the polymer containing 9.5 mole % HEMA  $2.1 \times 10^{21}$  and for all the other copolymers  $2.0 \times 10^{21}$ . The radii of gyration obtained by this method are given in Table C in the last column. The value of 912 Å. for polystyrene is in accord with previous results.

Two explanations of our high values are possible. First, aggregation might be taking place. Trementozzi and co-workers (36) obtained results for a polystyrene containing hydroxyl groups which show some similarity to those found in the present work. For a polymer which they estimated contained less than 0.1% by weight of hydroxyl groups, the light scattering of a toluene solution at 25°C. gave a weight average molecular weight of  $4.5 \times 10^6$  and a value of  $B$  of  $1.3 \times 10^{-4}$ . They also found that for the unfractionated polymer the light scattering of a dioxane solution at 25°C. gave a molecular weight of only  $0.72 \times 10^6$ . After acetylation, the molecular weight in both toluene and dioxane was  $0.76 \times 10^6$ , and the virial coefficients increased considerably. It was suggested that the low value of  $B$  was caused by intramolecular attraction and that the high molecular weight in toluene was caused by aggregation.

Since our aim is to crosslink the copolymers under conditions where the polymer is present as single molecules, it would be highly undesirable to have aggregates in the solutions. In dry dioxane at 25°C. the following results were obtained for the copolymer containing 9.5 mole % HEMA:

$$\begin{array}{ll} \bar{M}_w & 7.2 \times 10^6 \\ \langle R_g^2 \rangle_z / \bar{M}_w & 0.46 \text{ Å.}^2 \\ B & 6.3 \times 10^{-4} \text{ cc./gram} \end{array}$$

The increase in  $B$  is what might be expected for a solvent of higher dielectric constant. The most significant point in these results is that there is no evidence of a decrease in molecular weight. It is, therefore, unlikely that large hydrogen-bonded aggregates are present in the solutions.

The alternative and, in our view, more probable explanation of the high value of  $R_g$  for polystyrene lies in the nature of the molecular weight distribution of the polymers. The radius of gyration measured by light scattering is a  $z$ -average quantity and is higher for a polymer of broad

molecular weight distribution than for a monodisperse polymer. The number average molecular weight,  $M_n$  was therefore determined for the copolymer containing 3.8 mole % HEMA by measuring osmotic pressure in toluene solution using an automatic membrane osmometer (Hallikainen Instruments) and was found to be  $6.5 \pm 0.5 \times 10^5$  compared with a weight average of  $1.8 \times 10^6$  (see Table C). This gave a weight-to-number average ratio of about 3.0 for the two copolymers measured, indicating that they have a relatively broad molecular weight distribution.

We therefore conclude that the styrene-hydroxyethyl methacrylate copolymers used in this work have a relatively broad molecular weight distribution and that the effect of increasing hydroxyl content on the properties of dilute toluene solution is to contract the polymer molecule and decrease the polymer-solvent interaction without causing appreciable aggregation by intermolecular hydrogen bonding.

### Literature Cited

- (1) Alfrey, T., Goldberg, A. I., Price, J. A., *J. Colloid Sci.* **5**, 251 (1950).
- (2) Baker, J. W., Holdsworth, J. B., *J. Chem. Soc.* **1947**, 713.
- (3) Baker, J. W., Gaunt, J., *J. Chem. Soc.* **1949**, 9, 19, 27.
- (4) Baker, J. W., Davies, M. M., Gaunt, J., *J. Chem. Soc.* **1949**, 24.
- (5) Baker, W. O., Mason, W. P., Heiss, J. H., *J. Polymer Sci.* **8**, 129 (1952).
- (6) Breitenbach, J. W., Cabler, H., *Makromol. Chem.* **37**, 53 (1960).
- (7) Butler, G. B., Ingley, F. L., *J. Am. Chem. Soc.* **73**, 894 (1951).
- (8) Butler, G. B., Angelo, R. J., *J. Am. Chem. Soc.* **79**, 3128 (1957).
- (9) Cragg, L. H., Manson, J. A., *J. Polymer Sci.* **9**, 205 (1952).
- (10) Fineman, M., Ross, S. D., *J. Polymer Sci.* **5**, 259 (1950).
- (11) Flory, P. J., Fox, T. G., *J. Am. Chem. Soc.* **73**, 1904 (1951).
- (12) Gibbs, W. E., Barton, J. M., "Kinetics and Mechanisms of Polymerization," Vol. 1, "Vinyl Polymerization," G. E. Ham, Ed., p. 59, Arnold, London, 1967.
- (13) Greenshields, J. N., Peters, R. H., Stepto, R. F. T., *J. Chem. Soc.* **1954**, 5101.
- (14) Haward, R. N., Parker, B. M., White, E. F. T., Appendix to this paper.
- (15) Haward, R. N., Simpson, W., *J. Polymer Sci.* **18**, 440 (1955).
- (16) Heller, W., *J. Colloid Sci.* **9**, 547 (1954).
- (17) Hopkins, W., Ph.D. Thesis, Manchester, 1967.
- (18) Huggins, M. L., *J. Am. Chem. Soc.* **64**, 2716 (1942).
- (19) Krigbaum, W. R., Flory, P. J., *J. Am. Chem. Soc.* **75**, 1775, 5254 (1953).
- (20) Krigbaum, W. R., Carpenter, D. K., *J. Phys. Chem.* **59**, 1166 (1955).
- (21) Kuhn, W., *Kolloid-Zeit.* **68**, 2 (1934).
- (22) Kuhn, W., Balmer, G., *J. Polymer Sci.* **57**, 311 (1962).
- (23) Kuhn, W., Majer, H., *Makromol. Chem.* **18**, 239 (1955).
- (24) Nottley, N. T., Debye, P., *J. Polymer Sci.* **17**, 99 (1955).
- (25) Rohm and Hass Co., Special Products Department, *Bull. SP-261*.
- (26) Ruziska, L., Salomon, G., Meyer, K. E., *Helv. Chim. Acta* **17**, 882 (1934).
- (27) Salomon, G., *Trans. Faraday Soc.* **32**, 153 (1936).
- (28) Sato, M., *J. Am. Chem. Soc.* **82**, 3893 (1960).
- (29) Schulz, G. V., Blaschke, J., *Prakt. Chem.* **158**, 130 (1941).
- (30) Sigwalt, P., *Bull. Soc. Chim. France* **1959**, 54.

- (31) Simpson, W., Holt, T., Zetie, R. J., *J. Polymer Sci.* **10**, 489 (1953).
- (32) Simpson, W., Holt, T., *Proc. Roy. Soc.* **A238**, 154 (1956).
- (33) Sorenson, W. R., Campbell, T. W., "Preparative Methods of Polymer Chemistry," p. 134, Interscience, New York, 1961.
- (34) Stockmayer, W. H., Weil, L. L., "Advancing Fronts in Chemistry," B. S. Twiss, Ed., Rheinhold, New York, 1945.
- (35) Tanford, C., "Physical Chemistry of Macromolecules," p. 210, Wiley, New York, 1961.
- (36) Trementozzi, Q. A., Steiner, R. F., Doty, P., *J. Am. Chem. Soc.* **74**, 2070 (1952).
- (37) Williamson, G. R., Carrington Plastics Laboratory, private communication.
- (38) Ziegler, K., *Ber. A* **67**, 139 (1934).

RECEIVED April 22, 1968.

## Expandable Polystyrene Processes

A. R. INGRAM

Koppers Company, Inc., Research Department, Monroeville, Pa.

*Various processes are reviewed for making expandable polystyrene which can be molded or extruded into foam. Most processes employ aqueous suspension systems in which pentanes are introduced before, during, or after polymerization. Water-free systems may also be used. The requirements for particle size and shape are critical. In suspension polymerization, bead size is controlled by the agitation and dispersing agents. To reduce off-size particles, prescreened polystyrene beads or chopped filaments may be impregnated. Since pentane is not a solvent for polystyrene, its diffusion is hastened by raising the temperature and/or by adding solvents. Chemical and physical modifications of expandable polystyrene processes are considered in terms of expandability, cell structure, heat resistance, flammability, and solvent resistance of foams.*

In 1967 the total sales of polystyrene foam in the United States were about 193 million pounds (78). Foams molded or extruded from expandable polystyrene amounted to 145 million pounds. The recent growth rate of polystyrene foam in the United States is depicted in Figure 1. The lower section represents expandable polystyrene.

Expandable polystyrene consists of particles of styrene polymers with volatile organic liquids trapped among the rigid chains. The most significant property responsible for the commercial acceptance of expandable polystyrene is its ability to be steam-molded into such useful, light-weight, low-cost, closed-cell foams as beverage cups, packages, picnic chests, and ice buckets, as well as insulation board (121). The molding of foams is done in two steps. First, the particles are expanded in a continuous upward flow of steam to yield free-flowing individual pieces of foam (94). Then, after an aging period of several hours during which air diffuses into the expanded particles, they are placed in a slightly vented mold. The particles are then heated by steam at super-



atmospheric pressure injected into the mold so they expand to fill the empty spaces and fuse together. The molding operation is completed by circulating or spraying cold water in the jacket of the mold until the foam no longer exerts pressure. Expandable polystyrene may also be extruded into films, sheets, and boards.

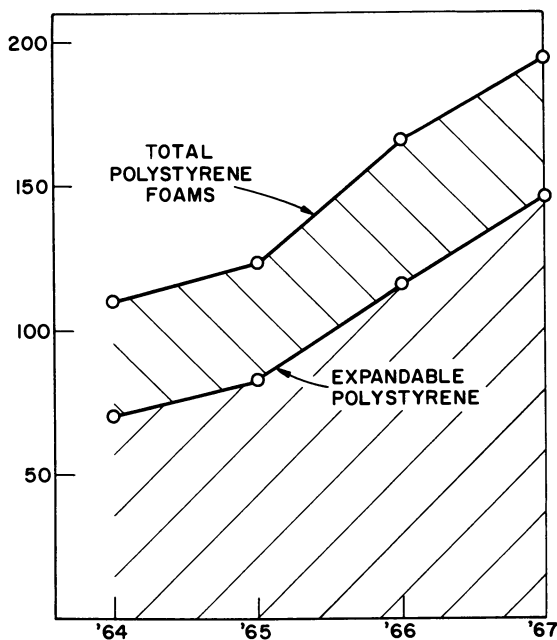


Figure 1. Four-year sales record of polystyrene foams (million pounds)

### Preparing Expandable Polystyrene

**Diffusion of Blowing Agents into Polystyrene.** IN CONTACT WITH ORGANIC LIQUIDS IN THE ABSENCE OF WATER. *Particles Plus Excess Liquid.* The first patent on the preparation of expandable polystyrene containing volatile hydrocarbons, applied for in Great Britain in 1944, covers the soaking of polystyrene particles, held in a cheesecloth bag, in a solution comprising a nonsolvent, petroleum ether (90–99 volume %), and a solvent (10–1%) such as acetone, ethyl acetate, or benzene (126). At 20°–25°C., impregnation was complete within 0.5 to 12 hours, depending on particle size and composition. A mixture of diethyl ether and ethanol is also claimed as rendering polystyrene expandable after three days of soaking therein (127). Nonvolatile additives may be incorporated in the polystyrene, hastening its impregnation by *n*-pentane, and avoiding the

use of solvents as disclosed above. Cited additives are rubbery isobutylene polymers, rubbery diene polymers (*e.g.*, butadiene-styrene elastomers), fatty acid salts or esters (*e.g.*, stearates), organic insoluble pigments, and inorganic pigments smaller than  $5\mu$  in diameter (22, 87). Ground polystyrene, screened through an 8-mesh sieve and onto a 20-mesh sieve, was stirred with an equal weight of *n*-pentane. In 24 hours the particles absorbed 4.7% by weight; in 48 hours, 7.7%. However, the presence within the polystyrene of intimately mixed 1% calcium carbonate of a particle size of  $0.1\mu$  increased the 24-hour absorption of *n*-pentane to 7.8% (87). While the above modifications of the polymer decrease absorption time effectively, they also increase the rate at which *n*-pentane diffuses out of the polymer, thereby shortening shelf life.

A difficulty with the above steeping processes is that the particles become softened and tend to agglomerate. Therefore, they are stirred vigorously and kept at relatively low temperatures. The addition of finely divided solids to the dispersion avoids agglomeration and permits the use of higher temperatures to hasten impregnation. Thus, a slurry of 24% polystyrene in pentane was stabilized by 5% (polystyrene basis) calcium carbonate and 2% calcium phosphate. After stirring at  $90^{\circ}\text{C}$ . for 3 hours, the beads contained 10% pentane and were not stuck together (120). By another process a 50% slurry in *n*-pentane was stabilized by 1% of calcium silicate and stirred for 0.5 hour at  $40^{\circ}\text{C}$ . and 40 p.s.i.g. under nitrogen (43). This product contained 8% *n*-pentane.

A mechanical device for impregnating polystyrene placed in the annular space between two cylinders has been disclosed (30).

*Particles Plus the Minimum Amount of Liquid.* A process without a dilution medium or antiagglomeration agent would be desirable. The first such process involves the continual rolling for 32 hours at  $70^{\circ}\text{C}$ . of a closed vessel containing 1000 parts of polystyrene particles with a solution comprising 65 parts of hexane, 5 parts of benzene, and 15 parts of methanol (122). Another process involves impregnation under carbon dioxide well above the softening point of the polymer: 900 parts of polystyrene and 80 parts of hexane under carbon dioxide at 10 atm. for 4 hours at  $140^{\circ}\text{C}$ . (125). This product was broken apart after cooling.

The absorption of butane into polystyrene proceeds more rapidly than pentane or hexane. Thus, the addition of the required amount (7%), plus an excess only for air-purging, to polystyrene (or to rubber-modified polystyrene) particles in a sealed container provides useful expandable polystyrene after agitation for 24 hours at room temperature (27). If the butane is mixed with a noncombustible gas of lower density, the explosion hazard is avoided (50).

*Molded Objects Immersed in Liquids.* Molded, non-foamed articles, such as drinking cups from rubber-modified polystyrene, are immersed

in absorbable liquid blowing agents. The molding is then heated, creating an insulating surface according to the location and amount of heat, as well as the extent of absorption of liquid (3, 107).

**IN CONTACT WITH ORGANIC VAPORS.** Finely divided polystyrene beads (22–48 mesh) supported on a screen suspended above the surface of pentane in a closed vessel absorb as much as 9.2% in 2 days at 30°C. In the same way, a styrene–acrylonitrile copolymer is rendered expandable by exposure to vapors of a 90/10 mixture of pentane and methylene chloride (5).

A graft copolymer sheet of 5 parts of rubber (25/75 styrene/butadiene) and 95 parts styrene may be kept for a week at  $-70^{\circ}\text{C}$ . among “dry ice” (carbon dioxide) to make it expandable (47).

**IN AQUEOUS SLURRIES.** Patent applications on the diffusion of pentane fractions of petroleum into slurries of polystyrene beads in water at elevated temperatures were made in both the United States and Germany in 1953. In the U.S. application the suspension was stabilized by a finely divided calcium phosphate and an anionic surfactant, and impregnation was carried out at 90°C. (24). In the German application, the suspension was stabilized by an emulsifying agent alone, and the impregnation was conducted at 80°C. (19). To permit the introduction of butanes rather than pentanes as blowing agent without creating excessive pressure in the reactor, methylene chloride or ethyl acetate (strong solvents) were first added to the slurry, then the polystyrene beads readily absorbed butane within 5 hours at room temperature (20). Reactor pressure was 30 p.s.i.g. The impregnation of polystyrene in aqueous suspension can be performed without a pressure vessel if a mixture of equal parts of petroleum ether and ethyl acetate is added slowly to the bead slurry (72). Addition time is 6 hours; soaking time, 18 hours. The use of poly(vinyl alcohol) as the sole or partial suspending agent is claimed to permit the rapid impregnation by pentane of polystyrene slurries at rather high temperatures—115° and 120°C. (49, 114). Instead of charging beads to be impregnated with pentane, one may charge ground or chopped strands of polystyrene. When the impregnation is conducted at very high temperatures, 130°–135°C., these particles become rounded, and the suspension is stable provided prescribed suspending agents (a mixture of carboxymethyl cellulose and the ammonium salt of sulfonated poly(vinyltoluene) are used. Pentane is added under pressure at the elevated temperature, preferably in a slow stream or by several small additions (128). In another modification of this process, the length/diameter dimensions of the cylindrical particles—*e.g.*, about 0.1-inch long  $\times$  0.02-inch diameter—are such that they become spherical as a result of being heated in a suspension stabilized by basic magnesium carbonate at

130°–135°C. The temperature of the suspension is then reduced, and pentane is added at a lower temperature, 118°C. (65).

In a process for obtaining simultaneously a rapid rate of diffusion of pentane and good foam-forming qualities, the autogenous pressure of the vessel is maintained constant by increasing temperature in the range 90°–120°C. within four hours (93).

**Polymerization of Styrene Solutions of Volatile Hydrocarbons.**  
ADDITION OF HYDROCARBON BEFORE POLYMERIZATION. *Bulk Polymerization.* Expandable polystyrene was prepared inadvertently in 1945 in an attempt to bulk copolymerize 10% isobutylene with styrene. The product formed a low density foam when heated (96). An early method (1950) for rendering polystyrene expandable by petroleum ether was to dissolve 6 parts of petroleum ether in a 40% solution of polystyrene in benzoyl peroxide-catalyzed styrene and to hold the mass for 28 days at 32°C. (124). In a recent version of this process, the monomer (chlorostyrene) and blowing agent (trichlorofluoromethane) in a poly(vinyl fluoride) bag were irradiated with  $\gamma$ -rays (105).

*Suspension Polymerization.* The first patent application on polymerizing a suspended styrene solution of petroleum ether (7%) was made in Germany in 1951. The suspending agent was poly(vinyl 2-pyrrolidone), the initiator was benzoyl peroxide (0.7%), and the temperature of polymerization was 82°C. (123). These products were used to develop the popular process for steam molding expanded beads (121). This system was improved by using special initiators to reduce the residual monomer content, in one case with a mixture of azobisisobutyronitrile and di-*tert*-butyl peroxide, and in the other by using a difunctional peroxide (17, 81). An objectionable feature of these processes is the formation of blisters, craters, and pock marks by pentane escaping from the particles at a critical viscosity during the latter stage of polymerization. This effect can be reduced greatly by increasing the pressure in the polymerization vessel by at least one-fifth of the original pressure by introducing an inert gas such as nitrogen, when the polymerization has reached the bead identity point—*i.e.*, where bead growth by coalescence has ceased (138).

ADDITION OF BLOWING AGENTS TO STYRENE SOLUTIONS OF POLYSTYRENE. If the pentane is added to a suspension polymerization of styrene after the bead identity point has been reached, the formation of blisters is avoided and the diffusion of pentane into the bead is rapid. Thus, the two objections to the “pentane-in-monomer” process and the “post-polymerization impregnation” processes are avoided (31, 119). The same system has also been used to introduce normally gaseous blowing agents, such as butane, propane, *sym*-dichlorotetrafluoroethane, propylene, butene, and butadiene (51, 91, 115).

The styrene monomer first may be polymerized to about 65% conversion in the absence of water, and then the blowing agent (cyclopentane) may be added with additional peroxide. This solution is suspended in water in the presence of potato starch, and the polymerization is finished (74). By another modification a styrene solution of "waste" polystyrene and peroxide is suspended by poly(vinyl alcohol) in water, and pentane is added to the suspension after the solids content of the oil phase is greater than 70% (133). Polystyrene particles may also be suspended in water by a mixture of poly(vinyl alcohol) and a phenyl sulfonate and then a mixture of equal parts of pentane and catalyzed styrene (8% each on polymer) is diffused into the polymer. The temperature is elevated, and the polymerization is completed (23).

**Suspension Polymerization Systems for Controlling Particle Size.** SUSPENDING AGENTS. Both types of suspension stabilizers—the finely divided water-insoluble solids and the soluble film formers—have been used extensively to prepare styrene polymers of a particle size between about 10 and 40 mesh. Examples of such materials are listed below:

**Finely Divided Solids:**

- Tricalcium phosphate with anionic surfactants (48)
- Tricalcium phosphate with sodium  $\beta$ -naphthalene sulfonate and sodium polyacrylate (35)
- Zinc oxide without or with ammonia (33, 34)
- Silica plus a diethanolamine adipic acid polymer (56)
- Bentonite plus gelatin (4)

**Water-Soluble High Molecular Weight Polymers:**

- Poly(vinyl 2-pyrrolidone) (123)
- Vinyl 2-pyrrolidone copolymers with alkyl acrylates (16)
- Poly(vinyl 2-pyrrolidone) (123)
- alkylnaphthalene sulfonic acid (97)
- Methyl cellulose (100)
- Hydroxyethyl cellulose (58)
- Ammonium poly(vinyltoluene sulfonate) plus anionic surfactant (66)

**AGITATION SYSTEM.** The particle size of polystyrene made in a suspension polymerization is influenced not only by the type of suspending agent but also is subject to mechanical factors such as shape and size of the vessel and speed of agitation. A review of such mechanical factors in large reactors (50 and 500 liters) was published recently (137).

**Deposition of Expandable Polystyrene from Solution.** Polystyrene is dissolved in a miscible blend of two liquids (80/20 pentane/dimethylformamide), and this solution is precipitated by addition to a non-solvent (methanol), whereby particles of polystyrene containing pentane are precipitated out (116).

The polymer may be dissolved in a water-immiscible liquid, then suspended into droplets, and the resulting suspension is partially stripped until a suspension of expandable particles is obtained. For example, a

solution of chlorinated polystyrene in methylene chloride is suspended by poly(vinyl 2-pyrrolidone), and the resulting suspension is simultaneously sparged and agitated by nitrogen (70).

**Quenched-Pellet Process.** This process consists of extruding a mixture of polystyrene and pentanes, chilling the extrudate to avoid foaming, and chopping the strand into particles of the desired size. The following features were disclosed in the first patent applications: (1) extrusion into a water bath at 50 p.s.i.g. pressure; (2) extrusion into a water bath to cool the strand instantly to below 50°C. at atmospheric pressure; (3) to hold the quenched pellets at an elevated temperature (50°C. to the plasticizing temperature) to relieve orientation strains (45, 77, 104). In the above processes pentane was injected into a molten stream of polystyrene. Several improvements and modifications of the apparatus to make the quenched pellets have been made—extrusion through a die made of or lined with polytetrafluoroethylene to broaden the permissible temperature range of extrusion (6); a conveyor system for passing continually the freshly chopped pellets through a normalizing bath to relieve orientation strains at 65°–85°C. (32); an extruder to facilitate mixing of pentane with polystyrene (109); replacement of the water bath by a chilled roll containing grooves in which the extrudate is cooled (21). Orientation strains were relieved by short exposure (0.5–15 sec.) above the heat plasticizing temperature (77°–99°C.) (28). The cell size of foam made from quenched pellets was reduced substantially by instituting cyclic shock waves in the unfoamed extrudate (68). In another method the pellets were treated to reduce cell size either by storing them at –10°C. or by agitating them until they appeared cloudy (73). The charge to the quenched pellet extruder may be in the form of expandable beads (69). However, because spherical beads tend to slip around the screw in the feed section, they do not extrude smoothly without “stuffing.” This problem was overcome by feeding expandable disks obtained from a modified suspension polymerization process (62). Considerable quantities (2–40%) of a light weight, finely divided, inexpensive filler, especially Wollastonite, may be incorporated without harming the foaming properties substantially (129). The quenched-pellet operation may be incorporated as the finishing step to a bulk polymerization of a styrene solution of pentane (83). The feed to the extruder also may be a mixture of equal parts of polystyrene particles and granulated polystyrene containing about 12% petroleum ether, impregnated with the assistance of methylene chloride (85). A particular feature of the quenched pellet process is its facility for incorporating colorants and nucleating agents. The latter additives are discussed later.

**Water-in-Monomer Polymerizations for Open-Celled Foams.** Porous polymers or mixed polymers of styrene are prepared by polymerizing the

monomer with water emulsified therein. These foams are open-celled rather than the typical closed-cell structure of the foams discussed above (14, 131).

### Composition of Expandable Polystyrene

**The Blowing Agent.** The blowing agent for most commercial expandable polystyrene has consisted of hydrocarbons obtained from the pentane boiling range of petroleum. Expandable polystyrene typically contains about 6.3 to 7.3% pentane. For each composition there is an optimum amount of blowing agent for complete foaming. Only slightly more (*i.e.*, to 1 part per 100 of polymer) than this amount leads to such undesirable properties as sweating, foam collapse, and excessive cell size (63). The tolerable amount of blowing agent decreases with the molecular weight of the polymer. A practicable volume of *n*-pentane (6.5% by weight) for foaming is identical with the free volume determined by the compressibility of amorphous polystyrene (60).

Expandable beads made in water suspensions must be dried at relatively low temperatures (*e.g.*, 50°–60°C. maximum) to avoid excessive evaporation of *n*-pentane (b.p., 36°C.). The loss of *n*-pentane in one hour is related to temperature and *n*-pentane content of the beads as shown in Table I (63).

**Table I. Loss of *n*-Pentane in 1 Hour from Expandable Beads at Varying Temperature**

Temperature, °C.	Loss (wt. %) from Beads with an <i>n</i> -Pentane Content of:			
	4.0%	5.0%	6.0%	7.0%
35	0.0	0.0	0.0	0.0
45	0.0	<0.1	<0.1	0.1
52.5	0.0	<0.1	<0.1	0.1
65	0.0	0.1	0.1	0.9

To reduce pentane losses in shipping, expandable beads are ordinarily transported in 50-gallon drums constructed from fiberboard with an inner liner of aluminum foil. In these containers the beads meet most expansion requirements for a few months, depending on storage conditions. When expandable beads (screened through a 10-mesh sieve and retained on a 25-mesh sieve) were exposed in open containers at 23°C., their *n*-pentane content decreased from 7.0 to 6.0% in 6–7 days.

Several other blowing agents have been disclosed, and many of these have particular advantages. Neopentane (tetramethylmethane), b.p., 9.5°C., is retained well by polystyrene and generates low density foam of extremely fine cell size (100). Isopentane (b.p., 28°C.) also

provides a smaller-celled foam than does *n*-pentane, and despite its lower boiling point it is held more tenaciously than is *n*-pentane (b.p., 36°C.) (63). In combination with selected plasticizers, isopentane provides expandability to very low densities without excessive collapse (134). As noted earlier, normally gaseous materials such as propane, butane, butene, and *sym*-dichlorotetrafluoroethane have been incorporated with polystyrene during its polymerization in suspension near the bead identity point.

Solid, gas-releasing blowing agents can also be used to expand polystyrene. Azobisisobutyronitrile may initiate polymerization, and the unused portion in the polymer will serve as a blowing agent when the polymer is heated above its plasticization temperature (92). Nitrogen-releasing blowing agents have been encapsulated in polystyrene by polystyrene by polymerizing the monomer on the surface of the blowing agent (52). Azodicarbonamide has been incorporated into polystyrene pellets by extruding them at a temperature below the decomposition point (86). Carbonate esters which release carbon dioxide have also been disclosed, employing an activator to promote the release of the gas—*e.g.*, sodium carbonate with succinyl monoglyceryl carbonate (26).

**The Polymer.** AMORPHOUS POLYSTYRENE. All of the expandable polystyrene referred to above is the amorphous type that is obtained by free radical initiation. This polymer is completely noncrystalline, and in the absence of impurities such as monomer and blowing agent it exhibits a glass-transition temperature of about 100°C. Both the rate of expansion and the extent of expansion are enhanced by reducing molecular weight, but the foam becomes less resistant to collapse on further steaming (63). Other polymeric modifications are discussed below.

ISOTACTIC POLYSTYRENE. The familiar steam molding of pre-expanded particles has so far not been applied successfully to isotactic polystyrene. However, the polymer has been foamed, according to three disclosed methods. For example, finely divided acetone-insoluble polymer, with a melting point in excess of 200°C., is blended with a liquid selected from methylene chloride, aromatic hydrocarbons, or halogenated aromatic hydrocarbons. This blend is then heated (84). A mixture of molten polymer and methyl chloride, propane, or butane is suddenly depressurized (8). Foam may also be generated in a continuous manner directly from a butyllithium-initiated polymerization conducted in the presence of a 4/1 blend of benzene and petroleum ether (15).

IRRADIATED POLYSTYRENE. The irradiation-induced crosslinking of expandable polystyrene with ionizing radiation in the range of 200–300 megarep raises the serviceability temperature of the foam in proportion



to the degree of radiation. Foams stable to 166°C. have been made in this manner (101).

**MIXED POLYMERS.** A mixture of 5 parts of polyethylene and 95 parts of expandable polystyrene is extruded and converted to quenched pellets. The pellets are expanded and converted into molded foams with improved resistance to solvents and water vapor transmission (29). There is a polyethylene skin on the surface.

**STYRENE COPOLYMERS. *Non-Crosslinked.*** Foams with improved resistance to gasoline and lubricating oils are obtained at reasonable costs by substituting acrylonitrile for 20–30% of the styrene in the polymer. Expandable copolymers have been made by the pentane-in-monomer process and by the impregnation of already formed pellets (16, 65). A difficulty with the former process is the formation of yellow beads with high residual acrylonitrile when one attempts to prepare copolymers of over 25% acrylonitrile. A difficulty with the latter process is the need to have a more expensive expanding agent—trichlorofluoromethane—to assist impregnation of pentane. A pentane-in-monomer process to overcome these objections was disclosed, whereby alkaline reagents were added at the bead identity point to hydrolyze the acrylonitrile in the water phase (61).

$\alpha$ -Methylstyrene (*e.g.*, 20%) in the copolymer improves the heat resistance of the molded foams (79). Copolymers of 30–60% methyl methacrylate are prepared by a partial conversion by bulk polymerization followed by suspension and addition of petroleum ether blowing agent (75).

Polymers or copolymers of mono- and/or dichlorostyrene are prepared by suspension polymerization in the presence of a volatile blowing agent (36).

***Crosslinked Polystyrene.*** Polystyrene lightly crosslinked during polymerization by 0.01–0.25% divinylbenzene provides foams, expanded by carbon dioxide or other gases, with greater expandability and resistance to collapse at elevated temperatures (102, 103). Other divinylbenzene copolymers are reported, employing as blowing agent saturated aliphatic or fluoroaliphatic volatile liquids, tetramethylsilane, and azobisisobutyronitrile (99, 106, 108).

Molded foam copolymers with 10–30% glycidyl acrylate may be crosslinked by heating in the presence of polyamines. Heat resistance may be increased to as high as 150°C. by this treatment (25). Use of certain allyl or diallyl esters to control the crosslinking of polystyrene to the desired very light extent has been disclosed as a means of obtaining foams of improved and regular cell structure (135). Block copolymers of polystyrene, polydiene (particularly polyisoprene), and polystyrene

have been foamed by sudden depressurizing of a solution in isopentane. These foams are particularly adaptable to crosslinking by irradiation (112).

**Postreacted.** The serviceability temperature of polystyrene may be increased significantly by hydrogenation of polystyrene before foaming (118). Polystyrene foams can be rendered infusible by alkylating the polymer with mixtures of mono- and dihalomethylated compounds in the presence of dehydrochlorination catalysts (2).

**Additives. SELF-EXTINGUISHING AGENTS.** Because of the extensive amount of information in this field, we make no attempt to list all contributions. However, the state of the art was reviewed in three papers in 1963 (39, 57, 67). The self-extinguishing agent for expandable polystyrene is usually a mixture of an aliphatic bromine compound and a relatively stable peroxide (37, 38, 130). For example, the self-extinguishing action of 5% acetylene tetrabromide alone with polystyrene is duplicated by only 0.50% acetylene tetrabromide in combination with 0.5% dicumyl peroxide (39). Other bromine compounds cited for their use in expandable polystyrene are 1,2-dibromotetrachloroethane, tris(2,3-dibromopropyl) phosphate, and hexabromocyclododecane (18, 67, 80). The first compound is incorporated into the polystyrene chain by a transfer mechanism. Among recently disclosed self-extinguishing agents of interest are 2,2,3,3-tetrabromobutanediol dinitrate which imparts self-extinguishing action at only 0.8% without the addition of a synergist and the bromine adducts of vegetable oils which are efficient self-extinguishing agents of low bromine content (10, 136).

Many free radical-generating compounds have been disclosed as synergists which may be used in place of peroxides to enhance the self-extinguishing action of bromine compounds. Examples of some of these materials are the disulfides, sulfenamides,  $\alpha, \alpha'$ -diphenyl- $\alpha$ -methoxybibenzyl, *N*-nitroso-*N*-methylaniline, tetraethyllead, pentaphenylphosphine, 1,2-diphenyltetramethylethane, tetraphenylhydrazine, and heavy metal salts or chelates (7, 9, 40, 41, 42, 55, 59, 71, 90, 132).

**PREPUFF ANTI-LUMPING AGENTS.** The tendency of expandable polystyrene to form agglomerates—*i.e.*, “lumps”—of prepuff during the pre-expansion step is a well-recognized problem. Lumping is overcome in varying degrees of success by moistening the beads with and without surfactants, by adding lubricants such as zinc stearate and by increasing the intensity of agitation in the pre-expander. Special additives have also been disclosed for pre-treatment of the beads to prevent lumping. For example, the beads may be contacted with a solution of perfluorooctanoic acid in water (139), with an emulsion of polysiloxane oil and water (64), with a solution of sodium stearate and citric acid (110), with an alcohol

solution of hydroxyoleamide (111), or with kaolin which has been coated with hydroxyethylated or hydroxypropylated amides of fatty acids (44).

**COLORANTS.** The above-mentioned quenched-pellet process is quite suitable for incorporating dyes or pigments to expandable polystyrene. Oil-soluble dyes may be transferred to the surface of expandable beads by immersion in an aqueous dye bath containing a carrier such as dimethylformamide or dimethyl sulfoxide (13). Oil-soluble dyes are more uniformly distributed in expandable polystyrene if they are incorporated in the prescribed manner in the impregnation of polystyrene in an aqueous suspension (82). Insoluble pigments may be incorporated into polystyrene by first wetting them with a styrene-ethylacrylate copolymer, then polymerizing a styrene dispersion of the pigment in an aqueous suspension stabilized by poly(vinyl alcohol) (46). In another method, expandable polystyrene is coated with pigment dispersed in a solution of a polymer in gasoline, thereby leaving on the surface of expandable polystyrene a coating of pigment dispersed in polymer (53).

**REGULATION OF CELL SIZE.** *Steam-Expanded Foam.* Several finely divided polymers have been mentioned as nucleating agents to reduce the cell size of polystyrene foam from the range of 20–50 mils in diameter down to less than 5 or preferably less than 2 mils. For this purpose, chlorinated wax or poly(vinyl propionate) may be dissolved in monomer (11, 117). A finely divided polymer, such as poly(vinyl chloride), may be formed by adding vinyl chloride monomer to the starting styrene-monomer charge (12). Various finely divided polymers, such as polyethylene wax or poly(vinyl chloride), may be dispersed in the monomer before polymerization (95). Physical means have also been used to effect a similar reduction in cell size. A slurry of expandable beads may be cooled very rapidly, in less than 15 minutes from 100°C. to below 25°C. (1, 88). The cell size of expandable beads may be reduced as desired by cooling to below -18°C., crushing (*e.g.*, from 1/4- to 3/16-inch thickness) or by prolonged soaking in surfactant solutions (97, 98).

*Extruded Foams.* The subject of extruded foams, including all extruded board and sheet, is too vast to include in this discussion. However, expandable polystyrene of the molding type is not suitable for extrusion because it produces a coarse-celled, brittle foam of high density. When certain nucleating agents, such as a mixture of sodium bicarbonate and citric acid or a 2/1 styrene/maleic anhydride copolymer, are incorporated, the surface cells are very small (*i.e.*, less than 3 mils) and the extrudate is not brittle (54, 113). Expandable polystyrene particularly suitable for making extruded foam consists of pentane-expandable quenched pellets containing encapsulated citric acid. Sodium bicarbonate is then added to these pellets immediately before feeding to the foam extruder (89). For extrusion it is not necessary to feed expandable polystyrene since

much commercial foam is produced by extruding either methyl chloride solutions of polystyrene or by feeding polystyrene, *per se*, and then pumping the volatile blowing agent into the extruder.

### **Conclusions**

The production and application in 1967 of 193 million pounds of polystyrene foam reflects considerable scientific, engineering, and commercial activity. The continuing growth of expandable polystyrene in this field is attributed to its ability to be steam molded economically into a variety of useful items.

Most expandable polystyrene processes involve aqueous suspension systems in which pentane fractions of petroleum are introduced before, during, or after polymerization of styrene. Water-free systems may also be used. Particle size is controlled by suspension polymerization or by chopping fine filaments. The "quenched pellet" process for expandable polystyrene can consume off-size particles and is a convenient way to add colorants and cell-nucleating additives.

Expandable polystyrene with improved properties has been obtained by copolymerization, postreaction, additives, or by physical means. Improvements have been achieved particularly in resistance to premature fusion of particles during expansion, in reducing cell size, in self-extinguishability, in attractive coloration, in resistance of foams to attack by gasoline and in dimensional stability of foams at elevated temperatures.

### **Acknowledgment**

The author expresses his appreciation to E. P. Meckly and associates in the Information Section of Koppers Research Department for assistance in preparing the bibliography.

### **Literature Cited**

- (1) Andrews, E. D., Francis, D. V., Rode, D. J., U. S. Patent **3,207,712** (1965).
- (2) Asahi Electro-Chemical Co., Ltd., Japanese Patent **2,148** (1967).
- (3) Aykanian, A. A., U. S. Patent **3,324,210** (1967).
- (4) Barber, E. G., Roper, A. N., British Patent **1,056,470** (1967).
- (5) Badische Anilin- & Soda-Fabrik A.-G., Belgian Patent **604,776** (1961).
- (6) Badische Anilin- & Soda-Fabrik A.G., British Patent **948,300** (1962).
- (7) Badische Anilin- & Soda-Fabrik A.G., Belgian Patent **642,915** (1964).
- (8) *Ibid.*, **661,324** (1965).
- (9) *Ibid.*, **678,791** (1965).
- (10) *Ibid.*, **691,252** (1967).
- (11) Badische Anilin- & Soda-Fabrik A.-G., French Patent **1,463,625** (1966).

- (12) Badische Anilin- & Soda-Fabrik A.-G., Netherlands Patent App. **6,516,742** (1966).
- (13) Bianco, J., U. S. Patent **3,020,247** (1962).
- (14) Bonin, V., Bartl, H., German Patent **1,160,616** (1964).
- (15) Borg-Warner Corp., Netherlands Patent Appl. **6,413,848** (1965).
- (16) Buchholz, K., U. S. Patent **2,888,410** (1959).
- (17) Buchholz, K., Grohmann, J., Stahnecker, E., Belgian Patent **668,325** (1965).
- (18) Buchholz, K., Stastny, F., U. S. Patent **3,001,954** (1961).
- (19) Buchholz, K., Stastny, F., Gaeth, R., U. S. Patent **2,950,261** (1960).
- (20) Cleland, W. J., Thomas, R. G., Seijo, E., U. S. Patent **2,893,963** (1959).
- (21) Collins, F. H., U. S. Patent **3,250,834** (1966).
- (22) Colwell, R., U. S. Patents **2,857,339, 2,857,340, 2,857,341, 2,857,342** (1958).
- (23) Compagnie Internationale pour le Commerce et L' Industrie, Belgian Patent **566,994** (1958).
- (24) D'Alelio, G. F., U. S. Patent **2,983,692** (1961).
- (25) *Ibid.*, **2,994,670** (1961).
- (26) *Ibid.*, **3,224,983** (1965).
- (27) Day, S. T., U. S. Patent **3,126,354** (1964).
- (28) Del Bene, S. J., U. S. Patent **3,121,132** (1964).
- (29) Del Bene, S. J., Fox, A. J., U. S. Patent **3,285,865** (1966).
- (30) de Romano, O., Belgian Patent **653,820** (1965).
- (31) Doak, K. W., U. S. Patent **3,192,169** (1965).
- (32) Dow Chemical Co., Belgian Patent **622,808** (1963).
- (33) *Ibid.*, **673,061** (1966).
- (34) *Ibid.*, **674,357** (1966).
- (35) *Ibid.*, **677,173** (1966).
- (36) Dow Chemical Co., Netherlands Patent Appl. **6,514,797** (1966).
- (37) Eichhorn, J., U. S. Patent **3,058,926** (1962).
- (38) Eichhorn, J., Bates, S. I., U. S. Patent **3,058,928** (1962).
- (39) Eichhorn, J., *J. Appl. Polymer Sci.* **8**, 2497 (1964).
- (40) Eichhorn, J., U. S. Patent **3,271,333** (1966).
- (41) *Ibid.*, **3,284,544** (1966).
- (42) *Ibid.*, **3,296,340** (1967).
- (43) Eng, A. A., U. S. Patent **3,304,274** (1967).
- (44) Ferrigno, T. H., U. S. Patents **3,300,437, 3,301,812** (1967).
- (45) Engels, E. F., U. S. Patent **3,026,273** (1962).
- (46) Geigy, S. A., Belgian Patent **669,399** (1965).
- (47) Griffin, J. D., Belgian Patent **651,577** (1965).
- (48) Grim, J. M., U. S. Patent **2,594,913** (1952).
- (49) Hall, W. E., Poshkus, A. C., U. S. Patent **3,088,925** (1963).
- (50) Harrison, J. M., U. S. Patent **3,127,360** (1964).
- (51) Hatano, I., Senuma, K., Kasamatsu, T., Nishino, M., U. S. Patent **3,265,643** (1966).
- (52) Hedman, E. A., Mather, S. R., U. S. Patent **3,138,478** (1964).
- (53) Hein, E., German Patent **1,221,008** (1966).
- (54) Houston, J. C., Tress, J. J., U. S. Patent **2,941,964** (1960).
- (55) Ilgmann, R., Rauschenbach, R. D., French Patent **1,411,363** (1965).
- (56) Imperial Chemical Industries, Ltd., Belgian Patent **674,949** (1966).
- (57) Ingram, A. R., *J. Appl. Polymer Sci.* **8**, 2485 (1964).
- (58) Ingram, A. R., Canadian Patent **718,088** (1965).
- (59) Ingram, A. R., U. S. Patent **3,274,133** (1966).
- (60) Ingram, A. R., *Wayne State Univ. Polymer Conf. Cellular Plastics Technol. Detroit, Mich.*, 1967.
- (61) Ingram, A. R., Gleason, E. H., U. S. Patent **3,288,731** (1966).
- (62) Ingram, A. R., Jurgeleit, H. W., U. S. Patent **3,222,343**.

- (63) Ingram, A. R., Wright, H. A., *Mod. Plastics* 41 (3), 152 (1963).  
(64) Jahn, A. K., U. S. Patent 3,086,885 (1963).  
(65) Jahn, A. K., British Patent 1,009,130 (1965).  
(66) Jahn, A. K., Gillard, E. J., U. S. Patent 3,043,817 (1962).  
(67) Jahn, A. K., Vanderhoff, J. W., *J. Appl. Polymer Sci.* 8, 2525 (1964).  
(68) Karpovich, J., U. S. Patent 3,072,584 (1963).  
(69) Kline, S. M., Lafferty, G. F., Canadian Patent 683,415 (1964).  
(70) Knobloch, H. E., Meyer, F., Stastny, F., U. S. Patent 3,117,941 (1964).  
(71) Laib, H., Burger, H., German Patent 1,244,396 (1967).  
(72) Lintner, J., Petrovicki, H., Schaffernack, F., U. S. Patent 3,085,073 (1963).  
(73) Lintner, J., Petrovicki, H., Schaffernack, F., Canadian Patent 663,596 (1963).  
(74) Marek, O., Mrazek, J., Tomka, M., Cerny, M., British Patent 978,631 (1964).  
(75) *Ibid.*, 1,013,215 (1965).  
(76) McMaster, E. L., Eichhorn, J., Nagle, F. B., U. S. Patent 3,058,927 (1962).  
(77) McMillan, W. J., Nicholls, G. L., U. S. Patent 3,026,274 (1962).  
(78) *Mod. Plastics* 45 (5), 84 (1968).  
(79) Motoishi, Y., Japanese Patent 16,437 (1967).  
(80) Mueller-Tamm, H., Buchholz, K., Stastny, F., U. S. Patent 3,093,599 (1963).  
(81) Mueller-Tamm, H., Grohmann, J., German Patent 1,163,025 (1964).  
(82) Nicholson, H. L., British Patent 1,064,490 (1967).  
(83) Ohlinger, H., Guenther, W., Single, W., Buchholz, K., Wild, H., U. S. Patent 3,287,286 (1966).  
(84) Overhults, W. C., British Patent 938,639 (1963).  
(85) Petrovicki, H., Schaffernack, F., Holl, K., Lintner, J., German Patent 1,248,934 (1967).  
(86) Pilz, E., *et al.*, East German Patent 51,424 (1966).  
(87) Platzer, N., U. S. Patent 3,072,581 (1963).  
(88) Pollard, E. G., Rubens, L. C., U. S. Patent 3,013,996 (1961).  
(89) Pottenger, C. H., U. S. Patent 3,089,857 (1963).  
(90) Priebe, E., Weber, H., Willersinn, H., German Patent 1,245,593 (1967).  
(91) Produits Chimiques Pechiney-Saint-Cobain, British Patent 1,063,333 (1967).  
(92) Reed, R. A., Spencer, R. C. H., Barb, W. G., British Patent 790,312 (1958).  
(93) Rode, D. J., Greenawald, G., U. S. Patent 3,342,760 (1967).  
(94) Rodman, H., Jr., U. S. Patent 3,023,175 (1962).  
(95) Roper, A. N., Barber, E. G., U. S. Patent 3,224,984 (1965).  
(96) Rosenthal, F., U. S. Patent 2,533,629 (1950).  
(97) Roth, M. H., U. S. Patent 2,816,827 (1957).  
(98) Roth, M. H., U. S. Patents 2,910,446, 2,911,381 (1959).  
(99) Rubens, L. C., U. S. Patent 2,848,428 (1958).  
(100) *Ibid.*, 2,878,194 (1959).  
(101) *Ibid.*, 2,952,594 (1960).  
(102) Rubens, L. C., *J. Cellular Plastics* 1, 311 (1965).  
(103) Rubens, L. C., U. S. Patent 2,848,427 (1958).  
(104) Rubens, L. C., Engels, E. F., U. S. Patent 3,026,272.  
(105) Rubens, L. C., Walsh, W. B., French Patent 1,476,888 (1967).  
(106) Rubens, L. C., Warren, J. S., U. S. Patent 3,033,805 (1962).  
(107) Russell, D. A., Hardy, E. E., U. S. Patent 3,262,625 (1966).  
(108) Scalari, F., Sabatini, G., Italian Patent 664,755 (1964).  
(109) Schroeder, C. W., Fuller, M. E., Canadian Patent 682,464 (1964).  
(110) Shell Int. Res. Mij. N.V., Belgian Patent 626,772 (1963).

- (111) Shell Int. Res. Mij. N.V., British Patent **1,029,397** (1966).
- (112) Shell Int. Res. Mij. N.V., Netherlands Patent Appl. **6,506,473** (1965).
- (113) Simpson, D. W., U. S. Patent **3,231,524** (1966).
- (114) Soc. Edison, Canadian Patent **738,490** (1966).
- (115) Soc. Edison, British Patent **1,062,011** (1967).
- (116) Spencer, F. R., U. S. Patent **3,018,257** (1962).
- (117) Stahnecker, E., Mueller-Tamm, H., Belgian Patent **627,053** (1963).
- (118) Stahnecker, E., Mueller-Tamm, H., Friederich, H., British Patent **1,015,709** (1966).
- (119) Stahnecker, E., Mueller-Tamm, H., Zuern, L., Grohmann, J., Buchholz, K., German Patent **1,152,261** (1963).
- (120) Stamicarbon, N.V., Belgian Patent **661,777** (1965).
- (121) Stastny, F., U. S. Patent **2,787,809** (1957).
- (122) Stastny, F., Buchholz, K., German Patent **951,299** (1956).
- (123) Stastny, F., Buchholz, K., U. S. Patent **2,744,291** (1956).
- (124) Stastny, F., Gaeth, R., U. S. Patent **2,681,321** (1954).
- (125) Stastny, F., Gaeth, R., German Patent **1,009,391** (1957).
- (126) Staudinger, H. P., Kelly, B. K., Cooper, A., British Patent **605,863** (1948).
- (127) Sunde, J., Norwegian Patent **95,882** (1960).
- (128) Ulmanis, E. B., British Patents **988,289, 988,290** (1965).
- (129) Urbach, H., Mueller-Tamm, H., Belgian Patent **623,387** (1963).
- (130) Vanderhoff, J. W., Jahn, A. K., U. S. Patent **3,058,929** (1962).
- (131) Will, G., U. S. Patent **3,256,219** (1966).
- (132) Willersinn, H., Rauschenbach, R. D., Ilgmann, R., French Patent **1,425,972** (1966).
- (133) Wolff, P., Kaaber, S. H., British Patent **1,021,250** (1966).
- (134) Wright, H. A., U. S. Patents **3,027,334, 3,027,335, 3,060,138** (1962).
- (135) *Ibid.*, **3,259,594, 3,259,595** (1966).
- (136) *Ibid.*, **3,359,220** (1967).
- (137) Yanishevskii, A. V., Voevodin, K. V., *J. Appl. Chem. U.S.S.R. (Eng. Transl.)* **40** (3), 533 (1967).
- (138) Zuern, L., Mueller-Tamm, H., Buchholz, K., U. S. Patent **3,324,052** (1967).
- (139) Zweigle, M. L., U. S. Patent **3,056,752** (1962).

RECEIVED April 1, 1968.

# Expandable Olefin-Sulfur Dioxide Copolymers from Suspension Polymerization

J. CHATELAIN

R & D Laboratory, Pechiney Saint-Gobain, 69-Saint-Fons, France

*A suspension polymerization process can be used to manufacture beads in polybutene-sulfone for use in the production of expanded cellular material. The solvent power of the reaction medium is important with respect to the homogeneity of the beads and to the diffusion of the blowing agent. Processing and properties of this new cellular material are examined briefly.*

This chapter describes the manufacture of expandable beads in the copolymer 1-butene-sulfur dioxide by suspension polymerization. The processing and properties of expandable beads and of molded articles are examined briefly.

## *Preparation of Expandable Beads*

**1-Butene-Sulfur Dioxide Copolymerization.** Polybutene sulfones are well known. Copolymerization of 1-butene with sulfur dioxide is characterized by certain features:

- (1) Copolymerization is initiated by free radical catalysts.
- (2) The copolymer contains an equimolecular ratio of the two reactants irrespective of their initial concentration.
- (3) Copolymerization is characterized by a ceiling temperature of 64°C. above which no polymerization takes place.

**Copolymerization Conditions.** It is necessary to use a 1-butene as pure as possible. 2-Butene and isobutene greatly inhibit the copolymerization reaction (Figure 1).

The copolymerization must be conducted below the ceiling temperature. Isopropyl percarbonate (IPP) has been chosen because of its



good reactivity between 45° and 55°C. Figure 2 shows the conversion of 1-butene-sulfur dioxide *vs.* time. The catalyst used is IPP at a concentration of 23 mg. active oxygen for 100 grams of 1-butene (molar ratio  $\text{SO}_2/1\text{-butene} = 2$ ).

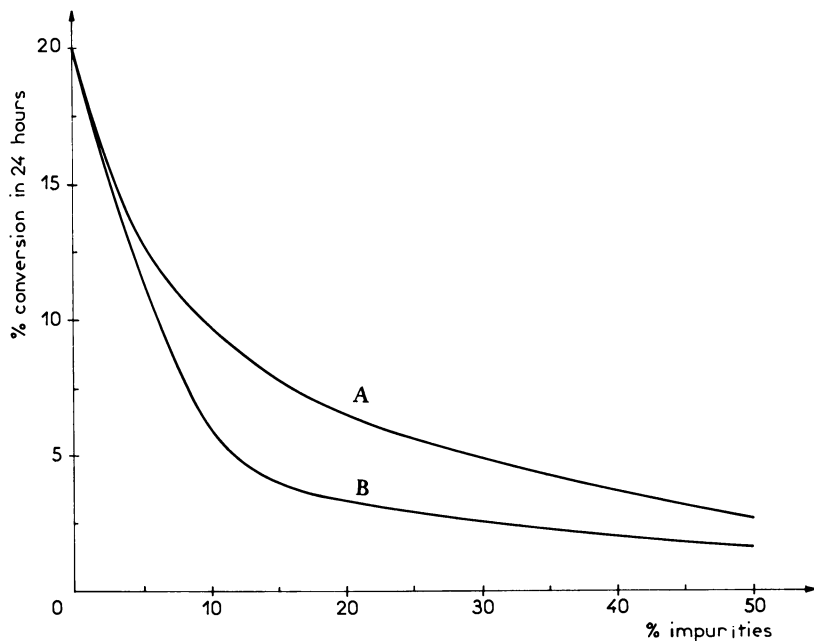


Figure 1. Dependence of reactivity by 1-butene- $\text{SO}_2$  mixture on impurities. Polymerization conducted at 84°C. by  $\gamma$ -radiation

A: 2-Butene  
B: Isobutene

A suspending agent unlikely to be modified by sulfur dioxide can be chosen among poly(vinyl alcohols) or cellulose derivatives.

Agitation conditions must be selected carefully. To achieve good expansion, it is necessary to obtain large beads; therefore, agitation must not be too turbulent, but owing to the high density of the beads (1.37), agitation must be sufficiently rapid to avoid block formation.

**Expandability.** Polybutene sulfone is insoluble in 1-butene but is soluble in sulfur dioxide. The higher the concentration of 1-butene in 1-butene-sulfur dioxide mixture, the lower is the solubility of the copolymer in this mixture. Even when copolymerization takes place with an excess of sulfur dioxide, the two monomers react in equimolecular

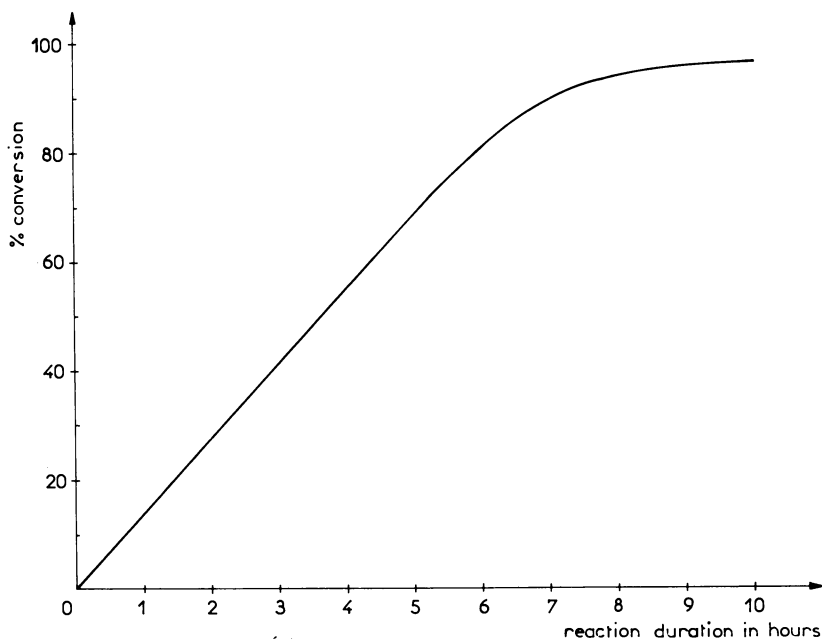
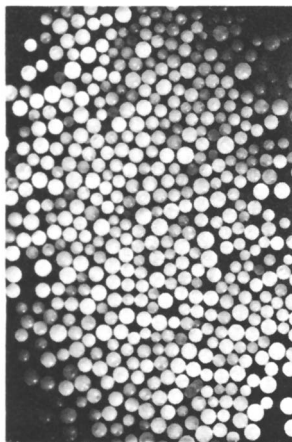


Figure 2. Conversion rate of 1-butene-SO<sub>2</sub> copolymerization at 48°C. using IPP as catalyst

ratio. Consequently, the concentration of sulfur dioxide increases continuously during copolymerization. After all 1-butene is consumed, the copolymer will be dissolved completely in the remaining sulfur dioxide. In other words, reaction begins in a precipitating medium, and as it proceeds, solubility of copolymer in the medium increases. At the end of the reaction, the situation is similar to that of polystyrene during polymerization: the copolymer is entirely soluble in the monomer. This dissolution allows the beads to be homogeneous.

At the end of copolymerization C-4 hydrocarbons are added before removal of the unreacted sulfur dioxide. Sulfur dioxide favors the diffusion of C-4 hydrocarbons into the beads and allows a good and homogeneous distribution. Finally, the unreacted sulfur dioxide is removed. Since sulfur dioxide dissolves polybutene sulfone, its diffusion rate is very high in contrast with the hydrocarbons which diffuse slowly and remain occluded in the beads.

After degassing the unreacted monomers, the remaining sulfur dioxide can be removed by washing the beads with water. After drying, the beads contain 6-7% hydrocarbons as expanding agent.



*Figure 3. Expandable polybutene sulfone beads ( $\times 2.5$ )*



*Figure 4. Expanded polybutene sulfone beads ( $\times 2.5$ )*

### ***Manufacture and Properties of Cellular Materials from Polybutene Sulfone***

**Manufacture.** Expandable polybutene sulfone beads are processed into expanded polybutene sulfone in three stages: preexpansion, maturation, and molding. Study of this process has shown that the use of steam for preexpansion and molding is favorable and allows a lower density than with hot air alone. Preexpansion is carried out in a continuous preexpander by a mixture of steam and hot air. Cooling of the beads

involves a decrease of internal pressure in the cells. Maturing requires storage of beads so they may absorb air to balance the internal pressure with atmospheric pressure. Molding is effected by introducing steam into the bead-filled mold. Cooling conditions must be controlled carefully before opening the mold. Figure 3 shows expandable beads, Figure 4 shows expanded beads, and Figure 5 shows a molded article in cross-section.

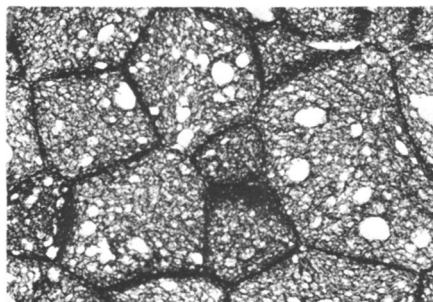


Figure 5. Microtome of expanded polybutene sulfone molded article ( $\times 7.5$ )

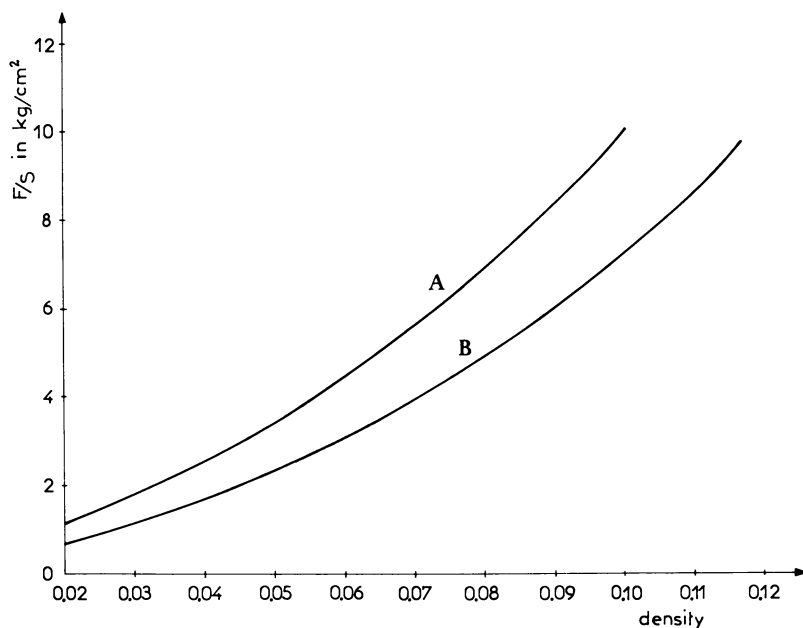


Figure 6. Compression resistance (25% crushing)

A: Expanded polystyrene  
B: Expanded polybutene sulfone

**Properties of Polybutene Sulfone Foam.** Many properties of polybutene sulfone foam are similar to those of polystyrene foam. Mechanical properties are a little lower for the same foam density, but the bulk density of polybutene sulfone is 1.37 compared with 1.05 for polystyrene. Figure 6 shows that mechanical properties vary in the same ratio as density. The insulating properties of polybutene sulfone foam are very good, somewhat better than polystyrene foam (Figure 7). Polybutene sulfone has a good solvent resistance as shown in Table I. In particular, styrene, benzene, and toluene do not attack polybutene sulfone but attack polystyrene.

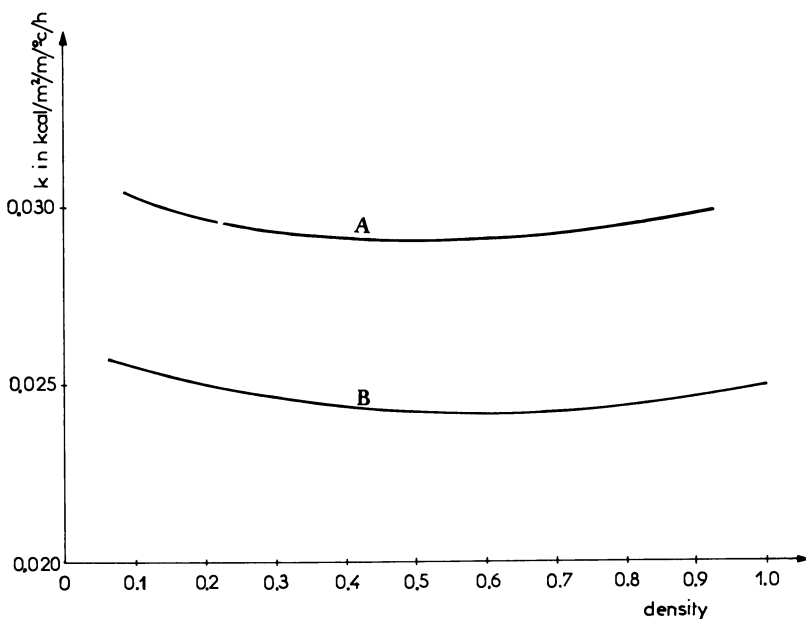


Figure 7. Thermal conductivity at 25°C.

A: Expanded polystyrene  
B: Expanded polybutene sulfone

Polybutene sulfone foam is also different from polystyrene foam in its combustion behavior, which is important for various applications. This foam burns without smoke production unlike polystyrene which burns with an abundant black smoke.

**Applications.** Polybutene sulfone foam can be used in all usual applications of rigid foams, in particular with the following obvious advantages over expanded polystyrene:

(1) Sandwich panels: polyesters can be coated directly on polybutene sulfone foam (styrene does not dissolve the foam).

Table I. Solvent Resistance<sup>a</sup>

<i>Solvent</i>	<i>EPBS</i>	<i>EPS</i>	<i>Solvent</i>	<i>EPBS</i>	<i>EPS</i>
Pentane	G	G	Chlorobenzene	G	B
Hexane	G	G	Nitrobenzene	B	B
Heptane	G	G	Styrene	G	B
Methyl chloride	B	B	Methanol	G	G
Chloroform	B	B	Ethanol	G	G
Carbon tetrachloride	G	B	2-Propanol	G	G
1,2- <i>trans</i> -Dichloroethylene	G	B	Ethyl ether	G	B
Trichloroethylene	G	B	Ethyl acetate	B	B
Acrylonitrile	B	B	Butyl acetate	B	B
Dichloroethane	B	B	Isoamyl acetate	G	B
Tetrachloroethane	B	B	Acetone	B	B
Benzene	G	B	Methyl ethyl ketone	B	B
Toluene	G	B	Cyclohexanone	B	B
Xylene	G	B	Dioxane	B	B
Dimethyl sulfoxide	B	G	Dimethylformamide	B	B
			Tetrahydrofuran	B	B

<sup>a</sup> G: good, B: bad, EPBS: expanded polybutene sulfone, EPS: expanded polystyrene.

(2) Metal molding by gasifiable pattern (no smoke during molding and total disappearance of pattern).

(3) Packaging: possibility of direct printing or painting on foam.

(4) Insulation: easy bonding by use of a wide choice of glues (good resistance to aromatic solvents and ability to be coated directly with vapor barrier).

In addition, better insulation properties allow the use of thinner panels of cellular material.

### Conclusion

Suspension copolymerization of 1-butene and sulfur dioxide can lead to expandable beads. The cellular material obtained has improved properties with respect to expanded polystyrene. The manufacture of expandable beads by suspension copolymerization is covered by a patent (1).

### Literature Cited

- (1) French Patent 1,453,275 (March 15, 1965).
- (2) French Patent 89,511 (Jan. 21, 1966) (addition to patent cited in Ref. 1).

## A Flame Resistant ABS-Type Polymer from Terpolymerization with a Novel Bromine-Containing Monomer

WILLIAM CUMMINGS and RONALD E. STARK

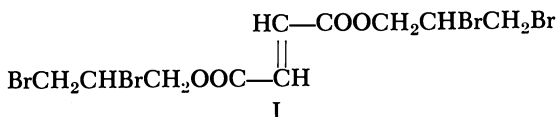
Uniroyal Chemical, Naugatuck, Conn.

*Bis(2,3-dibromopropyl) fumarate has been used as a fourth monomer in nitrile rubber- and graft-type ABS materials giving flame-resistant polymers. At least 10% bromine incorporation is required to pass the Underwriter's Laboratories Subject 94 test. The graft-type materials fail at 7-10% bromine only because of dripping. Both types pass the ASTM D-635 test with 7% or more bromine. For the impact strength to be equivalent to that of conventional ABS, the fourth monomer must be present in both the rubber and resin phases. Thermal stability is marginal but can be improved with typical PVC stabilizers.*

The ABS polymers (acrylonitrile-butadiene-styrene) have unusual properties which combine toughness with high strength, easy flow in processing, and good surface appearance (2). The rapid growth in the use of these polymers during their 19-year history is testimony to the usefulness of this combination of properties in a variety of applications.

In common with most thermoplastics, ABS polymers are not flame resistant. In principle, a flame-resistant ABS could be made by incorporating halogen- and/or phosphorus-containing structures either by (a) copolymerization of appropriate monomers or (b) addition of small molecules containing these structures as plasticizers. Recognizing that the second approach can involve a serious loss in heat deflection temperature, hardness, and occasionally impact strength (4), we have favored the copolymerization approach in the work described here.

The development of bis(2,3-dibromopropyl) fumarate (DBPF) (I) in these laboratories by Amidon and Bill (1):



provided a monomer which seemed to offer interesting possibilities as a fourth monomer in ABS-type polymers.

### Experimental

DBPF was prepared using either the procedure of Amidon and Bill (1) or of Cummings (3). The product was recrystallized from benzene-methanol, m.p., 67°–68°C. (uncorrected).

**Terpolymer Resins.** DBPF was dissolved in a mixture of styrene, acrylonitrile, and mercaptan (Table I). About one-tenth of this solution was added to a solution of sodium alkylbenzene sulfonate emulsifier (Nacconal NRSF, 2 parts) in deionized water (180 parts) at 60°C. Potassium persulfate (0.3 part) was added, followed by the remaining monomer mixture at a rate consistent with temperature control (60°C.) Gentle agitation and a nitrogen atmosphere were maintained throughout the polymerization. The latex was maintained at 60°C. until a solids determination indicated no further conversion (6–8 hours total polymerization time).

**Nitrile Rubbers.** Mixtures of butadiene, acrylonitrile, and DBPF were polymerized in bottles at 35°C. using the following recipe:

	<i>Parts</i>
Monomers	100
Water	180
Mixed tertiary mercaptans (C <sub>12</sub> , C <sub>14</sub> , C <sub>16</sub> )	1.3
Oleic acid	1.16
Sodium hydroxide	0.1
Sodium salt of alkylbenzene sulfonate (Nacconal NRSF)	2.85
Potassium persulfate	0.26
Divinylbenzene (commercial 42% solution)	1.5

Table II gives the feed ratios and the composition of the finished rubbers.

**Graft Polymers.** The procedure used was described by Cummings (3). To a quantity of commercially available polybutadiene latex (52.3% solids) containing 50 parts of rubber was added sufficient deionized water to increase the water content to 180 parts. The diluted latex was heated to 60°C. Potassium persulfate (0.3 part) and monomers (styrene, acrylonitrile, DBPF; 50 parts) were added, and poly-



merization was carried out with gentle stirring under a nitrogen blanket for five hours at 60°C.

**Preparation of Resin-Rubber Blends.** To a mixture of appropriate quantities of the resin and rubber latices was added sufficient quantities of an emulsion of 2,6-di-*tert*-butyl-*p*-cresol to furnish 1 p.p.h. of antioxidant. This mixture was flucculated by pouring it into a stirred 2% aqueous solution of calcium chloride held at 95°–98°C. After cooling to 60°–70°C., the resulting slurry was filtered. The polymeric crumb was washed with water and dried 16–24 hours at 60°C. Zinc stearate and tribasic lead silicate (1 p.p.h. each) were added during mixing on a mill at 149°–160°C. The Izod impact strength (ASTM D256-56), Rockwell R hardness (ASTM D785-51), and flame resistance (Underwriter's Subject 94) were measured on 1/4-inch compression molded test pieces.

**Table I. Styrene–Acrylonitrile–DBPF Terpolymers**

Resin	S-AN-DBPF		Parts Mixed tert-Mercaptans	[ $\eta$ ] <sup>b</sup>	Conversion, <sup>c</sup> %
	Charged	Polymer <sup>a</sup>			
1	63-10-27	64-10-26	0.25	0.70	98
2	73-10.5-16.5	74-10-16	0.22	0.76	98
3	55-20-25	60-20-20	0.25	1.10	95
4	55-20-25	57-19-24	0.25	1.32	98
5	55-20-25	62-20-18	0.25	1.44	91

<sup>a</sup> Weight ratios based on nitrogen and bromine analyses; styrene by difference.

<sup>b</sup> Deciliters/gram in dimethylformamide at 30.00°C.

<sup>c</sup> Estimated from terminal % solids.

**Table II. Butadiene–Acrylonitrile–DBPF Terpolymers**

<i>Butadiene–Acrylonitrile–DBPF Weight Ratio</i>		
<i>Charged</i>	<i>In Polymer<sup>a</sup></i>	<i>Hours to 76% Conversion</i>
66-34-0	68-32-0	24.5
70-25-5	70-24-6	21.5
65-25-10	64-24-12	20.0
60-25-15	61-23-16	17.0

<sup>a</sup> Weight ratios based on nitrogen and bromine analyses; butadiene by difference.

**Flammability Tests.** ASTM D-635. The specimen, 0.25 × 0.5 × 5 inches, was clamped horizontally with its transverse axis inclined at a 45° angle to the horizontal. A 1-inch blue, Bunsen burner flame was held to the end of the specimen for 30 sec. and then removed. If the specimen failed to burn, ignition was attempted again. If it did not burn after the second ignition, or if the flame extinguished before 4 inches of the specimen burned, the specimen was considered self-extinguishing. For the material being tested to be considered self-extinguishing and pass the test, 10 specimens were tested, and all had to pass.

UL SUBJECT 94. The same size sample was used as in ASTM D-635. The specimen was held vertically and ignited with a 1-inch blue, Bunsen

burner flame for 10 sec. To be classified self-extinguishing, and pass the test, there could be no glow or flame remaining 30 sec. after removing the flame. Also the sample could not drip burning particles capable of igniting a horizontal layer of cotton fibers placed 1 ft. below the specimen. Three specimens were tested, and all had to pass for the material to pass and be considered self-extinguishing.

### Discussion

Conventional ABS polymers are blends of poly(styrene-coacrylonitrile) with either poly(butadiene-coacrylonitrile) or a graft of poly(styrene-coacrylonitrile) onto a rubbery spine. To confer flame-resistance on either ABS system using DBPF as a fourth monomer, the major component should be a styrene-acrylonitrile-DBPF terpolymer since the resinous component is the major one. The composition of such a terpolymer is restricted by two considerations: (1) it should contain sufficient acrylonitrile to impart the resistance to solvent attack which is characteristic of ABS polymers, and (2) the amount of DBPF should be sufficient to give a useful level of flame resistance.

**Blends with Nitrile Rubbers.** The data in Table III show the importance of using a terpolymer rubber to obtain good impact strength in a blend with styrene-acrylonitrile-DBPF terpolymer resin. Blend No. 1 gives the properties of a conventional nitrile rubber blend type ABS. Blends 2-4, involving terpolymer resins with the same amount of the rubber used in Blend 1, have a much lower impact strength.

If, however, terpolymer resin is blended with terpolymer rubber (Blends 5-7), the impact strength approaches that of the conventional

**Table III. Blends of Styrene-Acrylonitrile-DBPF Resins with Nitrile Rubbers<sup>c</sup>**

Blend	No.	Resin		Rubber, %	Impact Strength (ft.-lbs./ in. of notch)	Hard- ness Rock- well R	Br, %	Flame Resist- ance <sup>b</sup>
		S-AN- DBPF <sup>a</sup>	BDE-AN- DBPF <sup>a</sup>					
1	-	73-27-0	68-32-0	25	7-8	98	0	—
2	1	64-10-26	68-32-0	25	1.5	89	12.1	Pass
3	2	71-10-19	68-32-0	25	1.3	86	8.8	Fail
4	3	60-20-20	68-32-0	25	2.3	95	9.3	Pass
5	4	57-19-24	70-24-6	25	5.8	87	12.1	Pass
6	4	57-19-24	64-24-12	25	7.1	93	13.0	Pass
7	4	57-19-24	61-23-16	25	4.7	95	13.6	Pass

<sup>a</sup> Terpolymer composition by analysis for N<sub>2</sub> and Br<sub>2</sub> (styrene and butadiene by difference).

<sup>b</sup> Underwriter's Laboratories Subject 94 test.

<sup>c</sup> Abbreviations: S = styrene, AN = acrylonitrile, DBPF = 2,3-dibromopropyl fumarate, BDE = butadiene.

ABS (Blend 1). It seems likely that better impact strength is obtained when both phases contain DBPF because of better interphase compatibility.

**Graft Blends.** The properties of ABS-type polymers involving mixtures of terpolymer resins and graft rubbers are shown in Table IV. As with the nitrile rubber types, there is a pronounced gain in impact strength at a given rubber level when DBPF is present in both phases (Blends 1 vs. 3 and 2 vs. 4).

**Table IV. Blends of Styrene-Acrylonitrile-DBPF Resins with Graft Rubbers<sup>c</sup>**

Blend	No.	Resin		Graft Polymer	BDE, %	Impact Strength (ft.-lbs./ in. of notch)	Hard- ness Rock- well R	Br, %	Flame Resist- ance <sup>b</sup>
		S-AN- DBPF	BDE-S-AN- DBPF <sup>a</sup>						
1	4	57-19-24	50-34-16-0	15	1.5	112	10.4	Fail	
2	4	57-19-24	50-34-16-0	25	3.7	98	7.4	Fail	
3	5	62-20-18	50-32-11-7	13	3.0	106	9.6	Fail (Drip)	
4	5	62-20-18	50-32-11-7	25	7.0	94	7.6	Fail (Drip)	

<sup>a</sup> Terpolymer composition by analysis for N<sub>2</sub> and Br<sub>2</sub> (styrene and butadiene by difference).

<sup>b</sup> Underwriter's Laboratories Subject 94 test.

<sup>c</sup> Abbreviations: S = styrene, AN = acrylonitrile, DBPF = 2,3-dibromopropyl fumarate, BDE = butadiene.

Improved interphase compatibility, owing to the greater similarity in constitution of the two phases, again seems a reasonable explanation of the effect.

**Flame Resistance.** Blends with nitrile rubbers (Table III) containing at least 10% bromine passed the comparatively stringent Underwriter's Subject 94 test. Graft blends having 7-10% bromine failed the Underwriter's test only because of dripping. They passed the ASTM D-635 test, as did all the nitrile rubber blend types.

Nitrile rubber Blend No. 3 (Table III) which contains 8.8% bromine and which failed the Underwriter's test, was mixed with 6 and 12 parts of tricresyl phosphate.

As Table V shows, the plasticizer improved flame resistance and made the compositions softer. Six parts of tricresyl phosphate increased the impact strength notably with little decrease in hardness. With 12 parts of this plasticizer present, the impact strength was intermediate, but the loss in hardness was serious.

**Table V. Effect of Tricresyl Phosphate on the Properties of a Nitrile Rubber Blend DBPF-Containing ABS**

Parts TCP <sup>b</sup>	Impact Strength (ft.-lbs./in. of notch)	Rockwell R, Hardness	Flame Resistance <sup>a</sup>
0	1.3	86	Fail
6	4.4	84	Borderline
12	2.7	79	Pass

<sup>a</sup> Underwriter's Laboratories Subject 94 test.

<sup>b</sup> Added to Blend 3 of Table III.

**Thermal Stability.** The ABS-type polymers containing sufficient DBPF to pass the Underwriter's test were notably less prone to discoloration during processing than unstabilized PVC. On the other hand, they discolored when subjected to processing conditions normally used for conventional ABS polymers. Tribasic lead silicate was as effective as any of the common PVC stabilizers in preventing this discoloration during milling.

### Summary

Use of bis(2,3-dibromopropyl) fumarate as a fourth monomer in either nitrile rubber- or graft-type ABS materials gives flame-resistant polymers. With either type, better impact strength is obtained when the fourth monomer is present in both the rubber and resin phases. The compositions are more thermally stable than poly(vinyl chloride) and can be stabilized by typical PVC stabilizers.

### Literature Cited

- (1) Amidon, R. W., Bill, J. C., U. S. Patent 3,151,183 (Sept. 29, 1964).
- (2) Basdekis, C. H., "ABS Plastics," Reinhold, New York, 1964.
- (3) Cummings, W., U. S. Patent 3,260,772 (July 22, 1966).
- (4) Lamon, D. A., Hoskins, E. J., "Physics of Plastics," P. D. Ritchie, Ed., Van Nostrand, Princeton, N. J.

RECEIVED April 1, 1968.

# Radiation-Grafted Polyelectrolytes on Polymer Surfaces

## Water Contact Angles as a Function of the Mobile Counter-Anion Species

ALLAN S. HOFFMAN, RON GOMES-CASSERES, and GEOFFREY D. PARFITT<sup>1</sup>

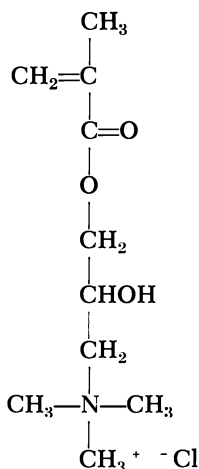
Department of Chemical Engineering, Massachusetts Institute of Technology, Cambridge, Mass.

*Nylon 6/6 film surfaces have been radiation grafted with a quaternized methacrylate monomer. The contact angle,  $\theta$  of pure water on the surface has been measured as a function of surface coverage and for one particular surface coverage as a function of the anion counterion species. Contact angles varied between ca. 23° and 76°, depending on treatment. Calculations of the various contributions to the free energy of interfacial adhesion between water and the grafted polyelectrolyte–microion surface indicate that the free energy of the double layer is the major factor leading to the lowest values of  $\theta$  observed (e.g., < 35°). In the absence of significant dissociation of the polycation–anion pair, measured contact angles are high, and the free energy of interfacial adhesion is made up mainly of van der Waals' interactions.*

**I**t is often desirable to increase the surface free energy of a synthetic polymer to alleviate such processing or end-use problems as static buildup, poor wettability, dyability, printability, or adherability, and poor stain-release or soil redeposition properties in textile applications. One method for accomplishing this is to graft copolymerize hydrophilic monomers onto the polymer molecules in the surface using ionizing radia-

<sup>1</sup> Permanent address: University of Nottingham, England.

tion to initiate the graft copolymerization. In the study reported here, a quaternized methacrylate monomer,



2-Hydroxy-3-methacryloyloxypropyltrimethylammonium chloride

has been radiation-grafted onto the surface of nylon 6/6 film to increase the "hydrophilicity" of the nylon surface. The associated increase in surface energy of the nylon has been investigated by measuring water contact angles on this surface. One would expect this measure of water wettability to be related directly to the processing or end-use problems enumerated above.

### *Experimental*

**Film Grafting and Treatment.** Two-mil nylon 6/6 extruded film was used in all studies. The films were washed successively in tetrachloroethylene, methyl ethyl ketone, acetone, and deionized water (3 baths). The washed samples were vacuum desiccated overnight at room temperature.

The films were then irradiated in air to the desired dose by passing under a 2.5-Mev. Van de Graaff accelerator. The delay time between irradiation and the start of the grafting varied between 5 and 10 min.

The grafting solution was composed of 1 part monomer, 2 parts water (deionized), and 6 parts dimethylformamide (DMF). The monomer was obtained as a powder of 91% (min.) purity from the Shell Chemical Co. and is known under their name of G-MAC Methacrylate. It was used without further purification. DMF was reagent-grade solvent and was used to increase penetration into the surface amorphous regions of the nylon, facilitating the grafting reaction. The irradiated specimens along with unirradiated control specimens were immersed in the grafting solution in a three-necked flask at room temperature. The contents of the flask were then frozen in liquid nitrogen, evacuated, and thawed under

vacuum; this process was repeated several times and took typically about 1 hour. Finally, the flask was filled with nitrogen to 1 atm., and heated to 70°C. for 1 hour. A reflux condenser returned all volatiles to the flask. After this, the samples were removed, rinsed in deionized water at room temperature, and washed in fresh deionized water for 10 min. at 70°C. (This procedure removed any homopolymer from the surface of the unirradiated control specimens).

After washing, the samples were placed in various 0.4*N* sodium salt solutions to exchange the chloride counterion with other anions; they were removed after about 3½ hours in these solutions, each rinsed several times in fresh deionized water at room temperature, vacuum dried and weighed.

**Contact Angle Measurement.** The contact angle of a drop of water on the film surface was estimated by a method developed by Bikerman (2), with slight modifications. The polymer film was first maintained in a flat position by placing on a plate fitted with many tiny holes through which a vacuum was drawn. Then several drops of water of very small volume (0.3μliter) were deposited on the polymer surface with a microsyringe (1μliter total volume, Hamilton Co.). Two mutually perpendicular diameters of each drop were measured by a Microstar light microscope (American Optical Co.) by viewing from above at 40× magnification. The contact angle was calculated knowing the drop volume  $V$ , and base diameter,  $\Delta_o$ , assuming that the drop approximates a spherical section and neglecting gravitational effects:

$$\frac{\Delta_o^3}{V} = \frac{24 \sin^3 \theta}{\pi(2 - 3 \cos \theta + \cos^3 \theta)} \quad (2)$$

Three drops were placed on each new surface to be studied, and the results for  $(\Delta_o^3/V)$  were averaged before calculating  $\theta$ .

To determine if the contact angles measured were "advancing" or equilibrium angles, the film on the vacuum-plate apparatus was vibrated strenuously in several cases with a vibrating glass etching pencil; no change in  $\theta$  was ever noted. It is assumed throughout that the angles calculated represent equilibrium contact angles. All films were equilibrated at 50% relative humidity before contact angles were measured. Repeat measurements on different days suggested that the precision of the results was not exceptional;  $\theta$  values varied over a  $\pm 3$ – $5^\circ$  range with greater precision for the higher  $\theta$  cases (which is not unexpected based on surface roughness considerations, *e.g.*, Ref. 37). When salt solutions were used, the techniques were the same as described above.

## Results

Figure 1 shows the effect of radiation dose on contact angle and weight pickup for Series A treated samples, with the Cl<sup>-</sup> counterion graft only. The weight gain and  $\theta$  level out at higher doses. This cannot correspond to an "ideal" monolayer since for the 2-mil film a "well-packed" monolayer would correspond to less than 0.01% weight gain. (Indeed, assuming 50 A.<sup>2</sup>/charged group, the weight gain is *ca.* 0.008% for a film

treated on both sides). It is probable that the grafting first occurs in the accessible amorphous regions (*i.e.*, interlamellar regions and at the fold surfaces of the nylon chain-folded lamellae) and that the surface is not "fully" treated until the continuing grafting reaction disrupts the surface crystallinity sufficiently such that the grafted polyelectrolyte eventually covers the whole surface.

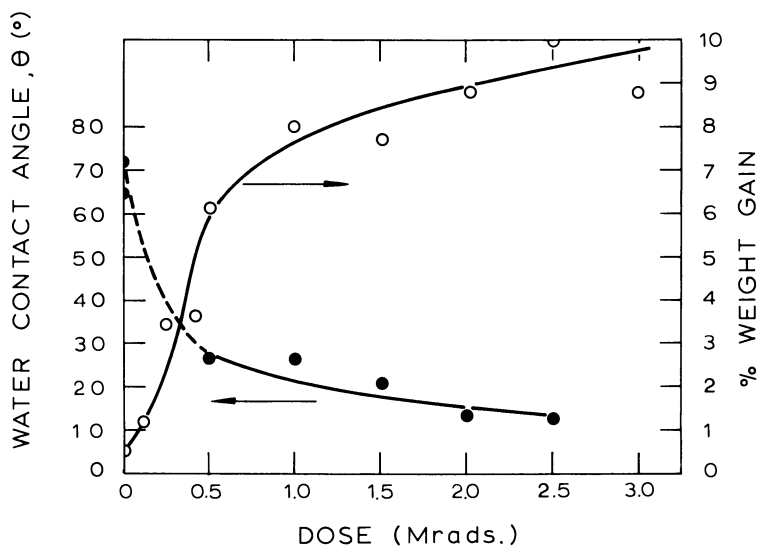


Figure 1. Effect of radiation dose on weight gain and water contact angle. Series A films,  $\text{Cl}^-$  counterion

Since the  $\text{Cl}^-$  counterion surface was expected to exhibit one of the lowest contact angles for water, a 2.5-Mrad dose was selected for the next series of films (Series B) wherein the counterion would be varied. These results, presented in Table I, show that the counterion species has a significant effect on the water contact angle. It is also apparent that, except perhaps in the case of NaOH, the various exchange solutions did not essentially alter the contact angle of water on the surface of the unirradiated nylon; furthermore, the grafting solution treatment with or without the monomer present did not change the water contact angle on the unirradiated nylon surface. No contact angle studies were made on irradiated (only) nylon since this control is thought to be meaningless in view of the subsequent film treatments.

One would have expected a lower contact angle for the irradiated  $\text{Cl}^-$  counterion sample based on the results of the first series (Figure 1). Such differences from one series to another reflect the over-all experimental difficulties involved in reproducing exactly the same procedure for each film series; they also reflect the over-all precision of the use of



**Table I. Effect of Counterion Species on Contact Angle, Series B Films**

<i>Counterion</i>	$\theta$ , degrees	$\theta$ (Control), <sup>a</sup> degrees	$\theta$ (Special Controls) degrees
F <sup>-</sup>	28	70	
Cl <sup>-</sup>	32	72	
IO <sub>3</sub> <sup>-</sup>	32	74	
CH <sub>3</sub> CO <sub>2</sub> <sup>-</sup>	36	78	
Br <sup>-</sup>	40	74	
OH <sup>-</sup>	46	64	
NO <sub>3</sub> <sup>-</sup>	48	72	
SCN <sup>-</sup>	58	70	
ClO <sub>4</sub> <sup>-</sup>	62	74	
I <sup>-</sup>	67	74	
Control 1 (Cl <sup>-</sup> ) <sup>b</sup>			72
Control 2 <sup>c</sup>			72
Control 3 <sup>d</sup>			av. = 76 (range 72-80)

<i>Radiation</i>	<i>Grafting Solution Treatment</i>	<i>Ion Exchange</i>
<sup>a</sup> No	No	Yes
<sup>b</sup> No	Yes	No (already in Cl <sup>-</sup> form)
<sup>c</sup> No	DMF-H <sub>2</sub> O only	No
<sup>d</sup> No	No	No

this contact angle measurement technique on a commercially extruded film surface.

### Discussion

**Counterion Interactions with Water and Polycations.** The wide range of contact angles measured for the different counterions is no doubt related to the extent of their interaction with water relative to that with the polycations.

There are various "degrees" of interaction that hydrated anions may exhibit with quaternary ions. For individual, monomeric quaternary ions Diamond (5) has emphasized the importance of what he calls "water structure-enforced" ion pairing as opposed to complexing, or to simple Bjerrum electrostatic ion pairing, or to "localized hydrolysis" ion pairing (between small anions and cations). For water structure-enforced ion pairing, larger, more poorly hydrated anions such as I<sup>-</sup>, ClO<sub>4</sub><sup>-</sup>, and SCN<sup>-</sup> form ion-pairs in aqueous solution with the larger quaternary ions in order to minimize the disturbance of the water-water interactions in the solvent region surrounding these ions. This type of ion pairing is not a direct result of electrostatic attraction.

For polyelectrolytes, two different models have been proposed to account for ion-binding phenomena (*e.g.*, Ref. 28). In one the counterions are occluded by the coiled polyelectrolyte, while in the other electrostatic binding occurs with localization of a counterion near a polyion charge. In addition, the nature of the binding is still in some "dispute" (22, 23, 29). For example, Strauss and Leung (35) have demonstrated the difference between localized or specific "site binding" and "ion-atmosphere binding" of counterions to polyelectrolytes. With both types of interaction only ion pairing is implied, but in the former case partial dehydration of the counterion may occur, while in the latter case the fully hydrated counterions interact electrostatically with the polyelectrolyte chains. (These two types of binding are comparable respectively to that occurring in (a) the "inner Helmholtz plane" of the Stern layer and (b) the outer Helmholtz plane and the Gouy diffuse double layer in a charged colloid, or the Debye-Hückel ionic atmosphere in dilute electrolyte solutions. It is clear that the extent of the first will affect that of the second.)

There is convincing evidence for "site binding" of anions to simple quaternary ions (7, 9, 21) and to "bolaform" ions (10). "Binding" of counterions to quaternary soap micelles is demonstrated on the basis of changes in the equivalent conductance or CMC values (1, 8, 24, 30). In one case, (32) for  $C_{12}H_{25}NH_3^+Cl^-$  micelles, it was concluded that the extent of dehydration of the  $Cl^-$  counterion at the micelle surface is insignificant. The order of decreasing binding is generally  $I^- > Br^- > Cl^-$ . Electrophoretic studies of Strauss and co-workers (34) have shown that the charge on a quaternized poly(vinyl pyridine) in KBr solutions may be neutralized and then reversed (to a negative charge) on increasing addition of KBr. Presumably increasing site binding of  $Br^-$  to the polycation charges is occurring at first, and eventually even excess  $Br^-$  ions are bound within the shear layer of the "neutralized" polymer molecule coils. Endothermic binding of  $I^-$  and  $NO_3^-$  (17) and charge transfer complex formation of  $I^-$  and  $Br^-$  (24) have also been noted with quaternary ions on dentin collagen and in soap micelles, respectively.

Anion-exchange resin studies have also shown evidence of site binding of anions by the fixed quaternary groups. Selectivity of one anion over another has been used as a relative measure of site binding (3, 13, 14). In one study, Gregor and co-workers (13) measured relative uptake of anions in a Dowex quaternary ion-exchange resin, and their results, in terms of moles of anion/1000 grams  $H_2O$  inside the resin, are correlated with our contact angle data in Figure 2. A good correlation is obtained, except for the  $OH^-$  counterion which has already been questioned owing to the low value of  $\theta$  for the control. They proposed that anion selectivity in ion-exchange resins was governed by "ion-pair" formation with the

fixed polycation and that ion-pairing increased with the size of the unhydrated anion, in an order similar to that of the Hofmeister Series. Recent studies have modified this viewpoint somewhat, and Reichenberg (28) and Diamond and Whitney (6) have pointed out that the most important factor governing selectivity is the relative degree and type of water structuring caused by the different anions rather than simply the anion size. Reichenberg (28) is able to correlate anion selectivity data in quaternary ion exchange resins ( $\text{ClO}_4^- > \text{I}^- > \text{Br}^- > \text{Cl}^-$ ) on the basis that the smaller or more basic anions which are strongly hydrated prefer to remain outside the field of the polycation. That is, despite the fact that they would gain more electrostatic free energy than would a larger, less basic anion upon close approach to the polycation, such a site-binding process would require so much energy to dehydrate the anion partially that the over-all free energy change would tend to be more positive for such a process. Nightingale (26) presents an excellent discussion of ion-water interactions, and our water contact angles appear to correlate well with the viscosity  $B$  coefficient of Jones and Dole (18).

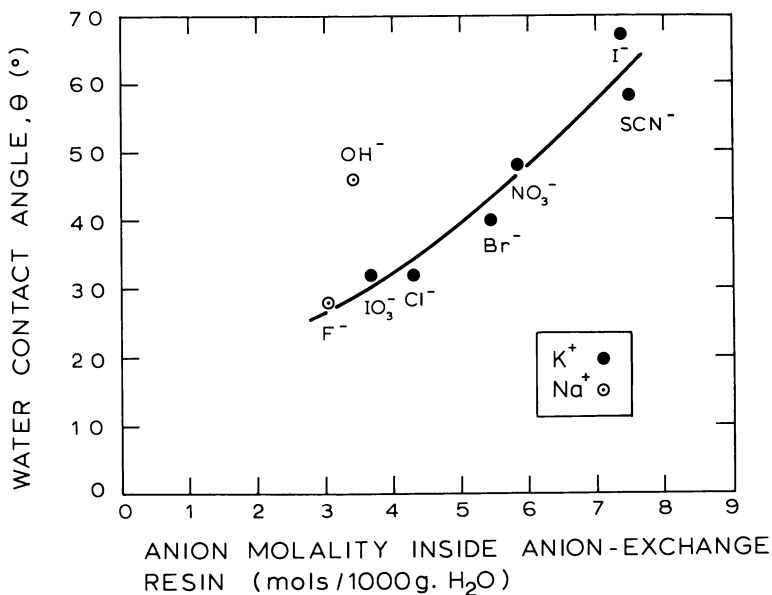
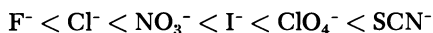


Figure 2. Correlation of water contact angles for different counterions with anion-exchange resin selectivity data of Gregor et al. (13)

It is also interesting that surface potentials measured for aqueous salt solutions indicate that the order of increasing negative potential or increasing closeness of the anion to the surface follows approximately

the same order as the contact angles measured here (15, 27):



Therefore, the anions which exhibit the highest contact angles are most likely to be closely associated ("site bound") with the polycation charges on the nylon surface. If such anions are unable to escape the local field of the polycation, the interfacial tension of the water-polymer interface should be increased over the case where the anion is hydrated more strongly and thus more likely to "escape" from the polymer surface into the water phase. This situation may be demonstrated by adding NaCl to the water droplet used to measure contact angles, for the case of the  $Cl^-$  counterion surface. A film (Series C) was especially prepared by irradiating and grafting the monomer, washing, drying, weighing, and then equilibrating at 50% relative humidity. The contact angle measured for pure, deionized water was  $23^\circ$  for this film specimen. Then the contact angles for NaCl solutions of increasing salt content were measured on this same surface. The results are presented in Table II and Figure 3.

**Table II. Effect of NaCl Concentration in Water Droplet on Contact Angle, Series C Film**

NaCl Concentration, equiv./liter	$\theta$ , degrees	$\gamma_{LV}$ , <sup>a</sup> dynes/cm.	$\gamma_{LV} \cos \theta$ , dynes/cm.
0	23	72.8	67.0
$10^{-3}$	26	72.8	65.4
$10^{-2}$	28	72.8	64.0
$10^{-1}$	36	73.0	58.6
1.0	39	74.6	58.0
2.5	42	77.2	57.1
5.0	46	81.6	56.7

<sup>a</sup> Data from Ref. 19. (Points for 2.5N and 5.0N estimated from this reference.)

The striking increase in contact angle with increasing salt content is caused mainly by the increased interfacial tension and presumably reflects the "original"  $Cl^-$  counterions being forced back to the surface as the polycation charges are screened by the large number of  $Cl^-$  ions available. It cannot be caused by the increase in surface tension of the salt droplet since the product of liquid droplet surface tension,  $\gamma_{LV}$  and  $\cos \theta$  is decreasing as  $\gamma_{LV}$  increases. Thus, since  $(\gamma_{LV} \cos \theta) = \gamma_{SV} - \gamma_{LS}$  (where  $\gamma_{SV}$  = solid surface tension in equilibrium with vapor from droplet and  $\gamma_{LS}$  = interfacial tension) and since  $\gamma_{SV}$  would not be expected to change much with increasing salt in the droplet, the decrease in  $(\gamma_{LV} \cos \theta)$  must be roughly equal in magnitude to the increase in  $\gamma_{LS}$ .

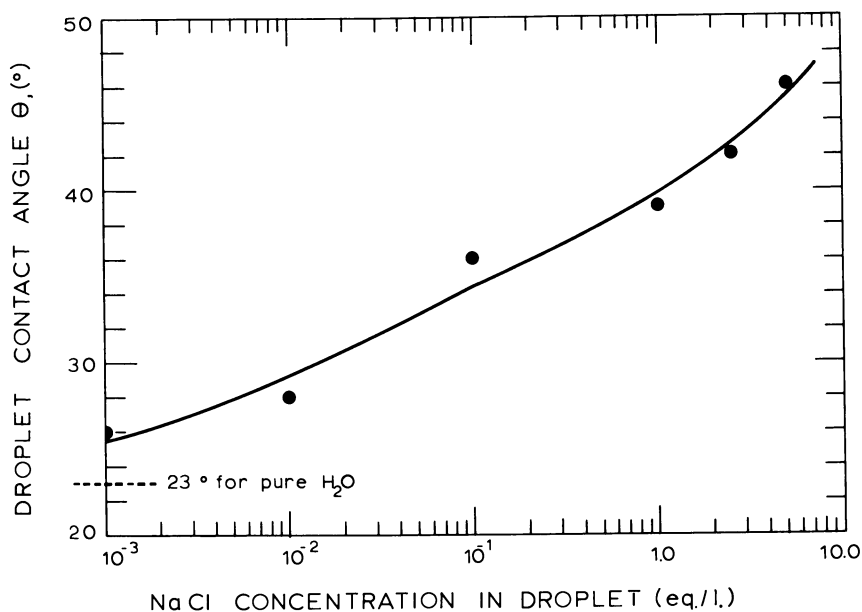


Figure 3. Effect of NaCl concentration on droplet contact angle. Series C films,  $\text{Cl}^-$  counterion

The spreading pressure,  $\pi_e$  of water vapor on the solid surface would decrease slightly owing to the lower vapor pressure of water over the droplets of increasing salt content, but this should not be a major factor since the most concentrated salt solution—5*N*—lowers the vapor pressure of water only 20% at 100°C. If the Young equation for pure water is subtracted from that for any salt concentration,  $\gamma_{SV}$  may be eliminated, and the relative increase in  $\gamma_{LS}$  may be calculated as:

$$\gamma_{LS} - \gamma_{LS}^o = (\gamma_{LV} \cos \theta)^o - \gamma_{LV} \cos \theta$$

where the superscript  $o$  refers to pure water, and all other terms refer to a particular salt concentration. These calculations are presented in Figure 4 as a function of droplet contact angle. Although the maximum calculated increase in interfacial tension is just over 10 dynes/cm., it is sufficient to double the contact angle from 23° to 46°. These results emphasize the tremendous influence that the degree of counterion site binding has on the wettability of a polyelectrolyte-grafted surface.

**Critical Surface Tensions.** The data in Table II may be plotted (Figure 5) as  $\cos \theta$  vs.  $\gamma_{LV}$ , according to the approach of Zisman (37). Then one may estimate the critical surface tension,  $\gamma_c$  of the undissociated polycation $^+ - \text{Cl}^-$  surface of this particular nylon film in equilibrium with saturated water vapor by extrapolating the last four data points (which

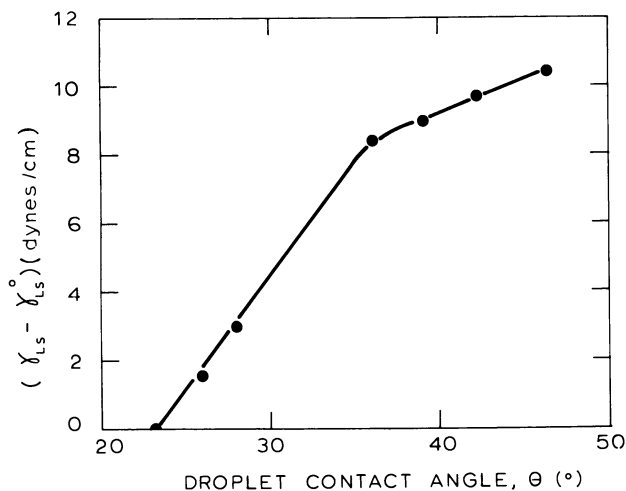


Figure 4. Relative increase in interfacial tension as a function of droplet contact angle for increasing NaCl concentrations. Series C films,  $Cl^-$  counterion

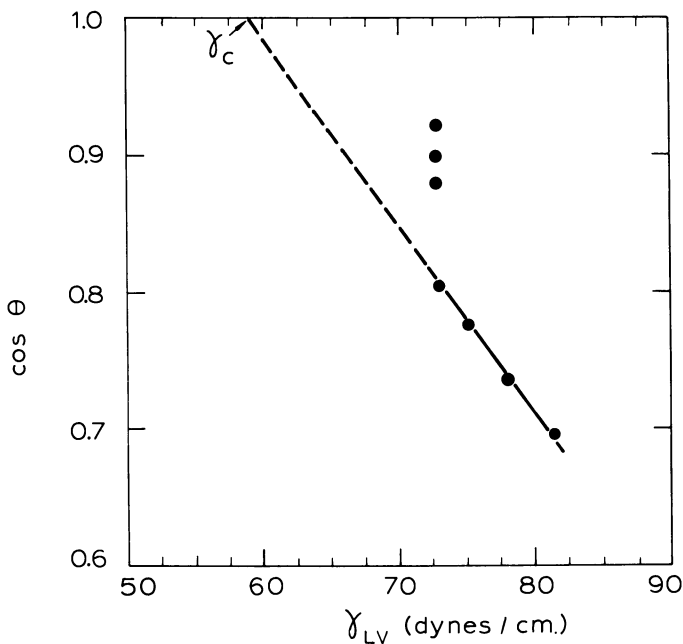


Figure 5. Estimation of critical surface tension,  $\gamma_c$ , for the undissociated  $Cl^-$  counterion surface

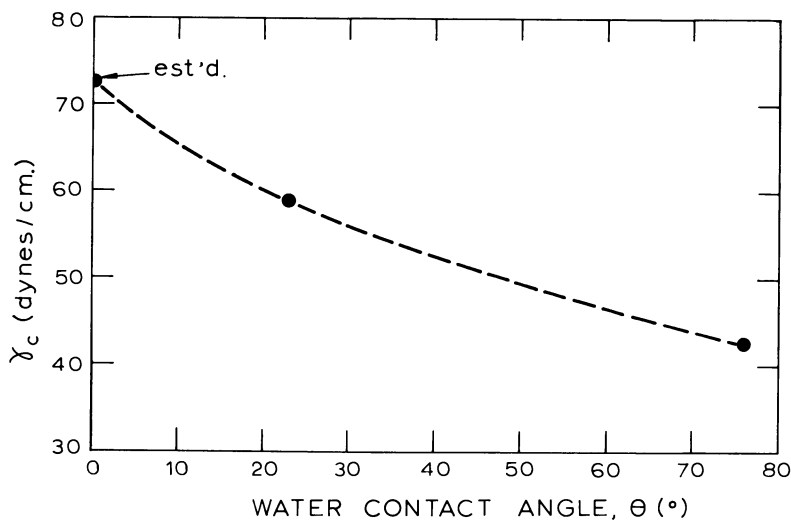


Figure 6. Estimated critical surface tensions as a function of water contact angle

Table III. Estimate of Critical Surface Tensions for Undissociated Poly  $R_4\bar{N}^+\bar{X}^-$  Surfaces<sup>a</sup>

Counterion, $X^-$	$\theta$ , degrees	$\gamma_c$ , <sup>b</sup> dynes/cm.
F <sup>-</sup>	28	57
Cl <sup>-</sup>	32	55
IO <sub>3</sub> <sup>-</sup>	32	55
CH <sub>3</sub> CO <sub>2</sub> <sup>-</sup>	36	54
Br <sup>-</sup>	40	52
OH <sup>-</sup>	46	50
NO <sub>3</sub> <sup>-</sup>	48	50
SCN <sup>-</sup>	58	47
ClO <sub>4</sub> <sup>-</sup>	62	46
I <sup>-</sup>	67	44

<sup>a</sup> Series B films.

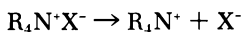
<sup>b</sup> Estimated from Figure 6.

are most likely to pertain to this *undissociated* surface condition) to  $\cos \theta = 1$ . This yields a value of  $\gamma_c \cong 59$  dynes/cm. If the contact angle of pure water on treated nylon surface were just  $0^\circ$ , one could assume that  $\gamma_c$  for this surface would be best approximated by the surface tension of water—*i.e.*, 72–73 dynes/cm. Finally, literature values for  $\gamma_c$  of an untreated nylon 6/6 surface are in the range of 43–43 dynes/cm. (9, 37). These three values of  $\gamma_c$  may be plotted against the corresponding contact

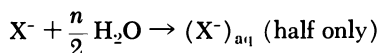
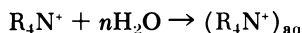
angles of pure water on the three surfaces, as shown in Figure 6. Then the critical surface tensions for the different *undissociated* polycation-anion surfaces in equilibrium with saturated water vapor may be estimated from this curve for the Series B film samples shown in Table I. These values are presented in Table III.

**Interfacial Energy of Adhesion.** When the polyelectrolyte-grafted nylon surface, in equilibrium with 50% relative humidity, is brought into contact with water or a salt solution, various interactions will occur; together they comprise the reversible work of adhesion or free energy of adhesion at the interface of these two phases. This free energy of adhesion should be composed of the following contributions:

- (1) Van der Waals' energy of interaction between water and:
  - (a) a site-bound  $R_4N^+X^-$  ion pair
  - (b) a covalently bonded  $R_4NX$
  - (c) polar groups as NH, OH, C=O on the nylon or polyelectrolyte backbones.
  - (d) nonpolar groups on the nylon or polyelectrolyte backbones.
- (2) Electrostatic energy needed to dissociate an ion pair



- (3) Free energies of hydration of the dissociated ions



- (4) Electrostatic free energy of interaction between the polyelectrolyte charges and the ionic atmosphere of loosely bound counterions.

- (5) Free energy associated with water structure changes at or near the interface.

- (6) Free energy associated with conformational changes of polycations.

Of the above contributions, 1, 3, and 4 will tend to lower the free energy of adhesion and favor wetting (lower  $\theta$ ); 2 will raise the free energy and oppose wetting (higher  $\theta$ ); the effects of 5 and 6 may go in either direction.

With respect to these last two terms, site binding of a water-structuring anion could result in an increase in  $H_2O-H_2O$  interactions and a decrease in the structuring of the bulk water above the surface, decreasing the free energy of the water. Furthermore, one would expect the polymer generally to gain in conformational entropy upon mixing with water, but if the degree of dissociation is very high the local charged groups along the chain may stiffen the chain, owing to mutual repulsion, leading to a decrease in conformation entropy.

On the other hand, one may also argue that the more strongly site-bound ion pairs could be expected to exhibit a greater tendency to struc-



ture water (and thus to exclude more water from the regions between the grafted chains in and under the nylon surface) owing to enhanced hydrophobic bonding along the polymer chain. Indeed, it has been suggested (14) that site-bound ion pairs within ion-exchange resins may actually cluster together in a kind of phase separation owing to van der Waals' interactions between them.

All these types of interactions could affect significantly the free energy of adhesion at the interface. It is impossible at this time to estimate these contributions to the free energy of adhesion, and they are omitted from the following discussion.

The interface may be modeled ideally as a planar positively charged surface on which a fraction of the counterions are site bound—*i.e.*, in the inner Helmholtz plane of the Stern layer. This is shown in Figure 7. The remaining counterions are assumed to remain hydrated and to form a Gouy-Chapman diffuse double layer extending into the water phase and starting at the outer Helmholtz plane. The total surface charge density is taken to be similar to that encountered with a gaseous monolayer of cetylpyridinium chloride on water, which would correspond to about 85 A.<sup>2</sup> per charged group (4). This yields a polycation charge density of  $1.2 \times 10^{14}$  charges/cm.<sup>2</sup>.

The specific case to be considered is that of the Cl<sup>-</sup> counterion surface in contact with a dilute salt solution—*e.g.*, at  $10^{-2}N$  NaCl where  $\theta = 28^\circ$  (Table II). Data of Stigter (33) show that the fraction of Cl<sup>-</sup> counterions outside the shear surface of dodecyl ammonium chloride micelles is about 0.4 in the range 0.02–0.05M NaCl plus surfactant at the critical micelle concentration (CMC). This value appears to rise toward 0.5–0.6 as NaCl concentration is lowered. Conductance data of Robins and Thomas (30) indicate that 73% of Cl<sup>-</sup> counterions are bound to 2-dodecyl aminoethanol hydrochloride micelles at the CMC in the absence of added salt.

It seems reasonable to assume that the fraction of counterions bound to a spherical micellar surface would be similar in magnitude to that for an ionized monolayer and therefore also similar to that for a charged planar surface since these surface charge densities should be roughly within a factor of two of each other. Therefore, it is assumed for the specific case considered here that about half of the Cl<sup>-</sup> ions are "tightly-bound," or about  $0.6 \times 10^{14}$  charges/cm.<sup>2</sup> are "closely associated" (site bound or covalently bonded) with their counterions and about  $0.6 \times 10^{14}$  charges/cm.<sup>2</sup> have a corresponding number of "loosely bound" counterions in the diffuse double layer.

The calculation of the van der Waals' energy of interaction of any of the four contributions (1a, 1b, 1c, 1d) requires knowledge of the dipole moments,  $\mu$ , polarizabilities,  $\alpha$  and average distance of separation,  $r$

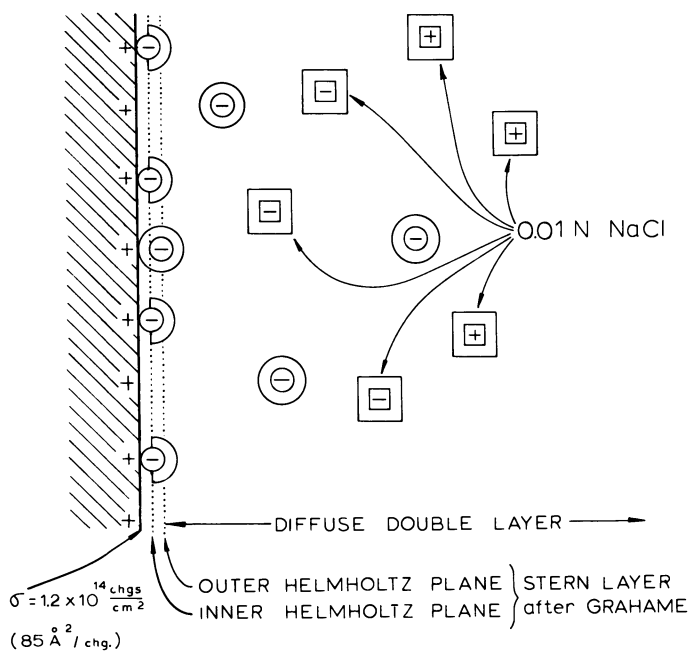


Figure 7. Interface model

Table IV. van der Waals' Interactions

Term <sup>a</sup>	$R_4N^+Cl^-$ (ergs/ion pair) $\times 10^{14}$	$R_4NCl$ (ergs/bond) $\times 10^{14}$
Orientation: $2/3 \left[ \frac{\mu_1^2 \mu_2^2}{kT} \right] (r^{-6})$	-1330	-130
Induction: $[\alpha_1 \mu_2^2 + \alpha_2 \mu_1^2] (r^{-6})$	-60	-3
Dispersion: $3/4 [\alpha_1 \alpha_2 (h\nu_o)_{av.}] (r^{-6})$	-75	-14
Total	$\sim -1500$	$\sim -150$

<sup>a</sup> Values assumed:

	$\mu$ , Debye	$\alpha$ , A. <sup>3</sup>	$r$ , A.	$h\nu_o$ , e.v.
H <sub>2</sub> O	1.84	1.48	2.5	16
R <sub>4</sub> NCl	1	2.6	2.5	16
R <sub>4</sub> N <sup>+</sup> Cl <sup>-</sup>	10	14	2.5	16

between water and the interacting groups. The ion pair,  $R_4N^+Cl^-$  values are estimated from literature values as follows:  $\mu = 10$  Debyes (based on dielectric measurements in dilute benzene solutions of tri- and tetrabutyl ammonium salts) (11);  $\alpha = \alpha_{R_4N^+} + \alpha_{Cl^-} \cong 14 \text{ A.}^3$  (28);  $r \cong 2.5 \text{ A.}$

(based on center-to-center distance of the bare  $\text{Cl}^-$  ion and the first layer of water molecules and assumed to apply for the ion pair,  $\text{R}_4\text{N}^+\text{Cl}^-$ -water distance) (25). The values of  $\mu$  and  $\alpha$  for covalently bonded  $\text{R}_4\text{NCl}$  are, for want of better data, taken to be those for  $\text{HCl}$  gas molecules, or  $\mu \cong 1$  Debye and  $\alpha \cong 2.6 \text{ \AA}^3$  (16). The average separation here should be about the same as for  $\text{R}_4\text{N}^+\text{Cl}^-$ , 2.5  $\text{\AA}$ . It is probable that contributions 1c and 1d will be much less than 1a or 1b, and they are neglected here.

The three van der Waals' interactions with water are then calculated for each ion pair or covalent  $\text{R}_4\text{NCl}$  bond, and the results are summarized in Table IV.

The dissociation energy of  $\text{R}_4\text{N}^+\text{X}^-$  into the individual ions may be estimated from literature data. Grahame (12) has shown that the specific adsorption potential of  $\text{Cl}^-$  ions onto a positively charged mercury interface will vary as a function of the charge density on the mercury surface. Between a charge density of 0 and  $0.6 \times 10^{14}$  charges/cm.<sup>2</sup> this specific adsorption potential varies from 120 to 200 mv. If an average value of 160 mv. is assumed, one calculates 26 ergs/cm.<sup>2</sup> to be the total energy (av.) needed to dissociate half the original ion pairs when the grafted nylon surface is contacted with water. This assumes, of course, that the values measured by Grahame for the aqueous  $\text{NaCl}$ - $\text{Hg}$  interface may be applied here.

After these ions are dissociated, some energy is recovered upon hydration of the  $\text{R}_4\text{N}^+$  cations and the corresponding  $\text{Cl}^-$  anions. Here it is assumed that since the original surface is in equilibrium with 50% relative humidity, each of the  $\text{Cl}^-$  ions is already half hydrated. Since the  $\text{R}_4\text{N}^+$  is relatively hydrophobic, it is not expected that it will hydrate extensively or that this hydration will be very energetic, and this term is neglected here.

The free energy of hydration of the  $\text{Cl}^-$  ion, based on standard states at 25°C. of 1 mole/liter for gaseous ions or an equivalent hypothetical molal solution for aqueous ions is about  $-84$  kcal./gram mole or  $-5.83 \times 10^{12}$  ergs/ion (31). Thus, for  $0.6 \times 10^{14}$  ions/cm.<sup>2</sup>, the energy contribution of  $\text{Cl}^-$  hydration to interfacial adhesion is  $1/2 (0.6 \times 10^{14}) (-5.8 \times 10^{12}) \cong -170$  ergs/cm.<sup>2</sup>.

The contribution of the free energy of the diffuse double layer,  $\Delta G_{\text{ddl}}$ , to the interfacial adhesion may be estimated as follows (36):

$$\Delta G_{\text{ddl}} = -\frac{8ckT}{\kappa} \left[ \cosh \frac{ze\psi}{2kT} - 1 \right]$$

where:  $c$  = salt concentration, 0.01M  
 $k$  = Boltzmann's constant  
 $T$  = temperature, °K.

$\kappa$  = Debye-Hückel parameter, estimated here as  $\kappa \cong \sqrt{c}/3 \text{ \AA}^{-1}$  (assuming the dielectric constant of the solvent medium inside the double layer is 80).

$z$  = valence of charges (= 1)

$e$  = electronic charge

$\psi$  = electrical potential at the outer edge of the Stern layer, calculated to be about 150 mv. from the following expression (36):

$$\sigma = \sqrt{\frac{DckT}{2\pi}} \left[ e^{\frac{ze\psi}{2kT}} - e^{-\frac{ze\psi}{2kT}} \right]$$

where:  $D$  = dielectric constant of water = 80

$\sigma$  = effective surface charge density at edge of Stern layer =  $0.6 \times 10^{14}$  charges/cm.<sup>2</sup>

This free energy is calculated to be

$$\Delta G_{\text{adl}} \cong -3900 \text{ ergs/cm.}^2$$

Thus, the total contribution estimated for the loosely bound Cl<sup>-</sup> ions is  $-3900 - 170 + 26$  or about  $-4000$  ergs/cm.<sup>2</sup>, while that for the tightly bound Cl<sup>-</sup> ions may vary between about  $-90$  and  $-900$  ergs/cm.<sup>2</sup> (i.e., if all the bound Cl<sup>-</sup> ions were site-bound ion pairs, their contribution to the free energy of adhesion would be  $(0.6 \times 10^{14}) \times (-1500 \times 10^{-14})$  or about  $-900$  ergs/cm.<sup>2</sup>. If all these Cl<sup>-</sup> ions were covalently bonded, this figure would be about  $-90$  ergs/cm.<sup>2</sup>).

In any case, it is clear that when even half the counterions are tightly bound to the surface, the contribution of the loosely bound ions to the free energy of adhesion is greater. (This is still true even if a value of 3  $\text{\AA}$ . is taken as the average separation in the van der Waals' calculations). The comparison is perhaps clearer when made on the basis of one ion or ion pair (Table V).

**Table V. Summary of Interfacial Energies**

Term	Energy, $\times 10^{14}$	
Electrostatic (double layer)	-6600	ergs/ $R_1N^+$
van der Waals' $R_1N^+Cl^-$	-1500	ergs/ $R_4N^+Cl^-$
Hydration	-300	ergs/ $Cl^-$
van der Waals' $R_1NCl$	-150	ergs/ $R_4NCl$
Dissociation	+40	ergs/ $R_1N^+ + Cl^-$

Thus, in general for any counterion species the free energy of adhesion will probably always be higher and the contact angle lower when more counterions are able to escape the local fields of the individual charges on the polyelectrolyte. Figure 8 depicts schematically this behavior for the different counterions. Therefore, for grafted polyquaternary cations on a nylon surface, the counterions F<sup>-</sup>, Cl<sup>-</sup>, and IO<sub>3</sub><sup>-</sup> are

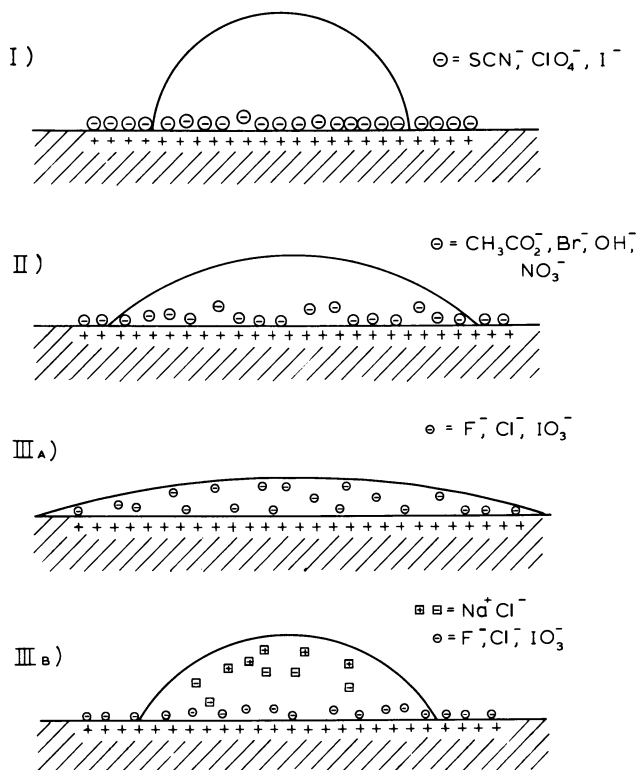


Figure 8. Schematic of drop configuration as a function of surface counterion and NaCl in drop

relatively strongly hydrated and loosely bound (ion-atmosphere binding),  $\text{I}^-$ ,  $\text{ClO}_4^-$ , and  $\text{SCN}^-$  are relatively weakly hydrated and tightly bound (covalent bonding), while  $\text{CH}_3\text{CO}_2^-$ ,  $\text{Br}^-$ ,  $\text{NO}_3^-$ , and  $\text{OH}^-$  (?) represent intermediate cases of association (ion-pair site binding) at the pure water–polyelectrolyte interface.

### Acknowledgment

The authors acknowledge the helpful assistance of K. Sidman and E. Kiran in the laboratory and thank K. Wright for irradiating the films.

### Literature Cited

- (1) Anacker, E. W., Ghose, H. M., *J. Phys. Chem.* **67**, 1713 (1963).
- (2) Bikerman, J. J., *Ind. Eng. Chem. (Anal. Ed.)* **13**, 443 (1941).
- (3) Boyd, G. E., Lindenbaum, S., Myers, G. E., *J. Phys. Chem.* **65**, 577 (1961).

- (4) Davies, J. T., *Proc. Roy. Soc. (London)* **A208**, 224 (1951).
- (5) Diamond, R. M., *J. Phys. Chem.* **67**, 2513 (1963).
- (6) Diamond, R. M., Whitney, D. C., "Ion Exchange," J. A. Marinsky, Ed., Vol. I., Chap. 8, Marcel Dekker, New York, 1966.
- (7) Evans, D. F., Kay, R. L., *J. Phys. Chem.* **70**, 366 (1966).
- (8) Ford, W. P. J., Ottewill, R. H., Parrevia, H. C., *J. Colloid Interface Sci.* **21**, 522 (1966).
- (9) Fort, T., *ADVAN. CHEM. SER.* **43**, 302-309 (1964).
- (10) Fuoss, R. M., Chu, V. F. H., *J. Am. Chem. Soc.* **73**, 949 (1951).
- (11) Geddes, J. A., Kraus, C. A., *Trans. Faraday Soc.* **32**, 585 (1936).
- (12) Grahame, D. C., *Chem. Rev.* **41**, 441 (1947).
- (13) Gregor, H. P., Belle, J., Marcus, R. A., *J. Am. Chem. Soc.* **76**, 1984 (1954).
- (14) *Ibid.*, **77**, 2713 (1955).
- (15) Haydon, D. A., "Recent Progress in Surface Science," J. F. Danielli *et al.*, Eds., Vol. 1, Chap. 3, Academic, London, 1964.
- (16) Hirschfelder, J. O., Curtiss, C. F., Bird, R. B., "Molecular Theory of Gases and Liquids," Wiley, New York, 1954.
- (17) Huget, E. F., Brauer, G. M., *Chem. Eng. News* p. 16 (July 1, 1968).
- (18) Jones, G., Dole, M., *J. Am. Chem. Soc.* **51**, 2950 (1929).
- (19) Jones, G., Ray, W. A., *J. Am. Chem. Soc.* **63**, 3262 (1941).
- (20) Kay, R. L., Evans, D. F., *J. Phys. Chem.* **69**, 4216 (1965).
- (21) Lindenbaum, S., Boyd, G. E., *J. Phys. Chem.* **68**, 911 (1964).
- (22) Mandel, M., *J. Polymer Sci., Pt. C* **16**, 2955 (1967).
- (23) Morawetz, H., "Macromolecules in Solution," Chap. VII, Interscience, New York, 1965.
- (24) Mukerjee, P., Ray, A., *J. Phys. Chem.* **70**, 2150 (1966).
- (25) Nightingale, E. R., *J. Phys. Chem.* **63**, 1381 (1959).
- (26) Nightingale, E. R., "Chemical Physics of Ionic Solutions," B. E. Conway, R. G. Barradas, Eds., Chap. 7, Wiley, New York, 1966.
- (27) Randles, J. E. B., *Discussions Faraday Soc.* **24**, 194 (1957).
- (28) Reichenberg, D., "Ion Exchange," J. A. Marinsky, Ed., Vol. I., Chap. 7, Marcel Dekker, New York, 1966.
- (29) Rice, S. A., Nagasawa, M., "Polyelectrolyte Solutions," Chaps. 5, 9, Academic, New York, 1961.
- (30) Robins, D. C., Thomas, I. L., *J. Colloid Interface Sci.* **26**, 407 (1968).
- (31) Robinson, R. A., Stokes, R. H., "Electrolyte Solutions," p. 70, Butterworth, London, 1959.
- (32) Stigter, D., *J. Phys. Chem.* **68**, 3603 (1964).
- (33) Stigter, D., *J. Colloid Interface Sci.* **23**, 379 (1967).
- (34) Strauss, V. P., Gershfeld, N. L., Spiera, H., *J. Am. Chem. Soc.* **76**, 5909 (1954).
- (35) Strauss, V. P., Leung, Y. P., *J. Am. Chem. Soc.* **87**, 1476 (1965).
- (36) Verwey, E. J. W., Overbeek, J. Th. G., "Theory of the Stability of Lyophobic Colloids," Elsevier, Amsterdam, 1948.
- (37) Zisman, W. A., *ADVAN. CHEM. SER.* **43**, 1-51 (1964).

RECEIVED August 20, 1968.

## Preparation of Permselective Membranes by Radiation Grafting of Hydrophilic Monomers into Polytetrafluoroethylene Films

A. CHAPIRO, G. BEX, A. M. JENDRYCHOWSKA-BONAMOUR, and T. O'NEILL

Laboratoire de Chimie des Radiations, C.N.R.S., 92-Bellevue, France

*Acrylic acid (AA) and vinyl pyridine (VP) were grafted into 0.05 and 0.1-mm. thick PTFE films by irradiating the latter immersed in aqueous solutions of the monomer. Selective inhibitors were used to minimize homopolymerization. The kinetics were investigated at different temperatures and radiation dose rates. AA was grafted in 50% aqueous solutions containing ferrous sulfate. VP was grafted in 80% aqueous solutions. The various kinetic results are discussed and compared with earlier data obtained when grafting styrene into PTFE. Polyfunctional membranes containing both AA and VP groups were prepared by grafting the two monomers in two successive steps. The resulting membranes were found to swell much more in water than membranes containing either AA or VP groups alone.*

A fairly abundant literature covers the graft copolymerization of polytetrafluoroethylene (PTFE). One of the main features which controls the kinetics of this reaction is the fact that PTFE does not dissolve or swell in any known reagent. Hence, grafting should be limited in principle to the surface of films, fibers, or molded objects made of PTFE (3, 6, 15). About 10 years ago it was found, however, that under suitable conditions styrene and methyl methacrylate can be grafted in the bulk of PTFE films by irradiating the latter immersed in a monomer or in a monomer solution (2, 4). This reaction was possible by a gradual penetration of the monomer through the successive grafted layers which swell in the reaction medium; the grafted front slowly moves inward into the

film. The process involves competition between the diffusion of the monomer and its conversion to polymer. Several studies were devoted to such systems using PTFE films and fibers. Grafting was achieved either by the "direct radiation method" (9, 14) or after preirradiation (7, 8, 12, 13, 17). Grafting was also found to occur "spontaneously" when PTFE films are immersed in a polymerizing monomer, the reaction being initiated either thermally or by peroxides (10). Most likely in such an event grafting occurs by chain transfer to the polymer.

More recently, we became interested in grafting hydrophilic monomers into PTFE films, thereby generating permselective membranes (5). A preliminary report on the kinetics of the grafting of acrylic acid and 4-vinylpyridine was presented a year ago (1). This chapter is devoted to a detailed kinetic analysis of the reaction.

### **Experimental**

PTFE films were irradiated with cobalt-60  $\gamma$ -rays in vacuum-sealed ampoules containing aqueous monomer solutions. The following reaction parameters were investigated: radiation dose and dose rate, reaction temperature, and film thickness. Selective inhibitors were used to minimize the homopolymerization of the monomer in the solution around the film.

Acrylic acid (of Compagnie Nobel-Bozel or Uglier) was used without further purification. 4-Vinylpyridine (Fluka) was distilled twice under vacuum (b.p., = 58°C. at 12 mm. Hg) and stored in a refrigerator under nitrogen. Small pieces of PTFE,  $10 \times 20$  to  $10 \times 40$  mm.<sup>2</sup> were cut from commercial films 0.1- and 0.05-mm. thick. They were immersed for 24 hours in either chromic acid or methanol at room temperature, washed, and dried under vacuum.

Irradiations were performed with cobalt-60  $\gamma$ -rays from a 1000-curie source. The sealed ampoules were either irradiated in air at 20°C. or in a water thermostat at different temperatures. Dosimetry was based on the oxidation of ferrous sulfate in 0.8N sulfuric acid, using  $G(\text{Fe}^{3+}) = 15.5$ .

After irradiation the grafted films were extracted in methanol for 8 to 16 hours and dried *in vacuo*. The grafting ratio is expressed by the weight ratio  $W/W_0$  of the grafted film to the original PTFE film. The ratio  $(W - W_0)/W_0$  is the weight increase in grams per gram of original material. After extensive drying, the films were again swollen in water and thereafter treated with 0.1N HCl or KOH. Their swelling ratio  $W_s/W$  was determined under these conditions ( $W_s$  is the weight of the swollen film). After drying, the films usually exhibited a weight increase corresponding to the theoretical addition of K or HCl to the active groups.

### **Results**

**Carboxylic Membranes.** PTFE films were irradiated in 50% aqueous solutions of acrylic acid. To prevent homopolymerization, 0.25% ferrous



sulfate (Mohr salt) was added to the reaction mixture. These reaction conditions were found to correspond to an optimum in our earlier work (5).

**INFLUENCE OF DOSE AND DOSE-RATE.** Figure 1 is a plot of the conversion curves obtained with 0.1-mm. thick films at 20°C. with different dose rates. The curves are composed of two portions: an initial rapid process with a short "induction period," followed by a slower process which sets in fairly suddenly. The curves exhibit a break at a critical degree of grafting which gradually increases with dose rate. No break is observed at the highest dose rate used. This effect has been described (1, 5). It seems to result from the following sequence of events. As the grafting proceeds, the PTFE chains uncoil gradually, and the polymer swells gradually in the reaction mixture. A limiting configuration is reached soon, however, which presumably corresponds to an elastic limit of the chains. At this point the grafted films swell only slightly in water, as was shown by direct measurements (1). If the grafting proceeds further, some of the polymeric chains may break under the mechanical forces developed by the swelling. This leads to more scattered results and to a greater swelling of the grafted films.

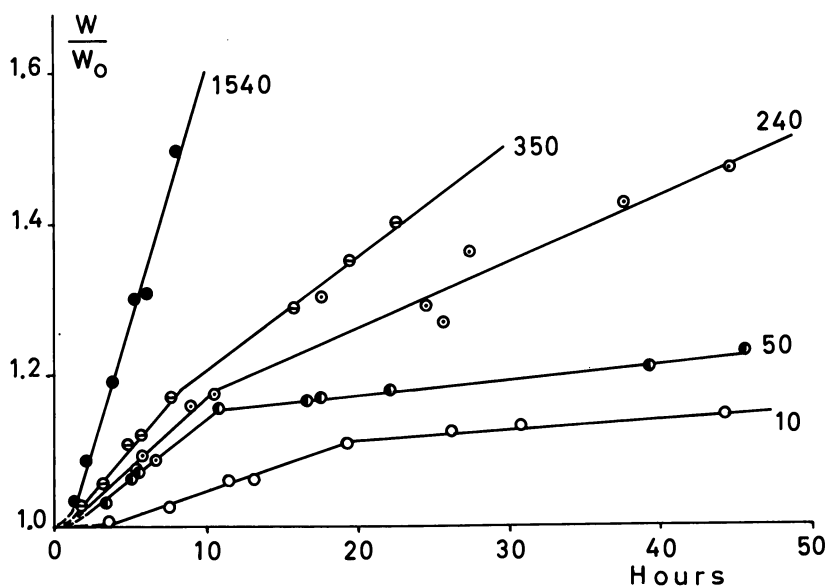


Figure 1. Weight increase of 0.1-mm. thick PTFE films irradiated in 50% aqueous solutions of acrylic acid at 20°C. and different dose rates (shown on curves)

At higher dose rates, a given grafting ratio is attained by a higher total dose since the rate follows approximately the square root relationship (*see below*). As a result, the PTFE chains then carry a larger number of shorter grafted branches, and this presumably helps their uncoiling. Experimental evidence shows that the above described effect vanishes at *ca.* 1000 rads per minute (*see* Figures 1, 2, and 4).

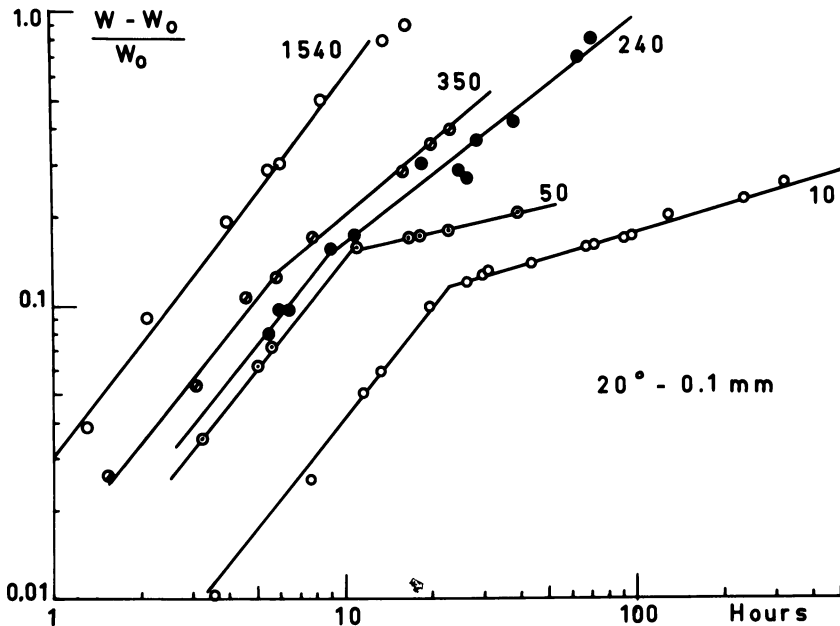


Figure 2. Log-log plot of weight increase of 0.1-mm. thick PTFE films irradiated in 50% aqueous solutions of AA at 20°C. and different dose rates (shown on curves)

To determine grafting rates, the conversion curves were plotted on a log-log diagram (*see also* Refs. 2 and 4). This plot is shown in Figure 2. The initial portions of the curves are straight lines with a constant slope  $\beta = 1.25$ . The weight increase of the films follows the relationship:

$$(W - W_0)/W_0 = Kt^{1.25}$$

which corresponds to a fairly small "autoacceleration index" (4).

The instantaneous grafting rate at 10% weight increase derived from the above results is plotted as a function of dose rate in Figure 3 on a log-log diagram. The plot obeys the following relationship:

$$R_{0.1} = KI^{0.45}$$

At 0°, 40°, and 60°C. the dose-rate exponents are approximately the same.

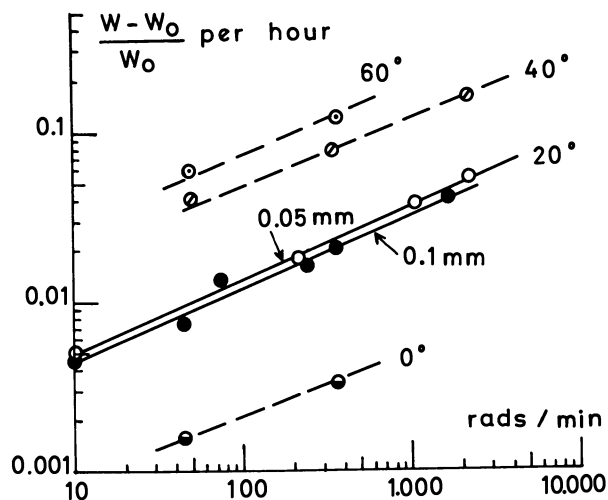


Figure 3. Influence of dose rate of  $\gamma$ -rays on the rate of grafting AA on PTFE films at different temperatures (0.1-mm. thick films except when indicated)

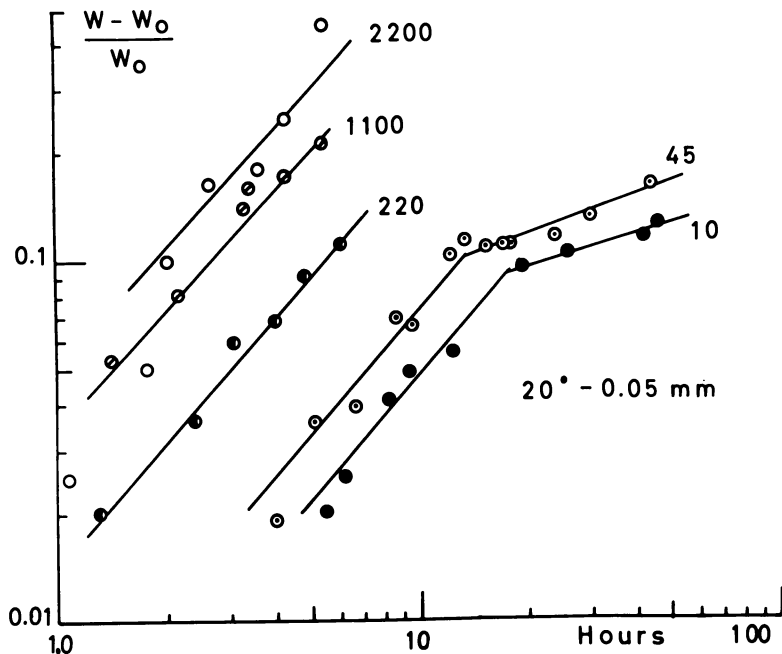


Figure 4. Log-log plot of weight increase of 0.05-mm. thick PTFE films irradiated in 50% aqueous solutions of AA at 20°C. and different dose rates (shown on curves)

Similar experiments were performed with 0.05-mm. thick films. The log-log plot of the conversion curves is shown in Figure 4. Here the autoacceleration index is  $\beta = 1.15$ . The break on the curves occurs at lower grafting ratios than for the 0.1-mm. films. The dose-rate exponent for the instantaneous rate at 10% weight increase is  $\alpha = 0.45$  as shown in Figure 3.

**INFLUENCE OF IRRADIATION TEMPERATURE.** Experiments were carried out at temperatures ranging from 0° to 95°C. and at various dose rates. The following points were clarified in this work:

(1) For a given dose rate the break in the conversion curves occurs at approximately the same conversion regardless of reaction temperature.

(2) For 0.1-mm. thick PTFE films, the autoacceleration index—*i.e.*, the slope of the initial portions of the conversion curves in log-log coordinates—remains approximately the same at all temperatures and dose rates. Figure 5 shows the data obtained at 350 rads/min. The autoacceleration index is 1.25–1.29. The Arrhenius plot of the instantaneous rates at 10% conversion is shown in Figure 6. This plot is based on the ratios  $R_t/R_{20^\circ\text{C}}$  of the rates measured at different temperatures and dose rates with respect to the corresponding rates at 20°C. It exhibits a break at a temperature of *ca.* 33°C. A transition point of PTFE has been reported at about the same temperature (11, 16). The activation energies are respectively 15.0 and 5.1 kcal./mole below and above 33°C.

(3) For 0.05-mm. thick PTFE films the results are more complex. Between 20° and 40°C. the rate increase is approximately the same as for the thicker films, and the conversion curves are parallel (Figure 7).

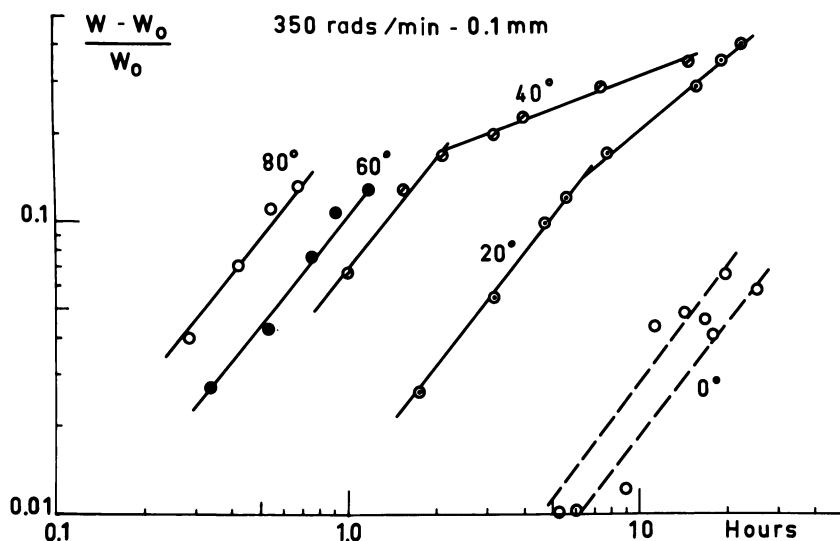


Figure 5. Log-log plot of weight increase of 0.1-mm. thick PTFE films irradiated at 350 rads/min. at different temperatures

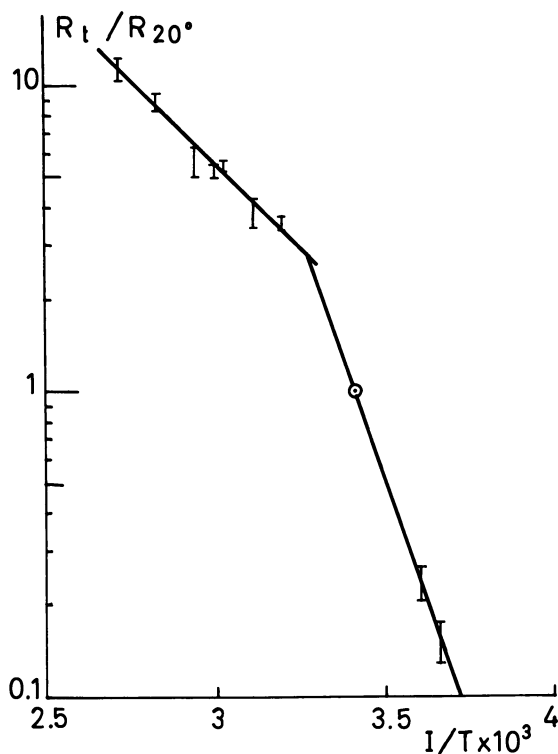


Figure 6. Arrhenius plot of the rate of grafting AA onto 0.1-mm. thick PTFE films

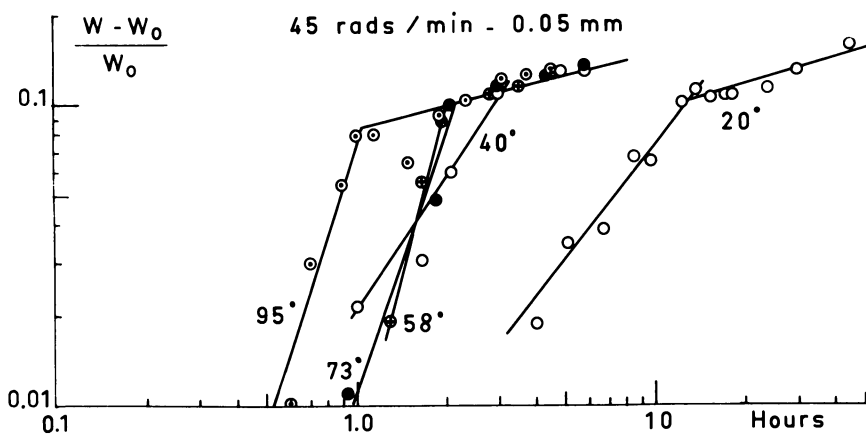


Figure 7. Log-log plot of weight increase of 0.05-mm. thick PTFE films irradiated at 45 rads/min. at different temperatures

Above 40°C. the autoacceleration index increases. The conversion curves obtained at 40°, 58°, and 73°C. cross, and the yields for a given dose are comparable. At 73° and 95°C. the autoacceleration index is 3.2 and the over-all activation energy determined on the basis of these two curves is 5.5 kcal./mole.

The break in the conversion curves occurs at 8–10% grafting. Above this critical value all experimental points obtained between 40° and 95°C. fall on the same line.

**INFLUENCE OF "SELECTIVE" INHIBITORS.** The use of a selective inhibitor is essential for grafting acrylic acid deeply into PTFE films because this monomer polymerizes with an unusually high rate (5), and if no inhibitor is present, the monomer is converted under irradiation into a hard block of polymer before grafting has even started on the surface of the film. In our standard experiments described above we used ferrous sulfate which inhibits homopolymerization efficiently. However, its solubility in the reaction mixture is low, 0.25% being close to the saturation point at 20°C. To explore further the influence of the inhibitor on the kinetics of grafting, experiments were carried out with cupric chloride at concentrations of 0.5, 2, 5, and  $50 \times 10^{-2}M$ . The results obtained with 0.1-mm. thick PTFE films at 20°C. and a dose rate of 200 rads/min. are shown in Figure 8. In contrast to the data shown in Figure 1, the initial portion of the conversion curves is autoretarded. A plot of these data on a log-log diagram leads to straight lines with slopes less than 1.

The grafting rates decrease as the concentration of  $CuCl_2$  rises. This effect demonstrates that the inhibitor not only interferes with homopolymerization but also affects the grafting process except perhaps in its initial stages (*see* Figure 8).

Grafting occurs faster in the presence of  $FeSO_4$  than at the lowest concentration of  $CuCl_2$  used, but the latter compound inhibits homopolymerization much more efficiently. At 20°C. and 2000 rads/min. the homopolymer formed in 50% aqueous solutions of acrylic acid amounts to 5% after 23 hours, in the presence of  $0.5 \times 10^{-2}M$   $CuCl_2$ , whereas more than 20% of homopolymer accumulate after 7.5 hours irradiation in the presence of 0.25% (or  $1 \times 10^{-2}M$ )  $FeSO_4$ .

**Anionic Membranes.** Solutions of 4-vinylpyridine (80%) in water were used in this work. Preliminary experiments had shown that most inhibitors affect the grafting process strongly. The kinetics were therefore investigated without any additive. Most experiments were carried out at a single dose rate: 28 rads/min.; a few irradiations were conducted at 157 rads/min.

**INFLUENCE OF DOSE AND DOSE RATE.** With 0.1-mm. thick PTFE films the grafting did not proceed homogeneously, despite the low dose rate used. All grafted films exhibited crumpled edges, as was observed earlier when PTFE films were grafted near the critical conditions, where

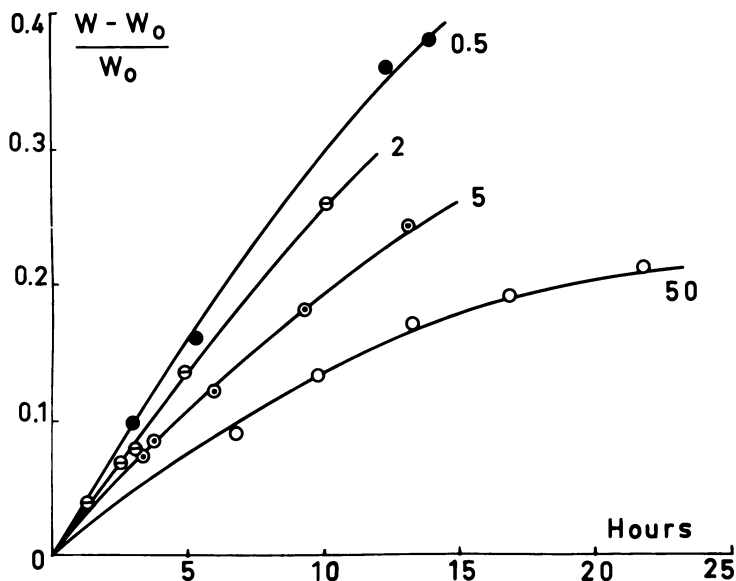


Figure 8. Weight increase of 0.1-mm. thick PTFE films irradiated at 20°C. and 2000 rads/min. in 50% aqueous solutions of AA containing various amounts of  $\text{CuCl}_2$  (concentrations expressed in moles/liter  $\times 10^2$ )

the reaction becomes diffusion controlled (2, 4). Systematic studies were therefore limited to 0.05-mm. thick films.

The conversion curves obtained at 20°C. exhibit marked auto-acceleration. Straight lines are again obtained on a log-log diagram, but the slopes are as high as 4.8 (Figure 9).

From experiments conducted at the two dose rates investigated the dose-rate exponent is estimated to be  $\alpha = 0.47$ . At the higher dose rate the reaction was diffusion controlled, heterogeneous films being obtained at elevated grafting ratios.

**INFLUENCE OF IRRADIATION TEMPERATURE.** Experiments were carried out at 20°, 30°, 35°, 40°, and 60°C. at 28 rads/min. The conversion curves are plotted in Figure 9 on a log-log diagram. The kinetics change suddenly between 30° and 35°C. Below 30°C. the acceleration index is 4.8; above 35°C. it drops to 1.9.

The activation energies, calculated on the basis of the instantaneous rates measured at 10% grafting, were found to be 6.6 kcal./mole in both ranges of temperatures where they could be determined: 20°–30° and 35°–60°C.

**INFLUENCE OF INHIBITORS.** Benzoquinone and ferrous sulfate were tried as selective inhibitors. In both cases the rate of grafting was

reduced strongly. Moreover, in the presence of an inhibitor the conversion curves of the grafting process at 20°C. are linear with dose up to high grafting ratios.

### Discussion

The various data obtained for the kinetics of graft copolymerization onto PTFE films demonstrate that this reaction is complicated by the fact that the rate of diffusion of the monomer may become the controlling factor. It seems interesting at this point to compare and discuss together the results obtained with the different monomers. Table I summarizes the data obtained for autoacceleration indexes ( $\beta$ ), dose-rate exponents ( $\alpha$ ), and over-all activation energies  $E$ , with styrene, acrylic acid, and vinylpyridine. Several conclusions can be derived from an examination of these data.

**Autoacceleration Indexes.** The values of  $\beta$  differ widely for the different systems, and moreover, their variation with temperature has a different character depending on the monomer under consideration.

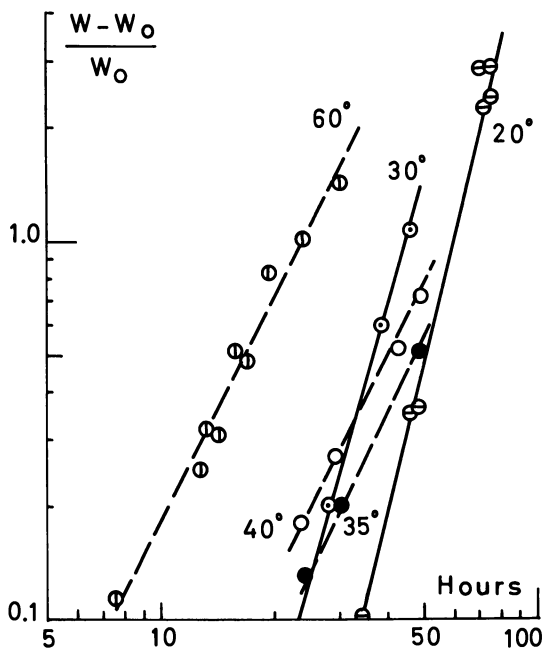


Figure 9. Log-log plot of weight increase of 0.05-mm. thick PTFE films irradiated at 28 rads/min. in 80% aqueous solutions of 4-VP at different temperatures (shown on curves)



**Table I. Autoacceleration Indexes,  $\beta$ , Dose-Rate Exponents,  $\alpha$ , and Over-all Activation Energies,  $E$ , for the Direct Radiation Grafting of Various Monomers into PTFE Films**

Monomer	PTFE Films, mm.	Irradiation Temperature, °C.	$\beta$	$\alpha$	$E$ , kcal./mole
Styrene	0.1	20	2.5-3.2	0.5	Depends on conversion at which rates are measured
	0.1	40	1.5-1.6	0.68	
	0.1	60	1.0-1.2	0.72	
Acrylic acid (+ 50% water + 0.25% Mohr salt)	0.1	0-33	1.25-1.29	0.45	15
	0.1	33-95	1.25-1.29	0.45	5.1
	0.05	20-40	1.15	0.45	~15
	0.05	73-95	3.2	0.45	~5.5
4-Vinylpyridine (+ 20% water)	0.05	20-30	4.8	~0.47	6.6
	0.05	35-60	1.9	—	6.6

With both styrene and vinylpyridine, the autoacceleration index decreases as the reaction temperature rises. This effect can be considered normal behavior of polymerizing systems in which the "gel effect" is operative. As the temperature rises, the termination step, which involves the interaction of two polymeric chains in a highly viscous medium, increases in rate, and the over-all reaction tends to become "normal." Ultimately, the stationary-state conditions may eventually apply.

This seems to be the case with styrene at 60°C. where  $\beta$  is almost unity—*i.e.*, where the reaction proceeds with a constant rate. The dose-rate exponent of this system indicates, however, more complicated kinetics.

A difference between these two systems is that in the case of styrene,  $\beta$  decreases gradually as the temperature rises, whereas with vinylpyridine a sudden change occurs between 30° and 35°C., which seems to be related to the transition point of PTFE.

With acrylic acid the situation is very different. For 0.1-mm. thick films  $\beta$  is independent of temperature, whereas for 0.05-mm. thick films  $\beta$  rises above 40°C. At low temperatures  $\beta$  is unusually small. This effect may be ascribed to the use of a selective inhibitor to prevent homopolymerization. It was shown above that in grafting vinylpyridine the autoaccelerated character of the reaction at 20°C. vanishes in the presence of inhibitors. Moreover, with acrylic acid the autoacceleration index is lower if a more efficient inhibitor ( $\text{CuCl}_2$ ) is used, and  $\beta$  decreases as the amount of inhibitor increases (Figure 8).

It is likely, therefore, that the autoacceleration would have been more pronounced if acrylic acid could be grafted on PTFE films without

using any inhibitor. The results obtained at 73° and 95°C. with the 0.05-mm. thick PTFE films are of interest in this respect. Here  $\beta$  rises to 3.2. This suggests that at elevated temperatures the inhibitor interferes less with the grafting process, and this in turn may be a consequence of the very rapid diffusion of the monomer.

Another peculiar feature of the grafting of acrylic acid is the break observed in the conversion curves particularly at low dose rates. The interpretation of this effect proposed above does not account for the fact that no break is observed with other monomers except at much higher grafting ratios (2, 4). These striking differences in kinetics for systems which in principle should exhibit comparable behavior are presumably related to differences in diffusion rates and polymer-polymer and polymer-monomer compatibilities. Little is known at present on the factors which govern these effects and on their influence on the kinetics.

**Influence of Temperature.** The reaction temperature necessarily plays a major role in grafting, where at least two reaction steps (chain propagation and termination) may become diffusion controlled. Indeed, grafting occurs faster at elevated temperatures, but here again each system exhibits a specific behavior.

With styrene, the autoacceleration index gradually changes with temperature which makes it impossible to define an activation energy since its apparent value depends strongly on the grafting ratio at which the rates are measured.

With both acrylic acid and vinylpyridine the kinetics change suddenly between 30° and 35°C., but the nature of this change is different for the two systems. With acrylic acid and 0.1-mm. thick PTFE films the autoacceleration index remains constant over the entire temperature range investigated (0°-95°C.), and only the Arrhenius plot exhibits a break at 33°C. This effect can be understood by assuming that the diffusion of the monomer into the partially grafted PTFE films requires a lower temperature coefficient in the PTFE structure prevailing above 33°C. than in the low temperature phase. For 0.05-mm. thick films a more profound change occurs at about the same temperature, resulting in a change of the autoacceleration index. From the discussion above one may accept that this effect involves a competition between the diffusion of monomer and inhibitor (ferrous sulfate).

For vinylpyridine the sudden decrease of  $\beta$  above 30°C. conforms with a faster termination step resulting from an increased mobility of the growing chains owing partly to a higher swelling of the films and partly to increased thermal motion. Here again, one has to assume easier diffusion of the monomer into the high temperature structure of PTFE.

### Polyfunctional Membranes

To explore further the characteristic properties of membranes derived from PTFE films, several attempts were made to graft mixtures of AA and VP or to graft the two monomers in two successive steps. Both techniques failed because a spontaneous reaction occurs when 4-VP is brought in contact with AA (or its polymer), leading to the formation of a reddish-brown polymer which is extracted readily by acidic or alkaline solutions.

Membranes containing both types of active groups were prepared successfully, however, by grafting the two monomers, one after the other, provided the intermediate membrane obtained in the first grafting step was neutralized before starting the second grafting operation.

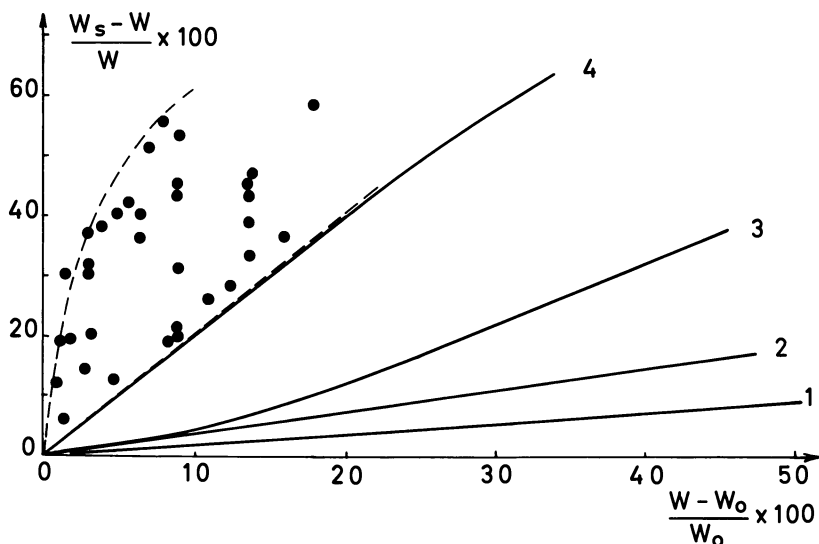


Figure 10. Percent swelling in water as a function of percent grafting for different membranes based on PTFE

- 1: 4-VP grafts (free pyridine)
- 2: AA grafts (free acid)
- 3: 4-VP grafts (hydrochloride)
- 4: AA grafts (potassium salt)

Closed circles pertain to difunctional membranes with various compositions

A number of difunctional membranes were thus obtained by either of the two following reaction sequences:

- (a) Grafting AA, neutralization by KOH, grafting 4-VP.
- (b) Grafting 4-VP, neutralization by HCl, grafting AA.

The kinetics of these reactions will be described elsewhere. We would like to present here some unusual properties of such difunctional membranes. The grafted films were treated with a solution of 0.1N KOH to convert the carboxylic groups into potassium salt. The resulting membranes swelled to a much larger extent in water than any of the other membranes studied. The swelling data are summarized in Figure 10. The percent swelling ( $W_s - W/W \times 100$ ) is plotted as a function of percent grafting ( $W - W_0/W_0 \times 100$ ) for the different types of membranes. The neutralized membranes always exhibit larger swelling ratios than either the acid or the alkaline forms (*see also* Refs. 1 and 5). For a given grafting ratio the carboxylic membranes swell more than the vinylpyridine grafts. All difunctional membranes examined exhibit larger swelling ratios than the neutralized carboxylic membranes. This unusual behavior of difunctional membranes is being investigated further.

#### Literature Cited

- (1) Bex, G., Chapiro, A., Huglin, M., Jendrychowska-Bonamour, A. M., O'Neill, T., *J. Polymer Sci., Pt. C* **22**, 493 (1968).
- (2) Chapiro, A., *J. Polymer Sci.* **34**, 481 (1959).
- (3) Chapiro, A., Magat, M., Sebban, J., French Patent **1,130,099** (1956).
- (4) Chapiro, A., Matsumoto, A., *J. Polymer Sci.* **57**, 743 (1962).
- (5) Chapiro, A., Seidler, P., *European Polymer J.* **1**, 189 (1965).
- (6) Chen, W. K. W., Mesrobian, R. B., Ballantine, D. S., Metz, D. J., Glines, A., *J. Polymer Sci.* **23**, 903 (1957).
- (7) Dobo, J., Somogyi, A., *Proc. Tihany Symp. Radiation Chem., Budapest, 1964*, p. 195.
- (8) Dobo, J., Somogyi, A., Czvikovsky, T., *J. Polymer Sci., Pt. C* **4**, 1173 (1964).
- (9) Dobo, J., Somogyi, A., Lakner, E., *Plaste Kautschuk* **7**, 393 (1960).
- (10) Lebel, P., Chen, W. K. W., Chapiro, A., *J. Polymer Sci., Pt. C* **4**, 1193 (1964).
- (11) McCrum, N. G., *J. Polymer Sci.* **34**, 355 (1959).
- (12) Munari, S., Vigo, F., Tealdo, G., Rossi, L., *J. Polymer Sci., Pt. B* **4**, 547 (1966).
- (13) Munari, S., Vigo, F., Tealdo, G., Rossi, L., *J. Appl. Polymer Sci.* **11**, 1563 (1967).
- (14) Odian, G., Acker, T., Rossi, A., Ratchik, E., *J. Polymer Sci.* **57**, 661 (1962).
- (15) Restaino, A. J., Reed, W. N., *J. Polymer Sci.* **36**, 499 (1959).
- (16) Schultz, A. K., *J. Chim. Phys.* **53**, 933 (1956).
- (17) Sinitsyna, Z. A., Tsvetkov, Yu. D., Bagdasaryan, Kh. S., Voevodskii, V. V., *Dokl. Akad. Nauk. SSSR* **129**, 631 (1959).

RECEIVED March 22, 1968.

## Cellulose Graft Copolymers

JETT C. ARTHUR, JR.

Southern Regional Research Laboratory, Southern Utilization Research and Development Division, Agricultural Research Service,  
U. S. Department of Agriculture, New Orleans, La. 70119

*Graft copolymerization reactions of fibrous cellulose with vinyl monomers were initiated at free radical sites formed on the cellulose molecule by interaction with radiation, by reaction with  $Ce^{4+}$  ions in acidic solution, or by H abstraction by  $\cdot OH$  radicals formed by reaction of  $Fe^{2+}$  ions with  $H_2O_2$  in aqueous solution. The effects of experimental conditions on the location of these sites on the cellulose molecule and on the reactions were studied by ESR spectroscopy. The molecular weights of the grafted copolymers and the distribution of the polymers within the fibrous cellulosic structure were determined. Some of the properties of the copolymers are discussed.*

The preparation and properties of cellulose graft copolymers have been of considerable interest in the textile, paper, and wood products industries for a number of years. Both free radical- and ionic-initiated graft copolymerization reactions of vinyl monomers with cellulose have been reported. The vinyl-cellulose copolymers have some of the properties of both the cellulosic fibers and the grafted polyvinyl copolymers (1, 3, 47).

The modification of the properties of cotton cellulosic textile products, through free radical-initiated graft copolymerization reactions with vinyl monomers, has been investigated at the Southern Laboratory for a number of years (6, 9). In this chapter, we summarize the basic mechanisms and principles involved in free radical reactions of cellulose, initiated by high energy radiation, ceric ion in acidic solution, and aqueous solutions of ferrous ion and hydrogen peroxide. Some of the properties of fibrous cotton cellulose graft copolymers are also presented.

**Mechanisms of Free Radical Formation**

The formation of free radicals on the cellulose molecule (Figure 1) can occur by the following possible processes: dehydrogenation, dehydroxylation, depolymerization, or cleavage of the glucopyranoside ring (4, 8, 10, 14, 29, 30, 32, 34). The location of the free radical sites on the cellulose molecule and within the fibrous structure will depend on the method of initiation of the formation of the free radical site and on the physical chemical properties of the cellulose which is reacting (5, 19, 22). For this discussion we are considering only fibrous cotton cellulose, which in its natural state is about 75–80% crystalline as determined by x-ray and has a high molecular weight and crystalline lattice type I.— $a = 8.35$  A.,  $b = 10.3$  A. (fiber period),  $c = 7.9$  A.,  $\beta = 84^\circ$  (angle between  $a$  and  $c$  axes), a monoclinic unit cell containing two cellobiose units (3, 59).

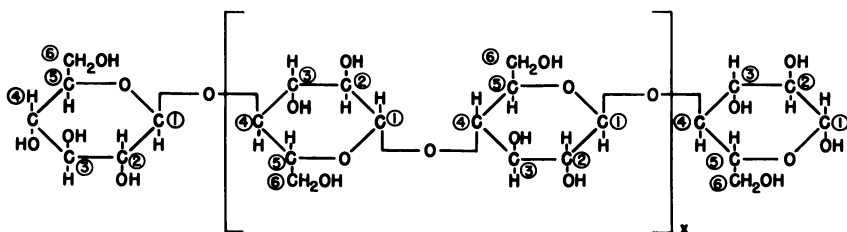


Figure 1. Cellulose molecule ( $x = 2000-2500$ )

The cellulose was purified by extracting with hot ethanol followed by boiling in dilute sodium hydroxide solution, washing with distilled water, then souring with dilute acetic acid, neutralizing with dilute ammonium hydroxide, and again washing with distilled water (50). After the purified cellulose was conditioned at  $21^\circ\text{C}$ . and 65% relative humidity, the resulting product had a moisture content of about 6–7%, cellulose content of about 93–94%, and a molecular weight of about 700,000 (39).

**Ionizing Radiation.** Energy localization from ionizing radiation in the cellulose molecule resulted in depolymerization, dehydrogenation, and destruction of glucopyranoside units to yield gaseous products of hydrogen, carbon monoxide, and carbon dioxide (2, 20, 21, 24, 28, 63). The dehydrogenation and depolymerization reactions initiated the formation of both short lived and trapped free radical sites on the cellulose molecule (22, 26, 44). When cellulose (lattice type I) with a low moisture content (about 0.5%) was irradiated in vacuum at about  $25^\circ\text{C}$ . by  $^{60}\text{Co}$   $\gamma$ -radiation, the ESR spectrum generated is that shown in Figure 2A. When cellulose with regain moisture content (about 7%) was irradiated in air, the ESR spectrum generated is that shown in Figure 2B.

When the irradiated cellulose, with a low moisture content, was contacted with moisture vapor, the ESR spectrum (Figure 2A) changed to a spectrum similar to that obtained for irradiated cellulose with regain moisture content (Figure 2B). At a given dosage the trapped radical concentration in cellulose, irradiated dry and then allowed to absorb regain moisture, was higher than the concentration in cellulose, irradiated containing regain moisture (26, 44). This indicated that increased intermolecular bonding occurred in the cellulose molecule on irradiation and thereby decreased the penetration of water molecules to the free radical sites. These trapped radicals were made accessible to initiate graft copolymerization reactions with vinyl monomers, dissolved in solvents which tended to swell the cellulosic structure (31, 33, 36).

The spectrum shown in Figure 2B, was relatively stable and consisted of three lines in an intensity ratio of about 1:1.8:1. Equal inter-

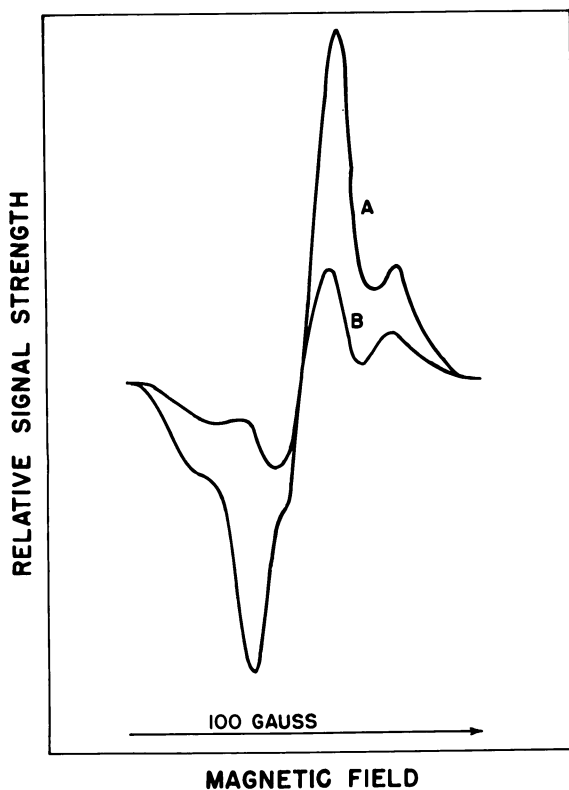


Figure 2. ESR spectra of  $\gamma$ -irradiated cellulose at 25°C.

A: Irradiated dry (about 0.5%  $H_2O$ ) in vacuo  
 B: Irradiated with about 6%  $H_2O$  in air

action of two equivalent hydrogen nuclear spins with a free radical would be required to give a three-line spectrum and ideally an intensity ratio of 1:2:1. Dehydrogenation at carbon C<sub>5</sub> (see Figure 1) would give a free radical which could interact with the two equivalent hydrogens on carbon C<sub>6</sub> to give a three-line spectrum. Two other possible free radicals on the cellulose molecule, which could give three-line spectra, would be formed on dehydroxylation of carbon C<sub>6</sub> or dehydrogenation of the hydroxyl group on carbon C<sub>6</sub>. However, the delocalizing energy available at carbon C<sub>5</sub>, arising from the presence of the ring oxygen atom, was greater than that at carbon C<sub>6</sub>. Consequently, after energy localization, the formation of a free radical on carbon C<sub>5</sub> by dehydrogenation would be the most probable stable free radical on the cellulose molecule to generate the three-line spectrum. The stability of the radical in the presence of water probably indicated that the radical formed is located in the more ordered regions of the fibrous cotton cellulose, which in its natural state is about 70–80% crystalline (22, 26).

The concentration of trapped radicals in the cellulose lattice depended on the radiation dosage and the amount of moisture present in the cellulose during irradiation. The trapped radical yield in irradiated cellulose, containing about 7% moisture, is shown in Table I. If cellulose was irradiated dry (about 0.5% moisture) and in vacuum, an initial yield of 2.5–3 times that shown was obtained; however, the concentration of the radicals decreased rapidly on exposure of the irradiated, dry cellulose to moisture (26).

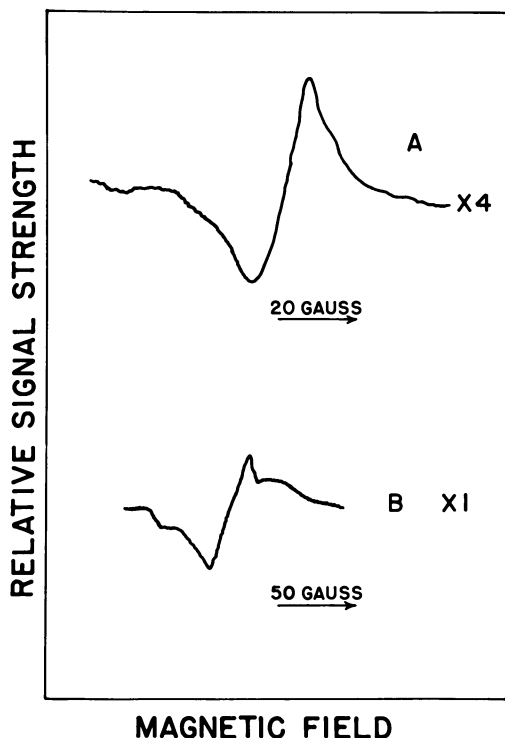
**Table I. Trapped Radical Yield on Irradiation of Cellulose<sup>a</sup>**

<i>Dosage,</i> <i>e.v./gram × 10<sup>-19</sup></i>	<i>Trapped Radicals,</i> <i>spins/gram × 10<sup>-16</sup></i>	<i>Trapped Radical Yield,</i> <i>spins/100 e.v.</i>
0.26	3.6	1.4
0.52	7.2	1.4
2.6	40	1.5
5.2	86	1.7

<sup>a</sup> Purified fibrous cotton cellulose, containing 7% moisture, irradiated at 25°C. in air with <sup>60</sup>Co  $\gamma$ -radiation.

**Ceric Ion Initiation.** Ceric ion in acidic solution formed a chelate with the cellulose molecule, probably by reaction through the hydroxyl groups on carbon C<sub>2</sub> and C<sub>3</sub>. There was a transfer of one electron from the cellulose molecule to Ce<sup>IV</sup>. Then Ce<sup>IV</sup> was reduced to Ce<sup>III</sup>, followed by release of Ce<sup>3+</sup> and anhydroglucose ring cleavage of the C<sub>2</sub>—C<sub>3</sub> bond. A short lived free radical was then formed on either carbon C<sub>2</sub> or C<sub>3</sub> and generated the ESR spectrum shown in Figure 3A. The decay of free radicals, formed on the cellulose molecule by ceric ion interaction, is





*Figure 3. ESR spectra of cellulose which has reacted with  $Ce^{4+}$  ion and/or acrylonitrile recorded at  $-100^{\circ}C$ .*

*A: Cellulose saturated with ceric ammonium nitrate (0.05M) in  $HNO_3$  (0.05M) for 20 seconds at  $25^{\circ}C$ ., then frozen at  $-100^{\circ}C$ .*

*B: Saturated as in A followed by copolymerization with acrylonitrile for 6 minutes at  $25^{\circ}C$ ., then frozen at  $-100^{\circ}C$ .*

shown in Figure 4. Termination could result from the reaction of  $Ce^{4+}$  ion with the free radical to yield  $Ce^{3+}$  ion and an oxidized product of cellulose. Reaction of solvent, usually  $H_2O$ , with the free radical could also terminate the radical (5).

**Hydroxyl Radical Initiation.** When  $Fe^{2+}$  ions were mixed with  $H_2O_2$ ,  $\cdot OH$  radicals were generated (19, 25, 27) according to the Haber-Weiss mechanism (45, 46). Fibrous cellulose was immersed in 0.1M  $FeSO_4$  for about 15 minutes to wet the fiber thoroughly and then dried in a flowing stream of nitrogen. This dried cellulose was placed in a quartz tube; then 0.3M  $H_2O_2$  was drawn onto the cellulose. Immediately, the tube and its contents were immersed in liquid nitrogen. The ESR spectrum generated was recorded at  $-110^{\circ}C$ . and is shown in Figure 5.

The ESR signal was very weak and short-lived. The spectrometer was operated at high amplification, and the signal was accumulated by a

time-averaging computer to obtain the ESR spectrum shown. The three intense lines appeared to be a triplet and could be attributed to a radical formed on abstraction of a hydrogen atom from the hydroxyl group on carbon C<sub>6</sub>. The two equivalent hydrogen atoms on carbon C<sub>6</sub> would split the ESR spectrum to form a triplet. The ESR spectrum was very sensitive to temperature; even at temperatures as low as  $-60^{\circ}\text{C}$ . the spectrum became very weak and undefined within a few minutes (19).

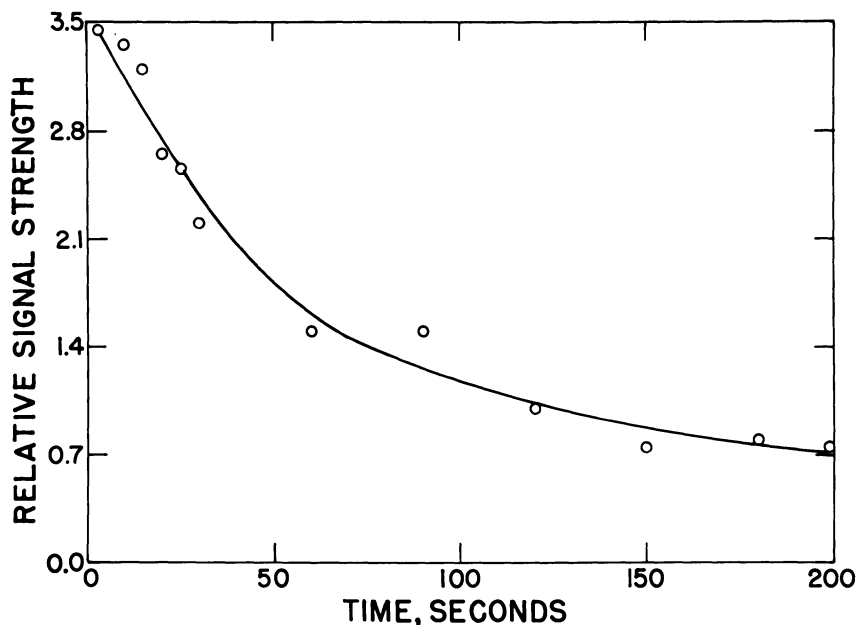


Figure 4. Decay of free radicals formed on cellulose by  $\text{Ce}^{4+}$  ion

See legend for Figure 3A; time measured from saturation of cellulose with  $\text{Ce}^{4+}$  ion at  $25^{\circ}\text{C}$ . until freezing at  $-100^{\circ}\text{C}$ . before recording spectrum

### **Copolymerization Reactions**

Two important factors in initiating graft copolymerization reactions of vinyl monomers with activated cellulose are: (1) the lifetime of the free radical sites and (2) the accessibility of the free radical sites to the monomers. For ceric ion initiation or hydroxyl radical initiation the lifetimes of the free radicals on the cellulose molecule were short (5, 19); therefore, the monomer should be present when the free radicals were formed. For ionizing radiation both short lived and long lived (trapped) free radicals were formed (22, 26, 44). Consequently, the activation reaction and the copolymerization reaction could either be conducted

simultaneously or consecutively. The short lived radicals formed were probably not too important in the copolymerization reaction since they would probably be quenched by the solvent for the monomer. For the long lived or trapped radicals, considering both the crystalline structure and morphology of fibrous cellulose (3, 59), the rate of diffusion of monomer to the free radical site was an important factor in the copolymerization reaction.

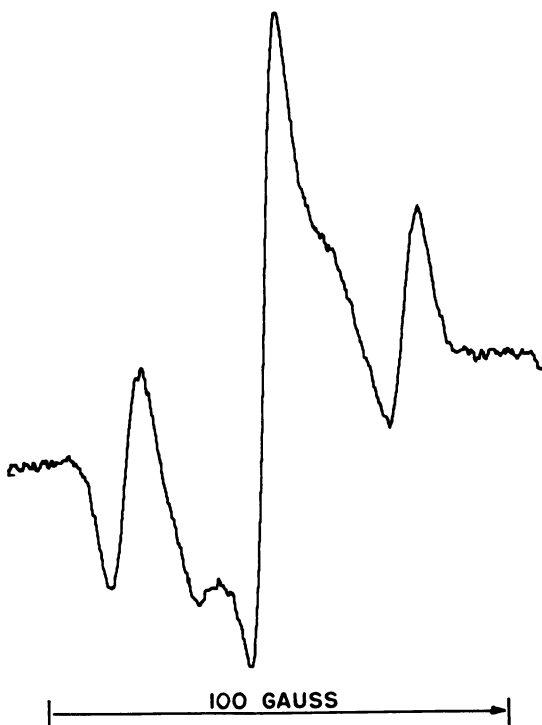


Figure 5. ESR spectrum of cellulose generated by  $\cdot\text{OH}$  radicals formed in  $\text{Fe}^{2+}\text{-H}_2\text{O}_2$  system recorded at  $-110^\circ\text{C}$ .

**Ionizing Radiation.** When the activation reaction and copolymerization reaction were conducted simultaneously, the fibrous cellulose was first treated with monomer solution and then irradiated. Usually some homopolymer was formed and was removed from the cellulose graft copolymer by extraction with solvent for the polymer. When the activation reaction and copolymerization reaction were conducted consecutively, the fibrous cellulose was first irradiated and then treated with monomer solution. As compared with the simultaneous procedure, formation of homopolymer was very low. The changes in the ESR spectra for irra-

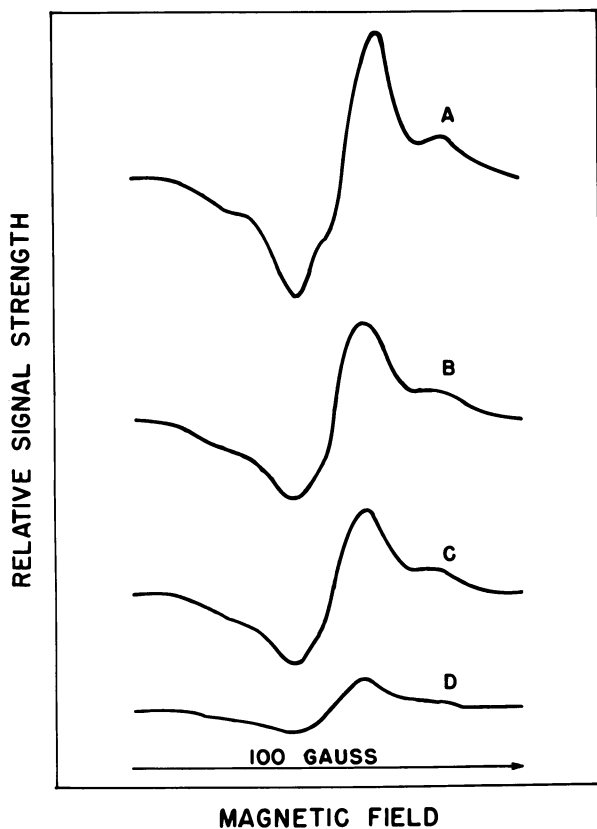


Figure 6. ESR spectra of  $\gamma$ -irradiated cellulose after copolymerization with acrylonitrile (15% monomer in 75% aqueous  $\text{ZnCl}_2$ ). Recorded at  $-100^\circ\text{C}$ .

- A:  $\gamma$ -Irradiated cellulose  
 B: A contacted with monomer solution and frozen immediately  
 C: A contacted with monomer solution for 34 minutes at  $25^\circ\text{C}$ ., then frozen  
 D: A contacted with monomer solution for 17 hours at  $25^\circ\text{C}$ ., then frozen

diated cellulose after treatment with monomer solution are shown in Figure 6. As the duration of the copolymerization reaction increased, the intensity of the ESR spectrum of the irradiated cellulose decreased. However, even after a lapsed time as long as 17 hours, a measurable fraction of the free radical sites, initially formed in the irradiated cellulose, remained as shown in Figures 6 and 7. About 35–40% of the initial concentration of free radical sites, as measured in spins per gram, were apparently located within the crystalline area of the fibrous cellulose and were not accessible to monomer solution (26).

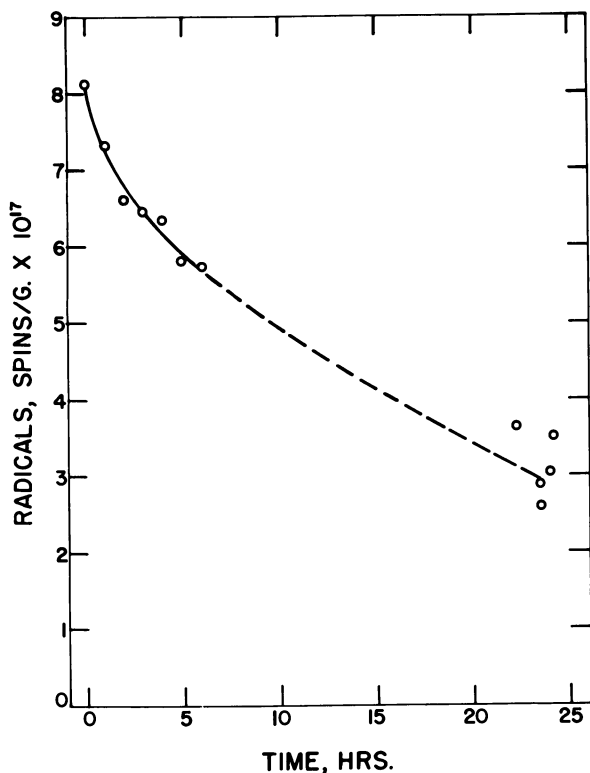


Figure 7. Decay of free radicals formed in  $\gamma$ -irradiated cellulose during copolymerization with acrylonitrile (15% monomer in 75% aqueous  $\text{ZnCl}_2$ ) at 25°C.

Radiochemical yields of the copolymerization reactions depended primarily on the type of monomer, solvent for the monomer, and concentration of the monomer used. Yields, ranging from  $10^3$  to  $10^5$  moles of monomer copolymerized per 100 e.v., were obtained (7).

**Ceric Ion Initiation.** Fibrous cellulose, which reacted with ceric ion solution for 20 seconds at 25°C. and then reacted with acrylonitrile monomer, generated the ESR spectrum shown in Figure 3B. On initiation of the copolymerization reaction there was a change in the number of lines in the ESR spectrum (compared with Figure 3A) and a broadening of the spectrum. A second free radical on the end of the growing polymer chain was apparently being recorded. During the initial stages of the copolymerization, the concentration of free radicals apparently increased and then decreased, as shown in Figure 8. The initial free radical site, formed on the cellulose molecule, was apparently retained on the end of the growing polymer chain. Then additional ceric ion coordinated with

the hydroxyl groups on the cellulose molecule, leading to the formation of more free radical sites. After the reaction had proceeded about 150 seconds, the termination reaction for the free radicals became predominant, and the free radical concentration decreased (5).

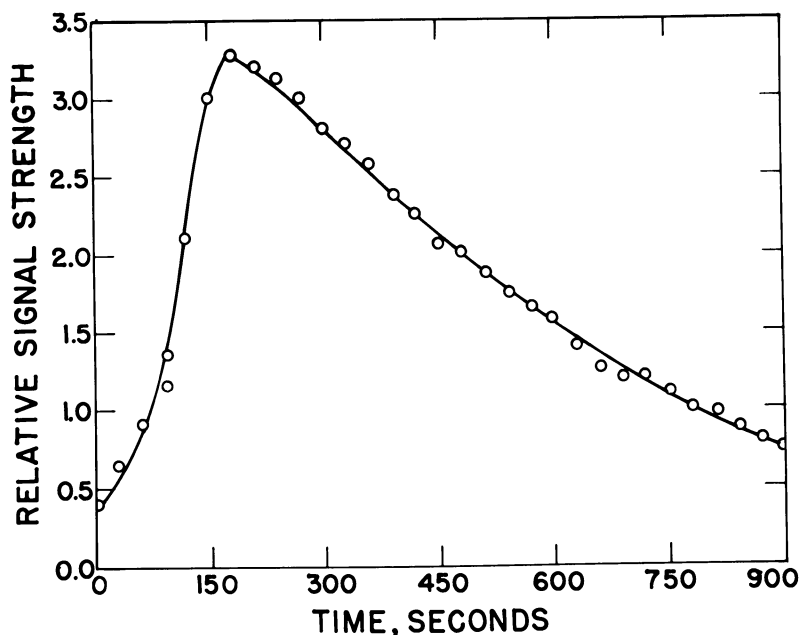
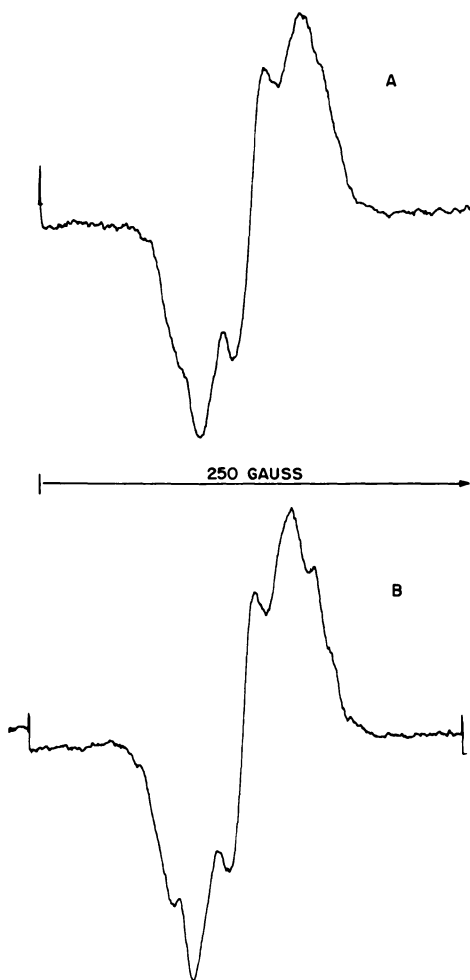


Figure 8. Rate of formation and decay of free radicals during copolymerization of acrylonitrile with cellulose initiated by  $Ce^{4+}$  ion at  $25^{\circ}C$ .

**Hydroxyl Radical Initiation.** Fibrous cellulose, which was allowed to react with ferrous ion solution and was then dried, was contacted at  $25^{\circ}C$ . with  $H_2O_2$  solution containing acrylonitrile. The graft polymerization reaction generated the ESR spectrum shown in Figure 9. The intensity of this spectrum was several times greater than that generated in cellulose by the  $Fe^{2+}-H_2O_2$  system alone (*see* Figure 5). The triplet spectrum disappeared during the copolymerization reaction, and an ESR spectrum, generated by the free radical on the growing polymer chain and probably by a free radical formed on oxidative depolymerization of the cellulose molecule, was recorded. The ESR spectrum appeared to be a combination of two singlet spectra (19).

### **Molecular Relationships**

The molecular relationships in cellulose graft copolymers depended on the method of free radical formation on the cellulose molecule and



*Figure 9. ESR spectra of cellulose after copolymerization with acrylonitrile initiated by  $\cdot\text{OH}$  radicals formed in  $\text{Fe}^{2+}\text{-H}_2\text{O}_2$  system. Recorded at  $-40^\circ\text{C}$ .*

*A: Attenuation 10 db.*

*B: Attenuation 13 db.*

the experimental conditions during copolymerization, as shown in Table II. The cellulose-poly(acrylonitrile) copolymer was selected to illustrate the possible variations in these molecular relationships. The molecular weights of the grafted poly(acrylonitrile) ranged from  $3.3 \times 10^4$  to  $1.1 \times 10^6$  (58). The method of free radical formation also initiated oxidative depolymerization of the cellulose molecule, as shown by the decrease in molecular weight of the irradiated cellulose (10, 32). It has also been

reported that the chemical redox systems initiated oxidative degradation of the cellulose molecule (38, 42, 43, 48, 49, 51–57, 62). In most cases the average number of molecules of poly(acrylonitrile) grafted per cellulose molecule was much less than one. When ionizing radiation (simultaneous steps) or chemical redox systems were used, one or more molecules of polymer were usually grafted per cellulose molecule.

**Table II. Effect of Method of Free Radical Formation and Conditions of Reaction on the Molecular Relationships in Cellulose Graft Copolymers**

Free Radical Formation	Monomer Solution <sup>a</sup>	Molecular Weight, $\times 10^{-5}$		Moles of Cellulose per mole of Grafted Polymer
		Cellulose <sup>b</sup>	Polymer <sup>c</sup>	
Ionizing Radiation—Simultaneous Steps				
$0.2 \times 10^6$ roentgens	32% AN in 80% aq. ZnCl <sub>2</sub> 0.9 hr.	3.6	5.1	5.0
$1.0 \times 10^6$ roentgens	30% AN in DMF, 4.7 hr.	1.4	0.33	0.94
Ionizing Radiation—Consecutive Steps				
$1.0 \times 10^6$ roentgens	15% AN in 75% aq. ZnCl <sub>2</sub> 2.5 hr.	1.4	11	26
$1.0 \times 10^6$ roentgens	32% AN in 80% aq. ZnCl <sub>2</sub> 7.5 hr.	1.4	5.9	19
$6.0 \times 10^6$ roentgens	32% AN in 80% aq. ZnCl <sub>2</sub> 7.5 hr.	0.37	8.5	86
Chemical Redox Initiation				
0.005M Ce <sup>4+</sup> in 0.05M HNO <sub>3</sub>	4% aq. AN 1 hr.	7.1	0.84	0.42
Fe <sup>2+</sup> /H <sub>2</sub> O <sub>2</sub>	8% aq. AN 0.5 hr.	7.1	0.84	0.40

<sup>a</sup> Conditions selected so that the copolymer contained about the same amount of cellulose, 77–82%; AN = acrylonitrile; DMF = *N,N*-dimethylformamide.

<sup>b</sup> Initial molecular weight of cellulose  $7.1 \times 10^5$ ; for ionizing radiation molecular weight of cellulose was determined at dosage indicated; no determination was made on possible oxidative depolymerization of cellulose by chemical redox systems.

<sup>c</sup> Based on poly(acrylonitrile) recovered from acid hydrolysis of copolymer and on intrinsic viscosity method.



### Morphology of Copolymers

The morphology of the fibrous cellulose graft copolymers depended on the method of initiation of free radical formation, experimental conditions during the copolymerization, chemical modification of the cellulose before reaction, and the type of monomer used (60). Variations in the shape of the fibrous cross section, in layering effects in the fiber, and in the location and distribution of the grafted copolymer in the fiber were observed by electron microscopy (61). Cotton cellulose-poly(acrylonitrile) copolymer was selected to show the possible variations in location and distribution of the grafted copolymer in the fiber.

With ionizing radiation (simultaneous steps procedure) with aqueous  $\text{ZnCl}_2$  as the solvent for the monomer the fibrous cross section was rounded, and the polymer was concentrated about midway between the inner and outer layers of the fiber (12, 13, 15, 16, 17), as shown in Figure 10A. When cellulose was cyanoethylated before irradiation and aqueous  $\text{ZnCl}_2$  was the solvent for the monomer, the fibrous cross section was rounded, and a uniform distribution of the polymer was obtained (18, 41), as shown in Figure 10B.

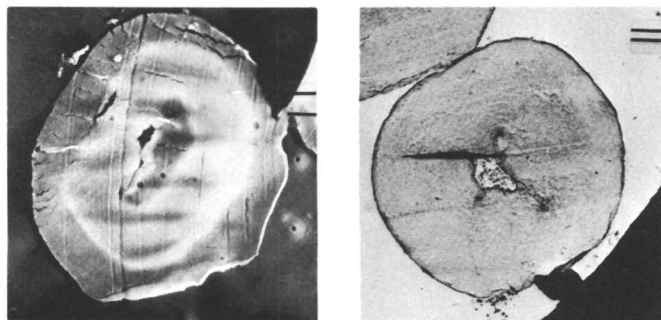
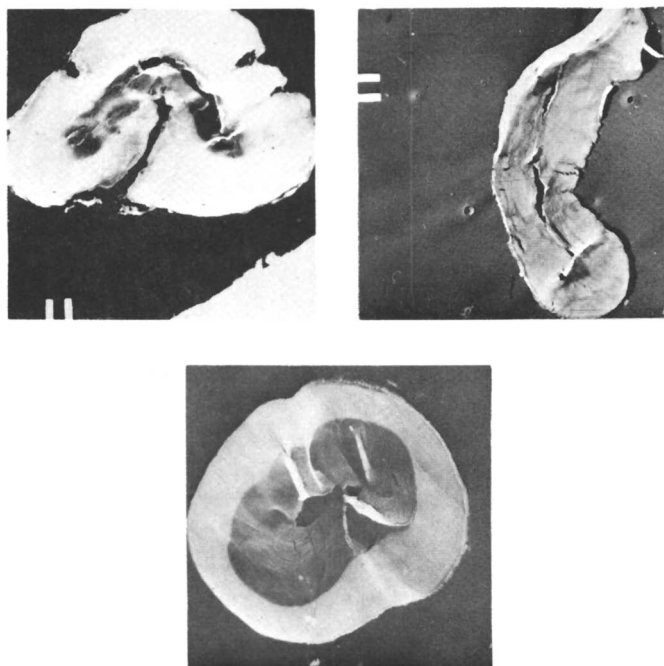


Figure 10. Poly(acrylonitrile)-cellulose copolymer using  $\gamma$ -radiation (simultaneous steps procedure)

A: Monomer solution: 32% acrylonitrile in 80% aqueous  $\text{ZnCl}_2$   
B: Cyanoethylated cellulose (D.S. 0.7); monomer solution: same as A

With ionizing radiation (consecutive steps procedure) with saturated aqueous  $\text{ZnCl}_2$  as solvent and a monomer concentration of 32%, the cross section of the fiber retained its natural shape, and polymer was distributed from the outer edge of the fiber towards the lumen area (33), as shown in Figure 11A. If more dilute aqueous  $\text{ZnCl}_2$  and a lower concentration of monomer were used, the cross section of the fiber was rounded, and the polymer was more concentrated in the outer layers of the fiber (31, 36), as shown in Figure 11C. When *N,N*-dimethylforma-



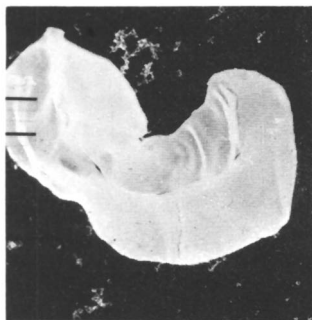
**Figure 11.** *Poly(acrylonitrile)-cellulose copolymer using  $\gamma$ -radiation (consecutive steps procedure)*

- A:** *Monomer solution: 32% acrylonitrile in 80% aqueous  $ZnCl_2$*   
**B:** *Monomer solution: 32% acrylonitrile in N,N-dimethylformamide*  
**C:** *Monomer solution: 15% acrylonitrile in 75% aqueous  $ZnCl_2$*

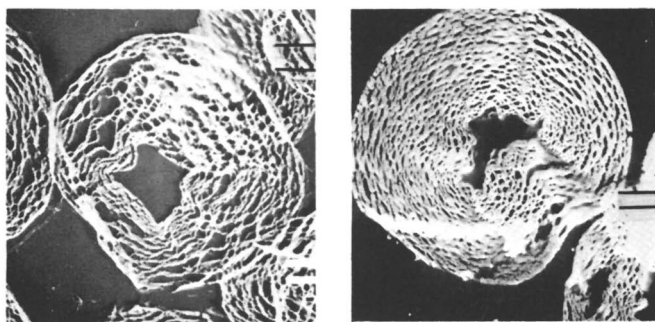
mide was used as the solvent, the fibrous cross section resembled that of native fiber, and a uniform distribution of the polymer was obtained (33) (Figure 11B).

When the chemical redox initiation procedure, either  $Ce^{4+}$  ion or  $\cdot OH$  radical, was used, the fibrous cross section also resembled that of native fiber, and a uniform distribution of the polymer was obtained (5, 19) as shown in Figure 12.

A layering or opening of the fibrous structure was obtained when the ionizing radiation (simultaneous steps procedure) was used, with styrene in methanol (11, 23, 40), as shown in Figure 13A. By the same procedure, alkyl methacrylates in methanol also caused layering of the fibrous structure. The extent of the layering effect increased as the molecular weight of the alkyl methacrylate increased (35, 37). The effect of poly(hexyl methacrylate) on the fibrous structure is shown in Figure 13B.



*Figure 12. Poly(acrylonitrile)-cellulose copolymer using  $Ce^{4+}$  ion initiated copolymerization reaction*



*Figure 13. Layering or opening effects in cellulose copolymers using  $\gamma$ -radiation (simultaneous steps procedure)*

*A: Monomer solution: 30% styrene and 70% methanol  
B: Monomer solution: 30% hexyl methacrylate and 70% methanol*

### ***Physical Properties***

The physical properties of the cellulose graft copolymers, prepared by free radical initiated processes, depended in part on the type of monomer used, the total amount of polymer grafted, and the location and distribution of the grafted polymer in the fibrous structure. There were no apparent relationships between the carbon on the cellulose molecule at which the copolymerization was initiated, the molecular weight of the grafted polymer, the fraction of cellulose molecules grafted, and the physical properties of the cellulose graft copolymers. To retain the fibrous nature of the cellulose, little or no stress could be applied to the grafted polymer to develop its properties. Consequently, the effects

of amorphous grafted polymer on the properties of cellulose graft copolymers were being observed.

Some of the important changes in physical properties of cellulose graft copolymers are summarized below.

**Fibers.** The elastic recovery properties of cotton fibers were changed by first cyanoethylating the cellulose and then graft copolymerizing acrylonitrile with the cellulose, when ionizing radiation was used to initiate the reaction. The values for permanent set, after elongation and relaxation of the fibrous copolymer, were less than for unmodified or cyanoethylated fibrous celluloses (1, 18). The effect of the distribution of the poly(acrylonitrile) in the fibrous structure was probably an important factor in determining this property (*see* Figure 10B).

**Yarns.** The properties of yarns, composed of cellulose graft copolymers (*see* Figures 10–13), were changed as compared with unmodified yarns. The copolymer yarns were thermoplastic and exhibited second-order transition points at about the same temperatures as the softening points of the grafted polymers. The copolymer yarns also had increased elongation-at-break, decreased average stiffness, and decreased breaking toughness, as compared with unmodified yarns. The poly(acrylonitrile)–cellulose yarns were rot resistant, as compared with unmodified yarns (1, 6, 9, 12, 13, 15, 16, 17, 23, 31, 33, 35, 36, 37, 40, 41, 47).

**Fabrics.** Fabrics composed of cellulose graft copolymers had increased flex and flat abrasion resistances as compared with untreated fabrics (1, 31, 35, 36, 37, 47).

### **Conclusion**

Cellulose graft copolymers, composed of cellulose and poly(vinyl monomer), were prepared by free radical initiated copolymerization reactions. From an analysis of ESR data the most likely site of grafting was on carbon C<sub>5</sub> of the cellulose molecule when ionizing radiation and the consecutive steps procedure were used. With the simultaneous-steps procedure, the grafting could also occur at carbon C<sub>6</sub>. With ceric ion initiation, the most likely site of grafting was at carbon C<sub>2</sub> or C<sub>3</sub>. Using ·OH radical initiation (Fe<sup>2+</sup>–H<sub>2</sub>O<sub>2</sub>), the most likely site of grafting was at carbon C<sub>6</sub>. The molecular weights of the grafted polymers varied over a range from about 3 × 10<sup>4</sup> to 1 × 10<sup>6</sup>. By chemical redox initiation, generally one or more grafted molecules were obtained per cellulose molecule. With ionizing radiation, generally less than one grafted molecule was obtained per cellulose molecule. The distribution of the grafted polymer in the fibrous structure was determined by experimental conditions during the copolymerizations. Some changes in physical proper-

ties of cellulose graft copolymers, as compared with unmodified cellulose, were decreased permanent set, development of thermoplasticity, decreased stiffness, increased rot resistance, and increased abrasion resistance.

### Literature Cited

- (1) Arthur, J. C., Jr., *Cotton Trade J., Intern. Ed.* **1964-1965**, 41.
- (2) Arthur, J. C., Jr., "Energy Transfer in Radiation Processes," G. O. Phillips, Ed., p. 29, Elsevier, Amsterdam, 1966.
- (3) Arthur, J. C., Jr., "Encyclopedia of Polymer Science and Technology," H. F. Mark, N. G. Gaylord, N. M. Bikales, Eds., Vol. 4, p. 244, Interscience, New York, 1966.
- (4) Arthur, J. C., Jr., *Textile Res. J.* **28**, 204 (1958).
- (5) Arthur, J. C., Jr., Baugh, P. J., Hinojosa, O., *J. Appl. Polymer Sci.* **10**, 1591 (1966).
- (6) Arthur, J. C., Jr., Blouin, F. A., *Am. Dyestuff Repr.* **51**, 1024 (1962).
- (7) Arthur, J. C., Jr., Blouin, F. A., *J. Appl. Polymer Sci.* **8**, 2813 (1964).
- (8) Arthur, J. C., Jr., Blouin, F. A., *Textile Res. J.* **34**, 733 (1964).
- (9) Arthur, J. C., Jr., Blouin, F. A., *U. S. At. Energy Doc.*, TID-7643, 319 (1962).
- (10) Arthur, J. C., Jr., Blouin, F. A., Demint, R. J., *Am. Dyestuff Repr.* **49**, 383 (1960).
- (11) Arthur, J. C., Jr., Daigle, D. J., *Textile Res. J.* **34**, 635 (1964).
- (12) Arthur, J. C., Jr., Demint, R. J., *Textile Res. J.* **30**, 505 (1960).
- (13) *Ibid.*, **31**, 988 (1961).
- (14) *Ibid.*, **32**, 108 (1962).
- (15) Arthur, J. C., Jr., Demint, R. J., U. S. Patent 3,109,798 (Nov. 5, 1963).
- (16) *Ibid.*, 3,157,460 (Nov. 17, 1964).
- (17) Arthur, J. C., Jr., Demint, R. J., McSherry, W. F., Jurgens, J. F., *Textile Res. J.* **29**, 759 (1959).
- (18) Arthur, J. C., Jr., Grant, J. N., *Textile Res. J.* **36**, 934 (1966).
- (19) Arthur, J. C., Jr., Hinojosa, O., Bains, M. S., *J. Appl. Polymer Sci.* **12**, 1411 (1968).
- (20) Arthur, J. C., Jr., Mares, T., *J. Appl. Polymer Sci.* **9**, 2581 (1965).
- (21) Arthur, J. C., Jr., Mares, T., George, M., *Textile Res. J.* **35**, 1116 (1965).
- (22) Arthur, J. C., Jr., Mares, T., Hinojosa, O., *Textile Res. J.* **36**, 630 (1966).
- (23) Arthur, J. C., Jr., Markezich, A. R., McSherry, W. F., *Textile Res. J.* **33**, 896 (1963).
- (24) Arthur, J. C., Jr., Stanonis, D. J., Mares, T., Hinojosa, O., *J. Appl. Polymer Sci.* **11**, 1129 (1967).
- (25) Bains, M. S., Arthur, J. C., Jr., Hinojosa, O., *J. Phys. Chem.* **72**, 2250 (1968).
- (26) Baugh, P. J., Hinojosa, O., Arthur, J. C., Jr., *J. Appl. Polymer Sci.* **11**, 1139 (1967).
- (27) Baugh, P. J., Hinojosa, O., Arthur, J. C., Jr., *J. Phys. Chem.* **71**, 1135 (1967).
- (28) Baugh, P. J., Hinojosa, O., Mares, T., Hoffman, M. J., Arthur, J. C., Jr., *Textile Res. J.* **37**, 942 (1967).
- (29) Blouin, F. A., Arthur, J. C., Jr., *Am. Dyestuff Repr.* **53**, 951 (1964).
- (30) Blouin, F. A., Arthur, J. C., Jr., *J. Chem. Eng. Data* **5**, 470 (1960).
- (31) Blouin, F. A., Arthur, J. C., Jr., *Polymer Preprints* **6**, 359 (1965).
- (32) Blouin, F. A., Arthur, J. C., Jr., *Textile Res. J.* **28**, 198 (1958).
- (33) Blouin, F. A., Arthur, J. C., Jr., *Textile Res. J.* **33**, 727 (1963).

- (34) Blouin, F. A., Arthur, J. C., Jr., Orr, R. S., Ott, V. J., *Textile Res. J.* **31**, 597 (1961).
- (35) Blouin, F. A., Cannizzaro, A. M., Arthur, J. C., Jr., Rollins, M. L., *Textile Res. J.* **38**, 811 (1968).
- (36) Blouin, F. A., Morris, N. J., Arthur, J. C., Jr., *Textile Res. J.* **36**, 309 (1966).
- (37) *Ibid.*, **38**, 710 (1968).
- (38) Bridgeford, D. J., *Ind. Eng. Chem., Prod. Res. Develop.* **1**, 45 (1962).
- (39) Conrad, C. M., Tripp, V. W., Mares, T., *J. Phys. Colloid Chem.* **55**, 1474 (1951).
- (40) Demint, R. J., Arthur, J. C., Jr., Markezich, A. R., McSherry, W. F., *Textile Res. J.* **32**, 918 (1962).
- (41) Demint, R. J., Arthur, J. C., Jr., McSherry, W. F., *Textile Res. J.* **31**, 821 (1961).
- (42) Duke, F. R., Forist, A. A., *J. Am. Chem. Soc.* **71**, 2790 (1949).
- (43) Duke, F. R., Bremer, R. F., *J. Am. Chem. Soc.* **73**, 5179 (1951).
- (44) Florin, R. E., Wall, L. A., *J. Polymer Sci.* **A1**, 1163 (1963).
- (45) Haber, F., Weiss, J., *Naturwiss.* **20**, 948 (1932).
- (46) Haber, F., Weiss, J., *Proc. Roy. Soc. (London)* **A147**, 332 (1934).
- (47) Immergut, E. H., "Encyclopedia of Polymer Science and Technology," Vol. 3, p. 242, Interscience, New York, 1965.
- (48) Iwakura, Y., Kurosaki, T., Imai, Y., *J. Polymer Sci.* **A3**, 1185 (1965).
- (49) Kaizerman, S., Mino, G., Meinhold, F., *Textile Res. J.* **32**, 136 (1962).
- (50) Kettering, J. H., Conrad, C. M., *Ind. Eng. Chem., Anal. Ed.* **14**, 432 (1942).
- (51) Landells, G., Whewell, C. S., *J. Soc. Dyers Colourists* **67**, 338 (1951).
- (52) *Ibid.*, **71**, 171 (1955).
- (53) Merz, J. H., Waters, W. A., *J. Chem. Soc.* **1949**, S15.
- (54) Mino, G., Kaizerman, S., *J. Polymer Sci.* **31**, 242 (1958).
- (55) Mino, G., Kaizerman, S., U. S. Patent **2,922,768** (Jan. 26, 1960).
- (56) Mino, G., Kaizerman, S., Rasmussen, E., *J. Am. Chem. Soc.* **81**, 1494 (1959).
- (57) Mino, G., Kaizerman, S., Rasmussen, E., *J. Polymer Sci.* **38**, 393 (1959).
- (58) Morris, N. J., Blouin, F. A., Arthur, J. C., Jr., *J. Appl. Polymer Sci.* **12**, 373 (1968).
- (59) Percival, E. G. U., "Structural Carbohydrate Chemistry," p. 221, J. Garnet Miller Ltd., London, 1962.
- (60) Rollins, M. L., Cannizzaro, A. M., Blouin, F. A., Arthur, J. C., Jr., *J. Appl. Polymer Sci.* **12**, 71 (1968).
- (61) Rollins, M. L., Moore, A. T., Goynes, W. R., Carra, J. H., deCruy, I. V., *Am. Dyestuff. Reprtr.* **54**, P512 (1965).
- (62) Richard, G. N., *J. Appl. Polymer Sci.* **5**, 539 (1961).
- (63) Sarkar, I. M., Arthur, J. C., Jr., George, M., *Textile Res. J.* **38**, 1145 (1968).

RECEIVED March 28, 1968.

## Mobility of Methyl Groups in Polycarbonate and in Poly- $\alpha$ -methylstyrene Analyzed by Nuclear Magnetic Resonance

R. KOSFELD, U. VON MYLIUS, and G. VOSSKÖTTER

Institute of Physical Chemistry of the RWTH, Aachen, Germany

*The high polymers polycarbonate and poly- $\alpha$ -methylstyrene were investigated by wide line NMR spectroscopy. The activation energies and correlation frequencies of the rotational motion of the methyl groups in the polymers are determined from the measured line-widths and second moments. These are too small for a classical leap process. With the model of the quantum mechanical rotator there is sufficient conformity at low temperatures only. At higher temperatures the results seem to point to a correlation spectrum. From the measured absorption lines, the line-widths and intensities of the components are determined by iteration. This makes it possible to state the number of the rotating and non-rotating methyl groups which are temperature dependent.*

Freezing of internal degrees of freedom has been observed frequently in high molecular substances below the glass transition temperature by NMR spectroscopy. Measurements have been carried out on polycarbonate (PC) by Kovarskaja *et al.* (7), Murakani *et al.* (9), and Slonin *et al.* (19), and on poly- $\alpha$ -methylstyrene (PMST) by Odajima *et al.* (10).

Most investigators studying freezing processes determine only line-widths and second moments of the experimentally determined resonance lines and compare them with the theoretically calculated values. Using these results they try to derive information about correlation times of molecules or molecule groups and about activation energies for thawing certain degrees of freedom of such microscopic systems. Certainly, more information can be obtained from NMR measurements, especially from

complicated absorption lines as in PC and PMST. Our studies were directed toward obtaining a better understanding of the freezing process. [The polycarbonate was supplied by Bayer, Uerdingen, Germany and the poly- $\alpha$ -methylstyrene by BASF, Ludwigshafen, Germany.]

### **Experimental Results**

Since the distance between two extremes of the measured absorption lines is defined as linewidth, Figure 1 shows the temperature dependence of the linewidths of PC. Figure 2 shows the course of the linewidths of PMST. The slight dip in the linewidth curve of the small component observed around 200°K. can be reduced to superposition by another absorption line with a larger linewidth.

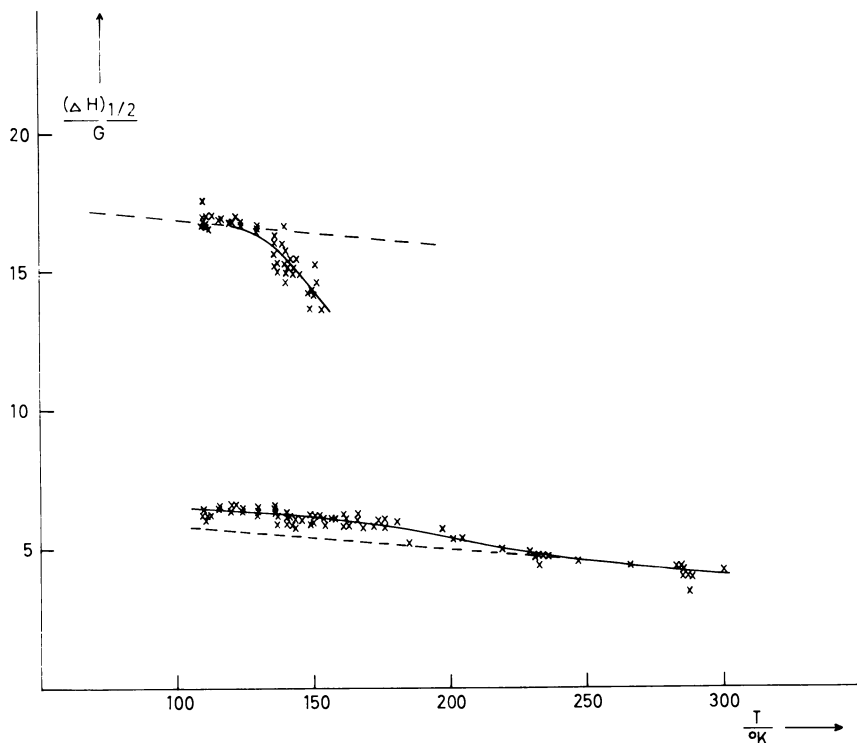


Figure 1. Linewidth  $(\Delta H)_{1/2}$  of polycarbonate as a function of temperature

It is well known that gaussian curves undergo a shift of their maxima by superposition in such a direction that their maxima move toward each other. The results for both linewidths below 150°K. show that minor linewidths are shifted to major values and major linewidths to minor



values. This is valid also for temperatures around 200°K., but here it is impossible to distinguish the two absorption lines because of the small intensity of the absorption line which has the major linewidth. However, around 200°K. a distinct decrease in linewidth of the minor component caused by the influence of the major component can be observed. Measurements with PMST give essentially the same results.

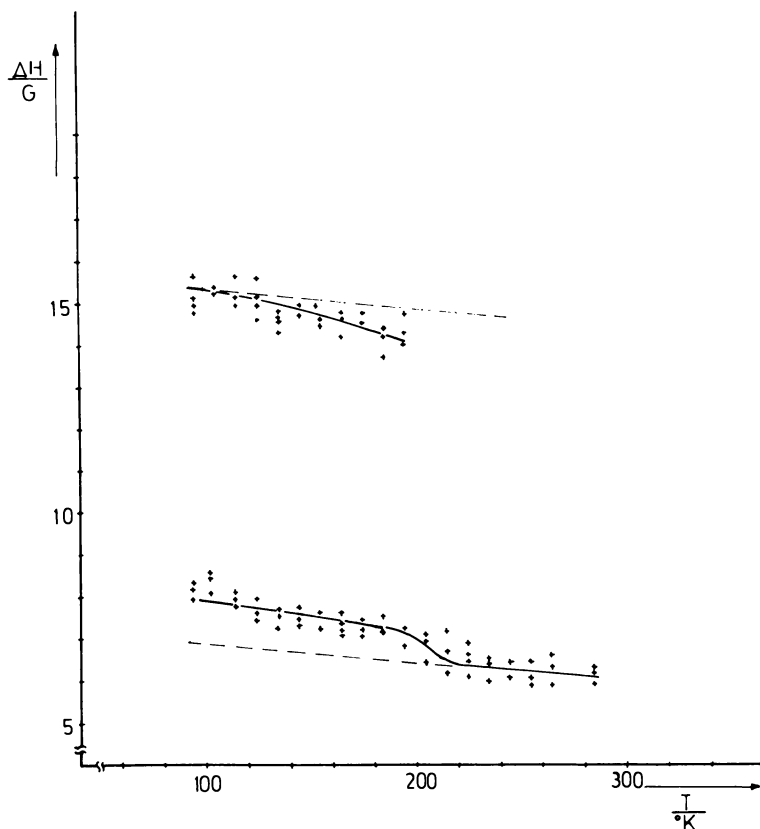


Figure 2. Linewidth  $(\Delta H)_{1/2}$  of PMST as a function of temperature

The temperature dependence of the second moment  $\overline{\Delta H^2}$  gives even more evidence of structural changes in the two substances. The second moment is defined by:

$$\overline{\Delta H^2} = \frac{1}{3} \frac{\int_{-\infty}^{+\infty} g^*(H)' (H - H_0)^3 dH}{\int_{-\infty}^{+\infty} g^*(H)' (H - H_0) dH} \quad (1)$$

where  $g^*(H)'$  is the differentiated, field dependent absorption curve. Corresponding to Equation 1 values of the second moment were determined from the experimentally obtained curves by a Stiltjes planimeter. Figure 3 shows the temperature dependence of the second moment of PC, and Figure 4 gives the temperature dependence of PMST.

The observed change of the second moment with temperature corresponds to a change of  $13.6 \text{ G}^2$  for PC and of  $10.4 \text{ G}^2$  for PMST.

### Discussion

To determine the molecular process which causes a change in the second moment of  $13.6 \text{ G}^2$  for PC and  $10.4 \text{ G}^2$  for PMST, it is necessary to calculate the second moment. According to Van Vleck (22) the second

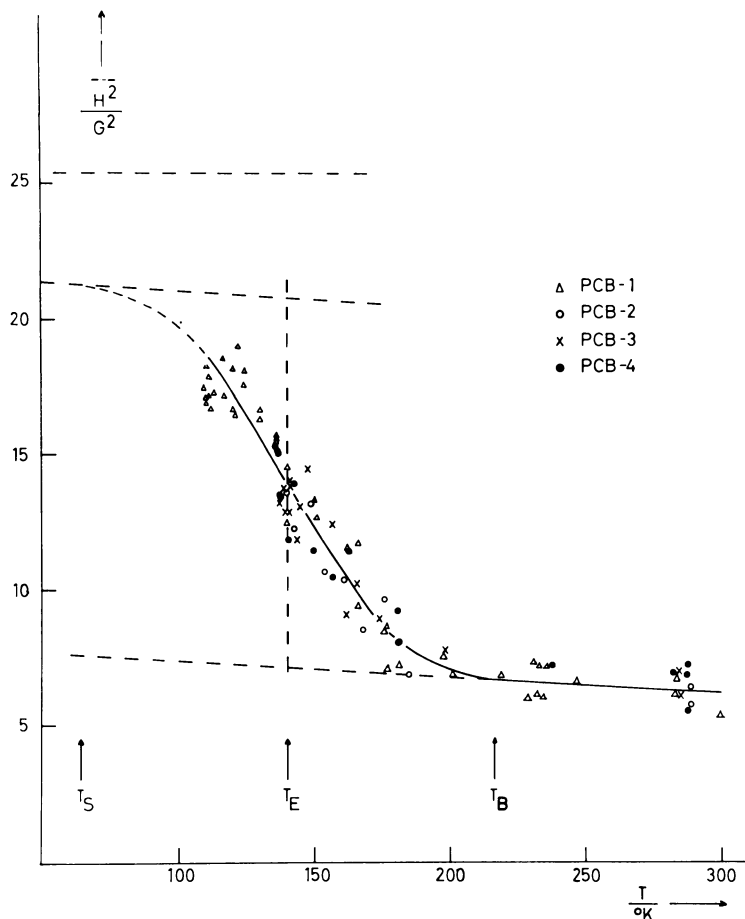


Figure 3. Second moment  $\Delta H^2$  vs. temperature for PC

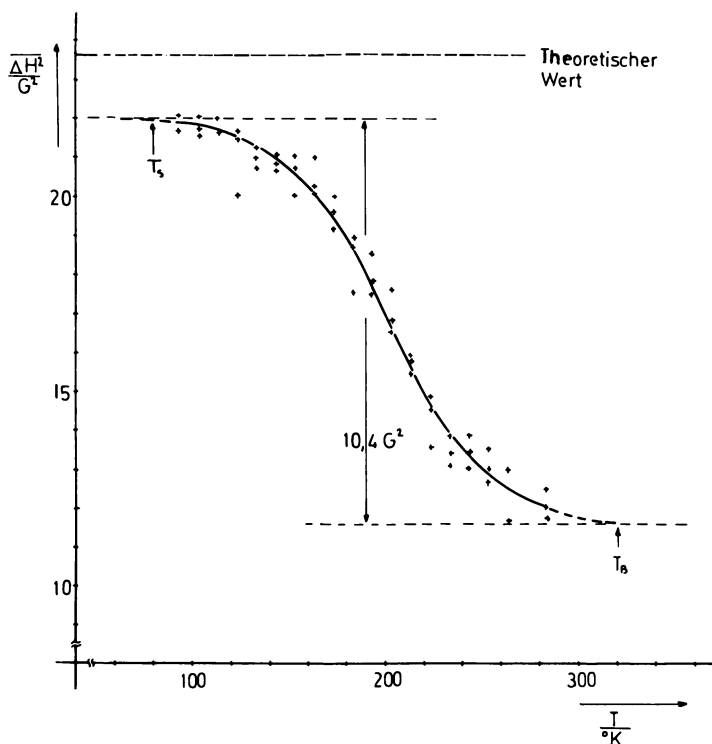


Figure 4. Second moment  $\Delta H^2$  vs. temperature for PMST

moment of a substance which contains only one type of nucleus capable of resonance and which is isotropic can be calculated from Equation 2.

$$\overline{\Delta H^2} = \frac{6}{5} I(I+1) g^2 \mu^2 N^{-1} \sum_{j>k} r_{jk}^{-6} \quad (2)$$

Here  $r_{jk}$  is the distance between the nuclei  $j$  and  $k$ ,  $g$  is the Landé-factor of the nuclei,  $I$  is the nuclear spin, and  $N$  is the number of nuclei which are summarized.

The following distances and angles are taken from published data (8, 21):

- (1) In the aromatic ring: a C—C distance of 1.39 Å, a C—H distance of 1.08 Å, and the C—C—C and C—C—H angles of 120°.
- (2) In the aliphatic chain: a C—C distance of 1.54 Å, a C—H distance of 1.09 Å, and C—C—C and C—C—H angles of 109°28'.
- (3) In the junction between aromatic and aliphatic part of the molecules: a C—C distance of 1.50 Å.

Considering these values, Equation 2 gives  $\overline{\Delta H^2} = 18.7 \text{ G}^2$  for the second moment of PC for internal molecular interactions. To calculate

the contribution of the interactions between the molecules, the results from x-ray measurements of Prietzschk (15) have been used. From his values for the unit cell of PC in the crystalline state, a  $\overline{\Delta H^2}$  value of 6.7 G<sup>2</sup> is calculated. A value of  $\Delta H^2 = 25.4 \text{ G}^2$  for the second moment for 100% crystalline polycarbonate was obtained. This value is marked by a dashed line in Figure 3.

For PMST a second moment for internal molecular interactions of 17.6 G<sup>2</sup> is calculated. The contribution of the interaction between the molecules was estimated only because no structural data of PMST are known. Compared with literature data for similar substances, a value of about 6.0 G<sup>2</sup> seems adequate. Thus, one obtains 23.6 G<sup>2</sup> for the second moment of PMST.

This value is marked by a dashed line in Figure 4. In calculating the second moment it was obvious that in PC as well as in PMST the largest contributions to this moment occur always when at least one of the interacting partners is a proton of a methyl group. Calculating the moment for this case a value of 17.4 G<sup>2</sup> for the internal molecular interactions of PC and a value of 13.5 G<sup>2</sup> for PMST were obtained.

According to Gutowsky and Pake (5) this moment decreases to one-fourth its value in a rigid methyl group if a rotational motion occurs in the molecule. For an initial methyl rotation 17.4 G<sup>2</sup> for PC should decrease to 4.4 G<sup>2</sup> and that from 13.5 G<sup>2</sup> should decrease to 3.4 G<sup>2</sup> for PMST respectively. This causes an increase of 13.0 G<sup>2</sup> for PC and of 10.1 G<sup>2</sup> for PMST. Considering further that for an initial CH<sub>3</sub> rotation the contributions of the interactions between the molecules decrease to the second moment, good conformity is obtained with the experimentally found values of 13.6 and 10.4 G<sup>2</sup> respectively. These results with PC and PMST show a freezing of methyl group rotation. Comparing these experimentally determined values with corresponding values found by Slonim *et al.* (19), a clear difference beyond experimental error is noticeable. Slonim *et al.* (19) corrected their values by considering the amplitude of the wobbling field. A correction like this does not reduce the difference found here since a modulation amplitude of 0.8 G, as used in our experiment, influences only insignificantly the size of the second moment compared with the values of Perlmann and Bloom (11), Andrew (1), and Visweswaramurthy (23).

Besides a miscalibration of the magnitude ( $H-H_0$ ) the main reason for the often large differences in the experimentally found second moments seems to be that the outer dropping sides of the resonance curves which do not emerge clearly from the noise level, make an important contribution to the second moment. It is difficult to decide at which point the integration according Equation 1 can be stopped without great errors.

Despite the relatively large differences between the values found here and those given by Slonim (19) there is a good agreement in the amount of increase of the second moment [ $13.6 \text{ G}^2$  from our experiments and with  $13.0 \text{ G}^2$  from Slonim (19)]. Good agreement is found between our measurements on PMST and those of Odajima *et al.* (10); therefore, no discussion of these values is necessary.

The freezing of methyl-group rotation is always observed in the temperature range  $60^\circ\text{--}300^\circ\text{K}$ . if the methyl groups are hindered by neighboring groups. This has been reported by Powles and Gutowsky (13) for low molecular weight substances. Gutowsky and Meyer (4) and Slichter (17) confirmed such results for different rubbers. Similar observations have been made by Sinnott (16) and Slichter and Mandell (18). Therefore, as shown by Odajima (10) with PMST, the hindering potential, which must be overcome by the methyl groups during rotation, must be estimated. For this purpose an equation derived by Powles and Gutowsky (14) is used:

$$\log a = 0.4343 \frac{\Delta E}{kT} - \log \nu^* \quad (3)$$

where:

$$a = \frac{2\pi\nu_0}{\gamma(\Delta H^2)^{1/2}} t_g \frac{(\overline{\Delta H^2} - \overline{\Delta H_h^2})}{(\Delta H_t^2 - \overline{\Delta H_h^2}) 2} \quad (4)$$

$\nu^*$  is a dimensionless number. It is determined by  $\nu_\infty = \nu^* \cdot \nu_0$ , with  $\nu_0 = 1 \text{ sec}^{-1}$ .

Between the activation energy  $\Delta E$ , the correlation frequency  $\nu_c$  and the correlation frequency  $\nu_{00}$  for infinite temperatures a dependence corresponding to the Arrhenius equation is assumed:

$$\nu_c = \nu_\infty \exp\left(-\frac{\Delta E}{kT}\right) \quad (5)$$

$\Delta H_h^2$  represents the second moment at  $T_B$  and  $\Delta H_t^2$  the value at  $T_S$  (see Figure 3).  $\log a$  is calculated as function of the reciprocal of absolute temperature. The values of the second moment were taken from Figures 3 and 4.

From the slopes of the resulting straight lines and from the abscissa intersection an activation energy  $\Delta E$  of 1.2 kcal./mole and a limiting frequency  $\nu_\infty$  of 1.26 MHz. for PC and 1.47 kcal./mole and 0.63 MHz. for PMST, respectively, are obtained. These values are too small.

According to the Transition State Theory (3) a limiting frequency of  $2.7 \times 10^6$  MHz. at very high temperatures for a classical leap process is obtained which is assumed from previous calculation. With Powles (12) and Odajima (10) the frequently observed low activation energies in polymers can be explained by a correlation spectrum. That means it is

necessary to assume not only one correlation frequency  $\nu_c$  but a correlation spectrum because of the many degrees of freedom in complicated high molecular weight substances.

Steiskal and Gutowsky (20) give another explanation for low molecular weight solid matter. They consider the methyl groups as quantum-mechanical rotators which overcome the hindering potential by a tunneling effect. The hindering potential which counteracts rotation is given by Equation 6.

$$V = \frac{V_0}{2} [1 + \cos(3\phi)] \quad (6)$$

$V_0$  is the potential height, and  $\phi$  describes the rotation of the methyl groups. Steiskal and Gutowsky (20) give the dependence of the tunneling frequency  $\nu_T$  of the reciprocal absolute temperature as parameter for  $V_0$ . Figure 5 gives these results.

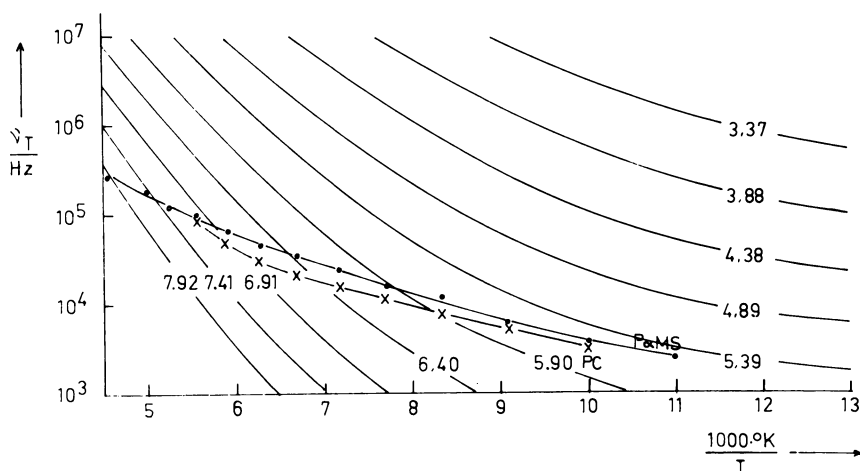


Figure 5. Comparison of the correlation frequencies calculated according Equation 7 with the averaged tunneling frequencies  $\nu_T$  calculated by Steiskal and Gutowsky for the methyl groups assumed as quantum-mechanical rotators as a function of the temperature for PC (x) and PMST (o). The potential height in units of kcal./mole is the parameter

To confirm whether or not the results reported here can be described by a tunneling effect, an equation is derived for the correlation frequency  $\nu_c$  from the Equations 3, 4, and 5 in the form:

$$\nu_c = \frac{\gamma}{2\pi} (\overline{\Delta H^2})^{1/2} t_g \left[ \frac{(\overline{\Delta H^2} - \overline{\Delta H_h^2})}{(\overline{\Delta H_t^2} - \overline{\Delta H_h^2})} \right]^{-1} \quad (7)$$

Using the temperature dependent values for the second moment from Figure 3 and 4 it is possible to calculate the correlation frequencies  $\nu_c$  from Equation 7. Assuming that the correlation frequencies  $\nu_c$  obtained this way were identical to the tunneling frequencies  $\nu_T$ , the calculated values for  $\nu_c$  were inserted in Figure 5. The correlation frequencies from Equation 7 are close to the theoretical curves at low temperatures. At high temperatures the  $\nu_c$  values differ more and more from the quantum mechanical model. This is understandable since the neighboring groups which constitute the real hindrance for methyl-group rotation become more mobile with increasing temperature. Therefore, methyl-group rotation is similar to a classical describable rotation diffusion.

This result shows clearly that the motion of methyl groups as they change from a frozen state to one of free motion can be described not only by the model of a quantum-mechanical rotator. Still the tunneling effect seems to give a possible explanation for the low rotation frequencies of the methyl groups and the corresponding hindering potential at low temperatures. Previously, it has been noted that the observed low activation energies compared with the classical model for a hindered methyl-group rotation point to a correlation spectrum. It is very difficult to determine correlation functions. Therefore, we will study in a way in which the behavior of the motion of the methyl groups can be described.

### *Separation of the Absorption Curves*

The shape of the absorption curves shows that the lateral extremes differ from the inner extremes. Extrapolation of the inner side of the lateral extremes to the value  $H_0$  gives curves which incline concavely to the abscissa. In performing a convex extrapolation corresponding to the inner extremes an intersection with the abscissa alongside  $H_0$  is obtained. This indicates that the absorption curves arise from the superposition of several curves, whose centers of symmetry are shifted with respect to  $H_0$ , at least for the lateral components.

As shown before, the splitting of the absorption curves to several components is caused by the freezing of methyl-group rotation. Andrew and Bersohn (2) have calculated the corresponding line shapes for an isolated rigid three-spin system in a powderlike substance. From this one expects for rigid methyl groups having no interactions between each other a spectrum of three line groups which are symmetrical to a center. If the spin groups interact with their neighboring groups, the lines broaden. The resulting line shape can be described approximately by three gaussian curves, two of which have identical shapes lying symmetrically to the third one. Gutowsky and Pake (5) and Kakiuchi *et al.* (6) confirmed these results of Andrew and Bersohn (2).

Corresponding to these results it is assumed that the line shape of the absorption curves of PC and PMST at low temperatures can be described by the expression:

$$I = C_o \exp [-\alpha_o (H - H_o)^2] + C_1 \{ \exp [-\alpha_1 (H - H_o + H_1)^2] + \exp [-\alpha_1 (H - H_o - H_1)^2] \} \quad (8)$$

$I$  is the intensity of the absorption curves depending on the field strength  $H$ ;  $C_o$  describes the intensity of the inner gaussian curve and  $C_1$  the intensity of the lateral gaussian curves;  $\alpha_o$  and  $\alpha_1$  are the corresponding shape parameters of the curves.  $H_o$  determines the position of the inner curve, and  $H_1$  determines the shift of the lateral curves corresponding to  $H_o$ . In this expression it is important that the inner gaussian curve is a superposition of several curves. It is composed of a contribution of the frozen methyl groups and a contribution of the still rotating methyl groups and benzol-ring protons. In PMST there is an additional contribution of the  $\text{CH}_2$  groups. The contribution of the rigid  $\text{CH}_3$  groups must be separated from this.

In the experiment the differentiated absorption curves are obtained. Therefore, we begin with the differentiated form of Equation 8. The differentiation of the field strength  $H$  is marked here by a comma. Accordingly, the intensity of the lateral extremes for the differentiated absorption curves is marked  $(I_1')_{1/2}$  and the intensity of the inner extremes  $(I_o')_{1/2}$ . The linewidths resulting from the distance of the extremes are marked  $(\Delta H_1)_{1/2}$  for the lateral gaussian curves and  $(\Delta H_o)_{1/2}$  for the inner curve. In this way the areas under the different gaussian curves defined by Equation 8 are determinable.

$F_o$  designates the area under the central gaussian curve and  $F_1$  that under one of the lateral curves. The total number of protons  $N$  in the sample is proportional to the area  $F$  under the complete absorption curve.  $F$  follows from the summation of  $F_o$  and  $2F_1$ . From this, the total number of protons  $N$  is:

$$N \sim (F_o + 2 F_1). \quad (9)$$

Since the protons in PC are bound at 3/7 in methyl groups and in PMST at 3/10, the number of protons in the methyl groups  $N_M$  are:

$$N_M = \frac{3}{7} N \quad (10)$$

and

$$N_M = \frac{3}{10} N. \quad (11)$$



The number of protons in the frozen methyl groups  $N_{\text{ME}}$  can be defined as being proportional to an area consisting of  $2F_1$  and a contribution  $F_2$  contained in  $F_o$ :

$$N_{\text{ME}} \sim (2F_1 + F_2) \quad (12)$$

For the relation  $N_{\text{ME}}/N_{\text{M}}$  for PC from Refs. 9, 10, and 12 and Equation 13:

$$\frac{N_{\text{ME}}}{N_{\text{M}}} = \frac{2F_1 + F_2}{3/7(F_o + 2F_1)} \quad (13)$$

and for PMST from Refs. 9, 11, and 12 and Equation 14:

$$\frac{N_{\text{ME}}}{N_{\text{M}}} = \frac{2F_1 + F_2}{3/10(F_o + 2F_1)} \quad (14)$$

is obtained.

Andrew and Bersohn (2) have shown that for rigid methyl groups the intensity of the spectrum in the central part of the absorption curve is twice as high as that of the lateral parts—*i.e.*,

$$F_2 = 2F_1 \quad (15)$$

If we determine the different areas by values of  $(I_1')_{1/2}$ ,  $(I_o')_{1/2}$ ,  $(\Delta H_1)_{1/2}$ , and  $(\Delta H_o)_{1/2}$ , we can transform Equation 13 by Equation 15, and we obtain the relation for PC:

$$\frac{N_{\text{ME}}}{N_{\text{M}}} = 9.33 \left[ \frac{(I_o')_{1/2} (\Delta H_o)_{1/2}^2}{(I_1')_{1/2} (\Delta H_1)_{1/2}^2} + 2 \right]^{-1} \quad (16)$$

From Equations 14 and 15 we obtain the corresponding relation for PMST:

$$\frac{N_{\text{ME}}}{N_{\text{M}}} = 13.33 \left[ \frac{(I_o')_{1/2} (\Delta H_o)_{1/2}^2}{(I_1')_{1/2} (\Delta H_1)_{1/2}^2} + 2 \right]^{-1} \quad (17)$$

With Equations 16 and 17 it is possible to determine the transition of methyl groups from the rotating state to the frozen state as functions of temperature from the experimental data.  $(\Delta H_o)_{1/2}$  corresponds to the linewidths for the inner component of the absorption curves as shown in Figures 1 and 2. These values are false, owing to the superposition of the lateral components. A correction is reported later. The values of the lateral components of the absorption curves marked in Figures 1 and 2—in these figures these parts of the curves were marked as the broad components—have lost the meaning of a linewidth. These values give the position of the lateral gaussian curves only. That means it is possible to calculate the shift of the lateral gaussian curves with respect to  $H_o$  from these values. A correction is also necessary to determine the

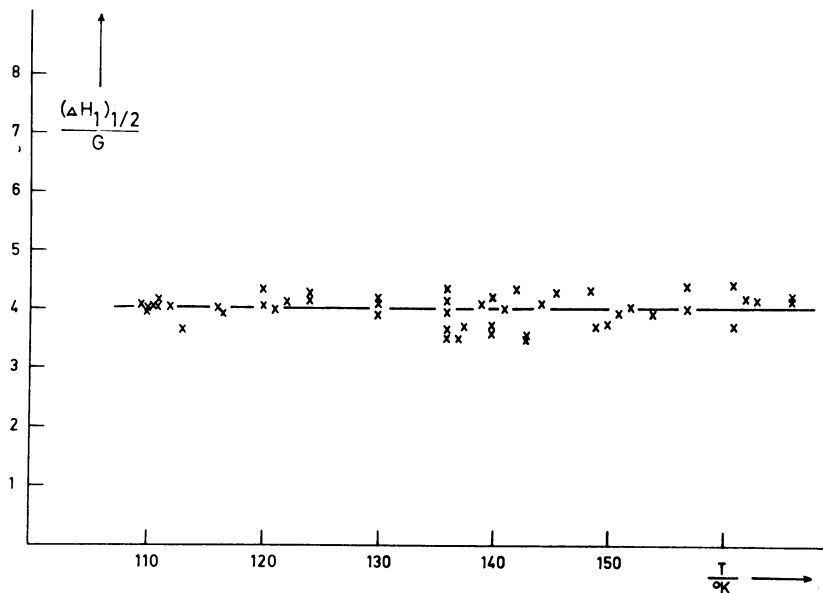


Figure 6. Temperature dependence of the corrected  $(\Delta H_1)_{1/2}$ -values for PC

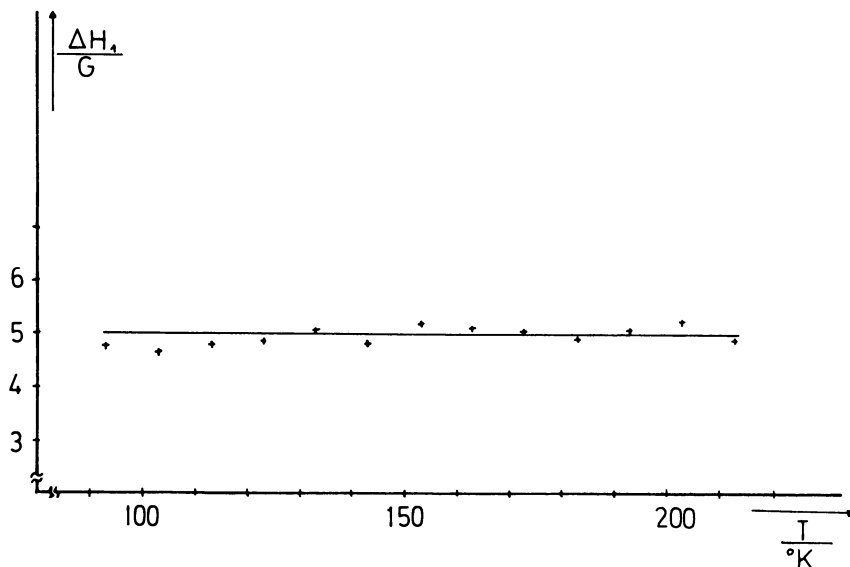


Figure 7. Temperature dependence of the corrected  $(\Delta H_1)_{1/2}$ -values for PMST

relation between the ordinates  $(I_1')_{1/2}/(I_o')_{1/2}$  of the lateral and inner extremes. At the position of the extreme value a contribution, which belongs to the dropping side of the component of the curve must be

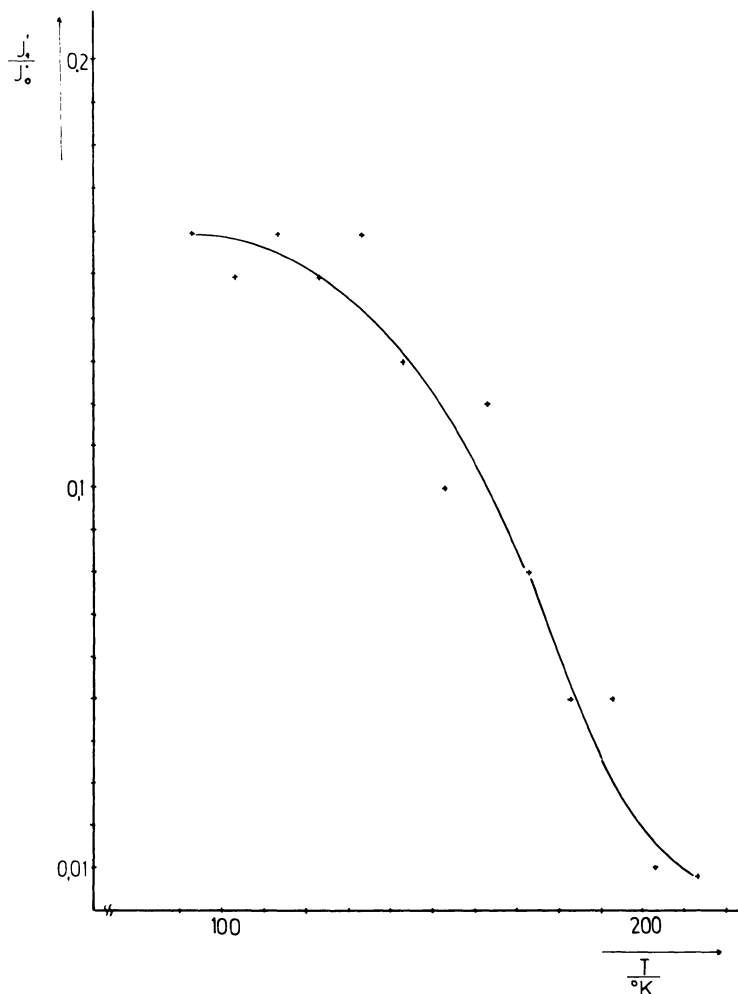


Figure 8. Intensity relation  $(I'_1)_{1/2}/(I'_0)_{1/2}$  of the lateral and central extremes for the differentiated absorption curves as a function of temperature for PMST

taken into account. Therefore, this correction must start with the differentiated form of Equation 8, where  $\alpha_0$ ,  $\alpha_1$ ,  $C_0$ , and  $C_1$  must be replaced by  $(I'_1)_{1/2}$ ,  $(I'_0)_{1/2}$ , and  $(\Delta H_1)_{1/2}$  and  $(\Delta H_0)_{1/2}$ . Thus, the values of  $(I'_1)_{1/2}$  and  $(I'_0)_{1/2}$  taken from the experimental curves are used to perform the correction mentioned above, according to differentiated Equation 8. Hence, corrected  $(I'_1)_{1/2}$  and  $(I'_0)_{1/2}$  values are obtained, which are used for a second correction. In this way the true intensity

values are iteratively approximated. This iteration must of course consider the correction of the linewidths.

First there is a question as to how  $(\Delta H_1)_{1/2}$ , the linewidth of the lateral gaussian curves, can be determined. A determination is not possible by the inflection point distance because the sides of the lateral curves near  $H_0$  are covered by the middle part of the spectrum. Therefore, a point of the absorption curve must be found which is shifted by  $0.5 (\Delta H_1)_{1/2}$  with respect to the position of the lateral extremes. In determining this point the contribution of the central gaussian curve similar to the determination of the intensities must be considered.

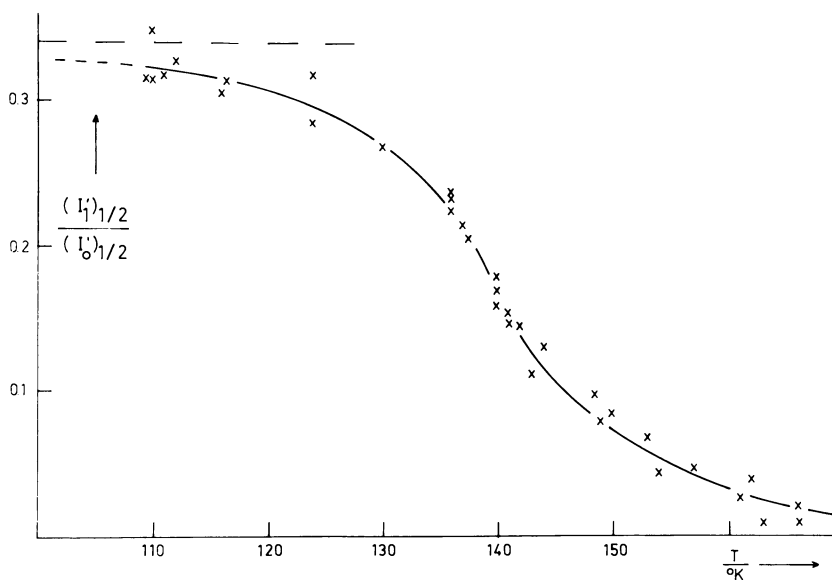


Figure 9. Intensity relation  $(I'_1)_{1/2}/(I'_0)_{1/2}$  of the lateral and central extremes for the differentiated absorption curves as function of temperature for PC

As mentioned above an increase of the linewidth occurs by the superposition of the lateral and central gaussian curves or by a shift of the extremes of the differentiated absorption curves, which is essentially the same. Again the real linewidths can be obtained iteratively only. For this purpose we begin with the twice-differentiated form of Equation 8 because the question after the shift of the extremes for the differentiated curves is identical to the question after the shift of the zeros for the twice-differentiated absorption curves. There the twice-differentiated Equation 8 is developed in a Taylor series at the positions of the extremes breaking off after the second term. At these positions the function is

approximated by straight lines, but it is easy to determine the shift of the zero by superimposing the straight lines. This indicates the direction and size of shift of the zeros for the twice-differentiated equation (Equation 8) and also gives a correction for the linewidths. Repetition of this performance gives finally the true linewidth. The corrected  $(\Delta H_0)_{1/2}$  values are nearly identical with the dashed extrapolation to low temperatures for the small linewidths in Figures 1 and 2.

Figures 6 and 7 give the corrected  $(\Delta H_1)_{1/2}$  values for PC and PMST. Figures 8 and 9 show the corrected intensity relation  $(I_1')_{1/2}/(I_0')_{1/2}$  for PC and PMST. The relation  $N_{ME}/N_M$  can be calculated from Equations 16 and 17 by the data obtained from Figures 1, 6, and 8 for PC and from Figures 2, 7, and 9 for PMST. Figure 10 displays these results for PC and for PMST.

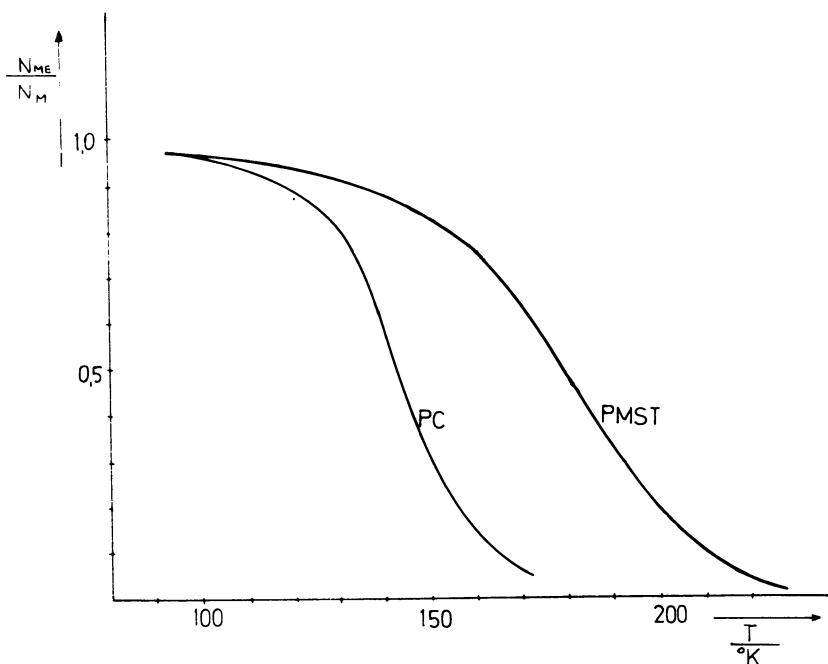
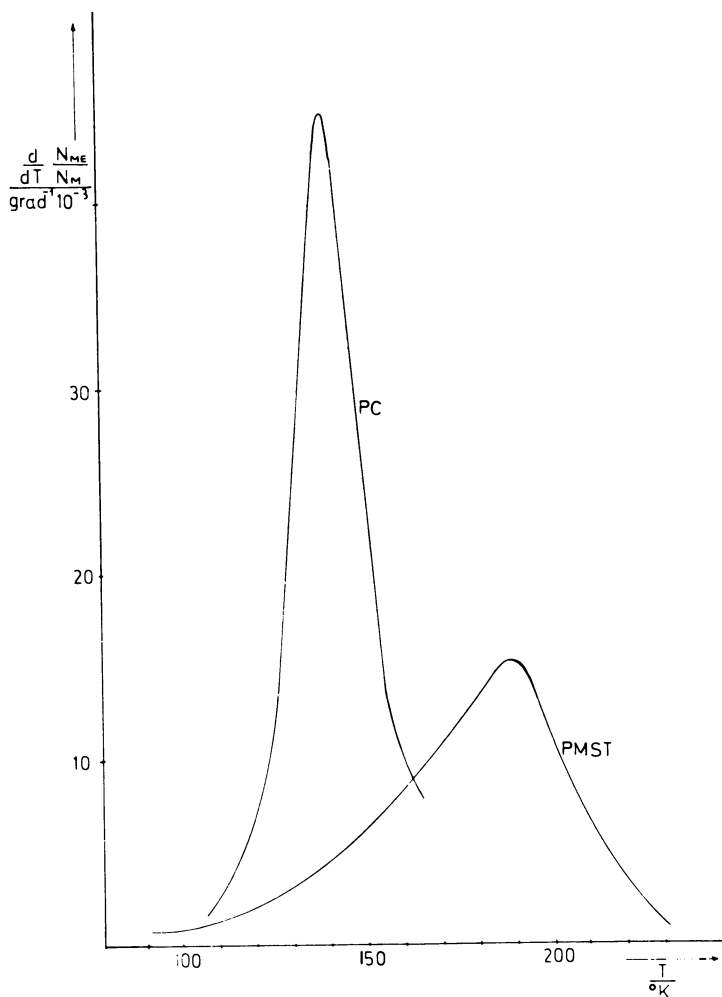


Figure 10. Number ( $N_{ME}$ ) of frozen methyl groups with respect to the total number ( $N_M$ ) of methyl groups as a function of temperature for PC and PMST

For low temperatures the curves must approach asymptotically the value 1. The physical meaning of these curves is as follows. It is possible to determine for each temperature in the transition range how many methyl groups in relation to the total number of methyl groups change from a frozen state to one of free rotation during a temperature increase

$\delta T$ . Yet it must be remembered that the decision as to when a methyl group is in a frozen or a state of free rotation is made by the NMR experiment in such a way that the methyl group under consideration does or does not cross a specific rotational frequency. This deciding rotational frequency has been introduced in Equation 7 as the correlation frequency  $\nu_c$ . According to Equation 7  $\nu_c$  is temperature dependent. Figure 5 shows the  $\nu_c$  values calculated from Equation 7 as a function of the reciprocal temperature.



*Figure 11. Number of methyl groups changing from a frozen state to rotation during a temperature variation as function of temperature for PC and PMST*

The NMR experiment not only answers the question of how many methyl groups are frozen and how many are moving freely but also how many cross the threshold defined by  $\nu_c$  during a small temperature variation  $\delta T$ . Therefore, differentiating  $N_{ME}/N_M = f(T)$  as a function of temperature as shown in Figure 10 relates the methyl group distribution to the different frequencies  $\nu_c$ .

The result of this differentiation is shown in Figure 11 for PC and for PMST. The functional relation given in these figures can be described as follows: For a rise in the temperature  $\delta T$  at a defined temperature  $T$  the NMR experiment forces the number of methyl groups to change from a rotational movement below  $\nu_c$  to a rotational movement above  $\nu_c$  according to  $\delta T$ . This number is related to the number of methyl groups occurring in a frequency interval  $\delta\nu$  above the frequency  $\nu_c$  given by the temperature  $T$ .

It is possible to demonstrate the relation between  $\nu$  and  $T$  giving an arbitrary assumed frequency distribution function  $f(T, \nu)$ . This is done in Figure 12 for two temperatures  $T$  and  $T + \delta T$  according to the function:

$$\frac{\Delta N}{N} = f(T, \nu) \delta\nu \quad (18)$$

$N$  is the total number of methyl groups,  $\Delta N$  the number of methyl groups occurring in the frequency interval  $\delta\nu$ . The number of methyl groups crossing the frequency  $\nu_c$  is represented by  $(\Delta N/N)\delta T$ . Figure 12 demonstrates this number by the area difference  $F_1 - F_2$ . From this it follows:

$$\begin{aligned} \left(\frac{\Delta N}{N}\right)_{\delta T} &= F_1 - F_2 \quad (19) \\ &= \int_0^{\nu_c} f(T, \nu) \, d\nu - \int_0^{\nu_c} f(T + \delta T, \nu) \, d\nu \\ &= - \int_0^{\nu_c} [f(T + \delta T, \nu) - f(T, \nu)] \, d\nu \end{aligned}$$

For small  $\delta T$   $f(T + \delta T, \nu)$  can be approximated by a Taylor series breaking off after the first term:

$$f(T + \delta T, \nu) = f(T, \nu) + \frac{\delta f(T, \nu)}{\delta T} \delta T \quad (20)$$

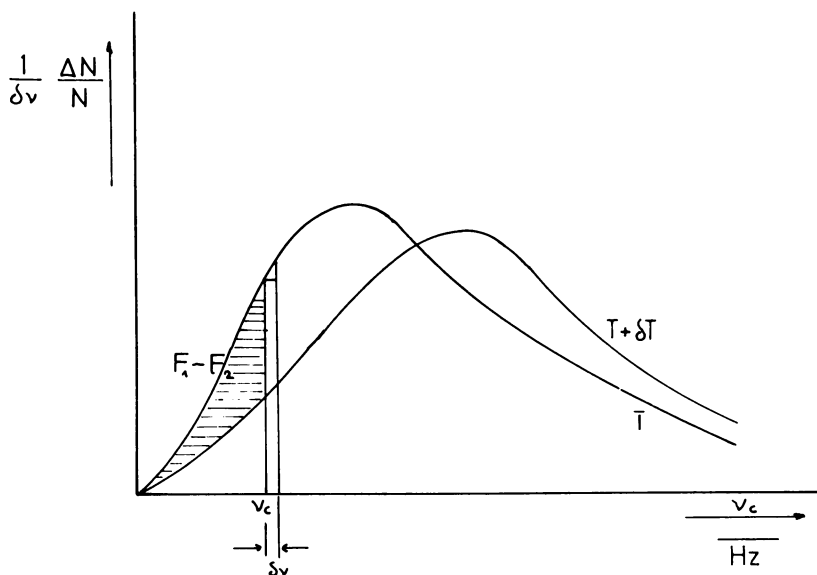


Figure 12. Frequency distribution function  $f(T, \nu)$  vs. temperature at two different temperatures

Equation 20 with Equation 19 leads to:

$$\left(\frac{\Delta N}{N}\right)_{\Delta T} = \delta T \int_0^{\nu_c} \frac{\delta f(T, \nu)}{\delta T} d\nu \quad (21)$$

When

$$\frac{\Delta N}{N} = \left(\frac{\Delta N}{N}\right)_{\delta T} \quad (22)$$

it follows from Equations 18 and 21:

$$f(T, \nu) \delta \nu = T \int_0^{\nu_c} \frac{\delta f(T, \nu)}{\delta T} d\nu \quad (23)$$

Assuming for a further interpretation (this is arbitrary) the unknown frequency distribution corresponding to a Maxwell distribution, from Equation 23 a relationship between  $\delta \nu$  and  $\delta T$  of the form:

$$\frac{\delta T}{2T} = \frac{\delta \nu}{\nu_c} \quad (24)$$

is obtained.



Therefore, if it is possible to find a frequency distribution function corresponding to experimental results, it would be possible to find a relation using Equation 24 which would correspond to a Maxwell distribution. With this equation the variable  $1/\delta T \times N_{ME}/N_M$  of Figure 11 should be transformed into the variable  $1/\delta v \times N_{ME}/N_M$ . If pairs of values using this performance corresponding to the intersection points of the correlation frequencies with the theoretically determined distribution (cf. Figure 5) are gained, the theoretically determined distribution function would be confirmed by experimental results.

The distinct maximum in Figure 11 at 140°K. for PC and at 186°K. for PMST demonstrates that the change of the number of methyl groups crossing the limiting frequency which is critical for line splitting occurs most frequently at this temperature. The temperature of 140°K. marked as  $T_E$  has been used already to extrapolate the second moment reported in Figure 3. For PMST this extrapolation was not necessary because the measurements could be made to sufficiently low temperatures.

It is not possible to derive the frequency distribution curves from the curves reported in the Figure 11. The only value of these demonstrations is that they uncover experimental criteria which are useful for examining a model describing the methyl group motion.

### Literature Cited

- (1) Andrew, E. R., *Phys. Rev.* **91**, 425 (1953).
- (2) Andrew, E. R., Bersohn, R., *J. Chem. Phys.* **18**, 159 (1950).
- (3) Glasstone, S., Laidler, F. K. J., Eyring, E. H., "The Theory of Rate Processes," McGraw-Hill, New York, 1941.
- (4) Gutowsky, H. S., Meyer, L. H., *J. Chem. Phys.* **21**, 2133 (1953).
- (5) Gutowsky, H. S., Pake, G. E., *J. Chem. Phys.* **18**, 162 (1950).
- (6) Kakiuchi, Y., Shono, H., Kigoshi, K., Komatsu, H., *J. Chem. Phys.* **19**, 1069 (1951).
- (7) Kovarskaja, E. M., Zigunova, I. E., Slonin, J. J., Urman, J. G., Nejman, M. B., "Sammelband Chimiceskie Svojstva: modifikacija, polimerov," SSSR, 1964.
- (8) Landolt, H., Börnstein, R., "Zahlenwerte und Funktionen," Teil 3, II, Springer-Verlag, Berlin, 1951.
- (9) Murakami, I., Kawai, A., Yamamura, H., *J. Sci. Hiroshima Univ., Ser. A-II*, **27**, 141 (1964).
- (10) Odajima, A., Woodward, A. E., Sauer, J. A., *J. Polymer Sci.* **55**, 181 (1961).
- (11) Perlman, M. M., Bloom, M., *Phys. Rev.* **88**, 1290 (1952).
- (12) Powles, J. G., *Polymer* **1**, 219 (1960).
- (13) Powles, J. G., Gutowsky, H. S., *J. Chem. Phys.* **18**, 162 (1950).
- (14) *Ibid.*, **23**, 1962 (1955).
- (15) Prietzschk, A., *Kolloid-Z.* **156**, 8 (1958).
- (16) Sinnott, K. M., *J. Polymer Sci.* **42**, 3 (1960).
- (17) Slichter, W. P., *Makromol. Chem.* **34**, 67 (1959).
- (18) Slichter, W. P., Mandell, E. R., *J. Appl. Phys.* **30**, 1473 (1959).

- (19) Slonin, I., Urman, J. G., Konovalov, A. G., Sammelband Chimiceskie Svostva: modifkacija polimerov lzd. AN SSSR (1964).
- (20) Steijskal, E. O., Gutowsky, H. S., *J. Chem. Phys.* **28**, 388 (1958).
- (21) Stuart, H. A., "Die Physik der Hochpolymeren," Vol. III, Springer-Verlag, Berlin, 1955.
- (22) Van Vleck, H. J., *Phys. Rev.* **74**, 1168 (1948).
- (23) Visweswaramurthy, S., *Indian J. Pure Appl. Phys.* **3**, 261 (1965).

RECEIVED March 25, 1968.

## New Polycondensation Polymers

GERHARD BIER

Dynamit Nobel AG, 521 Troisdorf Bez. Koln, Germany

*Although amorphous polyamides so far have not generated great interest in the plastics field, some new ones were synthesized and examined. The characteristic structural elements were the aromatic ring, the methyl-branched aliphatic chain, and the carbonamide group; these influence the glass temperature and crystallinity. The aromatic and carbonamide groups result in a relatively high glass temperature of the polyamides. The methyl branches of the aliphatic chain with ca. 10% in weight prevent crystallization and increase the glass temperature as compared with the unbranched compounds. The position of the carbonamide group also influences the glass temperature. A commercial product based on terephthalic acid and trimethylhexamethylenediamine is Trogamid T.*

The properties of a plastic can be affected by differences in structures—*i.e.*, mobility of the main chain, volume and arrangement (tacticity) of the lateral substituents, forces between the chains (*e.g.*, hydrogen bridges), crystallinity. Macromolecular products of distinctly different structures can lead to technical substances with similar properties and application. Nylon 6/6 and PEPT (polyethylene terephthalate) are common examples. In the fiber field crystallinity and intermolecular forces, both arising from geometrical configurations, are essential. The important factors are the hydrogen bridges for nylon 6/6 and the forces between the aromatic groups for PETP.

In synthesizing the most important polyesters and polyamides in thermoplastics—*i.e.*, polyesters: PETP, polycarbonates (11, 16) and polyamides: nylon 6, nylon 6/6 etc.—the emphasis for polyesters is on products with a high aromatic content (partially aromatic products), and for polyamides the emphasis is on purely aliphatic products.

Among the polyesters there are neither purely aliphatic nor fully aromatic products as commercial products which are available or suitable

as a thermoplastic material. As regards the polyamides, the partially aromatic and fully aromatic products are not within the manufacturers' production range. The fully aromatic products do not lend themselves to thermoplastic processing (7, 13). The answer for thermoplastic processing possibly could be a polyamide based on terephthalic acid and hexamethylenediamine. However, such a product would have a crystalline melting point of 371°C. necessitating a processing temperature too close to the decomposition temperature. A product of similar structure but without crystallinity might perhaps facilitate processing at lower temperatures. The following deals with a product likely to fill this obvious gap.

The starting point of our work has been studies by R. Gabler and co-workers in the former Zürich Research Institute of W. R. Grace & Co. (8). Dynamit Nobel learned of Gabler's work at a relatively early stage and acquired a license on the patents anticipated. One of the products described by Gabler has been developed by F. Blaschke, G. Schade, and H. Wemheuer *via* a pilot plant to a semicommercial production stage (discussed later). This product has the tradename Trogamid T. The laboratory studies described in the following section have been carried out by G. Renckhoff, W. Wolfes, and P. Janssen (synthesis) and A. Gardziella, R. Minke, E. Bessler, and W. Lessmann (product studies).

### ***Amorphous Polyamides Based on Terephthalic Acid***

As a dicarboxylic acid Gabler *et al.* used primarily terephthalic acid and in some cases isophthalic acid also. As diamine they used a number of branched aliphatic products, and the emphasis was on products having C-6 chain members separating the two NH<sub>2</sub> groups. Table I lists some of Gabler's products.

A mixture of the last two diamines in Table I is a commercial product of Scholven Chemie in Germany. The melting points given by Gabler have been determined visually. In view of the fact that the products are all amorphous the points are sinter points rather than melting points. More interesting than the sinter temperatures are the glass temperatures or second-order transition points which have been determined on some products submitted to us by Gabler (last two columns of Table I).

Glass temperatures have been determined by the DTA method with two different instruments (a Mettler differential thermoanalyzer and a Perkin-Elmer differential scanning calorimeter DSC 1) (9) in two different laboratories. They are listed in the two last columns of Table I. Small differences of 0°–7°C. were observed. This order of agreement was sufficient.

**Table I. Amorphous Polyamides Based on Terephthalic Acid by Gabler *et al.***

Diamine	Melting Point, Gabler	Glass Temperature/DTA	
		Minke	Gardziella
$\begin{array}{c} \text{C} \\   \\ \text{C} \\   \\ \text{N}-\text{C}-\text{C}-\text{C}-\text{C}-\text{C}-\text{N} \end{array}$	180	135	130
$\begin{array}{c} \text{C} \quad \text{C} \\ \diagdown \quad / \\ \text{C} \\   \\ \text{N}-\text{C}-\text{C}-\text{C}-\text{C}-\text{C}-\text{N} \end{array}$	217	150	143
$\begin{array}{c} \text{C} \\   \\ \text{C} \\   \\ \text{N}-\text{C}-\text{C}-\text{C}-\text{C}-\text{C}-\text{N} \\   \\ \text{C} \end{array}$	200	—	—
$\begin{array}{c} \text{C} \\   \\ \text{C} \\   \\ \text{N}-\text{C}-\text{C}-\text{C}-\text{C}-\text{C}-\text{N} \\   \\ \text{C} \end{array}$	200	139	139
$\begin{array}{c} \text{C} \quad \text{C} \\   \quad   \\ \text{N}-\text{C}-\text{C}-\text{C}-\text{C}-\text{C}-\text{N} \\   \\ \text{C} \end{array}$	227	148	145
$\begin{array}{c} \text{C} \quad \text{C} \\   \quad   \\ \text{N}-\text{C}-\text{C}-\text{C}-\text{C}-\text{C}-\text{N} \\   \\ \text{C} \end{array}$	—	159	153

The glass temperatures of all products fall within the range 130°–160°C. The partially aromatic polycarbonate has a glass temperature of 150°C.; the partially aromatic PETP has a glass temperature of 75°C. To determine the ratio of the aromatic to the aliphatic content, we assume four chain links for the benzene rings. Then the polycarbonate has the ratio: aromatic/aliphatic links = 4:6, the polyester has a ratio 4:2, and the polyamides (Table I) have a ratio 4:10. Despite the lower aromatic content the glass temperatures of some of the amorphous polyamide are

of the same order as those of the polycarbonate and higher than those of the crystalline terephthalic polyester (75°C.).

What then are the factors which cause the high glass temperature and the amorphous character? To answer this, we must analyze the structure of the polyamides. There are three structural components of the polyamides in question: (1) a branched aliphatic group, (2) an aromatic group, (3) two carbonamide groups. The influence exerted by these components is examined more closely in the following discussions. Trials to calculate glass temperatures of polyamides by summing the partial contributions of the components of polyamides are described by Beaman (2) and Askadskii (1).

**Branched and Unbranched Diamines.** To examine the influence of branching, polyamides based on adipic acid and terephthalic acid have been prepared with branched and unbranched diamines of equal chain length. Their melting points and glass temperatures are listed in Table II.

**Table II. Unbranched and Branched Aliphatic Chains in Polyamides**

Acid	Diamine	T <sub>m</sub>	T <sub>g</sub>
Adipic	N—C—C—C—C—C—C—N	264	50-57
Adipic	$\begin{array}{c} \text{C} \quad \quad \text{C} \\   \quad \quad   \\ \text{N}-\text{C}-\text{C}-\text{C}-\text{C}-\text{C}-\text{N} \\   \\ \text{C} \end{array}$ (isomer mixture)	am. <sup>a</sup>	65
Terephthalic	N—C—C—C—C—C—C—N	371	140
Terephthalic	$\begin{array}{c} \text{C} \quad \quad \text{C} \\   \quad \quad   \\ \text{N}-\text{C}-\text{C}-\text{C}-\text{C}-\text{C}-\text{N} \\   \\ \text{C} \end{array}$ (isomer mixture)	am.	148

<sup>a</sup> Am = amorphous.

The three methyl groups, which account for about 11.5 and 10.5% of the weight, eliminate crystallinity completely, both for the adipic acid-based aliphatic polyamide and the terephthalic acid-based aromatic-aliphatic polyamide.

A similar observation of reduced crystallinity caused by methyl side groups was noted by Yu and Evans (17), who find that the introduction of 2-methyl substituents in the 4,4' position in the heptanediamine yields an amorphous polyterephthalamide. The corresponding polyamide of

3,3'-dimethylhexamethylenediamine and terephthalic acid is not mentioned in the literature. In a du Pont patent (6) however, it is claimed in a generalized way, that polyamides of TPA and monomethyl- or dimethylhexamethylenediamines are suitable raw materials for fibers. Therefore, these should be expected to be crystalline.

A statistical ethylene-propylene copolymer with the ratio of 4 ethylene units to 3 propylene units (E.P. Rubber) has approximately the same degree of branching as the trimethyl nylon 6/6 of Table II.

The three methyl groups have no substantial influence on the glass temperature of our polyamides, but they do increase it a little even in the last sample in Table II despite the higher weight content of the aliphatic segment. In both cases we have three methyl side groups on 14 linear chain segments.

**Table III. Polyamides of TPA and Diamines with Different Structures and Similar Molecular Weights**

<i>Carbon Skeleton of Diamine</i>	$T_m, ^\circ\text{C.}$	$T_g, ^\circ\text{C.}$
—C—C—C—C—C—C—C—C—C—	371	115
<pre>       C       C                 —C—C—C—C—C—C—               C           </pre>	am.	150
<pre>       C         —C—C—C—C—C—C—C—               C           </pre>	am.	152
<pre>       C   C   C        \ / \ / \ /         C   C   C                            C   C   C          / \ / \ /         C   C   C           </pre>	am.	200

**Diamines of Equal Molecular Weight and Different Chain Structure.**

The branched diamines discussed previously have nine carbon atoms. Entirely different diamine structures can be built up from nine carbon atoms. Three products (diamines) with characteristically different carbon skeletons were available: an unbranched linear product (nonamethylenediamine), a branched product, (trimethylhexamethylenediamine), and a cycloaliphatic compound (IPD) with 10 carbon atoms. Polyamides

with terephthalic acid have been synthesized from all three diamines. The glass temperatures are listed in Table III. The product of Yu and Evans (17) is also included.

As expected, the arrangement of the carbon atoms in the diamine exerts a substantial influence on the crystallinity and the glass temperature. The unbranched linear diamine gives a crystalline product; the other diamines give amorphous polyamides. The diamine with the cycloaliphatic structure leads to products with obviously stiffened chains and thus relatively high glass temperatures. For comparison the polyamide of IPD and adipic acid has a  $T_g$  of 160°C. In this connection it would be interesting to study analogous polyamides having methyl substitution at the nitrogen instead of the carbon chain. We have not synthesized such products. However, they have been described by Shashoua and Eareckson (12) and by Saotome and Komoto (10). The authors do not state the glass temperatures in their publications.

**Influence of Aliphatic and Cyclic Structural Units.** The influence of cyclic structural units is evident from Tables II and III. Table II shows that replacing the adipic acid by terephthalic acid increases the melting point and the glass temperature by about 100°C. Table III shows that replacing the aliphatic chains by a cycloaliphatic chain of similar molecular weight increases the glass temperature by *ca.* 50°–100°C. Similar results are known from the polyester. We have listed some products in Table IV.

**Table IV. Polyesters of Ethylene Glycol and Dicarboxylic Acids**

	$T_m$ , °C.	$T_g$ , °C.
Adipic acid	50	–80
<i>trans</i> -Hexahydroterephthalic acid	64	25
Terephthalic acid	260	70–80
Naphthalene 1,4-dicarboxylic acid	170	64
Naphthalene 2,6-dicarboxylic acid	255	113

Here the differences in the melting temperatures and in the glass temperatures are even greater than in Tables II and III. Large differences are encountered on comparing a purely aliphatic polyester with a highly aromatic polyester (*cf.* Table V). A polyester of adipic acid and

**Table V. Aliphatic and Aromatic Polyesters**

<i>Dicarboxylic Acid</i>	<i>Diol</i>	$T_m$ , °C.	$T_g$ , °C.
Adipic acid	decanediol	71	–80
Adipic acid	bisphenol A	am.	63
Terephthalic acid	bisphenol A	315	200



decanediol has a glass temperature of *ca.*  $-80^{\circ}\text{C}$ . and a polyester of terephthalic acid and bisphenol A of about  $200^{\circ}\text{C}$ .

**Comparison of the Structural Units of Ester and Amide.** The effect of hydrogen bridges in polyamides has already been mentioned. For a more accurate demonstration of the influence of NH bridges, it would be necessary to compare polyamides with analogous high molecular weight ketones, which have a  $-\text{CH}_2$  unit instead of the NH chain link (Table VI). Such products are not yet described. Therefore, we have chosen the polyesters for comparison. These have an oxygen chain link instead of the NH chain link.

**Table VI. Structures of Aliphatic Chains**

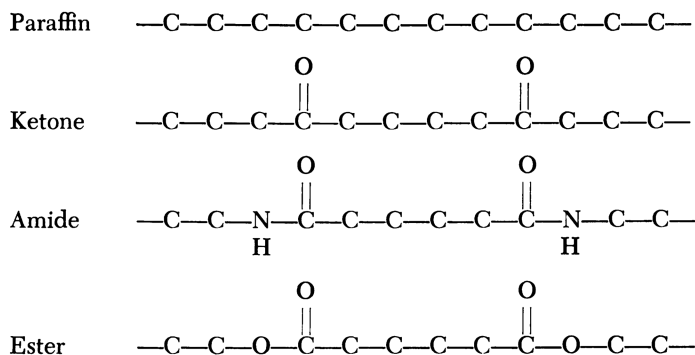


Table VII gives the  $T_g$  values of some polycondensation polymers, polyesters, and polyamides which we have synthesized.

For these polymers in Table VII the substitution of one oxygen link by one NH link per six chain members increases the glass temperature by  $100^{\circ}\text{C}$ . or more. The amide effect is much smaller when the subunits of the chains form very stiff molecules. This is true for polymers of high aromatic content. Thus, a polyamide of isophthalic acid (*m*-xylylenediamine) has a glass temperature of  $165^{\circ}\text{C}$ ., and a polyester of isophthalic acid (*m*-xylylene glycol) has a glass temperature of  $143^{\circ}\text{C}$ . (15). Here the difference in glass temperature is only slightly more than  $20^{\circ}\text{C}$ .

**Reverse Polyamides.** When using dicarboxylic acids and diamines of different carbon numbers—*e.g.*, C-6 dicarboxylic acid and C-10 diamine—products are obtained with melting points similar to a polyamide of C-6 diamine and C-10 dicarboxylic acid. Although no details are known, it can be assumed that the glass temperatures of these polyamides are similar. We have examined the problem with our amorphous partially aromatic polyamides, and we have synthesized and compared the following products shown in Table VIII.

**Table VII. Structures of Analogous Polyesters and Polyamides**

	<i>Dicarboxylic Acid</i>	<i>Diole or Diamine</i>	$T_m$	$T_g$
Polyester Polyamide	$C-C-C-C-C-C$	$C-C-C-C-C-C$	55 264	-70 50-57
Polyester Polyamide	$C-C-C-C-C-C$	$  \begin{array}{c}  C \quad C \\    \quad   \\  C-C-C-C-C-C \\    \\  C  \end{array}  $	am. am.	-70 65
Polyester Polyamide	$  \begin{array}{c}  C=C \\  / \quad \backslash \\  C-C \quad C-C \\  \backslash \quad / \\  C=C  \end{array}  $	$C-C-C-C-C-C$	148 371	45 140
Polyester Polyamide	$  \begin{array}{c}  C=C \\  / \quad \backslash \\  C-C \quad C-C \\  \backslash \quad / \\  C=C  \end{array}  $	$  \begin{array}{c}  C \quad C \\    \quad   \\  C-C-C-C-C-C \\    \\  C  \end{array}  $	am. am.	-15.-9 148

**Table VIII. Reverse Polyamides**

<i>Formula</i>	$T_g, ^\circ C.$
$  \begin{array}{c}  O \quad O \\     \quad    \\  -C \quad -C- \\    \quad   \\  \text{Benzene Ring} \quad \text{Benzene Ring} \\    \quad   \\  -C \quad -C- \\    \quad   \\  C \quad C  \end{array}  $	148
$  \begin{array}{c}  O \quad C \quad O \\     \quad   \quad    \\  -C \quad -C \quad -C- \\    \quad   \quad   \\  \text{Benzene Ring} \quad \text{Benzene Ring} \quad \text{Benzene Ring} \\    \quad   \quad   \\  C \quad C \quad C  \end{array}  $	125

There are real differences in  $T_g$  with this pair of reverse polyamides. We looked for further examples in the literature and found another pair given by Temin (15). In this example (Table IX) the differences are even larger than in our case.

Tables VIII and IX show that the position of the carbon-amide group is important. With both pairs of compounds, ours and the pair of Temin, higher glass temperatures of the polyamides are obtained if the carboxylic groups are attached to the ring. The products with the

Table IX. Reverse Polyamides

Formula	T <sub>g</sub>	Ref.
	130	15
	73	15
	(45-47)	10

methylene-amine group of the xylylenediamines have lower glass temperatures. For this phenomenon we have two explanations:

(1) The carbonyl groups in polyamides are fixed by hydrogen bonds. Polyamides with carbonyl groups at the ring form a larger compact bulk with six stiff chain links in the chain. For xylylenediamine the NH group is not fixed directly at the ring but is located at a methylene carbon, which in turn is attached to the ring. This methylene carbon will not be restricted in its flexibility by a hydrogen bridge; hence, there are only four rigid chain links.

(2) The carbonyl groups of terephthalic polyamides are in resonance with the ring. Therefore, they are less flexible than carbonyl group of aliphatic dicarboxylic acids. Xylylenediamine adipates don't have this resonance.

Table IX lists an additional substance, described by Saotome and Komoto (10). This polyamide is identical to one of the Temin polyamides, except for the substitution of the hydrogen at the NH group by a methyl group. Hence, this polyamide cannot form hydrogen bridges. Unfortunately, the glass temperature was not determined—only the softening point. Shashoua (12) described a similar product, a poly-

acid from terephthalic acid and *N,N'*-dimethylhexamethylenediamine. This product is crystalline, and its  $T_g$  is not given.

Table VII (polyester–polyamide) shows that in our series the polyamides have glass temperatures which are 100°C. or higher than those of polyester. Probably the differences of glass temperatures of 100°C. between polyamides and analogous polyesters are caused not only by the hydrogen bridges but also by polarity. It can be assumed that the polyamide with the *N*-methylamide structure (no H bridges) has a higher glass temperature than the analogous polyester.

Similar studies on reverse structures have been carried out by Goodman (9) on polyesters. He finds that products with carboxyl groups in the aromatic radical residue have higher crystalline melting points than the products with a reverse structure. However, he has studied only the crystalline melting points and not the glass temperatures. Thus, his particular investigation cannot be compared with ours. One must assume that the glass temperature is a more significant indication of mobility and flexibility of the macromolecules segments and of the forces between the macromolecules segments than the crystalline melting points. The latter is significant mainly for the degree of orientation and the crystalline forces.

In nylon 6 and nylon 6/6 practically all NH groups are bound by hydrogen bridges. In Trogamid T and other experimental samples there are many more free NH groups. However, the total free NH groups may be below 5% (3).

**Symmetry.** The influence which the geometrical and optical symmetry of the building units of polycondensation polymers exert on the structure of the macromolecules and the properties of the materials has been explored very little, and there are no studies available in our case. However, the diamine (TMD) used has an asymmetric structure and in addition an asymmetric carbon atom.

The 2,2,4- (or 2,4,4)-trimethylhexamethylenediamine has a head and a tail. Formally it can be incorporated into the chain according to principles known from vinyl polymers—*e.g.*, in a head-to-head arrangement to the dicarboxylic acid or head-to-tail arrangement. It is quite probable that our melt condensates have a statistical distribution of structure. The different reactivities of the two ends of the diamine may suggest that certain conditions could be visualized under which identical monomers can arrange to macromolecules of different structures. In addition to the modifications by the “head-tail” principle, the asymmetric carbon atom creates optical isomers, such as the *l* and the *d* form or a mixture of both.

Finally, our monomer TMD represents a mixture of two isomers, and the possibilities of the “head-tail” principle and of the *d,l* structure

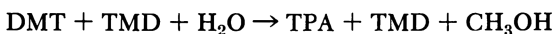
are true for each monomer. Trogamid T is indeed a copolyamide. Theoretically, many different block copolymers are available from our monomers.

### *Preparation of Amorphous-Aromatic-Aliphatic Polyamides*

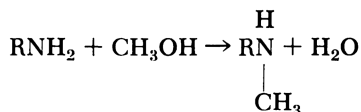
The approach through a melt condensation of the salt from the dicarboxylic acid and the diamine TMD has been studied primarily. There has been no systematic study of the approaches through interfacial polycondensation and solution polycondensation.

**Condensation via Terephthalic Acid.** The salt from the acid and the diamine is formed easily in the aqueous phase (8). Crystallization is effected by isopropyl alcohol addition. Recrystallization is unnecessary when pure starting components are used. The aqueous solution of the salt is heated under pressure, the solution water is distilled off, the condensation begins, the temperature is increased, and the pressure is lowered. The reaction is complete when the desired viscosity is reached.

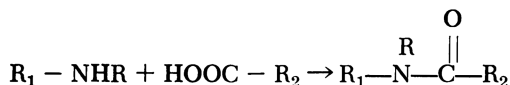
**Condensation via DMT.** Dynamit Nobel produces DMT but not terephthalic acid. Therefore, a process has been developed which starts directly from DMT:



Depending on the conditions, methylation of the amino group may take place to a certain extent:



In extreme cases it will be a dimethylation. It is desirable to operate in a way which ensures that little if any methylation reactions take place. A dimethylated product has a chain-terminating effect. Monomethylation leads to reduced reactivity and to a methylated amide group, which has no proton left for a hydrogen bridge



**Pilot Plant.** A schematic of the pilot plant is shown in Figure 1. In a first reactor the nylon salt is dissolved in water. The hot solution is transferred to Reactor 2. Here the polycondensation is performed to the desired degree. The final viscosity of the melt is in the range of 100,000 poises at 250°C. The hot melt is removed from the reactor, chilled, and pelletized. The molecular weight of the commercial product is around 20,000.

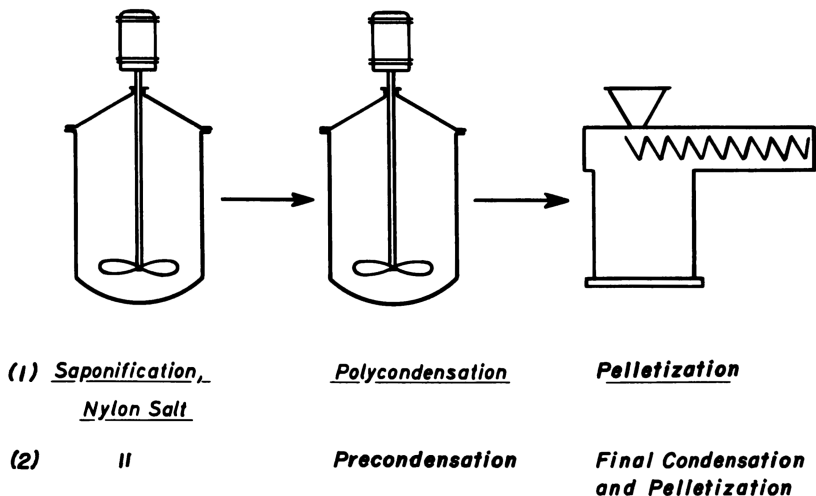
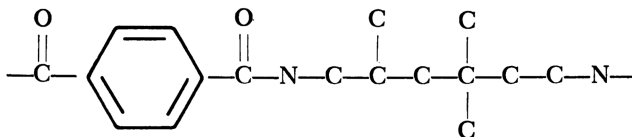


Figure 1. Production of Trogamid T by two methods

**Semicommercial Plant.** In the semicommercial plant only the first stage of the condensation is carried out in a reaction vessel with stirrer. The second phase of final condensation and granulation takes place in an extruder. (This stage of the process has been developed in our company by M. Wienand and K. Jensen.) To ensure a fully continuous operation, either two precondensers operating alternatively or a precondensator and one intermediate vessel are employed.

### Properties of Trogamid T

Following a discussion of the influence exerted by the various structural elements on the glass temperature, a more detailed discussion is now given of the product which is produced from DMT and a mixture of 2,2,4- and 2,4,4-trimethylhexamethylenediamine (Scholven Chemie) and has the formula:



This product was first reported in 1966 (4). Since then, knowledge has been widened through the studies of W. Pungs and J. Schneider. Here only a general characterization is given. Contrary to the classical nylons, Trogamid is a clear material, similar to polycarbonate.

**Mechanical Properties.** Trogamid T has high tensile strength, high stiffness, and medium notched impact strength. Under normal test conditions in air Trogamid T undergoes no stress corrosion. The dimensional stability under load is good.

**Thermal Properties.** Trogamid T has a glass temperature similar to that of polycarbonate. A molded and quickly quenched sample has a lower glass temperature than an annealed one. Obviously, annealing brings some order without creating crystallinity. The quenched and annealed samples may differ as to the extent of their hydrogen bridging. This subject has not been studied so far.

The expansion coefficient is also similar to that of polycarbonate, and the same is true for the torsional modulus *vs.* temperature as shown in Figure 2. Trogamid T has a good tensile strength (*ca.* 500 kg.) even at temperatures as high as 100°C.

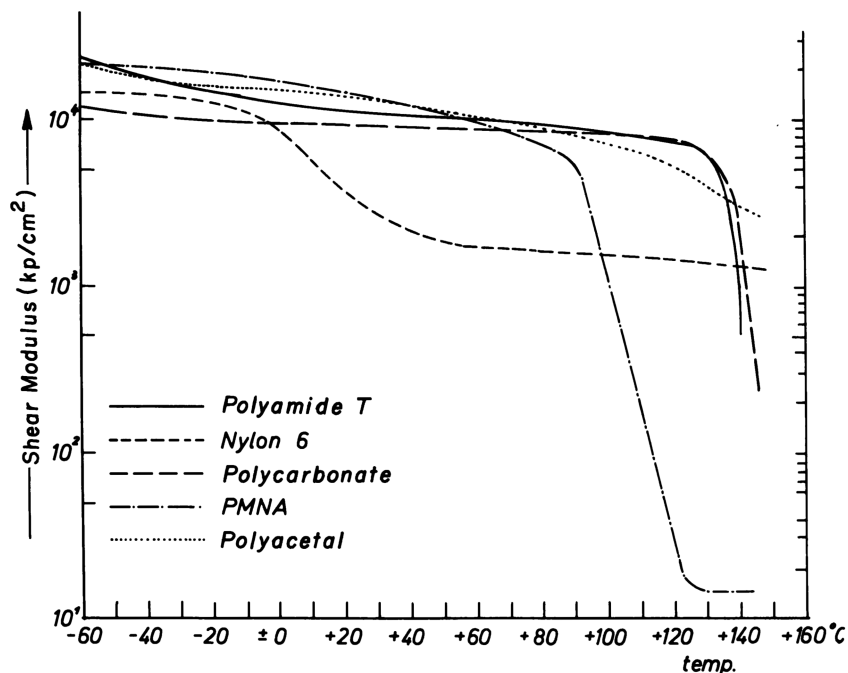


Figure 2. Torsional modulus *vs.* temperature

**Electrical Properties.** In its electrical insulating properties Trogamid T is similar to other polyamides. Its dielectric properties are not particularly striking. The electrical properties undergo slight change in relation to humidity, and prolonged water immersion has no appreciable

influence. Frequency has little effect on the dissipation factor and on the dielectric constant. The tracking resistance is good.

**Behavior in Water and Aqueous Solutions.** Like all polyamides Trogamid T absorbs water when stored in humid air or immersed in water. This absorption, however, is lower than that of nylon 6 and nylon 6/6 (Figure 3 and Table X).

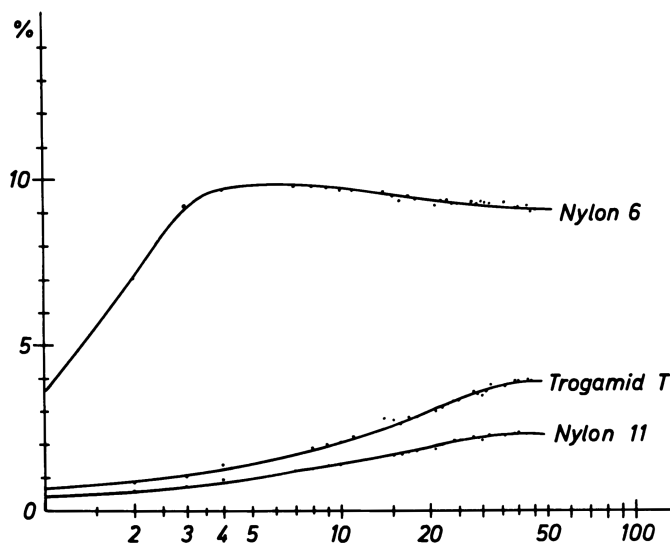


Figure 3. Water absorption in liquid water

Table X. H<sub>2</sub>O Absorption from Air

	Trogamid T	Nylon 6	Poly- acetal	Polycar- bonate	Poly- MM Ester
Water absorption from air, 65% humidity mg./gram	40	210	20	10	30

Moisture absorption affects the properties only to a small extent. However, the swelling ratio from water related to the absorbed water is smaller than for other polyamides.

In the different polyamides the absorbed water has the following apparent density: nylon 6 = 0.86, Rilsan = 0.72, Trogamid = 0.67. Immersion in water up to 80°C. has little influence on the properties. In boiling water, however, turbidity is observed, and this is especially evident in a thin film. An alkaline pH adjustment of the hot water reduces this phenomenon. The turbidity is not accompanied by degradation. Dried turbid material can be processed to clear specimen. Electronic



microscopic pictures of a Trogamid T sample, which had been heated in boiling water for many hours and had become turbid, show small punctures in the surface. Working with the crystalline polyterephthalate of linear diamines (and *N*-methylated diamines) Shashoua and Eareckson (12) have found higher water absorption data than we did with our amorphous polyamide from terephthalic acid and branched diamine. It is known from the literature of the classical polyamides, that the amorphous portions account for the water absorption. Thus, one would expect higher water absorption by the amorphous Trogamid T than by the crystalline polyamides of Shashoua and Eareckson, but it is just the reverse. However, the samples were different. Shashoua used fibers precipitated from solution, and we tested molded samples. Maybe the preparation of the samples influenced the water absorption.

**Behavior toward Organic Materials.** Trogamid T is soluble in some phenols, formic acid, dimethylformamide and in certain chloroform-methanol mixtures. Trogamid T undergoes swelling in lower aliphatic alcohols. Prolonged exposure to these alcohols leads to environmental stress corrosion. The resistance to lower ketones is limited. Trogamid T is resistant to ethers, esters, trichloroethylene, methylchloroform, carbon tetrachloride, hydrocarbons, oils and fats from mineral, vegetable, and animal sources, and PVC plasticizers and shows no stress corrosion.

**Behavior toward Gases.** Behavior toward gases is important in packaging applications. Table XI shows the permeability as compared with some other materials used for packaging.

Table XI. Gas Permeability

	$H_2O$ grams/cm. hr. torr $6 \times 10^{-9}$	$O_2$ cm. <sup>3</sup> /cm. sec. cm. Hg $\times 10^{12}$	$CO_2$ cm. <sup>3</sup> /cm. sec. cm. Hg $\times 10^{12}$
Polyethylene	0.6-1	100-120	400-450
Polypropylene	1.4-1.6	80-100	320-350
PVC	7-9	4-5	10-12
Nylon 6	20-40	6-8	40-50
Polyester	4-4.5	1.5	8-9
Polycarbonate	30-50	500	1500
Trogamid T	6	4	7

### Processing and Uses of Trogamid T

Trogamid T can be processed without difficulty by the normal methods used for thermoplastics (5). In this respect it offers fewer problems than polyacetal or polycarbonate, for example. Some Trogamid T properties can be improved by biaxial orientation. The effects, however, are lower than with crystalline polymers.

Trogamid T has low mold shrinkage and good dimensional stability. The weldability which is very good offers an obvious advantage over the crystalline polyesters and polyamides.

Mechanical properties (stiffness, impact, and shock resistance), electrical properties, clarity, ease of processing, sealing properties, dimensional stability, resistance to hydrocarbons and other organic liquids, resistance to plasticizers, greases, and oils are the characteristic properties desired. In its mechanical properties it approaches polycarbonate most closely. However, since polycarbonate is cheaper than Trogamid T, Trogamid T will be preferred only where polycarbonate cannot be used.

Typical applications for Trogamid T are flow meters or flow meter parts for gases and liquids, containers, parts in electrical equipment and appliances, optical equipment, measuring devices, printing machines.

### *Literature Cited*

- (1) Askadskii, A. A., *Polymer Sci. USSR* **9**, 471 (1967).
- (2) Beaman, R. G., *J. Appl. Polymer Sci.* **9**, 3949 (1965).
- (3) Bessler, E., Bier, G., *Makromol. Chem.* **122**, 30 (1969).
- (4) Cramer, F. B., Beaman, R. G., *J. Polymer Sci.* **21**, 237 (1956).
- (5) Doffin, H., Pungs, W., Gabler, R., *Kunststoffe* **56**, 542-546 (1966).
- (6) Du Pont, Magat, E. E., U. S. Patent **2,752,328** (1956).
- (7) Du Pont, Sweeny, W., U. S. Patent **3,287,324** (1966).
- (8) Gabler, R., Müller, H., Ashby, G. E., Agouri, E. R., Meyer, H-R., Kabas, G., *Chimia* **21**, 2, 65 (1967).
- (9) Goodman, I., *Angew. Chem.* **74**, 606 (1962).
- (10) Saotome, K., Komoto, H., *J. Polymer Sci. Pt. A1*, **5**, 107 (1967).
- (11) Schnell, H., *Angew. Chem.* **68**, 633 (1956).
- (12) Shashoua, V. E., Eareckson, W. M., *J. Polymer Sci.* **40**, 343-358 (1959).
- (13) Sokolov, L. B. *et al.*, *Plastičeskie Massy* **9**, 21 (1967).
- (14) Staudinger, H., *Ber.* **53**, 1073 (1920).
- (15) Temin, C. S., *J. Appl. Polymer Sci.* **9**, 471 (1965).
- (16) Whinfield, I. R., Dickson, J. T., British Patent **578,079** (1946).
- (17) Yu, A. J., Evans, R. D., *J. Polymer Sci.* **42**, 249 (1960).

RECEIVED March 18, 1968.

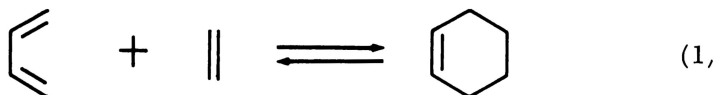
## The Diels-Alder Reaction in Polymer Synthesis

J. K. STILLE, F. W. HARRIS, H. MUKAMAL, R. O. RAKUTIS,  
C. L. SCHILLING, G. K. NOREN, and J. A. REED

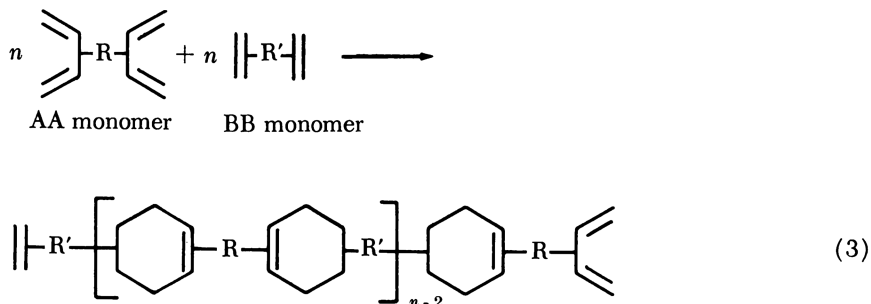
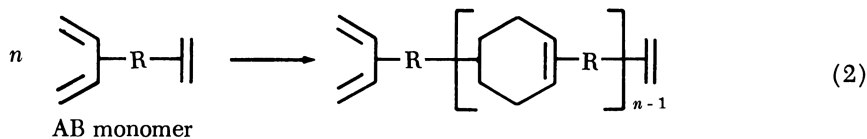
University of Iowa, Iowa City, Iowa 52240

*The synthesis of high molecular weight polymers through the Diels-Alder step-growth reaction has been investigated for the preparation of polyimides and polyphenylenes. The reaction of bicyclopentadienones with bismaleimides affords high molecular weight, soluble polyimides while the same reaction of the cyclopentadienones with diacetylenes produces colorless, soluble, phenylated polyphenylenes of high molecular weight and in quantitative conversions. The polymers are amorphous, form clear films, and are stable in air to 550°C. The reaction of bis-2-pyrones with the diacetylene dienophile also has been shown to give polyphenyls.*

The well-known 1,4-cycloaddition reaction of a 1,3-diene to a dienophile which forms a six-membered adduct, commonly known as the Diels-Alder reaction, or diene synthesis, is established as a useful synthetic organic reaction. Although this reaction provides a high yield of



adduct in certain cases, there are few reported syntheses of polymers which use it as a step-growth reaction (21). In theory, this polymerization reaction should be successful if a monomer which contains both the diene and dienophilic portions were subjected to the polymerization conditions. Alternatively, high molecular weight polymer should be obtained from the reaction of equimolar amounts of a bisdiene with a bisdienophile.

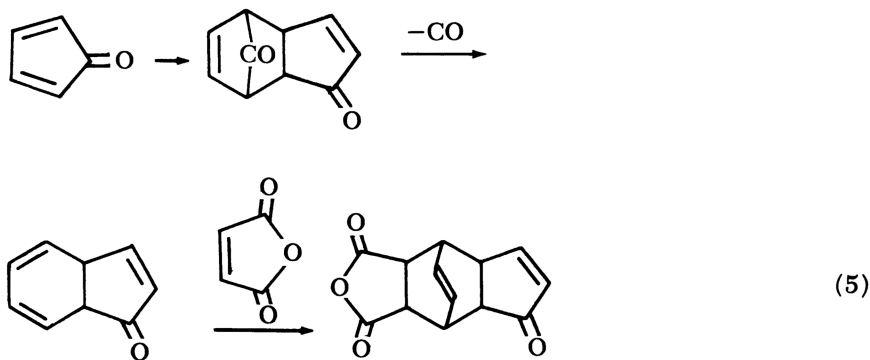
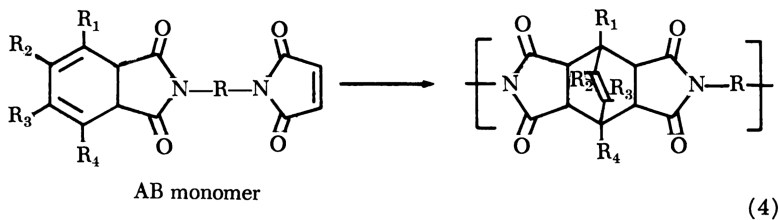
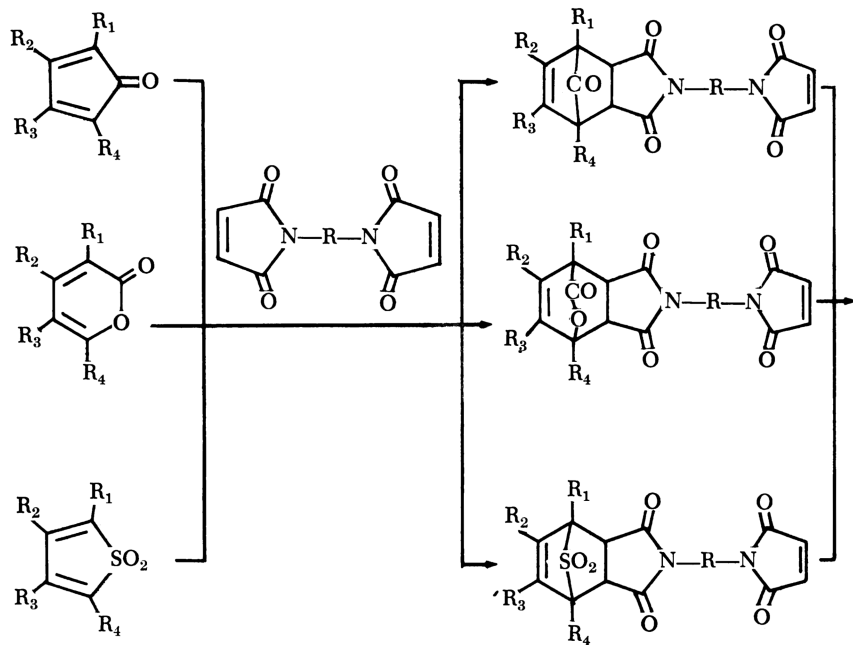


Not many high molecular weight polymers have been obtained from this reaction, however. In most cases, failure can be attributed to the reversal of the diene synthesis (23) (Reaction 1), a high frequency of side reactions, such as chain-growth polymerization of the diene (23, 25), or the insolubility of the rigid, ring-containing polymer which removes it from the reaction medium (3).

The most successful polymerizations carried out by using a Diels-Alder step-growth reaction are those which generate a highly reactive A-B monomer *in situ* by the reaction of a bismaleimide with cyclopentadienone (12), 2-pyrone (6, 13), or thiophene dioxide (5) derivatives. The intermediate 1:1 adduct loses carbon monoxide, carbon dioxide, or sulfur dioxide, respectively, all to generate the same type of reactive AB monomer, which is converted rapidly to polymer. High molecular weight polymers are obtained (Reaction 4).

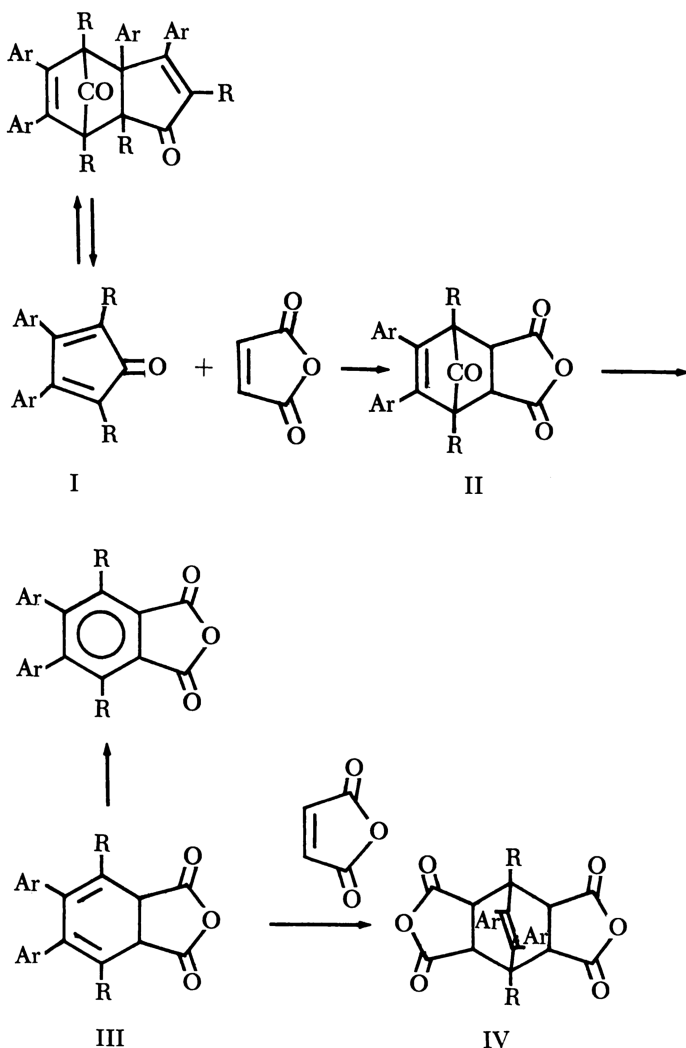
### *Cyclopentadienones*

Cyclopentadienones can undergo a variety of Diels-Alder reactions, depending on the substitution on the cyclopentadiene ring, the dienophile, and the reaction conditions (17). In general, cyclopentadienones containing up to two substituents, and in certain cases three substituents, are highly reactive and spontaneously form a "non dissociating" dimer (2) through a self-Diels-Alder reaction. Therefore, the reactions of these cyclopentadienones with dienophiles are Diels-Alder reactions of the dimer with the accompanying loss of carbon monoxide (Reaction 5).



Other trisubstituted and certain tetrasubstituted cyclopentadienones are not as self-reactive and form "dissociating dimers" in solution. The cycloaddition chemistry of these cyclopentadienones is that of the cyclo-

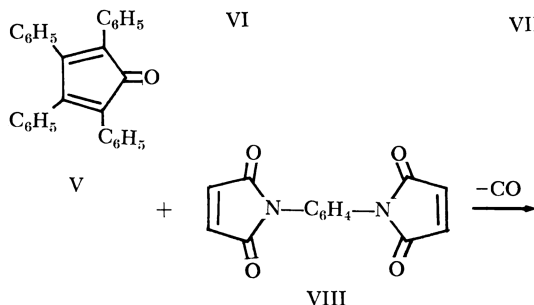
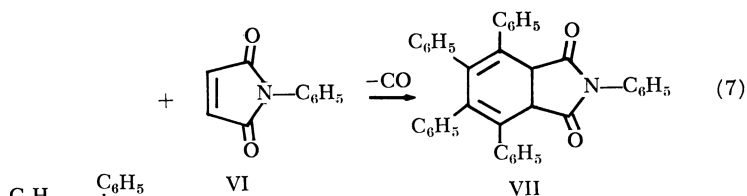
pentadienone monomer. Other tetrasubstituted cyclopentadienones exist only as monomers and also exhibit cycloaddition reactions as such. The difference in reactivity of the trisubstituted (“nondissociating” *vs.* “dissociating dimer”) and the tetrasubstituted (“dissociating dimer” *vs.* monomer) cyclopentadienones can be ascribed usually to steric and/or electronic effects. Tetrasubstituted “dissociating dimers” are those which contain small alkyl groups in the 2- and 5- positions (I, R = CH<sub>3</sub>) or contain alkyl groups in these positions which are not severely buttressed by Ar (*e.g.*, both Ar groups in I represented by the 1,8-naphthyl moiety).



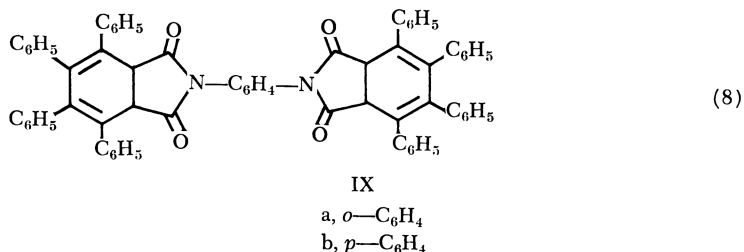
(6)

It is the reaction of the "dissociating dimer" or monomer that is of most interest in polymerization. Whether or not Reaction 6 proceeds to afford products II, III, or IV depends on the dienophile, the diene, and the reaction conditions. Cyclopentadienones which are "dissociating dimers" can be driven to IV in most cases by the appropriate dienophile at elevated temperatures. This is, in fact, the course of the polymerization reaction shown in Reaction 4. Monomeric cyclopentadienones, on the other hand, will often stop at the intermediate III, even under quite severe conditions. It is this reaction stage that is of particular interest to us for the study of Diels-Alder step-growth polymerizations.

**Polyimides.** The reaction of tetraphenylcyclopentadienone (V) (17) with *N*-phenylmaleimide (VI) in refluxing  $\alpha$ -chloronaphthalene (263°C.) for 1.5 hours or refluxing, 1,2,4-trichlorobenzene (213°C.) for 18 hours provides a quantitative yield of adduct VII (Reaction 7). Similarly, V reacts with *N,N'*-*o*- and *p*-phenylenebismaleimide (VIIIa,b) (8) to afford the diadducts IXa,b (Reaction 8).

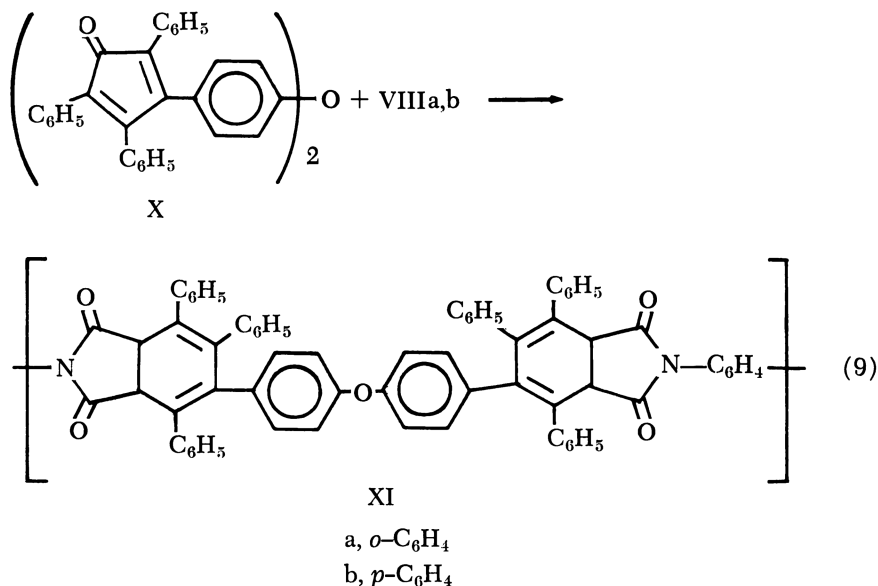


a, *o*-C<sub>6</sub>H<sub>4</sub>  
b, *p*-C<sub>6</sub>H<sub>4</sub>



IX  
a, *o*-C<sub>6</sub>H<sub>4</sub>  
b, *p*-C<sub>6</sub>H<sub>4</sub>

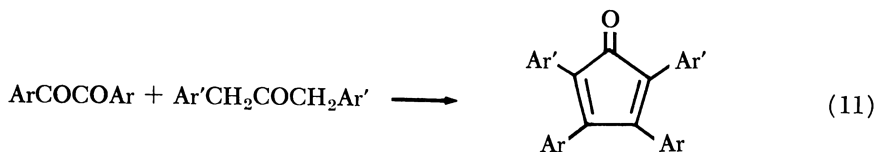
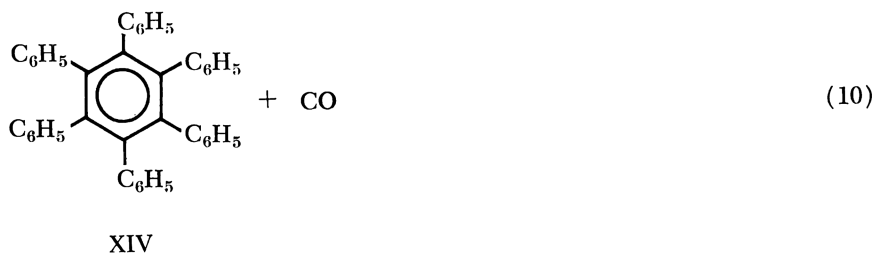
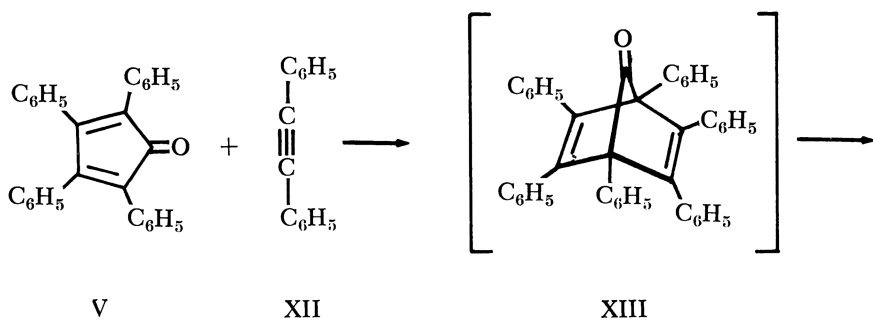
The analogous reactions of VIIIa,b with 3,3'-(oxydi-*p*-phenylene) bis(2,4,5-triphenylcyclopentadienone) (X) give the corresponding polyimides (XIa,b) in quantitative conversions (Reaction 9). Polymer XIb, obtained from the *p*-phenylenebismaleimide (VIIIb) reaches an intrinsic viscosity of 1.01 in 4 hours in refluxing 1,2,4-trichlorobenzene, while XIa attains an intrinsic viscosity of only 0.33 after 24 hours under the same conditions. Apparently there is considerable steric hindrance in the case of the *o*-isomer, and the result is a series of sharp kinks in the polymer chain. Polymer XI is soluble in DMF and forms clear, slightly yellow films. The polymer dehydrogenates slowly at elevated temperatures or more rapidly with chemical dehydrogenation reagents to form the totally aromatic polyimide.



**Polyphenyls.** Another means of carrying the cyclopentadienone Diels-Alder reaction to the monoadduct stage (III, Reaction 6) is to use an acetylenic dienophile and obtain a product which is no longer a diene but an aromatic. The reaction of tetraphenylcyclopentadienone (V) with diphenylacetylene (XII) affords hexaphenylbenzene (XIV) by loss of carbon monoxide from the intermediate adduct XIII (Reaction 10). In certain cases the intermediate adduct XIII can be isolated.

The preferred route to the synthesis of tetraarylated cyclopentadienones is the base-catalyzed condensation of benzils with benzyl ketones (Reaction 11) (17).

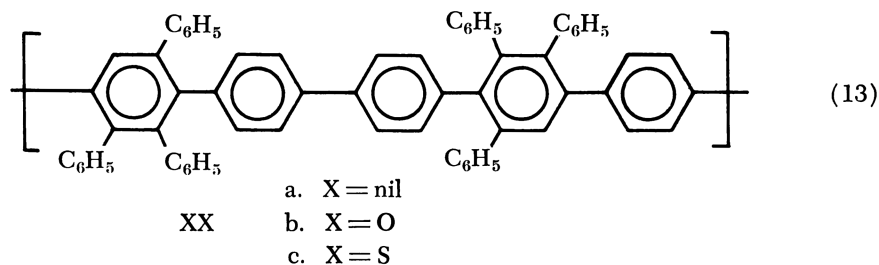
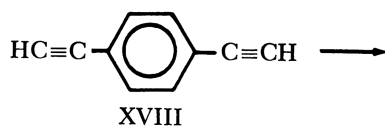
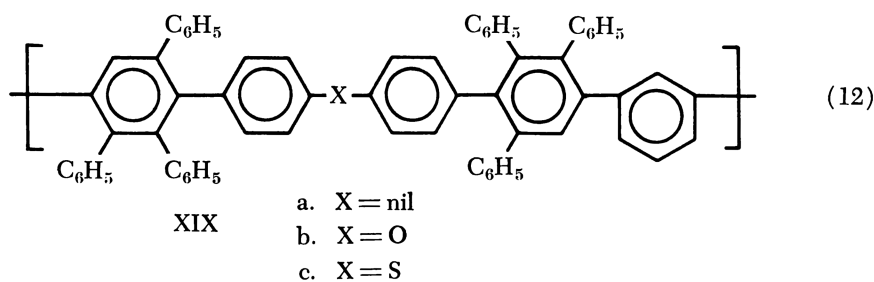
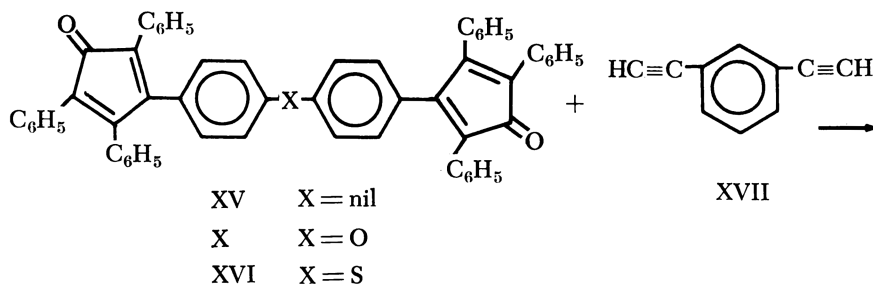




Of particular interest to the formation of polymers is the fact that many bistetracyclones have been synthesized by this method (17, 18). The reaction of bistetracyclones X, XV, and XVI with *m*- and *p*-diethynylbenzene (XVII and XVIII) in toluene at 225°C. for 24 hours, afforded the phenylated polyphenyls XIX and XX in quantitative conversions (16, 19, 22).

Molecular weights of 30,000–60,000 could be obtained. The polymers showed outstanding thermal stability (TGA 550°C. break, air or nitrogen), are all soluble in common organic solvents (up to 15 wt. %), form clear films, are colorless, and amorphous. The thermal decomposition of these polymers has been shown to take place by the loss of pendant phenyl groups as phenyl radicals. Thus, the thermal treatment of a film under nitrogen produces a crosslinked film which is still amorphous but insoluble; no appreciable main chain degradation takes place.

To achieve proper monomer balance, the monomers were purified with great care. The stoichiometry needed to achieve the highest molecular weight polymer (Table I) required 1% excess of bistetracyclone. This suggests either that there were impurities in the bistetracyclone that



escaped detection in chromatography or that some side reaction upset monomer balance.

Severe polymerization conditions (350°C., 48 hours), in fact, gave lower molecular weight polymers ( $[\eta] = 0.1$ ) and a small amount of black, insoluble precipitate. These results suggest that there was considerable degradation which interfered with monomer balance. Such

degradation reactions at elevated temperatures are known for many tetracyclones (17).

**Table I. Effect of Monomer Balance on Molecular Weight (Polymer XXb)**

Mole Ratio X:XVIII	$[\eta]$ , dl./gram <sup>b</sup>	$\bar{M}_n \times 10^{-4}$ <sup>a</sup>
1.02	0.61	3.6
1.01	0.64	4.1
1.00	0.58 <sup>c</sup>	2.9
0.98	0.38	1.9

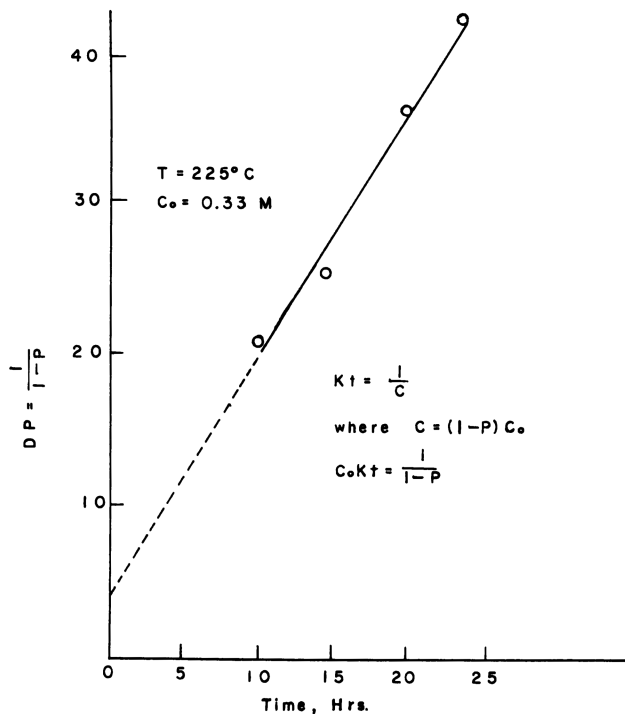
<sup>a</sup> At a concentration of 0.08M for each monomer.

<sup>b</sup> Taken at 25°C. in toluene.

<sup>c</sup> Obtained with a Hewlett-Packard high speed membrane osmometer using a superdense membrane at 29.5°C. in toluene.

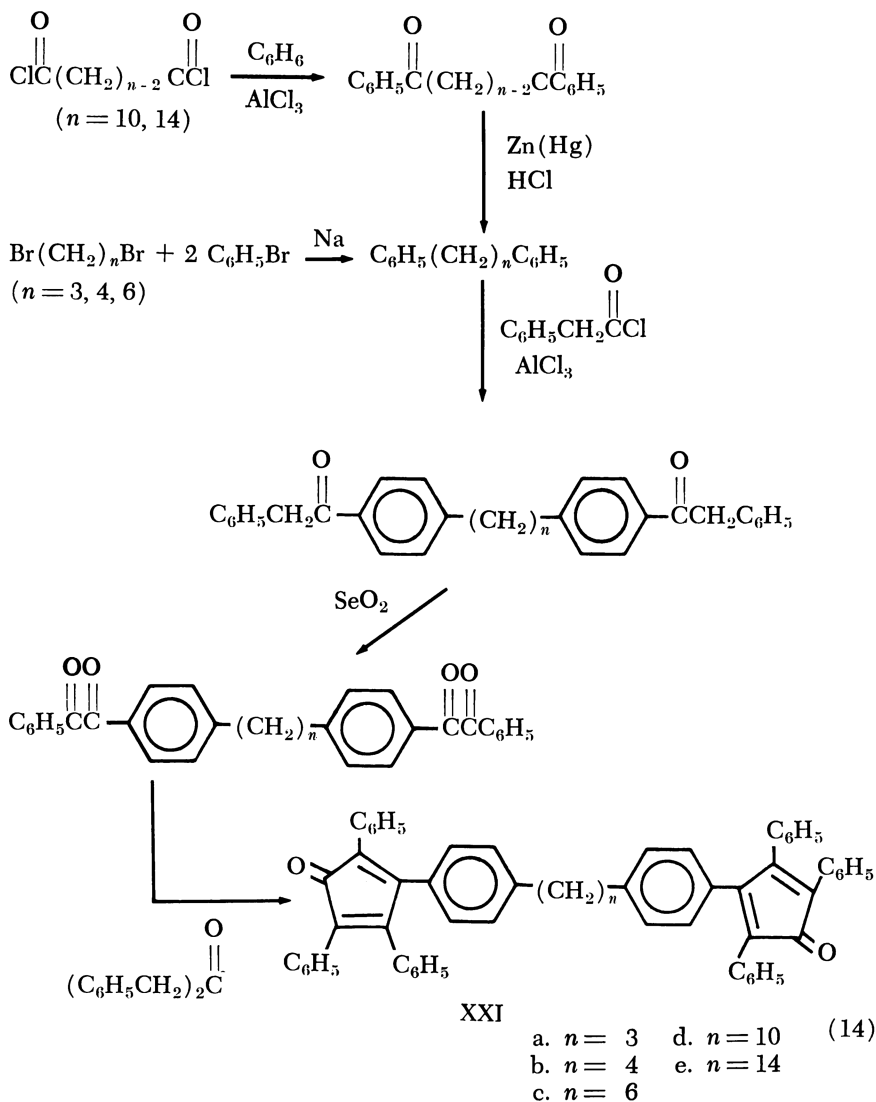
<sup>d</sup> When this reaction was run with a concentration of 0.01M for each monomer, the viscosity was 0.16.

The polymerization reaction is typical of step-growth reactions in that it follows second-order kinetics for the reaction of tetracyclone ends with acetylene ends (Figures 1 and 2).



*Figure 1. Reaction of X and XVIII (time vs. DP)*

In addition, several bistetracyclones linked by methylene units have been synthesized according to the scheme shown in Reaction 14.



The polymerization reactions of bistetracyclone monomers XXIa-e with both *m*- and *p*-diethynylbenzene (XVII and XVIII) produced a series of polymers (XXII, Reaction 15) containing short blocks of phenylene units connected by methylene chains. High molecular weight polymers were obtained (Table II), and a range of physical properties was observed.

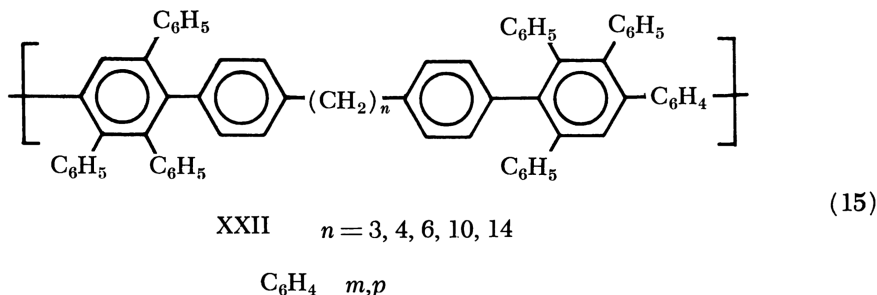
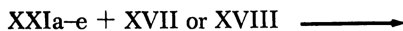


Table II. Polymer XXII

Polymer	$[\eta]^a$	$\bar{M}_n^b$
$\text{C}_3$ <i>m</i> -	0.35	46,500
<i>p</i> -	0.55	59,000
$\text{C}_4$ <i>m</i> -	0.61	58,400
<i>p</i> -	0.77	42,600
$\text{C}_6$ <i>m</i> -	0.71	56,800
<i>p</i> -	1.51	63,400
$\text{C}_{10}$ <i>m</i> -	0.60	48,500
<i>p</i> -	1.30	50,500
$\text{C}_{14}$ <i>m</i> -	0.48	31,300
<i>p</i> -	0.77	32,700

<sup>a</sup> Intrinsic viscosities in toluene at 25°C.

<sup>b</sup> Obtained with a Hewlett-Packard high speed membrane osmometer using a superdense membrane at 30°C. in toluene.

### 2-Pyrones

The Diels-Alder reaction of 2-pyrones has been used in polymer syntheses (6, 13) (Reaction 4). In these reactions the 2-pyrone is difunctional in that it consumes two moles of dienophile (Reaction 16). A practical way of stopping at the 1:1 adduct is to use an acetylenic monomer (24) (Reaction 17). Although 2-pyrone itself polymerizes on standing (1), phenyl-substituted 2-pyrones, including monophenyl 2-pyrones, are stable at ordinary temperatures.

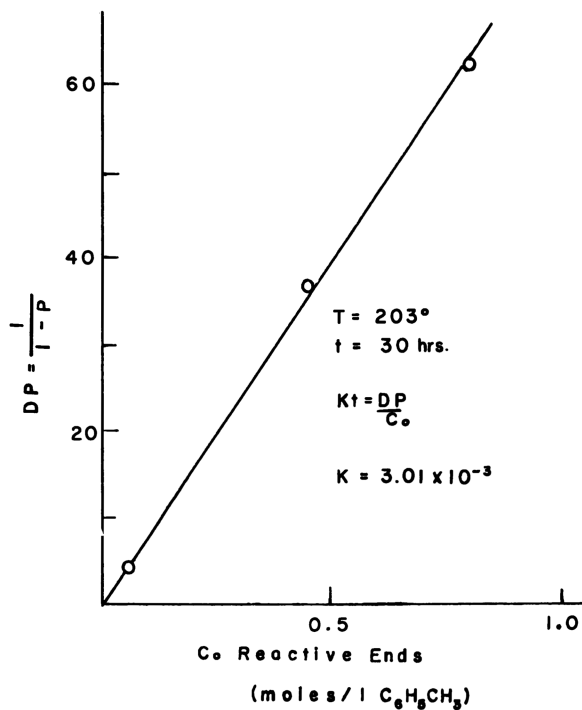
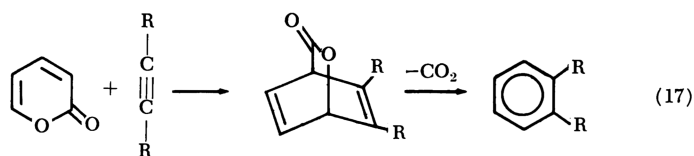
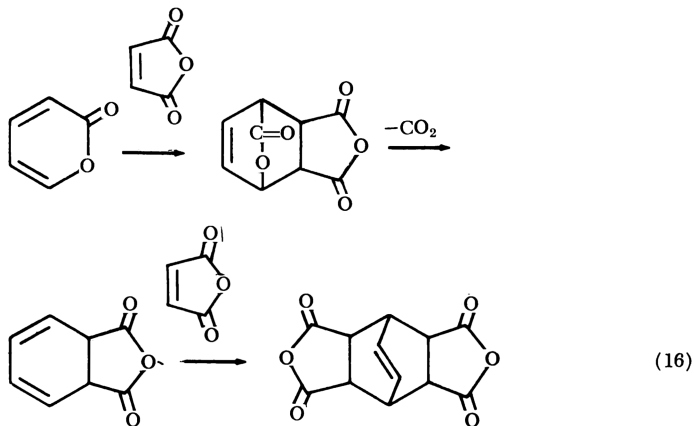
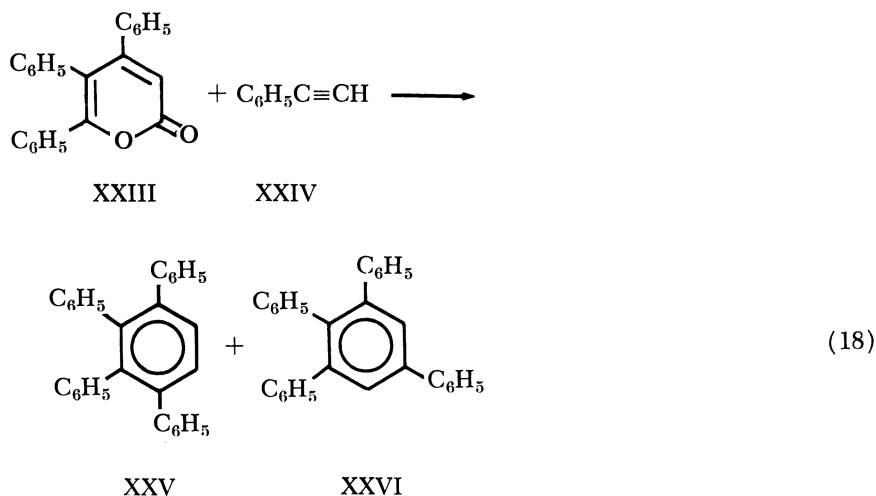


Figure 2. Reaction of X and XVIII (Co vs. DP)

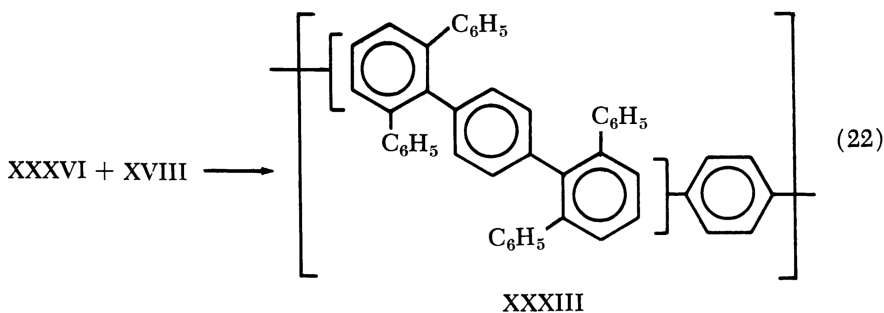
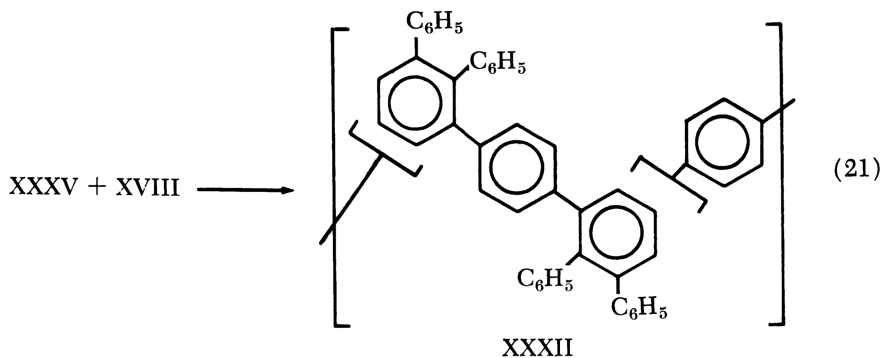
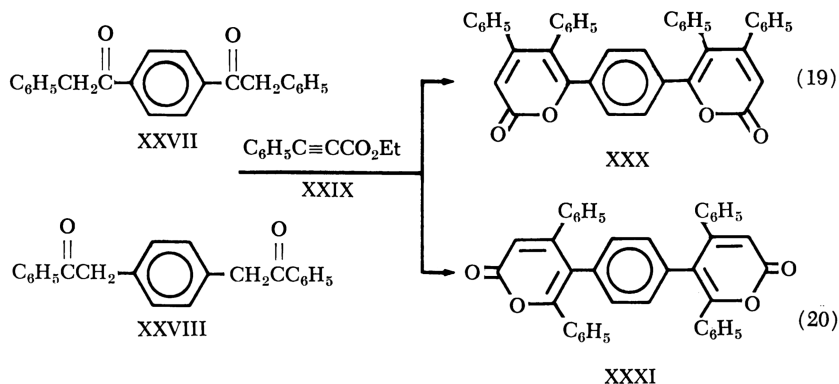
Since the thermal degradation in phenylated polyphenyls of the type XXa is caused by the loss of pendant phenyl groups, and since the reported (4, 7, 9, 10, 11, 14, 15) properties of *p*-polyphenylenes are quite different from those of XXa, the synthesis of an unphenylated polyphenylene by this pathway was of considerable significance. Only a few results employing this reaction have thus far been obtained. [The *p*-polyphenylenes reported are black or brown, insoluble, crystalline materials of lower thermal stability than XXa.]

If the diene fragment of the 2-pyrone and the acetylene dienophile are unsymmetrically substituted, the formation of two isomeric benzene products is possible. The model reaction between 4,5,6-triphenyl-2-pyrone (20) (XXIII) and phenylacetylene yields approximately equal amounts of 1, 2, 3, 4- (XXV) and 1,2,3,5-tetraphenylbenzene (XXVI). Therefore, this position isomerism would be expected to materialize during polymer formation when similar bispyrone monomers are polymerized with diethynylbenzene.



Bis-2-pyrones XXX and XXXI were prepared by utilizing the base-catalyzed Michael addition of bisdesoxybenzoins XXVII and XXVIII to ethyl phenylpropionate (XXIX) (20) (Reactions 19 and 20).

The polymerization of the bispyrones XXX and XXXI with *p*-diethynylbenzene (XVIII) in toluene at 225°–300°C. for 20–48 hours produced both soluble and insoluble fractions of polymers XXXII and XXXIII (Reactions 21 and 22). The soluble portions were only relatively low molecular weight ( $[\eta] = 0.1$ ). These materials did show the same excellent thermal stability as exhibited by the polyphenyls of type XIX and XX.



Hopefully, this type of synthesis will provide a *p*-polyphenylene of unquestionable structure so that its physical properties might be studied.

Although the utilization of the Diels-Alder synthesis as a step-growth reaction for polymerization requires, in most cases, rather unusual monomers, an occasional lengthy and trying synthesis, torturous purifications, and, in certain cases, difficult reaction conditions, it does afford high



molecular weight polymers with interesting and unusual structures which are not attainable by other means.

### *Acknowledgment*

This work was supported by the U. S. Army Research Office, Durham, N. C.

### *Literature Cited*

- (1) Albert, A., "Heterocyclic Chemistry," p. 268, Essential Books, Fair Lawn, N. J., 1959.
- (2) Allen, C. F. H., Van Allan, J. A., *J. Am. Chem. Soc.* **72**, 5165 (1950).
- (3) Bailey, W. J., Economy, J., Hermes, M. E., *J. Org. Chem.* **27**, 3295 (1962).
- (4) Cassidy, P. E., Marvel, C. S., Ray, S., *J. Polymer Sci. Pt. A*, **3**, 1553 (1965).
- (5) Chow, S-W., U. S. Patent **2,971,944** (Feb. 14, 1961).
- (6) *Ibid.*, **3,074,915** (Jan. 22, 1963).
- (7) Frey, D. A., Hasegawa, M., Marvel, C. S., *J. Polymer Sci. Pt. A*, **1**, 2057 (1963).
- (8) Kovacic, P., Hine, R. W., *J. Am. Chem. Soc.* **81**, 1187 (1959).
- (9) Kovacic, P., Hoppe, R. J., *J. Polymer Sci. Pt. A-1*, **4**, 1445 (1966).
- (10) Kovacic, P., Itsu, L. C., *J. Polymer Sci. Pt. A-1*, **4**, 5 (1966).
- (11) Kovacic, P., Marchionna, V. J., Koch, F. W., Oziomek, J., *J. Org. Chem.* **31**, 2467 (1966).
- (12) Kraiman, E. A., U. S. Patent **2,890,206** (June 9, 1959).
- (13) *Ibid.*, **2,890,207** (June 9, 1959).
- (14) Lefebvre, G., Dawans, F., *J. Polymer Sci. Pt. A*, **2**, 3277 (1964).
- (15) Marvel, C. S., Hartzell, G. E., *J. Am. Chem. Soc.* **81**, 448 (1959).
- (16) Mukamal, H., Harris, F. W., Stille, J. K., *J. Polymer Sci. Pt. A-1*, **5**, 2721 (1967).
- (17) Ogliaruso, M. A., Romanelli, M. G., Becker, E. I., *Chem. Rev.* **65**, 261 (1965).
- (18) Ogliaruso, M. A., Shadoff, L. A., Becker, E. I., *J. Org. Chem.* **28**, 2725 (1963).
- (19) Reid, W., Freitag, D., *Naturwiss.* **53**, 306 (1966).
- (20) Ruheman, S., *J. Chem. Soc.* **97**, 459 (1910).
- (21) Stille, J. K., *Fortschr. Hochpolym. Forsch.* **3**, (1), 48 (1961).
- (22) Stille, J. K., Harris, F. W., Rakutis, R. O., Mukamal, H., *J. Polymer Sci. Pt. B*, **4**, 791 (1966).
- (23) Stille, J. K., Plummer, L., *J. Org. Chem.* **2**, 4026 (1961).
- (24) Shusherina, U. P., Dmitrieva, U. D., Luk'ianets, E. A., Levina, R. A., *Usp. Khim.* **36**, 437 (1967).
- (25) Upsom, R. W., U. S. Patent **2,776,232** (Dec. 6, 1955).

RECEIVED April 8, 1968.

## Recent Advances in the Vapor Deposition Polymerization of *p*-Xylylenes

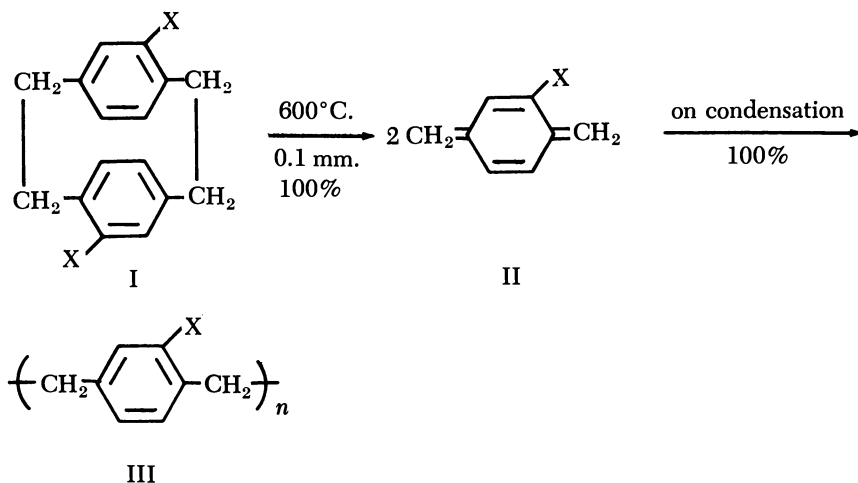
WILLIAM F. GORHAM

Union Carbide Chemicals and Plastics, Research and Development Department,  
P.O. Box 670, Bound Brook, N. J. 08805

*The process for preparing linear poly-p-xylylenes by pyrolytic polymerization of di-p-xylylenes has been extended to include the formation of p-xylylene copolymers. Pyrolysis of mono-substituted di-p-xylylenes or of mixtures of substituted di-p-xylylenes results in formation of two or more p-xylylene species. Copolymerization is effected by deposition polymerization on surfaces at a temperature below the threshold condensation temperature of at least two of the reactive intermediates. Random copolymers are produced. Molecular weight of polymers produced by this process can be controlled by deposition temperature and by addition of mercaptans. Unique capabilities of vapor deposition polymerization include the encapsulation of particulate materials, the ability to replicate very fine structural details, and the ability of the monomers to penetrate crevices and deposit polymer in otherwise difficultly accessible structural configurations.*

**A** new general synthetic method for preparing linear poly-*p*-xylylenes was reported recently (6, 7, 8, 9, 10, 11, 13). This new method involves the vacuum pyrolysis of di-*p*-xylylene or substituted di-*p*-xylylenes at temperatures of 600°–700°C. to form *p*-xylylenes and the subsequent condensation and spontaneous polymerization of these reactive species to form a family of linear polymers. The over-all reaction scheme is illustrated at the top of p. 644.

This process was shown to be general, and a large family of substituted poly-*p*-xylylenes prepared in which X equals hydrogen, halogen, alkyl, cyano, ester, acyl, and other groupings. Advantages of this process (6, 7, 8, 9, 10, 11, 13) over previous routes (4) to poly-*p*-xylylene include

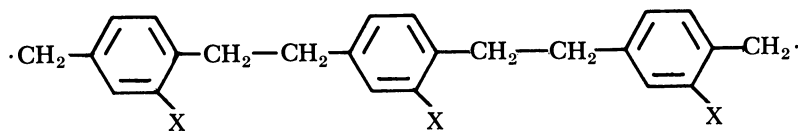


the quantitative nature of both reactions, the formation of linear rather than crosslinked polymers, and the absence of byproducts and telomers.

While all substituted di-*p*-xylylenes are pyrolyzed under substantially identical conditions, the temperatures of condensation and polymerization varied substantially, depending on the *p*-xylylene derivative under study. It was established that there is a threshold condensation temperature,  $T_c$ , above which the rate of condensation-polymerization was very slow under the system conditions (50–100  $\mu$ ) normally used. The  $T_c$ 's for several *p*-xylylene monomers were established as follows:

Monomer	$T_c$ , °C.
<i>p</i> -Xylylene	30
2-Methyl- <i>p</i> -xylylene	60
2-Ethyl- <i>p</i> -xylylene	90
2-Chloro- <i>p</i> -xylylene	90
2-Acetyl- <i>p</i> -xylylene	130
2-Cyano- <i>p</i> -xylylene	130
2-Bromo- <i>p</i> -xylylene	130
Dichloro- <i>p</i> -xylylene	130

In this series  $T_c$  is related to both molecular weight of the monomer and the polarity of the substituent(s) attached to the aromatic ring. It appears that the monomer must be able to condense on a surface and be available in sufficiently high concentration to react with its neighbors to form initially diradical intermediates such as IV containing at least three and probably four monomer units.



IV

Once this intermediate is formed, growth appears to be very rapid through addition of monomer units which condense near either radical site. High molecular weight polymers are then formed by a free radical addition mechanism.

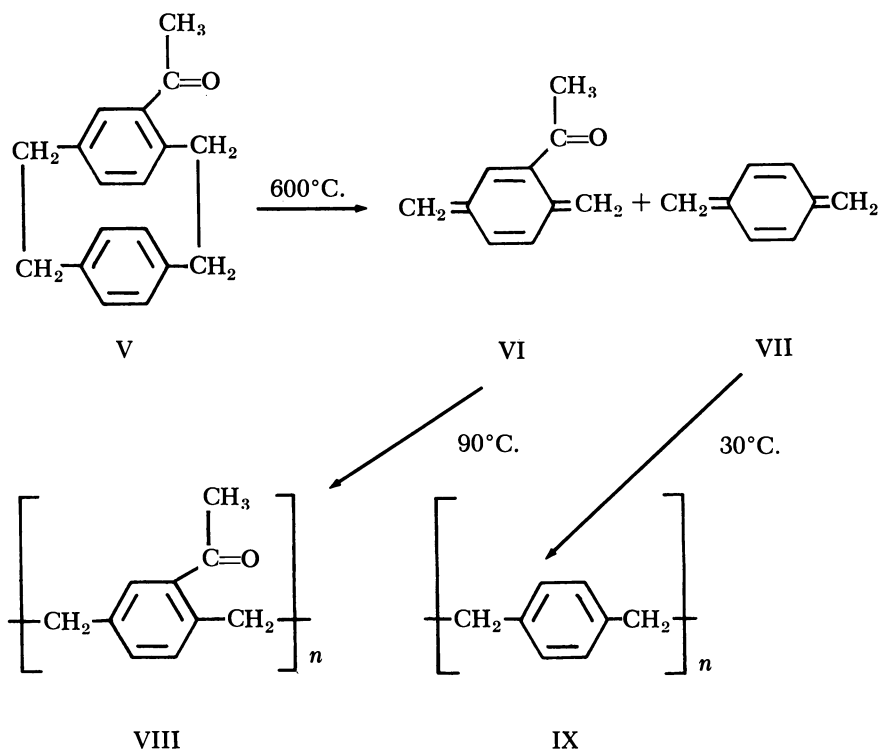
This polymerization route was first proposed by Szwarc (17). There is general agreement (4) that the original Szwarc proposal represents the most probable path. An excellent paper discussing the polymerization of *p*-xylylene has been published by Errede, Gregorian, and Hoyt (2).

Growth is terminated by coupling of radicals from two growing polymer molecules or by the reactive sites becoming buried in the polymer matrix. Polymers formed by the di-*p*-xylylene process have been shown (6, 7, 8, 9, 10, 11, 13) to be living polymers and exhibit radical concentrations of  $5\text{--}10 \times 10^{-4}$  mole of free electrons per mole of *p*-xylylene.

Pyrolysis of monosubstituted di-*p*-xylylenes, such as acetyl-di-*p*-xylylene (V) results in formation of two reactive *p*-xylylenes with different  $T_c$ 's. The two species were separated as their polymers by using the principle of threshold condensation temperature. The pyrolysis vapors containing the two monomers VI and VII were passed initially through a zone maintained at a temperature low enough to permit rapid condensation and polymerization of acetyl-*p*-xylylene, but substantially above the  $T_c$  of *p*-xylylene which passed through the first zone and polymerized in a final zone maintained at ambient temperature. In a sense, the monomers were fractionated on the basis of volatility, and the monomers were isolated in the form of their polymers. These transformations are illustrated at the top of p. 646.

### Copolymerization Studies

The earliest work on the copolymerization of *p*-xylylene type monomers was reported in the brilliant pioneering studies of M. Szwarc (17). He and Roper (5) studied the pyrolysis of mixtures of *p*-xylylene and pseudocumene and concluded that mixtures of *p*-xylylene and 2-methyl-*p*-xylylene were formed which copolymerized on condensation. Apparently no extensive work on copolymerization or the nature of the products was conducted.



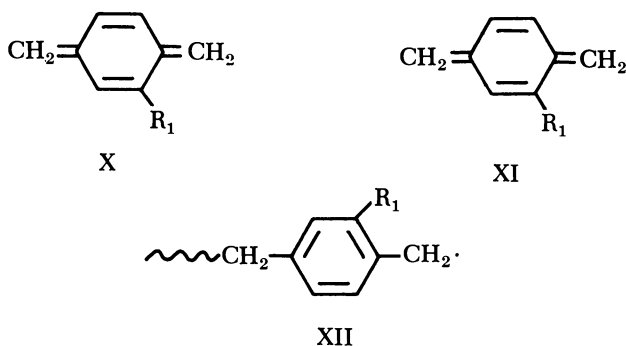
Other groups (1, 15) have also conducted studies on the copolymerization of substituted *p*-xylylenes by pyrolysis of mixtures of substituted *p*-xylylenes. Problems associated with the stability of many substituent groups at the elevated pyrolysis temperatures ( $\cong 900^\circ\text{C}.$ ) required to convert *p*-xylylenes to *p*-xylylenes have, however, prevented a general study of copolymerization.

The formation of *p*-xylylene monomers by pyrolysis of substituted di-*p*-xylylenes is a quantitative, clean process and provides an excellent starting point for generating mixtures of monomers and for studying their copolymerization. The formation of linear poly-*p*-xylylenes by the di-*p*-xylylene route is also a major advantage in characterizing the products formed.

Considerable flexibility is available in the di-*p*-xylylene process with regard to preparation of intermediates for generating monomers. Introduction of a substituent on one ring of di-*p*-xylylene (as, for example, acetyl-di-*p*-xylylene) provides a starting material which on pyrolysis yields two distinct monomers. Alternatively, disubstituted products, for

example dichloro, dibromo, or dialkyl derivatives, provide intermediates which on pyrolysis yield pure sources of a single monomer. The preparation of a broad range of substituted di-*p*-xylylenes has been reported (12, 13, 16, 18, 19, 20).

In considering the copolymerization of substituted *p*-xylylenes, such as X and XI, an important question is whether the growing polymer chain XII (which has just added a unit of monomer X) shows any preference for reacting with X or XI. The chain-propagating step involves addition of a radical to a highly reactive monomer to form a covalent bond and a



new radical site. Owing to the great reactivity of these molecules in the condensed phase, it is probable that XII shows little or no preference but will react with whichever is available at the radical site. Since the substituent groups R<sub>1</sub> and R<sub>2</sub> are quite far removed from the reaction site, it is also probable that steric and electronic effects are not nearly as important as in vinyl copolymerizations.

Assuming the above statements are correct, any two *p*-xylylene species should be capable of copolymerization in any desired ratio. This is somewhat of a simplification since it has been observed that for each substituted *p*-xylylene there is a definite ceiling condensation temperature above which it will not condense and polymerize at any appreciable rate. Thus, if the monomer does not condense, it is not available for copolymerization. This was demonstrated in the studies described earlier of the pyrolysis of acetyl-di-*p*-xylylene and separation of the monomers VI and VII on the basis of widely differing *T<sub>c</sub>*'s.

Therefore, to study copolymerization one must either utilize two monomers with approximately the same vapor pressure characteristics or maintain the initial polymerization zone at a temperature below the threshold condensation temperature of the more volatile species. Studies were conducted on the copolymerization of several sets of monomers.

### Experimental

**Conversion of Di-*p*-xylylenes to Poly(*p*-xylylenes).** The following equipment and procedure were used to convert di-*p*-xylylenes to poly-*p*-xylylenes. The pyrolysis reactions were carried out in a 24-inch section of 1-inch i.d. 96% silica tubing. The first 6 inches of the tube served as a distillation zone, and the following 18-inch section as the pyrolysis zone. The pyrolysis tube was connected by appropriate glass connections to a glass deposition chamber. Deposition chambers ranging in diameter from 1 to 6 inches and in length from 8 to 20 inches were used. The end of the chamber was connected by tubing through a dry ice trap to a 4 cu. ft./min. mechanical pump. A thermocouple or Pirani vacuum gage probe was placed in the system between the dry ice trap and the pump to record pressure and pressure changes.

In each experiment, a measured quantity of di-*p*-xylylene, ring-substituted derivatives, or mixtures were placed in a porcelain boat, and the boat was placed in the distillation zone. The system was then closed and evacuated to 1–100  $\mu$ , depending on the derivative in question. The di-*p*-xylylene was distilled at the rate of 1 gram every 3 or 4 minutes through the pyrolysis zone. To achieve this rate, the distillation zone was maintained at temperatures ranging from 140° to 220°C., depending on the derivative. The pyrolysis zone was heated to 600°C., the temperature being measured by the thermocouple in the middle of the furnace on the outside of the tube. The pyrolysis gases were then led into a deposition chamber. The glass joints leading from the pyrolysis zone to the deposition chamber were maintained at about 200°C. to prevent premature polymerization. The deposition chamber was usually held at room temperature, although with some derivatives it was heated as high as 100°C. to permit deposition of polymer over a fairly broad area.

A pressure rise of 5–100  $\mu$  is generally observed during a pyrolytic polymerization. At the end of the run the pressure falls back to the base pressure. The heating jacket on the distillation section of the pyrolysis tube is removed at this point to ensure that complete distillation of the charge has occurred. When it is established that the distillation is complete, the vacuum is broken, the equipment is dismantled, and the polymeric film is recovered from the walls of the deposition chamber.

**Preparation of Mixtures of *p*-Xylylenes and Separation into Polymer on the Basis of *T<sub>c</sub>*.** The distillation and pyrolysis steps were conducted as described above for di-*p*-xylylene and substituted di-*p*-xylylenes. The pyrolysis gases were led immediately into a deposition zone which consisted of a 24-inch section of 1-inch i.d. glass tubing. The initial 15-inch section of this tubing (Zone A) was heated to 90°–100°C. The final 9-inch section of the tubing (Zone B) was maintained at room temperature. The end of the deposition zone was connected *via* rubber tubing through the dry ice trap to the pump.

**Preparation of Copolymer of Chloro- and Butyl-*p*-xylylene.** Mixtures of dichloro-di-*p*-xylylene and butyl-di-*p*-xylylene were prepared and melted to ensure homogeneity. The mixture was placed in the distillation zone, and the reaction was carried out in the usual fashion. The copolymers formed in the initial polymerization zone which was maintained at 90°–100°C. Poly-*p*-xylylene formed in the final, air-cooled zone. At

the end of each run, the copolymers were removed mechanically and extracted with ether. In each run, the pyrolysis temperature was 600°C., the distillation temperature 100°–125°C., and the pressure of the system was 0.2 mm. The runs lasted 10–12 minutes. The following data were obtained:

	Run			
	A	B	C	D
Dichloro-di- <i>p</i> -xylylene (gram)	0.8	0.8	1.6	1.0
Butyl-di- <i>p</i> -xylylene (gram)	0.3	0.15	0.15	0.0
Weight of crude copolymer (gram)	0.95	0.88		0.97
Weight of extracted polymer (gram)	0.55	0.70	1.35	0.85
Theoretical % butyl <sup>a</sup>	18.5	10	5.5	0
Percent chlorine in polymer	18.9	22.5	22.8	25.8
Calculated % butyl <sup>b</sup>	25	12	11	0
Polymer melting point, °C.	210-215	220-225	230-235	270-280

<sup>a</sup> Based on monomer charge.

<sup>b</sup> Based on chlorine analysis of copolymer.

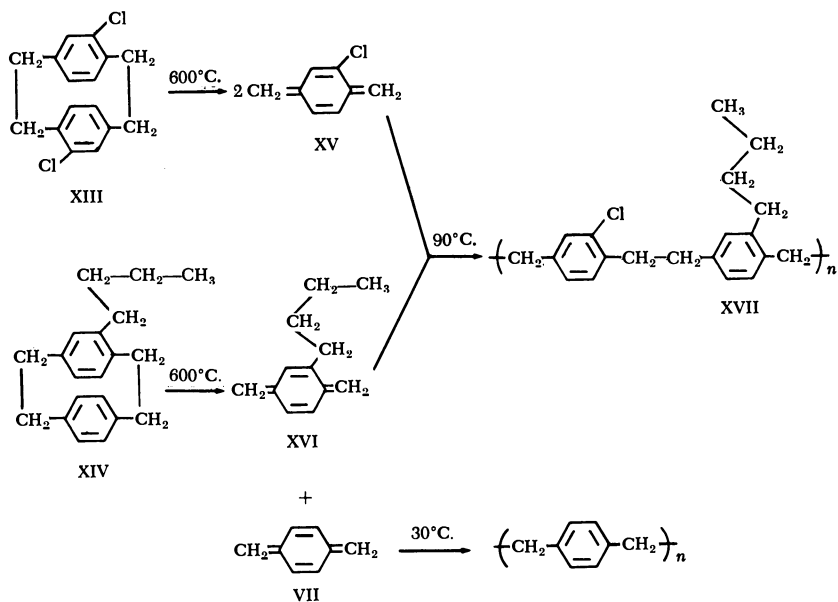
### Results and Discussion

**Copolymerization of Chloro- and Butyl-*p*-xylylene.** Mixtures of dichloro-di-*p*-xylylene (XIII) and butyl-di-*p*-xylylene (XIV) were pyrolyzed to form chloro-*p*-xylylene (XV), butyl-*p*-xylylene (XVI), and *p*-xylylene (VII). In the initial polymerization zone (*ca.* 90°C.) chloro-*p*-xylylene (XV) and butyl-*p*-xylylene (XVI) condensed and polymerized. Since this temperature is above the *T<sub>c</sub>* of *p*-xylylene at 0.3 mm., *p*-xylylene molecules passed through and condensed and polymerized in the final, air-cooled zone. In this way it was possible to study the copolymerization of chloro- and butyl-*p*-xylylenes starting from the mixtures of the three monomers XV, XVI, and VII.

Poly(chloro-*p*-xylylenes) containing (in theory) about 5, 10, and 20% butyl-*p*-xylylene were prepared in this way (*see* illustration on p. 650). The crystalline melting points of the products (XVII) were in the range 220°–250°C. compared with 290°C. for pure poly(chloro-*p*-xylylene). Solubility characteristics of the products and a sample of poly(chloro-*p*-xylylene) were studied by heating in  $\alpha$ -chloronaphthalene. The solution temperature is the minimum temperature required to dissolve the product with slow heating. The gel temperature is that at which the solution of the product in  $\alpha$ -chloronaphthalene sets to a gel on gradual cooling. Results were as follows:

	Run			
	A	B	C	D
Theoretical % butyl	18.5	10	5.5	0
Solution temp., °C.	170	185	210	215
Gel temp., °C.	65	68	71	105





The product from Run A was found to be completely soluble in *s*-tetrachloroethane at room temperature, whereas poly(chloro-*p*-xylylene) is insoluble in this solvent at all temperatures. These marked changes in solubility characteristics are considered excellent evidence for the formation of random copolymers rather than block copolymers or mixtures of homopolymers.

Chlorine analyses of the products were in the range expected for the copolymers. All experimental evidence indicated that copolymers were obtained rather than a mixture of two homopolymers.

**Copolymerization of Ethyl- and Chloro-*p*-xylylene.** The copolymerization of these monomers was studied by pyrolysis of a mixture of 1.35 grams of dichloro-di-*p*-xylylene and 0.27 gram of ethyl-*p*-xylylene at 600°C. and initial condensation of the pyrolysis products in a zone maintained at 90°C. and a pressure of about 0.3 mm. Under these conditions, chloro- and ethyl-*p*-xylylene would be expected to condense and polymerize, while *p*-xylylene would pass downstream to condense and polymerize in the final air-cooled zone. At the end of the run, the product was removed from the 90°C. zone, extracted with ether, and dried. A total of 1.5 grams of tough, high molecular weight product was obtained. Since the product weighed more than the initial charge of dichloro-*p*-xylylene, either a copolymer or a mixture of homopolymers was formed.

Physical property measurements provide strong evidence for the formation of a random copolymer rather than formation of either block

copolymers or mixtures of homopolymers. Stiffness-temperature measurements of the "copolymer" and of poly(chloro-*p*-xylylene) and poly(ethyl-*p*-xylylene) are shown in Figure 1. The presence of only one glass

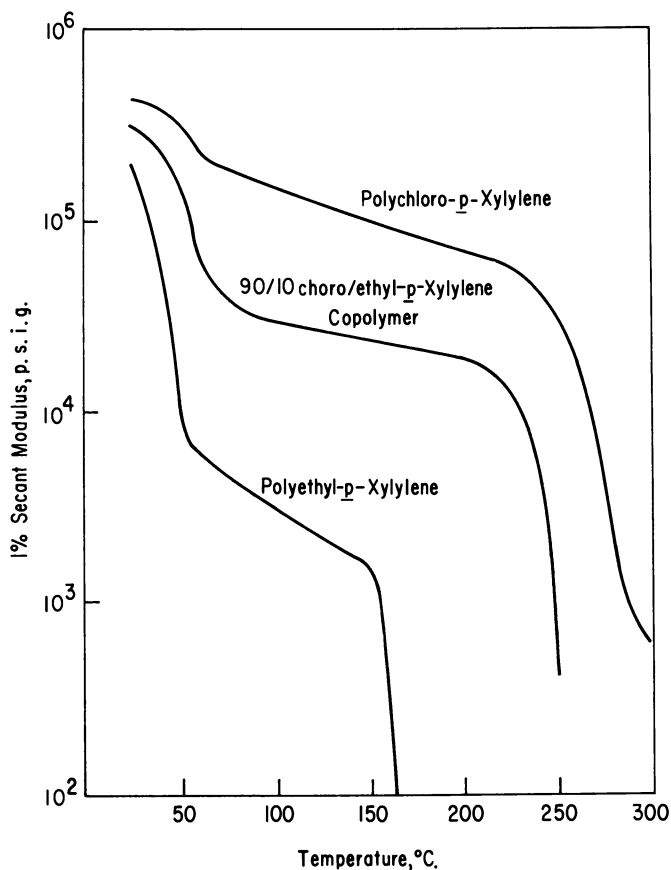
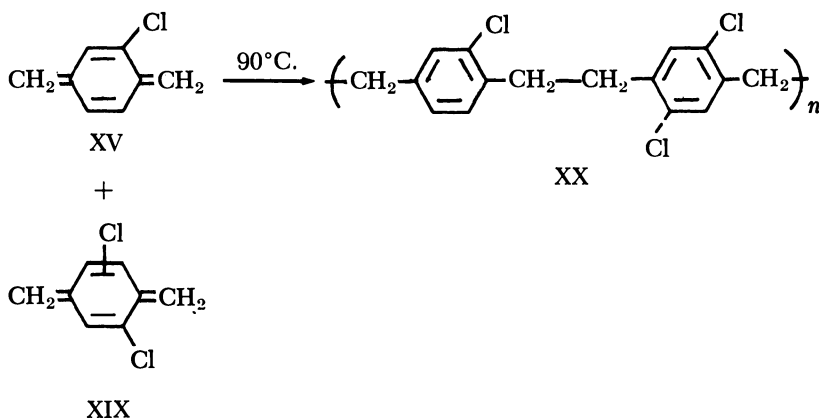
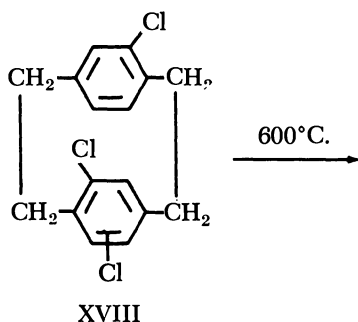


Figure 1. Temperature stiffness measurements of poly(*p*-xylylenes)

transition (65°C.), a lower level of crystallinity, and only one melting point (250°C.) are interpreted to indicate the formation of a random copolymer. It is interesting to note that incorporation of approximately 10 mole % ethyl-*p*-xylylene lowers the melting point of poly(chloro-*p*-xylylene) from 290° to 250°C. The incorporation of 10 mole % of 2-ethyl-*p*-xylylene as a block copolymer would be expected to have little or no effect on the crystalline melting point, and a mixture of two homopolymers would exhibit two melting points.

**Copolymerization of Chloro- and Dichloro-*p*-xylylene.** Trichloro-di-*p*-xylylene (XVIII) was obtained by chlorination of di-*p*-xylylene with three molar equivalents of chlorine. Pyrolysis yielded monomers XV and XIX, which were condensed and polymerized on a 90°C. surface. A quantitative yield of product was obtained. The product was transparent, tough, self-extinguishing, had a softening point above 280°C., and exhibited the correct elemental analysis for copolymer XX. Owing to the low solubility of the chlorinated poly-*p*-xylylenes, no attempts



were made to fractionate the product. This is an example of formation of a copolymer from a single starting material.

Copolymers of ethyl- and chloro-*p*-xylylene were also prepared by pyrolytic polymerization of mixtures of dichloro-di-*p*-xylylene and diethyl-di-*p*-xylylene at 50°C. This is an example of preparation of a copolymer by pyrolysis of a mixture of two disubstituted di-*p*-xylylenes.

All available evidence indicates that copolymers can be prepared from any two *p*-xylylenes provided that the polymerization is conducted

at a temperature at which each monomer will condense and polymerize separately. The results of characterization studies of the copolymers indicate that random copolymers are formed. The question of whether the monomers add in a head-to-head or head-to-tail fashion remains to be investigated.

### *Related Studies*

**Control of Molecular Weight.** Studies have been conducted on techniques for controlling the molecular weight of poly-*p*-xylylenes produced from di-*p*-xylylenes by the vacuum pyrolysis route. Earlier work by Szwarc (17), Errede (3), and Auspos (1) indicated that very reactive chain transfer agents were required to achieve a significant effect in the polymerization of *p*-xylylene derived from *p*-xylene. This general picture was confirmed in the present study.

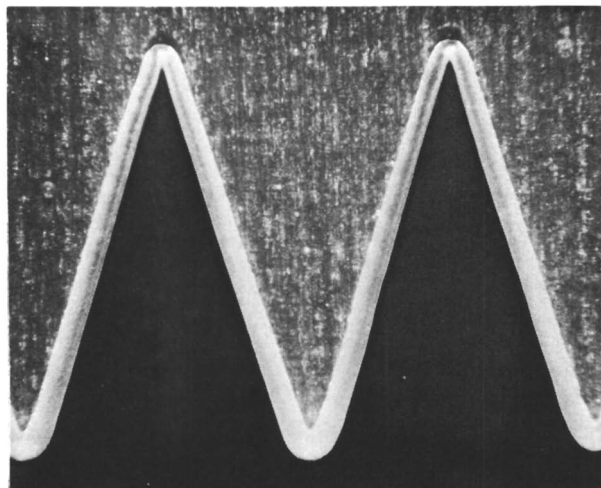
The effect of potential chain transfer agents was studied by co-condensation with the polymerizing *p*-xylylene species. It was established that it was necessary to match volatility of the agent with that of the *p*-xylylene. Apparently, the agent must be in the condensed phase near a polymerizing site to participate in a chain transfer reaction resulting in termination of one growing chain. Both aliphatic and aromatic mercaptans were useful in achieving significant changes in molecular weight as measured by the RV (reduced viscosity of 0.2% solution in  $\alpha$ -chloronaphthalene at 150°C.) of the product. Concentrations of 0, 1, and 2% of  $\beta$ -naphthylmercaptan in polymerizing chloro-*p*-xylylene resulted in poly(chloro-*p*-xylylene) with RV's of 1.34, 1.09, and 0.65, respectively. Similarly, concentrations of 0, 7, and 14% dodecylmercaptan in polymerizing chloro/butyl-*p*-xylylene resulted in 90/10 chloro/butyl-*p*-xylylene copolymer with RV's of 2.2, 1.02, and 0.85, respectively. Yields of carbon tetrachloride-insoluble polymer were lowered by the presence of the mercaptans, indicating the probable formation of soluble telomers.

**Unique Capabilities.** A number of unique features and capabilities of the *p*-xylylene polymerization process have been uncovered and elucidated. The reactive monomers will condense and polymerize on any solid surface placed in the condensation (deposition) zone. The chemical nature of the surface is unimportant, and many materials, including strong acids, bases, the alkali metals, metal hydrides, and chemically reactive compounds such as resorcinol, have been coated when placed in a deposition chamber.

The polymerization of *p*-xylylenes on condensation is extremely rapid and appears to proceed from gaseous monomer to solid polymer without passing through a viscous stage. The monomer behaves as a reactive plasma which surrounds solid objects placed in the deposition chamber.



*Figure 2. Mesh coated with poly(chloro-p-xylylene). Polymer is transparent inner rings. 16.5 ×*



*Figure 3. Sawtooth coated with poly(chloro-p-xylylene). 16.5 ×*

For these reasons uniform thickness films are deposited on all surfaces. Unique features which result are the deposition of uniform thickness coatings on sharp edges, in crevices, and around the inside of holes. A metallizing mask was coated with 1.5 mils of poly(chloro-*p*-xylylene). Figures 2 and 3 are magnifications of the coated saw tooth and coated

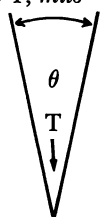
mesh. It is noteworthy that uniform thickness coatings are deposited over and around these structural features. In essence these structural features are replicated in the coating.

In a further elaboration of this feature the ability of the monomer to penetrate between closely positioned glass slides and into deep crevices was investigated. In the initial experiment, several pairs of 3 inch  $\times$  3 inch glass slides were placed in a polymerization zone, the distance between the parallel surfaces of the plates varied from 0.017 to 0.125 inch, and sufficient chloro-*p*-xylylene was introduced to deposit 1.0 mil poly(chloro-*p*-xylylene) on the walls of the chamber and exposed surfaces. The plates were placed perpendicular to the flow of the gaseous monomer. At the end of the experiment the samples were removed, and the thickness of the coating at the center point on the inside surface of the plates was examined with the following results:

<i>Distance Between Plates, inch</i>	<i>Coating Thickness at Center, mil</i>
1	1
0.125	0.8
0.0625	0.68
0.0312	0.34
0.017	0.04

In a second series of experiments, 3 inch  $\times$  3 inch glass slides were joined at one end, the side openings were closed with tape, and the angle of the open end ( $\theta$ ) varied from 90° to 1°. This experiment was designed to investigate the degree of penetration of the monomer-polymer into a crevice. The polymerization was conducted to deposit 1.0 mil poly(chloro-*p*-xylylene) on the walls of the chamber. The samples were removed at the end of the run, and the thickness of the film at the bottom point of the 3-inch crevice was measured.

$\theta$ , Angle of Opening (°)	Thickness at T, mils
90	1.0
20	0.75
10	0.70
5	0.62
1	<0.01



The diagram shows a downward-pointing triangle representing a crevice. The top horizontal edge is labeled with a double-headed arrow and the value 1.0. The angle at the top vertex is labeled with the Greek letter theta. The bottom vertex is labeled with a downward-pointing arrow and the letter T. The right side of the triangle is labeled with the value 0.62.

In both experiments a surprising degree of penetration of the polymerizable monomers into a difficultly accessible point was achieved. In the crevice experiment the thickness of the deposited polymer at the bottom of the crevice in all runs was more than 50% that deposited on the outer surface, except where the angle of opening was only  $1^\circ$  of arc.

**Particle Encapsulation.** A unique capability of the *p*-xylylene vapor deposition process has been uncovered in the area of encapsulation (12) of particulate solids. The particles or granules to be encapsulated are placed in a container which in turn is placed in the deposition chamber, and the nozzle from the pyrolysis tube is inserted in the mouth of the bottle. During the run the monomers pass from the pyrolysis zone through a nozzle into the bottle and polymerize on the surface of the tumbling particles or granules. Polymer is also formed on the inner surface of the bottle which is rotated at 50–150 r.p.m. Relatively simple equipment (Figure 4) has been used to study this phenomenon.

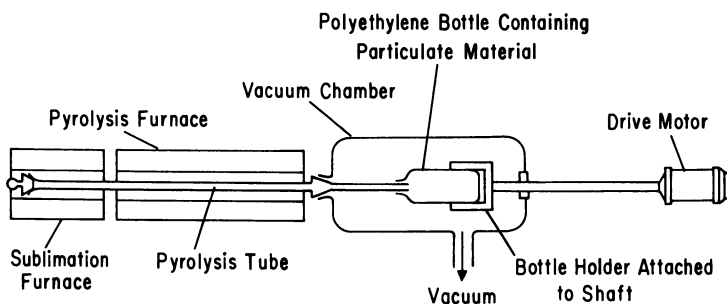


Figure 4. Apparatus for encapsulating particulate materials

Particles as small as 50–100 mesh can be encapsulated. It is essential to keep the particles in continuous motion—*e.g.*, by simple rotation of the bottle to maintain a tumbling bank—to prevent agglomeration and sticking. Since no solvents are involved and no liquid viscous stage is encountered during the polymerization, coherent, uniform coatings are deposited around each particle.

Particulate materials which have been studied in the encapsulation process include sodium chloride, sodium dichromate, lithium, sodium, lithium hydride, zinc, and lithium aluminum hydride. Typical experiments are described below.

**EXAMPLE 1: ENCAPSULATION OF LITHIUM ALUMINUM HYDRIDE WITH POLY(CHLORO-*p*-XYLYLENE).** In the distillation zone were placed 5.0 grams of dichloro-di-*p*-xylylene. In a 4-oz. polyethylene bottle were placed 10.0 grams (400 pellets) of lithium aluminum hydride (LAH). LAH was obtained from Metal Hydrides, Inc., as 1/8-inch diameter pellets. The bottle was positioned in the coating chamber, the system was

evacuated to 0.01 mm., the bottle was rotated at 75 r.p.m., and the coating was conducted over a 30-minute period. At the end of the run, the bottle was removed, and a total of 11.27 grams encapsulated pellets was recovered.

**EXAMPLE 2: ENCAPSULATION OF 3/16-INCH SODIUM HYDROXIDE PELLETS WITH POLY(CHLORO-*p*-XYLYLENE).** Fifty grams of sodium hydroxide pellets were encapsulated with polymerizing chloro-*p*-xylylene generated by pyrolysis of 5.0 grams of dichloro-di-*p*-xylylene over a 15-minute period. The bottle was rotated at 60 r.p.m. during the run. A pyrolysis temperature of 660°C. and system pressure of 50  $\mu$  were employed. A total of 51.97 grams of encapsulated pellets was recovered at the end of the run.

**EXAMPLE 3: ENCAPSULATION OF 20-MESH ZINC GRANULES WITH POLY(CHLORO-*p*-XYLYLENE).** Ten grams of 20-mesh zinc granules were encapsulated with polymerizing chloro-*p*-xylylene generated by pyrolysis of 2.0 grams of dichloro-di-*p*-xylylene over an 8-minute period. A pyrolysis temperature of 660°C. and a system pressure of 40  $\mu$  were employed. The bottle containing the granules was rotated at 60 r.p.m. during the run. A total of 10.35 grams of encapsulated granules was recovered.

**EXAMPLE 4: ENCAPSULATION OF LITHIUM WITH POLY(CHLORO-*p*-XYLYLENE).** Pellets of lithium were prepared by cutting approximately 1/4 inch lengths from 1/8 inch diameter lithium wire. Grease from the surface was removed by washing in heptane for 5 minutes, filtering and transferring the pellets to a 4-oz. polyethylene bottle. All handling and transfer operations were conducted under argon. A total of 0.42 gram of lithium pellets was encapsulated with polymerizing chloro-*p*-xylylene produced by pyrolysis at 660°C. of 1.5 grams of dichloro-di-*p*-xylylene over an 8-minute period. The pressure of the system during the encapsulation was 0.01 mm. The weight of the encapsulated particles was 0.465 gram. Two pellets were tested for perfection of encapsulation by placing in water and measuring hydrogen evolution. There was no measurable evolution after a 30-day test period.

Surprisingly high levels of protection were achieved in the encapsulated products when poly(chloro-*p*-xylylene) was used as the encapsulant.

In a typical experiment, 150 grams of sodium hydroxide pellets were encapsulated with 2.5% polymer. The pellets were 3/16" in diameter and of rather irregular contour. On the average there were 10 pellets per gram. Protection of the encapsulated pellets was measured by choosing 50 coated pellets from the production at random. Ten test tubes were filled with 20 ml. of distilled water, and a portion of universal pH indicator was added. Five pellets were placed in each tube. One uncoated pellet immersed in the test solution resulted in a pH change from 5 to 13 within ten seconds (color change of yellow to blue). pH changes in tubes containing encapsulated pellets were monitored. A tube is considered to have "failed" if the pH of the solution changes to any value above 7. This indicates an imperfection or pinhole in at least one of the pellets. In this test, pellets coated with 2.5% encapsulant exhibited no failures in any tube after 5 days, indicating a high level of protection.



Samples of commercial 20-mesh zinc were encapsulated with 3.5 and 7.5% poly(chloro-*p*-xylylene). No problems with sticking or agglomeration were encountered. The perfection of encapsulation was examined by immersion of 1 gram of encapsulated zinc from each run in 3*N* hydrochloric acid and measuring hydrogen evolution. One gram of uncoated zinc liberates 375 ml. of hydrogen within 30 seconds in this medium. There was no hydrogen evolution from any of the encapsulated samples during a 30-day test period, again indicating a very high level of protection and perfection of the coatings on the individual coated particles.

Attention was then turned to encapsulation of a more reactive species, lithium aluminum hydride (Example 1). Several batches were encapsulated readily with poly(chloro-*p*-xylylene) utilizing the standard tumbling process. Products with from 1–20 wt. % coating were prepared.

To evaluate the perfection of encapsulation, the coated pellets were immersed in pure methanol. Evolution of hydrogen from one or more points indicates the presence of a pinhole or other imperfection in the coating. Since the encapsulated pellets are denser than methanol, pinholes in individual pellets are detected easily by evolution of a stream of hydrogen bubbles rising from the pellet to the surface. Such pellets are removed. The test is continued for 15 minutes, and the percent of pinhole-free pellets is calculated. Typical data are presented in Table I.

**Table I. Effect of Weight Percent Poly (chloro-*p*-xylylene) Coating on Percent of Pinhole-Free LAH Pellets**

Run	Wt. % Coating	% of Pellets Pinhole-Free
A	5.5	82.5
B	9.5	94
C	11.2	98.25
D	15.5	100

**Table II. Effect of Weight Percent Poly (chloro-*p*-xylylene) Coating on LAH Pellets to Long Term Protection in 50/50 Methanol/Water**

Run	Wt. % Coating	Number of Pellets Tested	Duration of Test, days	Total Hydrogen Evolution, ml.
A	1	20	1½	500
B	5.7	20	21	85
C	9	20	26	30
D	15	20	29	13
E	19	5	150	0

It is seen that the percentage of pinhole-free pellets increases from 82 to 100% as the weight percent of coating is increased from 5–15%.

A second test conducted with the pellets was to measure long term protection against hydroxylic solvents. This was accomplished by immersing 20 pellets of each of several batches in 50/50 methanol/water and measuring hydrogen evolution with time. One uncoated pellet in this medium liberates 85 ml. of hydrogen within 15 seconds. Table II summarizes the important data.

### **Acknowledgments**

It is a pleasure to acknowledge the expert technical assistance of Charles E. White of the Union Carbide laboratories in the performance of this work. Physical property measurements and interpretations were conducted by Alexander Brown and Neale Merriam. It is also a pleasure to acknowledge guidance gained from many stimulating and provocative discussions held with William E. Loeb of these laboratories and D. J. Cram of the University of Southern California.

### **Literature Cited**

- (1) Auspos, L. A., Hoel, L. A., Hubbard, J. K., Kirk, W. M., Jr., Schaeffgen, J. R., Speck, S. S., *J. Polymer Sci.* **15**, 9 (1955).
- (2) Errede, L. A., Gregorian, R. S., Hoyt, J. M., *J. Am. Chem. Soc.* **82**, 5218 (1960).
- (3) Errede, L. A., Hoyt, J. M., *J. Am. Chem. Soc.* **82**, 436 (1960).
- (4) Errede, L. A., Szwarc, M., *Quart. Rev. (London)* **12**, 301 (1958).
- (5) *Ibid.*, p. 314, Ref. 33.
- (6) Gorham, W. F., *J. Polymer Sci. Pt. A-1*, 3027 (1966). For Patent References to this work, see Literature Cited Nos. (7-11) and (13) below.
- (7) Gorham, W. F., British Patent **883,939** (Dec. 7, 1961).
- (8) *Ibid.*, **883,941** (Dec. 7, 1961).
- (9) Gorham, W. F., German Patent **1,085,673** (July 21, 1960).
- (10) Gorham, W. F., U. S. Patent **3,342,754** (Sept. 19, 1964).
- (11) *Ibid.*, **3,288,728** (Nov. 29, 1966).
- (12) *Ibid.*, **3,117,168** (Jan. 7, 1964).
- (13) *Ibid.*, **3,221,068** (Nov. 30, 1965).
- (14) Gorham, W. F., Willard, H., U. S. Patent **3,300,332** (Jan. 24, 1967).
- (15) Kaufman, M. H., Mark, H. F., Mesrobian, R. B., *J. Polymer Sci.* **13**, 3 (1954).
- (16) Pollart, D. F., U. S. Patent **3,164,625** (Jan. 5, 1965).
- (17) Szwarc, M., *J. Polymer Sci.* **6**, 319 (1951).
- (18) Yeh, Y. L., U. S. Patent **3,349,142** (Oct. 24, 1967).
- (19) Yeh, Y. L., U. S. Patent **3,155,712** (Nov. 3, 1964).
- (20) Yeh, Y. L., U. S. Patent **3,153,103** (Oct. 13, 1964).

RECEIVED March 14, 1968.

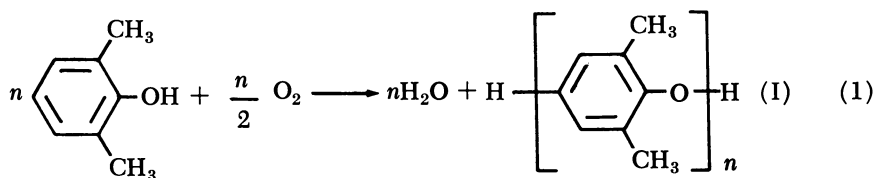
## Polyphenylene Oxides by Oxidative Coupling

GLENN D. COOPER and ARTHUR KATCHMAN

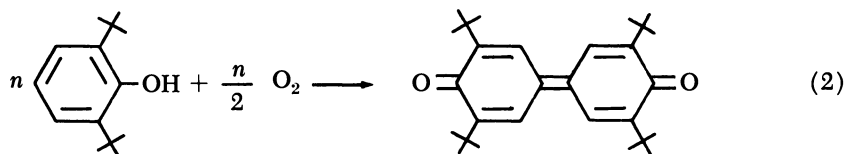
Plastics Department, General Electric Co., Selkirk, N. Y. 12158

*The oxidative coupling of 2,6-disubstituted phenols to poly-(arylene oxides) is a polycondensation reaction, in which polymer molecules couple with other polymer molecules as well as with monomer. Unstable quinone ketals formed by coupling of a polymeric aryloxy radical at the para position of the phenolic ring of a second radical are believed to be intermediates or the reaction. The ketals may be converted to polymeric phenols either by a series of intramolecular rearrangements or by disproportionation to aryloxy radicals, leading to a mobile equilibrium between polymer molecules of varying degree of polymerization. Both processes have been shown to occur, with their relative importance determined by the reaction conditions.*

In 1959 Hay (19) reported that 2,6-xylenol reacts with oxygen in the presence of a pyridine-cuprous chloride catalyst to yield a high molecular weight poly(1,4-arylene oxide) (Reaction 1).



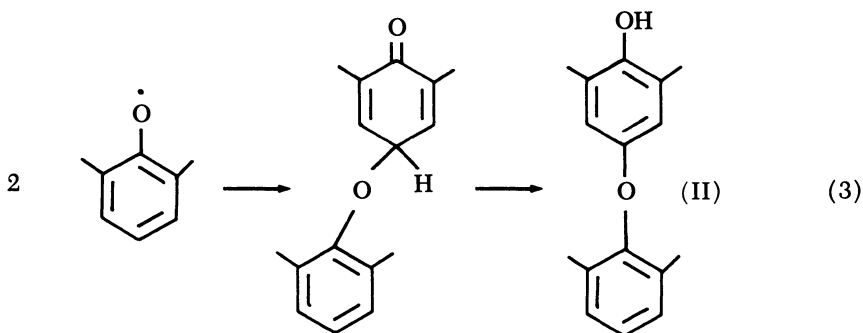
Other 2,6-disubstituted phenols react in the same manner, provided the substituents are not too large; oxidation of phenols with bulky ortho substituents, such as 2,6-di-*tert*-butylphenol, yields the diphenoquinone as the major product (16) (Reaction 2).



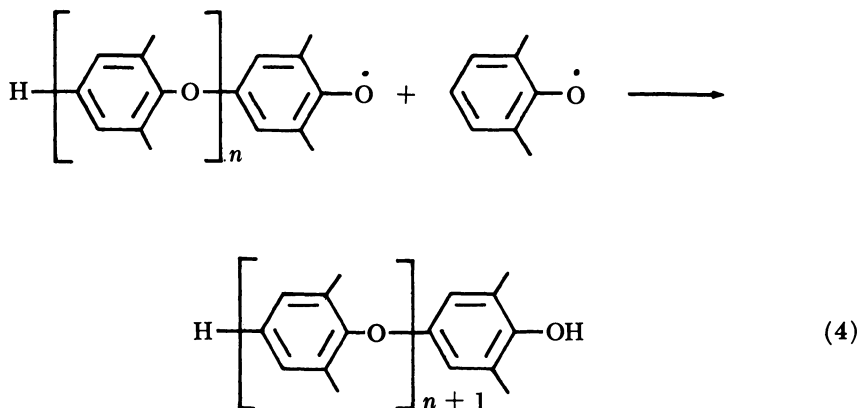
Many amine-copper complexes, as well as a few amine complexes of other metals, and certain metal oxides have since been shown to induce similar reactions (17, 18, 22, 23, 30). This chapter is concerned largely with the mechanism of oxidative polymerization of phenols to linear polyarylene ethers; most of the work reported has dealt with the copper-amine catalyzed oxidation of 2,6-xyleneol, which is the basis for the commercial production of the polymer marketed under the trade name PPO, but the principal features of the reaction are common to the oxidative polymerization of other 2,6-disubstituted phenols.

### Mechanism

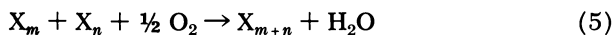
It has generally been accepted that aryloxy radicals are intermediates in the polymerization, largely because the effective reagents are those capable of one-electron transfer. This assumption has been confirmed recently by the identification of both monomeric and polymeric aryloxy radicals in the ESR spectra of polymerizing solutions of 2,6-xyleneol (21). The first step in the reaction is the oxidation of the phenol to the aryloxy radical by Cu(II). Carbon-oxygen coupling of two aryloxy radicals yields the cyclohexadienone, which tautomerizes to the dimer (II) (Reaction 3).



The simplest explanation for the formation of high molecular weight polymer through oxidative coupling of aryloxy radicals involves the successive addition of monomer units to the radicals derived from polymer phenols (Reaction 4).



Although reactions of this type must occur, there are at least two observations which cannot be explained on this basis. Endres and Kwiatek (12) reported that the dimer reacts to yield a polymer identical with that obtained from xylenol; the mixture of low molecular weight oligomers isolated from the reaction mixture at early stages of the polymerization behaves similarly. Since no xylenol is present, and hence there is no apparent source of the monomer radical, Reaction 4 cannot explain the polymerization completely. The variation in polymer molecular weight with conversion is also inconsistent with simple stepwise addition of monomer units. When the degree of polymerization is plotted against fractional polymer yield (Figure 1), a sharp increase is observed near the end of the reaction. This type of behavior is typical of polycondensation reactions in which polymer molecules couple with each other as well as with monomer molecules:



### Proposed Mechanisms for Coupling of Polymer Molecules

In polyesterification and other polycondensation reactions, polymer molecules condense with one another by the same mechanism by which they add monomer units. There is no immediately apparent explanation, however, for the coupling of two polyarylene ether molecules of structure I. Three possible routes were first outlined by Finkbeiner (13), and each has received some support since.

**Endlinking.** The most obvious path for Reaction 5 is by the attack of the phenolic oxygen of one polymer molecule at the para position of the terminal ring of another. This cannot be simply a homolytic aromatic

substitution with the polymeric aryloxy radical attacking the terminal ring of a polymeric phenol; if this were the case, aromatic ethers should act as chain stoppers, but no reduction of polymer molecular weight was observed when the reaction was carried out in 2,6-dimethyl anisole or in the methyl ether of the dimer as solvent (13). The coupling, if it occurs, therefore must be between two polymeric aryloxy radicals. The objection to this head-to-tail combination of polymeric aryloxy radicals is that no satisfactory resonance structure can be written which places the unpaired electron in the terminal ring. Bolon (4) prepared the stable radical from 2,6-di-*tert*-butyl-4-phenoxyphenol and found that there was no detectable spin transmission through even a single diaryl ether linkage.

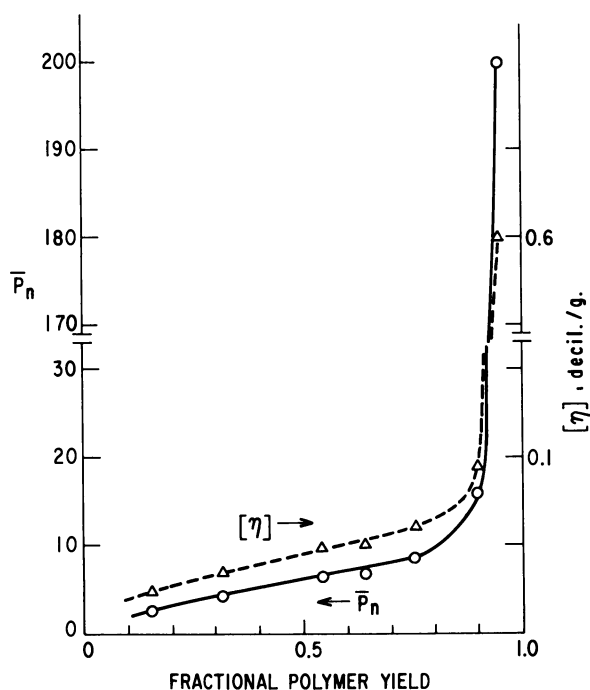
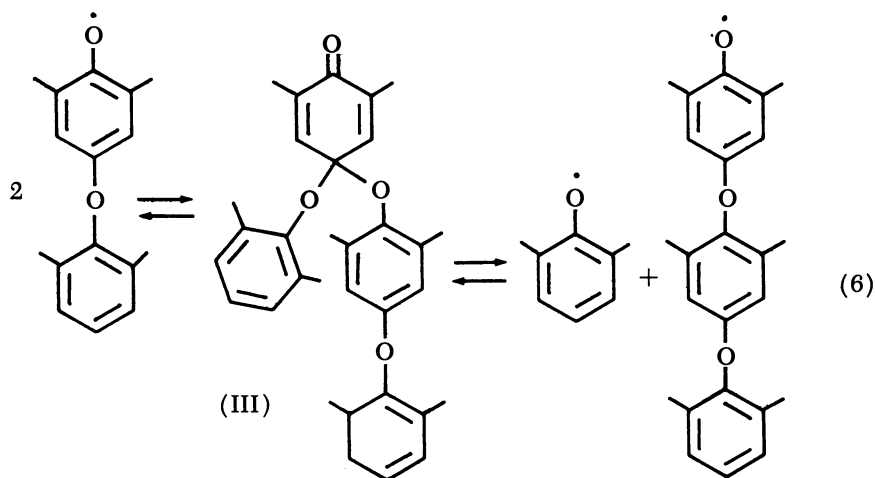


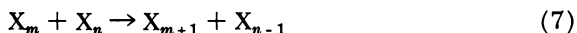
Figure 1. Variation of  $\bar{P}_n$  with conversion during oxidation of 2,6-xyleneol

**Quinone Ketal Redistribution.** This mechanism suggests that in the coupling of two aryloxy radicals the oxygen atom of one attacks at the para position of the phenolic ring of the second to yield the unstable quinone ketal. This rapidly decomposes either to yield the aryloxy radicals from which it was formed or two different aryloxy radicals, as shown

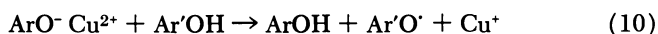
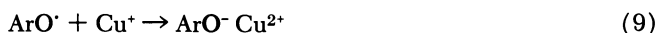
below for two dimer radicals:



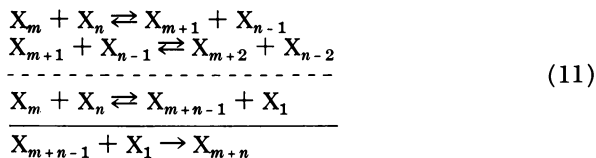
or, for any pair of radicals,



where the subscripts indicate the number of aromatic rings in each radical. This scheme must include steps allowing the reaction of aryloxy radicals with phenols to generate new aryloxy radicals, either directly or through oxidation-reduction reactions involving the catalyst.

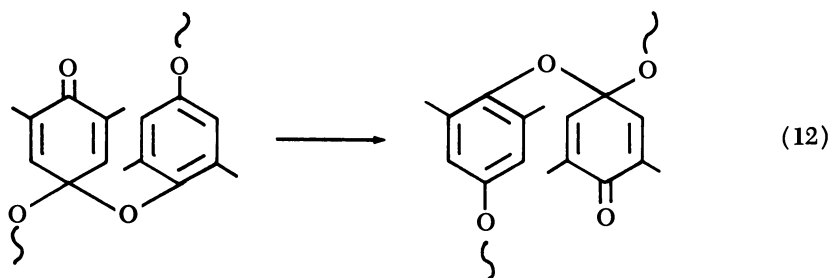


Reaction 7 does not change the average degree of polymerization of the system. If one of the radicals is a monomer radical, however, coupling according to Reaction 4 can occur, reducing the total number of molecules and increasing the average molecular weight. The net result of the formation of a monomer radical by disproportionation, followed by coupling with a polymer radical, is the same as would be produced by head-to-tail coupling of two polymer radicals, although the only growth step involves the addition of a single monomer unit.

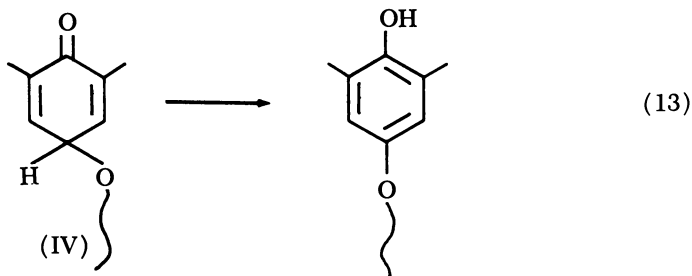


The sequence accounts satisfactorily for the production of polymer from low oligomers and for the shape of the DP-conversion curve in the oxidation of 2,6-xylenol. Formation of quinone ketals similar to III is, furthermore, a known reaction of hindered aryloxy radicals (1, 14). The major objection to this proposal is the great number of steps required to produce a monomer radical from two polymeric radicals of a high degree of polymerization.

**Quinone Ketal Rearrangement.** This mechanism likewise assumed the formation of quinone ketals as intermediates. Examination of models of III shows that the carbonyl oxygen of the ketal is within bonding distance of the para position of the next succeeding ring. Formation of a new carbon-oxygen bond, accompanied by the breaking of one of the ether linkages, leads to a new quinone ketal, in which the second ring has become the cyclohexadienone ring (Reaction 12).



A second rearrangement can place the third ring at the head of the sequence; if rearrangement proceeds until one of the terminal rings becomes the cyclohexadienone ring, enolization yields a polymeric phenol identical in every way, except for the order of succession of the rings, with that which would be produced by the direct head-to-tail coupling of aryloxy radicals (Reaction 13). The formation of a polymeric phenol





## QUINONE KETAL REARRANGEMENT MECHANISM

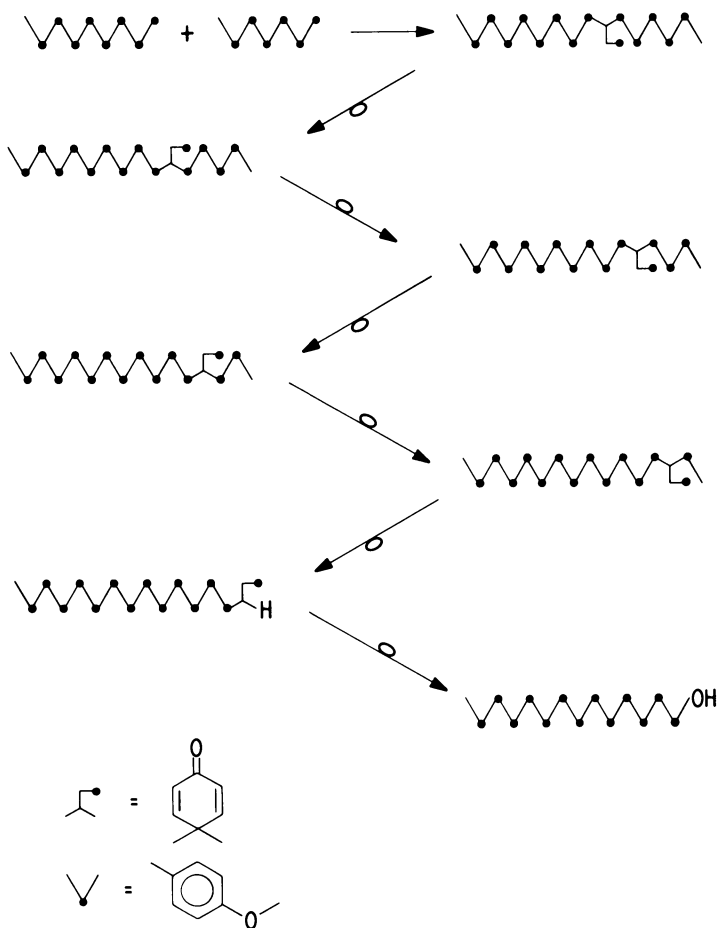
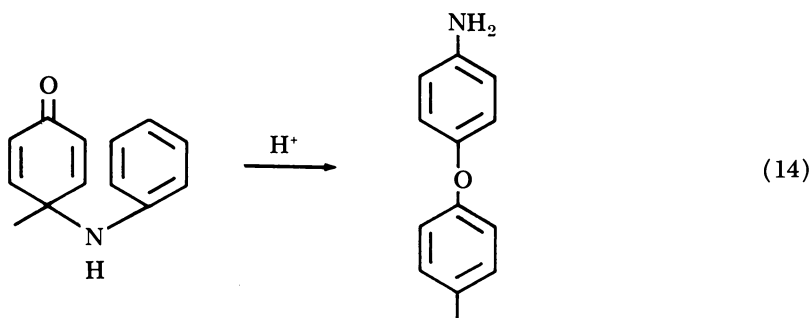


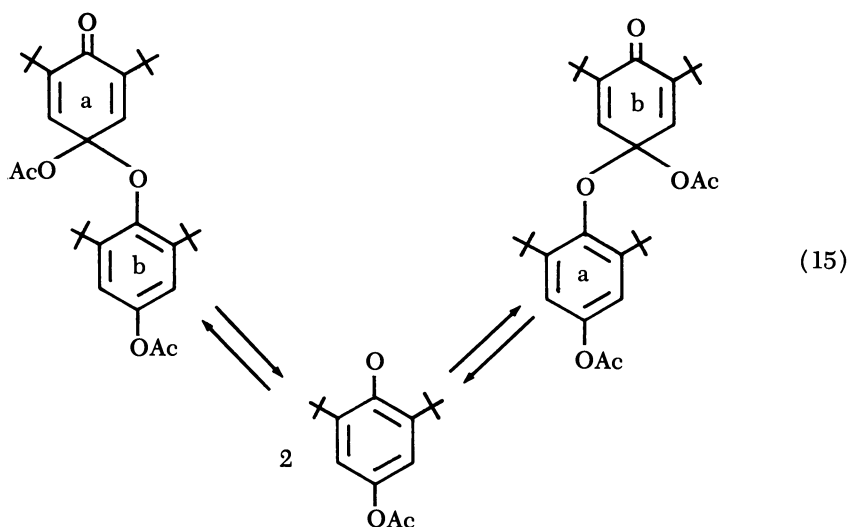
Figure 2. Coupling and rearrangement of polymeric aryloxy radicals

by coupling and rearrangement of two polymeric aryloxy radicals is illustrated schematically in Figure 2.

When Finkbeiner first proposed the ketal rearrangement mechanism, this type of reaction was unknown, but similar rearrangements of cyclohexadienones have been demonstrated since. Miller (25) has shown that the rearrangement of 4-anilino-cyclohexadienones to diaryl ethers is an intramolecular reaction, with a geometry almost identical to that of Reaction 12.



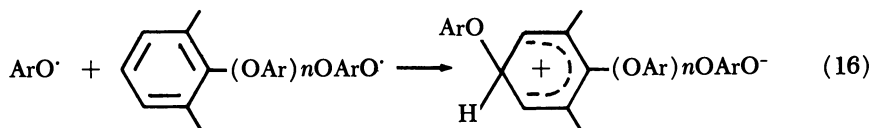
An even closer parallel is found in the work of Kreilick (33, 34), who prepared the ketal derived from 2,6-di-*tert*-butyl-4-acetoxyphe-*n*ol. From a study of the effect of temperature on line broadening in the NMR spectrum of this compound he concluded that rearrangement occurs both by dissociation to radicals and recombination and by a direct intramolecular process. The former corresponds to the key reaction of the redistribution mechanism, while the latter is entirely analogous to the ketal rearrangement mechanism (Reaction 15).



### Studies of Polymer Coupling Mechanism

The principal evidence in favor of Mechanism 1—endlinking of polymer radicals—is provided by Price's observation that when 2,6-xylenol labeled in the 4-position with tritium was oxidized, 23% of the

label was retained in the polymer (7). From this it was argued that polymer radicals coupled to give a "phenonium ion."



Proton migration before tautomerization would cause some of the label to be retained. However, migration could occur equally well during the addition of monomer units, a step common to all the proposed mechanisms (23). It must be concluded that this mechanism, although attractive because of its simplicity, lacks experimental verification.

Much of the evidence for the mechanism of polymer coupling rests on identification of the intermediate products of oxidation of low

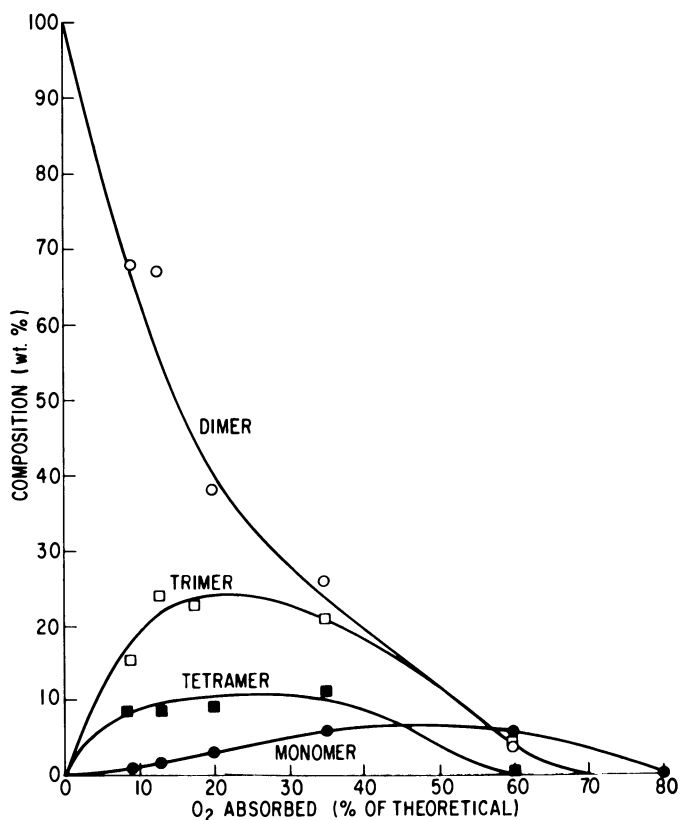


Figure 3. Composition of product from oxidation of 2,6-xyleneol dimer

oligomers. If either endlinking or ketal rearrangement operated exclusively, oxidation of the dimer would yield only tetramers, hexamers, and other species with an even number of aromatic rings. The products actually observed in this oxidation are shown in Figure 3 (10). The initial products are largely monomer and trimer; as the reaction proceeds, the concentration of monomer increases until at 50% completion monomer is by far the most abundant single species present.

Oxidation of trimer yields a mixture of monomer, dimer, trimer, and other low oligomers; monomer has been detected among the initial products of oxidation of a low molecular weight polymer fraction consisting largely of oligomers having six to nine rings. The formation of monomer, followed by its eventual disappearance, is strong evidence that the redistribution sequence outlined in Reaction 11 is a major route to polymer-polymer coupling in these instances. The importance of the redistribution processes is confirmed by the observation that adding monomer or a low oligomer to a polymerizing solution of 2,6-xyleneol causes a rapid reduction in solution viscosity, as the degree of polymerization of the polymer is reduced by redistribution with the monomer (Figure 4) (8).

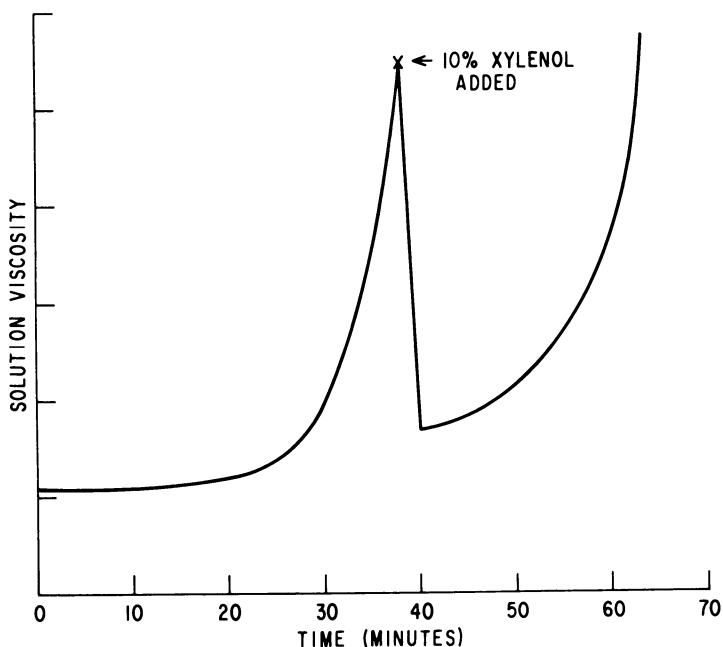
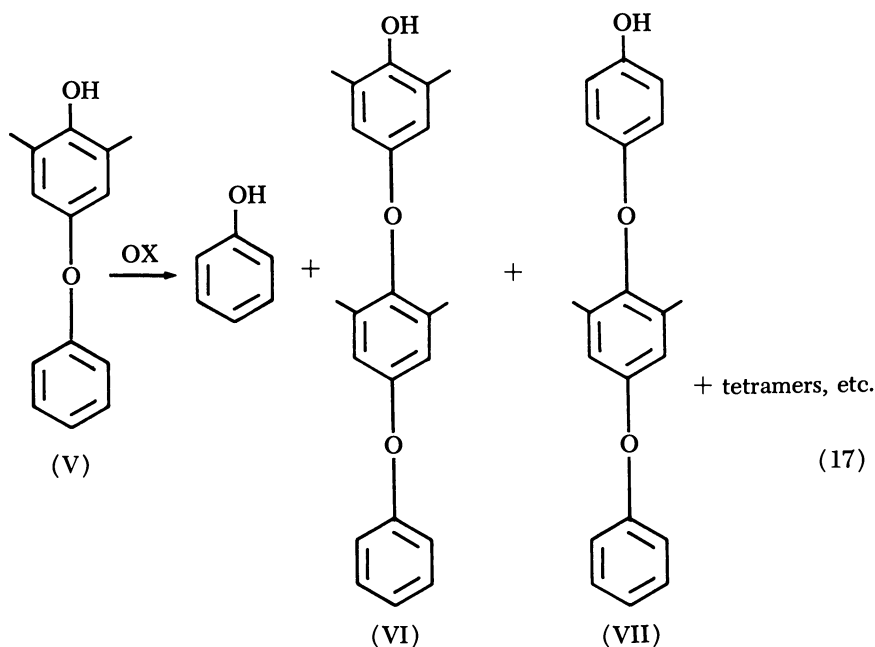


Figure 4. Effect of adding monomer to polymerizing solution of 2,6-xyleneol

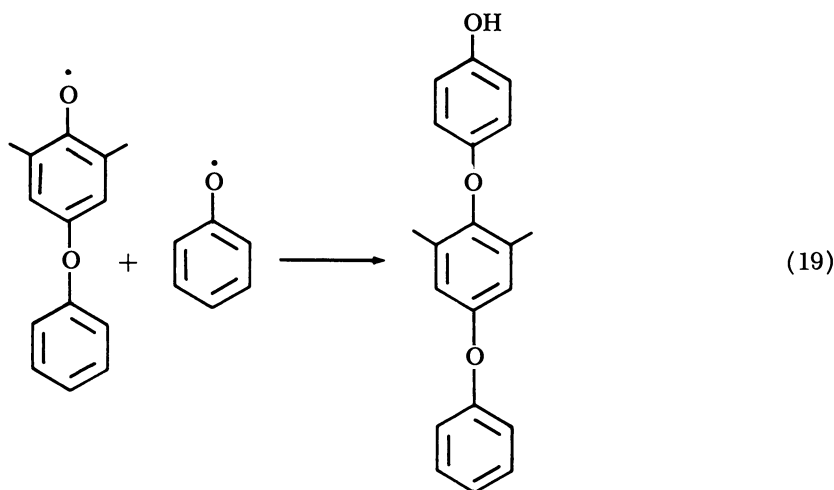
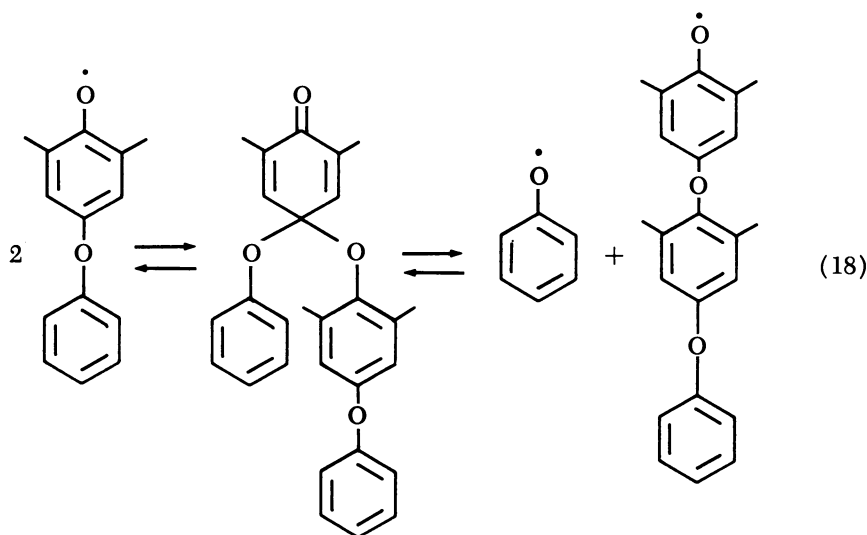
More information is available by examining the products of oxidation of "mixed dimers"—*i.e.*, dimers having different substitution patterns in the two rings. Cooper (9) showed that the initial products from oxidation of 2,6-dimethyl-4-phenoxyphenol (V) consisted largely of phenol and two trimers (Reaction 17).



Trimer VI and phenol are the products predicted from the first step of the redistribution reaction; trimer VII would be expected from coupling of some of the phenol with the starting dimer (Reactions 18 and 19).

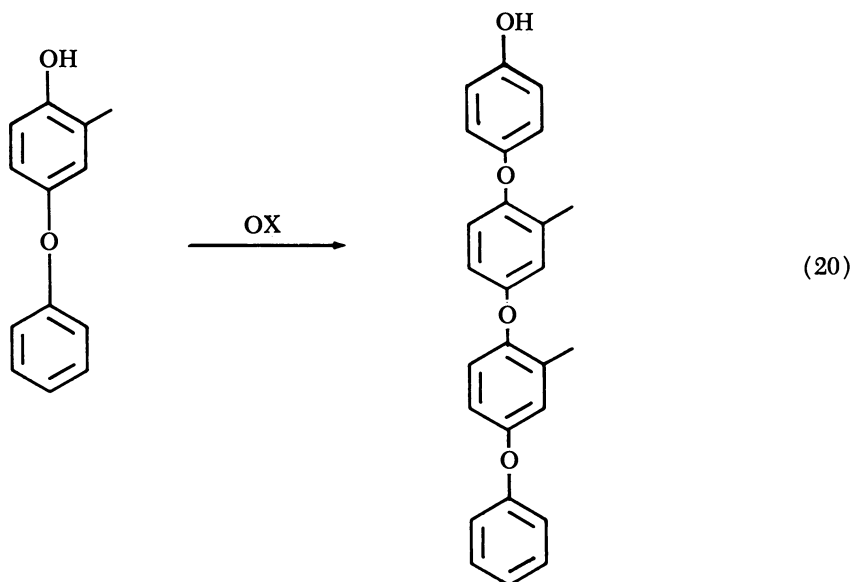
Similar results were obtained by Cooper and by Mijs *et al.* (24) from a number of other substituted dimers. With lightly substituted dimers, however, Mijs observed that at low temperatures the initial products consist almost entirely of tetramers; the tetramer, moreover, is that corresponding to the quinone ketal rearrangement, rather than to head-to-tail coupling (Reaction 20).

Recently, White (32) observed that under certain conditions ( $-15^{\circ}\text{C}$ ., large excess of amine base) oxidation of the dimer derived from 2,6-xyleneol with a limited amount of preoxidized copper complex yielded the tetramer as the major product, with small amounts of hexamer and only traces of monomer and trimer. The two rings are indistinguishable in this case, but there is little doubt, in view of the results of Mijs, that

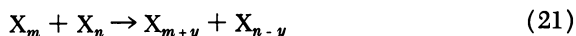


the tetramer was formed by rearrangement of the quinone ketal rather than by endlinking.

The experiments cited above show that redistribution, presumably *via* a quinone ketal intermediate, occurs during the oxidative polymerization of 2,6-xyleneol and must be responsible at least partially for the polycondensation characteristics of the reaction. Although the conditions under which Mijs and White demonstrated rearrangement are different from those usually employed for oxidative polymerization of xyleneol, it appears certain that this process also contributes to the coupling of polymer molecules. Redistribution and rearrangement are complementary reactions. Dissociation into aryloxy radicals can occur at any point



during the rearrangement so that redistribution need not occur solely by transfer of a single unit as in Reaction 7; rearrangement followed by dissociation provides a path by which any number of monomer units may be transferred in what is essentially a single step:



White has obtained evidence for this process by examining the products of redistribution of monomer with high polymer. At low temperatures the products first formed did not consist only of dimer, as would be expected if redistribution occurred solely by Reaction 7; trimer, tetramer, and higher oligomers were initially present in more than their equilibrium ratio to dimer, indicating that several rearrangement reactions preceded the dissociation of the ketal.

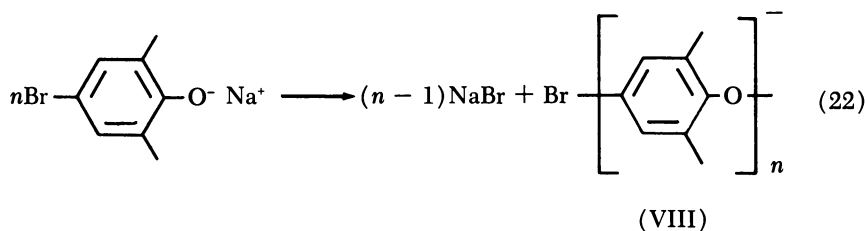
Although it is not ordinarily possible to separate the two processes, both rearrangement and redistribution undoubtedly occur during the oxidative polymerization of xylenol, with the relative contribution of each to polymer coupling determined by reaction conditions. The possibility that other reactions, such as the endlinking of Reaction 17, also contribute cannot be excluded, but no other reactions are required to explain the experimental observations.

The experiments discussed above deal with the copper-amine catalyzed oxidation of 2,6-xyleneol, but oxidation of xylenol by metal oxides takes place by the same mechanism (22). The oxidative coupling of other 2,6-disubstituted phenols has the same characteristics as the oxida-

tion of xylenol (low oligomers may be oxidized to linear polymer, a growth curve typical of a polycondensation process). Redistribution has been shown to accompany polymerization in all cases studied, so that it appears that all the oxidative polymerizations leading to linear poly(1,4-arylene oxides) proceed by essentially the same mechanism.

### *Other Condensations Leading to Poly(arylene oxides)*

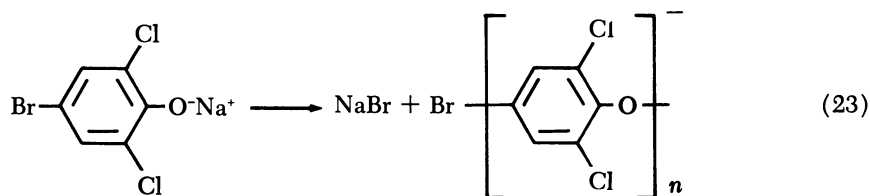
The term "oxidative polymerization" has been used above to describe the reaction in which the substituted phenol reacts with oxygen or another oxidizing agent to eliminate a molecule of hydrogen (usually appearing as water in the product) and form a poly(arylene oxide). Another route to linear poly(1,4-arylene) oxides is by the oxidative elimination of halide ion from certain 4-halophenoxides. This reaction was studied over a number of years by Hunter (20), who obtained low molecular weight, probably branched, polymers from a number of polyhalophenols. Recently, high molecular weight linear polymers have been obtained by this route. Two examples are of particular interest. Price (28) found that in a two-phase system consisting of aqueous base and a suitable polymer solvent 2,6-dimethyl-4-bromophenol reacted with traces of ferricyanide, benzoyl peroxide, or other initiators to form poly(2,6-dimethyl-1,4-phenylene oxide), identical except for the end groups, with that produced by oxidative polymerization of xylenol (Reaction 22).



In a two-phase system similar to that used by Price, Stamatoff (29) obtained from 2,6-dichloro-4-bromophenol a branched polymer having approximately the statistical ratio of ortho and para ether linkages. When the reaction was carried out using the anhydrous salt of the phenol in the presence of highly polar aprotic solvents, such as dimethyl sulfoxide, the product was the linear poly(2,6-dichlorophenylene oxide) (Reaction 23).

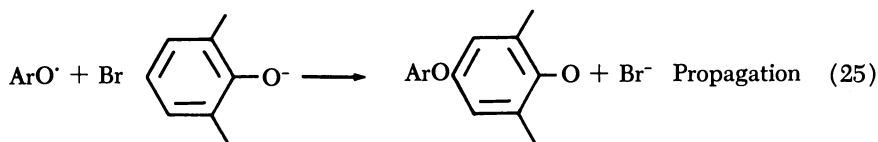
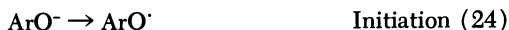
These condensations, like the oxidative coupling of phenols, presumably are free radical chain reactions with aryloxy radicals as intermediates, but the gross features of the two types of reactions are quite different. At low extents of oxidation the oxidative coupling reaction





yields only low oligomers, as expected of a polycondensation. Price and Shu, however, showed that when the oxidative dehalogenation reaction was carried out under nitrogen, an increase in initiator caused an increase in polymer yield but had little effect on molecular weight; high polymer was obtained even at low conversions (27). These are characteristics of a process involving stepwise addition of monomer units, as in radical-initiated vinyl polymerization.

Price proposed a mechanism in which the propagation step involves attack of the polymeric aryloxy radical on the monomer anion, displacing bromide ion and generating a new aryloxy radical; termination is by coupling (possibly ortho) of two radicals.



This sequence explains Price's observations adequately and seems to be required in this particular case. The oxidative elimination of halide ion from salts of phenols does not always follow this course, however. In the peroxide-initiated condensation of the sodium salt of 2,6-dichloro-4-bromophenol (Reaction 23) molecular weight continues to increase with reaction time after the maximum polymer yield is obtained (Figure 5) (8). Furthermore, Hamilton and Blanchard (15) have shown that the dimer of 2,6-dimethyl-4-bromophenol (VIII,  $n = 2$ ) is polymerized rapidly by the same initiators which are effective with the monomer. Obviously, polymer growth does not occur solely by addition of monomer units in either Reaction 22 or 23; some process leading to polymer-polymer coupling must also be possible. Hamilton and Blanchard explained the formation of polymer from dimer by redistribution between polymeric radicals to form monomer radicals, which then coupled with polymer, as in Reaction 11. Redistribution has indeed been shown to occur under

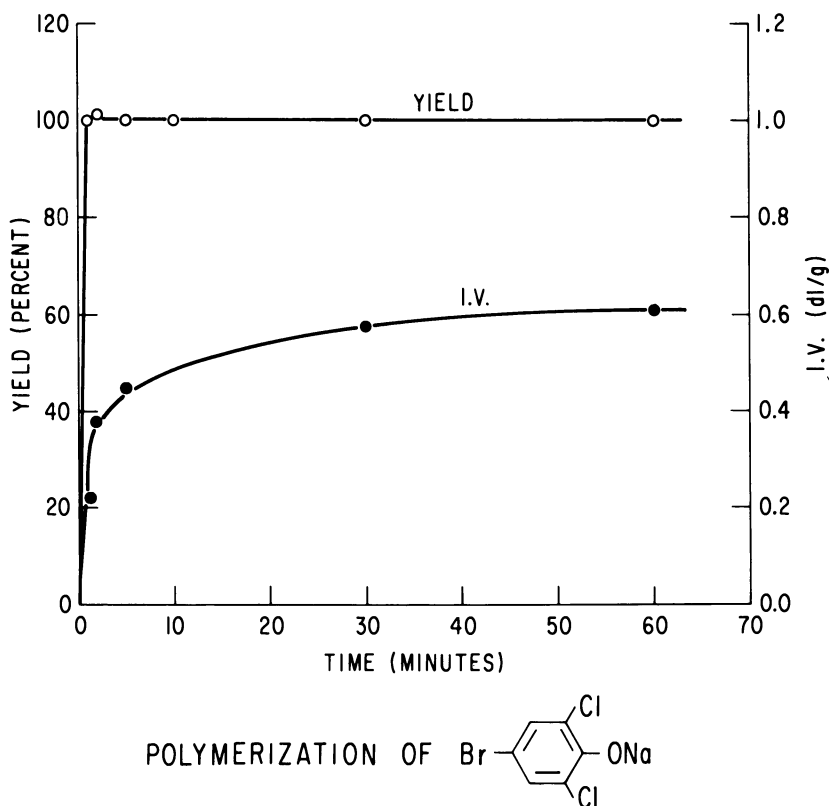


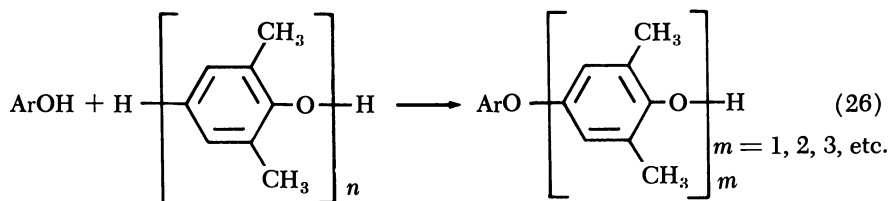
Figure 5. Yield and intrinsic viscosity of polymer in the peroxide-initiated condensation of sodium 2,6-dichloro-4-bromophenolate

the polymerization conditions in both Reaction 9 and 15, but it has not been established that it is important to the polymer growth reaction (8, 15).

### *Consequences of Redistribution*

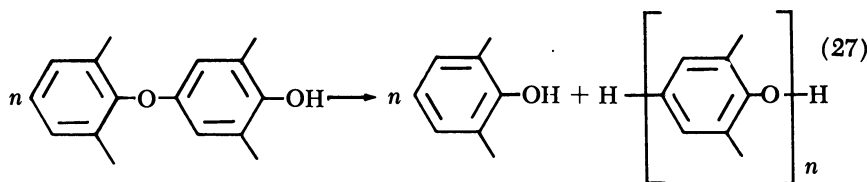
Redistribution reactions are common among condensation polymers having in the recurring unit a functional group capable of reacting with other groups or with the end groups of the polymer molecule, but it is surprising to find these reactions in the poly(arylene oxides), which have as the only functional group in the recurring unit the diaryl ether linkage, ordinarily an extremely unreactive group. The mechanistic studies cited above demonstrate, however, that redistribution of polymers of Structure I occurs with great ease.

**Redistribution of Monomer with Polymer.** Cooper *et al.* (11) showed that traces of oxidizing agents converted a mixture of equal weights of 2,6-xylenol and poly(2,6-dimethyl-1,4-phenylene oxide) to a mixture of monomer, dimer, trimer, and other low oligomers; the composition was identical with that obtained from pure dimer under the same conditions. Phenols other than xylenol may be used, yielding a mixture of low oligomers having the terminal unit derived from the added phenol and all others from the polymer (Reaction 26).



This procedure has been used by White (31) to prepare substituted diaryl ethers, many of them not readily available by other routes.

**Polymer-Polymer Redistribution.** The redistribution reaction causes no change in the over-all degree of polymerization of the system. If the monomer formed by redistribution is removed continuously, however, the molecular weight of remaining polymer necessarily increases. High polymer has been prepared in this way from the dimer II, xylenol being removed either by distillation or by extraction with alkali (3, 9):



At high temperatures redistribution of poly(arylene oxides) may occur in the absence of added initiators. This sometimes causes changes in molecular weight distribution. If the distribution is initially very broad, it is narrowed by heating; the opposite effect, broadening of an initially narrow distribution, should also be possible, but has not yet been observed. Figure 6 shows the effect of heating at 275°C. for 3 hours on the distribution of an artificial blend made by combining two polymers of widely different molecular weight. Redistribution is obviously extensive, although not complete, probably because of the presence of some polymer molecules not having the perfectly regular structure of I. No

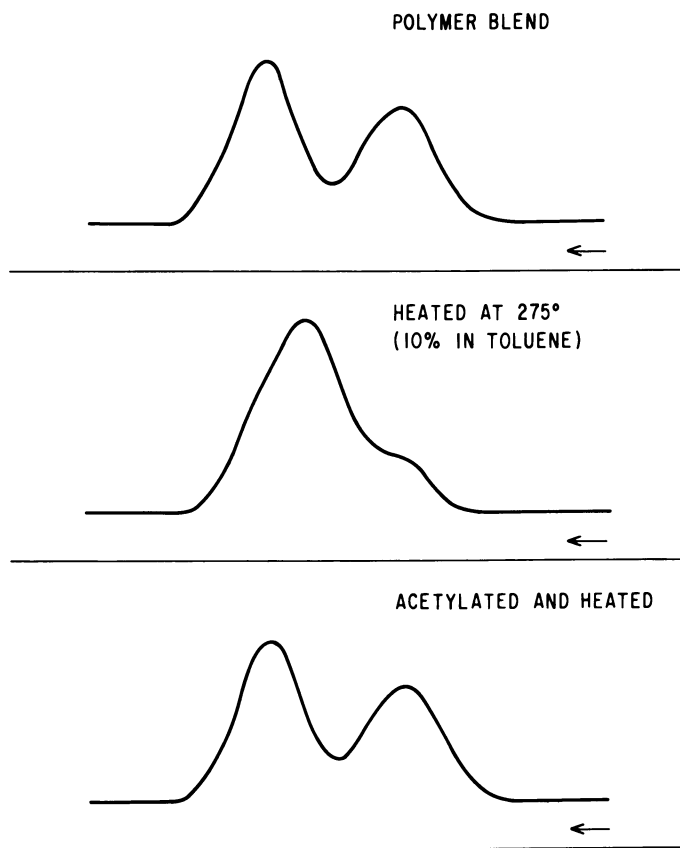


Figure 6. Gel permeation chromatograms showing redistribution of poly(2,6-dimethyl-1,4-phenylene) oxide

further changes in distribution were observed on continued heating. This thermal redistribution, like the other types mentioned above, is eliminated completely when the terminal hydroxyl groups are converted to ester or ether groups. Facile redistribution requires: (1) 2,6-disubstitution, (2) 1,4-arylene ether linkages, and (3) a free terminal hydroxyl group (8).

#### Literature Cited

- (1) Becker, H. D., *J. Org. Chem.* **29**, 3068 (1964).
- (2) Blanchard, H. S., Cooper, G. D., unpublished work.
- (3) Blanchard, H. S., Finkbeiner, H. L., Endres, G. F., *SPE Trans.* **2**, 110 (1962).
- (4) Bolon, D. A., *J. Am. Chem. Soc.* **88**, 3148 (1966).
- (5) Bolon, D. A., private communication.
- (6) Bolon, D. A., Gilbert, A. R., *Polymer Letters* **5**, 277 (1967).
- (7) Butte, W. A., Price, C. C., *J. Am. Chem. Soc.* **84**, 3567 (1962).

- (8) Cooper, G. D., *Natl. Conf. Redistribution Reactions*, N.Y. Acad. Sci., June 1967.
- (9) Cooper, G. D., "Abstracts of Papers," Western Regional Meeting, ACS, December 1965.
- (10) Cooper, G. D., Blanchard, H. S., Endres, G. F., Finkbeiner, H. L., *J. Am. Chem. Soc.* **87**, 3996 (1965).
- (11) Cooper, G. D., Gilbert, A. R., Finkbeiner, H. L., *ACS, Div. Polymer Chem. Preprints* **7**, 166 (1966).
- (12) Endres, G. F., Kwiatek, J., *J. Polymer Sci.* **58**, 593 (1962).
- (13) Finkbeiner, H. L., Endres, G. F., Blanchard, H. S., Eustance, J. W., *SPE Trans.* **2**, 110 (1962).
- (14) Forrester, A. R., Hay, J. M., Thomson, R. H., "Organic Chemistry of Stable Free Radicals," p. 281, Academic Press, New York, 1968.
- (15) Hamilton, S. B., Blanchard, H. S., *J. Org. Chem.*, in press.
- (16) Hay, A. S., *J. Polymer Sci.* **58**, 581 (1962).
- (17) Hay, A. S., U. S. Patent **3,306,875** (1967).
- (18) Hay, A. S., *Advan. Polymer Sci.* **4**, 496 (1967).
- (19) Hay, A. S., Blanchard, H. S., Endres, G. F., Eustance, J. W., *J. Am. Chem. Soc.* **81**, 6335 (1959).
- (20) Hunter, W. H., Dahlen, M. A., *J. Am. Chem. Soc.* **84**, 2459 (1932).
- (21) Huysmans, W. G. B., Waters, W. A., *J. Chem. Soc. (B)* **1967**, 1163.
- (22) Lidgren, B. O., *Acta Chem. Scand.* **14**, 1203, 2089 (1962).
- (23) McNelis, E., *J. Org. Chem.* **31**, 1255 (1966).
- (24) Mijs, W. J., von Lohuisen, O. E., Bussink, J., Vollbracht, L., *Tetrahedron* **23**, 2253 (1967).
- (25) Miller, B., *J. Am. Chem. Soc.* **86**, 1127 (1964).
- (26) Muller, E., Ley, K., *Ber.* **87**, 922 (1954).
- (27) Price, C. C., Shu, N. S., *J. Polymer Sci.* **61**, 135 (1962).
- (28) Staffin, G. D., Price, C. C., *J. Am. Chem. Soc.* **82**, 3632 (1960).
- (29) Stamatoff, G. S., U. S. Patent **3,257,358** (1966).
- (30) Van Dort, H. M., de Jonge, C. R. H. I., Mijs, W. J., *J. Polymer Sci., Pt. C* **22**, 431 (1968).
- (31) White, D. M., *J. Org. Chem.* **34**, 297 (1969).
- (32) White, D. M., "Abstracts of Papers," 155th Meeting, ACS, April 1968, T103.
- (33) Williams, D. J., Kreilick, R., *J. Am. Chem. Soc.* **89**, 3408 (1967).
- (34) *Ibid.*, **90**, 2775 (1968).

RECEIVED March 26, 1968.

# Polymerization of Primary Aromatic Diamines to Azopolymers by Oxidative Coupling

HARTWIG C. BACH

Monsanto Co., Textiles Division, Technical Center, P. O. Box 1507,  
Pensacola, Fla. 32502

W. BRUCE BLACK

Chemstrand Research Center, Inc., Durham, N. C.

*Catalyzed oxidative coupling of primary aromatic diamines yields linear polymers containing the oxidatively formed aromatic azo linkage. The generally applicable coupling reaction is conducted under mild conditions with oxygen (air) as the oxidant and a cupric ion/nitrogen base complex as the homogeneous catalyst. Tertiary amines such as pyridine as well as N,N-disubstituted amides such as dimethyl acetamide or hexamethyl phosphotriamide serve as activating catalyst ligands. Fully aromatic azopolymers exhibit good thermal stability to temperatures above 300°C.; they are colored and highly crystalline. A fiber of one of the compositions was spun. It showed good tensile properties (tenacity, 4.4 grams/denier; elongation, 9.0%; tensile modulus, 93 grams/denier) which were retained to a comparatively large degree at elevated temperatures and under the degrading influence of light.*

**D**uring the last decade, catalyzed oxidative coupling has gained widespread interest as a novel and general polymerization method. Various polymer systems of scientific and commercial interest have been prepared by this novel technique. Such polymer systems include: poly-(phenylene oxides) (9, 13, 25), of which poly(2,6-dimethylphenylene oxide) (PPO) is produced commercially; polyphenylenes (21); poly-

acetylenes (10, 11, 17, 18); polydisulfides (12), and polyazoaromatics (1, 2, 3, 19, 20, 30). The role of oxidative coupling in the biosynthesis of lignin (8), a naturally occurring polymer, has been recognized.

The reactions leading to the formation of these polymers—except polyphenylene—have one feature in common, although they otherwise differ greatly in mechanism: the crucial step in the reaction sequence is a one-electron transfer from the monomer to a transition metal ion serving as an electron acceptor. In addition to being an electron acceptor the transition metal ion is probably also involved in the coupling reaction by complexation of radical-like intermediates produced.

Most of the polymer-forming oxidative coupling reactions known are catalytic processes by virtue of the reoxidation of the transition metal ion with an oxidant, preferably oxygen (air). Cupric-cuprous complexes serve most prominently as catalysts (1, 2, 3, 9, 10, 11, 12, 17, 18, 19, 20, 30); manganese (24) and cobalt (6) complexes have also been used.

In the last few years, the catalyzed oxidative coupling of primary aromatic diamines has been investigated extensively in our laboratories (1, 2, 3) and also by Kotlyarevskii (19, 20, 30). Results of these investigations are reviewed in this chapter as well as the properties of the class of aromatic azopolymers.

### **Experimental**

Monomers not commercially available were prepared by known methods: 4,4'-bis(*p*-aminophenyl)-2,2'-bithiazole (22), 2,5-bis(*p*-aminophenyl)oxadiazole (22), *N,N'*-bis(*p*-aminophenyl)isophthalamide (27), *N,N'*-*m*-phenylenebis(*m*-aminobenzamide) (23), and 1,4-bis(*p*-aminophenyl)butadiene (16). Cuprous chloride was obtained by ascorbic acid reduction of  $\text{CuCl}_2$  according to Stathis (26).

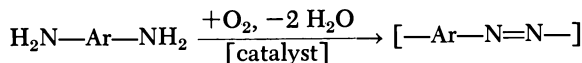
All polymerizations were conducted in a stirred, closed system, with oxygen at atmospheric pressure as the gas phase. Oxygen absorption was measured by an oxygen buret, which formed an integral part of the system. Depending on the reactivity of the diamine used, the reactions were run at room temperature or at slightly elevated temperatures (up to 90°C.) in pyridine, dimethyl acetamide, hexamethyl phosphortriamide, or mixtures of these.

In a typical example 0.5 gram (0.0025 mole) of  $\text{Cu}_2\text{Cl}_2$  was oxidized with oxygen in 50 ml. pyridine. After adding 3.46 grams (0.01 mole) of 4,4'-bis(*p*-aminophenyl)isophthalamide, the stirred reaction mixture absorbed 255 ml. of  $\text{O}_2$  in 195 minutes at 25°C. (theory: 244 ml. of  $\text{O}_2$  at 25°C.). The polymer was isolated in quantitative yield by coagulation in water.

Inherent viscosities were determined at 30°C. with solutions of 0.5 gram polymer in 100 ml. of concentrated  $\text{H}_2\text{SO}_4$ , dimethyl acetamide-pyridine, or dimethyl acetamide.

**Results and Discussion**

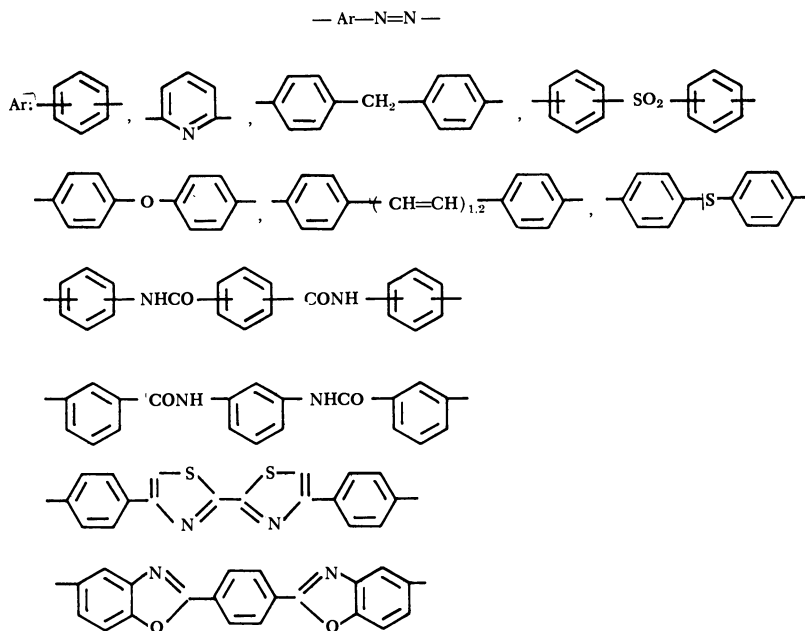
**Oxidative Coupling Reaction.** Catalyzed oxidative coupling of primary aromatic diamines with oxygen as the oxidant yields linear polymers according to the following scheme:



Ar: aromatic, heterocyclic, aromatic-heterocyclic, aromatic-aliphatic bi-valent radical

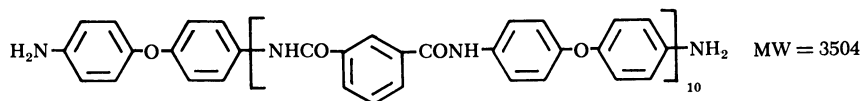
In studying this novel oxidative polymerization we investigated the following points in particular: (a) scope of the reaction, (b) side reactions, (c) catalysis, (d) molecular weights obtainable, (e) properties of aromatic azopolymers in bulk and fabricated form.

Catalyzed oxidative coupling is generally applicable to simple primary aromatic diamines as well as to diamines of a complex structure. The scope of the reaction is exemplified by some of the polymers prepared:

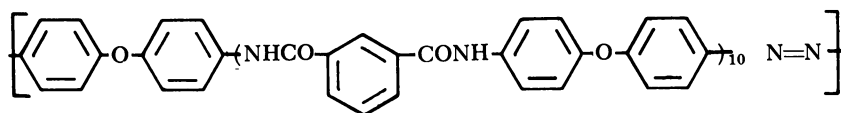


This oxidative polymerization also proved to be applicable to long chain prepolymers of a molecular weight of several thousand having terminal primary aromatic amine groups. For example, the following prepolymer

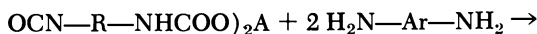




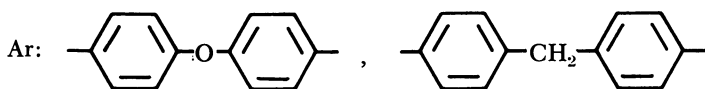
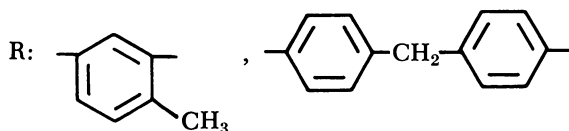
having an inherent viscosity of 0.28 (30°C., 0.5 gram of polymer in 100 ml. dimethyl acetamide/5% LiCl) was prepared by low temperature solution polycondensation of isophthaloyl chloride with a 10% molar excess of 4,4'-diaminodiphenyl ether. This prepolymer was treated in dimethyl acetamide (DMAc)/pyridine (6:1) solution with oxygen in the presence of the cupric-cuprous redox couple. By rapid low temperature oxidative polymerization the linear, high molecular weight azoblock copolymer



was obtained having an inherent viscosity of 2.8 (30°C., 0.5 gram of polymer in 100 ml. of DMAc/5% LiCl). A clear, strong and hot-drawable film could be cast from the polymer solution obtained. Similarly, predominantly aliphatic prepolymers with terminal aromatic amine end groups were prepared by successive reaction of aliphatic polyester or polyether diols with aromatic diisocyanates and aromatic diamines



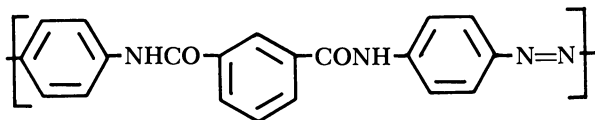
A: poly[ethylene(80%)/propylene(20%)] adipate      MW = 1900  
or poly(tetramethylene glycol)      MW = 1100



Addition of cuprous chloride to these prepolymers in a DMAc/pyridine solution and subsequent oxygenation led to the formation of high molecular weight polymers from which strong, elastic and hot-drawable

films were obtained by casting of the polymerization dope. The prepolymer solutions cast as controls did not yield coherent films.

Side reactions in the oxidative coupling of primary aromatic diamines to azopolymers could severely limit the molecular weights of polymers obtainable and disrupt their ordered, linear structure. To investigate this point the following polymer



was prepared by two independent routes: (a) oxidative coupling of bis(*p*-aminophenyl)isophthalamide, and (b) solution polymerization of 4,4'-diaminoazobenzene with isophthaloyl chloride. The polymers obtained were identical in their infrared spectra (1, 2, 3) and other properties; this is strong evidence that azolinkages are formed exclusively in the oxidative coupling of aromatic diamines.

The described oxidative polymerization is truly a catalyzed reaction. *p*-Phenylenediamine—an easily oxidizable aromatic amine—was subjected to oxygenation with and without cupric ion/nitrogen base complex present. Only the oxygenation in the presence of the catalyst yielded polymeric material; oxygen absorption was minimal without the catalyst.

In the oxidative coupling of primary aromatic diamines to azopolymers cupric ion/nitrogen base complexes serve as homogeneous catalysts. Such complexes are best prepared *in situ* by oxygenating a cuprous species, preferably CuCl or Cu<sub>2</sub>O/HCl, in the presence of the nitrogen base. Cupric salts investigated except for cupric acetate yielded inactive species.

The selection of the nitrogen base which also forms part of the solvent system is critically important. A suitable nitrogen base must fulfill the following requirements:

(a) It must yield an active catalyst which is soluble in the reaction medium.

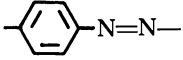
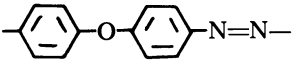
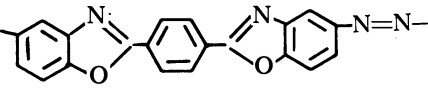
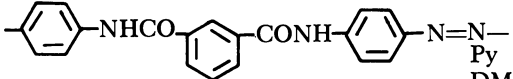
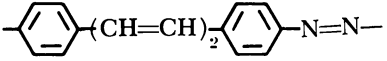
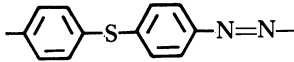
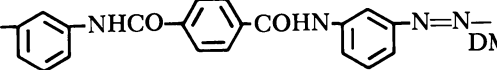
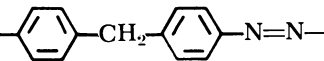
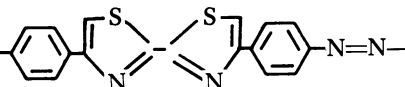
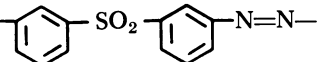
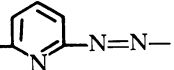
(b) It must be nonoxidizable by the cupric ion at the reaction conditions, therefore excluding secondary or primary amines.

(c) It must have at least some solubilizing power for the azopolymers prepared.

Pyridine, a tertiary amine, yields a very active catalyst complex, [Py<sub>2</sub>Cu<sup>II</sup>(OH)Cl] (7), for the coupling reaction giving high rates of oxidation at low temperatures. However, molecular weights of the azopolymers preparable in this medium proved to be somewhat limited (*see* Table I) owing to the generally low solubility of the azopolymers formed.

Use of DMAc (1, 2, 3)—an excellent solvent for aromatic condensation polymers—as a cosolvent gave polymers of considerably higher molecular weight. Some comparative results are given in Table I. Because of the greater polymer solubility and the consequently higher molecular weights possible, strong films of several compositions could be prepared directly from the polymerization solution.

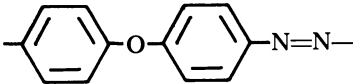
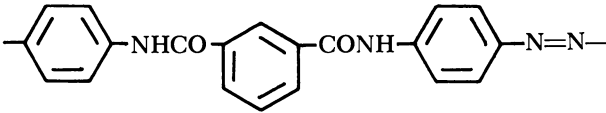
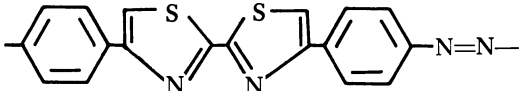
Table I. Aromatic Condensation Polymers

	Polymer	Reaction Medium	IV <sup>a</sup>
I		Py DMAc/Py (4:1)	0.23 0.41
II		Py DMAc/Py (4:1)	0.25 1.1
III		Py DMAc/Py (1:1)	0.37 0.81
IV		Py DMAc/Py (3:2)	0.64 2.1
V		DMAc/Py (4:1)	2.0
VI		DMAc/Py (4:1)	0.18
VII		DMAc/Py (4:1)	0.40
VIII		Py	0.55
IX		Py	0.67
X		Py	0.11
XI		Py	0.09

<sup>a</sup>Inherent viscosity (solution of 0.5 gram of polymer in 100 ml. of concentrated H<sub>2</sub>SO<sub>4</sub> at 30°C.).

In the investigation of catalyst-solvent systems it was found that not only tertiary amines but also *N,N*-disubstituted amides such as dimethyl acetamide (3) or hexamethyl phosphortriamide (HPT) yield catalytically active cupric-cuprous complexes. Some results obtained with these catalysts are shown in Table II.

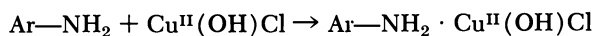
**Table II. Results on Catalyst-Solvent Systems**

Polymer	Solvent	IV <sup>a</sup>
	HPT DMAc	0.61 0.39
	DMAc	0.22
	DMAc	0.91

<sup>a</sup> Inherent viscosity (solution of 0.5 gram of polymer in 100 ml. of DMAc at 30°C.).

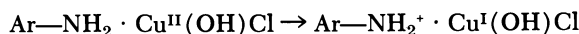
In the cupric ion-catalyzed reaction of primary aromatic diamines with oxygen four key steps can be recognized (shown for a monoamine with nitrogen base ligands left out for convenience):

(1) Complex Formation:



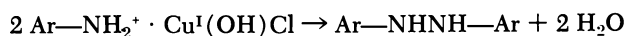
This first step would involve the displacement of a pyridine ligand by the aromatic amine. Some evidence points to this being the rate-determining step. A strict positive correlation between the basicity of the diamine relative to pyridine and the oxidative coupling rate (as measured by the oxygen absorption) was established (3).

(2) Electron Transfer:



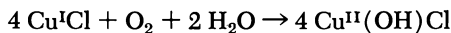
This step leads to an amine radical-cation or possibly to a complexed amine radical  $\text{Ar-NH} \cdot \text{Cu}^{\text{I}}\text{Cl}$ .

(3) Coupling:



The intermediately formed hydrazine linkages would be oxidized to azo-linkages in a subsequent reaction considerably faster than the oxidation of the amine as shown by Terent'ev (28, 29) for diphenylhydrazines.

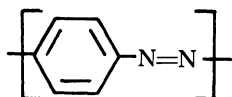
(4) Catalyst Reoxidation:



**Aromatic Azopolymers.** Through the described catalyzed oxidative coupling of primary aromatic diamines a great variety of aromatic azopolymers has become easily accessible. Therefore, an investigation of their properties in bulk as well as fabricated form seemed warranted.

**COLOR.** All aromatic azopolymers are colored owing to the strongly chromophoric azogroup. Even the azoblock copolymer derived from a phenyl oxide-isophthalamide backbone (discussed earlier) which has only one azogroup per repeat unit of a molecular weight of 3500 is bright yellow. Naturally, the shade of color of individual polymers depends on the structure of the repeat unit; as expected, fully conjugated polymers

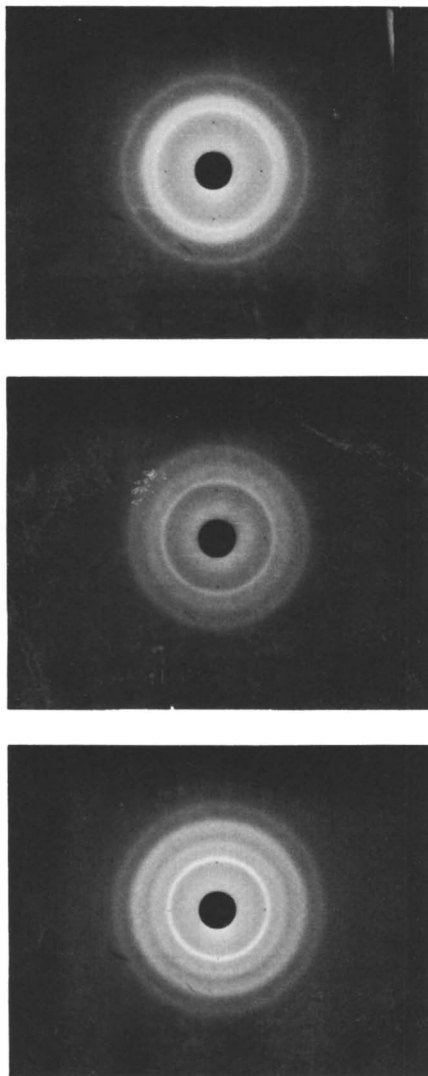
such as:



are essentially black.

**CRYSTALLINITY.** Aromatic azopolymers show a high degree of crystallinity without annealing. X-ray diffraction patterns of three representative polymers are shown in Figure 1. The high degree of crystallinity of as prepared poly(azophenylene oxide) is surprising in view of the fact that other polymers such as PPO (15) and Bakelite polysulfone (14) having a predominance of aromatic ether linkages in the backbone show little or no crystallinity unless they are annealed for several days in a suitable solvent (4).

**THERMAL STABILITY.** In contrast to their aliphatic analogs aromatic azocompounds are rather stable thermally. This stability is also characteristic of azopolymers. Figures 2 and 3 show TGA diagrams of polymers (II, IV, IX) in nitrogen and in air. [The seemingly higher stability of II in air when compared with a nitrogen atmosphere could possibly be explained by a weight-gain arising from oxidation, thus compensating for some of the weight loss caused by expulsion of  $\text{N}_2$ .] As shown, the polymers are stable to more than  $300^\circ\text{C}$ .; catastrophic weight loss ( $\geq 10\%$ ) begins in the range  $360^\circ\text{--}420^\circ\text{C}$ . Rapid thermal degradation is always accompanied by a strong exotherm. This exotherm combined with the narrow range ( $360^\circ\text{--}400^\circ\text{C}$ .) of its occurrence irrespective of polymer structure indicates that the first step in the degradation is the elimination of the azogroup as molecular nitrogen.



*Figure 1. X-ray diffraction patterns of representative polymers*

*Top: Polymer II*

*Middle: Polymer IV*

*Bottom: Polymer VIII*

Fully aromatic azopolymers described show no melting or softening up to the temperature of thermal degradation. Therefore, films and fibers must be prepared from solution; films cast are strong, tough and flexible.

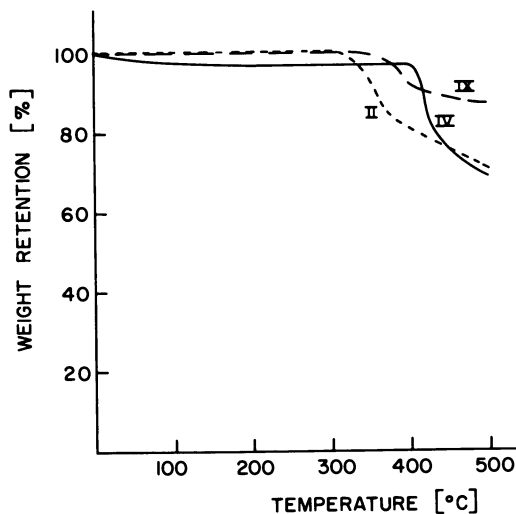


Figure 2. TGA in nitrogen; heating rate: 15°C./min.

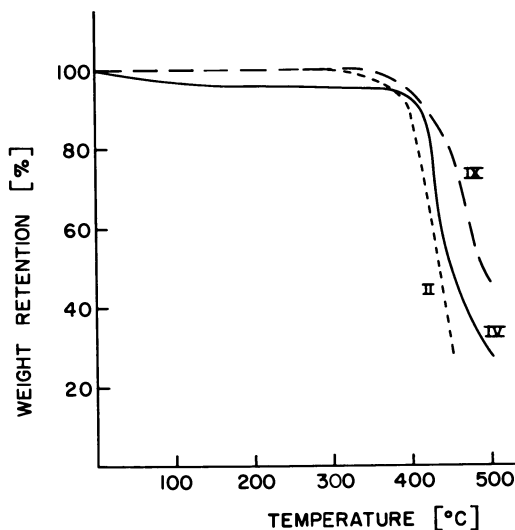


Figure 3. TGA in air. Heating rate: 15°C./min.

**FIBER PROPERTIES.** One of the polymers, the poly(isophthalamide) of 4,4'-diaminoazobenzene (IV), was selected for investigation of fiber properties of aromatic azopolymers. Table III shows standard tensile data of the "as spun" as well as the hot-drawn (1.5 $\times$ , 350°C.) fiber. As shown, this polymer has tensile properties fairly typical of an aromatic polyamide.

**Table III. Standard Tensile Data of an Azopolymer Fiber**

	<i>As Spun</i>	<i>Hot-Drawn</i>
Tenacity, grams/denier	2.5	4.4
Elongation, %	19.6	9.0
Tensile modulus, grams/denier	58	93

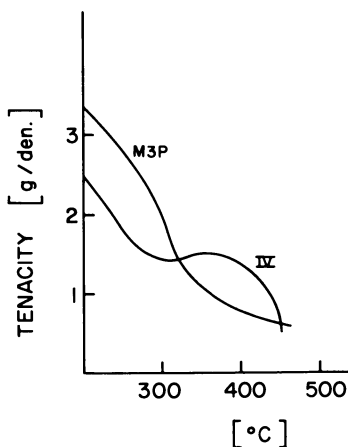
In view of the good stability of aromatic azopolymers at elevated temperatures, it is not surprising to find a fair retention of tensile properties up to about 400°C. (Table IV).

**Table IV. Tensile Properties at Varying Temperatures**

	<i>Fiber Temperature, °C.<sup>a</sup></i>				
	250	300	350	400	450
Tenacity, grams/denier	1.8	1.4	1.5	1.4	0.6
Elongation, %	5.7	8.7	6.6	4.8	1.4
Tensile modulus, grams/denier	47	37	39	40	47

<sup>a</sup> Fiber held 1 minute at temperature before test.

Figure 4 shows the retention of tenacity in percent of the original values compared with another aromatic polyamide, M3P, the polyterephthalamide of bis(*m*-aminobenzoyl)*m*-phenylenediamine (31).



*Figure 4. Retention of tenacity of polymer fibers at elevated temperature*

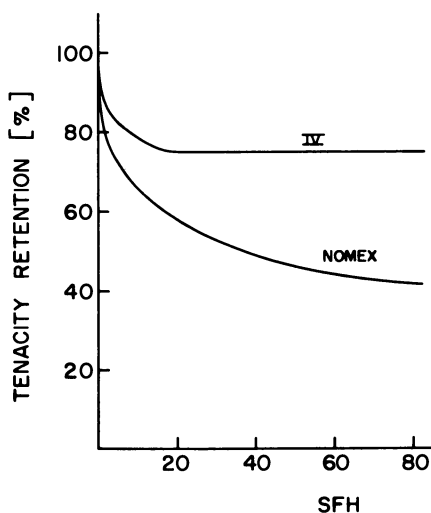
Fibers of Polymer IV show a comparatively strong resistance to light degradation (Table V). These values compare favorably with the



**Table V. Resistance of Fibers of Polymer IV to Light Degradation**

	<i>Standard Fading Hours<sup>a</sup></i>			
	0	20	40	80
Tenacity, grams/denier	4.4	3.3	3.3	3.3
Elongation, %	9.0	6.8	7.2	7.1
Tensile modulus, grams/denier	93	84	86	85

<sup>a</sup> Test according to A.A.T.C.C. Standard Test Method 16-A-1964 (Fade-Ometer, carbon arc).



*Figure 5. Retention of tenacity of polymer fibers upon exposure to light (carbon arc)*

strength retention (4) of a commercial aromatic polyamide as shown in Figure 5.

### **Conclusions**

As shown in recent investigations, catalyzed oxidative coupling of organic molecules provides a new and general route to a variety of hitherto only difficultly accessible polymer systems. While the literature on oxidative coupling reactions in polymer synthesis is already rather extensive, by further investigations of this reaction concept, particularly studies of the catalysis involved, oxidative coupling promises to rival conventional condensation and addition polymerization in importance.

### Acknowledgment

We wish to express our sincere appreciation to J. R. Sechrist for skillful and dedicated assistance, to H. S. Morgan and J. D. Fowler for spinning the fiber reported.

### Literature Cited

- (1) Bach, H. C., *ACS, Div. Polymer Chem., Polymer Preprints* **7**, 576 (1966).
- (2) *Ibid.*, **8**, 610 (1967).
- (3) Bach, H. C., Black, W. B., *J. Polymer Sci. Pt. C*, in press.
- (4) Butte, W. A., Price, C. C., Hughes, R. E., *J. Polymer Sci.* **61**, S 28 (1962).
- (5) Du Pont Co., New Product Technical Information NP-33 (1963).
- (6) Finkbeiner, H. L., "Abstracts of Papers," 155th National Meeting, ACS, April 1968, p. 206.
- (7) Finkbeiner, H., Hay, A. S., Blanchard, H. S., Endres, G. F., *J. Org. Chem.* **31**, 549 (1966).
- (8) Freudenberg, K., *Science* **148**, 595 (1965).
- (9) Hay, A. S., Blanchard, H. S., Endres, G. F., Eustance, J. W., *J. Am. Chem. Soc.* **81**, 6335 (1959).
- (10) Hay, A. S., *J. Org. Chem.* **25**, 1275 (1960).
- (11) *Ibid.*, **27**, 3320 (1962).
- (12) Hay, A. S., U. S. Patent **3,294,760** (1966).
- (13) Hunter, W. H., Olson, A. O., Daniels, E. A., *J. Am. Chem. Soc.* **38**, 1761 (1916).
- (14) Johnson, R. N. *et al.*, *J. Polymer Sci. A-1*, **5**, 2375 (1967).
- (15) Karasz, F. E., O'Reilly, J. M., *Polymer Letters* **3**, 561 (1965).
- (16) Katz, L., Hein, D. W., Pretka, J. E., Long, R. S., U. S. Patent **2,852,556** (1958).
- (17) Korshak, V. V., Sladkov, A. M., Kudryavtsev, Yu. P., *Vysokomolekul. Soedin.* **5**, 793 (1963).
- (18) Kotlyarevskii, I. L., Fisher, L. B., Dulov, A. A., Slinkin, A. A., *Izv. Akad. Nauk SSSR, Otd. Khim. Nauk*, **1960**, 950.
- (19) Kotlyarevskii, I. L., Terpugova, M. P., Andrievskaya, E. K., *Izv. Akad. Nauk SSSR, Ser. Khim.* **1964** (10), 1854.
- (20) Kotlyarevskii, I. L., Svartsberg, M. S., Fisher, L. B., Sanina, A. S., Bardamova, M. A., Terpugova, M. P., *IUPAC Symp., Prague 1965, Preprints*, p. 497.
- (21) Kovacic, P., Kyriakis, A., *J. Am. Chem. Soc.* **85**, 454 (1963).
- (22) Preston, J., *J. Heterocycl. Chem.* **2**, 441 (1965).
- (23) Preston, J., *J. Polymer Sci. A-1*, **4**, 529 (1966).
- (24) Shono, T., Yamanoi, K., Shinra, K., *Makromol. Chem.* **105**, 277 (1967).
- (25) Staffin, G. D., Price, C. C., *J. Am. Chem. Soc.* **82**, 3632 (1960).
- (26) Stathis, E. C., *Chem. Ind. (London)* **1958**, 633.
- (27) Stephens, C. W., U. S. Patent **3,049,518** (1962).
- (28) Terent'ev, A. P., Mogilyanskii, Ya. D., *Dokl. Akad. Nauk SSSR*, **103**, 91 (1955).
- (29) Terent'ev, A. P., Mogilyanskii, Ya. D., *Zh. Obshch. Khim.* **31**, 326 (1961).
- (30) Terpugova, M. P., Kotlyarevskii, I. L., Andrievskaya, E. K., *Izv. Akad. Nauk SSSR*, **1966** (4), 713.
- (31) Weiss, J. O., Morgan, H. S., Lilyquist, M. R., *J. Polymer Sci. Pt. C*, **19**, 29 (1967).

RECEIVED April 1, 1968.

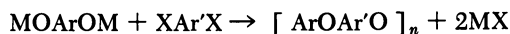
## The Kinetics of Solution Polycondensation of Aromatic Polyethers

S. R. SCHULZE and A. L. BARON

Celanese Plastics Co., Clark, N. J. 07066

*The kinetics of polycondensation by nucleophilic aromatic substitution in highly polar solvents and solvent mixtures to yield linear, high molecular weight aromatic polyethers were measured. The basic reaction studied was between a diphenoxide salt and a dihaloaromatic compound. The role of steric and inductive effects was elucidated on the basis of the kinetics determined for model compounds. The polymerization rate of the dipotassium salt of various bisphenols with 4,4'-dichlorodiphenylsulfone in methyl sulfoxide solvent follows second-order kinetics. The rate constant at the monomer stage was found to be greater than the rate constant at the dimer and subsequent polymerization stages.*

Recently, Johnson *et al.* (2) reported the synthesis of several aromatic polyethers by nucleophilic aromatic substitution reactions. These solution condensations take place between the diphenoxide salt of a bisphenol and an aromatic dihalide:



where M = alkali metal and X = halogen. The aromatic dihalide must have electron-withdrawing groups ortho or para to the halides to activate them sufficiently.

In this chapter we report on an investigation of the kinetics of this reaction with several monomers. Bunnett and Levitt have studied the kinetics of nucleophilic substitution between *p*-substituted bromobenzenes and sodium methoxide (1) and found these reactions to be second order. Therefore, for a polymer-forming reaction between difunctional reactants, one would expect a second-order reaction with respect to the concentra-

tion of functional (end) groups. The rate of reaction should therefore be written as

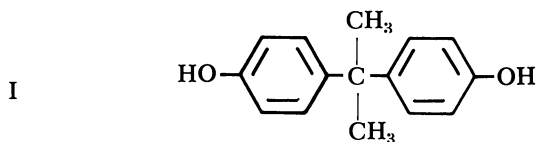
$$-\frac{d[\text{ArO}^-]}{dt} = k[\text{ArO}^-][\text{Ar}'\text{X}]$$

where the concentrations are expressed as equivalents of the functional groups per unit volume: phenoxide ( $\text{ArO}^-$ ) and aromatic halide ( $\text{Ar}'\text{X}$ ). Assuming equal concentrations of phenoxide and halide (which is necessary to achieve high molecular weight), this expression can be integrated to give:

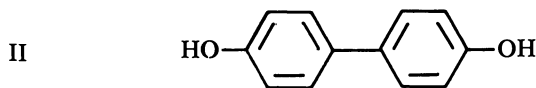
$$\frac{1}{C} = kt + \frac{1}{C_0}$$

where  $C$  = concentration of phenoxide (or halide) functional group, and  $C_0$  = initial concentration of functional group.

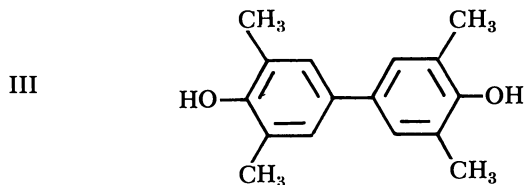
If the reaction rate of the functional groups is independent of the size of the molecule to which it is attached, the rate constant,  $k$ , should be truly constant during the polymerization. Thus, a plot of  $1/C$  vs.  $t$  should be linear with a slope equal to  $k$ . To test these ideas, the reaction rate of 4,4'-dichlorodiphenylsulfone with the potassium diphenoxide salts of three bisphenols was measured in dimethyl sulfoxide (DMSO) solvent. These bisphenols are shown below (I, II, and III).



2,2-Bis(*p*-hydroxyphenyl)propane (bisphenol A)



4,4'-Biphenol



3,5,3',5'-Tetramethyl 4,4'-biphenol

The reaction rates were measured by determining the concentration of phenoxide salt remaining at any given reaction time,  $t$ .

### Experimental

**Reagents.** "Para-Bis-A" polymerization-quality bisphenol-A (Dow Chemical Co.) was recrystallized once from toluene. Pfaltz and Bauer's 4,4'-dichlorodiphenylsulfone was recrystallized three times from ethanol. Reagent phenol (Baker) and 4,4'-biphenol (Eastman's white label) were used as received. Spectroquality methyl sulfoxide, dimethyl acetamide, and dimethylformamide (Matheson, Coleman, and Bell) were used as solvents. 3,5,3',5'-Tetramethyldiphenone and hexamethylphosphoramide (Aldrich) were used as received.

**Synthesis of 3,5,3',5'-Tetramethyl-4,4'-biphenol.** Tetramethyldiphenone (100 grams) was heated with 100 grams of zinc powder and 300 ml. glacial acetic acid in a 500 ml. round-bottomed flask with stirring for 60 minutes at 100°C. After cooling, the reaction mixture was added to 800 ml. water, and the acid was neutralized with 225 grams sodium carbonate. The solids were filtered, and the product was separated from excess zinc by solution in hot toluene. Decolorizing charcoal was added, the solution was filtered, and the product was allowed to crystallize. After two succeeding recrystallizations from toluene, white 3,5,3',5'-tetramethyl-4,4'-biphenol was obtained which melted at 223°–226°C. Elemental analysis: found: C, 79.9%; H, 7.85%; calculated: C, 79.3%; H, 7.49%.

**Polymerization.** A four-necked, 500-ml. round bottomed flask was equipped with a stirrer, nitrogen inlet gas-dispersion tube, thermometer, Barrett trap, condenser, and heating mantle. Bisphenol A (5.14 grams, 0.0225 mole), 231 ml. DMSO, and 40 ml. benzene were placed in the flask, and the Barrett trap was filled with benzene. The system was stirred and sparged with nitrogen for 10 minutes, and then 0.0450 mole KOH (45% solution) was added rapidly from a buret. As the nitrogen flow was maintained, the solution was heated to reflux (*ca.* 135°C.) for about one hour, or long enough to distill all water into the Barrett trap. The trap was emptied, and benzene was allowed to distill out of the DMSO solution (temperature rises to about 170°C.). The trap was removed, and a clean, dry, condenser was substituted. The flask was then transferred to an oil bath at 80°C. with a temperature control of  $\pm 0.25^\circ\text{C}$ . The system was sparged constantly with nitrogen to keep oxygen out of the solution. The polymerization reaction was begun by adding a DMSO—4,4'-dichlorodiphenylsulfone solution *via* a syringe. The solution was at 80°C., and the 50.0-ml. volume contained 6.46 grams (0.0225 mole) of the 4,4'-dichlorodiphenylsulfone. The resulting reaction solution volume was 300 ml., giving a phenoxide and chlorine functional group concentration of 0.15 mole/liter. (For reaction at other temperatures, the DMSO volume was adjusted to maintain a total volume of 300 ml.)

**Analytical.** Samples (5.00 ml.) for phenoxide analysis were withdrawn from the reacting solution at regular intervals with a syringe. The syringe was emptied immediately into a 250-ml. beaker containing a 25 ml. (pipetted) sample of 0.05*N* HCl in DMSO. The HCl–DMSO

solution immediately stopped the polymerization by reacting with the remaining phenoxide. This solution was then diluted with 25 ml. acetone and 50 ml. water. The excess HCl was determined by titration with 0.025N KOH (in methanol) using a pH meter. The amount of phenoxide remaining in the polymerizing solution was then calculated.

### Results and Discussion

**Polymerization Kinetic Theory.** The results for the polymerization of 4,4'-dichlorodiphenylsulfone with the potassium diphenoxide salts of bisphenol-A, 4,4'-biphenol, and 3,5,3',5'-tetramethyl-4,4'-biphenol are shown in Figures 1, 2, and 3, respectively. Each figure contains a plot of the inverse phenoxide concentration *vs.* time at several temperatures. In each case, there is an initial curved line, followed by the expected straight line. The transition from the curve to the straight line occurs at about the 50% conversion point, which corresponds to an average degree of polymerization of 2.0 (dimer stage). This suggested that the monomers have a higher reactivity than the growing chain. The initial high reactivity would be caused most likely by the highly unstable diphenoxide monomer. The proximity of the phenoxide salts in these monomers creates an instability which promotes a high reaction rate constant in the

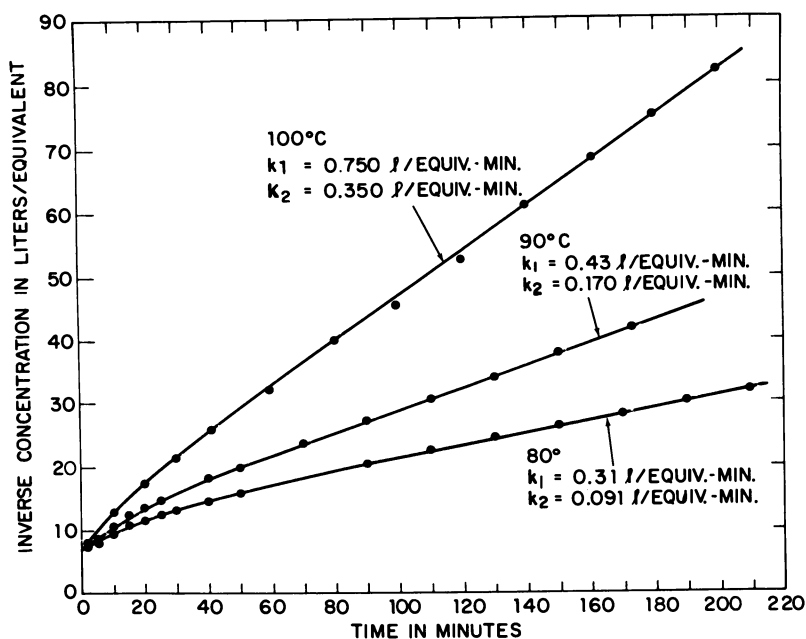
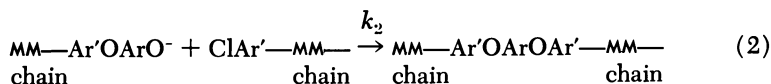


Figure 1. Polymerization of bisphenol A with 4,4'-dichlorodiphenylsulfone



Slow reaction (dimer and higher molecular weight stages):



In this theoretical analysis we have assumed an equal reactivity of both functional groups on 4,4'-dichlorodiphenylsulfone (*see* section on reaction rate of potassium phenoxide for a discussion of this assumption).

This reaction sequence can be treated kinetically in the following way.

Let  $C_c$  = concentration of chloro functional group  
 $C_p$  = concentration of all phenoxide functional groups  
 $C_{p1}$  = concentration of monomeric phenoxide groups  
 $C_{p2}$  = concentration of phenoxide groups on chain ends

Thus,

$$C_p = C_{p1} + C_{p2} \quad (3)$$

and

$$C_p = C_c \quad (4)$$

The kinetic equations are:

$$-\frac{dC_{p1}}{dt} = 2k_1C_{p1}C_c \quad (\text{disappearance of monomeric phenoxide}) \quad (5)$$

$$-\frac{dC_{p2}}{dt} = \begin{array}{c} k_2C_{p2}C_c \\ \text{Reaction} \\ \text{of } C_{p2} \end{array} - \begin{array}{c} k_1C_{p1}C_c \\ \text{Formation} \\ \text{of } C_{p2} \end{array} \quad (\text{disappearance of chain-ended phenoxide}) \quad (6)$$

A factor of 2 is introduced into Equation 5 since the reaction of one monomeric phenoxide group causes the adjoining phenoxide to become a chain-ended phenoxide. This also explains the presence of the term,  $k_1C_{p1}C_c$ , in Equation 6. By adding Equations 5 and 6, we obtain an equation for the total phenoxide reaction rate:

$$-\frac{dC_p}{dt} = C_c(k_1C_{p1} + k_2C_{p2}) \quad (7)$$

This can be converted into the following difference equation by appropriate substitutions:

$$\Delta C_p = -\Delta t \cdot C_p(k_1C_{p1} + k_2[C_p - C_{p1}]) \quad (8)$$

The difference equation from Equation 5 is:

$$\Delta C_{p1} = -\Delta t \cdot 2k_1C_{p1}C_p \quad (9)$$



The simultaneous equations, 8 and 9, were solved numerically by computer to yield the lines shown on each of the graphs. The appropriate values for  $k_1$  and  $k_2$  were determined by trial and error to achieve the best fit with the experimental data points shown.

**Comparison of Reaction Rate Constants.** The calculated values for  $k_1$  and  $k_2$  are listed in Table I. Figure 4 contains a plot of  $\log(k_2)$  vs.  $1/T$  for the reaction between bisphenol A-phenoxide salt and 4,4'-dichlorodiphenylsulfone. This yielded an activation energy of 20.3 kcal./mole with a standard deviation of 0.9 kcal./mole. The other activation energies in Table I were determined by using the values for  $k$  at just two temperatures and the following form of the Arrhenius equation:

$$E = \frac{RT_a T_b}{(T_a - T_b)} \ln \frac{k_a}{k_b}$$

where  $E$  = activation energy, and  $R$  = gas constant

**Table I. Reaction Rate Constants for Bisphenols Which React with 4,4'-Dichlorodiphenylsulfone in DMSO**

Bisphenol	Temperature, °C.	$k_2$	$k_1$	$E_{act 1}$	$E_{act 2}$
		(liter/equiv.-min.)		(kcal./equiv.)	
A	80.0	0.28	0.086	≈13	20.3
	79.8	0.19	0.060		
	80.0	0.31	0.091		
	90.1	0.43	0.170		
	89.5	0.54	0.176		
	100.0	0.75	0.350		
	110.0	<sup>a</sup>	0.812		
	120.0	<sup>a</sup>	1.44		
4,4'-Biphenol	80.0	0.43	≈0.022	≈14	19
	120.0	3.4	0.34		
Tetramethylbiphenol	80.0	0.24	≈0.002	≈12	—
	120.0	1.4	0.083		

<sup>a</sup> Could not be determined from data.

Most of the differences in the reaction rate constants for the various bisphenol reactants can be explained theoretically. The values for bisphenol A ( $k_1$ ) are probably less than for 4,4'-biphenol ( $k_1$ ) because the isopropylidene group on bisphenol A acts to stabilize the monomer by separating the charges. However, the values for bisphenol ( $k_2$ ) are greater than for 4,4'-biphenyl ( $k_2$ ) because the isopropylidene group has a secondary effect of mildly donating electrons to the phenyl ring. This tends to destabilize the phenoxide and give it a higher rate relative to the second phenoxide on 4,4'-biphenol.

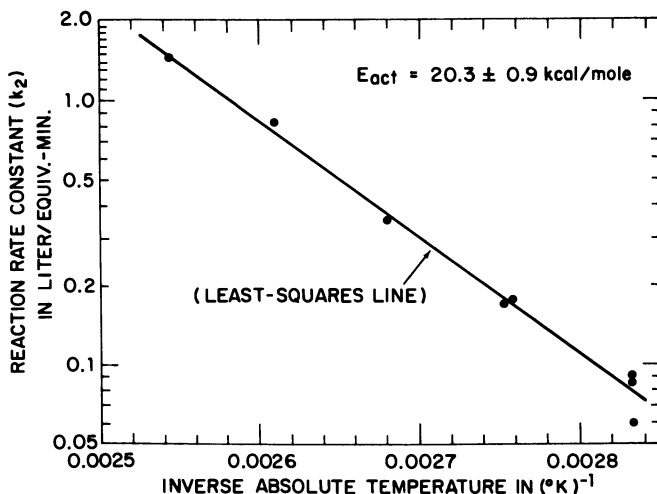


Figure 4. Reaction rate ( $k_2$ ) vs. temperature for bisphenol A-4,4'-dichlorodiphenylsulfone polymerization

As would be expected, the  $k$  values for tetramethylbiphenol are much lower than for 4,4'-biphenol owing to steric hindrance. The effect would be even greater if it were not for the slight, secondary, activating influence of the methyl groups owing to their electron donation to the phenyl ring.

**Other Explanations of Curved Second-Order Plot.** Other possible explanations for this kinetic behavior were explored. One explanation is that the KCl being produced in the reaction was changing the ionic character of the solvent and was thereby affecting the rate. This idea was tested by adding extra KCl to the solvent at the beginning of the reaction, but polymerization rate was unaffected.

A second possibility was that the increasing viscosity of the solution and/or increasing molecular chain length reduced the reaction rate by lowering the diffusion of reactants. However, if this were happening, it would reduce the rate at high conversions rather than at the beginning of the polymerization when only monomers and very short chains are present.

**Reaction Rate of Potassium Phenoxide.** As a test of the kinetics theory presented, the potassium salt of phenol was allowed to react with (1) *p*-chloronitrobenzene and (2) 4,4'-dichlorodiphenylsulfone.

In the first case, both reactants are monofunctional, so this reaction should yield a completely straight second-order plot. Figure 5 shows that this is the case. The high rate of this reaction (0.591 liter/mole-min.

at 40°C.) also indicates the great activating (electron withdrawing) power of the nitro group relative to the sulfone group.

In the second case, the phenoxide is monofunctional, but the chloromonomer is difunctional. This reaction provided a test of the relative reactivities of the two chlorines on 4,4'-dichlorodiphenylsulfone. Figure 5 does show a slight curvature which indicates a difference in the reactivities. Using Equations 8 and 9, the reaction rate constants ( $k_1$  and  $k_2$ ) were determined to be 0.10 and 0.053 liter/mole-min. Therefore, the assumption of equal chlorine reactivity (which was made in deriving these equations for the polymerization reaction) is not entirely correct. A complete theoretical analysis would be very involved; at least two more reaction rate constants would be necessary, and the experimental data obtained would not be sufficient to determine all of these constants.

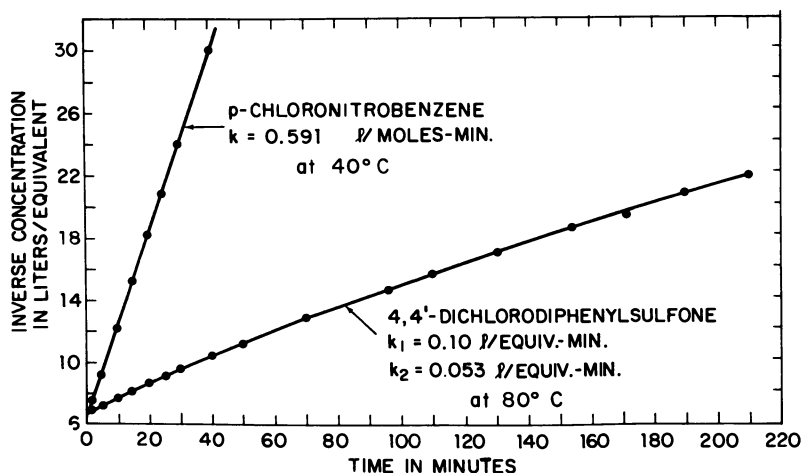


Figure 5. Reaction of potassium phenoxide with aromatic halides

**Error in Calculated Rate Constants.** The slope of the straight-line section in the reaction rate curves should be equal to the calculated values of  $k_2$ . To obtain an idea of the probable error in the calculated values for  $k_2$  (Table I), they can be compared with the slopes of these lines. The slopes (and standard errors) were determined by least-squares regression analysis. Table II lists the values for  $k_2$  from Table I, the least-squares slope, and the standard error of the least-squares value. In most cases,  $k_2$  agrees with the least-squares slope to within the standard error (4% or less).

Of course, the values for  $k_1$  cannot be compared in the same way. However, the error in  $k_1$  is probably greater in most cases.

**Table II. Error in Reaction Rate Constant**

<i>Bisphenol</i>	<i>Temperature,</i> °C.	$k_2$	<i>Least-Squares</i> <i>Slope</i>	<i>Standard</i> <i>Error</i>
A	80.0	0.086	0.086	0.003
	79.8	0.060	0.059	0.004
	80.0	0.091	0.090	0.002
	90.1	0.170	0.172	0.005
	89.5	0.176	0.178	0.002
	100.0	0.350	0.356	0.003
	110.0	0.812	0.813	0.010
	120.0	1.44	1.427	0.057
4,4'-Biphenol	80.0	0.022	0.024	0.001
	120.0	0.34	0.338	0.003
Tetramethylbiphenol	80.0	0.002	0.008	—
	120.0	0.083	0.082	0.001

**Effect of Solvent.** Besides polymerizing in DMSO solvent, we also polymerized bisphenol A with 4,4'-dichlorodiphenylsulfone in the following solvents: (a) mixtures of DMSO and chlorobenzene; (b) dimethylacetamide (DMAc); (c) dimethylformamide (DMF); (d) hexamethylphosphoramide. We found that the reaction rate constant ( $k_2$ ) was the same in the chlorobenzene-DMSO mixtures as in pure DMSO. However, if the chlorobenzene concentration was too high, the solubility of the bisphenol-A-diphenoxide salt was reduced, thereby precipitating some of the salt and effecting a slower polymerization. At a monomer concentration of 0.075M, the critical chlorobenzene concentration for precipitation was found to be between 35 and 50 vol. % at 100°C.

The polymerization appeared to proceed in each of the other solvents, although at a reduced speed owing to incomplete solubility of the phenoxide salt. In DMAc the salts were soluble enough to determine that the basic kinetic rate constant ( $k_2$ ) is the same as in DMSO. However, the solubility in the other solvents was too low to determine a rate constant.

### *Summary*

The polymerization rate of several diphenoxide salts with 4,4'-dichlorodiphenylsulfone has been measured in methyl sulfoxide and other solvents. The experimental data conforms to a second-order reaction model, which consists of a high reaction rate constant at the monomer stage, followed by a lower reaction rate constant at subsequent polymerization stages. Based on this kinetic model, the reaction rate constants and activation energies have been determined.

***Acknowledgment***

The authors acknowledge the excellent laboratory assistance of Dorothy D. Barksdale and James C. Krutzler.

***Literature Cited***

- (1) Bunnett, J. F., Levitt, A., *J. Am. Chem. Soc.* **70**, 2778 (1948).
- (2) Johnson, R. N. *et al.*, *J. Polymer Sci. Pt. A-1*, **5**, 2375-2398 (1967).

RECEIVED April 1, 1968.

## Preparation and Properties of Aromatic Polysulfonates

R. J. SCHLOTT, E. P. GOLDBERG,<sup>1</sup> F. SCARDIGLIA,<sup>2</sup> and D. F. HOEG

R. C. Ingersoll Research Center, Borg-Warner Corp., Des Plaines, Ill.

*Aromatic polysulfonates, reported recently by us, are thermoplastic materials possessing unique and previously unrecognized stability toward hydrolytic attack. The incorporation of the aromatic sulfonate linkage into co-polyester structures has been found to impart significant chemical stability to the copolymer. Engineering thermoplastics have been developed, based upon aromatic sulfonate copolyester, which possess an outstanding balance of mechanical properties. Materials produced by interfacial polycondensation were difficult to purify on a large scale and hence were thermally unstable. A low temperature solution polymerization technique using tertiary aliphatic amines as acid acceptors was developed. Polymers thus prepared exhibited much improved stability toward thermal processing. Precise control of molecular weight was achieved in laboratory and scaleup runs by using phenol.*

The preparation and properties of various aromatic polysulfonates have been described in the literature (1, 2, 3, 8, 12), especially in the patents of Conix. In later work, Thompson and Ehlers (13) reported on the thermal stabilities of a few aromatic polysulfonates. More recently (5) we described in detail the hydrolytic stability of these aromatic polymers and copolymers, pointing out the significant improvement in stability toward hydrolysis that is realized when the sulfonate linkage is incorporated into various ester compositions.

An extensive investigation was carried out in our laboratories of an aromatic sulfonate copolyester system, which led to the definition of a remarkable class of engineering thermoplastics. In this chapter we dis-

<sup>1</sup> Present address: Xerox Corp., Webster, N. Y.

<sup>2</sup> Present address: Velsicol Chemical Corp., Chicago, Ill.

cuss the synthesis, evaluation, and large scale preparation of one particularly attractive engineering thermoplastic, a sulfonate-carboxylate composition.

### *Experimental*

**Materials.** DIACID CHLORIDES. Isophthalyl and terephthalyl chlorides (Hooker Chemical, Trubeck [UOP Chemicals], and Eastman), as received, were usually yellow in the melt and contained free acid. Good results were obtained consistently only when these monomers were vacuum distilled and stored in dry flasks under nitrogen. No suitable analyses for trace acid content were found. Since the free acids are insoluble in methylene chloride, a good indication of the purity level is found by dissolving the acid chloride to 10% concentration in dry methylene chloride. The solution should be colorless and completely free of turbidity.

DISULFONYL CHLORIDES. 4,4'-Biphenyldisulfonyl chloride (BPDSC) is not commercially available in adequate purity for polymer work. Materials synthesized in this laboratory were used throughout.

Lab purifications worked out for lower quality BPDSC include repeated crystallizations from xylene or toluene until a white crystalline product is obtained, melting at 206°–207°C. to a clear, colorless melt.

BISPHENOLS. Bisphenol-A (BPA) (Dow [Parabis-A] and Union Carbide [bisphenol-HP]), as received, generally is of adequate purity. Pre-drying at 120°C./1 mm. was carried out to remove surface moisture.

An initial indication of purity is found by dissolving the BPA to 10% solids in 10% aqueous KOH. The solution should be clear and absolutely colorless.

SOLVENTS. Methylene chloride (Hooker, Dow Chemical, Stauffer, DuPont, Eastman, and Fisher) from most suppliers was satisfactory. After drying over sieves (Linde, Type 3A), the solvent generally contained <10 p.p.m. water, by Karl Fisher water titration.

Other chlorinated hydrocarbons, including *o*-dichlorobenzene, chlorobenzene and tetrachloroethylene, were similarly dried before use.

AMINES. Triethylamine (TEA) (Pennsalt and Eastman), like all tertiary alkylamines, is subject to light-catalyzed air oxidation. These contaminants are removed readily along with moisture by passing through a column of (or standing over) freshly activated silica gel. (Note: molecular sieves must not be used here—these seem to accelerate decomposition and color formation.) The amine should be dry and colorless before use. Other amines used in this work were obtained from Eastman and purified by distillation immediately before use.

**Polymerizations.** INTERFACIAL POLYCONDENSATION. A 1-liter glass reactor fitted with a thermometer, an addition funnel, a high speed, high shear stirrer (Dispersator) and (optionally) a dry ice condenser was charged with 22.8 grams (0.10 mole) of bisphenol-A and 250 ml. of water containing 8.8 grams (0.22 mole) of sodium hydroxide. Slow stirring was used to effect solution of the bisphenol-A. When complete, the mixture was cooled externally to 20°C., and 12 drops of 60% aqueous benzyltrimethylammonium chloride (BTAC) were added. A solution of 7.02

grams (0.02 mole) BPDSC and 16.24 grams (0.08 mole) of iso- and terephthalyl chlorides (50/50) dissolved in 250 ml. of methylene chloride was added quickly through the addition funnel, and the stirrer speed was increased to its maximum. A homogeneous emulsion quickly develops on mixing and rapidly becomes quite viscous. After about 20 minutes agitation, the stirring is stopped, and the emulsion is poured from the reactor.

Work-up of the emulsion, which usually breaks on standing, is effected by separation of the organic phase and precipitation by pouring into methanol with high shear agitation (Waring Blendor) and repeatedly washing the solid in the blendor with methanol and with water. Drying is accomplished overnight at 75°–125°C. in a vacuum oven. Additional purification may be carried out if desired by redissolving the polymer in methylene chloride, extracting the solution with water, filtering through filter aid, and reprecipitating and drying as before.

**POLYSULFONATE PREPARATION.** Into a carefully dried, 100-ml. resin reaction flask fitted with a paddle stirrer, thermometer, dropping funnel, and reflux condenser were placed 7.02 grams (0.02 mole) of BPDSC, 4.56 grams (0.02 mole) of BPA, and 50 ml. of dry methylene chloride. The reactor was fitted with an argon inlet to the top of the condenser to exclude moisture, and the stirrer was turned on to effect suspension of the insoluble solid monomers. Through the dropping funnel, 4.85 grams (0.048 mole) of freshly dried TEA were added slowly over a one-half hour period. The exothermic reaction produces sufficient heat to maintain a gentle reflux of methylene chloride at this rate of addition.

As amine was added, the bisphenol-A went into solution, followed by BPDSC as the reaction progressed. Finally, near the end of the amine addition, TEA hydrochloride began to precipitate as fine white needles.

At the end of the addition, external heat was applied by a heating mantle, and refluxing was continued for one hour. The viscous polymer solution was then cooled and poured into an equal volume of dilute (1%) aqueous hydrochloric acid and shaken. The organic layer was separated, extracted once with acid, then with equal volumes of water until the aqueous phase was neutral to pH paper.

The polymer was then precipitated by pouring into methanol in a Waring Blendor, collected by filtration, and dried *in vacuo* at 100°–200°C. overnight. The product had  $\eta$  sp/c-1.05 when measured in tetrachloroethane at 0.1 gram/dl. concentration.

**20% POLYSULFONATE-CARBOXYLATE.** Into a carefully dried, 500-ml. resin reaction flask fitted with stirrer, condenser, thermometer, and a dropping funnel and a condenser fitted with a nitrogen inlet were placed 22.8 grams (8.10 moles) of bisphenol-A, 7.02 grams (0.02 mole) of BPDSC, and 200 ml. of dry methylene chloride. To this stirred suspension were added dropwise 22.2 grams (0.22 mole) of freshly dried TEA. On completion of this step, all monomers were dissolved, and the pot mixture was a clear solution. The mixture was held with stirring one-half hour at 25°C. (Note: if phenol chain terminator is used, it is added at this point.)

A solution of 8.12 grams (0.04 mole) of IPC and 8.12 grams (0.04 mole) of TPC dissolved in 50 ml. of methylene chloride was added dropwise (clean, dry dropping funnel!) to the mixture over a one-half hour period, maintaining the temperature at 25°–30°C. by external cooling.



Finally, to effect quantitative transfer, the addition funnel was rinsed with 10 ml. of dry methylene chloride.

Toward the end of the acid chloride addition, TEA hydrochloride precipitated, and the solution became quite viscous, making stirring and removal of reaction heat more difficult. Hence, a large stirring paddle and a strong stirring motor (*e.g.*, an air-driven stirrer) were used.

The reaction mixture was held with stirring one hour, then quenched by pouring into an equal volume of dilute (1%) aqueous hydrochloric acid. Extraction, precipitation in methanol, and drying as before gave product having  $\eta$  sp/c 1.09 (TCE).

### Results and Discussion

**Physical Properties.** The polymer structure of interest, arrived at after evaluating thoroughly various copolymer compositions, is derived from bisphenol-A, 4,4'-biphenyldisulfonyl chloride (BPDSC), and the mixed isomeric phthalyl chlorides (Figure 1). The composition and properties of this three-component copolymer can be varied over a wide range simply by varying the proportions of the three acid chlorides employed.

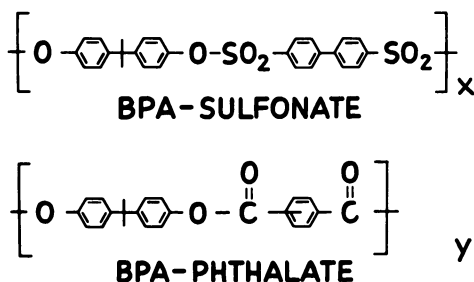


Figure 1. Sulfonate-carboxylate copolymer

The all-sulfonate system is a rigid, brittle material which crystallizes either in the solid state or from solution to become completely insoluble in common solvents. Only melt-pressed films can be made, and these exhibit the properties given in Table I.

Table I. Poly(BPA-4,4'-biphenyldisulfonate) Properties

$\eta$ sp/c	0.76
HDT (micro test)	175°C.
Yield, p.s.i.g.	9600
Ultimate p.s.i.g.	9820
Elongation, %	12
Izod Impact, ft. lbs./in. notch	0.4

In the terpolymer system crystallization is suppressed, resulting in amorphous, significantly tougher materials. The changes in properties over a range of sulfonate content are given in Figure 2. The BPA-50:50-isoterephthalate structure becomes more tractable by incorporating the biphenyldisulfonate linkage through lowered HDT and much improved in hydrolytic stability toward refluxing acids and bases. The hydrolytic weight loss curve in Figure 2 reflects the substantial improvement with sulfonate content in the resistance of molded bars to refluxing 10% aqueous caustic. These polymers are also quite stable toward refluxing 15% aqueous hydrochloric acid, where only slight (0.2 to 1.1%) weight gains are noted after one week.

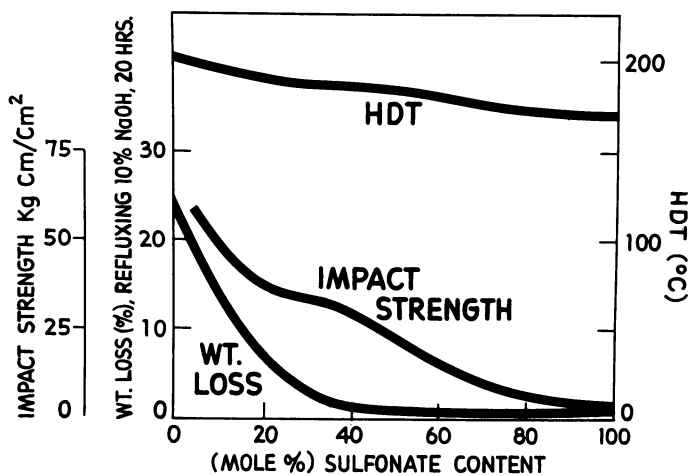


Figure 2. Effect of sulfonate content on properties

The structure chosen from this system for further development was the 20% sulfonate resin. It seemed to us to be a good compromise, possessing the best balance of physical properties for a general purpose material and having a good degree of hydrolytic stability.

Some properties of the 20% sulfonate are compared with two commercial engineering thermoplastics in Table II. The polysulfonate compares quite favorably in all points. Most notable, however, is the upper use temperature behavior. For example, the impact strength of Lexan polycarbonate is outstanding but only over a narrow temperature range. The impact behavior of the 20% sulfonate polymer, given in Figure 3, improves with temperature over the entire range to 400°F., far above the use temperature limit for Lexan. Similarly, the tensile strength is greater than 3500 p.s.i.g. at 350°F. (Figure 4).

**Table II. Mechanical Property Comparisons**

	20% "Polysulfonate"	Lexan	Polysulfone
Tensile strength, p.s.i.g.	10,150	8,500	10,200
Tensile modulus, p.s.i.g.	320,000	300,000	360,000
Tensile elongation, %	45	80	50-100
Flexural strength, p.s.i.g.	16,800	12,000	15,400
Impact strength ft. lbs./in.	6-8	13-16	1-2
HDT 10-mil def., 264 p.s.i.g., °C.	171	139	178
Hardness	124R	118R	120R
Flammability	self-ex	self-ex	self-ex

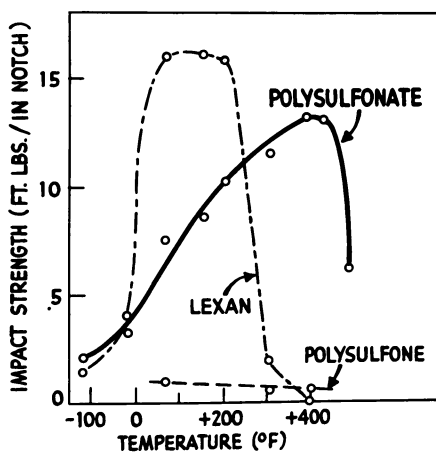


Figure 3. Izod impact vs. temperature

The aromatic polycarboxylates have generally been regarded as difficult to process at best. The sulfonate copolymer is similarly a high melt viscosity material. It can, however, be injection molded and extruded. In the interests of brevity we will not detail our experience in these areas, except to observe that only properly prepared and purified polysulfonates are stable to thermal processing, and predrying the resin prior to molding is preferred.

**Syntheses.** INTERFACIAL POLYCONDENSATION. Morgan has discussed low temperature polycondensations involving room temperature reactions of fast-reacting intermediates under interfacial conditions (11). In his many papers (9) concerning this method of polymer preparation, in the published work of Conix (1, 2, 3), and in our own patent (6), the application of interfacial polycondensation to polyphthalate and to polysulfonate preparation is well described. Hence, we dwell only briefly on the interfacial method to make available our observations particularly with regard to scaleup problems.

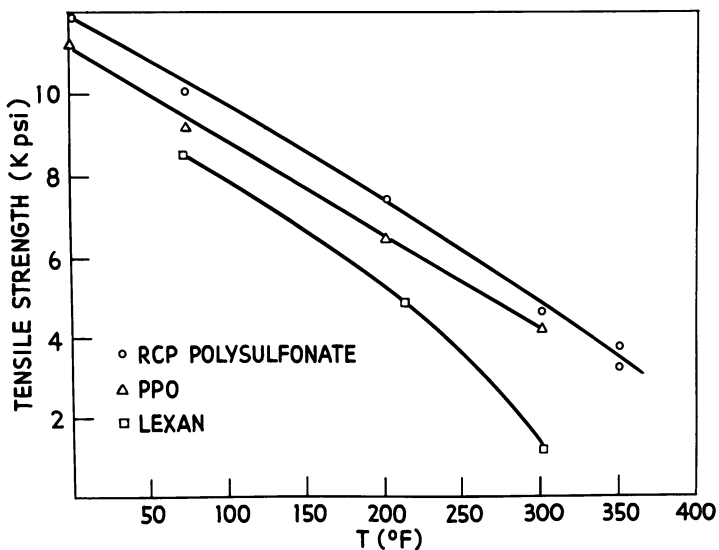


Figure 4. Tensile strength vs. temperature

The laboratory interfacial condensation of a mixture of iso- and terephthalyl chlorides and 4,4'-biphenyldisulfonyl chloride with bisphenol A is best carried out with methylene chloride as the solvent, as shown in Table III. A surfactant is required, and the best found for our work was benzyltrimethylammonium chloride (BTAC) (Table IV). The detailed mechanism of this polycondensation was investigated and will be presented in a later publication.

Table III. Effect of Solvent on Viscosity

Organic Phase	$\eta$
Toluene	0.21
<i>o</i> -Dichlorobenzene	0.34
<i>sym</i> -Tetrachloroethane	0.75
Methylene chloride	0.95

Table IV. Effect of Catalyst

Catalyst	$\eta$
None	<0.1
Triethylamine	0.34
Tetramethylammonium chloride	0.39
Benzyltrimethylammonium chloride	0.62

The preparation, given in the Experimental section, generally reproduces the systems outlined by previous workers and need not be considered further here.

Scaleup of the interfacial process presented us with unexpected difficulties. The resulting water-in-oil emulsion is not readily broken, and the washing-out of excess caustic and by-product salts is thereby inefficient if not completely impossible. As a result, the polymers were of poor quality and stability when prepared interfacially.

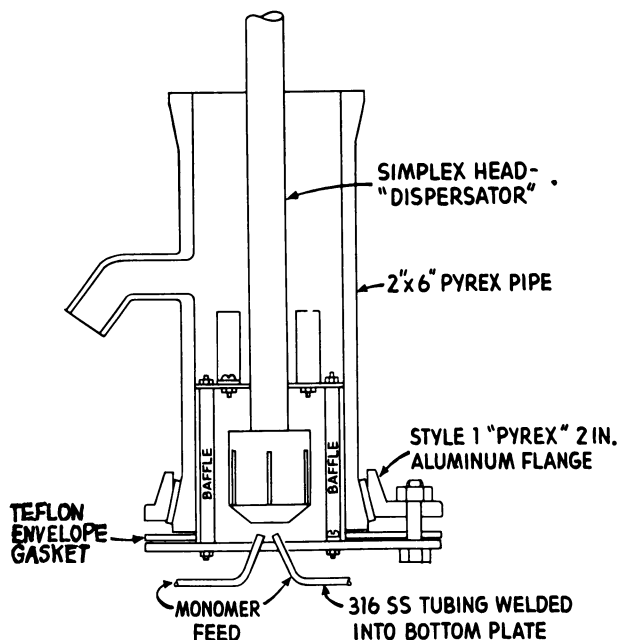


Figure 5. Continuous reactor for interfacial polymerization

The large scale work did provide the basis for a successful continuous polymerization reactor, shown in Figure 5. This reactor was quite effective, producing large amounts of polymer emulsion rapidly. When the effect of stirring rate was examined, we discovered that the immediately produced polymer was of relatively low viscosity (Table V). The emulsified polymer continued to "grow" on standing, reaching a maximum in about 30 minutes. The efficient stirring seems needed simply to bring the reactants into contact. Once established the emulsion is sufficiently stable to maintain the reaction unaided.

**Table V. Effect of Stirring (Continuous I-F Reaction)**

Stirring Speed, r.p.m.	$\eta_{sp}/0.1$	
	0 min.	30 min.
1500	0.30	0.64
3000	0.35	0.71
6200	0.35	0.73
9200	0.44	1.00

Since the interfacial method could not provide material pure enough to withstand thermal processing, we turned to a technique which would permit a simplified purification.

**SOLUTION POLYCONDENSATION.** The low temperature, amine-catalyzed condensation of diacid chlorides with diphenols in a single solvent system was one of a group of new polymer syntheses described by Morgan and co-workers (10). His method, termed "low temperature solution polycondensation" consists of combining fast reacting intermediates in an inert liquid medium and removing the acidic by-products by acid acceptors. Despite the sensitivity of such systems toward stoichiometry and reagent purity, great advantages are realized in the case of product purification compared with interfacial systems.

We examined the condensation of disulfonyl chlorides with diphenols, using aliphatic tertiary amines as acid acceptors and found that polysulfonates and copolymers could be obtained readily. This method, as described in our soon-to-be-issued U. S. patent, is directly applicable to the preparation of a wide variety of sulfur-containing polyesters.

Other workers have reported that tertiary aliphatic amines undergo a decomposition reaction with sulfonyl chlorides (8) and therefore would be unsatisfactory acid acceptors for these reactions. We have found no evidence that such a reaction occurs at any temperature in our system, and in fact aliphatic tertiary amines are excellent acid acceptors for such condensations.

The choice of amines is important, however, in that they must be strongly basic. Unlike the usual condensations of phosgene and of dicarboxylic acid chlorides, this system does not go at all well with weaker bases like pyridine, even when used in large excess. Pyridines and dialkylanilines form highly colored side products and do not promote the rapid formation of high polymer (Table VI).

The preparative method used in these syntheses and in the scaleup evaluation was a two-step sequential batch technique (Figure 6) (*see* Experimental). BPDSC and bisphenol A, both sparingly soluble, were suspended in methylene chloride. No reaction occurred until the acid acceptor was added slowly to this mixture. Once the initial exothermic

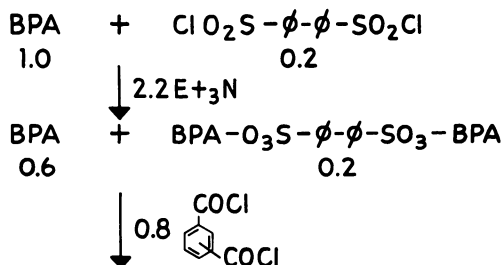
reaction was complete, to provide the BPA-BPDSC trimer, a mixture of phthalyl chlorides in methylene chloride was added at a rate which provided a gentle reflux. Near the end of this addition, the viscosity increase became quite apparent, and amine hydrochloride separated from solution.

Polymer work-up was straightforward—extraction with dilute aqueous HCl to remove the amine and its salts, followed by water extraction and then precipitation either in alcohol or in hot water.

**Table VI. Polysulfonate Preparation with Various Tertiary Amines**

<i>Acid Acceptor</i>	$pK_b^a$	<i>Polymer <math>\eta</math> sp/c</i>
Triethylamine	3.1	0.68
Tri- <i>n</i> -butylamine	3.1	0.35
Dioctadecylmethylamine	(3.2)	0.37
<i>N</i> -methylpiperidine	(3.6)	0.34
<i>N,N</i> -dimethylpiperazine	(4.5)	0.44
<i>N,N</i> -dimethylbenzylamine	5.0	0.37
<i>N</i> -methylmorpholine	6.6	0.31
Tribenzylamine	(8)	none
<i>N,N</i> -dimethylaniline	8.0	none
Pyridine	7.8	none

\*  $pK_b$  Values from H. K. Hall, Jr. (7).



*Figure 6. Sequential polymer formation (20% polysulfonate)*

**Table VII. Effect of Addition Order on Molecular Weight**

<i>Addition Order</i>	$\eta$ sp/c
Amine added to stirred monomers	0.56
BPA-TEA added to stirred acid chloride	0.55
Dilute solution of acid chlorides added to BPA/TEA	0.56
Sequential polymerization	0.68

The addition order was selected largely because of the difficulty of handling mixtures of soluble and insoluble monomers. Alternate orders

were examined, however, and polysulfonates could be obtained in all cases (Table VII). Thus, when all the monomers were stirred together and amine was added, exothermic polymerization occurred. Similarly, when a solution of the amine and BPA were added to a mixture of the stirred acid chlorides, the polymer was obtained in good yield.

The single limitation was that the acid chloride could not be present with free amine. When this combination occurred, either by addition of excess acid chlorides or by inadequate mixing so that localized excesses of acid chloride developed, an intense yellow color was produced which could not be dissipated by post reaction or by extraction. Other parameters examined for the sequential reaction included amine stoichiometry, temperature, hold terminal, and reagent purity.

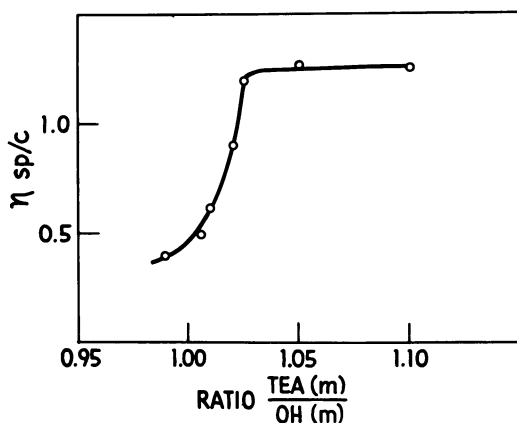


Figure 7. Effect of TEA/phenolic OH ratio on molecular weight

*Amine Stoichiometry* (Figure 7). It is necessary that a slight excess of amine be employed to achieve high molecular weight. The reasons for this are not at all clear. [A referee suggests this requirement for excess amine may reflect the effect of dissolved TEA:HCl on the polymerization. It may well be that the ionization of phenolic hydroxyls, *viz.*,  $[\sim\text{OH}] + [\text{TEA}] = [\sim\text{O}^-] + [\text{TEA} \cdot \text{H}^+]$  is repressed by the increasing TEA:HCl concentration. Additional TEA would be expected to overcome this effect.]

*Temperature.* The reaction was normally carried out over the range from 25° to 39°C.—the reflux temperature of methylene chloride. Good results were obtained at 10° and at 100°C. in dichlorobenzene, and there seems to be little reason to require any specific range. Since it was convenient to use solvent reflux as a secondary temperature control, the scaleup system was operated in the range 25°–39°C.



*Hold Time.* The time necessary for complete reaction was defined by measuring viscosity with hold time (Figure 8). While the reaction appears complete in about 30 minutes, the products obtained at that point were significantly less thermally stable compared with the two-hour reaction product from the pilot scale work. No evaluation of intermediate time products was made.

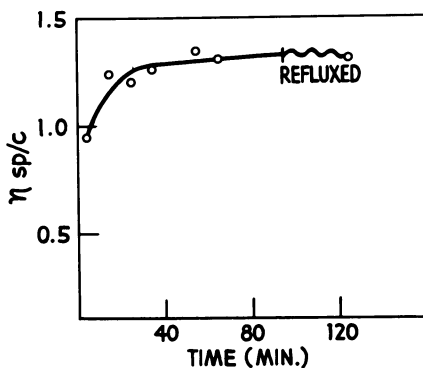


Figure 8. Effect of reaction hold time at 25°C. on molecular weight

*Reagent Purity.* The acid chlorides used were freshly distilled, and the solvent was sieve dried. The tertiary amine was distilled and stored over activated silica gel. The only contaminant examined was moisture. While small amounts (<5%) of water permitted the attainment of high molecular weight, the products were significantly poorer in thermal stability. We later found that up to 5% phthalic acid could be substituted for phthalyl chlorides and still give high molecular weight polymer. The appearance of a carbonyl shoulder at  $5.65\mu$  on the ester carbonyl absorption in the infrared spectra indicated the formation of anhydride linkages in the polymer. We reasoned that the major influence of water must be the production of free acid and incorporation into the polymer chain by formation of anhydride linkages (Figure 9). We found that such linkages resulted in poor stability, established by comparing viscosity changes on thermal aging.

Molecular weight control was accomplished by chain end-capping with phenol. This stabilized the polymer further by eliminating functionality at the polymer chain ends. The success of this technique depends on maintaining a balanced stoichiometry by substituting phenol for BPA stoichiometrically. The curve calculated from Flory (4) is shown in Figure 10, together with the experimental results over the range.

Within the limits of our ability to maintain stoichiometry by the weighing of reagents, the desired molecular weights can be achieved reproducibly, both in the lab and on the pilot (50-gal. reactor) scale.

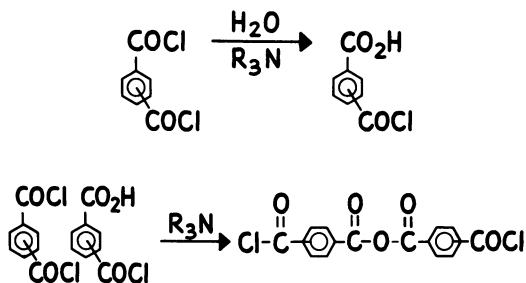


Figure 9. Probable source of thermal instability

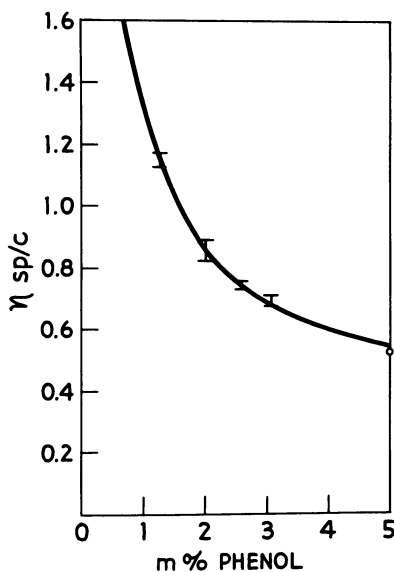


Figure 10. Phenol in molecular weight control

Using the process essentially as outlined, we produced nearly 2 tons of polysulfonate resin in the pilot scale work. The only major changes in the lab procedure, other than simplifying monomer handling for use on a large scale, were the use of a Podbielniak countercurrent liquid-liquid extractor for continuous aqueous washing of the polymer solution and precipitation in a hot water system followed by centrifuging and drying in an Aeromatic fluid bed drying unit. The improved extraction efficiency

realized with the Pod unit provided much cleaner and thereby more stable products than could be realized in the laboratory.

### Summary

The solution polycondensation process of Morgan has been extended for the first time to the preparation of aromatic polysulfonates, providing materials much improved in properties over those obtained by interfacial methods. The resulting BPA-phthalate-sulfonates are excellent engineering thermoplastics, exhibiting the properties of tough, rigid, higher impact materials. The resins provide an additional advantage as chemically resistant plastics by virtue of their unique stabilities towards aqueous acids and bases.

### Acknowledgment

The authors are indebted to R. H. Rosenberg and the chemical engineering staff for their many contributions, and to F. S. C. Chang for the extensive mechanical testing, solution properties research, and the processing studies carried out under his direction.

### Literature Cited

- (1) Conix, A. J., Laridan, U. L., *Angew Chem.* **72**, 116 (1960).
- (2) Conix, A. J., Belgian Patent **565,478** (1958).
- (3) *Ibid.*, Belgian Patent **600,053** (1961).
- (4) Flory, P. J., "Principles of Polymer Chemistry," Cornell University Press, Ithaca, 1953.
- (5) Goldberg, E. P., Scardiglia, F., Schlott, R. J., Hoeg, D. F., *Biennial Polymer Symp., 3rd, Case Inst. Technol.*, June 1966.
- (6) Goldberg, E. P., Scardiglia, F., U. S. Patent **3,262,914** (1966).
- (7) Hall, Jr., H. K., *J. Phys. Chem.* **60**, 63 (1956).
- (8) Jones, E. W., Whalen, H. F., *J. Am. Chem. Soc.* **62**, 1057 (1940).
- (9) Morgan, P. W., "Condensation Polymers," pp. 370, 372 Interscience, New York, 1965.
- (10) *Ibid.*, pp. 115-162.
- (11) Morgan, P. W., *ADVAN. CHEM. SER.* **34**, 191-199 (1962).
- (12) Shuto, Y., *J. Chem. Soc. Japan, Ind. Chem. Sect.* **67**, 367-370 (1964).
- (13) Thompson, D. W., Ehlers, G. F. L., *J. Polymer Sci.* **A2**, 1051 (1964).

# The Polymerization of $\beta$ -Carboxymethyl Caprolactam

HERBERT K. REIMSCHUESSEL

Corporate Research Laboratory, Allied Chemical Corp.,  
P. O. Box 309, Morristown, N. J. 07960

*The thermal polymerization of  $\beta$ -carboxymethyl caprolactam results in a novel polyimide which has been identified as a poly(2,6-dioxo-1,4-piperidinediyl)trimethylene. The formation of this structure is explained by a mechanism that consists in an initial isomerization of the caprolactam derivative to 3-(3-aminopropyl)glutaranhydride or its linear dimer and subsequent polymerization by condensation involving the terminal amino group and the anhydride moiety. Suggested reaction schemes and corresponding kinetic equations are based upon the premise that the extent of polymerization is represented by the concentration of imide linkages. Results of rate studies carried out at 210°–290°C. support the proposed mechanism.*

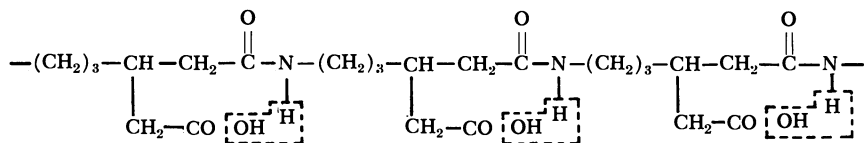
The polymerization of  $\beta$ -carboxymethyl caprolactam has been of interest not only because it resulted in the formation of a novel and interesting polymer structure but it demonstrated a new concept for synthesizing condensation polymers. For comparison, recall that the polymerization of the unsubstituted  $\epsilon$ -caprolactam results in an equilibrium in which the main product is a linear polyamide known as nylon 6. It is well known that its formation involves an initial ring opening and both condensation and stepwise addition reactions (2, 3, 7). The same is true also for the polymerization of known simple derivatives of  $\epsilon$ -caprolactam that may be derived by substituting a hydrogen atom in any of the five methylene groups by, for instance, an alkyl group. Regardless of which position from  $\alpha$  through  $\epsilon$  a substituent may occupy, the equilibrium between monomer and polymer shifts toward the monomer as the size of the substituent increases (1). In all these cases the polymer formed is a polyamide. On the other hand, the polymerization of the

**Table I. Structures of Monomers and the Repeat Units of the Respective Polymers**

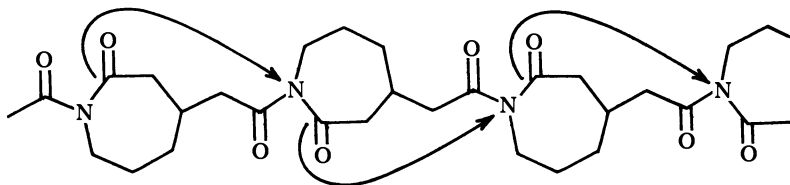
	<i>Monomer</i>	<i>Polymer Repeat Unit</i>
I		$-(\text{CH}_2)_5-\overset{\text{O}}{\parallel}{\text{C}}-\text{NH}-$
II		$-(\text{CH}_2)_m-\underset{\text{R}}{\text{CH}}-(\text{CH}_2)_n-\overset{\text{O}}{\parallel}{\text{C}}-\text{NH}-$ <p style="text-align: center;"><math>n = 4 - m \quad \text{O} \leq m \leq 4</math></p>
III		

$\beta$ -carboxymethyl caprolactam results in a polyimide which we identified recently as a poly(2,6-dioxo-1,4-piperidinediyl)trimethylene [4, 5]. Structures of both the monomers and the repeat units of the respective polymers are shown in Table I for  $\epsilon$ -caprolactam (I), a polymerizable alkyl caprolactam (II), and  $\beta$ -carboxymethyl caprolactam (III).

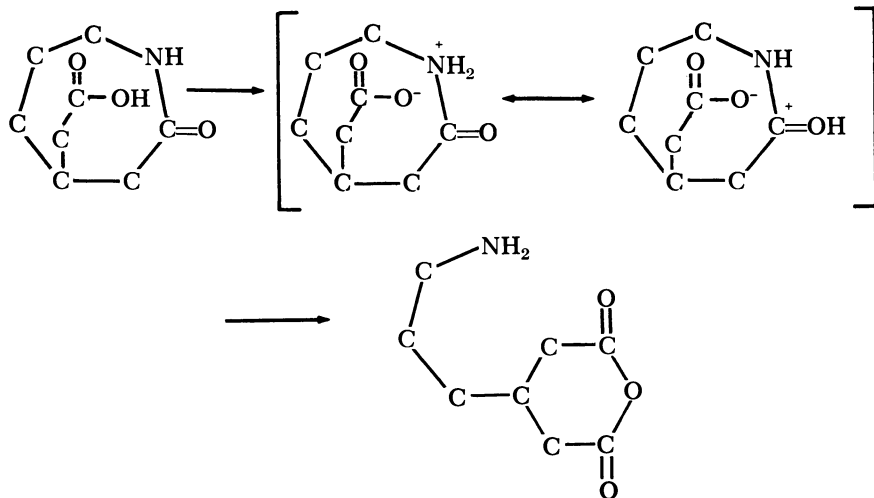
Comparing the structure of the monomer with that of the polymer as shown in Table I, we see that the polymerization of the  $\beta$ -carboxymethyl caprolactam must involve isomerization of the monomer ring system. This isomerization may be described by several possible processes, all of which are characterized by reaction between the amide and acid group of the  $\beta$ -carboxymethyl caprolactam. Based upon the results of our studies on the structure of this polymer (5) we may eliminate confidently those processes according to which the formation of the glutarimide moiety results either by intrachain cyclization or by trans-cyclization of certain intermediate polymer structures. The former would involve a polymer formed by a conventional ring opening polymerization:



whereas the latter would require a polymer formed by a simple polycondensation:



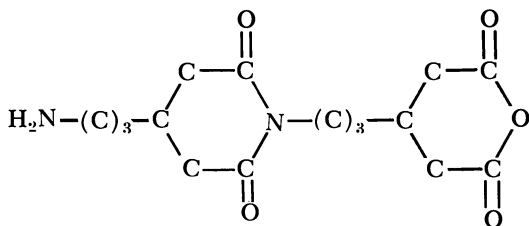
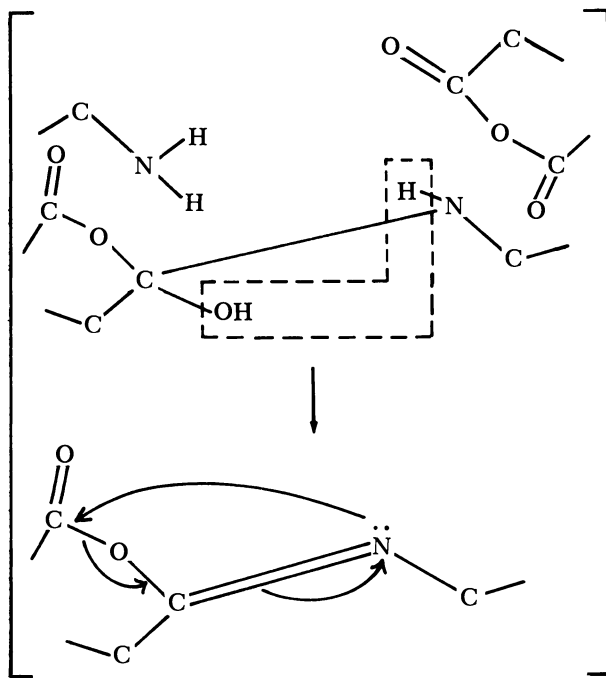
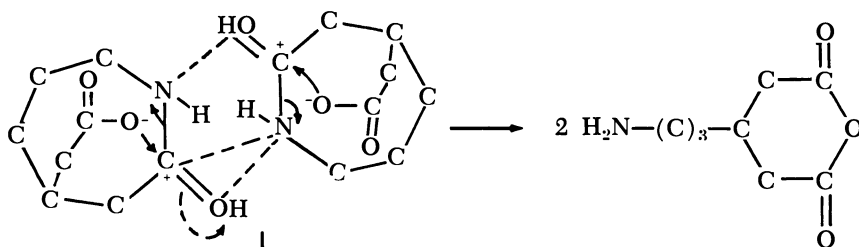
To explain the formation of the isomerized structure, we may consider a process that is initiated by an intramolecular protonation of the amide group, proceeds with opening of the lactam ring, and results in the formation of 3-(3-aminopropyl)glutaranhydride according to:



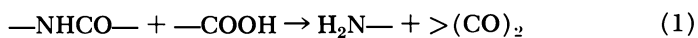
Another possible mechanism may involve intermolecular proton transfer and reactions as depicted on p. 720.

Polymerization could be envisaged by reaction of the anhydride group with the lactam moiety of the primary reaction product; since, however, amino end groups have been found in the polymer, transamidation as indicated in the above scheme must also occur. Although this mechanism cannot be eliminated completely from consideration, we do not feel that it plays a significant part in the conversion of the monomer.





To derive a kinetic expression the monomer conversion may in a first approximation for any of the considered mechanisms be represented by the simple chemical reaction, Reaction 1:

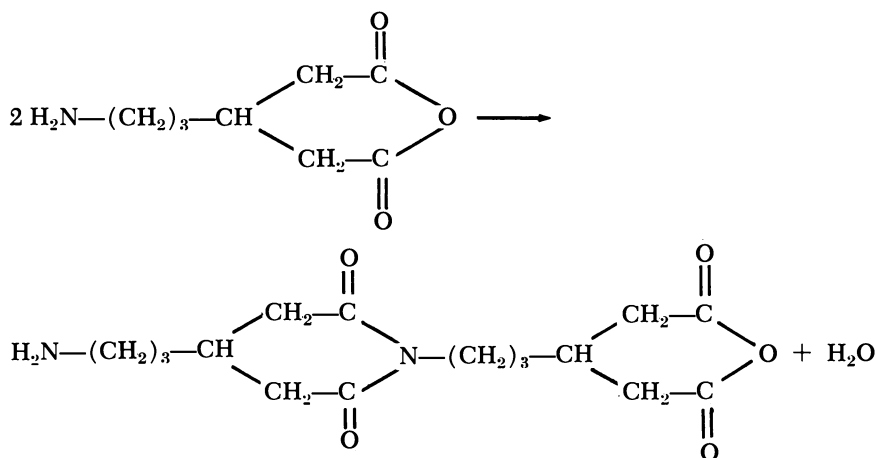




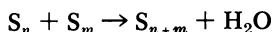
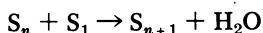
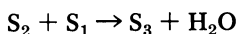
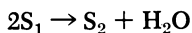
The concentration of the monomer ( $M$ ) is given by the relationship:

$$M = [-\text{NHCO}-] = [-\text{COOH}]$$

The growth of the polymer chains (polymerization) may be described by a condensation reaction between the anhydride and amine functions as depicted here for the formation of a linear dimer:



More generally the reactions for the chain growth may be represented by the following scheme:



Where  $S$  denotes a linear chain, and the subscript identifies the number of repeat units in this chain.

If we make the usual assumption that the reactivity of the functional groups is independent of the size of the respective molecules, chain growth may be represented by Reaction 2.



The concentrations of polymer molecules,  $c$ , (chains) and imide linkages,  $I$ , are given by the relationships

$$C = [-\text{NH}_2] = [\begin{array}{c} \text{O} \\ \parallel \\ \text{---}(\text{CO})_2\text{O} \end{array}]$$

$$I = [\begin{array}{c} \text{O} \\ \parallel \\ \text{---}(\text{CO})_2\text{N---} \end{array}] = [\text{H}_2\text{O}]$$

$I$  is a measure of the extent of reaction and depends upon both the concentrations of the monomer ( $M$ ) and the polymer molecules ( $c$ ). Mathematically this may be expressed by

$$I = I(M, c) \quad (3)$$

The derivative of this function with respect to time is then represented by Equation 4

$$\frac{dI}{dt} = \frac{\partial I}{\partial M} \frac{dM}{dt} + \frac{\partial I}{\partial c} \frac{dc}{dt} \quad (4)$$

Independent of any mechanism that may be considered, the concentration of imide linkages is given by the relationship

$$I = 1 - M - c = U - c$$

provided the concentrations are expressed in moles per mole of monomer as we have chosen to do in this work, and where  $U = 1 - M$  is the mole fraction of monomer converted to polymer. Considering this relationship, the rate of formation of imide linkages is then according to Equation 4

$$\frac{dI}{dt} = - \frac{dM}{dt} - \frac{dc}{dt} = \frac{dU}{dt} - \frac{dc}{dt} \quad (5)$$

According to Reaction 1 the rate of monomer conversion is given as

$$- \frac{dM}{dt} = k_1 M^2 = k_1 (1 - U)^2$$

while according to the Reaction 2 the rate at which the concentration of the linear species changes is as follows

$$- \frac{dc}{dt} = k_2 c^2$$

Substitution into Equation 5 gives, for the rate of polymerization,

$$\frac{dI}{dt} = k_1 (1 - U)^2 + k_2 c^2 \quad (6)$$

This equation is well suited to evaluate easily obtainable experimental data and will permit us to ascertain whether the formation of our polyimide can be explained by the proposed mechanism.

### **Experimental**

Polymerizations were carried out at temperatures of 210°, 220°, 230°, 240°, 250°, 270°, and 290°C. For each series about 10 small (8–10 mm. i.d.) polymerization tubes were used. Pure *β*-carboxymethyl caprolactam was placed into these tubes, and air was removed by alternate application

of vacuum and nitrogen. The tubes were connected to a manifold and immersed in a constant temperature oil bath. A nitrogen atmosphere was maintained throughout the polymerization. At various time intervals tubes were removed, quenched, and the reaction products were analyzed with respect to conversion and solution viscosities.

The experimental data are presented in Figures 1 and 2. Figure 1 shows the conversion  $U$  as a function of time for the various temperatures of polymerization. The conversion was determined by extracting the polymer sample with water. Since it was found that the water-soluble fraction was essentially pure  $\beta$ -carboxymethyl caprolactam,  $U$  was calculated from the value of the water insoluble weight fraction.

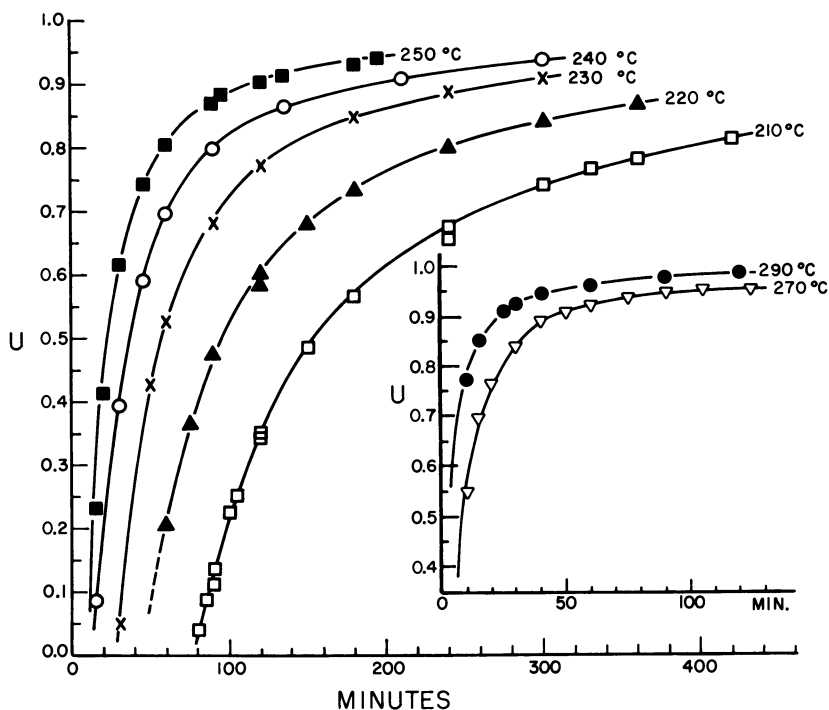


Figure 1. Experimental conversion-time curves

Figure 2 shows the viscosities of the polymer solutions as measured at  $25^\circ \pm 0.05^\circ\text{C}$ . in an Ubbelohde viscosimeter employing a concentration of 0.52 gram of polymer per 100 ml. of *m*-cresol. The viscosimeter had a flow time of more than 100 sec. for the pure solvent.

From the solution viscosities number average degrees of polymerization were calculated according to (6):

$$\log P_n = 2.008 + 1.241 \log \eta \quad (6)$$

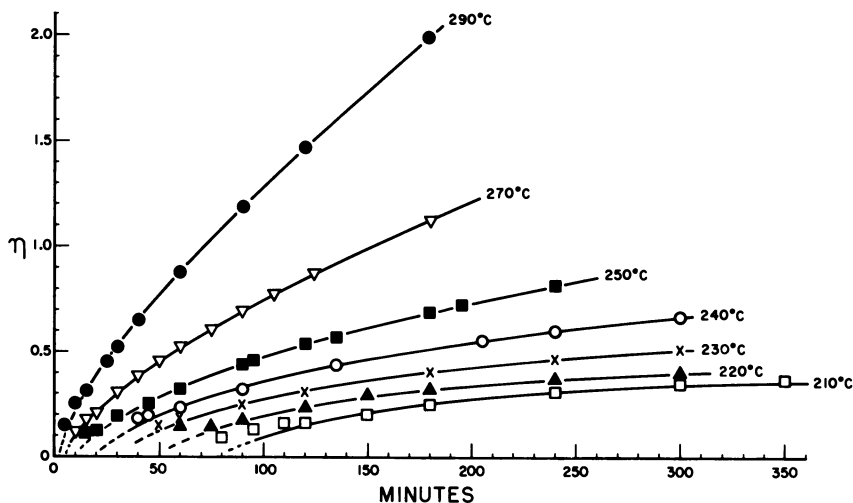


Figure 2. Viscosities of polymer solutions as a function of time

The concentration of polymer molecules was obtained according to

$$c = \frac{U}{P_n}$$

### Evaluation of Experimental Data

Inspection of the experimental conversion data as shown in Figure 1 revealed the existence of a distinct temperature-dependent induction period. To evaluate the measured conversion data, the respective term in Equation 6 was integrated using the boundary conditions  $U = 0$  at  $t = t_i$ , where  $t_i$  is the induction period

$$\int \frac{dU}{(1-U)^2} = \frac{1}{1-U} - 1 = k_1(t - t_i) \quad (7)$$

Figure 3 shows the plots of  $1/(1-U)$  vs. time. From the straight lines that start from the origin of the coordinate system used, values for  $k_1$  were estimated. It can be seen easily that the values for  $k_1$  are the reciprocal of the respective induction times  $t_i$ .

To evaluate data concerning the chain growth, the second term in Equation 6 was integrated, and  $\frac{1}{c}$  was plotted vs. time. Most of the plots in this case were curves such as shown in Figure 4, in which the data for polymerizations carried out at 210° and 220°C. were used. The shape of these curves indicates that at short reaction times the concentration of polymer chains ( $c$ ) increased as the time increased until

a maximum of chains was obtained; from this point on the number of chains decreased owing to condensation between end groups as the time increased. It is obvious that to estimate values for  $k_2$  only the linear (second) portion of these curves can be used. For the higher reaction temperatures the shape of the first portion of the curve could hardly be determined. In all cases, however, where a determination was possible we found that  $c$  was at a maximum at a time that corresponded to about  $2t_i$ . In this evaluation we therefore designated the concentration of chains at the time  $2t_i$  with  $c_m$ .

Figure 5 shows the linear portions of plots of  $\frac{1}{c}$  vs. time for all polymerization temperatures used.

The straight lines in Figure 5 are represented adequately by:

$$\frac{1}{c} - \frac{1}{c_m} = k_2 \Delta t \quad (8)$$

where  $\Delta t = t - 2t_i$  and  $c_m$  is a temperature-dependent quantity as defined above.

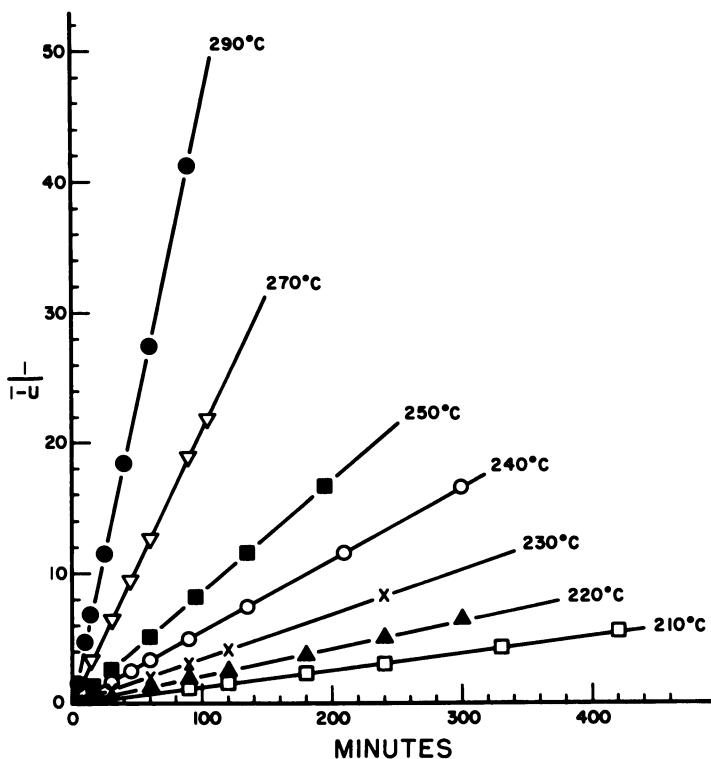


Figure 3. Second-order rate plot of conversion data

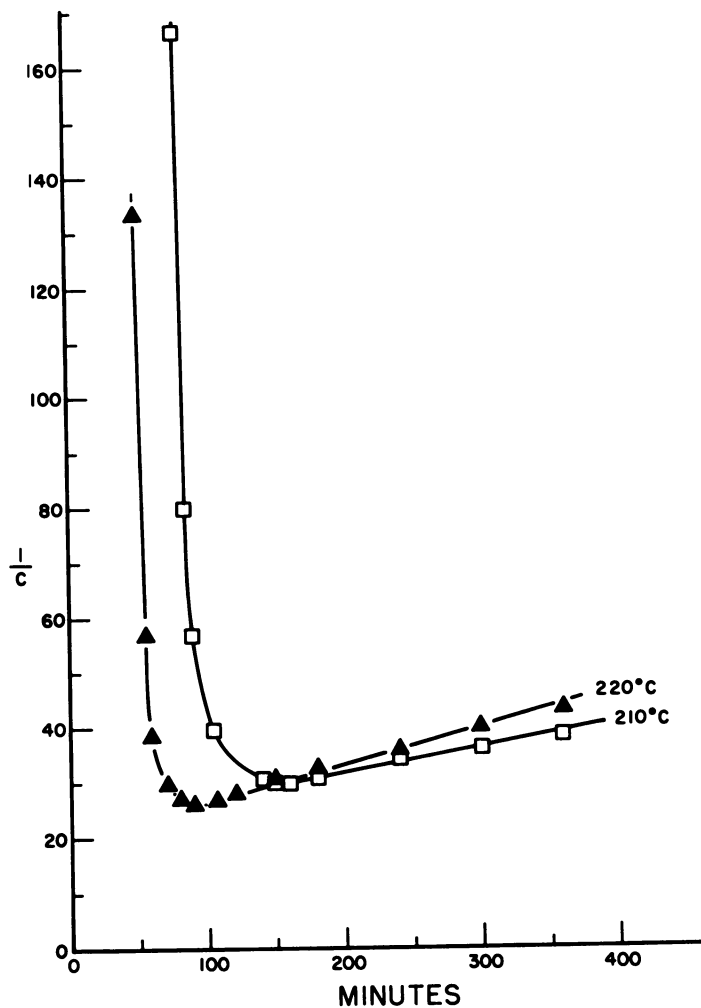


Figure 4. Plot of  $1/c$  vs. time for polymerization temperatures of  $210^\circ$  and  $220^\circ\text{C}$ .

The rate constants  $k_1$  and  $k_2$  were estimated from the plots in Figures 3 and 5. The values obtained were used to construct the Arrhenius plots shown in Figures 6 and 7.

The following relationships were derived from these plots:

$$k_1 = 74.9 \times 10^7 \exp(-23800/RT) \quad (9)$$

$$k_2 = 237.22 \times 10^7 \exp(-23800/RT) \quad (10)$$

from which follows

$$k_2/k_1 = 3.167 \quad (11)$$

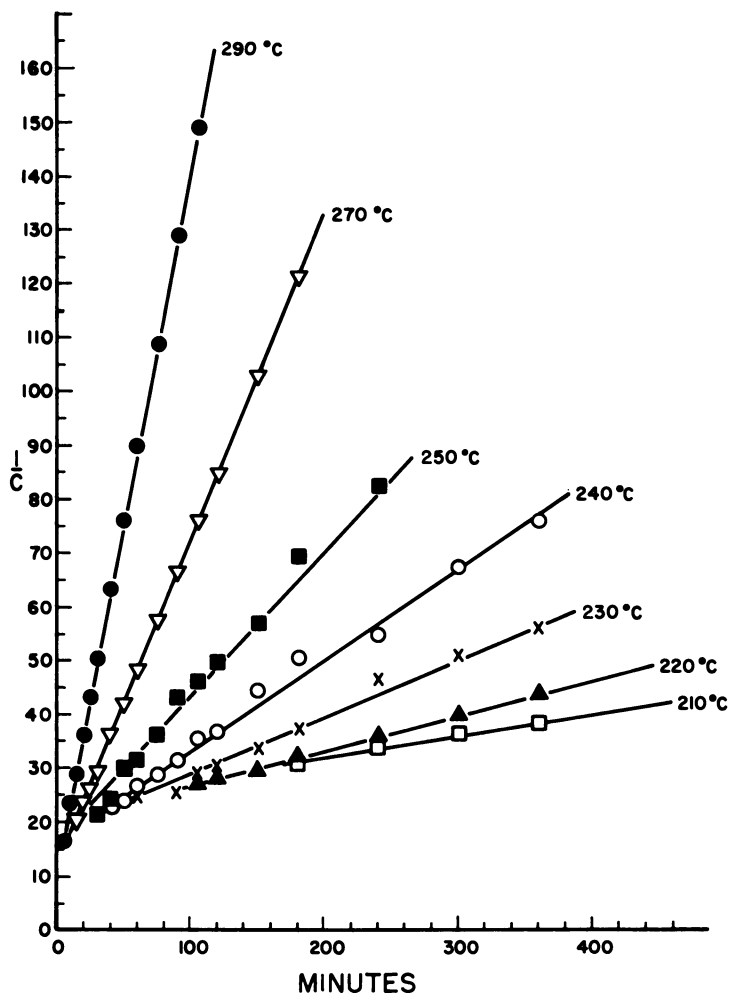


Figure 5. Second-order rate plots for chain growth

Equation 12 for  $c_m$  could be derived from Figure 8 showing a plot of  $\frac{1}{c_m}$  vs. the reciprocal of the absolute temperature

$$\frac{1}{c_m} = \frac{49.528 \times 10^3}{T} - 73.96 \quad (12)$$

Using Equations 7 through 12 rates of imide formation were calculated according to Equation 6 and plotted vs. time in comparison with experimental rates obtained by graphical differentiation of curves obtained from experimental data. The result is shown in Figure 9.

Solid lines represent the values calculated according to Equation 6 while the symbols are experimental values. This result shows that the polymerization of  $\beta$ -carboxymethyl caprolactam, involving both conversion of monomer and chain growth, may be explained by the mechanisms considered here. Since the disappearance of monomer follows second-order kinetics, the mechanism involving proton transfer between two intramolecular protonated monomer molecules seems to be the one that governs this reaction. We favor this mechanism over the others considered. Isomerization by an internal molecular rearrangement involving a single monomer molecule would also satisfy the experimental observations if one assumes that the reaction is acid catalyzed. In view of the complexity of the process which involves isomerization of one ring system into another, it is not surprising that application of our simplified reaction schemes does not lead to a rigorous description of all phases of this

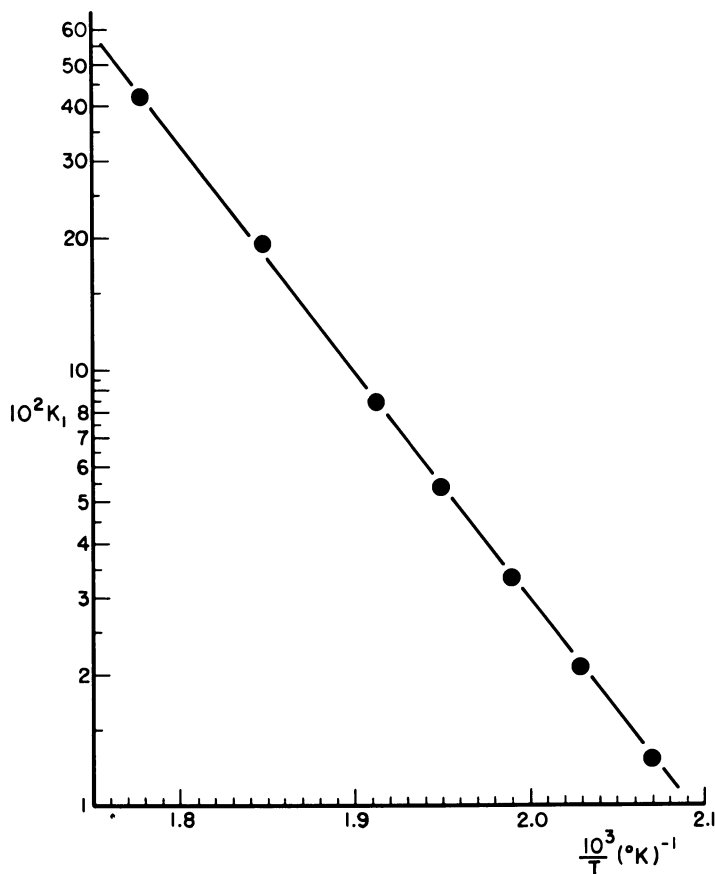


Figure 6. Arrhenius plot for  $k_1$



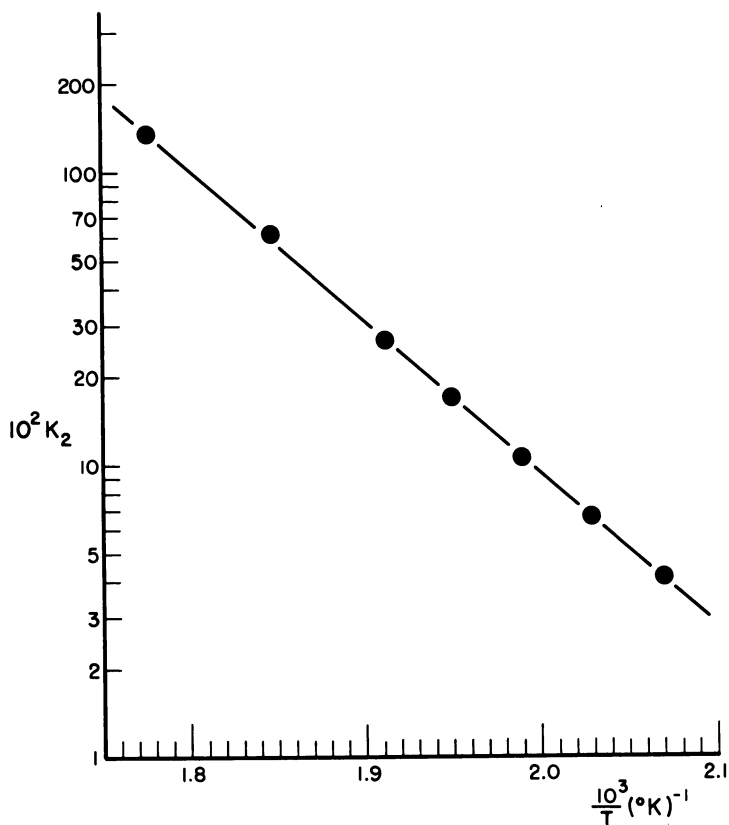


Figure 7. Arrhenius plot for  $k_2$

polymerization. Additional information is necessary to describe adequately all phases of this process.

The studies on this system, to date, have not indicated the existence of a temperature-dependent equilibrium similar to the one in which the polymerization of caprolactam results. Here essentially quantitative conversion was obtained independent of the polymerization temperature used. The final degree of polymerization, however, depends strongly on the temperature of polymerization; it increased when the polymerization temperature was increased. This may be explained by the increased mobility of the polymer molecules as a result of a temperature increase.

The final degree of polymerization ( $P_e$ ) has been defined as the highest that could be obtained at a given temperature and remained constant upon prolonged heating at this temperature.

To derive a relationship according to which  $P_e$  may be calculated for a given reaction temperature, let us consider Equation 8 and apply it to

the situation characterized by the absence of further chain growth. For this case follows

$$\frac{1}{c_r} - \frac{1}{c_m} = k_2 \Delta t_e \quad (8a)$$

Since the final conversion  $U_e \simeq 1$ , the term  $\frac{1}{c_c}$  in Equation 8a may be replaced by  $P_e$  and we may write

$$P_e - \frac{1}{c_m} = k_2 \Delta t_e \quad (13)$$

A plot of  $P_e - \frac{1}{c_m}$  vs.  $k_2$  resulted in a straight line as shown in Figure 10.

The slope of this line is  $\Delta t_e$  from which values for  $t_e$  (the time at which further polymerization at a given temperature stops) may be computed easily.

In combination with the expression found for  $c_m$  (Equation 12) Equation 14 has been derived from Figure 10. This equation represents the temperature dependence of  $P_e$ .

$$P_e = 18.621 \times 10^{11} \exp\left(-\frac{23800}{RT}\right) + \frac{49.528 \times 10^3}{T} - 28.21 \quad (14)$$

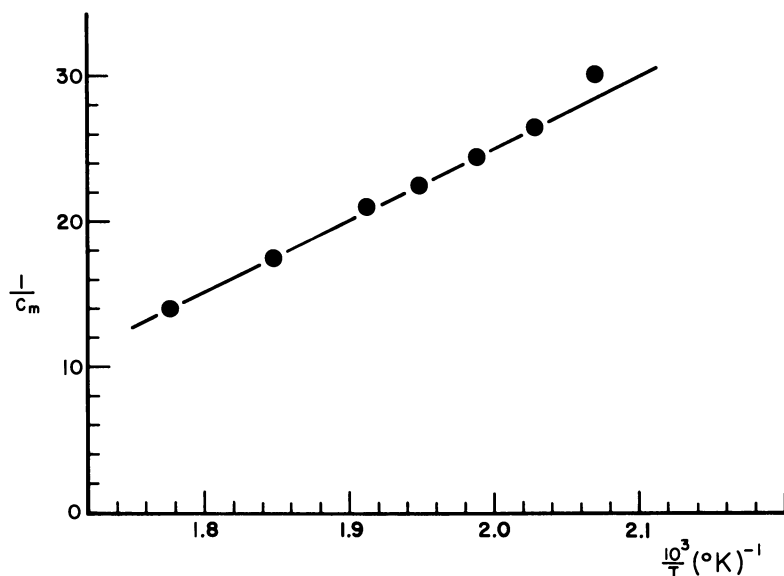


Figure 8. Temperature dependence of  $c_m$

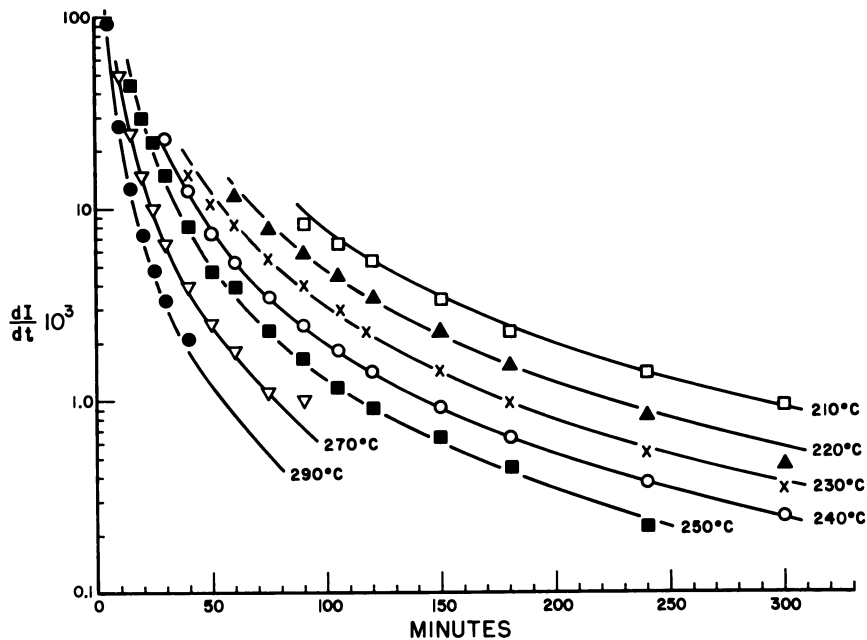


Figure 9. Experimental and calculated rate data

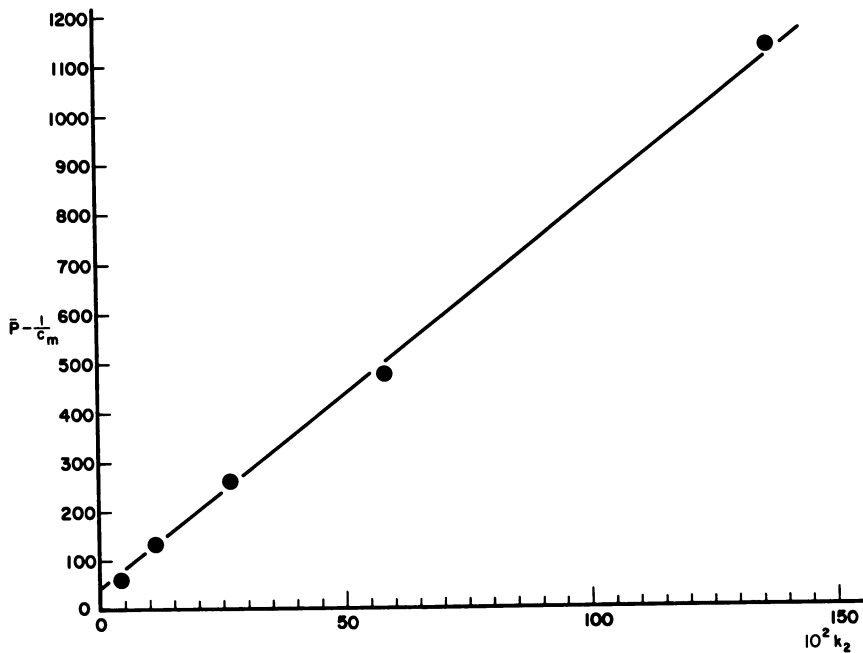


Figure 10. Temperature dependence of  $P_e$

A comparison of experimental data for  $P_e$  and calculated values according to Equation 14 is given in Table II.

Table II. Experimental and Calculated Values of  $P_e$

T, °C.	$P_e$	
	<i>calc.</i>	<i>exp.</i>
210	108	90
230	156	156
250	276	282
270	521	492
290	1139	1149

In conclusion, the results of our study indicate that the principal features of the formation of poly(2,6-dioxo-1,4-piperidinediyl)trimethylene by thermal polymerization of  $\beta$ -carboxymethyl caprolactam consists in an initial isomerization of the caprolactam derivative to a reactive species and subsequent polymerization of the latter by condensation. The reactive intermediate is in all probability either or both the 3-(3-aminopropyl)-glutaranhydride or its linear dimer. Both the conversion of the lactam by isomerization and the polycondensation follow second-order kinetics.

The conversion of an asymmetrical seven-membered ring structure into a symmetrical six-membered one that is highly stabilized by having become part of a macromolecule is considered to be the driving force in this polymerization.

#### Literature Cited

- (1) Cubbon, R. C. P., *Makromol. Chem.* **80**, 44 (1964).
- (2) Hermans, P. H., Heikens, D., van Velden, P. F., *J. Polymer Sci.* **30**, 81 (1958).
- (3) Kruissink, C. A., van der Want, C. M., Stavermann, A. J., *J. Polymer Sci.* **30**, 67 (1958).
- (4) Reimschuessel, H. K., *Polymer Letters* **4**, 953 (1966).
- (5) Reimschuessel, H. K., Roldan, L. G., Sibilía, J. P., *J. Polymer Sci. Pt. A-2* **6**, 559-574 (1968).
- (6) Walsh, E. K., Reimschuessel, H. K., unpublished data, 1967.
- (7) Wiloth, F., *Z. physik. Chem. N.F.* **11**, 78 (1957).

RECEIVED April 1, 1968.

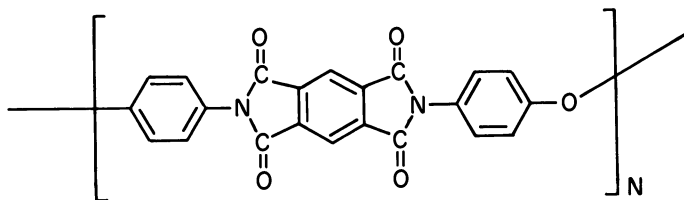
## Structure and Properties of a Heterocyclic Polymer

G. C. BERRY and S. P. YEN

Carnegie-Mellon University, Mellon Institute, 4400 Fifth Ave.,  
Pittsburgh, Pa. 15213

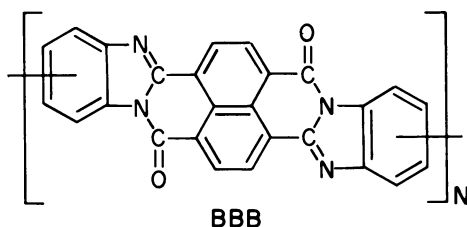
*Investigations on the heterocyclic polymer BBB prepared from naphthalene-1,4,5,8-tetracarboxylic acid and 3,3'-diaminobenzidine are described. These include infrared absorption studies of the structure of the polymer, fractionation of the polymer by exclusion chromatography on a porous substrate, and light scattering and dilute solution viscometry on fractions of the polymer dissolved in a strong acid. These data are interpreted to conclude that (1) in dilute solutions BBB behaves as a "flexible coil" macromolecule, perhaps with relatively free rotation about the single bond connecting the long, inflexible, nearly planar repeat units; (2) a sufficient amount of interchain complex formation occurs in the solid state to give the linear, noncrystalline polymer some of the physical properties of a highly crosslinked network polymer.*

New heterocyclic polymers designed especially for service at elevated temperatures have intriguing properties, some of which are in contrast to properties usually associated with linear noncrystalline polymers. These polymers have sometimes been described as "stiff chains" because of the long inflexible repeat units of which they are comprised. Relatively few quantitative studies have yet appeared in the dilute solution properties or the viscoelastic behavior of the new heterocyclic polymers—partly because of the difficulties inherent in working with the poorly soluble materials. Some studies on the polyimide with the (idealized) structure:

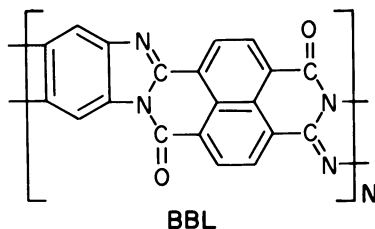


734

have suggested that in solution in sulfuric acid (29) this polymer behaves as a chain with nearly free rotation about its valence bonds, but in bulk it exhibits a dynamic modulus that lacks the transition temperatures usually observed for linear flexible chain polymers (10). This combined behavior is suggestive of some properties not commonly encountered with linear polymers and receives further comment below. We report here some of the first results from investigations still in progress on a heterocyclic polymer, BBB, prepared from the condensation reaction between naphthalene-1,4,5,8-tetracarboxylic acid and 3,3'-diaminobenzidine to give the (idealized) structure (26):



(Only the trans isomer of the repeating unit is illustrated, although probably both the cis and trans forms are present in the polymer.) A closely related polymer, BBL, discussed briefly below is prepared from 1,2,4,5-tetraminobenzene to give the (idealized) structure (27):



where again cis and trans isomers are presumed to exist in the polymer.

Both BBB and BBL have been developed for possible service at elevated temperature and exhibit excellent thermal stability as determined by the conventional measurement of weight loss as a function of increasing temperature or by weight loss as a function of time at an elevated temperature (26, 27). The increasing importance of new polymers comprised of large, relatively inflexible, repeating units presents new problems in interpreting the data ordinarily used to characterize macromolecules. For example, the question of definitions and experimentally useful measures of chain stiffness become increasingly important, especially for structures such as BBL. The importance of a few imperfect repeat units representing deviation from the idealized structure on thermal stability, mechanical

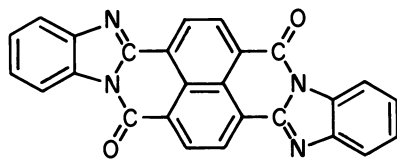
properties, and dilute solution properties requires investigation. The nature of the solid state of an amorphous linear polymer that behaves as a highly crosslinked network polymer presents significant problems. Is the polymer well below its glass transition temperature, or do factors not usually dominant now become critical? These are some of the questions that are central to the studies on heterocyclic polymers reported here. To anticipate our principal conclusions, it appears that:

(1) In dilute solution BBB behaves as a "flexible coil" macromolecule, perhaps with relatively free rotation about the single bond connecting the long, inflexible, nearly planar, repeat units.

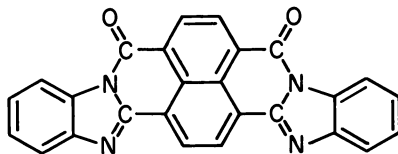
(2) A sufficient amount of strong interchain complex formation occurs in the solid state to give the linear, noncrystalline polymer some of the physical properties of a highly crosslinked network polymer.

### *Solubility of BBB and Fractionation of the Polymer*

One of the characteristic properties of BBB, BBL, and many other similar heterocyclic polymers is their limited solubility. As far as is now known, BBB is soluble only in strong acids such as concentrated sulfuric, benzenesulfonic, methanesulfonic, and concentrated phosphoric acid and in certain aqueous reagents discussed below, in which a chemical reaction modifies the polymer. The vat dyestuffs below:



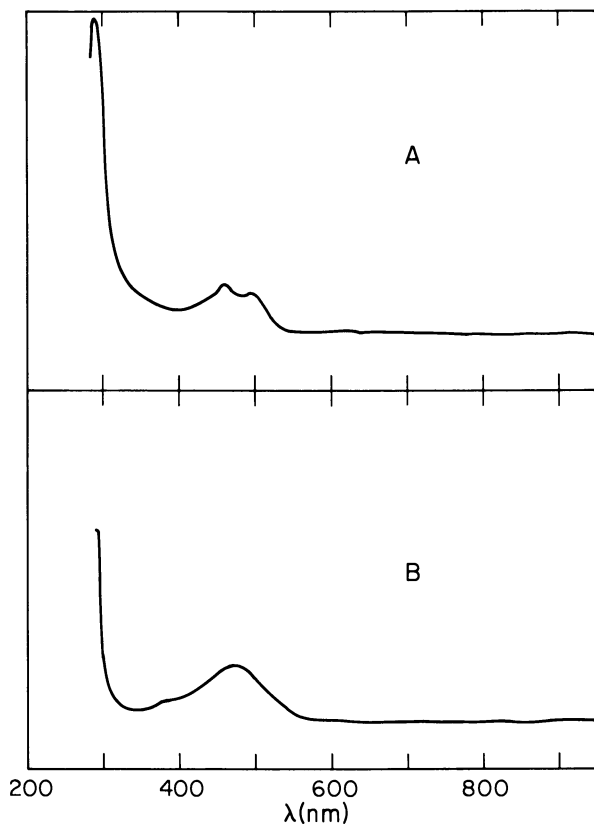
Vat Orange 7  
CI 71105



Vat Red 15  
CI 71100

are useful model compounds of the cis and trans repeating units of BBB. Keep in mind the similarity of BBB (and other heterocyclic polymers) to the more familiar dyestuffs since some of the chemical and physical properties of the latter, which have been fairly well studied (28), will also apply to the polymer. Both the cis and trans compounds exhibit nearly as poor solubility as BBB, although they do have limited solubility

in *o*-chlorophenol, pyridine, xylene, and a few other organic solvents. Figure 1 shows the electronic absorption spectra of Vat Orange 7 in two such organic solvents. The spectra of Vat Orange 7 adsorbed onto cellulose film (by a method described below) and of the dyestuff sublimed onto a quartz plate is illustrated in Figure 2. These spectra differ appreciably from those shown in Figure 3 obtained for a solution of Vat Orange 7 in 96% sulfuric acid (or for the model compound in other strong acids). For example, the maximum extinction coefficient of the visible absorption band is  $3.0 \times 10^4$  liters/mole cm. in *o*-chlorophenol and  $7.4 \times 10^4$  liters/mole cm. in 96% sulfuric acid for Vat Orange 7. The difference is attributed to protonation of the dyestuff which presumably acts as a multifunctional base in strong acid, as do many similar compounds (26, 28). The pyridine nitrogens and the carbonyl groups appear to be likely sites for the protonation.



*Figure 1. The electronic absorption spectra for solutions of model compound Vat Orange 7 in (A) xylene and (B) o-chlorophenol*



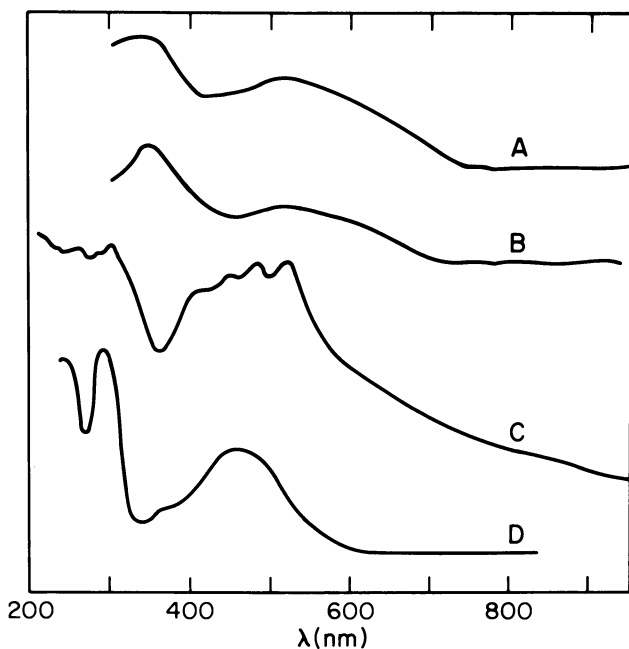


Figure 2. Electronic spectra of BBB and Vat Orange 7: (A) BBB suspended in a KBr pellet; (B) BBB adsorbed on cellulose; (C) Vat Orange 7 sublimed onto a quartz plate, and (D) Vat Orange 7 adsorbed on cellulose

Possible methods of determining the extent of protonation include absorption spectroscopy at a wavelength for which species with  $n$  and  $n-1$  protons have different extinction coefficients, freezing point depression, and electrical conductivity (15). Of these, we have utilized only spectroscopy, which has the disadvantage that only the equilibrium constants for the most highly protonated states are accessible if, as is usual, the species with low protonation are insoluble. In this method, the extinction coefficient  $\epsilon$  of the compound is determined as a function of the  $\text{H}_2\text{SO}_4$  content in the sulfuric acid solvent and correlated with the Hammett acidity function  $H_0$  (18) to give the  $pK_B$  value of the protonated species,

$$pK_B = H_0 + \log \frac{\epsilon_2 - \epsilon}{\epsilon - \epsilon_1}$$

where  $\epsilon_2$  and  $\epsilon_1$  are the extinction coefficients of the species with  $n$  and  $n-1$  protons, respectively. Efforts to determine  $pK_B$  for BBB and Vat Orange 7 are hampered by the tendency of these compounds to form colloidal dispersions in acids with less than 92%  $\text{H}_2\text{SO}_4$ . The effect is observed readily in solutions of BBB as a sudden marked change in the

extinction coefficient commencing in the low wavelength part of the spectrum and extending to the entire absorption spectrum as the  $\text{H}_2\text{SO}_4$  content of the acid is decreased. An estimate of  $\text{p}K_B = -7$  for Vat Red 15 was possible, however, since this compound remained in solution in 85%  $\text{H}_2\text{SO}_4$  solvent. (The unreliable values estimated from the data on solutions of Vat Orange 7 and BBB are consistent with this value of  $\text{p}K_B$ .) This magnitude is similar to that found for several polycyclic aromatic ketones (19) for which protonation of the carbonyl oxygen is postulated. It seems likely that this value represents only the protonation site of weakest basicity and that the compound is still multiply protonated when it precipitates from solution. On the basis of this behavior, we conclude that BBB is highly protonated in concentrated sulfuric acid

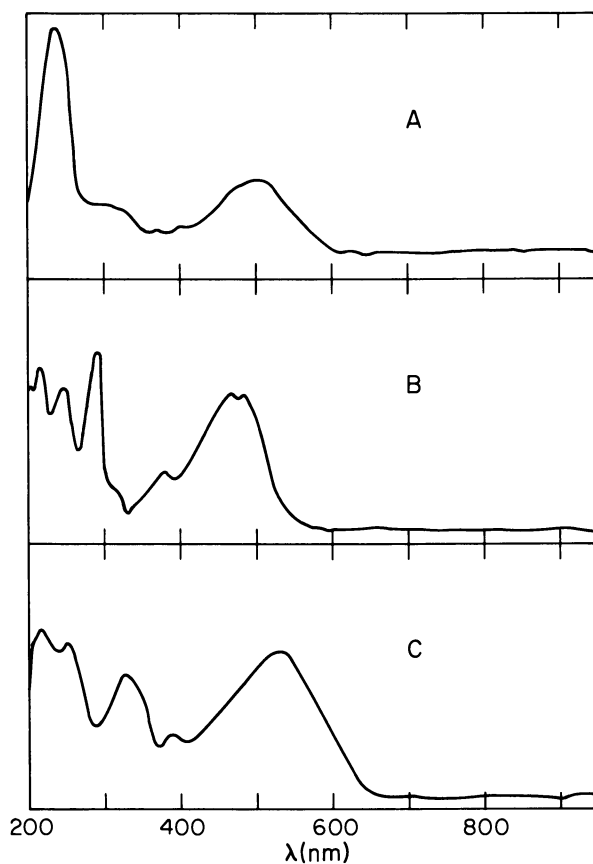


Figure 3. Electronic spectra of dilute solutions of BBB and its model compounds in solutions in 96% sulfuric acid: (A) Vat Red 15, (B) Vat Orange 7, and (C) BBB

to become a polyelectrolyte in the acid. Apparently the value of the acidity function  $H_0$  is not the only factor involved in the solubility of BBB and BBL in a particular acid, however, since methanesulfonic acid which is basic with respect to sulfuric acid appears to be a better solvent for both polymers than 96% sulfuric acid; similarly 85% phosphoric acid will dissolve BBB whereas sulfuric acid of composition with a comparable acidity function will not dissolve the polymer.

A method of fractionating BBB and similar polymers is desirable to obtain well defined polymers for dilute solution studies and other physical measurements and to elucidate the polymerization process. It is evident from the preceding discussion that the well established methods of fractionation that rely on the dependence of the solubility of the polymer on its chain length will be of little use in fractionating BBB. Attempts to fractionate BBB from solution in methanesulfonic acid by adding methanol or from solution in sulfuric acid by adding water confirm this conclusion. In both systems, addition of the nonsolvent did not cause immediate precipitation of the polymer, but instead the solution became increasingly turbid over a period of several hours. Once precipitated, the polymer could not be redissolved simply by increasing the temperature, and it was difficult to avoid almost complete precipitation and effect fractional precipitation. Finally, analysis of the "fractions" that were recovered revealed that essentially no fractionation had taken place.

Fortunately, it has been shown that chromatography on substrates with suitable-size pores can achieve a separation based on the molecular size of macromolecules in solution. (Recent papers based on this subject may be found in Ref. 20.) Samples of porous glass (kindly supplied by W. Haller (14, 17), National Bureau of Standards) with average pore diameters of 650 and 1700 Å. were used to construct chromatographic columns 50 cm. long and 1 cm. in diameter to evaluate this procedure for solutions of BBB in methanesulfonic acid, 96% sulfuric acid, and 85% phosphoric acid. Figure 4 is a block diagram of the apparatus. The effluent from the column is passed through a flow cell in a Beckman DU spectrophotometer equipped to record continuously the transmission at a fixed wavelength. The effluent is collected in 2.5-cc. increments in a siphon collector similar to that on the Waters GPC unit. A pulse is recorded on the strip chart at each discharge of the siphon collector to allow correlation of the effluent volume with the transmission. Fractionation was achieved in solutions in methanesulfonic acid and in 96% sulfuric acid, yielding fractions with  $5.0 > [\eta] > 1.6$  for a whole polymer with  $[\eta] = 2.6$  dl./gram, but appreciable absorption of the polymer on the glass substrate occurred in 85% phosphoric acid.

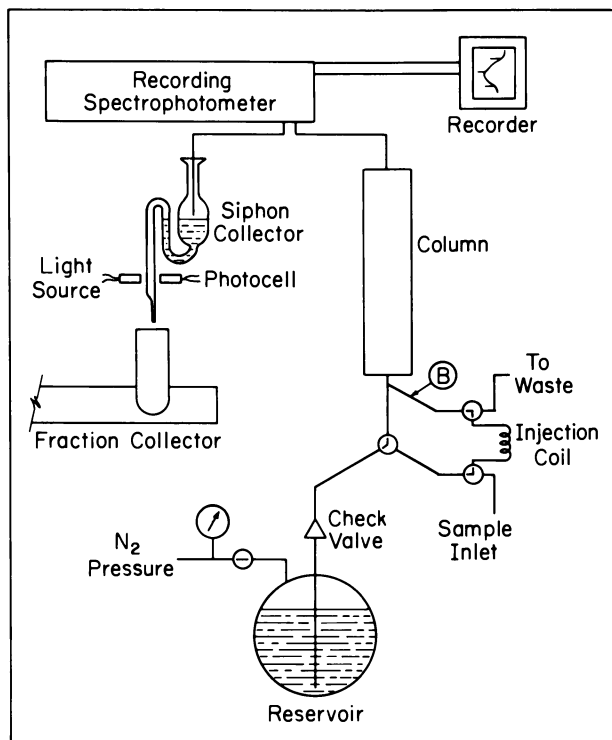


Figure 4. Schematic flow diagram of the preparative scale chromatography column

Although the exploratory results in columns constructed with glass supplied by Haller were very satisfactory, the glass was not available in sufficient quantity to construct large scale columns. Consequently, a large scale preparative column and a set of five analytical columns were constructed from the commercially available porous silica "Porasil" (*see* Experimental section for details of construction). The use of Porasil as a support for exclusion chromatography has been discussed recently by LePage *et al.* (21). The substrate in the preparative scale column was selected to fractionate a BBB polymer with  $[\eta] = 2.6$  dl./gram; the analytical column was designed to achieve separation over a wider range of species. Figure 5 illustrates the calibration of the analytical column with anionic polystyrene samples dissolved in butanone and in tetrahydrofuran. The abscissa is given at the ratio  $V_e/V_T$  of the maximum elution volume  $V_e$  to the total void volume  $V_T$  in the column. It is noteworthy that the product  $[\eta]M$  is independent of the solvent even though butanone is a relatively poor solvent for polystyrene, and tetrahydrofuran is a good solvent. This is to be expected if the separation is effected according to molecular size as generally supposed (4, 9).

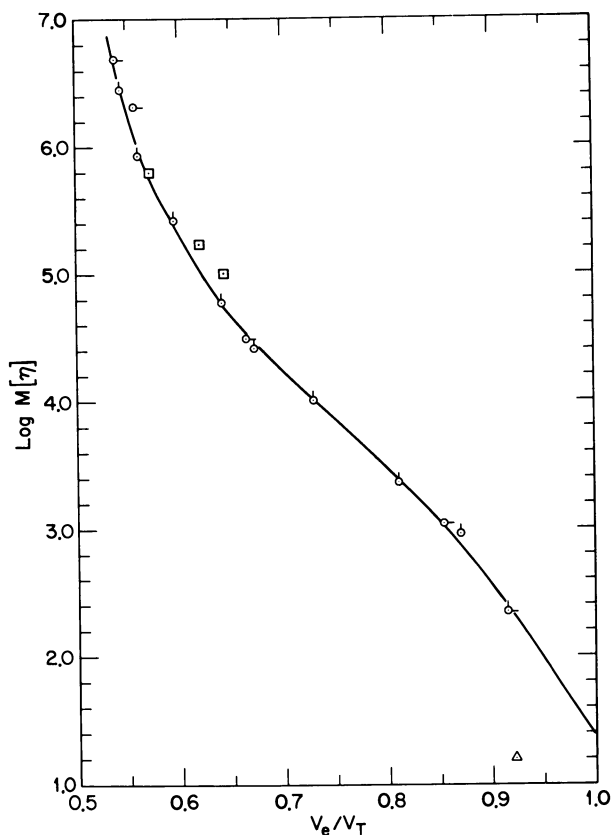


Figure 5.  $\text{Log } M[\eta]$  vs. the fractional elution volume  $V_e/V_T$  for anionic polystyrenes dissolved in toluene, ○, and in butanone, ○; and for BBB fractions dissolved in sulfuric acid, □

Figure 6, illustrating some data from the analytical column, shows chromatograms of two 0.5% solutions of unfractionated BBB samples with  $[\eta]$  equal to 2.6 and 0.2 dl./gram; Figure 7 shows chromatograms of three of the fractions of the unfractionated sample with  $[\eta] = 2.6$  that were obtained from the preparative column. The product  $[\eta]M$  for these three fractions correlates satisfactorily with the function relating  $[\eta]M$  with  $V_e/V_T$  found for the polystyrene fraction.

#### Miscellaneous Solvent Systems for BBB and BBL

The similarity of BBB and BBL to the vat dyestuffs suggests some alternate methods of forming solutions of these polymers by chemical modifications already well studied on the dyes. Both polymers can be

converted to a soluble form in aqueous solution containing 4 grams/liter sodium hydrosulfite, 10 grams/liter sodium hydroxide, and one-third pyridine by volume. The polymers are recovered easily by oxidation in air. It is assumed that the carbonyl oxygen is reduced by the sodium hydrosulfite, which is a commonly used reagent to effect reduction in vat dyestuffs (28). Both model compounds and the BBB and BBL polymers can be rendered soluble with this reagent. The intrinsic viscosity of a BBB sample with nearly the idealized structure (*cf. seq.*) shown above does not change after treatment with the reducing agent. This system has been found useful as a solvent for sedimentation velocity experiments in the ultracentrifuge, which cannot be carried out in sulfuric acid.

Treatment with fuming sulfuric acid produces an irreversible change in BBB but has no effect on BBL if the polymer is cyclized completely to give the structure indicated above. Further condensation may occur in solution in fuming sulfuric acid if the BBL is not formed completely before dissolution. Infrared analysis of the acid-treated BBB after precipitation in water shows the presence of sulfone and sulfonate groups, and gravimetric analysis shows that the polymer contains one sulfur

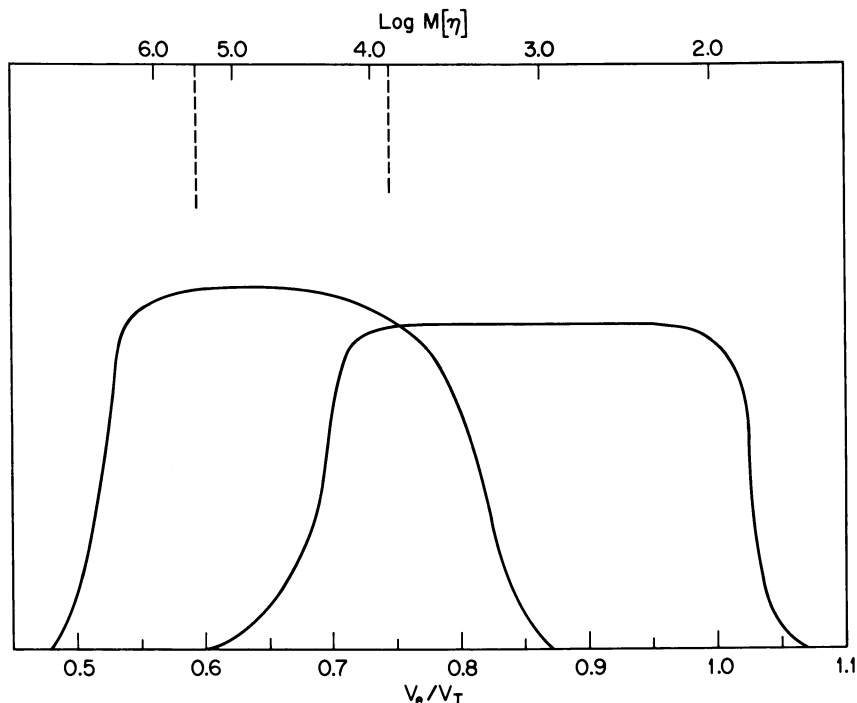


Figure 6. Optical density versus the fractional elution volume  $V_e/V_T$  and  $\log M[\eta]$  for two unfractionated samples of BBB. The dashed lines indicate the values of  $M[\eta]$  for the two samples

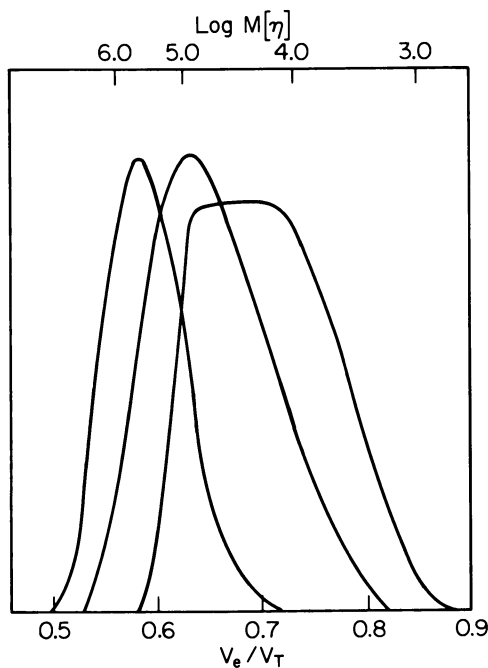
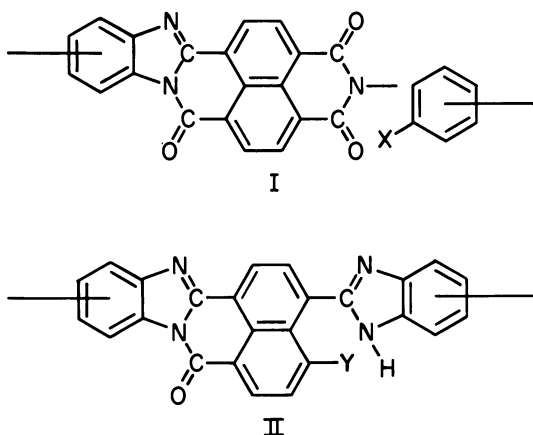


Figure 7. Optical density vs. fractional elution volume  $V_e/V_T$  and  $\log M[\eta]$  for the fractions of BBB

atom per repeating unit of the polymer. The acid-treated BBB is soluble in 0.1N sodium hydroxide.

### *Infrared Absorption Studies on BBB*

It is important to know to what extent the real polymer has the idealized structure that would result from polymerization without side reactions and completion of all desirable ring-forming reactions. Structural imperfections could include (a) branching, leading to complete insolubility if present in substantial amount, and/or (b) incomplete fusion of the ring structure of the heterocyclic repeat unit. Although side reactions that would lead to branching in a polymerization have been observed in condensation reactions involving pyromellitic dianhydride (3), these appear to be less likely with naphthalene-1,4,5,8-tetracarboxylic acid (2). Incomplete ring formation is of more concern here since the physical properties of the polymer may be sensitive to the presence of a few imperfect repeat units. The imperfect repeat units could contain either of the groups I or II, where X and Y can be amino



and carboxy groups, respectively, or can represent impurities in the monomers. The imide structure I can be detected in BBB through the characteristic strong absorption at  $1650\text{--}1660\text{ cm.}^{-1}$  that is evident in the spectra for the model compounds studied by Van Deusen *et al.* (27). This band is absent in the spectra of both the *cis* and *trans* model compounds of the repeat unit of BBB.

Spectra of KBr pellets of BBB usually do not have sufficient resolution to allow this band to be identified unambiguously and indicate that the imide content in the polymer is low. However, thin films of BBB can be rolled and examined in a cell in which the film can be evacuated and heated *in situ*. Figure 8 shows the results of a series of heat treatments *in vacuo*. Treatment at  $110^\circ\text{C.}$  results in considerable sharpening of the band at  $1660\text{ cm.}^{-1}$ . Exposure to water vapor causes the band to assume its original diffuse shape. Therefore, the presence of adsorbed moisture is the cause of the poor resolution in the original film. The intensity of the band after heating at  $110^\circ\text{C.}$  is a measure of the imide content in the polymer. The imide content of the polymer investigated in Figure 8 evidently is low, less than 5%.

Further heat treatment at temperatures below  $250^\circ\text{C.}$  causes a reduction in the imide content as measured by the absorption band at  $1660\text{ cm.}^{-1}$  and indicates completion of the remaining ring fusion. Continued heat treatment of the BBB film at temperatures in excess of  $600^\circ\text{C.}$  results in a drastic alteration in the spectrum. Separate studies on an Associated Electric Industries MS-9 mass spectrometer reveal that CO is evolved from BBB at temperatures in excess of  $600^\circ\text{C.}$ ; a concomitant weight loss accounted for by the loss of CO is observed for polymer samples heated *in vacuo*. Consistent with these results is a gradual diminution of the absorption band at  $1715\text{ cm.}^{-1}$ , together with its overtone at  $3400\text{ cm.}^{-1}$



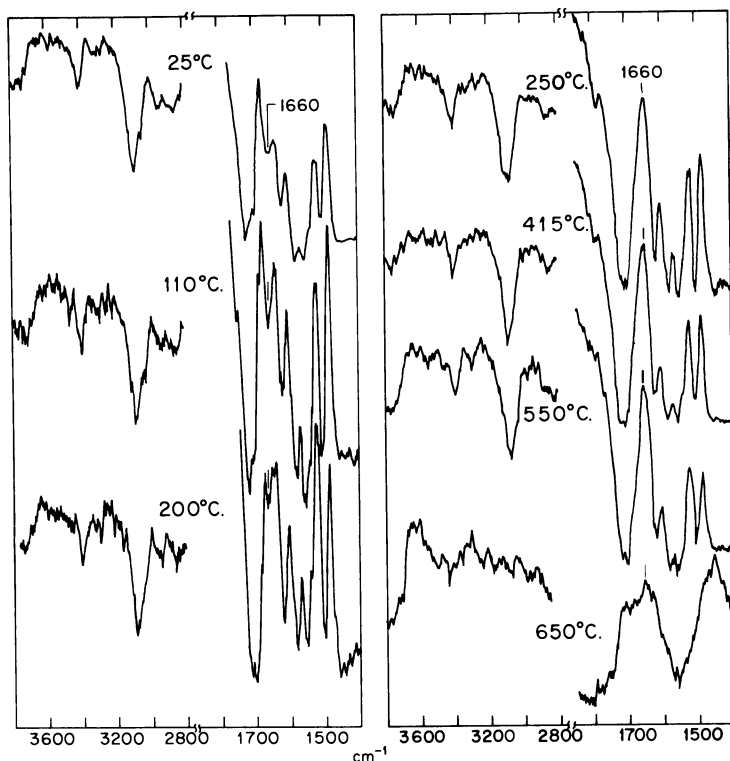


Figure 8. Infrared spectra for a BBB film heat treated in vacuo

when the film is held at 600°C. These bands are characteristic of the carbonyl group.

### **Physical Properties of BBB**

The dilute solution properties of BBB in strong acids can provide information on the chain conformation of the polymer. Figure 3 shows that light scattering studies cannot be carried out with the usual mercury vapor lamp with emissions of 4358 and 5461 Å. because of the strong absorption of BBB at these wavelengths. It is possible, however, to carry out measurements with a laser source of 6328 Å., although the scattered intensity still must be corrected for attenuation since the extinction coefficient is  $1.25 \times 10^3$  cc. gram<sup>-1</sup> cm.<sup>-1</sup> for BBB in methanesulfonic acid at this wavelength. (Since the extinction coefficient is appreciably higher for solutions of BBB in 96% sulfuric acid, light scattering measurements in that medium are very difficult.) Since the intensity of scattered light is proportional to the concentration  $c$  (neglecting second order effects in  $c$ ) and the attenuation is proportional to  $\exp(-\epsilon cl)$  increase of  $c$  to

values greater than  $c_m = (\epsilon l)^{-1} = (8 \times 10^{-4})l^{-1}$ , where  $l$  is the diameter of the light scattering cell, will not result in further increase in the intensity of the scattered light. Measurements were carried out with light scattering apparatus described elsewhere (5), modified by introducing

**Table I. Dilute Solution Parameters of BBB Polymer in Methanesulfonic Acid**

Sample	$10^{-4}M_w$	$10^{12}\langle s^2 \rangle, \text{cm.}^2$	$[\eta], \text{dl./gram}$
I-3	16.7	6.3 <sub>6</sub>	5.48
I-5	13.1	3.5 <sub>4</sub>	4.05
I-11	9.8	3.2 <sub>7</sub>	2.87
I-18	8.1	1.9 <sub>7</sub>	2.02
Whole I	9.73	2.6 <sub>4</sub>	2.66

a laser source. Small light scattering cells in which the solution could be centrifuged *in situ* were utilized (11) (see Experimental section for details). Since  $l = 1.2\text{--}1.4$  cm. for these cells, all concentrations were of the order  $5 \times 10^{-4}$  gram/cc. or lower in accordance with the comments above on  $c_m$ . Fortunately the high value of the refractive index increment  $dn/dc = 0.78$  cc./gram permits useful measurements to be carried out at these low concentrations. The light scattering data were analyzed according to the usual relations

$$Kc/R(u,c) = [1/MP(u)] + 2A_2c + O(c^2)$$

$$P^{-1}(u) = 1 + \frac{1}{3}u + O(u^2)$$

where  $u = [\langle s^2 \rangle (4\pi n/\lambda)^2] \sin^2\theta/2$ , with  $\langle s^2 \rangle$  the mean square radius of gyration,  $n$  the refractive index,  $\theta$  the scattering angle,  $\lambda$  the wavelength, and  $K$  the optical constant proportional to  $(dn/dc)^2$ . It was not possible to extract the second virial coefficient  $A_2$  from the data because, at the very low concentrations employed,  $c/R(u,c)$  is independent of  $c$  within experimental error. Values of  $M$ , and where possible  $\langle s^2 \rangle$  determined from the data are given in Table I. The uncertainty in the value of  $\langle s^2 \rangle$  increases with decreasing  $M$ , and  $\langle s^2 \rangle$  becomes difficult to determine with reasonable accuracy with the 6328 Å. light when  $10^{12}\langle s^2 \rangle = 1 \text{ cm.}^2$ .

Intrinsic viscosities of BBB in methanesulfonic acid were determined with a suspended level Ubbelohde viscometer by extrapolating the data for at least four concentrations to infinite dilution according to the simultaneous extrapolations:

$$\eta_{sp}/c = [\eta] + k'[\eta]^2c + O(c^2)$$

$$\ln \eta_{rel}/c = [\eta] - (\frac{1}{2} - k')[\eta]^2c + O(c^2)$$

Linear plots were obtained in every case over the interval  $1.2 < \eta_{rel} < 1.8$ .

The results are given in Table I. Values of  $k'$  vary from 0.3 to 0.5; these are typical for flexible coil polymers.  $[\eta]$  for the high molecular weight fractions could not be determined in 96% sulfuric acid apparently owing to considerable intermolecular aggregation as evidenced by a value of  $k'$  well in excess of unity and very poor reproducibility of results. This suggests there may be aggregation effects in the fractionation of BBB in the porous silica permeation column as well, although such effects should be minimal since the concentrations on the column are well below those necessary in the viscometric measurement. The value of  $[\eta]$  could be determined in concentrated sulfuric acid for the unfractionated polymer with  $[\eta] = 2.6$  dl./gram in methanesulfonic acid. Interestingly, a salting out effect is suggested in the slightly aqueous acid by an increase in  $[\eta]$  from 1.8 dl./gram in 96% sulfuric acid to 2.7 dl./gram in 100% sulfuric acid.

The values of  $M_w$  recorded in Table I have been used to plot  $M[\eta]$  vs.  $V_e/V_T$  on Figure 5 for the fractions of BBB studied (after correlation of  $[\eta_2]$  in methanesulfonic acid to  $[\eta_1]$  in 96% sulfuric acid by the relation  $[\eta_1] = 0.67 [\eta_2]$ ). The results are in reasonable agreement with the empirical relation between  $[\eta]M$  and  $V_e/V_T$  found with the polystyrene fractions.

The striking feature of the data given in Table I is that the exponent  $\nu$  in the Mark-Houwink relation

$$[\eta] = KM^\nu$$

exceeds unity even though the span in  $M$  covered is admittedly small. Four distinct and entirely independent reasons can be postulated for this behavior.

(1) An enormous excluded volume effect exists in methanesulfonic acid so that according to the relation

$$[\eta] = \Phi_0 \frac{\langle s^2 \rangle_0^{3/2}}{M} \alpha^3$$

we have

$$\nu = \frac{d \ln [\eta]}{d \ln M} = \frac{d \ln \Phi_0}{d \ln M} + \frac{d \ln (\langle s^2 \rangle_0 / M)^{3/2}}{d \ln M} + \frac{1}{2} + \frac{d \ln M}{d \ln \alpha^3}$$

with  $d \ln \alpha^3 / d \ln M$  exceptionally large. The expansion factor  $\alpha^2 = \langle s^2 \rangle / \langle s^2 \rangle_0$  is a measure of the increase of the molecular radius relative to the unperturbed value  $\langle s^2 \rangle_0$ .

(2) The excluded volume effect is not exceptionally large, but for the molecular weights of interest the unperturbed dimension  $\langle s^2 \rangle_0 / M$  has not yet reached its asymptotic level for large  $M$  and is still increasing with  $M$ .

(3) The BBB coil is so highly expanded that it behaves as a partially draining or free draining coil, in which case  $d \ln \Phi_0/d \ln M$  is very large. For a free draining coil we should put

$$[\eta] = \frac{N_A}{600} \frac{\langle s^2 \rangle_0}{M} \frac{M}{m_a} D_s$$

where  $N_A$  is Avagadro's number and  $D_s$  is the equivalent Stokes diameter of a hydrodynamic segment with molecular weight  $m_a$ . Thus  $[\eta]$  is proportional to  $M$  (excluded volume effects being neglected).

(4) The fractionation achieved on the porous silica substrate actually separates according to molecular size and not according to molecular weight. In fact, BBB cannot be considered as a homopolymer in this kind of separation, but must act as a "hexapolymer" comprised of the six repeat units illustrated schematically in Figure 9. In this case,  $\langle s^2 \rangle_0/M$  varies among the fractions not because of an inherent variation of  $\langle s^2 \rangle_0/M$  with  $M$ , but because the distribution of the repeat units is not the same for all fractions. In addition, and perhaps even more important, structural imperfections in the repeat units would greatly enhance this effect.

Of course, the observed behavior could result from some combination of these effects. The first possibility given above cannot be expected to explain the observed effect alone unless the BBB chain behaves in a far different way than other linear polymers for which  $\nu$  does not exceed *ca.* 0.80 (6, 7). Calculation of the Stokes diameter  $D_s$  from the data for  $[\eta]$ ,  $\langle s^2 \rangle$  and  $M$  in Table I yields values of the order 5 Å., which seems too low to be meaningful. Calculation of  $\Phi$  from the Fox-Flory relation (13)

$$\Phi = [\eta]M/\langle s^2 \rangle^{3/2}$$

together with the data in Table I yields values of  $\Phi \times 10^{-21}$  ranging from 45 to 80, compared with 40 both found experimentally for polystyrene (6) and 39.4 calculated theoretically (23). Thus, taking into account the uncertainty in the determination of  $\langle s^2 \rangle$ , the experimental values of  $\Phi$  suggest to us that BBB behaves essentially as a nondraining coil in methanesulfonic acid, despite the large value of  $\nu$ . Although additional data are needed, it seems probable that the extreme variation of  $\langle s^2 \rangle/M$  among the fractions implied by this conclusion can be accounted for by the effects of fractionation.

Calculation of the dimension  $\langle s^2 \rangle_{FR}/N$  of a chain with  $N$  segments with free rotation about valence bonds has not yet been carried out because of uncertainties in the dimensions of the six isomers of the repeat unit. The measured values of  $\langle s^2 \rangle$  correspond to  $\langle s^2 \rangle/N$  on the order of 100 Å.<sup>2</sup>, where a repeat unit is equated to a segment. It is expected that the freely rotating chain with fixed valence bonds will be a good model for BBB owing to the inappreciable steric interference to rotation about the single bonds connecting the repeat units. Such behavior has

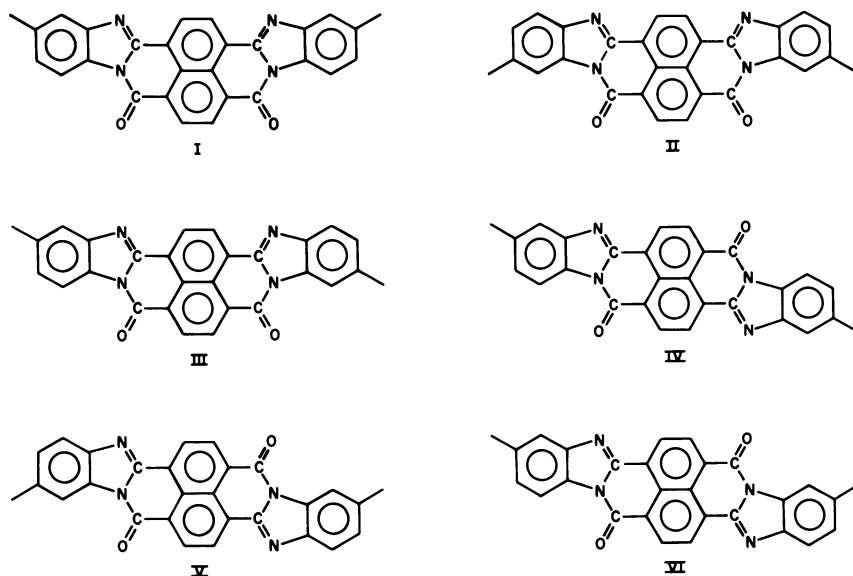


Figure 9. Schematic of BBB isomers

been inferred from data on  $[\eta]$  vs.  $M$  for unfractionated samples of the polyimide described in the introduction (29) and for other polymers containing groups in their backbone that tend to reduce hindrance to rotation about intrachain bonds (8, 30). If we naively use the simple relation

$$\frac{\langle s^2 \rangle}{N} = \frac{b^2}{6} \cdot \frac{1 + \cos \alpha}{1 - \cos \alpha}$$

applicable for a chain with free rotation about fixed valence bonds of length  $b$  which make an angle of  $\pi - \alpha$  with each other, we obtain  $(1 + \cos \alpha)/(1 - \cos \alpha) \simeq 2$  if  $b = 18$  A. Even though these correspond to a reasonable value of  $b$  and  $\cos \alpha = 1/3$ , the model is very crude since neither  $b$  nor  $\alpha$  can be considered as constant along the chain.

The possibility of intermolecular aggregation has been mentioned several times in the preceding discussion of the properties of BBB. For example, the electronic absorption spectra of solutions of BBB in sulfuric acid change markedly when the  $\text{H}_2\text{SO}_4$  content of the acid is decreased below *ca.* 92%. This behavior is accompanied by a marked increase in the dependence of the viscosity of dilute solutions on the polymer concentration, resulting in values of the Huggins  $k'$  constant greater than unity. In addition, the angular distribution of the scattered light reveals the presence of aggregated species by high intensity in the forward direction, and a rapid decrease as the scattering angle is increased. The x-ray

diffraction patterns shown in Figure 10 suggest that aggregation of BBB is also an important factor in the solid state. Thus, the diffraction patterns for the model compounds show them to be crystalline. In particular, the patterns for both model compounds reveal Bragg spacings in the neighborhood of 3.5 Å, which is characteristic of the interplanar separation of aromatic molecules with planar, or nearly planar, symmetry (25, 31). The polymer is apparently not crystalline, but the diffraction pattern in Figure 10 (bottom) shows a diffuse band centered at a Bragg spacing of 3.5–3.6 Å.

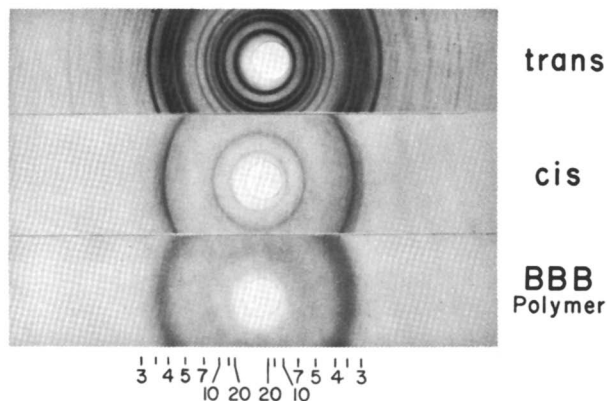


Figure 10. X-ray powder scattering patterns for the *trans* and *cis* model compounds of the BBB repeat unit and for BBB. The scale indicates Bragg spacings in Angstroms

It is not surprising that BBB is not crystalline in view of the six structural isomers possible for the repeat unit of the polymer. This spacing is interpreted as evidence for extensive short-range stacking of the repeat units of neighboring BBB chains giving the polymer some of the characteristics of a crosslinked network polymer. This interpretation is similar to that offered in explanation of the diffuse diffraction pattern observed for mixtures of polycyclic aromatic ketones. Thus, it has been shown that some planar polycyclic aromatic ketones that can easily be crystallized alone will not crystallize when mixed, even though they have similar over-all size and shape (1). It can be expected that the extra constraints imposed by the bonds connecting the repeat units in the polymer would inhibit further crystallization. It can be argued that an intermolecular spacing of about 3.5 Å is bound to occur in substance such as BBB simply because of considerations of packing the (nearly) planar repeat units into a dense solid and that no specific intermolecular bonding need be postulated. The mobility of such a molecular

arrangement would still be low because of the interlocking of the repeat units and their relatively large size. It should be noted, however, that neither the trans nor cis isomers of the model compounds can be melted to form liquids at atmospheric pressure. Thus,  $\Delta H_f/\Delta S_f$  is large so that the enthalpy of fusion  $\Delta H_f$  is relatively large or the entropy of fusion  $\Delta S_f$  is very small (or both). The entropy of fusion may be small because of the tendency of extended molecules to order simply on the basis of geometric arguments (12), but an appreciable value for  $\Delta H_f$  would not be unexpected for aromatic molecules of this type that can engage in an intermolecular electron transfer complex (22, 24). The fact that films can be formed from BBB by rolling, although the polymer will not flow under moderate shear stresses, supports the postulate of extensive inter-chain coupling; it is presumed that intermolecular bonds are broken and reformed under the influence of the high stresses encountered in rolling.

A similar kind of association may be responsible for the mechanical properties of the polyimide discussed at the beginning of this article. Thus, the "10-second modulus" shows only a gradual decrease over the temperature interval 30° to 450°C. rather than an abrupt decrease over a small temperature span, as is usually observed for linear amorphous polymers at temperatures near the glass transition (10). It was suggested that a small amount of crystallinity was responsible for this behavior, which is similar to the explanation advanced for the properties of BBB. Despite this indication of limited molecular mobility, the polyimide is reported to be ductile in elongation and thus again similar to BBB.

The model of the solid state of BBB discussed above is different from others proposed for heterocyclic condensation polymers. For example, the concepts of a material in a glassy state in which molecular mobility is hindered by considerations of volume do not apply, and marked changes in the mechanical properties with variation in temperature are not to be expected. Moreover, the properties of the solid state are not controlled by an inherent long range chain stiffness according to this model for BBB but rather by the inflexible planar character of short segments of the chain. It is expected that further studies including low angle x-ray scattering, and investigation of the viscoelastic properties of concentrated solutions of BBB will elucidate further the model proposed for BBB.

### **Experimental**

Some of the experimental details not discussed in the preceding text are gathered together in this section.

**Preparative-Scale Porous Silica Permeation Column.** The preparative-scale columns were constructed with a 4 foot length of 1.5-inch i.d. borosilicate glass pipe fitted with Teflon endplates as shown in Figure

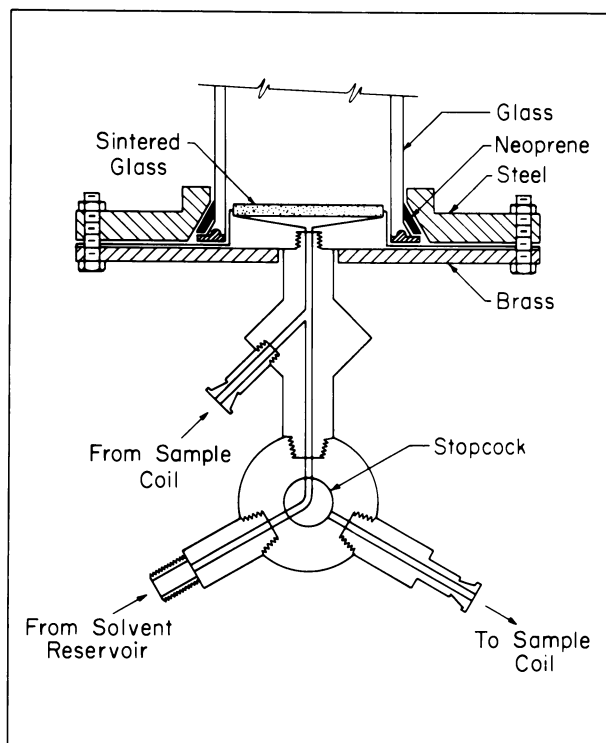


Figure 11. Schematic of the inlet end piece in cross section of the preparative scale porous silica chromatography column. All parts are Teflon unless otherwise noted. The thermostat jacket is not shown

11. The "Porasil" porous silica was added dry to the column through a funnel with a fine tip to disperse the powder evenly. The column used to fractionate the BBB polymer studied here contained 2/3 by volume "Porasil" D and 1/3 "Porasil" C. It was vibrated periodically during the filling operation with a hand vibrator and then again after it was completely packed. The columns were jacketed to permit operation above room temperature. Teflon tubing and valves equipped with Luer fittings (Hamilton Co.) were used in plumbing associated with the column with the exception of a 1/4-inch Teflon tube leading from the solvent reservoir to the column (*cf.* Figure 4) and the Teflon stopcock shown in Figure 11. A one-way Teflon valve (Mace Corp.) in the solvent inlet line prevented backflow of the solvent with the reservoir during the periodic filling of the reservoir. The reservoir was pressurized with dry filtered air at 8–10 p.s.i.g. to force the acid through the column at a flow rate of *ca.* 1 cc./min., no outgassing has been observed under these conditions on the preparative scale column. Samples injected on the column ranged from 1–2 grams/dl. in concentration; 20-cc. injection volumes were used. About 5 grams of polymer were processed and separated into



seven primary fractions. These were then recovered by precipitation in water, and each was reprocessed and separated into 22 fractions. Polymers so recovered from each of the seven primary fractions were then combined at like elution volumes to yield 22 final fractions. These were precipitated and washed extensively in water and dried under vacuum at 100°C.

**Analytical Scale Porous Silica Permeation Columns.** Five columns, each 110 cm. long, were constructed from heavy wall borosilicate glass tubing of 1/2-inch o.d. The tubes were fitted with Teflon plugs that extended past the end of the glass tubing as a 1/4-inch shaft. The Teflon shaft of the plug extended through a stainless steel tube-to-tube fitting with Teflon ferrules that provided a seal to the glass tube and to the Teflon shaft. A Luer-to-thread adapter (Hamilton Co.) was threaded into the Teflon shaft allowing the columns to be connected to Teflon tubing equipped with Luer fittings. The columns were jacketed to permit operation above room temperature. Each of the columns was packed with one grade of dry "Porasil" following the procedure given above. Porasils A, B, C, D, and E were used to construct the columns. Three-way Teflon valves (Hamilton Co.) were used in the construction of the injection loop. Injection volumes of 1–2 cc. were used.

The pressure drop across the set of five columns was very low (on the order of 20 p.s.i.g. at a flow rate of 5 cc./min.) with low viscosity organic liquids but was too high to permit safe operation at satisfactory flow rates with sulfuric acid with the pressure system utilized on the preparative-scale column. Thus, a glass/Teflon pump was constructed using standard 5-ml. glass syringes, Teflon tubing, Teflon one-way flow valves, and a Teflon pressure relief valve (Mace Corp.). One syringe was arranged to fill as the other pumped liquid through the column; thus serious pulsation of the flow in the column is prevented.

The columns were calibrated with anionic polystyrenes (Pressure Chemical Co.) in two solvents as described above. The pumping system and recording refractometer on the Waters gel permeation apparatus were used in this calibration. The resolution obtained was comparable with that typical with the Waters unit.

**Light Scattering and Viscosity Measurements.** All of the dilute solution studies reported above were carried out with one batch of methane-sulfonic acid (Eastman Co.) stored in the dark in an all-glass container under a blanket of nitrogen. (The acid as received varied in color from nearly colorless to light brown. The acid used was light yellow and had an absorption maximum of 283 nm. that tended to increase if the solvent was exposed to light for prolonged periods.) Light scattering measurements were carried out on an apparatus described elsewhere (5) except for a modification to allow interchangeable use of a mercury vapor lamp or a laser as the source. The modification involved only the mounting of the lamp; it did not alter the remaining optical or electronic features of the instrument.

Light scattering cells were of the type designed by Dandliker and Kraut (11) to permit the solution to be centrifuged in the cells for removal of dust. The cells were floated in sulfuric acid and centrifuged for 4–6 hours at 9000 r.p.m. in a Servall centrifuge equipped with a swinging bucket rotor. Cells suitable for use were selected from a hand-

blown batch. They varied in diameter from 12–15 mm. The effective diameter of each conically shaped cell was determined by measuring the attenuation of the scattering from a polystyrene sample in butanone accompanying the addition of one or two drops of a solution of crystal violet dye in butanone. The absorbance of the solutions was determined in a separate experiment with a standard 10-mm. absorption cell by using the light-scattering instrument as a spectrophotometer to avoid any mismatch of wavelength. Optical densities were adjusted to the levels typical of scattering experiments on solutions of BBB. The effective cell diameter is calculated easily from the data on absorbance in the 10-mm. cell and the attenuation of the scattering. Addition of the dye caused no change in the angular distribution of scattered light; thus, the geometric effect discussed by Frank and Ullman (14) can be neglected for the cells used here. (This effect can cause greater attenuation of light scattered in the forward direction than that scattered in the backward direction.)

The observed intensities of light scattered from BBB solutions were corrected for attenuation with data on the absorbance of each solution in a 10-mm. cell obtained by using the light-scattering apparatus as a spectrophotometer, together with the effective cell diameter discussed previously. This correction varied with solute concentration, being a factor generally between 1.1 and 5. (This correction is appreciably larger if 96% sulfuric acid is used as a solvent owing to small changes in the over-all shape of the absorption spectrum.) The absorption spectrum was also determined on each solution over the span 200–800 nm. to permit a check on the solute concentration and as a check on the solvent purity. Scattering data collected at four to six concentrations of the polymer over the angular range 25° to 135° were analyzed by conventional methods.

The refractive index increment  $dn/dc$  was measured on solutions of BBB used for light scattering studies. A differential refractometer described previously (5) except for the incorporation of a laser source was utilized. A very large value  $dn/dc = 0.785$  cc./gram was found for BBB. Comparably large values were found for the cis and trans model compounds, each of which had a value of  $dn/dc$  different from the polymer.

Intrinsic viscosities were determined with a Cannon-Ubbelohde semi-micro dilution viscometer, size 150, with a solvent flow time of 162 sec. for methanesulfonic acid at  $35.10 \pm 0.02^\circ\text{C}$ . The viscometer was modified slightly to permit operation under nitrogen; the liquid was forced up the capillary by nitrogen pressure before each flow-time determination. Dilutions were made by adding a weighed amount of solvent to the viscometer from a syringe equipped with a coarse filter. Concentrations were checked on the final dilution by measurement of the absorption spectra. Kinetic energy corrections were ignored because of the long flow times in the viscometer. All data were analyzed by dual plotting of  $\eta_{sp}/c$  and  $\ln \eta_{rel}/c$  as discussed in the text. The viscosities of solutions of BBB in methanesulfonic acid (or 96% sulfuric acid) were constant over a period of weeks.

### Acknowledgment

The authors acknowledge the contribution of K. G. Mayhan of the University of Missouri (Rolla) during his stay at Mellon Institute as a Visiting Fellow. This work has been supported in part by the Air Force Materials Laboratory under Contract No. AF33(615)-3884.

### Literature Cited

- (1) Akamatu, H., Nagamatsu, K., *J. Colloid Sci.* **2**, 593 (1947).
- (2) Arient, J., Dvořák, J., Šnobl, D., *Collections Czech. Chem. Commun.* **28**, 2749 (1963).
- (3) Arient, J., Haviličková, L., *Collections Czech. Chem. Commun.* **28**, 2534 (1963).
- (4) Benoit, H., Grubisic, Z., Rempp, P., Decker, D., Zilliox, J. G., *J. Chim. Phys.* **63**, 1507 (1966).
- (5) Berry, G. C., *J. Chem. Phys.* **44**, 4550 (1966).
- (6) *Ibid.*, **46**, 1338 (1967).
- (7) Berry, G. C., Fox, T. G., *J. Am. Chem. Soc.* **86**, 3540 (1964).
- (8) Berry, G. C., Nomura, H., Mayhan, K. G., *J. Polymer Sci.* **5**, 1 (1967).
- (9) Casassa, E. F., *J. Polymer Sci. Pt. B*, **5**, 773 (1967).
- (10) Cooper, S. L., Mair, A. D., Tobolsky, A. V., *Textile Res. J.* **35**, 1110 (1965).
- (11) Bandliker, W. B., Kraut, J., *J. Am. Chem. Soc.* **78**, 2380 (1956).
- (12) Flory, P. J., *Proc. Roy. Soc. London A* **234**, 60 (1956).
- (13) Fox, T. G., Flory, P. J., *J. Am. Chem. Soc.* **73**, 1904 (1951).
- (14) Frank, H. P., Ullman, R., *J. Opt. Soc. Am.* **45**, 471 (1955).
- (15) Gillespie, R. J., Robinson, E. A., "Non-Aqueous Solvent Systems," T. C. Waddington, Ed., Academic Press, New York, 1965.
- (16) Haller, W., *J. Chromatog.* **32**, 676 (1968).
- (17) Haller, W., *Nature* **206**, 693 (1965).
- (18) Hammett, L. P., *Chem. Rev.* **16**, 67 (1935).
- (19) Handa, T., *Bull. Chem. Soc., Japan* **28**, 483 (1955).
- (20) Johnson, J. F., Porter, R. S., Eds., *J. Polymer Sci. Pt. C*, **21**, 1968.
- (21) LePage, M., Bean, R., deVries, A. J., *J. Polymer Sci. Pt. C*, **21**, 119 (1968).
- (22) McGlynn, S. P., *Chem. Rev.* **58**, 1113 (1958).
- (23) Pyun, C. W., Fixman, M., *J. Chem. Phys.* **42**, 3838 (1964).
- (24) Schuyer, J., *Rec. Trav. Chim.* **75**, 878 (1956).
- (25) Stadler, H. P., *Acta Cryst.* **6**, 549 (1953).
- (26) VanDeusen, R. L., *J. Polymer Sci.* **B4**, 211 (1966).
- (27) VanDeusen, R. L., Goins, O. K., Sicree, A. J., *Am. Chem. Soc. Div. Polymer Chem., Preprints* **7**, 528 (1966).
- (28) Venkataraman, K., "The Chemistry of Synthetic Dyes," Academic Press, New York, 1952.
- (29) Wallach, M. L., *Am. Chem. Soc. Div. Polymer Chem., Preprints* **8**, 1170 (1967).
- (30) Wallach, M. L., *Makromol. Chem.* **103**, 19 (1967).
- (31) Yen, T. F., Erdman, J. G., Pollack, S. S., *Anal. Chem.* **32**, 1587 (1961).

RECEIVED July 19, 1968.

# INDEX

- A**
- ABS-type polymer, flame resistant 536  
 Acetaldehyde ..... 465  
 Acrylamide ..... 75  
 Acrylate esters ..... 277, 279, 281  
 Acrylic acid ..... 129  
 Acrylic monomers ..... 128  
 Acrylonitrile ..... 75, 94, 110, 113-5,  
 120-1, 129  
   -benzene mixtures ..... 28  
   bulk polymerization of ..... 25  
   heterogeneous polymerization of 33  
 Activation energies ..... 570  
 Activation temperature vs. molecu-  
 lar weight of ethylene polymer 398  
 Addition  
   copolymerization ..... 439  
   order vs. molecular weight ... 712  
   polymerization, free-radical ... 64  
 Adhesion, interfacial energy of ... 553  
 AFR ..... 268  
 Al-*i*-Bu<sub>3</sub>MeCl system ..... 297  
 Aliphatic chains, structures of ... 618  
 Alkenes ..... 126  
 Alkyl derivatives ..... 317  
 Alkyl vinyl ethers ..... 318  
 $\pi$ -Allylic complexes ..... 310  
 Al<sub>2</sub>Me<sub>6</sub>-Lewis base systems ..... 299  
 Al<sub>2</sub>Me<sub>6</sub>-MeCl complex ..... 293  
 AlMe<sub>3</sub>-MeCl system ..... 289  
 AlR<sub>3</sub>-Lewis base systems ..... 287  
 Alternating copolymerization ... 94  
 Aluminum chloride ..... 94  
 Amino radicals ..... 127  
 Amorphous polyamides ..... 614  
 Amorphous polystyrene ..... 521  
 Anionic emulsifier ..... 180, 182-5  
 Anionic free radical polymerizations 268  
 Anion free radical polymers of  
    $\alpha$ -olefins ..... 268  
 Anionic membranes ..... 567  
 Anions ..... 220  
 Anti-lumping agents ..... 523  
 Aromatic  
   azopolymers ..... 686  
   condensation polymers ..... 684  
   hydrocarbons ..... 287  
   polysulfonates ..... 703  
 Arylcarbonyl compounds ..... 47  
 Aryl derivatives ..... 317  
 Aryloxy radicals ..... 661  
 Autoacceleration indexes ..... 569-70  
 Azobisisobutyronitrile ..... 70  
 Azopolymer fiber ..... 689
- B**
- Batch polymerization ..... 16, 18  
 Batch reactors ..... 4, 14  
 BBB ..... 735  
 BCMO ..... 351  
 Benzene ..... 55-6  
   -acrylonitrile mixtures ..... 28  
 Benzoin ..... 61  
 Benzopyrylium derivatives ..... 317  
 Benzoyl peroxide ..... 70  
 Bicyclo[*n*.1.0]alkanes, polymeriza-  
 tion of ..... 434-5  
 4,4'-Biphenyldisulfonyl chloride .. 706  
 Bis( $\pi$ -allylnickel halides) ..... 307  
 3,3-Bischloromethyloxetane .... 351, 355  
 Bis( $\pi$ -crotylnickel chloride) ... 308-10  
 Bis( $\pi$ -crotylpalladium chloride) .. 252  
 Bisphenol-A ..... 706  
 Bisphenols ..... 693  
 Bistetracyclones ..... 634  
 Block polymerization ..... 268, 283  
 Block copolymers of polystyrene .. 522  
 Block polymers 271-3, 275, 278-82, 284  
 Block and random copolymers by  
   cationic copolymerization ... 350  
 Blowing agents ..... 514, 517, 520  
 Boron trifluoride dibutyl etherate . 360  
 BPDSC ..... 706  
 Branched carboxylic acids, vinyl  
   esters of ..... 178  
 Bromine-containing monomer, ter-  
   polymerization with a novel .. 536  
 Bulk polymerization ..... 324  
   of acrylonitrile ..... 25  
 Butadiene ..... 113, 115, 120, 126  
   emulsion polymerization of ... 309  
   initiated by the transition metal  
    $\pi$ -complexes, stereospecific  
   polymerization of ..... 306  
 Butenyllithium chloride ..... 251  
 Butenylmagnesium chloride ..... 251  
*tert*-Butyl hydroperoxide ..... 75, 127  
*n*-Butyl methacrylate ..... 75  
 Butyl peroxy isopropyl carbonate .. 70  
 Butyl-*p*-xylylene ..... 649
- C**
- Caprolactam, polymerization of  
 $\beta$ -carboxymethyl ..... 717

Carbathoxynitrene .....	426-7	Complexed monomers, copolymerization of metal halide .....	108
Carbon monoxide-chromium complex .....	395	Complexed monomers, homopolymerization of metal halide- ..	106
Carbonium ion polymerizations ..	287	Complexes, metal-crotyl .....	255
theory of initiation and propagation of .....	300	$\pi$ -Complexes, stereospecific polymerization of 1,3-butadienes initiated by metal .....	306
Carbonyl groups, pendant .....	94	Complex formation, catalysis of .....	104
Carboxylic acids, vinyl esters of branched .....	178	-radical processes .....	120
Carboxylic membranes .....	561	stability <i>vs.</i> copolymerizability ..	100
$\beta$ -Carboxymethyl caprolactam, polymerization of .....	717	Condensation <i>via</i> DMT .....	622
Carboxy-terminated polyisobutylene .....	448, 450	polymerization .....	17
Catalysis of complex formation ..	104	polymers, aromatic .....	684
Catalyst-solvent systems .....	685	<i>via</i> terephthalic acid .....	622
Catalysts, supported chromium oxide .....	387	Conjugated dienes .....	419
Catalyst systems .....	251	Contact angle <i>vs.</i> critical surface tensions ....	552
Catalyzed oxidative coupling ....	679	<i>vs.</i> NaCl concentration .....	549-50
Cationic polymerization .....	317	radiation dose <i>vs.</i> .....	544
and copolymerization of trioxane	359	Continuous variable approach ....	11
Cationic copolymerization, block and random copolymers by	350	Continuous stirred tank reactors .....	4, 14, 16, 18
of trioxane and 1,3-dioxolane ..	371	Copolymerizability, complex stability <i>vs.</i> .....	100
Cations .....	223	Copolymerization .....	645
Cellulose copolymerization of vinyl monomers with .....	579	addition .....	439
graft copolymers .....	574, 585	block and random copolymers by cationic .....	350
morphology of fibrous .....	586	with depropagation .....	439
trapped radical yield in .....	577	emulsion .....	178
Ceric ion initiation .....	577, 582	of ethylene and 1-olefins .....	396
Chain addition with termination ....	21	with ethylene oxide .....	365
growth .....	728	of metal halide-complexed monomers .....	108
propagation, topochemistry of ..	380	of olefins on chromium oxide catalysts .....	387
reaction with termination .....	13	reactivity ratios in .....	374
transfer .....	198	reversibility of .....	441
Chemical shifts of cyclopentane .....	297	ring opening .....	446
methyl chloride .....	298	trioxane .....	362-6
triisobutylaluminum .....	298	cationic .....	359
$\alpha$ -Chinaldoin .....	61	of VAc .....	138
Chloro- <i>p</i> -xylylene .....	649, 650, 652	of vinyl monomers with cellulose	579
( $C_4H_7NiCl$ ) <sub>2</sub> .....	315	with vinyl carboxylic acids ....	189
$C_4H_7NiX_2$ .....	311	Copolymers .....	194
Chromium complex, carbon monoxide- .....	395	Counter-anion species, water contact angles as a function of the mobile .....	542
Chromium content <i>vs.</i> reaction rate	394	Counterion, drop configuration <i>vs.</i> surface .....	558
Chromium oxide catalysts, polymerization and copolymerization of olefins on .....	387	Coupling constants .....	134, 143
Chromium oxide on silica-alumina, polymerization over nickel oxide- .....	396	mechanism, polymer .....	667
Chromium trioxide, stabilizing interaction between the support and .....	389	of polymer molecules .....	662
Coagulation by freezing and thawing .....	192	Crosslinking of styrene copolymers, internal .....	489
Comonomer in vinyl acetate .....	179	Critical surface tensions .....	550, 552
Complex copolymerization .....	120	<i>vs.</i> water contact angle .....	552
		Crystalline structures .....	473
		Crystallization during polymerization .....	380

- Crystal size ..... 233  
 Cocatalyst systems ..... 287  
 Crotyllithium ..... 252  
 CSTR ..... 4, 14  
 CTPIB ..... 451, 452  
 Cyclic formals ..... 351  
 Cyclization ..... 489  
 1,5,9-Cyclododecatriene ..... 400  
 extractable macrocyclics ..... 412  
 Cycloheptatrienyl derivatives ..... 317  
 1,5-Cyclooctadiene ..... 400  
 extractable macrocyclics ..... 411-2, 414  
 Cyclooctene ..... 400, 413  
 extractable macrocyclics ..... 410  
 Cycloolefins, metathesis of ..... 402  
 Cycloolefins, ring-opening polymerization of ..... 399  
 Cyclopentadienones ..... 629  
 Cyclopentane, chemical shifts of ..... 297  
 Cyclopropane hydrocarbon macro-molecules, preparation of ..... 423  
 Cyclopropane models ..... 437  
 Cyclopropanes ..... 421  
 NMR spectra of ..... 426  
 $\alpha$ -cyano- $\alpha$ -naphthyl pyruvic acid ethyl ester ..... 52-5
- D**
- DBPF ..... 537  
 Dead polymer ..... 149  
 Degree of polymerization, gegenion vs. .... 337  
 Depropagation, copolymerization with ..... 439  
 Deuteriochloroform ..... 53  
 Diamines ..... 615-6  
 to azopolymers, polymerization of primary aromatic ..... 679  
 Dichlorocyclopropanes, polymerization of ..... 431  
 primary aromatic ..... 681  
 1,1-Dichlorocyclopropanes, polymerization of ..... 430  
 Dichloro-*p*-xylylene ..... 652  
 Dicumyl peroxide ..... 69-70  
 initiator ..... 68  
 Diels-Alder reaction in polymer synthesis ..... 628  
 Diene polymerization ..... 250  
 Diene synthesis ..... 628  
 Dienes ..... 287  
 conjugated ..... 419  
 Dihalocarbenes ..... 420  
 Dihalocyclopropane models ..... 424  
 Dihalocyclopropanes ..... 420  
 preparation of ..... 422  
 Diketene ..... 466  
 Dilatometer ..... 29  
 Dimethylaminoethyl methacrylate ..... 280  
*p*-Dioxene-maleic anhydride ..... 97  
 1,3-Dioxolane ..... 351, 355  
 cationic copolymerization of ..... 371  
 living polymer of ..... 352
- Dissociating dimer ..... 631-2  
 Distribution vs. rate ..... 7  
 Di-*tert*-butyl peroxide ..... 69, 70  
 DMT, condensation vs. .... 622  
 DOL ..... 351  
 Donor-acceptor molecular complexes ..... 94  
 Dose rate ..... 567  
 exponents ..... 570  
 Drop configuration vs. surface counterion ..... 558  
 Dryness ..... 238  
 Dynamic allylic compounds ..... 251
- E**
- Eigenzeit transformation ..... 12  
 Electrical conductivity ..... 207  
 Electron micrographs ..... 26  
 Electron spin resonance ..... 33  
 HEMA ..... 490  
 Emerging polymer ..... 472  
 Emerging poly(vinyl chloride), globular structure of the ..... 469  
 Emulsifier, anionic ..... 180  
 Emulsion  
 -addition method ..... 180  
 copolymerization ..... 178  
 polymerization ..... 145, 179, 470  
 of 1,3-butadiene ..... 309  
 vinyl chloride ..... 158  
 -seeded polymerization ..... 176  
 Emulsions, freeze/thaw stability of polymer ..... 188  
 Encapsulation, particle ..... 656  
 End group analysis ..... 77  
 End-linking ..... 662  
 Equilibrium conversion of monomeric THF to polymer ..... 324  
 Equilibrium polymerization ..... 417  
 ESR ..... 125  
 Et<sub>3</sub>OBF<sub>4</sub> ..... 352  
 EVA copolymers ..... 477  
 Ethyl acrylate ..... 75  
 Ethylene ..... 268  
 glycol dicarboxylic acid, polyesters of ..... 617  
 and 1-olefins, copolymerization of oxide ..... 396  
 copolymerization with ..... 360  
 polymers, molecular weight of .. 365  
 -vinyl acetate copolymers, graft polymerization of vinyl compounds on ..... 477  
 2-Ethylhexyl acrylate ..... 65  
 Ethyl methacrylate ..... 75  
 Ethyl-*p*-chloroxylylene ..... 650  
 Expandable  
 beads ..... 529  
 olefin-sulfur dioxide copolymers ..... 529  
 polystyrene processes ..... 513  
 Extruded foams ..... 524

<b>F</b>	
Fenton's reagent .....	127-8
Flame resistant ABS-type polymer .....	536
Flammability tests .....	538
Foam, polybutene sulfone .....	534
Formation of macrocyclics .....	406
Free-radical	
addition polymerization .....	64
formation .....	575
inhibitors .....	77
initiated polymerization .....	94
polymerization .....	273
of immobilized chains .....	25
polymers of $\alpha$ -olefins, anionic ..	268
Freeze/thaw stability of polymer emulsions .....	188
Freezing and thawing, coagulation by .....	192
F/T stability .....	191
Furoin .....	56
$\alpha$ -Furoin .....	61
<b>G</b>	
GaCl <sub>3</sub> .....	315
Gas chromatography .....	409
Gegenion	
vs. degree of polymerization ..	337
vs. GPC results .....	345
vs. intrinsic viscosity .....	341, 344
vs. molecular weight distribution	342
vs. percent conversion .....	341-2
in tetrahydrofuran polymerization	335
Gel permeation chromatography ..	76
Geminate chain termination .....	35
Geminate pair, lifetime of a .....	40
Glass temperatures .....	613-4
Globular structure of the emerging poly(vinyl chloride) .....	469
Glycidyl acrylate .....	65
Glymated pair .....	246
Graft	
copolymers, morphology of fibrous cellulose .....	586
polymerization of vinyl compounds on ethylene-vinyl acetate copolymers .....	477
polymers .....	537
Grafting of monomer to surface-active agents .....	189
Growing particle size .....	162
Growing radicals .....	145
Growth of polymer particles .....	158
<b>H</b>	
HEMA .....	505
Heterocyclic polymer .....	734
Heterogeneous polymerization of acrylonitrile .....	33
Hexachloroantimonate salts .....	319
Hexamethylcyclotrisiloxane, solid state polymerization of .....	229
Hexapolymer .....	749
Homopolymerization .....	362
of metal halide-complexed monomers .....	106
reversibility of .....	440
Hydrogen peroxide .....	125
Hydroperoxide, <i>tert</i> -butyl .....	75
Hydrophilic monomers, radiation grafting of .....	560
Hydrophilicity .....	543
Hydroxyethyl methacrylate .....	490
Hydroxyl radical initiation .....	578, 583
<b>I</b>	
Immobilized chains, free radical polymerization of .....	25
Initial concentration, viscosity vs.	499
Initiation	
and propagation of carbonium ion polymerizations, theory of .....	300
with triphenylmethyl cation ..	318, 323
Initiation with tropylium ion ..	322, 330
Initiator .....	69
dicumyl peroxide .....	68
radicals, termination by .....	36
systems .....	127
Initiators .....	71
keto-enol tautomers as polymerization .....	46
for unsaturated polyester/styrene copolymerization systems ..	47
Interfacial	
energies .....	557
energy of adhesion .....	553
model .....	555
polycondensation .....	708
Internal crosslinking .....	490
of styrene copolymers .....	489
Internal cyclization .....	490
Intrinsic viscosity .....	501, 747
vs. gegenion .....	341, 344
Ionic polymerization, radiation-induced .....	202
Ionic polymerizations, mechanisms of propagation of .....	236
Ionizing radiation .....	542, 575, 580
Ion-pair dissociation constants ..	319
Irradiation temperature .....	565, 568
Isoprene .....	112, 114, 120
Isobutylene .....	287
Isobutyl vinyl ether .....	82
polymerization of .....	323
Isocyanate concentration, effect of	499
Isoolefins .....	287
Isotactic polystyrene .....	521
<b>K</b>	
Ketal redistribution, quinone .....	663, 665, 666
Keto-enol tautomers as polymerization initiators .....	46

- Kinetic  
 behavior of styrene polymeri-  
 zation ..... 204  
 chain length ..... 73  
 scheme ..... 209, 215
- Kinetics  
 of polymerization ..... 77  
 of solution polycondensation ... 692  
 of vinyl polymerization ..... 35
- L**
- Laplace transforms ..... 11  
 Levapren 450 ..... 478  
 Lewis acids ..... 309-10  
 Lewis base systems,  $Al_2Me_6$ - .... 299  
 Lewis base systems,  $AlR_3$ - .... 287  
 Lifetime of a geminate pair .... 40  
 Light scattering ..... 504, 508  
 Limiting polymer size  
 distribution ..... 153, 155  
 Liquid crystals ..... 466-8  
 Liquid rubbers ..... 448  
 Living polymers ..... 238  
 of 1,3-dioxolane ..... 352  
 Lowry case II ..... 443
- M**
- Macrocyclic extractables ..... 407  
 Macrocylics, formation of ..... 406  
 Macrocylics, selective formation of  
 Macromolecular polyenes ..... 416  
 methylene transfer to ..... 419  
 425  
 Markov process ..... 146  
 Mathematical techniques ..... 10  
 Mechanical stability ..... 191  
 Mechanisms for initiating polymeri-  
 zation by stable organic cations  
 ..... 317  
 Mechanisms of propagation of ionic  
 polymerizations ..... 236  
 Metal-allylic compounds ..... 261  
 Metalallyls, structure of ..... 250  
 Metal  
 -crotyl complexes ..... 255  
 $\pi$ -complexes, stereospecific poly-  
 merization of 1,3-butadiene  
 initiated by transition ..... 306  
 halides ..... 94  
 halide-complexed  
 monomers, copolymerization of  
 monomers, homopolymeriza-  
 tion of ..... 106  
 vinyl monomers, polymeriza-  
 tion of ..... 94  
 Metathesis of cycloolefins ..... 402  
 Methacrylates ..... 473  
*p*-Methacrylylhydroxybenzoic acid 466  
 Methacrylic acid ..... 129, 193  
 Methacrylic monomers ..... 128  
 Methyl acrylate ..... 75  
 Methyl chloride ..... 295  
 chemical shifts of ..... 298
- Methylene transfer to macromolec-  
 ular polyenes ..... 425  
 Methyl group exchange ..... 288  
 Methyl groups ..... 607  
 frozen ..... 606  
 in polycarbonate and poly- $\alpha$ -  
 methylstyrene, mobility of . 592  
 Methyl methacrylate ... 94, 118-9, 121  
 -ethyl acrylate-methacrylic acid  
 terpolymers ..... 194  
 and other vinyl monomers, poly-  
 merization of ..... 75  
 2-Methyl-1-pentene ..... 110  
 Methyl radicals ..... 127  
 $\alpha$ -Methylstyrene, pulse radiolysis of 219  
 2-Methyl-5-vinylpyridine ..... 269  
 Minimum film formation tempera-  
 ture ..... 193  
 Mobility of methyl groups in poly-  
 carbonate and in poly- $\alpha$ -  
 methylstyrene ..... 592  
 Model polyenes ..... 419  
 Models  
 dihalocyclopropane ..... 424  
 polybutadiene ..... 423  
*cis*-1,4-polyisoprene ..... 423  
 Molecular weight  
 addition order *vs.* ..... 712  
 distribution ..... 4, 9, 145  
 gegenion *vs.* ..... 342  
 of ethylene polymers ..... 397  
 activation temperature *vs.* ... 398  
*vs.* monomer balance ..... 636  
 Moments ..... 12  
 of the size distribution ..... 154  
 Monodispersed latexes ..... 169  
 Monomer  
 balance *vs.* molecular weight .. 636  
 concentration ..... 272  
 conversion, rates of ..... 376  
 -polymer redistribution ..... 676  
 reactivity ratios ..... 507  
 to surface-active agents, grafting  
 of ..... 189  
 Monomers, polymerization rates of  
 various ..... 396  
 Morphology of fibrous cellulose  
 graft copolymers ..... 586  
 Multichain polymers ..... 64  
 Multistate stereospecific polymeri-  
 zation mechanism ..... 250  
 MWD ..... 4
- N**
- NaCl *vs.* droplet contact angle .. 549-50  
 $\alpha$ -Naphthenoin ..... 56  
 Network quality *vs.* prepolymer  
 functionality ..... 449  
 Newton's method ..... 37  
 Nickel oxide-chromium oxide on  
 silica-alumina, polymerization  
 over ..... 396



Nitrile groups, pendant .....	94	Polycarbonate, mobility of methyl groups in .....	592
Nitrile rubbers .....	537	Polycondensation	
NMA .....	359	of aromatic polyethers, solution	692
NMR .....	592	interfacial .....	708
spectra of cyclopropanes .....	426	polymers .....	612
spectra of the oxonium salts .....	340	solution .....	711
spectroscopy .....	287	Polydiketone .....	466
nonionic emulsifier .....	180, 182	Polydispersed latexes .....	169
Numerical techniques .....	13	Polydisulfides .....	680
Nylon 6/6 .....	543, 612	Polyelectrolytes on polymer surfaces, radiation-grafted .....	542
<b>O</b>			
Olefin copolymerizations with alkylaluminum .....	287	Polyenes, macromolecular .....	419
Olefin polymerizations with alkylaluminum .....	287	Polyenes, model .....	419
$\alpha$ -Olefins, anionic free radical polymers of .....	268	Polyesters .....	466, 612, 619
Olefins on chromium oxide catalysts, polymerization and copolymerization of .....	387	of ethylene glycol dicarboxylic acid .....	617
1-Olefins, copolymerization of ethylene and .....	396	-styrene copolymerization systems, initiators for unsaturated .....	47
Olefin-sulfur dioxide copolymers, expandable .....	529	unsaturated .....	46
Organic cations, mechanisms for initiating polymerization by stable .....	317	Polyethers .....	197
Organic peroxide .....	268	solution polycondensation of aromatic .....	692
Organometallic compounds .....	251	Polyethylene .....	473
Oxidative coupling .....	679	Poly(ethylene oxide) .....	197
polyphenylene oxides by .....	660	Polyfunctional membranes .....	572
reaction .....	681	Polyisobutylene, carboxy-terminated .....	448, 450
Oxonium ion equilibria .....	328	<i>cis</i> -1,4-Polyisoprene models .....	423
Oxonium salts, NMR spectra of the .....	340	Polyisoprene structures .....	426
Ozonization .....	451, 453-61	Poly-1,5-octadienamer extractable macrocyclic fraction .....	415
<b>P</b>			
Particle encapsulation .....	656	Polymerization	
Particle size distribution .....	186	of acrylonitrile, bulk .....	25
Pendant nitrile and carbonyl groups .....	94	of acrylonitrile, heterogeneous .....	33
PEPT .....	612	of the bicyclo[ <i>n</i> .1.0]alkanes .....	434-5
Percent conversion, gegenion vs. .....	341-2	of $\beta$ -carboxymethyl caprolactam .....	717
Permeable membranes .....	560	crystallization during .....	380
Peroxides .....	270, 280	-depolymerization equilibrium .....	372
Phenylacetaldehyde .....	46	of 1,1-dichlorocyclopropanes .....	430-1
2-Phenyl-1,1-dichlorocyclopropane, polymerization of .....	433	diene .....	250
Phenylmethacrylamide .....	474	of immobilized chains, free radical .....	25
<i>p</i> -Phenylenediamine .....	683	initiators, keto-enol tautomers as .....	46
Phthalyl chlorides .....	706	of isobutyl vinyl ether .....	323
Polar groups .....	269	kinetic theory .....	695
Polar monomers .....	94, 274	kinetics of vinyl .....	35
Polyacetal .....	466	of metal halide-complexed vinyl monomers .....	94
Polyacetylenes .....	679	of methyl methacrylate and other vinyl monomers .....	75
Polyamides .....	612-3, 615-6, 619, 632	over nickel oxide-chromium oxide on silica-alumina .....	396
amorphous .....	614	of olefins on chromium oxide catalysts .....	387
reverse .....	618-9	of 2-phenyl-1,1-dichlorocyclopropane .....	433
Poly(arylene oxides) .....	673	of primary aromatic diamines to azopolymers .....	679
Polyazoaromatics .....	680	rates of various monomers .....	396
Polybutadiene models .....	423	reaction engineering .....	1
Polybutene sulfone foam .....	534	reproducibility of .....	70
Polybutene sulfones .....	529	of spiropentane .....	436

- Polymerization (*Continued*)  
 structural phenomena in ..... 465  
 suspension ..... 529  
 of tetrahydrofuran ..... 323  
 of tricentric systems ..... 430  
 of trioxane, cationic ..... 359  
 in two-phase systems ..... 145  
 of *N*-vinylcarbazole ..... 330-1  
 vinyl chloride emulsion ..... 158
- Polymer  
 concentration *vs.*  
   viscosity ..... 493, 497, 502  
 coupling mechanism ..... 667  
 emulsions, freeze/thaw stability  
   of ..... 188  
 flame resistant ABS-type ..... 536  
 growth ..... 469  
 latices ..... 179  
 molecules, coupling of ..... 662  
 oxidation, chemistry of ..... 462  
 particles, growth of ..... 158  
 polymer redistribution ..... 676  
 surfaces, radiation-grafted poly-  
   electrolytes on ..... 542  
 synthesis, Diels-Alder reaction in  
 Poly(methyl methacrylate) ..... 474  
 Poly- $\alpha$ -methylstyrene, mobility of  
   methyl groups in ..... 592  
 Polyoctamer extractable macro-  
   cyclic fraction ..... 415  
 Polyolefin ..... 268  
   molecules ..... 269  
 Polyoxymethylene copolymers ... 371  
 Poly(phenylene oxides) ..... 679  
   by oxidative coupling ..... 660  
 Polyphenylenes ..... 679  
 Polyphenyls ..... 633  
 Polypropylene polymers ..... 284  
 Polystyrene ..... 197, 472  
   block copolymers of ..... 522  
   processes, expandable ..... 513  
   salts ..... 240  
   polystyryl anions ..... 240  
 Polysulfonates, aromatic ..... 703  
 Polytetrafluoroethylene ..... 560  
 Polytetrahydrofuran ..... 335  
 Poly(tetramethylene oxide) ..... 335  
 Poly(vinyl alcohol) ..... 466  
 Poly(vinyl chloride), globular  
   structure of the emerging .... 469  
 Poly(vinyl isobutyl ether) ..... 320  
 Porofor N ..... 478  
 Porous silica permeation ..... 754  
 Postadditions ..... 190  
 Potassium phenoxide ..... 699  
 Prepolymer functionality, network  
   quality *vs.* ..... 449  
 Primary aromatic diamines ..... 681  
   to azopolymers, polymerization of 679  
 Primary radicals ..... 26  
 Propagation of carbonium ion poly-  
   merizations, theory of initiation  
   and ..... 300  
 Propylene ..... 121, 268
- Protonation ..... 737-8  
 Pseudo-steady state assumption .. 11  
 PSSA ..... 11  
 PTFE ..... 560  
 PTHF ..... 335  
 Pulse radiolysis ..... 208  
   of styrene and  $\alpha$ -methylstyrene . 219  
 Push-pull mechanism ..... 246  
 PVC particles ..... 469  
 Pyridine ..... 683  
 $\alpha$ -Pyridoin ..... 55  
 2-Pyrones ..... 638  
 Pyruvic acid ethyl ester,  $\alpha$ -cyano-  
    $\alpha$ -naphthyl ..... 52-5
- Q**
- Quinone ketal redistribution ..... 663  
 Quinone ketal rearrangement .... 665-6
- R**
- Radiation  
 dose *vs.* contact angle ..... 544  
 -grafted polyelectrolytes on  
   polymer surfaces ..... 542  
 grafting of hydrophilic monomers  
   -induced ionic polymerization .. 202  
 Radicals ..... 223  
   growing ..... 145  
 Radical transfer reactions ..... 197  
 Random copolymers by cationic co-  
   polymerization, block and ... 350  
 Rate *vs.* distribution ..... 7  
 Rates of monomer conversion .... 376  
 Rates of various monomers, poly-  
   merization ..... 396  
 Reactant ratio, viscosity change *vs.* 498  
 Reaction  
   engineering, polymerization .... 1  
   mechanisms ..... 9-10  
   rate, chromium content *vs.* .... 394  
   rate as a function of temperature 392  
 Reactivity ratios in copolymeri-  
   zation ..... 374  
 Reactivity ratios, estimating ..... 377  
 Reactor  
   batch ..... 4  
   continuous stirred tank ..... 4  
   tubular ..... 6  
 Redistribution ..... 675  
   monomer-polymer ..... 676  
   polymer-polymer ..... 676  
 Reproducibility of polymerizations 70  
 Resin-rubber blends ..... 538  
 Reverse polyamides ..... 618-20  
 Reversibility of copolymerization . 441  
 Reversibility of homopolymeri-  
   zation ..... 440  
 Ring opening copolymerizations .. 446  
 Ring opening polymerization of  
   cycloolefins ..... 399

S	T		
Scavenger studies .....	206	Temperature vs. polymerization	
Seed latexes .....	160-1	activity .....	392
Seeded emulsion polymerization of		Temperature, reaction rate as a	
vinyl chloride .....	158	function of .....	392
Seeding technique .....	158	Terephthalic acid .....	613-4, 622
Selective inhibitors .....	567	Termination by initiator radicals ..	36
Seyferth's method .....	420, 424	Terpolymerization .....	65
Silica permeation, porous .....	754	with a novel bromine-containing	
Slurry process .....	388	monomer .....	536
SO <sub>2</sub> .....	75	parameters .....	64
Sodium naphthalenide .....	241-2	Terpolymers .....	194
Solid state polymerization of hexa-		Tetrahydrofuran .....	351
methylcyclotrisiloxane .....	229	polymerization .....	323
Solution		gegenions in .....	335
polycondensation .....	711	Thawing, coagulation by freezing	
of aromatic polyethers .....	692	and .....	192
process .....	388	THF .....	327, 335, 351
viscosity .....	507	to polymer equilibrium conver-	
Spin densities .....	134	sion of monomeric .....	324
Spiropentane, polymerization of ..	436	Thenoin .....	56
Stability		$\alpha$ -Thenoin .....	61
F/T .....	191	Theory of initiation and propaga-	
mechanical .....	191	tion of carbonium ion poly-	
of polymer emulsions, freeze/		merizations .....	300
thaw .....	188	Thermogravimetric analysis .....	79
Stabilizing interaction between the		TiCl <sub>4</sub> .....	311
support and chromium trioxide	389	Time vs. viscosity .....	498
Steam-expanded foam .....	524	Titanous chloride .....	125
Stepwise addition without		TMD .....	621-2
termination .....	16	Topochemistry of chain propagation	380
Stereospecific polymerization of		Transacetalization .....	385
1,3-butadiene initiated by the		Transient free radicals .....	125
transition of metal $\pi$ -complexes	306	Transition metal $\pi$ -complexes, ster-	
Structural phenomena in polymeri-		eospecific polymerization of	
zation .....	465	1,3-butadiene initiated by the	306
Structure of metalalyls .....	250	Trapped radicals .....	32
Styrene .....	65, 75, 118-9, 121, 351, 355, 472	Trapped radical yield in cellulose	577
copolymerization systems, initi-		Trialkylaluminum .....	287
ators for unsaturated poly-		catalysts .....	300
ester- .....	47	Tricentric systems, polymerization	
copolymers, internal crosslinking		of .....	430
of .....	489	Triisobutylaluminum, chemical	
ethyl acrylate copolymers .....	194	shifts of .....	298
polymerization, kinetic behavior		Trimethylaluminum .....	295
of .....	204	spectra .....	291
pulse radiolysis of .....	219	Trioxane .....	360
Sulfonate-carboxylate composition	704	cationic copolymerization of ..	359, 371
Sulfones, polybutene .....	529	cationic polymerization .....	359
Sulfur dioxide .....	75	copolymerization of .....	362-6
Supported chromium oxide catalysts	387	Triphenylmethyl cation, initiation	
Support and chromium trioxide,		with .....	323
stabilizing interaction between		Triphenylmethyl derivatives .....	317
the .....	389	Trityl ion .....	319
Surface-active agents, grafting of		Trogamid T .....	613, 621, 623-6
monomer to .....	189	Tropylium derivatives .....	317
Surface area .....	27	Tropylium ion, initiation with ..	322, 330
Suspension polymerization .....	145, 529	Tubular reactor .....	6, 19
Symmetry .....	621	Two-phase systems, polymerization	
		in .....	145

- U**
- Unsaturated polyesters ..... 46
- Unsaturated polyester/styrene copolymerization systems, initiators for ..... 47
- V**
- van der Waals' interactions ..... 555
- Vapor deposition polymerization of *p*-xylylenes ..... 643
- Vat Orange 7 ..... 736
- Vat Red 15 ..... 736
- Versatic acids ..... 178
- Vinyl acetate ..... 75, 178, 180-1
- comonomer in ..... 179
- copolymers, graft polymerization of vinyl compounds on ethylene ..... 477
- N-Vinylcarbazole, polymerization of ..... 330-1
- Vinyl carboxylic acids, copolymerization with ..... 189
- Vinyl chloride ..... 126
- emulsion polymerization ..... 158
- seeded emulsion polymerization of ..... 158
- Vinyl ester monomer radicals ... 135
- Vinyl esters ..... 126, 132
- of branched carboxylic acids .. 178
- Vinyl ether-fumaronitrile ..... 97
- Vinyl ether-maleic anhydride ... 97
- Vinyl fluoride ..... 126
- Vinyl monomers ..... 46, 268
- polymerization of metal halide-complexed ..... 94
- polymerization of methyl methacrylate and other ..... 75
- Vinyl polymerization ..... 75
- kinetics of ..... 35
- in solution ..... 125
- Vinylpyridine ..... 75, 270
- 4-Vinylpyridine ..... 269
- Viscosity
- change
- vs.* reactant ratio ..... 498
- polymer concentration *vs.* ... 497
- in reaction, polymer concentration *vs.* ..... 493
- vs.* initial concentration ..... 499
- vs.* polymer concentration .... 502
- solution ..... 507
- vs.* time ..... 498
- W**
- Water contact angles as a function of the mobile counter-anion species ..... 542
- X**
- Xylylenes, vapor deposition polymerization of ..... 643
- Z**
- Zeta transforms ..... 12
- Ziegler type of polymerization ... 268
- Zimm plot ..... 503-4
- Zinc chloride ..... 94
- Zwitterion mechanism of ozonization ..... 452